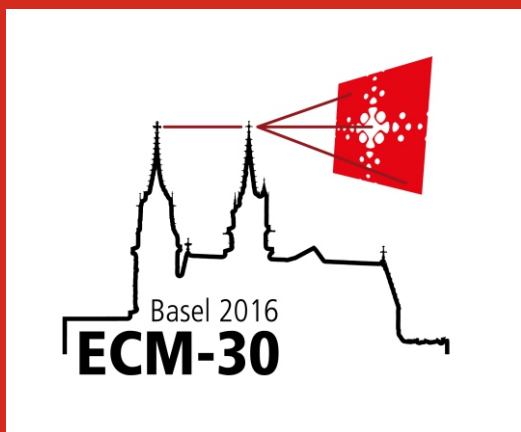


# 30<sup>th</sup> Meeting of the European Crystallographic Association



28 August - 1 September 2016

Congress Center Basel, Switzerland



# Book of abstracts



**30<sup>th</sup> Meeting of the European  
Crystallographic Association**

**Book of abstracts**





## Plenary lectures

### PL-1 Crystallography & Ribosomes, Antibiotics Resistance, Parasites, the Microbiome, Environmental issues, Origin of Life and More

Ada Yonath<sup>1</sup>

1. Weizmann Institute, Israel

email: ada.yonath@weizmann.ac.il

The current global escalation in resistance to antibiotics is a serious threat. Thus, it seems that the world is headed for a post-antibiotic era, in which common infections and minor injuries that have been treatable for decades could become fatal again. Ribosomes, the universal cellular machines that translate the genetic code into proteins, are paralyzed by many clinically useful antibiotics. Structures of ribosomes from genuine multi resistant pathogens, alongside those from eukaryotic parasites illuminated the antibiotics modes of action and highlighted issues associated with species specificity in susceptibility to antibiotics. These structures also showed that the ribosome's catalytic site is located at its core within a universally conserved semi-symmetrical region. The high conservation of this region implies its existence irrespective of environmental conditions and indicates that it might represent a prebiotic RNA entity with catalytic capabilities. Hence, it could be the kernel around which life originated and evolved.

**Keywords:** Ribosomes, biochemistry, biology

### PL-2 Self-Organization-driven Supramolecular Chemistry and Adaptive Chemistry

Jean-Marie Lehn<sup>1</sup>

1. ISIS, Université de Strasbourg, France

email: lehn@unistra.fr

Supramolecular chemistry is actively exploring systems undergoing self-organization, i.e. systems capable of spontaneously generating well-defined functional supramolecular architectures by self-assembly from their components, on the basis of the molecular information stored in the covalent framework of the components.

Supramolecular chemistry is intrinsically a dynamic chemistry in view of the lability of the interactions connecting the molecular components of a supramolecular entity and the resulting ability of supramolecular species to exchange their components. The same holds for molecular chemistry when the molecular entity contains covalent bonds that may form and break reversibly, so as to allow a continuous change in constitution by reorganization and exchange of building blocks. These features define a Constitutional Dynamic Chemistry (CDC) covering both the molecular and supramolecular levels.

CDC takes advantage of dynamic diversity to allow variation and selection and operates on dynamic constitutional diversity in response to either internal or external factors to achieve adaptation.

In particular, component selection on both the dynamic molecular and the supramolecular levels may be driven by the formation of an organized phase: - in 2D on a surface, - in soft matter (gel, liquid crystal), - as well as in 3D in a solid/crystal. Systems will be described and discussed that undergo such processes of self-organization-driven constitutional adaptation. They point to the emergence of an adaptive chemistry.

#### References

- Lehn, J.-M., *Supramolecular Chemistry: Concepts and Perspectives*, VCH Weinheim, 1995.  
 Lehn, J.-M., *From supramolecular chemistry towards constitutional dynamic chemistry and adaptive chemistry*, Chem. Soc. Rev., 2007, 36, 151.  
 Lehn, J.-M., Chapter 1, in *Constitutional Dynamic Chemistry*, ed. M. Barboiu, *Topics Curr. Chem.*, 2012, 322, 1-32.  
 Lehn, J.-M., *Perspectives in Chemistry – Steps towards Complex Matter*, Angew. Chem. Int. Ed., 2013, 52, 2836-2850.  
 Lehn, J.-M., *Perspectives in Chemistry – Aspects of Adaptive Chemistry and Materials*, Angew. Chem. Int. Ed., 2015, 54, 3276-3289.

**Keywords:** Supramolecular Chemistry, Adaptive Chemistry

## Keynote lectures

### KN-1 Colloids in the spotlight - watching crystal-crystal transitions in real time and real space

Peter Schurtenberger<sup>1</sup>

1. Lund University, Sweden

email: Peter.Schurtenberger@fkem1.lu.se

Colloids have frequently been used as attractive model systems to study processes such as nucleation and crystal growth, melting, or crystal-crystal transitions. The nature of solid-solid phase transformations has indeed been a long-standing question in areas such as metallurgy and condensed matter physics. They are not only interesting from a fundamental science viewpoint, but have many applications in materials. However, despite their importance and the numerous investigations existing, we still lack a deep understanding of the micro-structural changes and the underlying kinetic mechanisms. Here I will show that we can use thermoresponsive colloids as an ideal model system to study such phase transitions using confocal laser scanning microscopy, and achieve exquisite control over the relevant thermodynamic variables. In particular the application of an external electric field allows us to carefully tune the resulting interparticle interactions such that we can cycle through the complex phase diagram of these systems. This allows us to probe crucial features of phase transitions: kinetics of phase change in both forward and reverse directions, reversibility and irreversibility, and the stability of arrested states. We see path-dependent crystal-to-crystal phase transition kinetics with both diffusive and martensitic transformations controllable via an external electric field, and we observe kinetic arrest, with the time to transit to the equilibrium phase controllable via temperature. We believe that these two path dependent transitions provide a first direct evidence of colloidal analogues of diffusive and martensitic transformation respectively in a single 3-dimensional system.

**Keywords:** colloid crystals, crystal-crystal transition, diffusive transformation, martensitic transformation

### KN-2 Exploring crystalline molecular materials at high pressure

Francesca P.A. Fabbiani<sup>1</sup>

1. Georg-August-Universität Göttingen, GZG, Department of Crystallography

email: ffabbia@gwdg.de

Over the course of the past two decades, the number of high-pressure crystallographic studies on molecular materials reported in the literature has been increasing at an exponential rate. One of the reasons behind this surge is certainly the increasing ease with which these studies can be performed in the home laboratory and at large-scale facilities. Besides technology advances, the scientific community has realised that pressure is a powerful thermodynamic variable that allows modifying the structure, bonding and reactivity of all matter, *including molecular compounds*. High-pressure structural studies on such materials have managed to catch the attention and imagination of crystallographers and material scientists world-wide, opening up innumerable opportunities across several natural sciences disciplines. This is demonstrated by the observation that high-pressure crystallography is currently an integral part of several multidisciplinary research programs that aim at exploring and understanding the structure and property of molecular materials.

After a brief overview of recent and current trends in the field, I shall focus on a number of case studies, primarily involving molecular *organic* compounds. The aim here is to demonstrate the rich structural landscape that can be obtained when high-pressure crystallography and crystal growth techniques are combined with ambient-pressure studies. The examples will cover a range of topics, including a) "classical" high-pressure structural studies, *e.g.* studies of intermolecular interactions and of phase transitions but also of more exotic phenomena such as pressure-induced hydration, and b) practical applications of high-pressure techniques in the pharmaceutical industry.

**Keywords:** high pressure, polymorphism, molecular compounds, pharmaceuticals, crystallisation

## KN-3 Molecular Recognition in Chemical and Biological Systems: A Multi-Dimensional Approach

François Diederich<sup>1</sup>

1. ETH Zurich

email: [diederich@org.chem.ethz.ch](mailto:diederich@org.chem.ethz.ch)

We pursue a multi-dimensional approach towards deciphering and quantifying weak intermolecular interactions in chemical and biological systems. Experimental study in this research involves the investigation of protein-ligand interactions, synthetic host-guest complexation, and dynamic processes in designed unimolecular model systems, such as molecular torsional balances. It is complemented by computational analysis and exhaustive data base mining in the Cambridge Crystallographic Database (CSD) and the Protein Data Bank (PDB). Examples of intermolecular interactions quantified by this approach are orthogonal dipolar interactions, organofluorine interactions, stacking on peptide bonds, and halogen bonding. We also investigate the energetics of the replacement of conserved water molecules in protein co-crystal structures by ligand parts. This multi-dimensional approach is illustrated in examples taken from a variety of structure-based drug design projects. Lessons learned are directly applicable to ligand design and optimization in drug discovery and crop protection research, but equally to the assembly of synthetic supramolecular systems. Specific examples will include the replacement of water clusters in protein-ligand complexes of tRNA-guanine transglycosylase (TGT), a target against bacterial shigellosis dysenteriae. It is shown for protein kinase A (PKA), how the glycine-rich loop at the ATP binding site can be favorably addressed by establishing an intense cooperative interaction network. Ligand development against novel targets for antimalarials is illustrated for serine hydroxymethyl transferase (SHMT), a key enzyme from the folate cycle for which ligands had surprisingly not been reported previously. Protein crystallographic work has been essential in all three projects.

**Keywords:** Molecular Recognition

## KN-4 Emphasizing the difference between experimental and theoretical electron density in the solid state: new opportunities from anharmonic thermal motion to excited states

Birger Dittrich<sup>1</sup>

1. Heinrich-Heine Universität Düsseldorf, Anorganische Chemie und Strukturchemie, Universitätsstraße 1, Gebäude 26.42.01.21, 40225 Düsseldorf

email: [bdittri@gwdg.de](mailto:bdittri@gwdg.de)

Single-crystal X-ray Bragg diffraction to high scattering angle on suitable, high-quality samples contains detailed information on the electron-density distribution (EDD). Likewise, knowledge of the EDD can be obtained by theoretical methods.

The pseudoatom model [1] has been the method most frequently used for extracting experimental solid-state EDD and coming of age has been proclaimed [2]. However, many open questions beyond the well-established EDD topology remain, especially concerning structures so far considered unsuitable for precise experiments on grounds of incomplete de-convolution of displacement parameters and EDD.

Research opportunities related to this situation allow studying (1) temperature dependent changes in structure or EDD (e.g. due to rotational disorder, phase transitions, or dynamic Jahn Teller Distortion/ spin crossover), (2) effects of high-pressure, (3) visible-light excitation, (5) time dependence, (6) anharmonic thermal motion, (7) and/or disorder. Here differences between theory and experiment may be caused by other physical effects. The approximation of using suitable partitioned isolated-molecular ground-state EDD projected onto multipoles ("invariants") for describing crystal EDD is then often sufficient and permits to calculate differences on a grid, thereby directly showing how experimental signal and theoretical EDD differ for a particular system. Most importantly there is a change in philosophy involved first explored in [4], which could provide an impulse to rejuvenate charge density research: not the EDD but difference densities matter. They should be given more attention.

Examples of applications of this guiding principle will be given. Finally a (literally) exciting new application are "beyond Born-Oppenheimer" experiments, where tunable synchrotron radiation is exploited by probing EDD at and below the absorption edge using otherwise identical measurement conditions, requiring a d-block central atom in a coordination compound. Hard X-ray core-electron excitation/relaxation is faster than nuclear rearrangements, and the difference of the two diffraction patterns contains the information on these ultrafast processes.

[1] Stewart, R. F. (1976). *Acta Cryst.* A32, 565; Hansen, N. K. & Coppens, P. (1978). *Acta Cryst.* A34, 909

[2] Coppens, P. (2005). *Angew. Chem. Int. Ed.* 44, 6810

[3] Dittrich, B., et al. (2009). *Phys. Chem. Chem. Phys.* 11, 2601

[4] Dittrich, B. et al. (2015) *ChemPhysChem*, 16, 412

**Keywords:** charge density, multipole model, difference electron densities

**KN-5** The role of structure and biophysics in the discovery of allosteric kinase inhibitors: ABL001, a potent and specific inhibitor of BCR-ABL

Sandra W. Cowan-Jacob<sup>1</sup>

<sup>1</sup> Novartis, Switzerland

email: [sandra.jacob@novartis.com](mailto:sandra.jacob@novartis.com)

Protein kinases are one of the most successfully targeted protein families with over 30 different FDA-approved drugs on the market and many more undergoing testing in the clinic. Despite this success, there are many challenges to overcome to identify potent, selective inhibitors with good pharmacokinetics. An area that has not yet been exploited widely and that offers opportunities to overcome these challenges is the idea of targeting the kinases outside the ATP site.

Chronic myelogenous leukemia (CML) is characterized by a chromosomal translocation resulting in fusion of the BCR and ABL1 genes and constitutive activation of ABL1 kinase. This fatal disease has been transformed into a chronic condition for a majority of patients due to the discovery of tyrosine kinase inhibitors (TKI), targeting the ATP site of the kinase. However, there remains a subset of patients who develop resistance or who do not tolerate these drugs.

The molecular understanding of the regulation of ABL1 kinase enabled us to design biophysical and biochemical assays that could replicate the effects of blocking the kinase in a physiologically relevant inactive conformation. This resulted in the discovery of ABL001 which binds with single digit nM affinity to a pocket distant from the ATP site and is active against known clinically relevant mutations in CML. ABL001 is currently being evaluated in Phase I clinical trials.

This case study highlights an example of the synergy between biophysics and medicinal chemistry in delivering potentially better drugs, and also demonstrates how an improved molecular understanding of the target can lead to novel modes of targeting proteins.

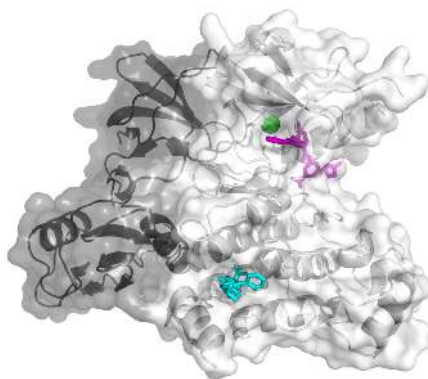


**Figure 1.** The structure of Abl (SH3-SH2-Kinase) in complex with an ATP site inhibitor (top) and a myristate site inhibitor (bottom), and showing the location of the T315I mutation (sphere in ATP binding site).

**Keywords:** kinase, allosteric, inhibitor, drug discovery

## KN-6 Organic crystal structure prediction – from fundamental research to industrial application

Marcus Neumann<sup>1</sup>

<sup>1</sup> Avant-garde Materials Simulation Deutschland GmbH, Freiburg, Germany

email: neumann@avmatsim.de

Crystal structure prediction is the task of deriving the observable three-dimensional crystal structures of organic molecules from their chemical structure alone. Prediction methods face the mathematical challenge of sampling a search space that grows exponentially with the number of degrees of freedom and the physical challenge of calculating lattice free energy differences with an accuracy that should be better than the order of magnitude of typical lattice energy differences between polymorphs.

The state-of-the-art was assessed by a series of blind tests in 1999, 2001, 2004, 2007, 2010 and 2015. In the last three blind tests, the highest success rate was scored with an approach implemented in the computer program GRACE. Dispersion-corrected density functional theory (DFT-D) calculations [1] are used to first generate reference data to which a tailor-made force field is fitted from scratch [2] for every chemical compound under consideration. The tailor-made force field is then used in conjunction with a Monte Carlo parallel tempering algorithm to generate crystal structures that are further optimized at DFT-D level. Statistical control mechanisms ensure that all crystal structures in a user-defined target energy window are found with a user-defined level of confidence.

The 2015 blind test [3] has demonstrated the ability of GRACE to perform crystal structure predictions using fully automated workflows, to handle two flexible molecules per asymmetric unit and to predict the crystal structure of the hydrate of a chloride salt.

Looking back on a dozen case studies published on drug-like molecules by various authors and an equal number of confidential studies with GRACE, a picture emerges how crystal structure prediction in an industrial working environment helps to rationalize crystallization behaviour, to understand solid-state forms, to solve crystal structures and to flag missing more stable forms. The emerging ability to find new crystal forms by rational crystallization experiment design based on the knowledge of the computed crystal energy landscape is illustrated by the example of Dalcetrapib [4].

[1] Neumann, M. A. and Perrin, M.-A. J. Phys. Chem. B 109: 15531-15541 (2005)

[2] Neumann, M. A. J. Phys. Chem. B 112: 9810-9829 (2008)

[3] Reilly, A. M. et al. Acta Cryst. B, submitted for publication (2016)

[4] Neumann, M. A. et al. Nature Communications 6, art7793 (2015)

**Keywords:** crystal structure prediction, in silico polymorph screening, crystal energy landscape

**KN-7 Electron nanodiffraction for structural biology**Jan Pieter Abrahams<sup>1</sup>

1. Biozentrum, University of Basel, Switzerland

email: jp.abrahams@unibas.ch

Cryo-electron microscopy (cryo-EM) is a powerful technique for studying the structure of macromolecular complexes. Radiation damage by the electron beam limits image contrast, and thus the resolution. But an EM can be switched to diffraction mode and recent experiments indicate that this delivers ten times better data with an electron dose that is 100 times lower, when using a hybrid pixel quantum area detector originally developed for high-energy physics. This allows full atomic structure determination using just a single protein nano-crystal with a diffracted volume of 0.03 cubic micrometer. The physics that explain this vast improvement equally applies to non-crystalline samples. These results indicate that switching to diffraction may allow structure determination of single macromolecules in solution, and ultimately in complex environments like those of the living cell. But collecting electron scattering data does have a major disadvantage: the phase information that is required for structure determination can only be inferred indirectly. For electron scattering data of crystals, methods that were originally developed for X-ray crystallography have proven to work. But in order to extend the method to non-crystalline samples, alternative phasing strategies have to be considered.

**Keywords:** Cryo-electron microscopy, Electron nanodiffraction

**KN-8 Driving Forces of Phase Transitions in Molecular Materials**Simon Parsons<sup>1</sup>

1. University of Edinburgh

email: s.parsons@ed.ac.uk

In two essays published in the March 2015 issue of *IUCrJ* Dunitz and Desiraju and co-workers present contrasting views of the way in which intermolecular interactions in crystal structures should be interpreted. Dunitz's view emphasises the importance of whole-molecule interaction energies, whereas Desiraju promotes the importance of individual atom-atom interactions, associating short atom-atom distances with specific intermolecular bonding. The contrast in between views, which is extremely important in the analysis of phase stability and the rationalisation of phase transitions, forms the subject of this Keynote. For example, application of pressure to trigonal  $\gamma$  glycine yields the monoclinic  $\epsilon$  phase, and we have studied this transition using neutron powder diffraction. Packing energy calculations using both the PIXEL method and symmetry-adapted perturbation theory yield consistent results which can be interpreted using Hirshfeld surface analysis and full interaction maps. The calculations provide detailed characterisation of the factors which promote the stability of the two phases under different external conditions, enabling the principal thermodynamic driving forces of the forward and reverse transitions to be identified. The crystal structures of amino acids have generally been interpreted in terms of strong  $\text{NH}\cdots\text{O}$  hydrogen bond formation between the ammonium and carboxylate groups of the zwitterionic molecules, supported by weaker dispersion or  $\text{CH}\cdots\text{O}$  interactions. The packing energy calculations reveal that this view should be modified substantially, to take into account the large *repulsive* intermolecular interactions (as promoted by Dunitz) which are associated with apparently highly-stabilising hydrogen bond geometry (emphasised by the Desiraju model).

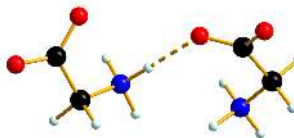


**Figure 1.** Repulsive H-bonded dimer in  $\gamma$ -glycine.  $\text{NH}\cdots\text{O} = 1.95$  Å,  $\angle\text{NH}\cdots\text{O} = 179^\circ$ , Energy =  $+18.5$  kJ mol<sup>-1</sup>.

**Keywords:** Hydrogen bonding, high pressure, amino acids, phase transitions, intermolecular energies

**KN-9** Crystalline Sponge Method for Absolute Structure DeterminationMakoto Fujita<sup>1</sup><sup>1</sup>. Department of Applied Chemistry, University of Tokyo, Tokyo, Japan

email: mfujita@appchem.t.u-tokyo.ac.jp

X-ray single crystal diffraction (SCD) analysis has the intrinsic limitation that the target molecules must be obtained as single crystals. Here, we report a new protocol for SCD analysis that does not require the crystallization of the sample.<sup>1-5</sup> In our method, tiny crystals of porous complexes are soaked in the solution of a target, where the complexes can absorb and orient the target molecules in the pores. The crystallographic analysis clearly determines the absorbed guest structures along with the host frameworks. As the SCD analysis is carried out with only one tiny crystal, the required sample amount is of the nano-to-microgram order. In this talk, following a general discussion,<sup>6-11</sup> the applications of the method for the absolute structure determination will be discussed. The absolute configurations of elatene (1) has still not been unequivocally confirmed because of its almost achiral meso-formed core structure that results in nearly zero [α]<sub>D</sub> specific rotation. This faint chirality was precisely discriminated by the crystalline sponge and its absolute structure was reliably determined (Fig. 1).<sup>11</sup> We will show a dozen of examples for absolute structure determination in asymmetric synthesis studies as well as in natural product chemistry.

References: 1) K. Biradha and M. Fujita, *Angew. Chem. Int. Ed.* **2002**, *41*, 3392-3395; 2) O. Ohmori, M. Kawano, and M. Fujita, *J. Am. Chem. Soc.* **2004**, *126*, 16292-16295; 3) Y. Inokuma, S. Yoshioka, J. Ariyoshi, T. Arai, Y. Hitora, K. Takada, S. Matsunaga, K. Rissanen, M. Fujita *Nature* **2013**, *495*, 461-466; 4) Y. Inokuma, S. Yoshioka, J. Ariyoshi, T. Arai, M. Fujita *Nat. Protoc.* **2014**, *9*, 246-252; 5) K. Ikemoto, Y. Inokuma, K. Rissanen, and M. Fujita *J. Am. Chem. Soc.* **2014**, *136*, 6892-6895; 6) T. R. Ramadhar, S.-L. Zheng, Y.-S. Chen and J. Clardy, *Acta Cryst.*, **2015**, *A71*, 46-58; 7) S. Yoshioka, Y. Inokuma, M. Hoshino, T. Sato, M. Fujita *Chem. Sci.* **2015**, *6*, 3765-3768; 8) N. Zigon, M. Hoshino, S. Yoshioka, Y. Inokuma, and M. Fujita, *Angew. Chem. Int. Ed.* **2015**, *54*, 9033-9037; 9) A. B. Cuenca, N. Zigon, V. Duplan, M. Hoshino, M. Fujita, and E. Fernández, *Chem. Euro J.* **2016**, *22*, 4723-4726; 10) M. Hoshino, A. Khutia, H. Xing, Y. Inokuma, M. Fujita, *IUCrJ* **2016**, *3*, 139-151; 11) V. Duplan, M. Hoshino, W. Li, T. Honda, and M. Fujita, *Angew. Chem. Int. Ed.* **2016**, *55*, 4919-4923.

**Keywords:** crystalline sponge method, absolute structure, absolute configurations, crystallography, metal-organic frameworks

**KN-10** Mechanical properties of nanostructures in the light of synchrotron radiationOlivier Thomas<sup>1</sup><sup>1</sup>. Aix-Marseille Université, CNRS IM2NP UMR7334

email: olivier.thomas@im2np.fr

Mechanical properties of nanostructures are different from those of bulk materials. In particular the yield stress is much larger when the size of objects decreases. Many issues are still being debated about the elementary mechanisms at work: what is the role of dislocation sources in these structures? What is the influence of surfaces on dislocation nucleation? ... X-ray diffraction is a very powerful tool to investigate mechanics in small dimensions. Indeed X-rays have the distinct advantage of being non-destructive and highly penetrating. Moreover the wavelength of hard X-rays is perfectly matched to lattice spacing, which makes X-ray diffraction very sensitive to strains. In this talk I will give a brief overview of recent developments, which have been made possible thanks to smaller beams (down to few 100 nms) and new 2D X-ray detectors (with high dynamic range and reading frequency). These new features allow for *in situ* mechanical testing of nanostructures. Specific examples will include coherent diffraction imaging of inversion domain boundaries in GaN nanowires and prismatic dislocation loops in Au nanoislands during *in situ* nanoindentation as well as micro-Laue diffraction of Au nanowires during *in situ* three-point bending.

*This work is funded by ANR under project MECANIX ANR-11-BS10-01401*

Z. Ren *et al.*, Scanning force microscope for in situ nanofocused X-ray diffraction studies, *J. Synch. Rad.* **21**, 1128 (2014).

C. Leclerc *et al.*, In situ bending of a Au nanowire monitored by micro Laue diffraction, *J. Appl. Cryst.* **48**, 291 (2015).

S. Labat *et al.*, Inversion Domain Boundaries in GaN Wires Revealed by Coherent Bragg Imaging, *ACS Nano* **9**, 9210 (2015).

**Keywords:** Mechanics, Nanowires, Coherent diffraction, Laue diffraction

## KN-11 Solving crystal structures with GSAS-II

Robert B. Von Dreele<sup>1</sup>

1. Advanced Photon Source, Argonne National Laboratory, Lemont, IL 60439 USA

email: vondreele@anl.gov

One of the goals in developing GSAS-II was to expand from the capabilities of the original General Structure Analysis System (GSAS) which largely encompassed just structure refinement and post refinement analysis. GSAS-II has been written almost entirely in Python loaded with graphics, GUI and mathematical packages (matplotlib, pyOpenGL, wx, numpy and scipy). Thus, GSAS-II has a fully developed modern GUI as well as extensive graphical display of data and results. However, the structure and operation of Python has required new approaches to many of the algorithms used in crystal structure analysis. The extensions beyond GSAS include image calibration/integration as well as peak fitting and unit cell indexing for powder data which are precursors for structure solution. Structure solution within GSAS-II begins with either Pawley extracted structure factors from powder data or those measured in a single crystal experiment. Both charge flipping and Monte Carlo-Simulated Annealing techniques are available; the former can be applied to (3+1) incommensurate structures as well as conventional 3D structures. This talk will highlight the features of GSAS-II with particular focus on the structure solution facilities. Supported by US DOE/OS/BES under Contract No. DE-AC-02-06CH11357.

**Keywords:** charge flipping, GSAS-II, Rietveld refinement, Python

## KN-12 Time-resolved femtosecond crystallography opens a new era in Structure Biology

Petra Fromme<sup>1</sup>

1. Arizona State University, School of Molecular Sciences and center for Applied Structural Discovery Biodesign Institute

email: PFromme@asu.edu

Time-resolved Serial Femtosecond Crystallography (SFX) provides a novel concept for structure determination, where X-ray diffraction “snapshots” are collected from a fully hydrated stream of nanocrystals at room temperature, using femtosecond pulses from the world’s first high energy X-ray free-electron laser, the Linac Coherent Light Source before the crystals are destroyed by the X-rays. The first proof of concept of serial femtosecond crystallography was achieved using Photosystem I, a larger membrane protein complex involved in Photosynthesis as a model system [1],[2]. In the time resolved SFX studies, the nano/microcrystals of Photosystem II [3] are fully active in water splitting and are cycled through the S-states by laser excitation “on the fly”. Conformational changes of the Mn<sub>4</sub>Ca cluster and its protein environment were observed for the first time in the transition from the dark to the double excited state [4], however the resolution was limited to 5Å resolution. Very recently we have achieved a breakthrough, which cuts the “Gordian Knott” that will lead to a paradigm shift in X-ray crystallography. We have been able to show that “single molecule” continuous X-ray diffraction can be obtained by SFX from Photosystem II microcrystals with minimal displacements of the PSII molecules by 0.8 Å, which is less than the bond length between two C atoms. These molecular continuous diffraction patterns were directly phased and the structure determined to a resolution way beyond the Bragg peaks [5]. The talk will also report on the development of compact femto and attosecond X-ray Sources at DESY (AXSiS) and at ASU (CXLS and CXFEL), which will provide unique new opportunities to study the ultrafast dynamics of reactions in photosynthesis with a combination of X-ray diffraction, X-ray spectroscopy and ultrafast optical spectroscopy. References: [1] Chapman, H.N., Fromme, P., Barty, A. et al Nature 2011, 470, 73-77 [2] Fromme P., Spence J.C. Curr Opin Struct Biol 2011, 21: 509-516 [3] Kupitz C, Grotjohann I, Conrad CE, Roy-Chowdhury S, Fromme R, Fromme P Philo Trans R Soc Lond B Biol Sci 2014, 369 [4] Kupitz, C, Basu, S, Grotjohann, I et al Nature 2014, 513, (7517), 261-5 [5] Ayer, K. et al. Nature 2016 **530**, 202-206



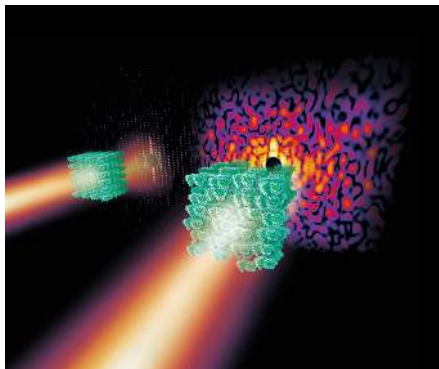


**Figure 1.** Artistic view of Bragg versus Continuous Diffraction from crystals (Credit: DESY, Eberhard Reiman)

**Keywords:** Free Electron Laser, time-resolved femtosecond crystallography, Photosynthesis, Photosystem II, continuous diffraction

## KN-13 Transition metal oxides: from structural complexity and topotactic oxygen diffusion pathways to energy applications

Werner Paulus<sup>1</sup>

1. Institut Charles Gerhardt, ICGM-UMR 5253 CNRS Université de Montpellier, 34000 Montpellier, France

email: werner.paulus@univ-montp2.fr

Understanding oxygen diffusion in solid oxides at the atomic scale is an important issue for the development of technological devices such as solid oxide fuel cells (SOFC), as well as membrane based air separators, oxygen sensors and catalytic converters to transform e.g. NO or CO from exhaust emissions into N<sub>2</sub> and CO<sub>2</sub> [1-2]. For SOFC e.g., the main drawback of long-term endurance is related to high operating temperatures of around 1000-1250 °C, presenting a key challenge in terms of fatigue due to compositional and microstructural degradation of the respective electrode/membrane materials.

Regarding electrodes materials with *mixed ionic and electronic* transport properties, two structure types are known today to undergo oxygen intercalation reactions at ambient temperature: the Ruddlesden-Popper series, such as the RE<sub>2</sub>MO<sub>4+d</sub> (RE = La, Nd, Pr; M = Cu, Ni, Co) members, and the layered double perovskites labeled AA'B<sub>2</sub>O<sub>5+d</sub> including the brownmillerite structure, such as SrMO<sub>2.5</sub> (M = Fe, Co). We recently demonstrated that oxygen mobility at ambient temperature in brownmillerites is intimately related to low energy phonon modes, which constituted the first evidence of a phonon-assisted oxygen diffusion mechanism [3-4].

We discuss here complex oxygen ordering phenomena during oxygen uptake or release reactions in non-stoichiometric oxides with Brownmillerite and K<sub>2</sub>NiF<sub>4</sub> type frameworks, essentially explored by *in situ* neutron scattering and synchrotron radiation. Oxygen doping frequently induces the generation of highly correlated systems for both, oxygen ordering but also for charge and orbital ordering, resulting in giant unit cells. We further discuss the interplay of highly correlated oxygen ordering and related changes in the lattice dynamics to better understand low temperature oxygen mobility, activated by a phonon-assisted diffusion mechanisms. Our studies allow to achieve a microscopic understanding of oxygen diffusion mechanism in solid oxides down to ambient temperature, which is equally important for the synthetic chemist to explore new, kinetically stabilized oxides not available by classical solid state methods [5].

1. Paulus W. et al. *JACS* 130, 47 (2008) 16080
2. Penkala B. et al. *Cat Sci & Tech*, 5 (2015) 4839
3. Ceretti M et al. , *J MatChem A*, 3, 42 (2015) 21140
4. Perrichon A. et al. *JPhysChem C*119 (2015) 1557
5. Houchati I. et al. *Chem. Mater.* 24 (2012) 3811

## KN-14 Colour X-ray Tomography

Bob Cernik<sup>1</sup><sup>1</sup>. School of Materials, The University of Manchester, UK

email: B.Cernik@manchester.ac.uk

The twentieth century saw a revolution in the field of X-ray imaging beginning with the acquisition of somewhat rudimentary 2D radiographs and finishing with the arrival of advanced CT systems capable of producing very high quality 3D images that can show the internal structure of an object. The most common uses of CT can be found in non-destructive testing; security scanning and in hospitals where modern spiral CT scanners can collect whole body images in minutes. CT works on the basic principle that an X-ray beam incident on an object is absorbed by differing amounts depending upon the composition of the material and the shape of the object. By measuring the transmitted X-rays we obtain 2D radiographs. If we then rotate or translate the sample a number of radiographs can be collected from which 3D, density contrast, images can be mathematically reconstructed. These images can be made sharper by the use of phase or diffraction contrast but are still dominated by absorptive processes. The main limitations of radiography and CT are that they lack insight into the chemical, atomic or crystallographic structure of the object under study. This information can be crucial to fully understanding in-situ chemical processes. Examples of this can be found in corrosion mechanics; alloying behaviour or catalytic reactions. This talk is targeted toward the development and use of bright and dark field colour X-ray imaging systems capable of forming 3D images of relatively large objects using high power, high energy, X-ray sources (from lab and synchrotron). The colour images generated have chemical or physical information in each voxel of the image. Two main approaches will be discussed using high energy monochromatic and white or pink beam radiation. The monochromatic approach is usually called XRD-CT and can be configured to deliver excellent spatial resolution. XRD-CT has recently been demonstrated to work well with PDF data delivering nanocrystalline maps. The energy dispersive methods are faster but have poorer spatial and energy resolution but are more likely to be adopted for non-destructive testing and security scanning applications. EDD imaging has been facilitated by the development of pixelated energy sensitive X-ray detectors and by the development of scattering geometries to improve the signal to noise ratio (SNR) of the weak signals that contain this chemical and structural information.

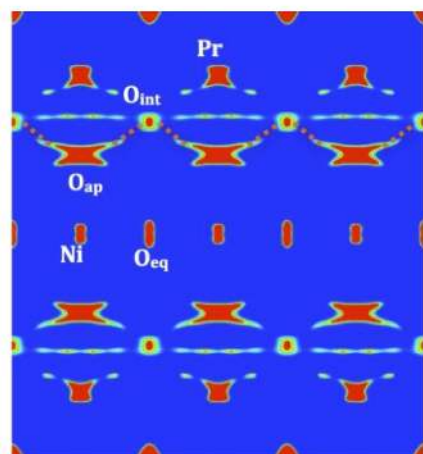
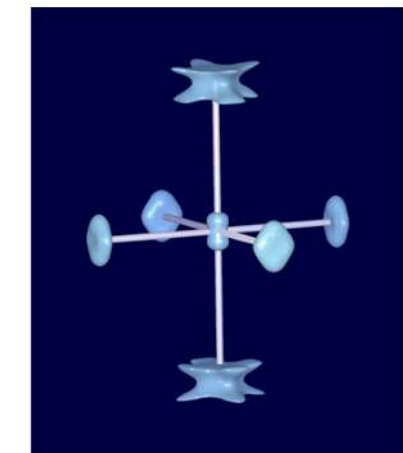


**Figure 1.** Nuclear density of  $\text{Pr}_2\text{NiO}_{4.25}$  @400°C from single crystal neutron diffraction and subsequent MaxEnt reconstruction. Top: Anharmonic double potential of the  $\text{O}_{\text{ap}}$  atoms of the  $\text{NiO}_6$  octahedra. Bottom: Dynamically activated oxygen diffusion pathway in the  $\text{Pr}_2\text{O}_3$  rock salt layer between  $\text{O}_{\text{int}}$  and  $\text{O}_{\text{ap}}$  sites [3]

**Keywords:** transition metal oxides, phonon assisted diffusion, oxygen intercalation, in situ diffraction, inelastic neutron scattering, SOFC

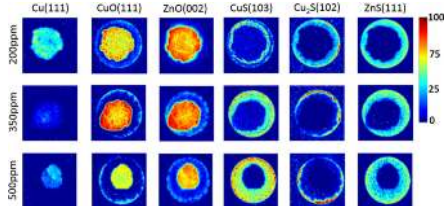


**Figure 1.** The figure shows how the crystalline phases within a 3D catalyst body ( $\text{Cu/ZnO/Al}_2\text{O}_3$ ) change after various levels of  $\text{H}_2\text{S}$  exposure. The 2D reconstructions were based on XRD-CT principles. Beale A M et al. JOURNAL OF CATALYSIS Vol 314, 94-100 (2014)

**Keywords:** X-ray imaging**KN-15** Every pixel countsSven Lidin<sup>1</sup>

1. Lund University, Sweden

email: sven.lidin@polymat.lth.se

Bragg scattering is a wonderful thing that permits us to determine the positions of individual atoms and even the shape of their electron densities with unrivalled accuracy, while the information carried by the part of the diffraction pattern that is non-Bragg is still largely considered a nuisance. Incommensurate satellites tell us about additional intra-crystalline ordering, structured diffuse scattering carries information about incipient ordering, strain and the shape of crystals while reflections from twinning and intergrowth helps us understand the material from an inter-crystalline point of view. These features have long been used in powder diffraction where it is difficult to sweep the extra information under the carpet, but in single crystal work we are used to presenting the data in integrated form where none of these disturbing features need be addressed. This is unfortunate and wasteful. First of all it has led to the debatable practice of selecting the “best” “single” crystals for experiments. If the study is about determining the electron density with the highest possible precision, this is clearly the way to go, but if we want information beyond that we are discarding a lot of data. We learn a lot about the “best” “single” crystal but less about the sample in general. We are like tourist agencies showing you images of altstadt Basel in glorious sunshine, having picked the “best” image rather than displaying the full truth of a town where, according to statistics, it rains two days out of three throughout the period april-september.

In the past, we were limited to evaluating Bragg scattering for the simple reason that sources were to weak, sensitivity of detectors was too low and that as a result of this, methods for the evaluation of non-Bragg data were largely lacking. Thanks to new detectors and sources and to the development in methods this has driven, we are now in a position where we can make full use of the total scattering from our samples. There are, however, two factors that limit us in this respect. The first is time. It is much more time consuming to perform a full scattering analysis that a standard single crystal structure determination. The second is evaluation. Through the practice of avoiding samples that display significant non-Brag effects we have set a standard for what is an acceptable experimental outcome. In this talk these issues will be discussed using a number of examples from pathological samples.



**Figure 1.** The tourist picture of Basel does not agree with the statistics for the average seasonal rainfall

**Keywords:** Bragg scattering, Structured diffuse scattering, Twinning, Incommensurabilities

## **KN-16** New methods for structural investigations of nanocrystalline and amorphous organic compounds

Martin U. Schmidt<sup>1</sup>

1. Institut für Anorganische und Analytische Chemie,  
Goethe-Universität, D-60438 Frankfurt am Main, Deutschland

email: m.schmidt@chemie.uni-frankfurt.de

Most methods for structure determination from powder diffraction data and Rietveld refinement only work, if the peaks of the simulated powder pattern overlap with those of the experimental diffractogram, i.e. if the lattice parameters of the structural model are very close to the correct ones. We developed a method for a Fit with DEviating Lattice parameters (FIDEL) [1]. The algorithm uses cross-correlation functions instead of a point-to-point comparison of the simulated and experimental diagrams. It can be used, e.g., as a pre-fit for a Rietveld refinement. The FIDEL method is also useful to fit, e.g., low-temperature crystal structures to a room-temperature powder diagram. Crystal structures can be solved from a non-indexed powder diagram by a crystal structure prediction with force fields, followed by FIDEL fit with subsequent automated Rietveld refinement. Structure determination from unindexed powder data is even possible directly with a FIDEL fit, starting from a large set of random crystal structures in various space groups with random values for lattice parameters, molecular position and orientation [1].

Local structures of crystalline, nanocrystalline and amorphous organic compounds can be investigated by analysis of the pair-distribution function (PDF) [2]. The pair-distribution function gives the probability of finding pairs of atoms separated by a distance  $r$ . Experimentally, the PDF is obtained by Fourier transformation of the intensities of a carefully measured powder diffractogram. Also electron powder diffraction data can be used [3,4]. The PDF is used to investigate local arrangements of neighbouring molecules, ordering lengths etc [5]. Examples will be shown. Recent software developments allow the fit of a crystal structural model to the PDF curve [6]. It is also possible to solve crystal structures from powder data by a PDF fit. The structure of allopurinol could even be successfully solved in P1 with four symmetrically independent molecules [6].

[1] S. Habermehl et al., *Acta Cryst.* B70 (2014), 347-359.

[2] D. Prill, P. Juhás, M.U. Schmidt, S.J.L. Billinge, J. *Appl. Cryst.* 48 (2015), 171-178.

[3] T.E. Gorelik, M.U. Schmidt, U. Kolb, S.J.L. Billinge, *Microsc. Microanal.* 21 (2015), 459-471.

[4] S. Billinge, C. Farrow, M. Kanatzidis, T.E. Gorelik, M.U. Schmidt, US-Patent 8921783 B2 (2014).

[5] M.U. Schmidt et al., *Acta Cryst.* B65 (2009), 189-199.

[6] D. Prill, P. Juhás, S.J.L. Billinge, M.U. Schmidt, *Acta Cryst.* A72 (2016), 62-72.

**Keywords:** Nanocrystalline organic compounds, Amorphous organic compounds, SDPD, FIDEL fit, Pair-distribution function, PDF fit

## MS1 SAXS in structural biology

Chairs: Bente Vestergaard, Dimitri Svergun

### MS1-O1 Disentangling Structural Heterogeneity in Highly Disordered Biomolecular Complexes

Pau Bernadó<sup>1</sup>

1. Centre de Biochimie Structurale, Montpellier

email: pau.bernado@cbs.cnrs.fr

During the last decade multiple bioinformatics analysis have revealed that many key proteins involved in signalling and cell control contain large disordered regions and, in some cases, are fully unstructured. The existence of proteins that despite not having permanent structural elements are fully functional have required the reformulation of the traditional structure/function paradigm, one of the historical bases of biological sciences. The study of the relationship between the dynamic structure of Intrinsically Disordered Proteins (IDPs) and their function represents an enormous challenge due to their inherent conformational plasticity. IDPs do not crystallize, and solution methods provide ensemble averaged structural parameters that must be interpreted in terms of ensembles. These difficulties have been partially overcome by applying integrative structural biology approaches where multiple complementary structural data are integrated to derive ensemble models embedding the structure and dynamics of IDPs or their complexes with other biomolecules. In this presentation the study of disordered biomolecular complexes involved in regulation of gene transcription and DNA processivity will be presented. These studies integrate SAXS and NMR data with models built based on partial crystallographic structures. Developments aiming at disentangling conformational and species heterogeneity, which are very common in this family of biomolecular complexes, will be explained. Derived models provide the structural bases of their biological function.

**Keywords:** SAXS, NMR, biomolecular complexes, polydispersity

### MS1-O2 Enzyme dynamics visualized by SAXS

David Albesa-Jové<sup>1</sup>, Marceo E. Guerin<sup>1</sup>

1. Structural Biology Unit - CIC bioGUNE, Derio, Spain; IKERBASQUE, Basque Foundation for Science, Bilbao, Spain

email: davidalbesa@gmail.com

Substrate specificity is a fundamental property of enzyme catalysis. Enzymes are characterized by their exceptional capacity to efficiently catalyze a great number of stereospecific chemical reactions in all organisms. A selective binding and stabilization of the transition state rather than more stable forms of substrates seems to be the major determinant of the chemical reaction step. To achieve such enzyme-transition state complex, a particular spatial arrangement of the active site is required, highlighting the importance of protein dynamics and conformational changes in substrate recognition and catalysis [1]. Specifically, protein conformational changes not only involve local reorganization of flexible loops and side-chain residues, but also, in many cases, domain motions and protein oligomerization events. In addition, as a consequence of protein-protein interactions, post-translational modifications, and non-covalent associations with small-molecule inhibitors or activators, protein dynamics critically modulate enzyme catalysis. Thus, the elucidations of the molecular mechanisms by which these events modulate the function and substrate specificity of enzymes represent a major challenge.

Combining Crystallography with Small-Angle X-ray Scattering (SAXS) can advance our understanding of these dynamic processes. During this talk we will focus on two cases where combining these techniques have proven important. The first, is the phosphatidylinositol mannosyltransferase PimA, an essential membrane-associated enzyme that initiates the biosynthetic pathway of key structural elements and virulence factors of the cell wall in *Mycobacterium tuberculosis* [2,3]. PimA shows an exceptional flexibility along the catalytic cycle, including  $\beta$ -strand-to- $\alpha$ -helix and  $\alpha$ -helix-to- $\beta$ -strand transitions [4]. The second case is the Rv2466c, a key oxidoreductase where the redox state regulates the enzyme conformation, mediating the reductive activation of TP053, a thienopyrimidine derivative that kills replicating and non-replicating *Mycobacterium tuberculosis* [5,6].

1. Khersonsky O, Tawfik DS. *Annu. Rev. Biochem.* 2010, **79**:471–505.

2. Guerin ME, et al. *J. Biol. Chem.* 2010, **285**:33577–33583.

3. Albesa-Jove D, et al. *Glycobiology* 2014, **24**:108–124.

4. Giganti D, et al. *Nat. Chem. Biol.* 2014, **11**:16–18.

5. Albesa-Jove D, et al. *ACS Chem. Biol.* 2014, **9**:1567–1575.

6. Albesa-Jove D, et al. *J. Biol. Chem.* 2015, **290**:31077–31089.

**Keywords:** Enzyme dynamics

## MS1-O3 From size exclusion to HIS-tags: Increasing sample purity for BioSAXS

Martha E. Brennich<sup>1</sup>, Stephanie Hutin<sup>2</sup>, Katharina Weinhäupl<sup>2</sup>,  
Paul Schanda<sup>2</sup>, Benoit Maillot<sup>1</sup>, Petra Pernot<sup>1</sup>, Adam Round<sup>3</sup>

1. ESRF-The European Synchrotron, Grenoble, France
2. Institute de Biologie Structurale, Grenoble, France
3. EMBL, Grenoble Outstation, France

email: brennich@esrf.fr

Small Angle X-ray scattering of proteins and nucleic acids (BioSAXS) is continuously gaining importance for structural biology. This has led to the development of dedicated, highly automated beamlines such as BM29 at the ESRF which provides a completely *in vacuo* setup with a flow-through capillary for samples and a sample changer robot for sample delivery.

For many macromolecules of interest, obtaining useful results is still challenging as complexes might disassociate or aggregates might form between purification and SAXS measurement, especially if buffer adjustments or transportation (including freezing and de-freezing) are required. Therefore, online size exclusion chromatography (SEC) directly at the beamline has by now become a standard approach to BioSAXS measurements. These experiments provide SEC-SAXS chromatograms that do not only allow us to obtain SAXS curves for different oligomeric species in a sample, but can also indicate conformational changes within a single species.

But in some cases, size exclusion is not the best approach as final purification step, as it requires high initial sample concentrations and fails to separate similarly sized molecules. In this presentation we show the combination of gradient-varying liquid chromatography techniques with SAXS: We use online nickel affinity chromatography to separate a complex of a chaperone protein with its target from the target and the chaperone protein alone, and ion exchange chromatography to purify and simultaneously concentrate a viral helicase complex while maintaining its monomeric state and moderate salt concentrations. Both these techniques demand careful considerations of the background correction, which will also be addressed in the talk.

**Keywords:** SAXS, liquid chromatography

## MS1-O4 High throughput and time resolved BioSAXS at the P12 beamline of EMBL Hamburg

Clement E. Blanchet<sup>1</sup>, Alessandro Spilotos<sup>1</sup>, Florian D.C.  
Wieland<sup>1</sup>, Martin A. Schroer<sup>1</sup>, Cy M. Jeffries<sup>1</sup>, Melissa A.  
Graewert<sup>1</sup>, Daniel Franke<sup>1</sup>, Nelly Hajizadeh<sup>1</sup>, Stefan Fiedler<sup>1</sup>,  
Dmitri I. Svergun<sup>1</sup>

1. EMBL Hamburg

email: clement.blanchet@embl-hamburg.de

Last decades saw a growing interest for SAXS from the structural biology community, underlining the need for dedicated instruments able to rapidly collect accurate SAXS data on weakly scattering, sensitive, and scarce samples. The EMBL BioSAXS beamline P12 (PETRA-III ring, Hamburg) is tailored for biological solution SAXS and offers services to about 100 user groups from the entire world every year.

The undulator and double crystal monochromator deliver a beam of energy tunable between 4 and 20keV with up to two 10<sup>13</sup> photons per seconds focused by bimorph mirrors down to the size of 200x100 µm<sup>2</sup>.

High throughput solution SAXS measurements are performed in an in vacuum flow through capillary. The samples are automatically loaded by a robotic sample changer, which also cleans and dries the capillary between measurements. The typical exposure time is one second and the full loading/cleaning cycle finished within 1 minute. Alternatively, an on-line size exclusion chromatography mode is available with additional spectrometers (UV/Vis, refractive index and RALS) attached for online purification and characterization.

For these experiments, particular care was taken to automate the measurements such that they can be performed with a minimal input from the user. Fully automated data collection by the sample changer robot is followed by the computation of the overall parameters of the solute (R<sub>g</sub>, p(r), MW and 3D low resolution shape) by the data analysis pipeline SASFLOW within minutes after data collection. This high level of automation allows one to conduct and analyze over 1000 measurements per day and also allows for permit remote and mail-in operation.

The sample environment can be rapidly exchanged to conduct "non-standard" SAXS experiments such as scanning SAXS, microfluidic chips, etc. The beamline is further being developed to allow for fast time resolved measurements. A multilayer monochromator, presently in commissioning, delivers the flux 5x10<sup>14</sup> photons per seconds allowing for data collection on biological samples within a few ms, and using the newly installed EIGER 4M detector, data can be collected at 750 Hz frame rate. A stopped flow device, already available at the beamline, allows time resolved data collection with a dead time of a few ms. Continuous flow chip and laser triggering devices are developed to further reduce the dead time and allow sub-ms time resolved SAXS experiments. Pilot time-resolved experiments conducted at P12 will be presented.

**Keywords:** SAXS, Biological macromolecules, time resolved experiments, automation, high brilliance synchrotron beamline

## MS1-O5 Structural insight into host cell surface retention of a 1.5-MDa bacterial ice-binding adhesin

Shuaiqi (Phil) Guo<sup>1</sup>, Luuk Olijve<sup>2</sup>, David Langelaan<sup>1</sup>, Sean Phippen<sup>1</sup>, Robert Campbell<sup>1</sup>, Steven Smith<sup>1</sup>, Ilja Voets<sup>2</sup>, Peter Davies<sup>1</sup>

1. Queen's University, Kingston, Canada

2. Eindhoven University of Technology, The Netherlands

email: 9sg52@queensu.ca

Repeats-In-Toxin (RTX) adhesins are a member of the biofilm-associated protein (Bap) family used by many Gram-negative bacteria to form multicellular communities. The largest RTX adhesin known to date is the 1.5-MDa *MpAFP* produced by the Antarctic bacterium *Marinomonas primoryensis*. The giant adhesin includes ice- and sugar-binding domains close to its C terminus, and ~120 extender domains that project the ligand-binding region ~ 0.6 µm away from the host. The role of *MpAFP* is to help its strictly aerobic host remain in the upper reaches of ice-covered seas and lakes, perhaps to gain better access to oxygen and other nutrients produced by photosynthetic microorganisms. Here we have focused on *MpAFP*'s ~ 50-kDa N-terminal region 1 (RI) that likely serves as the cell surface anchoring point for the adhesin. Bioinformatic analyses indicated that RI crosses the bacterium's outer membrane (OM), with its N terminus (RIN) localized in the periplasmic space, its C terminus (RIC) in the extracellular environment, while the intervening domain (RIM) spans the OM. RTX adhesins are exported to the cell surface via the Type I Secretion Pathway (TISS), however, the mechanism of surface retention is unclear due to a lack of detailed structural information. Here we solved the 30-kDa crystal structure of RIC to 1.9 Å. It has an extended shape with three tandemly linked Ca<sup>2+</sup>-dependent Immunoglobulin-like domains. We also determined the NMR structure of the 8-kDa periplasmic RIN, which has a novel β-sandwich fold with a triangular cross section. The SAXS envelope of the whole RI is an elongated, kinked rod, whose two ends are in good agreement with the RIN and RIC structures. By subtraction, the structure of the ~ 12-kDa intervening RIM is that of a thin cylinder with a diameter of ~18 Å and a height of ~ 40 Å. This shape is similar to the internal dimension of the TISS pore (ToIC) embedded in the OM. As ToIC restricts passage of folded proteins, all TISS substrates must stay unstructured until they enter the Ca<sup>2+</sup>-rich extracellular environment. Indeed, all *MpAFP* domains but RIN and RIM require millimolar Ca<sup>2+</sup> levels to fold. While RIM might interact with the interior of ToIC, RIN cannot pass ToIC due to steric hindrance, which prevents the total release of *MpAFP* from the cell surface. Since the RIN fold is conserved in many TISS Baps, this could be a general mechanism for these adhesins to stay attached to their hosts.

Supported by CIHR

**Keywords:** Biofilm-associated proteins, Calcium-binding proteins, Ice-binding proteins

## MS2 Development of new types of sample preparation (both XFEL & synchrotrons)

Chairs: Jörg Standfuss, Gwyndaf Evans

### MS2-O1 Fundamental Characterization of Liquid-Jet Sample Injectors for XFEL and Synchrotron Use

R. Bruce Doak<sup>1</sup>

1. Max-Planck-Institut fuer medizinische Forschung, Heidelberg

email: bruce.doak@mpimf-heidelberg.mpg.de

Structure determination of biological macromolecules has often been cited as a prominent motivation in the development of X-ray Free Electron Lasers (XFEL). During the protracted period of XFEL design and construction, however, no attention whatsoever was ever directed to the question of exactly how complex and fragile biological macromolecules were to be introduced, unaltered, into the XFEL X-ray beam. The question was anything but moot, given that the preferred environment for an XFEL beam is high vacuum whereas that of a biological species is liquid or lipidic solution, and that the XFEL and sample jets of interest were to have diameters in the micron or even sub-micron regime. To XFEL developers, the XFEL was the horse and everything else only a cart. Only after the XFEL horse was cantering at full speed down the road did construction of the sample injection cart finally begin. Strikingly enough, the forced rapid development of micron-sized liquid jet injectors proved quite successful, with innovative gas-focusing techniques being invented from scratch to generate microscopic liquid jets of both low and high viscosity sample media. This precipitous development necessarily precluded detailed investigations into the science and technology of the injectors and their jets, the overriding concern always being simply to get something working well enough for the next beamtime. Fundamental but crucial issues were simply skirted: What jet speeds are possible? How does the presence of biocrystals alter the hydrodynamic flow characteristics of the injector? What shear forces are imposed on biological species in transit through the injector? How do the injector streams turn on and off? How can sample consumption be reduced? Can sample settling be generically addressed, specifically for low viscosity samples in very small quantities (microliters)? Knowledge of this is sort crucial to further improvement and diversification of the sample injectors. Accordingly, with usable techniques now in place for liquid jet sample injection into both XFEL and synchrotron X-ray beams, injector developers are finally able to return to fundamental physical characterization of this sort. This talk will address a selection of ongoing measurements of this sort.



**Keywords:** XFEL Sample Injectors, Gas-Dynamic Virtual  
Nozzles, GDVN, High Viscosity Extrusion Injectors, HVE

## **MS2-O2** Enabling time-resolved structural studies of biological macromolecules

Arwen Pearson<sup>1</sup>

1. Hamburg Centre for Ultrafast Imaging, University of Hamburg

email: arwen.pearson@cfe1.de

In order to fully understand the mechanisms of biological processes, time-resolved methodologies that allow us to comprehend how function is linked to changes in molecular structure are required. Time-resolved X-ray crystallography provides a means of directly visualising structural rearrangements associated with function. Although time-resolved crystallography is a powerful tool it has not been widely applied to biomacromolecules, due to both the lack of beamlines where such experiments can be done as well as to the challenge of fast and uniform reaction initiation. To address these challenges we have developed a new multiplexing data collection method, based on the Hadamard transform, to make sub millisecond time-resolved data collection possible at standard macromolecular crystallography beamlines. We are also developing a suite of photochemical and rapid mixing tools for reaction initiation.

**Keywords:** time-resolved crystallography, rapid mixing, photocaging



## MS2-O3 Macromolecular Crystallography at SwissFEL

Isabelle Martiel<sup>1</sup>, Meitian Wang<sup>1</sup>, Ezequiel Panepucci<sup>1</sup>, Claude Pradervand<sup>1</sup>, Jörg Standfuss<sup>1</sup>, Christopher J. Milne<sup>1</sup>, Gerhard Ingold<sup>1</sup>, Bill Pedrini<sup>1</sup>, Rafael Abela<sup>1</sup>

1. Paul Scherrer Institute, Switzerland

email: isabelle.martiel@psi.ch

X-ray free electron lasers (XFELs) bear the promise of providing damage-free protein structures in a “diffract-before-destroy” approach. The Swiss free electron laser (SwissFEL) is currently under construction at the Paul Scherrer Institute, Switzerland. In the standard operation mode, the hard X-ray beamline will deliver 2-20 fs (rms) pulses at 100 Hz repetition rate, with photon energies in the range 2-12.4 keV and up to about 1 mJ/pulse. The start of operation is foreseen at the end of 2017. The hard X-ray experimental stations are conceived to offer state-of-the-art possibilities for femtosecond protein crystallography, with a variety of sample delivery methods and experimental conditions. At each station, femtosecond pump lasers will be available for time resolved studies.

The SwissFEL hard X-ray experimental station A (ESA) is designed for time resolved X-ray spectroscopy and serial femtosecond crystallography (SFX). It will cover the full photon energy range 2-12.4 keV, and the beam can be focused down to a size of 1  $\mu\text{m}$ . The experiments are done within a chamber at pressures ranging from vacuum to ambient. The chamber can host injectors to perform SFX measurements while delivering the sample with a liquid or viscous jet [1]. Simultaneous acquisition of diffraction images and single-shot X-ray emission spectra will be possible.

The SwissFEL hard X-ray experimental station B (ESB) is designed for time-resolved X-ray diffraction studies in the field of condensed matter physics. The beam can be focused down to a size of 2  $\mu\text{m}$ . The station also includes a general purpose table for alternative setups, one of which will be an in-house developed instrument for fixed-target protein crystallography, an important recently developed alternative to sample injection. The possible data acquisition schemes include synchrotron-like rotation measurements on a relatively small set of large crystals [2], as well as SFX on microcrystals deposited on a solid support [3] with fast scanning data acquisition, in the photon energy range 5-12.4 keV. An automatic sample changer will ensure high-throughput use of the XFEL beam. In-air and in-helium sample environments, as well as cryogenic and room-temperature conditions will be available.

[1] Kang, Y., et al. (2015). *Nature*, 523(7562), 561–567

[2] Cohen, A. E., et al. (2014). *Proc. Natl. Acad. Sci. U. S. A.*, 111(48), 17122–17127.

[3] Hunter, M. S., et al, (2014). *Sci. Rep.*, 4, 6026.

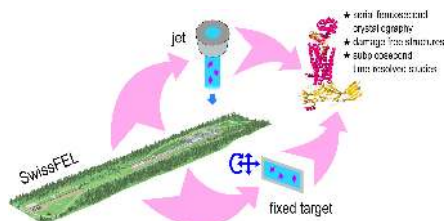


**Figure 1.** Sample delivery possibilities at SwissFEL. Structure of the rhodopsin-arrestin complex by femtosecond X-ray laser (PDB 4ZWJ, ref [1]).

**Keywords:** Free electron laser, macromolecular crystallography, serial crystallography, femtosecond crystallography, sample delivery, fixed target, jet

## MS2-O4 The newPin project: Towards a new sample holder standard for cryogenic macromolecular x-ray crystallography

Gergely Papp<sup>1</sup>, Christopher Rossi<sup>1</sup>, Clement Sorez<sup>1</sup>, Franck Elisasz<sup>1</sup>, Hassan Belrhali<sup>1</sup>, Matthew Bowler<sup>1</sup>, Florent Cipriani<sup>1</sup>

1. European Molecular Biology Laboratory, Grenoble Outstation, France

email: gpapp@embl.fr

The SPINE sample holder standard [1] has been essential for the automation of macromolecular X-ray crystallography (MX) in Europe. Motivated by the continuously increasing sample flow at MX beamlines and by the emergence of automated harvesters, studies are ongoing to define a compact and precise sample holder for frozen crystallography. Lead by the EMBL Grenoble, this “newPin” collaborative project is partly supported by the European FP7 program BioStruct-X ([www.embl.fr/newpin](http://www.embl.fr/newpin)) and includes most of the European synchrotrons, NSLS-II (USA), SPING8 (Japan), as well as the companies Molecular Dimension Ltd. and MiTeGen. First aim of this new standard is to reduce the transporting costs of frozen samples as well as puck turnover at beamlines. Second aim would be to facilitate crystal alignment at beamlines using a design that allows precise 3D positioning of the sample holder on its support. Ultimately, automated harvesting systems like “CrystalDirect” [2] could record the coordinates of the harvested crystals for a priori alignment at beamlines. Two sample holder models are proposed with a storage density of 36 samples per puck, newPin and miniSpine, which share a common handling robot gripper and uni-puck like Dewar slots. MiniSpine was selected for the first implementation of the future sample holder standard as it is easier to integrate at beamlines. It will be presented in detail together with compatible robotics and goniometer equipment. The results obtained at the ESRF/EMBL/INDIA BM14 beamline using the FlexED8 sample changer will be shown. The challenges to finalize and integrate this new standard at beamlines will be discussed.

[1] Acta Cryst. (2006) D62, 1251–1259

[2] Acta Cryst. (2012). D68, 1393–1399



**Figure 1.** newPin, miniSpine and SPINEplus sample holders and pucks

**Keywords:** sample holder, cryogenic sample holder, SPINE standard, sample changer, MX, macromolecular crystallography

## MS2-O5 Structure determination of a membrane protein with data collected from micro-crystals in lipidic cubic phase at room temperature in low background CrystalDirect™ crystallization plates.

Thomas R. Schneider<sup>1</sup>, Gleb Bourenkov<sup>1</sup>, Maria Martinez-Molledo<sup>1</sup>, Ivars Karpics<sup>1</sup>, Esben M. Quistgaard<sup>2</sup>, Guillaume Hoffmann<sup>3</sup>, Florent Cipriani<sup>3</sup>, Josan Marquez<sup>3</sup>, Rob Meijers<sup>1</sup>, Christian Loew<sup>1</sup>

1. European Molecular Biology Laboratory, Hamburg Outstation, c/o DESY, Notkestr. 85, 22603 Hamburg, Germany.

2. Laboratory Karolinska Institutet Biophysics/MBB Scheeles väg 2 SE - 17177 Stockholm, Sweden

3. European Molecular Biology Laboratory, Grenoble Outstation, 71 avenue des Martyrs, CS 90181, 38042 Grenoble Cedex 9, France.

email: thomas.schneider@embl-hamburg.de

Crystallization using the lipidic cubic phase (LCP) methodology in many cases is a decisive step towards obtaining high-resolution structural information for membrane proteins. However, harvesting crystals from LCP setups is notoriously difficult and frequently results in damaged or destroyed crystals. Furthermore, cryo-protection can be difficult, and data collection at cryogenic temperatures is often hampered by the LCP-matrix becoming opaque upon flash-cooling preventing optical crystal centering.

To overcome the above problems, we have grown crystals of a membrane transporter protein, PepT<sub>st</sub> (491 residues; Lyons et al. 2014), in CrystalDirect™ plates and collected *in situ* diffraction data at room temperature on the EMBL beamline P14 at PETRA III (DESY, Hamburg). The 5 µm micro-focus beam of P14 in combination with the low X-ray background of the CrystalDirect™ plates allowed to acquire diffraction data to 2.5 Å resolution from crystals with typical dimensions of 10 µm and embedded in LCP. Employing the serial helical scan data collection strategy (Gati, Bourenkov et al. 2014) as implemented in the high-precision MD3 diffractometer (ARINAX, Grenoble, France), 66 serial helical scans were performed on 19 crystallization wells delivering a total of 36013 frames containing more than 2 million reflections in 2 hours of beamtime.

The reflections were integrated, scaled, and merged into a 98% complete data set (space group C222<sub>1</sub>) containing 23105 reflections to 2.5 Å. Structure solution by molecular replacement and refinement using standard methods delivered high-quality electron density maps and a high-quality model ( $R_{\text{work}}/R_{\text{free}} = 0.219/0.235$ ) for the crystal structure of PepT<sub>st</sub> at room temperature.

Gati, Bourenkov et al. (2014) Lyons et al. (2014) EMBO Rep. 15(8):886-93



**Figure 1.** CrystalDirect™ crystallization plate mounted on the MD3 diffractometer for in situ data collection.

**Keywords:** in situ datacollection, LCP, serial crystallography

## MS3 Data collection and processing software (XFELS & synchrotrons)

Chairs: Adrian Mancuso, Thomas Schneider

### MS3-O1 MX data analysis developments at Diamond Light Source.

Gwynndaf Evans<sup>1</sup>, Melanie Vollmar<sup>1</sup>, Graeme Winter<sup>1</sup>, David Waterman<sup>2</sup>, James Parkhurst<sup>1</sup>, Richard Gildea<sup>1</sup>, Pierre Aller<sup>1</sup>, James Foadi<sup>1</sup>, Alun Ashton<sup>1</sup>

1. Diamond Light Source, Harwell Science and Innovation Campus, Didcot OX11 0DE, United Kingdom.

2. CCP4, Research Complex at Harwell, Rutherford Appleton Laboratory, Didcot OX11 0FA, UK

email: gwynndaf.evans@diamond.ac.uk

The Macromolecular Crystallography team at Diamond Light Source are providing their users with a broad suite of beamlines and capabilities all supported by automated data analysis engines running in the background, generating results that are accessible to remote users through web and app interfaces. The new VMX beamlines at Diamond and the Diamond XFEL-Hub will push the limits of performance of these pipelines and are demanding fundamental development of underlying software and algorithms, in particular raw data analysis, to handle broad bandpass beams and multicrystal analysis. The DIALS software is one such development that provides the flexibility to accommodate these challenges and together with new approaches to pipeline design and remote analysis services (in collaboration with CCP4) we aim to provide users with 'cloud' like access to collection and analysis.

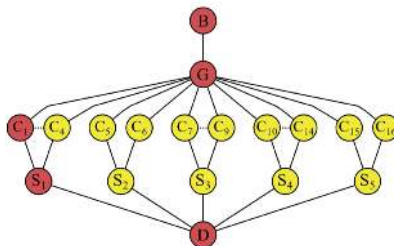


**Figure 1.** Global refinement model in DIALS enabling joint refinement of multi-scan multicrystal data sets or serial snapshot crystallography data. A single experiment consists of a path from top to bottom connecting one of each type of model. Key: B: beam, G: goniometer, C: crystal, S: scan and D: detector.

**Keywords:** data collection, data analysis, macromolecular crystallography, DIALS, automation, pipelines

## **MS3-O2** Hidden treasure in serial femtosecond diffraction

Anton Barty<sup>1</sup>

1. CFEL/DESY

email: anton.barty@desy.de

Serial Femtosecond Crystallography using X-ray free electron lasers has established itself as a technique ideally suited to the study small and radiation sensitive crystals by outrunning radiation damage, and for probing protein dynamics with sub-picosecond time resolution. A typical experiment involves exposing a stream of crystals to millions of individual femtosecond duration X-ray pulses, resulting in measurable diffraction patterns from thousands of individual protein micro- or nano-crystals each of which is exposed to the intense X-ray beam only once before being discarded. Combining these diffraction patterns yields intensity measurements for structure analysis, for example reflection intensities for conventional crystallographic analysis. In some cases it can also reveal hidden gems including diffraction beyond the resolution of observable Bragg peaks and continuous diffraction from individual asymmetric units. This has required the development of new data analysis techniques.

**Keywords:** serial femtosecond crystallography, Free electron laser, data processing

### MS3-O3 Processing XFEL Still Shots and Merging Multi-crystal Data

Nicholas K. Sauter<sup>1</sup>, Iris D. Young<sup>1</sup>, Aaron S. Brewster<sup>1</sup>

1. Lawrence Berkeley National Laboratory

email: nksauter@lbl.gov

The ability to avoid radiation damage with femtosecond X-ray pulses is a powerful argument for the use of X-ray free electron lasers (XFELs), with the important caveat that the observed diffraction consists entirely of partially recorded Bragg spots. Correcting the structure factor intensity to the full spot equivalent improves the quality of the final, merged data set that is created by mutually scaling hundreds or thousands of separate shots. However, several years after the initial XFEL results, efforts are still ongoing to produce optimal models of the spot partiality, with programs such as cctbx.xfel, DIALS, Prime, and ccpxfel each taking a slightly different approach. Data merging affects the final outcome, including the ability to phase with anomalous scattering data, and to discern high-resolution structural details. Examples will be shown from recent data collection at LCLS, including results from the new protein crystallography end station MFX.

**Keywords:** XFEL, diffraction

### MS3-O4 Data sets merging in serial crystallography

Rangana S. Warshamanage<sup>1</sup>, Vincent Olieric<sup>1</sup>, Chia-Ying Huang<sup>2</sup>, Martin Caffrey<sup>2</sup>, Kay Diederichs<sup>3</sup>, Meitian Wang<sup>1</sup>

1. Swiss Light Source, Paul Scherrer Institute, CH 5232 Villigen, Switzerland

2. Membrane Structural and Functional Biology Group, School of Medicine and School of Biochemistry and Immunology, Trinity College, Dublin 2, Ireland

3. Fachbereich Biologie, Universität Konstanz, D-78457 Konstanz, Germany

email: rangana.warshamanage@psi.ch

In synchrotron serial crystallography experiments by the IMISX method micro-crystals in the lipid mesophase are sandwiched between thin cyclic olefin copolymer windows [1,2] and measured *in situ* with an X-ray microbeam (Figure 1). Small rotations of crystals are achieved by turning the whole plate mounted on the goniometer. These rotations allow one to record full intensities of reflections. In this geometry, it is difficult to collect a complete data set from a single crystal. A full data set can be recorded by merging many partial data sets from randomly oriented crystals. However, prior to merging isomorphous data sets must be identified. The criteria used for this purpose rely on the correlation between an individual data set and the rest of the data [2]. Data set selection is carried out iteratively. This method can be used not only to identify isomorphous data sets but also to identify the data frames compromised by radiation damage. In this presentation, details of the method and our recent results will be presented.

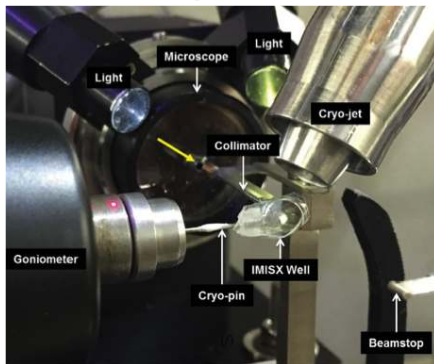


**Figure 1.** Experimental setup for IMISX data collection on beamline PXI (X06SA) at the Swiss Light Source.

**Keywords:** synchrotron serial crystallography, isomorphous data set, IMISX method

## MS3-O5 Experimental phasing with serial crystallography at XFEL and synchrotron radiation

Keitaro Yamashita<sup>1</sup>, Kazuya Hasegawa<sup>2</sup>, Dongqing Pan<sup>3</sup>,  
Tomohiro Murai<sup>1</sup>, Kunio Hirata<sup>1</sup>, Go Ueno<sup>1</sup>, Toru Nakatsu<sup>1,3</sup>,  
Hideo Ago<sup>1</sup>, Takashi Kumasaka<sup>2</sup>, Masaki Yamamoto<sup>1</sup>

1. RIKEN SPring-8 Center, Advanced Photon Technology Division, Sayo, Japan
2. JASRI/SPring-8, Research & Utilization Division, Sayo, Japan
3. Graduate School of Pharmaceutical Sciences, Kyoto University, Sakyo, Kyoto, Japan

email: k.yamashita@spring8.or.jp

X-ray crystallography is a powerful method to determine biomacromolecular structures at atomic resolution. However, there are still many challenging targets like membrane proteins, which are often reluctant to produce large well diffracting crystals. Serial crystallography is an emerging method for microcrystals. It has been first established at XFEL and known as serial femtosecond crystallography (SFX). After the success of SFX at XFEL, serial crystallography was imported to synchrotron radiations (SR). Fast read-out detectors and high-flux microbeam beamlines have made synchrotron serial crystallography (SSX) practical option.

Phase problem has been the critical problem in crystallography. While nowadays most structures are solved by the molecular replacement, there is still much demand for *de novo* structure determinations. SAD, the most popular experimental phasing method, utilizes the small anomalous difference (< ~5%) and therefore highly accurate data is essential. Barends *et al.* [(2014) *Nature*, **505**, 244-247] proved SAD method worked with SFX, but it required an enormous number of diffraction patterns. An efficient *de novo* phasing method is highly demanding.

Here we present the successful demonstration of experimental phasing with serial crystallography. We used microcrystals of mercury-bound luciferin-regenerating enzyme (LRE), a soluble protein, as a first sample. SFX datasets were collected at BL3, SACLA and processed using CrystFEL. SSX datasets were collected by raster-scanning of cryoloops (similar protocol to Gati *et al.* [(2014), *IUCr*, **1**, 87-94]) at BL41XU, SPring-8 and processed using CrystFEL or XDS as random snapshots. At SR, crystals can be rotated during X-ray exposure, which is potential advantage over XFELs. We studied the effect of crystal rotations and larger rotations per image to a certain degree resulted in higher anomalous signal and better statistics with the same number of images. In both SFX and SSX cases, the selection of diffraction images based on the data processing statistics was proven to be effective. We will discuss the data processing method using SAD-ability or anomalous signal as a data quality indicator.

**Keywords:** serial crystallography, SFX, SAD, phasing, data processing

## MS4 New developments in phasing and refinement

Chairs: Eleanor Dodson, Randy Read

### MS4-O1 Refinement without a model

Jon Agirre<sup>1</sup>, Kevin Cowtan<sup>1</sup>

1. York Structural Biology Laboratory, Department of Chemistry, University of York, YO10 5DD, England.

email: jon.agirre@york.ac.uk

Refinement is a problem of optimising the parameters of a model against observed data. When the data are limited in number (for example due to low resolution) or of low quality, the refinement becomes poorly determined, which manifests itself in weak convergence and a multiplicity of local minima.

One way to address the problem is through more parsimonious parameterisations of the model. We explore the use of control points to represent the positions and thermal motion of whole groups of atoms within the structure. This approach has significant potential for refining a homologous structure into low resolution electron density (for example from electron cryomicroscopy). It also has potential for increasing the radius of convergence of molecular replacement, and for providing an alternative characterisation of the domain motions, currently represented by TLS parameters or the generation of ensembles.

**Keywords:** refinement, model free, control points

**MS4-O2** New bulk-solvent models improves model-to-data fit and facilitates map interpretationPavel V. Afonine<sup>1</sup>, Paul D. Adams<sup>1</sup>

1. Lawrence Berkeley National Laboratory, Berkeley CA, USA

email: pafonine@lbl.gov

Bio-macromolecular crystals contain between 10 and 90% of solvent. This solvent is mostly disordered so it cannot be interpreted in terms of an atomic model. Owing to its simplicity and yet relatively good modeling power, flat bulk-solvent model is the most commonly used model to account for disordered solvent in modern crystallographic software packages such as CNS, CCP4 or Phenix. This model assumes electron density is constant anywhere in the unit cell where there is no atomic model placed. While this may be a reasonable approximation for some crystal structures or at initial stages of structure determination, it may be less accurate at final stages. Major deviations from the assumption of a flat model include: 1) local concentration of solvent component of specific types, such as lipid belts in membrane proteins, 2) unmodeled ligands, 3) partial occupancy of solvent in small isolated regions (between or inside macromolecules), and 4) lack of solvent in certain regions (hydrophobic cores).

These deviations manifest themselves as elevated R factors in the lowest resolution shells as well as residual features in difference maps: positive in cases when the flat solvent model is inadequate in accounting for distinct features, or negative when solvent model is used in regions with no solvent.

To overcome the limitations of the existing bulk solvent model we have proposed a non-uniform bulk-solvent model that allows for solvent variation across the unit cell volume. The new model splits initially binary (0/1) solvent masks into several masks by applying connectivity analysis. These masks are then split further into more masks based on analysis of difference maps. This final set of solvent masks is used to compute the individual bulk solvent contributions to the total model structure factor.

Tests on all deposited structures in PDB that have diffraction data and cross-validation flags available indicate systematic improvement of model-to-data fit with no signs of over-fitting as judged by the  $R_{\text{free}}$  factor. Tests on selected models demonstrate notable improvements in map quality especially for weak features such as ligands or solvent molecules.

All described tools will be available in *Phenix*.

**Keywords:** Refinement, bulk-solvent, maps

**MS4-O3** Fragon - rapid fragment-based molecular replacementHuw T. Jenkins<sup>1</sup>, Alfred A. Antson<sup>1</sup>

1. York Structural Biology Laboratory, Department of Chemistry, University of York, York, YO10 5DD

email: huw.jenkins@york.ac.uk

Calculating phases from small geometrically-ideal protein fragments presents an attractive method for structure determination when no suitable template structure for molecular replacement is available. Over 15 years ago ACORN could solve the structure of lysozyme by locating a 10-residue poly-alanine  $\alpha$ -helix (3.4% of the contents of the unit cell) and improving phases from this fragment through density modification [1]. More recently several approaches have been developed which use Phaser [2] to place either ideal  $\alpha$ -helices [3] or fragments from ab initio modeling [4,5] followed by multiple iterations of density modification and auto-building for each fragment to identify correctly placed fragments. The main drawback of this method is obvious – the vast majority of CPU time is spent attempting model building with phases from incorrectly placed fragments.

We have implemented a novel approach – Fragon – that also uses Phaser to place fragments (ideal  $\alpha$ -helices,  $\beta$ -strands or even single atoms) but tests solutions by artificial extension of the data to 1.0 Å resolution followed by density modification with ACORN. In many cases this can rapidly identify correctly placed fragments. Subsequent chain tracing with SHELXE into the density-modified maps provides a robust measure of success and enables comparison with previous approaches [3-6].

We generated a challenging test set (103 structures) of mixed  $\alpha/\beta$  folds at resolutions between 1.0 and 1.7 Å. Fragon solved 62% of the test cases searching for one or two ideal  $\alpha$ -helices of 7-14 residues. One further structure was solved from a single S atom to bring the final success rate to 63%. Fragon was also benchmarked against the test set used in previous approaches [4-6]. Fragon's success rate of 61% compares favourably with that of previous approaches of 54% [5] and 49% [6].

We will also describe application of Fragon to solve a previously unknown structure starting from ideal  $\beta$ -strands and a 54.5 kDa structure solved from a single P atom.

1. Foadi *et al.* (2000) *Acta Cryst.* D56:1137-47
2. McCoy *et al.* (2007) *J. Appl. Crystallogr.* 40:658-74
3. Rodríguez *et al.* (2009) *Nature Methods* 6:651-3
4. Bibby *et al.* (2012) *Acta Cryst.* D68:1622-31
5. Keegan *et al.* (2015). *Acta Cryst.* D71:338-343
6. Sammito *et al.* (2015) *Acta Cryst.* D71:1921-30



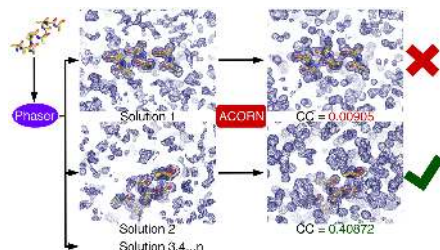


**Figure 1.** The Fragon process. The correct solution can be selected based on the correlation coefficient (CC) after density modification.

**Keywords:** Molecular replacement, Phasing, Fragments, Fragon

## MS4-O4 BORGES\_MATRIX: a tool to generate models for ab initio phasing and for structure interpretation.

Massimo D. Sammito<sup>1,2</sup>, Claudia L. Millán-Nebot<sup>2</sup>, Rafael J. Borges<sup>2,3</sup>, George M. Sheldrick<sup>1</sup>, Isabel Usón<sup>2,4</sup>

1. Georg August University of Göttingen, Dept. of Structural Chemistry, 37077 Göttingen, Germany
2. Crystallographic Methods, Institute of Molecular Biology of Barcelona (IBMB), Spanish National Research Council (CSIC), 08028, Barcelona, Spain
3. Dept. Physics and Biophysics, Biosciences Institute (IBB), São Paulo State University (UNESP), 18618-970, Botucatu, São Paulo, Brazil
4. Structural Biology, Catalan Institution for Research and Advanced Studies (ICREA), 08028, Barcelona, Spain

email: massimo.sammito@ibmb.csic.es

ARCIMBOLDO\_LITE [1] is a pipeline that combines the search of small fragments, like alpha helices, with PHASER [2], and density modification and autotracing with SHELXE [3]. Even though the model constitutes only a small percentage of the total scattering, the method has proven to be successful for high resolution cases (better than 2.1 Å). In order to correctly locate and extend the input search model it is required that its main chain matches very accurately the one of the final structure. This assumption is generally correct for helices but it does not hold true for composite secondary structure elements. Thus, exploiting the idea that there are common building blocks (such as three beta strands in a sheet, or two small parallel helices) common to unrelated protein structures, we developed BORGES [4], a tool to extract and use libraries of small local folds for phasing. Other bioinformatic tools are also available to search for similar structural occurrences of a fold [5,6], but they tend to retrieve continuous domains, and give a relatively general view of the fold. Our new program BORGES\_MATRIX implements a detailed description, based on discrete distributions of characteristic vectors to entail the local conformation of the main chain and to geometrically compare extracted models with a search template. Our method also extracts folds formed through crystallographic and non crystallographic symmetry, and does not require sequence information to retrieve similar occurrences. Recently, a library of three antiparallel strands was used to solve the structure of a viral all beta structure of 130 aa diffracting to 1.55 Å presenting a novel fold [7]. Beyond phasing, the program contributed to the understanding of the structural environment of the binding site by extracting and comparing similar occurrences of the local geometrical conformation.

- [1] Millán, C. *et al.* (2015). IUCrJ 2, 95-105.
- [2] McCoy, A. J. *et al.* (2007) J. Appl. Cryst. 40, 658-674
- [3] Sheldrick, G. M. (2010) Acta Cryst. D66, 479-485.
- [4] Sammito, M. *et al.* (2013) Nature Methods 10, 1099-101.
- [5] Holm L, *et al.* (2010) Nucl. Acids Res. 38, W545-549.
- [6] E. Krissinel *et al.* (2004). Acta Cryst. D60, 2256-268
- [7] Fedosyuk *et al.* (2016). PNAS submitted

**Keywords:** ab initio phasing, fragment libraries, structural bioinformatics



**MS4-05** Substructure determination from SAD data using phase retrieval techniquesPavol Skubak<sup>1</sup><sup>1</sup>. Faculty of Science, Leiden Institute of Chemistry, Biophysical Structural Chemistry, Leiden, NL

email: skubakp@gmail.com

The major current bottleneck for macromolecular structure solution from SAD data is determination of positions of the anomalously scattering atoms. The current programs for substructure determination are usually based on the "direct" methods developed for the structure solution of small molecules, obtaining the phase estimates from relations between intensities and phases of the reflections or from the Patterson function.

From a more general point of view, the X-ray crystallography phase problem belongs to the class of non-linear and non-convex inverse problems. Although no general solution is known for this class of inverse problems, they have been studied for decades and efficient phase retrieval algorithms were proposed for the special case of optical phase retrieval. Similarly to most "direct" methods implementations, the phase retrieval techniques perform iterative dual-space recycling. However, unlike the direct methods, the operations performed in either of the spaces alone cannot, even in principle, solve the phase problem.

Dumas & van der Lee (2008) showed that the simplest phase retrieval algorithm - charge flipping, as implemented in Superflip (Palatinus & Chapuis, 2007) - can be used for substructure determination from some SAD datasets. One disadvantage of this simple algorithm may be that it tends to diverge from the solution (Marchesini, 2007) for an inconsistent problem. Clearly, the problem of substructure determination from weak anomalous signals is strongly inconsistent due to the tiny signal-to-noise ratio of the data. The Relaxed Alternating Averaged Reflections (RAAR) algorithm (Luke, 2005) has been designed to elude the divergence while still retaining a high ability to escape local minima.

I have adapted the RAAR algorithm in a new program for Phase Retrieval from Anomalously Scattering Atoms (PRASA). The preliminary results show that the novel approach provides consistently better results than the charge flipping algorithm and is competitive with the state-of-the-art substructure determination programs. In the presentation, the advantages and disadvantages of this new approach will be discussed and its performance will be demonstrated on massive testing results on over 150 real SAD datasets.

Dumas C. & van der Lee A. (2008). *Acta Cryst.* **D64**, 864–873.

Palatinus L. & Chapuis G. (2007). *J. Appl. Cryst.* **40**, 786–790.

Marchesini S. (2007). *Rev. Sci. Instrum.* **78**, 011301.

Luke D. R. (2005). *Inverse Probl.* **21**, 37–50.

**Keywords:** anomalous scattering, substructure determination, SAD, phase retrieval, charge flipping, RAAR, phase problem

**MS5** Structural information in drug design

Chairs: Michael Hennig, Vincent Mikol

**MS5-01** Structural elucidation of ligand binding sites in family B GPCRs and their application in drug discovery

Ali Jazayeri<sup>1</sup>, Andrew Dore<sup>1</sup>, Daniel Lamb<sup>1</sup>, Harini Krishnamurthy<sup>1</sup>, Stacey Southall<sup>1</sup>, Asma Baig<sup>1</sup>, Andrea Bortolato<sup>1</sup>, Markus Koglin<sup>1</sup>, Nathan Robertson<sup>1</sup>, James Errey<sup>1</sup>, Stephen Andrews<sup>1</sup>, Alastair Brown<sup>1</sup>, Robert Cooke<sup>1</sup>, Malcolm Weir<sup>1</sup>, Fiona Marshall<sup>1</sup>

<sup>1</sup>. Heptares Therapeutics Ltd

email: ali.jazayeri@heptares.com

G protein-coupled receptors (GPCRs) comprise one of the most important families of drug targets owing to the multitude of roles they fulfil across many different physiological processes. Despite the huge amount of investment in GPCR drug discovery there remains significant opportunities for identification of novel or better drugs. One way to achieve this goal is to utilise structure based drug design (SBDD) strategies. However, GPCRs are generally challenging proteins for crystallisation and structure determinations primarily due to their hydrophobic nature, low expression levels and conformational flexibility. To facilitate application of SBDD approaches to GPCRs Heptares uses its proprietary StaR technology to thermostabilise GPCRs in a single conformational state. The purified StaRs can then be used for crystallisation to yield X-ray structures with multiple ligands as well as used in biophysical screening techniques. Using the StaR approach, we have solved structures of multiple Class B GPCRs in both agonist and antagonist conformations. This has led to the elucidation of the orthosteric and allosteric binding sites. The structural insight into multiple ligand binding sites has significantly increased our ability to design novel drugs to modulate the activities of these receptors.

**Keywords:** GPCR, structure based drug design, family B receptors, glucagon receptor, GLP-1 receptor

## MS5-O2 Crystal structures of the human doublecortin C-terminal and N-terminal domains in complex with specific antibodies

Armin Ruf<sup>1</sup>

1. Roche, Pharma Research and Early Development (pRED), Basel, Switzerland

email: armin.ruf@roche.com

Doublecortin is a microtubule-associated protein essential for human brain development and for proper transport of presynaptic vesicles. Missense mutations in the doublecortin gene cause defective cortical neuronal migration leading to the brain formation disorders X-linked lissencephaly (XLIS) and subcortical band heterotopia (SBH). Anti-doublecortin-antibodies are widely used research tools to detect neurogenesis. In order to enable better characterization of the doublecortin interaction with tubulin we raised novel domain specific antibodies against doublecortin. Only the antibody specific for the C-terminal domain prevented doublecortin binding to microtubules. The antibodies epitopes and binding geometries were observed in their crystal structures in complex with their doublecortin domains. With help of the specific antibody, the first crystal structure of the C-terminal domain of human doublecortin was determined. Several new structures of the doublecortin N-terminal domain illustrate the conformational flexibility of the linker region connecting the two domains, that is necessary for doublecortin function. Taken together, our results show that doublecortin interacts with microtubules by its C-terminal domain.

**Keywords:** protein crystallization, antibodies, drug discovery, drug design

## MS5-O3 Combining “dry” co-crystallization with in situ diffraction to facilitate ligand screening by X-ray crystallography

Gilles Labesse<sup>1</sup>, Muriel Gelin<sup>1</sup>, Vanessa Delfosse<sup>1</sup>, Frédéric Allemand<sup>1</sup>, François Hoh<sup>1</sup>, Yoann Sallaz-Damaz<sup>2</sup>, Michel Pirocchi<sup>2</sup>, William Bourguet<sup>1</sup>, Jean-Luc Ferrer<sup>2</sup>, Jean-François Guichou<sup>1</sup>

1. CNRS, UMR5048 – Université de Montpellier – INSERM, U1054, Centre de Biochimie Structurale, F-34090 Montpellier, France.

2. CNRS-CEA – Université Grenoble Alpes, IBS, F-38044 Grenoble, France

email: labesse@cbs.cnrs.fr

Structure-Based Drug Design is well established as a powerful technique to develop new binders for a given therapeutic target. Indeed, nanomolar ligands can be built from fragments showing millimolar affinity to the target. To optimally guide the drug-design process, one have to unravel protein-ligand interaction at atomic details.

Recently, structure determination has been dramatically accelerated. New beamlines have been recently set up to allow automatic data collections of a few hundred of macromolecular crystals per day. However, ligand deliveries is still a tedious and often limiting step.

We have recently developed a new method for pre-coating crystallization plates with the desired ligands. This lead to a solvent-free ligand delivery to protein crystals compliant with most (if not all) media used for protein crystal growth.

Ligand pre-coating prior to co-crystallization can be combined with in situ diffraction thanks to dedicated robotic suites compatible with 96-well plates[1] in order to make ligand screening by X-ray crystallography fully automatic. The use of this integrated approach to discover new ligands for important drug targets will be discussed [2].

[1] le Maire, Gelin, Pochet, Hoh, Pirocchi, Guichou, Ferrer & Labesse. (2011) In-plate protein crystallization, in situ ligand soaking and X-ray diffraction. *Acta Cryst. D67*, 747-755.

[2] Gelin, Delfosse, Allemand, Hoh, Sallaz-Damaz, Pirocchi, Bourguet, Ferrer, Labesse, Guichou. (2015) Combining “dry” co-crystallization and in situ diffraction to facilitate ligand screening by X-ray crystallography. *Acta Crystallogr D Biol Crystallogr. D71*, 1777-1787.

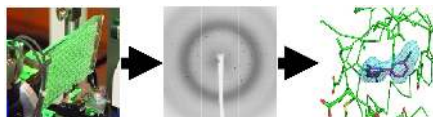


**Figure 1.** Toward automatic ligand screening using ligand pre-coating and *in situ* X-ray crystallography

**Keywords:** solvent-free co-crystallization; fragment approach ; therapeutic targets, drug design ; automation; solvent evaporation

## MS5-O4 Crystal structure of HDAC6: insights into molecular assembly, selective inhibition and microtubule deacetylation

Heinz Gut<sup>1</sup>, Yasuyuki Miyake<sup>1</sup>, Jeremy J. Keusch<sup>1</sup>, Longlong Wang<sup>1</sup>, Makoto Saito<sup>1</sup>, Daniel Hess<sup>1</sup>, Xiaoning Wang<sup>2</sup>, Bruce J. Melancon<sup>2</sup>, Paul Helquist<sup>2</sup>, Patrick Matthias<sup>1</sup>

1. Friedrich Miescher Institute for Biomedical Research, Maulbeerstrasse 66, 4058 Basel, Switzerland
2. Department of Chemistry & Biochemistry, University of Notre Dame, Notre Dame, Indiana 46556, U.S.A.

email: heinz.gut@fmi.ch

Histone deacetylases (HDACs) form a large family of enzymes catalyzing the removal of  $\epsilon$ -N acetyl groups from acetylated lysines on target proteins. HDACs are categorized into four classes with class I, II, and IV containing zinc-dependent enzymes (HDAC 1-11) and class III proteins using nicotinic adenine dinucleotide as cofactor (SIRT 1-7) [1]. HDAC6 is a unique class II member as it is the only histone deacetylase featuring two catalytic domains and a C-terminal ubiquitin binding domain. In addition, while most HDACs are located in the nucleus acting on acetylated histone peptides, HDAC6 is mainly found in the cytosol where it regulates acetylation states of a diverse set of proteins such as tubulin, cortactin, HSP90, and many more. HDAC6 is a major regulator of the aggresome pathway, influences microtubule dynamics and the function of regulatory T-cells, and plays a role in influenza virus infection [2,3,4]. It has been shown to be involved in several cancers, neurodegenerative diseases and inflammatory processes and is actively pursued as promising drug target by pharmaceutical companies and academic groups [5]. Although several HDAC6 specific inhibitors have recently been developed by combinatorial chemistry approaches, the lack of structural information prevented further structure-based drug design and understanding of selective inhibition over other HDAC family members. Here, we present high resolution crystal structures of HDAC6 inhibitor complexes which give insight into selective inhibition and which might have the potential to enlarge the chemical inhibitor space as well as making use of completely new  $\text{Zn}^{2+}$  binding groups. Additional structures reveal for the first time the interdomain assembly of the two catalytic domains and the positioning of the connecting linker, while functional analyses shed light onto the role of the two catalytic domains in microtubule deacetylation and catalysis.

[1] Seidel et al., *Epigenomics*, 2015, 7(1), 103 [2] Kawaguchi et al., *Cell*, 2003, 115(6), 727 [3] de Zoeten et al., *MCB*, 2011, 31(10), 2066 [4] Banerjee et al., *Science*, 2014, 346, 473 [5] Kalin and Bergman, *J.Med.Chem.*, 56, 6297

**Keywords:** Histone deacetylase, HDAC6, crystal structure, enzyme inhibition, drug design

## MS5-O5 Probing nucleotide-induced conformational changes and interaction studies of the GTPase EngA

Catarina S. Tomé<sup>1</sup>, Anne-Emmanuelle Foucher<sup>1</sup>, Ahcène Boumendjel<sup>2</sup>, Emmanuelle Neumann<sup>1</sup>, Jean-Michel Jault<sup>2</sup>, Dominique Housset<sup>1</sup>

1. Institut de Biologie Structurale, CEA/CNRS/UGA, Grenoble, France
2. Faculté de Pharmacie, Département de Pharmacochimie Moléculaire, UGA/CNRS, Grenoble, France
3. Institut de Biologie et Chimie des Protéines, CNRS/UCB, Lyon, France

email: catarinatome7@gmail.com

Microorganisms resistant to antibiotics and the geographic areas affected by drug resistance have been drastically increasing. Antimicrobial resistance has become one of the major concerns on public health and the return to the investment on new antibiotics is of major importance. One of the strategies has been to identify genes critical to the survival of bacteria as enzymes encoded by these genes represent potential targets for antibiotic design.

EngA is a GTPase conserved in bacteria and involved in ribosome biogenesis. While essential in bacteria, EngA does not have any human ortholog and can thus be targeted to selectively act on bacteria eradication. Our work aims at understanding how EngA interacts with the ribosome and to identify inhibitors for its function.

We have used a multitechnique approach to investigate ligand-induced conformational changes in EngA and unveil its role in ribosome binding. EngA has the unique feature among GTPases of bearing two G-domains (1).

We have probed conformational changes by SAXS and limited proteolysis and have observed a change in protein structure and a higher rate of proteolysis induced by GTP. The conformation adopted in solution in the presence of GTP does not relate with any of the crystal structures of EngA. Attempts to crystallize EngA in the GTP-bound form have resulted so far in 4 structures in different crystal form, but adopting the conformation observed for the GDP-bound state, despite the presence of GTP in one G-domain and some changes in switch regions. Some of the regions sensitive to proteolysis display different kinetics in the apo- and GTP-bound states. Analysis of these fragments may give us insights into which regions become more or less accessible.

Interactions studies confirmed better binding of EngA to the ribosome in the presence of GTP, suggesting the new conformation is more prone to bind the ribosome. Ongoing analysis of the complex by cryo-EM will allow us to visualise the EngA conformation when bound to the ribosome and will possibly help us characterize the interface.

In parallel, an ELISA assay is being set up to screen inhibitors in order to identify molecules able to block the interaction between EngA and the ribosome.

Our latest results will be presented at the conference.

1. Foucher AE, Reiser JB, Ebel C, Housset D, Jault JM. Potassium acts as a GTPase-activating element on each nucleotide-binding domain of the essential *Bacillus subtilis* EngA. *PLoS One*. 2012;7(10):e46795

**Keywords:** GTPase, ribosome, protein-protein interaction, conformational changes, X-ray crystallography, SAXS, cryo-EM,

## MS6 Molecular machines and big complexes

Chairs: Christoph Müller, Miquel Coll

### MS6-O1 Fuzzy Sarcomeric Z-disk Complex: $\alpha$ -Actinin-FATZ

Kristina Djinovic-Carugo<sup>1</sup>, Antonio Sponga<sup>1</sup>, Ariadna Rodriguez Chamorro<sup>1</sup>, Euripedes de Ribeiro<sup>1</sup>, Georg Mlynek<sup>1</sup>, Leo Geist<sup>1</sup>, Joan Lopez Arolas<sup>1</sup>, Robert Konrat<sup>1</sup>

1. Department of Structural and Computational Biology, Max F. Perutz Laboratories, University of Vienna

email: kristina.djinovic@univie.ac.at

The sarcomere is the minimal contractile unit in the cardiac and skeletal muscle, where actin and myosin filaments slide past each other to generate tension. This molecular machinery is supported by a subset of highly organised cytoskeletal proteins that fulfil architectural, mechanical and signalling functions, including the giant proteins titin, obscurin and nebulin as well as the cross-linking proteins  $\alpha$ -actinin and myomesin (1).

The cross-linking of actin and myosin at the boundaries of their filamentous structures is essential for the muscle integrity and function. In the Z-disks – the lateral boundaries of the sarcomere machinery – the protein  $\alpha$ -actinin-2 cross-links antiparallel actin filaments from adjacent sarcomeres, and additionally serves as a binding platform for a number of other Z-disk proteins. Among them is FATZ, also known as calsarcin and myozenin, which appears in the early stages of myofibrillogenesis together with  $\alpha$ -actinin-2 [1].  $\alpha$ -Actinin is an antiparallel dimer, where each subunit is composed of an N-terminal actin binding domain, which is connected by a neck region to the four spectrin-like repeats (rod), and a C-terminal calmodulin-like domain. FATZ is composed of conserved N- and C-terminal regions connected by an intrinsically disordered segment. FATZ is believed to act as an adaptor protein linking  $\alpha$ -actinin to other Z-disk proteins, but the structural information at molecular level on FATZ and complexes with any of its interaction partners still remains unknown.

We employed a combination of structural and biophysical approaches to elucidate the three-dimensional structure and dynamics of human  $\alpha$ -actinin-FATZ complex. Circular dichroism, NMR and small angle X-ray scattering data of FATZ alone and in complex with  $\alpha$ -actinin showed that FATZ is and IDP in solution, and that it does not fold upon binding. The non-bound portion displays pronounced structural plasticity and dynamics, characteristic of fuzzy complexes. Furthermore, the crystal structure shows that two stretches of FATZ interact in mostly extended conformation with the rod domain of  $\alpha$ -actinin, and that FATZ binding might displace the N-terminal lobe of the calmodulin-like domain from the position found in the structure of full length  $\alpha$ -actinin-2 [2], suggesting a specific role in the

hierarchy of Z-disk ultrastructure.

#### References

- [1] Stout et al. Cell Motil Cytoskeleton 2008; 65:353-67.
- [2] Ribeiro Ede et al. Cell 2014; 159:1447-60

**Keywords:** Striated muscle -Z-disk, actin based cytoskeleton, alpha-actinin:FATZ complex, intrinsically unstructured protein,

## MS6-O2 Macromolecular machines in genome maintenance

Thomä H. Nicolas<sup>1</sup>

1. Friedrich Miescher Institute for Biomedical Research  
Maulbeerstrasse 66 4058 Basel Switzerland

email: Nicolas.Thoma@fmi.ch

UV-exposure of the skin result in the covalent cross-links of neighboring DNA nucleotides, introducing mutations in the genome if left unrepaired. Patients suffering from Xeroderma pigmentosum (XP) fail to effectively repair these DNA lesions, resulting in heightened propensity to develop skin cancers (melanomas, squamous cell, & basal cell carcinomas). My lab has solved the structures of these protein complexes and delineated their mode of action in respect to the ubiquitin proteasome system. We provided the mechanism by which this molecular sunscreen works, and how it is lost in XP cancer patients. In the presence of this DNA repair machine skin cancer rates are suppressed by more 1000-fold providing a major means of safeguarding the genome.

**Keywords:** DNA repair, ubiquitin, ligases

## MS6-O3 The Architecture of Fully Reducing Polyketide Synthases

Dominik A. Herbst<sup>1</sup>, Roman P. Jakob<sup>1</sup>, Franziska Zähringer<sup>2</sup>,  
Timm Maier<sup>1</sup>

1. Department Biozentrum, University of Basel, Klingelbergstrasse 50/70, 4056 Basel, Switzerland

2. Present address: F. Hoffmann-La Roche AG, Grenzacherstrasse 124, 4070 Basel, Switzerland.

email: dominik.herbst@unibas.ch

Polyketides are a diverse family of potent bioactive microbial secondary metabolites and amongst the most successful compound classes in drug discovery, including many clinically relevant drugs. They are assembled via stepwise precursor elongation by giant polyketide synthases (PKSs)<sup>1</sup>. PKSs combine all enzymatic domains for a single-step of precursor elongation and modification in one module, which features a structural and functional separation into a product condensing and a modifying region as observed for fatty acid synthases. The product of each PKS module is determined by its specificity for the precursor and elongation substrate as well as the extent of product modification, encoded in the variable domain composition of the modifying region. The maximum extent of product modification is observed in reducing PKS, which employ two reductase and one dehydratase domain for full reduction of the intermediate to an elongated acyl chain. PKS modules either operate iteratively in iterative PKS or as part of a multimodular assembly line, with directed transfer of substrates between modules. The product diversity of PKS is thus directly encoded in their molecular organization.

Here, we report<sup>2</sup> a hybrid model of a reducing mycroceroic acid synthase-like PKS (MAS-PKS)<sup>3</sup>, which represents a large family of closely related mycobacterial PKS, based on overlapping crystal structures of its condensing and modifying regions. A comparison of a large set of experimentally observed MAS-PKS conformations provides a visualization of structural dynamics and conformational coupling in PKSs. Our data reveal a close relationship of individual domains of MAS-PKS and multimodular PKS. The modifying region of MAS-PKS adopts a unique dimeric linker-based organization devoid of stable interactions between different domain types. Comparative small angle X-ray scattering (SAXS) demonstrates that this architecture is common also to multimodular PKS. The linker-mediated construction principle provides a rationale for the characteristic variability of PKS modifying regions as a main contributor to the evolution of product diversity. Our comprehensive model of PKS architecture will contribute to the functional dissection and targeted re-engineering of PKSs for enabling combinatorial biosynthesis.

### References

- [1] Hertweck, C. (2009) *Angew. Chem. Int. Ed. Engl.* 48, 4688-4716.
- [2] Herbst, D.A., et al. (2016) *Nature* 531, 533-537.
- [3] Etienne, G., et al. (2009) *J Bacteriol.* 191, 2613-21.

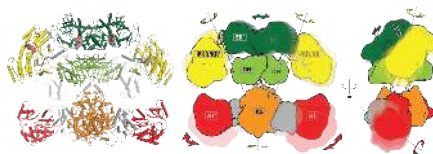


**Figure 1.** Hybrid model and conformational variability of a reducing mycroceroic acid synthase-like PKS.

**Keywords:** Polyketide Synthase, PKS, Molecular Machine, Architecture

## MS6-O4 Crystal structure of the 239 kDa nuclear export complex CRM1 - RanGTP - Snurportin1 - Nup214 - MBP

Ralf Ficner<sup>1</sup>, Thomas Monecke<sup>1</sup>, Sarah A. Port<sup>2</sup>, Manfred S. Weiß<sup>3</sup>, Ralph H. Kehlenbach<sup>2</sup>, Achim Dickmanns<sup>1</sup>

1. Department of Molecular Structural Biology, Institute for Microbiology and Genetics, GZMB, Georg-August-University Göttingen, Justus-von-Liebig-Weg 11, Göttingen, 37077, Germany
2. Department of Molecular Biology, Faculty of Medicine, GZMB, Georg-August-University Göttingen, Humboldtallee 23, 37073 Göttingen, Germany
3. Macromolecular Crystallography (HZB-MX), Helmholtz-Zentrum Berlin für Materialien und Energie, Albert-Einstein-Strasse 15, 12489 Berlin, Germany

email: rficner@uni-goettingen.de

In eukaryotic cells nucleocytoplasmic transport of macromolecules is a sophisticated active process. It proceeds through nuclear pore complexes (NPCs) mediated by soluble nuclear transport receptors of the karyopherin- $\beta$  superfamily termed importins and exportins. During passage through the NPC, importins and exportins transiently interact with the intrinsically disordered phenylalanine-glycine (FG-) repeat-domains of the nucleoporin proteins (Nups). These transient interactions with FG-Nups are necessary to overcome the nuclear envelope barrier and thus are crucial for all nuclear transport events. CRM1 is the major and most versatile nuclear exportin. Several crystal structures of different functional CRM1 complexes have been determined, revealing the structural basis for the cooperativity of cargo and RanGTP binding [1-3]. However, detailed structural insight into the interaction of CRM1 with the nuclear pore complex has remained an enigma.

Here, we present the crystal structure of a nuclear export complex comprising CRM1, the cargo Snurportin1 and the GTPase Ran, and a 117 amino acid FG-repeat containing fragment of Nup214 fused to MBP [4]. Optimization of protein constructs, seeding and the development of a sophisticated protocol including successive PEG-mediated crystal dehydration as well as additional post-mounting steps were pivotal to obtain well diffracting crystals and to solve the crystal structure [5]. The crystal structure, which was refined at 2.85 Å resolution, shows eight binding sites on CRM1 for Nup214 FG-motifs, with its intervening sequences loosely attached to the transport receptor. Interestingly, Nup214 binds to N- and C-terminal regions of CRM1, thereby clamping CRM1 in a closed conformation and stabilizing the export complex. The role of these hydrophobic pockets for the recognition of FG-motifs was analysed by means of biochemical and cell-based assays.

### References

- [1] Monecke et al. Science 324, 1087-91 (2009).
- [2] Monecke et al. PNAS 110, 960-5 (2013).
- [3] Monecke et al. FEBS J. 281, 4179-94 (2014).
- [4] Port, Monecke et al. Cell Rep. 13, 690–702 (2015).
- [5] Monecke et al. Acta Cryst. F71, 1481–1487 (2015).

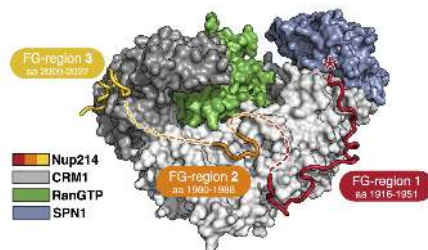


**Figure 1.** Structure of the quaternary export complex CRM1-RanGTP-Snurportin1-Nup214 reveals 3 binding regions for FG-repeats. The MBP fused to the N-terminus of the Nup214 fragment is not shown.

**Keywords:** Nucleocytoplasmic transport, crystal dehydration



## MS6-O5 Cooperative Motion Analysis of group II chaperonins at single molecule level using nanocrystal and time-resolved diffraction measurement

Hiroshi Sekiguchi<sup>1</sup>, Yohei Y. Yamamoto<sup>2</sup>, Masafumi Yohda<sup>2</sup>, Yuji C. Sasaki<sup>3</sup>

1. Japan Synchrotron Radiation Research Institute  
2. Tokyo University of Agriculture and Technology  
3. The University of Tokyo

email: sekiguchi@spring8.or.jp

Group II chaperonin, found in archaea and in the eukaryotic cytosol, is an indispensable protein that captures a nonnative protein and refolds it to the correct conformation in an ATP dependent manner. ATP-induced structural changes are essential for chaperonin activity and we had reported that the diffracted X-ray tracking (DXT) method could trace ATP induced conformational change of group II chaperonin at single molecule level (Sekiguchi et al., PLoS ONE 2013). In DXT, nanocrystal immobilized on one side of chaperonin-ring is used as motion tracer for structural change of chaperonin as shown in the figure. In this study, we analyzed how ATPase deficient mutant modulate dynamic motion of chaperonin, and cooperatively inter and intra communication of chaperonin ring. We found that although one ring of the asymmetric ring complex lacks ATPase activity, the other wild-type ring undergoes an ATP-dependent conformational change and maintains its protein-folding activity. The results clearly demonstrate that inter-ring communication is dispensable in the reaction cycle of group II chaperonins (Yamamoto et al., JMB 2014), despite the reaction cycle of group I chaperonins, for example GroEL-ES system in *E. coli*, is controlled by inter-ring allosteric communication.

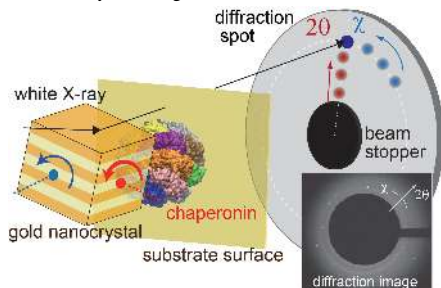


**Figure 1.** Schematic illustration of motion analysis of chaperonin by diffracted X-ray tracking.

**Keywords:** nanocrystal chaperonin dynamics

## MS7 Protein & glycobiology structure determination

Chairs: Jon Agirre, Gerlind Sulzenbacher

### MS7-O1 Structures of lytic polysaccharide monoxygenases and their interaction with polysaccharide substrates

Leila Lo Leggio<sup>1</sup>, Kristian E.H. Frandsen<sup>1</sup>, Jens-Christian N. Poulsen<sup>1</sup>

1. Department of Chemistry, University of Copenhagen, Denmark

email: leila@chem.ku.dk

The recent discovery of lytic polysaccharide monoxygenases has revolutionized our understanding of how polysaccharides are degraded in nature and our thoughts on how they could be most efficiently degraded in industrial processes. Cellulose, the main constituent of the plant cell wall, is the most abundant polysaccharide on earth, and as it is present in all plants is of particular interest for the production of second generation biofuels. Conventional cellulases are glycoside hydrolases, and catalyze the cleavage of the glycosidic linkage by using water molecule in mechanisms involving one or more carboxylate residues. In contrast, lytic polysaccharide monoxygenases (LPMOs) are metalloenzymes which cleave the glycosidic linkage by activating molecular oxygen through a mononuclear copper center held by the so-called histidine brace, thereby mediating oxidation at C1 or C4 (1,2).

Carbohydrate modifying enzymes are classified in the Carbohydrate Active Enzyme Database, CAZY, where LPMOs are now classified as Auxiliary Activities (3) in families AA9 (GH61 prior to discovery of their LPMO activity (4)), AA10 (CBM33 prior to discovery of their LPMO activity), AA11 and AA13. The initially characterized LPMOs had activity on the insoluble  $\beta$ -1,4-linked polysaccharides chitin and cellulose, but now LPMOs active on soluble  $\beta$ -1,4-linked oligo-/polysaccharides substrates, as well as active on  $\alpha$ -1,4-linked polysaccharides, have been both characterized biochemically and structurally (5-7).

This talk will provide an overview on the structural biology of LPMOs so far and focus primarily on substrate binding and specificity, in particular the structural differences between  $\alpha$ -1,4 and  $\beta$ -1,4- active LPMOs (5) and the very first LPMO substrate complexes which we recently obtained (7).

The results are largely from the CESBIC consortium collaborative project funded by the ERA-IB initiative, which additionally to the University of Copenhagen included Novozymes A/S, the University of Cambridge, University of York and the CNRS Marseille.

1. Vaaje-Kolstad et al. (2010) *Science* **330**:219-222.
2. Quinlan et al. (2011) *PNAS* **108**:15079-15084.



3. Levasseur et al (2013) *Biotechnology for biofuels* **6**:41.

4. Lo Leggio et al (2012) *CSBJ* **2**:e201209019.

5. Lo Leggio et al. (2015) *Nature Comm* **6**:5961.

6. Agger et al. (2014) *PNAS* **111**:6287-6292.

7. Frandsen et al (2016) *Nature Chemical Biology*, **12**:298-303.

**Keywords:** carbohydrate active enzyme; biofuel; lytic polysaccharide monooxygenase; metalloenzyme

## MS7-O2 Membrane Enzymes: the Structural basis of Phosphatidylinositol Mannosides Biosynthesis in Mycobacteria

Marcelo E. Guerin<sup>1,2</sup>

1. IKERBASQUE, Basque Foundation for Science, 48013, Bilbao, Spain

2. Structural Biology Unit, CIC bioGUNE, Bizkaia Technology Park, 48160 Derio, Spain

email: mrcguerin@gmail.com

Membrane enzymes constitute a large class of proteins with critical roles in a variety of cellular processes in all living organisms. They generate a significant amount of structural diversity in biological systems, which are particularly apparent in cell-pathogen interactions. Many of these enzymes are required to access a lipophilic substrate located in the membranes and to catalyze its reaction with a polar, water-soluble compound.<sup>[1]</sup> Here we focus on the membrane enzymes involved in the early steps of the phosphatidylinositol mannosides (PIMs) biosynthetic pathway, essential structural components of the cell envelope of *Mycobacterium tuberculosis*. Of particular relevance, we demonstrate the occurrence of a conformational switch during the catalytic cycle of the retaining glycosyltransferase PimA, the enzyme that start the pathway, involving both  $\beta$ -strand-to- $\alpha$ -helix and  $\alpha$ -helix-to- $\beta$ -strand transitions.<sup>[2, 3]</sup> These structural changes seem to modulate catalysis and are promoted by interactions of the protein with anionic phospholipids in the membrane surface. Our studies demonstrate that protein-membrane interactions might entail unanticipated structural changes in otherwise well conserved protein architectures, and suggests that similar changes may also play a functional role in other membrane-associated enzymes. Finally, we report the crystal structures of PatA, an essential membrane acyltransferase that transfers a palmitoyl moiety from palmitoyl-CoA to the 6-position of the mannose ring added by PimA, in the presence of its naturally occurring acyl donor palmitate and a nonhydrolyzable palmitoyl-CoA analog. The structures reveal an  $\alpha/\beta$  architecture, with the acyl chain deeply buried into a hydrophobic pocket that runs perpendicular to a long groove where the active site is located. Enzyme catalysis is mediated by an unprecedented charge relay system, which markedly diverges from the canonical HX<sub>2</sub>D motif. Our studies establish the mechanistic basis of substrate/membrane recognition and catalysis for an important family of acyltransferases, providing exciting possibilities for inhibitor design.<sup>[4]</sup>

### References

[1] Forneris, F. et al., *Science* **2008**, *321*, 213-216.

[2] Giganti et al., *Nat. Chem. Biol.* **2015**, *11*, 16-18. Highlighted in the News and Views Section: Brodhun F, Tittmann K. *Nat. Chem. Biol.* **2015**, *11*, 102-103.

[3] Albesa-Jove et al., *Angew. Chem. Int. Ed. Engl.* **2015**, *54*, 9898-9902.

[4] Albesa-Jove et al., *Nat. Commun.* **2016**, *7*, 10906.

**Keywords:** membrane enzymes, glycosyltransferase, acyltransferase, glycobiology, mycobacterium

## MS7-O3 Structural studies of medically-interesting protease inhibitors and lectins that belong to the $\beta$ -trefoil family

Alexander Wlodawer<sup>1</sup>, Jacek Lubkowski<sup>1</sup>, Alla Guschchina<sup>1</sup>, Dongwen Zhou<sup>1</sup>, Michal Jakob<sup>1</sup>, Barry R. O'Keefe<sup>1</sup>, Rodrigo da Silva Ferreira<sup>2</sup>, Yara A. Lobo<sup>2</sup>, Daiane Hansen<sup>2</sup>, Maria L.V. Oliva<sup>2</sup>

1. Center for Cancer Research, National Cancer Institute, Frederick, MD, USA

2. Departamento de Bioquímica, Universidade Federal de São Paulo, Brazil

email: wlodawer@nih.gov

Several related proteins that belong to the  $\beta$ -trefoil family have been investigated by X-ray crystallography as well as by biochemical and biophysical techniques. Two of them are potent inhibitors of trypsin-related enzymes. EcTI, isolated from the seeds of *Enterolobium contortisiliquum*, inhibits the invasion of gastric cancer cells through alterations in integrin-dependent cell-signaling pathway. BbKI, found in *Bauhinia bauhinoides* seeds, is a kallikrein inhibitor with a reactive site sequence similar to that of kinins, the vasoactive peptides inserted in kininogen moieties. A much weaker protease inhibitor isolated from the bark of *Crataeva tapia* tree (CrataBL) also functions as a lectin. The amino acids sequence of CGL, a lectin isolated from the sea mussel *Crenomytilus grayanus*, is significantly different from the other three proteins.

We determined high-resolution crystal structures of free EcTI and in complex with bovine trypsin, in the process re-determining the amino acid sequence. Modeling of the putative complexes of EcTI with several serine proteases and a comparison with equivalent models for other Kunitz inhibitors elucidated the structural basis for the fine differences in their specificity. The structure of free BbKI indicated that the presence of disulfide bonds is not necessary for stabilization of the fold of the members of this family. A model of a complex of BbKI with plasma kallikrein indicates the need for mutual rearrangement of the interacting molecules.

We have also determined the high-resolution crystal structure of glycosylated CrataBL. We have shown that, as a lectin, CrataBL binds only sulfated oligosaccharides, most likely heparin and its derivatives.

CGL displays antibacterial, antifungal, and antiviral activities, and displays high affinity for mucin-type receptors, abundant on some cancer cells. We determined its crystal structure and modeled the glycan-binding pockets, based on the location of the glycerol molecules bound in the three sites exhibiting quasi-threefold symmetry.

**Keywords:** protease inhibitors, lectins, crystal structures

## MS7-O4 Structure-function characterization reveals catalytic diversity in the galactose oxidase family

Saioa Urresti<sup>1</sup>, DeLu T. Yin<sup>2</sup>, Mickael Lafond<sup>2,3</sup>, Esther M. Johnston<sup>1</sup>, Fatemeh Derikvand<sup>2</sup>, Luisa Ciano<sup>1</sup>, Jean-Guy Berrin<sup>4</sup>, Bernard Henrissat<sup>5,6</sup>, Paul H. Walton<sup>1</sup>, Harry Brumer<sup>2</sup>, Gideon J. Davies<sup>1</sup>

1. Department of Chemistry, University of York, York (UK)

2. Michael Smith Laboratories and Department of Chemistry, University of British Columbia, British Columbia (Canada)

3. Institut des Sciences Moléculaires de Marseille, Aix-Marseille University, Marseille (France)

4. INRA, Biodiversité et Biotechnologie Fongiques, Marseille (France)

5. Architecture et Fonction des Macromolécules Biologiques, CNRS, Aix-Marseille University, Marseille (France)

6. INRA, USC, Marseille (France)

7. Department of Biological Sciences, King Abdulaziz University, Jeddah (Saudi Arabia)

email: saioa.urresti@york.ac.uk

Auxiliary Activity 5 family (AA5; <http://www.cazy.org>) comprises the well-studied glyoxal oxidase (AA5\_1) and galactose oxidase (AA5\_2) subfamilies. Despite all the known biochemical characterization, only a few structures are available for these copper radical oxidases. These enzymes employ molecular oxygen as a terminal electron acceptor to generate hydrogen peroxide (believed to be coupled to lignolytic peroxidases), independently of an organic cofactor (1,2) for their catalytic activity on galactose. This has increased the biological interest in the context of recalcitrant plant degradation by fungal saprotrophs and phytopathogens (2,3). With a combination of spectroscopic, crystallographic and biochemical studies, here we report the discovery of a new fungal AA5\_2 from *Colletotrichum graminicola* (CgrAlcOx). This enzyme, in contrast with its homologue, the fungal *Fusarium graminearum* galactose oxidase (FgrGalOx), shows poor oxidative capability on galactose, but efficiently catalyses the oxidation of aliphatic alcohols (4,5).

1. Pickl, M., Fuchs, M., Glueck, S.M. and Faber, K. The substrate tolerance of alcohol oxidases. Appl. Microbiol. Biotechnol. 99, 6617–6642 (2015).

2. Kersten, P. and Cullen, D. Copper radical oxidases and related extracellular oxidoreductases of wood-decay Agaricomycetes. Fungal Genet. Biol. 72, 124–130 (2014).

3. Leuthner, B., Aichinger, C., Oehmen, E., Koopmann, E., Müller, O., Müller, P., Kahmann, R., Böcker, M., Schreiber, P.H. A H<sub>2</sub>O<sub>2</sub>-producing glyoxal oxidase is required for filamentous growth and pathogenicity in *Ustilago maydis*. Mol. Genet. Genomics 272, 639–650 (2005).

4. Rogers, M.S., Tyler, E.M., Akyumani, N., Kurtis, C.R., Spooner, R.K., Deacon, S.E., Tamber, S., Firbank, S.J., Mahmoud, K., Knowles, P.F., Phillips, S.E., McPherson, M.J. and Dooley, D.M. The stacking tryptophan of galactose oxidase: a second-coordination sphere residue that has profound effects on tyrosyl radical behavior and enzyme catalysis. Biochemistry 46, 4606–4618 (2007).

5. Yin, D.T., Urresti, S., Lafond, M., Johnston, E.M., Derikvand, F., Ciano, L., Berrin, J.-G., Henrissat, B., Walton, P.H., Davies, G.J. and Brumer, H.

Structure-function characterization reveals new catalytic diversity in the galactose oxidase and glyoxal oxidase family. *Nature Comms.* 6, 10197-10209 (2015).

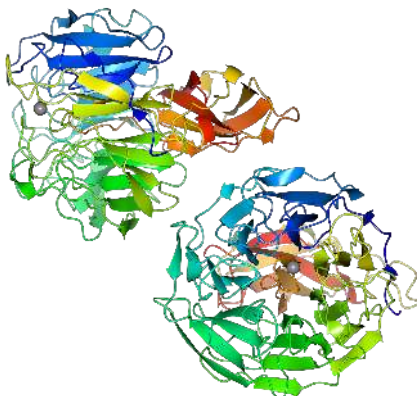


**Figure 1.** Lateral and rear view of the *FgrAlcOx* structure in complex with copper (pdb 5C92). The N terminus (blue to yellow) consists of seven Kelch motifs arranged in a  $\beta$ -propeller, enclosing the copper-binding site. The C terminus (orange to red) displays a nine-stranded  $\beta$ -barrel.

**Keywords:** Copper, EPR, eukaryotic expression, deglycosylation

## MS7-O5 Structure of the factor H-sialic acid complex links sialic acid recognition to atypical hemolytic uremic syndrome and reveals a novel conformation of the GM1 glycan

Bärbel Blaum<sup>1</sup>, Martin Frank<sup>2</sup>, Thilo Stehle<sup>1</sup>

1. Interfaculty Institute of Biochemistry, University of Tübingen, Germany

2. Biogenos AB, Gothenburg, Sweden

email: baerbel.blaum@uni-tuebingen.de

Complement factor H (FH) ensures down-regulation of the complement alternative pathway upon interaction with specific glycans on host cells, protecting the latter from attack by the host's complement system. There is long-standing evidence that the ubiquitous mammalian glycan cap sialic acid acts as such a self marker to FH, but the low affinity of the interaction and the structural diversity of sialylated glycans have hampered structural and functional investigations. Using ligand-based NMR spectroscopy we defined the FH sialoligosaccharide specificity and found that FH binds to glycans that spot Neu5Ac $\alpha$ (2-3)Gal caps. A previously reported crystal form of the two FH C-terminal domains 19 and 20 (1), which contain the sialic acid binding site, were refractory to glycan soaking. Co-crystallization attempts with the GM3 glycan yielded another unliganded crystal form of FH 19-20. Inspection of the protein packing in these two crystals forms prompted us to co-crystallize FH 19-20 with another FH ligand, the thioester domain (TED) of C3b, yielding FH19-20/C3b-TED crystals (2) that were successfully soaked with the GM3 and GM1 glycans. The atomic (2.2 Å resolution) structures of the ternary complexes suggest that sialic acid and the C3b TED together recruit FH to self-cells to which C3b attaches covalently by virtue of its reactive thioester bond - initiating local degradation of C3b on host cells that are covered with sialic acid (3). The structures revealed that numerous FH residues linked to atypical hemolytic uremic syndrome (aHUS), a rare hereditary disease that can lead to kidney failure, cluster in the sialic acid binding site, and their functional impairment with respect to sialic acid binding has since been confirmed (4). Our structures lend an etiological model to aHUS and also bear implications for complement evasion strategies by bacterial pathogens that cover themselves in host-derived sialic acid or recruit FH directly via its sialic acid binding site. Additionally, the complex structure with the GM1 glycan revealed a previously unreported GM1 conformation that escaped NMR-restrained modeling in the past but that is evident in the electron density and was confirmed by molecular dynamics simulations in the 10  $\mu$ s time scale (5). (1) Jokiranta T.S. et al, *EMBO J.* 2006. (2) Morgan H.P. et al, *Nat. Struct. Mol. Biol.* 2011. (3) Blaum B.S. et al, *Nat. Chem. Biol.* 2015. (4) Hyvärinen S. et al, *Blood* 2016. (5) Blaum B.S. et al., *Glycobiology* 2016.

**Keywords:** crystallography, glycobiology, ganglioside, NMR spectroscopy, innate immunity, molecular dynamics

## MS8 Membranes and membrane interacting proteins

Chairs: Han Remaut, Maïke Bublitz

### MS8-O1 Gating MscS: Structural basis of mechanosensation and the role of lipids in ion channel regulation

Christos Pliotas<sup>1</sup>, AC Dahl<sup>2</sup>, T Rasmussen<sup>3</sup>, KR Mahendran<sup>4</sup>, TK Smith<sup>1</sup>, P Marius<sup>1</sup>, J Gault<sup>4</sup>, A Rasmussen<sup>3</sup>, CV Robinson<sup>4</sup>, H Bayley<sup>4</sup>, MS Sansom<sup>2</sup>, IR Booth<sup>3</sup>, JH Naismith<sup>1</sup>

1. Biomedical Sciences Research Complex, School of Chemistry, University of St Andrews, St Andrews, United Kingdom
2. Department of Biochemistry, University of Oxford, Oxford, United Kingdom
3. Institute of Medical Sciences, University of Aberdeen, Aberdeen, United Kingdom
4. Department of Chemistry, University of Oxford, Oxford, United Kingdom

email: cp39@st-andrews.ac.uk

Organisms use lipid bilayers impermeable to ions and polar molecules, to compartmentalize. The exchange of molecules with the outside world occurs in a controlled manner via ion channels, which are pore-forming proteins and respond to specific stimuli. Mechanosensitive ion channels in bacteria gate in response to changes in the lateral tension in the lipid bilayer and act as pressure safety valves, to prevent lysis during extreme osmotic shock.

Despite years of efforts, the gating models proposed, failed to accurately describe the structural transitions these systems undergo during gating and identify an effective molecular trigger. A combination of experimental methods, spanning from biochemistry (site directed spin labeling) and biophysics (EPR and W-fluorescence spectroscopy, single molecule electrophysiology) to analytical chemistry (TLC, native and ES mass spectrometry) and structural biology (x-ray crystallography) along with computational (MD simulations) were introduced to elucidate gating of the mechanosensitive channel MscS at a molecular level.

Alkyl chains inside hydrophobic crevices are present in a new high-resolution x-ray MscS structure. Native and electrospray mass spectrometry demonstrate that purified protein contains endogenous lipids transferred from the parental *E. coli* strain, used for expression. W-fluorescence quenching shows that exogenously added phospholipids exchange between bulk lipid bilayer and TM hydrophobic pockets. MD simulations and structural analyses demonstrate that the volume of the pockets and the contained lipids decreases during channel opening, while exogenously added *lys*o-phospholipids (LPC) displace the endogenous phospholipids and trigger channel opening.

We propose a new gating model by which the extent of lipid partitioning within transmembrane pockets determines the conformation of MscS, a model with potential applicability to a wide range of membrane proteins. Our model is supported by single-channel recordings, in which LPC causes stable channel opening only when added from the cytosolic side of MscS, when the latter is embedded within planar lipid bilayers.

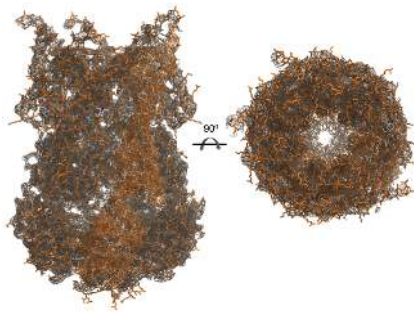


**Figure 1.** X-ray structure (side and top-pore views) of the MscS mechanosensitive ion channel (PDB 5AJI)

**Keywords:** mechanosensation, ion channels, mechanosensitive channels, MscS, lipids

## MS8-O2 The structure and function of calcium activated lipid scramblases and ion channels of the TMEM16 family

Raimund Dutzler<sup>1</sup>

1. Dept. of Biochemistry, University of Zurich

email: dutzler@bioc.uzh.ch

The TMEM16/Anoctamin family of membrane proteins is broadly expressed in eukaryotes and features a remarkable functional diversity. The family contains the long sought-after  $\text{Ca}^{2+}$ -activated chloride channels but also lipid scramblases or cation channels. We have determined the crystal structure of nhTMEM16, a fungal family member that operates as a  $\text{Ca}^{2+}$ -activated lipid scramblase [1]. Each subunit of the homodimeric protein encompasses ten transmembrane helices and structured cytosolic domains at the N- and C-terminus. The 'subunit cavity', a hydrophilic membrane-traversing cavity contained within each subunit that is exposed to the lipid bilayer acts as potential site of catalysis in both functional branches of the family. This cavity is sufficiently wide to accommodate the polar head groups of lipids and it contains residues that, upon mutation in the Cl<sup>-</sup>-channel TMEM16A, affect its ion selectivity. The 'subunit cavity' harbors a  $\text{Ca}^{2+}$ -binding site located within the hydrophobic core of the membrane. In this site two  $\text{Ca}^{2+}$  ions are coordinated by six conserved residues, five of which carry a negative charge. Mutations of these residues decrease the potency of  $\text{Ca}^{2+}$  in the activation of lipid scrambling in nhTMEM16 and ion conduction in TMEM16A. The nhTMEM16 structure thus reveals the general architecture of the family and its mode of  $\text{Ca}^{2+}$ -activation. It also provides insight into potential scrambling mechanisms and serves as a framework to unravel the conduction of ions in certain TMEM16 proteins acting as ion channels.

[1] Brunner, J.D., et al., *X-ray structure of a calcium-activated TMEM16 lipid scramblase*. *Nature*, 2014. **516**(7530): p. 207-12.

**Keywords:** lipid transport, calcium activation, anion selective ion channels, anoctamins

## MS8-O3 Crystal Structure of Mitochondrial Respiratory Complex I

Christophe Wirth<sup>1</sup>, Volker Zickermann<sup>2,3</sup>, Katarzyna Kmitya<sup>3</sup>, Ulrich Brandt<sup>2,4</sup>, Carola Hunte<sup>1</sup>

1. Institute for Biochemistry and Molecular Biology, ZBMZ, BIOS Centre for Biological Signalling Studies, University of Freiburg, Germany

2. Cluster of Excellence Frankfurt "Macromolecular Complexes", Goethe-University, Germany

3. Structural Bioenergetics Group, Institute of Biochemistry II, Medical School, Goethe-University, Frankfurt am Main, Germany

4. Radboud Center for Mitochondrial Medicine, Radboud University Medical Center, Nijmegen, The Netherlands

email: christophe.wirth@biochemie.uni-freiburg.de

Proton-pumping complex I is the largest membrane protein complex of the mitochondrial respiratory chain. The enzyme substantially contributes to energy conversion in eukaryotic cells as it couples oxidation of NADH and reduction of ubiquinone to pumping of four protons. It thus contributes to the generation of the electrochemical proton gradient across the inner mitochondrial membrane, which drives ATP synthesis. Complex I is a major source of deleterious reactive oxygen species (ROS) and its dysfunction is associated with many inborn and degenerative disorders.

We determined the X-ray structure of mitochondrial complex I (41 subunits and about 1MDa) from the strictly aerobic yeast *Yarrowia lipolytica* and shed light on its mechanism (1,2). With brominated competitive inhibitors and anomalous diffraction, we identified the binding site of the hydrophobic substrate quinone deeply buried in the hydrophilic domain of the complex. The site is connected to four putative proton translocation paths via a continuous axis of acidic and basic residues that runs centrally through the entire membrane embedded arm. The structure provides clues that the spatially separated redox reactions and proton pumping machinery are linked via conformational changes at and close to the quinone binding pocket. The same structural rearrangements may explain the active/deactive transition of complex I. The reversible transition is discussed as protection mechanism against excessive ROS formation in many eukaryotic species. Slow return to the A form was shown to attenuate reperfusion injury.

The function of many of the 30 accessory subunits of the mitochondrial complex I is not known. We identified the position of a single zinc ion present in *Y. lipolytica* complex I by anomalous diffraction and thereby located NUMM. This accessory subunit was shown to be required for the assembly of iron-sulfur cluster N4, a very late assembly stage of the complex (3).

1. Zickermann, V., Wirth, C., Nasiri, H., Siegmund, K., Schwalbe, H., Hunte, C. & Brandt, U. (2015). *Science* **347**, 44-49.

2. Wirth, C., Brandt, U., Hunte, C. & Zickermann, V. (2016). *Biochimica et biophysica acta*. 10.1016/j.bbabo.2016.02.013

3. Kmitya, K., Wirth, C., Wamau, J., Guerrero-Castillo, S., Hunte, C., Hummer, G., Kaila, V. R., Zwicker, K., Brandt, U. & Zickermann, V. (2015). *Proc Natl Acad Sci U S A* **112**, 5685-5690.

**Keywords:** Respiratory complex, Mitochondria, Membrane protein

## MS8-O4 Architecture and regulation of a redox-driven $\text{Na}^+$ -pump from the pathogen *Vibrio cholerae*

Gunter Fritz<sup>1</sup>

1. University of Freiburg, Institute of Neuropathology

email: guenter.fritz@uniklinik-freiburg.de

The human pathogen *Vibrio cholerae* maintains a  $\text{Na}^+$  gradient across the cytoplasmic membrane. The generated sodium motive force is essential for substrate uptake, motility, pathogenicity, or efflux of antibiotics. This gradient is generated by an integral membrane protein complex, the NADH:ubiquinone oxidoreductase (NQR). The NQR complex is conserved in many other bacterial pathogens and might therefore represent a novel and promising target in antibacterial therapy.

In order to get insights into the mechanism of redox driven  $\text{Na}^+$ -transport we have isolated and crystallized the NQR of *Vibrio cholerae* [1]. The crystals of the entire membrane complex diffract to 3.5 Å. Moreover, we determined independently the structures of the major soluble domains of subunits NqrA, C and F at 1.9 Å, 1.6 Å and 1.7 Å, respectively, completing large parts of the structure of the respiratory complex at high resolution [1]. The structural information allows the detailed analysis of the ion translocation pathway across the membrane and of the coupling between redox and translocation reactions. Moreover, we recently determined two additional structures of the complex in different states representing two further snapshots of the pumping cycle including a regulatory  $\text{K}^+$  binding site that facilitates large conformational changes required for  $\text{Na}^+$  pumping.

### References

[1] Steuber, J., Vohl, G., Casutt, M.S., Vorburger, T., Diederichs, K., Fritz, G. (2014) *Nature*, 516,62-67

[2] Steuber J., Vohl G., Muras V., Toulouse C., Claßen B., Vorburger T., Fritz G.(2015). *Biol. Chem.*, 396, 1015-30

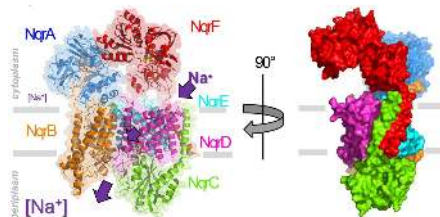


**Figure 1.** Overall structure of  $\text{Na}^+$ -NQR. The  $\text{Na}^+$ -NQR complex is composed of six subunits NqrA-F. The membrane plane is indicated by grey lines.

**Keywords:** respiratory complex, *Vibrio cholerae*

## MS8-O5 Molecular basis of secondary multidrug transport by X-ray crystallography

Vincent Debruycker<sup>1</sup>

1. Université libre de Bruxelles - Université d'Europe, Brussels, Belgium

email: vdebruyck@ulb.ac.be

The Major Facilitator Superfamily groups a vast number of secondary transporters that import or export distinct substrates. Among these, multidrug antiporters constitute a peculiar class, not only because of their multispecificity, recognizing structurally very diverse substrates, but also due to their transport mechanism, that relies on bilayer-mediated extrusion of cytotoxic compounds. Using X-ray crystallography, we investigate the molecular basis of secondary multidrug transport of *LmrP*, a Major Facilitator Superfamily multidrug transporter from *Lactococcus lactis*. Through extensive screening and optimization of the lipidation state of *LmrP* we were able to produce crystals of *LmrP*-ligand complex diffracting at resolution up to 3 Å. The protein has been co-crystallized with Hoechst 33342 in the outward open conformation. The structure unveils the presence of a lipid molecule in the substrate binding site and suggest a functional role of this lipid. In parallel to this, preliminary result show that point mutations and nanobodies targeting defined conformational state of *LmrP* are promising tools to determine the high resolution structure of distinct conformations of the transporter.

**Keywords:** multidrug resistance, MFS, membrane, transporter

## MS9 Enzyme reactions and dynamics in crystals

Chairs: Gunter Schneider, Arwen Pearson

### MS9-O1 Single Crystal Serial Crystallography to Capture Redox Enzyme Catalysis and Dynamics

Mike Hough<sup>1</sup>, Demet Kekilli<sup>1</sup>, Sam Horrell<sup>1</sup>, Florian S.N. Dworkowski<sup>2</sup>, Robin L. Owen<sup>3</sup>, Svetlana V. Antonyuk<sup>4</sup>, Robert R. Eady<sup>4</sup>, Samar Hasnain<sup>4</sup>, Richard W. Strange<sup>1</sup>

1. School of Biological Sciences, University of Essex, Wivenhoe Park, Colchester, CO4 3SQ
2. Swiss Light Source, Paul Scherrer Institut, CH-5232 Villigen PSI, Switzerland
3. Diamond Light Source Ltd, Harwell Science and Innovation Campus, Didcot OX11 0DE, UK
4. Institute of Integrative Biology, University of Liverpool, Crown Street, Liverpool, L69 7ZB

email: mahough@essex.ac.uk

Relating individual protein crystal structures to enzyme mechanisms remains a challenging goal for structural biology. The mechanisms of radiation damage to macromolecular crystals have become increasingly well-characterised [1] and attention is paid to minimising the deleterious effects. Alternatively, X-rays may be used to drive enzymes to particular redox states or intermediates. Serial crystallography using multiple crystals has recently been reported in both SR and XFEL experiments [2,3]. I will describe our approach to exploit rapid, shutterless X-ray detector technology on synchrotron MX beamlines to perform low-dose serial crystallography on a single Cu nitrite reductase crystal, allowing 10-50 consecutive X-ray structures at high resolution to be collected, all sampled from the same crystal volume.

This serial crystallography approach captures the gradual conversion of the substrate bound at the catalytic type 2 Cu centre, from nitrite to the product, nitric oxide, following reduction of the electron transfer type 1 Cu centre by X-ray generated solvated electrons. Significant, well defined structural rearrangements in the active site are evident in the series as the enzyme moves through its catalytic cycle, which is a vital step in the global denitrification process. We propose that such a serial crystallography approach is widely applicable for studying any redox or electron-driven enzyme reactions in a single protein crystal. It can provide a 'catalytic reaction movie' highlighting structural changes that occur during enzyme catalysis. Anticipated developments in the automation of data analysis and modelling are likely to allow seamless and near-real-time analysis of such data on-site at synchrotron crystallographic beamlines.

We describe such serial crystallographic experiments conducted at 100K [4] at the elevated cryogenic temperatures of 180-200K, exploiting previously

characterised changes in solvent viscosity and dynamics [5]. Finally, we extend our approach to crystals at room temperature, allowing a more complete protein conformational response to active site structural changes to be observed.

#### References

- [1] E. F. Garman & M. Weik (2015) *J. Synchrotron Rad.* 22, 195-200.
- [2] e.g. M. Suga, et al. (2015) *Nature* 517, 99-103.
- [3] e.g. C. Gati, G. et al. (2014) *IUCrJ* 1, 87-94.
- [4] M. Weik & J.-P. Colletier (2010) *Acta Cryst. Section D*, 66, 437-446.
- [5] S. Horrell, S. V. et al. (2016) *IUCrJ* (submitted).

**Keywords:** serial crystallography, nitrite reductase, enzyme catalysis, copper, radiation damage, dynamics



## MS9-O2 Time-Resolved Serial Femtosecond Crystallography On Photoswitchable Fluorescent Proteins

Martin Weik<sup>1</sup>, COQUELLE Nicolas<sup>1</sup>, SLIWA Michel<sup>2</sup>, WOODHOUSE Joyce<sup>1</sup>, SCHIRO Giorgio<sup>1</sup>, ADAM Virgile<sup>1</sup>, AQUILA Andrew<sup>3</sup>, BARENDT Thomas<sup>4</sup>, BOUTET Sébastien<sup>3</sup>, BYRDIN Martin<sup>1</sup>, DOAK Bruce<sup>4</sup>, FELIKS Mikolaj<sup>1</sup>, FIESCHI Franck<sup>1</sup>, FOUCAR Lutz<sup>4</sup>, GUILLON Virginia<sup>1</sup>, HILPERT Mario<sup>1</sup>, HUNTER Mark<sup>3</sup>, JAKOBS Stefan<sup>3</sup>, KOGLIN Jason<sup>3</sup>, KOVACSOVA Gabriela<sup>4</sup>, LEVY Bernard<sup>6</sup>, LIANG Mengning<sup>3</sup>, NASS Karol<sup>4</sup>, RIDARD Jacqueline<sup>6</sup>, ROBINSON Joseph<sup>3</sup>, ROOME Christopher<sup>4</sup>, RUCKEBUSCH Cyni<sup>1</sup>, THEPAUT Michel<sup>1</sup>, CAMMARATA Marco<sup>7</sup>, DEMACHY Isabelle<sup>6</sup>, FIELD Martin<sup>1</sup>, SHOEMAN Robert<sup>4</sup>, BOURGEOIS Dominique<sup>1</sup>, COLLETIER Jacques-Philippe<sup>1</sup>, SCHLICHTING Ilme<sup>4</sup>, WEIK Martin<sup>1</sup>

1. Institut de Biologie Structurale, Grenoble, France
2. Laboratoire de Spectrochimie Infrarouge et Raman, Lille, France
3. Linac Coherent Light Source, Menlo Park, USA
4. Max-Planck-Institut für Medical Research, Heidelberg, Germany
5. Max Planck Institute for Biophysical Chemistry, Göttingen, Germany
6. Laboratoire de Chimie-Physique, Orsay, France
7. Department of Physics, University of Rennes, France

email: weik@ibs.fr

Reversibly photoswitchable fluorescent proteins (RSFP) are essential tools in advanced fluorescence microscopy of live cells (such as PALM and RESOLFT). They can be repeatedly toggled back and forth between a fluorescent (*on*) and a non-fluorescent (*off*) state by irradiation with light at two different wavelengths. Mechanistic details of photoswitching, in particular on the ultra-fast photochemical time scale, remain largely unknown. Our consortium combines time-resolved serial femtosecond crystallography (TR-SFX) at X-ray free electron lasers, ultrafast absorption spectroscopy in solution and simulation methods to study *off-to-on* photoswitching intermediates in two RSFP on the picosecond to microsecond time scale. Two major bottlenecks had to be passed before TR-SFX could be conducted, *i.e.* the production of well-diffracting microcrystals in large quantities and efficient inline pre-illumination to photoswitch RSFP microcrystals from the *on* to the *off* state prior to injection. First pump-probe TR-SFX experiments were conducted at both the LCLS and SACLA that, together with time-resolved absorption spectroscopy, provide first insight into a possible sequence of events involved in photoswitching.

**Keywords:** time-resolved serial femtosecond crystallography, XFEL, microcrystals, fluorescent proteins, chromophore

## MS9-O3 Changes in metal coordination are required to regulate activity of bacterial phosphodiesterases, implicated in c-di-GMP regulated biofilm dispersal

Andrew Hutchin<sup>1,2</sup>, Dom Bellini<sup>2,3</sup>, Sam Horrell<sup>2,4</sup>, Curtis W. Phippen<sup>1</sup>, Yuming Cai<sup>1</sup>, Richard W. Strange<sup>4</sup>, Armin Wagner<sup>2</sup>, Jeremy S. Webb<sup>1</sup>, Martin A. Walsh<sup>2,3</sup>, Ivo Tews<sup>1</sup>

1. Centre for Biological Sciences, University of Southampton, UK
2. Diamond Light Source, Harwell Science and Innovation Campus, Didcot, UK
3. Research Complex at Harwell, Harwell Science and Innovation Campus, Didcot, UK
4. Institute of Integrative Biology, Faculty of Health and Life Sciences, University of Liverpool, UK

email: ajh4g10@soton.ac.uk

Many chronic infections are underpinned by the ability of bacteria to transition to the biofilm life-style, which is up to 1000 fold more tolerant to antibiotics. Both biofilm formation and dispersal are controlled by the secondary messenger bis-(3'-5') cyclic dimeric guanosine monophosphate (c-di-GMP); high levels of c-di-GMP are associated with biofilm formation, while a reduction in c-di-GMP induces biofilm dispersal<sup>(1)</sup>. Future pharmaceutical strategies may interfere with these mechanisms. We look at biofilm dispersal, studying c-di-GMP hydrolysis by bacterial phosphodiesterases of the EAL type.

Structures of the EAL type enzymes are readily observed in the substrate bound state (c-di-GMP). These structures pose the question of full enzyme activation; while dimerisation is known to play a key role, many of the structures are observed as dimers<sup>(2,3)</sup>. We present an analysis of these dimers and show that dimerisation alone is insufficient for activation.

Our study of the *Pseudomonas aeruginosa* protein MorA demonstrates that dimerisation is linked with reorganisation of the catalytic site, by unwinding of a helical segment (figure 1)<sup>(3)</sup>. However, this structure is again observed in the substrate bound state. We now present further evidence from phosphodiesterase structures in complex with the hydrolysis product 5'-phosphoguanlyl-(3'-5')-guanosine. Observed differences in metal coordination in the catalytic centre may represent the final layer of enzyme activation. Understanding the full catalytic potential of EAL-type phosphodiesterases is required to explore this class of enzymes in drug design.

1. Schirmer T, Jenal U. "Structural and mechanistic determinants of c-di-GMP signalling." *Nat Rev Microbiol.* 2009; 7 (10): 724–35.
2. Sundriyal A, Massa C, Samoray D, Zehender F, Sharpe T, Jenal U, Schirmer T. "Inherent regulation of EAL domain-catalyzed hydrolysis of second messenger cyclic di-GMP." *J Biol Chem.* 2014; 289 (10): 6978–90.
3. Winkler A, Udvarhelyi A, Hartmann E, Reinstein J, Menzel A, Shoeman RL, Schlichting I. "Characterization of elements involved in allosteric light regulation of phosphodiesterase activity by comparison of different functional BIRP1 states." *J Mol Biol.* 2014; 426 (4): 853–68.
4. Phippen CW, Mikolajek H, Schlaefli HG, Keevil CW, Webb JS, Tews I. "Formation and dimerization of



the phosphodiesterase active site of the *Pseudomonas aeruginosa* MorA, a bi-functional c-di-GMP regulator." *FEBS Lett.* 2014; 588 (24): 4631–6.



**Figure 1.** EAL domain dimerisation induces a change in the length of the R-helix; this brings a pair of aspartic acid side chains (Asp 1310 and Asp 1311) closer to the catalytic centre. These amino acids are involved in metal coordination and thus required for catalytic activity.

**Keywords:** EAL domain, cyclic-di-GMP signalling, phosphodiesterase, metal-ion catalysis, biofilm

## MS9-O4 pH Dependent conformational change of bound maltose observed in the crystal of $\beta$ -amylase at room temperature.

Bunzo Mikami<sup>1</sup>, Youna Kang<sup>1</sup>, Kimihiko Mizutani<sup>1</sup>, Nobuyuki Takahashi<sup>1</sup>

1. Kyoto University

email: mikami@kais.kyoto-u.ac.jp

$\beta$ -Amylase catalyzes the liberation of maltose from the non-reducing ends of  $\alpha$ -1, 4-glucan such as starch and glycogen. In contrast to  $\alpha$ -amylase,  $\beta$ -amylase produces  $\beta$ -anomeric maltose, and is classified as an inverting enzyme. In soybean  $\beta$ -amylase (SBA), the hydrolysis of the  $\alpha$ -1, 4-glucosyl linkage is proceeded by two catalytic residues, Glu186 (acid) and Glu380 (base). The enzyme has two mobile loops, flexible loop (residue 96-103) and inner loop (residue 341-345) near the active site. The conformation of these loops change from open to closed form and from apo to product form, respectively, during enzyme action. In this paper, we are intended to determine the structural changes of SBA/maltose complex in a different pH media. In order to control pH correctly, we have determined the crystal structure at room temperature to avoid the undesirable effect of freezing and cryo-protectant such as glycerol. SBA was expressed in expression system of *E. coli*, and was purified and crystallized by a hanging-drop vapor diffusion against 1 ml of the bottom solution containing 45% saturated ammonium sulfate, 0.1 M sodium acetate buffer, pH 5.4. The obtained crystals were packed in glass capillaries after soaked with 200mM maltose in the different pH buffer (0.1 M acetate, PIPES or Tris buffer, pH 3-9), containing 45% saturated ammonium sulfate. The diffraction data sets were collected at BL26B1/B2 beam-lines in SPring-8. Each crystal data was collected with 98-100 % completeness and  $R_{\text{merge}}$  of 0.04-0.05 up to 1.6-1.7 Å resolution. The models were refined with SHELXL program including protein anisotropic B-factors. The refined models contains one molecules of SBA comprising 492 amino acid residues, 3-7 sulfate ions and 403-450 water molecules with  $R = 0.12$ - $0.13$  and  $R_{\text{free}} = 0.14$ - $0.16$ . At pH 5.4, two maltose molecules were located at the subsites -2~-1 and +1~+2 with  $\alpha$ -anomer boat form at subsite -1, whereas  $\alpha/\beta$ -anomer chair forms were clearly found at pH 4.0 (Fig. 1). This indicates that the glucose residue at subsite -1 is distorted to boat form by the deprotonation of a protein residue with  $pK_a = 4.5$  in the active site. The pH dependency of the conformational change of maltose in mutant proteins, K295A and T342V were also analyzed. It is suggested that the sugar conformational change from chair to boat form occurs by the increased nucleophilicity of the catalytic water near subsite -1.

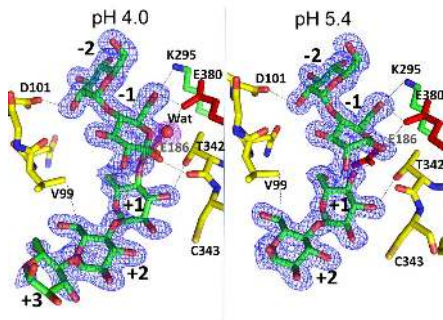


**Figure 1.** The effect of pH on the binding mode of maltose in the active site of SBA.

**Keywords:**  $\beta$ -amylase, capillary measurement

## MS9-O5 Lipidic cubic phase injector is a viable crystal delivery system for time-resolved serial crystallography

Przemyslaw Nogly<sup>1</sup>, Valerie Panneels<sup>1</sup>, Garrett Nelson<sup>2</sup>, Cornelius Gati<sup>3</sup>, Tetsunari Kimura<sup>4</sup>, Christopher Milne<sup>5</sup>, Despina Milathianaki<sup>6</sup>, Minoru Kubo<sup>4</sup>, Wenting Wu<sup>1</sup>, Chelsie Conrad<sup>7</sup>, Jesse Coe<sup>7</sup>, Richard Bean<sup>3</sup>, Yun Zhao<sup>2</sup>, Petra Bath<sup>8</sup>, Robert Dods<sup>8</sup>, Rajiv Harimoorthy<sup>9</sup>, Kenneth Beyerlein<sup>3</sup>, Jan Rheinberger<sup>1</sup>, Daniel James<sup>2</sup>, Daniel DePonte<sup>6</sup>, Chufeng Li<sup>2</sup>, Leonardo Sala<sup>5</sup>, Garth Williams<sup>6</sup>, Mark Hunter<sup>6</sup>, Jason E. Koglin<sup>6</sup>, Peter Bernsten<sup>8</sup>, Eriko Nango<sup>9</sup>, So Iwata<sup>9</sup>, Henry Chapman<sup>3</sup>, Petra Fromme<sup>7</sup>, Matthias Frank<sup>10</sup>, Rafael Abela<sup>7</sup>, Sébastien Boutet<sup>6</sup>, Anton Barty<sup>7</sup>, Thomas A. White<sup>7</sup>, Uwe Weierstall<sup>7</sup>, John Spence<sup>2</sup>, Richard Neutze<sup>8</sup>, Gebhard Schertler<sup>1</sup>, Jörg Standfuss<sup>1</sup>

1. Laboratory for Biomolecular Research, Paul Scherrer Institute, 5232 Villigen, Switzerland
2. Department of Physics, Arizona State University, 85287 Tempe AZ, USA
3. Center for Free-Electron Laser Science, Deutsches Elektronen-Synchrotron DESY, 22607, Hamburg, Germany
4. Biometal Science Laboratory, RIKEN Spring-8 Center, 679-5148 Hyogo, Japan
5. SwissFEL, Paul Scherrer Institute, 5232 Villigen, Switzerland
6. Linac Coherent Light Source (LCLS), SLAC National Accelerator Laboratory, 94025 Menlo Park, USA
7. Department of Chemistry and Biochemistry, and Center for Applied Structural Discovery, Biodesign Institute, Arizona State University, 85287-1604 Tempe, USA
8. Department of Chemistry and Molecular Biology, University of Gothenburg, Gothenburg, Sweden
9. SACLAS Science Research Group, RIKEN/Spring-8 Center, 679-5148 Hyogo, Japan
10. Lawrence Livermore National Laboratory, 94550 Livermore, USA

email: [przemyslaw.nogly@psi.ch](mailto:przemyslaw.nogly@psi.ch)

Serial femtosecond crystallography (SFX) using X-ray free-electron laser (XFEL) sources is a newly developed method with considerable potential for time-resolved pump probe experiments. I will present a lipidic cubic phase SFX structure of the light-driven proton pump bacteriorhodopsin (bR) to 2.3 Å resolution and a method to investigate protein dynamics with modest sample requirement. Time-resolved serial femtosecond crystallography (TR-SFX) with a pump-probe delay of 1 ms yields Fourier difference maps ( $F - F_0$ ) compatible with the dark to M state transition of bR. Importantly the method is sample efficient and reduces sample consumption to a few milligrams of protein per collected time point. Accumulation of M intermediate within the crystal lattice is confirmed by time-resolved visible absorption spectroscopy. The impact of radiation damage free data collection using femtosecond XFEL pulses on the study of structural intermediates is discussed and compared with serial millisecond crystallography (SMX) at a synchrotron source. This study provides an important step towards characterizing the dynamics of complete photocycles of retinal proteins and demonstrates the feasibility of a sample efficient viscous medium jet in TR-SFX.

Nogly, P., Panneels, V., Nelson, G., Gati, C., Kimura, T., Milne, C., Milathianaki, D., Kubo, M., Wu, W., Conrad, C., Coe, J., Bean, R., Zhao, Y., Bath, P., Dods, R., Harimoorthy, R., Beyerlein, K.R., Rheinberger, J., James, D., DePonte, D., Li, C., Sala, L., Williams, G., Hunter, M., Koglin, J.E., Bernsten, P., Nango, E., Iwata, S., Chapman, H.N., Fromme, P., Frank, M., Abela, R., Boutet, S., Barty, A., White, T.A., Weierstall, U., Spence, J., Neutze, R., Schertler, G. & Standfuss, J. *Lipidic cubic phase injector is a viable crystal delivery system for time-resolved serial crystallography*. (2016) under revision.

Nogly, P., James, D., Wang, D., White, T. A., Zatspein, N., Shilova, A., Nelson,

G., Liu, H., Johansson, L., Heymann, M., Jaeger, K., Metz, M., Wickstrand, C., Wu, W., Bath, P., Berntsen, P., Oberthuer, D., Panneels, V., Cherezov, V., Chapman, H., Schertler, G., Neutze, R., Spence, J., Moraes, I., Burghammer, M., Standfuss, J. & Weierstall, U. *Lipidic cubic phase serial millisecond crystallography using synchrotron radiation*. (2015) IUCr 2.

**Keywords:** time-resolved crystallography, bacteriorhodopsin, X-ray Free Electron Laser

## MS10 H-bonding & weak interactions in crystals: neutrons and X-rays

Chairs: Boris Zakharov, Hazel Sparkes

### MS10-O1 Nanoscale hydrogen bond network revealed by neutron scattering

Heloisa N. Bordallo<sup>1</sup>

1. The Niels Bohr Institute - University of Copenhagen - Copenhagen - Denmark

email: bordallo@nbi.ku.dk

Neutron science is the science of everyday life, providing a microscopic view of the materials we rely on for modern life. Neutrons, similarly to X-rays, penetrate matter. However, unlike X-rays, neutrons interact with matter in a different manner, thus allowing the identification of elements with very low molecular weight, including hydrogen. Thus while X-rays is one of the most important characterization methods in solid state chemistry and materials science, neutron diffraction is more commonly used to provide information on proton distribution within the structure. For this reason, both X-rays and neutron diffraction, complemented by neutron spectroscopy, which brings information about hydrogen mobility, can contribute for better understanding of complex structures. In this talk I will discuss on this promising approach by presenting a couple of specific examples. The first is related to a number of differences in the structural and dynamical behavior of D-alanine when compared to L-alanine<sup>[1]</sup> and the second to the interplay of molecular flexibility and hydrogen bonding manifested in the polymorphs of paracetamol.<sup>[2]</sup> Finally I will give a brief overview in how this approach can extend to the study of highly intricate pore structures.<sup>[3]</sup>

[1] E. Belo, P.T.C Freire, J. E. M. Pereira, D. N. Argyriou, T. Seydel, H.N. Bordallo (2016) Manuscript in preparation.

[2] N. Tsapatsaris, B.A. Kolesov, J. Fischer, E.V. Boldyreva, L. Daemen, J. Eckert, and H.N. Bordallo (2014) Polymorphism of Paracetamol: A new understanding of molecular flexibility through local methyl dynamics. *Molecular Pharmaceutics* **11**, 1032-1041.

[3] A.R. Benetti, J. Jacobsen, B. Lehnhoff, N.C.R. Momsen, D.V. Okhrimenko, M.T.F. Telling, N.Kardjilov, M. Strobl, T. Seydel, I. Manke and H.N. Bordallo (2015) How mobile are protons in the structure of dental glass ionomer cements? *Sci. Rep.* **5**, 8972 (8 pages)

**Keywords:** hydrogen bond dynamics, flexibility, conformational change

**MS10-O2** Molecular Interactions in Pharmaceutical CompoundsKatharina Edkins<sup>1</sup><sup>1</sup>. School of Medicine, Pharmacy and Health, Durham University, United Kingdomemail: [katharina.fucke@durham.ac.uk](mailto:katharina.fucke@durham.ac.uk)

Small organic molecules, especially in the pharmaceutical sciences, tend to crystallise in a plethora of different crystal forms, either as pure compounds or with the inclusion of solvent molecules. Due to their changed physico-chemical characteristics, such as melting point, compressibility, solubility and thus bioavailability, and physical and chemical stability, different crystal forms can pose a problem to the manufacture of medicines.<sup>[1]</sup> It is thus crucial to understand the crystallisation behaviour and manufacturability of these compounds in order to avoid problems in the life-time of the medicine and costly recalls comparable to ritonavir<sup>[2]</sup> or rosiglitone.<sup>[3]</sup> Bioactive molecules and pharmaceuticals typically have multiple functional groups, enabling them to interact with receptors and thus show pharmacological action. In the solid-state, the interactions through these functional groups are the driving forces of molecular recognition. By applying X-ray and neutron diffraction methods as well as thermoanalysis, vapour sorption and spectroscopic analysis in combination with computational techniques, we are probing the strong and weak interactions within the crystal forms and during the crystallisation in order to understand and predict their characteristics.

[1] R. Hilfiker, *Polymorphism: In the Pharmaceutical Industry*, Wiley-VCH Verlag GmbH & Co. KGaA, Weinheim, Germany, **2006**. [2] S. R. Chemburkar, J. Bauer, K. Deming, H. Spiwek, K. Patel, J. Morris, R. Henry, S. Spanton, W. Dzik, W. Porter, J. Quick, P. Bauer, J. Donaubauer, B. A. Narayanan, M. Soldani, D. Riley and K. McFarland, *Organic Process Research & Development* **2000**, 4, 413-417. [3] I. B. Rietveld and R. Ceolin, *Journal of Pharmaceutical Sciences* **2015**, 104, 4117-4122.

**Keywords:** Polymorphism, Pharmaceutical, Molecular recognition**MS10-O3** High resolution neutron and X-ray diffraction RT studies of an H-FABP – Oleic acid complex: study of the internal water cluster and the ligand binding by a transferred multipolar electron density distribution

Alberto Podjarny<sup>1</sup>, Eduardo I. Howard<sup>2</sup>, Benoit Guillot<sup>3</sup>, Matthew P. Blakeley<sup>4</sup>, Michael Haertlein<sup>5</sup>, Martine Moulin<sup>6</sup>, Andre Mitschler<sup>1</sup>, Alexandra Cousido-Siah<sup>1</sup>, Firas Fadel<sup>1</sup>, Wanda Valsecchi<sup>6</sup>, Takashi Tomizaki<sup>7</sup>, Tania Petrova<sup>8</sup>, Julien Claudot<sup>3</sup>

1. IGBMC, CNRS, INSERM, UoS, Illkirch, France
2. IFILYSIB, CONICET, UNLP, La Plata, Argentina
3. CRM2, CNRS, U.Lorraine, Vandoeuvre-les-Nancy, France
4. ILL, Grenoble, France
5. PBS, Grenoble, France
6. IQFB, UBA, Buenos Aires, Argentina
7. SLS, Villigen PSI, Switzerland
8. IMPB, RAS, Pouchino, Russia

email: [apodjarny@gmail.com](mailto:apodjarny@gmail.com)

Crystal diffraction data of heart fatty acid binding protein (H-FABP) in complex with oleic acid were measured at room temperature with high resolution X-ray and neutron protein crystallography (0.98 Å and 1.90 Å resolution respectively). These data provided very detailed information about the cluster of water molecules and the bound oleic acid in the H-FABP large internal cavity. The jointly refined X-ray/neutron structure of H-FABP was complemented by a transferred multipolar electron density distribution using the parameters of the ELMAM2 library. The resulting electron density allowed a precise determination of the electrostatic potential in the fatty acid (FA) binding pocket. Bader's quantum theory of atoms in molecules was then used to study interactions involving the internal water molecules, the FA and the protein. This approach showed H-H contacts of the FA with highly conserved hydrophobic residues known to play a role in the stabilization of long chain FAs in the binding cavity. The determination of water hydrogen (deuterium) positions allowed the analysis of the orientation and electrostatic properties of the water molecules in the very ordered cluster. As a result, a significant alignment of the water molecules permanent dipoles with the protein electrostatic field was observed. This can be related to the dielectric properties of hydration layers around proteins, where the shielding of electrostatic interactions depends directly on the rotational degrees of freedom of the water molecules in the interface.

**Keywords:** Neutron protein crystallography ; High resolution room temperature X-ray crystallography; Fatty acid binding protein; Protein hydration layer ; AIM Topological properties

## MS10-O4 Targeting transthyretin amyloidosis: Joint neutron and X-ray diffraction analysis of a pathogenic protein

Ai Won Yee<sup>1,2</sup>, Martine Moulin<sup>1,2</sup>, Matthew Blakeley<sup>3</sup>, Edward Mitchell<sup>2,4</sup>, Michael Haertlein<sup>1</sup>, Jonathan Cooper<sup>3</sup>, Trevor Forsyth<sup>1,2</sup>

1. Life Sciences group, Institut Laue-Langevin, Grenoble, France
2. EPSAM, Keele University, UK
3. Large Scale Structures group, Institut Laue-Langevin, Grenoble, France
4. European Synchrotron Radiation Facility, Grenoble, France
5. Laboratory of Protein Crystallography, Drug Discovery Group, Wolfson Institute for Biomedical Research, UCL, UK

email: yee@ill.fr

Transthyretin (TTR) amyloidosis is the most common hereditary form of amyloidosis that is characterised by extracellular deposition of insoluble amyloid fibrils derived from misfolded protein in one or more organ systems in the body.<sup>1</sup> It is an irreversible and progressive disease and is fatal within 10 years of onset. Autosomal dominant mutations<sup>2</sup> in the TTR gene alter the protein stability leading to tetramer dissociation and favouring an abnormal monomeric structure, which in turn polymerises into unknown intermediates and finally into amyloid fibrils.<sup>3</sup>

Up to date, more than 200 X-ray crystal structures are available for TTR, but there is no consistent model to conclude the molecular assembly of the fibril building blocks and the triggering factors for this process. Neutron protein crystallography is a powerful tool that strongly complements X-ray structural studies by revealing key details of hydrogen atom interactions within the protein. Looking at the differences in hydrogen bonding, protonation states and hydration of two TTR mutants – S52P and T119M, which play opposite roles in the protein stability,<sup>4,5</sup> will provide key insights into how they destabilise the tetramer and promote amyloidotic aggregation.

### References:

1. Planté-Bordeneuve V, Said G. *Lancet Neurol*. 2011;10(12):1086-1097.
2. Saraiva MJM. Database on Transthyretin Mutations. 2013:1-24.
3. Damas AM, Saraiva MJ. *J Struct Biol*. 2000;130(2-3):290-9.
4. Mangione PP, Porcari R, Gillmore JD, et al. *Proc Natl Acad Sci U S A*. 2014;111(4):1539-44.
5. Sebastião MP, Lamzin V, Saraiva MJ, Damas A M. *J Mol Biol*. 2001;306:733-44.

**Keywords:** amyloid, transthyretin, neutron, x-ray

## MS10-O5 Bond Formation, Interactions and Reactions in *Peri*-Substituted Naphthalenes.

John D. Wallis<sup>1</sup>, Amelie Wannebroucq<sup>1</sup>, Gizem Saritemur<sup>1</sup>, Nerea Mercadal<sup>1</sup>, Laura Nomen Miralles<sup>1</sup>, Mateusz B. Pitak<sup>2</sup>, Simon J. Coles<sup>2</sup>

1. School of Science and Technology, Nottingham Trent University, Clifton Lane, Nottingham NG11 8NS, UK
2. National Crystallography Service, School of Chemistry, University of Southampton SO17 1BJ, UK.

email: john.wallis@ntu.ac.uk

Crystal structures of *peri*-naphthalenes containing a dimethylamino group and an alkene, e.g. **1-4**, show either attractive interactions or bond formation between the *peri*-substituents depending on the electrophilicity of the alkene. Charge density measurements have been used to characterise these interactions and bonds. Using the “Atoms in Molecules” approach, the values of the electron density and the Laplacian at the (3,-1) critical monitor the progress of bond formation. It is of note that the inter-group bond in zwitterion **3** (1.647 Å) is not fully formed.

In naphthalene **5** the neighbouring dimethylamino group modifies the properties of the aldehyde group which can be protonated or acylated on oxygen. A series of related ketones also protonate on oxygen, though for the *t*-butyl and phenyl ketones protonation on nitrogen with formation of a hydrogen bond to the carbonyl pi system is preferred.

Initial investigations show two types of interaction between *peri*-oriented carboxylate and aldehyde groups in anion **6**: either a Bürgi-Dunitz type interaction of carboxylate oxygen with the aldehyde carbonyl group, or direction of the aldehyde hydrogen atom at the face of the carboxylate group.

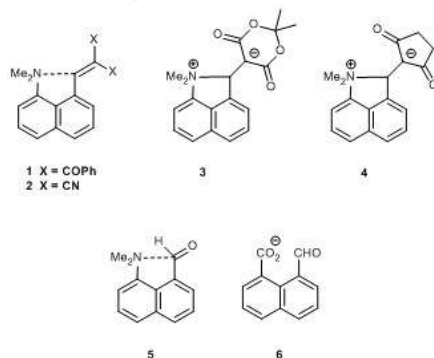


**Figure 1.** Structures of *peri*-naphthalene derivatives.

**Keywords:** Interactions, charge density measurements, long bonds.

## MS11 Hybrid approaches and validation (X-ray and electron microscopy)

Chairs: Felix Rey, Mathieu Botte

### MS11-O1 How reliable are atomic models based on cryo-EM reconstructions? Improvements in model fitting and validation.

Piotr Neumann<sup>1</sup>, Niels Fischer<sup>2</sup>, Holger Stark<sup>2</sup>, Ralf Ficner<sup>1</sup>

1. Department of Molecular Structural Biology, Institute for Microbiology & Genetics GZMB, Georg-August-Universität Göttingen, Justus-von-Liebig-Weg 11, 37077 Göttingen, Germany  
2. 3D Electron Cryomicroscopy Group, Max-Planck-Institute for Biophysical Chemistry, Am Fassberg 11, 37077 Göttingen, Germany

email: pneuman2@uni-goettingen.de

Recent developments in the field of single particle electron cryo-microscopy (cryo-EM) made it possible to obtain 3D reconstruction based atomic models with the overall quality comparable to X-ray crystal structures. However in comparison to X-ray crystallography, the level of structural details is often less uniformly spread across the entire cryo-EM reconstruction, what causes the major difficulty in obtaining reliable atomic models for not well defined or flexible regions. This raises the need of developing new tools for “multi-resolution” fitting of atomic models and their validation or customization of the usage of existing programs.

Our analysis of local Real Space Correlation Coefficient (RSCC) of over 50 near-atomic resolution structures deposited in the Electron Microscopy Data Bank (EMDB) revealed that only a few of those fit the deposited cryo-EM map at a level commonly accepted for X-ray crystal structures (Figure 1). Among the best fitting atomic models is the structure of 70S ribosome from *Escherichia coli* determined at 2.65-2.9 Å resolution (PDB ID: 5AFL<sup>[1]</sup>) obtained by cryo-EM reconstruction and a pseudo-crystallographic refinement approach employing manual model adjustments, density-guided modeling and energy optimization using the Rosetta package and efficient conformational sampling with the usage of customized “distance-slacked chemical” restraints. Testing the newly established refinement protocol employing customized chemical restraints on the set of analyzed cryo-EM based atomic models will be discussed. Interestingly, re-refinement of analyzed structures revealed significant discrepancies in the highest resolution limit determined by cryo-EM gold-standard FSC and X-ray crystallography derived criteria indicating the need of employing validation techniques assessing to which resolution limit reliable structural features extend.

<sup>[1]</sup> Niels Fischer, Piotr Neumann, Andrey L. Konevega, Lars V. Bock, Ralf Ficner, Marina V. Rodnina & Holger Stark, Structure of the E. coli ribosome-EF-Tu complex at <3 Å resolution by Cs-corrected cryo-EM, (2015), Nature 520, 567–570.

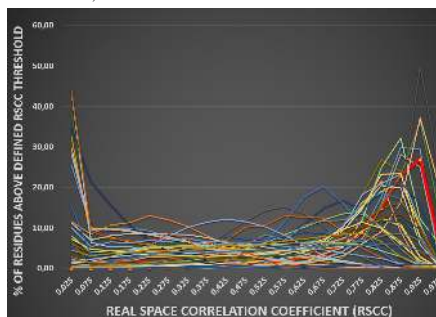


**Figure 1.** Histogram of RSCC of analyzed cryo-EM structures (5AFL structure is highlighted in red).

**Keywords:** cryo-EM, model fitting and refinement, validation

## MS11-O2 Cholesteryl esters are a new class of ligands for lipid antigen presentation by CD1c proteins

Ivo Tews<sup>1</sup>, Salah Mansour<sup>2</sup>, Chris Cave-Ayland<sup>3</sup>, Moritz Machelett<sup>1</sup>, Barbara Sander<sup>3</sup>, Tim Elliott<sup>2</sup>, Chris Skylaris<sup>3</sup>, Jon Essex<sup>3</sup>, Stephan Gadiola<sup>2</sup>

1. Centre for Biological Sciences, Institute for Life Sciences B85, University of Southampton, Southampton SO17 1BJ, UK
2. Clinical and Experimental Sciences, Faculty of Medicine, University of Southampton, Tremona Road, Southampton, SO16 6YD, UK
3. Chemistry, University of Southampton, Southampton SO17 1BJ, UK

email: ivo.tews@soton.ac.uk

Presentation of lipid antigens to T cells is negotiated by CD1 proteins (Cluster of differentiation 1). CD1 proteins are a family of MHC class I-like glycoproteins, distinguished into five different classes that differ in substrate specificity and intracellular trafficking. Determining their individual substrate specificity and unique features is instrumental to understanding their roles in host defense and immune regulation.

We have studied the CD1c isoform and determined the 2.4 Å structure of CD1c in the presence of lipid ligands, differentiating this isoform from other CD1 proteins. The ligands are enclosed in binding pockets, resulting in significant changes in shape of CD1c between ligand bound and unbound forms. Computational simulations starting with this structure explore the lipid-binding pocket to suggest the potential of CD1c to present acylated sterols.

We confirmed the prediction for two lipid classes: cholesteryl esters similar to those accumulating in foamy macrophages and in solid tumors, relevant in the context of autoimmune disorders and cancer, and acylated sterol glycosides relevant in bacterial infections such as lime disease and tuberculosis. The findings open up new avenues for research into the role of CD1c in human immunity.

Mansour S, Tocheva AS, Cave-Ayland C, Machelett MM, Sander B, Lissin NM, Molloy PE, Baird MS, Stübs G, Schröder NW, Schumann RR, Rademann J, Postle AD, Jakobsen BK, Marshall BG, Gosain R, Elkington PT, Elliott T, Skylaris CK, Essex JW, Tews I, Gadola SD. "Cholesteryl esters stabilize human CD1c conformations for recognition by self-reactive T cells." *Proc Natl Acad Sci USA*. 113 (2016), E1266-75.

**Keywords:** Immunity, glycoprotein, CD1, lipid, antigen

## MS11-O3 Structure of the full-length VEGFR-1 extracellular domain in complex with VEGF-A

Sandra Markovic-Mueller<sup>1,2</sup>, Edward Stuttfeld<sup>3</sup>, Mayanka Asthana<sup>4</sup>, Tobias Weinert<sup>1</sup>, Spencer Bliven<sup>1</sup>, Kenneth N. Goldie<sup>4</sup>, Kaisa Kisko<sup>1</sup>, Guido Capitani<sup>1</sup>, Kurt Ballmer-Hofer<sup>1</sup>

1. Paul Scherrer Institute, Laboratory of Biomolecular Research, 5232 Villigen PSI, Switzerland
2. leadXpro AG, PARK innovAARE, 5234 Villigen, Switzerland
3. Biocenter, University of Basel, Basel, Switzerland
4. Center for Cellular Imaging and Nano Analytics (C-CINA), Biocenter, University of Basel, Basel, Switzerland

email: sandra.markovic@leadxpro.com

Vascular Endothelial Growth Factors (VEGFs) regulate blood and lymph vessel development and are thus essential for vessel homeostasis. VEGFs activate three receptor tyrosine kinases (RTKs), VEGFR-1, -2, and -3. Mutation of these receptors gives rise to distinct disease profiles documenting signal diversity among VEGF receptors. Aberrant expression of a soluble splice variant of VEGFR-1, encompassing only the extracellular domain (ECD) and acting as a ligand trap, is associated with vascular defects such as the placental deficiency preeclampsia, or corneal avascularity. This variant is thus a potentially interesting target for drug development. A low resolution structure of the full-length VEGFR-2 ECD/VEGF-A complex based on single particle electron microscopy and small angle X-ray scattering data revealed the location of VEGF binding and domain arrangement of the membrane proximal part of the receptor. Here we describe the structure of the full-length VEGFR-1 ECD in complex with VEGF-A at 4 Å resolution. We combined X-ray crystallography, single particle electron microscopy, and molecular modeling for structure determination and validation. The structure reveals the molecular details of ligand-induced receptor dimerization, in particular of homotypic receptor interactions in Ig-domains 4, 5, and 7. Thermodynamic and mutational analyses of ligand binding and receptor activation confirm the functional relevance of these homotypic contacts and identify them as potential therapeutic sites to allosterically inhibit VEGFR-1 activity. This structural and functional information will be central for developing novel, highly specific VEGFR inhibitors.

**Keywords:** low resolution X-ray crystallography, negative staining EM, SAXS, native-SAD, modeling, receptor tyrosine kinases



## MS11-O4 Protein-ligand interaction energy for crystallographic model building and validation

Daria Beshnova<sup>1</sup>, Joana Pereira<sup>1</sup>, Victor Lamzin<sup>1</sup>

1. Hamburg Outstation, European Molecular Biology Laboratory, c/o DESY, Notkestrasse 85, Hamburg, 22607, Germany

email: beshnova@embl-hamburg.de

As the number of crystallographic studies undertaken by non-experts is increasing, the availability of powerful validation techniques to verify the correctness of built models before their deposition in the PDB is essential. While for protein models existing approaches allow detection of many classes of errors, for ligand-protein structures the validation protocols are less well developed and the electron density is often difficult to interpret.

We propose a new addition to the crystallographic ligand building in electron density maps that is based on the estimation of the inter-molecular energy of the ligand-protein complex. We will demonstrate that taking into account three major energetic terms - van der Waals, hydrogen-bonding and electrostatic interactions - helps enhance the interpretation of electron density maps. During ligand fitting the method allows to identify the ligand conformation with the most plausible ligand-protein contacts and the lowest energy. The method can also be applied for validation of fitted ligands or deposited protein-ligand complexes and can be used as additional scoring criterion for guessing the ligand identity in difference electron density maps.

**Keywords:** inter-molecular energy, crystallographic model building, validation

## MS11-O5 DipSpace and DipCheck: A Distance Geometry-Based Description of Protein Main-Chain Conformation

Joana Pereira<sup>1</sup>, Victor Lamzin<sup>1</sup>

1. EMBL Hamburg

email: joana.pereira@embl-hamburg.de

The knowledge of the structures of biological macromolecules is imperative for the understanding of their function in cellular processes and their role in human diseases. Deciphering and validating these structures is therefore essential for biological research.

By searching for a convenient notation of polypeptide conformation, Ramachandran *et al.* suggested the use of two main-chain torsion angles,  $\varphi$  and  $\psi$ , which provide elegant description of protein local conformational space. However, a 2D description of the polypeptide conformational space is a simplification and does not account for the natural variation of the interatomic and angle-bonded distances of the protein backbone. It also lacks the information about the stretched geometry around the  $C\alpha$  atom: the stretching angle  $\tau$ . Therefore, validation methods such as WHAT\_CHECK or MolProbity check for the Ramachandran angles as well as for the stretching angles, bond angles, bond lengths and the possibility for clashes.

Here, we propose a new distance-based 3D space for the description of protein polypeptide conformation, at a given  $C\alpha_i$  position using a 5-atom representation of a dipeptide unit ( $C\alpha_{i-1}-O_{i-1}-C\alpha_i-O_i-C\alpha_{i+1}$ ). We consider the apparent planarity of the trans-peptide unit, which arises from the fact that the almost double-bonded nature of the peptide bond forces the  $\omega$  torsion angle to be around  $180^\circ$ . The polypeptide chain can thus be seen as a set of connected peptide planes defined by the positions of its  $C\alpha_i$ ,  $O_i$  and  $C\alpha_{i+1}$  atoms. T

he method is based on the premise that molecular conformation can be defined by the relative position of atoms in the 3D space and on the chirality of asymmetric atomic groups, and accounts for all conformations that a dipeptide unit can adopt as well as for the natural variations of bond lengths and bond angles. The resulting Euclidian orthogonal 3D space, DipSpace, in combination with a chirality measure, allows description of protein stereochemistry and points to residues in an unusual conformation which may not be detectable with other approaches. The method was implemented within a tool, DipCheck, whose application to the validation of protein models will be demonstrated.

**Keywords:** validation, backbone description, distance geometry



## MS12 Biophysical characterization and crystallization

Chairs: Rob Meijers, Bernadette Byrne

### MS12-O1 The magnesium transporter A, a bacterial P-type ATPase dependent on cardiolipin and selectively sensitive to free magnesium *in vitro*

Jens Preben Morth<sup>1,2</sup>, Harmonie Perdreau-Dahl<sup>1,2</sup>, Saranya Subramani<sup>1,2</sup>

1. Centre for Molecular Medicine, Nordic EMBL Partnership, University of Oslo, 0318 Oslo, Norway  
2. Institute for Experimental Medical Research, Oslo University Hospital Ullevaal, 0407 Oslo, Norway

email: j.p.morth@ncmm.uio.no

Three classes of Magnesium transporters have been identified in Bacteria and Archaea; CorA, MgtE and MgtA/MgtB (Groisman et al., 2013). CorA and MgtE are constitutively expressed. CorA and MgtE are both magnesium efflux transporter. Influx is believed to be mediated by MgtA. The magnesium transporter A (MgtA) is a specialized P-type ATPase, that import  $Mg^{2+}$  into the cytoplasm. In both *Salmonella typhimurium* and *Escherichia coli*, the virulence determining two-component system PhoQ/PhoP regulates the transcription of the *mgtA* gene by sensing  $Mg^{2+}$  concentrations in the periplasm, along with low pH and the presence of cationic peptides. This study demonstrates, for the first time, that MgtA is highly dependent on anionic phospholipids and in particular, cardiolipin, the *in vitro* kinetic experiments performed on detergent solubilized MgtA suggest that cardiolipin act as a magnesium chaperone. We further show that MgtA is highly sensitive to free  $Mg^{2+}$  ( $Mg^{2+}_{free}$ ) levels in the solution. MgtA is activated when the  $Mg^{2+}_{free}$  concentration is reduced below 10 mM and is strongly inhibited above 1 mM, indicating that  $Mg^{2+}_{free}$  acts as product inhibitor. Furthermore, colocalization studies confirm that MgtA is found in the cardiolipin lipid rafts in the membrane. Combined, our findings indicate that MgtA may act as a sensor as well as a transporter of  $Mg^{2+}$  (Subramani et al., 2016). Initial crystals have been obtained, using the Hilide method for membrane protein crystallization (Gourdon et al., 2011). The approach of Hilide method will be discussed in this context.

Groisman, E. A.; Hollands, K.; Kriner, M. A.; Lee, E. J.; Park, S. Y.; Pontes, M. H. Bacterial  $Mg^{2+}$  homeostasis, transport, and virulence. *Annual review of genetics* **2013**, 47, 625-46.

Subramani, S.; Perdreau-Dahl, H.; Morth, J. P. The magnesium transporter A is activated by cardiolipin and is highly sensitive to free magnesium *in vitro*. *Elife* **2016**,

5, 10.7554/eLife.11407.

Gourdon, P.; Andersen, J. L.; Hein, K. L.; Bublit, M.; Pedersen, B. P.; Liu, X. Y.; Yatime, L.; Nyblom, M.; Nielsen, T. T.; Olesen, C.; Möller, J. V.; Nissen, P.; Morth, J. P. Hilide—Systematic Approach to Membrane Protein Crystallization in Lipid and Detergent. *Crystal Growth & Design* **2011**, 11, 2098.

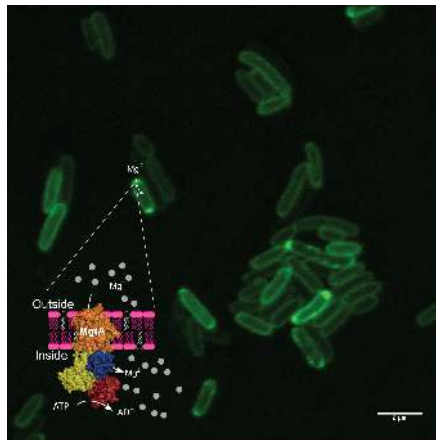


**Figure 1.** Overexpressed MgtA-GFP in *E. coli* is visualized in the background. The fluorescence intensity indicates polar localization. The cartoon describes ATP dependent magnesium (grey) uptake through the P-type ATPase MgtA. Cardiolipin (pink) is believed to be co-localized in the poles and activate MgtA.

**Keywords:** MgtA, P-type ATPases, Hilide, Magnesium homeostasis, cardiolipin, membrane protein

## MS12-O2 New Pipelines for Automated High Throughput Ligand Screening

Irina Cornaci<sup>1</sup>, Mari Ytre-Arne<sup>2</sup>, Guillaume Hoffmann<sup>1</sup>, Vincent Mariaule<sup>1</sup>, Peter Murphy<sup>1</sup>, Matthew Bowler<sup>3</sup>, Didier Nurizzo<sup>3</sup>, Gordon Leonard<sup>3</sup>, Bjørn Dalhus<sup>2</sup>, José A. Márquez<sup>1</sup>

1. EMBL Grenoble
2. Department for Medical Biochemistry, Oslo University Hospital, Oslo, Norway
3. The European Synchrotron Radiation Facility, Grenoble, France

email: cornaci@embl.fr

While both crystallization and data collection can be performed in a highly automated, high-throughput fashion, the numbers of ligands that can be investigated with macromolecular crystallography is strongly limited by manual crystal soaking and mounting. Here we describe a novel generations of pipelines for automated, high-throughput ligand screening with X-ray crystallography. They are based on the combination of the EMBL CrystalDirect technology, enabling completely automated crystal harvesting and cryo-cooling and the MASSIF beamline at ESRF, a fully automated hands-off data collection facility. In addition to automated crystal cryo-cooling and harvesting, the CrystalDirect Technology provides an opportunity to automate soaking experiments through controlled diffusion<sup>1</sup>. This approach supports a gentler delivery (lower osmotic stress) and enables the achievement of higher final ligand concentrations. These new ligand screening pipelines were applied to screen small-molecule libraries targeting proteins of high biomedical relevance leading to the identification and structural characterization of novel ligand protein complexes. These high-throughout, automated, ligand screening pipelines can help streamline the process of structure-based drug design by removing critical bottlenecks and are available to European scientists through the E.C funded H2020 iNEXT project.

<sup>1</sup> Zander U, Hoffmann G, Cornaci I, Marquette J-P, Papp G, Landret C, Seroul G, Sinoir J, Röwer M, Felisaz F, Rodríguez-Puente S, Mariaule V, Murphy P, Mathieu M, Cipriani F, Márquez J. *Automated harvesting and processing of protein crystals through laser photoablation*. Acta Cryst. 2016. D72, 454-466

**Keywords:** ligand screening, high-throughput

## MS12-O3 DNA Structure and Dynamics – A Combinational Approach

James P. Hall<sup>1,2</sup>, Sarah P. Gurung<sup>1,2</sup>, Paraic M. Keane<sup>1,2,3,4</sup>, Fergus E. Poynton<sup>5</sup>, David J. Cardin<sup>1</sup>, Thomas Sorensen<sup>2</sup>, Graeme Winter<sup>2</sup>, Thorfinnur Gunnlaugsson<sup>3</sup>, Igor V. Sazanovich<sup>1</sup>, Mike Towrie<sup>4</sup>, John M. Kelly<sup>3</sup>, Susan J. Quinn<sup>6</sup>, John A. Brazier<sup>7</sup>, Christine J. Cardin<sup>1</sup>

1. Department of Chemistry, University of Reading, Whiteknights, Reading, RG6 6AD, UK
2. Diamond Light Source, Harwell Science and Innovation Campus, Fermi Avenue, Didcot, Oxford, OX11 0DE
3. School of Chemistry, Trinity College, University of Dublin, Dublin 2, Ireland
4. Central Laser Facility, Research Complex at Harwell, Science & Technology Facilities Council, Rutherford Appleton Laboratory, Didcot, Oxfordshire, OX11 0QX, UK
5. Trinity Biomedical Science Institute, Trinity College Dublin, Dublin 2, Ireland
6. School of Chemistry, University College Dublin, Dublin 4, Ireland
7. Department of Pharmacy, University of Reading, Whiteknights, Reading, RG6 6AD, UK

email: james.hall@reading.ac.uk

DNA is an incredibly flexible and versatile molecule. It can adopt a number of different structures ranging from the iconic Watson-Crick double helix to the 4-stranded I-motif. The structure adopted by different DNA sequences strongly affects the dynamics observed in the solution environment. DNA can be damaged by UV light or the introduction of ligands designed to induce DNA damage. As such, linking data from a crystal structure, which gives a static picture of the biomolecule, with spectroscopic measurements is key in establishing how DNA behaves and why.

Here we present our research into the structure and dynamics of DNA and DNA-ligand complexes, using a variety of techniques including circular dichroism<sup>1</sup>, X-ray crystallography<sup>2</sup> and ultrafast transient infra-red spectroscopy<sup>3</sup>. By combining these techniques together, we can determine how DNA behaves, and why, under many different conditions and in multiple sample environments.

1. Gurung, S., Schwarz, C., Hall, J.P., Cardin, C.J. & Brazier, J.A. *Chem. Commun.*, 2015, **51**, 5630-5632.
2. Niyazi, H., Hall, J.P., O'Sullivan, K., Winter, G., Sorensen, T., Kelly, J.M. & Cardin, C.J. *Nature Chem.* 2012, **4**, 621-628.
3. Hall, J.P., Poynton, F.E., Keane, P.M., Gurung, S.P., Brazier, J.A., Cardin, D.J., Winter, G., Gunnlaugsson, T., Sazanovich, I.V., Towrie, M., Cardin, C.J., Kelly, J.M. & Quinn, S.J. *Nature Chem.* 2015, **7**, 961-967.

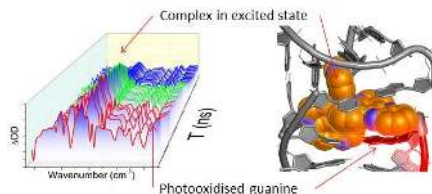


**Figure 1.** (Left) Transient infra-red spectroscopic measurements recorded from crystal fragments. (Right) This is combined with the knowledge of the crystal structure to assign a specific damage

site.

**Keywords:** DNA, photooxidation, time-resolved spectroscopy

## MS12-O4 Racemic DNA Crystallography: advantages and applications

Pradeep K. Mandal<sup>1,2</sup>, Gavin W. Collie<sup>1,2</sup>, Suresh C. Srivastava<sup>3</sup>,  
Brice Kauffmann<sup>4,5,6</sup>, Ivan Huc<sup>1,2</sup>

1. Université de Bordeaux, CBMN (UMR5248), Pessac 33600, France

2. CNRS, CBMN (UMR5248), Pessac 33600, France

3. ChemGenes Corporation, 33 Industrial Way, Wilmington, MA 01887, USA

4. CNRS, Institut Européen de Chimie et Biologie (UMS3033), Pessac 33600, France

5. INSERM, Institut Européen de Chimie et Biologie (US001), Pessac 33600, France

6. Université de Bordeaux, Institut Européen de Chimie et Biologie (UMS3033), Pessac 33600, France

email: pk.mandal@iecb.u-bordeaux.fr

The use of racemic mixtures of naturally chiral macromolecules such as proteins and nucleic acids can significantly increase the chances of crystallization. Racemates allow molecular contacts to be formed in a greater number of ways and give access to centrosymmetric space groups. The benefits of applying racemic crystallographic methods to proteins are considerable (1). Curiously, however, racemic DNA crystallography had not been established despite the commercial availability of L- deoxyribo-oligonucleotides. We present a study into racemic DNA crystallography over a diverse range of sequences and folded conformations including duplexes, four-way Junctions and G-quadruplexes. This study revealed a strong propensity of racemic DNA mixtures to form racemic crystals (2). The crystals obtained from racemic mixtures were invariably achiral, showing a preference for the space group P1(bar) and the structures determined were nearly identical to those determined from classical D-enantiopure solutions (2). Following this proof-of-concept, we evaluated the racemic crystallographic approach for the crystallization of an intractable, biologically relevant DNA sequence – that of the Pribnow box consensus sequence 5'-TATAAT-3' in a duplex with its complementary sequence. Four high-quality crystal structures were determined with resolutions in the range of 1.65 – 2.3 Å, providing insights into the racemic crystallization process as well as structural details of this biologically relevant sequence (3). The racemic crystallization technique provides an attractive alternate to conventional crystallization using D-enantiopure solutions alone. It shows potential for the study of native DNA sequences beyond the classical model sequences, and thus may be of interest to those investigating structural aspects of fundamental biological processes and structure-based DNA-directed drug development programs. This work was supported by the European Union's Seventh Framework Programme through the European Research Council (Grant Agreement No. ERC-2012-AdG-320892, post-doctoral fellowship to PKM).

### References:

- (1) Yeates, T. O. & Kent, S. B. H. (2011). *Annu. Rev. Biophys.*, **41**, 41–61.
- (2) Mandal, P. K., Collie, G. W., Kauffmann, B. & Huc, I. (2014). *Angew. Chem. Int. Ed.*, **53**, 14424–14427.
- (3) Mandal, P. K., Collie, G. W., Srivastava, S. C., Kauffmann, B. & Huc, I. (submitted).

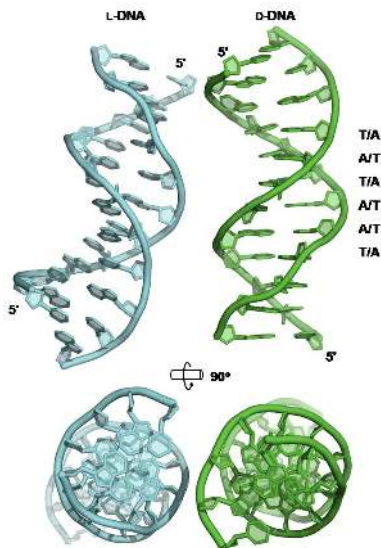


**Figure 1.** Crystal structure (in space group *Pbc*, resolution 1.65 Å) of a DNA duplex containing the Pribnow box consensus promoter sequence 5'-TATAAT-3' with its complementary strand. Right: asymmetric unit, containing one complete D-DNA duplex (green). Left: L-DNA symmetry mate (cyan).

**Keywords:** Racemic crystallography, DNA, X-ray diffraction, DNA crystallography

## MS12-O5 An all-in-one lanthanide complex to overcome the two major bottlenecks in protein crystallography.

Sylvain Engilberge<sup>1</sup>, Louise Lassalle<sup>1</sup>, Sebastiano Di Pietro<sup>2</sup>, François Riobé<sup>2</sup>, Olivier Maury<sup>2</sup>, Eric Girard<sup>1</sup>

1. Institut de Biologie Structurale, UMR5075 CEA-CNRS-UJF, EPN Campus, 71 avenue des Martyrs, 38044 Grenoble Cedex 9

2. UMR5182 CNRS-ENS Lyon-Université Lyon 1, 46 allée d'Italie, 69364, Lyon cedex

email: sylvain.engilberge@ibs.fr

Protein crystallography remains the major technique for protein structure determination. Among 117438 structures deposited on the protein data bank (April 2016), 89 % had been solved using X-ray crystallography. However, protein crystallography is still limited by two major bottlenecks: Obtaining protein crystals and solving the phase problem.

Since 2000, we developed lanthanide complexes for structure determination of macromolecules, exploiting the high-phasing power of lanthanide elements [1-7]. Recently, we produced a new complex with luminescent properties. Unexpectedly, this lanthanide complex ([Ln]) showed nucleant properties making it the first nucleant, luminescent and phasing agent.

To demonstrate the effects of this new molecule, we selected 8 proteins with different molecular weights and different oligomeric states. Among these 8 proteins, two were of unknown structure including one with an unknown fold.

We performed comparative crystallization screening at the HTX lab crystallization plate form (EMBL – Grenoble) with and without [Ln]. We showed that [Ln] significantly increases the number of crystal hits and more importantly, it provides unique crystallization conditions. In many cases the incorporation of [Ln] significantly increases the crystal quality as shown in Figure 1.

The luminescence properties of [Ln] have been used for crystals detection and may be exploited for crystal centering on synchrotron beam line.

The structures of the 8 proteins have been determined using anomalous based phasing methods.

In conclusion, this new all-in-one lanthanide complex allows to overcome the two majors bottlenecks in protein crystallography.

[1] E. Girard et al. *Acta Cryst D*, 59, (2003), 118.[2] E. Girard et al. *Acta Cryst D*, 59, (2003), 1914.[3] R. Talon et al. *J. Synch. Rad.*, 18, (2011), 74. [4] G. Pompidor et al. *Acta Cryst D*, 66, (2010), 762.[5] G. Pompidor et al. *Angew. Chem. Int. Ed.*, 47, (2008), 3388. [6] E. Dumont et al. *Phys. ChemChemPhys.*, 15, (2013), 18235. [7] A. D'Aléo et al. *ChemPhysChem.*, 8, (2007), 2125.

We acknowledge financial support from the Agence Nationale de la Recherche (ANR-13-BS07-0007-02 Ln23).

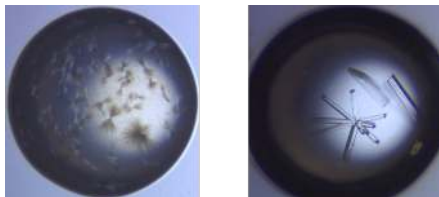


**Figure 1.** Crystallization drops obtained for the same protein without (left) and with the all in one lanthanide complex (right).

**Keywords:** Crystallization, Nucleation, Phasing, Anomalous, Luminescence, Lanthanide complex

## MS13 Hot structures in biology

Chairs: Mariusz Jaskolski, Udo Heinemann

### MS13-O1 How Bacteria Make Rocket Fuel: Structure and Mechanism of Hydrazine Synthase

Thomas R.M. Barends<sup>1</sup>

<sup>1</sup> Max Planck Institute for Medical Research, Heidelberg, Germany

email: [thomas.barends@mpimf-heidelberg.mpg.de](mailto:thomas.barends@mpimf-heidelberg.mpg.de)

The last few decades have seen major changes in our understanding of the global biological nitrogen cycle, largely due to the discovery of the *anammox* pathway. This *anaerobic ammonium oxidation* pathway constitutes a shortcut in the nitrogen cycle that allows bacteria to directly combine nitrite ( $\text{NO}_2^-$ ) with ammonium ( $\text{NH}_4^+$ ), resulting in nitrogen gas ( $\text{N}_2$ ) and water ( $\text{H}_2\text{O}$ ), and which yields energy for the cell. It has been estimated that anammox is responsible for up to 50% of the nitrogen gas production in some ecosystems. Moreover, the process is increasingly being used in energy-efficient waste water treatment plants.

Interestingly, the anammox pathway relies on the highly reactive intermediate hydrazine ( $\text{H}_2\text{N-NH}_2$ ), known to most people only as rocket fuel. The synthesis of hydrazine constitutes the first step in the formation of the highly stable triple bond in nitrogen gas, and is performed by the enigmatic hydrazine synthase complex.

We have studied hydrazine synthase with an array of biophysical methods: X-ray crystallography, solution small-angle X-ray scattering, analytical ultracentrifugation and EPR spectroscopy. We find that the hydrazine synthase multienzyme complex forms crescent-shaped heterohexamers with two distinct active sites connected by a tunnel. The active sites contain entirely novel features and together, the data suggest a mechanism for biological hydrazine synthesis that relies on hydroxylamine as an intermediate.

**Keywords:** protein crystallography

## MS13-O2 Challenges at low resolution: crystal structure of the yeast Vps34 complex II.

Nicolas Soler<sup>1</sup>, Ksenia Rostislavleva<sup>1</sup>, Yohei Ohashi<sup>1</sup>, Lufei Zhang<sup>1</sup>, Els Pardon<sup>2,3</sup>, John E. Burke<sup>1</sup>, Glenn R. Masson<sup>1</sup>, Chris Johnson<sup>1</sup>, Jan Steyaert<sup>2,3</sup>, Nicholas T. Ktistakis<sup>4</sup>, Roger L. Williams<sup>1</sup>

1. MRC Laboratory of Molecular Biology, Cambridge, UK
2. Structural Biology Research Center, VIB, Brussels, Belgium.
3. Structural Biology Brussels, Vrije Universiteit Brussel, Brussels, Belgium.
4. The Babraham Institute, Cambridge, UK

email: nicolas@nicolassolver.eu

Vps34 is a phosphatidylinositol 3-kinase that regulates intracellular vesicle trafficking in endocytic sorting, cytokinesis and autophagy. In cells, the enzyme occurs in two large protein complexes known as complex I and complex II. The full-length 385 kDa yeast endosomal complex II, which consists of Vps34, Vps15, Vps30 and Vps38, could be crystallized using a nanobody that binds to Vps34 and the 4.4 Å structure was subsequently solved. The Y-shaped complex shows Vps34 and Vps15 closely engaging in one arm and Vps30 and Vps38 form the other arm. Hydrogen-Deuterium Exchange Mass Spectrometry (HDX-MS) revealed dynamics of the complex and showed that conformational changes accompany membrane binding and lipid kinase activity. HDX-MS identified a loop in Vps30 that controls the activity on the enzyme on lipid membranes. Determining the structure at this resolution required careful MAD data collection for a tantalum cluster to give excellent phases, which revealed the general shape of the complex. Most of the structure had to be built de novo into this electron density map. However, this process was assisted by first segmenting the structure into elements then employing an automated script using secondary structure profiling results (HHPRED) to place pieces of known structure into the local density. The model was then completed and finalised with manual model building.

**Keywords:** Vps34, complex II, autophagy, endosomal sorting, nanobody, low resolution.

## MS13-O3 X-Ray Crystal Structure of a Chromatosome

Curt A. Davey<sup>1</sup>, Zenita Adhireksan<sup>1</sup>, Qiuye Bao<sup>1</sup>, Sivaraman Padavattan<sup>1</sup>

1. School of Biological Sciences, Nanyang Technological University, 60 Nanyang Drive, Singapore 637551

email: davey@ntu.edu.sg

Linker histones are essential proteins in higher eukaryotes that promote chromatin compaction through binding to the nucleosome. Condensing nucleosomes into highly compact states is required for gene regulation, maintaining genomic integrity and generating mitotic chromosomes for cell division. Nonetheless, the biological relevance of different types of condensed nucleosomal structures observed *in vitro* is controversial, and we lack a unified understanding of how linker histones bind to nucleosomes and promote compaction in the cell.

The first atomic model of the nucleosome core (particle) was published in 1997 [1], paving the way for the structural solution of a great variety of nucleosome core constructs composed of variant/modified histones and different DNA sequences [2,3]. This has consequently revolutionized our understanding of nucleosome activity, and yet nearly two decades later we are still lacking an atomic level understanding of how linker histones interact with nucleosomes.

As with the nucleosome core particle, the challenge in solving the first structure of a chromatosome—the nominal assembly of a nucleosome and linker histone—has been in the discovery of constructs that yield well diffracting crystals. To overcome this obstacle, we developed an approach that promotes ordered lattice formation, which appears to have general utility for structural studies of nucleosomal assemblies. Here we will describe the 2.7 Å resolution X-ray structure of a chromatosome composed of a full length H1 variant. The structure reveals a hitherto unknown mode for linker histone-induced condensing of nucleosomes, which rationalizes *in vivo* data and provides a simple model behind chromatin compaction.

[1] K. Luger, A.W. Mäder, R.K. Richmond, D.F. Sargent & T.J. Richmond. 1997. Crystal structure of the nucleosome core particle at 2.8 Å resolution. *Nature*. **389**: 251-60.

[2] S. Tan & C.A. Davey. 2011. Nucleosome structural studies. *Curr. Opin. Struct. Biol.* **21**: 128-136.

[3] E.Y.D. Chua\*, D. Vasudevan\*, G.E. Davey, B. Wu & C.A. Davey. 2012. The mechanics behind DNA sequence-dependent properties of the nucleosome. *Nucleic Acids Res.* **40**: 6338-6352.

**Funding:** Ministry of Education Academic Research Fund Tier 2 (grant MOE2015-T2-2-089); Ministry of Education Academic Research Fund Tier 3 Programme (grant MOE2012-T3-1-001).

**Keywords:** Nucleosome, Linker histone, Chromatin, Chromatosome, DNA compaction

**MS13-O4 Zinc dependent  
3'-nucleases/nucleotidases from plants,  
fungi and bacteria – varied roles and  
specificity**

Jan Dohnalek<sup>1</sup>, Tomas Koval<sup>1</sup>, Lars H. Østergaard<sup>2</sup>, Petra Lipovova<sup>3</sup>, Jarmila Duskova<sup>1</sup>, Tereza Skalova<sup>1</sup>, Maria Trundova<sup>1</sup>, Karla Fejfarova<sup>1</sup>, Jan Stransky<sup>1</sup>

1. Institute of Biotechnology CAS, Biocev, Průmyslová 595, 252 50 Vestec, Czech Republic
2. Novozymes A/S, Krogshoejvej 36, 2880 Bagsvaerd, Denmark
3. Institute of Chemical Technology, Technická 5, 16628 Prague, Czech Republic

email: dohnalek@ibt.cas.cz

S1-P1 3'-nucleases/nucleotidases (EC 3.1.30.1) are small, mostly alpha-helical enzymes relying on the active centre formed by three zinc ions and surrounded by varied nucleotide binding sites [1]. These extracellular enzymes are employed in various roles in plants, fungi and bacteria but typically not in mammals. These enzymes are utilized in plants in apoptotic processes, tissue development and senescence, in protozoan parasites for securing nutrients and a similar role is expected in some gram-negative bacteria. The purpose of the enzyme in a given organism seems to lead to modification of substrate specificity. Tomato TBN1 has almost universal ability to cleave nucleic acids – single strand, double strand DNA, RNA and structured RNA and this is reflected by the appearance of the enzyme surface [2, 3]. Fungal S1 nuclease shows basically strict ssDNA preference. The enzyme specificity is defined by the width of the cleft, presence of nucleotide binding sites and distribution of electrostatic potential.

We have determined a series of complexes with a fungal enzyme showing a range of ligand-protein interactions. The required enzyme specificity/substrate promiscuity is connected with particular arrangement of surface sites. S1-P1 nuclease is also present in gram negative bacteria and protozoan parasites pathogenic to humans [e.g. 4]. We have cloned, expressed and purified nuclease from a human pathogen and proved its activity. Recent results leading aimed at clarification of specificity features, stabilization of the enzyme in bacteria and inhibition potential, will be presented.

The project is supported by MEYS CR (LG14009, LQ1604 NPU II), CZ.1.05/1.1.00/02.01/09 BIOCEV provided by ERDF and MEYS, and CSF (15-05228S).

#### References

1. Romier C., Dominguez R., Lahm A., *et al. Proteins* 1998, vol. 32, no. 4, 414–424.
2. Koval' T., Lipovová P., Podzimek T., *et al. Acta Cryst.* 2013, vol. D69, no. 2, 213–226.
3. Stránský J., Koval' T., Podzimek T., *et al. Acta Cryst.* 2015, vol. F71, 1408–1415.
4. Guimarães-Costa A.B., DeSouza-Vieira T.S., Paletta-Silva R., *et al. Infect. Immun.* 2014, vol. 82, no. 4, 1732–40.

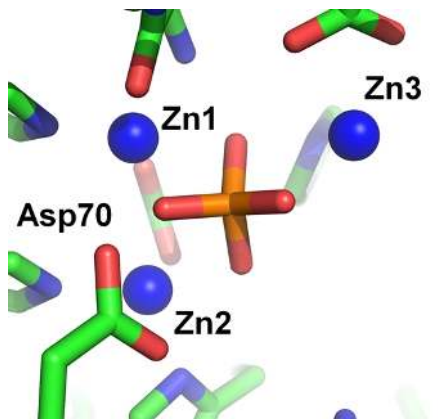


**Figure 1.** Complex of TBN1 and phosphate ion: mimic of product binding mode (PDB ID 4JDG).

**Keywords:** nuclease, 3'nuclease, zinc, S1-P1 nuclease, pathogen, substrate promiscuity



## MS13-O5 Structure and dynamics of the polymyxin-resistance-associated response regulator PmrA in complex with the promoter DNA

Chwan-Deng Hsiao<sup>1</sup>

1. Institute of Molecular Biology, Academia Sinica

email: hsiao@gate.sinica.edu.tw

PmrA, an OmpR/PhoB family response regulator (RR), manages genes for antibiotic resistance. Phosphorylation of OmpR/PhoB RR induces the formation of a symmetric dimer in the N-terminal receive domain (REC), promoting 2 C-terminal DNA-binding domains (DBDs) to recognize the promoter DNA to elicit adaptive responses. Recently, determination of the KdpE-DNA complex structure revealed a unique asymmetric REC-DBD interface that may be necessary for transcription activation. Here, we report the 3.2-Å resolution of the crystal structure of the PmrA-DNA complex, which reveals a similar yet different asymmetric REC-DBD interaction. However, this asymmetric interface is transiently populated in solution, as revealed by relaxation dispersion NMR, and is not crucial in supporting gene expression, as evidenced by the b-galactosidase reporter assay. The interdomain dynamics of the protein, together with the DBD-DBD interface, may help PmrA search for the most suitable conformation for interacting with RNA polymerase holoenzyme to activate downstream gene transcription.

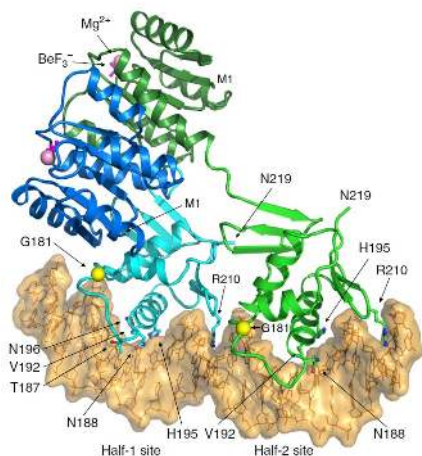


**Figure 1.** Structure of the BeF<sub>3</sub><sup>-</sup>-activated PmrA dimer in complex with the promoter DNA. The PmrA molecule that recognizes half-1 site is denoted as PmrA-1 and half-2 site as PmrA-2.

**Keywords:** Two-component systems, response regulator, crystal structure

## MS14 Biominerological crystallography and bioinspired inorganic materials

Chairs: Wolfgang Schmahl, Fernandez-Diaz Lurdes

### MS14-O1 Learning from Sea Shells – Bio-Inspired Approaches Toward Mesoscale Architectures in Functional Spinel Oxides

Anna S. Schenk<sup>1</sup>, Sabine Eiben<sup>2</sup>, Miriam Goll<sup>1</sup>, Lukas Reith<sup>1</sup>, Elisabeth John<sup>1</sup>, Alex N. Kulak<sup>3</sup>, Fiona C. Meldrum<sup>3</sup>, Christina Wege<sup>2</sup>, Sabine Ludwigs<sup>1</sup>

1. Institute of Polymer Chemistry, University of Stuttgart, Pfaffenwaldring 55, 70569 Stuttgart, Germany
2. Institute of Biomaterials and Biomolecular Systems, University of Stuttgart, Pfaffenwaldring 57, 70569 Stuttgart, Germany
3. School of Chemistry, University of Leeds, Woodhouse Lane, LS2 9JT, Leeds, United Kingdom

email: anna.schenk@ipoc.uni-stuttgart.de

Despite drawing on a limited pool of available elements, nature has developed sophisticated mechanisms to fabricate nanostructured minerals under environmental conditions. Biominerals characteristically represent organic/inorganic composite materials with hierarchical organization spanning multiple length scales, where these complex architectures often lead to astounding properties adapted to suit a specific function. Unsurprisingly, the study of biominerals has therefore inspired a substantial body of research activities, which are aiming to transfer key concepts of biological mineralization, e.g. the use of structure-directing organic matrices and confined reaction environments, into artificial systems. This approach is particularly exciting in view of the growing demand for eco-efficient synthetic routes for the preparation of technologically relevant materials showing inherent functional properties.

We here explore bio-inspired strategies to generate mesoscale architectures in spinel cobalt(II,III) oxide (Co<sub>3</sub>O<sub>4</sub>) and related mixed metal spinels, where these compounds represent a highly promising class of materials for a wide range of applications, particularly in the field of heterogeneous catalysis. In this context, the catalytic activity of the functional oxide largely depends on its morphology, nanostructure and surface area. Specifically, we precipitate thermally unstable cobalt hydroxide carbonate precursors under biomimetic conditions in the presence of either synthetic water-soluble polymers with flexible chains or tobacco mosaic viruses (TMV), where the latter represent plant-derived nanoscopic biotemplates with a rigid-rod supramolecular structure. Calcination at relatively moderate temperatures converts the mineral precursors into the functional spinel oxide phase, while retaining the



gross morphology induced by the structure-directing additives. We demonstrate that highly unusual  $\text{Co}_3\text{O}_4$  structures such as thin films or micrometer-sized tubular superstructures composed of elongated nanoparticles can be generated based on bio-inspired concepts.

The products of the polymer- or virus-mediated mineralization reactions are analyzed before and after calcination using a range of imaging, spectroscopic and x-ray scattering techniques. With the aim to ultimately establish structure-property relationships, the electrocatalytic activity of the resulting materials is investigated with respect to model reactions such as electrolytic water splitting.

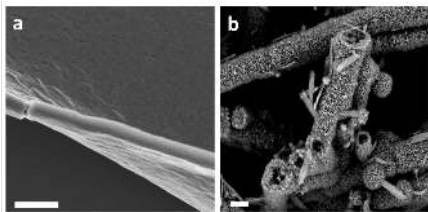


**Figure 1.** Bio-inspired mineralization of basic cobalt carbonate mediated by the water-soluble polyelectrolyte poly(vinylamine) (a) and tobacco mosaic viruses as biotemplates (b). Scale bars = 1  $\mu\text{m}$ .

**Keywords:** bio-inspired mineralization, biotemplates, mesostructure, functional materials, small-angle x-ray scattering

## MS14-O2 Complex biomimetic self-assembly in simple inorganic precipitation systems

Matthias Kellermeier<sup>1</sup>

<sup>1</sup> Material Physics, BASF SE, D-67056 Ludwigshafen, Germany

email: matthias.kellermeier@basf.com

Biomimetalization provides spectacular examples for the concerted organization of inorganic matter into delicate superstructures with extraordinary properties designed for specific functions. Mimicking these processes in vitro is an overarching goal in material science and other areas of research. However, the currently achieved performance of bioinspired man-made materials does often not approach the natural counterpart yet – essentially due to the complexity of the phenomena leading to biomineral formation. Therefore, simplified model systems are needed to understand and ultimately control the fundamental mechanisms of self-assembly at various time and length scales.

Silica “biomorphs” are one such model system. They form upon crystallization of alkaline-earth metal carbonates in silica-rich environments at high pH and display structural and morphological features strongly reminiscent of biominerals and other living forms – although no organic matter is involved in their formation. This contribution is meant to give an overview on the fascinating world of silica biomorphs and related structures. It is shown that the interplay of simplest components can lead to the spontaneous development of highly complex architectures if conditions are carefully controlled. A number of recent experimental observations shed light on the processes at work and suggest that dynamic reaction coupling drives self-assembly at the nanoscale, while even more peculiar mechanisms seem to govern the evolution of complex shapes at the micrometer level and beyond. Eventually, different approaches to benefit from the structural concept of silica biomorphs are highlighted along with possible implications for material science and early life detection.

### References

- [1] M. Kellermeier, H. Cölfen, J. M. Garcia-Ruiz, *Eur. J. Mineral.* 2012, 32, 5132.
- [2] J. Opel, M. Hecht, K. Rurack, J. Eiblmeier, W. Kunz, H. Cölfen, M. Kellermeier, *Nanoscale* 2015, 7, 17434.
- [3] J. Opel, F. P. Wimmer, M. Kellermeier, H. Cölfen, *Nanoscale Horizons* 2016, 1, 144.

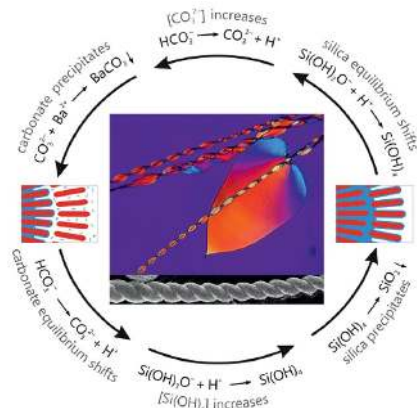


Figure 1.

**Keywords:** Biomorphs, biomimetic materials, crystallization, silica, carbonate

### MS14-O3 Biomimetic formation of calcite in intermixed gelatin/agarose hydrogels: Aggregate co-orientation and Mg content

Xiaofei Yin<sup>1</sup>, Fitriana Nindiyasari<sup>1</sup>, Erika Griesshaber<sup>1</sup>, Lurdes Fernández-Díaz<sup>2,3</sup>, Andreas Ziegler<sup>4</sup>, Wolfgang W. Schmahl<sup>1</sup>

1. Department für Geo- und Umweltwissenschaften, Ludwig-Maximilians-Universität, 80333 Munich, Germany
2. Departamento de Cristalografía y Mineralogía, Universidad Complutense de Madrid, 28040 Madrid, Spain
3. Instituto de Geociencias (UCM, CSIC). C/ José Antonio Novais 2, 28040 Madrid, Spain
4. Central Facility for Electron Microscopy, University of Ulm, 89069 Ulm, Germany

email: xiaofei.yin@campus.lmu.de

Crystal aggregation and orientation in carbonate biological hard tissues such as shells and teeth is organic matrix mediated, a structure consisting of membranes (1A, star) and fibrils (1A, arrow). The gel fibril network creates pores where local crystallization environments resemble those formed by extracellular, biological matrices. In previous studies we investigated in single gel systems the effect of agarose and gelatin on calcite nucleation and aggregate formation<sup>[1]</sup>. Gel was always occluded into the aggregate and imposed a marked effect on crystal co-orientation and aggregate formation. In Mg-free growth environments, either single crystals or radial aggregates with very few subunits formed. Was Mg added to the growth medium, the amount of internal boundaries increased as well as the number of subunits in the aggregate.

In this paper we discuss the effect on calcite nucleation, growth and aggregate formation of MIXED hydrogel systems. A very first attempt to use a mixture of hydrogels was conducted by Simon *et al.*<sup>[2]</sup>. In our experiments we use agarose/gelatin mixtures to crystallize  $\text{CaCO}_3$  using the double-diffusion method. Mineral microstructure and texture is determined with high-resolution EBSD, the occlusion of gels and characteristics of their distribution is visualized with an FE-SEM on microtome polished, etched and critical point dried sample surfaces. In gel/mineral composites grown in 1:1 agarose/gelatin hydrogels (1B), the hydrogel fabric is characterized by thick fibrils, a high variety of pore sizes and numerous walls. Hydrogels in gel/mineral composites grown in 2:1 agarose/gelatin gels (1C) are dense and consist of thick fibrils but also gel membranes (1C, stars and rectangles). When hydrogels with a 1:1 agarose:gelatin ratio are used (1B), calcite grows as hopper crystals bounded by terraced {104} faces. In an agarose:gelatin ratio of 2:1 used (1C), calcite crystals appear elongated along their *c*-axis and bounded by extremely terraced very rough and curved {104} surfaces that seem to correspond to steep rhombohedra. In both cases, crystals consist of rhombohedral sub-blocks (size < 1  $\mu\text{m}$ ) arranged in an approximately equal orientation. Differences in the occluded gel fabric are the consequence of hydrogel strength and crystallization pressure.

[1] F. Nindiyasari *et al.*, *Cryst. Growth Des.* **15**, 2667-2685, 2015

[2] P. Simon *et al.*, *Eur. J. Inorg. Chem.* **35**, 5370-5377, 2011

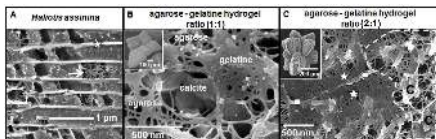


**Figure 1.** Characteristics of extracellular carbonate hard tissue (1A) and hydrogel (1B, 1C) matrices.

**Keywords:** EBSD, calcite-hydrogel aggregate, extracellular matrix, gelatin, agarose

## MS14-04 Polar ordering of macromolecular chains in biomimetic composite materials and natural tissues

Martin Sommer<sup>1</sup>, Matthias Burgener<sup>1</sup>, Hanane Aboulfadi<sup>1</sup>, Jürg Hulliger<sup>1</sup>

<sup>1</sup> Department of Chemistry and Biochemistry, University of Bern, Freiestrasse 3, CH-3012 Bern, Switzerland

email: martin.sommer@dcb.unibe.ch

The state of alignment of macromolecules in biomimetic materials and natural tissues will be discussed by investigating a mechanism of electrical polarity formation: An *in vitro* grown biomimetic fluorapatite (FAP)/gelatin composite is analyzed for its polar properties by second harmonic (SHGM) and scanning pyroelectric microscopy (SPEM). Growth media containing biological macromolecules do not only influence the morphology, but can also have a significant impact on the polarity of a composite [1]. Hexagonal prismatic seed crystals of FAP formed in gelatin represent a monodomain polar state due to aligned mineralized gelatin molecules [1]. Later growth stages, expressing a dumbbell morphology, develop into a bipolar state because of surface recognition by gelatin functionality.

Other inorganic materials like  $\text{CaCO}_3$  (calcite),  $\text{CaSO}_4$  and  $\text{CaC}_2\text{O}_4$  formed analogous composites when grown in a gelatin matrix. In addition, all of these composites revealed a similar behavior regarding polarity formation as compared to FAP. Subsequently the gelatin matrix was replaced by other gels, such as agar-agar and carrageenan, which developed the same kind of bipolar state. By growing the inorganic components in tetramethylorthosilicate (TMOS, nonpolar gel), SPEM experiments did not reveal any polarity. In all grown composites, the only present organic and polar material are the polar gel macromolecules. Single crystals of the investigated inorganic components, e.g. FAP and  $\text{CaCO}_3$ , are centrosymmetric. Therefore, the only possible origin of polarity in these biomimetic composites is due to the incorporated macromolecules.

Comparing SPEM data of natural hard tissues (teeth and bone) with biomimetic FAP/gelatin, calcite/gelatin and other investigated composites, a surprising analogy in view of growth-induced states of polarity is found: The development of polarity *in vivo* and *in vitro* can be explained by a Markov-type mechanism of molecular recognition during the attachment of macromolecules. Furthermore, SHGM was able to reveal the polar structure of tissues by the application of phase sensitive experiments and the use of a polar reference crystal [2].

[1] Burgener, M.; Putzeys, T.; Gasthi, M. P.; Busch, S.; Aboulfadi, H.; Wübbenhorst, M.; Kniep, R.; Hulliger, J. *Biomacromolecules* **2015**, 16, 2814-2819.

[2] Aboulfadi, H.; Hulliger, J. *J. Struct. Biol.* **2015**, 192, 67-75.

**Keywords:** polarity, polarity formation, biomimetic, composite materials, natural tissues

## MS14-O5 BioMOFs: are we getting alternative carriers for improved drug storage and release?

Silvia Quaresma<sup>1</sup>, Vânia André<sup>1,2</sup>, Teresa Duarte<sup>1</sup>

1. Centro de Química Estrutural, Instituto Superior Técnico, Universidade de Lisboa, Av. Rovisco Pais, 1049-001 Lisbon, Portugal

2. CICECO, Universidade de Aveiro, 3010-193 Aveiro, Portugal

email: [silvia.quaresma@tecnico.ulisboa.pt](mailto:silvia.quaresma@tecnico.ulisboa.pt)

We are engaged in a challenging project that proposes to synthesize new “bio-inspired” metal organic frameworks, BioMOFs, using safe metals and having active pharmaceutical ingredients (API) as linkers and/or guests. This is a new approach that has been proposed as a way to tackle the common drawbacks, such as low drug-storage capacity, too rapid delivery and high toxicity, presented in the traditional systems, used for controlled release of drugs, such as mesoporous silicas [1-4]. This type of compounds is traditionally synthesized by solvothermal methods, but in this project we are deeply engaged in using “green” techniques such as mechanochemistry.

In this work we will present results obtained with azelaic acid, a well-known API commonly used to treat skin disorders and flufenamic acid, a non-steroidal anti-inflammatory drug when using these as linkers in the network. The novel compounds are being characterized and we are strongly dependent on powder diffraction data (collected at the ESRF) for structure solution.

Muconic acid, a rigid and GRAS spacer, is one of the ligands that we are using to synthesize new BioMOFs having the API as guest. New compounds were successfully synthesized and characterized and we are now exploring the addition of a second GRAS ligand.

This is an on-going work using different synthetic and characterization approaches. However preliminary results are encouraging and may lead to very promising applications in the pharmaceutical field.

**Acknowledgements:** Authors acknowledge funding to Fundação para a Ciência e a Tecnologia (PEST-OE/QUI/UI0100/2013, RECI/QUE-QIN70189/2012, SFRH/BPD/78854/2011 and SFRH/BD/100024/2014).

1. P. Horcajada, et al, 2006. *Angew. Chem. Int. Ed.*, 45(36), 5974-5978

2. S. Keskin, et al, 2011. *Ind. Eng. Chem. Res.*, 50 (4), 1799-1812

3. A. C. McKinlay, et al, 2010. *Angew. Chem. Int. Ed.*, 49, 6260 – 6266

4. P. Horcajada, et al, 2012, *Chem. Rev.*, 112 (2), 1232-1268

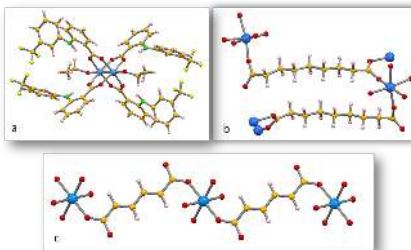


**Figure 1.** Molecular structure view of some new compounds obtained with: a) Flufenamic acid and Cu; b) Azelaic acid and Mg and c) Muconic acid and Mg

**Keywords:** BioMOFs, Drug delivery, azelaic acid, flufenamic acid, muconic acid

## MS15 Minerals and materials

Chairs: Frederic Hatert, Roland Nilica

### MS15-O1 How crystallography can assist process mineralogy – two metallurgical examples

Volker Kahlenberg<sup>1</sup>, Clivia Hejny<sup>1</sup>, Johan P.R. deVilliers<sup>2</sup>

1. University of Innsbruck, Institute of Mineralogy and Petrography
2. University of Pretoria, Department of Materials Science and Metallurgical Engineering

email: Volker.Kahlenberg@uibk.ac.at

Process mineralogy can be considered a special branch of applied mineralogy. It combines *processing* of minerals with traditional *mineralogical* knowledge in order to assist mineral exploration and to predict and optimize how the relevant ores can be best mined and processed. Process mineralogy is not only an indispensable tool for ore characterization but in also of vital importance for the design and tailoring of the whole manufacturing including refining of semi-finished products. A thorough understanding of the relevant reactions involved is a necessity not only from an engineering point of view but also to meet the constantly growing demands to reduce operational costs and to account for environmental aspects.

The production processes related to metallurgy are frequently based on complex high-temperature reactions which are far away from equilibrium. Analysis of the resulting multi-phase assemblages is usually also rather complex because they may depend not only temperature but on other parameters such as oxygen fugacity as well. In order to characterize the specific compounds completely and to understand their formation conditions and stabilities chemical analysis using microprobe techniques alone are frequently not sufficient and crystallographic information obtained from single-crystal or powder diffraction data can be of great help. Furthermore, crystallographic input can be used to do ab-initio calculation of thermodynamic properties of less-common compounds encountered.

In the present contribution two examples from an ongoing collaboration between the Universities in Innsbruck (Austria) and Pretoria (South Africa) will be presented. They are related to (i) iron-ore sintering involving so-called SFCA-phases as well as (ii) producing low carbon ferrochrome from chromite using aluminothermic reduction.

**Keywords:** process mineralogy, SFCA-phases, beta-alumina compounds

### MS15-O2 Crystal chemistry of layered Pb hydroxocarbonate minerals

Oleg I. Siidra<sup>1</sup>, Diana O. Zinyakhina<sup>1</sup>, Anatoly N. Zaitsev<sup>1</sup>, Rick Turner<sup>2</sup>, Mike Rumsey<sup>3</sup>, Igor V. Pekov<sup>4</sup>, Nikita V. Chukanov<sup>5</sup>, Sergey V. Krivovichev<sup>1</sup>, Erik Jonsson<sup>6</sup>

1. Saint-Petersburg State University
2. Imbuia Holdings
3. Natural History Museum
4. Moscow State University
5. Institute of Problems of Chemical Physics
6. Geological Survey of Sweden, Department of Mineral Resources

email: o.siidra@spbu.ru

Oleg Siidra, Diana Zinyakhina, Anatoly Zaitsev, Rick Turner, Mike Rumsey, Nikita Chukanov, Sergey Krivovichev, Igor Pekov, Erik Jonsson.

Pb carbonate minerals containing additional hydroxyl groups receive considerable attention due to their importance to the environment. These phases widely form as lead corrosion technological products. Majority of Pb hydroxocarbonates demonstrate layered structural architectures and include: hydrocerussite, plumbonacrite and recently discovered grootfonteinite, abellaite and  $\text{NaPb}_3(\text{OH})_3(\text{CO}_3)_4$  mineral phase from Lavrion slags. There were several reports on hydrocerussite physical properties and chemistry previously (e.g. Anthony *et al.*, 2003; Olby, 1966). Structural data on powdery synthetic samples of  $2\text{PbCO}_3 \cdot \text{Pb}(\text{OH})_2$  were reported in Marinetto *et al.*, 2002. However single-crystal X-ray data for natural samples of layered Pb hydroxocarbonates were unavailable till very recent time. We have worked with many samples of "hydrocerussite" from several localities within our ongoing projects on  $\text{Pb}^{2+}$  oxysalts crystal chemistry: Merehead quarry, England; Långban, Sweden; Lavrion, Greece; Kombat, Namibia. Structural studies allowed identification of grootfonteinite from Kombat and unknown yet as a mineral  $\text{NaPb}_3(\text{OH})_3(\text{CO}_3)_4$  from Lavrion slags. Several different polytypes for hydrocerussites from Merehead were also identified. Each of above mentioned Pb hydroxocarbonates demonstrates unique but related structure type, which in turn can be transformed via various mechanisms one to each other.

This work was supported by St. Petersburg State University through the internal grant 3.38.238.2015 and RFBR 15-35-20632.

**Keywords:** lead, carbonates, minerals, layered materials, oxysalts

**MS15-03** Phase diagrams of  
 $\text{Ba}_2\text{M}^{2+}\text{Te}^{6+}\text{O}_6$ : insight into the interplay  
 between crystal structure and magnetic  
 dimensionality

Alexandra S. Gibbs<sup>1,2,3</sup>, Kevin S. Knight<sup>1</sup>, Paul J. Saines<sup>4,5</sup>, James R. Hester<sup>6</sup>, Hidenori Takagi<sup>2,3,7</sup>

1. ISIS Pulsed Neutron and Muon Source, Rutherford Appleton Laboratory, Harwell Oxford, Didcot, OX11 0QX, United Kingdom
2. Department of Physics, The University of Tokyo, Hongo 7-3-1, Bunkyo-ku, Tokyo, 113-0033 Japan
3. Max Planck Institute for Solid State Research, Heisenbergstrasse 1, 70569 Stuttgart, Germany
4. School of Physical Sciences, University of Kent, Canterbury, CT2 7NH, United Kingdom
5. Department of Chemistry, University of Oxford, Inorganic Chemistry Laboratory, South Parks Road, Oxford OX1 3QR, United Kingdom
6. Bragg Institute, ANSTO, Locked Bag 2001, Kirrawee DC, NSW 2232, Australia
7. Institute for Functional Materials and Quantum Technologies, University of Stuttgart, Pfaffenwaldring 57, 70569 Stuttgart, Germany

email: alexandra.gibbs@stfc.ac.uk

$\text{Ba}_2\text{M}^{2+}\text{Te}^{6+}\text{O}_6$  ( $\text{M}^{2+}=\text{Ni}, \text{Cu}, \text{Zn}$ ) adopt structures composed of triplets of face-sharing  $\text{TeO}_6$  and  $\text{MO}_6$  octahedra linked by corner-sharing  $\text{TeO}_6$  octahedra [1,2]. This leads to a crystal structure composed of 1D chains along the *c*-axis and a 2D network in the *ab*-plane. We will present detailed high resolution neutron diffraction studies of the thermal phase diagrams of all three compounds, focusing on the relationship between crystal structure and magnetic dimensionality in this family.

At ambient temperature,  $\text{Ba}_2\text{NiTeO}_6$  and  $\text{Ba}_2\text{ZnTeO}_6$  crystallise in space group  $R\bar{3}m$  whilst  $\text{Ba}_2\text{CuTeO}_6$  has a distorted monoclinic  $C2/m$  structure (Figure 1).  $\text{Ba}_2\text{CuTeO}_6$  and  $\text{Ba}_2\text{NiTeO}_6$  display clear differences in magnetic dimensionality.  $\text{Ba}_2\text{NiTeO}_6$  is a strongly frustrated antiferromagnet with  $T_N=8.5$  K [3].  $\text{Ba}_2\text{CuTeO}_6$ , on the other hand, shows quasi-1D two-leg  $S=1/2$  spin ladder behaviour above  $T\sim 25$  K followed by 'marginal' magnetic ordering at  $T^{\text{mag}}=16$  K. Our previous work implies that the system is in close proximity to a quantum critical point induced by inter-ladder coupling [2].

It could be easily assumed that the different crystal structure of  $\text{Ba}_2\text{CuTeO}_6$  compared to  $\text{Ba}_2\text{NiTeO}_6$  and nonmagnetic  $\text{Ba}_2\text{ZnTeO}_6$  at ambient temperature is related to the Jahn-Teller effect of the  $\text{Cu}^{2+}$  ion. However, using high-resolution neutron diffraction the phase diagrams of the three compounds have been mapped by us and reveal a more complex and interesting picture [3]. The phase diagram of  $\text{Ba}_2\text{CuTeO}_6$  reveals a high-temperature Jahn-Teller transition and unexpected low-temperature monoclinic-to-triclinic transition undetectable by specific heat measurements.  $\text{Ba}_2\text{NiTeO}_6$  shows no structural phase transitions down to  $T=1.8$  K whereas in  $\text{Ba}_2\text{ZnTeO}_6$  a transition to  $C2/m$  below  $T\sim 165$  K is found. The discovery of an intrinsic structural instability towards the  $C2/m$  phase displayed by Jahn-Teller inactive  $\text{Ba}_2\text{ZnTeO}_6$  (but not by  $\text{Ba}_2\text{NiTeO}_6$ ) requires a re-examination of the interplay between crystal structure, Jahn-Teller distortions and magnetic dimensionality in these compounds opening up a new route to understanding the exotic magnetism present in this family.

[1] P. Köhl and D. Reinen, Z. Anorg. Allg. Chem 409, 257-352 (1974).

[2] A. S. Gibbs, A. Yamamoto, A. N. Yaresko, K. S. Knight, H. Yasuoka, M. Majumder, M. Baenitz, P. J. Saines, J. R. Hester, D. Hashizume, A. Kondo, K. Kindo and H. Takagi, arXiv:1511.01477 (2015).

[3] A. S. Gibbs, K. S. Knight, P.J. Saines, J. R. Hester and H. Takagi, to be submitted.

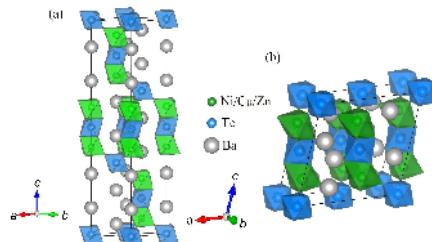


**Figure 1.** The room temperature structures of (a)  $\text{Ba}_2\text{NiTeO}_6$  and  $\text{Ba}_2\text{ZnTeO}_6$  and (b)  $\text{Ba}_2\text{CuTeO}_6$ .

**Keywords:** transition metal oxides, phase transitions, neutron diffraction, magnetism

# MS15-04 Crystal structure and polymorphism of NaSrVO<sub>4</sub>: the first A<sup>I</sup>B<sup>II</sup>X<sup>V</sup>O<sub>4</sub> larnite related structure from X-ray powder data

Gwilherm Nenert<sup>1</sup>

1. PANalytical B. V., Lelyweg 1, 7602 EA Almelo, The Netherlands

email: gwilherm.nenert@panalytical.com

The crystal chemistry of A<sup>I</sup>B<sup>II</sup>XO<sub>4</sub> (A<sup>I</sup> = alkali ion, B<sup>II</sup> = alkali-earth ion, X = P, V, As) is very rich and leads to numerous polymorphic phases which belong to 8 different structures types: olivine, arcanite, glaserite, tridymite, α-K<sub>2</sub>SO<sub>4</sub>, β-Na<sub>2</sub>SO<sub>4</sub> and γ-Na<sub>2</sub>SO<sub>4</sub> [1]. Among the various families (X = P, V, As), the phosphates have been the most widely investigated. Besides the purely interest from a crystal chemistry point of view, the research activities related to this family of materials is driven mainly due to their ferroelectric and ferroelastic properties and possible applications as phosphors for LEDs [1,2].

Within the rich crystal chemistry of this family, no structural data have demonstrated the occurrence of the larnite/belite structure [3]. The larnite/belite structure has been widely investigated due to its importance for Portland cement and its rich polymorphism [4]. All the materials related to the larnite structural type have the general formula A<sup>I</sup>B<sup>II</sup>X<sup>IV</sup>O<sub>4</sub> (A, B = Ca, Sr, Eu; Ba; X = Si, Ge, Ti) [4]. Upon doping on the A, B and X sites, some alkaline ions can be incorporated into the structure giving rise to belite [5] and flamite [6].

NaSrVO<sub>4</sub> has been mentioned in the past but with conflicting results and without providing any structural model [3, 7]. These contradicting results and the absence of report on the crystal structure motivated us to reinvestigate this material. We present here its crystal structure, as determined and refined from laboratory powder X-ray diffraction data. This is the first crystal structure reported among the larnite/belite structural type exhibiting the chemistry A<sup>I</sup>B<sup>II</sup>X<sup>V</sup>O<sub>4</sub>. Similarly to other larnite structures, we observe a rich polymorphism in the temperature range 25 – 900°C and we report one polymorph which was not previously reported in the larnite family.

- [1] V. A. Isupov, *Ferroelectrics*, **2002** 274:1, 203-283.
- [2] S. Choi, *et al.* *Optical Letters*, **2013** 38, 1346-1348.
- [3] S. Drai, *et al.*, **1974**. *Journal of Solid State Chemistry*, **10**, 95-101
- [4] H. F. W. Taylor, **1990** *Cement Chemistry*, Academic Press.
- [5] M. Catti, *et al.* **1983**. *Acta Crystallogr., Sect. B: Struct. Sci.*, **39**, 674-679; S. Deganello, **1973**. *Acta Cryst. B* **29**, 2593-2597; J. Felsche **1971**. *Die Naturwissenschaften*, **58**, 218-219; C. M. Midgley **1952**. *Acta Cryst.* **5**, 307-312.
- [6] F. Gfeller, *et al.* **2015**. *European Journal of Mineralogy* **27**, 755-769.
- [7] R. Klement, P. Kresse **1961**. *Zeitschrift für anorganische und allgemeine Chemie*, **310**, 53-68.

**Keywords:** larnite, belite, vanadate, powder diffraction, NaSrVO<sub>4</sub>

# MS15-05 Ordering phenomena in minerals: the Verwey phase of natural magnetite

Giuditta Perversi<sup>1</sup>, James C. Cumby<sup>1</sup>, Elise Pachoud<sup>1</sup>, Jon P. Wright<sup>2</sup>, J. Paul Attfield<sup>1</sup>1. Centre for Science at Extreme Conditions and School of Chemistry, University of Edinburgh, United Kingdom  
2. European Synchrotron Radiation Facility, France

email: g.perversi@sms.ed.ac.uk

Transition metal oxides can feature mixed valence cations, spin ordering and direct interactions between *d*-orbitals. This makes them intrinsically susceptible to the formation of atomic clusters with direct metal-metal interactions (*orbital molecules*).

The most significant example of orbital molecule behaviour is in the Verwey phase of magnetite (Fe<sub>3</sub>O<sub>4</sub>). Cooling magnetite below ~125 K causes remarkable changes to its conductivity, magnetisation and heat capacity; this is called the Verwey transition, commonly used for detection and quantification of magnetite in minerals. The transition is also accompanied by a structural change, whose specifics were only determined in 2012: the *Fd-3m* high-temperature structure distorts to a monoclinic *Cc* supercell; the change of physical properties is due to a cooperative bond distortion that brings together three neighbouring Fe sites in a linear Fe<sup>3+</sup>-Fe<sup>2+</sup>-Fe<sup>3+</sup> arrangement, delocalizing the extra electron provided by Fe<sup>2+</sup>. This bonded cluster is a three-atom orbital molecule, called a '*trimeron*' (Fig.1). [1] The trimeron formation is one of the most complex electronically ordered ground states known, and as such is notoriously susceptible to the effects of non-stoichiometry, through both oxidation effects and cation substitution. [2]

We investigated the low-temperature behaviour of a sample of natural magnetite from Ouro Preto, Brazil, crushed to provide a microcrystal of 60 × 50 × 25 μm from the bulk of the rock. Electron Probe Microanalysis showed a relatively low dopant content (< 0.5% total impurities, mainly Al and Si). SQUID magnetization measurements identified a lowering of the transition temperature to T<sub>v</sub> = 119 K. The structural transition was studied with single crystal synchrotron XRD at the ESRF, and we were able to apply the established trimeron model to the data, with some relevant variations that show us an influence of the stoichiometry also on the structural arrangement.

On this basis, we claim evidence of long-range electronic order as a natural occurrence in the magnetite system. Therefore, we suggest that the Verwey transition may contribute to geophysical processes in rocky bodies that can easily cycle above and below ~125 K (i.e.: meteorites, iron-rich planets, etc.). [3]

**References:** [1] M.S. Senn, J.P. Wright and J.P. Attfield, *Nature* **481**, 173 (2012); [2] J. M. Honig, *J Alloy Compd* **229**, 24 (1995); [3] G. Perversi, J. Cumby, E. Pachoud, J. P. Wright and J.P. Attfield, *Chem. Comm.* **52**, 4864 (2016)



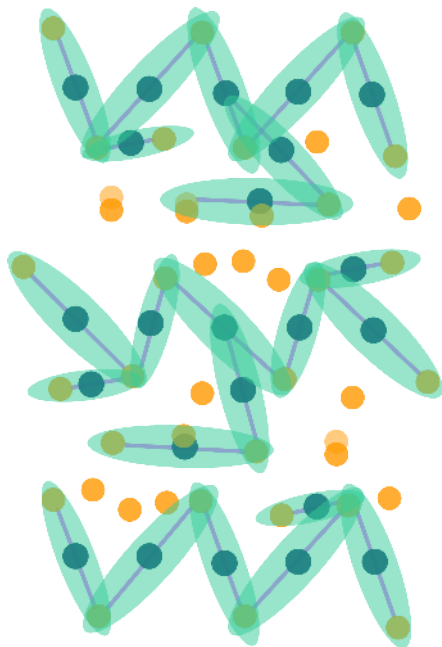


**Figure 1.** Trimeron arrangement in the low-temperature *Cc* structure. Fe<sup>2+</sup> in blue, Fe<sup>3+</sup> in yellow, delocalization region is indicated in green. Only octahedral cations are displayed.

**Keywords:** Single crystal XRD, low-temperature, phase transition, Verwey transition, ordering, distortions, minerals, magnetite

## MS16 Structure-property relationships in high pressure crystallography

Chairs: Andrzej Grzechnik, Paul Attfield

### MS16-O1 The large-volume press at ID06 of the ESRF for structure-properties research at extreme conditions

Wilson Crichton<sup>1</sup>

1. ESRF

email: [crichton@esrf.fr](mailto:crichton@esrf.fr)

Here we highlight, using examples from our in-house and User repertoire, the opportunities for research into the structures, phase transitions, stabilities and properties of materials under extreme conditions. We draw on a range of samples – both powder and single-crystal – and scientific domains to illustrate our talk. We will describe the various modes of operation of the press and the detection system: from 1- and 2-stage compressions with continuous data collections for phase diagram mapping, for estimation of equations of state, for high through-put reconnaissance studies to deformation studies for the collection of the mechanical response of materials under high strain. Highlights of ancillary measurements that augment the information available from diffraction and imaging alone; e.g. ultrasonics will also be commented on.

**Keywords:** high-pressure, powder diffraction, structures, phase diagrams, materials



**MS16-O2** New chemistry of hydrogen-rich systems uncovered with the help of extreme conditionsYaroslav Filinchuk<sup>1</sup>

1. Université Catholique de Louvain

email: Yaroslav.Filinchuk@uclouvain.be

The demand for materials with high energy density has shifted the research focus from metal hydrides to much lighter systems based on *p*-elements bound to hydrogen atoms. First seen as merely ionic salts, light complex hydrides based on Al, B and N soon revealed complicated structural chemistry driven by directional interaction between metal cations and complex hydride anions [1]. For example, an unexpected outcome of the directional metal-borohydride interaction are the porous [2, 3] and dense [2, 4, 5] frameworks containing less electropositive Mg and Mn, where the BH<sub>4</sub> units serve as linear linkers.

The dense phases with high volumetric hydrogen density can be obtained by relatively modest hydrostatic pressure. Already at pressures of 1 GPa, achievable in laboratory steel dies, the amorphous Mg(BH<sub>4</sub>)<sub>2</sub> can be synthesized, as well as the dense form of Mn(BH<sub>4</sub>)<sub>2</sub>. Both phases can be quenched to ambient pressure. The search for the complex order of the BH<sub>4</sub> anions, studied for the first time with neutron powder diffraction under high pressures, will be presented.

The porous hydride phases show remarkable capacity for the loading of guest molecules. In particular, condensation of the molecular hydrogen in the porous γ-Mg(BH<sub>4</sub>)<sub>2</sub> leads to twice as high hydrogen density in the pores as in the liquid hydrogen, making it the highest local hydrogen density achieved so far in a porous system.

Finally, I would like to draw the attention to the recent developments in the reactive ball milling followed simultaneously by X-ray powder diffraction. This technique allows for *in situ* monitoring the mechano-chemical reactions, including formation of high-pressure phases. Our recent developments (see also the dedicated contribution [6]), involving 3D printing of milling jars, are aiming to improve the data quality for the needs of structure solution.

[1] Rude L.H. et al. *Phys. Stat. Sol. A*, **2011**, 208, 1754.  
[2] Filinchuk Y. et al. *Angew. Chem. Int. Ed.*, **2011**, 50, 11162. [3] Richter B. et al. *Dalton Trans.*, **2015**, 44, 3988. [4] Ban V. et al. *J. Phys. Chem. C*, **2014**, 118, 40, 23402. [5] Tumanov N. et al. *Chem. Mater.*, **2016**, 28, 274. [6] Ban V., Tumanov N., Sadikin Y., Filinchuk Y., Černý R., Casati N. Last advances in *in situ* monitoring of mechanochemical reactions by X-ray diffraction // ECM 30, Basel, 28 Aug. - 1 Sep. **2016**.

**Keywords:** hydrides, extreme conditions, new materials, porous and dense

**MS16-O3** New coordination chemistry and properties revealed by high pressure crystallographyAlexander J. Blake<sup>1</sup>, Jeremiah P. Tidey<sup>1</sup>, Alice E. O'Connor<sup>1</sup>, Jonathon McMaster<sup>1,2</sup>, Martin Schröder<sup>1,2</sup>, David R. Allan<sup>3</sup>

1. University of Nottingham

2. University of Manchester

3. Diamond Light Source

email: a.j.blake@nottingham.ac.uk

The results of our initial experiments in high pressure crystallography provided vital signposts for our subsequent studies, leading to the discovery of unusual and usually unpredicted phenomena. The coordination compounds we have studied under pressure include macrocyclic complexes of thioether [1–3] and oxathioether [4, 5] ligands, cyclometallated Pt(II) complexes, gold complexes [7] and extended polyiodides.

For example, we studied the salt [Ag([18]aneS<sub>6</sub>)]I<sub>7</sub> which is known to adopt a highly unusual and visually striking structure [8] – see Figure 1. The complex cation templates the formation of a distorted cubic cage consisting of iodine molecules (I<sub>2</sub>) and iodide ions (I<sup>−</sup>). The iodines and iodides form an extended polymeric matrix in which the cations reside. In response to moderate pressure, [Ag([18]aneS<sub>6</sub>)]I<sub>7</sub> undergoes a distinct phase change involving desymmetrisation of the cubic cage and the evolution of a discrete I<sub>3</sub><sup>−</sup> anion. The resulting phase is stable over the pressure range 11–36 kbar.

This contribution will describe how pressure can effect significant changes to coordination complexes, including to their structures, conformations, spectroscopic properties and degrees of association.

## References

1. D. R. Allan, A. J. Blake, D. Huang, T. J. Prior, M. Schröder, *Chem. Commun.* 2006, 4081.
2. D. R. Allan, D. Bailey, N. Bird, A. J. Blake, N. R. Champness, D. Huang, C. P. Keane, J. McMaster, T. J. Prior, J. P. Tidey, M. Schröder, *Acta Crystallogr., Sect. B* 2014, **70**, 469.
3. H. L. S. Wong, D. R. Allan, N. R. Champness, J. McMaster, M. Schröder, A. J. Blake, *Angew. Chem. Int. Ed.* 2013, **52**, 5093.
4. J. P. Tidey, A. E. O'Connor, A. Markevich, E. Bichoutskaia, J. J. P. Cavan, G. A. Lawrance, H. L. S. Wong, J. McMaster, M. Schröder, A. J. Blake, *Cryst. Growth Des.* 2015, **15**, 115.
5. J. P. Tidey, H. L. S. Wong, J. McMaster, M. Schröder, A. J. Blake, *Acta Crystallogr., Sect. B*, 2016, submitted.
6. J. P. Tidey, H. L. S. Wong, M. Schröder, A. J. Blake, *Coord. Chem. Rev.* 2014, **277–278**, 187.
7. A. E. O'Connor, T. L. Easun, N. Mirzadeh, S. K. Bhargava, M. Schröder, A. J. Blake, *ChemComm* 2016, DOI: 10.1039/C6CC00923A.
8. A. J. Blake, R. O. Gould, S. Parsons, C. Radek, M. Schröder, *Angew. Chem. Int. Ed. Engl.* 1995, **34**, 2374.

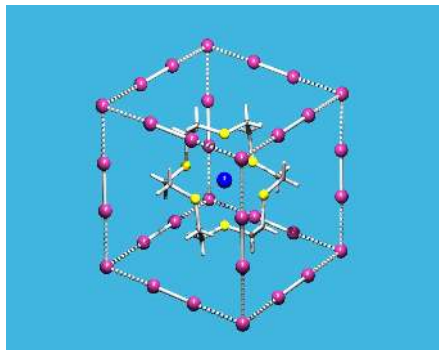


**Figure 1.** The complex cation in  $[\text{Ag}(\text{I}8\text{aneS})]\text{I}_2$  templates the formation of a distorted cube comprising iodine molecules and iodide ions.

**Keywords:** pressure dependence, spectroscopic properties, geometric distortion, conformation, disorder

## MS16-O4 Pressure-Tuning of Guest Species and Magnetic Response in Mn- and Fe-based Formate Frameworks

Scott C. McKellar<sup>1</sup>, Christopher H. Woodall<sup>2</sup>, Michael R. Probert<sup>3</sup>, Gavin A. Craig<sup>4</sup>, Konstantin V. Kamanov<sup>2</sup>, Mark Murrie<sup>4</sup>, Euan K. Brechin<sup>1</sup>, Stephen A. Moggach<sup>1</sup>, Simon Parsons<sup>1</sup>

1. EaStCHEM School of Chemistry and the Centre for Science at Extreme Conditions, University of Edinburgh, Edinburgh, UK

2. Centre for Science at Extreme Conditions, University of Edinburgh, Edinburgh, UK

3. School of Chemistry, Newcastle University, Newcastle-upon-Tyne, UK

4. WestCHEM, School of Chemistry, University of Glasgow, Glasgow, UK

email: scott.mckellar@ed.ac.uk

The synthesis of a microporous solid that behaves as a magnet at room temperature remains an open challenge. The combination of magnetism and porosity has recently become a hot topic, as reflected in an increasing number of studies.<sup>1</sup> Porosity provides a means for tuning magnetic properties in functional materials where the long range ordering temperature (ferro- or antiferromagnetic) can be varied depending on the metal-ligand exchange and guest content. Metal formates ( $[\text{M}_3(\text{HCOO})_6](\text{G})$ ;  $\text{M}(\text{II}) = \text{Mn, Fe, Co, Ni}$ ,  $\text{G} = \text{guest}$ ) are a family of metal-organic frameworks (MOFs) which display permanent porosity and guest-dependent magnetic properties.<sup>2</sup> For example, exchange between various small organic guest molecules causes the critical ordering temperature ( $T_c$ ) to vary between 4.8 and 9.7 K for  $[\text{Mn}_3(\text{HCOO})_6]$  and 15.6 to 20.7 K for  $[\text{Fe}_3(\text{HCOO})_6]$ .

The ability to enhance  $T_c$  is desirable in order for materials to be applicable in real-world applications. One approach to structure and magnetic property modification is through the application of high pressure. Here, in the first study of a porous magnetic material to resolve both structural and magnetic changes, we have performed a combined high-pressure single-crystal X-ray diffraction (XRD) and high-pressure SQUID magnetometry investigation of  $[\text{Mn}_3(\text{HCOO})_6]$  and  $[\text{Fe}_3(\text{HCOO})_6]$ . Upon application of pressures  $<20$  kbar to  $[\text{Mn}_3(\text{HCOO})_6]$  and  $[\text{Fe}_3(\text{HCOO})_6]$ , we have observed large changes around the metal coordination spheres, which cause an increase in  $T_c$ , dependent on the guest species. By using different solvents (methanol/water, tetrahydrofuran, pentane/isopentane, Fluorinert FC70) as pressure-transmitting liquids, the structural and magnetic response can be correlated not only to the type of metal but to the nature and quantity of guest present in the framework pores. The variation in  $T_c$  is caused in part by twisting of the M-O-M angles of the host framework: materials with larger guests induce larger M-O-M angles and a lower  $T_c$  under ambient conditions, but this changes with the application of pressure, depending on the pressure-transmitting liquid. Since metal-metal or metal-ligand distances or the bridging group geometry are all sensitive to pressure, this is an extremely effective method for investigating magneto-structural correlations.

[1]Kurmo0(2009)Chem. Soc. Rev.,38,1353.

[2]Wang et al.(2007)Polyhedron,26,2207

**Keywords:** high-pressure crystallography, metal-organic framework, magnetism

## MS16-O5 Structural basis for sensitivity to molecular oxygen of oxidases and fluorescent proteins investigated by high pressure crystallography

Bénédicte Lafumat<sup>1</sup>, Eve de Rosny<sup>2</sup>, Peter Van der Linden<sup>1</sup>, Philippe Carpentier<sup>1</sup>, Antoine Royant<sup>1,2</sup>, Gordon Leonard<sup>1</sup>

1. European Synchrotron Radiation Facility (ESRF)

2. Institut de Biologie Structurale (IBS)

email: benedicte.lafumat@esrf.fr

Molecular oxygen plays a key role in many fundamental biological processes. Investigations of oxygen-dependent proteins require determining O<sub>2</sub> binding sites, diffusion routes to active sites and reaction mechanisms. The position and traffic of dioxygen cannot always be reliably decipher by using oxygen mimic, as halide ions, in high resolution X-ray crystal structures. Protein high pressure crystallography allows exploring dynamics and conformational sub-states of proteins but additionally enable the direct population and determination of oxygen molecule positions in biological macromolecules at high resolution [1]. In this work, specific pressure cells have been designed to cryo-cool protein crystals under Helium, Oxygen or Krypton pressure [2]. The enzymes Urate oxydase (UOX) and Glucose oxidase (GOx), and a representative series of FPs comprising the photosensitizer Killerred have been crystallized, pressurized and cryo-cooled using the O<sub>2</sub>, He and Kr pressure-cells. The GOx present a fundamental bactericide role in natural process by generating hydrogen peroxide and additionally is widely used in food and pharmaceutical industries as major component of glucose biosensors and biofuel cells. Killerred is a Reactive Oxygen Species (ROS) generating fluorescent protein which is proposed for fundamental biomedical and biotechnological applications, such as for cancer photodynamic therapy. X-ray crystallography together with in-crystallo UV-visible spectroscopy and Raman spectroscopy as complementary techniques, allow us to propose a comprehensive molecular redox mechanisms for the GOx [3]. In addition, our data reveal new insights into the mechanism that is responsible for the ROS generation by the fluorescent protein KillerRed that explain its photosensitization properties.

[1] Collins et al (2011) Annual Review of Biophysics. **40**, 81-98; [2] Van der Linden et al (2014) J. Appl. Cryst. **47**, 584-92; [3] Kommoju et al (2011) Biochemistry. **50**(24), 5521-34; [4] Carpentier et al (2012) J. Am. Chem. Soc. **134**, 18015-21

**Keywords:** Oxidases, Fluorescent proteins, High pressure crystallography, Molecular oxygen

## MS17 Minerals, materials and polymorphs

Chairs: Håkon Hope, Elisa Nauha

### MS17-O1 Understanding the polymorphic phase transitions of linear amino acids using in situ characterisation

Mireille Smets<sup>1</sup>, Sander Brugman<sup>1</sup>, Ernst van Eck<sup>1</sup>, Joost van den Ende<sup>1</sup>, Hugo Meekes<sup>1</sup>, Elias Vlieg<sup>1</sup>, Herma Cuppen<sup>1</sup>

1. Institute for Molecules and Materials, Radboud University, Heyendaalseweg 135, 6525 AJ Nijmegen, The Netherlands

email: m.smets@science.ru.nl

Polymorphism is a common phenomenon for molecular crystals. Here we aim to understand the mechanisms involved in transitions between polymorphic forms in the solid state. Ultimately, the understanding will allow for the control of polymorphic forms by promoting or inhibiting transitions, which is important for prolonging the shelf life of polymorphic forms of active pharmaceutical ingredients (API). The established classification of phase transitions cannot explain several phenomena in molecular systems, such as cooperative motion<sup>1</sup>. This mechanism has been inferred to explain thermosolient behaviour<sup>2</sup>. I will present the *in-situ* characterisation of the reversible  $\alpha$ - $\beta$  and  $\alpha$ - $\gamma$  phase transitions of DL-norleucine (NLE) and the  $\alpha$ - $\beta$  transition of DL-methionine (MET). Although all polymorphs involved have been reported in the literature, little is known about the *transition* between the structures. I will show that the transition behaviour in these linear amino acids can be explained by cooperative motion.

NLE is an amino acid with three known polymorphic forms, which consist of zwitterionic H-bonded bilayers. The three monoclinic structures differ in the stacking of the bilayers ( $\beta \leftrightarrow \alpha$ ,  $\alpha \leftrightarrow \gamma$ ) and in the conformation of the molecules ( $\alpha \leftrightarrow \gamma$ )<sup>3</sup>. MET has two known polymorphic forms ( $\beta$  &  $\alpha$ ) with different bilayer stacking and different conformations<sup>4</sup>.

We studied the transitions using complementary *in situ* techniques (DSC, SCXRD, solid-state NMR, polarisation microscopy) to get a full picture of the phase transitions. Especially solid-state NMR proved to be a powerful technique, due to its sensitivity to changes in the environment of atoms. The  $\alpha$ - $\gamma$  phase transition of NLE behaves as a typical first order phase transition with the nucleation and growth mechanism. The  $\alpha$ - $\beta$  phase transition of NLE is difficult to observe and occurs very irregularly. It shows coexistence and a large dependence on crystal quality and defect density that suggests cooperative motion<sup>5</sup>. This is in agreement with molecular dynamics simulations<sup>6</sup>. The  $\alpha$ - $\beta$  transition of MET shows intermediate behaviour and is consistent with kinetic hindrance.

- 1.Brandel *et al*, *Chem. Mat.* **27**,6360-6373 (2015).
- 2.Naumov *et al*, *Chem. Rev.* **115**,12440-12490 (2015).
- 3.Coles *et al*, *Cryst. Growth & Des.* **9**,4610-4612 (2009).
- 4.Göribitz *et al*, *Acta Cryst E*, **70**,337-340 (2014), *Acta Cryst E*, **71**,o398-o399 (2015).
- 5.Smets *et al*, *Cryst. Growth Des.* **15**,5157-5167 (2015).
- 6.Van den Ende, Smets, *et al*, *Faraday Discuss.* **179**,421-436 (2015).

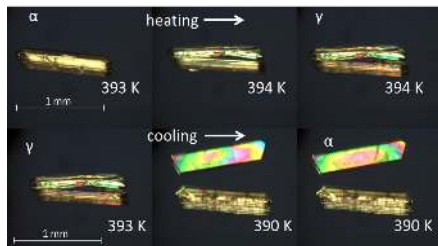


**Figure 1.** Thermal stage polarisation microscopy snapshots of a single crystal of DL-norleucine at different temperatures during the  $\alpha \leftrightarrow \gamma$  transition. During the transition, the crystal delaminates because of the anisotropic lattice expansion.

**Keywords:** solid-state phase transitions, polymorphism, amino acids, in situ characterisation

## MS17-O2 Structural studies of M-type ferrites used as template layers for the growth of oriented Y-type ferrites through chemical solution deposition method

Radomir Kuzel<sup>1</sup>, Josef Bursík<sup>2</sup>, Dorota Pulmannová<sup>2</sup>, Robert Uhrecký<sup>2</sup>, Milan Dopita<sup>1</sup>

1. Charles University in Prague, Faculty of Mathematics and Physics, Ke Karlovu 5, Praha 2, Czech Republic
2. Institute of Inorganic Chemistry, Czech Academy of Sciences, Rez near Prague, Czech Republic

email: kuzel@karlov.mff.cuni.cz

Thin films of trigonal  $\text{Ba}_2\text{Zn}_2\text{Fe}_{12}\text{O}_{22}$  (Y-type) ferrite were prepared by the chemical solution deposition using  $\text{SrTiO}_3(111)$  substrates covered with hexagonal magnetoplumbite (M-Type) seed layers. Seven M phases with different chemical composition, magnetic character and lattice misfit (-0.8 % to -7.0 %) values were investigated in their use as template and buffer layers. The films were studied by X-ray diffraction, atomic force microscopy and electron back-scatter diffraction. X-ray diffraction analysis in parallel beam setup with Eulerian cradle was concentrated on the precise determination of lattice parameters, studies of preferred orientation by symmetric and asymmetric scans ( $\omega$  and  $\chi$ ) and studies of possible stresses for all the layers by measurement of reflections at different inclinations  $\chi$  and  $\psi$ . For this, correct reference values of lattice parameters are required in particular for non-cubic phases. For most of the phases tested, the values are either completely missing in PDF4+ database or often a number of values can be found there for a single phase. Therefore some data analysis of PDF4+ with respect to the statistics and/or also to the stoichiometry was performed.

For all the seed layers strong out-of-plane (0001) orientation of M- and Y-films was observed but with somewhat different degree. The in-plane orientation depended on misfit between the M-interlayer and substrate and also M-interlayer and the top Y-film. The optimum growth was reached using  $\text{SrTiO}_3(111)/(\text{BaSr})(\text{GaAl})_{12}\text{O}_{19}$ ,  $\text{SrTiO}_3(111)/\text{Ba}(\text{FeAl})_{12}\text{O}_{19}$  and  $\text{SrTiO}_3(111)/\text{SrGa}_{12}\text{O}_{19}$  substrate/seed layer architectures. In general, the best results were achieved when the misfit values between the seed layer and substrate, and between the seed layer and top Y-layer are approximately equal and when the surface of seed layers are formed by hexagons. Then single domain perfect hexagon-on-hexagon orientation was observed for M-film. For Y-layer also the in-plane orientation  $(001)_Y \parallel (111)_{\text{STO}}$  and  $[100]_Y \parallel \text{STO}$  was observed but six maxima detected in  $\chi$ -scans instead of three confirmed in-plane obverse/reverse twinning. The results demonstrated the possibilities of the intelligent material design (namely anisotropy manipulation) for this important class of magnetic materials by proper design of key constituents: lattice misfits and surface topography of seeding structures.

**Keywords:** powder diffraction, oriented thin films, preferred orientation

## MS17-03 Pore Shape Determination in Mesoporous Ordered Silica Films

Gerhard Popovski<sup>1</sup>, Roland Morak<sup>1</sup>, Parvin Sharifi<sup>2</sup>, Heinz Amenitsch<sup>3</sup>, Oskar Paris<sup>1</sup>

1. Montanuniversitaet Leoben
2. Max-Planck-Institut fuer Kohlenforschung,
3. Graz University of Technology

email: gerhard.popovski@unileoben.ac.at

Mesoporous materials are often templated by organic materials that give a scaffold for precursor molecules. The organic material is removed by a calcination step, which leads to shrinkage of the whole structure. In the case of thin films the shrinkage is largely inhibited in two dimensions leading to a uniaxial deformation of pore lattice and of the pores themselves.

Grating incidence small angle x-ray scattering (GISAXS) of ordered mesoporous films show well-defined Bragg peaks. The deformation of the lattice can be determined from the positions of the Bragg-peaks after correction for reflection and refraction effects at the film interfaces. The intensities of the peaks can be corrected for geometric effects, i.e. the rotational symmetry around the surface normal and the curvature of the Ewald-sphere intersecting the peaks at different positions in reciprocal space. It is then possible to approximate the corrected peak intensities by a model for elliptically shaped cross sections of the pores. The pores are found to be deformed similar to the lattice. Pores and lattice are slightly more deformed in spin coated films than in dip-coated ones.

**Keywords:** mesoporous films, GISAXS

## MS17-04 Control of porosity through temperature and pressure

Jan A. Gertenbach<sup>1</sup>, Simon A. Herbert<sup>2</sup>, Tia Jacobs<sup>2</sup>, Agnieszka Janiak<sup>2</sup>, Thomas Degen<sup>1</sup>, Len J. Barbour<sup>2</sup>

1. PANalytical BV, Almelo, The Netherlands
2. Stellenbosch University, Stellenbosch, South Africa

email: jan.gertenbach@panalytical.com

Gaining control of phase transformations offers the possibility of tailoring the properties of polymorphic materials[1]. X-ray powder diffraction is ideally suited to studying such structural modifications, particularly since the bulk material is analysed, allowing the averaged structural features of the material to be correlated with its bulk physical properties, in this case the porosity. In addition, rapid X-ray diffraction data collection allows the determination of intermediate phases, onset points of reactions and information about the reversibility of processes involved. The material studied here exists in four distinct polymorphic forms, each porous to a differing extent. Control of the desired polymorph, and hence the desired porosity is achieved by manipulation of temperature and pressure. The X-ray diffractograms were modelled by Rietveld refinement using the HighScore Plus software[2] to study the structural processes during the phase transformations. The physical properties determined by sorption measurements were modelled using Partial Least Squares Regression (PLSR) analysis, and this data compared to the output from the Rietveld structural study.

[1] see for example Herbert, S.A. *et al. J. Am. Chem. Soc.*, **2013**, 135, 6411.

[2] Degen, T. *et al. Powder Diffr.*, **2014**, 29, S13.

**Keywords:** porosity, gas storage, polymorphism

## MS18 Structures of minerals, planetary and carbon materials at Earth and planetary conditions

Chairs: Tiziana Boffa-Ballaran, Marco Merlini

### MS18-O1 Discovering new materials, minerals and phenomena with evolutionary algorithms

Artem R. Oganov<sup>1,2</sup>

1. Skolkovo Institute of Science and Technology, Russia  
2. Stony Brook University, USA

email: artem.oganov@stonybrook.edu

Thanks to powerful evolutionary algorithms, in particular the USPEX method, it is now possible to predict both the stable compounds and their crystal structures at arbitrary conditions, given just the set of chemical elements. Recent developments include major increases of efficiency and extensions to low-dimensional systems and molecular crystals and new techniques called evolutionary metadynamics and Mendelevian search.

Some of the results that I will discuss include:

1. Theoretical and experimental evidence for a new partially ionic phase of boron,  $\gamma$ -B and an insulating and optically transparent form of sodium.
2. Predicted stability of “impossible” chemical compounds that become stable under pressure – e.g.  $\text{Na}_3\text{Cl}$ ,  $\text{Na}_2\text{Cl}$ ,  $\text{Na}_3\text{Cl}_2$ ,  $\text{Na}_4\text{Cl}_3$ ,  $\text{NaCl}_3$ ,  $\text{NaCl}_7$ ,  $\text{Mg}_3\text{O}_2$  and  $\text{MgO}_2$ .
3. New chemistry of planet-forming systems Mg-Si-O and N-H-O.
4. Fate of carbon inside the Earth.
5. Novel surface phases (e.g. boron surface reconstructions).
6. Prediction of new ultrahard materials and computational proof that diamond is the hardest possible material.

**Keywords:** crystal structure prediction, computational materials discovery, high-pressure geochemistry

### MS18-O2 Super-deep diamonds and their mineral inclusions: an overview

Fabrizio Nestola<sup>1</sup>

1. Department of Geosciences, University of Padova, Via G. Gradenigo 6, I-35131 Padova (Italy)

email: fabrizio.nestola@unipd.it

Natural diamonds and their mineral inclusions play a crucial role in Earth Sciences as they could be considered as open windows to the deep Earth. Indeed, they are thought to crystallize between about 120 and 1000 km depth. Diamonds formed between 120 and about 200-250 km depth are called “lithospheric”, whereas those crystallized much deeper are the so called “super-deep diamonds”. This last category of diamonds is extremely rare and represents only 6% of the diamond production. Among the most common mineral inclusions found in super-deep diamonds are ferropervicite ( $\text{Mg,Fe}$ )O,  $\text{CaSiO}_3$  walsbyite-type structure and jeffbenite ( $\text{Mg,Fe}$ )<sub>2</sub>Al<sub>2</sub>Si<sub>2</sub>O<sub>12</sub> (Kaminsky 2012; Nestola et al. 2016). Although, such inclusions are considered stable at very high-pressure conditions reaching the Earth’s lower mantle depth (below about 660 km depth), it is still questionable if their diamond hosts could be placed actually in the lower mantle (between 660 and 900-1000 km depth) or “just” in the deepest regions of the upper mantle (about 300-400 km depth). However, a very rare mineral, ringwoodite ( $\text{Mg,Fe}$ )<sub>2</sub>SiO<sub>4</sub>, was recently found included within a Brazilian diamond (Pearson et al. 2014) providing a strong constraint on their depth of crystallization being ringwoodite stable only between about 525 and 660 km depth. Here, I will provide an overview on the super-deep diamonds and their mineral inclusions focusing on the most recent discoveries and their geological meaning.

#### References

- Kaminsky, F. (2012) Mineralogy of the lower mantle: a review of “super-deep” mineral inclusions in diamond. *Earth Science Reviews*, 110, 127-147.
- Nestola, F., et al. (2016) Tetragonal Almandine-Pyroxene Phase, TAPP: finally a name for it, the new mineral jeffbenite. *Mineralogical Magazine*, 10.1180/minmag.2016.080.059
- Pearson, D.G., et al. (2014) Hydrous mantle transition zone indicated by ringwoodite included within diamond. *Nature*, 507, 221-224.
- FN is supported by the ERC Starting Grant INDIMEDEA (agreement no. 307322)

**Keywords:** Diamond, mineral inclusions, lower mantle, upper mantle

## MS18-O3 Water-rock interactions in carbonaceous chondrites: a meso to nanoscale study of alteration processes in an anoxygenic environment

Agnes Elmaleh<sup>1</sup>, Benoît Baptiste<sup>1</sup>, Serena C. Tarantino<sup>2</sup>, Bertrand Devouard<sup>3</sup>, Franck Bourdelle<sup>4</sup>, Florent Caste<sup>1</sup>, Karim Benzerara<sup>1</sup>, Hugues Leroux<sup>5</sup>, Nicolas Menguy<sup>1</sup>, Martine Gérard<sup>1</sup>, Jonathan Wright<sup>6</sup>

1. Institut de Minéralogie, de Physique des Matériaux et de Cosmochimie (UPMC-CNRS)
2. Dipartimento di Scienza della terra e dell'ambiente (Università di Pavia)
3. Cerege (Université Aix Marseille-CNRS)
4. LGCgE (Université Lille 1)
5. Unité Matériaux et Transformations (Université Lille 1 - CNRS)
6. European Synchrotron Radiation Facility

email: agnes.elmaleh@impmc.upmc.fr

Here we will focus on the early processes of serpentinisation in small bodies of the solar system by presenting a mineralogical study of carbonaceous chondrites. CI-CM chondrites are among the most primitive objects of the solar system, with elemental compositions of refractory elements close to that of the solar photosphere. From a mineralogical point of view, these meteorites mostly consist of phyllosilicates attesting to early water-rock interactions. From mineralogical and petrological observations, it has long been proposed that the bulk of mineral hydration occurred in these meteorites parent bodies after ices that accreted with rock material have melted. CM chondrites, which are the most common among carbonaceous chondrites, have a particular interest for better understanding the processes involved, and their consequences in terms of the conditions that prevailed on small bodies that may have contributed to the water budget of terrestrial planets. Indeed, a relative preservation of primary anhydrous minerals (20-30 vol%), mostly Mg-rich olivine, pyroxene and Fe,Ni-alloys and minor sulfides and refractory oxides, gives the possibility to assess the reactions leading to secondary phases, mostly Fe<sup>2+</sup>, Fe<sup>3+</sup>-rich Mg-, Al-bearing serpentines as well as carbonates, sulfates, oxides and sulfides. We will illustrate the complementarity of approaches based on one hand on nanoscale investigations of the structure, valence state of Fe and composition of secondary phases using STXM-XANES at the Fe L<sub>2,3</sub>-edges coupled with TEM investigations, and on the other hand on an evaluation of the mineralogy of primary and secondary assemblages and their relationships as a function of the degree of alteration mainly using micro-focused XRD and preliminary results of computed tomography XRD (XRD-CT). From these results, we will specifically address the questions of the transformations of primary minerals by illustrating the role of the early alteration of Fe,Ni-alloys on the control of the mineralogy of serpentines, and that of the fluid-assisted evolution of secondary products as alteration proceeds, which presents an analogy with hydrothermal terrestrial processes. We will show how structural studies of serpentines can yield a better understanding of the oxidation processes that prevailed in this anoxygenic environment. Finally, we will briefly illustrate the insight provided into asteroidal processes by an experimental approach of the formation of chondritic serpentines.

## MS18-O4 Structures of meteoritic diamond nanocrystals

Peter Nemeth<sup>1,2</sup>, Laurence A.J. Garvie<sup>3</sup>, Peter R. Buseck<sup>2,4</sup>

1. Institute of Materials and Environmental Chemistry, Research Center for Natural Sciences, Hungarian Academy of Sciences, H-1117 Budapest, Magyar Tudósok Körútja 2, Hungary.
2. School of Earth and Space Exploration, Arizona State University, Tempe, Arizona 85287-1404, USA
3. Center for Meteorite Studies, Arizona State University, Tempe, Arizona 85287-6004, USA
4. School of Molecular Sciences, Arizona State University, Tempe, AZ 85287-1604, USA

email: nemeth.peter@ttk.mta.hu

Meteoritic diamond nanocrystals can provide information on stellar nucleosynthesis<sup>1</sup> as well as shock processes occurring during cosmic and terrestrial impacts<sup>2</sup>. According to published data, these crystals are structurally inhomogeneous and consist of ordinary cubic (c-) diamond (space group: Fd-3m) plus a variety of sp<sup>3</sup>-bonded diamond polymorphs including *h*- (lonsdaleite), *i*-, *m*-, and *n*-diamond. These structures have received considerable attention because they are thought to indicate diagnostic formation conditions. In particular, the polymorphs have been widely used as indicators of asteroidal impacts and linked to mass extinctions such as the dinosaurs and mammoths. However, pure crystals, even tiny ones, of the polymorphs have never been reported. Furthermore, the diagnostic features of the polymorphs have been controversial, which posed serious problems with their identifications. In order to elucidate the structures of diamond nanocrystals, and thus to approach the issue of diamond polymorphs, we studied samples from the Canyon Diablo, Gubba, Murchison, and Orgueil meteorites as well as from the Popagai crater using an ultrahigh-resolution transmission electron microscope (uHRTM). We found that diamond nanocrystals are intimately twinned and faulted. Combinations of {113} and {111} twins as well as {111} stacking faults produce uHRTM images and d-spacings that match those attributed to *h*-, *i*-, and *m*-diamond. The diagnostic features of *n*-diamond in TEM images can arise from crystal-thickness effects. Our data and interpretations strongly suggest that the reported diamond polymorphs are all actually *c*-diamond containing intimate twins and stacking faults<sup>3,4</sup>. This finding calls for reevaluation of implications regarding impact origins based on nanosized diamond polymorphs. The results also imply that defects are widespread in diamond nanocrystals, and these defects can give rise to a surprisingly diverse nanometer-scale structural complexity (Figure 1).

<sup>1</sup>Huss GR (2005) Meteoritic nanodiamonds: Messengers from the stars. *Elements* 1(2):97-100.  
<sup>2</sup>Hough, RM, *et al.* (1997) Diamonds from the iridium-rich K-T boundary layer at Arroyo el Mimbral, Tamaulipas, Mexico. *Geology* 25: 1019-1022. <sup>3</sup>Németh P, *et al.* (2014) Lonsdaleite is faulted and twinned cubic diamond and does not exist as a discrete material. *Nat. Commun.* 5:5447. <sup>4</sup>Németh P, Garvie LJA & Buseck PR (2015) Twinning of cubic diamond explains reported nanodiamond polymorphs. *Sci. Rep.* 5 (18381).

**Keywords:** meteorites, serpentinisation, synchrotron radiation

*Acta Cryst.* (2016). A72, s71

s71



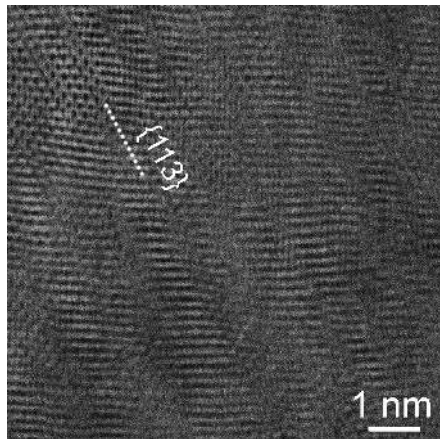


**Figure 1.** Structural complexity occurs in diamond as a result of {113} twins. Sample: Canyon Diablo meteorite.

**Keywords:** diamond nanocrystals, diamond polymorphs, asteroidal impact, twins, stacking faults, structural complexity

## MS18-O5 Structural trend of alkaline carbonates under high pressure

Pavel N. Gavryushkin<sup>1,2</sup>, Altyna Behtenova<sup>1,2</sup>, Zakhar I. Popov<sup>3</sup>,  
Konstantin D. Litasov<sup>1,2</sup>, Anton Shatskiy<sup>1,2</sup>

1. V.S. Sobolev Institute of Geology and Mineralogy SB RAS, Novosibirsk 630090, Russia

2. Novosibirsk State University, Novosibirsk 630090, Russia

3. National University of Science and Technology MISIS, Moscow 119049, Russia

email: gavryushkin@igm.nsc.ru

The high-pressure behavior of alkaline carbonates is of practical interest due to the catalytic activity of these compounds in the process of diamond's crystals growth. The fundamental interest is in the construction of the high-pressure structural trend and its comparison with such trends of other  $A_2CO_3$  carbonates and  $A_2B$  binary compounds. We determine this trend based on complex experimental and theoretical investigation of high-pressure behavior of  $Li_2CO_3$ ,  $Na_2CO_3$  and  $K_2CO_3$ . Theoretical investigation is based on the evolutionary crystal structure prediction algorithms (USPEX package) and density functional theory (VASP package), pressure range 0-100 GPa. Experiments were performed in the large-volume multi-anvil apparatus installed at the BL04B1 beamline of the Spring-8 synchrotron radiation facility, pressure range 2-30 GPa.

The sequence of theoretically revealed transitions is presented in Fig.1. All cation arrays of the high-pressure structures are of  $AlB_2$ -type, ideal or deformed. The simplest high pressure behavior is observed for  $Li_2CO_3$ , which directly transforms to ideal (hexagonal)  $AlB_2$ -type at 8 GPa and stable in this form up to 100 GPa.  $Na_2CO_3$  transforms to ideal  $AlB_2$ -type at 5 GPa and then to deformed monoclinic (P2/m)  $AlB_2$ -type at 35 GPa.  $K_2CO_3$  does not adopt ideal  $AlB_2$ -type and at 12 GPa transforms to triclinic (P-1), and then to monoclinic phase (C2/c) at 53.5 GPa. The last one is the analogue of P2/m-phase of  $Na_2CO_3$ . The presented results are in good agreement with results of our experiments, according to which ambient  $\gamma$ - $Na_2CO_3$  transforms to ideal  $AlB_2$ -structure at 12 GPa, and  $\gamma$ - $K_2CO_3$  transforms to a new phase at 12 GPa. The transformation of  $\gamma$ - $Li_2CO_3$  into ideal  $AlB_2$ -structure was observed in the experiments of Grzechnik and co-authors [Grzechnik *et al.*, 2003] above 10 GPa.

Thus, according to our results cation arrays of alkaline carbonates transform from anti- $CaF_2$  ( $Li_2CO_3$ ) and from  $Ni_2In$  ( $Na_2CO_3$ ,  $K_2CO_3$ ) types to  $AlB_2$ -type. This trend is consistent with that of alkaline sulfides (selenides, tellurides), which under compression goes through the series of phase transitions: anti- $CaF_2$ --- $PbCl_2$ --- $Ni_2In$ --- $AlB_2$ . The correspondence of these two trends is supported by the fact that  $PbCl_2$ -type structure was revealed in our calculations as the possible phase of  $Na_2CO_3$  stable under ambient conditions.

**References** Grzechnik, A., P. Bouvier, and L. Farina (2003), High-pressure structure of  $Li_2CO_3$ , *J. Solid State Chem.*, 173(1), 13-19.

$Li_2CO_3$ :  $\gamma$ - $Li_2CO_3$  (anti- $CaF_2$ )  $\xrightarrow{8\text{ GPa}}$   $P6_3/mcm$  ( $AlB_2$ )  
 $Na_2CO_3$ :  $\gamma$ - $Na_2CO_3$  ( $Ni_2In$ )  $\xrightarrow{5\text{ GPa}}$   $P6_3/mcm$  ( $AlB_2$ )  $\xrightarrow{35\text{ GPa}}$   $P2/m$  ( $AlB_2$ -deformed)  
 $K_2CO_3$ :  $\gamma$ - $K_2CO_3$  ( $Ni_2In$ )  $\xrightarrow{12\text{ GPa}}$   $P1$  ( $AlB_2$ -deformed)  $\xrightarrow{53.5\text{ GPa}}$   $C2/c$  ( $AlB_2$ -deformed)

**Figure 1.** High-pressure phase transitions of  $Li_2CO_3$ ,  $Na_2CO_3$ , and  $K_2CO_3$ .



**Keywords:** pressure, crystal structure prediction, DFT, experiment, synchrotron radiation

## MS19 Solid state oxygen fuel cell, hydrogen storage & battery materials

Chairs: Bernhard Frick, Kristina Edstroem

### MS19-O1 Structure and dehydration mechanism of the proton conducting brownmillerite $\text{Ba}_2\text{In}_2\text{O}_5$

Maths Karlsson<sup>1</sup>, Johan Bielecki<sup>1,2</sup>, Stewart F. Parker<sup>3</sup>, Lars Börjesson<sup>1</sup>, Laura Mazzei<sup>1</sup>, Adrien Perrichon<sup>1</sup>

1. Department of Physics, Chalmers University of Technology
2. Department of Cell and Molecular Biology, Uppsala University
3. ISIS Facility, STFC Rutherford Appleton Laboratory

email: maths.karlsson@chalmers.se

Proton conducting oxides are currently accumulating considerable attention due to their potential as efficient electrolytes in various electrochemical technologies, including intermediate temperature solid oxide fuel cells [1]. An important material is the brownmillerite structured oxide  $\text{Ba}_2\text{In}_2\text{O}_5$ , which may be described as an oxygen deficient variant of the perovskite structure, with alternating layers of  $\text{InO}_6$  octahedra and  $\text{InO}_4$  tetrahedra. Like many other oxygen-deficient oxides,  $\text{Ba}_2\text{In}_2\text{O}_5$  transforms upon hydration into a hydrogen-containing material,  $\text{Ba}_2\text{In}_2\text{O}_5(\text{H}_2\text{O})_x$ , which show proton conducting properties. In this contribution, I will report on detailed investigations of the local structure and dehydration mechanism of  $\text{Ba}_2\text{In}_2\text{O}_5(\text{H}_2\text{O})_x$ , using a combination of variable temperature Raman spectroscopy together with inelastic neutron scattering and computer simulations [2,3]. The results suggest that  $\text{Ba}_2\text{In}_2\text{O}_5(\text{H}_2\text{O})_x$  evolves upon heating from a perovskite-like structure for the fully hydrated material ( $x = 1$ ) at room temperature, through a partially hydrated intermediate phase, appearing at ca. 370 °C, to an essentially fully dehydrated ( $x \approx 0$ ) brownmillerite material at 600 °C. The dehydration process appears to be a two-stage mechanism characterized by a homogenous release of protons below the hydrated-to-intermediate phase transition, whereas at higher temperatures a preferential desorption of protons originating in the nominally tetrahedral layers is observed.

[1] L. Malavasi, C. A. J. Fisher, M. S. Islam, *Chem. Soc. Rev.* **39** (2010) 4370-4387.

[2] J. Bielecki, S. F. Parker, D. Ekanayake, S. M. H. Rahman, L. Börjesson, M. Karlsson, *J. Mater. Chem. A* **2** (2014) 16915-16924.

[3] J. Bielecki, S. F. Parker, L. Mazzei, L. Börjesson, M. Karlsson, *J. Mater. Chem. A* **4** (2016) 1224-1232.

**Keywords:** Proton, conducting, oxide, fuel cells, SOFC, neutron scattering, Raman spectroscopy

**MS19-O2** *In operando* pair distribution function analysis and solid-state NMR studies of antimony anodes for sodium-ion batteries

Phoebe K. Allan<sup>1,2,3</sup>, John M. Griffin<sup>2</sup>, Joshua M. Stratford<sup>2</sup>, Ali Darwiche<sup>4</sup>, Olaf J. Borkiewicz<sup>5</sup>, Kamila M. Wiaderek<sup>5</sup>, Andrew J. Morris<sup>6</sup>, Karena W. Chapman<sup>5</sup>, Peter J. Chupas<sup>5</sup>, Clare P. Grey<sup>2</sup>

1. Diamond Light Source, Diamond House, Harwell Science & Innovation Campus, Didcot, Oxfordshire, OX11 0DE, UK
2. University of Cambridge, University Chemical Laboratory, Lensfield Road, Cambridge, CB2 1EW, UK
3. Gonville and Caius College, Trinity Street, Cambridge, CB2 1TA, UK
4. Université Montpellier II, 2 Place Eugène Bataillon - CC 1502, 34095 Montpellier CEDEX 5, France
5. Advanced Photon Source, Argonne National Laboratory, IL60439, USA
6. Theory of Condensed Matter Group, Cavendish Laboratory, University of Cambridge, J. J. Thomson Avenue, Cambridge

email: phoebe.allan@diamond.ac.uk

Sodium-ion batteries have attracted attention recently because of the high natural abundance of sodium compared to lithium, making them particularly attractive in applications such as large-scale grid storage where low cost and sustainability, rather than light weight is the key issue. Several materials have been suggested as cathodes but far fewer studies have been done on anode materials and, because of the reluctance of sodium to intercalate into graphite, the anode material of choice in commercial lithium-ion batteries, the anode represents a significant challenge to this technology. Materials which form alloys with sodium, particularly tin and antimony, have been suggested as anode materials; their ability to react with multiple sodiums per metal-atom give potential for high gravimetric capacities. However, relatively little is known about the reaction mechanism of these materials in the battery, primarily due to drastic reduction in crystallinity during (dis)charging conditions, but also because the structures formed on electrochemical cycling may not be alloys known to exist under ambient conditions.

We present a study of antimony-based anodes for sodium-ion batteries, using *in situ* pair distribution function (PDF) analysis combined with *ex situ* solid-state nuclear magnetic resonance studies<sup>1</sup>. Inclusion of diffuse scattering in analysis is able to circumvent some of the issues of crystallinity loss, and gain information about the local structure in all regions, independent of the presence of long-range order in the material. As a result, we separate the crystalline and amorphous phases present in the Na-Sb system and probe the nature of previously unknown amorphous intermediate phases. This analysis has been linked with *ex situ* <sup>23</sup>Na solid-state NMR experiments to examine the local environment of the sodium; these show evidence of known Na<sub>3</sub>Sb phases but indicate additional metastable phases are present at partial discharge. The electrochemical signatures are linked with structural processes taking place in the battery to show that the different electrochemical profile observed on the second sodiation is a result of complex multiphase electrode formed after the first desodiation as the amorphous and crystalline phases take different sodiation pathways.

<sup>1</sup> P. K. Allan, J.M. Griffin, A. Darwiche, O.J. Borkiewicz, K.M. Wiaderek, K.W. Chapman, A.J.

Morris, P.J. Chupas, L. Monconduit, C.P. Grey, *J. Am. Chem. Soc.* (2016) **138**, 2352

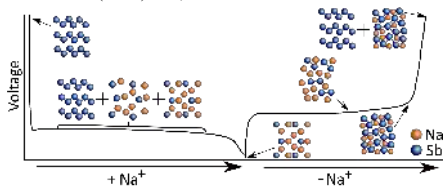


**Figure 1.** Schematic of the sodiation processes in antimony anodes

**Keywords:** pair distribution function analysis, batteries, *in operando*

## MS19-O3 Quasi-Elastic Neutron Scattering Studies on Solid Electrolytes for all-solid-state Lithium Batteries

Didier Blanchard<sup>1</sup>, Jon Steinar G. Myrdal<sup>1</sup>, Dadi Sveinbjörnsson<sup>1</sup>, Peter NGene<sup>2</sup>, Petra de Jongh<sup>2</sup>, Tejs Vegge<sup>1</sup>

1. Department of Energy, Technical University of Denmark (DTU), Denmark

2. Inorganic Chemistry and Catalysis, Debye Institute for Nanomaterials Science, Utrecht University, The Netherlands

email: dibi@dtu.dk

The development of better batteries is paramount for market penetration of electrical vehicle and integration of renewable energy sources into the grid. For today's best technology, state-of-the-art lithium-ion battery, limited improvement in capacity and cost are expected because of the use of organic liquid or gel electrolytes limiting the choice of electrode materials and exposing to safety concerns. A choice alternative is to use solid electrolytes instead.

The high temperature phase of lithium borohydride ( $\text{LiBH}_4$ ), hexagonal crystal structure at temperature above 383 K, is a fast  $\text{Li}^+$  conductor ( $\sigma \sim 10^{-4} \text{ W}^{-1} \cdot \text{cm}^{-1}$ ).<sup>[1]</sup> This property is kept at room temperature by stabilizing the hexagonal phase with Li halides<sup>[2]</sup> or confining  $\text{LiBH}_4$  in nanoporous scaffolds.<sup>[3]</sup>

We have studied the  $\text{Li}^+$  diffusion in  $\text{LiBH}_4$  with Density Functional Theory (DFT) coupled to Quasi-Elastic Neutron Scattering (QENS). DFT shows that lithium defects such as Frenkel pairs are easily formed at room temperature ( $E_f = 0.44 \text{ eV}$ ) and low energy barriers (0.3 eV) are found between stable defect sites, giving rise to high defect mobility (Fig.1-a). The most favorable mechanism for the  $\text{Li}^+$  conduction is calculated to occur in the hexagonal plane. The QENS results at 380 K show long range diffusion of  $\text{Li}^+$ , with jump lengths of one unit cell in the hexagonal plane and rates in agreement with DFT. At 300 K, QENS reveals jumps of shorter length ( $\sim 2 \text{ \AA}$ ), which could correspond to jump of  $\text{Li}^+$  interstitials to intermediate lattice sites, in agreement with DFT.<sup>[4]</sup>

QENS was also used to probe the dynamic of the  $\text{BH}_4^-$  anions in  $\text{LiBH}_4$  confined in nanoporous  $\text{SiO}_2$ . Four quasi-elastic components were found in two different temperature domains. At low temperature,  $< 170 \text{ K}$ , the components are an order of magnitude broader than those at high temperature, however still below the phase transition (Fig.1-b). The narrower components are associated with reorienting  $\text{BH}_4^-$  anions in crystalline  $\text{LiBH}_4$ , while the broader components, with much more rapidly reorienting  $\text{BH}_4^-$ , can be associated with the fraction of  $\text{LiBH}_4$  located at the  $\text{SiO}_2$  surfaces, reflecting a disruption of the bulk crystal lattice. It suggests that the high  $\text{Li}^+$  conductivity takes place at the interface between  $\text{LiBH}_4$  and  $\text{SiO}_2$ .

[1] Matsuo *et al.*, *Appl. Phys. Lett.* **2007**, 91, 224103.

[2] Sveinbjörnsson *et al.*, *J. Phys. Chem. C* **2013**, 117, 3249.

[3] Blanchard *et al.*, *Adv. Funct. Mater.* **2014**, 1.

[4] Myrdal *et al.*, *J. Phys. Chem. C* **2013**, 117, 9084.

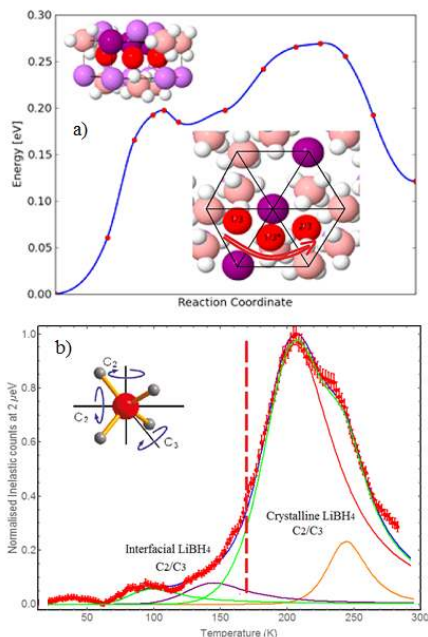


**Figure 1.** a) DFT energy path for interstitial Li diffusion. b)  $\text{LiBH}_4/\text{SiO}_2$  neutron inelastic temperature scans. The four quasi-elastic components correspond to reorientational diffusion of the  $\text{BH}_4^-$  along the  $C_2$  -  $C_3$  axis for the interfacial  $\text{LiBH}_4$  (low temp.) and crystalline  $\text{LiBH}_4$  (high temp.).

**Keywords:** Battery, Quasi-elastic Neutron Scattering, Density Functional Theory, all-solid-state battery, solid electrolyte

## MS19-O4 Characterization of cation ordering, oxygen vacancy distribution and proton sites in hexagonal and cubic

### BaTi<sub>1-x</sub>Sc<sub>x</sub>O<sub>3-δ</sub>

Paul F. Henry<sup>1,2</sup>, Nico Torino<sup>2</sup>, Habibur S.M. Rahman<sup>2</sup>, Christopher S. Knee<sup>2</sup>, Sten G. Eriksson<sup>2</sup>, Stefan T. Norberg<sup>2</sup>, Tor S. Bjørheim<sup>3</sup>, Reidar Haugsrud<sup>4</sup>, Sam Callear<sup>4</sup>, Ron Smith<sup>4</sup>

1. European Spallation Source ERIC, Lund, Sweden
2. Chalmers University of Technology, Gothenburg, Sweden
3. University of Oslo, Norway
4. STFC, Didcot, UK

email: paul.henry@ess.se

Proton conducting oxides find applications as electrolyte materials in fuel cells, steam electrolyzers and hydrogen and humidity sensors. Proton conducting fuel cells, which use H<sub>2</sub> as a fuel, stand out as a promising technology for future clean energy generation. However, its success relies on the discovery of novel electrolyte materials with high protonic conduction at intermediate temperatures (200 – 600 °C). Acceptor doped perovskites are actively studied in the search for improved proton conducting materials. We have synthesized and characterized the proton conducting properties of the series BaTi<sub>1-x</sub>Sc<sub>x</sub>O<sub>3-δ</sub> (0.1 ≤ x ≤ 0.8). [1,2] The series shows a transition from a 6H perovskite structure at low scandium doping to a cubic phase for x ≥ 0.5. All the doped series show hydration behavior indicative of filling oxide ion vacancies within the structure and that protons are the dominant charge carriers below 600 °C. The conductivity of the materials with the 6H structure is significantly lower than those with the cubic structure. X-ray data suggest different oxygen vacancy ordering within the 6H perovskite structure at low doping levels, whereas the vacancies are distributed randomly in the cubic structure with no evidence of long range ordering of the Ti and Sc ions on the B-site. However, due to the weak scattering from oxygen *cf.* the transition metals and barium, coupled with the similar scattering power of the Ti and Sc, the presence of cation and/or oxygen ion order and the driving force for the phase transition to the cubic structure are unknown. Moreover, the origin of the poorer conductivity of the 6H *cf.* the cubic structure upon hydration is also unknown and is likely related to the proton sites and the exchange pathways within the material. Neutron powder diffraction (NPD) and recent *in situ* studies using combined NPD/thermogravimetric analysis resolving these key questions will be presented and coupled to DFT calculations.

[1] S.M.H. Rahman, I. Ahmed, R. Haugsrud, S.G. Eriksson, C.S. Knee. (2014) *Solid State Ionics*, **255**, 140-146.

[2] S.M.H. Rahman, S.T. Norberg, C.S. Knee, J.J. Biendicho, S. Hull, S.G. Eriksson, (2014) *Dalton Transactions*, **43**, 15055.

**Keywords:** neutron, powder diffraction, structure

## MS19-O5 Lattice dynamics of the ionic superconductor Li<sub>4</sub>C<sub>60</sub>: Inelastic neutron scattering and Powder Averaged Lattice Dynamics (PALD) investigations.

Stéphane ROLS<sup>1</sup>, Daniele Pontiroli<sup>2</sup>, Matteo Aramini<sup>2</sup>, Mattia Gaboardi<sup>2</sup>, Chiara Cavallari<sup>1,2</sup>, Mauro Riccò<sup>2</sup>, Emmanuelle Suard<sup>1</sup>, Mark R. Johnson<sup>1</sup>, Didier Richard<sup>1</sup>

1. Institut Laue Langevin, Grenoble, FRANCE
2. Dipartimento di Fisica e Scienze della Terra, Università degli Studi di Parma, Parma, ITALY

email: rols@ill.fr

The two-dimensional polymer structure and lattice dynamics of the superionic conductor Li<sub>4</sub>C<sub>60</sub> (ionic conductivity of 10<sup>-2</sup> S/cm at room temperature [1]), are investigated by neutron diffraction and neutron spectroscopy. The peculiar bonding architecture of this compound is confirmed through the precise localization of the carbon atoms involved in the intermolecular bonds. The spectral features of this phase are revealed through a combination of *ab initio* lattice dynamics calculations and inelastic neutron scattering experiments. The neutron scattering observables are found to be in excellent agreement with the simulations, the latter predicting a partial charge transfer from the Li atoms to the C<sub>60</sub> cage. The absence of a well-defined band associated with the Li atoms in the experimental spectrum suggests that this species is not ordered even at the lowest temperatures. The calculations also predict an unstable Li sublattice at a temperature of ~200 K, which we relate to the large ionic diffusivity of this system : low-frequency optic modes of the Li ions couple to the soft structure of the polymer [2].

[1] M. Ricco et al., Phys. Rev. Lett., **102** (2009) 145901.

[2] S. Rols et al. Phys. Rev. B, **92** (2015) 014305

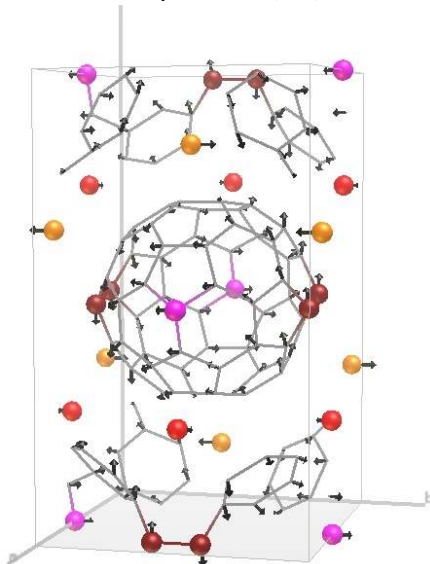


**Figure 1.** Optic low frequency hybrid mode, involving  $C_{60}$  deformation and Li translations.

**Keywords:** superionic conductor, inelastic neutron scattering, fullerenes, DFT

## MS20 Materials for energy conversion and harvesting

Chairs: Manuel Hinterstein, Siegbert Schmid

### MS20-O1 A structural perception about intrinsic point defects in kesterite type compound semiconductors

Susan Schorr<sup>1</sup>

<sup>1</sup> Helmholtz-Zentrum Berlin für Materialien und Energie

email: susan.schorr@helmholtz-berlin.de

The understanding of the interplay between structural, chemical and electronic properties of kesterite type compound semiconductors, applied as absorber materials in photovoltaic devices, can give crucial informations aiding the continuous improvement of device efficiencies. Various reasons are discussed about efficiency losses in the bulk material of kesterite type based solar cells. These absorber layers, which are  $Cu_2ZnSn(S, Se)_4$ , exhibit in general a off-stoichiometric composition (Cu-poor, Zn-rich). The presence of secondary phases and deep defect levels caused by intrinsic point defects are efficiency limiting factors. The present study reports a detailed crystallographic investigation about cationic point defects in off-stoichiometric  $Cu_2ZnSnS_4$  and  $Cu_2ZnSnSe_4$ . Both compounds crystallize in the kesterite type structure (space group I-4). The basis of the systematic study are series of powder samples synthesized by solid state reaction. Their chemical composition has been determined by WDX spectroscopy (electron microprobe analysis). Due to the isoelectronic character of  $Cu^+$  and  $Zn^{2+}$  it is necessary to apply neutron powder diffraction to investigate the distribution of the three cations on the four cationic sites of the kesterite type structure. Rietveld refinements and the average neutron scattering length analysis method have been used to evaluate the neutron diffraction data. The kesterite type structure can be described by a stacking sequence of cation layerd Cu/Sn - Cu/Zn - Sn/Cu - Cu/Zn - Cu/Sn perpendicular to the crystallographic z-direction. An off-stoichiometric composition, for instance Cu-poor, originates from the propensity of the structure to stabilize copper vacancies, the charge balancees being commonly insured by appropriate substitutions on the cationic sites. If the oxidation states of the cations and anions are retained going from stoichiometric to an off-stoichiometric composition, a number of specific substitutions can be envisioned to account for the charge

balance in the off-stoichiometric material. These substitutions lead to the formation of point defects in the crystal structure. The presented study shows, that the point defects, expected by this model, are found experimentally in the synthesized compounds. This demonstrates the ability of the kesterite type phase to tolerate large deviations from stoichiometric composition without collapse of the structure.

**Keywords:** compound semiconductors, point defects, neutron diffraction

## MS20-O3 Interaction of water with (silico)aluminophosphate zeotypes: A comparative investigation using dispersion-corrected DFT

Michael Fischer<sup>1,2</sup>

1. Fachgebiet Kristallographie, FB Geowissenschaften, Universität Bremen, Germany

2. MAPEX Center for Materials and Processes, Universität Bremen, Germany

email: michael.fischer@uni-bremen.de

Porous aluminophosphates (AIPOs) and silicoaluminophosphates (SAPOs) with zeolite-like structures have received considerable attention as potential adsorbents for heat transformation applications using water adsorption/desorption cycles.<sup>(1,2)</sup> While experimental investigations have been reported for some materials like AIPO-18 (AEI topology) and SAPO-34 (CHA topology), more systematic insights into the relationships between structure and water adsorption properties are lacking. In this contribution, dispersion-corrected density-functional theory (DFT-D) calculations are employed to study the interaction of water with a variety of AIPOs and SAPOs, allowing for an identification of the structural features that tend to enhance the affinity towards water.

In the first part, the results of DFT-D calculations for six topologically different AIPOs and their SAPO analogues are presented. Structurally, the systems differ in the pore size and in the shape of the main pores (elongated vs. nearly spherical). For the AIPOs, the calculations predict rather similar adsorbent-water interaction energies for all systems, indicating a minuscule influence of pore size and topology on the affinity towards water. However, considerable differences are observed in the response of the framework to the adsorbed water molecules. In the SAPO materials, the structural environment of the framework proton strongly influences the interaction strength at low water loadings (one H<sub>2</sub>O per proton), whereas the interaction energies at high water loadings (near saturation) depend primarily on the silicon content.

In the second part of the contribution, the influence of structural heterogeneities (e.g. silicon islands) and defects on the affinity of SAPO-34 towards water is assessed on the basis of DFT-D calculations. A rather pronounced effect is found at low water loadings: Here, heterogeneities in the silicon distribution tend to create particularly strong adsorption sites, whereas the interaction with water is reduced considerably in defective models. At high water loadings, however, the average interaction strength is affected only slightly when compared to the defect-free reference system which contains isolated silicon atoms.<sup>(3)</sup>

### References:

- (1) A. Ristić, N. Z. Logar, S. K. Henninger and V. Kaučič, *Adv. Funct. Mater.*, 2012, **22**, 1952–1957.
- (2) J. Jänchen and H. Stach, *Solar Energy*, 2014, **104**, 16–18.
- (3) M. Fischer, *Phys. Chem. Chem. Phys.*, 2015, **17**, 25260–25271.

**Keywords:** thermal energy storage, zeolites, density-functional theory, computational chemistry

# MS20-O4 TiO<sub>2</sub> nanocontainers and nanospheres as photocatalysts for CO<sub>2</sub> reduction and photoelectrochemical water splitting: Structural modification.

Nelly Hérault<sup>1</sup>, Veerabhadra Rao Kaliginedi<sup>2</sup>, Peter Broekmann<sup>2</sup>, Katharina M. Fromm<sup>1</sup>

1. Department of Chemistry, University of Fribourg, Chemin du Musée 9, 1700 Fribourg.

2. Departement für Chemie und Biochemie, Freiestrasse 3, 3012 Bern.

email: nelly.herault@unifr.ch

CO<sub>2</sub> gas is one of the major factors of the climate imbalance. The reduction of CO<sub>2</sub> by photocatalysis is proposed to convert CO<sub>2</sub> gas into more valuable molecules (such as CH<sub>4</sub>, CH<sub>3</sub>OH etc.)<sup>1</sup> because solar energy, being an alternative, cheap and environmentally friendly source of energy, can be used as power supply<sup>1</sup>. For this process, titanium dioxide-based materials with various structures are commonly used as photocatalysts<sup>2,3</sup>. Furthermore, the photocatalytic water splitting using the TiO<sub>2</sub>-based materials could be a great option for hydrogen production to obtain clean and renewable energy sources<sup>4</sup>.

In this project, the TiO<sub>2</sub> nanocontainers and nanospheres (Figure 1 (A), (B)) with different crystalline structures are investigated because the crystalline phase, the size and the shape of TiO<sub>2</sub> may have an influence on its band gap energy and consequently on its photocatalytic properties<sup>5</sup>. Moreover the embedment of silver nanoparticles into the TiO<sub>2</sub> material is explored. Indeed, the presence of silver islands may enhance its photoactivity<sup>6</sup>.

The objective of this study (Figure 1 (C)) is the correlation between the morphology of the TiO<sub>2</sub>-based materials and their photocatalytic properties for the CO<sub>2</sub> reduction and the photoelectrochemical water splitting.

<sup>1</sup> W-N. Wang, J. Soulis, Y. J. Yang, P. Biswas, *Aerosol Air Qual. Res.* 14, 533-549 (2014)

<sup>2</sup> T. Wang, X. Meng, P. Li, S. Ouyang, K. Chang, G. Liu, Z. Mei, J. Ye, *Nano Energy*, 9, 50-60 (2014)

<sup>3</sup> P-Q. Wang, Y. Bai, J-Y. Liu, Z. Fan, Y-Q. Hu, *Catal. Commun.* 29, 185-188 (2012)

<sup>4</sup> M. Ni, M.K.H. Leung, D.Y.C. Leung, K. Sumathy, *Renew. Sustainable Energy Rev.* 11, 401-425 (2007)

<sup>5</sup> Y. Ma, X. Wang, Y. Jia, X. Chen, H. Han, C. Li, *Chem. Rev.* 114, 9987-10043 (2014)

<sup>6</sup> D. Kong, J. Ziang Yie Tan, F. Yang, J. Zeng, X. Zhang, *Appl. Surf. Sci.* 277, 105-110 (2013)

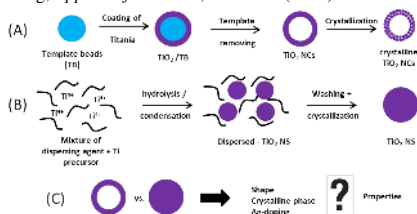


**Figure 1.** Synthesis of (A) TiO<sub>2</sub> nanocontainers, (B) TiO<sub>2</sub> nanospheres and (C) the study objectives

**Keywords:** TiO<sub>2</sub> nanocontainers, TiO<sub>2</sub> nanospheres, photoreduction of CO<sub>2</sub>, photoelectrochemical water splitting

**MS20-O5** Structure and magnetocaloric properties of Gadolinium borohydridesPascal Schouwink<sup>1</sup>, Emilie Didelot<sup>1</sup>, Young-Su Lee<sup>2</sup>, Thomas Mazet<sup>3</sup>, Radovan Cerný<sup>1</sup>

1. University of Geneva
2. Korea Institute of Science and Technology
3. Université de Lorraine

email: pascal.schouwink@gmail.com

Recently, a thorough understanding of the building principles underlying inorganic metal borohydrides has promoted the search for functional materials outside the well-known field of hydrogen storage.<sup>1</sup> In particular, we can follow very simple design strategies based on a close structural relationship to metal oxides and halides. The low molecular mass per unit of the borohydride anion can be seen as a useful property for energy-related applications in general, where light and dense materials are often favoured. Here, we have explored if borohydrides may be potential magnetic coolers. We begin our investigations on these applications with the exploration of Gd-compounds, Gadolinium being the active magnetic ion in many benchmark cryogenic coolers. The results show that, as assumed from previous studies on Mn(BH<sub>4</sub>)<sub>3</sub>, the exchange interaction is very low across the BH<sub>4</sub> linker, and these materials can hence be considered paramagnetic salts down to very low temperatures. We present an illustrative and purposeful series of novel double-cation metal borohydride salts with a high spin density per unit mass, K<sub>j</sub>Gd(BH<sub>4</sub>)<sub>j+3</sub> (j = 0, 1, 2, 3), where the molar magnetic entropy change increases with j, while the number of Gd-Gd nearest neighbours decreases simultaneously, from 6 in Gd(BH<sub>4</sub>)<sub>3</sub> to 0 in the double perovskites K<sub>2</sub>Gd(BH<sub>4</sub>)<sub>6</sub>, Cs<sub>2</sub>Gd(BH<sub>4</sub>)<sub>6</sub> as well as in the novel structure type K<sub>2</sub>Gd(BH<sub>4</sub>)<sub>5</sub>. For j = 0, 1, 3 the coordination polyhedron around Gd is an octahedron, whereas the 5-fold coordination is reported in two different geometries for j = 2 in K<sub>2</sub>Gd(BH<sub>4</sub>)<sub>5</sub>, which results in a remarkable magnetic entropy change -ΔS<sub>m</sub> of 54.6 J kg<sup>-1</sup> K<sup>-1</sup> (9T). The differences in j lead to different dimensionalities of the Gd-BH<sub>4</sub> substructure, which comprises 2D and 3D networks as well as isolated polyanions, and are reflected in magnetization measurements. In the currently investigated compounds Potassium is used as a second counter-cation in order to build the double cation salts. There is room to improve the gravimetric magnetic entropy change by substituting K<sup>+</sup> for molecules lighter in weight such as NH<sub>4</sub><sup>+</sup>. Such cationic substitutions are known to occur readily in complex hydrides<sup>1</sup> and a perspective will be presented on the synthesis and the potential behaviour of such materials.

**Keywords:** Borohydride, Magnetocaloric effect, Powder Diffraction, DFT

**MS21** Structural disorder and materials' properties at ambient and non-ambient conditions

Chairs: Dmitry Chernyshov, Vaughan Gavin

**MS21-O1** Lattice dynamics and elastic properties from thermal diffuse scatteringBjörn Wehinger<sup>1,2</sup>, Alexei Bosak<sup>3</sup>, Dmitry Chernyshov<sup>4</sup>,  
Alessandro Mirone<sup>3</sup>, Michael Krisch<sup>3</sup>

1. Laboratory for Neutron Scattering and Imaging, Paul Scherrer Institute, Villigen, Switzerland
2. Department of Quantum Matter Physics, University of Geneva, Switzerland
3. European Synchrotron Radiation Facility, Grenoble, France
4. Swiss-Norwegian Beamlines at European Synchrotron Radiation Facility, Grenoble, France

email: bjorn.wehinger@unige.ch

Diffuse scattering from thermally populated phonons contains important details on the lattice dynamics. The intensity distribution of thermal diffuse scattering across reciprocal space allows for the identification and localization of phonon anomalies and naturally encodes the phonon eigenvectors [1]. In this presentation, the audience will be introduced to the theoretical background, recent developments on model calculations and the use of pertinent software for computing the intensity distribution in 3D reciprocal space [2]. Important aspects of the experimental implementation and data treatment are discussed and the methodology is illustrated by a representative set of recent examples [3-5]. I will show how distinct features in the lattice dynamics leave their footprint in the intensity distribution, such as soft and low energy phonon modes (see Figure 1), similarities in the electronic potential and symmetry relations upon phase transitions. Finally, the possibility for extracting the full elasticity tensor from thermal diffuse scattering is discussed and an outlook to application at high pressures is presented.

[1] A. Bosak *et al* 2015 In-between Bragg reflections: thermal diffuse scattering and vibrational spectroscopy with x-rays *J. Phys. D: Appl. Phys.* **48** 504003

[2] B. Wehinger and A. Mirone 2013-2016, ab2tds, <https://forge.epn-campus.eu/html/ab2tds/Introduction.html>

[3] B. Wehinger, A. Bosak, and P. T. Jochym 2016 Soft phonon modes in rutile TiO<sub>2</sub> *Phys. Rev. B* **93**, 014303

[4] B. Wehinger *et al* 2015 Lattice dynamics of α-cristobalite and the Boson peak in silica glass *J. Phys.: Condens. Matter* **27** 305401

[5] B. Wehinger *et al* 2014 Diffuse scattering in metallic tin polymorphs *J. Phys.: Condens. Matter* **26** 115401



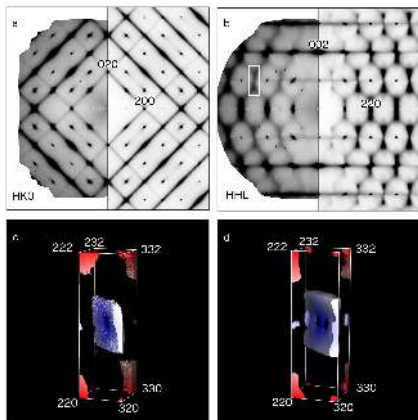


**Figure 1.** TDS from TiO<sub>2</sub> [3]. Reconstructions from experiment (left part of panels a and b) are compared to model calculations using density functional perturbation theory. (c) and (d) iso-intensity distribution of TDS in 3D around  $Q = (2.5 \ 2.5 \ 1)$  as obtained from experiment and calculation, respectively.

**Keywords:** diffuse scattering, lattice dynamics, elasticity

## MS21-O2 3D Single Crystal Diffuse Scattering - Measurement and Interpretation

Hans-Beat Bürgi<sup>1,2</sup>, Ruggero Frison<sup>2</sup>, Thomas Weber<sup>3</sup>

1. Department of Chemistry and Biochemistry, University of Berne, Switzerland

2. Department of Chemistry, University of Zürich, Switzerland

3. X-Ray Platform, Department of Materials, ETH Zürich, Switzerland

email: hans-beat.buergi@krist.unibe.ch

The useful and interesting properties of many crystalline materials are due to crystal defects. Defects manifest themselves by diffuse scattering interspersed between the Bragg reflections. The total scattering, Bragg and diffuse, contains information on the periodic portion of the total scattering density including its chemically unreasonable parts and the nature of the underlying crystal defects as well as the correlation between them.

Nowadays reasonably accurate measurement of complete 3D total scattering is possible at synchrotrons with their high flux of X-rays and low-noise, energy discriminating pixel detectors. Several neutron scattering facilities provide stations for measuring 3D diffuse scattering patterns. Careful data processing is mandatory, especially with respect to background corrections. Diffuse data sets may contain millions to hundreds of millions of observations. Their handling and interpretation thus requires substantial computing resources.

Interpretation of such data relies primarily on two tools [1]: 1) analysis of the 3D-PDF, i.e. the Fourier Transform (FT) of the total scattering intensity. The 3D-PDF is the non-periodic Patterson function of the disordered crystal just like the FT of the Bragg intensities is the periodic Patterson function  $P$  of an ordered crystal. With a good model of the average, periodic structure usually available, the  $3D-\Delta PDF = 3D-PDF - P$  is usually more informative. It represents the deviations from periodicity in terms of inter-nuclear vectors, their intensity and a between-atoms temperature factor. 2) The disordered structure may be modeled with Monte Carlo (MC) simulations constrained to match the average structure. In practice it is often useful to alternate between MC modeling and the  $3D-\Delta\Delta PDF = 3D-\Delta PDF(\text{exp}) - 3D-\Delta PDF(\text{MC model})$ .

The information from 3D total scattering patterns is necessarily superior to that of 1D powder patterns as is the information from 3D single crystal Bragg data compared to powder diagrams. The general comments above will be illustrated with a 3D-PDF/MC interpretation of X-ray and neutron data measured for the same compound.

[1] For a recent review see: T.R. Welberry, T. Weber, *Cryst. Rev.* **22** (2016) 2-78.

**Keywords:** Disorder, Diffuse scattering, Pair Distribution Function, Monte Carlo simulation

**MS21-O3** Guest – induced polymorphism and quenching of disorder in the Hofmann spin-crossover compound  $\text{Fe}(\text{Pz})\text{Pt}(\text{CN})_4$  studied by *in-situ* powder diffraction.

Céline Besnard<sup>1</sup>, Delgado Pérez Maria Teresa<sup>2</sup>, Tissot Antoine<sup>3</sup>, Schouwink Pascal<sup>1</sup>

1. Laboratoire de cristallographie, University of Geneva, Switzerland
2. Département de Chimie Physique, University of Geneva, Switzerland
3. INSTITUT LAVOISIER CNRS : UMR8180, Université de Versailles Saint-Quentin-en-Yvelines, France

email: celine.besnard@unige.ch

The Hofmann-chlorate  $\text{Fe}(\text{Pz})\text{Pt}(\text{CN})_4$  has received significant attention due to its spin transition with a large hysteresis at room temperature and the possibility of bidirectional light switching. The spin-crossover behaviour, and hence colour change, can be modulated by means of absorbed gas species<sup>1</sup>, making this family of compounds very attractive materials for the design of gas sensors. The tetragonal crystal structure of both the HS and the LS state is formed by 2D layers of  $\text{Fe}(\text{Pt})(\text{CN})_4$  linked by the pyrazine ligands. In both guest-free HS and LS structure, disordered pyrazine molecules rotate around the Fe-Fe axis. As expected, most bulky guest molecules stabilize the HS state due to steric effects. Interestingly, the reverse was observed for  $\text{C}_3\text{H}_4$ -absorption, which was theoretically attributed to the molecule-specific sorption site, which in this case suppresses the rotational movement of the pyrazine rings<sup>2</sup>.

In order to get a better insight on the chemical sensitivity of the spin crossover properties, we have experimentally studied the effects of different gas molecules of various sizes (ethylene  $\text{C}_2\text{H}_4$ , propadiene  $\text{C}_3\text{H}_2$  and dimethylether  $\text{C}_2\text{H}_6\text{O}$ ) on the thermal spin-crossover transition. The samples were loaded in glass capillaries at a gas pressure of 1 bar, and synchrotron radiation X-ray powder diffraction data were recorded *in-situ* as a function of temperature and applied gas pressure. In agreement with the literature, the unloaded sample undergoes a phase transition with a small hysteresis ( $T_{\text{down}}^{(283)}$  and  $T_{\text{up}}^{(309\text{K})}$ ). While the smallest guest molecule  $\text{C}_2\text{H}_4$  shifts this tetragonal – tetragonal transition by a small  $\Delta T$  ( $T_{\text{down}}^{(265\text{K})}$ ,  $T_{\text{up}}^{(278\text{K})}$ ), the absorption of the larger dimethyl ether and propadiene (loaded at 350K) causes a structural transformation to a monoclinic HS phase, whose structure was solved from the *in-situ* powder diffraction data. In this structure, pyrazine disorder is quenched. Additionally, the spin transition is significantly shifted to lower temperatures ( $T_{\text{down}}^{(207\text{K})}$ ,  $T_{\text{up}}^{(290\text{K})}$  for propadiene and  $T_{\text{down}}^{(250\text{K})}$  for DME)<sup>3</sup>. This exciting results illustrate that the geometry of gas molecules has a large impact on the guest-host interaction even in this very simple member of the Hofmann-family.

1 M. Ohba and others *Angew. Chem. Int. Ed.*, 2009, **48**, 4767–4771. 2 H. Ando and others *Chem. Phys. Lett.*, 2011, **511**, 399–404.

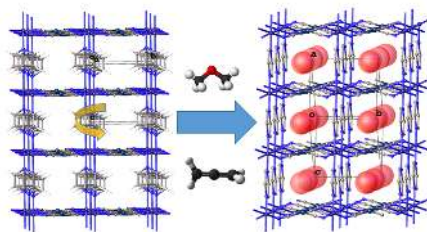


**Figure 1.** The absorption of dimethyl ether and propadiene causes a structural transformation to a monoclinic phase in which the pyrazine rotational disorder is quenched.

**Keywords:** spin crossover, *in situ* powder diffraction, gas sorption

**MS21-O4 Structural disorder in spinel-like nanoparticles probed by total scattering****Keywords:** Spinel Disorder; Total Scattering; Modulation Enhanced DiffractionAntonio Cervellino<sup>1</sup>, Ruggero Frison<sup>2,3</sup>, Lucia Pagliari<sup>4</sup>, Monica Dapiaggi<sup>4</sup>, Norberto Masciocchi<sup>5</sup>, Antonietta Guagliardi<sup>3</sup>

1. Swiss Light Source, Paul Scherrer Institut, CH-5232 Villigen, Switzerland
2. University of Zurich, CH-8057, Zurich, Switzerland
3. Istituto di Cristallografia - CNR and To.Sca.Lab., I-22100 Como, Italy
4. Dipartimento di Scienze della Terra, Università di Milano, I-20133 Milano, Italy
5. Dipartimento di Scienza e Alta Tecnologia and To.Sca.Lab., Università dell'Insubria, I-22100 Como, Italy

email: antonio.cervellino@psi.ch

Nano-crystalline spinel-like oxides are today widely studied because of their application in many different fields like information technology (ferrofluids, data storage), medicine (drug delivery, medical imaging) and chemistry (catalysis) [1]. Within this class Magnetite ( $\text{Fe}_3\text{O}_4$ ) has a prominent role, however, a detailed understanding of some of its structural and micro-structural aspects – especially at the nanoscale – is still missing and the currently proposed structural models are not yet exhaustive of its magnetic properties. As is well-known the  $\text{Fe}^{2+}$  occupying the tetrahedral site is unstable under normal conditions, thus Magnetite is most often observed in a partially oxidised state. We studied the oxidation process of magnetite nano-particles (NP) revealing a partial ordering of the iron vacancies created during the oxidation process, leading to a partial phase transition of the NPs volume. As a second example we studied the cation disorder in the direct spinel Gahnite ( $\text{ZnAl}_2\text{O}_4$ ) at very small NPs sizes, and we observed an important Zn-Al inversion disorder, with an inversion parameter  $x=0.34$ , higher than previously reported [3]. Our studies were performed by means of total scattering X-ray powder diffraction data (collected at the MS-Powder X04SA beamline [4] of the SLS synchrotron at PSI, Villigen, CH) and Debye scattering equation analysis [5]. In addition, for the cation disorder in  $\text{ZnAl}_2\text{O}_4$  we performed for the first time using Total Scattering Anomalous Modulation Enhanced Diffraction [6] measurements at the Zn K-edge.

[1] Laurent S. et al., Chem. Rev., 2008, 108, 2064; Z. Li, S. Zhang, W. E. Lee, J. Eur. Ceram. Soc. 27, 3407, 2007

[2] Morales M. P. et al., Chem. Mat., 1999, 11, 3058.

[3] L. Cornu, M. Gaudon, V. Jubera, J. Mat. Chem. C (2013) 1, 5419-5428

[4] P. R. Willmott, D. Meister, S. J. Leake et al., J. Synchrotron Rad. (2013) 20, 667-682.

[5] A. Cervellino, R. Frison, F. Bertolotti and A. Guagliardi, J. Appl. Cryst. (2015). 48, 2026-2032.

[6] D. Chernyshov, W. van Beek, H. Emerich, M. Milanesio, A. Urakawa, D. Viterbo, L. Palin and R. Caliendo, Acta Cryst. (2011). A67, 327-335

**MS21-O5 Local order in cadmium cyanide.**Arkadiy Simonov<sup>1</sup>, Chloe Coates<sup>1</sup>, Andrew L. Goodwin<sup>1</sup>

1. Oxford University

email: arkadiy.simonov@chem.ox.ac.uk

Local order in cadmium cyanide. Cadmium cyanide  $\text{Cd}(\text{CN})_2$  is a material with exceptionally strong isotropic negative thermal expansion coefficient. This unusual property is currently not well understood, despite a related compound  $\text{Zn}(\text{CN})_2$  was very extensively studied. On the one hand, the negative thermal expansion can be attributed to the effects of vibration modes which include cadmium off-centering. Such modes have negative Grüneisen parameter and thus cause unit cell shrinkage as their amplitude increases. On the other hand, cadmium off-centering can also be caused by crystal disorder. In the average structure of  $\text{Cd}(\text{CN})_2$  cyano groups are disordered by a mirror plane, so each atomic position contain 1:1 mixture of carbon and nitrogen. In the real structure, position of cadmium atoms will be determined by the local orientation of neighboring cyano groups. Thus the volume of the  $\text{Cd}(\text{CN})_2$  crystal is influenced both by short range order and atomic vibrations.

In the current contribution we analyse single crystal diffuse scattering from  $\text{Cd}(\text{CN})_2$ . The crystal shows very strong diffuse scattering in the form of very broad rods along  $\langle 111 \rangle$  type directions and wide planes perpendicular to  $\langle 110 \rangle$  (see figure below). The diffuse scattering is analyzed using three dimensional pair distribution function (3D- $\Delta$ PDF) in the program Yell. The 3D- $\Delta$ PDF method is advantageous in the current case because it allows to investigate both static and dynamic short range order in a unified fashion.

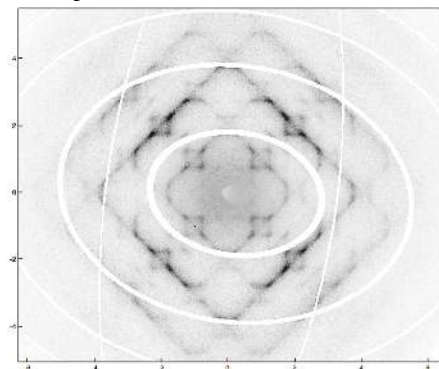


Figure 1. Diffuse scattering from  $\text{Cd}(\text{CN})_2$ ,  $hk\frac{1}{4}$  section.

**Keywords:** diffuse scattering, 3D- $\Delta$ PDF, disorder, local order

**MS22 Beyond multipolar refinement**

Chairs: Alessandro Genoni, Simon Grabowsky

**MS22-O1 Quasi-harmonic Treatment of Thermal Effects on Electron Charge and Momentum Densities of Solids from *Ab initio* Calculations**Alessandro Erba<sup>1</sup>

1. Chemistry Department, University of Torino, via Giuria 5, 10125 Torino (Italy)

email: alessandro\_erba@virgilio.it

The inclusion of thermal effects on computed properties of solids from *ab initio* calculations still represents a challenge to state-of-the-art quantum-chemical methods, particularly so when the limitations of the harmonic approximation (HA) to the lattice potential have to be overcome. When the HA is used, indeed, the vibrational contribution to the free energy of the crystal is assumed to be independent of volume. As a consequence, a variety of physical properties would be wrongly described [1]: null thermal expansion, elastic constants independent of temperature as well as the bulk modulus, equality of constant-pressure and constant-volume specific heats, infinite thermal conductivity as well as phonon lifetimes, etc.

If the explicit calculation of anharmonic phonon-phonon interaction coefficients remains a rather computationally demanding task, with implementations often limited to a molecular, non-periodic context, a simpler, though effective, approach for correcting most of the above mentioned deficiencies of the HA is represented by the so-called quasi-harmonic approximation (QHA) [2].

In this contribution, I discuss a series of *ab initio* techniques, as they have been implemented into the CRYSTAL program, for the inclusion of thermal effects on several (structural, elastic, thermodynamic and electronic) properties of solids beyond the HA, by explicitly accounting for thermal lattice expansion [3-6]. In particular, the QHA is used to study thermal effects on the EMD of crystalline LiF [7]. Preliminary results are also presented of a study where the QHA is applied to compute atomic anisotropic displacement parameters (ADPs) and dynamic X-ray structure factors of the urea molecular crystal, from dispersion-corrected lattice dynamical *ab initio* calculations [8].

**References**

- [1] N. W. Ashcroft and N. D. Mermin, *Solid State Physics*, Saunders College, Philadelphia, USA (1976).
- [2] R. E. Allen and F. W. De Wette, *Phys. Rev.*, **179**, 873-886 (1969).
- [3] A. Erba, *J. Chem. Phys.*, **141**, 124115 (2014)

[4] A. Erba, M. Shahrokhi, R. Moradian and R. Dovesi, *J. Chem. Phys.*, **142**, 044114 (2015)

[5] A. Erba, J. Maul, R. Demichelis and R. Dovesi, *Phys. Chem. Chem. Phys.*, **17**, 11670-11677 (2015)

[6] A. Erba, J. Maul, M. De la Pierre and R. Dovesi, *J. Chem. Phys.*, **142**, 204502 (2015)

[7] A. Erba, J. Maul, M. Itou, R. Dovesi and Y. Sakurai, *Phys. Rev. Lett.*, **115**, 117402 (2015)

[8] A. Erba, J. Maul and B. Civalleri, *Chem. Commun.*, **52**, 1820-1823 (2016)

**Keywords:** thermal effects, quasi-harmonic approximation, ab initio calculations, Compton profiles, ADPs

## MS22-O2 Probability densities in different spaces: when multipolar-atom model is just not enough.

Jean-Michel Gillet<sup>1</sup>, Zeyin Yan<sup>1</sup>, Iurii Kibalin<sup>2</sup>, Bolivard Voufack<sup>3</sup>, Nicolas Claiser<sup>3</sup>, Maxime Deutsch<sup>3</sup>, Beatrice Gillon<sup>2</sup>, Claude Lecomte<sup>3</sup>, Pietro Cortona<sup>4</sup>, Alessandro Genoni<sup>4</sup>, Yoshiharu Sakurai<sup>5</sup>, Masayoshi Itou<sup>5</sup>, Masahisa Itoh<sup>6</sup>, Marek Brancewicz<sup>3</sup>, Naruki Tsuji<sup>3</sup>, Arsen Gukasov<sup>2</sup>, Florence Porcher<sup>2</sup>, Mohamed Souhassou<sup>3</sup>

1. Laboratoire SPMS, UMR CNRS 8580, CentraleSupélec, Université Paris-Saclay, France

2. Laboratoire Léon Brillouin CEA/CNRS, France

3. Laboratoire CRM2, UMR CNRS 7036, Université de Lorraine, France

4. Laboratoire SRSMC, CNRS & Université de Lorraine, France

5. JASRI/ Spring8, Japan

6. Gunma University, Japan

email: Jean-michel.gillet@centralesupelec.fr

In many situations, multipolar-atom refinement model is still the most efficient means of reconstructing charge density in position space from high resolution X-ray diffraction (XRD) data. Furthermore, polarized neutron diffraction (PND), which is a unique technique for the study of unpaired electron in magnetic systems, has also benefited from the great versatility of the multipole on pseudo-atom model. Providing that the description on "magnetic atoms" allows for a differentiation depending on the spin state, we have demonstrated that a **joint analysis** of polarized neutron and X-ray diffraction data is also possible. A wealth of other experimental data has been made available by a development of more powerful sources. For example, magnetic X-ray diffraction (MXRD) or magnetic Compton scattering (MCS) are such techniques that have developed almost independently with the advent of efficient insertion devices in synchrotron facilities. Because MCS relies on an incoherent inelastic process it is better adapted to a representation in momentum space. Such a technique is thus a valuable means for observing the most delocalized unpaired electrons. There have been numerous demonstrations that a mere incoherent addition of atom centred contributions is not well adapted to momentum space description. As a consequence, the ambition to gather data from XRD, PND, MXRD and MCS constitutes a new motivation to explore beyond multipole on pseudo-atom models. The talk will address this new and exciting challenge through our latest results concerning spin and charge densities in YTiO<sub>3</sub>.

Financial support from ANR (MTMED project) and CNRS are gratefully acknowledged.

Ref: "First spin-resolved electron distributions in crystals from combined polarized neutron and X-ray diffraction experiments" IUCrJ (2014), Volume 1, Part 3, Pages 194-199, M. Deutsch, B. Gillon, N. Claier, J.-M. Gillet, C. Lecomte and M. Souhassou,

**Keywords:** X-ray diffraction, polarized neutron diffraction, magnetic Compton scattering, ab-initio computation, charge density, spin density, position space, momentum space, ferromagnet

**MS22-O3** Electron Density of a Layered Transition Metal DichalcogenideHidetaka Kasai<sup>1,2</sup>, Kasper Tolborg<sup>2</sup>, Mattia Sisti<sup>2</sup>, Venkatesha R. Hathwar<sup>2</sup>, Mette O. Filsoe<sup>2</sup>, Simone Cenedese<sup>2</sup>, Kunihiisa Sugimoto<sup>3</sup>, Jacob Overgaard<sup>2</sup>, Eiji Nishibori<sup>1</sup>, Bo B. Iversen<sup>2</sup>

1. Faculty of Pure and Applied Sciences, TIMS and CiRiSE, University of Tsukuba
2. Center for Materials Crystallography, Department of Chemistry and iNANO, Aarhus University
3. Japan Synchrotron Radiation Research Institute

email: kasai.hidetaka@chem.au.dk

Electron density (ED) studies enable us to understand chemical bonding features in materials. While accurate experimental ED has provided information on bonding in a variety of materials, it is still a great challenge to evaluate weak interactions e.g. in layered structures. Layered transition metal dichalcogenides (TMDs) have attracted much attention because of their unique properties e.g. as topological insulators [1], charge density wave systems [2], electrode materials for ion batteries [3], and thermoelectric materials [4]. The generalized formula is  $MX_2$ , where M is a transition metal and X is a chalcogen (S, Se and Te). The layered structure exhibits strong covalent intralayer bonding and weak van der Waals (vdW) interaction between adjacent layers. The weak vdW interaction also enables stacking different TMDs layers [5] as well as application of a monolayer or a few-layer TMDs [6]. Understanding the weak interaction in TMDs is important not only for fundamental science but also for application. Recently the interlayer interaction in  $SnS_2$  was discussed using high pressure techniques [7]. In the present study, we evaluate the weak interlayer interaction in TMDs using experimental X-ray ED. We measured single crystal diffraction data of  $TiS_2$  (Space Group:  $P-3m1$ ) to a resolution of  $\sin\theta/\lambda = 1.67 \text{ \AA}^{-1}$  at 20 K using 50 keV X-ray with the image plate detector at BL02B1 of SPring-8. The ED was modelled with the extended Hansen-Coppens multipole model [8], which includes refinement of core electron density features. In the presentation, we will discuss the weak interlayer interaction based on the ED.

- [1] X. Qian et al., *Science* **346**, 1344 (2014).
- [2] J. Okamoto et al., *Phys. Rev. Lett.* **114**, 026802 (2015).
- [3] A. Unemoto et al., *Chem. Mater.* **27**, 5407 (2015).
- [4] C. Wan et al., *Nature Mater.* **14**, 622 (2015).
- [5] A. K. Geim and I. V. Grigorieva, *Nature* **499**, 419 (2013).
- [6] M. Chhowalla et al., *Nature Chem.* **5**, 263 (2013).
- [7] M. Ø. Filsoe et al., *Dalton Trans.* **45**, 3798 (2016).
- [8] A. Fischer et al., *J. Phys. Chem. A* **115**, 13061 (2011).

**Keywords:** Electron density, layered structure, multipole model**MS22-O4** Experimental Electron Density of Low-Barrier Hydrogen Bonds in  $H_3Co(CN)_6$ Kasper Tolborg<sup>1</sup>, Bo B. Iversen<sup>1</sup>

1. Center for Materials Crystallography, Department of Chemistry, Aarhus University

email: tolborg@chem.au.dk

Hydrogen bonding is the most important directional intermolecular interaction with importance in a wide range of fields across natural science. Electron density studies may quantify hydrogen bonding behavior in compounds with very strong hydrogen bonds and explain their importance for particular properties.

Recent PDF studies on  $H_3Co(CN)_6$ , which has one of the shortest N-H-N hydrogen bonds known in the literature, has shown a significant effect of isotope substitution on the negative thermal expansion (NTE) behavior of the crystals, i.e. the protonated compound has a significantly larger NTE than the deuterated compound [1]. In this study, the experimental electron density distribution in  $H_3Co(CN)_6$  is evaluated using synchrotron single crystal X-ray diffraction and neutron powder diffraction.

Single crystal X-ray diffraction were measured at BL02B1, Spring8, Japan on both protonated and deuterated samples at 20K and 100K with resolutions up to  $1.67 \text{ \AA}^{-1}$ . These are combined with powder neutron diffraction data to get a better description of the hydrogen position and thermal parameters.

The X-ray data have been modelled with the extended Hansen-Coppens multipole formalism [2] and the resulting density is analyzed by the Quantum Theory of Atoms in Molecules. The Co-CN interaction is found to be of intermediate character, with very similar properties as those reported for transition metal carbonyls in the literature [3]. This is interesting, since the formal charges are very different in two cases.

The properties along the bond path for the hydrogen bond is very dependent on the position of hydrogen. A symmetric arrangement as proposed for hydrogen at low temperature, gives two shared interactions very similar to the ones seen for the O-H-O low-barrier hydrogen bond in Benzoylacetone [4], explaining the origin of the negative thermal expansion as arising from a covalently bonded network. An asymmetric arrangement gives more shared character to the donor atom bonding and more closed shell character to the acceptor atom, making the crystal more molecular of nature.

1. Keen, D. A., et al., *J. Phys.: Condens. Matter* **2010**, 22, 404202-404208
2. Fischer, A. et al., *J. Phys. Chem. A* **2011**, 115, 13061-13071
3. Farrugia et al., *J. Phys. Chem. A* **2005**, 109, 8834-8848
4. Madsen et al., *J. Am. Chem. Soc.* **1998**, 120, 10040-10045

**Keywords:** Hydrogen Bonds, Electron Density, Negative Thermal Expansion



## MS22-O5 Electrostatic Potential of Dynamic Charge Densities

Christian B. Hübschle<sup>1</sup>, Sander van Smaalen<sup>1</sup>

1. Laboratory of Crystallography, University of Bayreuth

email: chuebsch@moliso.de

The computer program PRIOR, which is part of the BayMEM suite [1] is able to calculate a dynamic electron density from a multipole model [2]. Such a density or the result of a maximum entropy method (MEM) calculation can be used to calculate a electrostatic potential by a modified version of the PRIOR program.

The idea of the algorithm is based on the reciprocal part of an Ewald summation [3]. The application of the  $U_{ij}$  parameter to the nuclear density in the above equation improves the convergence of the summation so that a calculation in direct space is unnecessary, which make this approach quite fast.

We will show applications to boron and boron rich compounds.

[1] L. Palatinus, S. van Smaalen and M. Schneider. *Acta Crystallogr.* (2003) A59 459-469.

[2] S. Mondal, S. J. Prathapa and S. van Smaalen. *Acta Crystallogr.* (2012) A68 568-581.

[3] P. Ewald (1921). "Die Berechnung optischer und elektrostatischer gitterpotentiale." *Annals Phys.* 64, 253-287.

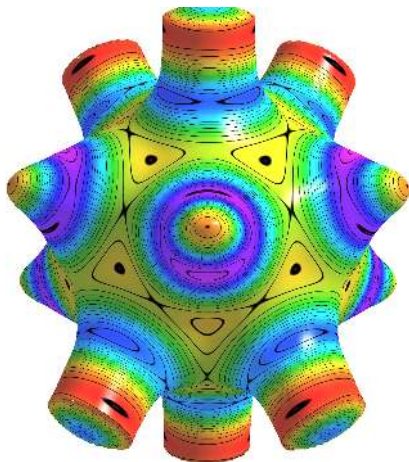


**Figure 1.** Electrostatic potential of the dynamic charge density of  $\alpha$ -boron mapped on an iso density surface.

**Keywords:** electrostatic potential, boron, dynamic density

## MS23 Charge and spin density of materials at extreme conditions

Chairs: Nicola Casati, Philippe Guionneau

### MS23-O1 Anagostic Interactions under Pressure: Attractive or Repulsive?

Wolfgang Scherer<sup>1</sup>

1. Universität Augsburg

email: wolfgang.scherer@physik.uni-augsburg.de

The expression "anagostic interactions" was introduced to distinguish *sterically enforced*  $M\cdots H-C$  contacts ( $M = Pd, Pt$ ) in square-planar transition metal  $d^8$  complexes from *attractive*, agostic interactions. This classification raised the fundamental question whether axial  $M\cdots H-C$  interaction in planar  $d^8-ML_4$  complexes represent (i) repulsive anagostic 3c-4e  $M\cdots H-C$  interactions or (ii) attractive 3c-4e  $M\cdots H-C$  hydrogen bonds.

We reveal, however, that square-planar  $d^8-ML_4$  complexes might display subtle but noticeable *local* Lewis acidic sites in axial direction in the valence shell of the metal atom. These sites of local charge depletion provide the electronic prerequisites to establish **weakly attractive** 3c-2e  $M\cdots H-C$  agostic interactions in contrast to earlier assumptions in the literature (see above). We therefore suggest as a new characterization method to probe the response of these  $M\cdots H-C$  interactions under pressure via combined high pressure IR and diffraction studies [1].

[1] W. Scherer, A. C. Dunbar, J. E. Barquera-Lozada, D. Schmitz, G. Eickerling, D. Kratzert, D. Stalke, A. Lanza, P. Macchi, N. P. M. Casati, J. Ebad-Allah, Ch. Kuntscher, *Angew. Chem. Int. Ed.* **2015**, 54, 2505-2509.

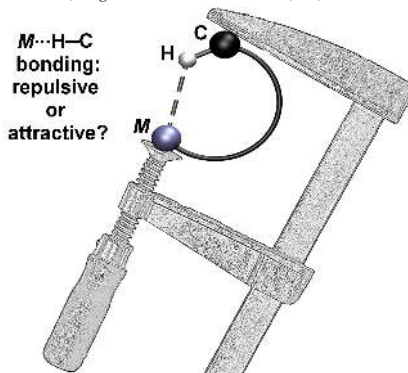




**Figure 1.**

**Keywords:** high pressure, bond activation, agostic interactions, charge density

**MS23-O2 Charge Density Studies of Switchable Molecular Materials at Extreme Conditions: What; How & Why?**

Helena J. Shepherd<sup>1</sup>

1. University of Kent

email: H.J.Shepherd@kent.ac.uk

Spin crossover (SCO) is the phenomenon of switching between high-spin (HS) and low-spin (LS) states shown by certain complexes of first row (d4 - d7) transition metals. It is accompanied by changes in colour, magnetism, optical and mechanical properties of the material, and may be induced by some perturbation such as a change in temperature, light irradiation, pressure, the presence of guest molecules etc. [1]. These characteristics present interesting opportunities for applications in sensing, display and actuating technologies [2]. The subtle electronic redistribution of electron density within these materials results in substantial structural reorganisation of the material, driven by changes in volume of the metal coordination sphere in excess of 25%.

In-situ high pressure and/or light-irradiation during structural studies of SCO materials have created new understanding of this fascinating class of switchable molecular materials, and although by no means routine, incorporation of such extreme conditions into the X-ray diffraction experiment is now reasonably common [3,4]. Charge density studies provide an opportunity to study the coupling between electronic and structural effects in these out-of-equilibrium processes, providing complimentary insights. Combining charge-density studies with extreme conditions, while experimentally very demanding, will allow development of the next generation of materials with improved switchable functionality. This presentation will evaluate the benefits, as well as the challenges, to be encountered in performing these kinds of cutting-edge experiments.

**References:**

- [1] A. Bousseksou et al. Chem. Soc. Rev., 2011,40, 3313-3335
- [2] G. Molnar et al. J. Mater. Chem. C, 2014,2, 1360-1366
- [3] Helena J. Shepherd et al. Phys. Rev. B 84, 144107
- [4] Sébastien Pillet, Helena J. Shepherd et al. Phys. Rev. B 86, 064106

**Keywords:** Extreme Conditions, Charge Density, Functional Molecular Materials

**MS23-O3** Copper-pyrazine magnetic polymers under high pressure

Arianna Lanza<sup>1,2</sup>, Rebecca Scatena<sup>2</sup>, Leonardo H.R. Dos Santos<sup>2</sup>, Mariusz Kubus<sup>3</sup>, Karl W. Krämer<sup>2</sup>, Lukas Keller<sup>3</sup>, Tom Fennell<sup>3</sup>, Björn Wehinger<sup>3</sup>, Alun Biffin<sup>3</sup>, Christian Rüegg<sup>3</sup>, Nicola Casati<sup>1</sup>, Piero Macchi<sup>2</sup>

1. Laboratory of Synchrotron Radiation, Paul Scherrer Institute, Switzerland
2. Department of Chemistry and Biochemistry, University of Bern, Switzerland
3. Laboratory for Neutron Scattering and Imaging, Paul Scherrer Institute, Switzerland

email: arianna.lanza@dcb.unibe.ch

Coordination polymers based on copper ions linked by pyrazine (pyz) and halide bridges are easy to synthesize and crystallize. Depending on the stoichiometry, the counter ions and the reaction conditions, a wide variety of polymers has been obtained, showing different topologies and magnetic properties.[1]

Their characteristics and chemical simplicity make them suitable models for a systematic investigation of the variation of the material properties as a function of composition or pressure-induced structural modifications. Pressure may trigger phase transitions or even chemical reactions in these species. The most commonly observed phenomena are: a) orientational changes of the pyz spacers; b) orbital reordering and consequent re-orientation of the Jahn-Teller distortion; c) attachment/detachment of ancillary ligands. These phenomena (especially orbital reordering) have important consequences for the dimensionality of the magnetic exchange network.[1,2]

Recently, the magnetic properties of some Cu-pyz based materials have been examined and correlated with the topological and integrated properties of their electron and spin density distribution.[3]

In this talk, we will focus on  $[(\text{CuF}_2(\text{H}_2\text{O})_x)(\text{pyz})]$  ( $x=1,2$ ) and  $[(\text{Cu}(\text{pyz})_2\text{X})\text{Y}]$  ( $\text{X}=\text{halide}; \text{Y}=\text{BF}_4^-$ ), investigated up to 15 GPa with single crystal and powder X-ray diffraction and theoretical charge and spin density calculations. The role of the ligands in the super exchange mechanisms and the experimental coupling constants will be rationalized by systematic electron density analysis on the room pressure and high pressure phases.

[1] Lanza, A.; Fiolka, C.; Fisch, M.; Casati, N.; Skoulatos, M.; Rüegg, C.; Krämer, K. W.; Macchi, P. *Chem. Comm.* **2014**, 50, 14504.

[2] Halder, G. J.; Chapman, K. W.; Schlueter J. A.; Manson, J. L. *Angew. Chem.-Int. Ed.*, **2011**, 50, 419.

[3] Dos Santos L.H.R.; Lanza A.; Barton A.M.; Brambleby J.; Blackmore W.J.A.; Goddard P.A.; Xiao F.; Williams R.C.; Lancaster T.; Pratt F.L.; Blundell S.J.; Singleton J.; Manson, J.L.; Macchi, P. *J. Am. Chem. Soc.*, **2015**, 137 (7), 2280.

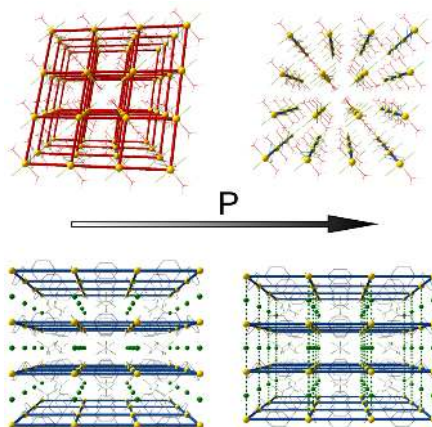


**Figure 1.** High pressure can alter the dimensionality of the magnetic exchange in Cu-pyz based quantum magnets. Thick lines represent magnetic exchange pathways and different colours indicate H-bonds-, pyz- or X- mediated interactions, (in red, blue and green, respectively).

**Keywords:** high-pressure, quantum magnets, spin density

## MS23-O4 Hydrogen maleate salts: Precise and accurate determination of the hydrogen atom position in short hydrogen bonds using X-ray diffraction at extremely low temperatures

Simon Grabowsky<sup>1</sup>, Lorraine Andrade Malaspina<sup>1</sup>, Magdalena Woinska<sup>2</sup>, Eiji Nishibori<sup>3</sup>, Kuniyoshi Sugimoto<sup>4</sup>, Alison J. Edwards<sup>5</sup>, Dylan Jayatilaka<sup>6</sup>

1. The University of Bremen
2. University of Warsaw
3. University of Tsukuba
4. Japan Synchrotron Radiation Research Institute
5. Australian Nuclear Science and Technology Organization
6. The University of Western Australia

email: simon.grabowsky@uni-bremen.de

Hydrogen maleate salts offer the unique opportunity to follow a pseudo-reaction pathway of a proton transfer not only in theoretical simulations but also experimentally because the hydrogen position in the strong and short intramolecular O-H...O hydrogen bond is highly flexible dependent on the cation. There are numerous crystal structures of hydrogen maleate salts in the literature showing that the O...O distance is constant around 2.45 Å, but the O-H distances vary from 0.83 Å/1.63 Å in highly asymmetric hydrogen bonds to 1.22 Å in symmetric hydrogen bonds with a large variety of intermediate distances. This means that snapshots along a pseudo-reaction pathway can be measured and with the symmetric hydrogen bonds, even a model for a possible transition state is accessible. Experimental electron-density modelling of high-resolution low-temperature (20 K) synchrotron X-ray data of nine different compounds (4-aminopyridinium, 8-hydroxyquinolinium, barium, calcium, potassium, lithium, magnesium, sodium and phenylalaninium hydrogen maleates) measured at SPring-8, Japan, will give electronic information on the pseudo-reaction mechanism.

For these detailed electron-density analyses, it is crucial to obtain accurate positional and displacement parameters of the hydrogen atoms. It is a widespread notion that this can only be achieved using neutron-diffraction techniques. Therefore we have collected Laue-diffraction neutron data at the Bragg institute of ANSTO, Australia. Using those data as a reference, we will show that we can obtain hydrogen atom positions and bond lengths involving hydrogen atoms with the same accuracy and precision from X-ray data as from neutron data - even from X-ray data of routinely achievable resolution - if an advanced X-ray refinement technique is used. This new technique is called Hirshfeld Atom Refinement (HAR) [1].

[1] S. C. Capelli, H.-B. Bürgi, B. Dittrich, S. Grabowsky, D. Jayatilaka: Hirshfeld atom refinement. *IUCr* 2014, 1, 361-379.

**Keywords:** hydrogen maleate salts, Hirshfeld atom refinement, hydrogen atom parameters from X-ray diffraction

## MS23-O5 Charge density of the semiquinone radical anion

Krešimir Molčanov<sup>1</sup>, Christian Jelsch<sup>2</sup>, Emmanuel Wenger<sup>2</sup>, Vladimir Stilinović<sup>3</sup>, Biserka Kojić-Prodić<sup>1</sup>

1. Rudjer Bošković Institute
2. Université de Lorraine
3. Faculty of Science, University of Zagreb

email: kmolcano@irb.hr

Semiquinones are a class of stable organic radical anions; especially stable are ones with four electronegative substituents such as halogens, which enhance delocalisation of the unpaired electron. Therefore, they are potential candidates for design of functional materials with fine-tuned magnetic properties.

Here we present a detailed study of electron density and delocalisation in two polymorphs of N-methylpyridinium (N-MePy) salt of tetrachlorosemiquinone (CA) radical anion (N-MePy·CA), which are especially interesting due to their stability and semiconductivity [1]. In the diamagnetic polymorph closely bound radical dimers occur, similar to previously known K·CA·Me<sub>2</sub>CO [2] and similar alkali salts of 5,6-dichloro-2,3-dicyanosemiquinone (DDQ) [3], and the crystals are diamagnetic due to spin pairing. In the orthorhombic polymorph radicals are equidistant, leading to 1D antiferromagnetic coupling between the spins.

Electronic delocalisation in the semiquinones is particularly interesting because it is somewhere between aromatic (fully delocalised  $\pi$  electrons) and quinoid (distinguishable single and double bonds), as confirmed by previous crystallographic [2,3] and computational studies. However, exact bond orders of C-C and C-O bonds have not yet been experimentally determined. Also, study of charge density reveals subtle differences between diamagnetic (triclinic) and antiferromagnetic (orthorhombic) phases, which will enable more insight into the phenomenon of magnetic exchange between organic molecules.

This is the first experimental study of electronic structure of ionic semiquinones and is complemented by periodic DFT studies.

[1] K. Molčanov, V. Stilinović, N. Maltar-Strmečki, A. Šantić, B. Kojić-Prodić, D. Pajić, L. Androš Dubraja, presentation on the ECM29 (Rovinj, Croatia, 2015), *Acta Crystallogr. A*, **A71**, s136.

[2] K. Molčanov, B. Kojić-Prodić, D. Babić, D. Žilić, B. Rakvin, *CrystEngComm*, **13** (2011), 5170.

[3] K. Molčanov, D. Babić, B. Kojić-Prodić, J. Stare, N. Maltar-Strmečki, L. Androš, *Acta Crystallogr. B*, **70** (2014), 181.

**Keywords:** semiquinone radical, charge density, spin coupling, electron delocalisation

## MS24 Inorganic and metal-organic magnetic structures

Chairs: Georg Eickerling, Bo Iversen

### MS24-O1 Elucidating the magnetic behaviour of a unique linear Fe(I)-complex using the electron density

Jacob Overgaard<sup>1</sup>, Maja K. Thomsen<sup>1</sup>, Phil Bunting<sup>2</sup>, James P.S. Walsh<sup>1,3</sup>, Jeffrey R. Long<sup>2</sup>

1. Department of Chemistry, Aarhus University, Denmark

2. Department of Chemistry, University of California, Berkeley, USA

3. Department of Chemistry, Northwestern University, Evanston, USA

email: jacob@chem.au.dk

Single-molecule magnets (SMM) are able to preserve an induced magnetization after external magnetic field, but in contrast to the domains that explain magnetism in bulk ferromagnets, in SMMs this has a purely molecular origin. Such tiny magnets are naturally in high demand as they have potential technological applications in e.g. spin-based electronics. Lanthanide-based SMMs offer promising candidates for this purpose.<sup>1</sup> However, cheap and earth-abundant metals such as iron are obviously desirable alternatives to lanthanide-based materials. The SMM behaviour is due to a bi-stable magnetic ground state ( $\pm M_{J_{\text{gs}}}$ ) in which the two levels are separated by an energy barrier, thus a barrier hindering magnetic relaxation. The presence of such a barrier is due to molecular magnetic anisotropy, which for a transition metal complex can be tuned through variation of the ligand field. The premier mononuclear transition metal-based SMM so far discovered took combines two unusual features of an iron complex, namely two-coordinate Fe(I),<sup>2</sup>  $[\text{Fe}(\text{C}(\text{SiMe}_3)_5)]^-$  (Figure 1). This complex has a record high effective relaxation barrier ( $U = 226(4) \text{ cm}^{-1}$ ). Based on *ab initio* calculations the authors found that the low coordination number and the low oxidation state result in a very weak ligand field and also find that the  $d_{z^2}$ -orbital is lower in energy than the other  $d$ -orbitals. This is unexpected from a basic crystal field theory viewpoint. We have therefore derived the experimental electron density of this compound, as well as its di-valent analogue, and in this presentation we use these densities to discuss and assess the molecular magnetic properties.

[1] See, for example: Meihaus, K. R. and Long, J. R., *J. Amer. Chem. Soc.*, **2013**, *135*, 17952–17957.

[2] Zadrozny, J. M., Xiao, D. J., Atanasov, M., Long, G. J., Grandjean, F., Neese, F., Long, J. R., *Nature Chem.*, **2013**, *5*, 577-581.



**Figure 1.** ORTEP drawing of the  $[\text{Fe}(\text{C}(\text{SiMe}_3)_5)]^-$  anion at 100 K. Atoms are depicted as 50 % probability ellipsoids. Orange, petrol blue and grey refer to iron, silicon and carbon, respectively. Hydrogen atoms have been omitted for clarity.

**Keywords:** Electron density, single molecule magnet, synchrotron radiation, topological analysis

**MS24-O2 Spin, charge and momentum densities of YTiO<sub>3</sub> perovskite**

Mohamed Souhassou<sup>1</sup>, Voulack Bolivard<sup>1</sup>, Nicolas Claïser, Maxime Deutsch, Claude Lacomte, Jean Michel Gillet<sup>2</sup>, Pietro Cortona<sup>2</sup>, Zeyin Yan<sup>2</sup>, Iurii Kibalin<sup>3</sup>, Béatrice Gillon<sup>3</sup>, Florence Porcher<sup>3</sup>, Arsen Gukasov<sup>3</sup>, Yoshiharu Sakurai<sup>4</sup>, Masayoshi Ito<sup>4</sup>, Masahisa Itoh<sup>5</sup>

1. CRM2 Université de Lorraine Nancy France
2. Laboratoire SPMS, CentraleSupélec, Université Paris-Saclay, France
3. Laboratoire Leon Brillouin, CEA/CNRS, France
4. JASRI/ SPring8, Japan
5. Gunma University, Japan

email: Mohamed.Souhassou@univ-lorraine.fr

High resolution X-ray (XRD) and polarized neutron diffractions (PND) are routinely used to model charge and spin densities of localized electrons, while inelastic Compton scattering (ICS) is a valuable mean for determining delocalized electrons. Our objective is to construct a unique electron density model common to these three experimental data sets. We have demonstrated that a joint refinement of a multipolar model based on polarized neutron and X-ray diffraction data is possible and brings more insight in the electron distribution [1]. The inclusion of ICS data implies to go beyond the atom centered model to take into account bicentric terms. As the multipolar model is thus no more adapted, a new model based on atomic orbitals under development will be discussed and applied to a YTiO<sub>3</sub> perovskite crystal. This compound is ferromagnetic at low temperature (below 29K), suggesting that a single d electron (0.84mB/mol) mainly localized on the Ti atom gives rise to the magnetic interactions.

Reference 1. "First spin-resolved electron distributions in crystals from combined polarized neutron and X-ray diffraction experiments". Maxime Deutsch, Béatrice Gillon, Nicolas Claïser, Jean-Michel Gillet, Claude Lecomte, and Mohamed Souhassou, *IUCrJ*. 2014 May 1; 1(Pt 3): 194–199.

**Keywords:** charge spin densities , xray diffraction, polarised neutron diffraction, magnetic compton scattering, joint refinement, magnetic materials

**MS24-O3 New antiferromagnets [CuX(pyz)<sub>2</sub>](BF<sub>4</sub>) with X = Cl and Br.**

Mariusz Kubus<sup>1,2</sup>, Arianna Lanza<sup>2</sup>, Nicola Casati<sup>3</sup>, Piero Macchi<sup>2</sup>, Lukas Keller<sup>1</sup>, Christoph Fiolka<sup>2</sup>, Jürg Schefer<sup>1</sup>, Christian Rüegg<sup>1</sup>, Karl Krämer<sup>2</sup>

1. Laboratory for Neutron Scattering and Imaging, Paul Scherrer Institute, CH-5232 Villigen PSI, Switzerland
2. Department of Chemistry and Biochemistry, University of Bern, Freiestrasse 3, CH-3012 Bern, Switzerland
3. Laboratory for Synchrotron Radiation – Condensed Matter, Paul Scherrer Institute, CH-5232 Villigen PSI, Switzerland

email: mariusz.kubus@psi.ch

The structures of new compound [CuX(pyz)<sub>2</sub>](BF<sub>4</sub>) with X = Cl<sup>-</sup> and Br<sup>-</sup> and pyz = pyrazine were determined by single crystal X-ray diffraction. These tetragonal compounds crystallize in space group *P4/nbm*. They are built from [Cu(pyz)<sub>2</sub>]<sup>2+</sup> layers which are connected by X<sup>-</sup> ions along the *c*-axis. Charge is compensated by BF<sub>4</sub><sup>-</sup> ions in the voids of the 3D coordination compound. The antiferromagnetic interactions between the Cu<sup>2+</sup> ions are mainly two-dimensional (2D) located within the [Cu(pyz)<sub>2</sub>]<sup>2+</sup> layers. This results in a broad maximum of the magnetic susceptibility around 9 K. Towards lower temperature a kink is observed at 4 K which indicates long-range 3D magnetic order. The magnetic unit cell is doubled along the *c*-axis (*k* = 0,0,1/2) and the ordered magnetic moment amounts to  $\mu_x = 0.76(8) \mu_B/\text{Cu}^{2+}$  at 1.5 K. The moments are antiferromagnetically coupled along the *b*- and *c*-axes. Long-range 3D magnetic order is observed below  $T_N = 3.9(1)$  K. A fit of a 2D Heisenberg model to the magnetic susceptibility data results in  $J_{||} = 9.6$  K.

**Keywords:** 2D antiferromagnet, copper, pyrazine, DMC, XRD, ESR

**MS24-O4 Structural and magnetic properties of the low dimensional fluoride** **$\beta\text{-FeF}_3 \cdot 3\text{H}_2\text{O}$** 

Stjepan Prugovečki<sup>1</sup>, Gwilherm Nénert<sup>1</sup>, Oscar Fabelo<sup>2</sup>, Kerstin Forsberg<sup>3</sup>, Claire V. Colin<sup>4</sup>, Juan Rodríguez-Carvajal<sup>2</sup>

1. PANalytical B.V., Twentepoort Oost 26, 7609 RG Almelo
2. Institut Laue Langevin, 71 Avenue des Martyrs, 38000 Grenoble, France
3. School of Chemical Science and Engineering, Royal Institute of Technology, Teknikringen 42, SE 100 44 Stockholm, Sweden
4. Institut Néel, 25 rue des martyrs, BP 166, 38042 Grenoble, France

email: stjepan.prugovecki@panalytical.com

The anisotropy inherent in low-dimensional (1-D) solid-state compounds leads to a variety of interesting magnetic, electronic, and optical properties, with applications including single-chain magnets for data storage, (1) multiferroics for bifunctional materials (2,3) and nonlinear optical materials for second harmonic generation (4,5). Certain types of 1-D materials containing isolated chains exhibit nearly ideal magnetic properties, acting as experimental models for Ising and Heisenberg spin chains, furthering our understanding of magnetic exchange in highly correlated systems (6). One of the strategies for building these 1-D magnetic materials is to incorporate small one- or three-atom linkers between magnetic centers to facilitate exchange along the chains or networks (7,8). Many of these compounds are known, but very few have been created using iron centers, and most rely on relatively large bridging ligands to separate the magnetically coupled components within the structure. We report on the structural and magnetic properties of the low-dimensional fluoride  $\beta\text{-FeF}_3 \cdot 3\text{H}_2\text{O}$  using SQUID magnetometry, X-ray and neutron diffraction. The structure consists of 1D-chains of corner-linked  $\text{Fe}[\text{F}_4(\text{H}_2\text{O})_5]$  octahedra running parallel to [001] and isolated water molecules. A dense network of hydrogen bonds strongly connects the Fe-F chains. The structural formula is  $\text{Fe}[\text{F}_{0.5}(\text{H}_2\text{O})_{0.5}]_4 \cdot 4\text{H}_2\text{O}$ . This material exhibits a very pronounced 1D character with a very broad maximum around 150 K in the magnetic susceptibility. Below  $T_N = 20$  K, long range magnetic order appears characterized by  $k = (0 \ 0 \ 1/2)$ . From magnetic susceptibility, the intrachain magnetic coupling is estimated to be 18 K, while the interchain magnetic interaction is estimated to be about 3 K. We discuss this non negligible interchain coupling in light of the crystal structure of this material.

- (1) Zhang, W.-X.; et al., RSC Adv. 2013, 3, 3772–3798.
- (2) Xu, G. C.; et al. J. Am. Chem. Soc. 2010, 132, 9588–9590.
- (3) Xu, G. C.; et al. J. Am. Chem. Soc. 2011, 133, 14948–14951.
- (4) Kandasamy, et al. Cryst. Growth Des. 2007, 7, 183–186.
- (5) Anbuezhayan, M. et al. Mater. Res. Bull. 2010, 45, 897–904.
- (6) Coulon, C.; et al. R. In Single-Molecule Magnets and Related Phenomena; Winpenny, R., Ed.; Springer-Verlag: Berlin, Germany, 2006
- (7) Wang, X.-Y.; et al. Chem. Commun. 2008, 281–294.

- (8) Sun, H.-L.; Wang, et al. Coord. Chem. Rev. 2010, 254, 1081–1100.
- (9) G. Nénert, et al., Dalton Transactions 44 (31), 14130–14138

**Keywords:** 1-D magnetic materials , X-ray diffraction, neutron diffraction, interchain coupling

## MS24-O5 Synthesis and Characterization of Asymmetric Tetranuclear Nickel Chains without Disordered Ligand Phenomenon in Crystallography

Lien-Hung Tsou<sup>1</sup>, Marc Sigrist<sup>2</sup>, Ming-Hsi Chiang<sup>2</sup>, Er-Chien Horng<sup>1</sup>, Chun-hsien Chen<sup>1</sup>, Gene-Hsiang Lee<sup>1</sup>, Shie-Ming Peng<sup>1,2</sup>

1. Department of Chemistry, National Taiwan University, No. 1, Sec. 4, Roosevelt Rd., Taipei, Taiwan (R.O.C.)  
2. Institute of Chemistry, Academia Sinica, 128 Academia Road, Section 2, Nankang, Taipei, Taiwan (R.O.C.)

email: d01223123@ntu.edu.tw

The new ligand, 2-(2-(5-phenylpyridyl)amino)-1,8-naphthyridine (Hphpyany), was synthesized by the reaction of 2-chloro-1,8-naphthyridine with 2-amino-5-phenylpyridine in the presence of potassium *tert*-butoxide under palladium(0)-catalyzed condition. The linear tetranickel metal complexes,  $[Ni_4(\text{phpyany})_4(\text{Cl})_2](\text{CF}_3\text{SO}_3)_2$  **1**,  $[Ni_4(\text{phpyany})_4(\text{Cl})_2](\text{BF}_4)_2$  **2**,  $[Ni_4(\text{phpyany})_4(\text{NCS})_2](\text{ClO}_4)_2$  **3** and  $[Ni_4(\text{phpyany})_4(\text{NCS})_2](\text{CF}_3\text{SO}_3)_2$  **4** were synthesized and have been crystallographically characterized. All of the complexes consist of four phpnyan<sup>-</sup> ligands, wrapped around a linear tetranickel core, in the same orientation. The remarkably short Ni-Ni distances (ca. 2.33 Å) for **1** and **3** indicate partial metal-metal bonding, which can be viewed as both complexes containing one mixed-valence  $Ni_2^{3+}$  unit. Magnetic susceptibility measurements reveal that the  $Ni_4^{2+}$  complexes exhibit antiferromagnetic interactions ( $J = -42 \text{ cm}^{-1}$  for **1** and  $-46 \text{ cm}^{-1}$  for **3**) between the  $Ni^{2+}$  and the  $Ni_2^{3+}$  units, while the  $Ni_4^{2+}$  complexes **2** and **4** exhibit antiferromagnetic interactions ( $J = -33 \text{ cm}^{-1}$  for **2** and  $-35 \text{ cm}^{-1}$  for **4**) between the two terminal  $Ni^{2+}$  ions. The results of the cyclic voltammetry indicate the presence two reversible redox couples at  $E_{1/2}^{(1)} = 0.07 \text{ V}$ ,  $E_{1/2}^{(2)} = -0.80 \text{ V}$  for **1**, and at  $E_{1/2}^{(1)} = 0.12 \text{ V}$ ,  $E_{1/2}^{(2)} = -0.74 \text{ V}$  for **3**. The products of the oxidation process  $E_{1/2}^{(1)}$  of **1** and **3** are the corresponding oxidized species **2** and **4**, respectively. The value of conductance is  $9.39 (\pm 0.301) \times 10^{-4} G_0$  and the value of resistance is  $13.7 (\pm 4.4) \text{ M}\Omega$  for **4** were measured by means of the STM break-junction. This represents the first conductance measurement of a linear tetranickel chain.

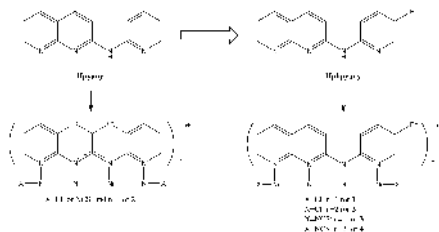


**Figure 1.** Crystallographic disordered ligand on C and C' (left bottom) and schematic diagram for complexes **1**, **2**, **3** and **4** (right bottom).

**Keywords:** Metal-metal interactions, Nitrogen ligands, Electrochemistry, Magnetic properties, Single molecular conductance

## MS25 Quasicrystal and approximant: structure and properties

Chairs: Cesar Pay Gomez, Emilie Gaudry

### MS25-O1 Computational Self-Assembly of Complex Crystals

Julia Dshemuchadse<sup>1</sup>, Michael Engel<sup>1,2</sup>, Pablo F. Damasceno<sup>3,4</sup>, Carolyn L. Phillips<sup>4,5</sup>, Sharon C. Glotzer<sup>1,4,6,7</sup>

1. Department of Chemical Engineering, University of Michigan, Ann Arbor, Michigan, USA
2. Department of Chemical and Biological Engineering, Friedrich-Alexander-Universität Erlangen-Nürnberg, Erlangen, Germany
3. Department of Cellular and Molecular Pharmacology, University of California, San Francisco, California, USA
4. Applied Physics Program, University of Michigan, Ann Arbor, Michigan, USA
5. Argonne National Laboratory, Argonne, Illinois, USA
6. Department of Materials Science and Engineering, University of Michigan, Ann Arbor, Michigan, USA
7. Biointerfaces Institute, University of Michigan, Ann Arbor, Michigan, USA

email: djulia@umich.edu

Complex structures can be found in all classes of materials and across multiple length scales. We seek to understand why and how these geometries arise – both aperiodic ones [1], as well as periodic structures with hundreds or thousands of atoms or particles per unit cell (e.g., [2]). We computationally study particles interacting via isotropic pair potentials and analyze the structures into which they self-assemble. We simulate a wide range of systems using the highly parallel molecular dynamics code HOOMD-blue [3], tuning different system parameters and observing the variation in the thermodynamic crystal phases. We report a rich variety of self-assembled structures, ranging from the expected and well-known sphere packings and other simple structure types, to giant-unit cell structures and quasi-crystals [1]. The resulting phase diagrams and selected structures will be presented – some that are ubiquitous in atomic systems, as well as previously unknown ones.

[1] M. Engel, P. F. Damasceno, C. L. Phillips, S. C. Glotzer, *Nature Mater.* **14**, 109-116 (2015).

[2] J. Dshemuchadse, D. Y. Jung, W. Steurer, *Acta Crystallogr. B* **67**, 269-292 (2011).

[3] J. A. Anderson, S. C. Glotzer, <http://arXiv.org/abs/1308.5587> (2013). <http://codeblue.umich.edu/hoomd-blue>

**Keywords:** soft matter crystallography, complex structures, aperiodic structures, self-assembly



**MS25-O2** Magnetic properties of Au-based Tsai-type approximantsRyuji Tamura<sup>1</sup>

1. Department of Materials Science and Technology, Tokyo University of Science

email: tamura@rs.noda.tus.ac.jp

The discovery of the icosahedral quasicrystals (QCs) [1] has shed light on the existences of closely-related crystals called “approximants”, which are also made of the same icosahedral clusters found in QCs. Tsai-type approximants containing rare-earth (R) icosahedra are of particular interest in view of their magnetic properties since they provide unique localized spin systems, i.e., periodic arrangement of R spin icosahedra. As a result of extensive investigations on a number of binary and ternary Tsai-type approximants, various magnetic orders including antiferromagnetic, ferromagnetic and spin-glass transitions have been observed and the origin of such different behaviours has now become an interesting issue. Moreover, recently, a composition-driven spin glass to ferromagnetic transition has been observed in Au-Al-Gd [2], which indicates that the magnetic order of approximants is governed by the oscillating nature of the RKKY interaction. This observation will give us a hint on how to tune the magnetic order of approximants as well as QCs. In this talk, we will give an overview of the magnetic transition phenomena in the approximants composed of R spin icosahedra and discuss the behaviours of spin icosahedra embedded in a bcc lattice, in terms of the RKKY interaction, local anisotropy and frustration. Recent new findings will be also presented.

[1] D. Shechtman, *et al.*, *Phys. Rev. Lett.* 53, 1951 (1984).

[2] A. Ishikawa *et al.*, *Phys. Rev. B* 93, 024416 (2016).

**Keywords:** quasicrystal, approximant, magnetism

**MS25-O3** Atomic structure and phason modes of the Sc-Zn icosahedral quasicrystal

Marc de Boissieu<sup>1,2</sup>, Tusnetomo Yamada<sup>3</sup>, Hiroyuki Takakura<sup>4</sup>,  
Holger Euchner<sup>5</sup>, Cesar Pay-Gomez<sup>6</sup>, Alexey Bosak<sup>7</sup>, Pierre  
Fertey<sup>8</sup>

1. Univ. Grenoble Alpes, SIMAP, F-38000, Grenoble, France
2. CNRS, SIMAP, F-38000, Grenoble, France
3. IMRAM, Tohoku University, Miyagi 980-8577, Japan
4. Division of Applied Physics, Faculty of Engineering, Hokkaido University, Hokkaido 060-8628, Japan,
5. Institute of Materials Science and Technology, Vienna University of Technology, Vienna 1040, Austria
6. Department of Chemistry, Ångström Laboratory, Uppsala University, Uppsala 751 21, Sweden
7. ESRF-The European Synchrotron, Grenoble F-38000, France,
8. Synchrotron SOLEIL, Gif-sur-Yvette F-91192, France,

email: marc.de-boissieu@simap.grenoble-inp.fr

The detailed atomic structure of the binary icosahedral i-ScZn<sub>7/33</sub> quasicrystal has been investigated by means of high-resolution synchrotron single-crystal X-ray diffraction and absolute scale measurements of the diffuse scattering. The average atomic structure has been solved using the measured Bragg intensity data based on a six dimensional model that is isostructural to the i-YbCd<sub>7/33</sub> one. The structure is described with a quasiperiodic packing of large Tsai-type rhombic triacontahedron clusters and double Friauf polyhedra (DFP), both resulting from a close-packing of a large (Sc) and a small (Zn) atom. The difference in chemical composition between i-ScZn<sub>7/33</sub> and i-YbCd<sub>7/33</sub> was found to lie in the icosahedron shell and the DFP where in i-ScZn<sub>7/33</sub> chemical disorder occurs on the large atom sites, which induces a significant distortion to the structure units. The intensity in reciprocal space displays a substantial amount of diffuse scattering with anisotropic distribution, located around the strong Bragg peaks, that can be fully interpreted as resulting from phason fluctuations, with a ratio of the phason elastic constants  $K_2/K_1 = -0.53$ , i.e. close to a three-fold instability limit. This induces a relatively large perpendicular (or phason) Debye-Waller factor, which explains the vanishing of “high-Q<sub>perp</sub>” reflections.

**Keywords:** quasicrystals, structure, phasons

## MS25-O4 The oxidic two-dimensional quasicrystal and its approximant: X-ray analysis of the atomic structure

Holger L. Meyerheim<sup>1</sup>, Sanjiev K. Nayak<sup>2</sup>, Rene Hammer<sup>2</sup>,  
Sumalay Roy<sup>1</sup>, Waheed Adeagbo<sup>2</sup>, Stefan Förster<sup>2</sup>, Katayoon  
Mohseni<sup>1</sup>, Wolfram Hergert<sup>2</sup>, Wolf Widra<sup>1,2</sup>

1. Max-Planck-Institut f. Mikrostrukturphysik, Weinberg 2,  
D-06120 Halle/S. (Germany)

2. Institut f. Physik, Martin-Luther-Universität Halle-Wittenberg,  
D-06099 Halle/S. (Germany)

email: hmeyerhm@mpi-halle.mpg.de

Very recently a new type of quasicrystal has been discovered based on an oxide phase, closely related to barium titanate ( $\text{BaTiO}_3$ ) [1]. The two-dimensional (2D) oxide quasicrystal (OQC) and its periodic approximant (AP) were grown in situ under ultra-high vacuum conditions on Pt(111) and investigated by scanning tunneling microscopy (STM) which provided clear evidence for the presence of different tilings. For both, the OQC and the AP only one kind of protrusion could be observed by STM which are arranged in a 2D pattern identified as Stampfli-Gähler tiling [2,3] for the OQC and the Kepler tiling [4] for the AP, respectively. The tiling of the AP is composed of squares and triangles while in the OQC also rhombs exist. The tilings are fundamental to distinguish between the OQC and the AP. Despite the precise analysis of the tilings, their metric and the approximate stoichiometry of the phases, no detailed structural information is available on the atomic scale. For instance, a straightforward assignment of the protrusions observed in STM to one of the atomic species (Ba, Ti, O, Pt) is not possible. To this end we have carried out a surface x-ray diffraction study to elucidate the geometric structure of the AP which also allows to develop a model for the OQC structure.

Figure 1 shows the z-projected charge density contour plot calculated on the basis of 44 superlattice reflections. Four unit cells with lattice parameters  $a=13.1$  Å,  $b=12.9$  Å,  $\gamma=90.5^\circ$  are shown. Superimposed are the approximate atomic positions derived from the least squares fit ( $R=13\%$ ). We find that the protrusions observed by STM are related to titanium atoms (blue) which are surrounded by three oxygen atoms approximately forming a triangle. Furthermore, barium atoms (yellow) are located at the origin of the unit cell (plane group  $p2$ ). Further barium atoms are located in the vicinity of two out of four edges of the squares (triangles) leading to  $\text{BaTiO}_3$  stoichiometry if no vacancies are present. The relation of the AP to the OQC structure will be discussed.

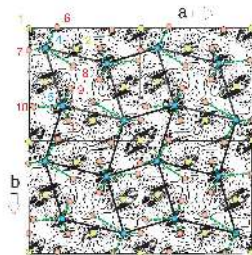


**Figure 1.** Z-projected charge density contour plot  $\rho(x,y)$  of the approximant structure showing four unit cells. The Kepler tiling is indicated by the solid black lines.

**Keywords:** Oxide Quasicrystal, Approximant, Surface x-ray diffraction, Bariumtitanate

[1] S. Förster, K. Meinel, R. Hammer, M. Trautmann, and W. Widra, *Nature* 502, 215 (2013)

[2] P. Stampfli, *Helv. Phys.* 59, 1260 (1986)

[3] F. Gähler in: *Quasicrystalline Materials* (World Scientific, 1988)

[4] J. Kepler: *Harmonices Mundi* (1619)

The authors acknowledge support and hospitality of the ESRF staff during their stay in Grenoble. This work is supported by the Deutsche Forschungsgemeinschaft (DFG) through SFB 762.

**MS25-05** Z-module dislocations in complex intermetallic phasesAbdullah Sirindil<sup>1</sup>, Loïc Perrière<sup>2</sup>, Sylvie Lartigue-Korinek<sup>2</sup>,  
Marianne Quiquandon<sup>1</sup>, Richard Portier<sup>1</sup>, Denis Gratias<sup>1</sup>

1. IRCP Chimie-Paristech, 11 rue Pierre et Marie Curie, 75005 Paris FRANCE

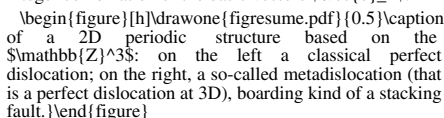
2. ICMPE - CNRS 2-8, rue Henri Dunant - 94320 THIAIS-FRANCE Thiais, France

email: abdullah.sirindil@chimie-paristech.fr

Several intermetallic phases have structures where the atoms are located on the sites of a Z-module, i.e. at positions  $\sim \mathbf{x}_i$  that are linear integer combination of  $N > d$  vectors  $\sim \mathbf{e}_k$  arithmetically independent, where  $d$  is the dimension of the physical space:

$$\mathbf{x}_i = \sum_{k=1}^N n_i^k \mathbf{e}_k$$

These structures are best analyzed as cuts of large periodic objects in a space of dimension  $N > d$ . These objects can carry high dimensionnal  $N$ -dim dislocations the Burgers vectors of which are linear integer combination of the basic vectors  $\mathbf{e}_k$ .

Example of a 2D periodic structure based on the  $\mathbb{Z}^3$  module on the left a classical perfect dislocation; on the right, a so-called metadislocation (that is a perfect dislocation at 3D), boarding kind of a stacking fault.

We shall illustrate on simples examples the basic properties of these  $\mathbb{Z}$ -module dislocations also designated by  $\{\text{it metadislocations}\}$ , as a function of the relative values of the rank  $N$  of the module and the dimension  $d$  of the physical space. In particular, when the  $\mathbb{Z}$ -module is superabundant, it is possible to build original dislocations the Burgers vector of which is entirely perpendicular to the physical space. These metadislocations are therefore insensitive to any stress fields and behave thus as "scalar" as we shall denominate them. These new defects will be exemplified in simple low dimensional cases.

**Keywords:** approximants, Z-modules, dislocations**MS26** Incommensurate modulated and composite phases

Chairs: Michal Dusek, Artem Abakumov

**MS26-01** Incommensurate charge order and charge-density wavesSander van Smaalen<sup>1</sup>

1. University of Bayreuth, Laboratory of Crystallography

Example: sander.van\_smaalen@uni-bayreuth.de

Charge order is an important phenomenon in functional materials. For example, in doped manganites,  $\text{Mn}^{3+}/\text{Mn}^{4+}$  charge order is intimately connected with the colossal magnetoresistance effect [1]. In magnetite ( $\text{Fe}_3\text{O}_4$ ), low-temperature  $\text{Fe}^{2+}/\text{Fe}^{3+}$  charge order has been shown to involve a pattern of trimers  $\text{Fe}^{3+}-\text{Fe}^{2+}-\text{Fe}^{3+}$  and isolated  $\text{Fe}^{2+}$  in a supercell of the cubic spinel structure type of magnetite [2]. Several types of interactions may drive a material into the charge-order state. On the other hand, a charge-density wave (CDW) was originally believed to occur exclusively by the Peierls mechanism in so-called quasi-one-dimensional (1D) electronic crystals containing weakly interacting metallic chains. Nesting by a single  $\mathbf{q}$  vector of flat, co-planar portions of the Fermi surface drive the system into a charge-modulated state with wave vector  $\mathbf{q}$ , which is generally incommensurate to the crystal lattice [3]. The CDW is intrinsically coupled to a periodic lattice distortion (PLD) of the same period, which can easily be measured by diffraction techniques. This simple interpretation of the CDW state has recently been questioned, and the role of electron-phonon interactions has been stressed. Alternative mechanisms will be required for so-called strongly coupled CDW systems, which lack an obvious anisotropy of their metallic electrical conductivity, like  $\text{RNiC}_2$ ,  $\text{R}_2\text{Ir}_2\text{Si}_{10}$ ,  $\text{R}_2\text{Ir}_2\text{Si}_4$  and  $\text{CuV}_2\text{S}_4$  ( $\text{R}$  = rare earth element) [4,5]. Here, I will discuss the crystallography of charge-ordered and CDW systems, with particular emphasis on the consequences of aperiodic crystal structures for understanding the ordered states.

**Literature**

[1] C. Sen, G. Alvarez & E. Dagotto, Phys. Rev. Lett. **98**, 127202 (2007). Competing Ferromagnetic and Charge-Ordered States in Models for Manganites: The Origin of the Colossal Magnetoresistance Effect.

[2] M. S. Senn, J. P. Wright & J. P. Attfield, Nature **481**, 173 (2012). Charge order and three-site distortions in the Verwey structure of magnetite.

[3] S. van Smaalen, Acta Cryst. A **61**, 51-61 (2005). The Peierls transition in low-dimensional electronic crystals.

[4] A. Wölfel, Liang Li, S. Shimomura, H. Onodera & S. van Smaalen, Phys. Rev. B **82**, 054120 (2010).

Commensurate charge-density wave with frustrated interchain coupling in  $\text{SmNiC}_2$ .

[5] S. Kawaguchi, H. Ishibashi, N. Tsuji, J. Kim, K. Kato, M. Takata & Y. Kubota, *J. Phys. Soc. Jpn* **82**, 064603 (2013). Structural Properties in Incommensurately Modulated Spinel Compound  $\text{CuV}_2\text{S}_4$ .

**Keywords:** charge-density wave, charge order, aperiodic crystals

## MS26-O2 Incommensurate oxides and sulfides

Berthold Stöger<sup>1</sup>

<sup>1</sup> TU Wien

email: bstoegeer@mail.tuwien.ac.at

The defining property of a crystal has for a long time been its three-dimensional periodicity. With the advent of X-ray diffraction, a seemingly equivalent property of crystals emerged, namely their discrete diffraction pattern. But already in 1927 Dehlinger [1] observed sharp "lattice ghosts" in cold-formed metals, which are incompatible with lattice periodicity. These additional reflections emerge from structural modulations of a basic structure with an incommensurate periodicity.

The superspace approach [2] provides the necessary theoretical foundation to conveniently describe such incommensurately modulated phases and their diffraction patterns. It resulted in an explosion of the number of known incommensurates [3] and the realization that quasiperiodicity is distinctly less rare than one might expect. Nevertheless, the existence of incommensurates still appears mysterious and counterintuitive.

To demonstrate the ubiquity and variety of these phases, several incommensurate oxides and sulfides are presented. The thortveitite family is made up of transition metal diphosphates, diarsenates or divanadates with the general formula  $M_2X_2O_7$  ( $X=\text{P, As, V}$ ). The members feature a complex crystal chemistry with commensurately and incommensurately modulated phases. The modulation is a dynamic phenomenon as evidenced by a complex phase transition behavior. Analogous phenomena are observed in the condensed phosphates and arsenates  $\text{Ti}_5\text{P}_3\text{O}_{14}\text{H}_8$  and  $\text{Rb}_3\text{AlsAs}_3\text{O}_{12}$  and the orthophosphate  $\text{K}_3\text{PO}_4 \cdot 3\text{H}_2\text{O}$ .

In the ditellurates(IV)  $M\text{Te}_2\text{O}_5$  ( $M=\text{Ca, Sr, Cd}$ ) and their solid solutions, on the other hand, modulation is due to an occupational modulation of the O atoms. Accordingly, these phases do not feature structural phase transitions. Such complex static occupational modulations are likewise observed in natural sartorite and roschinite sulfosalts. Here, the modulation periodicities depend on subtle variations of the composition.

[1] U. Dehlinger, *Am. Mineral.* **1927**, 65, 615.

[2] P. M. De Wolff, *Acta Crystallogr.* **1974**, A30, 777.

[3] H. Z. Cummin, *Phys. Rep.* **1990**, 185, 211.

**Keywords:** incommensurate modulation, phase transition, oxides, sulfides

**MS26-O3** Structural phase transitions in the organic-inorganic hybrid perovskites  
 $(\text{C}_6\text{H}_{11}\text{NH}_3)_2[\text{PbX}_4]$  (X=I, Br)

Sébastien Pillet<sup>1</sup>, Bendeif El Ulmi<sup>1</sup>, Yangui Aymen<sup>2,3</sup>, Triki Smail<sup>4</sup>, Abid Younes<sup>4</sup>, Boukheddaden Kamel<sup>2</sup>

1. Laboratoire de Cristallographie, Résonance Magnétique et Modélisations, UMR-CNRS 7036, Institut Jean Barriol, Université de Lorraine, BP 239, 54506 Vandœuvre-lès-Nancy, France
2. Groupe d'Etudes de la Matière Condensée, UMR CNRS 8653-Université de Versailles Saint Quentin En Yvelines, 45 Avenue des Etats-Unis, 78035 Versailles, France
3. Laboratoire de Physique Appliquée, Faculté des Sciences de Sfax, Route de Soukra km 3.5 BP 1171, 3018 Sfax, Tunisia
4. Laboratoire de Chimie, Electrochimie Moléculaires, Chimie Analytique, UMR CNRS 6521-Université de Bretagne Occidentale, BP 809, 29285 Brest, France

email: sebastien.pillet@univ-lorraine.fr

Organic-inorganic hybrid perovskites have recently emerged as highly efficient optoelectronic materials, and are being intensively investigated and developed for high performance photovoltaics, photodetections, light-emitting diodes and laser devices. These materials exhibit a structural topology derived from the  $\text{ABX}_3$  perovskite structure, consisting of a corner-sharing  $\text{BX}_6$  octahedral network completed by organic A cations. Depending on the size of the organic cation, 3D, 2D, and 1D systems have been reported.

The compounds  $(\text{C}_6\text{H}_{11}\text{NH}_3)_2[\text{PbX}_4]$  (X=I, Br, Cl) exhibit a 2D structural architecture with semi-conducting inorganic layers of corner-sharing  $\text{PbX}_6$  octahedra separated by bilayers of  $\text{C}_6\text{H}_{11}\text{NH}_3^+$  cations. The optical properties (absorption and photoluminescence) have been investigated as a function of temperature, and show very interesting and unusual behaviors, such as white light emission, which are connected to structural phase transitions [1-3]. Single crystals of the three compounds and of the solid solutions  $(\text{C}_6\text{H}_{11}\text{NH}_3)_2[\text{PbI}_{4-x}\text{Br}_x]$  have been investigated through x-ray diffraction as a function of temperature. The corresponding structural phase diagram is very rich, displaying a different sequence of commensurate-incommensurate phase transitions for the bromine and iodine derivatives, characterized by a distortion and modulation of the inorganic perovskite layer. The mixed-halide series  $(\text{C}_6\text{H}_{11}\text{NH}_3)_2[\text{PbI}_{4-x}\text{Br}_x]$  obtained by gradual substitution of Br by I exhibits a morphotropic structural transition, which allows tuning the optical properties.

The complete structural phase diagrams and phase transitions will be described and discussed in connection to the temperature dependence of optical properties.

#### References

- [1] A. Yangui, S. Pillet, D. Garrot, S. Triki, Y. Abid, and K. Boukheddaden, *J. Appl. Phys.*, (2015), **117**, 115503.
- [2] A. Yangui, D. Garrot, J. S. Lauret, A. Lusson, G. Bouchez, E. Deleporte, S. Pillet, E. E. Bendeif, M. Castro, S. Triki, Y. Abid, and K. Boukheddaden, *J. Phys. Chem. C*, (2015), **119**, 23638–23647.
- [3] A. Yangui, S. Pillet, A. Mlayah, A. Lusson, G. Bouchez, S. Triki, Y. Abid, and K. Boukheddaden, *J. Chem. Phys.* (2015), **143**, 224201.

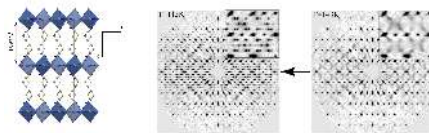


**Figure 1.** (left) crystal structure of  $(\text{C}_6\text{H}_{11}\text{NH}_3)_2[\text{PbI}_4]$ . (right) commensurate-incommensurate structural phase transition.

**Keywords:** hybrid perovskite, phase transition, incommensurate structure

## MS26-O4 Probing the nuclear and magnetic structure of a complex ferromagnetic semiconductor

John B. Claridge<sup>1</sup>, Jonathan Alaria<sup>1</sup>

1. University of Liverpool

email: j.b.claridge@liv.ac.uk

The large diversity of structural, electronic, and magnetic phases offered by compounds made up of two or more interpenetrating sublattices (composite structure) such as misfit layer chalcogenides offer the possibility to tune materials functionality using crystal chemistry concepts [1]. The structural and physical properties of the columnar composite crystal  $A_pCr_2X_{4+p}$  ( $A = Ba, Sr, Eu, Pb$ ;  $X = S, Se$ ;  $p \approx 0.29$ ) have not been studied in details.[2] The difficulty in interpreting the observed physical properties and the uncertainty about the exact chemical composition led to the reinvestigation of the crystal structure by Brouwer and Jellinek [2]. They concluded that the crystal structure of this family of materials could be described as an intergrowth of three structural units which have a common hexagonal basal plane, but different c axes. A three-dimensional network ( $B_{21}X_{36}$ ) of triply twined strips of  $CrX_6$  octahedra with a lattice constant of  $c_0$  creates hexagonal tunnels containing  $A_6B_2X_6$  chains with a lattice parameter  $c_6$  and the triangular tunnels  $A_3X$  chains with a lattice parameter  $c_3$ . Here we solve the crystal structure of the  $Ba_{2.71}Cr_2Se_{7.73}$  in the superspace group  $P6/m(00\gamma)s0(00\gamma_2)00$  (175.2.81.3 in the tables of Stokes and Campbell) using neutron powder diffraction, showing it is not a commensurate supercell but incommensurately modulated and study the evolution of the structural parameters on cooling through the magnetic transition observed at 110 K. This material is a ferromagnetic semiconductors at low temperature, with a measured Seebeck coefficients as large as 100  $\mu V/K$  at room temperature. It is thus likely to have low thermal conductivity on account of its complex structure and is thus of interest for thermoelectric applications.

[1] J. Rouxel, A. Meerschaut and G. A. Wiegiers, *J. Alloys Comp.*, 229 144 (1995)

[2] R. Brouwer and F. Jellinek, *J. Physique Colloque*, 38 C-7 (12) c7.36 (1977)

**Keywords:** composite phase, magnetic structure, incommensurate, neutron diffraction

## MS26-O5 Incommensurately modulated crystal structures of $Cu_3Si$

Cinthia A. Corrêa<sup>1,2</sup>, Petr Brázda<sup>1</sup>, Jaromír Kopeček<sup>1</sup>, Mariana Klementová<sup>1</sup>, Lukáš Palatinus<sup>1</sup>

1. Institute of Physics of the Czech Academy of Sciences, Na Slovance 2, Prague 8, Czech Republic

2. Department of Physics of Materials, Charles University in Prague, Ke Karlovu 5, Prague 2, Czech Republic

email: cinthiacac@gmail.com

The phase diagram of Cu-Si [1-3] has three polymorphs for Cu<sub>3</sub>Si:  $\eta''$  at room temperature,  $\eta'$  and  $\eta$  at high temperature. Several models of crystal structure for these phases were proposed [4-6]. However, there are still considerable uncertainties on the structure of these phases, and especially the crystal structures of  $\eta''$  and  $\eta$  remain essentially unknown. We have undertaken a systematic study of bulk samples with varying composition to elucidate the complex phase diagram and definitely resolve the ambiguities in the structural description of all phases in the diagram. Samples with composition  $Cu_{72}Si_{23}$ ,  $Cu_{76}Si_{24}$  and  $Cu_{78}Si_{25}$  were prepared by arc-melting and were measured by single crystal and powder X-ray diffraction. The average structure found is the same for the three compositions:  $P6_3/mmc$ ,  $a=4.06$  Å,  $c=14.66$  Å. The structures at room temperature have two dimensional incommensurate modulations, with modulation vectors  $q_1=(\alpha,\beta,1/3)$  and  $q_2=(\alpha,\beta,\alpha,1/3)$ . However, while the samples with composition  $Cu_{77}Si_{23}$  yields diffraction pattern with  $\alpha=\beta=0.251$  and point group, both  $Cu_{76}Si_{25}$  and  $Cu_{76}Si_{24}$  have point group, with the direction of the modulation vectors shifted away from the diagonal with  $\alpha=0.280$  and  $\beta=0.206$ . The structure of the former phase is different from the previously reported structure of  $\eta'$ -Cu<sub>3</sub>Si [6] in a doubled c lattice parameter and a different distribution of Cu and Si in the structure. The structure of the latter phase was observed for the first time, and differs from the phase with higher symmetry only in the arrangement of the modulated layers. Thermal analysis performed on the  $Cu_{76}Si_{24}$  sample showed additional phase transition, reported in the literature previously [5,7], but not reported in the published phase diagrams. Diffraction experiments at high temperature are currently in progress.

[1] Olesinski, R. W., Abbaschian, G. J., *Bulletin of Alloy Phase Diagrams* 7 (2), 1986.

[2] Sufryd, K. *et al.*, *Intermetallics* 19, 1479-1488, 2011.

[3] Okamoto, H., *Journal of Phase Equilibria and Diffusion* 33 (5), 2012.

[4] Solberg, J. K., *Acta Crystallographica A* 34, 684-698, 1978.

[5] Wen, Y. C., Spaepen, F. *Philosophical Magazine* 2007, 87, 5581-5599.

[6] Palatinus, L. *et al.*, *Inorg. Chem.* 2011, 50, 3743-3751.

[7] Mattern, N. *et al.*, *Journal of Alloys and Compounds* 429, 211-215, 2007.

This work is supported by the Czech Science Foundation, project No. 15-08842J, and by the Grant Agency of Charles University in Prague, project No. 366216.

**Keywords:** Cu<sub>3</sub>Si modulated structure, single crystal X-ray, thermal analysis

## MS27 Dynamical refinement of electron diffraction data

Chairs: Mauro Gemmi, Richard Beanland

### MS27-O1 Structure refinement using precession electron diffraction tomography and dynamical diffraction theory

Lukas Palatinus<sup>1</sup>

1. Institute of Physics of the CAS, Na Slovance 2, 182 21 Prague, Czechia

email: palat@fzu.cz

Electron diffraction techniques have made an enormous progress over the last decade. Currently it is possible to solve simple to medium sized crystal structures almost routinely using electron diffraction tomography techniques, and many examples of solving quite complex structures are also available. The bottle neck in the structure analysis work flow from electron diffraction was the optimization and validation of the structure model by structure refinement.

Recently, a possibility to perform full least-squares refinement of crystal structures against electron diffraction tomography data was studied in a series of works [1,2,3]. It was shown that it is indeed possible to obtain reliable structure models with good figures of merit from electron diffraction tomography data. The best results are obtained, if the data are recorded as a tilt series of diffraction patterns (electron diffraction tomography, EDT) combined with the precession of electron beam. On a series of test cases it was shown that the structure models deviate from the reference X-ray or neutron refinements on average by 0.02Å [3].

The method of structure refinement against electron diffraction tomography data (dynamical refinement for short), has been implemented in the crystallographic computing system Jana2006 [4] and made freely available to the scientific public. In the last months, considerable experience is being gained with this technique in several groups and on various materials. The results are encouraging. It has been shown that using this method it is possible to perform detailed crystallographic analyses of crystal structures, including the detection of partially occupied position, the refinement of site occupancies, determination of absolute structure and the use of difference Fourier synthesis to detect fine details of the structures, including the positions of hydrogen atoms. First applications of the technique have already been published [5,6] and more are in preparation.

[1] L. Palatinus et al., Acta Cryst. A69 (2013) 171.

[2] L. Palatinus et al., Acta Cryst. A71 (2015) 235.

[3] L. Palatinus et al., Acta Cryst B71 (2015) 740.

[4] V. Petricek et al., Z. Kristallgr. 229 (2014) 345.

[5] C. A. Correa et al., J. Alloys Comp. 672 (2016) 505.



[6] M. Colmont et al., Inorg. Chem. 55 (2016) 2252.

**Keywords:** electron diffraction, structure refinement, precession

## **MS27-O2** Accurate unit cell determination from rotation electron diffraction data

Wei Wan<sup>1</sup>, Hong Chen<sup>1</sup>, Jie Su<sup>1</sup>, Sven Hövö<sup>1</sup>

<sup>1</sup>. Bezeli Center EXSELENT on Porous Materials and Inorganic and Structural Chemistry, Department of Materials and Environmental Chemistry, Stockholm University, 106 91 Stockholm, Sweden

email: wei.wan@mmk.su.se

3D electron diffraction tomography (EDT), for example automated diffraction tomography (ADT)[1] and rotation electron diffraction (RED) [2-3], have been very successful as a complimentary method to X-ray crystallography in studying complex structures of crystals of sub-micrometer sizes. However, due to lower data quality the EDT methods often need to be combined with powder X-ray diffraction (PXRD) for complete structure determination. For example, unit cell parameters and structure models are usually refined against PXRD data for better accuracy.

In this work we focus on improving the accuracy of unit cell determination from RED data. Depending on data quality, the errors in unit cell determination from RED data can reach 1-2% in lengths and 1-2 degrees in angles. This may lead to difficulties in the initial identification of crystal symmetry and subsequent structure solution. As RED uses difference vectors among the reflections from reciprocal space reconstruction for unit cell determination, the accuracy of unit cell determination is dependent on the accuracy of the reconstructed reflection positions. We developed a procedure where the unit cell parameters are refined against the inter-reflection distances in 2D electron diffraction frames. This makes use of the fact that after data processing all the indices of the reflections in the original 2D frames are known and the refinement can be done using the known inter-reflection indices. We show with a test data that after correcting the geometric distortions of the 2D frames [4], the inter-reflection distances can be measured accurately and the refined unit cell parameters reach an accuracy of ~0.1% in lengths and 0.1-0.2 degrees in angles.

[1] U. Kolb et al, Ultramicroscopy 107 (2007) 507

[2] D.L. Zhang, et al, Z. Kristallogr. 225 (2010) 94

[3] W. Wan et al, J. Appl. Crystallogr. 46 (2013) 1863

[4] E. Mugnaioli et al, Am. Mineral. 94 (2009) 793

**Keywords:** rotation electron diffraction, unit cell

## MS27-O3 Study of partial occupancies and Jahn-Teller distortions in $(\text{Na}, \square)_5[\text{MnO}_2]_{13}$ by XRPD Rietveld and electron diffraction dynamical refinements

Enrico Mugnaioli<sup>1,2</sup>, Mauro Gemmi<sup>2</sup>, Marco Merlini<sup>3,4</sup>, Michele Grogorkiewicz<sup>1</sup>

1. Dipartimento di Scienze Fisiche, della Terra e dell'Ambiente, Università degli Studi di Siena, Siena, Italy
2. Center for Nanotechnology Innovation@NEST, Istituto Italiano di Tecnologia, Pisa, Italy
3. Dipartimento di Scienze della Terra, Università degli Studi di Milano, Milano, Italy
4. ESRF, European Synchrotron Radiation Facility, Grenoble, France

email: enrico.mugnaioli@unisi.it

Manganese octahedral molecular sieves (OMS) are characterized by framework structures made of channels walled by  $\text{MnO}_6$  octahedra and hosting different ionic species. A variable manganese oxidation state is found together with a wide structural variety of framework connectivity and pore sizes [1]. OMS are extensively investigated because their mixed electronic/ionic conductive properties, which in turn depend on structurally related features, like  $\text{Mn}^{4+}$ - $\text{Mn}^{3+}$  ordering and coordination number of extra-framework ions. Nonetheless, a systematic structure characterization of OMS by X-ray methods is hampered by difficulty in growing single crystals and achieving pure synthetic products.

$(\text{Na}, \square)_5[\text{MnO}_2]_{13}$  is a well-known electrode material, whose structure has long been associated with a romanèchite-like framework. Recently, the structure of  $(\text{Na}, \square)_5[\text{MnO}_2]_{13}$  was re-determined *ab initio* by precession-assisted Electron Diffraction Tomography (EDT) in space group  $C2/m$ , resulting in a completely novel framework hosting 3 independent Na sites inside the channels [2].

The structure was subsequently refined vs laboratory and synchrotron XRPD data by Rietveld method, and vs EDT data by both kinematical and dynamical methods [3]. Laboratory XRPD data and EDT kinematical refinement confirmed the correctness of the *ab initio* model, but  $\text{MnO}_6$  octahedra proved rather distorted and no information about possible crystallographically-related distribution of  $\text{Mn}^{3+}$  in the framework could be obtained.

Conversely, structures refined on the basis of synchrotron XRPD data ( $R_w=0.051$ ,  $R_p=0.037$ ,  $R_2=0.036$ ) and EDT dynamical refinement ( $R_{\text{Fobs}}=0.07$ ) converged on very close models. The average and maximum discrepancies between the two coordinate sets were 8 and 21 pm respectively (3 and 5 pm respectively for Mn atoms). Na coordination shells were well-defined and occupancies refined to values close to expected stoichiometry. One  $\text{MnO}_5$  square pyramid and two  $\text{MnO}_6$  octahedra were characterized by longer average interatomic distances and Jahn-Teller distortion, consistent with manganese in oxidation state (3+). Distribution and multiplicity of  $\text{Mn}^{3+}$  and Na sites in the structure satisfactorily explain the electro-chemical behavior of  $(\text{Na}, \square)_5[\text{MnO}_2]_{13}$ , which could not be understood assuming the former romanèchite model.

[1] Pasero, M. (2005). *Rev. Mineral. Geochem.* **57**, 291–305.

[2] Mugnaioli, E. *et al.* (2016). *J. Power Sources*, under revision.

[3] Palatinus, L. *et al.* (2013). *Acta Cryst.* **A69**, 171–188.

**Keywords:** electron diffraction tomography (EDT), dynamical refinement, synchrotron Rietveld refinement, octahedral molecular sieves (OMS), electrode materials

**MS27-O4** Localization of hydrogen atoms in organic molecules using dynamical refinement of electron diffraction dataPetr Brazda<sup>1</sup>, Mariana Klementova<sup>1</sup>, Lukas Palatinus<sup>1</sup><sup>1</sup>. Institute of Physics of the CAS, v.v.i.

email: brazda@fzu.cz

Although, localization of hydrogen atoms in data from electron diffraction has been reported in special cases [1,2] reliable *ab initio* determination of hydrogen positions from single nano-crystals has not been achieved to the best of our knowledge. Our work focuses on pharmaceuticals and pharmaceutical co-crystals. The stability of these compounds under electron beam irradiation is low and data collection requires low-dose technique at low-temperature. Precession assisted electron diffraction tomography on single nano-crystals was used for data acquisition. Data were processed using programs PETS, Jana2006 and Dyngo. In favourable cases like in the case of paracetamol form I (S. G.  $P2_1/n$ ), it was possible to localize a few of the hydrogen atoms in difference Fourier maps after kinematical refinement of the structure ( $R(\text{obs}) = 20\%$ ). Dynamical approach provided an improved difference Fourier map, which revealed the complete set of hydrogen atoms (Figure 1). Dynamical refinement of the structure without the hydrogen atoms resulted in the  $R(\text{obs})$  factor of 12 %. An addition of the hydrogen atoms into the model led to an addition improvement of the  $R(\text{obs})$  slightly below 10 %, demonstrating the sensitivity of the result to the presence of the hydrogen atoms in the model.

[1] Electron diffraction techniques, J. M. Cowley, Volume 1, Chapter 6 and references therein, Oxford University Press 1992.

[2] J. Hadermann et al. Chem. Mater. 24 (2012) 3401.

This work is supported by the Czech Science Foundation, project No. 16-10035S.

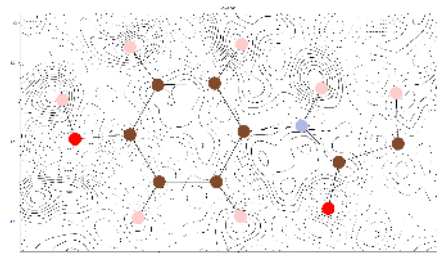


**Figure 1.** Difference Fourier map of the best plane through the paracetamol molecule overlayed by the structure obtained after refinement of the model with added hydrogen atoms.

**Keywords:** hydrogen atoms localization, single crystal electron diffraction, dynamical refinement

**MS27-O5** Improving rotation electron diffraction data quality by data mergingYunchen Wang<sup>1</sup>, Xiaodong Zou<sup>1</sup>, Wei Wan<sup>1</sup>

<sup>1</sup>. Berzelii Center EXSELENT on Porous Materials and Inorganic and Structural Chemistry, Department of Materials and Environmental Chemistry, Stockholm University, SE-106 91 Stockholm

email: yunchen.wang@mmk.su.se

Automated three-dimensional electron diffraction methods, for example automated diffraction tomography (ADT)[1] and rotation electron diffraction (RED) [2-3], can be used to collect and process completed 3D electron diffraction data from nanometer sized crystals and have been very successful in application of solving complex structures. However, limited crystal tilting range and steps, electron beam damage and dynamical scattering of electrons degrade the RED data quality and result in high  $R$  values and inaccurate structural parameters from refinement. Often structure models obtained from RED data are refined against powder X-ray diffraction data for confirmation and better accuracy.

Here we propose an approach for improving RED data quality through merging multiple datasets collected from different crystals with different orientations. Individual datasets are first processed using RED following the standard procedure. The initial model for the refinement is obtained by direct methods using SHELXS. The HKL lists from the individual datasets are merged together for refinement with the initial model using SHELXL. To study the effects of merging datasets on data quality, we performed refinement by sequentially including the individual datasets from a test sample. We show that the number of observed reflections increases and the  $R$  values decrease while more datasets are merged. The structural parameters after refinement are improved by merging more datasets. The apparent improved data quality may be attributed partly to the increased data completeness and resolution, and reduced effects of dynamic effects through averaging. These factors will be examined carefully to evaluate their potential in improving RED data.

[1] U. Kolb et al, Ultramicroscopy 107 (2007) 507

[2] D.L. Zhang, et al, Z. Kristallogr. 225 (2010) 94

[3] W. Wan et al, J. Appl. Crystallogr. 46 (2013) 1863

**Keywords:** RED, electron diffraction, data quality

## MS28 New approaches in electron crystallography

Chairs: Louisa Meshi, Xiaodong Zou

### MS28-O1 When Precession Electron Diffraction Tomography goes dynamical

Philippe BOULLAY<sup>1</sup>, Gwladys Steciuk<sup>1</sup>, Olivier Pérez<sup>1</sup>, Sébastien Petit<sup>1</sup>, Moussa Zaarour<sup>2</sup>, Svetlana Mintova<sup>2</sup>, Karl Rickert<sup>3</sup>, Kenneth R. Poeppelmeier<sup>3</sup>, Wenrui Zhang<sup>4</sup>, Haiyan Wang<sup>4</sup>, Mariana Klementova<sup>5</sup>, Lukas Palatinus<sup>5</sup>

1. Laboratoire de Cristallographie et de Sciences des Matériaux (CRISMAT) UMR CNRS 6508, ENSICAEN, 6 Boulevard Maréchal Juin, 14050 Caen, France

2. Laboratoire de Catalyse et de Spectroscopie (LCS), ENSICAEN, 6 Boulevard Maréchal Juin, 14050 Caen, France

3. Department of Chemistry, Northwestern University, Evanston, Illinois, 60208, USA

4. Department of Materials Science and Engineering, Texas A&M University, College Station, Texas 77843, USA

5. Institute of Physics of the AS CR, Na Slovance 2, Prague, Czech Republic

email: philippe.boullay@ensicaen.fr

The use of electron diffraction (ED) data for the refinement of crystal structures as routinely as what is done in X-ray diffraction (XRD) has long appeared to be inaccessible. While the strong electron/matter interaction allows studying crystals of nanometer size, the kinematic approximation is not valid, which makes the analysis of the diffracted intensity more complex than for XRD. More complex, but not impossible, as the formalism to describe dynamic conditions in ED is known since long. However, its use by programs aiming structural refinements using ED patterns obtained from parallel beam met no success despite several attempts. [1]

In 2013 [2], L. Palatinus and co-authors have studied the feasibility of refining crystal structures from few zone axis patterns considering the dynamic conditions of diffraction, and shown, the importance of Precession Electron Diffraction (PED) [4] to get better convergence. Early in 2015, the Prague group reached a decisive step by implementing in JANA2006 a module dedicated to ED and such “dynamical refinements” [5]. Integrated in an interface familiar to most structural crystallographers, this module now allows to process PED data collected in a “tomography mode” [6] aiming to reach a high level of data completeness. Several groups across Europe have joined forces to test and validate this new approach and offer the community a reliable and functional tool. [7]

From structure solution to structure refinement (kinematical then dynamical), Precession Electron Diffraction Tomography (PEDT) is a mature technique readily to be used in any materials science laboratory. In the present communication, we will show what astonishing results can be achieved and what are the limitations using examples from incommensurate

modulated structures, thin films and zeo-type materials. No doubt that combining PEDT data and “dynamical refinements” will allow to solve and refine an increasing number of structures on materials inaccessible by other diffraction techniques.

[1] J. Jansen et al. *Acta Cryst.* **A54** (1998) 91 and A.P. Dudka et al., *Crystallogr. Rep.* **53** (2008) 530.

[2] L. Palatinus et al., *Acta Cryst.* **A69** (2013) 171.

[3] L. Palatinus et al., *Acta Cryst.* **A71** (2015) 235.

[4] R. Vincent et al., *Ultramicroscopy* **53** (1994) 271.

[5] V. Petricek et al., *Z. Kristallg.* **229** (2014) 345.

[6] U. Kolb et al., *Ultramicroscopy* **107** (2007) 507.

[7] L. Palatinus et al., *Acta Cryst.* **B71** (2015) 740.

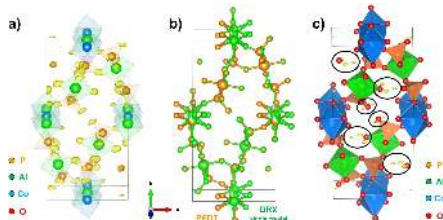


**Figure 1.** Co-AIPO zeo-type material: a) density map from PEDT data, b) structure from single crystal XRD (green) and PEDT “dynamical” (orange), c) residues in the Fourier difference map after dynamical refinement of PEDT data. Residues inside black circles would correspond to hydrogens.

**Keywords:** dynamical refinement, incommensurate modulated structures, thin films, zeo-type materials

## MS28-O2 MicroED: Three Dimensional Electron Diffraction of Microscopic Crystals

Tamir Gonen<sup>1</sup>

1. Group Leader, Howard Hughes Medical Institute, Janelia Research Campus, Ashburn VA 20147 USA

email: gonent@janelia.hhmi.org

My laboratory studies the structures of membrane proteins that are important in maintaining homeostasis in the brain. Understanding structure (and hence function) requires scientists to build an atomic resolution map of every atom in the protein of interest, that is, an atomic structural model of the protein of interest captured in various functional states. In 2013 we unveiled the method MicroED, electron diffraction of microscopic crystals, and demonstrated that it is feasible to determine high-resolution protein structures by electron crystallography of three-dimensional crystals in an electron cryo-microscope (CryoEM). The CryoEM is used in diffraction mode for structural analysis of proteins of interest using vanishingly small crystals. The crystals are often a billion times smaller in volume than what is normally used for other structural biology methods like x-ray crystallography. In this seminar I will describe the basics of this method, from concept to data collection, analysis and structure determination, and illustrate how samples that were previously unattainable can now be studied by MicroED. I will conclude by highlighting how this new method is helping us understand major brain diseases like Parkinson's disease.

**Keywords:** MicroED; CryoEM; Electron Diffraction; Crystallography; nanocrystals

## MS28-O3 Protein nano-crystallography using optimized quantum area direct electron detectors like the Medipix and Dectris families.

Eric van Genderen<sup>1</sup>, Max T.B. Clabbers<sup>2</sup>

1. Paul Scherrer Institute - LBR, Switzerland

2. Center for Cellular Imaging and NanoAnalytics (C-CINA), Biozentrum, University of Basel, Switzerland

email: ericvangenderen@gmail.com

In recent years new detectors became available for imaging in Electron Microscopy e.g. FEI Falcon and Gatan K2, the DE-series. These detectors gave a huge boost to imaging of tissues, cells and protein complexes. Recently these detectors, together with advances in image processing and computing power, made it possible to break the 2.5 Ångström resolution barrier in imaging of single bio-molecular complexes (Bartesaghi, Nature 2015: the 'resolution revolution' (Kühlbrandt, Nature 2014). These detectors have some drawbacks when it comes to diffraction studies: they are not very radiation hard and have a low dynamic range. These characteristics make it almost impossible to perform a good very low dose diffraction experiment, and one was still dependent on CCD cameras which are characterized by electronic noise, dark currents and noise coming from other sources than electrons (like the huge X-ray background that is present in any EM).

We have recently demonstrated that quantum area electron detectors like the Medipix have a similar impact when switching to diffraction mode [van Genderen, 2016]. We have solved the crystal structures of organic compounds from nano-crystals using electron diffraction with as low a dose as 0.013e-/Å<sup>2</sup>s. This enabled us to collect sufficient data for structure solution from a single nano-crystal even at room temperature.

I will discuss our recent progress on electron nano-crystallography, how these types of detectors will tear down the boundaries of electron diffraction of organic materials, why we think that diffraction will overcome the resolution problems that single particle faces and what role specialized diffraction cameras play in this process.

**van Genderen, E.,** Clabbers M.T.B., Pratim Das, P., Stewart, A., Nederlof, I., Barentsen, K.C., Portillo, J., Pannu, N.S., Nicolopoulos, S., Gruene, T., Abrahams, J.P. Ab initio structure determination of nanocrystals of organic pharmaceutical compounds by electron diffraction at room temperature using a Timepix quantum area direct electron detector. **Acta Cryst. A72**, 236-242 (2016)

**van Genderen, E.,** Li Y-W, Nederlof, I., Abrahams, J.P. Lattice filter for processing image data of 3D protein nano-crystals. **Acta Cryst. D72**, 34-39 (2016)

Nederlof, I., **van Genderen, E.,** Li, Y.W., Abrahams, J.P. A Medipix quantum area detector allows rotation electron diffraction data collection from submicrometre three-dimensional protein crystals **Acta Cryst. D69**, 1223-1230 (2013)

**Keywords:** Nano-crystallography, electron microscopy, electron diffraction detectors, continuous rotation, proteins

**MS28-O4** Serial snapshot crystallography using electron diffractionStef Smeets<sup>1</sup>, Xiaodong Zou<sup>1</sup>, Wei Wan<sup>1</sup>

1. Inorganic and Structural Chemistry, Department of Materials and Environmental Chemistry, Stockholm University, Sweden

email: stef.smeets@mmk.su.se

Can electron diffraction be used to process serial snapshot crystallography? In an attempt to answer this question, we are developing a strategy to collect and process such data on materials that are sensitive to the electron beam, and thus difficult to measure using the conventional methods that rely on long exposure of the same crystal. To avoid beam damage, crystals are measured only once, but by combining snapshots from several sets of randomly oriented crystals, a complete data set can be assembled, and structures of materials that are difficult to analyse otherwise become accessible. This method relies on the ability to reliably retrieve crystal orientations from a snapshot, and this is challenging: (1) accurate orientations have to be retrieved from a single frame, (2) reliable peak positions should be extracted, (3) the unit cells are small, limiting the number of observations per frame, and (4) crystals may overlap, so it should be possible to determine the orientations of multiple crystals from a single frame. We previously developed a strategy to process serial snapshot data based on the broad-bandpass mode that will be offered at the SwissFEL[1] free-electron laser that can overcome several of these problems. The indexing algorithm that we developed can find the orientations of up to 15 crystals at once, and look for several unit cells simultaneously.

To see if such an approach can work with electron diffraction data, we modified our algorithm and applied it to data collected using the rotation method[2] on samples of the mineral garnet, zeolite silicalite-1[3], and isolated crystals of a powder containing 5 different polymorphs of a Ni-Se-O-Cl system[4]. The indexing routine was applied frame by frame, and can find the orientations of these crystals with over 90% success rate. For the multiphasic sample, our algorithm can reliably distinguish between the different polymorphs. This enables automatic screening of beam-sensitive materials for known and unknown phases. The data collection procedure can include precession to increase resolution, improve reflection integration, and reduce dynamical effects. Although our interest is in inorganic materials, the method may also be applied to other beam-sensitive compounds.

[1] Dejoie *et al.* (2015) *IUCrJ*, **2**, 361; [2] Wan *et al.* (2013) *J. Appl. Cryst.* **46**, 1863; [3] Su *et al.* (2014) *Micropor. Mesopor. Mat.* **189**, 115; [4] Yun *et al.* (2014) *J. Appl. Cryst.* **47**, 2048

**Keywords:** serial snapshot crystallography, electron diffraction, beam-sensitive materials

**MS28-O5** Fast electron diffraction tomography on beam sensitive materials at room temperature: pharmaceuticals and zeolitesMauro Gemmi<sup>1</sup>, Enrico Mugnaioli<sup>1</sup>, Jeremy David<sup>1</sup>, Camilla Tossi<sup>1</sup>, Athanassios Galanis<sup>2</sup>, Partha Pratim Das<sup>2</sup>, Mihaela Pop<sup>3</sup>, Coda Iordache<sup>1</sup>, Stavros Nicolopoulos<sup>2</sup>

1. Center for Nanotechnology Innovation @NEST, Istituto Italiano di Tecnologia, Pisa Italy.

2. Nanomegas, Brussels, Belgium

3. TeraCrystal SRL, Cluj Napoca Romania.

email: mauro.gemmi@iit.it

Collecting electron diffraction data suitable for structure solution on beam sensitive materials is a challenging task. Pharmaceuticals and zeolites belong to extremely beam sensitive materials and in most of the cases they amorphize after few minutes when exposed to an electron beam strong enough for collecting a readable electron diffraction pattern with a conventional CCD. Here we present a method that couples the fast electron diffraction tomography (FEDT) [1] procedure with the Timepix single electron detection device [2]. In FEDT the patterns, in precession mode, are collected sequentially by the detector while the crystal is tilting. Due to the fast read-out and high sensitivity of the Timepix detector the FEDT data collection can be carried out with the crystal tilting at a speed of 2°/s or higher without any loss of reciprocal space volume. Crystals can be searched in STEM avoiding beam damage caused by the continuous TEM illumination. During diffraction data collection at room temperature, the electron dose rate can be reduced to the minimum available by the microscope settings, and weak diffraction reflections can be recorded thanks to the zero noise level of the Timepix, after the inelastic background is cut-out by the in-column energy filter. The high stability of the goniometer allows data collection of 90° of reciprocal space coverage in about 30-45 seconds. We demonstrate the efficiency of the method on the structure solution of the cowlesite zeolite, which degrades too fast under the beam for a standard steady-step data acquisition. As a further test for the efficiency of FEDT+Timepix procedure, the structure solution of a pharmaceutical compound is also presented together with the comparison of the crystal model refined by single crystal x-ray diffraction, in order to show the accuracy of electron data on such a compound.

## References

[1] Gemmi M, La Placa MGI, Galanis AS, Rauch EF, Nicolopoulos S (2015) *J. Appl. Cryst.* **48**, 718-727.

[2] Van Genderen E, Clabbers MTB, Das PP, Stewart A, Nederlof I, Barentsen KC, Portillo Q, Pannu NS, Nicolopoulos S, Gruene T, Abrahams JP (2016) *Acta Cryst.* **A72**, 236-242.

**Keywords:** precession, electron diffraction tomography

## MS29 Molecular interactions in crystal packing and molecular assemblies

**Keywords:** crystal engineering, intermolecular interactions, silver, two-fold coordination

Chairs: Kari Rissanen, Doris Braun

### MS29-O1 The silver bond

Carl Henrik Görbitz<sup>1</sup>

<sup>1</sup>. Department of Chemistry, University of Oslo

email: c.h.gorbitz@kjemi.uio.no

Hydrogen bonds, halogen bonds and metal coordination are the main tools used by the crystal engineer to design and synthesize new materials. Metal coordination is above all used for construction of metal-organic frameworks (MOFs), where metal ions or metal ion clusters serve as network hubs that are linked by organic, usually bifunctional struts.

Silver is special in being involved in more than one half of all X-M-X fragments (X = O or N, M = any metal) in the Cambridge Structural Database, where the metal is bonded to only two ligands. While this might not be a desirable property for a MOF hub, such links mimic hydrogen bonds, and the “silver bond” could therefore nevertheless represent an interesting addition to the crystal engineering toolbox. Despite the substantial number of Ag-containing crystal structures available, systematic efforts into this matter seem, however, largely to be lacking. The present investigation focuses on the potential of silver in the establishment of robust, three-dimensional structures. As an example, a dipeptide, L-Val-L-Leu, has been crystallized as a normal zwitterion and as the isostructural silver analogue, the latter forming larger and better diffracting crystals.

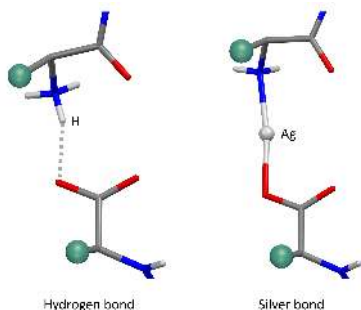


**Figure 1.** Regular hydrogen bond in the crystal structure of the dipeptide L-Val-L-Leu (left) and a silver bond in the isostructural silver analogue (right). Amino acid side chains are shown as small spheres for clarity.



**MS29-O2** Molecular interactions and configurational entropy determining the macroscopic polar state of molecular crystalsJuerg Hulliger<sup>1</sup>, Luigi Cannavacciuolo<sup>1</sup>, Khadidja Brahimi<sup>1</sup><sup>1</sup> University of Bern, Department of Chemistry and Biochemistry, Freiestrasse 3, 3012 Bern, Switzerland

email: juerg.hulliger@iac.unibe.ch

Advanced physical characterization of as grown molecular crystals made of dipolar molecules by scanning pyroelectric and phase sensitive second harmonic microscopy has revealed the true macroscopic polar state of molecular crystals: Supported by configurational entropy, i.e. 180° orientational disorder, molecular crystals (and similarly organized materials) grow into a *bi-polar macroscopic state* (for a review, see [1] or basics [2]). This means, experimentally at least two adjacent domains showing opposite average polarization may be observed. Theoretically, this phenomenon is well understood by analytical models (Markov chain, 2D anisotropic Ising model), force field based calculations for defect energies and Monte Carlo (MC) simulations. Both the thermalized state (concerning 180° disorder) of nano sized seeds and e.g. layer by layer grown crystals were investigated by MC. In case of a *seed* undergoing 180° disorder, a bi-polar state is found. In case of a kinetically controlled nucleation of a *mono polar seed*, growth should lead to a *reversal transition*, experimentally confirmed for bi-phenyls [3]. For 4-iodo-4'-nitro-biphenyl (INBP) the reversal of molecular axes 2 takes place over a transition zone of about 150 micron. The combination of anomalous X-ray scattering & pyroelectric measurements allows us to determine the absolute polarity of such bi-polar objects. The experimentum crucis supporting the *reversal* mechanism consisted in the investigation of solid solutions by adding symmetrical molecules (e.g. 4,4'-di-iodo-biphenyl) to the nutrient. Here, the absolute polarity of the as grown bi-polar state was found to be inverted. The result is in agreement with qualitative arguments about main intermolecular interactions at attachment sites [3]. Force field calculations for para substituted benzenes undergoing 180° orientational disorder at growing faces have provided quantitative data in favour of a *reversal transition*. When analysing the source for driving energies, we find that the main part for the electrostatic interaction stems from a dipolar to quadrupole interaction.

[1] J. Hulliger et al., New J. Chem. 37, 2229-2235, 2013

[2] J. Hulliger et al., Cryst. Growth Des. 12, 5211-5218, 2012

[3] M. Burgener et al., CrystEngCom 15, 7652-7656, 2013

**Keywords:** macroscopic polar state, orientational disorder, molecular crystals**MS29-O3** One-dimensional chains in PGM complexes- understanding metallophilic interactionsCarla Pretorius<sup>1</sup>, Andreas Roodt<sup>2</sup><sup>1</sup> University of the Free State<sup>2</sup> University of the Free State

email: cpretorius87@gmail.com

Research in the field of supramolecular chemistry has delivered several novel compounds with exciting optical, magnetic and conductive properties in recent years. Of particular interest in our current work is the use of metallophilic interactions as part of the arsenal library in the construction of large network structures. Metallophilicity has been defined as the interaction between electron densities of large closed-shell or pseudo closed-shell metal centres with d<sup>8</sup> and d<sup>10</sup> electron configurations with similar energies as hydrogen-bonding. Interactions of this kind facilitate the growth of infinite 1-D metallic chains between neighbouring metal centres along one direction of the crystal lattice. Materials containing such interactions often display tunable physical properties such as dichroism that can be directly influenced by changes to the interactions.

The current project was focused on an analogous series of complexes containing Rh(I) and Pt(II) metal centres with metallophilic interactions. Three classes of ligand systems were chosen for the study (Scheme 1 (a)) with accompanying illustration of the metallophilic interactions found in [Rh(piv)(CO)<sub>2</sub>] (piv= 1,1,1-trifluoro-5,5-dimethyl-2,4-hexanedionato) (b). Crystals of **1** with Rh(I) have been characterized by red-green dichroism with Rh...Rh distances of 3.264(3) Å whilst the Pt(II) analogue exhibits green-purple dichroism and Pt...Pt distances of 3.160(1) Å. In contrast Rh(I) complexes of **3** have much longer metallophilic interactions with Rh...Rh distances (3.641(1) Å) and red-yellow dichroism associated with the bulk material.

Several novel Rh(I) and Pt(II) complexes will be presented that display unique metallophilic interactions relating not only the importance of ligand choice in these systems but also the effect of different metals in the establishment of metallophilic interactions. In turn, the differences in chemical systems will be correlated to changes in the physical properties of the compounds thereby establishing a framework by which the design of future materials with desirable properties may be undertaken. Studies investigating the solid-state UV/Vis properties, charge transfer and excited state structures, fluorescence and mechanical effects such as pressure on the metallophilic interactions will also be highlighted.

# MS29-O4 Insights into molecular spreading and bridging in chromosome condensation from the complex structure of Spo0J and *par*

Yuh-Ju Sun<sup>1</sup>

1. National Tsing Hua University, Institute of Bioinformatics and Structural Biology, Taiwan ROC

email: yjsun@life.nthu.edu.tw

In the chromosome partitioning system (*parABS*), the partition protein (ParB) and its regulatory protein (ParA) act cooperatively through *parS* DNA to facilitate chromosome segregation. ParB oligomer and *parS* interact together to form a high-order nucleoprotein that is required for the loading of the structural maintenance of chromosomes proteins onto the chromosome for chromosomal DNA condensation. Spo0J is a member of ParB superfamily. The binding of *parS* and Spo0J from *H. pylori* (*HpSpo0J*) was characterized. The *HpSpo0J*-*parS* complex structure was determined by Se-MAD method. The overall structure of *HpSpo0J* is in an elongated shape including a flexible N-terminal domain for protein-protein interaction and a conserved DNA-binding domain for *parS* binding. A structure model for molecular spreading and bridging in chromosome condensation is proposed.

**Keywords:** Chromosome partitioning system, *parABS*

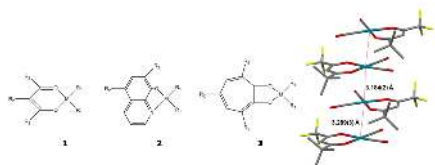


**Figure 1.** a) Selected Rh(I) and Pt(II) complexes (M = Rh, Pt; R = CO, COHCH<sub>3</sub>; R' = substituents); b) metallophilic interactions in [Rh(piv)(CO)<sub>2</sub>] in an extended 1-D chain along the *a*-axis.

**Keywords:** Metallophilic interactions, 1-D chains, Platinum, Rhodium

## MS29-O5 Crystal-Packing and Spin-CrossOver in some Molecular Solids. Trends and new Features.

Philippe Guionneau<sup>1</sup>, Arnaud Grosjean<sup>1</sup>, Elodie Tailleux<sup>1</sup>,  
Mathieu Marchivie<sup>1</sup>, Sabine Lakhroufi<sup>1</sup>, Patrick Rosa<sup>1</sup>, Guillaume  
Chastanet<sup>1</sup>

1. CNRS, Univ. Bordeaux, ICMCB, UPR9048, 87, Avenue du  
Docteur Schweitzer, F-33600 Pessac, France

email: Philippe.Guionneau@icmcb.cnrs.fr

One of the key-stones of modern science is the ability to determine the crystal structures of materials. To this end, diffraction techniques are in constant improvement always pushing the frontiers of investigation. For example, if focusing only on the **spin crossover (SCO)** molecular material field [1], recent X-ray diffraction developments permit to investigate local structures in materials that are not strictly crystalline, structural modifications at the picoseconds time scale or crystal structures under external perturbations as pressure or light irradiation [2-4]. As a result **a very fine description of the structure-properties relationships in molecular SCO solids can be achieved**. [5, 6].

In this context, we will present a multi-scale description of the SCO mechanism in molecular solids (Fig. 1) based on the **crystal-packing analysis** and focusing on **structural movies** showing the sample breathing of the **intermolecular interactions** and on the full determination of (pressure-temperature-light) **phase diagrams**. In addition, recent X-Ray diffraction on powders has revealed a potential **structural fatigability** upon cycling in a SCO compound. This fatigability, connected with some properties of the crystal-packing, will also be discussed [7].

[1] P. Gütllich, AB Gaspar, Y. Garcia, *Beilstein J. Org. Chem.*, **2013**, 9,342–391 [2] P. Durand, S. Pillet et al. *J. Mater. Chem. C*, **2013**, 1, 1933 [3] H. Cailleau, M. Lorenc, et al. *Acta Cryst.*, **2010**, A66, 189 [4] P. Guionneau and E. Collet in *Spin-Crossover Materials: Properties and Applications*, John Wiley & Sons Ltd, Oxford UK, **2013**, Chapter 20, 507 [5] M.A. Halcrow, *Chem. Soc. Rev.*, **2011**, 40, 4119 [6] P. Guionneau, *Dalton Trans.*, **2014**, 43, 382 [7] A. Grosjean et al., *Eur. J. Inorg. Chem.*, **2016**, DOI: 10.1002/ejic.201501164

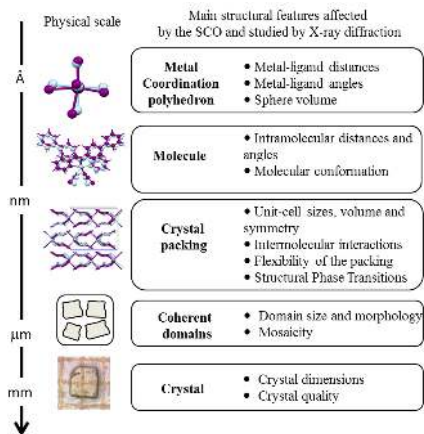


Figure 1. Physical scales and the related modifications due to the spin crossover in a molecular crystal (adapted from ref [6])

**Keywords:** X-ray diffraction, structure-properties relationship, spin-crossover, iron, molecular materials

## MS30 Hydrogen bonding from theory to applications

Chairs: László Fábián, Nikolett Bathori

### MS30-O1 Crystal Engineering: From Form to Function

Michael Zaworotko<sup>1</sup>

1. University of Limerick

email: Michael.Zaworotko@ul.ie

That composition and structure profoundly impact the properties of crystalline solids has provided impetus for exponential growth in the field of crystal engineering<sup>1</sup> over the past 25 years. This lecture will address how crystal engineering has evolved from structure design (form) to control over bulk properties (function).

Strategies for the generation of two classes of functional crystalline materials will be addressed:

**Multicomponent pharmaceutical materials**, MPMs, such as cocrystals<sup>2</sup> have emerged at the preformulation stage of drug development. This results from their modular and designable nature which facilitates the discovery of new crystal forms of active pharmaceutical ingredients, APIs, with changed physicochemical properties. The concept of “ionic cocrystals” will be explained and a case study addressing brain bioavailability of lithium will be presented.

**Hybrid Ultramicroporous Materials**, HUMs, are built from metal or metal cluster “nodes” and combinations of organic and inorganic “linkers”. Two families of HUMs that afford exceptional control over pore chemistry, pore size and binding energy, will be detailed. Benchmark selectivity for CO<sub>2</sub> capture in these HUMs with pcu or mmo (see Figure) topology has been observed<sup>3</sup> thanks to the strong electrostatics associated with pores lined by the inorganic components of these nets. New results that address other applications of HUMs will be presented and discussed.

1. (a) Desiraju, G.R. *Crystal engineering: The design of organic solids* Elsevier, 1989; (b) Moulton, B.; Zaworotko, M.J. *Chemical Reviews* 2001, 101, 1629-1658.

2. Duggirala, N.; Perry, M.L.; Almarsson, Ö.; Zaworotko, M.J. *Chem. Commun.* 52, 640-655, 2016.

3. Nugent, P.; Belmabkhout, Y.; Burd, S.D.; Cairns, A.J.; Luebke, R.; Forrest, K.; Pham, T.; Ma, S.; Space, B.; Wojtas, L.; Eddaoudi, M.; Zaworotko, M.J. *Nature* 2013, 495, 80-84, 2013.

**Keywords:** crystal engineering

### MS30-O2 Organic Hydrates: Chemistry, H-Bonding & Packing

Peter A. Wood<sup>1</sup>, Neil Feeder<sup>1</sup>, Colin R. Groom<sup>1</sup>, Andrew G.P. Maloney<sup>1</sup>

1. The Cambridge Crystallographic Data Centre

email: wood@ccdc.cam.ac.uk

The occurrence and understanding of hydrates (water-containing crystals) is of particular importance in the field of pharmaceutical research and industry. Hydrate formation is common for Active Pharmaceutical Ingredients (API), with one experimental polymorph screening study [1] reporting that 38% of molecules screened form hydrates and another account [2] indicating hydrates to occur for as many as 75% of drugs. This presentation will address the topic of hydration likelihood and water coordination patterns in organic hydrates, in particular with reference to pharmaceutical hydrates. We focus on the relative frequencies of hydration of specific types of molecules, re-evaluate the frequencies of occurrence and types of water coordination environment in these subsets and comment on the onward use of this information for structure evaluation and prediction.

[1] Stahly, G. P., *Crystal Growth & Design* 2007, 7, 1007-1026.

[2] Infantes, L.; Chisholm, J.; Motherwell, W. D. S., *CrystEngComm* 2003, 5, 480-486.

**Keywords:** hydrates, crystal engineering, hydrogen bonding

**MS30-O3 Gold as a hydrogen-bond acceptor**Catharine Esterhuysen<sup>1</sup><sup>1</sup> Dept. Chemistry and Polymer Science, University of Stellenbosch, Private Bag X1, Matieland, Stellenbosch, 7602

email: ce@sun.ac.za

Although hydrogen bonds are the most common and well-known intermolecular interactions, a wide variety of other, fascinating interactions that play a role in stabilising crystal structure packing have been identified. For instance, Au(I) complexes are well-known for forming aurophilic interactions, which are inter- or intramolecular Au...Au interactions of a similar strength to hydrogen bonds, with Au...Au distances similar to those found in gold metal.[1] In the intervening thirty years since these interactions were identified they have been extensively studied, and are known to have their origin in relativistic effects.[2] They are also of interest since they are often luminescent and exhibit unusual electronic properties. It has recently been shown that the auride ion, Au<sup>-</sup>, can also act as a hydrogen bond acceptor.[3] However there appears to be a lack of experimental evidence for a hydrogen bonding to Au(I) acceptors, since identification of these interactions in crystal structures is complicated by the simultaneous presence of other hydrogen bonding interactions.[4] Here we present quantum mechanical evidence utilising Density Functional Theory confirming that a number of different hydrogen bond donors do form interactions with a variety of Au(I) complexes, which can therefore be classified as Lewis bases.[5] We also show that a secondary interaction (usually a hydrogen bond) is required to fully stabilise the interaction, as observed experimentally.

The nature of these interactions will be described utilising results obtained with the Atoms in Molecules (AIM) and Noncovalent Interactions (NCI) methodologies, while the role that relativistic effects play in stabilising such interactions will be explored.

[1] (a) H. Schmidbaur, F. Scherbaum, B. Hubert, G. Müller, *Angew. Chem. Int. Ed. Engl.*, 1988, **27**, 419. (b) S. S. Pathaneni, G. R. Desiraju *J. Chem. Soc., Dalton Trans.*, 1993, 319-322.

[2] (a) Pyykkö, P., *Chem. Rev.*, 1997, **97**, 597-636; Pyykkö, P., *Angew. Chem. Int. Ed. Engl.*, 2004, **43**, 4412-4456. [

3] E. S. Kryachko, *J Mol. Struct.*, 2008, **880**, 23-30.

[4] H. Schmidbaur, H. G. Raubenheimer, L. Dobrańska, *Chem. Soc. Rev.* 2014, **43**, 345 – 380.

[5] F. Groenewald, J. Dillen, H. G. Raubenheimer, C. Esterhuysen, *Angew. Chem. Int. Ed.* 2016, **55**, 1694 –1698.

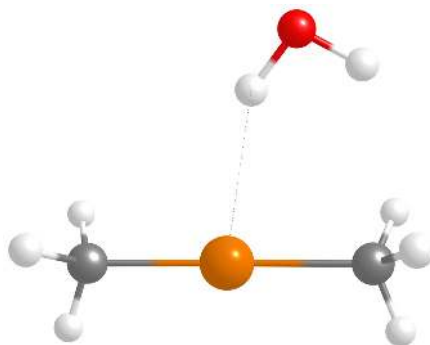


**Figure 1.** Au(CH<sub>3</sub>)<sub>2</sub><sup>-</sup> forming a hydrogen bond with water

**Keywords:** Gold, DFT

**MS30-O4** Supramolecular reactivity in the solid state: Step-wise assembly of ternary cocrystals through hydrogen and halogen bondingFilip Topić<sup>1</sup>, Dominik Cinčić<sup>2</sup>, Vladimir Stilić<sup>2</sup>, Kari Rissanen<sup>1</sup>

1. Department of Chemistry, Nanoscience Center, University of Jyväskylä, Finland  
 2. Department of Chemistry, Faculty of Science, University of Zagreb, Croatia

email: filip.f.topic@jyu.fi

In the field of crystal engineering, cocrystals have been among the most pursued topics in the last two decades.[1] Devising rational strategies for systematically assembling them has been one of the greatest challenges, even more so for cocrystals consisting of more than two components. Whereas both mechanochemical assembly and disassembly of the binary cocrystals have been studied [2,3], the supramolecular reactivity of ternary cocrystals is still almost unexplored [4].

Given our interest in the orthogonality of hydrogen and halogen bonding in the context of supramolecular chemistry, we focused our interest on the combination of thioureas, phosphine oxides and various halogen bond donors. These types of molecules are known to form binary cocrystals through hydrogen (thiourea and phosphine oxide) or halogen bonds (thioureas or phosphine oxides with different halogen bond donors), and we hypothesized that the combination of all three might yield ternary cocrystals.

Our initial studies revealed successful formation of a number of ternary cocrystals, primarily sustained by N–H...O hydrogen bonds between thioureas and phosphine oxides and C–I...S halogen bonds between thioureas and halogen bond donors. Next, reactivity studies were performed in the following way: First, for a given set of three components A, B, C, each two were ground together to probe for the formation of binary cocrystals AB, BC and AC. Subsequently, each of the resulting mixtures or cocrystals was ground with the third component from the set to probe for the formation of ternary solid ABC. These experiments revealed a spectrum of possible outcomes, from component sets where all of AB, BC, AC and ABC were successfully formed, to such cases where only binary cocrystal AB was detected, with all other combinations only yielding various mixtures. Structures of the obtained binary and ternary cocrystals, as well as the results of the mechanochemical experiments, will be discussed.

References: [1] Aakeröy, C. B. *Acta Cryst.* **2015**, B71, 387–391. [2] Cinčić, D., Friščić, T., Jones, W. J. *Am. Chem. Soc.*, **2008**, 130, 7524–7525. [3] Karki, S., Friščić, T., Jones, W. *CrystEngComm*, **2009**, 11, 470–481. [4] Only briefly mentioned in: Bolla, G., Nangia, A. *Chem. Commun.* **2015**, 11, 470–481.

**Keywords:** crystal engineering, mechanochemistry, ternary co-crystals, hydrogen bonding, halogen bonding

**MS30-O5** Hydrogen-bonded cocrystals of the drug metformin: From molecular interactions analysis to supramolecular synthesis and characterization of Met-bis(DCA), a pharmaceutical cocrystal with enhanced anti-leukemic activityPaola Gilli<sup>1</sup>, Valerio Bertolasi<sup>1</sup>, Aleksandar Cvetkovski<sup>2</sup>

1. Department of Chemical and Pharmaceutical Sciences and Centre for Structural Diffractionometry, University of Ferrara, Via Borsari 46, 44121 Ferrara, Italy  
 2. Faculty of Medical Sciences, Goce Delcev University, Krste Misirkov bb, 2000 Stip, Macedonia

email: paola.gilli@unife.it

*N,N*-dimethylbiguanide, metformin (Met) in the medical literature, is a widely used active pharmaceutical ingredient (API) of the biguanide class. Besides being the drug of first choice for oral therapy of type 2 diabetes, its anticancer activity is the subject of active research. Met can exist in three resonance-stabilized forms, *i.e.* as neutral molecule (Met), monoprotonated (MetH<sup>+</sup>) or diprotonated (MetH<sub>2</sub><sup>2+</sup>) cation, with dissociation constants in water typical of biguanides:  $pK_{a1} \sim 12.40$ ;  $pK_{a2} = 2.96$ .

We have investigated the crystal chemistry of Met in series of pharmaceutical cocrystals (PCC) prepared using various acids as cofomers (CF), with particular focus on Generally Recognized as Safe (GRAS) compounds, nutraceuticals and APIs. By cocrystallization under different conditions we obtained 33 PCCs of a quality suitable for structural determination, 27 containing MetH<sup>+</sup> and 6 MetH<sub>2</sub><sup>2+</sup>. The delocalized biguanide fragment is never found to be planar and the hydrogen bond (H-bond) is the dominating molecular interaction. Crystal packing analysis reveals that Met and CF molecules are linked by extended H-bond networks with a number of conserved patterns (dimers, rings, ribbons, sheets, *etc.*). The H-bond strength is increasing with decreasing  $\Delta pK_a$  according to the  $PA/pK_a$  equalization principle. All complexes formed by Met with acidic compounds are salts, as predictable from the thermodynamic acid-base constants. As a consequence of the high value of  $pK_{a1}$  (12.40), neutral Met is easily protonated at the iminic nitrogen even by weak acids, giving rise to 1:1 ionic adducts consisting of monoprotonated MetH<sup>+</sup> and one anion, but since  $pK_{a2}$  is much smaller (2.96), only strong acids succeed in protonating the secondary amino nitrogen, forming 1:2 ionic adducts consisting of diprotonated MetH<sub>2</sub><sup>2+</sup> and two anions.

As successful application, we report the crystal engineering, supramolecular synthesis, crystal structure determination and in vitro biological activity testing of two new PCCs of Met with the antileukemic drug dichloroacetic acid (DCA,  $pK_a = 0.9$ ) in 1:1 (1, MetH<sup>+</sup>•DCA<sup>-</sup>) and 1:2 (2, MetH<sub>2</sub><sup>2+</sup>•2DCA<sup>-</sup>) ratio, respectively. The activity of 1 resembles closely the 1:1

physical mixture of NaDCA and Met.HCl, while **2** displays a significantly higher activity and induces a synergistic apoptotic cell death on primary cells of human patients. To our best knowledge, **2** is the first PCC displaying a synergistic enhancement of the anticancer activity of two APIs.

**Keywords:** hydrogen bond, molecular interactions, pharmaceutical cocrystals, metformin, carboxylic acids, DCA

## MS31 Crystal energy landscapes: computation and uses

Chairs: Anthony Reilly, Marcus Neumann

### MS31-O1 Computed Crystal Energy Landscapes: A First Step towards Digital Drug Product Design?

Susan M. Reutzel-Edens<sup>1</sup>

1. Lilly Research Laboratories

email: reutzel-edens\_susan\_m@lilly.com

Drug product design generally begins with identifying, oftentimes through crystallization screening, solid forms in which to isolate and store the drug substance. When performed under different conditions, crystallization can yield different forms (polymorphs, solvates) with different sizes and morphologies, thus providing an opportunity to engineer particles to desired specifications. To meet the design requirements for the drug product, a solid form must be selected from potentially numerous options discovered through crystallization screening. However, the path to even one commercially-viable form can, in some cases, be lengthy and difficult. Under immense pressure to shorten development timelines and reduce costs, the pharmaceutical industry is keen on right-sizing the time and effort spent on finding suitable solid forms. By contrast, faced with the potential for a product failure should a new, more stable (less soluble) crystal form suddenly appear in a marketed product, finding the most stable crystal form is non-negotiable. In this presentation, the challenges in experimental solid form screening are discussed and the use of computed crystal energy landscapes for enhancing the effectiveness of experimental solid form screens is explored.

**Keywords:** crystal structure prediction, polymorph, solid form screening, pharmaceutical



## MS31-O2 Accurate and Affordable Lattice Energy Calculations: A Solved Problem?

Alexandre Tkatchenko<sup>1,2</sup>

1. University of Luxembourg
2. Fritz-Haber-Institut der Max-Planck-Gesellschaft, Berlin, Germany

email: tkatchen@fhi-berlin.mpg.de

The 6th blind test of crystal structure prediction organized by the Cambridge Crystallographic Data Centre (CCDC) has highlighted the growing maturity of lattice energy calculations based on first-principles density-functional approaches when applied to real-world molecular crystals. Despite clear and significant progress, the existing first-principles calculations are still facing considerable challenges for predicting lattice energies of polymorphic molecular crystals.

In this context, I will summarize the widely used first-principles methods and their successes and failures when applied to the calculation of lattice energies. A particular attention will be paid to the recent exciting finding that many-body dispersion (MBD) effects can play a crucial role in the relative stabilities of molecular crystals of pharmaceutical interest [1]. These findings provide novel control mechanisms in the development and design of intricate polymorphic forms of molecular crystals.

[1] Chem. Sci. 6, 3289 (2015); Angew. Chem. Int. Ed. 52, 6629 (2013); Phys. Rev. Lett. 113, 055701 (2014); Proc. Natl. Acad. Sci. 109, 14791 (2012); Science 351, 1171 (2016).

**Keywords:** Lattice energies, polymorphs, density functional theory, electronic structure, dispersion

## MS31-O3 Organic crystal polymorphism: A benchmark for dispersion corrected mean field electronic structure methods

Jan Gerit Brandenburg<sup>1</sup>, Stefan Grimme<sup>2</sup>

1. Department of Chemistry, University College London, 20 Gordon Street, London, United Kingdom.
2. Mulliken Center for Theoretical Chemistry, University of Bonn, Beringstr. 4-6, 53115 Bonn, Germany.

email: g.brandenburg@ucl.ac.uk

We analyze the energy landscape of the 6<sup>th</sup> crystal structure prediction blind test targets with various ab initio and semiempirical methodologies. A new benchmark set of 59 crystal structures (termed POLY59) for testing quantum chemical methods based on the blind test target crystals is presented.

We focus on different means to include London dispersion interactions within the density functional theory (DFT) framework. We show the impact of pair-wise dispersion corrections like the semi-empirical D2 scheme, the Tkatchenko-Scheffler TS method, and the density dependent dispersion correction dDsC.

Recent methodological progress includes higher order contributions in both the many-body and multipole sense. We use the D3 correction with Axilrod-Teller-Muto type three-body contribution, the many body dispersion MBD, and the nonlocal van der Waals density functional vdW-DF2. The density functionals with D3 and MBD correction provide an energy ranking of the blind test polymorphs in excellent agreement with the experimentally found structures. As computationally less demanding method, we test our recently presented minimal basis Hartree-Fock method (HF-3c) and a density functional tight binding Hamiltonian (DFTB). Considering the speed-up of three to four orders of magnitudes, the energy ranking provided by the low-cost methods is very reasonable. We compare the computed geometries with the corresponding X-ray data where TPSS-D3 performs best. The importance of zero-point vibrational energy and thermal effects on crystal densities is highlighted.

Related references:

- [1] S. Grimme, A. Hansen, J. G. Brandenburg, C. Bannwarth, *Chem. Rev.*, **2016**, in press.
- [2] J. G. Brandenburg, S. Grimme, *Acta Cryst. B.*, **2016**, submitted.
- [3] A. M. Reilly, *et al.*, *Acta Cryst. B.*, **2016**, submitted.
- [4] J. G. Brandenburg, S. Grimme, *Top. Curr. Chem.*, **2014**, 345, 1-23.

**Keywords:** crystal structure prediction, density functional theory, London dispersion interaction

**MS31-O4** Generation of crystal structure landscapes using known crystal structuresGregory P. Shields<sup>1</sup>, Jason C. Cole<sup>1</sup>, Colin R. Groom<sup>1</sup>, Murray G. Read<sup>1</sup>, Ilenia Giangreco<sup>1</sup>, Patrick McCabe<sup>1</sup>, Anthony M. Reilly<sup>1</sup>

1. Cambridge Crystallographic Data Centre

email: shields@ccdc.cam.ac.uk

We have developed an algorithm whereby a target molecule is shape matched to molecules in known crystal structures, which are then used as starting analogues for optimising putative crystal structures of the target molecule with a simple force field. Remarkably, this process generates the experimentally-observed crystal structure for over 90% of the molecules in a test set of around 300  $Z' = 1$  crystal structures of drug-like molecules. Many of the target molecules require fewer than 1000 analogues to generate the experimental crystal structure. While challenges remain for  $Z' > 1$  structures, conformational flexibility and ranking, this procedure shows promise for fast crystal-structure landscape generation and should complement existing structural-informatics tools for assessing organic solid forms.

This presentation will discuss how over 800,000 known crystal structures in the Cambridge Structural Database (CSD) can be used to predict the crystal structures of unknown systems.

**Keywords:** Crystal structure prediction; shape searching; Cambridge Structural Database

**MS31-O5** *Ab initio*  $^{35}\text{Cl}$  solid state NMR-based crystallography of active pharmaceutical ingredients.Angeles Pulido<sup>1</sup>, David A. Hirsch<sup>2</sup>, Robert W. Schurko<sup>2</sup>, Graeme M. Day<sup>1</sup>

1. School of Chemistry, University of Southampton, Southampton, United Kingdom

2. Department of Chemistry and Biochemistry, University of Windsor, Windsor, Canada N9B 3P4

email: mjp1m12@soton.ac.uk

Active pharmaceutical ingredients (APIs) are commonly commercialised in the form of HCl salts; but, as crystalline solids, they frequently exhibit polymorphism. The polymorphic forms may have different physico-chemical properties and the use of the undesired polymorph in a drug could produce catastrophic consequences, not to mention the economic cost. Therefore, knowledge about API polymorphism and accurate structural determination are of great importance in drug development. Structural resolution of polymorphic structures by X-ray diffraction (XRD) can be challenging, especially if single-crystal samples are not available (*e.g.*, for drugs with an API in an amorphous phase).

In this contribution, we show that experimental  $^{35}\text{Cl}$  solid state NMR spectroscopy— and computational —crystal structure prediction and first principles NMR calculations— techniques can be successfully combined to study HCl API polymorphism. We establish a protocol for *ab initio* chlorine- $^{35}\text{Cl}$  solid state NMR crystallography of HCl APIs, see Figure 1. Crystal structure prediction techniques were used to produce a set of computationally generated trial crystal structures for a test set of HCl APIs and to inform about HCl APIs polymorphism trends. First principles  $^{35}\text{Cl}$  solid state NMR shielding and quadrupolar tensors were calculated, within the periodic DFT-D/GIPAW framework, on a subset of low energy predicted crystal structures and the deviation of calculated  $^{35}\text{Cl}$  NMR tensor parameters from the experimentally determined values allows the selection of a few predicted crystal structures as potential matches to the experimentally known reference structure. The true structure can be selected unambiguously from the set of computationally generated crystal structures when information about DFT-D relative stability is included. Moreover, the reliability of periodic DFT-D calculated dipolar and quadrupolar  $^{35}\text{Cl}$  NMR parameters of HCl APIs as well as the potential and limitations of *ab initio*  $^{35}\text{Cl}$  solid state NMR crystallography on HCl APIs structure resolution will be discussed.

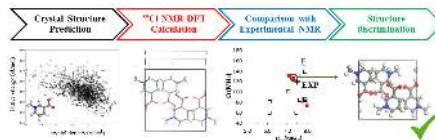


**Figure 1.** Schematic representation of the protocol for *ab initio*  $^{35}\text{Cl}$  solid state NMR crystallography of HCl salts of active pharmaceutical ingredients.

**Keywords:** Crystal structure prediction, NMR crystallography,  $^{35}\text{Cl}$  NMR, DFT calculated  $^{35}\text{Cl}$  NMR, Active Pharmaceutical Ingredients.

## MS32 Polymorphs, cocrystals, solvates, salts: a jungle for scientists and industries

simultaneous explorations of computationally and experimentally generated solid form landscapes for understanding the structural basis of phase transitions in anhydrate/hydrate systems.

[1] Braun, DE et al., Cryst. Growth Des. Submitted.

[2] Braun, DE et al., Mol. Pharmaceutics, 13, 1012–1029, 2016.

**Keywords:** hydrate, polytypism, screening

Chairs: Catharine Esterhuysen, Martin Schmidt

### MS32-O1 Thymine and Orotic Acid - small molecules with unusual hydrates and intriguing solid state phenomena

Doris E. Braun<sup>1</sup>, Ulrich J. Griesser<sup>1</sup>

1. Institute of Pharmacy, University of Innsbruck, Innrain 52c, 6020 Innsbruck, Austria

email: doris.braun@uibk.ac.at

The two structurally related model compounds, thymine [1] and orotic acid [2], show both unique solid state phenomena, with solvate/hydrate formation playing a key role in accessing anhydrous forms and desolvation conditions inducing order-disorder/polytypism and influencing polymorph purity. The solid forms have been studied by a combination of complementary experimental techniques (moisture sorption analysis, thermal analysis, isothermal calorimetry, spectroscopy, X-ray diffractometry) and computational modelling (crystal energy landscape calculations).

Anhydrate polymorphs of thymine (TYM) emerged in an experimental search for solid forms, which was guided by crystal structure prediction studies. The packing mode of three of the four anhydrides, A<sup>o</sup> – C, only differ in the location of the oxygen and hydrogen atoms and are homeoenergetic. Forms A<sup>o</sup> and B are ordered phases, whereas C shows disorder (X-ray diffuse scattering). The computationally generated structures provide models for stacking faults, so that intergrowth is likely. Anhydrate A<sup>o</sup> was identified as the thermodynamically most stable form at ambient conditions. The forms B and C are metastable but show high kinetic stability. The hydrate of thymine is stable only at water activities > 0.95 at temperatures ≤ 25 °C. It was found to be a stoichiometric hydrate despite being a channel hydrate with an unusual water/thymine molar ratio of 0.8. Depending on the dehydration conditions, either anhydrate C or D is obtained. The hydrate is the only known precursor to form D.

The monohydrate of orotic acid (OTA) is a highly stable hydrate, which dissociates above 135 °C and loses only a small part of the water when stored over desiccants (25 °C) for more than one year. Depending on the desolvation conditions of the hydrate or DMSO solvate variability in the crystallinity/ordering of anhydrous OTA is observed, which is also suggested by the computed low energy crystal structures. The variability in anhydrate crystals is of practical concern as it affects the moisture dependent stability of the anhydrate with respect to hydration. These studies highlight the value of

## MS32-O2 Selection of Solid State Forms for New Chemical Entities: Challenges, Opportunities and Lessons

Christoph Saal<sup>1</sup>

1. Merckgroup, Darmstadt, Germany

email: christoph.saal@merckgroup.com

Over the last decades, selection of solid-state forms – including pharmaceutical salts, polymorphs and co-crystals – has become a crucial step at the transition from research to development. Respective solid-state forms represent efficient ways of optimizing physico-chemical parameters of pharmaceutical research compounds. Clearly, in this context solubility and bioavailability play a key role as pharmaceutical industry has to develop more and more low-soluble new chemical entities. However, these are not the only parameters to be considered, as behavior of a solid-state form with regard to manufacturability, processability and stability also have to be considered. In the end, the selection of a salt form is based on a manifold of different aspects, which have to be carefully balanced. The lecture gives an introduction into solid state form selection based on scientific knowledge. Experiences gained by several specific examples where selection of a suitable solid-state form has been challenging – and even sometimes surprising properties of solid state forms became crucial – are discussed.

**Keywords:** Abstract\_ECM\_CS

## MS32-O3 Pharma: improving and controlling properties. Cocrystals, bio-inspired MOFs and Ionic Liquids. Gabapentine a case study.

Maria Teresa Duarte<sup>1</sup>, Vânia André<sup>1</sup>, Sílvia Quaresma<sup>1</sup>, Inês Martins<sup>1</sup>

1. Centro de Química Estrutural, Instituto Superior Técnico, Universidade de Lisboa

email: teresa.duarte@tecnico.ulisboa.pt

Up to now pharmaceutical industry has relied predominantly on crystalline solids, for the delivery of active pharmaceutical ingredients (APIs), however major drawbacks exist in particular their propensity to exhibit polymorphism, their thermal and shelf stability and their solubility. These issues can have a strong impact on the physico-chemical properties of the different solid forms, causing severe bioavailability and drug efficacy problems as well as commercial losses and patent issues. Gabapentin, an amino acid-based drug used to treat neurodegenerative diseases, presenting three polymorphic forms that easily interconvert, has been extensively studied in our laboratory [1-4]. Here we present the work done in its polymorphic control and reactivity, recently recurring to ionic liquids as crystallization solvents and final pharma products. Studies on their multicomponent forms crystal forms presenting enhanced properties at different pH and new gabapentin coordination networks will be extensively presented and discussed. Our results are very exciting and their applications in the pharmaceutical field particularly promising.

1. D. Braga, F. Grepioni, L. Maini, K. Rubini, M. Polito, R. Brescello, L. Cotarca, M. Teresa Duarte, V. André, M.F.M. Piedade *New J. Chemistry* 32 (10), 1788-179, 2008 2. V. André, M. Teresa Duarte, P. P. Santos, A. Fernandes, *Crystal Growth & Design.*, 11, 2325-2334, 2011 3. S. Quaresma, V. André, A. Antunes, L. Cunha-Silva, M. Teresa Duarte, *Crystal Growth & Design*, 13, 5007-5017, 2013 4. S. Domingos, V. André, S. Quaresma, I. Martins, F. Piedade, M. Teresa Duarte, *Journal of Pharmacy and Pharmacology* 67 (6), 830-846, 2015

**Keywords:** Gabapentin, polymorphism, cocrystals, ionic liquids, MOFs

## MS32-O4 Traversing the solid form jungle using the power of the Cambridge Structural Database

Neil Feeder<sup>1</sup>

1. The Cambridge Crystallographic Data Centre

email: feeder@ccdc.cam.ac.uk

The solid form jungle can be a place of high risk or untold opportunity. Uncontrolled crystal form polymorphism can have a critical impact on formulated product robustness, particularly exemplified by the pharmaceutical cases of Norvir<sup>TM</sup> [1] and Neupro<sup>TM</sup> [2], which were withdrawn from the market after the unexpected appearance of a more stable polymorph. However a detailed understanding of that same solid form landscapes can provide us with an opportunity to generate materials with desired properties by choice through crystal engineering[3].

At the CCDC we are developing structural informatics approaches that can mitigate solid form risk and move us towards the notion of solid form by design. Here the vast knowledge base of over 800,000 crystal structures of the CSD and the millions of discrete data points on the geometry of intermolecular interactions contained therein are mined to explore likely crystal packing landscapes. Such an approach complements ab-initio energy calculations yet offers the advantage of being applicable across all solid form types and accessible to solid state scientists rather than just computational specialists. For example, we have developed a CSD based Hydrogen-Bond Propensity tool which would have clearly predicted the likely existence of a more stable polymorph of ritonavir (Norvir<sup>TM</sup>) [4].

Our structural informatics approach to solid form understanding is being developed under the guidance of the Crystal Form Consortium (CFC); a partnership between the CCDC and global pharmaceutical/agrochemical companies. Here we will describe the tools and methodologies developed under the CFC currently available within the CSD-Materials and CSD-Enterprise packages.

In this presentation we will review and demonstrate the impact that structural knowledge derived from the CSD can have on formulated product development as well as broad applications to crystal engineering.

[1] J. Bauer, et al., Pharm. Res., (2001), 18, 859-866.

[2] S. Cajigal, Neurology Today, (2008), 8, 1 & 8.

[3] P. T. A. Galek et al., CrystEngComm, (2009), 11, 2634-2639.

[4] G. R. Desiraju J. Am. Chem. Soc., (2013), 135 (27), 9952–9967.

**Keywords:** Solid Form, Crystal Engineering, Polymorphism, Co-Crystals

## MS32-O5 In the jungle, the mighty jungle, the crystals grow tonight!

Ulrike Werthmann<sup>1</sup>

1. Boehringer Ingelheim GmbH, Germany

email: ulrike.werthmann@boehringer-ingelheim.com

*The process of crystal formation can sometimes be described as a walk through a dense jungle with no clear trail or map to guide you. Unexpected effects and unanticipated formation of “fancy crystals” are observed and this makes the life as scientist within a pharmaceutical industry very exciting! To get orientated in this “jungle” it is necessary to explore a broad experimental space to achieve the goal of identifying the form of an active pharmaceutical ingredient (API) with the most favorable properties for drug development. Using a High Throughput Crystallization Approach (µL-scale) the crystallization conditions can be defined. A large number of different crystallization conditions may be tested and up to 384 experiments can be performed within one run using 96-well plate formats (4 plates). Different solvents and solvent mixtures in combination with a variety of counter ions (for ionisable drugs) and/or cocrystal formers lead to a quick overview of the crystallization behavior of the API. This screening tool may be utilized for polymorph screening as well as for salt- and co-crystal-screening. All solid forms resulting out of this HT-screen (approx. 3mg /well) need to be analyzed by e.g. X-ray powder diffraction to check whether the compound crystallized or not. Furthermore, in order to characterize the resulting crystalline forms and to draw conclusions from the large amount of data (more than 100 patterns from a single experiment), a specific software tool is needed to handle and maintain an overview of the resulting “data jungle”. A case study will be presented to get a bit better orientation in the mighty jungle of crystal formation.*

**Keywords:** API, HT-crystallization, Pharmaceutical Industry

## MS33 Hot structures of small molecules

Chairs: Marijana Dakovic, Andreas Roodt

### MS33-O1 How to fill MOFs with different flavours

Alessia Bacchi<sup>1</sup>, Paolo Pelagatti<sup>1</sup>, Davide Balestri<sup>1</sup>, Stefano Canossa<sup>1</sup>, Patrick Scilabra<sup>1</sup>

1. Dipartimento di Chimica, Università di Parma, Italy

email: alessia.bacchi@unipr.it

The scope of this work is to find a systematic way to embed small molecular aggregates inside porous crystalline materials, with the multiple aims to explore the structural aspects of nanoconfinement, and of the stabilization of guest molecules inside the cavities of the structure. The feasibility of this approach stems from both the recent report that describes the structural determination of single molecules trapped inside a microporous framework [1] and the various reports showing the inclusion of species such as metal nanoparticles or polyoxometalates into mesoporous MOFs [2]. MOFs are highly versatile materials that are made by connecting metal ions with prefixed coordination geometry with rigid ligands acting as spacers, hence affording three-dimensional coordination polymers. The accurate design of the building units allows to design porous MOFs, obtaining cavities of considerable size, which usually accommodate loosely bound solvent molecules. The guest that we are considering here are some important compounds for the human health and nutrition which occur as liquids at room temperature, some organometallic precursors of inorganic oxides, and organometallic compounds potentially active in catalysis. We initially focused on a collection of already known MOFs, and we determined the interaction mode of some of the guests inside the pores (Figure 1), and the results will be shown. We then moved to the design of new organic linkers in order to better tune the topology and functionality of the MOF network. In particular, we aimed to decorate the inner cavities with hydrogen bond and halogen bond active functional groups, which could serve as anchoring points for the guests. A small library of linkers was synthesized: one group is composed by flexible aminocarboxylic linkers, the second one is characterized by rigid amidic bonds and pyridine as coordinative function. These ligands were used for the synthesis of novel MOFs; due to the nature of the ligands these frameworks resulted quite flexible. Their structure and inclusion properties will be illustrated.

[1] Y. Inokuma et al., *Nature*, **2013**, 495, 461–466 [2] C. Rösler, R. A. Fischer, *CrystEngComm*, **2015**, 17, 199–217 [3] H.C. Zhou et al., *J. Am. Chem. Soc.*, **2007**, 129, 1858–1859

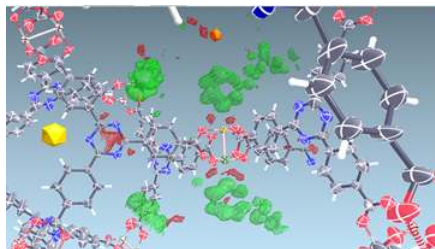


**Figure 1.** Experimental electron density of nicotine included inside the MOF known as PCN6 [3].

**Keywords:** crystal engineering, MOF, inclusion compounds

## MS33-O2 Solid-state transition-metal photoactive materials - tracing structure-property relationships via combined spectroscopic and crystallographic approaches

Katarzyna N. Jarzemska<sup>1</sup>, Radosław Kamiński<sup>1</sup>

1. Biological and Chemical Research Centre, Department of Chemistry, University of Warsaw, Żwirki i Wigury 101, 02-089 Warsaw, Poland

email: katarzyna.jarzemska@gmail.com

Coordination complexes can be described as 'hot' small molecules due to their rich electronic and luminescent properties.<sup>1</sup> Especially interesting here are d<sup>8</sup> or d<sup>10</sup> transition-metal systems, which frequently constitute the active sites of both biological and chemical catalysts, have versatile applications in solar-energy conversion and other fields ranging from molecular electronics and photocatalysts to light-emitting diodes (LEDs) and biolabels. It is, thus, of high importance to sensibly control optical properties of such materials at the molecular level, in order to apply this knowledge to generate materials with particular properties across all the size scales from molecules to bulk materials, relevant for specific applications.

It occurs that short metal-metal contacts usually determine the nature of the lowest lying emissive states, and so are crucial to understand physical properties of the respective materials. In this contribution we shall present our most recent results regarding the analysis of charge transfer processes and structure-property relationships of selected coinage metal complexes (Cu, Ag, Pt, Ni, Fe, etc.) in the solid state.<sup>2-5</sup> For the purpose of our investigations we combined advanced spectroscopic and crystallographic techniques supported by theoretical calculations.

(1) Yam, V. W.-W.; Lo, K. K.-W. *Chem. Soc. Rev.* **1999**, 28, 323. (2) Jarzemska, K. N.; Kamiński, R.; et al. *Inorg. Chem.* **2014**, 53, 10594; Koshevoy, I. O.; Shakirova, et al. *Dalton Trans.* **2011**, 40, 7927. (3) Filatov, A. S.; Hietsoi, O.; Sevryugina, Y.; Gerasimchuk, N. N.; Petrukhina, M. A. *Inorg. Chem.* **2010**, 49, 1626. (4) Trzop, E.; Fournier, B.; Jarzemska, K.; Sokolow, J.; Kamiński, R.; et al. *Acta Cryst.* **2014**, A70, C776. (5) Jarzemska, K. N.; Chen, Y.; et al. *Phys. Chem. Chem. Phys.* **2014**, 16, 15792.

**Keywords:** coordination complexes, charge transfer, photocrystallography

## MS33-O3 Structural differences in enantiopure and racemate organometallic complexes. Application to $[(\eta^5\text{-C}_5\text{Me}_5)\text{RhCl(PN)}]^{\text{+n}}$ complexes

Fernando J. Lahoz<sup>1</sup>, Pilar García-Orduña<sup>1</sup>, María Carmona<sup>1</sup>, Ricardo Rodríguez<sup>1</sup>, Daniel Carmona<sup>1</sup>

1. Institute for Chemical Synthesis and Homogeneous Catalysis (ISQCH), CSIC - University of Zaragoza, C/ Pedro Cerbuna, 12, 50009 Zaragoza (Spain)

email: lahoz@unizar.es

The use of metal-based catalysts is one of the most powerful strategies for synthesizing enantioenriched compounds by asymmetric catalysis. Our lab is focused in the development and structural characterization of different types of coordination complexes, based on 2<sup>nd</sup> and 3<sup>rd</sup> row late transition metals, and in their potential application as homogeneous catalyst precursors, trying to establish a clear correspondence between specific structural parameters and chemical and catalytic activity. This approach usually relies on organometallic complexes where the metal atoms are stereogenic centers. The asymmetric environment around the metal, i.e., the catalyst pocket in which catalysis occurs, may control the achieved enantioselectivity [1-3]. Therefore, the synthesis, isolation and the detailed structural characterization of enantiopure catalysts are primary goals in this research line.

Among the methodologies for enantiomer resolution, crystallization processes have been widely investigated, since Pasteur's famous separation of the sodium ammonium tartrate enantiomers [4]. Here we report on the characterization of a family of  $[(\eta^5\text{-C}_5\text{Me}_5)\text{RhCl(PN)}]^{\text{+n}}$  complexes in different crystals. The metal is always a stereogenic center, and depending on the chiral nature of the employed ligand, the new compounds are mixtures of diastereomers and epimers at the metal. We have been able to obtain and separate red single crystals of enantiopure *R* and *S* at the metal derivatives, together with orange racemate crystals containing both *R* and *S* enantiomers.

A systematic analysis of their crystal and molecular structures has been performed; the pertinent structural parameters concerning metal bonding, ring puckering of chelate ligands' metallacycles, or intramolecular N-H...Cl interactions have been analysed. The presence of solvent molecules in some crystals and their influence in intermolecular interactions will be discussed through Hirshfeld surface and two-dimensional fingerprint plot analysis.

[1] D. Carmona, P. Lamata, A. Sánchez, P. Pardo, R. Rodríguez, P. Ramírez, F.J. Lahoz, P. García-Orduña, L.A. Oro, *Dalton Trans.* **2014**, 43, 15546. [2] D. Carmona, I. Méndez, R. Rodríguez, F.J. Lahoz, P. García-Orduña, L.A. Oro, *Organometallics* **2014**, 33, 443. [3] A. Becerra, R. Contreras, D. Carmona, F.J.



Lahoz, P. García-Orduña, *Dalton Trans.* **2013**, 42, 11640.  
 [4] L. Pasteur; *Annales de Chimie et de Physique*, **1848**, 3, 442.

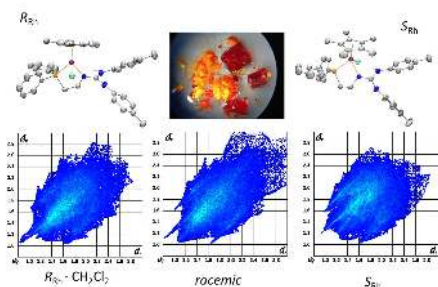


**Figure 1.** Molecular structure of R and S at-metal epimers in enantiopure crystals. Red (enantiopure) and orange (racemic) crystals. Fingerprint plots of rhodium complexes in the three crystals.

**Keywords:** Enantiopure, Racemic, Metal complexes,

## MS33-O4 Expanding the horizons of sky blue nitrosocarboranes

Georgina M. Rosair<sup>1</sup>, Samuel L. Powley<sup>1</sup>, Louise Schaefer<sup>1</sup>, Wing Y. Man<sup>1</sup>, David Ellis<sup>1</sup>, Alan J. Welch<sup>1</sup>

<sup>1</sup>. Institute of Chemical Sciences, Heriot Watt University, Edinburgh, UK

email: G.M.Rosair@hw.ac.uk

Nitrosocarboranes are a beautiful sky blue colour in contrast to most other carborane derivatives which are colourless. However it is the ability of NO to act as both a one electron and three electron donor that inspires our use of this substituent. Since the number of polyhedral skeletal electron pairs has a key role in the structure of carboranes, NO with its one and three electron donor possibilities has potential to effect changes in carborane structure and chemistry. In this work [1] both mono and bis(carborane) nitroso species have been studied (see example below left). In all cases the nitroso group bonds to the carborane as a one electron substituent (C–N–O angle ca. 113 degrees). An unexpected challenge arose in that two of the species (e.g. Fig. 1 left) are liquid at room temperature so structure determinations were performed on crystals grown *in situ* on the diffractometer from liquid samples. Glass Lindemann 0.3mm capillaries are the only additional equipment required for a standard data collection (in addition to patience and manual dexterity).

Both mono- and dinitroso derivatives of *meta* carborane and 1,1'-bis(*m*-carborane) were synthesised and structurally characterised. However the mononitroso derivative of bis(*o*-carborane) could not be prepared by the same method, instead the colourless hydroxylamine derivative was formed. Reasons behind this were explored and identified. The dinitroso *ortho*-carborane and bis(*o*-carborane) species were also elusive with alternative products proposed. Another strategy was employed for these *ortho* compounds; since the NO group can undergo Diels-Alder cycloaddition reactions with a cyclic 1,3-diene, we prepared derivatives of the unobtainable dinitroso *ortho*-carborane and bis(*o*-carborane) (Fig. 1, right)

1. S. L. Powley, L. Schaefer, W. Y. Man, D. Ellis, G. M. Rosair and A. J. Welch, *Dalton Trans.*, 2016, **45**, 3635.

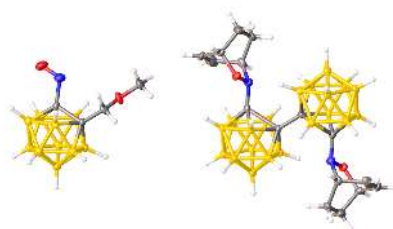


**Figure 1.** [1-NO-2-CH<sub>3</sub>OCH<sub>3</sub>-1,2-*closo*-C<sub>2</sub>B<sub>10</sub>H<sub>10</sub>] left and isolated derivative of dinitroso bis(*o*-carborane) (right).

**Keywords:** Nitroso, carborane, in-situ crystallography

**MS33-O5 Silolyl-FeCp complexes: is there a way to sila-ferrocene?**Petra Bombicz<sup>1</sup>, Csaba Fekete<sup>2</sup>, Réka Mokrai<sup>2</sup>, László Nyulászi<sup>2</sup>, Ilona Kovács<sup>2</sup><sup>1</sup>. Institute of Organic Chemistry, Research Centre for Natural Sciences, Hungarian Academy of Sciences, Magyar Tudósok körútja 2, Budapest, H-1117, Hungary<sup>2</sup>. Department of Inorganic and Analytical Chemistry, Budapest University of Technology and Economics, Szt. Gellért tér 4, Budapest, H-1111, Hungary

email: bombicz.petra@ttk.mta.hu

One of the milestones in organometallic chemistry is the synthesis of ferrocene by Kealy and Pauson in 1951 [1,2] and the determination of its structure by Wilkinson and Woodward in 1952 [3]. These achievements opened up the way to the use of metallocenes in applied and material science from polymerization catalysis to UV fluorescent materials [2]. Nowadays several metallocenes are known in which not just the central iron atom is replaced by other transition metals but also the ligands are changed to heterocyclopentadienyl analogues containing other main group elements such as P, As or Sb [4,5]. Notwithstanding, the number of known metallocenes possessing silicon or germanium containing heterocycles is small.

The reaction of 1-chlorosilols and K[Fe(CO)<sub>2</sub>Cp] in THF yielded two new η<sup>1</sup>-silolyl-FeCp(CO)<sub>2</sub> complexes in good yield. We report the molecular and crystal structures of the complexes, and their attempted transformation (by heating or UV irradiation) to the metallocenes. The reason for the increased stability of these carbonyl complexes can be attributed to the increased σ-electron donating behaviour of the silicon to the central Fe, while the aromaticity of the silolyl ligand seems to have less influence [6].

**References:**

- [1] Kealy, T. J.; Pauson, P. L. "A New Type of Organo-Iron Compound". *Nature* 168(4285): 1039-1040. 1951.
- [2] Pauson, P. L. "Ferrocene-how it all began". *J. Organomet. Chem.* 637–639: 3–6. 2001.
- [3] G. Wilkinson, M. Rosenblum, M. C. Whiting, R. B. Woodward. "The Structure of Iron Bis-Cyclopentadienyl". *Journal of the American Chemical Society* 74(8): 2125–2126. 1952.
- [4] R.S.P. Turbervill, A.R. Jupp, P.S.B. McCullough, D. Ergöçmen, J.M. Goicoechea. "Synthesis and Characterization of Free and Coordinated 1,2,3-Tripnictolide Anions" *Organometallics* 32. 2234-2244. 2013.
- [5] M. Fleischmann, S. Welsch, H. Krauss, M. Schmidt, M. Bodensteiner, E.V. Peresypkina, M. Sierka, C. Gröger, M. Scheer. "Complexes of Monocationic Group 13 Elements with Pentaphospha- and Pentaarsaferrocene" *Chem. Eur. J.* 20 3759-3768. 2014.
- [6] C. Fekete, R. Mokrai, P.Bombicz, L. Nyulászi, I. Kovács: „η<sup>1</sup>-silolyl-FeCp(CO)<sub>2</sub> complexes. Is there a way to sila-ferrocene?" *Journal of Organometallic Chemistry* 799-800. 291-298. 2015.

**Keywords:** sila-ferrocene, silolyl-FeCp complexes**MS34 Molecular recognition, supramolecular chemistry and crystal engineering**

Chairs: Chiara Massera, Carl Henrik Görbitz

**MS34-O1 Sense and flexibility: self-assembly, host-guest chemistry and solid state dynamic behaviour of cyclic peptoids**Consiglia Tedesco<sup>1</sup>, Eleonora Macedi<sup>1</sup>, Alessandra Meli<sup>1</sup>, Francesco De Riccardis<sup>1</sup>, Vincent J. Smith<sup>2</sup>, Leonard J. Barbour<sup>2</sup>, Irene Izzo<sup>1</sup><sup>1</sup>. Università di Salerno, Dipartimento di Chimica e Biologia "A. Zambelli", via Giovanni Paolo II, 84084 Fisciano, Italy<sup>2</sup>. Stellenbosch University, Department of Chemistry and Polymer Science, Private Bag X1, 7602 Matieland, South Africa

email: ctedesco@unisa.it

The design and synthesis of artificial systems able to mimic biological functions is the aim of extensive research activity in the field of molecular nanotechnology. Cyclic peptoids for their biostability and potential diversity seem to be the ideal candidates to evoke biological activities and novel chemical properties [1].

Peptoids differ from peptides in the backbone position of the side chains, which are attached to the nitrogen atoms. Due to the lack of the amide proton, CH<sub>2</sub>–OC hydrogen bonds and CH–π interactions, play a key role in the solid-state assembly of cyclic α-peptoids: face to face or side by side arrangement of the macrocycles mimic β-sheet secondary structure in proteins [2,3].

Interestingly, the side chains may act as pillars: they may extend vertically with respect to the macrocycle plane and determine the columnar arrangement of the peptoid macrocycles [3].

Moreover, the peculiar conformational flexibility of cyclic peptoids is the key to their solid state dynamic behaviour. A cyclic peptoid compound, strategically decorated with propargyl and methoxyethyl side chains, undergoes a reversible single-crystal-to-single-crystal transformation upon guest release/uptake (see figure). The extensive and reversible alteration in the solid state is connected to the formation of an unprecedented "CH–π zipper", which can reversibly open and close, thus allowing for guest sensing [4].

This contribution shows how easily tunable cyclic peptoids may lead to functional materials, that feature both robustness and adaptivity, at the frontier between materials science and biology.

This research has received funding from the People Programme (Marie Curie Actions) FP7/2007-2013/ under REA grant agreement n°PIRSES-GA-2012-319011.

[1] a) Schettini R., De Riccardis F., Della Sala G., Izzo I. *J. Org. Chem.* **81**, 2494 (2016); b) Lepage M. L. *et al. Chem. Eur. J.* **22**, 5151 (2016).

[2] a) Izzo I., Ianniello G., De Cola C., Nardone B., Erra L., Vaughan G., Tedesco C., De Riccardis F. *Org. Lett.* **15**, 598 (2013); b) Maulucci N. *et al. Chem. Commun.* 3927 (2008).

[3] Tedesco C., Erra L., Izzo I., De Riccardis F. *CrystEngComm* **16**, 3667 (2014).

[4] Meli A., Macedi E., De Riccardis F., Smith V. J., Barbour L. J., Izzo I., Tedesco C. *Angew. Chem. Int. Ed. Engl.* **55**, 4679 (2016).

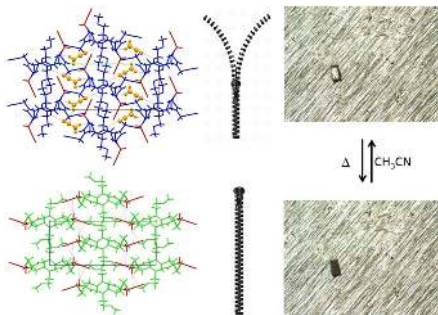


**Figure 1.** Single crystal to single crystal transformation upon acetonitrile release and uptake for the cyclic peptoid cyclo-(Nme-Npa)<sub>4</sub>, Nme = N-(methoxyethyl)glycine, Npa = N-(propargyl)glycine. Open CH- $\pi$  zipper in the acetonitrile inclusion compound and closed CH- $\pi$  zipper in the desolvated form.

**Keywords:** Crystal Engineering, Host-Guest Chemistry, Cyclic Peptoids, CH- $\pi$  interactions

## MS34-O2 Supramolecular chemistry of the *p*-carboxylatocalix[4]arenes

Scott J. Dalgarno <sup>1</sup>

<sup>1</sup> Heriot-Watt University, Riccarton, Edinburgh, EH14 4AS

email: S.J.Dalgarno@hw.ac.uk

Calixarenes have been used widely in supramolecular chemistry for a variety of reasons, some of which include their conformational versatility and ease of synthetic modification. The *p*-carboxylatocalix[4]arenes (*p*CO<sub>2</sub>[4]s) have received relatively little attention as molecular building blocks, which is surprising as they hold great potential in the formation of both discrete and polymeric metal-organic systems. In recent times we have been exploring the synthesis of *p*CO<sub>2</sub>[4]s in either cone or pinched-cone conformations, simultaneously varying the numbers of upper-rim carboxylic acid groups present at selected positions. These changes have marked effects on the resulting metal-directed assembly, as evidenced by the formation of either coordination polymers or discrete capsules.<sup>1-4</sup> The talk will outline these developments before moving on to discuss very recent exploration of the synthesis and metal-directed assembly of partial-cone *p*CO<sub>2</sub>[4]s.<sup>5</sup> In the first result obtained with this new conformer, the divergent nature of the molecule gives rise to an interesting discrete assembly that may itself act as a building block for directed assembly.

1. P. P. Cholewa, C. M. Beavers, S. J. Teat, S. J. Dalgarno, *Chem. Commun.*, **2013**, 49, 3203; 2. P. P. Cholewa, C. M. Beavers, S. J. Teat, S. J. Dalgarno, *Cryst. Growth Des.*, **2013**, 13, 2703; 3. P. P. Cholewa, C. M. Beavers, S. J. Teat, S. J. Dalgarno, *Cryst. Growth Des.*, **2013**, 13, 5165; 4. P. P. Cholewa, S. J. Dalgarno, *CrystEngComm*, **2014**, 16, 3655; 5. R. E. Fairbairn, S. J. Teat, K. J. Gagnon, S. J. Dalgarno, *CHIMIA*, **2015**, 69, No. 9.

**Keywords:** Supramolecular Chemistry, Calixarenes, Directed Assembly, Host-Guest Chemistry

**MS34-O3 Structural Layers in High-Z' Molecular Crystals**Carolyn P. Brock<sup>1</sup>

1. University of Kentucky

email: cpbrock@uky.edu

More than 280 organic crystal structures archived in the CSD and having more than four molecules in the asymmetric unit and  $R < 0.075$  have been investigated in detail and found to be reliable. A surprising discovery is that approximately 25 – 30% of them include easily recognizable structural layers.

There is no standard definition of a structural layer. Layers are obvious if two-dimensional regions of van der Waals contacts separate more densely packed molecular slabs; such layers are particularly obvious if they include strong intermolecular interactions such as hydrogen bonds. If there is a two-dimensional network of hydrogen bonds then layers can be described even if there is some interpenetration, such as by protruding phenyl rings. Likewise, parallel H-bonded chains are often described as forming a layer.

Layers can also be described if two-dimensional regions have higher approximate local symmetry than does the crystal as a whole. Such layer symmetry, which is often quite exact, is broken by the stacking. It has proved useful to describe such layers using the layer groups tabulated in Volume E of *International Tables*.<sup>1</sup> Some layer groups occur much more frequently than do others.

In some structures composed of stacked layers at least one of the layers is related to the others by rotation about an axis normal to or lying within the layer. Two sets of molecular polytypes have been found in which the same layer is stacked in different ways.

The most unusual structures are those in which two quite different layer types alternate. The H-bonding patterns in the two layers may differ and/or their symmetries may vary. One of the layers may incorporate a solvent molecule or one layer may be enantiomerically pure while the other is racemic.

It seems that these layered structures must provide hints about possible mechanisms of crystal nucleation and growth.

It is a pleasure to acknowledge the CCDC's very powerful visualization program *Mercury*<sup>2</sup>, without which this study would have been impossible.

<sup>1</sup>Kopský, V.; Litvin, D. B. *International Tables for Crystallography, Vol. E, Subperiodic Groups*, 2002, Dordrecht, The Netherlands: Kluwer Academic Publishers.

<sup>2</sup>Macrae, C. F., et al. *J. Appl. Cryst.*, 2008, 41, 466 – 470.

**Keywords:** crystal packing, high-Z' structures

**MS34-O4 From versatile hydrogen- and halogen-bond acceptors to elastic bending of metal-containing architectures**Marijana Đaković<sup>1</sup>, Mladen Borovina<sup>1</sup>, Željka Soldin<sup>1</sup>, Ivan Kodrin<sup>1</sup>, Aleksandar Višnjevac<sup>2</sup>, Christer B. Åakeröy<sup>3</sup>

1. Department of Chemistry, Faculty of Science, University of Zagreb, Zagreb, Horvátovac 102a, Croatia

2. Ruđer Bošković Institute, Bijenička 54, 10000 Zagreb

3. Department of Chemistry, Kansas State University, Manhattan, KS, USA

email: mdjakovic@chem.pmf.hr

In order to use weak interactions as effective tools in deliberate synthesis of desired metal-containing supramolecular assemblies a very detailed understanding of the importance of different noncovalent interactions is required [1,2]. Thanks to their comparable strengths and directionalities, hydrogen and halogen bonds have emerged as key synthetic tools in this context [3].

To establish similarities and possible mimicry of the two types of interactions we have carried out a structural examination of a series of metal-based halide complexes with pyridine-type ligands equipped with functionalities capable of forming of either hydrogen or halogen bonds. Our results indicate that synthon-transferability from system to system, regardless of the building-block dimensionality, is a genuine possibility. Some surprising physical properties, including elastic bending (Fig.1), will be discussed against a backdrop of weak interactions using a combination of experiment and theory.

**References:** [1] I. Kodrin, Ž. Soldin, C.B. Åakeröy, M. Đaković, *Cryst. Growth Des.*, 2016, 16, 2040-2051. [2] M. Đaković, D. Vila-Viçosa, M. J. Calhorda, Z. Popović, *CrystEngComm*, 2011, 13, 5863–5871. [3] C.B. Åakeröy, M. Baldrighi, J. Desper, P. Metrangolo, G. Resnati, *Chemistry*, 2013, 48, 16240-16247.

**Acknowledgment** This work has been fully supported by Croatian Science Foundation under the project UIP-11-2013-1809.



**Figure 1.** Elastic bending in crystals of  $[\text{CdBr}_2(1\text{-pz})_2]_n$ .

**Keywords:** hydrogen bond, halogen bond, elastic bending

## MS34-O5 Mechanisms of Guest Exchange and Selectivity in Host-Guest Systems

Luigi R. Nassimbeni<sup>1</sup>

1. University of Cape Town

email: luigi.nassimbeni@uct.ac.za

Halogenated organic host-guest compounds have been exposed to organic guest vapours in order to elucidate the mechanism of guest exchange. In the case of the inclusion compound tetrakis(4-bromophenyl)ethylene (H1) with dichloroethane (DCE), the kinetics of guest exchange with methyl iodine (MeI) vapour was monitored and the crystal structure of the intermediate product elucidated. The latter contains both guests DCE and MeI in distinct positions in an expanded unit cell. When the guests exchanged are Benzene and Piperidine, the guests occupy the same sites and the mechanism is one of isomorphous replacement.

The mechanism controlling synergistic effects of enhanced selectivity in host-guest chemistry have yielded interesting results. This is when two similar host compounds are exposed simultaneously to a target mixture of similar guests with a view to separating one particular guest. We have investigated the isomers of xylene, picolines and lutidines and explained the results in terms of the non-bonded interactions that occur in the crystal structures.

**Keywords:** Mechanism, Guest-exchange, Selectivity

## MS35 Simulation of dynamics in molecular compounds

Chairs: Anders Østergaard Madsen, Markus Meuwly

## MS35-O1 Lattice Vibrations in Molecular Crystals: Polymorphism and Phase Transitions

Jonas Nyman<sup>1</sup>, Graeme M. Day<sup>1</sup>

1. University of Southampton

email: jn1m12@soton.ac.uk

It is possible to predict how molecules will crystallise by performing an exhaustive search of all possible molecular packing alternatives and identifying the most energetically favourable crystal structures. The development of methods for Crystal Structure Prediction (CSP) is a rapidly growing field within computational chemistry. The most common methods rely on computing the cohesive energy between the molecules, while ignoring effects due to temperature and pressure. Lattice vibrational calculations can be used to account for thermal contributions to the lattice free energy and hence have the potential of improving the outcome of crystal structure predictions and may reveal the temperature-dependence of the stabilities of alternative crystal forms, such as polymorphs, cocrystals and solvates, see Figure 1.

We have implemented computationally very efficient methods that facilitate large scale application of harmonic and quasi-harmonic lattice dynamics to hundreds of polymorph pairs or to entire landscapes of predicted crystal structures. A benchmarked and highly accurate anisotropic force field is used to perform rigid-molecule vibrational calculations to obtain Gibbs lattice free energies of molecular crystals. Special care is taken in dealing with phonon dispersion in a way rarely affordable with electronic structure methods. Methods that dramatically improve the sampling of the first Brillouin zone will be presented.

I will also present results demonstrating that polymorphs of organic molecular crystals tend to have very similar thermochemical properties, which has important consequences for the prediction and development of molecular materials.

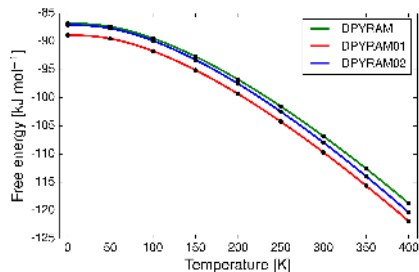


**Figure 1.** Lattice free energy curves of three polymorphs of 2,2'-dipyridylamine (CSD ref. DPYRAM) calculated with quasi-harmonic lattice dynamics in a highly accurate anisotropic force field.

**Keywords:** lattice dynamics, polymorphism, crystal structure prediction, phase transition, Brillouin zone integration

## MS35-O2 Diffuse scattering, spectroscopy and ab initio density functional theory

Matthias J. Gutmann<sup>1</sup>

<sup>1</sup> Rutherford Appleton Laboratory, ISIS Facility, Chilton Didcot, Oxfordshire OX11 0QX, United Kingdom

email: matthias.gutmann@stfc.ac.uk

Diffuse scattering in a crystal arises from any local deviation from long-range order and can be dynamic or static in origin. Most of the time, phonons are the main cause and this is known as thermal diffuse scattering. Phonons can be obtained from density functional theory and examples will be shown, where such calculations are compared with diffuse scattering from single crystals and phonon spectra from powdered samples. When using neutrons it is possible under certain circumstances to observe phonon excitations directly in a diffraction pattern. This leads to rather peculiar diffuse scattering which breaks the symmetry of the diffuse scattering and an example of this will be shown [1]. The second part will focus on benzil. Diffuse scattering in benzil has been the subject of a number of studies using X-rays and neutrons [2,4]. So far mostly Monte-Carlo modelling has been applied to the room-temperature phase [2]. Such a model has allowed least-squares refinement against joint X-ray and neutron data [3]. Here, we use an alternative approach to model the thermal diffuse scattering using ab-initio phonons. The study is extended to the diffuse scattering in the low temperature phase. The ab-initio models are compared to neutron spectroscopic data in the two phases leading to a complete assignment of the phonons. In a previous neutron experiment [4], interesting inelastic effects were observed, leading to peculiar modification of the diffuse scattering and ascribed to direct phonon excitations. However, this effect could not be simulated so far. Here, we employ a recently developed methodology to give a complete account of this effect [1].

[1] M. J. Gutmann, G. Graziano, S. Mukhopadhyay, and K. Refson, *J. Appl. Cryst.* 48, 1122 (2015).

[2] T. R. Welberry, D. J. Goossens, A. J. Edwards and W. I. F. David, *Acta Cryst.* A57, 101 (2001)

[3] D. J. Goossens, T. R. Welberry, A. P. Heerdegen, and M. J. Gutmann, *Acta Cryst.* A63, 30 (2007).

[4] T. R. Welberry, D. J. Goossens, W. I. F. David, M. J. Gutmann, M. J. Bull and A. P. Heerdegen, *J. Appl. Cryst.* 36, 1440 (2003)

**Keywords:** diffuse scattering, neutron, X-ray

### MS35-O3 Predicting Urea Crystal Shapes Grown from Solution with Molecular Dynamics Simulations

Zoran Bjelobrk<sup>1</sup>, Matteo Salvalaglio<sup>2</sup>, Michele Parrinello<sup>3,4</sup>, Marco Mazzotti<sup>1</sup>

1. Institute of Process Engineering, ETH Zürich, Switzerland
2. Department of Chemical Engineering, University College London, United Kingdom
3. Department of Chemistry and Applied Biosciences, ETH Zürich, Switzerland
4. Facoltà di Informatica, Istituto di Scienze Computazionali, Università della Svizzera Italiana, Switzerland

email: zoranb@ethz.ch

Crystallization is a common purification method for the production of active pharmaceutical ingredients and fine chemicals. The shape of crystalline particles influences downstream unit operations such as filtering and tableting, as well as physical and chemical properties such as solubility and bioavailability. Hence, control of the crystal shape is of crucial interest in the manufacturing of pharmaceutical compounds.

The macroscopic growth morphology of crystals is determined by the relative growth rates of the individual crystal faces [1]. Therefore, an atomistic description of the crystal surface dynamics, including the interaction of the crystal surface, solute, solvent and additives, allows for the prediction of crystal shapes grown from solution [2].

In this work, we examine the morphology of urea crystals grown from different solutions through the combination of molecular dynamics simulations and theory together with dedicated experiments [2, 3]. The free energies of adsorption of the liquid phase molecules onto the particular crystal faces are evaluated with advanced simulation methods comprising well-tempered metadynamics and variationally enhanced sampling [4]. From the molecular dynamics simulations and theory we are able to predict the steady-state crystal habits of urea in dependence of solvent, additive concentration, and supersaturation.

[1] A. A. Chernov *Sov. Phys. Crystallogr.* **1962**, *7*, 728–730.

[2] M. Salvalaglio et al. *Angew. Chem. Int. Ed.* **2013**, *52*, 13369–13372.

[3] M. Salvalaglio et al. *J. Am. Chem. Soc.* **2012**, *134*, 177221–17233.

[4] O. Valsson et al. *Phys. Rev. Lett.* **2014**, *113*, 090601.

**Keywords:** crystallization, molecular dynamics, urea

### MS35-O4 Computational dehydration of an organic hydrate using molecular dynamics simulations

Anders S. Larsen<sup>1</sup>, Jacco van de Streek<sup>1</sup>, Jukka Rantanen<sup>1</sup>, Kristoffer E. Johansson<sup>1</sup>

1. Department of Pharmacy, University of Copenhagen

email: anders.larsen@sund.ku.dk

Organic crystal structures can dehydrate to an anhydrous product, which might be completely different on important parameters such as solubility and stability. Our goal is to computationally investigate dehydration of these organic crystals at the molecular level.

Our method is based on classical molecular dynamics (1), which is able to calculate the time evolution of a crystal structure. The energy of the system is calculated with the force field COMPASS (2). The method for dehydrating the crystal is to remove the water molecules periodically during the simulation, this has proven a quite effective way to force the crystal into an anhydrous state. The time interval between the removal of the water molecules is 10 picoseconds and 2-5 are removed at a time. The systems we have investigated are prednisolone (3) and ampicillin trihydrate (4). In the bulk simulations with Prednisolone, water molecules showed great mobility in the water channels at 300 K. This is a result of the hydrophobic nature of the channels and it confirms the non-stoichiometric nature of the Prednisolone crystal structure. For ampicillin trihydrate the water molecules did not diffuse through the crystal or along the channels, instead the hydrogen bonding network stayed largely intact at 300 K, with the hydrogen bonding pattern extending along the channel. Although thermal motion might move the water molecule far from its equilibrium position and thus weakening the hydrogen bond, it will always return to its original position.

Water molecules are periodically removed with the previously described protocol which results in a severely disordered dehydration intermediate. As more water molecules are removed the disorder decreases. After all the water molecules are gone the crystal transform into a new anhydrate structure. Molecular dynamics is capable of describing the qualitative aspects of hydrates and shows promise for investigation of dehydration at the molecular level.

#### References

1. A. Nemkevich, H. Bürgi, M. A. Spackman and B. Corry, *Phys. Phys. Chem.* **2010**; *12*: 14916-14929.
2. H. Sun, *J. Phys. Chem. B* **1998**; *102*: 7338-7364.
3. S. R. Byrn, P. A. Sutton, B. Tobias, J. Frye and P. Main, *J. Am. Chem. Soc.* **1988**; *110*: 1609-1614
4. J. C. Burley, J. van de Streek and P. W. Stephens. *Acta Cryst* **2006**; *E62*: o797-0799.

**Keywords:** Molecular Dynamics, Dehydration



## MS35-O5 The application of tailor-made force fields and molecular dynamics for NMR crystallography

Xiaozhou Li<sup>1</sup>, Marcus A. Neumann<sup>2</sup>, Jacco van de Streek<sup>1</sup>

1. Department of Pharmacy, University of Copenhagen, Universitetsparken 2, DK-2100 Copenhagen, Denmark

2. Avant-garde Materials Simulation GmbH, Rosa-Luxemburg-Strasse 14, D-79100 Freiburg, Germany

email: xiaozhou.li@sund.ku.dk

The NMR crystallography method, which utilises solid-state NMR (SS-NMR) spectroscopy, possibly in combination with powder X-ray diffraction and *ab initio* chemical shift calculations, is becoming attractive in the elucidation of the structural and dynamic aspects of molecular crystals.<sup>[1]</sup> SS-NMR experiments are usually conducted at ambient temperature, and represent a time and space average. *Ab initio* SS-NMR calculations, however, are usually based on static density functional theory (DFT) calculations at zero Kelvin, leading to discrepancies between experimental and calculated chemical shifts.

For *in silico* calculations, the thermal motion of molecular crystals can be introduced by molecular dynamics (MD) if a force field that can properly describe the energy potential of the system of interest is available. Traditional force fields, which are generally not transferable for a wide spectrum of systems, may not represent the correct potential or configuration of a molecular crystal.<sup>[2]</sup> Tailor-made force fields (TMFFs) are an option to overcome such a limitation: the force fields are parameterised against DFT reference data for individual molecules.<sup>[3]</sup> Dispersion-corrected DFT (DFT-D) is well-known for its accuracy and transferability for the reproduction of molecular crystals.<sup>[4]</sup>

We will present a computational study, which aims to evaluate the performance of a tailor-made force field for the effects of thermal motion on *ab initio* chemical shift calculations, by comparing the chemical shifts calculated for crystal structure candidates obtained from crystal structure prediction using three different approaches: static DFT-D energy minimisations, motional averaging with an existing benchmark (the COMPASS force field)<sup>[5]</sup> and motional averaging with the TMFF. The crystal structure of cocaine free base will be used as an example.

### References

- [1] R. K. Harris *et al.*, NMR crystallography. (2009) John Wiley & Sons, Chichester.
- [2] A. Nemkevich *et al.*, Phys. Chem. Chem. Phys., (2010) **12**, 14916-14929.
- [3] M. A. Neumann, J. Phys. Chem. B, (2008) **32**, 9810-9829.
- [4] J. van de Streek and M. A. Neumann, Acta Cryst., (2010) **B66**, 544-558.
- [5] H. Sun, J. Phys. Chem. B (1998) **102**, 7338-7364.

**Keywords:** Molecular dynamics, Tailor-made force field, Density functional theory, NMR crystallography

## MS36 Crystallography in solid state reactions and catalysis

Chairs: Fernando Lahoz, Krešo Bučar

### MS36-O1 Designing single-crystal-to-single-crystal Diels-Alder reactions: the role of nonbonded interactions

Demetrius C. Levendis<sup>1</sup>, Sanaz Khorasani<sup>1</sup>, Delbert Botes<sup>1</sup>, Manuel A. Fernandes<sup>1</sup>

1. Molecular Sciences Institute, School of Chemistry, University of the Witwatersrand, Johannesburg

email: demetrius.levendis@wits.ac.za

Electron donor/acceptor (EDA) interactions influence the way in which pairs of dithiin and anthracene molecules assemble, forming heteromolecular crystals of charge-transfer (CT) complexes that can potentially react in the solid state.

Typically the crystal structures consist of stacks of alternating electron donor and acceptor molecules in a 1:1 ratio. These crystals can then undergo a thermally induced solid-state (SS) Diels – Alder reaction in a single-crystal-to-single-crystal (SCSC) fashion<sup>1-3</sup>, with the dithiin molecules as the dienophiles and anthracenes as the diene (see Figure 1: R = allyl, cyclobutyl or phenyl; X = Br or Me). Examination of close contacts in one such crystal, AD:9BrA (R = allyl, X = Br), indicates that the diene can theoretically react with the dienophile above or below it within a stack as the reaction distances are less than 3.5 Å in both directions.

A single crystal was selected and allowed to react at 30 °C, analyzed at various states of conversion by single-crystal X-ray diffraction, and was found to react by approximately 10% every 6 days, with the reaction occurring in a single direction along the CT stack axis. The solid-state reaction creates a void space which leads to a molecular conformational change within the crystal. The reaction occurs topochemically when fewer than 28% or more than 80% of the molecules have reacted, with minimal motion during the reaction. In the conversion range of 28 – 80%, the reaction occurs in an almost topotactic manner with significant molecular motion and associated crystal deterioration.

Consequently, the single crystal shows significant signs of deterioration after approximately 28% conversion but remained intact upon further reaction and was found to anneal as 100% conversion was approached, leading to the formation of new intermolecular interactions not

present in the starting crystal.

In this paper we discuss the central role of the nonbonded interactions (which differ according to the substituents on the dithiin and anthracene molecules) in determining the nature of the reaction cavity, the direction in which and the extent to which the reaction occurs.

[1] J. H. Kim, S. M. Hubig, S. V. Lindeman, J. K. Kochi, *J. Am. Chem. Soc.*, 2001, 123, 87-95. [2] S. Khorasani, M.A. Fernandes, *Cryst. Growth Des.*, 2013, 13, 5499–5505. [3] S. Khorasani, D. Botes, M.A. Fernandes, D.C. Levendis, *CrystEngComm.*, 2015, 17, 8933-8945.

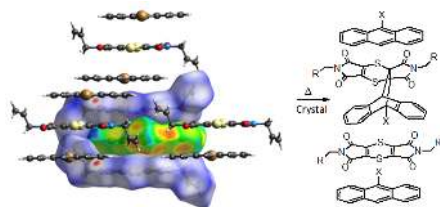


**Figure 1.** Packing in the crystal structure of AD:9BrA (bis (N-allylimino)-1,4-dithiin: 9-bromoanthracene). The Diels-Alder product forms in the reaction cavity initially in a topochemical fashion, influenced by intermolecular interactions.

**Keywords:** solid-state reaction, Diels-Alder, topochemical, reaction cavity, charge-transfer complex, molecular recognition

## MS36-O2 The Emergence of Medicinal Mechanochemistry

Tomislav Friscic<sup>1</sup>

1. McGill University

email: tomislav.friscic@mcgill.ca

This presentation will highlight how the overlap of previously unrelated areas of solid-state mechanochemical synthesis,<sup>[1]</sup> i.e. screening for API solid forms, organic synthesis by milling, and mechanochemical screening for molecular recognition, enables the emergence of a new research discipline in which different aspects of pharmaceutical and medicinal chemistry are addressed through solid-state reactivity, rather than the conventional solution-based routes. This nascent area of *medicinal mechanochemistry*<sup>[2]</sup> is likely to have a strong impact on future pharmaceutical and medicinal chemistry, by offering not only access to materials and reactivity that are sometimes difficult or even impossible to access from solution, but also by providing a general answer to the demands of pharmaceutical industry for cleaner, safer and efficient synthetic solutions.<sup>[3,4]</sup>

[1] James *et al.* *Chem. Soc. Rev.* **2012**, 41, 413.

[2] Tan, Loots, Friscic, *Chem. Commun.* **2016**, 52, DOI:10.1039/C6CC02015A

[3] Bonnamour, Métro, Martinez, Lamaty, *Green Chem.* **2013**, 15, 1116.

[4] Tan *et al.* *Chem. Commun.* **2014**, 50, 5248.

**Keywords:** Solid-state reactions, pharmaceutical materials, drugs, mechanochemistry

# MS36-O3 Last advances in *in situ* monitoring of mechanochemical reactions by X-ray diffraction

Voraksmy Ban<sup>1</sup>, Nikolay Tumanov<sup>2</sup>, Yolanda Sadikin<sup>3</sup>, Yaroslav Filinchuk<sup>2</sup>, Radovan Černý<sup>3</sup>, Nicola Casati<sup>1</sup>

1. Paul Scherrer Institute, 5232 Villigen, Switzerland

2. Institute of Condensed Matter and Nanosciences, Université catholique de Louvain, place L. Pasteur 1, 1348 Louvain-la-Neuve, Belgium

3. Laboratory of Crystallography, Department of Quantum Matter Physics, University of Geneva, Quai Ernest-Ansermet 24, 1211 Geneva, Switzerland

email: voraksmy.ban@psi.ch

The *in situ* characterization of materials is a widespread technique as it gives an accurate description of the sample in a particular state without disturbing the system and adding supplemental parameters/errors in the measurement. It allows to describe and understand phenomena during a process but it also plays a key role to the development of new materials. The renewed interest of mechanochemistry as an eco-friendly synthetic route has inspired creative methodologies to probe reactions.

One of the last methodologies was developed by Friščić *et al.* and for the first time the progress of milling reactions was monitored by synchrotron X-ray diffraction [1]. Recently, they were able to detect and unveil a new topology intermediate during the mechanochemical synthesis of the metal-organic framework ZIF-8 [2]. Nevertheless, such setup has limitations: it is only adapted for high-energy synchrotron X-rays providing diffraction patterns in a squeezed Q-range with strongly overlapping Bragg peaks and does not yield high quality data. With the aim of improving such situation, we developed a completely different setup yielding higher resolution powder diffraction data and providing continuously a representative part of the bulk for probing [3,4]. The particular geometry of the ball mill designed at Materials Science beamline (SLS, Switzerland) shows a significant improvement of diffraction data quality (Fig.1): new intermediates were precisely identified during ball milling syntheses and crystal structures might be solved from it. Moreover with this novel design, it will be easier and more efficient to couple it with other analytical techniques e.g. infra-red/Raman spectroscopies [5] or laser diffraction analysis. Such setup will be available to users at the MS beamline.

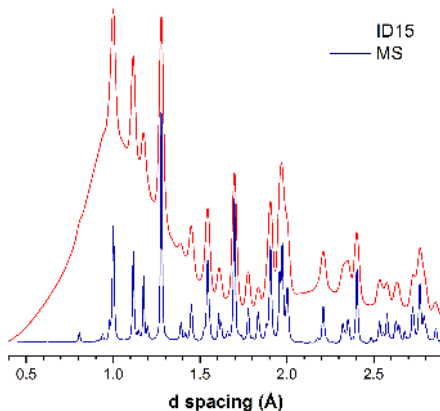


**Figure 1.** Comparison of data collected with the shaker mill at ID15 and our ball mill setup at MS beamline

**Keywords:** Mechanochemistry, *in situ* technique

[1] T. Friščić *et al.* Nat Chem, 2013, 5, 66-73

[2] A. D. Katsenis *et al.* Nat Chem, 2015, 6, 1-8

[3] N. Casati, V. Ban, M. Lange, Patent EP15197992

[4] V. Ban, N. Tumanov, Y. Sadikin, Y. Filinchuk, R. Černý, N. Casati manuscript in preparation

[5] L. Batzdorf *et al.* Angew. Chem. Int. Ed., 2015, 54, 1799-1802

## MS36-O4 Hindered reduction of NiO on Al containing carriers studied by *in situ*

Lars F. Lundegaard<sup>1</sup>, Ramchandra R. Tiruvalam<sup>1</sup>, Christoffer Tyrsted<sup>1</sup>, Anna Carlsson<sup>2</sup>, Fernando Morales-Cano<sup>1</sup>, Charlotte V. Ovesen<sup>1</sup>

1. Haldor Topsøe A/S, Haldor Topsøes Alle 1, 2800 Lyngby, Denmark
2. FEI Company, Achtseweg Noord 5, NL-5651 GG Eindhoven, The Netherlands

email: lafl@topsoe.dk

Steam reforming of natural gas using Ni-based catalysts is an important process in production of synthesis gas and hydrogen. Activation of the catalyst is carried out by reducing NiO to Ni in a mixture of steam and hydrogen (or hydrocarbons) from as low as 450°C. Full reduction and stability are vital for optimal performance and lifetime of the catalyst system. A detailed understanding of the reduction process is therefore of great importance in relation to plant operation.

To better understand this process, reduction behavior of NiO supported on industrial-like steam reforming carriers was studied under wet reduction conditions (1% H<sub>2</sub> + 3% H<sub>2</sub>O, in He) using *in situ* X-ray diffraction (XRD), temperature programmed reduction (TPR) and scanning transmission electron microscopy (STEM) mapping.

It is found that the interaction of NiO with the support greatly influences the reduction behavior. When free MgO is in the carrier, it will react with Ni<sup>2+</sup> during impregnation and calcination to form a Ni<sub>1-x</sub>Mg<sub>x</sub>O solid solution, which results in increasingly high reduction temperatures with increased Mg content.

Increased reduction temperatures are also observed when the calcination temperature during preparation is increased. In this case, the higher reduction temperatures are caused by migration of Al-species from the support to the surface of the NiO particles during calcination.

Calcination at 850°C results in NiO particles completely covered by Al-species, forming a thin (<3nm) protective surface spinel, resulting in reduction temperatures above 700°C. Based on the observed data, it is proposed that Al-species are mobile during calcination already at 450°C. Formation of the protective surface spinel seems to be a general feature for Al-containing carriers as similar reduction behavior is observed on both MgAl<sub>2</sub>O<sub>4</sub>, calcium aluminate, and  $\alpha$ -Al<sub>2</sub>O<sub>3</sub> carriers.[1]

[1] Lundegaard, L. F., Tiruvalam, R. R., Tyrsted, C., Carlsson, A., Morales-Cano, F., and Ovesen, C. V. *Catalysis Today*, 2015, available online, article in press. (doi:10.1016/j.cattod.2015.08.055)

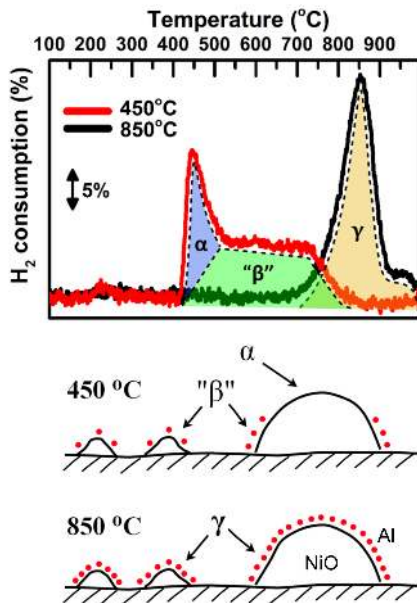


Figure 1. TPR results on Ni/MgAl<sub>2</sub>O<sub>4</sub> catalysts calcined at 450°C (red curve) and 850°C (black curve). The mechanism resulting in the different contributions ( $\alpha$ ,  $\beta$  and  $\gamma$ ) is proposed below.

**Keywords:** NiO reduction, Al migration, *in situ* XRD

**MS36-O5** *In situ* diffraction studies during transition metal catalysisClaudia Weidenthaler<sup>1</sup>, JoChi Tseng<sup>1</sup><sup>1</sup>, Max-Planck-Institut für Kohlenforschung, Kaiser-Wilhelm-Platz 1, 45470 Mülheim an der Ruhr

email: cweiden@gwdg.de

Transition metal compounds are nowadays tested as substituents for noble metal catalysts. Ammonia is an excellent hydrogen carrier and the decomposition of ammonia would be an elegant way to generate hydrogen for fuel cell applications without formation of CO<sub>x</sub>. The most active catalyst so far is Ru on carbon nanotubes, but bimetallic compounds or metal nitrides are also under investigation as potential catalysts for ammonia decomposition. Noble metals are rather expensive and limited in availability. In contrast, metal nitrides are much cheaper and easy to prepare by the nitridation of metal oxides. In this work we study different transition metal catalysts during the decomposition of ammonia. Starting from transition metal oxides, the catalyst formation was studied by *in situ* X-ray diffraction under reaction conditions. Crystallographic studies with respect to phase changes, crystal structure variations, and microstructure properties have been performed [1,2]. The behavior under reaction conditions and the catalytic activity can significantly differ for each catalyst system: while some transition metal oxides reduce during the reaction with ammonia to the metals, others form nitrides after reduction. Changes of the chemical composition associated with structure changes as well as alterations of the microstructure properties of the catalyst in terms of domains size or defect variations may influence the catalytic activity. So far, iron oxides and cobalt alumina spinels were investigated as precursors for ammonia decomposition. In case of iron oxides nitrides are formed during the reaction with ammonia while for cobalt oxides metals form after activation [3,4]. Molybdenum-based catalysts are a very good example that various factors govern activity. Structure changes as well as changes of specific surface areas, and defect concentrations have to be considered [1,2]. In this work we also present studies on the use of bimetallic catalysts (Fe-Co, Fe-Ni) for ammonia decomposition. The formation of metal nitrides, metals and/or alloys during the reactions is monitored by *in situ* XRD using in-house laboratory instruments. The structural changes and detailed reaction pathways were studied by the evaluation of the diffraction data.

[1] Tagliazucca et al., J. Catal. 2013, 305, 277. [2] Tagliazucca et al., Phys. Chem. Chem. Phys. 2014, 16(13), 6182. [3] Feyen et al., Chem.-Eur. J. 2011, 17, 598. [4] Gu et al. J. Phys. Chem. C. 2015, 30, 17102.

**Keywords:** transition metal catalysts, ammonia decomposition, *in situ* diffraction

**MS37** Molecular compounds and MOFs at ambient conditions and under high pressure

Chairs: Francesca Fabbiani, Wendy Queen

**MS37-O1** The Effect of Pressure, Guest Uptake and Structural Flexibility on Porous Framework MaterialsStephen Moggach<sup>1</sup><sup>1</sup>, University of Edinburgh, Scotland

email: s.moggach@ed.ac.uk

In recent years the development of new methods of storing, trapping or separating light gases, such as CO<sub>2</sub>, CH<sub>4</sub> and CO has become of outmost importance from an environmental and energetic viewpoint. Porous materials such as zeolites and porous organic polymers have long been considered good candidates for this purpose. More recently, metal organic frameworks (MOFs) have attracted further interest with many aspects of their functional and mechanical properties investigated. The porous channels found in MOFs are ideal for the uptake of guests of different shapes and sizes, and with careful design they can show high selectivity for particular species from a mixture. Adsorption properties of MOFs have been thoroughly studied, however obtaining in depth 'structural' insight into the adsorption/desorption mechanism is not so common place. For example, out of ca. forty thousand published framework structures there are less than 10 entries in which CO<sub>2</sub> molecules have been unambiguously located experimentally within the pores.

Over the last 6 years, we have been using high-pressure crystallographic techniques to explore the uptake of guest species in the pores of MOFs. We do this, by taking advantage of the fact that the small molecules that encompass the pressure transmitting fluids used frequently in high-pressure crystallographic studies, can penetrate the pores on increasing pressure. This has revealed unexpected flexibility, explain unusual adsorption phenomena under milder gas pressures, and increase reactivity in MOFs. The potential for using high-pressure to explain structure-property relationships has also been revealed in porous magnetic materials. Here, we will give an overview of the effect of high-pressure on both micro and nanoporous materials, and in-particular, highlight some recent work on gas-loaded framework materials.

**Keywords:** high-pressure, MOFs, porous

**MS37-O2** Role of pressure transmitting media in structural transformations of molecular crystals at high pressuresBoris Zakharov<sup>1,2</sup>, Sergey V. Goryainov<sup>3</sup>, Yurii V. Seryotkin<sup>1,2,3</sup>, Nikolay A. Tumanov<sup>4</sup>, Elena V. Boldyreva<sup>1</sup>

1. Institute of Solid State Chemistry and Mechanochemistry SB RAS (Novosibirsk, Russia)

2. Novosibirsk State University (Novosibirsk, Russia)

3. V.S. Sobolev Institute of Geology and Mineralogy (Novosibirsk, Russia)

4. Institute of Condensed Matter and Nanosciences, Université catholique de Louvain (Louvain-la-Neuve, Belgium)

email: b.zakharov@yahoo.com

Molecular compounds are interesting both from fundamental and applied point of view since many of them are promising as materials with piezoelectric, ferroelectric and non-linear optical properties. Some of them can serve as biomimetics. Due to these facts studies of polymorphism of molecular compounds are important for crystal engineering and crystallization theory. High pressure is one of the most powerful tools to influence polymorphism of molecular compounds. However, the control of high-pressure polymorphism is not a trivial task. Generally, it is not possible to predict which phase will be formed at a selected (T, P) point based on a thermodynamic phase diagram. As a result of the kinetic control of nucleation and nuclei growth, different phases can form, depending on the choice of the starting polymorph, the hydrostatic medium, the compression/decompression protocol and the choice of pressure transmitting media. The last effect is the most intriguing due to the fact that proper pressure transmitting media do not react chemically with studied molecular compound. Despite that pressure transmitting medium was shown to influence the product of high-pressure transformation of molecular compounds. In this contribution we illustrate this phenomenon in relation to an antidiabetic drug, chlorpropamide. In addition to the commercially available  $\alpha$  polymorph, which is thermodynamically stable, four other polymorphs ( $\beta$ -,  $\gamma$ -,  $\delta$ -,  $\epsilon$ -) can be preserved indefinitely long under ambient conditions. The variety of polymorphs makes chlorpropamide very interesting for high-pressure research. The chlorpropamide polymorphs were studied by diffraction and spectroscopic techniques. We compared the phase transitions in solid polymorphs immersed in different pressure transmitting media. We also studied the effects of pressure, when several different polymorphs were present simultaneously in the same diamond anvil cell. A plethora of interesting effects was observed. The same polymorph of chlorpropamide was shown to undergo transformations into different polymorphs depending on selected pressure transmitting medium (without recrystallization), as well as to recrystallize into other forms, depending on the presence of other polymorphs in the same diamond anvil cell.

The work was supported by a grant from RSF (14-13-00834).

**Keywords:** structural transformations, high pressures, polymorphism

**MS37-O3** Pressure induced chemisorption in isorecticular Metal Organic FrameworksPiero Macchi<sup>1</sup>, Arianna Lanza<sup>1</sup>, Luzia German<sup>1</sup>, Martin Fisch<sup>1</sup>, Nicola Casati<sup>2</sup>

1. Department of Chemistry and Biochemistry, University of Bern

2. Swiss Light Source, Paul Scherrer Institute, Villigen, Switzerland

email: piero.macchi@deb.unibe.ch

MOFs with stereochemically accessible unsaturated metal centres may enable chemisorption of small molecules at the metal sites, to be distinguished from the classical physisorption occurring through weaker interactions between the guest and the internal active surface of the MOF.

Chemisorption and framework flexibility are desirable features for the design of promising catalysts, selective sieves or absorbents. Moreover, by varying metal centers, oxidation states, organic linkers, guest molecules, stereochemical features etc., the potential and complexity of MOFs can be tuned towards the desired properties. Efforts to rationalize the synthesis of frameworks with specific features would therefore benefit from comparative studies involving systematic variations of their structure, which can be induced by external stimuli (temperature, pressure) as well as chemical modifications.

In this work, we investigated the role of controlled structural modifications on the physico-chemical properties of a family of isostructural MOFs. We discuss here about isomorphous, iso-reticular MOFs based on  $M^{II}$  connectors ( $Co^{II}$ ,  $Zn^{II}$  or  $Mn^{II}$ ) and benzotriazole-5-carboxylato (btca) linkers that were found to selectively react with guest molecules (like methanol or dimethylformamide) trapped in the channels during the sample preparation or after an exchange process. A mild compression or cooling are enough to induce a reversible nucleophilic addition of the guest molecules to the metal ion. Depending on the guest or the metal, the coordination may increase stepwise up to saturation. A preliminary study on the  $CoII$  MOF was recently published.<sup>1</sup>

[1] Lanza, A.; Germann, L. S.; Fisch, M.; Casati, N.; Macchi, P. J. Am. Chem. Soc., 2015, 137, 13072–13078



**Figure 1.** Schematic representation of the ligand addition stimulated by the crystal contraction in  $[Co_3(OH)_2btca]$

**Keywords:** MOFs, high pressure crystallography, chemisorption

## MS37-O4 High-pressure effects in carbohydrate-based crystals

Ewa Patyk<sup>1</sup>, Andrzej Katrusiak<sup>1</sup>

1. Department of Materials Chemistry, Adam Mickiewicz University, Umultowska 89b 61-614, Poznań, Poland

email: ewapatyk@amu.edu.pl

Carbohydrates create one of the most important groups of organic compounds. Their diverse properties result in their wide application in various industries. Lately, a new group of metal-organic frameworks based on  $\gamma$ -cyclodextrin molecules ( $\gamma$ -CD-MOF) was introduced,<sup>1</sup> allowing new ways of implementation of carbohydrates. All sugars, regardless the size, share the same characteristic feature, *i.e.* multiple hydrogen donors and acceptors taking part in creation of extensive hydrogen-bond network. It was recently shown that even slight structural change in their unique code of hydroxyl groups can result in quite different high-pressure behavior and stability.<sup>2,3</sup> Yet, some of the observed pressure effects are consistent for all mono- and disaccharides studied till know.<sup>2,4</sup> The information gathered for simple carbohydrates can be of an importance when more complex systems build of well-known monosaccharides are investigated at high pressure. In this research a high pressure study of  $\gamma$ -CD-MOF was performed in order to determine its stability and compare its behavior with the  $\alpha$ -D-glucose.

For this study the Merrill-Bassett diamond-anvil cell<sup>5</sup> (DAC) was used. Either single crystals of the sample obtained at ambient conditions were placed in the DAC along with the cellulose fiber to fix it position, or it was recrystallized *in situ* at high pressure. In all cases a small ruby chip was placed inside the DAC to measure the pressure. All sample crystals were measured with 4-circle diffractometer and either X-ray or synchrotron radiation.

Collected data allowed to determine the pressure stability of both compounds and to investigate how extreme conditions influence their H-bonding pattern and aggregation, as well as to compare these effects in both systems.

This research is a part of Preludium Programme No 2015/17/N/ST5/01927, founded by the National Science Centre, Poland.

1. Saldone, R. A., Forgan, R. S., Furukawa, H., Gassensmith, J. J., Slawin, A. M. Z., Yaghi, O. M. & Stoddart, J. F. (2010). *Angew. Chem. Int. Ed.* **49**, 8630–8634.

2. Patyk, E. & Katrusiak, A. (2015). *Chem. Sci.* **6**, 1991–1995.

3. Patyk, E., Jenczak, A. & Katrusiak, A. (2016). *PCCP- in press*.

4. Patyk, E., Skumiel, J., Podsiadło, M. & Katrusiak, A. (2012). *Angew. Chem. Int. Ed.* **51**, 2146–2150.

5. Merrill, L. & Bassett, W. A. (1974). *Rev. Sci. Instrum.* **45**, 290–294.

**Keywords:** high pressure, carbohydrates, glucose,  $\gamma$ -CD-MOF



**MS37-O5** A Series of Highly Stable  
Isorecticular Lanthanide Metal-Organic  
Frameworks with Tunable Luminescence  
Properties Solved by Rotation Electron  
Diffraction and X-ray Diffraction

Xiaodong Zou<sup>1,2</sup>, Qingxia Yao<sup>1,2</sup>, Antonio Bermejo Gómez<sup>2,3</sup>, Jie Su<sup>1,2</sup>, Vlad Pascanu<sup>2,3</sup>, Yifeng Yun<sup>1,2</sup>, Haoquan Zheng<sup>1,2</sup>, Hong Chen<sup>1,2</sup>, Leifeng Liu<sup>1,2</sup>, Hani N. Abdelhamid<sup>1,2</sup>, Belén Martín-Matute<sup>2,3</sup>

1. Department of Materials and Environmental Chemistry, Stockholm University, SE-106 91 Stockholm, Sweden

2. Berzelii Center EXSELENT on Porous Materials, Stockholm University, SE-106 91 Stockholm, Sweden

3. Department of Organic Chemistry, Stockholm University, SE-106 91 Stockholm, Sweden

email: xzou@mmk.su.se

Systematic design and control of pore size, shape and functionality in metal-organic frameworks (MOFs), without changing the underlying topology, has attracted large attention.[1] The isorecticular synthesis of MOFs has been mostly achieved with metal clusters and organic linkers of various sizes. In fewer cases, isorecticular MOFs built from inorganic chains have been synthesized, mainly by combining transition metals with ditopic or tetratopic linkers. Here we present a new series of porous isorecticular lanthanide-based MOFs (LnMOFs) (denoted SUMOF-7I, -7II, -7III and -7IV; Ln = La, Ce, Pr, Nd, Sm, Eu and Gd) synthesized by combining Ln-carboxylate inorganic chains and tritopic organic linkers of variable sizes [2].

The structure of SUMOF-7I was solved by single crystal X-ray diffraction (SXRD). The crystals of other SUMOFs were too small to be studied by SXRD. Therefore, we applied the rotation electron diffraction (RED) method, which has shown to be very powerful for structure solution of unknown inorganic crystals [3]. The structures of SUMOF-7II and -7III were solved by combining RED with powder X-ray diffraction (PXRD). The SUMOF-7s display 1D pseudo-hexagonal channels with the pore diameter gradually enlarged from 8.4 Å to 23.9 Å, as a result of increasing sizes of the organic linkers (Fig. 1). SUMOF-7I, -7II and -7III show extraordinary thermal stability and remarkable tolerance towards hot water, organic solvents, and aqueous media with pH values ranging from 2 to 11. *In-situ* SXRD study shows that the water molecules coordinated to lanthanide ions in SUMOF-7I could be removed by heating, and re-coordinated to lanthanide ions when the activated crystal was exposed to air for one day. The luminescent properties of these materials can be tuned by doping with different ratios of lanthanide ions as well as by incorporating guest dye molecules in the pores. The combination of tunable pore apertures, accessible metal sites, high thermal and chemical stability, and tunable luminescence properties, makes the SUMOF-7 series a very promising platform for applications in optical sensing, heterogeneous catalysis, and photocatalysis.

[1] W. Lu, Z. Wei, Z.-Y. Gu, H.-C. Zhou *et al. Chem. Soc. Rev.* **2014**, *43*, 5561-5593.

[2] Q. Yao, A. Bermejo-Gómez, B. Martín-Matute, X.D. Zou *et al. Chem. Mater.* **2015**, *27*, 5332-5339.

[3] W. Wan, J.L. Sun, J. Su, S. Hovmöller, X.D. Zou, *J. App. Crystallogr.* **2013**, *46*, 1863-1873.

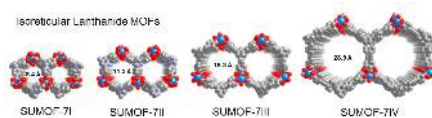


**Figure 1.** Crystal structures of SUMOF-7I to -IV. The free diameter of the pore aperture is given, taking into account the van der Waals radii of the atoms.

**Keywords:** metal-organic framework, isorecticular MOFs, structure determination, electron diffraction, in-situ XRD, luminescence property

## MS38 Nanomaterials & graphene

Chairs: Adrià Gil-Mestres, Michael Woerle

### MS38-O1 Shape, Chemical and Crystalline Structure of Nanocrystals and their Impact on the Supercrystal Structure of Colloidal Superlattices

Rainer T. Lechner<sup>1</sup>

1. Institut fuer Physik, Montanuniversitaet Leoben, Franz-Josef-Strasse 18, A-8700 Leoben, Austria

email: Rainer.Lechner@unileoben.ac.at

The chemical synthesis of nanocrystals (NCs) has led to a pronounced improvement in the optical properties and the chemical stability of semiconducting NCs [1]. The optical emission of NCs can be drastically increased by stabilising the core with a hard protective shell [1]. For the cationic exchange based shell growth of PbS/CdS NCs [2], we have recently shown that metastable crystal phases in the CdS shell influences significantly the photoluminescence (PL). This was only achieved by retrieving the chemical profile of NCs in sub-nanometer resolution by using anomalous small angle x-ray scattering (ASAXS) in combination with the analysis of powder diffraction data by wide angle x-ray scattering (WAXS) [2]. In a current synchrotron study we have investigated CdSe/CdS core/shell NCs by recording ASAXS and WAXS spectra. We revealed that the epitaxial core/shell structure depicts again a sharp chemical interface. With increasing core diameter, however, the CdSe/CdS NCs deviate significantly from a spherical shape. By means of a recently developed shape retrieval method [3], we could reveal an elliptical NC shape with pronounced surface facets for the largest core/shell series. In combination with the WAXS data we could relate this anisotropic shape to specific crystallographic directions.

The NC's shape can also significantly influence the super-crystal structure of colloidal superlattices [1], when the NCs are used as building blocks. This we have shown, when we investigated with in-situ synchrotron SAXS the template free self-assembly of colloidal supercrystals based on nearly monodisperse Bi NCs [4]. The retrieved 3D mean shape [3] of the Bi NCs looks like a strongly faceted oblate ellipsoid and can be related to the rhombohedral crystal structure of Bi. Many sharp Bragg peaks prove the formation of well-ordered supercrystals, but we want to reveal if this superlattice structure can be directly related to the NC shape. Thus, we used the derived shape as input for a modeling of the crystallization process based on molecular dynamic simulations. Simulations and experiments show a good agreement and thus we are able to link the supercrystal structure via the NC-shape to the atomic Bi crystal

structure.

[1] M. V. Kovalenko et al., ACS Nano 9, 1012-1057 (2015) [2] R.T. Lechner, et al., and O. Paris, Chem. Mater. 26, 5914-5922 (2014) [3] M. Burian, et al., and R.T. Lechner, J. Appl. Cryst. 48,857-868 (2015) [4] M. Yarema, et al., JACS 132, (2010)

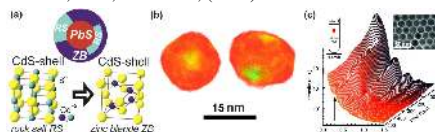


**Figure 1.** (a) Crystalline core/shell structure of PbS/CdS NCs derived by WAXS [3]. (b) From SAXS data derived elliptical and faceted shape of CdSe/CdS NCs. (c) *In-situ* SAXS study of the 3D self-assembly of colloidal supercrystals using Bi-NCs (see inset TEM) as building blocks.

**Keywords:** core/shell nanocrystals, colloidal supercrystals, synchrotron SAXS/WAXS

## MS38-O2 Layered and 2D materials: electronic properties and structural instabilities from first principles

Pablo Ordejón<sup>1</sup>, Enric Canadell<sup>2</sup>, Jose Angel Silva-Guillen<sup>3</sup>,  
Bogdan Guster<sup>1</sup>, Francisco Hidalgo<sup>1</sup>, Miguel Pruneda<sup>1</sup>

1. Institut Català de Nanociència i Nanotecnologia - ICN2, The Barcelona Institute of Science and Technology and CSIC, Campus de la UAB, 08193 Bellaterra, Barcelona (Spain)
2. Institut de Ciència de Materials de Barcelona - ICMAB-CSIC, Campus de Bellaterra, 08193 Barcelona, Spain
3. Fundación IMDEA Nanociencia, c/ Faraday 9, Campus Cantoblanco, 28049 Madrid, Spain

email: pablo.ordejon@icn2.cat

I will present recent work on the understanding of the electronic properties of layered materials and their 2D relatives by means of first principles electronic structure calculations. In particular, I will focus on the correlation between the crystal structure and the electronic properties, with special emphasis on the structural instabilities with an electronic origin. This will be done in connection to recent experimental studies that have been able to demonstrate the presence of charge density waves (CDW) in several 2D materials like NbSe<sub>2</sub> and TiSe<sub>2</sub>. I will also discuss the correlation between the electronic structure and the experimental STM images and STS spectra on some of these systems, which provide crucial insight for the understanding of their CDW and superconducting instabilities.

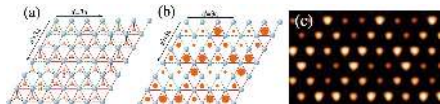


**Figure 1.** (a) 3x3 CDW structure of single-layer NbSe<sub>2</sub>. Blue (orange) balls represent Nb (Se) atoms. (b) Schematic STM image predicted for the 3x3 CDW structure taking only into account the height of the different Se atoms. (c) STM image obtained from first principles.

**Keywords:** 2D materials, DFT, first principles, charge density waves, structural instabilities, electronic structures, low dimensional solids, surfaces.

## MS38-O3 Preferred orientation of Li<sup>+</sup> diffusion in nano-LiMnPO<sub>4</sub>

Nam Hee Kwon<sup>1</sup>, Nam Hee Kwon<sup>1</sup>, Hui Yin<sup>1</sup>, Tatiana Vavrova<sup>1</sup>,  
Fabio Edafe<sup>1</sup>, Divine Mouck-Makanda<sup>1</sup>, Katharina M. Fromm<sup>1</sup>

1. University of Fribourg, Chemistry department, Chemin du Musée 9, CH-1700 Fribourg, Switzerland

email: namhee.kwon@unifr.ch

Transition metal containing olivine-structured materials, LiMPO<sub>4</sub> (M=Fe, Mn, Co, Ni), are considered to be useful as cathode material for lithium ion batteries. They show an excellent structural stability *versus* Li<sup>+</sup> insertion/extraction due to the strong covalent P-O bond<sup>1</sup>. Particularly, LiMnPO<sub>4</sub> is attractive because of its high cell voltage (4.1 V vs. Li<sup>+</sup>/Li), providing 20 % higher energy density than the commercial LiFePO<sub>4</sub>. LiMnPO<sub>4</sub> consists of slightly distorted LiO<sub>6</sub> and MnO<sub>6</sub> octahedra and PO<sub>4</sub> tetrahedra (Fig. 1)<sup>2,6</sup>. LiO<sub>6</sub> octahedra are edge-shared with PO<sub>4</sub> tetrahedra. Since the Li<sup>+</sup> diffusion occurs along the *b*-axis via edge-sharing LiO<sub>6</sub> octahedra and hence in one preferred orientation of the crystal structure, a morphology control is important to tune the length of the Li<sup>+</sup> channels in a single particle<sup>3</sup>. We therefore synthesized various shapes and sizes of nano-LiMnPO<sub>4</sub> (Fig. 2) to examine the preferred direction of the Li<sup>+</sup> diffusion in single LiMnPO<sub>4</sub> particles. The electron diffraction patterns were indexed using transmission electron microscopy to determine the (hkl)-planes and hence the orientation of the *b*-axis in the nanoparticles. Furthermore, the Li<sup>+</sup> diffusion coefficients were determined using electrochemical techniques. According to our measurements for each different shape of nano-LiMnPO<sub>4</sub>, the Li<sup>+</sup> diffusion occurs always along the shortest facet dimension in a single nanoparticle. The resulting specific capacity was different depending on the shape of LiMnPO<sub>4</sub> particles although the total specific surface areas were the same. This study helps to design the desired shapes and sizes of LiMnPO<sub>4</sub> for obtaining high energy Li-ion batteries.

<sup>1</sup> A. K. Padhi, K. S. Nanjundaswamy, J. B. Goodenough, *J. Electrochem. Soc.* 144 (1997) 1188-1194.

<sup>2</sup> C.E. Zaspel, T.E. Grigereit, J.E. Drumheller, *Phys. Rev. Lett.*, 74 (1995) 544-765.

<sup>3</sup> N.-H. Kwon, K.M. Fromm, *Electrochim. Acta* 69 (2012) 38-44.

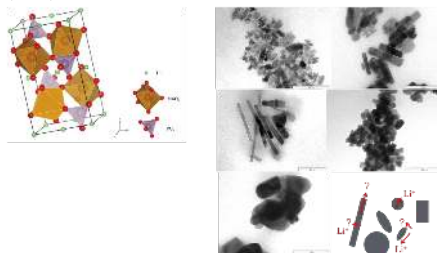


**Figure 1.** The crystal structure of LiMnPO<sub>4</sub> with Pnma space group. Fig. 2. TEM images show the various shapes and sizes of LiMnPO<sub>4</sub> nanoparticles. The scale bar is 200 nm.

**Keywords:** Nano-LiMnPOsub4, Li+ diffusion, crystal structure, lithium ion battery

## MS38-O4 X-ray studies on polymers and composites: the combination of 2D WAXS, SAXS and X-ray imaging techniques

Antonia Neels<sup>1</sup>, Rolf Kaufmann<sup>1</sup>, Monika Bauer<sup>2</sup>, Sara Dalle Vacche<sup>3</sup>, Yves Leterrier<sup>3</sup>, Alex Dommann<sup>1</sup>

1. Center for X-ray Analytics, Empa, Dübendorf, CH
2. Polymeric Materials, Brandenburg University of Technology Cottbus – Senftenberg, D
3. Laboratory for Polymer and Composite Technology, EPFL, Lausanne, CH

email: antonia.neels@empa.ch

Polymers, elastomers, composites, foams and textiles find their applications in growing industrial markets such as aerospace, automotive, building products, electronics, energy and medicine. While some of these polymer materials are amorphous, a large proportion exhibit local order with regularly arranged chains (crystallite domains) leading to varying amounts of crystallinity and hence can be characterized by X-Ray diffraction techniques. Structural information beside phase identification and quantification can be obtained for the polymer crystallinity, the polymer orientation, the crystalline microstructure and the non-crystalline periodicity and size. Structural variations, such as those induced by e.g. inorganic phases as in composites can be monitored by dynamic studies through in-situ experiments at process conditions (temperature, humidity, mechanical load). Preferred orientation or texturing is a dominant effect in polymers, especially in processed parts. Orientation is also the dominant feature in controlling the mechanical and physical properties of polymers which is of major interest for researchers and manufacturers. For the study of those orientation behaviors, a combination of SAXS and WAXS transmission experiments are conducted using a BRUKER Nanostar and an IPDS-II X-ray machine; both containing a 2D detector.

Investigations have been made for different synthetic polymer fiber and composite systems[1,2]. The figure 1 shows 2D images obtained for a carbon fibre reinforced polymer system with a strong texturing. The evaluation of the WAXS 2q range reveals information about the crystal structure parameters and the crystalline domain size (a). In contrast, integrating the azimuth ( $360^\circ$  in  $\Phi$  at  $2\theta$   $12.02^\circ$  for C(002)) gives the possibility to quantify polymer ordering through the determination of peak width (FWHM). SAXS enables the study of nano-particle and nano domain sizes in dependence of their orientation distributions (b). X-ray phase contrast imaging (XPCI) reveals materials voids and cracks (c).

[1] Polymer, **55**, 5695-5707 (2014).

[2] Journal of Polymer Science, Part B: Polymer Physics, **52**, 496–506 (2014).



**Figure 1.** 2D images from WAXS (a), SAXS (b) and X-ray phase contrast imaging (c).

**Keywords:** SAXS, WAXS, X-ray phase contrast imaging, 2D detection techniques

## MS38-O5 Nano- x-ray fluorescence of individual GaAs/InGaAs/GaAs core-shell nanowires grown by molecular beam epitaxy on silicon (111)

Ali Al Hassan<sup>1</sup>, Ryan B. Lewis<sup>2</sup>, Hanno Küpers<sup>2</sup>, Danial Bahrami<sup>1</sup>, Abbas Tahraoui<sup>2</sup>, Lutz Geelhaar<sup>2</sup>, Ullrich Pietsch<sup>1</sup>

1. Naturwissenschaftlich- Technische Fakultät der Universität Siegen, 57068 Siegen, Germany  
2. Paul-Drude-Institut für Festkörperelektronik, Hausvogteiplatz 5-7, 10117 Berlin, Germany

email: ali\_al\_hassan@live.com

The growth of GaAs/InGaAs/GaAs core-shell nanowires (NWs) on silicon is a challenging route to combine opto-electronics with the silicon technology. Due to discrepancy in the lattice parameters of core (GaAs) and shell (InGaAs) materials, X-ray diffraction (XRD) measurements taken on NW ensembles with momentum transfer perpendicular to the NW axis show a shift in the InGaAs Bragg peak as shell thickness is varied. This shift can be the result of either a complex strain field or in-homogenous indium distribution. As the composition of indium and the strain field cannot be distinguished by XRD, the spatial homogeneity of the Indium distribution in the shell layers of individual core-shell NWs was probed by means of X-ray fluorescence (XRF) analysis using a 50nm x 50nm sized white x-ray beam. For low indium contents within the InGaAs layer (nominal values of 15% and 25%), the Indium distribution along the six side facets and the NW axis is almost homogeneous (Figure 1, d,e) with slight Indium fluctuation (Figure 1, f). On the other hand, NWs with 60% of indium show the growth and random distribution of indium-rich aggregates (Figure 1, a) at the core circumference (Figure 1, b) with an approximated indium fluctuation of 33% (Figure 1, c).

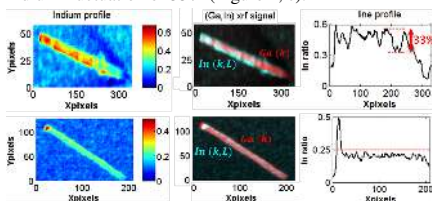


**Figure 1.** a) formation of In-rich aggregates for a NW with 60% of indium. b) distribution of the aggregates at the core circumference. c) Line profile through the aggregates. d,e) homogenous distribution of indium for NWs with 25% of indium content. e) Line profile along the NW presented in (d).

**Keywords:** Nano- x-ray fluorescence - single nanowire heterostructures - indium spatial distribution.

## MS39 X-Ray diffraction on the $\mu$ s to ps time scale

Chairs: Semën Gorfman, Michael Wulff

## MS39-O1 Time-resolved X-ray microdiffraction for ferroelectric heterostructures

Ji Young Jo<sup>1</sup>

1. Gwangji Institute of Science and Technology

email: jyjo@gist.ac.kr

The responses of ferroelectric heterostructures to external electric fields provide intriguing functionalities including the switching of remnant polarization and electromechanical distortion. Especially these functionalities of ferroelectric thin films can be greatly modified by a misfit strain arising from a lattice mismatch between substrate and film substance over a wide range of timescale. In this presentation, I will discuss our recent studies to resolve the electromechanical responses of ferroelectric thin films using a synchrotron time-resolved x-ray microdiffraction technique (Fig. 1).[1-2]

**Keywords:** Time-resolved X-ray microdiffraction, Ferroelectric

**MS39-O2 Laser driven acoustic vibrations in nanowires studied by time-resolved GIXD.**

Dmitry Khakhulin<sup>1</sup>, Tomas Stankevic<sup>2</sup>, Peter Vester<sup>3</sup>, Simon O. Mariager<sup>4</sup>, Peter Krogstrup<sup>5</sup>, Michael Wulff<sup>5</sup>, Robert Feidenhans<sup>1,3</sup>

1. European XFEL GmbH and the Hamburg Centre for Ultrafast Imaging, Hamburg, Germany
2. MAX IV Laboratory, Lund, Sweden
3. Niels Bohr Institute, Copenhagen, Denmark
4. Paul Scherrer Institute, Villigen, Switzerland
5. European Synchrotron Radiation Facility, Grenoble, France

email: dmitry.khakhulin@xfel.eu

Unique mechanical, thermal and electronic properties of semiconductor nanowires (NW) make them attractive as fundamental building blocks for nanoelectromechanical devices offering extremely high precision for force, mass and strain sensing [1]. Laser driven eigen acoustic vibrations in NWs are defined by their composition, geometry and elastic properties. A single ultrashort laser pulse may simultaneously induce various eigen modes in NWs depending of the excitation conditions.

Acoustic oscillations in nanostructures are usually investigated either by transient optical reflectivity or in case of the slowest modes directly by electron microscopy and stroboscopic imaging. None of these techniques give direct insight into acoustic displacements on the atomic scale. Time-resolved pump-probe x-ray diffraction makes it possible to track the laser induced ultrafast lattice dynamics with great spatial and temporal resolution and has been successfully applied for a number of studies on coherent acoustic phonons in bulk crystals, thin films [2], superlattices [3], and nanostructures [4, 5].

In this contribution we present studies on laser induced acoustic vibrations in crystalline free-standing semiconductor core-shell NWs by time-resolved pump-probe grazing incidence x-ray diffraction (GIXD). Tracking the motion of Bragg peaks on an area detector as a function of the pump-probe delay we were able to record the NWs lattice dynamics with atomic resolution on the sub-nanosecond timescale. Three fundamental acoustic vibrations namely radial breathing, extensional (along the axis) and bending modes generated by a single laser pulse were observed (Fig.1) and characterised. Analysis of the transient lattice displacement magnitudes and frequencies complemented by numeric simulations indicates the dominant mechanism of strain generation and elastic constants of the NWs.

**References**

- [1] K. Ekinici and M.L. Roukes, *Rev. Sci. Instrum.*, **76**, 061101 (2005).
- [2] M. Nicoul et al., *Appl. Phys. Lett.* **98** 191902 (2011).
- [3] M. Woerner et al., *Appl. Phys. A* **96**, 83 (2009).
- [4] S.O. Mariager et al., *Nano Lett.*, **10**, 2461 (2010).
- [5] J. N. Clark et al., *Science*, **341**, 56 (2013).

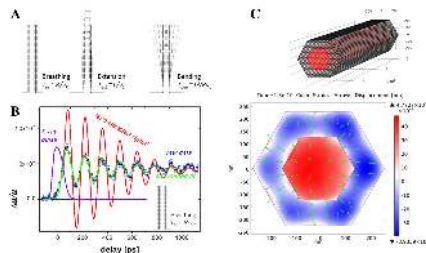


**Figure 1.** A: the 3 fundamental acoustic vibration modes of a NW; B: relative lattice displacement measured for the radial breathing mode (blue dots) and de-convoluted signal (red line); C: FEM modeling mesh on the top and the calculated transient strain distribution in the core-shell NW at 130 ps delay.

**Keywords:** pump-probe diffraction, nanowires, acoustic oscillations

**MS39-O3** Simulations of single-pulse Laue diffraction from proteins with radiation from synchrotron and XFEL sourcesVictoria Kabanova<sup>1</sup>, Marius Schmid<sup>2</sup>, Friedrich Schotte<sup>3</sup>, Marco Cammarata<sup>4</sup>, Michael Wulff<sup>1</sup>

1. European Synchrotron, 71, avenue des Martyrs, 38000 Grenoble, France

2. University of Wisconsin-Milwaukee, Physics Department, 3135 North Maryland Avenue Milwaukee, WI 53211, USA.

3. National Institutes of Health, Lab. of Chemical Physics, NIDDK, Bethesda, Maryland 20892-0520, USA

4. Department of Physics, University of Rennes 1, IPR, UMR 6251, 35042 Rennes, France.

email: victoria.kabanova@esrf.fr

Laue diffraction is the method of choice for measuring ultrafast structural changes in proteins initiated by light. The advantage is that Laue exploits the high intensity of the white beam and that the diffracted intensities are fully recorded with a stationary crystal. In practice, the precision is limited by the signal to noise ratio which depends on many parameters: crystal quality, crystal size, pulse intensity, the fraction of the sample volume activated by the light pulse etc. The time resolution is 100 ps for synchrotrons (SRs) and 100 fs for XFELs. The pulse intensities vary from  $1 \times 10^9$  to  $1 \times 10^{10}$  for SRs and to  $1 \times 10^{11}$  to  $1 \times 10^{12}$  for XFELs. Finally, the bandwidths are 0.1% for XFELs and 2.5-3.5 % for SRs.

With the extreme intensity of the XFEL pulse, high quality Laue data can be obtained from micron size crystals by serial crystallography [1]. The number of reflections is limited by the narrow bandwidth; in practice there are 50-100 reflections per image. The crystal is destroyed but the diffraction is generated before this happens. The SR pulse requires larger crystals, 10-300 mm, to get sufficient diffracted intensity [2]. SR Laue with micro crystals is prone to radiation damage: if a  $10^{10}$  ph pulse at 15 keV is focused to  $\varnothing 10$  mm on a  $10 \times 10 \times 10$  mm<sup>3</sup> crystal of myoglobin crystal, the temperature rises by 12.4 K which is often acceptable. For a  $5 \times 5 \times 5$  mm<sup>3</sup> and  $\varnothing 5$  mm focus, the temperature rise is 49.5 K! The lattice is damaged during the 100 ps exposure.

Motivated by the enormous gain in brilliance with the Extremely Bright Lattice (EBS) at the ESRF (Sep 2020), we are studying the gains from the increased photon density and having a tuneable focus from compound refractive lenses. What is the resolution as a function of crystal size at the EBS? To shed light on this question, we have calculated Laue patterns and intensities including the diffuse background from myoglobin crystals of different size. The simulations use the spectrum from a U14 cryo-undulator ( $E_e = 15$  keV,  $10^{10}$  ph/pulse, 2.3% bw, spot  $\varnothing$  5-100 mm). The Laue patterns are simulated for the Rayonix HS170 detector used at ID09 which has a pixel size of 44.3 mm and point-spread function of 100 mm. The resolution as a function of crystal size and pulse intensity will be presented.

[1] T.R. Barends et al., Science, 350, 445-450, 2015.

[2] F. Schotte et al., Science, 300, 1944-1947, 2003.

**Keywords:** Laue diffraction, single-pulse experiment, radiation damage, undulator radiation**MS39-O4** Time-resolved photocrystallography on a laboratory diffractometer on the millisecond time scaleDominik Schaniel<sup>1</sup>, Nicolas Casaretto<sup>1</sup>, Sébastien Pillet<sup>1</sup>, Bertrand Fournier<sup>1</sup>, Pascal Parois<sup>1</sup>, Paul Allé<sup>1</sup>, Emmanuel Wenger<sup>1</sup>

1. Université de Lorraine, CRM2, Vandoeuvre-les-Nancy, France

email: dominik.schaniel@univ-lorraine.fr

We have developed a laboratory x-ray diffraction instrument allowing for time-resolved photocrystallography by coupling a ns Nd-YAG pulsed LASER to a fast x-ray pixel detector (XPAD). The very first convincing results have been obtained on time-resolved photoswitching of nitrosyl complexes with this setup. In metal-nitrosyl complexes like sodiumnitroprusside (SNP,  $\text{Na}_2[\text{Fe}(\text{CN})_5\text{NO}]2\text{H}_2\text{O}$ ) photoinduced nitrosyl linkage isomers can be generated by irradiation with light in the visible spectral range. Their lifetime varies from a few nanoseconds to several tens of milliseconds at room temperature and increases with decreasing temperature. On the example of the prototype substance SNP we show that the variation of the intensities of Bragg reflections can be monitored with a time-resolution of 2 ms after pulsed LASER excitation. The photogeneration of the side-on bonded nitrosyl isomer (MSII) and its relaxation back to the ground state could be tracked in this manner at a temperature of 180 K, where the lifetime of SII is of the order of 100 ms. Further examples include ruthenium nitrosyl complexes with lifetimes of the photogenerated linkage isomers of a few milliseconds at room temperature. These proof-of-principle experiments open the way to other applications of this time-resolved photocrystallographic setup.

**Keywords:** photocrystallography



### MS39-05 X-ray study of femtosecond structural dynamics of the charge-density wave compound 1T-TaS<sub>2</sub>

Sylvain Ravy<sup>1</sup>, Claire Laulhé<sup>2</sup>, Tim Huber<sup>3</sup>, Gabriel Lantz<sup>3</sup>, Laurent Cario<sup>4</sup>, Benoît Corraze<sup>4</sup>, Etienne Janod<sup>4</sup>, Andres Ferrer<sup>5</sup>, Jochen Rittmann<sup>3</sup>, Simon Mariager<sup>3</sup>, Jeremy A. Johnson<sup>3</sup>, Sebastian Gruebel<sup>5</sup>, A. Luebecke<sup>5</sup>, L. Huber<sup>5</sup>, Martin Kubli<sup>5</sup>, Matteo Savoini<sup>5</sup>, Vincent Esposito<sup>5</sup>, Vincent Jacques<sup>1</sup>, Gerhard Ingold<sup>5</sup>, Paul Beaud<sup>5</sup>, Steven L. Johnson<sup>3</sup>

1. Laboratoire de Physique des Solides, CNRS, Univ. Paris-Sud, Université Paris-Saclay, 91405 Orsay, France
2. Synchrotron-SOLEIL, l'Orme des merisiers, Saint-Aubin - BP48, 91192 Gif-sur-Yvette, France
3. Institute for Quantum Electronics, Physics Department, ETH Zurich, CH-8093 Zurich, Switzerland
4. Institut des Matériaux Jean Rouxel, CNRS, Université de Nantes, 44322 Nantes, France
5. Swiss Light Source, Paul Scherrer institute, CH-5232 Villigen, Switzerland

email: sylvain.ravy@u-psud.fr

1T-TaS<sub>2</sub> is a 2D metallic compound which undergoes a series of electronically driven phase transitions toward charge density wave (CDW) and Mott phases. In this paper, we present femtosecond pump-probe X-ray diffraction experiments, carried out at the X05LA beamline of the Swiss Light Source in two of the low-temperature phases of 1T-TaS<sub>2</sub>.

In the low temperature Mott phase, we study the coherent phonon induced by the infrared 800 nm laser pulse, while in the so-called near-commensurate CDW phase, we have studied the mechanism of the phase induced phase transition toward another incommensurate phase, where a fast coarsening process is clearly observed.

**Keywords:** ultra-fast , diffraction , charge-density wave

### MS40 New detectors for high energy x-ray applications

Chairs: Heinz Graafsma, Lothar Strüder

#### MS40-01 Hard X-ray photon counting with “LAMBDA” high-Z detectors

David Pennicard<sup>1</sup>, Milijana Sarajlic<sup>1</sup>, Sergej Smoljanin<sup>1</sup>, Florian Pithan<sup>1</sup>, Heinz Graafsma<sup>1,2</sup>

1. DESY
2. University of Mid Sweden

email: david.pennicard@desy.de

Photon-counting hybrid pixel detectors are now the technology of choice for a wide range of X-ray scattering experiments, due to their excellent signal-to-noise ratio and high speed. However, most photon-counting detectors use silicon as a sensor material, limiting their detection efficiency in hard X-ray experiments. By replacing the silicon sensor with a “high-Z” (high atomic number) semiconductor, these detectors can also be applied to hard X-rays.

“LAMBDA” is a photon-counting hybrid pixel detector with a relatively small pixel size (55µm), high-speed readout at 2000 fps (deadtime-free), and a modular design that makes it possible to build large detector areas. Prototype LAMBDA systems using different high-Z semiconductors – GaAs, CdTe and Ge – have been built and tested to compare their performance. GaAs and CdTe both show some nonuniformities, but display sufficiently good performance for some experiments; in particular, GaAs shows good stability with time and irradiation, and good image quality after flat-field correction. Ge is at an earlier stage in development, but shows improved image quality.

A 2-megapixel LAMBDA system for hard X-ray detection has been built using GaAs sensors. This system has been used at the PETRA-III synchrotron to perform high-speed diffraction experiments, demonstrating a combination of high speed and sensitivity. For example, in experiments studying compression of Bi during rapid compression in a diamond anvil cell, it was possible to observe changes of phase on sub-millisecond timescales.

**Keywords:** pixel detector, high energy, photon counting

**MS40-O2** White beam Laue diffraction of polycrystalline materials using 3D energy dispersive detector (pnCCD)Ullrich Pietsch<sup>1</sup>

1. University of Siegen, Department of Physics

email: pietsch@physik.uni-siegen.de

Energy-dispersive CCD detectors, as the charged-coupled pnCCD, operating in the single photon counting mode (SPC) using white or pink beam spectra allows for simultaneous position and energy dispersive detection of scattered photons. This approach is well suited for Laue-type diffraction experiments because it provides structure data from a fixed sample position without sample rotation. In this presentation we report on pnCCD application using hard x-rays ( $30 < E < 140\text{keV}$ ) where bare silicon detectors are typically less sensitive. This deficit is partially compensated by coupling the silicon chip with a scintillator crystal converting the not directly counted photons into electrons and fluorescence photons of low energy. Due to the flat curvature of Ewald sphere at high photon energies a large number of Bragg reflections become accessible at same time. Each of the measured Laue spots can be indexed based on the knowledge on Bragg angles and diffraction energies. In case of polycrystalline materials and considering the respective crystal system we are able to assign each of the Laue spots to one or another of the illuminated grains. Grain defects can be classified via evaluation of streaking Laue spots as function of photon energy. These unique capabilities allows for the measurement of lattice parameter variations caused by local strains.

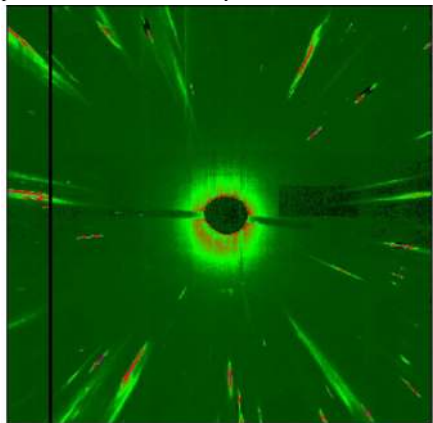


**Figure 1.** Laue pattern of a polycrystalline Ni sample measured in spectral range between 30 and 140 keV. Streaking is changing as function of tensile load

**Keywords:** white beam Laue diffraction, 3D energy-dispersive detector, polycrystalline material

**MS40-O3** High-resolution XRD investigation of SiGe/Si heterostructures for novel X-ray detectorsIvan Marozau<sup>1</sup>, Fabio Isa<sup>2</sup>, Arik Jung<sup>2</sup>, Giovanni Isella<sup>3</sup>, Hans von Känel<sup>2</sup>, Philippe Niedermann<sup>1</sup>, Olha Sereda<sup>1</sup>

1. CSEM SA

2. Laboratory for Solid State Physics, ETH Zurich

3. L-NESS and Department of Physics, Politecnico di Milano

email: imu@csem.ch

Imaging sensors directly coupled to complex readout units form an area of immense technological interest. One example concerns devices for X-ray imaging and inspection, ranging from medical diagnostics and cancer therapy to non-destructive testing of all kinds of goods (quality assurance, security). However, the development of semiconductor X-ray detectors monolithically integrated on a CMOS platform encounters lots of difficulties associated with crystal defects, layer cracks and wafer bowing. A new approach towards detector fabrication that involves epitaxial growth of thick three-dimensional Ge and SiGe crystal arrays on patterned Si(001) substrates has allowed to solve these problems [1].

We will present a high-resolution XRD study of such SiGe crystals heteroepitaxially grown on pillar-patterned Si(001) substrates. The Ge content in the heterostructures is gradually increased through the pillar height from 0.05 at. % at the interface with the substrate to ~80 at. % at the surface. We will show analysis of the reciprocal space maps (RSMs) measured around the symmetrical (004) and asymmetrical (115) Bragg reflections in order to investigate the strain gradient in the grown SiGe crystals. The results of the calculations of the in-plane and out-of-plane strain as well as the Ge content in the top layer of SiGe will be presented.

[1] C.V. Falub, H. von Känel, F. Isa, R. Bergamaschini, A. Marzegalli, D. Chrastina, G. Isella, E. Müller, P. Niedermann, L. Miglio, *Science*, **335**, 1330 (2012).

**Keywords:** X-ray detectors, monolithic integration, SiGe crystals, high-resolution XRD

## MS40-O4 PILATUS3 R CdTe large-area detectors for laboratory applications

Marcus Müller<sup>1</sup>, Tilman Donath<sup>1</sup>, Michael Rissi<sup>1</sup>, Clemens Schulze-Briesche<sup>1</sup>

1. DECTRIS Ltd.

email: marcus.mueller@dectris.com

The PILATUS3 X CdTe detector series for synchrotron applications was introduced by DECTRIS in 2015. Detectors in this series are available with an active area of up to 254 by 298 mm<sup>2</sup> and frame rates of up to 500 Hz. This year, DECTRIS introduces the PILATUS3 R CdTe detector series for laboratory applications.

The laboratory series of CdTe detectors features an active area of up to 84 by 106 mm<sup>2</sup> and a maximum frame rate of 20 Hz. The large, high-quality CdTe sensor achieves high efficiency not only for Cu, but also Mo and Ag radiation and the detector is calibrated for use over the entire energy range. Photon counting in each pixel provides noise-free images with no dark signal or readout noise. In contrast to scintillator-based detectors, this direct-conversion CdTe detector exhibits a sharp point-spread function, with counts confined to the 172 by 172 µm<sup>2</sup> pixel of photon incidence.

This presentation will give an overview of the experimental characterization of detector properties such as quantum efficiency, point-spread function, and count rate capability. Furthermore, first results from laboratory diffraction experiments will be presented.

**Keywords:** Cadmium Telluride, Hybrid Pixel Detectors, Hybrid Photon Counting, Pixel array detectors

## MS40-O5 Modern CPAD Detector Technology for Higher Energy X-rays

Holger Ott<sup>1</sup>, Juergen Graf<sup>2</sup>, Tobias Stuerzer<sup>1</sup>, Michael Ruff<sup>3</sup>

1. Bruker AXS GmbH, Karlsruhe, Germany

2. INCOATEC GmbH, Geesthacht, Germany

3. Bruker AXS Inc., Madison, USA

email: holger.ott@bruker.com

Higher energy X-rays result in a compressed diffraction pattern and enable higher resolution to be achieved, which is particularly advantageous for charge density studies or when the diffraction geometry is restricted, for example by a high-pressure cell. Other advantages include strongly reduced extinction and reduced absorption, which is proportional to about  $\lambda^3$ .

Recent advances in X-ray source and mirror technology have provided the home-lab market with viable solutions for higher energy X-rays, namely the Ag K $\alpha$  (0.56089 Å) IµS 3.0 and the In K $\alpha$  (0.51359 Å) METALJET. These high flux density systems with small, focused beams overcome the decrease in the absolute scattering power of the crystal, which is proportional to  $\lambda^3$ .

The higher energy X-rays challenge modern detectors, and especially Si-sensor based HPAD detectors. HPAD detectors suffer from low DQE and parallax effects due to the thick sensors employed. The latest generation of CPAD (Charge Integrating Pixel Area Detector) on the other hand, with their thin and extremely efficient high Z-element scintillators, overcome these challenges, and provide the ideal solution for shorter wavelength experiments.

This presentation will focus on recent advances in X-ray detector hardware and software development, and will highlight experiments where higher energy X-rays are advantageous, as outlined above.

**Keywords:** CPAD, detector technology, high pressure, strong absorbers, indium wavelength

## MS41 The use of X-ray, electron and neutron scattering in nanoscience

Chairs: Christian Lehmann, Julian Stangl

### MS41-O1 Complementarity of TEM to bulk diffraction techniques for structures at nanoscale

Joke Hadermann<sup>1</sup>

<sup>1</sup> University of Antwerp

email: Joke.Hadermann@uantwerpen.be

When a structure cannot be satisfactorily solved/refined from X-ray or neutron diffraction, advanced transmission electron microscopy techniques (but also sometimes the conventional ones) can often help. Typical problems might arise from local order, weak reflections disappearing in background noise, atoms that scatter weakly in XRD. ... Using examples of problems we faced in the structure solution and refinement of different inorganic materials, the possibilities of several transmission electron microscopy techniques will be exposed.

First of all, high angle annular dark field (HAADF) scanning transmission electron microscopy (STEM) and annular bright field (ABF) STEM can be used to directly visualize the structure, much more easily understandably than was possible with conventional high resolution transmission electron microscopy. This can then be combined with high resolution energy dispersive X-ray analysis (EDX) and electron energy loss spectroscopy (EELS) with which we can do spectroscopy at atomic resolution. We will show some representative examples where these techniques were used: to characterize the cation order in  $\text{Sr}_2\text{Fe}_2\text{TeO}_9$  (unexpectedly different from literature), to solve intricate modulations and to map the different coordinations of the same element in crystallographic shear plane structures<sup>1</sup>, to detect previously unnoticed atoms in  $[\text{K}_2\text{Nb}_2\text{O}_7]^{2-}$ , to display small shifts of light atoms in  $(\text{Bi,Pb})\text{FeO}_3$ <sup>2</sup>, ...

Furthermore, the conventional technique of electron diffraction underwent an update into electron diffraction tomography<sup>3</sup>, giving for each crystal a set of hkl with intensities reliable enough for structure solution and often even refinement. This can be used a.o. for characterizing nanocrystals, for the structure solution and refinement with elements that interact weakly with X-rays but more strongly with electrons, for samples where different phases cannot be separated (for example charged battery materials), ... Here, we will show a case where all these difficulties occurred in combination and where the structure could only be successfully refined using electron diffraction tomography, i.e. charged and discharged lithium based battery materials.

References: <sup>1</sup>D. Batuk et al., Acta Cryst. B71(2015)127–143; <sup>2</sup>R. Paria Sena et al., Dalton Transactions 45 (2016)973–979; <sup>3</sup>W. Dachraoui, Chem. Mater. 24(2012)1378–1385; <sup>4</sup>U. Kolb et al, Ultramicroscopy 107(2007)507–513

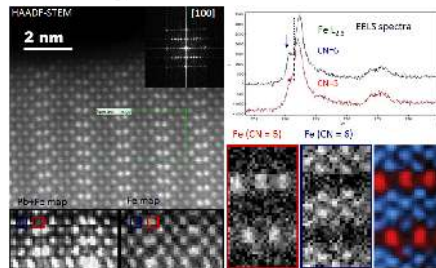


**Figure 1.** HAADF-STEM image of the  $\text{Pb,Sr,Bi,Fe,O}_{16}$  structure with an Fe elemental map and maps of the Fe cations in octahedral (blue) and square pyramidal (red) coordination.<sup>1</sup>

**Keywords:** TEM, EDT, Lithium, battery, perovskite

## MS41-O2 X-ray imaging of single nano-structures: from focused beams to coherent imaging and ptychography

Vincent Favre-Nicolin<sup>1</sup>, Ondrej Mandula<sup>1,2,3,4</sup>, Marta Elzo Aizarna<sup>1,2,4</sup>, Joel Eymery<sup>2,4</sup>, Francesca Mastropietro<sup>1,2,5</sup>, Gerardina Carbone<sup>1,6</sup>, Francois Andrieu<sup>7</sup>, Julien Claudon<sup>2,4</sup>, Jean-Michel Gerard<sup>2,4</sup>

**Keywords:** coherent diffraction imaging, nanostructure, ptychography, semiconductors

1. ESRF-The European Synchrotron, Grenoble, France
2. Univ. Grenoble Alpes, INAC-SP2M, Grenoble, France
3. Fondation Nanosciences, Grenoble, France
4. CEA, INAC-SP2M, Grenoble, France
5. Univ. Aix-Marseille, Institut Fresnel, France
6. Max IV Laboratory, Lund University, Sweden
7. Univ. Grenoble Alpes, CEA-LETI, Grenoble, France

email: favre@esrf.fr

The quantitative study of nano-structures has seen remarkable developments in the last 20 years, either using electron microscopy or synchrotron X-ray beams. The latter notably allow to study the structure of single objects with a resolution around 10 nm, giving access not only to the 2D and 3D electronic density, but (using the Bragg geometry) to the inhomogeneous strain of deformed crystal lattices.

We will present examples of X-ray nano-diffraction studies notably on semi-conductor nano-structures: (i) 70nm-thick silicon-on-insulator (SOI) lines and layers, where the strain is used to enhance the conductive properties, and (ii) GaAs nanowire with embedded InAs quantum dots used as source for single photon emission.

Finally, we will also discuss the future of coherent imaging techniques, which will become more accessible with the development of more user-friendly algorithms and software for data analysis, and the prospect of more brilliant sources giving several orders of magnitude improvement in the available coherent flux.

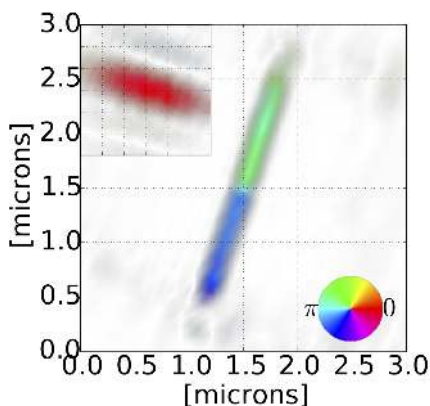


**Figure 1.** Reconstruction of a GaAs nanowire with an  $\sim 1.7$  monolayer InAs insertion in Bragg geometry. The brightness corresponds to the amplitude, the colour to the phase of the complex image - corresponding to a  $\sim 0.027$  nm shift of the crystalline lattice. Inset: reconstructed X-ray probe.

# MS41-O3 Twin domain mapping in topological insulator $\text{Bi}_2\text{X}_3$ (X=Se,Te) by scanning XRD and electron backscattering diffraction

Dominik Krieger<sup>1</sup>, Petr Harcuba<sup>1</sup>, Andreas Lesnik<sup>2</sup>, Gunther Springholz<sup>3</sup>, Guenther Bauer<sup>3</sup>, Václav Holy<sup>1</sup>

1. Charles University in Prague, Faculty of Mathematics and Physics, Czech Republic
2. Institut für Experimentelle Physik, Otto-von-Guericke Universität Magdeburg, Germany
3. Johannes Kepler University Linz, Institute of Semiconductor and Solid State Physics, Austria

email: dominik.krieger@gmail.com

3D topological insulators are a new kind of matter with inverted bulk band gap and Dirac cone-like surface states [1].  $\text{Bi}_2\text{X}_3$  with X=Se and Te are prime members of this material class and were shown to exhibit the predicted topological properties [2]. For electrical devices made from these materials large area high quality thin films are required which, however, commonly show the formation of twin defects as can be seen in Figure panel a. Horizontal (c-plane) twin defects were shown to influence the electronic properties [3] whereas little is known about vertical twin defects. We have investigated the horizontal and vertical twin defect formation in molecular beam epitaxy grown  $\text{Bi}_2\text{Se}_3$  and  $\text{Bi}_2\text{Te}_3$  thin films by scanning x-ray diffraction (SXRD) [4] and electron backscatter diffraction (EBSD). With EBSD we directly obtain the crystal orientation in the vicinity of the surface as shown in Figure panel b. Scanning x-ray diffraction probes the bulk of the thin films and thus complements the surface sensitive electron imaging techniques. For SXRD a focused x-ray beam (~150 nm diameter) is used and with the samples mounted on piezo-scanners the XRD intensity is mapped in real space. Performing measurements at the asymmetric (10-1.20) Bragg peak the XRD intensity (Figure panel c) therefore reveals that defects separating the two twin domains are not strictly vertical but that one twin domain might also overgrow another second one. Based on these results we are able to present a strategy to reduce the surface density of such defects which has important implications for the study of topological surface states.

[1] H. Zhang, C.-X. Liu, X.-L. Qi, X. Dai, Z. Fang and S.-C. Zhang, *Nature Physics* 5, 438–442 (2009) doi:10.1038/nphys1270

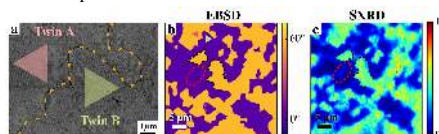
[2] Y. L. Chen, J. G. Analytis, J.-H. Chu, Z. K. Liu, S.-K. Mo, X. L. Qi, H. J. Zhang, D. H. Lu, X. Dai, Z. Fang, S. C. Zhang, I. R. Fisher, Z. Hussain and Z.-X. Shen, *Science* 325, 178–181 (2009) doi:10.1126/science.1173034

[3] H. Aramberri, J. I. Cerdá, and M. C. Muñoz, *Nano Lett.*, 15, 3840–3844 (2015) doi:10.1021/acs.nanolett.5b00625

[4] J. Stangl, C. Mocuta, A. Diaz, T. H. Metzger, and G. Bauer, *ChemPhysChem* 10, 2923–2930 (2009) doi:10.1002/cphc.200900563

**Figure 1.** Twin formation in  $\text{Bi}_2\text{Te}_3$  thin films. a) Scanning electron micrograph of a twin boundary (dashed line) separating two twinned areas. b) Electron backscatter diffraction (EBSD) inplane orientation map showing the twin domains in the very same area as bulk sensitive scanning XRD measurement c).

**Keywords:** scanning x-ray diffraction, electron backscatter diffraction, twin domain, topological insulators



## MS41-O4 Investigation of layered and porous nanomaterials by diffraction tomography, simulations and HRTEM

Yaşar Krysiak<sup>1</sup>, Bastian Barton<sup>1</sup>, Haishuang Zhao<sup>1</sup>, Reinhard Neder<sup>2</sup>, Ute Kolb<sup>1</sup>

1. Institute of Inorganic Chemistry and Analytical Chemistry, Johannes Gutenberg University, Jakob-Welder-Weg 11, D-55128 Mainz, Germany

2. Chair for Crystallography and Structural Physics, Friedrich-Alexander-Universität Erlangen-Nürnberg, Staudtstr. 3, D-91058 Erlangen, Germany

email: krysiak@uni-mainz.de

Layered and porous nanomaterials are frequently characterized by disorder, pseudo symmetry and stress/strain effects, which often give rise to unique properties but make structural analysis difficult. For such materials, automated electron diffraction tomography<sup>[1]</sup> (ADT) can deliver 3D structure information at atomic resolution. For instance, a super structure in CaCO<sub>3</sub> polymorph vaterite or twinned domains for boron oxynitride could be solved with ADT.<sup>[2,3]</sup>

Currently, we aim for a more complete description of nanomaterial structures, including non-periodic effects through a combination of TEM imaging, ADT and structure simulation and modeling.

ADT data can be directly used for an *ab-initio* structure solution of the average structure. Disorder and distortion or intergrown phases are simulated using the DISCUS software package<sup>[4]</sup> through accurate analysis of the structure's variance. The results are compared to TEM holograms<sup>[5]</sup> reconstructed from focal series.

Zeolite Beta<sup>[6]</sup> was chosen as a test sample. The intergrown polymorphs A and B could be solved *ab-initio* from one single ADT dataset by integrating the relative reflection intensities with two distinct lattices. The disorder type was identified by exit wave reconstruction and confirmed by DISCUS simulations. Based on these results it was possible to solve the non-periodic structure of an unknown zeolite *ab-initio*.

The 3D atomic structure of different compounds forming highly distorted and disordered nanoparticles could be successfully described by combining ADT, layer shift simulations and TEM imaging. In future, we aim to fit the simulations automatically to the experimental diffraction data and to apply this method to different compounds such as alloys, organic pigments, and photoactive organics.

[6] J. M. Newsam, M. M. J. Treacy, W. T. Koetsier, C. B. D. Gruyter, *Proc. R. Soc. Lond. Math. Phys. Eng. Sci.* **1988**, 420, 375–405.

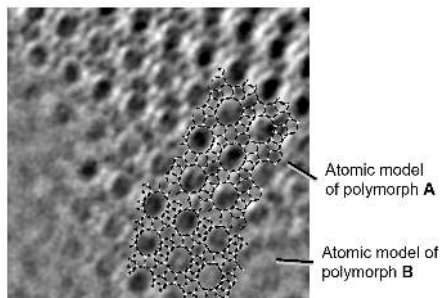


**Figure 1.** Intergrown polymorphic mixture of Zeolite Beta A and B: HRTEM hologram combined with structure solution models.

**Keywords:** automated electron diffraction tomography, disorder simulations, TEM holography, zeolite beta

[1] E. Mugnaioli, T. Gorelik, U. Kolb, *Ultramicroscopy* **2009**, 109, 758–765.

[2] E. Mugnaioli, I. Andrusenko, T. Schüler, N. Loges, R. E. Dinnebier, M. Panthöfer, W. Tremel, U. Kolb, *Angew. Chem.* **2012**, 124, 7148–7152.

[3] S. Bhat, L. Wiehl, L. Molina-Luna, E. Mugnaioli, S. Lauterbach, S. Siculo, P. Kroll, M. Duerschnebel, N. Nishiyama, U. Kolb, et al., *Chem. Mater.* **2015**, 27, 5907–5914.

[4] T. Proffen, R. B. Neder, *J. Appl. Crystallogr.* **1997**, 30, 171–175.

[5] B. Barton, B. Jiang, C. Song, P. Specht, H. Calderon, C. Kisielowski, *Microsc. Microanal.* **2012**, 18, 982–994.



## MS41-O5 Strain mapping in Ge microstructures using X-ray white beam Laue microdiffraction

Samuel TARDIF<sup>1,2</sup>

1. CEA-INAC

2. Université Grenoble Alpes

email: samuel.tardif@gmail.com

Strain-engineering of the band structure in germanium in currently intensively investigated to achieve a direct bandgap material suitable for a CMOS-compatible laser source. Theory predicts that the required tensile strain is relatively large ( $> 2\%$  biaxial or  $> 4\%$  uniaxial), yet such strain values have already been achieved using strain concentration in patterned suspended membranes.<sup>1-2</sup> A local probe of the full strain tensor would therefore be much needed to measure the actual strain distribution across the pattern. We have used X-ray Laue micro-diffraction ( $\mu$ Laue) at beamline BM32 at the European Synchrotron Radiation Facility to measure the strain tensor in different suspended Ge structures. We combined this technique with energy resolved measurements, such as rainbow-filtering<sup>3,4</sup> or direct energy determination using a silicon drift detector on a Bragg peak. The combination of the measurement of the deviatoric strain tensor with at least one measurement of a Bragg energy allowed us to measure the full strain tensor, *i.e.* including the hydrostatic part. Several conclusions were drawn from such measurements. First, the experimental results were confronted to numerical calculations of the full strain tensor obtained from the generalized Hooke's equation using the measured deviatoric strain tensor and the assumption of no normal stress on the free surfaces of the membranes. The excellent agreement evidenced the absence of changes in the values of the Ge elastic parameters up to 5% uniaxial strain. Experimental maps of all strain components were also consistent with Finite Element Method simulations. Furthermore, a comparison of the strain values measured by X-ray scattering with the spectral shift of the phonon modes measured using Raman spectroscopy showed a non-linear strain-shift relation for uniaxial strain larger than 3%. The non-linear dependence of the Raman shift on the strain was also observed in *ab initio* calculations. Finally, we show that experimental results in stretched Ge nanowires have allowed plotting the position of their direct bandgap as a function of strain and a remarkable agreement with the theoretical calculations was obtained.<sup>51</sup> M. Suess et al., *Nature Photonics* **7**, 466-472 (2013)<sup>2</sup> A. Gasseng et al., *Appl. Phys. Letters* **107**, 191904 (2015)<sup>3</sup> O. Robach et al., *Acta Cryst. A* **69**, 164-170 (2013)<sup>4</sup> S. Tardif et al., *arXiv:1603.06370* (2016)<sup>5</sup> K. Guilloy et al., *Nano Letters* **15**, 4 (2015)

**Keywords:** X-ray Laue micro-diffraction, strain mapping, strained Ge

## MS42 Advances in neutron scattering under non-ambient conditions

Chairs: Jiri Kulda, Stefan Klotz

### MS42-O1 The role of oxygen packing in the structural transformations of oxide glasses

Anita Zeidler<sup>1</sup>, Philip S. Salmon<sup>1</sup>

1. Physics Department, University of Bath

email: a.zeidler@bath.ac.uk

Liquid and glassy oxide materials play a vital role in multiple scientific and technological disciplines. Here we investigate the structural transformations in silica, a building block of geophysically relevant silicates, as well as germania and B<sub>2</sub>O<sub>3</sub>. We show that an interplay between experiment<sup>2</sup> and simulation leads to a new understanding of the pressure induced changes within these materials. A new structural map is devised for predicting the likely regimes of topological change. It is shown that this can be applied to a range of oxide materials. The information obtained can be used to forecast when changes may occur to the transport properties and compressibility of, e.g., fluids in planetary interiors, and is a prerequisite for the preparation of new materials following the principles of rational design.

**Keywords:** high pressure, glass, oxygen packing

## MS42-O2 Neutron Diffraction Studies of Gas Hydrates

John Loveday<sup>1</sup>

1. SUPA, School of Physics and Astronomy and Centre for Science at Extreme Conditions, The University of Edinburgh

email: J.Loveday@ed.ac.uk

The gas hydrates are a group of compounds which are of wide importance. They are model systems for the study of interactions between water and other molecules and can thus provide fundamental insight into such interactions. Gas hydrates also provide a cheap and environmentally benign way to store and transport gases and are thus potentially crucial to the task of decarbonising the energy economy. Finally, gas hydrates are common in nature and their behaviour affects phenomena as diverse as the Earth's paleoclimate and the magnetic fields of Uranus and Neptune.

High pressure studies of gas hydrates provide valuable insight into all of these areas. At low pressures most gas hydrates adopt one of three related cage structures. The application of modest pressures reveals a rich and varied structural landscape that provides deeper insight into water-gas interactions. New gas hydrate structures provide potential new materials for hydrogen storage and carbon sequestration. And, information on high pressure is directly relevant to models of planetary formation and evolution. In my talk I will illustrate some of these aspects with recent neutron diffraction studies of gas hydrates.

**Keywords:** neutron, diffraction, high-peressure

## MS42-O3 Matrix transformation temperature in boron containing Co-Re alloys for high temperature gas turbine applications

Pavel Strunz<sup>1</sup>, Debashis Mukherji<sup>2</sup>, Přemysl Beran<sup>1</sup>, Ralph Gilles<sup>3</sup>, Lukas Karge<sup>3</sup>, Michael Hofmann<sup>3</sup>, Markus Hoelzel<sup>4</sup>, Joachim Rösler<sup>2</sup>

1. Nuclear Physics Institute of the CAS, CZ-25068 Řež near Prague, Czech Republic
2. TU Braunschweig, Institut für Werkstoffe, Langer Kamp 8, 38106 Braunschweig, Germany
3. TU München, Heinz Maier-Leibnitz Zentrum (MLZ), Lichtenbergstraße 1, 85747 Garching, Germany
4. TU Darmstadt, Materialwissenschaft, Petersenstraße 23, 64287 Darmstadt, Germany

email: strunz@ujf.cas.cz

Co-Re-based alloys [1] are being developed to supplement single crystal Ni-based superalloys in future gas turbines which will operate with increased gas entry temperatures. The stability of the matrix at the foreseen metal operation temperatures ( $\geq 1200^\circ\text{C}$ ) is a very important concern for the alloy development.

Neutron diffraction was proved to be a valuable tool to study both the matrix transformation and minority phases stability in situ at high temperatures. Neutron measurements showed in the past that the low temperature hcp Co-solid solution matrix undergoes an allotropic transformation to a fcc structure above  $1100^\circ\text{C}$  [2]. The transformation temperature depends on the alloy composition.

It is known that an addition of boron (50-1000 ppm) to the alloy largely increases its ductility, which is desirable for the application of the Co-Re alloys. The boron influence on structure and microstructure was therefore tested on Co-17Re-23Cr alloy. The alloy contains, beside the matrix phase, only sigma phase (Cr<sub>2</sub>Re<sub>3</sub>) and (for boron containing alloy) also borides.

First, it was found in situ at high temperatures using neutron diffraction (MLZ Garching) that the boron content changes significantly the hcp  $\rightarrow$  fcc transformation temperature. For the reference alloy (Co-17Re-23Cr) without boron, the transformation hcp  $\rightarrow$  fcc starts at around  $1400^\circ\text{C}$  on heating, while a small addition of boron to the reference alloy lowers significantly the transformation temperatures by more than 50K [3].

As the cycling through the hcp-fcc transformation temperature during operation of the components produced from the alloy could be a problem for the microstructural stability, the boron-content influence on the matrix transformation temperature deserved more attention. Therefore, its influence on the hcp-fcc transformation temperature was investigated in more detail using neutron diffraction.

It was found by studying samples with boron content 0-1000 ppm (wt.) that the temperature of hcp-fcc transformation in Co-Re alloys is not changing monotonically with increasing boron content. After the initial decrease, the temperature significantly increases for the samples with high content of boron. Possible reason could be an interplay between amount of boron in the matrix and amount of sigma phase which binds hcp-stabilizing element Re.

[1] J. Rösler et al, Adv.Eng.Mater. 9, 2007, 876

[2] D. Mukherji et al, J.Mater.Lett. 64, 2010, 2608

[3] D. Mukherji et al, Kovove Mater. 53, 2015, 287

**Keywords:** High-temperature materials, Co-Re alloys, Neutron scattering

## **MS42-O4** Neutron Total Scattering of Crystalline Materials in the Gigapascal Regime

Craig L. Bull<sup>1</sup>, Helen Y. Playford<sup>1</sup>, Matthew G. Tucker<sup>1</sup>

1. ISIS Facility, STFC, Rutherford Appleton Lab

email: [craig.bull@stfc.ac.uk](mailto:craig.bull@stfc.ac.uk)

Neutron total scattering of disordered-crystalline materials provides direct experimental access to the local (short-range) structure. The ways in which this local structure agrees (or disagrees) with the average (long-range) crystal structure can provide important insight into structure-property relationships. High-pressure neutron diffraction using the Paris-Edinburgh (P-E) pressure cell allows experimenters to explore the ways in which materials are affected by pressure, can reveal new synthetic routes to novel functional materials and has important applications in many areas, including geology, engineering and planetary science. The combination of these two experimental techniques poses unique challenges for both data collection and analysis. In this paper it is shown that, with only minor modifications to the standard P-E press setup, high-quality total scattering data can be obtained from crystalline materials in the gigapascal pressure regime on the PEARL diffractometer at ISIS. The quality of the data is assessed through the calculation of coordination numbers and the use of reverse Monte Carlo (RMC) refinements. The time required to collect data of sufficient quality for detailed analysis is assessed and is found to be of the order of 8 hours for a quartz sample. Finally, data from the perovskite  $\text{LaCo}_{0.35}\text{Mn}_{0.65}\text{O}_3$  is presented and reveals that PEARL total scattering data offers the potential for the extraction of local structural information from complex materials at high pressure.

**Keywords:** neutron, high-pressure, total scattering

## MS42-O5 Stroboscopic neutron powder diffraction at HRPT, SINQ

Denis Sheptyakov<sup>1</sup>, Vladimir Pomjakushin<sup>1</sup>, Lucien Boullet-Roblin<sup>2</sup>, Claire Villevieille<sup>2</sup>, Gerd Theidel<sup>3</sup>, Mark Könncke<sup>4</sup>, Roman Bürge<sup>4</sup>

1. Laboratory for Neutron Scattering and Imaging, Paul Scherrer Institute, 5232 Villigen PSI, Switzerland
2. Electrochemistry Laboratory, Paul Scherrer Institute, 5232 Villigen PSI, Switzerland
3. Laboratory for Particle Physics, Paul Scherrer Institute, 5232 Villigen PSI, Switzerland
4. Laboratory for Scientific Developments and Novel Materials, Paul Scherrer Institute, 5232 Villigen PSI, Switzerland

email: denis.cheptakov@psi.ch

At HRPT, the high-resolution powder neutron diffractometer at SINQ\*, a new mode of operation has been realized and tested. This stroboscopic measurements mode is intended for studies of crystal or magnetic structure transformations occurring in short (available time binning down to 10 milliseconds), but multiply repeating processes triggered by some external effect, e.g. voltage, magnetic field, thermal heat pulse, etc. The diffraction data corresponding to different time slices after a certain repeating strobo signal are stored in the different histogram memory blocks (up to about 70000 independent diffraction patterns). In our tests, we could successfully slice time down to 10 milliseconds with overall duration of experiment of several hours, so the processes, or existence ranges of phases on the order of tens of milliseconds, seconds, minutes etc., - can now be addressed efficiently by neutron diffraction at HRPT. The first real studies, including the operando investigation of ultrafast charging-discharging cycles of a commercial Li-ion battery (LiFePO<sub>4</sub> vs. graphite) will be presented.

\* <https://www.psi.ch/sinq/hrpt/hrpt>

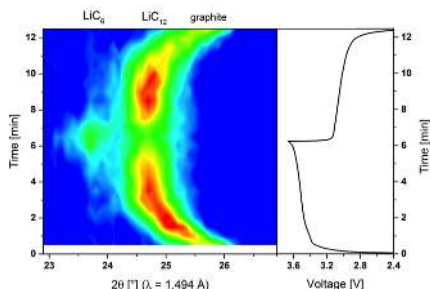


**Figure 1.** Selected sections of the stroboscopic neutron powder diffraction patterns corresponding to 120 charge-discharge cycles of a battery, showing transition between graphite, LiC<sub>12</sub> and LiC<sub>6</sub> phases and back. Overall charge-discharge time is approximately 12 min. Data binned with 30 seconds per pattern.

**Keywords:** stroboscopic, neutron diffraction

## MS43 Combining x-ray diffraction and other techniques for in situ and operando studies

Chairs: Helmut Ehrenberg, François Fauth

### MS43-O1 Revealing Secrets of Lithium-Ion Battery Operation by Neutron Scattering

Martin J. Muehlbauer<sup>1,2,3</sup>, Anatoliy Senyshyn<sup>3</sup>, Michael Knapp<sup>1,2</sup>, Helmut Ehrenberg<sup>1,2</sup>

1. Helmholtz-Institute Ulm for Electrochemical Energy Storage (HIU), P.O. Box 3640, D-76021 Karlsruhe, Germany
2. Institute for Applied Materials (IAM), Karlsruhe Institute of Technology (KIT), Hermann-von-Helmholtz-Platz 1, D-76344 Eggenstein-Leopoldshafen, Germany
3. Heinz Maier-Leibnitz Zentrum (MLZ), Technische Universität München, Lichtenbergstr. 1, 85748 Garching, Germany

email: martin.muehlbauer@kit.edu

Powering innumerable portable devices lithium-ion batteries are part of our everyday life for decades already. Although lithium-ion chemistry does a good job powering consumer electronics and tools, there are still some processes inside lithium-ion batteries that are not understood completely. Especially an increasing number of applications related to electromobility and energy storage calls for further improvements of their life span, energy/power density and rate capability. Therefore, single cells or even integrated batteries have to be investigated under real operating conditions to unravel details occurring in the millimetre to micrometre domain and reaching down to a nanometre or even atomic length scale. Neutrons offer a capability to conduct in operando investigations on standard size Li-ion cells even in combination with additional sample environment, e.g. to study temperature effects. For low temperatures an intercalation behaviour differing from the one at room temperature has been observed inside the graphitic anode [1]. Neutron radiation is not only sensitive for light elements but also enables to distinguish neighbouring elements. Therefore, structural changes, phase transitions and cation exchange reactions, e.g. in cathode materials, may be traced during intercalation and deintercalation of lithium providing detailed information about battery operation [2]. Inhomogeneities of the state of charge inside 18650-type Li-ion cells were pointed out by neutron imaging and neutron diffraction experiments. They could be quantified by spatially resolved neutron diffraction on a macroscopic length scale as inhomogeneities of the lithium concentration inside the

anode for fully charged cells [3]. Here a correlation between the cell design and the lithiation state of the graphitic anode has been found.

Results based on electrochemical cell characterization, neutron imaging and scattering techniques will be presented. They will be discussed in terms of their influence for the design and operation of Li-ion cells, i.e. cell geometry (tab positions), cell balancing or operating temperature.

[1] A. Senyshyn, M.J. Mühlbauer, O. Dolotko, H. Ehrenberg., Journal of Power Sources 282 235-240 (2015).

[2] O. Dolotko, A. Senyshyn, M.J. Mühlbauer, K. Nikolowski, H. Ehrenberg, Journal of Power Sources, 245 197-203 (2014).

[3] A. Senyshyn, M.J. Mühlbauer, O. Dolotko, M. Hofmann, H. Ehrenberg, Nature Scientific Reports, 5, 18380 (2015), doi: 10.1038/srep18380.

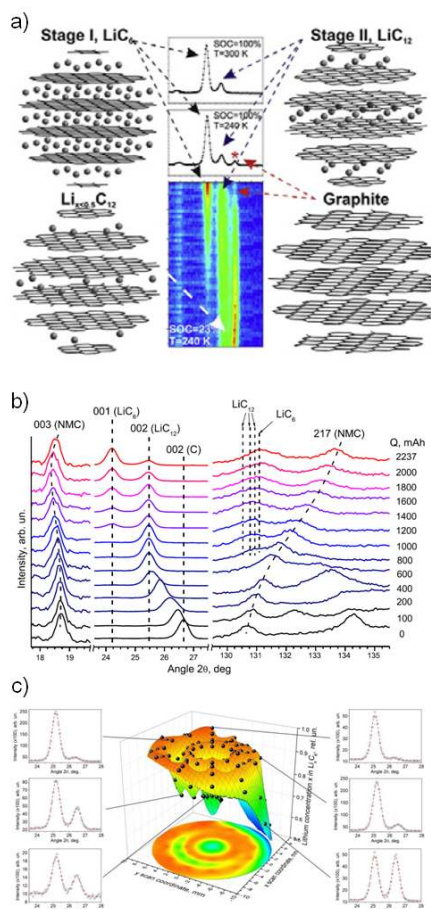


**Figure 1.** a) In operando neutron diffraction during discharge at 240 K, intercalation behaviour differs from room temperature [1]; b) diffraction data at different state of charge point out cation mixing in NMC cell [2]; c) spatially resolved lithium concentration inside the anode of a charged Li-ion cell [3]

**Keywords:** Li-Ion Battery, Neutron, Scattering, Diffraction

**MS43-O2** New insight on structural and redox processes involved upon cycling of  $\text{Na}_3\text{V}_2(\text{PO}_4)_2\text{F}_3$ , an attractive positive electrode material for Na-ion batteries

Thibault Broux<sup>1,2,3</sup>, Bianchini Matteo<sup>1,2,4</sup>, Fauth François<sup>5</sup>, Simonelli Laura<sup>5</sup>, Stievano Lorenzo<sup>3,6</sup>, Suard Emmanuelle<sup>4</sup>, Masquelier Christian<sup>2,3</sup>, Croguennec Laurence<sup>1,3</sup>

1. CNRS, University of Bordeaux, Bordeaux INP, ICMCB UPR 9048, F-33600 Pessac, France
2. LRCNS, CNRS-UMR 7314, University Picardie Jules Verne, F-80039 Amiens Cedex 1, France
3. RS2E, FR CNRS 3459, F-80039 Amiens Cedex 1, France
4. Institut Laue-Langevin, F-38000 Grenoble, France
5. CELLS - ALBA synchrotron, E-08290 Cerdanyola del Vallès, Barcelona, Spain
6. ICG, CNRS-UMR 5253, University of Montpellier, F-34095 Montpellier Cedex 5, France

email: Thibault.Broux@icmcb.cnrs.fr

As electrode materials for batteries are operating in non-equilibrium conditions a deeper understanding of the structural and redox processes occurring upon cycling can be achieved using *operando* techniques. In order to do this a versatile electrochemical cell has been developed for X-ray experiments allowing real-time data collection upon charge/discharge (*i.e.* upon lithium or sodium extraction/insertion from/into the electrodes), either by lab X-ray and synchrotron X-ray powder diffraction or by X-ray absorption spectroscopy [1]. This unveils dynamics features that are not accessible by other means and gives a greater picture of the electrodes' functioning from electronic and atomic point of view.

Concerning  $\text{Na}_3\text{V}_2(\text{PO}_4)_2\text{F}_3$ , recent structural characterization of the fully charged material  $\text{Na}_3\text{V}_2(\text{PO}_4)_2\text{F}_3$  via *operando* synchrotron X-ray diffraction performed at the ALBA synchrotron (Barcelona, Spain) suggests charge disproportionation of  $2\text{V}(+IV)$  into  $\text{V}(+III)$  and  $\text{V}(+V)$ . Indeed structural features combined with bond valence sums show two different vanadium environments consistent with such a hypothesis [2]. To further support this observation *operando* X-ray absorption near edge spectroscopy (XANES) at the vanadium K-edge in fluorescence mode has been performed at ALBA which gives relevant information on local environment and electronic configuration of the vanadium, especially through the pre-edge peaks' investigation. The obtained data have been analyzed via principal component analysis and multivariate curve resolution which constitute a novel approach to characterize electrode materials in operating conditions.

Furthermore impact of the cycling rate and temperature on the phase diagram observed upon sodium deintercalation and re-intercalation from/in  $\text{Na}_3\text{V}_2(\text{PO}_4)_2\text{F}_3$  will be also extensively discussed.

1. Leriche, J. B.; Hamelet, S.; Shu, J.; Morcrette, M.; Masquelier, C.; Ouvrard, G.; Zerrouki, M.; Soudan, P.; Belin, S.; Elkaïm, E. and Baudelet, F., *J. Electrochem. Soc.* **2010**, 157, A606-A610.

2. Bianchini, M.; Fauth, F.; Brisset, N.; Weill, F.; Suard, E.; Masquelier, C. and Croguennec, L., *Chem. Mater.* **2015**, 27(8), 3009-3020.

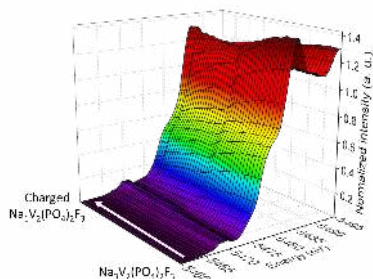


**Figure 1.** Vanadium K-edge XANES raw data collected *operando* upon charge of the battery  $\text{Na}/\text{Na}_3\text{V}_2(\text{PO}_4)_2\text{F}_3$

**Keywords:** Na-ion Battery, *operando* synchrotron X-ray powder diffraction, *operando* XANES, NVPF

### MS43-O3 In situ analysis of mechanochemical reactions using combined X-ray diffraction and Raman spectroscopy

Franziska Emmerling<sup>1</sup>, Lisa Batzdorf<sup>1</sup>, Franziska Fischer<sup>1</sup>, Hannes Kulla<sup>1</sup>, Manuel Wille<sup>1</sup>

1. Bundesanstalt für Materialforschung und -prüfung

email: franziska.emmerling@bam.de

Mechanochemistry is increasingly used for synthesizing various materials including metal organic compounds and cocrystals.[1-3] Although this synthesis approach offers a fast and pure synthesis in high yields, there is a lack in understanding the mechanisms of milling reactions. The necessary data can only be obtained in *in situ* experiments, which were only recently established for milling reactions.[4,5] Herein, we present a novel setup enabling a combined *in situ* investigation of mechanochemical reactions using synchrotron XRD and Raman spectroscopy (see Fig.1). The specific combination allows to study milling processes comprehensively on the level of the molecular and crystalline structure and thus obtaining reliable data for mechanistic studies. Besides well-known MOFs like ZIF-8, the formation process of new metal phosphonates [6] and model cocrystals [7] could be studied in detail. The synthesis pathway of the different compounds could be revealed. The results prove that the presented method combination is applicable for a wide range of materials and will provide the necessary understanding to tune and optimize mechanochemically synthesized compounds.

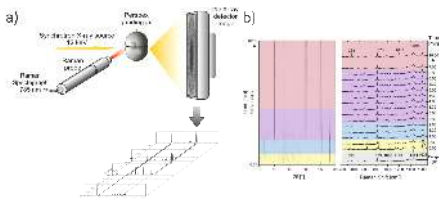


**Figure 1.** a) Schematic diagram of the experimental setup for collecting Raman spectra and XRD powder patterns during the mechanochemical synthesis. b) Synthesis process of the metal organic framework (H<sub>4</sub>Im)[Bi(1,4-bdc)<sub>3</sub>] followed *in situ* by synchrotron XRD (left) and Raman spectroscopy (right).

**Keywords:** *in situ*, mechanochemistry, Raman spectroscopy

### MS43-O4 Operando Study of Ceria Based Solid Oxide Electrochemical Cells

Catherine Dejoie<sup>1</sup>, Fabiano Bernardi<sup>2</sup>, Yi Yu<sup>3,4</sup>, Nobumichi Tamura<sup>3</sup>, Martin Kunz<sup>3</sup>, Matthew Marcus<sup>3</sup>, Chunjuan Zhang<sup>4</sup>, Bryan Eichhorn<sup>4</sup>, Zhi Liu<sup>3,5</sup>

1. ESRF - The European Synchrotron, Grenoble, France

2. Instituto de Física, Universidade Federal do Rio Grande do Sul, Porto Alegre, Brazil

3. Advanced Light Source, Lawrence Berkeley National Lab, Berkeley, USA

4. Department of Chemistry and Biochemistry, University of Maryland, College Park, USA

5. School of Physical Science and Technology, ShanghaiTech University, Shanghai, China

email: catherine.dejoie@esrf.fr

Many physical and chemical properties of ceria can be attributed to the tolerance of the fluorite structure to a high concentration of oxygen ion vacancies, which allows ceria to change oxidation states over a wide temperature range at low  $P_{O_2}$ . On ceria surface, oxygen vacancies can rapidly formed and re-oxidized, giving ceria an enhanced ability to release and store oxygen and to split H<sub>2</sub>O in catalytic reactors. In the bulk, oxygen vacancies are the predominant charge carriers, which makes ceria one of the most important oxygen ion conducting solid electrolytes in solid oxide fuel cells (SOFCs). Therefore, the abilities to monitor the oxygen vacancy number at the surface and in bulk at a given pressure, temperature, and gas environment are important and highly desirable to explore and create new ceria based materials and devices. By using ambient pressure photoelectron spectroscopy (AP-XPS) on a 50 nanometers thin ceria electrode [1], it has been shown that the electrochemically active region undergoes a pronounced Ce<sup>4+</sup> to Ce<sup>3+</sup> surface oxidation change during operation, suggesting that the surface reaction kinetics and lateral electron transport in thin ceria are co-rate limiting processes. Combining AP-XPS, micro X-ray absorption spectroscopy (micro-XAS) and X-ray microdiffraction (micro-XRD), we have investigated the water splitting process occurring at the ceria/gold interface of a 1 micron thick ceria SOEC cell, *in situ*. A shift of the cell parameters of ceria is observed under operation, in relation with the formation of oxygen vacancies. This is an evidence of a long-range process and the reduction of ceria in the bulk. Comparison of the oxygen vacancy number extracted from micro-XRD and micro-XAS experiments shows that ceria is mainly under a crystalline form. Furthermore, the active region extends on the other side of the ceria/gold interface, which means that reduction also occurs on top of gold. Thus, the electron transport in ceria may not be rate limiting in a thicker ceria electrode [2]. Finally, we show that the phase diagram of deficient ceria (CeO<sub>2-x</sub>, 0 < x < 0.2) is not valid anymore for such a non-equilibrium system. Such knowledge on structure and oxygen vacancy changes will be important in order to understand the ion transport and the degradation of electrodes in working electro-chemical cells (fuel cells and batteries).

[1] Zhang C., et al. *Nature Mater.* 2010, 9, 944. [2] Zhang, C. et al. *J. Am. Chem. Soc.* 2013, 135, 11572.

**Keywords:** ceria, micro-XRD, solid oxide electrochemical cell



## MS43-O5 Combined measurements of atomic displacements, lattice strain and macroscopic polarization in ferroelectrics

Semën Gorfman<sup>1</sup>, Hugh Simons<sup>2</sup>, Hyeokmin Choe<sup>1</sup>, Ullrich Pietsch<sup>1</sup>, Michael Ziolkowski<sup>1</sup>, Jacob Jones<sup>3</sup>

1. University of Siegen, Department of Physics, Siegen, Germany
2. Department of Physics, Technical University of Denmark, Denmark
3. Department of Materials Science and Engineering, North Carolina State University, Raleigh, NC, USA.

email: gorfman@physik.uni-siegen.de

Polycrystalline ferroelectrics offer a cost-effective route to produce materials with enhanced dielectric and electro-mechanical coefficients. They are the backbone of many sensors, actuators, non-linear optics and power conversion devices. Understanding the microscopic mechanism of these functionalities is the key to the optimization and discovery of new materials with enhanced properties.

The existing techniques lack the capability to measure polarization-strain coupling. This presentation shows the novel efficient technique [1], which introduces time-resolved and resonant synchrotron X-ray diffraction to simultaneously measure the atomic displacements, lattice strain and macroscopic polarization in a polycrystalline ferroelectric under cyclic electric fields. The time-resolved X-ray diffraction implements a stroboscopic data acquisition strategy operating on the principle of a multi-channel analyser, and providing an ideal platform for the investigation of repetitive processes down to the nanosecond time scale [2]. X-ray diffraction measurements are combined with the polarization measurements (electric field-polarization hysteresis loop). Most significantly, the structural inversion in individual crystallites of ferroelectric ceramics was observed through the Friedel pair contrast. This is a significant methodological innovation: because the hkl and -h-k-l powder rings exactly overlap with one another, the conditions at which the violation of Friedel's law can be observed using powder diffraction are very rare. These conditions can only be realized if: 1) a structure of individual powder grains can be actively inverted during the measurement and 2) the intensity of powder diffraction patterns is high enough to detect this small difference.

We demonstrate this approach using a high-energy (30 keV) X-ray beam on a material in which differentiating between multiple polarization reversal mechanisms remains a significant challenge: tetragonal 0.94-BaTiO<sub>3</sub>-0.06-BiZn<sub>0.5</sub>Ti<sub>0.5</sub>O<sub>3</sub> (BT-BZT) perovskite-based polycrystalline ferroelectrics. The approach offers significant opportunities for probing dynamics of intrinsic polarization using resonant X-ray scattering.

[1] S. Gorfman, H. Simons, T. Iamsasri, S. Prasertpalichat, D.P. Cann, H. Choe, U. Pietsch, Y. Watier, J.L. Jones. Scientific Reports, 20829, (2016)

[2] S. Gorfman, H. Choe, V. V Shvartsman, M. Ziolkowski, M. Vogt, J. Strempler, T. Łukasiewicz, U. Pietsch, and J. Dec, Phys. Rev. Lett. 114, 097601 (2015)

**Keywords:** ferroelectrics, time-resolved X-ray diffraction, high-energy powder diffraction, in-situ measurements

## MS44 Total scattering: pdf analysis and diffuse scattering in X-Ray, neutron and electron diffraction

Chairs: Václav Holý, Cinzia Giannini

### MS44-O1 Confined liquid structure and chemical kinetics from total neutron scattering

Tristan G.A. Youngs<sup>1,2</sup>, Marta Falkowska<sup>1,2</sup>, Daniel T. Bowron<sup>1</sup>, Chris Hardacre<sup>2</sup>

1. ISIS Facility, STFC Rutherford Appleton Laboratory, UK
2. Queen's University Belfast, Belfast, UK

email: tristan.youngs@stfc.ac.uk

Catalysis is, to put it mildly, extremely important. Around 80% of industrial chemical processes rely on a catalyst at some point, and 90% of all man-made materials use a catalyst in at least one step of the reaction. That said, there are still no experimental techniques that allow the structure and kinetics of (heterogeneous) catalytic processes to be resolved in situ. Here I will show the use of total neutron scattering in the determination of relevant information for the hydrogenation of benzene over Pt/MCM-41. I will begin with the structure of the reactant and product liquid, show how the chemical kinetics of the underlying processes can be obtained, and touch on the experimental determination of confined liquid structure.

**Keywords:** total scattering, catalysis, liquid structure, kinetics

**MS44-O2 Correlated disorder in relaxor ferroelectrics**Jiri Hlinka<sup>1</sup><sup>1</sup>. Institute of Physics, The Czech Academy of Science, Prague, Czech Republic

email: hlinka@fzu.cz

The aim of this contribution is report our insights in the correlated occupational and displacement disorder in perovskite ferroelectric crystals of relaxor type.

We begin by exposing our recent investigation of the short-range correlations in the distribution of cations in perovskite B-sites of lead magnesium niobate single crystal, the enigmatic model ferroelectric relaxor material. This analysis is based on the resonant x-ray diffuse scattering data taken in a sizeable volume of the reciprocal space, including both discrete diffraction peaks and continuous x-ray diffuse scattering, and on subsequent direct numeric reconstruction of the average atomic occupation around a given Nb<sup>5+</sup> cation up to the distance of several nanometers. Example of the experimental data is shown in Fig. 1.

We then discuss these results in the context of other experimental and theoretical studies of the B-site distribution in lead magnesium niobate single crystal, as well as its relation to the A-site displacement disorder and the implications for the peculiar dielectric properties of lead magnesium niobate single crystal and similar materials.

This work was supported by the Czech Science Foundation (project 15-09142S).

**References**

[1] M. Kopecky, J. Kub, J. Fabry, and J. Hlinka, *Phys. Rev. B*, **93**, 054202 (2016).

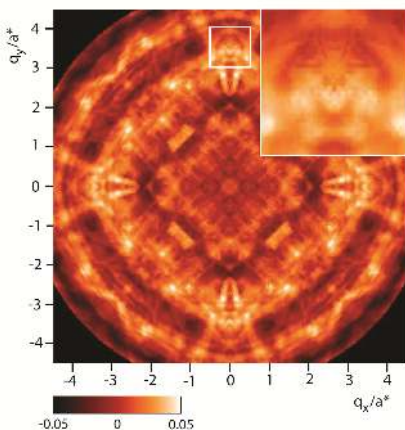


**Figure 1.** The intensity map of the anomalous part of the x-ray diffuse scattering from the PMN single crystal in the (0 0 0.25a\*) plane of the reciprocal space. The inset shows enlarged part of the scattering intensity from the marked regions.

**Keywords:** diffuse scattering, resonant x-ray scattering, short-range correlations, disorder, relaxor, lead magnoniobate

**MS44-O3 Mapping of reciprocal space with ferroelectrics under electric field**Dmitry Chernyshov<sup>1</sup>, Tikhon Vergentev<sup>2</sup>, Robert Cernik<sup>3</sup>, Alexei Bosak<sup>4</sup>, Semen Gorfman<sup>5</sup>

1. Swiss-Norwegian BeamLines at the European Synchrotron Radiation Facility, Grenoble, France
2. Peter the Great Saint Petersburg Polytechnic University, St.-Petersburg, Russia
3. School of Materials, The University of Manchester, Oxford Rd, Manchester, M13 9PL, United Kingdom
4. European Synchrotron Radiation Facility, Grenoble, France
5. Department of Physics University of Siegen, Siegen, Germany

email: dmitry.chernyshov@esrf.fr

Ferroelectric materials are widely used for piezoelectric applications. These materials show strong enhancement of electromechanical properties close to a solid state phase transition point or morphotropic phase boundary. Mapping of reciprocal space is a perfect tool to characterize the composite nature of the materials, in-situ measurements under electric field allow to see the ferroelectrics in action and provide a ground for understanding of microscopical mechanisms underlying macroscopic behavior. A compact setup for single crystal E-field diffraction experiments in a transmission mode has been recently developed [1]. Temperature and electric field evolution of diffraction patterns, both Bragg and diffuse, for PMN-PT and PIN-PMN-PT ferroelectrics studied with new setup indicates that the compounds predominantly consist from a twinned monoclinic phase. Role of lattice strain and ferroelectric domains is discussed on the basis on experimentally measured total diffraction response. Further development of the method implies a combination of dielectric spectroscopy with large volume reciprocal space mapping of diffuse and Bragg scattering.

[1] Vergentev T Yu, Dyadkin V and Chernyshov D Yu J. Surf. Invest. X-ray Synchrotron Neutron Tech. 9 436 (2015)

## MS44-O4 Pair Distribution Function calculated from electron diffraction data

Tatiana E. Gorelik<sup>1</sup>

<sup>1</sup> University of Mainz

email: gorelik@uni-mainz.de

Structure description through Pair Distribution Function (PDF) analysis has attracted particular interest in the last years with the declination of the technology towards nanocrystalline and amorphous materials. The structure of these materials cannot be described by a set of lattice basis vectors and atomic coordinates, but by a continuous function representing the probability to find atoms at a particular distance - PDF. Experimentally, the PDF is calculated from continuous scattering data, as a rule X-ray, or neutron diffraction. The employment of electron diffraction data for the PDF analysis, although not being completely new, survives a renaissance within the last years. Electron diffraction data for the PDF calculation is collected in a Transmission Electron Microscope (TEM), which has to be operated in a special way in order to collect optimal data for PDF. 2D electron diffraction patterns should be integrated into the 1D intensity profile, which then after a proper normalization will be transformed into a PDF. Specifics of electron diffraction data handling as well as the limitation of the method will be discussed. PDFs calculated from electron diffraction data for different materials will be presented and type of structural information extracted from the PDFs will be discussed.

**Keywords:** Total scattering, electron diffraction, pair-distribution function

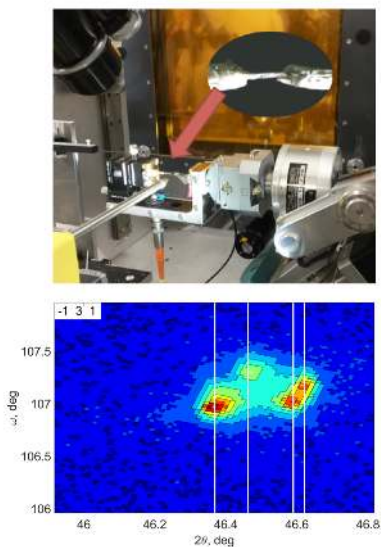


**Figure 1.** Top: The cell for the electric fields diffraction experiments. The single crystal sample is fixed between two needle contacts with conducting glue (insert). Bottom: a splitting of  $[-1\ 3\ 1]$  pseudo-cubic node for PMN-33PT ferroelectric indicative for a monoclinic phase.

**Keywords:** reciprocal map, ferroelectrics, electric field

## MS44-O5 Searching for Ti-clusters in $\text{Mg}_{0.7}\text{Ti}_{0.3}$ thin film

Hyunjeong Kim<sup>1</sup>, Kohta Asano<sup>1</sup>, Kouji Sakaki<sup>1</sup>, Yumiko Nakamura<sup>1</sup>, Akihiko Machida<sup>2</sup>, Naoyuki Maejima<sup>2</sup>, Tetsu Watanuki<sup>2</sup>, Herman Schreuders<sup>3</sup>, Bernard Dam<sup>3</sup>

1. National Institute of Advanced Industrial Science and Technology, Tsukuba, Ibaraki 305-8565, Japan
2. National Institutes for Quantum and Radiological Science and Technology, Sayo, Hyogo 679-5148, Japan
3. Delft University of Technology, Julianalaan 136, NL-2628 BL Delft, The Netherlands

email: hj.kim@aist.go.jp

Mg-rich  $\text{Mg}_{1-x}\text{Ti}_x$  thin film absorbs a large amount of hydrogen in ambient conditions. When in the hydride phase, it absorbs ~87% of solar radiation with low thermal emissivity [1, 2]. This makes Mg-rich  $\text{Mg}_{1-x}\text{Ti}_x$  thin film very attractive for a switchable smart coating material for solar collectors. Lattice parameters of  $\text{Mg}_{1-x}\text{Ti}_x$  thin film vary as if it is solid solution alloy following Vegard's law [2]. However, their optical and electrical properties are not well explained by such a simple structural model. Indeed, a more complex model like nanosized Ti-clusters embedded in Mg-matrix is required [2]. However, there has been no clear evidence for the existence of such nano-clusters in this material.

To resolve Ti-clusters, we obtained the X-ray atomic pair distribution functions (PDFs) of  $\text{Mg}_{0.7}\text{Ti}_{0.3}$  thin film during the hydrogenation process at BL22XU at SPring-8. The PDF before hydrogenation is well explained by a hexagonal close packed (hcp) structural model over a wide interatomic distance range. At the early stage of hydrogenation, a part of the PDF is gradually transformed into a face centered cubic (fcc) structure. Change occurs only in the low- $r$  region and the high- $r$  region of the PDF stays in an hcp structure. Such change in the PDF is expected: it has been proposed that when the  $\text{Mg}_{0.7}\text{Ti}_{0.3}$  thin film is hydrogenated, Ti clusters absorb hydrogen first transformed into an fcc structure while the Mg-matrix stays in a hcp structure [2]. The Mg-matrix absorbs hydrogen later. Our PDF study suggests that the average size of Ti-clusters in  $\text{Mg}_{0.7}\text{Ti}_{0.3}$  thin film is ~30 Å.

This work is partly supported by Photon and Quantum Basic Research Coordinated Development Program from the Ministry of Education, Culture, Sports, Science and Technology, Japan.

[1] D. M. Borsa et al., Appl. Phys. Lett. 88, 241910 (2006).

[2] D. M. Borsa et al., Phys. Rev. B 75, 205408 (2007).

**Keywords:** nano-clusters, thin film, x-ray atomic pair distribution function

## MS45 Measuring data quality

Chairs: Phil Evans, Alexandre Urzhumtsev

## MS45-O1 Processing and data quality in serial femtosecond crystallography

Thomas A. White<sup>1</sup>

1. Center for Free-Electron Laser Science, Deutsches Elektronen-Synchrotron DESY, Notkestraße 85, 22607 Hamburg, Germany

email: thomas.white@desy.de

Five years since the first publication describing serial femtosecond crystallography (SFX) [1], the technique is becoming an established technique for probing radiation-sensitive samples as well as for investigating macromolecular dynamics with high time resolution. Developments in data processing, combined with improvements to detector technology and sample delivery, mean that in 2016 we expect to be routinely able to see new information of biochemical interest, for example the electron densities of ligands absent from the structural models, in maps made using around a tenth of the data volume and measurement time which was required only a few years ago. The modern SFX analysis "toolkit" includes algorithms to resolve indexing ambiguities which arise in merohedral point groups in serial crystallography experiments [2], new methods for increasing the precision of the final intensity measurements, and much more besides. In this talk, I will detail the latest results in this area, in the context of CrystFEL, currently the most widely-used SFX data processing software [3].

[1] H. N. Chapman, P. Fromme et al. "Femtosecond X-ray protein nanocrystallography". Nature 470 (2011) p73-77. doi:10.1038/nature09750

[2] W. Brehm and K. Diederichs. "Breaking the indexing ambiguity in serial crystallography". Acta Cryst. D70 (2014) p101-109.

[3] T. A. White, V. Mariani, W. Brehm, O. Yefanov, A. Barty, K. R. Beyerlein, F. Chervinskii, L. Galli, C. Gati, T. Nakane, A. Tolstikova, K. Yamashita, C. H. Yoon, K. Diederichs and H. N. Chapman. "Recent developments in CrystFEL". J. Appl. Cryst. 49 (2016) p680-689. doi:10.1107/S1600576716004751

**Keywords:** serial femtosecond crystallography, XFEL, data processing

## MS45-O2 New ways to assess the quality of single and multiple (complete and partial) X-ray diffraction datasets

Kay Diederichs<sup>1</sup>

1. Universität Konstanz

email: Kay.Diederichs@uni-konstanz.de

The subject says it all. New ways of collecting data at synchrotrons and X-FEL source require new approaches to diffraction data analysis. In 2012, we described the properties of the  $CC_{1/2}$  indicator, but the opportunities to use this and related quantities have not yet been fully exploited.

Here, we describe novel ways to obtain insight into the relationships between - in particular - multiple partial datasets measured in Serial Synchrotron Crystallography experiments. It turns out that these quantities are useful also for the assessment of single datasets when these have "weak" data in certain rotation ranges of the experiment.

**Keywords:** accuracy, precision, partial datasets, completeness, model quality, radiation damage

## MS45-O3 Empirical correction for resolution- and temperature-dependent errors caused by factors such as thermal diffuse scattering

Regine Herbst-Irmer<sup>1</sup>, Benedikt Niepötter<sup>1</sup>, Dietmar Stalke<sup>1</sup>

1. Institute of Inorganic Chemistry, Georg-August-University Göttingen

email: rherbst@shelx.uni-ac.gwdg.de

Charge density investigations of several compounds conducted at multiple temperatures show two disturbing features. First, the models derived from these high resolution datasets at different temperatures differ significantly. Additionally, residual density appears close to or even at the atomic positions, especially for datasets measured at 100 K. This indicates significant errors that could be caused by thermal diffuse scattering (TDS).

TDS mainly results in an underestimation of the atomic displacement parameters. However, smaller but nevertheless important errors occur in other parameters as well [1]. Hence the heights of the maxima in the electron density are changed at the same location [2, 3]. First order TDS leads to peak broadening in the diffraction experiment.

A reduction of the integration box size leads to a substantial improvement in quality and diversity of the models. At the same time it indicates TDS to cause these errors. However, this method is very time-consuming and an alternative is needed.

It is possible to estimate the TDS contribution by analyzing the peak profile [4]. Extending this idea programs were developed to assess the TDS contribution to the measured intensities for data collected with point detectors [5, 6].

In endeavouring to improve the method, it was noticed that the refinement of resolution-dependent scale factors can be employed as a validation tool to detect such errors. In a nested interval approach a correction factor [7] is determined that minimizes these errors and improves the model quality [8].

[1] Alexandropoulos, N. G., Cooper, M. J., Suortti, P. & Willis, B. T. M. (2006). *International Tables for Crystallography*, Vol. C, edited by E. Prince, pp. 653–665, 1st online ed. Chester: International Union of Crystallography.

[2] Tsirelson, V. G. & Ozerov, R. P. (1996). *Electron Density and Bonding in Crystals: Principles, Theory and X-ray Diffraction Experiments in Solid State Physics and Chemistry*. Bristol, Philadelphia: Institute of Physics Publishing.

[3] Helmholdt, R. B. & Vos, A. (1977). *Acta Cryst.* **A33**, 38–45.

[4] Jennings, L. D. (1970). *Acta Cryst.* **A26**, 613–622.

[5] Blessing, R. H. (1987). *Crystallogr. Rev.* **1**, 3–58.

[6] Stash, A. & Zavodnik, V. (1995). *Crystallogr. Rep.* **41**, 404–412.

[7] Zavodnik, V., Stash, A., Tsirelson, V., de Vries, R. & Feil, D. (1999). *Acta Cryst.* **B55**, 45–54.

[8] Niepötter, B., Herbst-Irmer, R. & Stalke, D. (2015). *J. Appl. Cryst.*, **48**, 1485–1497.

**Keywords:** data quality, thermal diffuse scattering

## MS45-O4 Background modelling in the presence of ice rings

James M. Parkhurst<sup>1,2</sup>, Andrea Thorn<sup>2</sup>, Graeme Winter<sup>1</sup>, David Waterman<sup>3</sup>, Luis Fuentes-Montero<sup>1</sup>, Richard Gildea<sup>1</sup>, Garib Murshudov<sup>2</sup>, Gwyndaf Evans<sup>1</sup>

1. Diamond Light Source
2. LMB, Cambridge
3. CCP4

email: james.parkhurst@diamond.ac.uk

In macromolecular crystallography, integration programs are used to estimate the intensities of individual Bragg reflections. In the simple case of “summation integration”, this is typically done by labelling each pixel in the neighbourhood of a Bragg peak as either foreground or background; the reflection's intensity is then estimated as the total number of counts in the foreground region minus the total background estimated in the foreground region. The background in the foreground region is estimated from the surrounding background pixels.

Typically, the background is modelled as either a constant (Kabsch 2010) or a plane (Leslie 1999) in the region of the reflection peak. In most cases, these models are reasonably appropriate for the data. However, they may not be appropriate when there are additional features in the background, most notably ice rings; the shape of the background at the peak of an ice ring is not well modelled by a constant or plane.

156 Pilatus datasets were selected from the JCSG database. In total, 15 datasets were observed to have ice rings. The data were processed with DIALLS (Waterman et al. 2013) and scaled with POINTLESS and AIMLESS (Evans and Murshudov 2013). Analysis of the distribution of intensities as a function of resolution revealed that, at ice ring resolutions, the reflection intensities were being systematically over-estimated. This indicates that the reflection backgrounds at ice ring resolutions were being systematically under-estimated.

We present a simple method, implemented in the DIALLS framework, for modelling the background in the presence of ice rings. The method involves the creation of a global background model that describes the expected shape of the background at every pixel in the image. This method is shown to result in better background estimates (and consequently intensity estimates) for reflections recorded on ice rings than the simple constant or planar models.

Leslie, A. G. W. (1999). *Acta Crystallogr. D. Biol. Crystallogr.* 55, 1696–1702.

Evans, P. R. & Murshudov, G. N. (2013). *Acta Crystallogr. D. Biol. Crystallogr.* 69, 1204–1214.

Kabsch, W. (2010). *Acta Crystallogr. Sect. D Biol. Crystallogr.* 66, 133–144.

Waterman, D. G. et al. (2013). CCP4 newsletter on protein crystallography, 49, 16–19

**Keywords:** Integration, Background, Ice Rings

# MS45-O5 At home accurate XRD measurements with an hybrid pixel X-ray detector: a comparison with CCD, APS-CMOS commercial detectors and theoretical model

measurements, electron density, multipolar refinements

Claude Lecomte<sup>1</sup>, Emmanuel Wenger<sup>1</sup>, Paul Alle<sup>1</sup>, Emmanuel Aubert<sup>1</sup>, Slimane Dahaoui<sup>1</sup>, Dominik Schaniel<sup>1</sup>

1. Université de Lorraine

email: [claudel@univ-lorraine.fr](mailto:claudel@univ-lorraine.fr)

The new generation of X-ray detectors, the hybrid pixel area detectors or 'pixel detectors', are based on direct detection and single-photon counting processes. Large linearity range, high dynamic and extremely low noise leading to unprecedented high signal-to-noise ratio for bi-dimensional X-ray detectors, fast readout time (high frame rates) and electronic shutter are among their intrinsic characteristics which render them very attractive. As shown in our previous study on sodium nitroprusside crystals [Wenger et al. *Acta Cryst B*, 2014], it was demonstrated that these detectors are promising at laboratory sources for quasi-static experiments and accurate electron density measurements [Alle et al., *Physica Scripta*, 2016]. In this study, four different electron density models of a weakly scattering pure organic compound, the 4-benzyloxy-3-methoxybenzaldehyde ( $C_{15}H_{14}O_3$ ) have been refined against experimental structure factors obtained from commercial CCD and CMOS type X-ray detectors, an XPAD hybrid pixel detector and theoretical structure factors from DFT calculations. Atom coordinates, thermal displacement parameters, critical points, electron density values, laplacien, valence populations and electrostatic potential will be discussed and compared.

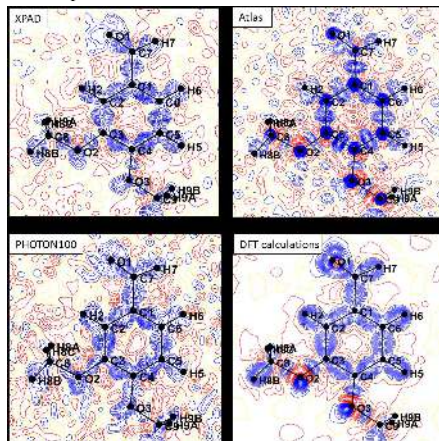


**Figure 1.** Electron density deformation maps in the C1-C6 plane from the three different detectors data sets and from DFT calculations. Max Res = 0.96 Å<sup>-1</sup> With all I > 0 reflections. Isocontours: 0.05 e/Å<sup>3</sup>

**Keywords:** X-ray detectors, hybrid pixel detector, CCD detectors, CMOS detectors, laboratory accurate X-ray intensity



## MS46 Computational tools for theoretical chemistry in crystallography

Chairs: Martin Lutz, Martyn Winn

1. D. Jayatilaka, D. J. Grimwood, *Acta Cryst A* **57**, 76 (2001).
2. W. L. Clinton, A. J. Galli, L. J. Massa, *Phys. Rev.* **177**, 7 (1969).
3. A. Genoni, *J. Phys. Chem. Lett.* **4**, 1093 (2013).
4. A. Genoni, *J. Chem. Theory Comput.* **9**, 3004 (2013).
5. B. Meyer, P. Macchi, A. Genoni, *submitted*.
6. N. Casati, A. Kleppe, A. J. Jephcoat, P. Macchi, *Nat. Commun.* **7**, 10901, doi:10.1038/ncomms10901 (2016).

**Keywords:** X-ray Constrained Wave Function, Electron Density, Extremely Localized Molecular Orbitals, Valence Bond Theory

### MS46-O1 Recent Advancements in the Development of X-ray Constrained Wave Function Strategies

Alessandro Genoni<sup>1</sup>

1. CNRS & Université de Lorraine, Laboratoire SRSNC - UMR 7565, Vandœuvre-lès-Nancy, France

email: Alessandro.Genoni@univ-lorraine.fr

As well known, the wave function is a fundamental entity that intrinsically contains all the information of a system in the most compact way. For this reason the possibility of determining wave functions from experimental data has been a tantalizing perspective that motivated different research groups over the years.

Among the modern strategies proposed in this context, the X-ray constrained wave function (XC-WF) method introduced by Jayatilaka [1] is undoubtedly the most noteworthy. This technique can be considered as the most promising advancement of the pioneering strategies introduced by Clinton *et al.* [2] and it consists in extracting single Slater determinants that, other than minimizing the Hartree-Fock energy of the systems, reproduce sets of experimental structure factors within a predefined accuracy.

In our group, the XC-WF approach has been extended in order to extract Extremely Localized Molecular Orbitals (ELMOs) from experimental X-ray diffraction data [3-4], namely Molecular Orbitals that are strictly localized on small molecular fragments (e.g., atoms or bonds) and that are consequently very close to the traditional chemical picture of molecules. Determining XC-ELMOs is straightforward and the new strategy can be seen as an alternative tool to determine experimental electron densities, combining the quantum mechanical rigor of the wave function-based approaches with the chemical interpretability of the popular multipole model.

More recently, always starting from the concept of ELMOs, we have also devised a preliminary X-ray constrained Valence Bond method. This technique, other than being the first attempt of introducing a multi-determinant wave function *ansatz* in the Jayatilaka approach, has allowed us to successfully study the charge distribution of the syn-1,6:8,13-Biscarbonyl[14]annulene at different pressures [5], theoretically confirming the partial rupture of the aromaticity experimentally observed when pressure is increased [6].

An overview of our techniques recently developed in the framework of the XC-WF approach will be presented.

## MS46-O2 Synergistic 'Substrate Activation' and 'Oxygen Activation' in Salicylate Dioxygenase from QM/MM Simulations

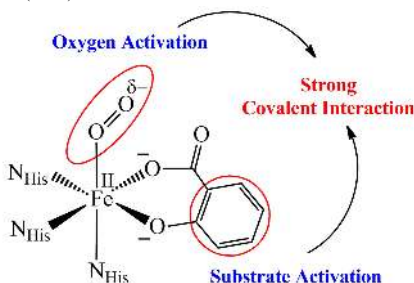
Johannes Kaestner<sup>1</sup>, Subhendu Roy<sup>1</sup>

1. University of Stuttgart, Institute for Theoretical Chemistry

email: kaestner@theochem.uni-stuttgart.de

Salicylate 1,2-Dioxygenase (SDO) is the first enzyme discovered to catalyze the oxidative cleavage of a monohydroxylated aromatic compound, salicylate, in contrast to the well-known electron-rich substrates. We have investigated the mechanism of dioxygen activation in SDO by QM/MM calculations. Our study reveals that the non-heme Fe<sup>II</sup> center in SDO activates salicylate and O<sub>2</sub> synergistically by a strong covalent interaction to facilitate the reductive cleavage of O<sub>2</sub>. A covalent Salicylate-Fe<sup>II</sup>-O<sub>2</sub> complex is the reactive oxygen species in this case, where the electronic structure is best described as between the two limiting cases, Fe<sup>II</sup>-O<sub>2</sub> and Fe<sup>II</sup>-O<sub>2</sub><sup>-</sup> with partial electron transfer from the activated salicylate to O<sub>2</sub> via the Fe center. Thus, SDO employs a synergistic strategy of 'substrate activation' and 'oxygen activation' to carry out the catalytic reaction, which is unprecedented in the family of iron dioxygenases. Moreover, O<sub>2</sub> activation in SDO happens without the assistance of a proton source. Our study essentially opens up a new window in the mechanism of O<sub>2</sub> activation.

[1] S. Roy and J. Kästner Angew. Chem. Int. Ed. 55, 1168 (2016)



(His = Histidine)

**Figure 1.** Dioxygen is activated in Salicylate 1,2-Dioxygenase (SDO) by a strong covalent interaction with the non-heme iron cofactor and the substrate.

**Keywords:** DIOXYGENASE, METALLOENZYMES, QM/MM, ACTIVATION

## MS46-O3 Topological collections and knowledge bases for applications in crystal engineering of coordination compounds

Eugeny V. Alexandrov<sup>1</sup>, Alexander P. Shevchenko<sup>1</sup>, Vladislav A. Blatov<sup>1</sup>

1. Samara Center for Theoretical Materials Science, Samara State Aerospace University named after academician S.P. Korolyev (National Research University), Moskovskoye Shosse 34, Samara 443086, Russia

email: aleksandrov\_ev1@mail.ru

Using ToposPro program package<sup>1</sup> the complete database of metal coordination centers, ligands (more than 150 000) and topological types of coordination networks (more than 100 000) were created for more than 400 000 crystal structures of coordination compounds (0D-3D) presented in CSD.<sup>2</sup> A number of possible applications of the databases for investigation and design of coordination compounds were highlighted. The databases help in finding the relations between composition, structure, and properties of complexes in terms of structural descriptors. Consequently, the criteria for statistical analysis and estimation of the results reliability are provided. Further, we have outlined the concept of the knowledge based approach for prediction of new crystal structures using the relations in a complete set of descriptors for properties. It has been shown how knowledge based approach can be applied for finding correlations between coordination characteristics and topological parameters in cyanometallates<sup>3,4</sup> malonates, and other MOFs<sup>5-7</sup> as well as for understanding the adsorption properties of MIL-53(Al).<sup>8</sup>

E.V.A. thanks the Russian government (grant No. 14.B25.31.0005), Russian Foundation for Basic Research (grants No. 13-07-00001, 14-03-97034, 16-37-00147), Russian Science Foundation (grant No. 16-13-10158), and Russian Ministry of Science and Education for support.

1 V.A. Blatov, A.P. Shevchenko, D. M. Proserpio, *Cryst. Growth Des.*, **2014**, *14*, 3576.

2 Cambridge Structural Database. Cambridge Crystallographic Data Centre, 12 Union Road, Cambridge, UK.

3 E.V. Alexandrov, A. P. Shevchenko, A. A. Asiri, V. A. Blatov, *CrystEngComm*, **2015**, *17*, 2913.

4 E.V. Alexandrov, A.V. Virovets, V.A. Blatov, E.V. Peresypkina, *Chem. Rev.*, **2015**, *115*, 12286.

5 E.V. Alexandrov, V.A. Blatov, A. V. Kochetkov, D. M. Proserpio, *CrystEngComm*, **2011**, *13*, 3947.

6 E.V. Alexandrov, V.A. Blatov, D. M. Proserpio *Acta Cryst.*, **2012**, *A68*, 484.

7 E.V. Alexandrov, V.A. Blatov, D. M. Proserpio, *J. Struct. Chem.*, **2014**, *55*, 1308.

8 B.R. Saifutdinov, V.I. Isaeva, E.V. Alexandrov, L.M. Kustov, *Russ. Chem. Bull., Int. Ed.*, **2015**, *64*, 1039.

**Keywords:** Knowledge base, expert system, topological analysis, coordination networks, crystal design, large-scale screening, crystal structure prediction

## MS46-O4 Harnessing the power of the Cambridge Structural Database in your own way: the CSD Python API

Andrew G.P. Maloney<sup>1</sup>, Seth B. Wiggin<sup>1</sup>, Paul C. Sanschagrin<sup>2</sup>

1. The Cambridge Crystallographic Data Centre, 12 Union Road, Cambridge, CB2 1EZ, UK

2. The Cambridge Crystallographic Data Centre, Piscataway, NJ, 08854, USA.

email: maloney@ccdc.cam.ac.uk

The Cambridge Structural Database (CSD) has been in existence for over 50 years and currently includes over 820,000 organic and organometallic crystal structures. The Cambridge Crystallographic Data Centre (CCDC) provides an extensive suite of desktop software to search, analyse, and make use of the data. However, the available methods and approaches in these tools are restricted to what CCDC has included. With the release of the CSD Python API, researchers and developers can now make use of CSD data and techniques in their own methods and approaches. This makes it possible to do analyses that were not possible, very difficult, or very tedious to do before in a much more effective way. Several examples of such analyses and approaches with real scientific impact will be presented. Examples of using the CSD Python API with other scientific Python tools will also be presented.

**Keywords:** Cambridge Structural Database, Python, Data Analysis

## MS46-O5 An Enhanced Hirshfeld Test - Validating Atomic Vibrations in Crystal Structures

Jens Luebben<sup>1</sup>, Birger Dittrich<sup>1</sup>, George Sheldrick<sup>2</sup>

1. Heinrich-Heine-University Duesseldorf, Germany

2. Georg-August-University Goettingen, Germany

email: jens.luebben@chemie.uni-goettingen.de

The current routine procedure for publishing crystal structures of small molecules includes structure validation via the the IUCr CheckCIF service. [1] Part of that procedure is the Hirshfeld test [2] which ensures that the atomic vibrations, encoded as Atomic Displacement Parameters (ADPs), are physically reasonable. While the Hirshfeld test is fast and efficient at finding potential problems in the structural model, there exist a number of borderline cases where the test is not able to find implausible ADPs. In other cases the CheckCIF routine might raise alerts where the structure is actually perfectly fine.

An improved procedure will be presented which aims to address these problems. The procedure is based on the Hirshfeld test and inspired by the 'RIGU' restraint from the Shelxl [3] program. This is achieved by analyzing the ADPs characteristics in all three spacial dimensions instead of only validating its expansion in bond direction and taking the atomic masses applied to a harmonic oscillator model into account.

This procedure achieves its goal of finding problematic ADPs in cases that are not found by the traditional Hirshfeld test and is able to reasonably evaluate the ADPs of atoms with significantly different atomic masses e.g. carbon – hydrogen bonds in neutron diffraction studies.

[1] Spek *Acta Cryst* (2015). **C71**, 9-18.

[2] Rosenfield et al., *Acta Cryst* (1978). **A34**, 828–829.

[3] Thorn et al., *Acta Cryst.* (2012). **A68**, 448-451.

**Keywords:** Validation, ADPs

## MS47 Teaching & Education

Chairs: Helen Stoeckli-Evans, Howard Flack

### MS47-O1 It is never too early, or too late to start

Elena V. Boldyreva<sup>1,2</sup>, Sergey G. Arkhipov<sup>1,2</sup>, Evgeniy A. Losev<sup>2</sup>,  
Denis A. Rychkov<sup>1,2</sup>, Adam L. Michalcuk<sup>1,3</sup>, Ivana  
Lapsanska<sup>1,3</sup>, Colin R. Pulham<sup>3</sup>

1. Novosibirsk State University

2. Institute of Solid State Chemistry and Mechanochemistry SB RAS

3. School of Chemistry, University of Edinburgh

email: eboldyreva@yahoo.com

Education tends to become more and more narrow. Knowledge about the world around and inside is being segmented into an ever-growing number of fields and sub-fields: mathematics, physics, chemistry, biology, planetary sciences, geology, mineralogy, and the list goes on. Not only are the humanities, sciences and arts taught separately, but there is also a growing trend not to teach all of these subjects to the same child. Instead, education is restricted to a narrow focus from an early age, limiting the breadth of skills and interests of any individual. As a result of this education technique, people tend to lose a general view of the world as a whole. Not only is this destructive for the individual, but places great limits on the development of society and culture.

Crystallography is a unique and fascinatingly multidisciplinary field that offers numerous links between the arts and sciences, between maths and chemistry, biology and physics. The objects of crystallography are beautiful, its language is strict and logical, yet open to intuition, and its applications are variable. Crystallography is, in some respects, a “meta-science”, affording those that study it an integrated, harmonious vision of nature. As such, crystallography is an excellent subject to pursue for life-long education, and an exemplary discipline around which to focus public engagement efforts in both the sciences and arts.

In the present contribution we suggest a concept of using crystallography as a tool for a wholesome, balanced education that starts with children aged 3-6 years old and ends with seniors. At no point is a background in the sciences assumed. Some aspects of this concept have already been successfully tested in Novosibirsk, Russia, and in Edinburgh, UK. Others are yet to be implemented; we welcome volunteers to join us in this educational experiment. In particular, we discuss examples of communicating science to kids, of using crystallographic texts during French and English lessons. We also emphasise the co-teaching of crystallography and art, where the principles of each discipline are mutually reinforced. Hands-on sessions, drawing, and crystal growing can be ideally combined with the solving of mathematical problems, performing chemical and physical experiments, exploring natural objects (minerals,

plants, food), and the discussion of modern materials and devices. Educational formats depend on the target audience and desired outcome.



Figure 1. Tiling - an art or science?

**Keywords:** public engagement, school education, multi-disciplinary teaching

## MS47-O2 A cross-field perspective on Symmetry & Crystal to introduce Crystallography

Jean-Louis Hodeau<sup>1</sup>, Christophe Bouchard<sup>1</sup>, Sabine Douillet<sup>1</sup>,  
Florence Fernandez<sup>1</sup>, Laurent Joubert<sup>1</sup>, Yvonne Soldo<sup>1</sup>, Stephanie  
Zaccaro<sup>1</sup>

1. Institut Neel, CNRS & Univ. Grenoble Alpes, 38042 Grenoble, France

email: hodeau@neel.cnrs.fr

Crystallography uses two important tools, a concrete object: crystal, and an abstract description: symmetry. To illustrate the science of crystallography to the public, examples using the symmetry and crystal will be illustrated.

Symmetry as proportion and light played an important role in aesthetics (symmetry means "right measures / proportions" in Greek). Vitruvius developed the virtues of proportion and symmetry in architecture and in nature, as shown by Leonardo da Vinci in its "human body" drawing. Architecture makes extensive use of symmetry: symmetry is present in Islamic mosques, Chinese pagodas, Hindu temples and Gothic cathedrals. Tiling patterns are also a great example of symmetry, as shown in Islamic cultures in the Middle Ages.

Crystals shapes and facets comply geometric rules. Studying their symmetries allows us to differentiate the crystals. In the 19th century German and French researchers developed symmetry to classify all the crystals. They introduce the concepts of lattice, axis, center, and mirror plane of symmetry. Crystallographers have given a new meaning to the word symmetry itself, which had hitherto been reserved for architectural purposes. This classification of crystals according to their symmetry and lattice structure is still with us today. The symmetry links the shape of the crystals to their atomic structure and it is important for studying the physical properties of crystals. This abstract relationship between crystal and symmetry was confirmed in 1912, together with the periodicity of the crystal, by the first X-ray diffraction experiments.

We can use the crystal and the symmetry to focus public interest on crystallography and to show children and students the importance of observations, models and representations in scientific approaches. As an illustration, we will present several workshops using the facilities of Physiquarium and KaleidoLab. The capacity of KaleidoLab to generate models is used for the creation of "on-live" wallpapers and videos.

This presentation is the result of different actions: Voyage dans le Cristal exhibition (\*) Krystalopolis website (\*\*) and KaleidoLab workshop (\*\*\*) and we thank colleagues who contributed to these actions, Marc DeBoissieu, Dominique Cornuejols, Thibaut David, Yannick Lacaze, René Guinebretière.

\* <http://www.ivcr2014.org/resource-materials/voyage>

\*\* <http://www.krystalopolis.fr/>

\*\*\*

[http://neel.cnrs.fr/IMG/KaleidoLab\\_Symetrie-cest-quoi\\_14dec15-ss-son\\_avec-3music\\_06.mp4](http://neel.cnrs.fr/IMG/KaleidoLab_Symetrie-cest-quoi_14dec15-ss-son_avec-3music_06.mp4)



**Figure 1.** Children can play with mosaics to cover surface with identical shapes. These tiles with different symmetries allow the public to discover symmetry rules. The shape of the tiles is related to the symmetry of the lattice. © IUCrJournals & KaleidoLab; Hodeau & Guinebretière, JAC 48, 1276 (2015)

**Keywords:** Crystallography, Teaching, Education, History

### MS47-03 The power of using 827,948 crystal structures in education

Suzanna C. Ward<sup>1</sup>, Amy A. Sarjeant<sup>2</sup>

1. The Cambridge Crystallographic Data Centre, 12 Union Road, Cambridge, CB2 1EZ, UK
2. The Cambridge Crystallographic Data Centre, Piscataway, NJ, 08854, USA

email: ward@ccdc.cam.ac.uk

The Cambridge Structural Database (CSD) contains over 800,000 experimentally determined small molecule crystal structures and this wealth of structural data can be a powerful tool in education. As well as providing the three dimensional structure of molecules, the CSD contains statistical information about symmetry, packing, coordination environments, bond distributions, and intermolecular interactions together with associated information such as physical properties and crystallization conditions.

This talk will focus on how structural data can be used in chemical education by using specific examples to illustrate how teachers can use the CSD to demonstrate key chemical concepts and principles. Students can learn a lot from this collection of structures, but given the vastness of the CSD identifying key structures that are most appropriate for a class is not always a simple process. We will therefore demonstrate, using examples, how the CSD teaching database, compiled to represent a diverse range of chemistry, can be used in the classroom to augment the learning experience of students in schools and universities worldwide.

Finally, we will reflect on the structural chemistry resources that are already available to educators and explore how these might evolve over the next 50 years of the CSD.

**Keywords:** Chemical Education, Teaching, Cambridge Structural Database, Structural Chemistry

### MS47-04 Improved access to raw diffraction data and its impact on crystallographic education and teaching

John R. Helliwell<sup>1</sup>, Brian McMahon<sup>2</sup>

1. School of Chemistry, University of Manchester, Manchester, M13 9PL, UK
2. IUCr 5 Abbey Square, Chester CH1 2HU, UK

email: john.helliwell@manchester.ac.uk

Raw diffraction images are expected to be useful for improving numerous research applications that crystallographers engage with. There are two main aspects to this 'raw data revolution' relevant to education. Firstly, researchers will learn the protocols associated with archived, open, raw diffraction data, to accompany their processed diffraction data and derived coordinates that are expected to be found in the curated databases. Also funding agencies are looking at an Open Science protocol to improve speed of discovery for societal challenges, from the start of a funded project. Secondly routine access to raw data will impact crystallographic teaching such as for our important European Crystallography School. For the archiving of our raw data the IUCr global Diffraction Data Deposition Working Group has examined the issues and prospects for linking raw diffraction data sets to publications. Important strides have been made in the structural biology area and by the ICDD for powder diffraction data. Long time pioneers of raw diffraction data archiving are at the National Crystallography Service at Southampton University UK. At the neutron and synchrotron facilities major pioneering efforts include assigning digital object identifiers (DOIs) to all data sets by the facility, across all techniques; this is being done at ISIS and now also at the ESRF. At the PDB the submission of an entry now routinely includes the opportunity for depositors to provide details of raw data DOIs. Another major development is that IUCr Journals (e.g. IUCrJ, J. Appl. Cryst., Acta Crystallographica D, F) have started linking their publications with raw diffraction data sets in the data repositories. In our own research, as an example, some thirty crystal structure studies on the binding of anti-cancer compounds (platin) to histidine in a protein (Tanley et al. (2012). Acta Cryst. F68, 1300-1306 have the associated raw data deposited at the University of Manchester eScholar repository (doi:10.15127/1.215887, <https://www.escholar.manchester.ac.uk/uk-ac-man-scw:215887>) so that there is Gold Open Access to the publications, the PDB files and the raw data. These form a complete set of our research in this area. Other colleagues in this specific medically oriented research topic, and who are providing raw diffraction data on the platins binding to proteins and nucleic acids, have been invited to contribute to this data archive.

**Keywords:** Raw diffraction data; Data archiving; Open Science; Open Data.

## MS47-O5 The educational and outreach programme of the IUCr

Michele Zema<sup>1</sup>

1. International Union of Crystallography, UK

email: michele.zema@uniprv.it

The International Year of Crystallography has seen an incredible variety of activities worldwide, which have ignited a fire in the new generation, most especially in parts of the developing world where structural science is still an infant science. The IUCr has actively developed a broad programme of initiatives, ranging from the launch of a new journal, IUCrJ, to activities for schoolchildren, from professional-level workshops and training sessions to international summit meetings to shape future policy, and much more.

The new IUCr educational and outreach programme will build on the successes of IYCr2014. A dedicated fund has been opened to support the continuation of these initiatives and everyone can contribute. The main aims of the IUCr Outreach programme are as follows:

- to continue to increase awareness of crystallography, its fundamental role in the different branches of science and its contribution to the global economy via events directed at the general public, the younger generation and the media;

- to build capacity in crystallography and related fields of science in the developing regions of the world, particularly in (but not limited to) Latin America, Africa and South East Asia, by promoting high-quality educational initiatives and developing research activities, possibly in collaboration with industry;

- to forge collaborations with governmental, scientific and educational institutions and organizations aimed at facilitating strategic projects for the development of crystallography in all parts of the world and for its inclusion in curricula for secondary- and tertiary-level education.

The main initiatives will be presented, including the IUCr Crystal growing competition for schoolchildren, which is now at its third edition, the IUCr-UNESCO OpenLabs, which have been implemented in more than 20 countries so far, the recent developments concerning IUCr publications, and strategies for collaborative projects with other bodies.

**Keywords:** crystallography teaching

## MS48 Crystallography in art and cultural heritage

Chairs: Alicja Rafalska-Lasocha, Helen Stoeckli-Evans

## MS48-O1 MAKING GOLD: Recent Developments and New Perspectives

Anke Zürn<sup>1</sup>

1. Artist Researcher based in Biel/Bienne, Switzerland

email: zuern@visual-chemistry.net

End 2011 I left the natural science context, to perform artistic research on topics related to materials science independent from scientists' research obligations, as artists' research methods and working goals embrace also the inclusion of emotions, contradictions, ambiguities, incertitudes, and celebrate uniqueness and non-reproducibility. In Basel I will present my ongoing art projects "MAKING GOLD", "AROUND THE LAKES", and "LOOKING FOR NEW DIAMONDS", while providing a short "golden" glance at artistic research as such.

The projects MAKING GOLD and AROUND THE LAKES both embrace natural dyes and historic lake pigments. The lake pigments are manufactured by adding metal salts and eventually also inorganic substrates to dye extracts from different plant species or insects. Generally any complex forming metal ions could be applied to precipitate the lake pigments; I prefer the use of aluminium, iron, calcium, magnesium, and eventually copper containing salts. Common substrates are lime stone, gypsum, aluminosilicates, or aluminium oxides and hydroxides. AROUND THE LAKES combines several projects, all of which canvass freshly produced lake pigments literally as coloured "LAKES" on a coated wooden plate, canvas or paper, referring thus to watercolour painting techniques as well as to the visual research experiments published by Friedlieb Ferdinand Runge<sup>1)</sup>. MAKING GOLD involves the production of lake pigments with wet ground mica and uses the glimmer effects of the flake-like particles to also explore emotions evoked by a "golden glamour". LOOKING FOR NEW DIAMONDS refers to model building traditions in crystallography and chemistry, and addresses the impact of sensuous components on the research process itself. All three projects are highly context sensitive and reflect emotional and economic values of materials, limited raw material resources and related luxury goods or materials trade. At the same time all projects investigate practice-based research approaches, trace visual and sensuous components of researching, and explore the unity of production and perception, the intimate relation of the research and working process with its aesthetic experience.

1) Friedlieb Ferdinand Runge, "Der Bildungstrieb der Stoffe: veranschaulicht in selbstständig gewachsenen



Bildern (Fortsetzung der Musterbilder)", 1855, Oranienburg, Selbstverlag.



**Figure 1.** MAKING GOLD: Exhibition view, Anke Zürn, August 2014, Espace Libre, Biel/Bienne, Switzerland.

**Keywords:** gold, colours, pigments, cultural heritage, art, research

## **MS48-O2** Micro-XRPD, XRPD tomography and MA-XRPD: three related methods to better understand structural alterations in cultural heritage materials

Koen H. Janssens<sup>1</sup>, Frederik Vanmeert<sup>1</sup>, Steven De Meyer<sup>1</sup>, Geert Van der Snickt<sup>1</sup>

<sup>1</sup>. University of Antwerp, Department of Chemistry

email: koen.janssens@uantwerpen.be

The (inner) structure of paintings may reveal changes made by the artists themselves or by others following them. Traditionally, this inner structure is examined by means of X-ray radiography and Infrared Reflectography. Both methods make use of deeply penetrative radiation; both give rise to black and white images that to some extent reflect the composition at or below the surface of the paintings. More powerful equivalents of these two methods are Macroscopic X-ray fluorescence imaging (MA-XRF) and hyperspectral imaging in the Visual and Near Infra-red (VNIR) region, allowing to collect a richer set of (spectroscopic) image data and construct false color images of paintings from which valuable information about the paint composition (at/below the surface) can be gleaned.

In many historical paintings, unwanted chemical transformations take place that may influence the general outlook/colors of part of a painting. Micro/nanoscale spectrometric methods such as Raman/Infra-red microscopy and various forms of Electron Microscopy are useful to understand these transformations. Also the (combined) use of synchrotron radiation based methods such as microscopic X-ray fluorescence, X-ray absorption spectroscopy and X-ray diffraction is highly relevant to reconstruct the degradation mechanism of painters' pigments such as chrome yellow or red lead. We recently were able to unravel the transformation process that converts red lead (minium) in lead white (cerussite) via XRPD tomography by the identification of the intermediate crystalline phase, called plumbonacrite.

With the purpose of rendering the elemental mapping capability of MA-XRF more pigment-specific, based on a micro-focussed X-ray source equipped with focussing and monochromatizing mirrors, we have recently constructed a MA-XRPD scanning setup and have evaluated the possibility of using this for recording high-specific distributions of painters' pigments and some of their degradation products in a non-destructive manner.

By discussing a number of case studies involving 17<sup>th</sup> and 19<sup>th</sup> century paintings or paint samples from painters such as J. De Heem, E. Munch, H. Matisse and V. Van Gogh, the usefulness of highly-specific non-invasive analytical imaging at the macroscopic scale in combination with microscopic multimodal examination of minute paint fragments will be discussed and their relevance both for art historians and art conservators highlighted.

**Keywords:** Microscopic XRPD, Macroscopic XRPD imaging, synchrotron radiation, Van Gogh, XRPD tomography

### MS48-O3 Crystallographic interpretation of mineral decompositions via Rietveld refinement strategy for clustering ancient ceramics

Mohammadamin Emami<sup>1,2</sup>

1. Department of conservation and archaeology, Art University of Isfahan, Isfahan, Iran
2. Department of Building Material Chemistry, University Siegen, Germany

email: emami@chemie.uni-siegen.de

Ceramics in the antiquity have a very complex structure according to their mineralogical constituents and their accidental or experimental manufacturing processes. The sintered body of such objects suggest a well-organized technological now-how at this time. Ceramics are always classified by archaeologists according to their external features and therefore the investigations are done mostly comparatively.

This study focuses on the exact quantitative phase composition of a collection of ceramics from 1250 millennium BC. Mineralogical properties of the crystalline phases are studied by means of polarization microscopy and X-ray diffraction inclusive Rietveld refinement strategy in order to get information about the different crystalline phase constituents via different firing conditions due to the – thermodynamically – mineralogical stability exchange.

According to the crystalline phase decompositions which have been carried out in the ceramic texture, the technology has been changed by means of different firing condition. Clustering the data proved that the manufacturing process mostly changed due to the firing condition and not only by means of raw material usage. Due to the results, ceramics can be classified in archetypal groups.

**Keywords:** ceramics, Rietveld refinement

### MS48-O4 Provenancing of clay-based pigments in paints using quantitative X-ray micro-diffraction analysis

Petr Bezdička<sup>1</sup>, David Hradil<sup>1,2</sup>, Janka Hradilová<sup>2</sup>

1. Institute of Inorganic Chemistry of the CAS, v.v.i., ALMA Laboratory, CZ-25068 Husinec - Rez
2. Academy of Fine Arts in Prague, ALMA Laboratory, U Akademie 4, 17022 Praha 7, Czech Republic

email: petrb@iic.cas.cz

One of the main reasons why individual clay minerals are not being properly detected in colour and preparatory layers of paintings regardless of their often significant contents is a missing methodology of its analysis. None of the micro-spectroscopic or spectrochemical analytical methods frequently used in the field leads to reliable differentiation of clay minerals due to their variable chemical composition, structural similarities and low Raman scattering. For their identification, it is necessary to employ powder X-ray micro-diffraction that is the only microanalytical method that allows a reliable differentiation of individual clay minerals' structures in colour and ground layers of paintings. It has not yet been satisfactorily tested for correct and unambiguous discrimination of clay structures in paint layers and, eventually, for reliable quantitative analysis of their relative contents. To overcome this lack of knowledge, several sets of laboratory experiments with model mixtures and reference samples imitating real paint layers have been performed and general rules for proper discrimination of clay structures have been described. Besides the common limitations of micro-pXRD (e.g. worse resolution, small size of irradiated area etc.), the accuracy of quantitative microanalysis of clay minerals in mixtures with other minerals in earth pigments is characterised by total bias values in the range of 3 – 10 wt. %. While in the case of conventional Bragg-Brentano geometry, the total bias does not exceed 6 wt. %. However, a more critical issue seems to be the effect of heterogeneity of natural materials, which tends to be more pronounced in small irradiated volumes. In our study, the newly determined accuracy of quantitative microanalysis was found to be sufficient for differentiation of red earths from two historical sources in Bavaria and Bohemia, respectively, both in reference samples and in micro-samples of Baroque grounds of paintings by, e.g., the famous Czech painter Karel Škréta. Further, as a specific sign of material's origin, randomly ordered illite-smectite interstratified structures were differentiated from pure smectites in painting grounds used by Baroque Venetian painters. These and other examples demonstrate the practical usability of this methodological approach for the comparative studies on paintings focusing on differentiating their regional provenance.

**Keywords:** x-ray powder micro-diffraction, clays, artworks, quantitative phase analysis

## MS49 How to...: crystallization for small and large molecules

### MS49-O2 How to... enhance the success of protein crystallization

Naomi E. Chayen<sup>1</sup>

<sup>1</sup>. Computational and Systems Medicine, Department of Surgery and Cancer, Faculty of Medicine, Imperial College London, London SW7 2AZ, UK

email: [n.chayen@imperial.ac.uk](mailto:n.chayen@imperial.ac.uk)

Protein crystals play a pivotal role in facilitating rational drug design and other industrial applications. The past decade has seen momentous progress in the miniaturisation, automation and analysis of crystallization experiments. However, production of high quality crystals still presents a major barrier to structure determination; it is often the case that no crystals are formed at all or that clusters of useless crystals are obtained. There is no 'magic bullet' that will guarantee the yield of useful crystals, hence rational approaches leading to the development of new and improved technologies for attaining high quality crystals is of crucial importance to progress [1,2]. This talk will present strategies for increasing the chances of success and highlight a variety of practical methods that have led to successful crystallization when standard crystal growth procedures had failed. These methods involve active influence and control of the crystallization environment in order to lead crystal growth to the desired result [e.g. 3-6]. Many of the techniques can be automated and adapted to high throughput experiments and several have been patented and commercialised. **References** [1] Chayen and Saridakis (2008) *Nature Methods* 5, 147-153. [2] Chayen, Helliwell and Snell *Macromolecular Crystallization and Crystal Perfection*, Oxford University Press, Oxford, UK (2010). [3] Saridakis *et al.* (2011) *Proc. Natl. Acad. Sci. U.S.A.* 108, 11081-11086. [4] Khurshid *et al.* (2014) *Nature Protocols* 9 (2014)Pages: 1621-1633. [5] Govada *et al.* (2016) *Scientific Reports - Nature* 6:20053 DOI: 10.1038/srep20053 [6] <http://www.imperialinnovations.co.uk/CRMIP>

**Keywords:** proteins, crystallization, nucleation, protein crystallization

Chairs: Aurelien Crochet, Andrew Maloney

### MS49-O1 Some Tricks for the Single Crystal Growth of Small Molecules

Bernhard Spingler<sup>1</sup>

<sup>1</sup>. Department of Chemistry, University of Zurich, Switzerland

email: [spingler@chem.uzh.ch](mailto:spingler@chem.uzh.ch)

While there exist helpful articles that describe the crystallization of small molecules for X-ray analysis<sup>1</sup>, it is our experience that some systems still present a challenge to be crystallized. We have summarized our assembled knowledge of the crystallization of small molecules over the last 15 years in a tutorial that is intended to be inspiring for the beginner as well as the more advanced chemist.<sup>2</sup> The techniques described in this tutorial are all being applied at room temperature. In more recent times, we have studied the influence of the temperature upon the formation of molecular single crystals as well as the possibility of growing high quality crystals from few milligrams of material within few hours by thermal recrystallization.

(1) Jones, P. G. *Chem. Brit.* **1981**, 17, 222; van der Sluis, P.; Hezemans, A. M. F.; Kroon, J. J. *Appl. Cryst.* **1989**, 22, 340; Hulliger, J. *Angew. Chem. Int. Ed.* **1994**, 33, 143.

(2) Spingler, B.; Schnidrig, S.; Todorova, T.; Wild, F. *CrystEngComm* **2012**, 14, 751.

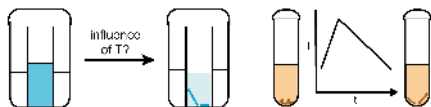


**Figure 1.** Different ways of obtaining single crystals. Left: Vapour diffusion at a constant temperature; right: thermal recrystallization.

**Keywords:** Single crystal growth, molecular compounds, crystallization, solvent/antisolvent

**MS49-O3** Toward the mitigation of growth rate dispersion through pretreatment of seed crystalsAshwin Kumar Rajagopalan<sup>1</sup>, Fabio Saluatori<sup>1</sup>, David R. Ochsenbein<sup>1</sup>, Marco Mazzotti<sup>1</sup>

1. Institute of Process Engineering, ETH Zurich, Sonneggstrasse 3, CH-8092 Zurich, Switzerland

email: ashwinr@ethz.ch

Crystals grown under identical conditions are found to have different growth rates independent of size, which leads to an often undesired broadening of the particle size distribution. Multiple potential causes of this phenomenon, known as growth rate dispersion (GRD) in crystallization literature, have been identified and are used to model systems that exhibit this phenomenon. Namely, differences in the number and structure of dislocations in crystals, lattice strain, and surface roughness are plausible candidates for GRD[1]. Recently, a modeling approach was proposed for the observed GRD of  $\beta$  L-glutamic acid in water that takes into account both non-spherical particle shape and the non-static nature of a generic growth affecting property, both on the level of single crystals and that of particle ensemble; this model was successfully used to quantitatively describe multiple sets of experiments subjected to a range of operating conditions[2]. In that work, it was hypothesized that performing pretreatments like temperature cycling on seed crystals would lead to a reduction of GRD due to refaceting, or healing of the surface of crystals; however, the efficacy of these methods have not yet been studied in detail. Populations of  $\beta$  L-glutamic acid crystals subjected to temperature cycles (or not) are characterized in terms of particle size and shape distribution using an in-house built stereoscopic imaging setup and in terms of growth of single crystals using a hot-stage microscopy setup. A deeper insight on the effect of temperature cycling on the surface of the treated crystals will be provided by surface analysis using surface characterization methods. The studies performed on single crystals and particle ensemble along with surface characterization of these crystals pre- and post-temperature cycling will shed more light on the underlying consequences of GRD and will provide a framework to test the validity of the model that was developed previously to describe GRD.

**References:**

- [1] R. I. Ristic, J. N. Sherwood, and K. Wojciechowski, "Assessment of the strain in small sodium chlorate crystals and its relation to growth rate dispersion," *J. Cryst. Growth*, vol. 91, no. 1–2, pp. 163–168, 1988.
- [2] D. R. Ochsenbein, S. Schorsch, F. Saluatori, T. Vetter, M. Morari, and M. Mazzotti, "Modeling the facet growth rate dispersion of  $\beta$  L-glutamic acid-Combining single crystal experiments with nD particle size distribution data," *Chem. Eng. Sci.*, vol. 133, pp. 30–43, 2014.

**Keywords:** crystallization, growth rate dispersion, seed crystal pretreatment, temperature cycling

**MS49-O4** Microseed matrix-screening (rMMS): introduction, theory, practice and a new technique for membrane protein crystallization in LCPPatrick D. Shaw Stewart<sup>1</sup>, Stefan Kolek<sup>1</sup>, Bastian Brauning<sup>2</sup>

1. Douglas Instruments Ltd

2. Technische Universität München, Germany

email: patrick@douglas.co.uk

Random Microseed Matrix-Screening (rMMS), where seed crystals are added automatically to random crystallization screens, is a significant recent breakthrough in protein crystallization [1]. During the eight years since the method was published, theoretical understanding of the method has increased [2 - 4], and several important practical variations of the basic method have emerged [5, 6]. We will briefly describe some of these variations, including cross-seeding, and introduce a novel method of making LCP seed stocks by scaling up LCP crystallization conditions. We will also describe a method of generating seed gradients across a plate so that the number of crystals in each LCP bolus can be varied, with a practical example.

[1] D'Arcy, A., Villard, F. and Marsh, M. "An automated microseed matrix-screening method for protein crystallization." *Acta Crystallographica Section D: Biological Crystallography* 63.4 (2007): 550-554.

[2] Shaw Stewart, P. D., Kolek, S. A., Briggs, R. A., Chayen, N. E., & Baldock, P. F. (2011). Random microseeding: a theoretical and practical exploration of seed stability and seeding techniques for successful protein crystallization. *Crystal Growth & Design*, 11(8), 3432-3441.

[3] D'Arcy, A., Bergfors, T., Cowan-Jacob, S. W., & Marsh, M. (2014). Microseed matrix screening for optimization in protein crystallization: what have we learned? *Acta Crystallographica Section F: Structural Biology Communications*, 70(9), 1117-1126.

[4] Shaw Stewart, P. D. & Mueller-Dieckmann, J. (2014). Automation in biological crystallization. *Acta Crystallographica Section F: Structural Biology Communications*, 70(6), 686-696.

[5] Obmolova, G., Malia, T. J., Teplyakov, A., Sweet, R. W., & Gilliland, G. L. (2014). Protein crystallization with microseed matrix screening: application to human germline antibody. *Fabs. Structural Biology and Crystallization Communications*, 70(8).

[6] Abuhammad, A., Lowe, E. D., McDonough, M. A., Shaw Stewart, P. D., Kolek, S. A., Sim, E., & Garman, E. F. (2013). Structure of arylamine N-acetyltransferase from *Mycobacterium tuberculosis* determined by cross-seeding with the homologous protein from *M. marinum*: triumph over adversity. *Acta Crystallographica Section D: Biological Crystallography*, 69(8), 1433-1446.

**Keywords:** Random Microseed Matrix Screening; LCP seed stocks. Membrane protein crystallization

## MS49-O5 The Highs And Lows Of Extreme Conditions Crystallisation

Michael R. Probert<sup>1</sup>

1. Newcastle University

email: michael.probert@ncl.ac.uk

Classical crystallisation of compounds commonly occurs through the evaporation of a solvent from a solution of dissolved material. This solution is allowed to become supersaturated, enabling nucleation and crystal formation/growth to occur. Although this approach is highly successful there are situations where alternative methods need to be employed. One example is observed when the desired product exists in the liquid phase under standard conditions; evaporation in this case then only leads to the loss of material, and not a crystalline material suitable for diffraction studies.

It is well understood that perturbing a material from nominally ambient conditions, via the application of pressure or reduced temperatures, can lead to a change in phase. If the perturbations are suitably controlled they can lead to the spontaneous crystallisation of samples that are liquid at room temperature and pressure. The large degree of flexibility in thermodynamic variables and the way in which they are applied in this method affords many, subtly different, routes to the solid state. This in turn opens up a pathway to a polymorphic playground of possibilities.

The techniques of in-situ crystallisation via high pressure and low temperature will be explained and highlighted with example case studies. This 'how to ...' will demonstrate the practicalities, optimisations and tricks that will enable users to enhance their success rates with these techniques.

**Keywords:** crystallisation, extreme conditions, high pressure, low temperature

## MS50 History of ECA, history of crystallography: contributions to and of crystallography

Chairs: Menahem Kaftory, Peter Paufler

## MS50-O1 History of crystallography in Switzerland

Dieter Schwarzenbach<sup>1</sup>

1. École Polytechnique Fédérale, SB-DO, Le Cubotron, CH-1015 Lausanne

email: dieter.schwarzenbach@epfl.ch

Laue's experiment in 1912 of the diffraction of X-rays by crystals led to one of the most influential revolutions in the history of science: the determination of crystal structures, the first structures being those of NaCl by W.L. Bragg, and diamond by W.L. Bragg and W.H. Bragg in 1913. The visualisation of matter with a sort of microscope possessing atomic resolution revolutionized chemistry and solid-state physics. By the early 1920s, the physics of X-ray diffraction was worked out, including atomic form and temperature factors, dynamical diffraction, application of space group symmetry, and the determination of simple structures. By the 1970s, the technical developments of X-ray tubes, cameras, detectors, diffractometers, computers and powerful software have enabled the art of structure determination to become a tool for chemical analysis. Since then, ever increasing efficiency of diffraction experiments and structure determination has resulted in service crystallography and an ever increasing demand for diffraction methods. Swiss contributions may be found in the early history of crystallography. Moritz Anton Kappeler, town physician of Lucerne, published an influential treatise on crystals in 1723. Debye and Scherrer moved to Zürich soon after their invention of powder diffraction. The most noteworthy Swiss contribution to early crystallography is certainly Paul Niggli's influential "Zürich School of Crystallography" in the Earth Sciences of the ETH and the University from 1920 to the retirement of Niggli's successor Fritz Laves in 1976. Its pioneering work was in the fields of space group symmetry (the precursor of the International Tables), geometrical crystallography (domains of influence of symmetry elements, homogeneous space partitions) and crystal chemistry, rather than in structure determination. The tradition of the "Zürich School", but also including structure determination (e.g. sulfo salts), was continued by Niggli's student Werner Nowacki at the University of Bern. Chemical Crystallography and structures of organic compounds were imported from the UK when J.D. Dunitz arrived at ETH Zürich in 1957. However, diffraction methods were applied to chemical problems early on by

pioneering chemists at the Universities of Bern (topochemistry by V. Kohlschütter and basic salts of divalent metals by W. Feitknecht) and Geneva (K.H. Meyer, fibers and polymers). From the 1970s onward, Swiss crystallography has developed similarly to elsewhere.

**Keywords:** Kappeler, Laue, Bragg, Scherrer, Niggli, Laves, Nowacki

## MS50-02 Crystallography in the Courtroom

Joel Bernstein<sup>1,2,3</sup>

1. New York University Abu Dhabi
2. New York University Shanghai
3. Ben-Gurion University of the Negev

email: joel.bernstein@nyu.edu

Over nearly the last twenty years there has been a major increase in the awareness of the intellectual property implications and manifestations of the existence of multiple solid forms (polymorphs, solvates, hydrates and amorphous) of commercially important materials (e.g. pharmaceuticals, pigments, high energy materials), due in part, at least, to a number of high profile litigations involving some leading pharmaceutical products. The prosecution of these litigations involves the recruitment of expert witnesses, who are called by the opposing sides to inform the court of the scientific principles issues in the legal conflict as well as to provide evidence in support of the party that has retained them. Due to the nature of the subject matter, many crystallographers have been retained as witnesses. The scientific subjects often deal with fundamental questions on the definition of chemical and physical terms, the precision, accuracy and interpretation of various analytical methods employed in the identification and characterization of different crystal forms, and the similarities and differences in the *modus operandi* of scientists and lawyers. Quite often colleagues and friends can find themselves on the opposite sides of a courtroom, due to differences in scientific opinion or interpretation of data involved in the litigations. These discussions frequently involve legitimate differences in scientific opinion with the courts left to decide either on which side is “right”, or perhaps which side is most convincing. A number of examples of these litigations will be described and discussed.

**Keywords:** patents, litigations, polymorphs, crystal forms, expert witnesses

## MS50-O3 Absolute structure

Howard D. Flack<sup>1</sup>

1. University of Geneva

email: crystal@flack.ch

The presentation will cover the history, development and current best practices in the treatment of non-centrosymmetric crystal structures. A full text on this subject was prepared for the International Year of Crystallography (Flack, 2014).

The origins of absolute-structure determination, starting from Friedel's 1913 proof that the intensities of the opposites  $hkl$  and  $-h-k-l$  are identical, are traced. The important structural principles derived from the study of chiral, but pseudo-mirror symmetric, methypylon are described. For the present time, the use of the average and difference intensities of the opposites  $hkl$  and  $-h-k-l$  are stressed. This leads to the use of *Friedif*,  $2AD$  and selected  $D$  plots, of  $R_{\text{merge}}$  and the  $D$ -Patterson.

Flack, H. D. (2014). *Chimia*, **68**, 26-30.

**Keywords:** Absolute configuration, Absolute structure, Flack parameter, Resonant scattering

## MS50-O4 History of Direct Methods: a personal account

Davide Viterbo<sup>1</sup>

1. Università del Piemonte Orientale, DISIT, viale T. Michel 11, Alessandria, Italy

email: davide.viterbo@uniupo.it

Having started my research in Crystallography in 1962, I could not live the birth of direct methods, but I had the invaluable chance of having accounts from many of the "founding fathers" (Figure 1).

My story will start from Harker and Kasper inequalities in 1948 as the first useful method to derive phases from measured intensities: in the same year they were applied by Gillis to solve a structure. Then in 1950 Karle and Hauptman generalized inequalities in a determinant form. In 1952 Sayre derived his famous equation and Okaya, Nitta and Zachariases proposed the use of symbols. In 1953 the monograph by Karle & Hauptman introduced important concepts and the use of probability methods, further developed also by Cochran, Woolfson, Bertaut and Klug in the following years. In 1966-67 Isabella Karle, using symbolic addition, solved a non-centrosymmetric structure and triggered the growth of the use of DM, also thanks to the development of computing software and hardware. Then in 1968 Woolfson proposed the multisolution method and with his co-workers developed the very successful MULTAN program. In 1970-71 he organized the schools on "Direct and Patterson methods of solving crystal structures" in Parma and York, that opened the route to the schools in Erice in 1974.

The final part will consider the exceptional developments of DM up to the late 80's, thanks to the works by Beurskens, Hauptman, Giacovazzo, Main, Sheldrick, Schenk, Woolfson and their co-workers.



**Figure 1.** J. Karle, D. Sayre, M. Woolfson, , H. Hauptman, F. Bertaut

**Keywords:** Direct Methods, History



## MS50-O5 The Artwork of Maurits C. Escher and Crystallography

Henk Schenk<sup>1</sup>

<sup>1</sup> University of Amsterdam, The Netherlands

email: h.schenk@uva.nl

Maurits C. Escher (1898-1972) is one of the world's most famous graphic artists. He was also one of the few artists to lecture at an IUCr Congress - perhaps the only one. The scientific interest in Escher's work for crystallographers is based on his hobby of making drawings of regular divisions of the plane. Moreover, as crystallographers study objects in three dimensions, it might well be that the way in which Escher played with the third dimension in his graphic art is also a reason behind their appreciation of his work.

In 1936, Escher visited the Alhambra and was fascinated by the regularity of the mosaic patterns there. He sketched many of them in detail. This led to his hobby of making original symmetrical drawings, but now with recognizable objects rather than ornaments, mostly animals. He used these periodic drawings (some of which are reproduced in part in the figure) as studies for making his woodcuts and other graphic art, even in one case a biscuit tin. For example, drawing No. 4 with puppets in three colours shows up in his woodcut *Metamorphosis I* (1937), woodcut *Development 1* (also 1937) relates to drawings 14 and 15, and his famous woodcut *Day and Night* (1938) is based on drawing 18. By 1940 his passion had resulted in 30 symmetrical drawings. He created a total of 137 of these patterns during his lifetime, and many of his other works are based on them.

Escher also developed 'a personal layman's theory on color symmetries'. His contact with crystallographers resulted in an exhibition at the Cambridge IUCr Congress in 1960, which gave Caroline MacGillavry the idea of collecting a group of patterns that could be of help in teaching plane-group symmetry. The Teaching and the Executive Committees of the International Union of Crystallography (IUCr) embraced this idea, as did Escher. Caroline selected 40 of the drawings to form the book. One plane group was not represented, so a pattern was specially created by Escher to fill the gap. This took place when Lodovico Riva and I were students in Caroline's group, so we met Escher himself. Caroline wrote texts to accompany each plate, and so the book *Symmetry Aspects of M. C. Escher's Periodic Drawings* was created and first published in 1965. Over 60,000 copies of the book were sold, making it the most popular IUCr publication ever.

In the lecture the artwork of Escher will be presented, but the emphasis will be on the symmetrical drawings, their symmetry and colour symmetry.



Figure 1. Six symmetrical drawings by Escher

**Keywords:** Escher, symmetrical drawings, plane groups, colour symmetry

## MS1 SAXS in structural biology

Chairs: Bente Vestergaard, Dimitri Svergun

### MS1-P1 Current Status of the Liquid-Metal-Jet X-ray Source Technology and SAXS applications

Emil Espes<sup>1</sup>, Björn A.M. Hansson<sup>1</sup>, Oscar Hemberg<sup>1</sup>, Mikael Otendal<sup>1</sup>, Göran Johansson<sup>1</sup>, Per Takman<sup>1</sup>, Tomi Tuohimaa<sup>1</sup>

1. Excillum AB

email: [emil.espes@excillum.com](mailto:emil.espes@excillum.com)

High-end x-ray scattering techniques such as SAXS and GISAXS rely heavily on the x-ray source brightness for resolution and exposure time. Traditional solid or rotating anode x-ray tubes are typically limited in brightness by when the e-beam power density melts the anode. The liquid-metal-jet technology has overcome this limitation by using an anode that is already in the molten state.

We have previously demonstrated prototype performance of a metal-jet anode x-ray source concept [1-3] with unprecedented brightness in the range of one order of magnitude above current state-of-the-art sources. Over the last years, the liquid-metal-jet technology has developed from prototypes into fully operational and stable X-ray tubes running in many labs over the world. Small angle scattering has been identified as a key application of the x-ray tube technology, since this application benefits greatly from small spot-sizes and high-brightness, to achieve a high flux x-ray beam with low divergence. Multiple users and system manufacturers have since installed the metal-jet anode x-ray source into their SAXS set-ups with successful results [4, 5].

The influence of the size of the x-ray source and its distance to the x-ray optics on the divergence will be discussed, and how to minimize the divergence in your SAXS experiments. This presentation will review the current status of the technology specifically in terms of stability, lifetime, flux and brightness. It will also discuss details of the liquid-metal-jet technology with a focus on the fundamental limitations of the technology. It will furthermore refer to some recent SAXS and GISAXS data from users of the metal-jet x-ray tube technology.

#### References

- [1] O. Hemberg *et al*, Appl. Phys. Lett. 83, (2003), 1483.
- [2] M. Otendal *et al*, Rev. Sci. Instr. 79, (2008), 016102.
- [3] T. Tuohimaa *et al*, Appl. Phys. Lett. 91, (2007), 074104
- [4] A. Schwamberger *et al*, Nuclear Instruments and Methods in Physics Research B 343 (2015) 116–122
- [5] U. Rücker, Deutsche Tagung für Forschung mit Synchrotronstrahlung, Neutronen und Ionenstrahlen an Großgeräten 2014, Bonn

**Keywords:** metaljet, saxs, home-lab, tabletop, x-ray source, x-ray tube, brightness, flux

**MS1-P2 In-line purification systems for structural analysis**Melissa A. Graewert<sup>1</sup><sup>1</sup>. EMBL Hamburg

email: graewert@embl-hamburg.de

Once the average protein sample is subjected to structural studies such as small-angle X-ray scattering (SAXS), it has undergone a number of procedures to ensure that it is of sufficient quantity as well as quality. Most purification protocols typically include an affinity purification step and/or ion-exchange chromatography step as well as size-exclusion chromatography (SEC). A number of beamlines now offer in-line SEC systems to generate a monodisperse sample stream from challenging samples. The SAXS data quality can thereby be improved by removing aggregates and/or separating individual species comprised within the sample. Three big challenges that arise with this approach are i) dealing with radiation damage, ii) strong (8-10 fold) dilution of the sample as well as iii) identification of suitable scattering frames for background subtraction. We could show that the parallel collection of biophysical data such as UV-Vis, differential refractometry and static light scattering has helped in the challenge of finding optimal regions for buffer subtraction (Graewert et al. 2015). In addition, we have now explored the advantage of this set-up for using other commonly applied purification processes such as affinity chromatography. Importantly, the data collected with differential refractometer detector helps follow the scattering behavior of ligand during the elution step which alters especially when a gradient is applied. Alternatively, the use of an on-column tag removal system has emerged as a very promising approach. The clear advantage of such an in-line purification procedure compared to SEC-SAXS is given with the prevention of the strong sample dilution.

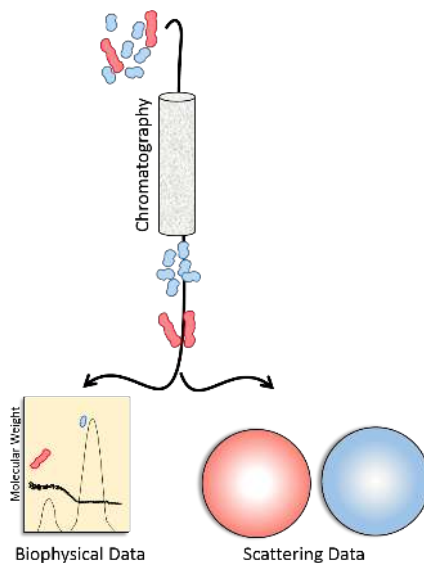


Figure 1.

**Keywords:** in-line purification, alternative methods, biophysical characterization

# MS1-P3 Small-Angle-X ray-Scattering (SAXS) studies of the low-resolution structure of the ribosomal GTPase EFL1, the SBDS protein and their complex

Dritan Siliqi<sup>1</sup>, Davide Altamura<sup>1</sup>, Abril Gijbsers<sup>2</sup>, Eugenio de la Mora<sup>3</sup>, Cinzia Giannini<sup>1</sup>, Teresa Sibillano<sup>1</sup>, Michele Saviano<sup>1</sup>, Nuria Sanchez-Puig<sup>2</sup>

1. Istituto di Cristallografia-CNR, Via G. Amendola 122/O, 70126 Bari, Italy

2. Instituto de Química, Departamento de Química de Biomacromoléculas, Universidad Nacional Autónoma de México, Ciudad Universitaria, 04510 México

3. Institute de Biologie Structurale, 71 av. des Martyrs, 38044 Grenoble, France

email: dritan.siliqi@ic.cnr.it

Ribosome biogenesis is closely linked to the cell growth and proliferation. Dysregulation of this process causes several diseases collectively known as ribosomopathies. One of them is the Shwachman-Diamond Syndrome, and the SBDS protein mutated in this disease participates with EFL1 in the cytoplasmic maturation of the 60S subunit. Recently, we have shown that the interaction of EFL1 with SBDS resulted in a decrease of the Michaelis-Menten constant ( $K_M$ ) for GTP and thus SBDS acts as a GEF for EFL1<sup>1</sup> (1). Subsequent studies demonstrated that SBDS debilitates the interaction of EFL1 with GDP without altering that for GTP (2). The interaction of EFL1 alone or in complex with SBDS to guanine nucleotides is followed by a conformational rearrangement. Understanding the molecular strategy used by SBDS to disrupt the binding of EFL1 for GDP and the associated conformational changes will be key to understand their mode of action and alterations occurring in the disease. In this study, we aim to show the conformational changes resulting from the interactions between EFL1 and its binding partners, the SBDS protein and the guanine nucleotides using SAXS technique (3). SAXS provided structural information of the proteins (Fig.1) and their conformational changes (4,5).

The authors acknowledge financial support PGR2015/2016 "Con il contributo del Ministero degli Affari Esteri e dalla Cooperazione Internazionale, Direzione Generale per la Promozione del Sistema Paese".

1. Gijbsers, A., García-Márquez, A., Luviano, A. and Sánchez-Puig, N. (2013) *Biochemical and Biophysical Research Communications*. **437**:349-354.

2. García-Márquez, A., Gijbsers, A., de la Mora, E. and Sánchez-Puig, N. (2015). *The Journal of Biological Chemistry* **290**:17669-17678.

3. Svergun, D. Koch, Michel H.J., Timmins, P.A. and May, R.P (2013). "Small Angle X-Ray and Neutron Scattering from Solutions of Biological Macromolecules". Oxford University Press

4. Petoukhov, M.V., Franke, D., Shkumatov, A.V., Tria, G., Kikhney, A.G., Gajda, M., Gorba, C., Mertens, H.D.T., Konarev, P.V. and Svergun, D.I. (2012). *J. Appl. Cryst.* **45**, 342-350.

5. Tria, G., Mertens, H. D. T., Kachala, M. & Svergun, D. I. (2015). *IUCrJ* **2**, 207-217.

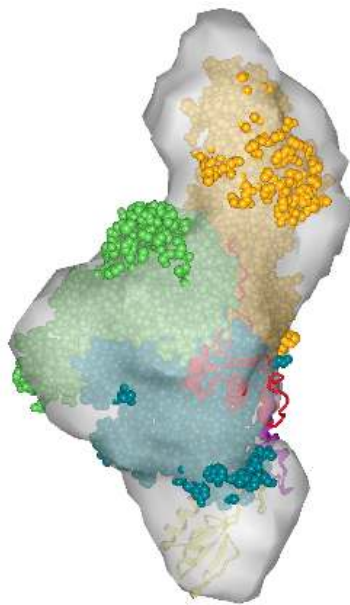


**Figure 1.** Efl1-Sdo1 complex model fitted into SAXS map. SAXS map obtained from ab-initio model [DAMMIF: Franke, D. and Svergun, D.I. (2009) *J. Appl. Cryst.*, **42**, 342-346]. Complex model obtained by a simultaneous docking into SAXS map [Sculptor: Birmans *et al* (2011). *J. Struct Biol.* **173** 428-435]

**Keywords:** Shwachman-Diamond Syndrome, Elongation factor-like 1, ribosomopathy, biosaxs

## MS2 Development of new types of sample preparation (both XFEL & synchrotrons)

Chairs: Jörg Standfuss, Gwyndaf Evans

### MS2-P1 Structure Determination of Membrane (and Soluble) Proteins Using In Meso In Situ Serial X-ray Crystallography at Room and Cryogenic Temperatures

Chia-Ying Huang<sup>1</sup>, Nicole Howe<sup>1</sup>, Vincent Olieric<sup>2</sup>, Rangana Warshamanage<sup>2</sup>, Piyee Ma<sup>1,3</sup>, Ezequiel Panepucci<sup>2</sup>, Xiang Liu<sup>4</sup>, Brian Kobilka<sup>4,5</sup>, Kay Diederichs<sup>6</sup>, Meitian Wang<sup>2</sup>, Martin Caffrey<sup>1</sup>

1. Membrane Structural and Functional Biology Group, School of Medicine and School of Biochemistry and Immunology, Trinity College, Dublin 2, D02 R590, Ireland
2. Swiss Light Source, Paul Scherrer Institute, Villigen, CH-5232, Switzerland
3. Laboratory of Structure and Function of Biological Membranes, Center for Structural Biology and Bioinformatics, Université Libre de Bruxelles, 1050 Brussels, Belgium
4. School of Medicine, Tsinghua University, Beijing, 100084, China
5. Department of Molecular and Cellular Physiology, Stanford University School of Medicine, Stanford, CA 94305, USA
6. Fachbereich Biologie, Universität Konstanz, Box 647, D-78457 Konstanz, Germany

email: cyhuang107@gmail.com

The lipid cubic phase continues to grow in popularity as a medium in which to generate crystals of membrane and soluble proteins for high-resolution X-ray structure determination (1, 2). To date, the PDB includes 313 records with 105 unique structures attributed to the *in meso* method (2). The most successful *in meso* protocol uses glass sandwich crystallization plates, but they are challenging to harvest crystals from. Here, we present a novel *in meso in situ* serial crystallography (IMISX) method which employs a thin cyclic olefin copolymer (COC) windowed plate for *in situ* data collection (3). The bolus of mesophase in which crystals grow on the plate contains tens to hundreds of crystals that are clearly visible with an in-line microscope at macromolecular crystallography synchrotron beamlines at both room and cryogenic temperatures. The data acquisition software DA+ GUI at the PX I (X10SA) and PXII (X06SA) beamlines at the Swiss Light Source (SLS) provides a semi-automated 'select and collect' protocol for serial crystallographic data collection with IMISX samples. The method has been demonstrated with  $\beta_2$ AR, AlgE, PepT<sub>st</sub> and DgkA as model membrane proteins and with lysozyme and insulin as test soluble proteins at room and/or at cryogenic temperatures (3, 4). Structures were solved by molecular replacement or by experimental phasing using bromine and native sulfur SAD methods to

resolutions ranging from 1.5 to 2.8 Å with micrometer-sized crystals and nano-gram to micro-gram quantities of protein. The IMISX and IMISXcryo method work with readily available, inexpensive materials and are compatible with high-throughput *in situ* serial data collection at macromolecular crystallography synchrotron beamlines.

1. Caffrey, M., Cherezov, V. (2009) Nature Protocols. 4:706-731.
2. Caffrey, M. (2015) Acta Cryst. F71, 3-18.
3. Huang, C.-Y. et al. (2015) Acta Cryst. D71, 1238-1256.
4. Huang, C.-Y. et al. (2016) Acta Cryst. D72, 93-112.

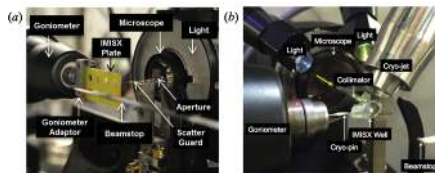


Figure 1. Experimental setup for IMISX data collection at 293 K (a) and 100 K (b)

**Keywords:** AlgE,  $\beta_2$ -adrenergic receptor, bromine SAD, DgkA, experimental phasing, GPCR, *in meso*, *in situ*, insulin, lipid cubic phase, mesophase, membrane protein, PepT<sub>st</sub>, serial crystallography, sulfur SAD

**MS2-P2** Microfluidic devices for fast time-resolved studiesDiana C.F. Monteiro<sup>1</sup>, Sebastian Bommel<sup>1</sup>, Ramakrishna Vasireddi<sup>1</sup>, Mohammad Vakili<sup>1</sup>, Martin Trebbin<sup>1</sup>

1. Centre for Ultrafast Imaging (CUI) - Universität Hamburg

email: diana.monteiro@uni-hamburg.de

Microfluidics enable the precise control of liquid volumes on the nanoliter scale within micron-sized channels. These very well defined flow conditions make this technology predestined for fundamental time-resolved investigations of biomacromolecules at microfocused X-ray sources.<sup>1</sup> This approach has many advantages compared to more traditional set-ups in terms of sample consumption, accuracy of measurements and the ability to access time-scales down to 10s of  $\mu$ s for time-resolved (TR) studies.

Microfluidic devices can be manufactured using a number of different polymers, such as PDMS, COCs or polyimide films (Kapton®), each having different optical and mechanical properties and varying ease of manufacture. With the advent of more powerful and brighter X-ray sources, Kapton and COCs have received great interest as materials for X-ray compatible devices due to their low-background and high stability. Alternatively, microfluidic liquid jet devices offer a free-flowing sample stream for XFELs and highly brilliant synchrotron sources.<sup>2</sup>

The precise control of reaction conditions have been demonstrated for the synthesis of nanoparticles<sup>3</sup> as well as in time-resolved structural studies of biomacromolecules using X-ray scattering<sup>4b</sup> and diffraction<sup>5</sup> as well as spectroscopy.<sup>6</sup> For TR studies, the reaction processes can be initiated by light activation (down to femtoseconds) or rapid mixing, where the time-resolution is only dependent on the diffusion rates of small molecules through the sample thickness (<1 $\mu$ m in laminar flow conditions, >10s  $\mu$ s).

Our group specializes in the design, manufacture and implementation of microfluidic devices, providing sample environments that address specific experimental condition requirements. Alongside this tailored approach, and in collaboration with local synchrotron facilities, we are making standardized microfluidic set-ups for TR biomacromolecular structural studies for general users.

1.(a) Toft, K. N.; *et al.*; *Analytical Chemistry* **2008**, *80* (10), 3648-3654; (b) Pollack, L. *Biopolymers* **2011**, *95* (8), 543-549.

2.Trebbin, M.; Kruger, K.; DePonte, D.; Roth, S. V.; Chapman, H. N.; Forster, S. *Lab on a Chip* **2014**, *14* (10), 1733-1745.

3.Lazarus, L. L.; *et al.*; *Lab on a Chip* **2010**, *10* (24), 3377-3379.

4.Rahman, M. T.; *et al.*; *RSC Advances* **2013**, *3* (9), 2897-2900.

5.Chapman, H. N.; *et al.*; *Nature* **2011**, *470* (7332), 73-77.

6.Park, H. Y.; *et al.*; *PNAS* **2008**, *105* (2), 542-547.

7.Levantino, M.; *et al.*; *Curr Opin Struct Biol* **2015**, *35*, 41-8.

**Keywords:** Microfluidics, time-resolved, SAXS

**MS2-P3** Developing and optimizing serial crystallography for static and dynamic structural biologyDominik Oberthür<sup>1</sup>, Juraj Knoska<sup>1,2</sup>, Max Wiedorn<sup>1,2</sup>, Carolin Seuring<sup>1,3</sup>, Kenneth Beyerlein<sup>1</sup>, Lars Gumprecht<sup>1</sup>, Anton Barty<sup>1</sup>, Alke Meents<sup>1</sup>, Sasa Bajt<sup>4</sup>, Henry N. Chapman<sup>1,2,3</sup>

1. Center for Free-Electron Laser Science, Deutsches Elektronen-Synchrotron DESY, Notkestraße 85, 22607 Hamburg, Germany

2. Department of Physics, University of Hamburg, Luruper Chaussee 149, 22761 Hamburg, Germany

3. Centre for Ultrafast Imaging, Luruper Chaussee 149, 22761 Hamburg, Germany

4. Photon Science, Deutsches Elektronen-Synchrotron DESY, Notkestraße 85, 22607 Hamburg, Germany

email: dominik.oberthuer@desy.de

In time resolved studies, the use of micron- or sub-micron sized protein crystals not only allows for uniform laser excitation of all unit-cells in the X-ray beam, but for mix-and-inject (Schmidt, 2013) studies of enzymatic reactions that cannot be photo-induced. The small dimensions allow for fast enough diffusion of substrate into the crystals, such that those reactions can be induced homogeneously at a defined time delay to the X-ray probe. This has strong implications for sample preparation: in case of such experiments one deliberately strives to grow micro- or even 'invisible' nano-crystals of proteins that would otherwise form larger crystals as well. Mix-and-inject experiments require furthermore a narrow size distribution of the crystals and fast mixing of the crystal suspension with substrate solution.

Serial crystallography methods, now established at both XFEL (Chapman, 2011) and third generation synchrotron sources (Gati, 2013; Stellato, 2014; Nogly, 2015) are very well suited for such time-resolved experiments (Tenboer, 2014; Barends, 2015), making it possible to reveal the dynamic nature of biological macromolecules and their interactions at near-atomic spatial resolution and on ultrafast timescales, even for extremely radiation sensitive samples.

Here we describe promising new crystallization methods for such experiments, the CFEL-pipeline for crystal characterization prior to the crystallographic experiment and novel sample delivery methods for reduced sample consumption, increased data collection efficiency and designed for mix-and-inject experiments.

Barends, T.R. *et al.*, (2015) Direct observation of ultrafast collective motions in CO myoglobin upon ligand dissociation. *Science* **350**, 445-50.

Chapman, H. N. *et al.*, (2011) Femtosecond X-ray protein nanocrystallography. *Nature* **470**, 73-77.

Gati, C. *et al.*, (2014) Serial crystallography on in vivo grown microcrystals using synchrotron radiation. *IUCrJ* **1**.

Nogly, P. *et al.*, (2015) Lipidic cubic phase serial millisecond crystallography using synchrotron radiation. *IUCrJ* **2**.

Schmidt, M., (2013) Mix and Inject. *Advances in Condensed Matter Physics* **2013**, 1-10.

Stellato, F. *et al.*, (2014) Room-temperature macromolecular serial crystallography using synchrotron radiation. *IUCrJ* **1**, 204-212.

Tenboer, J. et al., (2014) Time-resolved serial crystallography captures high-resolution intermediates of photoactive yellow protein. *Science* 346, 1242-1246.

**Keywords:** Serial Crystallography, SFX, Structural Biology, Sample Preparation, Time Resolved

## MS2-P4 Ultrathin membrane chips as X-ray transparent supports for serial crystallography

Nadia Opara<sup>1,2,3</sup>, Stefan Arnold<sup>2,3</sup>, Thomas Braun<sup>2,3</sup>, Henning Stahlberg<sup>2,3</sup>, Celestino Padeste<sup>1,3</sup>

1. LMN, Paul Scherrer Institute, 5232 Villigen PSI, Switzerland

2. C-CINA, Biozentrum, University of Basel, 4058 Basel

3. SNI, University of Basel, 4056 Basel, Switzerland

email: nadia.opara@psi.ch

Free electron lasers (FELs) allow collection of crystal diffraction data in serial femtosecond crystallography experiments (SFX), which are promising for studies of dynamic phenomena occurring in the femto- to nanosecond range. As the very intense radiation interacting with the sample leads to its destruction data need to be collected in the so-called "diffract-before-destroy" regime [1,2].

Protein crystals usually contain high amounts of water. Loss of the solvent leads to the deformation of the well-ordered structure of the crystal and reduced quality of the diffraction patterns. Therefore, protection from dehydration during measurements is essential. This can be achieved *via* flash cooling, keeping the sample in humidified atmosphere or by enclosure in watertight packaging.

*In situ* crystallization on microfabricated silicon chips with ultrathin silicon nitride membranes was used to produce protein crystals placed at defined position in required yields. The nanoliter volume cavities in the silicon chip can be filled with crystallization solution in manual or automatic manner (subnanoliter precision dispensing unit). Using vapor diffusion-based crystallization we obtained required size of crystalline sample for time-resolved tests at an FEL, which also allowed screening experiments of different crystal habits on one single chip. Assembly of two chips sealed with double-sided adhesive to form an array of sample chambers proved to be sufficient to preserve high quality of the grown crystals for the FEL experiments [Fig. 1.]. *In situ* crystallization is a promising alternative to the deposition of the crystal suspension on the fixed target support [3] or liquid-jet/injector based methods.

### References:

- [1] I. Schlichting, *IUCrJ* 2 (2015) 246-255.
- [2] J. Coe et al. *Protein Pept Lett.* 2016 23(3) 255-72.
- [3] A. Zarrine-Afsar et al. *Acta Cryst.* (2012). D68. 321-323.

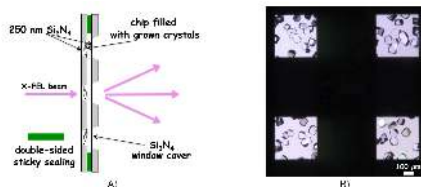


**Figure 1.** A) Solid support asymmetric sandwich for FEL data collection, B) *In situ* grown lysozyme crystals on nanomembrane chip. Scale bar: 100  $\mu$ m. The density of the crystals has been optimized for a time-resolved measurement on defined size sample at room temperature.



**Keywords:** serial femtosecond crystallography, microfabricated silicon chips, in situ protein crystallization

## **MS2-P5** LB Nanotemplate as optimal nanotechnology for Synchrotron Radiation (SR), Cryo Electron Microscopy (Cryo-EM) and X-ray Free Electron Lasers (XFELs).

Eugenia Pechkova<sup>1,2</sup>, Claudio Nicolini<sup>1,2</sup>

1. Laboratories of Biophysics and Nanotechnology, Department of Experimental Medicine, University of Genova, Via Pastore, 3, 16132 Genova, Italy

2. Nanoworld USA and Fondazione ELBA-Nicolini, Largo Redaelli, 7, 24020 Pradalunga, Bergamo, Italy

email: eugenia.pechkova@gmail.com

The methods of 3D protein structure resolution had significant progress in the recent years. However, many protein structures of high industrial, pharmaceutical and fundamental life science interest are still unsolved. The production of the protein crystal as well as its quality (order, intensity of diffraction, radiation stability) remains the major problem in the protein crystallography. Serial femtosecond crystallography with use of XFELs allows data collection from nm to micrometer-sized crystals, but the problems such as low hit rate and high quantity protein nanocrystals needed have to be solved. In Cryo-EM image recording by direct detectors as well as processing software make possible to obtain 3D macromolecular reconstructions at near-atomic resolution. Radiation damage and conformational heterogeneity of the sample make high resolution a major challenge. Therefore, common problems to all these advanced techniques is both radiation damage and difficult sample preparation. Langmuir-Blodgett (LB) protein nanotechnology is a novel approach for highly ordered, radiation stable protein sample preparation for all above methods of analysis. The numerous nanocrystallographic studies confirm exceptional radiation stability and quality of the crystals grown by homologous protein LB nanotemplate, including those failed to be obtain by classical methods. Moreover, highly ordered LB protein multilayer can bypass the bottleneck of protein crystallization. Further, homogeneously oriented LB film with the natural protein conformation offer the elegant solution to Cryo-EM problem. The property of the LB nanocrystals and LB multilayers can be used in all three frontier methods of analysis aiming to optimal protein 3D atomic structure resolution.

Pechkova E, Nicolini C, Protein nanocrystallography: a new approach to structural proteomics, Trends in Biotech 2004, 22, 117-122

Pechkova E et al, 3D atomic structure of a catalytic subunit mutant of human protein kinase CK2, Acta Cryst D 2003, 59, 2133-2139 Pechkova E et al, Radiation stability of proteinase K grown by LB nanotemplate method, J Struct Biol 2009, 168, 409-418

Pechkova E et al, In situ GISAXS: I. Experimental setup for submicron study of protein nucleation and growth, Biophys J 2010, 99, 1256-1261

Nicolini C et al. LB nanotemplate crystallization combined to laser-microfragmentation uniquely characterize proteins crystals by synchrotron microdiffraction. Am J Biochem Biotechnol 2014, 10, 22-30

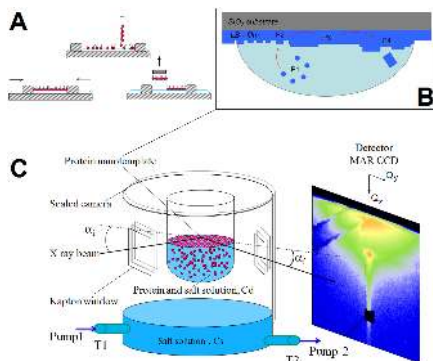


**Figure 1.** A. Formation of LB nanotemplate. B. The temporal model of LB nanotemplate method. Protein solution, P1, leads to protein association on the LB film states, P2 and P3, and to the crystal formation P4 detaching from the film in the drop. C. In situ submicron GISAXS of LB nanotemplate flow cell.

**Keywords:** Langmuir-Blodgett Nanotemplate, Protein Nanocrystallography, Synchrotron Radiation, XFELs, Cryo-EM.

## MS3 Data collection and processing software (XFELs & synchrotrons)

Chairs: Adrian Mancuso, Thomas Schneider

### MS3-P1 Computing Infrastructure, Software Optimization for High Data-Rate MX, and Real-Time Analysis

Herbert J. Bernstein<sup>1</sup>, Kaden Badalian<sup>2</sup>, Jean Jakoncic<sup>3</sup>, Edwin Lazo<sup>3</sup>, Sean McSweeney<sup>3</sup>, Wuxian Shi<sup>4</sup>, Robert M. Sweet<sup>3</sup>

1. Rochester Institute of Technology, School of Chemistry and Materials Science, Rochester NY, USA
2. SUNY Binghamton University, Binghamton, NY USA
3. Brookhaven National Laboratory, Upton, NY USA
4. Case Western University, Cleveland, OH USA

email: yayahjb@gmail.com

The very high data rates and data volumes now being seen with the new generation of pixel array x-ray detectors at synchrotron beam-lines require tuning and reorganization of computing infrastructure, and well-established processing pipelines, to make much more aggressive use of parallelism and to avoid unnecessary motion of data. Standard cluster environments, such as SGE, need to be retuned to work on much shorter time scales than usual. Standard spot-finding approaches need to be revised to make more use of “regions of interest”, binning, and image summing when appropriate. Multiple conversions of images need to be avoided and compressions need to be very carefully chosen to balance the need for compact data streams against competing demands for CPU access. Data, that once could have resided on single ordinary rotating disks, now need to be in memory as much as possible, on SSDs, or when necessary, on heavily striped RAIDS of rotating disks. Networks need to be several times faster than in the past. Each of the major processing flows, such as in DIALS and XDS, need to be retuned to allow as much parallel processing of images as possible. We appreciate the cooperation shown by Dectris, the DIALS group, especially Nicholas K. Sauter, Graeme Winter, Gwyndaf Evans, and James Parkhurst, and by the XDS project, especially Kay Diederichs, as well as by collaborators at many other facilities.

**Keywords:** pixel-array detectors, Eiger, cluster environments, SGE, compression, binning, summing, DIALS, XDS

## MS3-P2 Two-dimensional protein crystallography at FELs

Cecilia M. Casadei<sup>1</sup>, Bill Pedrini<sup>1</sup>

1. Paul Scherrer Institute

email: cecilia.casadei@psi.ch

Membrane proteins are involved in a number of crucial and diverse biological functions ranging from cross-membrane transportation to signal reception. The structural characterization of these macromolecules is hindered by the difficulty in producing well diffracting three-dimensional crystals, limiting the range of application of conventional X-ray crystallography in these systems.

Membrane proteins arrange favorably in periodic monolayers in a lipidic environment. This configuration presents the advantage that molecules are found in a close-to-physiological arrangement. In addition, the use of ultrashort free electron laser (FEL) X-ray pulses allows to largely outrun radiation damage phenomena in biological samples at ambient temperature.

Two-dimensional (2D) protein crystals of bacteriorhodopsin proved to give rise to diffraction spots to resolution of 4 Å at the Linac Coherent Light Source FEL, where the variable geometrical configuration of the experiment opens up to the possibility of collecting diffraction intensities along reciprocal space Bragg rods (B. Pedrini *et al.*, *Phil. Trans. R. Soc. B* **369**, 2014). The main bottleneck resides to date in 2D data processing and reduction due to the absence of dedicated software in conventional X-ray crystallography software suites.

The most recent advancements in 2D crystallography data treatment will be presented with particular focus on the opportunities and challenges of using intensities collected along reciprocal space rods.

**Keywords:** 2D-crystallography, membrane proteins, FEL

## MS3-P3 FIP-BM30A at the ESRF: an automated beamline for protein crystallography with unique features

Jean-Luc Ferrer<sup>1</sup>, Yoann Sallaz-Damaz<sup>1</sup>, Xavier Vernede<sup>1</sup>, Michel Pirocchi<sup>1</sup>, Christophe Berzin<sup>1</sup>, Monika Budayova-Spano<sup>1</sup>, Pascale Israel-Gouy<sup>1</sup>, Franck Borel<sup>1</sup>, David Cobessi<sup>1</sup>

1. Institut de Biologie Structurale, Grenoble, France

email: jean-luc.ferrer@ibs.fr

FIP-BM30A is an automated beamline for protein crystallography at the ESRF. But it is also a very flexible beamline, that can host a large variety of experiments, such as on-line absorption spectroscopy, humidity controlled, micro-ship *in situ* diffraction, Etc.

From the seminal work accomplished on beamline FIP-BM30A (ESRF) in 2000<sup>1</sup> to the present developments, robot based systems significantly changed the crystallography experiment strategy. They open possibilities for new strategies, give a high flexibility to the experimental setup, and make automation and remote control much easier. The robotized platform in operation on FIP-BM30A, named G-Rob, plays as a fully integrated, multi-purpose automated and remotely controlled diffractometer. G-Rob integrates several functions: classical sample changer; goniometer for frozen samples or capillaries [1], including frozen sample transfer from a storage Dewar; crystallization trays handling for *in situ* screening and data collection on crystallization plates and microchips [2]; beam monitoring; on line crystal fluorescence/absorption; crystal harvesting; Etc. Thanks to its tool changer, the robot arm can go automatically from one application to another. G-Rob can be easily upgraded with new functions. As an example of this flexibility, the G-Rob system on FIP-BM30A was recently expended with a new functionality: a dual gripper for SPINE-format sample holder, that makes possible the sample dismounting/mounting operation in a single trajectory, reducing this way the cycle time for sample exchange by a factor ~2.

Among the last results obtained with G-Rob are: (i) Automated structure resolution at room temperature (*in situ*), for the analysis of protein dynamic; (ii) Automated structural screening for the fragment based drug design strategy. New functions are also under development, such as the remote controlled robotized crystal harvesting [3].

Another, but important, feature of beamline FIP-BM30A is a new web-based user interface, named WIFIP. With this interface, several users can share the control of the experiment, from sample handling to data reduction, through a web browser, on the beamline or from the lab or home. Web-based technology makes the access easy, and the communication very fluid, even with a limited bandwidth.

[1] Jacquamet *et al.*, *Acta Cryst. D*, 2004, 60, 888-894.

[2] Jacquamet *et al.*, *Structure*, 2004, 12, 1219-1225.

[3] Heidari Khajepour *et al.*, *Acta D*, 2013, 69, 381-387.

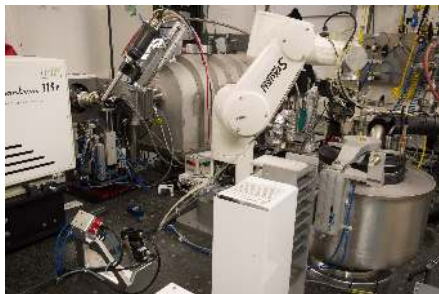


**Figure 1.** Overview of the robotized setup on beamline FIP-BM30A at the ESRF.

**Keywords:** beamline, macromolecular crystallography, automation, robot-based, crystallization, harvesting

## MS3-P4 Improved beam delivery and new data collection tools on the macromolecular crystallography beamline I04 at Diamond Light Source

Ralf Flaig<sup>1</sup>, Pierpaolo Romano<sup>1</sup>, Jonathan Blakes<sup>1</sup>, Chris Bloomer<sup>1</sup>, Graham Duller<sup>1</sup>, Sandra Gayadeen<sup>1</sup>, Michael Hillman<sup>1</sup>, James O'Hea<sup>1</sup>, Geoff Preece<sup>1</sup>, Graeme Winter<sup>1</sup>, David R. Hall<sup>1</sup>

<sup>1</sup>. Diamond Light Source, Harwell Science and Innovation Campus, Didcot, UK, OX11 0DE

email: ralf.flraig@diamond.ac.uk

Diamond Light Source [1] currently operates five beamlines for macromolecular crystallography (MX) and soon seven beamlines will serve the MX user community [2]. I04, a widely tuneable (5-25 keV, core range 6-17 keV) SAD/MAD station [3] is constantly evolving with the aim to provide the user with state of the art tools for data collection, especially to enable structure solution from increasingly difficult and challenging samples. Since early 2015 the beamline is using an array of compound refractive lenses in a translocator-like device allowing the user to change the beam size from 10 (h) x 5 (v) up to 110 (h) x 100 (v) microns over a wide energy range and thus be better able to match the beam size to the crystal size or be able to select more precisely the best part of the crystal. Using these small beam sizes, especially with small sample sizes, requires much more stringent schemes in terms of reliable beam delivery with respect to beam intensity and position than were envisaged for the original beamline design, including the monochromator. In addition, reliable beam diagnostics to monitor beam intensity and position over a wide beam size and energy range were not available at the beamline. We therefore have started a programme to improve beam delivery and have recently installed a new double crystal monochromator (DCM) which was designed inhouse based on existing proven technology and experience gained. The aim is to provide a system that is more stable, also taking into account possible future changes e.g. an increase in ring current, a lower emittance storage ring lattice and a new insertion device with higher power output. Alongside this, we have installed new beam position and intensity monitors that we will use in conjunction with a beam delivery feedback system. We are also looking into an improved goniometry and sample test system. As part of this we are planning the installation of the SmarGon multi-axis goniometer, which will enable better and faster sample centring, improved helical scan performance and provide us with new scientific capabilities for multi-sweep data collection strategies using multiple crystal orientations. Alongside these upgrades in beamline hardware we are also working on the development of the user software interface in order to streamline the user experiments.

### References

- [1] <http://www.diamond.ac.uk>
- [2] <http://www.diamond.ac.uk/Mx.html>
- [3] <http://www.diamond.ac.uk/Beamlines/Mx/I04.html>

**Keywords:** Diamond Light Source, macromolecular crystallography, beamlines, experimental phasing, data collection, multi-axis goniometry, monochromator, beam diagnostics, feedback

## MS3-P5 Introducing DUI, a graphical interface for DIALS

Luis Fuentes-Montero<sup>1</sup>, James Parkhurst<sup>1</sup>, Markus Gerstel<sup>1</sup>,  
Richard Gildea<sup>1</sup>, Graeme Winter<sup>1</sup>, Melanie Vollmar<sup>1</sup>, David  
Waterman<sup>2</sup>, Gwyndaf Evans<sup>1</sup>

1. Diamond Light Source Ltd, Harwell Science and Innovation  
Campus, Didcot, OX11 0DE, UK

2. CCP4, Research Complex at Harwell, Rutherford Appleton  
Laboratory, Didcot OX11 0FA, UK

email: luis.fuentes-montero@diamond.ac.uk

Given the usefulness of DIALS[1] as an integration software package and its command line utility nature, there is an obvious need for a tool that runs DIALS commands in a user-friendly and interactive way. There is also a need for visualization tools to help users diagnose the integration process. The aim of the DIALS User Interface (DUI) is to provide these tools to run and control DIALS. It should also act as a tool in teaching DIALS and data processing in general.

The DUI's layout has some features in common with iMOSFLM[2] and also follows the same workflow principals. The DUI's flexibility enables both the running of complicated commands with many parameters and simple commands using default parameters. The program is conceived in such a way that the user may never need to use the keyboard. While the user is adjusting parameters and choosing options with the mouse, the DUI is writing in real time the command line that should be run accordingly. The program generates graphics to help the user inspect the results. These graphics remain available in HTML5 format for later reuse, either for analysis or for publication.

The DUI is particularly helpful when an automated pipeline tool like Xia2[3] fails or gives unexpected results. It allows the user to run DIALS but in a controlled way, with the user taking over decision making.

### References:

[1] David G. Waterman, Graeme Winter, James M. Parkhurst, Luis Fuentes-Montero, Johan Hattne, Aaron Brewster, Nicholas K. Sauter, Gwyndaf Evans (2013) "The DIALS framework for integration software", CCP4 newsletter, n 49, pg 16-19

[2] T. Geoff G. Battye, Luke Kontogiannis, Owen Johnson, Harold R. Powell and Andrew G. W. Leslie (2011) "iMOSFLM: a new graphical interface for diffraction-image processing with MOSFLM", Acta Cryst D, Vol 67, Part 4 pg 271-281

[3] G. Winter "xia2: an expert system for macromolecular crystallography data reduction" (2010) J. Appl. Cryst, Vol 43, pg 186-190

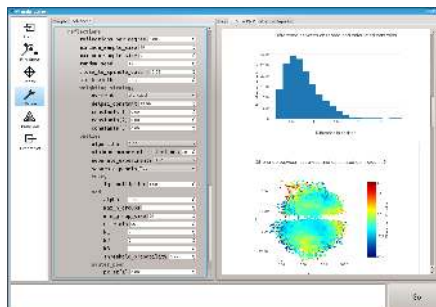


Figure 1. DUI showing diagnostic graphics after running refine job

**Keywords:** data integration, graphical user interface, data processing, software, DIALS, CCP4, macromolecular crystallography, collaboration

## MS3-P6 Novel data collection and processing strategies for the next generation X-ray source MAX IV

Jie Nan<sup>1</sup>, Mikel Eguiraun<sup>1</sup>, Fredrik Bolmsten<sup>1</sup>, Antonio Milan Ote<sup>1</sup>, Alberto Nardella<sup>1</sup>, Thomas Ursby<sup>1</sup>, Johan Unge<sup>1</sup>, Marjolein MGM Thunnissen<sup>1</sup>, & Uwe Mueller<sup>1</sup>

1. MAX IV Laboratory

email: jie.nan@maxiv.lu.se

MAX IV is the first 'fourth-generation' synchrotron in the world [1] and it will start to produce the brightest light from this summer and onwards. As the first MX beamline at MAX IV, BioMAX will not only have highly brilliant X-ray beam but also high performance hardware [2,3], including the next generation hybrid pixel-array detector EIGER 16M, a newly developed fast sample changer ISARA and a high precision MD3 diffractometer.

To take full advantage of these cutting edge technologies and to provide a more user friendly software interface particularly for the arising remote access, a new web-based version of a beamline and experiment control software MXCuBE3 has been being developed by MAX IV in strong collaboration with the ESRF. The software will support both single sample and *in situ* plate manipulation with modern acquisition methods, such as mesh scan and raster scan. Users can carry out their experiments through web browsers from any place and any operating system, without installation of any additional software.

Following these high throughput experiments, a fast and accurate data processing pipeline becomes critical to meet the high data rate. While testing and comparing various existing processing pipelines that utilize XDS and Dials, we are also seeking new approaches that can handle the diffraction images. Finally, the experimental meta-data and processing results will be stored in our ISPyB server and users can access them via web browsers.

[1] D. Castelvetti. (2015) *Nature*.

[2] M.M.G.M. Thunnissen et al. (2013) *J. Phys. Conf. Ser.*

[3] M.M.G.M. Thunnissen et al. (2015) *Acta Cryst. A*

**Keywords:** BioMAX, MAX IV, data collection, data processing

## MS3-P7 Pushing the Limits of a Beamline Endstation

Darren A. Sherrell<sup>1</sup>

1. Diamond Light Source

email: darren.sherrell@diamond.ac.uk

The recently upgraded endstation at beamline I24, Diamond Light Source greatly facilitates novel modes of data collection. The endstation can accommodate *in situ* 96 well crystal plates using a horizontal goniometer, conventional cryo-cooled rotation kappa data collection on a low sphere of confusion vertical goniometer, and the high speed serial delivery of crystals on fixed targets such as a silicon chip. The small beamsizes ( $\sim 2 \times 5 \mu\text{m}^2$ ) and high flux ( $> 1 \times 10^{12}$  ph s<sup>-1</sup>) available at the beamline has necessitated the development of new approaches to motion control, data collection and data analysis for the full potential and flexibility of the new endstation to be realised.

The difficulty in aligning micro-crystals on pins, *in situ* and in fixed targets in the X-ray beam and then the short duration of the diffraction experiment raises different and interesting technological challenges. The new endstation at 24 couples state-of-the-art commercially available hardware, with bespoke motion programs and novel software interfaces to allow high speed, high precision novel experiments. I will describe I24's versatile endstation design, and the advances in each of many techniques that have been achieved by our group. The techniques couple traditional techniques with serial approaches at both synchrotron and XFEL sources.

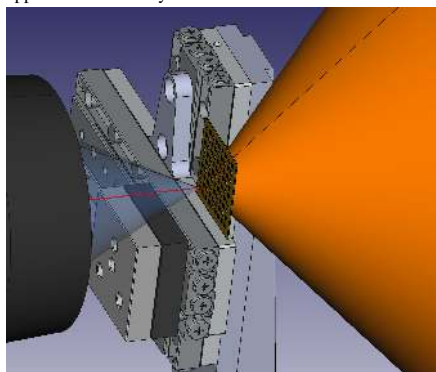


**Figure 1.** CAD drawing of a fixed target array with 2Å diffraction cone and focus cone of the on-axis objective lens.

**Keywords:** *In situ*, serial crystallography, microfocus, sample delivery, XFEL

## MS3-P8 Getting the Most of the Sample with Small Beams and Fast Detectors

Martin Savko<sup>1</sup>, Gavin Fox<sup>1</sup>, Enrico Stura<sup>1,2</sup>, William Shepard<sup>1</sup>

1. Synchrotron SOLEIL, France
2. Département d'Ingénierie et d'Etude des Protéines, CEA, Saclay, France

email: savko@synchrotron-soleil.fr

Combining fast sensitive detectors, high performance goniometers and small X-ray beams opens new venues in exploring the information content in the samples.

The photon budget available to explore the sample is limited, and to fully benefit from a fortuitous combination, the experimenter needs to weigh up the characteristics of the beam, the detector and the sample.

Holistic approaches to sample characterization, which combine optical imaging with X-ray techniques (fluorescence, diffraction and tomography), has a potential to provide a fuller appreciation of the spatial distribution of the sample properties and can provide a useful guidelines in the design of the experiment.

The increased data flow from the fast detectors also poses the new challenges for real time evaluation, and the computing infrastructure, which has always been important in the macromolecular crystallography experiments, becomes even more essential component in the overall workflow.

Here we present the practical choices made and the current solutions available on the Proxima 2A microfocus beamline at Synchrotron SOLEIL for the experiments performed using the newly commissioned Eiger X 9M detector.

**Keywords:** microbeam, Eiger, data processing

## MS3-P9 The automated expert processing system XDSAPP

Karine M. Sparta<sup>1</sup>, Uwe Mueller<sup>2</sup>, Udo Heinemann<sup>3,4</sup>, Manfred S. Weiss<sup>1</sup>

1. Helmholtz-Zentrum Berlin, Macromolecular Crystallography, Berlin, Germany
2. MAX IV Laboratory, Lund University, Lund, Sweden
3. Macromolecular Structure and Interaction, Max Delbrück Center for Molecular Medicine, Berlin, Germany
4. Chemistry and Biochemistry Institute, Freie Universität Berlin, Berlin, Germany

email: karine.sparta@helmholtz-berlin.de

In the last decade, macromolecular crystallography (MX) has experienced constant improvements of beamline efficiency at synchrotron sources around the world, leading to exposure times below one second per image and complete data collection within a few minutes. At the Helmholtz-Zentrum Berlin (HZB), we operate three MX beamlines, two of which are equipped with Pilatus detectors and sample changers [1], enabling fast high throughput experiments to be performed routinely.

We have developed the expert software XDSAPP (XDS Automation and Plotting Protocols) [2] to support users in the analysis of their diffraction data during measurement at our beamlines with minimal effort and time. It constitutes a convenient interface to XDS [3] and further relevant software such as POINTLESS from the CCP4 suite [4, 5], XDSSTAT [6], SFCHECK [7] and PHENIX.XTRIAGE [8], needed for automated decision-making. All important statistics from the XDS output files are represented graphically.

Originally developed as a Tcl/Tk graphical user interface (GUI), a completely new version has been made available for download since February 2014. Its new GUI has been designed to provide users with a much simplified and more intuitive way of handling diffraction data sets [9].

XDSAPP is used in more than 500 research groups distributed in 43 countries and is freely available to academic users from [www.helmholtz-berlin.de/bessy-mx](http://www.helmholtz-berlin.de/bessy-mx).

### References

- [1] Mueller, U. *et al.* (2015). *Eur. Phys. J. Plus* **130**, 141-150.
- [2] Krug, M. *et al.* (2012). *J. Appl. Cryst.* **45**, 568-572.
- [3] Kabsch, W. (2012). *Acta Cryst.* **D66**, 125-132.
- [4] Collaborative Computational Project (1994). *Acta Cryst.* **D50**, 760-763.
- [5] Winns, M.D. *et al.* (2011). *Acta Cryst.* **D67**, 235-242.
- [6] Diederichs, K. (2006). *Acta Cryst.* **D62**, 96-101.
- [7] Vaguine, A. *et al.* (1999). *Acta Cryst.* **D55**, 191-205.
- [8] Adams, P.D. *et al.* (2010). *Acta Cryst.* **D66**, 213-221.
- [9] Sparta, K. *et al.* (2016). *J. Appl. Cryst.* **49**.

**Keywords:** XDSAPP, software, data processing



## MS3-P10 Data acquisition and analysis software at the Swiss Light Source macromolecular crystallography beamlines

Justyna A. Wojdyla<sup>1</sup>, Ezequiel Panepucci<sup>1</sup>, Jakub Kaminski<sup>1</sup>, Simon Ebner<sup>1</sup>, Xiaoliang Wang<sup>1</sup>, Jose Gabadinho<sup>1</sup>, Meitian Wang<sup>1</sup>

1. Swiss Light Source, Paul Scherrer Institut, Villigen, Switzerland

email: justyna.wojdyla@psi.ch

Data acquisition software is an essential component of modern macromolecular crystallography (MX) beamlines, allowing for efficient use of beamtime at synchrotron facilities. Coupled with automatic data processing routines it allows assessment of data quality on the fly. Developed at the Paul Scherrer Institut, the DA+ data acquisition software is implemented at all three MX beamlines. DA+ consists of services and components written in Python and Java, which are connected via messaging and streaming technologies. The major components of DA+ are the user interface, acquisition engine, hardware/detector and online processing. The DA+ provides a simple and easy to use GUI, which supports standard, as well as advanced data acquisition protocols, such as multi-orientation SAD, energy interleaved MAD, raster scan and serial crystallography. Automatic data processing routines utilize freely available crystallographic data analysis programs and deliver near real time results for data collected with PILATUS (CBF format) and EIGER (HDF5 format) detectors. Resulting metadata are stored and analyzed in the dedicated MongoDB database. The software architecture enables exploration of the full potential of the latest instrumentations at beamlines. For example, real time evaluation of continuous raster scan data collected with a EIGER 16M detector at high frame-rate and delivered via streaming interface has been implemented at X06SA beamline recently.

**Keywords:** data acquisition, user gui, automatic data processing, Eiger, database

## MS3-P11 High-speed detectors enable synchrotron serial crystallography

Andreas Förster<sup>1</sup>

1. DECTRIS

email: andreas.foerster@dectris.com

With the recently introduced EIGER, hybrid photon counting enters a new dimension of spatial and temporal resolution and expands the field of x-ray experimentation. The absence of detector noise in combination with an image bit depth of 32 bit and high spatial resolution ensure uncompromised data quality. Continuous read-out with frame rates in the hundreds of hertz and a pixel size of 75 µm open EIGER detectors to various time-resolved and high-throughput experiments.

A short outline of the differences between EIGER and PILATUS3 will highlight key aspects of the new detector technology. The main focus of the presentation will be on synchrotron serial crystallography. This novel approach to data collection brings strategies developed at X-ray free-electron lasers (XFEL) to synchrotron beamlines. Appropriate sample supports (e.g. mesh loops or mesophase sandwiches) can be automatically screened for the presence of crystals by their diffraction [1]. Identified crystals are targeted for the acquisition of partial datasets that are then merged until sufficient data has been acquired for structure solution. Alternatively, crystals can be injected into the beam in glass capillaries, grease matrices, lipidic cubic phase jets [2] or on standing ultrasonic waves [3]. Individual diffraction images from non-oriented crystals can be merged to yield complete datasets.

Synchrotron serial crystallography allows the study of crystals of sizes formerly thought to require highly restrictive XFELs for their structural study. The crystals can be prepared in aqueous solutions as well as in lipidic mesophases [4] and at room temperature as well as at cryogenic temperatures [5], and can be presented to the beam in a variety of ways. To be successful, the new methods critically depend on noise-free detectors operating at high speed, like EIGER.

1. U. Zander *et al.* (2015) *Acta Cryst.* **D71**, 2328-2343
2. S. Muniyappan *et al.* (2015) *Bio Design* **3**, 98-110
3. T. Tomizaki (2016) personal communication
4. P. Nogly *et al.* (2015) *IUCrJ.* **2**, 168-176
5. C.-Y. Huang *et al.* (2016) *Acta Cryst.* **D72**, 93-112

**Keywords:** HPC detectors, synchrotron serial crystallography

## MS3-P12 Rapid data acquisition using an ultrasonic acoustic levitator and a next-generation pixel detector at room temperature

Takashi Tomizaki, Soichiro Tsujino<sup>1</sup>

<sup>1</sup>. Paul Scherrer Institut

email: takashi.tomizaki@psi.ch

A new data acquisition method was developed using an ultrasonic acoustic levitator and a next-generation pixel array detector in order to collect dataset rapidly at room temperature. Spinning of crystals in the levitated liquid droplet caused by the acoustic streaming and a rapid frame rate of few thousand Hz with the Eiger X detectors allow us to collect a dataset less than few hundred millisecond. We conducted the proof of principle experiments using lysozyme crystals and demonstrated the successful solution of the crystal structure. No damage due to the acoustic pressure was observed. Diffraction experiments were set up at the beamline X06SA, Swiss Light Source, Paul Scherrer Institut. Diffraction images were collected at 133 Hz with the Eiger X 16M detector and processed by CrystFEL data processing suite because of a smooth transition of rotation axis during the exposure. Details of the diffraction experiments, comparisons of structures solved by different methods and possible applications with this method will be presented.

**Keywords:** acoustic droplet levitation, room temperature, pixel array detector

## MS3-P13 Big EP: Automated structure solution pipeline deployment at Diamond Light Source

Irakli Sikharulidze<sup>1</sup>, Graeme Winter<sup>1</sup>, David R. Hall<sup>1</sup>

<sup>1</sup>. Diamond Light Source, Harwell Science and Innovation Campus, Didcot, Oxfordshire OX11 0DE, United Kingdom

email: irakli.sikharulidze@diamond.ac.uk

Automated processing of macromolecular crystallography data is an important component in effective use of valuable synchrotron beamtime. Providing feedback to experimenters during data collection allows better decision making regarding quality of their samples and experimental setup. The combination of increasing computational power and the development of automated structure solution pipelines makes it feasible to attempt solving structures during experimental sessions. Extensive computational and storage facilities at Diamond Light Source<sup>1</sup> has enabled deployment of a sophisticated data processing infrastructure<sup>2-4</sup>. Big EP is the latest in this line of software packages at Diamond that attempts to extend and exploit these resources to automatically build macromolecular models using the autoSHARP<sup>5</sup>, Phenix AutoSol/AutoBuild<sup>6,7</sup> and Crank<sup>2,8</sup> structure solution pipelines. Output of multiple trials using the SHELX<sup>9</sup> software suite and experimental records available in ISpyB<sup>2</sup> database are extensively used to identify datasets that pass selection criteria and to infer required input parameters for running the pipelines. Current computing infrastructure at Diamond results in Big EP successfully handling around one hundred suitable datasets a week and has provided users with useful starting models for further refinement.

<sup>1</sup> <http://www.diamond.ac.uk/mx>

<sup>2</sup> Delagenière, S. *et al.* (2011) ISPyB: an information management system for synchrotron macromolecular crystallography. *Bioinformatics*, 27, 3186–3192.

<sup>3</sup> Fisher, S. J. *et al.* (2015) *SynchWeb*: a modern interface for ISPyB. *J. Appl. Cryst.*, 48, 927–932.

<sup>4</sup> Winter, G. *et al.* (2013) Decision making in *xia2*. *Acta Cryst. D69*, 1260–1273.

<sup>5</sup> Vornrhein, C. *et al.* (2007) Automated structure solution with autoSHARP. *Methods Mol. Biol.* 364, 215–30.

<sup>6</sup> Terwilliger, T. C. *et al.* (2009) Decision-making in structure solution using Bayesian estimates of map quality: the PHENIX AutoSol wizard. *Acta Cryst. D65*, 582–601.

<sup>7</sup> Terwilliger, T. C. *et al.* (2008) Iterative model building, structure refinement and density modification with the PHENIX AutoBuild wizard. *Acta Cryst. D64*, 61–69.

<sup>8</sup> Skubák, P. & Pannu, N. S. (2013) Automatic protein structure solution from weak X-ray data. *Nat. Commun.* 4, 2777.

<sup>9</sup> Sheldrick, G. M. (2008) A short history of SHELX. *Acta Cryst. A64*, 112–122.

**Keywords:** macromolecular crystallography, automated structure solution, parallel computing

### MS3-P14 Tailor-made beams for macromolecular crystals on P14 at PETRAIII

Anna Polyakova<sup>1</sup>, Gleb Bourenkov<sup>1</sup>, Ivars Karpics<sup>1</sup>, Stefan Felder<sup>1</sup>, Fang Liu<sup>1</sup>, Thomas R. Schneider<sup>1</sup>

1. EMBL-Hamburg

email: anna.polyakova@embl-hamburg.de

The newest addition to the beamline optics of the P14 beamline at PETRAIII for macromolecular crystallography is a translocator (Vaughan et al, 2011) consisting of compound refractive lenses (CRLs). Acting as an additional focusing device, the CRLs produce beams with increased flux and different focal properties across a wide energy range. For example, the CRLs will enable adjustment of the beam size to match crystals in the size range of 100-500  $\mu\text{m}$  with an up to 50X increase in flux. The translocator allows the number of CRLs in the beam path to be easily changed, adjusting the focal distance and hence the beam size to match the dimensions of protein crystals of a wide range of sizes. The main objective of this study is to establish the conditions required to adjust the beam to crystals in the size range of 10-500  $\mu\text{m}$ . Following characterisation of the beam size and flux as obtained by employing different combinations of CRLs, the quality of the diffraction data from several macromolecular crystal systems is evaluated in order to establish optimum conditions. Diffraction data is collected from standard test systems (e.g. lysozyme, insulin, trypsin), as well as more challenging crystals from collaborators from the Karolinska Institute in Sweden. In addition, we aim to make the use of the CRLs available to P14 users through the beamline control software MxCuBE (Gabadinho et al, 2010), enabling rapid and easy adjustment of the beam size. Initial experiments have shown that the CRLs can be successfully used to adjust the size of the beam at P14 in the 20 to 150 micron range for X-ray energies between 6.1-12.7 keV. Diffraction data acquired at various energies have also shown that high quality native and anomalous data can be collected with CRLs in the beam path. These results show promise of the CRLs soon to be made available to P14 users, enabling them to optimise data quality for given crystals by matching the beam properties to the crystal. The project is performed in a collaboration with the groups of Gunter Schneider and Robert Schnell (Karolinska Institute, Stockholm) and is funded by the RAC programme.

Vaughan, G. B. M., et al. (2011). X-ray translocators: focusing devices based on compound refractive lenses. *Journal of Synchrotron Radiation*, 18(Pt 2), 125–133.

Gabadinho, J., et al. (2010). MxCuBE: a synchrotron beamline control environment customized for macromolecular crystallography experiments. *Journal of Synchrotron Radiation*, 17(5), 700–707.

**Keywords:** X-ray optics, compound refractive lenses, data collection

### MS3-P15 P13 and P14, the EMBL Beamlines for Macromolecular Crystallography at PETRA III

Isabel Bento<sup>1</sup>, Gleb Bourenkov<sup>1</sup>, Michele Ciani<sup>1</sup>, Guillaume Pompidor<sup>1</sup>, Johanna Kallio<sup>1</sup>, Ivars Karpics<sup>1</sup>, Anna Polyakova<sup>1</sup>, Stefan Fiedler<sup>1</sup>, Thomas R. Schneider<sup>1</sup>

1. European Molecular Biology Laboratory, Hamburg Outstation, Notkestrasse 85, 22607 Hamburg, Germany

email: ibento@embl-hamburg.de

EMBL is operating two beamlines for macromolecular crystallography on PETRA III (DESY, Hamburg). Both beamlines are fully tunable and provide a wide range of beam conditions. High flux X-ray beams with adjustable dimensions between 5 and 200  $\mu\text{m}$  are available in the energy range between 4 and 18 keV. To demonstrate the capability of the beamlines, we will describe and discuss typical experiments including:

- Structure solution via S-SAD phasing using 4 keV X-rays on P13.
- Structure solution using SAD phasing at 6.5 keV on multiple crystals with linear dimensions < 10  $\mu\text{m}$ .
- Structure solution by molecular replacement from data collected using serial helical scans on micro-crystals presented to the beam at room temperature in CrystalDirect<sup>TM</sup> plates.
- Rapid (< 3 min) data collection using a CRL-collimated X-ray beam with a 'top-hat' profile.

As a CrystalDirect Harvester system will be installed at EMBL Hamburg in June 2016, we hope to be able to present first results with crystals harvested with this system by the time of the meeting.

**Keywords:** Beamlines for Macromolecular Crystallography, SAD phasing, Serial Synchrotron Crystallography

## MS4 New developments in phasing and refinement

Chairs: Eleanor Dodson, Randy Read

### MS4-P1 *ContaMiner*: a webserver for early identification of unwantedly crystallised protein contaminants

Stefan T. Arold<sup>1</sup>, Arnaud Hungler<sup>1</sup>, Afaque Momin<sup>1</sup>, Kay Diederichs<sup>2</sup>

1. King Abdullah University of Science and Technology  
2. Fachbereich Biologie, Universität Konstanz, M647, D-78457 Konstanz, Germany

email: stefan.arold@kaust.edu.sa

Solving the phase problem in protein X-ray crystallography relies heavily on the identity of the crystallised protein, especially when molecular replacement (MR) methods are used. Yet, it is not uncommon that a contaminant crystallises instead of the protein of interest. Such contaminants may be bacterial proteins, protein fusion tags or proteins added during the purification steps. Many contaminants easily co-purify, crystallise and give good diffraction data. Identification of contaminant crystals may take much time, since the presence of the contaminant is unexpected, and its identity unknown. We have established a webserver, titled '*ContaMiner*' that allows fast MR-based screening of crystallographic data against a database of currently 57 potential contaminants. The web-based *ContaMiner* (available at [strube.cbrc.kaust.edu.sa/contaminer/](http://strube.cbrc.kaust.edu.sa/contaminer/)) currently returns results in 2-4h. Alternatively, the program is available in a GitHub repository and can be installed locally. *ContaMiner* enables systematic screening of novel crystals at synchrotron beamlines, and it would be valuable as a routine safety check for 'crystallisation and preliminary X-ray analysis' publications. Thus, in addition to potentially saving X-ray crystallographers much time and efforts, *ContaMiner* might minimise the risk of publishing erroneous data.

**Keywords:** diffraction, contaminant, crystal, molecular replacement

### MS4-P2 HKL2MAP 0.5 – new features for phasing with SHELXC/D/E

Fabio Dall'Antonia<sup>1</sup>, Thomas R. Schneider<sup>1</sup>

1. European Molecular Biology Laboratory, Hamburg Outstation

email: fabio.dallantonia@embl-hamburg.de

Crystallographic phasing (SAD, MAD, SIR, SIRAS) with the programs SHELXC, -D and -E <sup>[1]</sup> is a widely used path in macromolecular structure determination, in particular at synchrotron beam-lines, due to the fast feedback on phasing success. Along with the introduction of novel and powerful SHELXC/D/E features during the last years – e. g. substructure site refinement and backbone auto-tracing – the graphical user interface (GUI) HKL2MAP <sup>[2]</sup> has evolved and became a very popular tool for the control of the SHELX suite workflow and the graphical visualization of results.

Here, we present the latest developments of HKL2MAP with a focus on input data preparation. Ultimately, the performance of substructure determination in experimental phasing (SHELXD) as well as the resulting protein phase quality, that is, interpretability of electron density maps after density modification (SHELXE), depend on the accuracy of the processed diffraction data – in particular for methods based on anomalous differences. In this context, HKL2MAP/SHELXC provide an interface between data processing software and the phasing tasks.

Yet unaccounted for in our software so far, the monitoring of accuracy criteria over the course of data collection (*i. e.*, frame number) and the justified rejection of frame regions are possible measures that can crucially improve the quality of data subjected to SHELXC/D/E – which is sometimes the vital step for phasing success. HKL2MAP 0.5 now employs a preprocessor module for graphical visualization of frame-based XDS <sup>[3]</sup> statistics, namely the mean unmerged  $I/\sigma(I)$  vs. frame number and the derived  $R_{\text{decay}}$  <sup>[4]</sup> vs. frame distance. Furthermore, the new design of the GUI allows for truncation of frame ranges before submitting unmerged data to SHELXC. The new GUI and its functions are demonstrated and case studies of application presented.

HKL2MAP is free for academic users and can be obtained by online registration at [webapps.embl-hamburg.de](http://webapps.embl-hamburg.de).

#### References:

- [1] Sheldrick, G. M. (2010). *Acta Cryst.* **D66**, 479-485.
- [2] Pape, T. & Schneider, T. R. (2004). *J. Appl. Cryst.* **37**, 843-844.
- [3.a] Kabsch, W. (2010). *Acta Cryst.* **D66**, 125-132.
- [3.b] Kabsch, W. (2010). *Acta Cryst.* **D66**, 133-144.
- [4] Diederichs, K. (2006). *Acta Cryst.* **D62**, 96-101.

**Keywords:** HKL2MAP, Experimental phasing, SAD, MAD, SHELX

**MS4-P3** Experimental phase determination of the structure factorGyula Faigel<sup>1</sup>, Gabor Bortel<sup>1</sup>, Miklos Tegze<sup>1</sup>

1. Wigner RCP 1525 Budapest, POB 49, Hungary

email: gf@szfki.hu

Structure determination of crystalline substances is mostly done by x-ray diffraction. In these experiments an almost parallel probe beam is scattered by the sample, which is rotated to many orientations to fulfill Bragg condition and to measure enough reflections. This arrangement makes the study of time dependent structural changes, and experiments at non-ambient conditions very difficult, especially in the short time scale. In addition, in these traditional diffraction experiments the phase of the scattered wave is lost, which makes structure solution non trivial. These difficulties could be overcome by using point like inside x-ray sources within the sample. In this case a so called Kossel line pattern is formed [1]. Theoretical description of this pattern was worked out by Max von Laue [2]. Later, more detailed studies showed that not only the position and magnitude of Bragg reflections, but also their phase can be determined by measuring the fine structure of Kossel lines [3,4]. Although this was known for a long time, experimental realization of measuring the fine structure of several lines in parallel has not been presented. In this work we demonstrate experimentally for GaAs that phases can be directly determined from the profile of the Kossel lines [5,6]. These measurements are interesting not only theoretically, but they would facilitate structure solution of samples within extreme conditions, such as high pressure, high and low temperatures, high magnetic fields and extremely short times. The parallel measurement of many diffraction lines on a stationary sample will allow a more efficient use of the new generation of x-ray sources the X-ray free electron lasers (XFELs).

[1] Kossel W, Loeck V and Voges H, (1935) *Z. Physik* **94** 139

[2] Laue M. Von, (1935). *Ann. Phys., Lpz.* **23**, 705.

[3] J. M. Cowley, *Acta Cryst.* (1964). **17**, 33

[4] J. T. Hutton, G.T. Trammell J.P. Hannon, *Phys Rev.* (1985), **B31**, 743

[5] G. Bortel, G. Faigel, M. Tegze and A. Chumakov, *J. Synchrotron Rad.* (2016). **23**, 214–218

[6] G. Faigel, G. Bortel, M. Tegze, *Scientific Reports*, (2016), **6**:22904, DOI: 10.1038

**Keywords:** Kossel line, phase determination, diffraction

**MS4-P4** BioMEX Solutions: An expert facility for structure solution in macromolecular X-ray crystallographyRonan Keegan<sup>1</sup>

1. STFC Rutherford Appleton Laboratory

email: ronan.keegan@stfc.ac.uk

Macromolecular crystallography is an indispensable tool for researchers in many different fields of science. Much effort has been put into automating the procedure but more often than not the structure solution process requires manual effort and some degree of experience with the software techniques. Even with manual intervention, the process of eliciting a structural model from a set of X-ray images can be far from trivial. Problems such as twinning, pseudo symmetry and anisotropic data can all complicate the procedure and often frustrate the efforts of the researcher.

In sharp contrast to the situation 10-15 years ago, most structural biologists consider crystallography as a black-box tool designed to produce the structural information required for an understanding of the biological process being studied. However, solving a structure can take several months of valuable research time if the quality of the X-ray data is not sufficient for straightforward computational protocols. In such cases, structure solution becomes a burdensome routine, consuming effort to the disadvantage of project's main goals. BioMEX Solutions is a new service being established in the UK by the Science and Technology Facilities Council. It is designed to act like a facility giving access to a network of experts with many years of experience working with difficult X-ray data sets and a depth of knowledge that is hard to find elsewhere.

BioMEX offers a range of services from the initial data processing to structure completion and analysis/validation. There are many benefits to using our service and it optimizes the chances of successfully deciphering a solution from the X-ray data. Our experts have the skills to produce the best model that the data will allow for and in the quickest possible time. It frees up the valuable time of research staff to concentrate on the more important questions that the structural information is being used for. All of the processing done by our experts is documented and provided to the user in a form suitable for writing a publication or report, and may also be treated as a useful educational resource.

**Keywords:** Structure solution, data processing, phasing, refinement

## MS4-P5 Native SAD data collection environment at the Photon Factory BL-1A

Naohiro Matsugaki<sup>1,2</sup>, Yusuke Yamada<sup>1,2</sup>, Dorothee Liebschner<sup>1</sup>, Ayaka Harada<sup>1</sup>, Masahiko Hiraki<sup>3</sup>, Miki Senda<sup>1</sup>, Toshiya Senda<sup>1</sup>

1. Structural Biology Research Center, KEK
2. Photon Factory, KEK
3. Mechanical Engineering Center, KEK

email: naohiro.matsugaki@kek.jp

Native SAD (Single-wavelength anomalous dispersion) phasing, which utilizes naturally-included light atoms in macromolecules as anomalous scatterers, is an attractive crystallographic method for de-novo structural solution because no derivative crystals are required. The method appeared more than 30 years ago, however, it is still not ready to apply even at the latest synchrotron MX beamlines. Considering SAD phasing with heavy atoms is currently quite popular in MX, it is obvious the difficulty is in measuring accurately weak anomalous signal from light atoms. Using longer wavelength is required to enhance anomalous signals from light atoms, on the other hand causes experimental problems: severe beam absorption by the sample or air in the beam path, smaller angle of incident beam into the detector, etc. To overcome the absorption problem, a standing helium chamber was introduced on the long wavelength beamline BL-1A at the Photon Factory in order to perform diffraction experiment completely under helium environment. Helium cold stream is continuously supplied onto the sample position and recycled to keep the gas consumption minimum. A dedicated sample changer was developed to minimize the contamination of air during the sample exchange. The whole beamline system allows performing native SAD experiments feasible at long wavelength even above 3 Å. The problem of 'small angle of incident beam into the detector' is mitigated by placing two area detectors in V-shape. Two Eiger X4M detectors were installed with the newly developed supporting system which allows to exchange the V-shape and the standard horizontal configurations. A mini-kappa goniometer was installed at the same time to increase the completeness of the data and to reduce the systematic error due to the beam absorption by the sample. The current status of the beamline as well as successful de-novo structural solutions using the wavelength ranging from 2.7 Å to 3.5 Å will be reported.

**Keywords:** native SAD phasing, macromolecular crystallography beamline

## MS4-P6 ARCIMBOLDO\_SHREDDER's contribution to MR: Phasing with fragments from distant homologs

Claudia L. Millán-Nebot<sup>1</sup>, Massimo D. Sammito<sup>1,2</sup>, Andrey F.Z. Nascimento<sup>1,3</sup>, Isabel Usón<sup>1,4</sup>

1. Crystallographic Methods Group, Structural Biology Department, Institut de Biologia Molecular de Barcelona (IBMB-CSIC), Carrer Baldri Reixac 15, 3 A17, 08028 Barcelona, Spain
2. Structural Chemistry, Institut für Anorganische Chemie, University of Göttingen, Tammannstrasse 4, 37077 Göttingen, Germany
3. Alba Synchrotron, Carrer de la llum 2-26, Cerdanyola, 08192 Spain
4. Structural Biology, ICREA at IBMB-CSIC, Carrer Baldri Reixac 15, 3 A17, 08028 Barcelona, Spain

email: cmncr@ibmb.csic.es

Most macromolecular structures are solved by molecular replacement, provided suitable search models are available. Distant homologs provide templates that may be too different to succeed, notwithstanding the overall correct fold or their featuring areas with close enough fragments. Successful ways to tackle this problem rely on the degree of conservation to select and improve search models, as implemented in Sculptor<sup>1</sup> or Ensembler<sup>2</sup>.

ARCIMBOLDO<sup>3</sup> combines the search of small and accurate fragments with PHASER<sup>4</sup>, with their expansion through density modification and autotracing with SHELXE<sup>5</sup>. ARCIMBOLDO\_SHREDDER<sup>6</sup> uses fragments derived from distant homologs in a process driven by the experimental data. The following aspects will be illustrated in the solution of new and test structures:

- Model generation: contiguous polypeptide stretches, three dimensional volumes or structural unit
- Optimal fragment size to retrieve a minimum signal
- Model trimming against the rotation function
- Model optimization through gyre refinement against the rotation function
- Combination of partial fragment solutions with ALIXE (7)

ARCIMBOLDO\_SHREDDER can be downloaded from <http://chango.ibmb.csic.es/ARCIMBOLDO>.

### References:

- 1) Bunkoczi, G. & Read, R. J. (2011). *Acta Cryst.* D67, 303-312.
- 2) Bunkoczi, G., Echols, N., McCoy, A. J., Oeffner, R. D., Adams, P. D. & Read, R. J. (2013). *Acta Cryst.* D69, 2276-2286.
- 3) Millán, C., Sammito, M. & Usón, I. (2015). *IUCr J* 2, 95-105.
- 4) McCoy, A. J., Grosse-Kunstleve, R. W., Adams, P. D., Winn, M. D., Storoni, L. C. & Read, R. J. (2007). *J. Appl. Cryst.* 40, 658-674.
- 5) Sheldrick, G. M. (2010). *Acta Cryst.* D66, 479-485. Sammito, M., Meindl, K., de Ilarduya, I. M., Millán, C., Artola-Recolons, C., Hermoso, J. A. and Usón, I. (2014). *FEBS J*, 281: 4029-4045.

6) Millán, C., Sammito, M., García-Ferrer, I., Goulas, T., Sheldrick, G.M. and Usón, I. (2015). *Acta Cryst D* 71, 1931-1945.

**Keywords:** phasing, molecular replacement, small fragments, clustering, ARCIMBOLDO

## **MS4-P7** Fast iodide-SAD phasing for membrane protein structure determination

Igor Melnikov<sup>1</sup>, Vitaly Polovinkin<sup>2,3</sup>, Kirill Kovalev<sup>4</sup>, Vitaly Shevchenko<sup>3</sup>, Mikhail Shevtsov<sup>4</sup>, Valentin Borshechvskiy<sup>4</sup>, Vadim Cherezov<sup>5</sup>, Gordon Leonard<sup>1</sup>, Valentin Gordeliy<sup>2,3,4</sup>, Alexander Popov<sup>1</sup>

1. European Synchrotron Radiation Facility, F38043Grenoble, France
2. Institut de Biologie Structurale, Université Grenoble Alpes, Grenoble, France
3. Institute of Complex Systems (ICS), ICS-6, Structural Biochemistry, Research Center Jülich, Jülich, Germany
4. Laboratory for Advanced Studies of Membrane Proteins, Moscow Institute of Physics and Technology, Dolgoprudniy, Russia
5. Department of Chemistry, Bridge Institute, University of Southern California, Los Angeles, California 90089, USA

email: igor.melnikov@esrf.fr

Membrane proteins are hard to investigate. Each step of X-ray crystallographic pipeline from protein production to structure solution is non-trivial. In particular, experimental phasing techniques have shown their ineffectiveness in case of either soaking or co-crystallization of membrane protein crystals. A fast, easy and universal method is presented here for membrane protein structure determination. Four structures of target membrane proteins from four different largest classes have been solved via single-wavelength anomalous diffraction of iodide-soaked crystals. The method is highly efficient for various data collection strategies: standard and serial crystallography at synchrotron and XFEL sources.

**Keywords:** SAD, crystal soaking, iodide, membrane protein



## MS4-P8 Current and future potential of contact predictions for X-ray crystallography

Felix Simkovic<sup>1</sup>, Jens M.H. Thomas<sup>1</sup>, Olga Mayans<sup>1,2</sup>, Daniel J. Rigden<sup>1</sup>

1. Institute of Integrative Biology, University of Liverpool, Liverpool, L69 7ZB, United Kingdom  
2. Department of Biology, Universität Konstanz, 78457 Konstanz, Germany

email: hlfsimko@liv.ac.uk

Protein structures and protein-protein interactions are naturally constrained through contacting amino acids. Maintained under evolutionary pressure, a pair of contacting amino acids can remain invariant, accept only highly conservative changes over time, or accept more drastic mutations at one position when the other simultaneously alters in a coordinated fashion. Successful detection of these contacting residues, through the analysis of evolutionary covariance, is now reliably possible in suitable cases due to a new statistical treatment of the data that strongly reduces false positive predictions [1]. Such suitable cases are those where homologous sequences are sufficient in number and diversity - a limit expected to be surpassed by many more protein families in years to come [2]. Contact predictions provide great yet mostly unexplored opportunities to X-ray crystallography.

One benefit was recently demonstrated advancing *ab initio* Molecular Replacement (MR). The benefits of contact information in *ab initio* MR were successfully demonstrated using a software pipeline called AMPLE [3]. It was shown that a much larger target range is made tractable by guiding *ab initio* structure predictions with predicted residue contacts. Much larger - chain lengths up to 225 residues - and more  $\beta$ -rich protein targets were solved successfully using search model ensembles based on contact-guided *ab initio* structure predictions.

Additionally, further applications of contact data in the field of X-ray crystallography will be presented. Such applications can range from domain parsing to guide construct design [4] to the 3D-assembly of monomers into oligomeric search models for MR [5]. The use of contact information can also guide the interpretation of crystal structures by highlighting covarying and therefore functionally or structurally important interfaces or residues eg [6].

[1] Marks, D. S., Hopf, T. A., & Sander, C. (2012). *Nat. Biotechnol.* 30, 1072–1080.

[2] Kamisetty, H., Ovchinnikov, S., & Baker, D. (2013). *P. Natl. Acad. Sci. USA* 110, 15674–15679.

[3] Bibby, J., Keegan, R. M., Mayans, O., Winn, M. D. & Rigden, D. J. (2012). *Acta Cryst. D* 68, 1622–1631.

[4] Rigden, D.J. (2002). *Protein Eng.* 15, 65–77.

[5] Ovchinnikov, S., Kamisetty, H. & Baker, D. (2014). *Elife* 3, e02030.

[6] Nicoloudis, J. M., Lau, S.-Y., Schärfe, C. P. I., Marks, D. S., Weihofen, W. A., & Gaudet, R. (2015). *Structure* 23, 2087–2098.

**Keywords:** Molecular Replacement, AMPLE, Protein structure prediction, Evolutionary covariation

## MS4-P9 Combining unconventional MR with AMPLE *ab initio* models and experimental phasing

Adam J. Simpkin<sup>1</sup>, Olga Mayans<sup>2</sup>, Daniel J. Rigden<sup>1</sup>, Martin Savko<sup>3</sup>, William E. Shepard<sup>3</sup>, Ronan Keegan<sup>4</sup>

1. Institute of Integrative Biology, University of Liverpool, Liverpool, L69 7ZB, United Kingdom  
2. Fachbereich Biologie, Universität Konstanz, D-78457 Konstanz, Germany  
3. PROXIMA 2, Synchrotron SOLEIL, l'Orme des Merisiers, Saint Aubin, BP 48, 91192 Gif-sur-Yvette, France  
4. Research Complex at Harwell, STFC Rutherford Appleton Laboratory, Didcot OX11 0FA, England

email: hlasimpk@liv.ac.uk

In recent years the combination of molecular replacement (MR) with single anomalous dispersion (SAD) via MRSAD, has been shown to solve structures that neither individual technique was able to [1, 2]. Whilst this success highlights the advantages of MRSAD, a partial model is required for MR which may not be available from conventional sources.

A potential way of generating these partial models is AMPLE [3]. AMPLE is a pipeline that uses a cluster-and-truncate approach on *ab initio* models to solve the structures of small proteins via unconventional MR. As *ab initio* modelling predicts the three dimensional structure of a protein independently of homolog structures, it can be used to make models for novel folds and structures. In the case of small proteins, the modelling of these features is often enough to solve them via MR, however in larger structures it may not. The modelling of features can nonetheless contain some useful information about the structure and in combination with experimental phasing information, could lead to a solution.

An attractive method of experimental phasing for crystallographers when a solution cannot be found by more traditional means is sulphur-SAD (S-SAD) as it requires no changes to crystal preparation. However, because S-SAD experiments are often demanding on data quality and because some proteins contain only a low sulphur content ratio, it is often hard to get phases out of S-SAD experiments. Indeed, as of 2015, only 80 *de novo* S-SAD structures have been deposited in the wwPDB [4]. Using AMPLE in combination with S-SAD therefore provides a potential route through which the success rate of S-SAD can be improved. We describe preliminary experiments exploring this approach, and enhancements to the underlying MR pipeline MrBUMP that facilitate the work.

[1] Busby, J. N., Lott, J. S., & Panjikar, S. (2016). *Acta Cryst. D* 72(2), 182–191

[2] Skubák, P. & Pannu N. S., (2013). *Nat. Commun.* 4, 2777

[3] Bibby, J., Keegan, R. M., Mayans, O., Winn, M. D., & Rigden, D. J. (2012). *Acta Cryst. D* 68, 1622–1631

[4] Weinert, T et al. (2015). *Nat. Methods*. 12, 131–133

**Keywords:** Molecular replacement, Experimental phasing, AMPLE, MRSAD.

**MS4-P10** Mask-based approach to phasing single-particle diffraction data

Alexandre Urzhumtsev<sup>1,2</sup>, Natalia L. Lunina<sup>3</sup>, Tania E. Petrova<sup>3</sup>, Manfred W. Baumstark<sup>4</sup>, Vladimir Y. Lunin<sup>3</sup>

1. IGBMC, Illkirch, France

2. Université de Lorraine, Nancy, France

3. IMPB RAS - Branch of KIAM RAS, Pushchino, Russia

4. University of Freiburg, Germany

email: sachu@igbmc.fr

We suggest a new *ab initio* phasing method [1] which is particularly appropriate for diffraction data from a single particle. A test with a known structure resulted in phases that have 97% correlation with the exact ones in the full 25 Å resolution shell. Currently such data are phased mostly by 'solvent-flattening type' iterative procedures [2] based on the object's property to have a finite support. In our method, in addition to this feature, we use the connectivity of biological macromolecules and prior information in the form of probability distributions. The random search procedures allow a wide exploration of configurational space of possible phase solutions.

Instead of the search for the phase sets giving connected images as used previously [3], we start from a random generation of connected binary envelopes of a given volume. For each envelope, we calculate its structure factors and accept the corresponding phase set only if the amplitudes are very similar to the experimental values. Typically, from near a million of envelopes generated a hundred phase sets are selected, their values are aligned to their common origin and averaged.

Recent advances in the X-ray diffraction experiments lead to a possibility to register X-rays scattered by large isolated biological particles in all directions. In practice, the original continuous diffraction pattern is sampled at grid points in reciprocal space. This makes the phase problem equivalent to one for an imaginary crystal with the large unit cell containing a particle and a large volume of empty space ("solvent"). The smaller the sampling step, the larger the unit cell and the "solvent fraction". Using a known structure, we investigated the effect of the sampling step on the accuracy of the phase problem solution. Reducing the sampling step, it is shown that an expected improvement of the accuracy of the solution continues even beyond the Nyquist limit. On the other hand, the method is also efficient when the sampling corresponds to a unit cell which size is close to that occurring in crystallographic studies.

1. Lunin VY *et al.* (2016) *Acta Cryst.*, **D72**, 147

2. Fienup J. (1982). *Appl. Optics*, **21**, 2758

3. Lunin VY, Lunina NL, Urzhumtsev A. (2000) *Acta Cryst.*, **A56**, 375

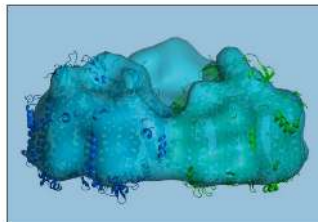


**Figure 1.** Image of trimer PS-I (Jordan *et al.* (2001) *Nature*, 411, 909) shown by 25 Å resolution *ab initio* phased Fourier synthesis calculated with the simulated magnitudes. Two of three monomers in the atomic model are shown (the 3<sup>rd</sup> is removed for clarity).

**Keywords:** *ab initio* phasing, single particle, connected masks, pattern sampling

## MS4-P11 Evaluation of MRSAD phasing protocols

Riccardo Pederzoli<sup>1</sup>, Fabio Dall'Antonia<sup>1</sup>, Isabel Bento<sup>1</sup>, Michele Cianci<sup>1</sup>, Thomas R. Schneider<sup>1</sup>

1. EMBL (European Molecular Biology Laboratory) - c/o DESY, Building 25a, Notkestrasse 85, 22607, Hamburg, Germany

email: rpederzoli@embl-hamburg.de

Molecular Replacement in combination with Single Anomalous Diffraction (MRSAD) is a crystallographic phasing method that can lead to structure solution starting from weak anomalous signal and/or poor MR search models, where both the SAD and MR methods alone would fail. The advent of MRSAD has been triggered by the need to reduce the MR intrinsic model bias, in particular at low resolution, and by the increasing availability of high-resolution structures for components of larger biological complexes.

To explore the capabilities and limitations of currently available MRSAD protocols, we have tested these on known crystal structures where we assume that only a part of the crystallographic unit cell is known and can be placed by molecular replacement.

Our model system is Cdc23<sup>NTerm</sup>, a dimeric protein of which the structure has been recently determined via S-SAD at 3.1 Å resolution<sup>1</sup>. Also, a monomeric, 1.9 Å-resolution structure has been obtained in 2013 by Se-SAD<sup>2</sup>. MRSAD has been tested on the low-resolution structure using different search models. The pipeline involves MR- and MRSAD-phasing, followed by model building/density modification with three different programs. To assess the results, the deposited PDB model has been used as a reference. The success of the protocol has been judged on the number of residues built into the electron density map, on the phase quality as evaluated via the Mean Phase Error (MPE) and real-space map correlation coefficients against the reference.

Numerically, the improvements from MR to MRSAD are limited to a few degrees in terms of MPE. However, the visual inspection of electron density maps and the analysis of the real space correlation coefficients have shown that the electron densities produced with MRSAD phases are clearly superior to those produced from MR or SAD phases alone.

As a next step of the study, we will apply the same strategy to larger macromolecular complexes.

1. Cianci, M. *et al.* (2016), *Acta Cryst.* **D72**, 403-412

2. Zhang, Z. *et al.* (2013), *J. Mol. Biol.* **425**, 4236-4248.

**Keywords:** Molecular Replacement, Single Anomalous Diffraction, MRSAD

## MS4-P12 Advances in nucleic acid model building with ARP/wARP 7.6

Grzegorz Chojnowski<sup>1</sup>, Victor Lamzin<sup>1</sup>

1. European Molecular Biology Laboratory (EMBL), c/o DESY, Notkestrasse 85, Hamburg 22607, Germany

email: gchojnowski@embl-hamburg.de

Nucleic acids perform a variety of functions in a living cell beyond their protein coding capacity. In particular, non-coding RNAs (ncRNAs) have been identified to be involved in many cellular processes ranging from the regulation of gene transcription to the catalysis of chemical reactions. Many known ncRNAs form compact three-dimensional structures, therefore understanding of their function in the cell requires knowledge of their molecular structure.

Over the years the ARP/wARP software has been continuously advancing and used by more than 15,000 researchers for building structural models of proteins with or without nucleic acids or small-molecule ligands. Nucleic acid model building was introduced in ARP/wARP relatively recently and it is algorithmically analogous to the protein chain tracing. In brief, the procedure starts with the detection of candidate positions of backbone phosphates. Subsequently, phosphate-ribose-phosphate units are placed in electron density with the use of graph theory and pattern recognition approaches. Finally, the bases are added to the backbone and the built chain fragments undergo restrained real-space refinement in the electron density.

Now we present a considerable revision of the nucleic acid model building module in ARP/wARP. The phosphate group detection, which is crucial for the successful polynucleotide tracing, has been complemented with the new machine learning algorithm. It now performs better at lower resolution and in poorly defined density regions. Moreover, the tracing of the nucleic acid backbone has been advanced in an iterative manner, similar to the protein chain tracing. Compared to previous version of ARP/wARP (7.5) the new revision resulted in an overall increase in the number of nucleotides built by 15%, while maintaining the high level of accuracy of the built models.

**Keywords:** nucleic acids, model building

## MS5 Structural information in drug design

This study was supported by BioStruct-X (No.283570) of European Community's 7th Framework Programme; the MedInProt program of the Hungarian Academy of Sciences; OTKA grants NK101072, K82092 and PD104344. We acknowledge SLS and EMBL-Hamburg for providing synchrotron radiation beamtime.

**Keywords:** calmodulin, protein/peptide complex, taxon-specific interactions, *Plasmodium falciparum*

Chairs: Michael Hennig, Vincent Mikol

### MS5-P1 Probing calmodulin - peptide interactions of different species with the same target peptide

Zsolt Dürvanger<sup>1</sup>, Tünde Juhász<sup>2</sup>, Károly Liliom<sup>2</sup>, Veronika Harmat<sup>1,3</sup>

1. Institute of Chemistry, Eötvös Loránd University, Budapest, Hungary

2. Institute of Enzymology, Research Centre for Natural Sciences, Hungarian Academy of Sciences, Budapest, Hungary

3. MTA-ELTE Protein Modelling Research Group, Budapest, Hungary

email: Drvanger@caesar.elte.hu

Calmodulin is a small calcium-binding protein that plays a key role in signal transduction pathways of all eukaryotic cells. The protein undergoes large conformational changes upon calcium binding, consequently its target binding hydrophobic residues become solvent accessible. These conformational changes create the possibility of calcium-dependent interactions with its target proteins. Some antimalarial drugs were reported to inhibit calmodulin action, suggesting that *Plasmodium falciparum* (a malaria causing parasite) calmodulin could be a target of antimalarial drug development. Though calmodulin is a highly conserved protein, structural differences between calmodulins from different organisms could provide a way of targeting calmodulin of disease causing organisms.

We solved the structure of mammalian calmodulin in complex with melittin, a well-known calmodulin binding model peptide, and refined the structure to 2.7Å resolution. Recently we determined the structure of *Plasmodium falciparum* calmodulin in complex with melittin, which provides the opportunity to compare the structures of calmodulin from two different organisms in complex with the same model peptide. Mammalian calmodulin shows 89% sequence identity with *P. falciparum* calmodulin, with the majority of the differing residues being on the surface, away from the protein – peptide interface. Despite the high sequence identity and the highly similar crystallization conditions, the structures of the two complexes differ significantly. While the orientation of the peptide is similar within the complexes, determined by a cluster of positively charged residues on the C-terminal part of the peptide, differences exist considering the backbone conformation and anchoring residues of the peptide. Moreover, the relative orientation of the two lobes of calmodulin shows a large difference, resulting in a more compact structure in the case of the mammalian calmodulin. Possible taxon-specific differences of the interactions are discussed.

## MS5-P2 Electron Nanocrystallography for Organic and Macromolecular Structure Determination

Tim Gruene<sup>1</sup>, Eric van Genderen<sup>1</sup>

I. Paul Scherrer Institute

email: tim.gruene@psi.ch

Electron crystallography has a long tradition in material science and also in 2D crystallography. Electrons interact much more strongly with matter and they cause about three orders of magnitude less radiation damage per diffracted quantum than X-rays. Crystals with a few to a few hundred nanometre thickness can be used for structure determination. These features have important applications for organic and (also macromolecular) structure determination: Often compounds, that represent themselves as powders to X-ray sources, consist of single nanocrystals suitable for structure determination with electron diffraction. In addition, crystal defects like disorder increase with crystal size so that data from nanocrystals can produce better quality models.

We recently exploited a quantum hybrid electron detector, Timepix, to determine the crystal structure of two organic compounds from single crystals at room temperature [1]. Here I will present our progress since this publication. We have improved the experimental procedure and developed methods to reduce systematic errors to such an extent that the data quality allows structure resolution with the default options of shelx. Both structure solution and refinement can be carried out simply with well established programs like shelx/shelxl. My presentation will include the effects of dynamic scattering that is often used as argument why electron diffraction was not practical to solve the structures of organic or macromolecular compounds.

Currently electron nanocrystallography is at a stage comparable with X-ray crystallography 3-4 decades ago. As we exploit a vast pool of experience from X-ray crystallography, electron nanocrystallography will soon become a new standard tool for biomolecular structure determination covering those systems that fail X-ray diffraction.

[1] van Genderen et al., *Acta Cryst* (2016), A72, 235-24

**Keywords:** Electron Nanocrystallography, Dynamic Scattering

## MS5-P3 Targeting Epigenetic Vulnerabilities of Cancer Cells by Exploiting Chromatin Structure and Chemistry

Zenita Adhikarsan<sup>1</sup>, Gabriela E. Davey<sup>1</sup>, Zhujun Ma<sup>1</sup>, Giulia Palermo<sup>2</sup>, Tina Riedel<sup>2</sup>, Benjamin S. Murray<sup>3</sup>, Alexey A. Nazarov<sup>4</sup>, Christian G. Hartinger<sup>5</sup>, Ursula Röthlisberger<sup>5</sup>, Paul J. Dyson<sup>2</sup>, Curt A. Davey<sup>1</sup>

1. School of Biological Sciences, Nanyang Technological University, 60 Nanyang Drive, Singapore 637551

2. Institut des Sciences et Ingénierie Chimiques, Ecole Polytechnique Fédérale de Lausanne (EPFL), CH-1015 Lausanne, Switzerland

3. Department of Chemistry, University of Hull, Cottingham Road, Hull, HU6 7RX, United Kingdom

4. Moscow State University, Department of Chemistry, Leninskie gory, 119991 Moscow, Russia

5. School of Chemical Sciences, University of Auckland, Private Bag 92019, Auckland 1142, New Zealand

email: zenita@ntu.edu.sg

Pronounced differences in the gene expression profiles between healthy and cancerous cells coincide with extensive epigenetic distinctions in chromatin, and yet the therapeutic landscape of chromatin is largely unexplored. We thus hypothesize that compounds capable of recognizing specific features of chromatin could enable targeting weak points of cancer cells [1-3]. Recent years have witnessed a resurgence of interest in developing new metal-based anticancer agents that are more effective and have fewer side effects, with focus shifting towards metals that are alternatives to the traditional platinum. We have so far characterized the nucleosome binding activity of over 50 different non-Pt drugs and therapeutic candidates, including various Ru-, Os-, Rh- and Au-based compounds. We observe that only one specific class of Ru agent preferentially forms DNA adducts, while the rest have an apparent preference for reaction at histone protein sites. In conjunction with studies on Pt compounds, this has revealed principles for selective targeting of different protein and DNA sites within chromatin and corresponding relationships to cytotoxicity and impact on cancer cell function. Moreover, newly designed binuclear antitumor compounds target a key regulatory site on the nucleosome, which alters chromatin structure in vitro and appears to kill cancer cells by interfering with chromatin dynamics. Beyond this, we have also discovered that two unrelated histone-targeting agents, in combination, display synergistic antitumor activity, and we can link this to a novel mechanical mechanism involving allosteric modulation in the nucleosome.

[1] C.A. Davey. 2015. Exposure to Metals Can Be Therapeutic. *Chimia*. **69**: 125-130.

[2] B. Wu\*, M.S. Ong\*, M. Groessl, Z. Adhikarsan, C.G. Hartinger, P.J. Dyson & C.A. Davey. 2011. A Ruthenium Antimetastasis Agent Forms Specific Histone Protein Adducts in the Nucleosome Core. *Chem. Eur. J.* **17**: 3562-3566.

[3] Z. Adhikarsan\*, G.E. Davey\*, P. Campomanes\*, M. Groessl, C.M. Clavel, H. Yu, A.A. Nazarov, H.F. Yeo, W.H. Ang, P. Dröge, U. Röthlisberger, P.J. Dyson & C.A. Davey. 2014. Ligand Substitutions between Ruthenium-Cymene Compounds Can Control Protein versus DNA Targeting and Anticancer Activity. *Nat. Commun.* **5**: 3462.

**Funding:** Ministry of Health National Medical Research Council (grant NMRC/1312/2011); Ministry of Education Academic Research Fund Tier 3 Programme (grant MOE2012-T3-1-001).

E-mail for correspondence: davey@ntu.edu.sg

**Keywords:** chromatin, nucleosome, metal-based compound, anticancer drug

## MS5-P4 Structure analysis of arylpiperazine derivatives displaying affinity towards 5-HT<sub>1A</sub> and 5-HT<sub>7</sub> receptors

Mateusz Jabłoński<sup>1</sup>, Katarzyna Rzęsikowska<sup>1</sup>, Justyna Kalinowska-Tłuścik<sup>1</sup>

1. Faculty of Chemistry, Jagiellonian University, Ingardena 3, 30 - 060 Kraków, Poland

email: jablonskikrystalografia@gmail.com

Serotonin (5-HT, 5-hydroxytryptamine) is one of the evolutionary oldest biogenic monoamines, which regulates various physiological functions in the human body. The serotonin receptor family was divided into 7 main classes among which, depending on the classification, at least 14 distinct classes may be distinguished. Six out of seven main classes belong to the G protein-coupled receptors (GPCRs) family. The member of the last main class, 5-HT<sub>7</sub> receptor, was found to be involved in regulation of temperature, circadian rhythm and proper functioning of memory. The lack of an accurate experimental structural data for most 5-HT receptor family members is a challenge in the process of designing selective and safe agonists and antagonists for individual classes. The selectivity problem is particularly important and visible in designing selective 5-HT<sub>1A</sub> and 5-HT<sub>7</sub> ligands, because the 5-HT<sub>7</sub> receptor shares a high sequence similarity to 5-HT<sub>1A</sub> receptor, especially in the binding pocket region.

Arylpiperazine is one of the most universal fragments found in ligands acting on various central nervous system receptors. Arylpiperazines are also a noteworthy scaffold component in 5-HT receptor ligands. Depending on the aryl part and its potential substituents, they can demonstrate diverse intrinsic activity and manifest different selectivity among the distinct 5-HT receptor classes. Substituents may variously affect the electronic features of the aromatic ring, which may result in different preferential mutual orientation of the aryl ring in regards with the piperazine moiety.

In this work, structures of selected long chain arylpiperazine derivatives are presented. Each compound contains a theophylline moiety connected to the piperazine with an alkyl linker. The crystal structure analysis is accompanied by molecular docking and structure-affinity relationship investigation.

**Keywords:** long chain arylpiperazines, serotonin receptors, structure-activity relationship, molecular docking

## MS5-P5 Identification of inhibitors for the DEDDh family of exonucleases and a unique inhibition mechanism revealed by crystal structure analysis of CRN-4 bound with MES

Yu-Yuan Hsiao<sup>1</sup>, Kuan-Wei Huang<sup>1</sup>, Kai-Cheng Hsu<sup>2</sup>, Lee-Ya Chu<sup>3</sup>, Jinn-Moon Yang<sup>4</sup>, Hanna S. Yuan<sup>3</sup>

1. Institute of Molecular Medicine and Bioengineering, National Chiao Tung University, Hsinchu 30068, Taiwan.
2. Graduate Institute of Cancer Biology and Drug Discovery, College of Medical Science and Technology, Taipei Medical University, Taipei, Taiwan.
3. Institute of Molecular Biology, Academia Sinica, Taipei, Taiwan 11529, ROC.
4. Institute of Bioinformatics and Systems Biology, National Chiao Tung University, Hsinchu, 30050, Taiwan.

email: mike0617@nctu.edu.tw

**ABSTRACT** The DEDDh exonuclease family contains more than 7000 members which play essential roles in nucleic acids metabolism in prokaryotes and eukaryotes. Recently, some DEDDh exonucleases proved to have important functions in viral infection and replication, such as NP exonuclease of Lassa fever virus (LV NP), can serve as antiviral drug targets. However, there is no systematic characterization of inhibitors for the DEDDh exonucleases. Here, we used two DEDDh exonucleases, RNase T and CRN-4, as model systems to identify potential DEDDh exonucleases inhibitors, including PV6R, PCMPS, DTNB and ATA. IC50 value analysis have shown PCMPS, DTNB and ATA, can inhibit the exonuclease activity of LV NP efficiently. Moreover, we determined the crystal structure of CRN-4 in complex with a weak inhibitor, 2-morpholin-4-ylethanesulfonate acid (MES). MES induces a conformational change in the active site of CRN-4, preventing substrate degradation. Combining structural information and molecular docking of inhibitors in CRN-4 help us to identify important inhibitor-binding residues and provide clues to design more effective inhibitors for DEDDh exonucleases. Taken together, both biochemical and structural studies on potential inhibitors of the DEDDh exonucleases are helpful for antiviral therapy.

**Keywords:** Nuclease, Inhibitors, Protein-inhibitor complex, crystal structure, nuclease inhibitor, antiviral drug.

## MS5-P6 Industrial integration at the French national synchrotron facility SOLEIL

Tiphaine Huet<sup>1,2</sup>, Gilbert Bey<sup>3</sup>, Laurent M. Vuillard<sup>2</sup>, Gilles Ferry<sup>2</sup>, Leonard M.G. Chavas<sup>1</sup>, Andrew W. Thompson<sup>1</sup>

1. Synchrotron SOLEIL, L'Orme des Merisiers, Saint-Aubin - BP 48, 91192 Gif-sur-Yvette Cedex, France.
2. Institut de Recherche SERVIER, 125 chemin de ronde, 78290 Croissy-sur-Seine, France.
3. NovAliX-LBS3, Synchrotron SOLEIL, SOLEIL L'Orme des Merisiers, Saint-Aubin - BP 48, 91192 Gif-sur-Yvette Cedex, France.

email: tiphaine.huet@synchrotron-soleil.fr

Synchrotron SOLEIL is a French national synchrotron facility, located on the Saclay Plateau in the Paris suburbs. It is a multi-disciplinary instrument and a research laboratory, with the mission to provide research programs, to develop state-of-the-art instrumentations targeted to specific experiments, and to make those available to the scientific community. SOLEIL differentiates itself from other complementary synchrotron facilities as a unique tool for performing both academic research and industrial applications developed on site and across a wide range of disciplines among which physics, biology, and chemistry. Based on a state-of-the-art synchrotron source, both in terms of brilliance and stability, SOLEIL is used by over 5,000 researchers coming from France and abroad.

Industrial applications at SOLEIL have recently been reinforced by the opening of an industrial laboratory specialised in structural biology within SOLEIL, working in the vicinity of the biology village and macromolecular crystallography *PROXIMA* beamlines. Both *PROXIMA-1* and *PROXIMA-2A* end-stations provide with the required instrumentation for high-throughput diffraction measurements on crystallographic samples. The presence of a structural biology unit from the industrial group SERVIER (LBS3) laboratory in close proximity to these instruments offers to SOLEIL's industrial collaborators both rapid access beam time and on site expertise. This proximity allows industrial applications to develop fast and practical solutions to redundant problems in sample preparation for structural studies, reduce their product-to-market downtimes and enhance their R&D programmes.

**Keywords:** industry, drug design,



**MS5-P7** Crystal structures of *Trypanosoma brucei* hypoxanthine \u2013 guanine \u2013 xanthine phosphoribosyltransferase

David Terán<sup>1</sup>, Dana Hocková<sup>2</sup>, Michal Česnek<sup>2</sup>, Dianne T. Keough<sup>1</sup>, Luke W. Guddat<sup>1</sup>

1. The School of Chemistry and Molecular Biosciences, The University of Queensland, Brisbane, 4072 QLD, Australia

2. Institute of Organic Chemistry and Biochemistry, Academy of Sciences of the Czech Republic, v.v.i. Flemingovo nám. 2, CZ-166 10 Prague 6, Czech Republic

email: david.teranmera@uq.net.au

Human African Trypanosomiasis (HAT) is a deadly infectious disease caused by the protozoan parasite *Trypanosoma brucei*. Due to the debilitating side-effects and emerging resistance to the current drugs available for this disease, new therapeutic targets and medications urgently need to be found. One potential new target is 6-oxopurine phosphoribosyltransferase (PRTase) an enzyme in the purine salvage pathway, whose activity appears to be essential for the production of nucleoside monophosphates required for incorporation into DNA and RNA in protozoan parasites. To begin evaluation of this enzyme as a potential drug target we have shown it can utilize the three naturally occurring 6-oxopurine bases, guanine, hypoxanthine and xanthine as substrates. Hence, we classify the enzyme as a HGXPRTase. Acyclic nucleoside phosphonates (ANPs) have previously been identified as a class of compounds that inhibit human and *Plasmodium* HG[X]PRTases. We have demonstrated that several acyclic nucleoside phosphonates (ANPs) are good inhibitors of this enzyme with  $K_i$  values as low as 2  $\mu$ M. Five crystal structures of *Tbr*HGXPRT (1.5-2.9 Å resolution) have been determined. These are in complex with products of reaction, GMP and IMP and with three ANPs. Two of the ANPs that bind to the enzyme induce an unusual conformational change at the location where pyrophosphate, a product of the reaction, would be expected to bind to the enzyme. Such a change has not been observed in structures of the human enzyme suggesting a possible route to selective inhibition.

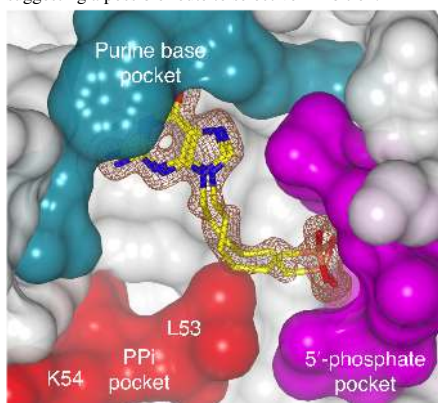


**Figure 1.** Surface structure representation of the *Tbr*HGXPRT.MIC-612 complex.  $F_o - F_c$  "omit" electron density for MIC-612 is overlaid.

**Keywords:** *Trypanosoma brucei*, purine salvage, acyclic nucleoside phosphonates

**MS5-P8** Needle Finder: A search engine for retrieving and evaluating hidden structural features and much more.

Wilhelm Stark<sup>1</sup>, Nunzio Putrino<sup>2</sup>, Karin Rüegg<sup>3</sup>, Manfred Drozd<sup>4</sup>,  
Dominique Brodbeck<sup>1</sup>, Markus Degen<sup>1</sup>

1. Fachhochschule Nordwestschweiz
2. Future-IT-Com
3. Tradeware
4. peakmarks

email: wilhelm.stark@fhnw.ch

How can we retrieve hidden structural features in the world of bio-molecular structures in short time, without inspecting every single structure file manually? The task would turn in an impossible mission, if we do not merge together a powerful infrastructure, great ideas and improvements of data quality. Especially, if we take into account the steadily increasing amount of data.

We are developing a tool box, which allows users to find the details of a piece of information within over a billion rows secure, fast and reliable in minutes if not seconds. For this reasons we put the sample on two real-world questions. They consist in retrieving well defined amino acid patterns we know they must exist. But before we run the tests, we hadn't a clue where to find them in the over 100'000 protein structures. The content driven relational database is the core part of our tool box. Beside the facts that the programs have found the exact name of the PDB-files, they also spotted – as welcomed side effects – the exact position within each protein structure, the sets of coordinates, atom serial number and much more. Moreover, the program also listed exactly those rows which stored inconsistent patterns, instead of the expected resolutions of the protein structures. Let's estimate the time to be spent for the same tasks, in case we were requested to do it without the help of the needle finder. For the purpose of the calculation we establish as a basic assumption that it takes us one minute for the download of each PDB-file including a brief inspection of the file content. Having more than 100'000 PDB coordinate files to inspect by an eight hour working day we need more than 200 working days. The estimation does not include to keep track and to trace what we have done so far, not mentioning that any kind of calculation has been done. We simply cannot afford it any longer. What's about you?

inspect	Manual	download	and
	Needle-Finder		
1 File	1 minute		
100'000 Files	200 working days		
(8h/day)	<b>5 minutes by sequential execution;</b>		
less			

**10seconds by paallel processes**

**MS5-P9** Structural and functional study of the antibody against influenza viruses' RNA polymerase to discover a new medicine for the influenza disease

Kanako Sugiyama<sup>1</sup>, Hisashi Yoshida<sup>1</sup>, Takeshi Urano<sup>2</sup>,  
Sam-Yong Park<sup>1,3</sup>

1. Influenza Drug Design Project, Kanagawa academy of science and technology
2. Department of Biochemistry, Shimane University School of Medicine
3. Department of Medical Life Science, Yokohama-city university

email: pp-sugiyama@newkast.or.jp

As you know, the influenza virus causes the influenza disease. Especially some viruses called the high-pathogenic influenza virus leads death of a large number of farm animals and could be a factor of a human pandemic if it modified to have the ability of the infection to humans. We tried to discover a new medicine against influenza viruses. And then we found the structure of the binding region between RNA polymerase subunits of the H1N1 influenza A virus few years ago. The results of our study published in the papers below.<sup>1,2</sup>

After that, we are studying more information about the RNA polymerase. We made some new antibodies against the RNA polymerase. One of it can repress the growth of several types of influenza A viruses. We introduce the structural and functional study of the anti-RNA polymerase antibody. The results of this research show a new possibility of a medicine against all kind of influenza A viruses.

1 Sugiyama, K. *et al.* Structural insight into the essential PB1-PB2 subunit contact of the influenza virus RNA polymerase. *The EMBO journal* **28**, 1803-1811 (2009).

2 Obayashi, E. *et al.* The structural basis for an essential subunit interaction in influenza virus RNA polymerase. *Nature* **454**, 1127-1131, (2008).

**Keywords:** Influenza virus, RNA polymerase, Antibody, Crystal structure

than

**Keywords:** Biological Structures, information retrieval, bigdata, database,

## MS5-P10 Study of metal coordination sphere parameters derived from the open access Crystallography Open Database

Antanas Vaitkus<sup>1</sup>, Andrius Merkus<sup>1</sup>, Saulius Gražulis<sup>1,2</sup>

1. Vilnius University Institute of Biotechnology, Saulėtekio av. 7, LT-10222 Vilnius, Lithuania

2. Vilnius University Faculty of Mathematics and Informatics, Naugarduko 24, LT-03225 Vilnius, Lithuania

email: antanas.vaitkus90@gmail.com

Metal coordination sites in proteins have been a subject of research for several decades now. Numerous works with the interest in specific chemical elements as well as wider scope databases have been published both on-line and off-line. Usually one of the two approaches is taken when compiling the datasets – the results are either calculated directly from the protein structures or they are derived from the structures of small molecules. In most cases the same data processing algorithms can be applied with minimal modifications; however, it is the data source that plays a far greater role than it appears at first glance.

The most popular protein structure data source for this kind of calculations is the Protein Data Bank (PDB) database. Among the benefits of using the PDB is its open access nature that allows any interested parties to check and reproduce the published results. However, the PDB is not drawback-free either; for example, grouping structures by the type of coordinating metal often results in unsatisfactory sample sizes.

The use of small molecule structure data sources presents an almost mirror image of the pros and cons – the number of high resolution structures containing metal coordination spheres is much greater, but all of the data sources used in this type of research so far are proprietary databases and as a result makes the research unreproducible without acquiring the database license.

To overcome this limitation the open access Crystallography Open Database (COD) was used as the source to automatically compile a set of metal coordination sphere parameters. The entire COD was scanned for structures containing metal coordination spheres and the selected entries were further processed by calculating coordination parameters such as the coordination number, ligand-metal-ligand angles and metal-ligand distances, as well as comparing the configuration of the coordination sphere with a list of idealised geometry templates.

The gathered results are accessible via the MySQL database interface as well as an interactive website where the coordination sphere information can be viewed grouped by a combination of various parameters like the chemical type of the coordinating metal, the chemical type of the coordinated ligands and the best fitting idealised geometry. An option to produce a normal distribution mixture model of the examined interatomic distances and angles is also provided.

**Keywords:** Metal coordination spheres, database

## MS5-P11 Structural and functional studies of the *Mycobacterium tuberculosis* VapBC30 toxin-antitoxin system

Sang Jae Lee<sup>1</sup>, In-Gyun Lee<sup>1</sup>, Bong-Jin Lee<sup>1</sup>

1. The Research Institute of Pharmaceutical Sciences, College of Pharmacy, Seoul National University

email: sjlee33@snu.ac.kr

*Mycobacterium tuberculosis* is the causative agent of tuberculosis and contains an unusually high number of VapBC systems. The VapBC system, which is implicated in dormant state formation, virulence, and stress response, is an interesting target for the rational design of an antimicrobial peptide against tuberculosis. Here, we report that the *M. tuberculosis* VapC30 toxin regulates cellular growth through both magnesium and manganese ion-dependent ribonuclease activity and is inhibited by the cognate VapB30 antitoxin. We also determined the 2.7-Å resolution crystal structure of the *M. tuberculosis* VapBC30 complex, which revealed a novel process of inactivation of the VapC30 toxin via swapped blocking by the VapB30 antitoxin. Our study on *M. tuberculosis* VapBC30 leads us to design two kinds of VapB30 and VapC30-based novel peptides which successfully disrupt the toxin-antitoxin complex and thus activate the ribonuclease activity of the VapC30 toxin. Our designed peptides mimic the helical regions of the VapB30 or VapC30 in the heterodimer interface of the VapBC30 complex, and they were capable of disrupting the interactions between VapBC30 complex *in vitro*. Our approach may form a foundation for the design of antimicrobial peptides targeting toxin-antitoxin systems, and the designed peptides may prove to be viable candidates in the development of anti-tuberculosis drugs.

**Keywords:** Rv0623, Rv0624, toxin-antitoxin systems, VapBC30, antimicrobial peptides, *Mycobacterium tuberculosis*

## MS5-P13 Neutron crystallographic studies of cancer-related human carbonic anhydrase IX reveal details of hydrogen-bonding in inhibitor binding.

Zsö Fisher<sup>1</sup>, Katarina Koruza<sup>2</sup>, Brian Mahon<sup>3</sup>, Cynthia Okoh<sup>3</sup>, Wolfgang Knecht<sup>4</sup>, Robert McKenna<sup>3</sup>

1. Scientific Activities Division, European Spallation Source, Lund, Sweden
2. Biology Department, Lund University, Lund, Sweden
3. Department of Biochemistry and Molecular Biology, University of Florida, Gainesville FL, USA
4. Biology Department, Lund Protein Production Platform, Lund University, Lund, Sweden

email: zoe.fisher@esss.se

Human carbonic anhydrase IX (HCA IX) expression in aggressive tumours, under hypoxic conditions, is an indicator of metastasis and poor cancer patient prognosis. As such, HCA IX has emerged as an important cancer imaging, diagnostic, and therapeutic target. Medicinal efforts to develop specific inhibitors for HCA IX are complicated by the presence of 14 other HCA isoforms that share both a common structural fold and exhibit high sequence similarity. It has been well established that ligand (inhibitor) binding to a target protein is mediated through numerous interactions that may include: H-bonding directly and/or through intervening waters, electrostatic interactions with charged or polar amino acid side chains, metal coordination, energetic changes through water displacement, aromatic stacking, or other hydrophobic interactions. As the magnitude of X-ray scattering from an atom depends on the atomic number (Z) for that element, the light atoms in protein crystals contribute very little, if at all, to X-ray scattering data, making the observation of hydrogen atoms almost impossible. Neutron diffraction offers a highly complementary approach in that the neutrons are scattered from atomic nuclei of all elements to a similar extent. In practice this means that the nuclear density maps for C, N, D (the isotope of H), and O atoms all appear to a similar extent, even at medium (~2 Å) resolution. In this way neutron crystallography offers a powerful approach to observe the details of ligand binding that involves H atoms. Our goal is to determine the atomic details of new promising drug leads, complexed to HCA IX, by neutron protein crystallography. Saccharin was recently identified as a promising lead compound in that it demonstrates HCA IX specificity. Comparing neutron crystal structures of unbound and inhibitor-bound HCA IX provides a unique opportunity to directly investigate how saccharin binds through H-bonding, the role of water displacement, and how the making/breaking of H-bonds modulates binding and isoform specificity. It is expected this fine structural detail, that is unique to neutron crystallography, can then be applied for rational drug design.

**Keywords:** hydrogen bond, neutron crystallography, carbonic anhydrase

## MS6 Molecular machines and big complexes

Chairs: Christoph Müller, Miquel Coll

### MS6-P1 Solving the structure of a mammalian acylaminoacyl-peptidase

Anna Kiss-Szemán<sup>1</sup>, Veronika Harmat<sup>1,2</sup>, Dóra K. Menyhárd<sup>2</sup>

1. Eötvös Loránd University, Institute of Chemistry, Laboratory of Structural Chemistry and Biology address: Pázmány Péter sétány 1/A, H-1117, Budapest, Hungary tel.:(+36-1) 372-2500/6547
2. MTA-ELTE Protein Modelling Group, address: Pázmány Péter sétány 1/A, H-1117, Budapest, Hungary tel.:(+36-1) 372-2500/6547, fax: (+36-1) 372-2592 web: prof.chem.elte.hu

email: kszemanna@chem.elte.hu

Acylaminoacyl-peptidases (AAP) catalyse the hydrolysis of oligopeptides, while they function as exopeptidases (processing N-terminal acylated peptides) and endopeptidases too. The mammalian enzyme – present also in the human liver – is a key protein in the upstream regulation of the proteasome [1]. For members of its enzyme family two basic ways of substrate selection have been discovered so far: flexible domain movement between opened and closed form, or multimerization of rigid monomers. The formation of multimers is linked to the shielding of the "sticky edge" of a  $\beta$ -sheet - to avoid aggregation. A. *pernix* AAP forms dimers capable for a gating mechanism by domain movements providing size selection of the substrates; in contrast, in P. *horikoshii* AAP formation of hexamers with a complex channel system is responsible for  $\beta$ -edge shielding and for the size selection too [2]. The goal of our study is to determine how the tetrameric structure of the mammalian AAP is formed: whether to shield the  $\beta$ -edge, or size selection or both. The mammalian enzyme was purified from porcine (*Sus scrofa*) liver. We found two crystal forms with their unit cell dimensions being similar: 1) The first reproducible crystals were thin plates diffracting to 5.5 Å. 2) Using additives a new crystal form was obtained diffracting to 2.8 Å, but pseudomerohedrally twinned. The crystallographic phase problem was solved by molecular replacement, using the structure of PhAAP hydrolase domain and a 7-bladed polyalanine propeller domain. Model building and refinement is in progress. Characteristic interactions of the "sticky edge" of a hydrolase domain are formed with the propeller domain of the neighbouring monomer were identified as well as specific interactions responsible for tetramer formation. We propose the role of the insertion found in the third blade of the propeller to be that of shielding the direct entrance to the catalytic triad. This study was supported by BioStruct-X (No.283570) of European Community's 7th Framework Programme; the MedInProt program of the Hungarian Academy of Sciences; OTKA grants NK101072 and PD101095. We acknowledge ESRF and EMBL-Hamburg for providing

synchrotron radiation beamtime.

[1] Palmieri G. et al. *PLoS ONE* 6(10):e25888 (2011)[2] Menyhard D.K. et al. *J Biol Chem* 288 (24):17884-94 (2013)

**Keywords:** acylaminoacyl-peptidase,  $\beta$ -edge aggregation, multimerization, substrate size selection

## MS6-P2 Structural characterization of dihydroorotase domain in yeast CAD multienzyme

Yujung Jeon<sup>1,2</sup>, Ian Ross<sup>2</sup>, Michael Landsberg<sup>1</sup>, Ben Schultz<sup>1</sup>, Ben Hankamer<sup>2</sup>, Bostjan Kobe<sup>1,2</sup>

1. School of Chemistry and Molecular Biosciences, The University of Queensland

2. Institute of Molecular Biosciences, The University of Queensland

email: yujung.jeon@uqconnect.edu.au

Carbamoyl phosphate synthetase II (CPS II), aspartate transcarbamoylase (ATC), and dihydroorotase (DHO) are three enzymes involved in the first three steps of de novo pyrimidine biosynthesis. In bacteria, these proteins are present in individual enzymes and function independently; however, in eukaryotes they are often found in a covalently linked form. In mammals, the enzymes are present as a large, multienzyme complex called CAD (CPS II-ATC-DHO, 243 kDa) and this complex has been proposed to form a homo-hexamer of ~1.5 MDa in the cellular environment. It is known that over-expression of CAD is required for proliferation and is associated with tumour cell development; thus, understanding the structural basis of the complex will be useful in cancer biology.

CAD in yeast, called URA2, is a bifunctional protein that has CPS II and ATC activity only. The DHO domain is substituted with pseudo-DHO amino acids sequence, which has lost its enzyme activity. The separately translated active DHO (URA4) compensates this loss of function, and this is homologous to bacterial type II DHO. This suggests the sequential gene duplication and fusion events occurred for CAD; thus, studying yeast URA2 may help understanding the molecular evolution. Crystal structure of the pseudo-DHO domain was determined at high resolution (1.2 Å) and biochemical studies such as enzyme assay, MALS, and SAXS were performed. The protein presents in equilibrium between dimer and hexamer in solution, and this suggests its potential role of the domain in hexamerisation of the CAD complex in cellular environment despite its inactivity.

**Keywords:** enzyme

**MS6-P3 X-ray Crystallographic Analysis of the Chromatosome**Sivaraman Padavattan<sup>1</sup>, Zenita Adhireksan<sup>1</sup>, Qiuye Bao<sup>1</sup>, Curt A Davey<sup>1</sup><sup>1</sup>. School of Biological Sciences, Nanyang Technological University, 60 Nanyang Drive, Singapore 637551

email: spadavattan@ntu.edu.sg

The packaging of eukaryotic DNA into chromatin consists of the nucleosome as the basic repeating unit. The nucleosome has a core region, comprised of ~146 base pairs of DNA wrapped around a protein octamer of core histones, in addition to a variable length of linker DNA. The linker DNA connecting adjacent nucleosome core regions is on average ~50 base pairs in length in higher eukaryotes and can be occupied by a linker histone. By modulating chromatin structure, dynamics and recognition by other nuclear factors, the core and linker histones regulate genomic function. The first atomic model of the nucleosome core (particle) was published in 1997 [1], paving the way for the structural solution of a great variety of nucleosome core constructs composed of variant/modified histones and different DNA sequences [2,3]. This has consequently revolutionized our understanding of nucleosome activity, and yet 19 years later we are still lacking an atomic level understanding of how linker histones interact with nucleosomes.

In mammals, there are 11 linker histone variants, which can display cell type and cellular status dependent expression, site-specific localization in the nucleus as well as specific interactions with different nuclear factors to foster gene-specific regulation. In addition, the linker histones can undergo an enormity of post-translational modifications that further expand the regulatory landscape. Nonetheless, the general function of the linker histones is largely that of compacting nucleosomes into condensed chromatin states, which are generally repressive to gene expression. An atomic model of the chromatosome, the minimal assembly of a nucleosome with a linker histone, could significantly advance our understanding of chromatin function, and we present here the first X-ray crystal structure of a chromatosome [4].

[1] K. Luger, A.W. Mäder, R.K. Richmond, D.F. Sargent & T.J. Richmond. 1997. *Nature*. 389: 251-60.

[2] S. Tan & C.A. Davey. 2011. *Curr. Opin. Struct. Biol.* 21: 128-136.

[3] E.Y.D. Chua\*, D. Vasudevan\*, G.E. Davey, B. Wu & C.A. Davey. 2012. *Nucleic Acids Res.* 40: 6338-6352.

[4] Z. Adhireksan\*, Q. Bao\*, S. Padavattan, C.A. Davey. In preparation.

**Funding:** Ministry of Education Academic Research Fund Tier 2 (grant MOE2015-T2-2-089); Ministry of Education Academic Research Fund Tier 3 Programme (grant MOE2012-T3-1-001).

E-mail for correspondence: davey@ntu.edu.sg.

**Keywords:** Chromatin, Chromatosome, Nucleosome and Linker histones

**MS6-P4 Unique base pairing interactions at the third position of codon-anticodon helix**Alexey Rozov<sup>1</sup>, Natalia Demeshkina<sup>1</sup>, Eric Westhof<sup>2</sup>, Marat Yusupov<sup>1</sup>, Gulnara Yusupova<sup>1</sup><sup>1</sup>. Institut de génétique et de biologie moléculaire et cellulaire, Illkirch, France<sup>2</sup>. Institut de Biologie Moléculaire et Cellulaire, Université de Strasbourg, Strasbourg, France

email: rozov@igbmc.fr

Post-transcriptional modifications at the wobble position of tRNAs play a substantial role in deciphering the degenerate genetic code on the ribosome. The number and variety of modifications suggest different mechanisms of action during mRNA decoding of which only a few were described so far. Uridine at the wobble positions of various tRNAs is almost always modified in bacteria and eukaryotes<sup>1</sup>. In many cases tRNAs with the modified uridines read two codons ending with purines A or G and in some rare cases modifications help to recognize all four nucleotides A, G, C and U at the third codon position<sup>2</sup>. Previously it was shown that preferential form of the third wobble pair with a fully modified uridine approached a standard Watson-Crick-like geometry if this uridine was paired with guanosine<sup>3,4</sup>. Here we describe a new type of a base pair at the third wobble position of a codon-anticodon duplex in the 70S ribosome decoding center. Our structures demonstrate that the reversed "wobble" pair mnm<sup>5</sup>s<sup>2</sup>U34•G(+6) adopts its own geometry, different from the standard G34•U(+6) pair<sup>5</sup> at the third codon-anticodon position. We show that mnm<sup>5</sup>s<sup>2</sup>U forms an unusual pair with guanosine at the wobble position that expands general knowledge on the degeneracy of the genetic code and specifies a powerful role of tRNA modifications in translation.

1. Machnicka, M.A. et al. MODOMICS: a database of RNA modification pathways--2013 update. *Nucleic Acids Res* **41**, D262-7 (2013).

2. Grosjean, H., de Crécy-Lagard, V. & Marck, C. Deciphering synonymous codons in the three domains of life: co-evolution with specific tRNA modification enzymes. *FEBS Lett* **584**, 252-64 (2010).

3. Vendeix, F.A. et al. Human tRNA(Lys3)(UUU) is pre-structured by natural modifications for cognate and wobble codon binding through keto-enol tautomerism. *J Mol Biol* **416**, 467-85 (2012).

4. Weixlbaumer, A. et al. Mechanism for expanding the decoding capacity of transfer RNAs by modification of uridines. *Nat Struct Mol Biol* **14**, 498-502 (2007).

5. Crick, F.H. Codon-anticodon pairing: the wobble hypothesis. *J Mol Biol* **19**, 548-55 (1966).

**Keywords:** translation, ribosome, decoding

**MS6-P5 Helical Foldamers as Hosts for Rod-like Guests****Keywords:** helical foldamers, oligourethanes, X-ray studiesBarbara Wicher<sup>1</sup>, Xiang Wang<sup>1</sup>, Yann Ferrand<sup>1</sup>, Ivan Huc<sup>1</sup>

1. Univ. Bordeaux, CBMN, UMR 5248, Institut Européen de Chimie Biologie, 2 rue Escarpiot 33607 Pessac, France and CNRS, CBMN, UMR 5248, Institut Européen de Chimie Biologie, 2 rue Escarpiot 33607 Pessac,

email: b.wicher@iecb.u-bordeaux.fr

Biomolecular machines, such as kinesin or the ribosome, have always been a paragon for chemists trying to obtain more and more advanced supramolecular architectures. During decades of research, organic chemists have developed a wide range of prototypes of artificial molecular machines. However, the design and synthesis of molecules able to execute particular tasks remains a challenge.<sup>[1]</sup>

During the course of our studies we have synthesized aromatic oligoamide foldamers able to fold and self-assemble into double helices. Their inner cylindrical hollow was designed to be complementary to linear oligourethanes around which the helices can wind.<sup>[2,3]</sup> Kinetic studies showed that these foldamers can shuttle along rod-like guest molecules in a sort of sliding motion with varying rates according to the length of the rods. We showed that the molecular structure of the guest determines the supramolecular pathway used by the helical shuttle.

In this poster, we will present several crystal structures of an oligoamide double helix forming pseudo-rotaxane architectures upon winding around rod-like guest molecules. X-ray studies revealed that helix-rod intermolecular hydrogen bonds and also the shape and size of the internal cavity of the double helix can adapt to accommodate differences in the structure of guest molecules. This flexibility allows the same oligoamide helix to be an excellent host for a large variety of guest molecules.

[1] Erbas-Cakmak et al (2015), Chem. Rev. 115, 10081-10206.

[2] Gan et al (2011), Science, 331, 1172-1175.

[3] Ferrand et al (2011), Angew. Chem. Int. Ed. 50, 7572-7575.

This work was supported by European Research Council under the European Union's Seventh Framework Programme (grant agreement no. ERC-2012-AdG-320892, post-doctoral fellowship to B.W.)

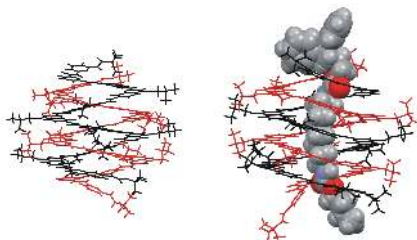


**Figure 1.** Oligoamide in a double helix form without (left) and with (right) rod-like guest molecule.



## MS6-P6 X-ray structure of *Triatoma virus* empty capsid: insights into the mechanism of uncoating and RNA release in dicistroviruses

Rubén Sánchez-Eugenía<sup>1</sup>, Aritz Durana<sup>1</sup>, Ibai Lopez-Marijuan<sup>1</sup>, Gerardo A. Martí<sup>2</sup>, Diego M.A. Guérin<sup>1,3</sup>

1. Biofisika Institute (UPV/EHU, CSIC), Bº Sarriena s/n, Leioa 48940, Bizkaia, Spain

2. Centro de Estudios Parasitológicos y de Vectores (CEPAVE-CCT-La Plata-CONICET-UNLP), Boulevard 120 e/61 y 62, 1900 La Plata, Argentina

3. Departamento de Bioquímica y Biología Molecular, Facultad de Ciencia y Tecnología, Universidad del País Vasco (UPV/EHU), Bº Sarriena S/N, 48940 Leioa, Bizkaia, Spain.

email: r.sanchez.eugenia@gmail.com

In viruses, uncoating and RNA release are two key steps of successfully infecting a target cell. During these steps, the capsid must undergo the necessary conformational changes to allow RNA egress. Despite their importance, these processes are poorly known in the *Dicistroviridae* family. Here we solved by X-ray crystallography the atomic structure of *Triatoma virus* empty particle (PDB code 5L7O), which is the resulting capsid after RNA release. It is observed that the overall shape of the capsid and of the three individual proteins is maintained in comparison with the mature virion. Furthermore, no channels indicative of RNA release are formed in TrV empty particle. However, the most prominent change in the empty particle in comparison with the mature virion is the loss of order in the N-terminal domain of VP2 protein. In mature virions this domain swaps with its two-fold related VP2 N-terminal domain located in an adjacent pentamer stabilizing the binding between pentamers. The loss of these interactions allows us to propose that RNA release may take place through the partial disassembly of TrV capsid into pentameric subunits. The fewer number of stabilizing interactions between pentamers and the lack of formation of new holes support this model. This model differs from the currently accepted model for rhinoviruses and enteroviruses in which genome externalization occurs by the extrusion of the RNA through capsid channels.

**Keywords:** Dicistroviridae, RNA release, uncoating, capsid disassembly

## MS7 Protein & glycobiology structure determination

Chairs: Jon Agirre, Gerlind Sulzenbacher

## MS7-P1 Crystal structure and biophysical characterization of ligand-free and -bound RNases 4 and 6, members of the human RNase A superfamily

Jacinthe Gagnon<sup>1</sup>, Sabina Sarvan<sup>2</sup>, Donald Gagné<sup>1</sup>, Jean-François Couture<sup>2</sup>, Miljan Simonović<sup>3</sup>, Nicolas Doucet<sup>1</sup>

1. INRS - Institut Armand-Frappier, Canada

2. Department of Biochemistry, Microbiology and Immunology, Faculty of Medicine, University of Ottawa, Canada

3. Department of Biochemistry and Molecular Genetics, University of Illinois at Chicago, U.S.A.

email: jacinthe.gagnon@iaf.inrs.ca

In addition to strictly conserved ribonucleolytic activities, ribonuclease (RNase) A superfamily members have been associated to a variety of biological functions such as anti-bactericidal, cytotoxic, angiogenic, immunosuppressive, anti-tumoral and/or anti-viral activities. Human RNase A members comprise eight rapidly evolving homologous enzymes with varying degrees of structural similarity and enzymatic activities. While the crystallographic and/or NMR structures of RNases 1-5 and 7 have already been elucidated, the structural characterization of RNases 6 (or RNase k6) and RNase 8 are still unresolved.

In this study, we have successfully crystallized human RNase 6 in presence of phosphate anions. We compare its crystalline structure with RNase A (bovine) and RNase 4. Despite many structural similarities with RNase A, we emphasized on a number of differences that may account for the different functions among the human RNases. Moreover, we have identified the phosphate binding residues and ionic binding architecture within the catalytic pocket of RNase 6. A new phosphate-binding site located within loop 4 and involving His67 was also uncovered.

The biophysical properties of RNases 4 and 6 were analyzed via NMR titration and isothermal titration calorimetry with two different ligands: 3'-UMP and 5'-AMP. The results were compared to RNase A and correlated to their unliganded crystal structures and their structures in presence of the ligand 5'-AMP.

Resolving the crystal structure of human RNases provides valuable insights into understanding its biological function in human, which may find applications in various fields such as drug design.

**Keywords:** Crystal structure, human ribonucleases, RNase 4, RNase 6, enzymes, ligand

**MS7-P2** Klf4 and Grhl1: Two distinct ways of achieving DNA target site recognitionUdo Heinemann<sup>1</sup>, Qianqian Ming<sup>1</sup>, Yvette Roske<sup>1</sup>, Anja Schütz<sup>1</sup>

1. Max Delbrück Center for Molecular Medicine, Berlin

email: heinemann@mdc-berlin.de

Cell- and tissue-specific gene expression is controlled at the transcriptional and translational levels. Transcription factors bind to target sites on double-stranded DNA that are characterized by distinct nucleotide sequence motifs. Recently, we have studied two human transcription factors, Klf4 and Grhl1, that appear to utilize different molecular strategies for achieving target site recognition.

Krueppel-like factor-4 (Klf4) belongs to a family of zinc-finger transcription factors and is indispensable for the terminal maturation of epithelial tissues (1). In combination with the transcription factors Sox2, Oct4 and c-Myc, Klf4 has the potential to revert differentiated cells to a pluripotent cell-like state (2). The crystal structure of the Klf4 zinc finger region bound to target DNA shows the arrangement of three CCHH zinc fingers in the DNA major groove and the formation of multiple DNA sequence specific hydrogen bonds between protein side chains and DNA base pairs (3).

Mammalian Grainyhead-like-1 (Grhl1) is grouped within a family of transcription factors along with Grhl2, Grhl3 and the CP2 factors for which no structural information was available until recently. These protein play important roles in early embryogenesis, have documented functions in adult mice and are linked to human disease (4, 5). The crystal structure of the DNA-binding domain of human Grhl1 (Grhl1 DBD) unexpectedly revealed a fold closely resembling the central tumor suppressor p53. Subsequent structure analysis of the DNA target site-bound Grhl1 DBD showed a mode of DNA sequence readout that relies on a small number of direct hydrogen bonds between the protein and DNA bases and additional contacts to the DNA backbone. This binding mode is fully supported by DNA binding assays using mutated Grhl1 variants and DNA target sites.

## References

1. Shields, J.M. & Yang, V.W. (1998) *Nucleic Acids Res.* 26, 796.
2. Takahashi, K., Tanabe, K., Ohnuki, M., Narita, M., Ichisaka, T., Tomoda, K. & Yamanaka, S. (2007) *Cell* 131, 861.
3. Schuetz, A., Nana, D., Rose, C., Zocher, G., Milanovic, M., Koenigsmann, J., Blasig, R., Heinemann, U. & Carstanjen, D. (2011) *Cell. Mol. Life Sci.* 68, 3121.
4. Rifat, Y., Parekh, V., Wilanowski, T., Hislop, N.R., Auden, A., Ting, S.B. & Jane, S.M. (2010) *Dev. Biol.* 345, 237.
5. Wang, S. & Samakovlis, C. (2012) *Curr. Topics Dev. Biol.* 98, 35.

**Keywords:** Transcription factors, Krueppel-like factor-4 (Klf4), Grainyhead-like-1 (Grhl1), protein-DNA binding, DNA sequence recognition

**MS7-P3** Structure of the EnvZ periplasmic domain with CHAPS reveals the mechanism of porin inactivation by bile saltsEunha Hwang<sup>1</sup>, Hae-Kap Cheong<sup>1</sup>, Young Ho Jeon<sup>2</sup>, Chaejoon Cheong<sup>1</sup>

1. Division of Bioconvergence Analysis, Korea Basic Science Institute (KBSI), Ochang, Chungbuk, Republic of Korea

2. College of Pharmacy, Korea University, Sejong, Republic of Korea

email: hwang0131@kbsi.re.kr

The EnvZ-OmpR two-component system senses external osmolarity and responds to environmental signals through the regulation of the outer membrane porins OmpF and OmpC. Although extensive studies for the EnvZ signaling have been reported, the structure of the periplasmic sensor domain at atomic resolution is not available yet. Here, we present the first crystal structure of the EnvZ periplasmic domain (EnvZ-PD) with CHAPS. The asymmetric unit contains a single monomer of EnvZ-PD and two molecules of CHAPS. The structure of EnvZ-PD showed similar folding topology to the PDC domains of PhoQ, DcuS, and CitA, but distinct orientations of helices and  $\beta$ -hairpin structures. Size exclusion chromatography and cross-linking experiment suggest that EnvZ-PD is in monomer-dimer equilibrium state in solution. It is likely that the CHAPS molecules hinder the dimerization of EnvZ-PD by changing the orientation of  $\beta$ -hairpin. When CHAPS is replaced by sodium cholate, a major component of bile salts, the overall folding of EnvZ-PD is retained. In vivo  $\beta$ -galactosidase assay showed that ompC-lacZ gene expression was dose-dependently inhibited by the addition of CHAPS and sodium cholate. These results provide an insight into the inactivation mechanism of porins in the EnvZ/OmpR signaling pathway, which is caused by the presence of bile salts.

**Keywords:** EnvZ

## MS7-P4 Crystal structure of the soluble domain of RC1339/APRc from *Rickettsia conorii*, a retropepsin-like aspartic protease

Alla Gustchina<sup>1</sup>, Mi Li<sup>1,2</sup>, Rui Cruz<sup>3,4</sup>, Marisa Simões<sup>3,4</sup>, Pedro Curto<sup>3,5</sup>, Juan Martínez<sup>2</sup>, Carlos Faro<sup>3,4</sup>, Isaura Simões<sup>3,4</sup>, Alexander Wlodawer<sup>1</sup>

1. Macromolecular Crystallography Laboratory, National Cancer Institute, Frederick, MD, USA
2. Basic Science Program, Leidos Biomedical Research, Frederick National Laboratory for Cancer Research, Frederick, MD, USA
3. Center for Neuroscience and Cell Biology, University of Coimbra, Coimbra, Portugal
4. Biocant, Biotechnology Innovation Center, Cantanhede, Portugal
5. Vector-Borne Diseases Laboratories, School of Veterinary Medicine, Louisiana State University, Baton Rouge, LA, USA

email: gustchia@mail.nih.gov

The common secondary structure template among domains/monomers of pepsin-like aspartic proteases and retropepsins supports the view that these proteases are evolutionarily related, and that pepsins may have arisen by gene duplication and fusion of an ancestral form of retropepsins. The nature of this primordial single-lobed aspartic protease has been the matter of debate over the years, mostly due to the lack of compelling evidence for the presence of these enzymes in prokaryotes. However, this argument has been first challenged with finding pepsin homologs in a restricted number of bacteria and the observation that at least one of these genes encodes an active enzyme. More recently, we reported the identification of a gene coding for a membrane-embedded, single-lobed aspartic protease, highly conserved in the genomes of 55 species of *Rickettsia*. Using *Rickettsia conorii* gene homolog rc1339, we provided evidence that the encoded product (APRc), indeed shares several enzymatic properties with viral retropepsins (Cruz, et al., *PLoS Pathog.*, **10**, e1004324, 2014).

These resemblance of enzymatic features suggested that APRc might indeed represent a more primordial form of retropepsins. In this work, crystal structures of two constructs of the soluble domain of RC1339/APRc from *Rickettsia conorii* have been determined in three different crystal forms. The results clearly show that the fold of APRc monomer is closely related to the fold of retropepsins, but the quaternary structure of the dimer differed from the canonical retropepsins. The observed dimer is most likely an artefact of expression and/or crystallization since it cannot support the previously reported enzymatic activity of APRc.

Overall, our results support the concepts that APRc may indeed represent a putative common ancestor of monomeric and dimeric aspartic proteases, as well as possible existence of a different evolutionary pathway for these enzymes.

**Keywords:** aspartic proteases, bacterial proteases, dimerization

## MS7-P5 Purification of *Z. mobilis* levansucrase for structural studies

Burcu Kaplan Türköz<sup>1</sup>, Dicle Dilara Akpınar<sup>1</sup>, Filiz Döner<sup>1</sup>

1. Ege University, Faculty of Engineering, Department of Food Engineering, Bornova, Izmir, Turkey

email: bkapan@sabanciuniv.edu

Levansucrases (Lsc) are enzymes, which have both sucrose hydrolysis and transfructosylation activity. Several microorganisms produce the enzyme, which have different product specificities. Among those identified from Gram-negative bacteria preferably produce short chain fructans; fructooligosaccharides (FOS). Gram-positive Lsc, on the other hand, are shown to produce mainly levan, long fructan polymers (1). Levan is a valuable polysaccharide used in food, biomedical and chemical industries (2). FOS are used as low calorie sweeteners and were shown to be effective prebiotics (3). Lsc produced by the gram-negative *Zymomonas mobilis* was shown to produce both FOS and levan depending on the reaction conditions such as substrate concentration and temperature (4). In order to understand the molecular details of this dual product formation ability, we are interested in solving the atomic structure of the native enzyme. To achieve this goal, we first optimized *Z. mobilis* growth conditions to maximize the production of the extracellular Lsc (5). In this study, the extracellular enzyme will be purified and crystallized for structural studies. Lsc was concentrated from the high volume cell free supernatant by salting out and active enzyme was obtained. This crude enzyme will be further purified by ion exchange and size exclusion chromatography. The crystallization of purified Lsc will be investigated using crystallization screens and in the presence of different substrate concentrations. Obtaining the crystal structure of this unique enzyme will allow us to compare its structural differences with only levan or only FOS producing levansucrases. The results might help understand the details of the enzyme's ability to produce both fructans and give valuable information for targeted enzyme design to increase the production of the desired polymer; levan or FOS.

**Acknowledgements:** This work is supported by TÜBİTAK-TÖVAG (grant number:214O174).

**References:** 1. Wuerges, J., et al. 2015, Journal of Structural Biology, 191(3), 290–298. 2. Srikanth, R., 2015, Carbohydrate Polymers, 120, 102–14. 3. Sangeetha, P. T., 2005, Trends in Food Science & Technology, 16(10), 442–457. 4. Santos-Moriano, P., 2015, Journal of Molecular Catalysis B: Enzymatic, 119, 18–25. 5. Erdal, Ö., 2016, M.Sc. Thesis, Ege University (TR)

**Keywords:** Levansucrase, Levan, Fructooligosaccharides, Crystallization

**MS7-P6** Structural analysis of human polo-like kinase 1 polo box domain in complex with peptide inhibitors

Hyee-Yeon Kim<sup>1</sup>, Woo Cheol Lee<sup>2</sup>, Ravichandran N Murugan<sup>1</sup>,  
Mija Ahn<sup>1</sup>, Jeong Kyu Bang<sup>1</sup>

1. Protein Structure Group, Korea Basic Science Institute, Ochang, Chungbuk 28119, South Korea

2. Department of Bio-Analytical Science, University of Science and Technology, Daejeon 34133, South Korea.

email: hyeyeon@kbsi.re.kr

Human polo-like kinase 1 (Plk1) is a serine/threonine-protein kinase 13(STPK13), which is overexpressed in human tumor cells. Plk1 consists of N-terminal kinase domain and C-terminal two polo-box domains. Polo-box domain (PBD) interacts with phosphoserine/phosphothreonine (pS/pT)-containing motif and is critical for tumorigenesis. Based on the crystal structure of hPlk1-PBD and PLHSpT, we designed a series of PLHSpT-derived peptide analogues to improve the binding affinity. To examine the interaction mode between hPlk1-PBD and peptide inhibitors in detail, hPlk1-PBD protein was purified and crystallized with peptide analogues. Here, we report the crystal structures of hPlk1-PBD in complex with several peptide inhibitors.

**Keywords:** polo-like kinase 1

**MS7-P7** Structural studies of the virulence factor peptidoglycan-associated lipoprotein from a Gram-negative pathogen

Eun-Hee Kim<sup>1</sup>, Kwon Joo Yeo<sup>1</sup>, Woo Cheol Lee<sup>1</sup>, Eunha Hwang<sup>1</sup>, Saeyoung Lee<sup>2</sup>, In-Geol Choi<sup>2</sup>, Hye-Yeon Kim<sup>1,3</sup>

1. Protein Structure Group, Korea Basic Science Institute, Ochang, Chungbuk 28119, South Korea

2. College of Life Sciences and Biotechnology, Korea University, Seoul 02841, South Korea

3. Department of Bio-Analytical Science, University of Science and Technology, Daejeon 34133, South Korea

email: keh@kbsi.re.kr

*Acinetobacter baumannii* is a multi-drug resistant Gram-negative pathogen that causes hospital-acquired infection of immunocompromised patients. Peptidoglycan-associated lipoprotein (Pal) of Gram-negative bacteria is one component of the Tol-Pal system, which plays an important role in the integrity of the outer membrane and it is found in the outer membrane vesicle used to deliver virulence effectors into host cells. *A. baumannii* Pal (AbPal) is composed of an N-terminal motif that is required for delivery and anchoring to the outer membrane and a C-terminal OmpA-like domain. OmpA-like domains interact noncovalently with peptidoglycan via a unique bacterial amino acid, *meso*-diaminopimelic acid (*meso*-DAP).

Incorporation of a D-amino acid moiety in the peptidoglycan structure has been suspected to be a method which bacteria can evade the host immune system. Specific binding to D-amino acid by this domain is of particular interest in terms of pathogenicity {Walsh, 1989 #31} {Walsh, 1989 #31}. However, the enantiomeric specificity of OmpA-like domains for the interaction with peptidoglycan has not been studied.

Here, we report molecular basis for the interaction with *meso*-DAP of peptidoglycan by OmpA-like domain of AbPal using X-ray crystallography, NMR spectroscopy, isothermal titration calorimetry (ITC), and site-directed mutagenesis. We performed the NMR backbone assignment of AbPal and firstly solved the crystal structure of AbPal in complex with *meso*-DAP or *LL*-DAP to evaluate a key determinant region for the stereospecific interaction with peptidoglycan. Our findings provide a foundation for the development of antibacterial agents that disrupt stability of cell wall of Gram-negative pathogen.

**Keywords:** peptidoglycan-associated lipoprotein, X-ray crystallography, NMR spectroscopy, ITC

## MS7-P8 A Closer Look at the Parallel RNA Double Helix Poly(rA)

Anna V. Luebben<sup>1</sup>, Jingwei Xie<sup>2</sup>, Nozhat Safae<sup>2</sup>, Kalle Gehring<sup>2</sup>,  
George M. Sheldrick<sup>1</sup>, Birger Dittrich<sup>3</sup>

1. Georg-August-University Göttingen Germany  
2. McGill University, Montreal Canada  
3. Heinrich-Heine University, Düsseldorf Germany

email: aluebbe@gwdg.de

As early as 1961, Rich, Davies, Crick and Watson proposed a parallel double helix RNA structure for poly(rA) on the basis of diffuse fibre diffraction photographs [1], using similar arguments to those used to deduce the antiparallel double helix structure for DNA. It took over 50 years before this could be confirmed by a crystal structure determination [2]. However the solution of this structure by *ab initio* direct methods required one week on an eight-CPU workstation.

We recently obtained synchrotron data from better quality crystals of significantly higher resolution and completeness. With the new data the structure can be solved in a much shorter time and the data quality appears to be sufficient for a charge density analysis using the Invariom approach [3].

[1] Rich, Davies, Crick and Watson, *J. Mol. Biol.* **1961**, 3, 71-86.

[2] Safae, Noronha, Rodionov, Kozlov, Wilds, Sheldrick and Gehring, *Angew. Chem. Int. Ed.* **2013**, 52, 10370-10373.

[3] Dittrich, Hübschle, Pröpper, Dietrich, Stolper and Holstein, *Acta Cryst.* **2013**, B69, 91-104.

**Keywords:** parallel double helix, RNA, charge density, direct methods

## MS7-P9 Structural insights into ObcA, an enzyme for oxalogenesis

Sangkee Rhee<sup>1</sup>, Juntaek Oh<sup>1</sup>, Ingyu Hwang<sup>1</sup>

1. Seoul National University, KOREA

email: srheesnu@snu.ac.kr

Bacterial quorum sensing (QS), a cell-to-cell communication process in many *Proteobacteria*, controls the gene expression for bacterial population-wide characteristics, including bioluminescence, motility, and virulence-related factors. Recently, QS has been recognized to provide further benefits at the population level by regulating the production of public goods, the function of which could be beneficial to all members of the group. In *Burkholderia* species, oxalic acid was recently identified as an excreted public good for the QS-dependent growth. In these species, QS-mediated oxalogenesis via the oxalate biosynthetic component (obc) is a cellular event indispensable for the survival of bacteria in the stationary phase. In *B. glumae*, obc consists of two genes encoding ObcA and ObcB for coordinating the production of oxalic acid, as well as acetoacetate and CoA, by using oxaloacetate and acetyl-CoA as substrates. In ObcA, oxaloacetate serves as a nucleophile by forming an enolate intermediate mediated by Tyr322 as a general base, which then attacks the thioester carbonyl carbon of acetyl-CoA to yield a tetrahedral adduct between the two substrates. Therefore, ObcA catalyzes its reaction by combining the enolase and acetyltransferase superfamilies, but the presence of the metal-coordination shell and absence of general acid(s) likely produces an unusual tetrahedral CoA adduct as a stable product. These results provide the structural basis for understanding the first step in oxalogenesis and the mechanistic features of ObcA. This work was supported by Next Generation BioGreen 21 program of Rural Development Administration (Plant Molecular Breeding Center) of Republic of KOREA.

**Keywords:** Enzyme catalysis, oxalate production

## MS7-P10 Optimizing expressed cyclic peptide library generation: a quantitative and structural study

Sabine Schneider<sup>1</sup>, Sabrina Harteis<sup>1</sup>, Leonhard Kick<sup>1</sup>, Maximilian Koch<sup>1</sup>

1. Technical University of Munich

email: sabine.schneider@mytum.de

In recent years peptides have been rediscovered as potential drugs, due to the increasing demand for the discovery of new therapeutic molecules. Particularly cyclic peptides (CPs) belong to the most effective, high-affinity drug-like agents, which exhibit a wide range of biological activities. CPs are extremely variable in the structures and conformations they adopt and, owing to the cyclisation they are exceptional stable. In the last decade, methods have been developed to genetically encode and express libraries of CPs, taking advantage of the protein-splice reaction carried out by split-inteins. In combination with an *in vivo* screening assay this provides a powerful tool for the straightforward identification of the active members against a chosen target. In this split-intein mediated ligation of proteins and peptides (SICLOPPS), [1] However the efficiency and velocity of the cyclization reaction strongly depends on the split-intein used and target sequence to be cyclized. [2] This results in great variation of the amount of CP produced and bias of the library towards certain sequences.

Here we compare efficiency as well as sequence bias of CP generation of natural split-inteins DnaE from *Synechocystis sp. PCC6803* and *Nostoc punctiforme*. Using synthetic <sup>13</sup>C-labeled reference peptides and liquid chromatography mass spectrometry we quantitatively determined the cyclization efficiency *in vivo* of different hexameric target sequences. In order to elucidate the molecular mechanisms for the observed target sequence preferences, we determined the crystal structures of the pre-splice complexes of the split-inteins with different CP sequences. These data will help to assess the potential quality and bias of the genetically encoded CP screening library generated using split inteins.

### Literature

- [1] A. Tavassoli and S. J. Benkovic, Nat. protocols 2007, 2, 1126-33.
- [2] G. Volkmann and H. D. Mootz, Cell. Mol. Life Sci., 2013, 70, 1185-1206

**Keywords:** split-intein, cyclic peptide, peptide library

## MS7-P11 Structural features of NPC1L1 and NPC1 proteins in complex with cholesterol: comparison between X-ray crystal structure and docking study

HyEjin Yoon<sup>1</sup>, EunSook Joo<sup>2</sup>, Soonmin Jang<sup>3</sup>, Se Won Suh<sup>1</sup>

1. Department of Chemistry, Seoul National University

2. Faculty of Biotechnology, Jeju National University

3. Department of Chemistry, Sejong University

email: yoonhj@snu.ac.kr

Cholesterol homeostasis in the human body is maintained by *de novo* synthesis, intestinal absorption, and biliary and fecal excretion. The absorption of dietary cholesterol in intestine is mediated with NPC1L1 (Niemann-Pick type C1 like 1), a polytopic transmembrane protein of 1332 amino acids, which shares sequence homology with NPC1 (Niemann-Pick type C1). Like its homolog, NPC1L1 was predicted to have a typical signal peptide and 13 membrane-spanning domains, which is in consistent with recent experimental data. The X-ray crystallography structure of this domain without cholesterol (PDB id: 3QNT) shows it has a conserved N-terminal "NPC1" domain, and extensive N-linked glycosylation sites.

Since its discovery, several studies demonstrated the importance of NPC1L1 as one of the key players in both dietary cholesterol absorption and biliary cholesterol re-absorption. On the other hands, NPC1 and NPC2 are main players of cholesterol control in lysosome and it is known that mutation of one of these proteins leads to disease, called Niemann-Pick disease type C (NPC) disease. The crystal structures of N-terminal domain (NTD) of NPC1 were determined with and without cholesterol (PDB id: 3GKI and 3GKH).

The structure of NPC1L1 in complex with cholesterol can provides insights into the mechanism of the cholesterol mediation by NPC1L1 and we attempted to get the NPC1L1-cholesterol complex structure with molecular docking study. Comparison of the resulting complex structure with that of NPC1-cholesterol complex can give better understand of the role of conserved "NPC1" domain absorption of cholesterol in small intestine. In this study, we have re-determined the crystal structure for NPC1L1 protein. We will propose the structure of NPC1L1 in complex with cholesterol and the role of NPC1L1-cholesterol complex in bulk cholesterol endocytosis of enterocyte membrane. We believe the current study can contribute the development of cholesterol absorption inhibitor for hypercholesterolemic patient ultimately.

**Keywords:** NPC1L1, cholesterol

**MS7-P12** Structural analysis of response regulator spr1814 from *Streptococcus pneumoniae* in the absence and presence of the phosphoryl analog beryll fluoride

Ae Kyung Park<sup>1,2</sup>, Han Woo Kim<sup>1,3</sup>, Hyun Park<sup>1,3</sup>, Young Min Chi<sup>2</sup>

1. Division of Polar Life Sciences, Korea Polar Research Institute, Incheon 406-840, Republic of Korea
2. Division of Biotechnology, College of Life Sciences, Korea University, Seoul 136-713, Republic of Korea
3. Department of Polar Sciences, University of Science and Technology, Incheon 406-840, Republic of Korea

email: parkak@kopri.re.kr

Organisms that live in a changing environment sense and respond to a wide variety of stimuli through a complex network of signalling systems. Of these, two-component systems (TCSs) are the common pathways by which bacteria sense and respond to their environments. Typical bacterial TCSs consists of a membrane-bound histidine kinase (HK) and a cytosolic cognate response regulator (RR) protein. In the simplest form, a HK catalyzes its own auto-phosphorylation of conserved histidine residue and the phosphoryl group is relayed to the conserved aspartic acid residue of RR. Phosphorylated RRs in turn undergo a conformational change that induces the appropriate cellular response. In general, phosphorylated RRs function as transcription factors triggering the expression of target genes. According to the structure of the DNA-binding domain, spr1814, the RR that is studied here, belongs to the NarL/FixJ subfamily, which is characterized by a helix-turn-helix (HTH) DNA-binding domain, and accounts for approximately 19 % of all response regulators. Until now, there have only been four full-length structures of NarL/FixJ subfamily identified. Despite of a similar overall structure in terms of their receiver and effector domains, different contacts between domains have been observed. The most extensive interdomain interactions were found to occur in NarL, DosR and VraR in very distinct manners, but few contacts were observed in StyR. Although they have different domain arrangements, the NarL/FixJ subfamily RRs have been suggested to release the blockage of the effector domain from the receiver domain upon phosphorylation. Here, we determined the crystal structure of full-length spr1814 in the presence and absence of a phosphate analog beryllium fluoride. This allows us to describe the conformational changes of spr1814 upon phosphorylation. The phosphorylation of conserved aspartic acid residue of N-terminal receiver domain triggers a structural perturbation at the  $\alpha 4$ - $\beta 5$ - $\alpha 5$  interface, leading to the domain reorganization of spr1814, and this is achieved by a rotational change in the C-terminal DNA-binding domain.

**Keywords:** Response regulator, a phosphate analog beryllium fluoride

**MS7-P13** Structural and mechanistic insights into a *Bacteroides vulgatus* retaining *N*-acetyl- $\beta$ -galactosaminidase that uses neighbouring group participation

Christian Roth<sup>1</sup>, Marija Petricevic<sup>2</sup>, Alan John<sup>3,4</sup>, Ethan D. Goddard-Borger<sup>3,4</sup>, Gideon J. Davies<sup>1</sup>, Spencer J. Williams<sup>2</sup>

1. Department of Chemistry, University of York, Heslington, York, UK
2. School of Chemistry and Bio21 Molecular Science and Biotechnology Institute, University of Melbourne, Parkville, Victoria, Australia.
3. ACRF Chemical Biology Division, The Walter and Eliza Hall Institute of Medical Research, Parkville, Victoria, Australia
4. Department of Medical Biology, University of Melbourne, Parkville, Victoria, Australia.

email: christian.roth@york.ac.uk

*Bacteroides vulgatus* is a member of the human microbiota whose abundance is increased in patients with Crohn's disease. We show that a *B. vulgatus* glycoside hydrolase from the carbohydrate active enzyme family GH123, BvGH123, is an *N*-acetyl- $\beta$ -galactosaminidase that acts with retention of stereochemistry, and through a 3-D structure in complex with Gal-thiazoline, provide evidence in support of a neighbouring group participation mechanism.

**Keywords:** glycoside hydrolase, crystal structure, neighbouring group participation



## MS8 Membranes and membrane interacting proteins

[3] Small et al., 2014 [4] Wisniewski et al., 1995 [5] Westermark et al., 1995 [6] Gursky et al., 1996 [7] Gwynne et al., 1974

**Keywords:** XRR, surface, membrane, surface-pressure, pH-value, amyloid, apolipoprotein A1

Chairs: Han Remaut, Maïke Bubltz

### MS8-P1 pH- and surface pressure-depend adsorption of human apolipoprotein A1 at solid/liquid- and gas/liquid-interfaces

Susanne Dogan<sup>1</sup>, Michael Paulus<sup>1</sup>, Paul Salmen<sup>1</sup>, Yury Forov<sup>1</sup>,  
Christopher Weis<sup>1</sup>, Metin Tolan<sup>1</sup>

1. Fakultät Physik / DELTA, Technische Universität Dortmund, Germany

email: susanne.dogan@gmx.net

In natural cells, proteins face a very complex environment, in which crowding and confinement can affect the conformational stability and the adsorption behavior of proteins or lead to aggregation. Interactions of proteins with solid surfaces are major issues in a number of fields of research such as biology, medicine, or biotechnology [1, 2]. Apolipoprotein A1 (apoA1) is an important protein of high density lipoproteins (HDLs) and plays a vital role in reverse cholesterol transport. Reduced plasma levels of HDL and apoA1 are the key risk factors for atherosclerosis and cardiovascular disease [3]. Lipidfree apoA1 is the main constituent of amyloid deposits found in atherosclerotic and senile plaques [4, 5]. Due to its anisotropic surface, apoA1 is able to interact with surfaces or interfaces via different interaction mechanisms. We investigated the adsorption behaviour of apoA1 at hydrophilic silicon dioxide surfaces as a function of the pH-value and the surface pressure-depend adsorption behaviour at DOTMA/DOPC-monolayer by means of x-ray reflectivity (XRR). The pH-depend adsorption behavior of apoA1 was examined at BL9 at the synchrotron light source DELTA (Dortmund, Germany) at the solid/liquid-interface (pH-value 3-7). Surface pressure-depend adsorption measurements were conducted at the gas/liquid-interface using a Langmuir trough with a Bruker-AXS D8 diffractometer (20-30 mN/m). The pH-depend measurements show that apoA1 adsorbs in different conformations depending on the microenvironment. Between pH 4 and pH 6, an adsorption window with different electron densities and layer thicknesses is determined. The adsorption within this window is mainly driven by electrostatic interactions, since the protein and surface are oppositely charged in the region of these pH-values. The protein is described as a molten globule with a loosely fold state [6] which are able to adsorb. With lowering the pH-value in the acidic region the protein undergoes molecular transitions where the  $\alpha$ -helical segments are reduced and the protein gets into a random coil state [7]. At the monolayer apoA1 causes a complete reduction of the electron density without changing the layer thickness. It seems that apoA1 adsorbs, penetrates and finally solubilizes the lipids into solution. [1] Kasemo et al., 2002 [2] Castner et al., 2002

**MS8-P2** Structural Analysis of a Soluble Fragment of the Membrane Fusion Protein HlyD in a Type I Secretion System of *Escherichia coli*.

Nam-Chul Ha<sup>1</sup>, Jin-Sook Ahn<sup>1</sup>

<sup>1</sup>. Department of Agricultural Biotechnology, CALS, Seoul National University

email: hanc210@snu.ac.kr

The protein toxin HlyA of *Escherichia coli* is exported without a periplasmic intermediate by the type I secretion system (TISS). The TISS is composed of an inner membrane ABC transporter HlyB, an outer-membrane channel protein TolC, and a membrane fusion protein HlyD. However, the assembly of the TISS remains to be elucidated. In this study, we determine the crystal structure of a part of the C-terminal periplasmic domain of HlyD. The long  $\alpha$ -helical domain consisting of three  $\alpha$  helices and a lipoyl domain was identified in the crystal structure. Based on the HlyD structure, we modeled the hexameric assembly of HlyD with a long  $\alpha$ -helical barrel, which formed a complex with TolC in an intermeshing cogwheel-to-cogwheel manner, as observed in tripartite RND-type drug efflux pumps. These observations provide a structural blueprint for understanding the type I secretion system in pathogenic Gram-negative bacteria.

**Keywords:** HlyD, TISS, Hexamer, Toxin secretion, *E. coli*

**MS8-P3** Structure of complete rotary ATP synthase and its role as new drug target against tuberculosis

Thomas Meier<sup>1</sup>

<sup>1</sup>. Imperial College London

email: t.meier@imperial.ac.uk

$F_1F_0$ -ATP synthases are paradigmatic molecular machines, which use the transmembrane electrochemical ion gradient to power ATP synthesis. The enzymes belong to the class of rotary ATPases, which all share a common architecture principle, consisting of a rotor and stator entity. While ions are shuttled through the  $F_0$  complex of the enzyme, torque is generated at the rotor/stator and transferred to the  $F_1$ -catalytic subunits for ATP synthesis. In the opposite direction, ATP hydrolysis can be used to drive ion pumping. I am going to present the structure of complete ATP synthase taking advantage of the combined approach of X-ray crystallography and cryo-electron microscopy. I will also focus on biochemical and structural investigations of the ATP synthase with respect to the development of new antibiotics in the fight against infectious diseases such as tuberculosis.

**Keywords:** Bioenergetics, X-ray crystallography, electron microscopy

## MS8-P4 Unconventional Molecular Replacement approaches for ab initio phasing of transmembrane helical protein targets

Jens M.H. Thomas<sup>1</sup>, Felix Simkovic<sup>1</sup>, Ronan M. Keegan<sup>2</sup>, Olga Mayans<sup>3</sup>, Daniel J. Rigden<sup>1</sup>

1. Institute of Integrative Biology, University of Liverpool
2. Research Complex at Harwell, STFC Rutherford Appleton Laboratory
3. Department of Biology, Universität Konstanz

email: jens.thomas@liv.ac.uk

Transmembrane helical proteins are underrepresented in the PDB due to the experimental difficulties associated with their protein expression and crystallisation. This results in a small pool of structures being available for conventional homology-based Molecular Replacement (MR) and places a premium on the development of unconventional homology-independent approaches.

AMPLE is a pipeline for using unconventional models in automated MR. It has been particularly successful in its cluster and truncate approach to creating search ensembles from ab initio molecular models<sup>[1]</sup>. Recent work has focussed on exploring the viability of different approaches to the clustering and truncation. By exploring multiple clusters and using TM scoring, we have been able to double the success rate of AMPLE on a difficult set of test cases without an increase in processing time.

Using the new approach, and combining it with intermolecular contact prediction<sup>[2]</sup> to improve the modelling, we have been exploring the effectiveness of AMPLE on a selection of alpha-helical transmembrane proteins. Our work has demonstrated that AMPLE is a powerful method to use on this class of protein, outperforming a baseline approach based on short alpha-helices, and able to solve the majority of cases in our test set with an average runtime of less than two days on a single processor.

Jens M. H. Thomas, Felix Simkovic, Olga Mayans and Daniel J. Rigden

1. Routine phasing of coiled-coil protein crystal structures with AMPLE. Jens MH Thomas, Ronan M Keegan, Jaclyn Bibby, Martyn D Winn, O Mayans & DJ Rigden. (2015). IUCr J 2/2,198-206

2. Protein structure prediction from sequence variation. Marks, D. S., Hopf, T. A., & Sander, C. (2012). Nat. Biotechnol. 30, 1072–1080.

**Keywords:** Automated Molecular Replacement, Helical Transmembrane Proteins, AMPLE

## MS9 Enzyme reactions and dynamics in crystals

Chairs: Gunter Schneider, Arwen Pearson

### MS9-P1 CckA regulation by c-di-GMP: how to steer a bacterial histidine kinase into the phosphate mode

Badri N. Dube<sup>1</sup>, Urs Jena<sup>2</sup>, Tilman Schirmer<sup>1</sup>

1. Focal Area of Structural Biology and Biophysics, University of Basel, CH-4056 Basel, Switzerland.
2. Focal Area of Infection Biology, University of Basel, CH-4056 Basel, Switzerland.

email: b.dube@unibas.ch

Cyclic diguanosine monophosphate (c-di-GMP) is a ubiquitous signaling molecule coordinating, amongst others, bacterial development and behavioural programs<sup>1</sup>. Recently, we have shown that histidine kinase CckA from *Caulobacter crescentus* is regulated by c-di-GMP in that it inhibits its kinase and stimulates its phosphatase activity<sup>2</sup>. Thus, the phosphorylation state of CtrA, the ultimate target of the CckA signaling pathway and a master transcription factor controlling cell replication, is controlled indirectly by the cellular c-di-GMP concentration.

In order to unravel the molecular mechanism of c-di-GMP induced reversal of CckA activity, we have biophysically (MALS, ITC) and structurally investigated various constructs of CckA. Interestingly, in the full-length context CckA binds c-di-GMP with low micro-molar affinity only in presence of ADP and not of ATP, whereas, the isolated catalytic domain (CA) binds c-di-GMP with medium affinity irrespective of the mononucleotide state. Thus, c-di-GMP binding appears to depend on the functional state (domain constellation) of the enzyme and, in this way, stabilize the ADP complexed form.

Crystal structures of the CA domain in complex with c-di-GMP/ATP and of the DHp-CA enzyme core in complex with ADP have been determined. The first structure shows c-di-GMP bound with one of its guanine bases to a specific binding pocket on the CA domain, whereas the second base is not involved in any interactions. In the context of the DHp-CA double domain structure, the second base would come to lie close to helix 1 of the DHp domain suggesting c-di-GMP mediated cross-linking. Taken together, we propose that c-di-GMP binding stabilizes a domain constellation, which allows access and dephosphorylation of the cognate receiver domain and, at the same time, prevents formation of the auto-kinase constellation.

#### References:

- 1- Romling U, Galperin MY, Gomelsky M. Cyclic di-GMP: the first 25 years of a universal bacterial second messenger. Microbiol Mol Biol Rev. 2013; 77(1):1-52.

2- Lori, 2- C; Ozaki, S; Steiner, S; Böhm, R; Abel, S; Dubey, B N; Schirmer, T; Hiller, S; Jenal, U (2015). Cyclic di-GMP acts as a cell cycle oscillator to drive chromosome replication. *Nature*. 2015; 523, 236- 239.

**Keywords:** Bi-functional enzyme, Histidine kinase, c-di-GMP, signalling, Crystal structure

## MS9-P2 Structural view of fungal glutathionyl-hydroquinone reductases

Claude DIDIERJEAN<sup>1,2</sup>

1. University of Lorraine, UMR 7036 CRM2, Vandoeuvre-les-Nancy, France

2. CNRS, UMR 7036 CRM2, Vandoeuvre-les-Nancy, France

email: [claudio.didierjean@univ-lorraine.fr](mailto:claudio.didierjean@univ-lorraine.fr)

**Mathieu Schwartz<sup>1</sup>, Thomas Perrot<sup>2</sup>, Arnaud Hecker<sup>2</sup>, Claude Didierjean<sup>1</sup>, Eric Gelhaye<sup>2</sup>, Frederique Favier<sup>1</sup>**

University of Lorraine, Nancy, France <sup>1</sup>UMR-CNRS 7036 CRM2 ; <sup>2</sup>UMR-INRA 1136 IAM.

Glutathione transferases (GSTs) constitute a widespread super-family of enzymes with highly specific to overlapping functions. These enzymes have been extensively studied in mammals because of their roles in xenobiotic conjugation. Despite this, GST functions are largely unexplored, especially in microorganisms. Our work focused on fungal glutathionyl-hydroquinone reductases (GHRs). These singular GSTs catalyze the reduction of hydroquinones-SG (Xun *et al.*, 2010), and are present in all kingdoms but animals. The first GHR structure to be described in the saprotrophic fungus *Phanerochaete chrysosporium* (PcGHR1) has unveiled original features. An original dimerization mode led us to establish a new structural class named Xi (GSTX) (Meux *et al.*, 2011).

Here we report the crystal structures of two GHRs, TvGHR1 from the basidiomycete *Trametes versicolor* and ScECM4 from the yeast *Saccharomyces cerevisiae*, at 2.28 and 1.45 Å resolution, respectively. TvGHR1 and ScECM4 share the classical GST fold which consists in a thioredoxin N-terminal domain and an all  $\alpha$  C-terminal domain. Besides the features that have been uncovered in PcGHR1, additional secondary structures were found in the yeast ScECM4 structure. Like its characterized homologs, ScECM4 is specific to the reduction of quinones conjugated with glutathione (Lallement *et al.*, 2014). TvGHR1 is more polyvalent because it also reduces substrates rather accepted by Omega-class GSTs like phenylacetophenone-SG. Compared with known GHR structures, TvGHR1 exhibits a larger substrate binding site with an original motif that could explain the substrate versatility. Phylogenetic analyses revealed that fungal GHRs could be separated in two families : the 'classic' GHRs and the 'atypical' GHRs that exhibit motif variations as observed in TvGHR1. Furthermore, the conservation of GHRs in fungi suggests that they could fulfill a crucial role. Their diversification in wood-degrading basidiomycetes agrees with the hypothesis that GHRs would play a role in the metabolism of phenolic compounds (Belchik & Xun, 2011).

Belchick S.M. & Xun L., *Drug Metab Rev.* 2011, **43**(2), 307 ; Lallement *et al.*, *FEBS Lett.* 2015, **589**, 37; Meux *et al.*, *J. Biol. Chem.* 2011, **286**(11), 9162 ; Xun *et al.*, *Biochem. J.* 2010, **428**(3), 419.

**Keywords:** glutathionyl-hydroquinone, reductase, fungi, glutathione transferase

**MS9-P3** PLA<sub>2</sub>-like membrane perturbation mechanism: extracting the most of crystallography dataRafael J. Borges<sup>1,2</sup>, Ney Lemke<sup>1</sup>, Massimo Sammito<sup>2</sup>, Claudia Millán<sup>2</sup>, Isabel Usón<sup>1</sup>, Marcos M.R. Fontes<sup>1</sup>

1. Dept. of Physics and Biophysics, Biosciences Institute (IBB), São Paulo State University (UNESP), Botucatu, São Paulo, Brazil
2. Dept. of Structural Biology, Institute of Molecular Biology of Barcelona (IBMB), Spanish National Research Council (CSIC), Barcelona, Spain
3. Dept. of Structural Biology, Catalan Institution for Research and Advanced Studies (ICREA), Barcelona, Spain

email: rjborges@ibb.unesp.br

Venomics has been an invaluable tool to biomedicine by aiding comprehension of physiological mechanisms and drug design. Particularly, secreted phospholipases A<sub>2</sub> (PLA<sub>2</sub>s) had their catalytic mechanism first inferred evaluating three high resolution crystallographic structures PLA<sub>2</sub>s from Chinese cobra and bee venom in different states<sup>1</sup>. A subtype of PLA<sub>2</sub>s, the PLA<sub>2</sub>-like, also named as PLA<sub>2</sub>-homologue due to its similar tertiary structure and common ancestor, does not possess catalytic activity but still presents a high myotoxicity and a wide range of pharmacological activities<sup>2,3</sup>. The PLA<sub>2</sub>-like versatility has related to its capability to perturb different biological membrane, breaking ionic homeostasis and inducing series physiological events that leads to cell death<sup>3</sup>. Although a lot has been discovered by functional and structural experiments, PLA<sub>2</sub>-like exact mechanism of action is not fully understood<sup>2,3</sup>. Herein, we investigated their molecular mechanism by evaluation of global and local characteristics of crystallographic models. We gathered all snake venom PLA<sub>2</sub>-like structures available in Protein DataBank in the most probable dimer in solution using ProtCID database<sup>4</sup>. We evaluated models by hydrophobic channel accessibility through MOLE 2.0<sup>5</sup>, by presence or absence of hydrophobic ligands and by the geometrical orientation of one monomer to the other. The geometrical orientation was extracted from the rotation matrix after monomer superimposition using lsqkab program<sup>6</sup> available in CCP4 suite<sup>7</sup>. By these global and local structural evaluations, we identified different native and complex states relating monomer-monomer geometry to hydrophobic channel aperture and closure.

## References

1. Scott, D. L. *et al. Science* **250**, 1541–1546 (1990).
2. Fernandes, C. A. H., *et al.* Borges, R. J., Lomonte, B. & Fontes, M. R. M. *Biochim. Biophys. Acta* (2014). doi:10.1016/j.bbapap.2014.09.015
3. Lomonte, B., Angulo, Y., Sasa, M. & Gutiérrez, J. M. *Protein Pept. Lett.* **16**, 860–876 (2009).
4. Xu, Q. & Dunbrack, R. L. *Nucleic Acids Res.* **39**, D761–770 (2011).
5. Sehnal, D. *et al.* MOLE 2.0: advanced approach for analysis of biomacromolecular channels. *J. Cheminformatics* **5**, 39 (2013).
6. Kabsch, W. *Acta Crystallogr. Sect. A* **32**, 922–923 (1976).
7. Winn, M. D. *et al. Acta Crystallogr. D Biol. Crystallogr.* **67**, 235–242 (2011).

**Keywords:** Phospholipase A<sub>2</sub>, geometry, hydrophobic channel**MS9-P4** Structural insights into the catalytic reaction trigger and inhibition of D-3-hydroxybutyrate dehydrogenaseHiroki Kanazawa<sup>1,2</sup>, Md. Mominul Hoque<sup>1,3</sup>, Masaru Tsunoda<sup>1</sup>, Kaoru Suzuki<sup>1</sup>, Tamotsu Yamamoto<sup>4</sup>, Gota Kawai<sup>5</sup>, Jiro Kondo<sup>2</sup>, Akio Takénaka<sup>1,5</sup>

1. Faculty of Pharmacy, Iwaki Meisei University, Chuodai-ino, Iwaki 970-8551, Japan
2. Department of Materials and Life Sciences, Sophia University, Kioto-cho, Chiyoda-ku, Tokyo 102-8554 Japan
3. Department of Biochemistry and Molecular Biology, University of Rajshahi, Rajshahi-6205, Bangladesh
4. Asahi Kasei Pharma Corporation, Tagata-gun, Shizuoka 410-2323, Japan
5. Research Institute, Chiba Institute of Technology, Tsudanuma, Narashino, Chiba 275-0016, Japan

email: h.kanazawa@eagle.sophia.ac.jp

It's known that acetyl-CoA which carries an acetyl group as energy source for the TCA cycle is prepared through the two different pathways, glycolysis and  $\beta$ -fatty acid oxidation. However, excess amount of acetyl-CoA is converted to acetoacetate in liver, and further converted to D-3-hydroxybutyrate as a water-soluble form. These two ketone bodies are transported *via* bloodstream to peripheral organisms which consume lots of energy, and then acetyl-CoA is reproduced. It is D-3-hydroxybutyrate dehydrogenase which catalyzes the reversible conversion. In order to clarify the structural mechanisms of the catalytic reaction with the cognate substrate D-3-hydroxybutyrate and of the reaction inhibition with inhibitors, the enzyme from *Alcaligenes faecalis* has been X-ray analyzed in the liganded states with the substrate, and with two kinds of inhibitors, malonate and methylmalonate.

Four subunits form a tetrameric enzyme. In each subunit, the substrate is trapped on the nicotinamide plane of NAD<sup>+</sup> bound in a central part of the enzyme. The OMIT map definitively shows that the bound ligand is D-3-hydroxybutyrate but not acetoacetate. The carboxylate group of the substrate forms four hydrogen bonds with Gln94, Gln196, Lys152 and His144. The methyl group prefers to accommodate in the nearby hydrophobic pocket, so that the OH group of substrate is facilitated to form a hydrogen bond with the hydroxy group of Tyr155 (Fig. 1a). In this geometry, an active H atom attached to the C<sup>3</sup> atom of the substrate in the *sp*<sup>3</sup> configuration is positioned at a distance of 3.1 Å from the nicotinamide C<sup>4</sup> atom in a direction of the plane normal. In addition, the donor-acceptor relationship of the hydrogen bonds suggests that the Tyr155 OH group is allowed to ionize by the two donations from the Ser142 OH and the ribose OH groups. A structural comparison of the enzymes with/without ligands suggests that the domain movement to form a hydrogen bond with the substrate facilitates the active H-atom movement of the substrate as the trigger of the catalytic reaction. In the complexes with inhibitors (Fig. 1b,c), however, their principal carboxylate groups interact with the enzyme, while the interactions of other groups are changed. The crucial determinant for inhibition is that the inhibitors have no active H atom at C<sup>3</sup>. In addition, the second determinant is the Tyr155 OH group which is perturbed by the inhibitors to donate the H atom for hydrogen-bond formation, losing the nucleophilicity.

**Keywords:** Reaction mechanism, D-3-Hydroxybutyrate dehydrogenase, Substrate, Inhibitor

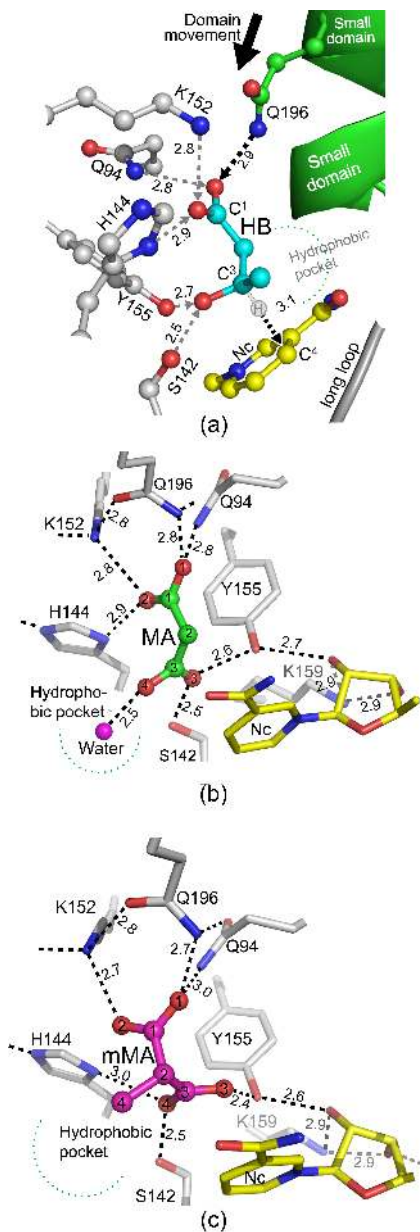


**Figure 1.** Interaction geometries of substrate/inhibitor binding sites found in substrate-complex (a), malonate-complex (b) and methylmalonate-complex (c). Broken lines indicate possible hydrogen bonds. Dotted half circles show the hydrophobic pocket surrounded by His144, Ala186, Trp187 and Trp257.

## MS9-P5 Structures of the photosensory core module of bacteriophytochrome Agp1 from two crystal forms reveal plasticity of the Pr state

Norbert Krauß<sup>1,2</sup>, Soshichiro Nagano<sup>2,3</sup>, Patrick Scheerer<sup>4</sup>, Kristina Zubow<sup>2</sup>, Norbert Michael<sup>5</sup>, Katsuhiko Inomata<sup>6</sup>, Tilman Lamparter<sup>1</sup>

1. Karlsruher Institut für Technologie, Botanisches Institut (Germany)
2. Queen Mary University of London, School of Biological and Chemical Sciences (United Kingdom)
3. Justus-Liebig-Universität Gießen, Institut für Pflanzenphysiologie (Germany)
4. Charité - Universitätsmedizin Berlin, Institut für Medizinische Physik und Biophysik (Germany)
5. Technische Universität Berlin, Institut für Chemie (Germany)
6. Kanazawa University, Division of Material Science (Japan)

email: norbert.krauss@kit.edu

Agp1 is a canonical biliverdin-binding bacteriophytochrome from the soil bacterium *Agrobacterium fabrum* that acts as a light-regulated histidine kinase and uses the red-light-absorbing Pr form as the dark adapted state [1]. At the level of the tertiary structure, the structural changes that occur during photoconversion from Pr to the far-red-absorbing Pfr form are characterised by a transition in the so-called tongue region of the PHY domain from an antiparallel  $\beta$ -sheet in Pr to a partially  $\alpha$ -helical structure in Pfr and rearrangements within the long  $\alpha$ -helix that connects the GAF and the PHY domain. Based on those crystal structures of photosensory core modules (PCMs) where the protein subunits are arranged as parallel dimers, suggestions have been made as to how changes in the quaternary structure of the PCM associated with photoconversion lead to modulation of the activity of the histidine kinase output module [2, 3, 4]. Here we present crystal structures of the PCM of Agp1 at 2.70 Å resolution and of a surface-engineered mutant at 1.85 Å resolution in Pr. Whereas in the mutant structure the dimer subunits are found to be in anti-parallel orientation, the wild-type structure contains parallel dimers, which structurally differ significantly from the parallel dimers of the PCMs of other phytochromes in Pr. Comparison of the two Agp1-PCM structures reveals relative orientations between the PAS-GAF bidomain and the PHY domains to be different, due to movement about two hinges in the GAF-PHY connecting  $\alpha$ -helix and in the tongue region that indicates pronounced structural flexibility which may give rise to a dynamic Pr state even at the level of the quaternary structure. The high

resolution of the mutant structure enabled us to detect a sterically strained conformation of the chromophore at pyrrole ring A and its side chain that we attribute to the tight interaction with Pro461 of the PRxSF motif in the tongue region and the restricted conformational degrees of freedom which are due to the covalent linkage between biliverdin (BV) and Cys20. Based on this observation and on additional biochemical data we discuss the potential reasons for the crucial role which the tongue region plays in Pr-to-Pfr photoconversion.

### References:

- [1] T. Lamparter et al., *Proc. Natl. Acad. Sci. U. S. A.* **99**, 11628-11633 (2002)
- [2] H. Takala et al., *Nature* **509**, 245-248 (2014)
- [3] X.J. Yang et al., *Structure* **23**, 1179-1189 (2015)
- [4] E.S. Burgie et al., *Structure* **24**, 448-457 (2016)

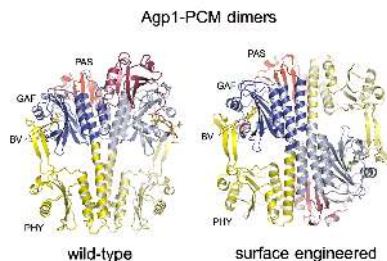


**Figure 1.** Structures of parallel (left) and anti-parallel dimers (right) of the photosensory core modules (PCMs) of wild-type Agp1 and a surface-engineered mutant, respectively. The domains of the PAS-GAF-PHY tridomains are shown in different colours.

**Keywords:** phytochrome, histidine kinase, dynamic quaternary structure



## MS9-P6 Neutron macromolecular crystallography at the FRM II - Or: what can neutrons do for you

Andreas Ostermann<sup>1</sup>, Tobias E. Schrader<sup>2</sup>, Michael Monkenbusch<sup>3</sup>, Bernhard Laatsch<sup>4</sup>, Philipp Jüttner<sup>1</sup>, Winfried Petry<sup>1</sup>, Dieter Richter<sup>3</sup>

1. Heinz Maier-Leibnitz Zentrum (MLZ), Technische Universität München, Lichtenbergstr. 1, 85748 Garching, Germany
2. Jülich Centre for Neutron Science JCNS, Forschungszentrum Jülich GmbH, Outstation at MLZ, Lichtenbergstr.1, 85747 Garching, Germany
3. Institute for Complex Systems ICS, Forschungszentrum Jülich GmbH, 52425 Jülich, Germany
4. Forschungszentrum Jülich GmbH, Engineering and Technology (ZEA-1), 52425 Jülich, Germany

email: Andreas.Ostermann@frm2.tum.de

The research reactor Heinz Maier-Leibnitz (FRM II) is a modern high flux neutron source which feeds at the present 27 state of the art instruments. The newly build neutron single crystal diffractometer BIODIFF is especially designed to collect data from crystals with large unit cells. The main field of application is the structure analysis of proteins, especially the determination of hydrogen atom positions. BIODIFF is a joint project of the Forschungszentrum Jülich (FZJ/JCNS) and the Forschungs-Neutronenquelle Heinz Maier-Leibnitz (FRM II). Typical scientific questions addressed are the determination of protonation states of amino acid side chains in the active center of enzymes and the characterization of the hydrogen bond network between the protein and an inhibitor or substrate. BIODIFF is designed as a monochromatic instrument. By using a highly orientated pyrolytic graphite monochromator (PG002) the diffractometer is able to operate in the wavelength range of 2.4 Å to about 5.6 Å. Contaminations of higher order wavelengths are removed by a neutron velocity selector. To cover a large solid angle and thus to minimize the data collection time the main detector of BIODIFF consists of a neutron imaging plate system in a cylindrical geometry. A Li/ZnS scintillator CCD camera is available for additional detection abilities. The main advantage of BIODIFF is the possibility to adapt the wavelength to the size of the unit cell of the sample crystal while operating with a clean monochromatic beam that keeps the background level low. BIODIFF is equipped with a standard Oxford Cryosystem "Cryostream 700+" which allows measurements in the temperature regime from 90K up to 500K.

**Keywords:** Protonation states, enzyme function, neutron macromolecular crystallography, water structure

## MS9-P7 Structural Insight of Hyperthermostable Cellulase from The Archaea *Pyrococcus horikoshii*

Han-Woo KIM<sup>1</sup>, Ae Kyung Park<sup>1</sup>, Kazuhiko Ishikawa<sup>2</sup>

1. Korea Polar Research Institute
2. National Institute of Advanced Industrial Science and Technology

email: hwkim@kopri.re.kr

**A hyperthermophilic membrane related  $\beta$ -1,4 endoglucanase (family 5, cellulase) from *Pyrococcus horikoshii* was found to be capable of hydrolyzing crystalline cellulose at high temperatures. This hyperthermophilic enzyme has promise for applications in biomass utilization, but we have no information regarding the substrate-recognition mechanism of the enzyme. To examine its mechanism, we determined the crystal structure of its active domain at a resolution of 1.95 Å. From analysis of its structure and the reaction products, it was clarified that this endocellulase has a unique characteristic of releasing cellobiose from the reducing end of the cellulose substrate. This unique action results from the specific recognition of the reducing end of the substrate by the subsite of the active domain. The enzyme-ligand structure and mutation analysis reveal that the variant residue, Ile162, located at the subsite -1 position may have a hydrophobic role in forming the Michaelis complex. The structure of the wild type enzyme-cellobiose complex also provides insight into the retaining mechanism of EGPh**

**Keywords:** cellulase, hyperthermostable, *Pyrococcus horikoshii*

## MS9-P8 Structural basis for ascorbate production by dehydroascorbate reductase in *Oryza sativa* L. japonica

Jun Hyuck Lee<sup>1,2</sup>, Il-Sup Kim<sup>3</sup>, Chang Woo Lee<sup>1,2</sup>, Ae Kyung Park<sup>1</sup>, Hyun Park<sup>1,2</sup>, Ho-Sung Yoon<sup>3</sup>, Han-Woo Kim<sup>1,2</sup>

1. Division of Polar Life Sciences, Korea Polar Research Institute
2. Department of Polar Sciences, University of Science and Technology
3. Department of Biology, Kyungpook National University

email: junhyucklee@kopri.re.kr

Ascorbate (ascorbic acid or vitamin C) is a strong antioxidant molecule as well as a cofactor for several enzymatic reactions. Dehydroascorbate reductase (DHAR) catalyzes the GSH-dependent reduction of oxidized ascorbate (dehydroascorbate, DHA) in plants to produce ascorbate. Therefore, DHAR functions in the detoxification of reactive oxygen species (ROS). In previous studies involving transgenic rice, we found that DHAR overexpression resulted in improved growth and increased grain yield. In order to clarify the molecular mechanisms of DHAR, we determined the crystal structures of DHAR from *Oryza sativa* L. japonica (OsDHAR) in the native, ascorbate-bound, and GSH-bound forms. These structures represent the first molecular view of the OsDHAR enzyme and the binding sites for ascorbate and GSH within OsDHAR. In addition, the residues involved in ascorbate and GSH recognition were identified at atomic resolution; structural comparisons with other homologous structures (CLIC1 and GSTs) are also discussed. We suggest a detailed enzymatic reaction mechanism for OsDHAR.

**Keywords:** ascorbate, dehydroascorbate reductase, *Oryza sativa* L. japonica, X-ray crystallography

## MS10 H-bonding & weak interactions in crystals: neutrons and X-rays

Chairs: Boris Zakharov, Hazel Sparkes

## MS10-P1 Crystal structure and hydrogen bonds pattern of a new hydrated hexachloridoindate based on piperazinium

Ratiba Belhouas<sup>1</sup>, Sofiane Bouacida<sup>1,2</sup>, Boubakeur Fantazi<sup>1</sup>, Chaouki Boudaren<sup>1</sup>

1. Unité de recherche CHEMS, Université Mentouri Constantine, 25000, Algeria
2. Département SM, Université LBM, Oum El Bouaghi, Algeria

email: belhouas.ratiba@yahoo.fr

A new hybrid compound based on piperazinium and hexachloridoindate(III) was synthesized by aqueous solution reaction and characterized by X-ray diffraction.

The asymmetric unit of (C<sub>4</sub>H<sub>12</sub>N<sub>2</sub>)<sub>3</sub>-[InCl<sub>6</sub>]<sub>2</sub>·4H<sub>2</sub>O, consists of one and half independent piperazinium cations, and hexachloridoindate anion and two molecules of water.

The In(III) ion is six-coordinated and forms a quasi-regular octahedral arrangement. In the crystal, alternating layers of cations and anions are arranged parallel to (101) and are linked with the water molecules via intra- and intermolecular N—H...O, O—H...Cl, C—H...O and N—H...Cl hydrogen bonds, forming a complex three-dimensional network. Additional stabilization within the layers is provided by weak intermolecular C—H...Cl interactions.

**Keywords:** crystal structure, piperazinium cation, hexachloridoindate anion, hydrogen bond.

## MS10-P2 An *ab-initio* fully deuterated tiny crystal (1x0.25x0.20mm) allows Neutron data collection at room temperature up to 1.90Å

Andre Mitschler<sup>1</sup>, Eduardo Howard<sup>2</sup>, Matthew Blakeley<sup>3</sup>, Takashi Tomizaki<sup>4</sup>, Michael Haertlein<sup>5</sup>, Martine Moulin<sup>5</sup>, Alexandra Coudido-Siah<sup>1</sup>, Alberto Podjarny<sup>1</sup>

1. IGBMC, CNRS, INSERM, UoS, Illkirch, France
2. IFILYSIB, CONICET, UNLP, La Plata, Argentina
3. ILL, Grenoble, France
4. SLS, Villigen PSI, Switzerland
5. PBS, Grenoble, France

email: mitschler@gmail.com

The crystal structure of Heart Fatty Acid Binding Protein (H-FABP) (M.W. = 15 kDa) complexed with its natural oleic acid ligand was jointly refined with X-ray and Neutron diffraction data measured both at RT up to 0.98 and 1.90Å respectively. The H---H contacts (as D---D) occurring in the binding of the long fatty acid (16 C) to the highly conserved hydrophobic protein residues, together with the ordered water cluster (as D<sub>2</sub>O) present inside the large internal protein cavity could be analyzed in fine details, [E. I. Howard *et al.*, (2016). *IUCrJ.* 3, 115-116., PDB entry 5ce4]. The perdeuterated protein has been over-expressed in the Deuteration Laboratory at ILL, Grenoble-France using d<sub>5</sub>-glycerol as a carbon source [J. B. Artero *et al.*, (2005). *Acta Cryst. D61*, 1541-1549.]. Subsequent crystallization was achieved in D<sub>2</sub>O. These perdeuterated crystals must be sheltered against air moisture (to avoid replacement of deuterium by hydrogen atoms) especially during their mounting in quartz capillaries, by using protecting D<sub>2</sub>O amounts on each side of the crystal within the capillary, which is finally closed tightly with a two-component glue. The quasi-Laue neutron data were collected at RT at ILL, Grenoble-France on the new LADI-III beamline [M. P. Blakeley *et al.*, (2010). *Acta Cryst. D66*, 1198-1205.]. Interestingly, the ratio of our tiny crystal volume (0.05mm<sup>3</sup>) vs. the crystal asymmetric unit-cell volume (34.000 Å<sup>3</sup>), is the smallest ratio (14x10<sup>-14</sup>) of any Neutron Protein Crystallography (NPC) study published so far [M. P. Blakeley *et al.*, (2015). *IUCrJ.* 2, 464-474.]. X-ray diffraction data from another perdeuterated crystal of the same crystallization batch were collected also at RT at the Swiss Light Source (SLS) Synchrotron on the X06SA beamline. Both data processing statistics are given in the poster.

**Keywords:** Neutron protein crystallography, hFABP, perdeuteration

## MS10-P3 Synthesis, X-ray structural study and theoretical investigation of new coordination complexes based on benzimidazole derivatives.

Sofiane BOUACIDA<sup>1,2</sup>, Sahki Ferial<sup>2</sup>, Bouraoui Abdelmalek<sup>2</sup>, Merazig Hocine<sup>2</sup>

1. Département sciences de la matière, université Oum El Bouaghi, 04000 Oum El Bouaghi Algeria.
2. Unité de Recherche de Chimie de l'Environnement et Moléculaire Structurale, Université des frères Mentouri. Constantine 25000, Algeria.

email: bouacida\_sofiane@yahoo.fr

Benzimidazole derivatives are reported to be physiologically and pharmacologically active and have shown different biological activities such as antioxidant, antifungal, antitumoral, anti-inflammatory and antimicrobial. The ability of benzimidazole derivatives to form stable complexes with metal ions, had given a place to a variety of metal-ligand coordination modes. Several research teams have examined the coordination behavior of benzimidazole derivatives towards transition metal ions and others studies have explored the biological activity of coordination compounds containing benzimidazole entity.

A ligand, 2-(1*H*-benzo[d]imidazole-2-yl)quinoline and its Cobalt and Manganese complex have been synthesized. The molecular structure of ligand and its Co(II) and Mn(II) complex are determined by single crystal X-ray diffraction technique. We report here the synthesis, crystallographic study, hydrogen bond interactions and theoretical investigation of two new coordination complexes based on benzimidazole derivative. In order to provide a better understanding of the bonding and the electronic structure of the ligand and their neutral complexes, we have carried out DFT calculations. The optimized structures reproduce those observed experimentally, while the reduced ones undergo remarkable geometrical parameters.

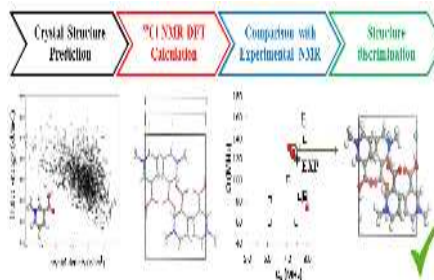


**Figure 1.** ORTEP of molecular structure of organic ligand and their coordination complexes.

**Keywords:** Benzimidazole derivatives, single crystal, hydrogen bond, theoretical investigation

# MS10-P4 Charge density studies and topological analysis of X-H...S hydrogen bonds

Anita M. Grzeskiewicz<sup>1</sup>, Maciej Kubicki<sup>2</sup>

1. Adam Mickiewicz University, Poznań, Poland

2. Adam Mickiewicz University, Poznań, Poland

email: aniw@amu.edu.pl

From many, many years hydrogen bonds - due to their great importance in biological systems - have been extensively studied in terms of geometry, energy and many others aspects. One of the method of studying hydrogen bond is Bader's quantum theory – Atoms in Molecules. This analysis permits to characterize interatomic interactions by means of the topological properties of charge density in the critical point. There are several articles that point out some relevant systematic relationship between the topological properties at the critical point and geometric parameters of HB[1-5]. However they mostly concern the X-H...O interactions. We have decided to perform similar research in case of sulfur atom as an acceptor of different type of HBs. To do that we have determined the experimental charge density distribution in crystals of 4 different thioamides (2-mercaptobenzothiazole, 5-chloro-2-mercaptobenzothiazole, thiobarbituric acid and 4-amino-6-hydroxy-pyrimidine-2-thione), in order to obtain a good basis for determining the aforementioned dependence. The results of analysis will be presented in the communication.

References [1] Espinosa, E., Molins, E. & Lecomte, C. *Chemical Physics Letters* **285**, 170–173 (1998). [2] Espinosa, E., Souhassou, M., Lachekar, H. & Lecomte, C. *Acta Crystallographica Section B Structural Science* **55**, 563–572 (1999). [3] Espinosa, E., Lecomte, C. & Molins, E. *Chemical Physics Letters* **300**, 745–748 (1999). [4] Ranganathan, A., Kulkarni, G. U. & Rao, C. N. R. *Journal of Molecular Structure* **656**, 249–263 (2003). [5] Munshi, P. & Row, T. N. G. *CrystEngComm* **7**, 608–611 (2005).

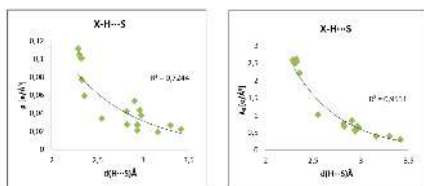


**Figure 1.** Exponential fitting of  $\rho$  (electron density in the critical point)  $\lambda_c$  (positive curvature of the electron density in the critical point) and against hydrogen ... sulfur distance [ $d(\text{H}\cdots\text{S})$ ]

**Keywords:** weak hydrogen bonds, sulfur, charge density, topological analysis

# MS10-P5 Intermolecular interactions in 4-[[[(4Z)-5-oxo-2-phenyl-4,5-dihydro-1,3-oxazol-4-ylidene] methyl} phenyl acetate: Insights from Crystal Structure and Hirshfeld Surface Analysis

Mukesh M. JOTANI<sup>1</sup>

1. Department of Physics, Bhavan's Sheth R. A. College of Science, Ahmedabad, Gujarat, 380 001, INDIA

email: mmjotani@rediffmail.com

The 1,3-oxazole ring is known to have the biological activity in its own right and serves as useful intermediate in the synthesis of biologically important imidazole molecules. The investigations for the title molecule (I) is the part of ongoing research on crystallographically important organic molecules. The colourless, block shape single crystals obtained by slow evaporation from ethanol solution were used for X-ray diffraction experiment. Intensity data were measured at 100 K on Agilent Technologies Super Nova diffractometer using CuK $\alpha$  ( $\lambda$  = 1.5418 Å). The structure was solved using direct methods and refined by full-matrix least-squares on  $F^2$  using SHELX programs. The Hirshfeld surfaces generated using *Crystal Explorer* and the two dimensional fingerprint plots provide the visual representation of crystal packing interactions in the structure. The molecule has Z-configuration about central olefinic bond, and the overall U-shaped conformation. The crystal structure of (I) determined at 100 K shows clear distinction from that at 293 K as the intermolecular interactions can be described more precisely due to improvement in thermal as well as geometrical parameters. The collective influence of intramolecular C-H...N and C-H...O interactions with the respective S(6) and S(5) graph-set motifs, intermolecular C-H...O interaction having  $R^2_2$ , (14) graph-set, C-O... $\pi$  and  $\pi$ - $\pi$  stacking along b-axis stabilize the crystal structure of (I) at 100 K in contrast to the presence of only C-O... $\pi$  interaction at 293 K. The intermolecular C-H...O interactions appear as bright-red spots near H7 and O3 atoms, and the inter atomic short C...C contacts as faint spots near corresponding atoms on the Hirshfeld surface mapped over  $d_{\text{norm}}$ . The C-O... $\pi$  and  $\pi$ - $\pi$  interactions in the crystal are identified from Hirshfeld surfaces mapped with shape-index and curvedness respectively. The significant features appearing in the two dimensional fingerprint plots are complementary to describe the role of intermolecular interactions in the crystal packing of title molecule (I). The intermolecular interactions were further assessed by a new descriptor enrichment ratio (ER) based on Hirshfeld surface analysis. Nearly same ER values for significantly contributing inter atomic contacts at 293 K and 100 K with the exception for C...C contacts also justify the determination of crystal structure of (I) at 100 K so as to describe the crystal packing interactions more precisely.

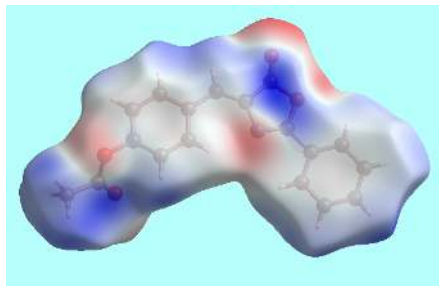


**Figure 1.** View of Hirshfeld surface mapped over electrostatic potential.

**Keywords:** Oxazoles, Intermolecular interactions, Hirshfeld surface Analysis, Fingerprint plots.

## MS10-P6 Inside “false tobacco”

Agata E. Owczarzak<sup>1</sup>, Maciej Kubicki<sup>1</sup>

<sup>1</sup>. Faculty of Chemistry, Adam Mickiewicz University in Poznań, Poland

email: agataowczarzak@gmail.com

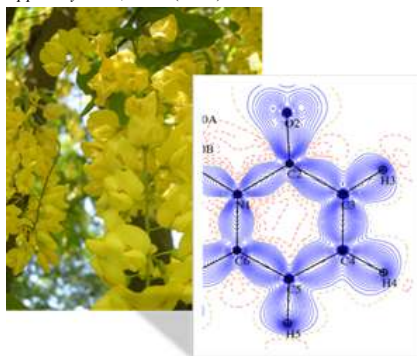
Tobacco smoking kills around 6 million people each year and it's one of the main public health threats. Smoking cessation with Cytisine is healthy and very effective. Cytisine is natural alkaloid obtained from *Laburnum anagyroides*, during the Second World War the levels of this plants were called "false tobacco". It's a partial agonist at the  $\alpha 4\beta 2$  nAChR (nicotinic acetylcholine receptors) and plays the part of nicotine substitute. Nicotine and cytisine have similar a mechanism action, but cytisine substance has low toxicity in contrast to nicotine. Therefore, cytisine has been applied in nicotine replacement therapy in the form of Tabex® Desmoxan® Chantix® etc. Moreover, cytisine derivatives have been explored as potential drugs Alzheimer's and Parkinson's diseases[1]. It is important to note that still, a thorough understanding of structural requirements of  $\alpha 4\beta 2$  agonists is lacking. High resolution X-ray crystallography can be used as main tool in analysis of structure relationships-activity. In this work will be present the analyse charge density distribution and intermolecular interactions in the cytisine and some of its new derivatives. The structures have been refined using Hansen-Coppens multipolar model [2] implemented in MoPro software [3], using several different strategies to obtain the best model of crystals. We will concentrated on a comparison of the multipole parameters and topological analyses in free base, protonated form and N-substituted cytisine.

This work is supported by a grant from the Polish National Science Center, 2013/11/B/ST5/01681

[1] P. Tutka, W. Zatonski, *Pharmacological Reports* 58, 777-798 (2005).

[2] N. Hansen, P. Coppens, *Acta Crystallographica Section A* 34, 909-921 (1978).

[3] C. Jelsch, B. Guillot, A. Lagoutte, C. Lecomte, *J. Appl. Cryst.* 38, 38-54 (2005).



**Keywords:** cytosine, charge distribution, electron density, topological analysis, hydrogen bond, weak interactions

## MS10-P7 Pressure induced C-H agostic interactions in a Uranium complex

Alessandro Prescimone<sup>1,2</sup>, Simon Parsons<sup>2</sup>, Polly L. Arnold<sup>2</sup>

1. University of Basel
2. University of Edinburgh

email: alessandro.prescimone@unibas.ch

The diuranium(III) compound [UN<sup>III</sup>2]2(μ-η(6):η(6)-C6H6) (N<sup>II</sup>=N(SiMe3)2) has been studied using variable, high-pressure single-crystal X-ray crystallography, and density functional theory. In this compound, the low-coordinate metal cations are coupled through π- and δ-symmetric arene overlap and show close metal-CH contacts with the flexible methyl CH groups of the sterically encumbered amido ligands. The metal-metal separation decreases with increasing pressure, but the most significant structural changes are to the close contacts between ligand CH bonds and the U centers. Although the interatomic distances are suggestive of agostic-type interactions between the U and ligand peripheral CH groups, QTAIM (quantum theory of atoms-in-molecules) computational analysis suggests that there is no such interaction at ambient pressure. However, QTAIM and NBO analyses indicate that the interaction becomes agostic at 3.2 GPa.

**Keywords:** extreme conditions, agostic interactions, high pressure, Uranium

# MS10-P8 Syntheses, Molecular Structures and Supramolecular Assembly in Three Mixed-Ligands Cobalt(II) Complexes

*trans*-[Co(HOOC-(C<sub>6</sub>H<sub>4</sub>)-COO)<sub>2</sub>(H<sub>2</sub>O)<sub>2</sub>(C<sub>3</sub>N<sub>2</sub>H<sub>4</sub>)<sub>2</sub>]  
*cis-mer*-[Co(C<sub>8</sub>H<sub>4</sub>O<sub>4</sub>)(H<sub>2</sub>O)<sub>2</sub>(C<sub>3</sub>H<sub>4</sub>N<sub>2</sub>)<sub>3</sub>]<sub>2</sub>·H<sub>2</sub>O  
 and  
*trans*-[Co(H<sub>2</sub>O)<sub>2</sub>(C<sub>3</sub>N<sub>2</sub>H<sub>4</sub>)<sub>4</sub>][OOC-C<sub>4</sub>H<sub>2</sub>S]-COO]

Balegroune Fadila<sup>1</sup>, Benkanoun Aouaouche<sup>1</sup>, Dahaoui Slimane<sup>2</sup>,  
 Triki Smail<sup>3</sup>

1. Laboratoire de Cristallographie-Thermodynamique, Faculté de Chimie, U.S.T.H.B, Alger, Algérie
2. CRM2, UMR-CNRS 7036 Jean Barriol Institut, Université de Lorraine, Nancy, France
3. Laboratoire de Chimie, Electrochimie Moléculaires et Chimie Analytique, UMR CNRS 6521, UBO, BP 809, Brest Cedex, France

email: fbalegroune@yahoo.fr

Carboxylate ligands, alone or combined with nitrogen ligands such as imidazole, have proven to be excellent candidates for the coordination polymers construction and multidimensional supramolecular structures [1-2]. Continuing our work on mixed ligand carboxylate complexes [3], three compounds from reactions between of cobalt salts, aromatic dicarboxylic acids and imidazole were synthesized, characterized by IR and TGA and their structures determined by single crystal XRD. Our syntheses have not achieved to expected mixed coordination polymers but led to 0D complexes. All the three crystallize in centrosymmetric spaces groups P2<sub>1</sub>/n, P-1 and P2<sub>1</sub>/c. The asymmetric unit consists of one Co(II) ion, one terephthalato dianion, three imidazole molecules, two coordination water molecules, one lattice water for complex 1, one Co(II) ion located on a center of inversion, one hydrogenisophthalato ligand, one imidazole molecule and one coordination water molecule for the second complex. In the salt complex, the structure consists unit of a [Co(H<sub>2</sub>O)<sub>2</sub>(C<sub>3</sub>N<sub>2</sub>H<sub>4</sub>)<sub>4</sub>]<sup>2+</sup> cation and a thiophenato ligand [OOC-C<sub>4</sub>H<sub>2</sub>S-COO]<sup>2-</sup>. All Co<sup>2+</sup> cations have a slightly distorted octahedral environment with all ligands adopting monocoordination mode except the dianion [OOC-C<sub>4</sub>H<sub>2</sub>S-COO]<sup>2-</sup> which remains uncoordinated. In the complex [Co(C<sub>8</sub>H<sub>4</sub>O<sub>4</sub>)(H<sub>2</sub>O)<sub>2</sub>(C<sub>3</sub>H<sub>4</sub>N<sub>2</sub>)<sub>3</sub>], the backbone of the architecture is an helical hydrogen-bonded ladder composed of alternating R<sub>2</sub><sup>4</sup>(10), R<sub>3</sub><sup>3</sup>(8) and R<sub>2</sub><sup>2</sup>(6) heterosynthons running along [010]. In [Co(HOOC-(C<sub>6</sub>H<sub>4</sub>)-COO)<sub>2</sub>(H<sub>2</sub>O)<sub>2</sub>(C<sub>3</sub>N<sub>2</sub>H<sub>4</sub>)<sub>2</sub>], the hydrogen bond network is not as dense as the previous complex but there are files of R<sub>2</sub><sup>2</sup>(8) synthons parallel to the [100] direction and connected by R<sub>2</sub><sup>2</sup>(16) synthons. In the complex salt, water molecules and cationic molecules are linked by hydrogen bonds forming R<sub>4</sub><sup>4</sup>(8) synthons, running in parallel lines at the b axis. This interconnected by thiophen dianion, engaged itself in a dense network of hydrogen bonds, in the three directions to form a three-dimensional supramolecular architecture. [1] Chen, P. K., Che, Y-X & Zheng, J-M. (2007). *Inorg.*

*Chem. Comm.*, 10, 187-190. [2] Fu, X-C., Wang, X-Y., Li, M-T., Wang, C-G. & Deng, X-T. (2006). *Acta Cryst.*, C62, m343-345. [4] Benkanoun, A., Balegroune, F., Guehria-Laidoudi, A., Dahaoui, S. & Lecomte, C. (2012). *Acta Cryst.*, E68, m480-m481.

**Keywords:** 0 D structures, Supramolecular assembly, Crystal structure



## MS11 Hybrid approaches and validation (X-ray and electron microscopy)

an easy task, all 54 atom positions in the unit cell were determined. It should be noted that despite the drastic compositional differences, the new  $\text{Th}_2\text{Ni}_{10}\text{Al}_{15}$  phase can be related to the orthorhombic phase discussed above since they both belong to a family of so-called layered structures.

**Keywords:** Intermetallics, Aluminides, Structure solution, Electron Crystallography, DFT calculations, Symmetry

Chairs: Felix Rey, Mathieu Botte

### MS11-P1 Structural changes as a function of transition metal's (T) type in the $\text{ThT}_2\text{Al}_{20}$ alloys

Louisa Meshi<sup>1</sup>, Gili Yaniv<sup>1</sup>, Asaf Uziel<sup>1</sup>, Avraham Bram<sup>1</sup>, Arnold E. Kiv<sup>1</sup>, Arie Venkert<sup>2</sup>, David Fuks<sup>1</sup>

1. Department of Materials Engineering, Ben-Gurion University of the Negev, 84105 Beer-Sheva, Israel

2. Nuclear Research Center - Negev, P.O. Box 9001, 84190 Beer-Sheva, Israel

email: louisa@bgu.ac.il

Strong inter-linkage exists between the physical/chemical properties-chemical composition and crystal structure of the materials. In order to gain improved properties - composition and/or structure should be changed. Such researches are normally done either via theoretical route (i.e. prediction) or experimental (i.e. "trial and error"). Experimental route is time and resource consuming. Prediction (basing on energy landscapes) is not always possible, especially when system of an interest exhibits complex electronic structure, such as A-T-Al (where A-actinide and T-transition metal) containing *f*-electron elements. In these systems,  $\text{AT}_2\text{Al}_{20}$  alloys were intensively studied with a purpose to find aluminides with heavy fermion properties. Our study concentrated on the  $\text{ThT}_2\text{Al}_{20}$  system (where T-*3d* transition metal) in order to formulate a general "rule of thumb" which will allow to estimate the symmetry of the Al-rich ternary structure forming in these systems. Such prediction will shorten the research time spent on search for the heavy fermion materials with interesting magnetic and electrical properties. We have proved experimentally (using a combination of X-ray diffraction and conventional electron microscopy) and theoretically (applying Density Functional Theory) that ternary aluminides structure's symmetry changes abruptly as a function of atomic number of T (i.e.  $Z_T$ ). At T=Mn, the symmetry decreases from cubic ( $22 \leq Z_T \leq 25$ ) to orthorhombic ( $25 \leq Z_T \leq 27$ ). At  $Z_T=28$  (i.e. T=Ni) three new structures were formed. Despite the prolonged heat treatment, equilibrium was not achieved. Applying Electron Diffraction Tomography method (known as EDT) for structure characterization of these phases - geometry of all phases was proposed. Full structure solution of the major  $\text{Th}_2\text{Ni}_{10}\text{Al}_{15}$  phase was performed using manually collected EDT dataset. This phase was found to be orthorhombic, *Immm*, with lattice parameters  $a=3.992\text{Å}$ ,  $b=11.172\text{Å}$  and  $c=17.343\text{Å}$ . Although Th, as heavy scatterer, did smear the Fourier difference map so that finding Al atom positions was not

**Keywords:** Bcl-2, apoptosis, Bok

## MS12 Biophysical characterization and crystallization

Chairs: Rob Meijers, Bernadette Byrne

### **MS12-P1** Structural and Functional Characterisation of Bok, a Pro-apoptotic Bcl-2 Effector Protein

Angus D. Cowan<sup>1,2</sup>, Peter M. Colman<sup>1,2</sup>, Peter E. Czabotar<sup>1,2</sup>

1. Structural Biology Division, Walter and Eliza Hall Institute of Medical Research, 1G Royal Parade, Parkville, Victoria 3052, Australia

2. Department of Medical Biology, University of Melbourne, Parkville, Victoria 3052, Australia

email: [cowan.a@wehi.edu.au](mailto:cowan.a@wehi.edu.au)

The Bcl-2 protein family regulates the essential cell death program known as intrinsic or mitochondrial apoptosis. A delicate balance of pro-survival and pro-apoptotic Bcl-2 proteins controls the critical process of mitochondrial outer membrane permeabilisation (MOMP) that results in the release of Cytochrome *c* from the intermembrane space and the subsequent death of the cell.

The pro-apoptotic effector proteins Bax and Bak facilitate MOMP and are kept in check by pro-survival proteins such as Mcl-1, Bcl-X<sub>L</sub> and the founding member and namesake of the family, Bcl-2. Pro-apoptotic BH3-only proteins such as Bim and Bid can both directly activate Bax and Bak and inhibit the function of pro-survival proteins. When pro-survival proteins are overwhelmed due to upregulation of BH3-only proteins in response to stress signals, activated Bax and Bak oligomerise on the mitochondrial outer membrane leading to MOMP.

Until recently, Bax and Bak were thought to be absolutely required for MOMP. However, recent work from the lab of Douglas Green has identified the previously enigmatic Bcl-2 protein Bok as a bone fide pro-apoptotic effector protein with the ability to permeabilise the mitochondria as well as membrane-mimicking liposomes. Interestingly, in contrast to Bax and Bak, Bok appears to be constitutively active and regulated by ER-associated degradation rather than by other Bcl-2 proteins.

We have solved the X-ray crystal structure of a homolog of human Bok that may provide clues in regards to its atypical property of constitutive activation. Additionally, we have performed our own biophysical characterization of Bok using a liposomal system and surface plasmon resonance. We find that, in agreement with recently published work, Bok is constitutively active and interacts only weakly with other Bcl-2 proteins.

## MS12-P2 New approach to protein crystallization. Investigation of various crystallization stages of lysozyme.

Yuliya A. Dyakova<sup>1,2</sup>, Alexander E. Blagov<sup>1,2</sup>, Margarita A. Marchenkova<sup>1,2</sup>, Yuriy V. Pisarevskiy<sup>1,2</sup>, Pavel A. Prosekov<sup>1,2</sup>, Vladimir V. Volkov<sup>1</sup>, Mikhail V. Kovalchuk<sup>1,2,3</sup>

1. Shubnikov Institute of Crystallography of Russian Academy of Sciences

2. National Research Centre "Kurchatov Institute"

3. St. Petersburg State University

email: juliaadi@yandex.ru

Nowadays protein crystallization is an extensive area of the scientific research, but a very important and difficult challenge in this area is to find the proper crystallization conditions. Currently the crystallization conditions are usually obtained by trial-and-error methods; hence, the possibility to obtain high X-ray diffraction (XRD) quality protein crystals is not so predictable.

In this work the processes of lysozyme crystals growth on different substrates have been studied in situ by XRD technique. Lysozyme crystals on substrates were grown using the sitting-drop method in a specially designed sealed crystallization cell with chemically fixed inner environment. This crystallization cell is suitable for optical and XRD studies in a wide incident-angle range, which enables researchers to perform in situ studies of the protein crystals growth and their properties in the native state (1).

An initial crystallization stage is of great importance for both the crystallization conditions search and obtaining high-quality crystals.

*We proposed and experimentally demonstrated a deep relation between an oligomer formation and the best crystallization conditions for tetragonal lysozyme.*

We selected elements in the crystal structure of tetragonal lysozyme crystals, which are ordered oligomers, and assumed that these oligomers can function as growth units in crystal growth.

The study of lysozyme conformation was conducted under different temperatures and concentration of protein. We also investigated the effect of substitution in the crystallization solution of ordinary water (H<sub>2</sub>O) to heavy water (D<sub>2</sub>O).

The results showed a noticeable presence of lysozyme dimers and octamers under crystallization conditions and the total absence of oligomers under conditions where crystal growth was impossible. Fig. 1 We identified the structures of possible crystal growth units of tetragonal lysozyme and revealed the relationship between the formation of certain types of oligomers in solution and the optimum crystallization conditions. Hence, our approach could be useful for studying protein crystallization mechanisms (2).

Based on the results presented in the paper, thin films were prepared by lysozyme area of about 1 cm square.

This study was supported in part by the RFBR (project no. 15-29-01142\_ofi\_m, 16-32-60144\_mol\_a-dk)

1- Kovalchuk, M. V. and all // *Crystallogr. Rep.* 2014, 59, 679

2- Mikhail V. Kovalchuk and all // *Crystal Growth & Design.* 2016, 16 (4), 1792

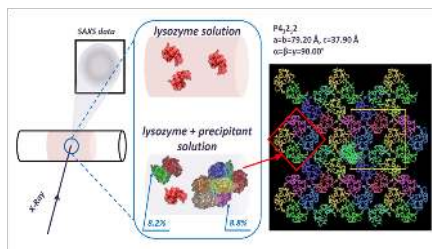


**Figure 1.** Scheme study of the initial stages of crystallization of lysozyme by SAXS. A projection of the tetragonal HEWL structure perpendicular to the 4-fold axis. The octamers are proposed as growth 'building blocks'.

**Keywords:** crystal growth unit, protein solution, small angle X-ray scattering, molecular modelling, lysozyme, X-ray diffraction

**MS12-P3** Structural and dynamics studies of human phenylalanine hydroxylase, a highly regulated allosteric enzymeMarte I. Flydal<sup>1,2</sup>, Martín Alcorlo<sup>3</sup>, Lars Skjærven<sup>1</sup>, Ines Muñoz<sup>4</sup>, Knut Teigen<sup>1</sup>, Juan A. Hermoso<sup>3</sup>, Aurora Martínez<sup>1</sup>

1. Department of Biomedicine, University of Bergen, Bergen, Norway
2. Department of Neurology, Haukeland University Hospital, Bergen, Norway
3. Department of Crystallography and Structural Biology, Institute of Physical Chemistry "Rocasolano", CSIC, Madrid, Spain
4. Macromolecular Crystallography Group, Spanish National Cancer Research Centre (CNIO), Madrid, Spain

email: marte.flydal@uib.no

Phenylalanine hydroxylase (PAH) is a tetrahydrobiopterin (BH<sub>4</sub>)-dependent enzyme that catalyses the rate-limiting step in the degradation of phenylalanine (L-Phe). Excessive amounts of L-Phe is toxic to the brain and in patients with the disease phenylketonuria (PKU), a dysfunctional PAH thus leads to irreversible brain damage if the patient does not follow a life-long diet with restricted protein content. Understanding the conformation and dynamics of the enzyme, as well as the misfolding and instability changes caused by the more than 800 PKU-associated loss-of-function mutations, is an essential requirement in the search of therapeutic strategies towards PKU, such as pharmacological chaperones. Mammalian PAH is a large tetrameric (200 kDa) enzyme and each of the identical subunits consists of three domains: an N-terminal regulatory domain (RD), a central catalytic domain (CD) and a C-terminal oligomerization domain (OD). In the inactive state, the long, unstructured N-terminus of the RDs covers the active site entrances. However, upon L-Phe binding, the flexible hinges between the domains promote a large conformational change resulting in displacement of the N-terminus, a cooperative increase in activity and stabilization of the high-activity state. We are at present investigating the conformation and dynamics of human PAH using structural techniques such as X-ray crystallography and SAXS, in combination with binding studies and molecular dynamics simulations. We are interested in unveiling the catalytic mechanism of human PAH as well as the regulatory conformational events elicited by its substrate and cofactor BH<sub>4</sub>. Also, we are investigating how the structure and dynamics are affected by recurrent PKU mutations as a base in the design of novel therapies for PKU. Our recent results on this matter will be presented.

**Keywords:** X-ray crystallography, SAXS, molecular dynamics simulations, phenylketonuria

**MS12-P4** DNA I-motifs: Beyond the Double HelixSarah P. Gurung<sup>1,2,3</sup>, James P. Hall<sup>1,2,3</sup>, John A. Brazier<sup>4</sup>, Graeme Winter<sup>1</sup>, Thomas Sorensen<sup>1,2</sup>, Christine J. Cardin<sup>2,3</sup>

1. Diamond Light Source Ltd., Harwell Science and Innovation Campus, Didcot, Oxfordshire, OX11 0DE, UK
2. The Research Complex at Harwell, Rutherford Appleton Laboratory, Didcot, Oxfordshire, OX11 0FA, UK
3. Dept. of Chemistry, University of Reading, Whiteknights, Reading, Berkshire, RG6 6AD, UK
4. School of Pharmacy, University of Reading, Whiteknights, Reading, Berkshire, RG6 6AD

email: s.p.gurung@pgr.reading.ac.uk

I-motifs are four-stranded DNA structures made up of cytosine-rich sequences.<sup>1</sup> These structures are held together by hemi-protonated cytosine<sup>+</sup>-cytosine base pairs (Fig. 1A) to form an intercalated motif (hence the name i-motif), therefore, proving to be more stable in acidic conditions. This unique property helped produce the first DNA molecular motor to be driven by pH changes. Cytosine-rich sequences have also been detected in promoter regions of several oncogenes, making i-motifs an attractive subject for gene transcription modulation along with DNA nanotechnology.

The i-motif can form as either an inter- or an intramolecular structure (Fig. 1B). However, only six i-motif crystal structures have been reported to date; all of which are tetramolecular, even though i-motifs *in vivo* would exist as intramolecular. UV and synchrotron radiation CD (srCD; beamline B23 at Diamond Light Source) spectroscopy were used to study the structural stability of intramolecular i-motifs. Our results showed that i-motifs with shorter loop lengths exhibit the highest stability.<sup>2</sup> Crystallisation trials based on these initial results will be reported along with previously recorded i-motif crystals grown in new conditions. I will also be reporting the diffraction of d(CCCT)<sub>n</sub> crystals (Fig. 1C) at 0.68 Å at beamline I02, illustrating the advances in modern-day DNA crystallography via synchrotron radiation. Combination of results from the mentioned instrumental approaches shows that these methods are actually complementary.

**References**

1. Gehring, K., Leroy, J. L. & Gueron, M. A tetrameric DNA structure with protonated cytosine-cytosine base pairs. *Nature*, **363**, 561–565 (1993).
2. Gurung, S. P., Schwarz, C., Hall, J. P., Cardin C. J. & Brazier, J. A. The importance of loop length in the stability of i-motif structures. *Chem. Comm.*, **51**, 5630-32 (2015).

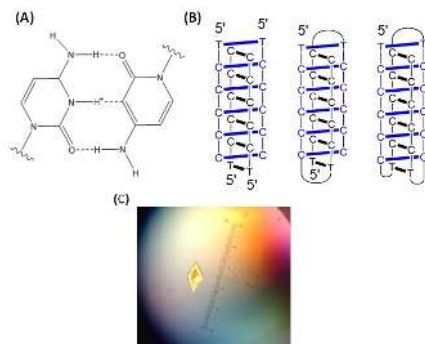


**Figure 1.** (A) Cytosine<sup>+</sup>- cytosine base pairing in i-motifs. (B) Schematic diagrams of tetramolecular (left) bimolecular (middle) and intramolecular (right) i-motifs. (C) 30x25x15 micron crystal of d(CCCT)<sub>4</sub>.

**Keywords:** i-motif, DNA, biophysical

## MS12-P5 Crystallography Platform at the Pasteur Institute

Ahmed Haouz<sup>1</sup>, Patrick Weber<sup>1</sup>, Cedric Pissis<sup>1</sup>, Rafael Navaza<sup>1</sup>,  
Frederick Saul<sup>1</sup>

1. Institut Pasteur, PF crystallography, CNRS-UMR 3528, 25 Dr Roux, 75724, Paris France

email: ahaouz@pasteur.fr

The goal of the crystallography platform is to provide research teams working in the field of macromolecular crystallography at Institut Pasteur with the expertise and technology for high throughput crystallization, X-ray diffraction measurements, and crystallographic computing as a core facility. Our second mission is to offer expertise in bio-crystallography, from crystallization of selected targets to resolution of 3D crystal structures by participating as a partner in research projects involving structural studies of single proteins and protein complexes. These projects arise from direct collaboration with research groups at Institut Pasteur and outside organisations.

Depending on the expertise of the users, three options can be offered: service provision, instrument allocation, and scientific collaboration. Service provision, which corresponds to the automated crystallization experiments performed in standard conditions, is the option used by the crystallographers. If initial crystallization trials are successful, the platform assists users to reproduce and optimize the crystallization conditions in order to obtain suitable crystals for X-ray data collection.

Since 2010, the platform has been involved in more than 24 scientific collaborations in association with 14 research units from 8 scientific departments of the Institut Pasteur and 6 laboratories from other institutions (French or foreign), leading to our co-authorship of 32 peer-reviewed publications. These projects cover many disciplines related to infectious diseases and human health, including defense mechanisms against pathogens, antibiotic resistance, regulation pathways, genetic disorders and drug design.

In our poster, we present the instrumentation and robotics available in the platform and a summary of results obtained during the last five years.

**Keywords:** High throughput, crystallization, pipeline

## MS12-P6 Best architecture of protein crystal. Database of protein-polymer interactions showing a unique role of PEG in protein crystallization

Hašek Jindřich<sup>1</sup>, Skálová Tereza<sup>1</sup>, Kolenko Petr<sup>1</sup>, Dušková Jarmila<sup>1</sup>, Koval Tomáš<sup>1</sup>, Stránský Jan<sup>1</sup>, Švecová Leona<sup>1</sup>, Trundová Marie<sup>1</sup>, Dohnálek Jan<sup>1</sup>

1. Institute of Biotechnology of Academy of Sciences, BIOCEV, Vestec 25242, Czech Republic

email: hasekjh@seznam.cz

Protein molecules regularly ordered in crystal remain highly solvated and are continuously in dynamic equilibrium with solution. The stability of molecules in crystal is ensured by the 3D scaffold formed by intermolecular contacts between adhesive patches of neighbor molecules, whereas 30-80 % of crystal content remains dynamically disordered. That is why the stability of the 3D skeleton, i.e. **protein crystal architecture (PCA)** is so important.

Large surface of protein molecules has usually many adhesive patches and thus we often observe different PCAs of the same protein (polymorphism). Each PCA has its own set of compatible adhesion modes and its own optimal solvent content in crystal. When incompatible adhesion modes are combined during crystal growth, one gets virtually non-diffracting solid phase.

**Principle of dominating adhesion mode** plays a key role in the control of diffraction quality of crystal. It says that well diffracting crystals grow only when incompatible adhesion modes are suppressed. This can be achieved either by rational composition of crystallization solution using **protein surface shielding agents (PSSA)** [J.Synchr.Radiation (2011)18,50-52] or by chemical modification of the protein surface, or complexation with high affinity ligands.

Analysis of already solved structures allows planned strengthening of dominant or weakening of non-compatible adhesion modes and a control of the diffraction quality of growing crystals. Theory of protein-protein adhesion modes shows why the poly(ethyleneglycol type polymers (PEGs) are the most successful precipitants [Z.Kristallogr.(2006)23,613-619].

**Database of protein-polymers interactions (DPPI)** [Z.Kristallogr.(2011)28,475-480] contains about 4000 of experimentally observed PEG-protein interfaces. It consists of a set of protein structures crystallizing with PEG and the script allowing easy visualization of PEG activities on protein surfaces. Seeing the PEG fragments interfering with protein-protein interfaces, with different types of salts, blocking competitive crystal contacts, protein oligomerization, crystallization, or biological activity, helps to understand the dynamic processes during crystal growth and allows rationalization of its performance on molecular basis. **DPPI** is available from [hasekjh@seznam.cz](mailto:hasekjh@seznam.cz).

The project is supported by BIOCEV CZ.1.05/1.1.00/02.0109 from the ERDF, CSF project 15-15181S of the CSF, grant LG14009 of MSMT, BioStruct-X (EC FP7 project 283570) and Instruct of ESFRI.

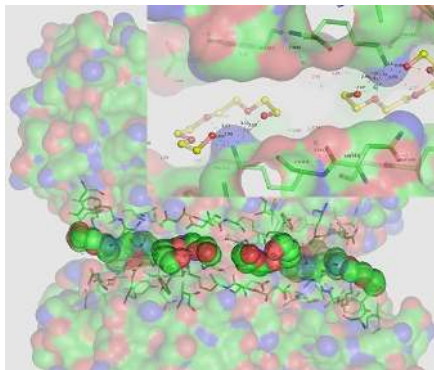


**Figure 1.** PEG induced adhesion mode as a leading motif for crystallization. The insert shows a typical crown ether conformation of polyether caused by interaction of five oxygens to lysine from one side. It induces strong hydrophobic interaction to the neighbor molecule on the opposite side. PDB code 3NBT.

**Keywords:** Protein crystal architecture, protein surface shielding agents, protein-protein interfaces, PEG-protein interactions, polymorphism, best diffraction, adhesion mode

## MS12-P7 Isolation, purification and crystallization of a novel bidirectional NK activating ligand CD160 in complex with herpesvirus entry mediator HVEM

Ivana Nemčovičová<sup>1,2</sup>, Marek Nemčovič<sup>3</sup>, Marcela Kúdelová<sup>1</sup>,  
Dirk M. Zajonc<sup>2</sup>

1. Biomedical Research Center at the Slovak Academy of Sciences, Dúbravská cesta 9, Bratislava, SK 84505, Slovakia
2. La Jolla Institute, 9420 Athena Circle, La Jolla, CA 92037, United States
3. Institute of Chemistry at the Slovak Academy of Sciences, Dúbravská cesta 9, Bratislava, SK 84505, Slovakia

email: ivana.nemcovicova@savba.sk

Many pathogens have evolved countermeasures to avoid detection and clearance by natural killer (NK) cells [1,2], however, regulatory mechanisms limiting cytokine activation of NK cells that reduce non-specific tissue damage remain poorly defined. CD160 is a 27 kDa glycoprotein which was initially identified with the monoclonal antibody BY55 [2]. Its expression is tightly associated with peripheral blood NK cells and CD8<sup>+</sup> T lymphocytes with cytolytic effector activity [2,3,4]. The cDNA sequence of CD160 predicts a cysteine-rich, glycosylphosphatidylinositol-(GPI)-anchored protein of 181 amino acids with a single Ig-like domain weakly homologous to KIR2DL4 molecule [Fig.1C]. It was found that TNF receptor herpesvirus entry mediator (HVEM) preferentially engages CD160 trimer to costimulate activation, while a viral ortholog of HVEM specifically binds to B and T lymphocyte attenuator (BTLA) to suppress this signaling. Thus, regulation of CD160 bidirectional binding may represent a common mechanism of immune regulation targeted by multiple pathogens, which by extension is a potential target for therapeutic manipulation. We have found that CD160 is expressed at the cell surface as a tightly disulfide-linked multimer. The homology model of CD160 antigen domain [Fig.1B] shows cysteine-rich region that was found to be responsible for CD160 tight-timer formation even under reduced conditions. CD160 trimer forms stable complex with HVEM, while monomeric form refused to binds its cognate ligand. We have attempted crystallization of HVEM and CD160 molecules in singles, as well as in complex. Protein crystals shown in Fig.1A were grown by using PEG ion and Morpheus crystal screens and successfully tested for X-ray diffraction.

IN is Marie Curie Fellow financed by Programme SASPRO, co-funded by European Union and the Slovak Academy of Sciences. The authors gratefully acknowledge the contribution of the Slovak Research and Development Agency under the project APVV-14-0839 and the contribution of the Scientific Grant Agency of the Slovak Republic under the grant 2/0103/15.

1. Vivier E, et al., *Science* 2011, 331, 44–49
2. Anumanthan A, *J Immunol* 1998, 161(6), 2780–90
3. Agrawal S, et al., *J Immunol* 1999, 162(3), 1223–26
4. Klopocki E, *Am. J. Hum. Gen.* 2007, 80(2), 232–40

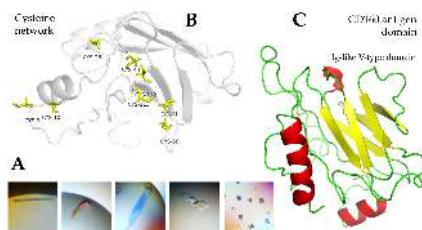


**Figure 1.** A, protein crystals of CD160, CD160-HVEM complex and HVEM; B, The network of intramolecular cysteines within CD160 ectodomain; C, The homology model of CD160 structure showing Ig-like V-set type domain and surrounding helix.

**Keywords:** NK cells, CD160 antigen, herpesvirus entry mediator HVEM



## MS12-P8 Molecular Dynamics and Monte Carlo Simulation for Protein Nanocrystallography.

Claudio Nicolini<sup>1,2</sup>, Eugenia Pechkova<sup>1,2</sup>

1. Nanoworld USA and Fondazione ELBA-Nicolini, Largo Redaelli, 7, 24020 Pradalunga, Bergamo, Italy

2. Laboratories of Biophysics and Nanotechnology, Department of Experimental Medicine, University of Genova, Via Pastore, 3, 16132 Genova, Italy

email: clannicolini@gmail.com

In the molecular dynamics (MD) method there is a polyatomic molecular system in which all atoms are interacting like material points, and behavior of the atoms is described by the equations of classical mechanics. This allows simulations of the system of the order of 106 atoms in the time range up to 1 microsecond. Despite of some limitations such approximation may describe the dynamics of macromolecules at the atomic level. However, this method does not consider the chemical reactions and the formation or breaking of chemical bonds. For these purposes there are approaches which combine classical and quantum mechanics simulations. The behavior of each atom can be described as Newton's equation of motion. In the present communication, we describe how MD can be applied for studying Langmuir-Blodgett (LB)-based protein crystals. Using MD analysis, we show how LB-based crystals and space ones can be compared with classically grown crystals. From our simulations LB crystals follow the trends of microgravity crystals, i.e. higher resolution, lower content of water, lower B-factor and higher number of reflections. Development of new approach using MD and Monte Carlo simulation allowing proper estimation of Radiation Damage (RD) occurring to the protein structure. Since RD represents a major problem in all advanced methods of 3D atomic structure determination (SR, XFELs, Cryo-EM), this goal is of high impact in evaluation of the resulting structures. The object of this research also is to solve the protein 3D atomic structure using Monte Carlo integration of high-quality diffraction intensities from which experimental phases could be determined. Monte Carlo simulation and MD can therefore play a major role in protein nanocrystallography and structural nanoproteomics.

Bozdaganyan M et al, LB Identification of best crystallization methods by molecular dynamics, CREGE 2014, 24, 311-324

Pechkova E, A Review of the strategies for obtaining high-quality crystals utilizing nanotechnologies and microgravity, CREGE 2014, 24, 325-339

Nicolini C et al, Molecular Dynamics (MD) Protocol, Nature Protocol Exchange 2016, doi.org/10.1038/protex.2016.016

Nicolini C, Pechkova E, New Trends in Protein Nanocrystallography by Cell Free Expression, APA Microarrays, LB Nanotemplate and Montecarlo Simulation, J Micro Biochem Technol 2014, 6, 366-369

Pechkova E, Nicolini C, From art to science in protein crystallization by means of thin film technology, Nanotechnology 2002, 13, 460-464

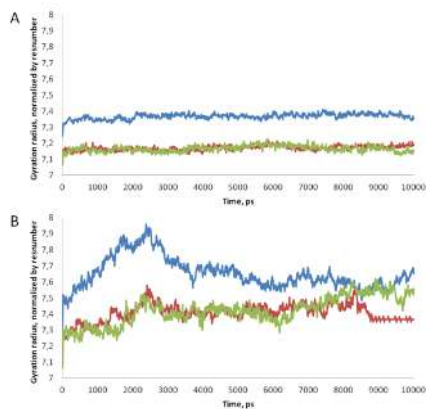


**Figure 1.** Normalized gyration radius of proteins crystallized by different techniques at 300 K (A) and 500 K (B). Blue line is classically (Hanging Drop) crystallized proteins, red is LB and green is space grown crystals.

**Keywords:** Molecular Dynamics, Monte Carlo Simulation, Radiation Damage, Protein Nanocrystallography

## MS12-P9 An X-ray Crystallographic Approach to Obtain an Atomic Model of a High Mobility Group N Protein-Nucleosome Assembly

Sailatha Ravi<sup>1</sup>, Curt A. Davey<sup>1</sup>

1. School of Biological Sciences, Nanyang Technological University, 60 Nanyang Drive, Singapore 637551.

email: sailatha001@e.ntu.edu.sg

Nucleosomes, comprising ~146 bp of DNA wrapped around a histone octamer along with adjoining linker DNA, form the basic repeating units of chromatin. Chromatin architectural proteins are nuclear factors that modulate genomic activities by modifying chromatin structure. Linker histone proteins are one type of chromatin architectural factor that interact with nucleosomes to foster compact states of chromatin, such as heterochromatin, which is generally associated with silenced genes. The ubiquitous and abundant High Mobility Group N (HMGN) proteins comprise a distinct family of chromatin architectural proteins that compete with linker histones to induce gene accessibility and maintain active states of chromatin. Unlike many transcription factors that recognize specific DNA sequences, HMGN proteins bind specifically to nucleosomes with high affinity irrespective of the underlying DNA sequence. This property has been attributed mainly to a highly conserved cluster of arginine residues, which bind to the acidic patch regions on the nucleosome. Moreover, under physiological ionic strength conditions, two molecules of HMGN bind co-operatively to a single nucleosome, and mixed pairs of variants will not associate with a given nucleosome. However, the mechanistic details of HMGN activity remain unclear. Here, we aim to obtain the first atomic model for an HMGN protein-nucleosome complex to shed light on the exact binding mode of HMGN proteins, their co-operative and homo-pairing association properties and potential structural alterations induced in the nucleosome.

HMGN proteins are unstructured prior to binding nucleosomes, but we have successfully overexpressed and purified the *Homo sapiens* HMGN1, HMGN2, HMGN3a, HMGN3b, HMGN4 proteins using a recombinant bacterial expression system. Biochemical assays have confirmed that all proteins are active in co-operatively binding to nucleosomes, with a variety of different DNA constructs tested. We have recently obtained crystals of an HMGN1-nucleosome complex that show diffraction beyond 4 Å, and we are currently optimizing growth, harvest and stabilization conditions to improve diffraction towards atomic model building resolution.

**Funding:** Ministry of Education Academic Research Fund Tier 2 (grant MOE2015-T2-2-089); Ministry of Education Academic Research Fund Tier 3 Programme (grant MOE2012-T3-1-001).

E-mail for correspondence: davey@ntu.edu.sg

**Keywords:** High Mobility Group N protein, nucleosomes, X-ray crystallography, chromatin architectural proteins

## MS12-P10 Characterization of RAGE-ligand interactions

Roya Tadayon<sup>1</sup>, Stephan Giesler<sup>1</sup>, Tomas Leanderson<sup>2</sup>, Günter Fritz<sup>1</sup>

1. Institute of Neuropathology, Neurozentrum, University of Freiburg, Breisacher Str. 64, 79106 Freiburg, Germany  
2. Immunology Group, Lund University, Lund, Sweden

email: roya.tadayon@uniklinik-freiburg.de

**The Receptor for Advanced Glycation End products (RAGE)** is a pattern recognition receptor and key in the innate immune response. It binds diverse ligands and initiates a downstream pro-inflammatory signaling cascade. Hyper-activation of RAGE has been linked to chronic inflammatory disorders, diabetic complications, tumor outgrowth, and neurodegenerative disorders. We are studying the structure of this unique receptor and of several of its ligands in order to understand the molecular basis for ligand recognition. Key ligands of RAGE are Danger-Associated Molecular Pattern molecules (DAMPs) like **HMGB1** and several members of the so-called S100 protein family, like **S100A9**, **S100B** and **S100A8/A9**. Depending on the nature of the ligand, its concentration and its affinity to the receptor, the cellular response evoked upon RAGE-ligand interaction is different. In order to characterize the RAGE-ligand interactions in more detail we analyzed their binding properties in vitro by microscale thermophoresis, surface plasmon resonance and isothermal calorimetry. Moreover, we elucidated the structural properties of S100A9, revealing that the metal ions  $\text{Ca}^{2+}$ - and  $\text{Zn}^{2+}$  induce major conformational changes exposing hydrophobic residues to the solvent, which are required for high-affinity binding to RAGE. Furthermore, we aim to develop strategies to interfere with RAGE activation. We study the binding of small molecules to S100A9 that are able to block S100A9-RAGE interaction. These data might guide the development of new strategies in the treatment of several disorders mentioned above.

**Keywords:** Receptor for advanced glycation end products, S100 Proteins, HMGB1

**MS12-P11** A method for high-throughput, low volume soaking of protein crystals in rapid screening fragment librariesPaul Thaw<sup>1</sup>

1. TTP Labtech

email: paul.thaw@ttplabtech.com

Co-crystallisation is a common method for producing protein-ligand complex structures. It is especially useful when drug-like compounds trigger conformational changes in proteins. This can result in variations in the growing conditions or crystal form and may necessitate wider screening strategies for co-crystallisation in general. Alternatively, soaking protein crystals with ligands is the fastest route to high-throughput structure if the starting crystal form is easy to grow reproducibly, able to accommodate the desired ligand and is robust to physical and chemical changes. This poster will describe a miniaturised, high-throughput soaking method developed by Dr. David Hargreaves, AstraZeneca, UK for screening a fragment-based lead generation (FBLG) library. This automated screening method uses TTP Labtech's mosquito<sup>®</sup> Crystal enabling small volumes of fragment libraries (10-25 nL) to be prepared systematically. The mosquito<sup>®</sup> liquid handler was used to make up a variety of soaking solutions containing fragment library cocktails at high concentrations, high affinity ligand soaks at lower concentrations and gradients of compound concentrations. Having already grown crystals in a standard crystallisation plate the solutions were prepared and transferred quickly and automatically reducing potential errors and improving reproducibility. The success of this soaking method relied on the accuracy and reproducibility of mosquito Crystal's low volume pipetting which is in the range of 25 nL to 1,200 nL. This reduced material cost and, together with its ease-of-use makes this method a highly attractive initial high-throughput screen for all structure-based compound screening.

**Keywords:** protein crystallography, soaking, fragment based drug design

**MS12-P12** Humidity Induced Phase Transitions of HEW Lysozyme Investigated by Microcrystalline Powder DiffractionRoman Trittbach<sup>1</sup>, Roman Trittbach<sup>1</sup>, Gwilherm Nenert<sup>1</sup>, Detlef Beckers<sup>1</sup>, Thomas Degen<sup>1</sup>, S Logotheti<sup>2</sup>, F Karavassili<sup>2</sup>, A Valmas<sup>2</sup>, S. Trampari<sup>3</sup>, Irene Margiolaki<sup>2</sup>

1. PANalytical B. V., Lelyweg 1, 7602 EA Almelo, The Netherlands

2. University of Patras, Greece

3. Kapodistrian University of Athens, Greece

email: roman.trittibach@panalytical.com

Proteins often crystallize in microcrystalline precipitates. The protein molecules are then surrounded by solvent and their packing arrangement is retained by limited intermolecular contacts. A change in the crystal environment first affects the bulk solvent that fills the intermolecular space, with resulting changes in the crystal structure. In literature it is reported that protein crystals in controlled humidity environments show a large change in unit-cell parameters when the humidity is decreased [1-2]. When a protein crystal is carefully dehydrated, it is in a metastable state in which the crystal initially still retains the original packing structure [2]. Further dehydration may cause the collapse of the crystal lattice: the crystal no longer maintains its packing structure because of the loss of a large amount of bulk solvent. However in some crystals, the dehydration induces a molecular arrangement change resulting in a new crystal structure. This has been already reported for hen egg-white (HEW) lysozyme [3]. While dehydration can induce structural changes, this is also likely to happen upon hydration of the same crystals.

Here, we present our results of microcrystalline tetragonal and monoclinic HEWL samples on a laboratory X-ray powder diffractometer including in situ measurements under variable relative humidity conditions. The observed gradual structural changes as well as phase transitions upon dehydration and hydration of HEWL are analyzed in the relative humidity range 50% - 95%. D

ehydration and hydration processes are reversible in humidity cycles in the range of 95% rH to 75% rH. Without stabilizing PEG the lower limit for dehydration of tetragonal HEWL is around 75% rH. With PEG the tetragonal HEWL samples remain crystalline below 75% rH, but show phase transitions and larger variations of the cell parameters. Below 75% rH a new tetragonal polymorph was discovered.

[1] R. Kiefersauer, , *et al. J. Appl. Cryst.* **2000**, *33*, 1223–1230.

[2] I. Dobrianov, *et al. J. Cryst. Growth*, **1999** *196*, 511–523.

[3] K. Harata, T. Akiba, *Acta Cryst. D* **2007** *63*, 1016–1021

**Keywords:** protein, HEWL, Lysozyme, humidity, polymorphism

**MS12-P13** How multivalent salts help proteins crystallizeFajun Zhang<sup>1</sup>, Georg Zoche<sup>2</sup>, Thilo Stehle<sup>2,3</sup>, Frank Schreiber<sup>1</sup>

1. Institut für Angewandte Physik, Universität Tübingen
2. IFIB, University of Tübingen
3. Department of Pediatrics, Vanderbilt University School of Medicine, Nashville, USA

email: fajun.zhang@uni-tuebingen.de

Knowledge of the protein structure is considered a precondition for understanding their function. Crystallography remains the most powerful tool in that context, but crystal structure determination of macromolecules is often hampered by a lack of crystals suitable for diffraction. In our work, we have studied the crystallization of human serum albumin (HSA) and bovine beta-lactoglobulin (BLG) in the presence of yttrium chloride (and other multivalent salts) to yield high quality crystals with new crystal packing. We demonstrate that trivalent salts can be used to optimize crystallization conditions for globular proteins along general physical insights. We have revealed that negatively charged proteins at neutral pH in the presence of trivalent salts undergo a "reentrant condensation" phase behavior [1-3], i.e. a phase-separated regime occurs in between two critical salt concentrations,  $c^* < c^{**}$ , giving rise to a metastable liquid-liquid phase separation (LLPS) [3,4]. Crystallization from the condensed regime follows different mechanisms. Near  $c^*$ , crystals grow following a classic nucleation and growth mechanism; near LLPS binodal, crystallization follows a two-step mechanism, i.e. crystals growth follows a metastable LLPS [4-8]. The yttrium ions are not only used to engineer crystallization, but are an integral part of the crystal lattice and can therefore be used to solve the phase problem using anomalous dispersion methods. The structure analysis demonstrates the specific binding of yttrium ions to surface-exposed glutamate and aspartate side chains contributed by different molecules in the crystal lattice. By bridging molecules in this manner, contacts between molecules are formed that enable the formation of a stable crystal lattice. Based on this bridging effect, an ion-activated patchy colloidal model was proposed to rationalize the phase behaviour observed experimentally [9].

**References** [1] F. Zhang et al., *Phys. Rev. Lett.* 2008, **101**, 148101 [2] F. Zhang et al., *Proteins* 2010, **78**, 3450 [3] F. Zhang et al., *Soft Matter* 2012, **8**, 1313 [4] F. Zhang et al., *J. Appl. Cryst.* 2011, **44**, 755 [5] F. Zhang et al., *Faraday Discuss.* 2012, **159**, 313 [6] F. Roosen-Runge et al., *J. Phys. Chem. B* 2013, **117**, 5777 [7] A. Sauter, et al. *JACS*, 2015, **137**, 1485 [8] A. Sauter, et al. *Faraday Discuss.* **179**, 41 [9] F. Roosen-Runge et al. *Scientific Reports*, 2014, **4**, 7016.

**Keywords:** protein crystallization, nonclassical nucleation, liquid-liquid phase separation, multivalent salt

**MS12-P14** Structural and ligand-binding properties of fatty acid-binding proteins (pFABP4 and pFABP5) in the gentoo penguinChang woo Lee<sup>1,2</sup>, Jung Eun Lee<sup>2</sup>, Hyun Park<sup>1,2</sup>, Il-Chan Kim<sup>2</sup>, Jun Hyuck Lee<sup>1,2</sup>

1. Department of Polar Sciences, University of Science and Technology, Incheon 406-840, Republic of Korea
2. Division of Polar Life Sciences, Korea Polar Research Institute, Incheon 406-840, Republic of Korea

email: justay@kopri.re.kr

Fatty acid-binding proteins (FABPs) are small, widely expressed intracellular proteins located in various tissues. FABPs facilitate the solubilization and transport of fatty acids and other hydrophobic substances by directly interacting with ligands. Here, we report the crystal structures of ligand-unbound pFABP4, linoleate-bound pFABP4, and palmitate-bound pFABP5 from the gentoo penguin (*Pygoscelis papua*) at 2.1, 2.2, and 2.3 Å resolution, respectively. The pFABP4 and pFABP5 structures were comprised primarily of 10-stranded  $\beta$ -barrels and two short  $\alpha$ -helices forming a cap region. Inside the  $\beta$ -barrel, a hydrophobic cavity containing the ligand binding site was observed. A ligand binding test using 8-anilino-1-naphthalene-sulfonic acid indicated that pFABP4 has relatively high affinity for linoleate compared with pFABP5. In contrast, pFABP5 has high affinity for palmitate compared with pFABP4. Structure comparison revealed the largest difference in the  $\beta$ 3- $\beta$ 4 loop region. Upon palmitate binding to pFABP5, the  $\beta$ 3- $\beta$ 4 loop was moved by 4 Å compared to linoleate-bound pFABP4. Moreover, several sequences (A76/L78, T30/M32, underlining indicates pFABP4 residues) caused structural changes and different affinities for linoleate and palmitate. Structural comparisons, combined with a ligand-binding assay, provide insight into the mechanism of the ligand specificities of pFABP4 and pFABP5.

**Keywords:** Fatty acid-binding protein,  $\beta$ -barrel protein, crystal structure, Gentoo penguin (*Pygoscelis papua*), X-ray crystallography

## MS12-P15 Crystallization of heat shock protein essential for protein disaggregation

Marta Orlikowska<sup>1</sup>, Krzysztof Liberek<sup>2</sup>, Grzegorz Bujacz<sup>1</sup>

1. Institute of Technical Biochemistry, Lodz University of Technology, Poland

2. Department of Molecular and Cellular Biology, University of Gdańsk

email: martaorlikowska07@gmail.com

The process in which a newly synthesized polypeptide chain transforms itself into a perfectly folded protein depends both on the properties of the amino-acid sequence and on multiple contributing influences from the crowded cellular milieu. Uncovering the mechanism of protein folding and unfolding is one of the grand challenges of modern science. The three-dimensional arrangement of the polypeptide chain decide about the specific biological function of the protein in the cell. Only correctly folded proteins are fully functional, randomly arranged polypeptide chain doesn't have biological activity. The state of protein folding is controlled and regulated by the protein quality control system. The system is formed by chaperones involved in protein folding and the proteasomal degradation system. The proper functioning of the system is required because its dysfunction may lead to neurodegenerative diseases. The prion-related illnesses such as Creutzfeldt-Jakob disease, amyloid-related illnesses such as Alzheimer's disease as well as intracytoplasmic aggregation diseases such as Huntington's and Parkinson's disease those are neurodegenerative diseases whose pathogenesis is associated with protein aggregation of incorrectly folded proteins. Many chaperones are heat shock proteins. Their expression is increased when cells are exposed to elevated temperatures or other stress conditions. The project focuses on the protein Hsp104 which belongs to the Hsp100 family and the AAA+ superfamily. Hsp104 is important in the cell due to its ability to solubilize and refold proteins trapped in aggregates formed during heat stress [1]. It achieves this in cooperation with the Hsp70 chaperone system. The active form of the protein is a ring-shaped hexamer, which is thought to drive protein disaggregation by directly translocating substrates through its central channel. However, there is still no general consensus regarding the domain organization within the hexameric molecular machine. Substantial efforts have been made to elucidate the location of domain M, but the results are contradictory [2,3]. We aim to learn the orientation of the unique M domain by solving the crystal structure of Hsp104 using X-ray crystallography.

[1] Liberek, K. et al., EMBO J. 2008, 27, 328-335.

[2] Lee, S. et al. J. Struct. Bio., 2004, 146, 99-105.

[3] Wendler, P. et al., Cell. 2007, 28, 1366-1377.

This work was supported by Grant 2013/08/S/NZ1/00750 from National Science Center (NCN)

**Keywords:** crystallization, heat shock protein

## MS13 Hot structures in biology

Chairs: Mariusz Jaskolski, Udo Heinemann

### MS13-P1 Bacterial Resistance to Silver: The Role of SilE Protein

Valentin Chabert<sup>1</sup>, Maggy Hologne<sup>2</sup>, Olivier Walker<sup>2</sup>, Katharina M. Fromm<sup>1</sup>

1. University of Fribourg, Switzerland

2. Université Claude Bernard, Lyon, France

email: valentin.chabert@unifr.ch

Silver has been used for hundreds of years for its antimicrobial properties. Since the emergence of many multi-resistant bacterial strains against classical antibiotics, the research of new silver compounds is now at its apogee. While these drugs have been shown to be highly able to kill bacteria, some of these pathogens have developed a resistance to high concentrations of Ag<sup>+</sup>. This resistance is provided by the plasmid pMG101, which encodes for eight proteins that act together in an efflux pump system to deal with silver ions. Among these, the SilE protein is the only one of which its mode of action is actually unknown.

To identify the role of SilE in this bacterial machinery, two approaches have been intended in our group. While one way is to study the interaction of the whole protein with silver ions, the other is based on a bottom-up approach, investigating the interaction of silver ions with short peptide sequences of this protein. By NMR studies of these peptide models, we were able to highlight a potential methionine participation in the complexation of Ag<sup>+</sup> by SilE.

S. Silver, L. T. Phung, G. Silver, *J. Ind. Microbiol. Biotechnol.* **2006**, 33, 627-634.

S. Eckhardt, P. S. Brunetto, J. Gagnon, M. Priebe, B. Giese, K. M. Fromm, *Chem. Rev.* **2013**, 113, 4708-4754.

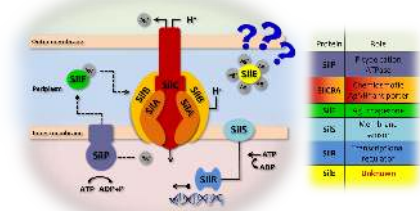


**Figure 1.** Proteins products of pMG101 silver resistance genes.

**Keywords:** Bacterial resistance, Silver(I), Metalloprotein, Methionine

## MS13-P2 MCPiP3 (ZC3H12C) Regulates the Innate Immune Response by Acting as a Ribonuclease.

Ankur Garg<sup>1</sup>, Osamu Takeuchi<sup>2</sup>, Udo Heinemann<sup>1</sup>

1. Crystallography, Max-Delbrück Center for Molecular Medicine in the Helmholtz Association-Berlin, Germany  
2. Laboratory of Infection Prevention, Virus Research Institute, Kyoto University, Japan

email: ankur.garg@mdc-berlin.de

During inflammation, different innate pattern recognition receptors like Toll-like receptors (TLR) and RIG-I like receptors sense the infection, and then the inflammatory response is orchestrated by pro-inflammatory cytokines such as tumor necrosis factor (TNF), interleukin (IL)-1 and IL-6 which ultimately result in elimination of pathogens (1). Cytokine levels are tightly controlled at transcriptional and post-transcriptional level by various proteins, because a cytokine storm could lead to immunodeficiency and autoimmune disorders (2).

The MCPiP3 (macrophage chemotactic protein-induced proteins) family (also known as ZC3H12 family) of proteins are ribonucleases containing a CCCH-type zinc finger. These proteins play an important role in innate immune response by regulating cytokine levels through targeting their mRNAs (3). MCPiP1 (Regnase1) has recently been shown to recognize specific stem-loop structures in the 3' untranslated region (UTR) of translationally active mRNAs for IL6 and other immunological factors and lead to their degradation by utilizing the helicase activity of UPF1 (4).

MCPiP3 (ZC3H12C) is another member of the family which has also been reported to be involved in cytokine regulation by mRNA degradation. Moreover, it is highly expressed in precursor B-lymphocytes and is also involved in lymphocyte differentiation, as MCPiP3 knock-out mice show severe defects in lymphocytes. A crystal structure for the RNase domain of ZC3H12C has been determined at a resolution of 1.9 Å which shows a Rossmann-fold like structure with an Mg<sup>2+</sup> ion bound in the catalytic site. Initial RNase assays show that the protein variants used in structure analysis are catalytically active.

Overall, we are trying to understand the structure-function relation of MCPiP3 which will enable us to understand how it recognizes its target mRNA and how it coordinates with other family members in order to regulate the lymphocyte maturation and inflammatory responses.

### References;

- 1) Medzhitov et al. Origin and physiological roles of inflammation. *Nature*, 454, 428-435 (2008).
- 2) Takeuchi et al. Pattern recognition receptors and inflammation. *Cell*, 140, 805-820 (2010).
- 3) Xu et al. Structural study of MCPiP1 N-terminal conserved domain reveals a PIN-like RNase. *Nucleic Acids Research*, 40, 6957-6965 (2012).
- 4) Mino et al. Regnase-1 and roquin regulate a common element in inflammatory mRNAs by spatiotemporally distinct mechanism. *Cell*, 141, 1-16 (2015).

**Keywords:** Macrophage activation, Innate immune response, B-lymphocyte differentiation, CCCH Zinc-finger, Ribonuclease

## MS13-P3 Crystal Structure of the cytoplasmic portion of histidine kinase SrrB from *Staphylococcus aureus*

Wen-Yih Jeng<sup>1,2</sup>, Ya-Jin Jheng<sup>1,2</sup>, Chia-I Liu<sup>3</sup>, Chieh-Shan Lee<sup>1,2</sup>, Te-Jung Lu<sup>4</sup>

1. University Center for Bioscience and Biotechnology, National Cheng Kung University, Tainan 701, Taiwan  
2. Department of Biochemistry and Molecular Biology, National Cheng Kung University, Tainan 701, Taiwan  
3. School of Medical Laboratory Science and Biotechnology, Taipei Medical University, Taipei 110, Taiwan  
4. Department of Medical Laboratory Science and Biotechnology, Chung Hwa University of Medical Technology, Tainan 717, Taiwan

email: wyjeng@mail.ncku.edu.tw

*Staphylococcus aureus* is one of the major causes of nosocomial infections today. *S. aureus* infection is considered to be the reason for the increasing number of antibiotic-resistant strains. Furthermore, *S. aureus* can produce slime layer or multilayered biofilm embedded with the glycocalyx on the surface of various biomaterials. *S. aureus* can persist in clinical settings and increase resistance to antimicrobial agents through biofilm formation. The staphylococcal respiratory response regulator SrrAB (synonym, SrrSR), a two-component system has been identified as a global regulator of the aerobic-anaerobic shift of metabolism in *S. aureus*. SrrB is a histidine kinase which responds to environmental stimuli by regulating its cognate response regulator SrrA. Under low-oxygen growth conditions, the staphylococcal regulator SrrAB induces *ica* locus transcription and polysaccharide intercellular adhesion (PIA) production, known as a major component of biofilm. SrrB is a transmembrane sensor protein consisted of 588 residues (66.7 kDa). N-terminal hydrophilic region of SrrB is located extracellularly, while the C-terminal phosphoacceptor, dimerization, and ATPase domains are located intracellularly. Here, we report the crystal structure of cytoplasmic portion of SrrB (SrrBc) from *S. aureus* in a dimeric form at 1.78 Å resolution. The overall structure of SrrBc forms a unique homodimer which is mediated by two pairs of long dimerization  $\alpha$ -helices. To the rear of dimerization helices is the ATP binding domain of SrrB which consists of three parallel  $\alpha$ -helices, one short anti-parallel  $\beta$ -sheet, one core mixed type  $\beta$ -sheet and a disordered ATP-lid region. Moreover, one disulfide bond (Cys469 and Cys506) is located within the core  $\beta$ -sheet to stable the structure. Finally, based on previous studies and our crystal structure, we propose that the redox state of this disulfide bond in the ATP binding domain of SrrB might play a key role to mediate the interaction between SrrB and SrrA, thus alter the target gene of SrrAB in transcription level in *S. aureus*.

**Keywords:** biofilm, multiple antibiotic resistant, two-component system, MRSA, VISA, PIA



## MS13-P4 Structural studies of AggC, an novel O-GlcNAc transferase involved in protection of virulence-associated cell proteins in *Staphylococcus aureus*

Chia-I Liu<sup>1</sup>, Wen-Yih Jeng<sup>2</sup>, Tzu-Ping Ko<sup>3</sup>, Andrew H.-J. Wang<sup>3,4</sup>

1. School of Medical Laboratory Science and Biotechnology, College of Medical Science and Technology, Taipei Medical University, Taipei 10031, Taiwan
2. University Center for Bioscience and Biotechnology, National Cheng Kung University, Tainan 70101, Taiwan
3. Institute of Biological Chemistry, Academia Sinica, Taipei 11529, Taiwan
4. Graduate Institute of Translational Medicine, College of Medical Science and Technology, Taipei Medical University, Taipei 10031, Taiwan

email: ponpiqq@gmail.com

Glycosylation of bacterial cell wall proteins play a critical role in bacterial pathophysiology. Two novel O-linked glycosyltransferases (OGTs), AggB and AggC, decorate all SD (serine-aspartate) repeats of adhesins with N-acetylglucosamine (GlcNAc) moieties, which containing the virulence factors ClfA (a fibrinogen-binding clumping factor A), ClfB, SdrC (SD repeats C), SdrD, SdrE of *S. aureus* and SdrF, SdrG, SdrH of *S. epidermidis*. Recently, it has been demonstrated that glycosylated SD repeats proteins can facilitate bacterial adhesion, immune evasion, colonization, persistence and invasion of host tissue. This specific modification also promotes *S. aureus* replication in the bloodstream of mammalian hosts. AggB and AggC modify all SD repeats proteins by an ordered mechanism, with AggC appending the sugar residues proximal to the target SD repeats, followed by additional modification by AggB. Here we report two crystal structures of *S. aureus* AggC, as a binary complex with citrate (2.8 Å) and as a ternary complex with UDP and GlcNAc (2.2 Å). The structures provide clues to the enzyme catalytic mechanism, implying how AggC recognizes target peptide sequences, and reveal the fold of the unique  $\beta$ -meander domain and a core catalytic domain with GT-B fold. Structure-based mutagenesis of AggC was also performed to explore the roles of amino acids involved in substrate binding. In summary, this information will accelerate the rational design of biological experiments to investigate AggC functions and also help the design of inhibitors as a therapeutic target.

**Keywords:** serine-aspartate (SD) repeats, glycosyltransferase, virulence factor, X-ray Crystallography

## MS13-P5 Structural basis for photoactivation of a light-regulated adenylate cyclase from the photosynthetic cyanobacterium *Oscillatoria acuminata*

Mio Ohki<sup>1</sup>, Kanako Sugiyama<sup>1</sup>, Fumihiko Kawai<sup>1</sup>, Shigeru Matsunaga<sup>2</sup>, Mineo Iseki<sup>3</sup>, Sam-Yong Park<sup>1</sup>

1. Drug Design Laboratory, Graduate School of Medical Life Science, Yokohama City University, 1-7-29 Suehiro, Tsurumi, Yokohama, 230-0045, Japan
2. Central Research Laboratory, Hamamatsu Photonics K.K., 5000, Hirakuchi, Hamakita-ku, Hamamatsu, Shizuoka 434-8601, Japan
3. Faculty of Pharmaceutical Sciences, Toho University, Funabashi, Chiba, 274-8510, Japan

email: mio-ki67@tsurumi.yokohama-cu.ac.jp

Cyclic-AMP is one of the most important second messengers, regulating many crucial cellular events in both prokaryotes and eukaryotes, and precise spatial and temporal control of cAMP levels by light shows great promise as a simple means of manipulating and studying numerous cell pathways and processes. The photoactivated adenylate cyclase (PAC) from the photosynthetic cyanobacterium *Oscillatoria acuminata* (OaPAC) is a small homodimer eminently suitable for this task, requiring only a simple flavin chromophore within a BLUF domain. These domains, one of the most studied type of biological photoreceptor, respond to blue light and either regulate the activity of an attached enzyme domain or change its affinity for a repressor protein. BLUF domains were discovered through studies of photo-induced movements of *Euglena gracilis*, a unicellular flagellate, and gene expression in the purple bacterium *Rhodobacter sphaeroides*, but the precise details of light activation remain unknown. Here we describe crystal structures and the light regulation mechanism of the previously undescribed OaPAC, showing a central coiled-coil transmits changes from the light-sensing domains to the active sites with minimal structural rearrangement. Site-directed mutants show residues essential for signal transduction over 30 Ångströms across the protein. The use of the protein in living human cells is demonstrated with cAMP-dependent luciferase, showing a rapid and stable response to light over many hours and activation cycles. The structures determined in this study will assist future efforts to create artificial light-regulated control modules as part of a general optogenetic toolkit.

**Keywords:** cAMP, optogenetics, photoactivation, structural biology



## MS13-P6 Structural Basis of Selective Aromatic Pollutant Sensing by MopR, an NtrC Family Transcriptional Regulator

Shamayeeta Ray<sup>1</sup>, Santosh Panjikar<sup>2,3</sup>, Ruchi Anand<sup>4</sup>

1. IITB-Monash Research Academy, Mumbai 400076, Maharashtra, India
2. Department of Biochemistry and Molecular Biology, Monash University, Victoria 3800, Australia
3. Australian Synchrotron, Victoria 3168, Australia
4. Department of Chemistry, Indian Institute of Technology, Bombay, Mumbai 400076, Maharashtra, India

email: shamayeeta.ray@gmail.com

Phenol and its derivatives are harmful to both terrestrial and aquatic life as they are carcinogenic, and embryotoxic in nature and their exposure, even in small quantities can be lethal. In recent years due to heavy industrial discharge these pollutants are released as major waste into the environment. Soil bacteria like *Pseudomonas* sp., possess transcription regulators like XylR, DmpR and MopR that facilitate the natural catabolic degradation of these aromatic pollutants and hence have been used extensively over the years for design of effective biosensors that can detect these pollutants even at low levels. These proteins possess a modular architecture and are classified under the NtrC family of transcriptional regulators as they harbor a central AAA+ domain whose activity is regulated by the N-terminal sensor domain (1). Here, we have determined the crystal structure of the sensor domain of MopR (MopR<sup>AB</sup>), from *Acinetobacter calcoaceticus*, in complex with phenol and its derivatives and investigated its binding profile using mutagenesis studies and various biophysical methods (2). The crystal structure of MopR<sup>AB</sup>, which is the first structure from its family, possesses a unique fold and harbors a novel zinc motif that had remained elusive over the years. Based on the structure, we propose that the phenol binding pocket is dynamic in nature and is only formed when the ligand molecule occupies the binding site, triggered by the movement of the zinc-binding domain. The crystal structure is of great importance as it opens doors for selective and accurate design of broad-based/specific biosensors using rational approach. Over the past twenty years, plethora of efforts have been devoted to engineering of efficient aromatic biosensors based on these regulators. However, in the absence of any structure, most of the studies have failed to identify the exact sensor determinants. Our structure helps in not only identifying the correct pocket architecture but also aids in explaining the effects observed by other groups who have attempted to tweak the sensitivity of the sensor domain via either random mutagenesis or by creation of hybrid sensor domains. Moreover, based on the structure, we have been successful in undertaking preliminary studies, which serve as a stepping stone towards design of specific/broad based biosensors.

**References** (1) Shingler V. (2003) *Environ. Microbiol.* **5**, 1226-1241. (2) Ray S. et.al. *Manuscript under review in ACS Chemical Biology*.

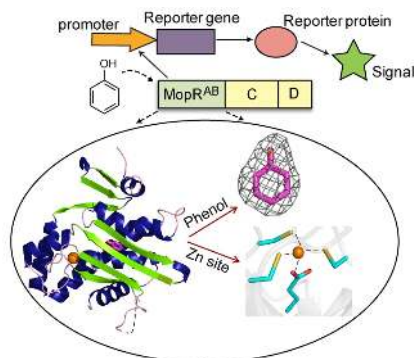


Figure 1. Crystal Structure of MopR<sup>AB</sup> in complex with phenol

**Keywords:** MopR , aromatic biosensor , phenol , XylR , DmpR , NtrC

## MS13-P7 Structures of amyloid a-synuclein and impact on our understanding of Parkinson's disease

Bente Vestergaard<sup>1</sup>

1. University of Copenhagen

email: bente.vestergaard@sund.ku.dk

Protein amyloid fibrillation is associated with a number of grave diseases, most notably the neurodegenerative Alzheimer's and Parkinson's diseases (1). Structural investigation of protein fibrillation is however inherently challenging. A number of spatially and temporally diverse structural species co-exist during the fibrillation reaction, in an equilibrium that is highly sensitive to experimental conditions. Isolation of individual species is thus not possible. At the same time understanding of the structural species formed during the fibrillation pathway are key to understanding the molecular principles behind the process, and accumulating evidence links such intermediate species to cytotoxic activity, central to the progressive, degenerative diseases. We use small angle X-ray scattering (SAXS) to investigate the fibrillation reaction. Formation of a-synuclein (aSN) fibrils is associated with Parkinson's disease. We have previously characterized the low-resolution structure of intermediately formed aSN oligomers (2) and reveal that these oligomers are building blocks of the fibril structure (3). We have recently demonstrated, that early amyloidogenic aSN species can disrupt lipid model systems, and that lipid:protein co-aggregates in a non-amyloid state are formed in this context (4) while the effect on lipid membranes varies depending on the lipid composition (5). While the methodology behind the data analysis has been well elaborated both by us (6), and others (e.g. 7), the need for a robust, objective and (semi-)automated analysis system is evident, and our latest efforts in this direction will be presented. We apply the newly developed software to the analysis of a familial mutant of aSN, revealing the occurrence of intermediate species, which have a radically different nature than those previously characterized (manuscript submitted). Although the software has been developed aiming for the analysis of fibrillating systems, it is generally applicable to any developing, heterogeneous macromolecular system.

1. Eisenberg & Jucker (2012) Cell, 148, 1188-1203
2. Giehm et al. (2011) PNAS, 108, 3246-3251
3. Perdersen et al. (2015) Scientific Reports, 5, 10422
4. van Maarschalkerweerd et al (2014) Biomacromolecules 15, 3643-3654
5. van Maarschalkerweerd et al. (2015) FEBS Letters 589, 2661-2667
6. Langkilde & Vestergaard (2012) Methods. Mol. Biol. 849, 137-155
7. Lorenzen et al. (2014) JACS 136, 3859-3868

**Keywords:** Parkinson's disease, amyloid, heterogeneous systems, data decomposition

## MS13-P8 Crystal structure of a human Fab in complex with a dominant antigen from *Neisseria meningitidis*.

Jacinto Lopez Sagaseta<sup>1</sup>

1. GSK Vaccines

email: jlopez.sagaseta@gmail.com

López-Sagaseta J.<sup>a</sup> Bottomley M.J.<sup>a</sup>

<sup>a</sup> GlaxoSmithKline Vaccines S.r.l., Via Fiorentina 1, 53100 Siena, Italy. jacinto.x.lopez-sagaseta@gsk.com

Anchored yet exposed to the outside moiety of the bacterial shell, Factor H binding protein (fHbp) is one of the main antigenic components of *Neisseria meningitidis*, one of the causative agents of meningitis, an infectious disease that can cause a fatal outcome or permanent disability within 24 hours of infection. Though there have been described up to three different variants of fHbp, it is fHbp variant 1 (fHbp-1), the subclass showing the highest prevalence amongst MenB strains, and also, one of the actual components of Bexsero, the current licensed vaccine against serogroup B Meningococci (MenB). In order to define the structural basis that underlie the recognition of this highly immunogenic antigen and the broad strain coverage offered by Bexsero, we have determined the crystal structure of a complex between a human Fab and fHbp-1 at a resolution of 2.2 Å. The Fab has been originated from an immunization study that included a recombinant form of fHbp-1, and importantly, it is cross-reactive against all of them. The cross-reactive epitope spans along the c-terminal beta barrel of fHbp and encompasses residues that are highly conserved across the different fHbp variants. The hypervariable CDR3 loop of the heavy chain dominates the recognition of the antigen. This crystal structure represents the first evidence, at the atomic level, of the recognition of *Neisseria meningitidis* fHbp by a human Fab raised in an individual upon vaccination, and provides the basis behind the broad strain coverage of the current vaccine against MenB. In addition, the information gathered from this structure will be of high value for future structure-based antigen design.

**Keywords:** STRUCTURAL BASIS; MENINGITIS; VACCINATION; IMMUNE RESPONSE.

## MS13-P9 Unexpected Active Site in *Trypanosoma brucei* Flap Endonuclease

Faizah AlMalki<sup>1,2</sup>, Sarah Oates<sup>3</sup>, Svetana Sedelnikova<sup>1</sup>, Jon Sayers<sup>3</sup>, Peter Artymiuk<sup>1</sup>

1. University of Sheffield, MBB Department, UK
2. Taif University, Biology & Biotechnology Department, Saudi Arabia
3. University of Sheffield, Medical School, UK

email: faalmalki459@gmail.com

Flap endonuclease (FEN) and 5'--3' exonucleases form a class of nucleolytic enzymes that are metalloenzymes using two metal ions in their activity. The primary function of these enzymes is as a 5' exo- and endonucleases that is required during the DNA replication procedure. According to the recent studies, FEN proteins are involved in multiple DNA metabolism and repair pathways which make them a new drug targets. *Trypanosoma brucei* (Tb) parasitic is the causative agent of sleeping sickness and its flap endonuclease enzyme shares more than 50% sequence identity with the human flap endonuclease (FEN-1). The crystal structure of TbFEN enzyme has been solved for the first time in our lab using X-ray crystallography and computational techniques. It has the same architecture as the other FEN family members which is composed of four main parts: the N-terminal region, the C-terminal region, a helical arch that is disordered in our structure and the active site. The structure has been complexed with calcium ions present in the crystallization buffer. According to the electron density map, there are two calcium ions separated by less than 4 Å and coordinated with four acidic residues for each ion are present in M1 and M2 sites in the active site. Another calcium ion 3.8 Å apart from the one in M1 sit has been observed in a new place underneath of the arch and coordinated with two amino acids from the same molecule and other two glutamic residues from neighbouring molecule to create unexpected before active site. This active site is presented and reported in FEN family members for the first time. The number and placement of metal ions is still a topic of hot debate in FEN family enzymes. This work will enable us to compare the Trypanosomal FEN structure with the human FEN one in the hope of designing molecules that will inhibit the former but not the later. The aim of this is to provide potential lead molecules for anti-protozoan drug design avoiding the toxicity and drug resistance that may occur from using current drugs.

**Keywords:** Flap endonuclease, *Trypanosoma brucei*, DNA replication and repair

## MS14 Biomineralogical crystallography and bioinspired inorganic materials

Chairs: Wolfgang Schmahl, Fernandez-Diaz Lurdes

### MS14-P1 Synergistic antimicrobial effect of silver and other metals in bimetallic complexes

Paula C. Corcosa<sup>1</sup>, Aurélien Crochet<sup>1</sup>, Katharina M. Fromm<sup>1</sup>

1. Department of Chemistry, University of Fribourg, Chemin du Musée 9, 1700 Fribourg, Switzerland

email: paula.corcosa@unifr.ch

The precious metal silver is aging for its excellent antimicrobial properties as throwing silver coins in fountains is not only a lovely old tradition.<sup>[1]</sup> It has been recognized to play an important role concerning medical applications, for example the coating of implants with Ag<sup>0</sup> or Ag<sup>+</sup> coordination compounds to avoid infection due to bacterial biofilms formation.<sup>[2]</sup>

The research of the FROMM group with respect to antimicrobial silver compounds was focused on silver coordination networks, meaning short PEG oligomers functionalized with (iso)-nicotinic acid as ligands.

Thus, the aim of the recent project is to create new Ag<sup>+</sup> complexes with bioinspired ligands, for example pyridylalanine or picolinic acid as well as with derivatives of phenylalanine or aminobenzoic acid. Furthermore, we try to synthesize bimetallic complexes combining silver and another metal such as Zn<sup>II</sup> or Cu<sup>II</sup> with the ambition to generate synergistic antimicrobial effects and to elucidate structural characteristics.

<sup>[1]</sup> Fromm, K. M. *Nat. Chem.* **2011**, 3, 178.

<sup>[2]</sup> Vig Slenters, T. *et al. Materials* **2010**, 3, 3407-3429.

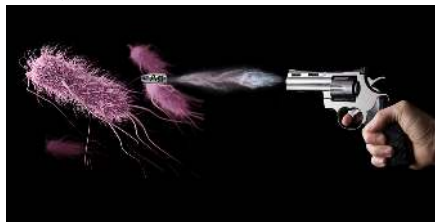


**Figure 1.** Silver fights against bacteria

**Keywords:** Bimetallic complexes, Silver, Bioinspired ligands

## MS15 Minerals and materials

## MS15-P2 New topology of cesium aluminum borophosphate: synthesis, crystal structure and IR-spectroscopy investigation

Vladislava I. Belik<sup>1</sup>, Larisa V. Shvanskaya<sup>1</sup>, Elena Y. Borovikova<sup>1</sup>

I. M.V. Lomonosov Moscow State University

email: vladislava.belik@mail.ru

Chairs: Frederic Hatert, Roland Nilica

MS15-P1 Synthesis and characterization of  $\text{Sb}_3\text{O}_4\text{F}$ ,  $\text{Y}_{0.49}\text{Sb}_{2.51}\text{O}_4\text{F}$ , and other Sb-O-F compoundsSk Imran Ali<sup>1</sup>, Mats Johansson<sup>2</sup>

1. Post-doc research fellow, Stockholm University S-10691 Stockholm Sweden

2. Prof., Department of Materials and Environmental Chemistry, Stockholm University S-10691 Stockholm Sweden

email: skimran1984@gmail.com

Six different  $\text{Sb}^{3+}$ -O-F compounds have previously been reported. Two are orthorhombic, designated as L- and M-SbOF,<sup>1</sup> one is cubic denoted as H-SbOF, one is glass<sup>1</sup> and the remaining two phases are monoclinic denoted as  $\alpha\text{-Sb}_3\text{O}_4\text{F}$ ,  $\beta\text{-Sb}_3\text{O}_4\text{F}$ .<sup>2</sup> One more compound,  $\text{Sb}_3\text{O}_4\text{F}$ , is theoretically predicted from the  $\text{Sb}_3\text{F-Sb}_3\text{O}_3$  phase diagram, however, it is not yet found experimentally. All the Sb-O-F compounds show framework type of structures. The main structural unit consists of different kinds of  $\text{SbO}_3\text{E}$ ,  $\text{SbO}_2\text{FE}$ ,  $\text{SbF}_4\text{E}$ ,  $\text{SbOF}_3\text{E}$ ,  $\text{SbO}_4\text{E}$  polyhedral units, where  $\text{Sb}^{3+}$  is equipped with a lone-electron-pair, E.

H-, L-, M- and the amorphous form of SbOF are synthesized by solid state reactions at different temperatures from mixtures of  $\text{Sb}_3\text{F}$  and  $\text{Sb}_2\text{O}_3$  (1:1 ratio). The compounds  $\alpha\text{-Sb}_3\text{O}_4\text{F}$  and  $\beta\text{-Sb}_3\text{O}_4\text{F}$  were synthesized in an aqueous solution of  $\text{NH}_4\text{F}$  and  $\text{SbF}_3$  with molar ratio of 0.05:1.<sup>1</sup> Synthesis via hydrothermal techniques haven't previously not been reported for these compounds.

In this study  $\text{Sb}_3\text{O}_4\text{F}$ , a new  $\text{Sb}^{3+}$ -O-F compound, has been synthesized by hydrothermal techniques. We have also synthesized  $\text{Y}_{0.5}\text{Sb}_{2.5}\text{O}_4\text{F}$  by introducing  $\text{YF}_3$  as one of the reactants. The structural characterization is made from single crystal data will be extensively discussed. Single crystals of the two previously known compounds M-SbOF and  $\alpha\text{-Sb}_3\text{O}_4\text{F}$  were also synthesized by the same technique differing from the previously known solid state synthesis. A comparison is made with previously reported compounds in the  $\text{Sb}^{3+}$ -O-X system (X = F, Cl, Br, I).

[1] A. S. Astrom, *Acta chem. Scand.*, 1971, **25**, 1519–1520.

[2] A. A. Udovenko, L. A. Zemnukhova, E. V. Kovaleva and G. A. Fedorishcheva, *Russ. J. Coord. Chem.*, 2004, **30**, 618–624.

[3] A. V. Kalinchenko, F. V., Borzenkova, M.P., and Novoselova, *Zh. Neorg. Khim.*, 1983, **28**, 2426.

**Keywords:** Hydrothermal synthesis, Transition metal oxo-halides, Single crystal X-ray diffraction

Borophosphates have received much attention because of their fascinating structural architectures and potential applications in sorption, catalysis, optics and ion exchange. An open-framework cesium aluminum borophosphate,  $\text{CsAl}_2\text{BP}_6\text{O}_{20}$ , with novel topology of layered anionic borophosphate partial structure was synthesized by solid state reaction method. The crystal structure was determined from single-crystal X-ray data ( $R_p = 0.043$ ): S.G. *Pbca*,  $a = 11.815(2)$ ,  $b = 10.042(2)$ ,  $c = 26.630(4)$  Å,  $Z = 8$ ,  $V = 3159.5(10)$  Å<sup>3</sup>. The structure contains the 16-member ring borophosphate layers stacked along [001] (Fig.1) and interconnected by aluminum octahedra. The resulting three-dimensional framework is characterized by channels running parallel to [021] and [100] directions formed by six- and five-membered rings, respectively. Cs ions reside within these channels. The topological relations between the  $\text{CsAl}_3(\text{P}_3\text{O}_{10})_2$  [1] and  $\text{CsAl}_2\text{BP}_6\text{O}_{20}$  structures are discussed.

The MID-FTIR spectrum (Fig.1) of new borophosphate corresponds well to revealed crystal structure. Its interpretation can be made on the basis of characteristic vibrations of  $\text{PO}_2$ ,  $\text{PO}_3$  and  $\text{BO}_4$  groups, P-O-P and B-O-P bridges. The high frequency bands between 1280–1230  $\text{cm}^{-1}$  are attributed to the antisymmetric vibrations of O-P-O bonds  $\nu_2(\text{PO}_2)$ . The bands in the region 1205–1150  $\text{cm}^{-1}$  are assigned to symmetrical vibrations of O-P-O bonds  $\nu_1(\text{PO}_2)$ . The bands in the region from 1140 to 930  $\text{cm}^{-1}$  belong to the asymmetrical stretching vibrations of  $\text{PO}_2$ ,  $\text{PO}_3$  and  $\text{BO}_4$  units. Strong bands at 930–900  $\text{cm}^{-1}$  and weak bands at 775–680  $\text{cm}^{-1}$  can be, respectively, attributed to the antisymmetric and symmetric stretching vibrations of P-O-P and B-O-P bridges. The low-frequency region (650–400  $\text{cm}^{-1}$ ) is quite complex: bending vibrations of  $\text{PO}_3$  and  $\text{BO}_4$  units and Al-O stretching vibrations contribute to the absorption in the 650–450  $\text{cm}^{-1}$  region.

The  $\text{CsAl}_2\text{BP}_6\text{O}_{20}$  presents a first example of borophosphates with anionic partial structure containing the triphosphate groups and characterizing by B:P equal to 1:6.

[1] Lesage J., Guesdon A., Raveau B. // *J. Solid State Chem.* 2005. V. 178. P. 1212.

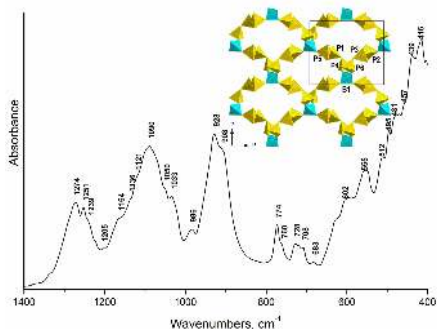


**Figure 1.** The 2D borophosphate anionic partial structure and infrared absorption spectrum of  $\text{CsAl}_2\text{BP}_6\text{O}_{20}$ .

**Keywords:** New topology of borophosphate, solid state reaction method

## MS15-P3 Mixed alkali/alkaline earth trielides of the $\text{BaAl}_4$ -type structure: A combined synthetic, crystallographic and theoretical case study for the 'coloring' in polar intermetallics

Martha Falk<sup>1</sup>, Carolin Meyer<sup>1</sup>, Matthias Kledt<sup>1</sup>, Caroline Röhr<sup>1</sup>

1. Institut für Anorganische und Analytische Chemie, Universität Freiburg

email: martha@almandine.chemie.uni-freiburg.de

The 'coloring' [1], the distribution of different atoms  $M$  among the apical/basal site of the pyramids in the  $\text{BaAl}_4$ -type (d), has already been extensively investigated for hundreds of ternary  $\text{TM}p$ -block compounds (cf. references in [2-4]). Concerning the electronic stability the optimized 'bond energy' of 14 ve/fu is sufficiently proven [5,6], even though the structure type occurs from 12 to almost 15 ve/fu. Using metallic  $M$  and ionic  $A^{n+}$  radii, the ratio  $r_M:r_A$  of the  $\text{BaAl}_4$ -type ranges from 0.89 to 1.04 [4].

The 'coloring' of the  $M$  anion by the triels, which differ both in size and electronegativity  $\chi$ , have been systematically investigated for the Ba series (Al/Ga/In),  $\text{SrGa}_4$  to  $\text{SrAl}_4$  (+In, [7]) (14 ve/fu) as well as for the Ga-containing K/Rb tetraindides (13 ve/fu). Carefully performed powder/single crystal structure analysis of distinct compounds (black symbols) reveal the  $\text{ThCr}_2\text{Si}_2$  ordering only ( $I4/mmm$ ), no indications towards the  $\text{CaBe}_2\text{Ge}_2$  or other 1:1:3 ordering variants are observed.

The calculated (FP-LAPW DFT) Bader volumes ( $V_{\text{BB}}$ ) of the binary trielides indicate no significant size differences for  $M_a$  and  $M_b$ , but a substantial more negative charge ( $q$ ) of  $M_a$ , due to the larger Coulomb interaction  $M_a-A$ . Accordingly, all Ga-phases show a strong preference for the electronegative Ga to occupy the  $M$  site (red curves in (a) and (b)). The preference is more restrictive for shorter  $A-M$  contacts, i.e. smaller  $r_A$  (e.g. difference Sr/Ba in (a)). The calculated 'coloring energy' ([5],  $\Delta E_{\text{tot}} = \text{CaAl}^b\text{Ga}^a \leftrightarrow \text{CaGa}^b\text{Al}^a$ , 0.46 eV) is by far larger than the difference of the  $M_a-M_a$  bond energies for Al/Ga (0.14 eV).

For mixed Al/In compounds (c) the  $M$  distribution changes with  $r$ : For smaller Sr with higher 'site energy'  $A-M_a$ , In with larger  $\chi$  occupies the  $M_a$  site. In contrast, for  $A=\text{Ba}$  the less electronegative element Al occupies this site. This change of the site preference could be verified by the calculations. It is a striking example for the important contribution of Coulomb interactions in the lattice energy of polar intermetallics.

[1] G. J. Miller, *Eur. J. Inorg. Chem.* 523 (1998)

[2] Q. Lin et al., *Z. Anorg. Allg. Chem.* **641**, 375 (2015)

[3] T.-S. You et al., *Bull. Korean. Chem. Soc.* **34**, 1656 (2013)

[4] M. Wendorff, C. Röhr, *Z. Naturforsch.* **68b**, 307 (2013)

[5] U. Häussermann et al., *J. Am. Chem. Soc.* **124**, 4371 (2002)

[6] M. Wendorff, C. Röhr, *Z. Anorg. Allg. Chem.* **631**, 338 (2005)

[7] C. Meyer, K. Köhler, C. Röhr, *Z. Kristallogr. Suppl.* **35**, 86 (2015)

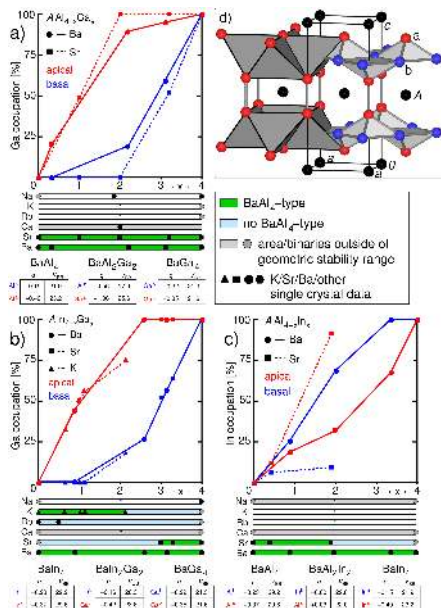


**Figure 1.** Triel-distribution in ternary compounds (investigated by means of single crystal data, black symbols) of the series AAl<sub>4</sub>Ga<sub>2</sub> (a), AIn<sub>4</sub>Ga<sub>2</sub> (b), AAl<sub>4</sub>In<sub>2</sub> (c) forming the BaAl<sub>4</sub>-type structure (d).

**Keywords:** Trielides, Gallides, Indides, Aluminides, Synthesis, Bandstructure Calculation

## MS15-P4 Twinning and pseudosymmetry in CsLan<sub>2</sub>F compounds with cation arrays equivalent to the hexagonal Laves phase Zn<sub>2</sub>Mg

Karen Friese<sup>1</sup>, Nicholas Khaidukov<sup>2</sup>, Andrzej Grzechnik<sup>3</sup>

1. Jülich Centre for Neutron Science-2, Forschungszentrum Jülich GmbH, 52425 Jülich, Germany
2. Kurnakov Institute of General and Inorganic Chemistry, Leninsky Prospect, 119991 Moscow, Russia
3. Institute for Crystallography, RWTH-University Aachen, Jägerstr. 17-19, 52066 Aachen, Germany

email: k.friese@fz-juelich.de

Ternary rare earth fluorides are of interest for a wide range of optical applications like e.g. lasers, scintillators, luminescent materials or efficient up- and downconverters e.g. [1]. The understanding and interpretation of their optical properties relies on an unambiguous structure determination. However, structure determination is frequently difficult due to the occurrence of complex twinning. One of the underlying reasons for this is the close relationship of the materials to high symmetry structures like fluoride, pyrochlore or tavorite [2-4].

Surprisingly ternary fluorides with general composition ALan<sub>2</sub>F<sub>7</sub> with A=K,Rb,Cs and Lan=rare earths and Y have been described in a large variety of different space groups, although the main structural motifs are very similar. It is also striking that for many of the described structures discussions about the correct space groups are ongoing.

We have investigated the compounds CsLan<sub>2</sub>F<sub>7</sub> with Lan=Nd,Gd,Tb,Er,Yb,Lu and Y with single crystal x-ray diffraction using synchrotron radiation. All the compounds show a pseudo-hexagonal metrics with  $a \approx b \approx 15.5\text{--}16.5$  Å,  $c \approx 12.3\text{--}12.7$  Å and  $\gamma \approx 120^\circ$ . A detailed analysis of the data shows that the structures are best described in the monoclinic space group P112<sub>1</sub>/b taking into account additional six-fold twinning. To better understand the underlying reasons for the frequent occurrence of twinning in the samples we performed a detailed analysis of the pseudosymmetry of the crystal structures, which showed that, in particular the cation array has a very high pseudosymmetry with respect to space group P6<sub>3</sub>/mmc with lattice parameter  $a_{\text{hex}} = 1/2a$ ,  $c' = c$ . Surprisingly, the resulting cation array in this high symmetry structure shows atomic positions which are equivalent to the ones observed in the hexagonal Laves phases Zn<sub>2</sub>Mg. An analysis of the pseudosymmetry of the structures of the known ALan<sub>2</sub>F<sub>7</sub> compounds shows the same highly symmetrical cation array.

[1] Advanced Inorganic Fluorides: Synthesis, Characterization and Applications, ed. T. Nakajima, B. Zemva, A. Tressaud, Elsevier, 2000.

[2] M. Bevan & S. E. Lawton, Acta Crystallogr. B42, 1986, p. 55-58.

[3] S. E. Ness, D. J. M. Bevan, & H. J. Rossell, Eur. J. Solid State Inorg. Chem. 25, 1988, 509-516.

[4] K. Friese, J.-Y. Gesland, & A. Grzechnik, Z. Kristallogr. 220, 2015, 614-621.

**Keywords:** ternary fluorides; twinning; pseudosymmetry; Laves phases



## MS15-P5 Lattice distortions in $\text{PrNiO}_3$ across the metal-to-insulator transition analyzed using the “*amplimodes*” approach

Dariusz J. Gawryluk<sup>1</sup>, Juan Rodriguez-Carvajal<sup>2</sup>, Maria T. Fernandez-Diaz<sup>3</sup>, Philippe Lacorre<sup>2</sup>, Marisa Medarde<sup>1</sup>

1. Laboratory for Scientific Developments and Novel Materials Paul Scherrer Institut, CH-5232 Villigen PSI (Switzerland)  
2. Institut Laue-Langevin, F-38042 Grenoble (France)  
3. Univ Maine, Univ Bretagne Loire, IMMM, CNRS, UMR 6283, F-72085 Le Mans 9 (France)

email: dariusz.gawryluk@psi.ch

The most significant feature of the  $\text{RNiO}_3$  perovskite family ( $R=Y$  or rare earth  $\neq \text{La}$ ) is a metal to insulator phase transition at a critical temperature ( $T_{\text{MIT}}$ ) which systematically increases by decreasing the size of the  $R$ . The electronic localization at  $T_{\text{MIT}}$  is associated with a subtle structural phase transition, which involves the splitting of the single Ni site of the high temperature metallic phase (SG  $P6mm$ ) into two non-equivalent sites, and decreases the symmetry of the unit cell from orthorhombic to monoclinic (SG  $P2_1/n$ ). The mechanism(s) at the origin of the MIT in this system is presently subject of an intense debate. However, several experimental results such a gigantic  $^{16}\text{O}$ ,  $^{18}\text{O}$  isotope effect on  $T_{\text{MIT}}$  point out towards a strong coupling between the lattice and the electronic degrees of freedom.

Here we report a detailed neutron powder diffraction study aimed to re-investigate the evolution of the crystal structure of the first member of the series ( $\text{PrNiO}_3$ ). For this purpose we collected high resolution data at the constant- $\lambda$  diffractometer D2B (ILL, Grenoble, France), and high- $Q$  data at the time-of-flight diffractometer SEPD (IPNS, Argonne National Laboratory, USA). The two sets of data were simultaneously refined using a common structural model and the novel “*amplimodes*” formalism [2,3] implemented in the Rietveld analysis suite FullProf [4]. Instead of describing the asymmetric unit with fractional atomic coordinates, this formalism involves a parametrization of the structural distortions in terms of symmetry-allowed distortion modes, defined as correlated atomic displacements which transform according to the irreducible representations of parent SG. The amplitudes of the different breathing, rotation and distortion modes are obtained directly in Å from the fit, allowing the identification of the main distortion modes involved in the transition. In the case of  $\text{PrNiO}_3$  we could successfully identify such modes, their amplitudes, and the magnitude of the anomalies that they undergo at  $T_{\text{MIT}}$ . We could also observe the appearance of an additional breathing mode below  $T_{\text{MIT}}$  directly related with the Ni positions splitting and the concomitant charge redistribution.

**Acknowledgment:** This research was supported by the NCCR MARVEL, funded by the Swiss National Science Foundation.

**References:** [1] D. Orobengoa et al., J. Appl. Cryst. **A42**, 820 (2009); [2] J.M. Perez-Mato et. al., Acta Cryst **A 66**, 558 (2010); [3] J. Rodriguez-Carvajal, Physica B **192**, 55 (1993).

**Keywords:** amplimodes, perovskite structure, rare earth nickelates, metal to insulator transition

## MS15-P6 Role of lithium diffusion on thermal expansion of $\text{Li}_{0.4}\text{WO}_3$ bronze

Thorsten M. Gesing<sup>1</sup>, M. Shahidur Rahman<sup>1</sup>, Ashfia Huq<sup>2</sup>, M. Mangir Murshed<sup>1</sup>

1. Chemische Kristallographie fester Stoffe, Institut für Anorganische Chemie und MAPEX Center for Materials and Processes, Universität Bremen, Leobener Straße /NW2, D-28359 Bremen, Germany  
2. Chemical and Engineering Materials Division, Oak Ridge National Laboratory, Oak Ridge, Tennessee 37831, USA

email: gesing@uni-bremen.de

Diffusion of interstitial cations in ionic conductors plays roles on the thermal expansion [1,2], which is of prime importance for the functionality of the materials at a given temperature. Herein we report the anomalous lattice thermal expansion of  $\text{Li}_{0.4}\text{WO}_3$  bronze. The polycrystalline sample was produced by solid state synthesis in a silica tube at low pressure and 973 K. The sample was characterized by in-house X-ray and time-of-flight neutron powder diffraction (NPD) as well as Raman spectroscopy. The as-synthesized  $\text{Li}_{0.4}\text{WO}_3$  crystallized in the  $Im\bar{3}$  space group [3], where the  $6b$  position (8-fold) is partially occupied by lithium and the  $2a$  (12-fold) is found to be vacant. In the  $6b$  site four planar oxygen atoms construct a smaller aperture of 26.7 pm, and the  $2a$  site a larger cavity of 39.5 pm for possible lithium diffusion. Temperature-dependent NPD data Rietveld refinement showed that the  $\text{Li}^+$  cations preferentially diffuse from the  $6b$  into  $2a$  site between 300 K and 500 K, which supports the ionic conductivity of some  $\text{LiWO}_3$  bronzes at high temperatures [4] and diffusion based phase transition at ambient condition [3]. Thus at this temperature regime a statistical equilibrium (dynamic disorder) exists between two occupancy possibilities for  $\text{Li}^+$  cations, leading to increase the  $\text{LiO}_n$  coordination as well as the averaged Li-O distance from 245 pm ( $6b$ , shortest distance 219 pm) to 265 pm ( $2a$ ). A sharp minimum was observed at 425 K for the temperature-dependent lattice thermal expansion coefficient (TEC) which does not show high temperature saturation. The low-temperature metric expansion could be modeled using a single Debye temperature. The observed data clearly depart from this model line once in the mid-range due to lithium diffusion and again at high-temperatures due to strong anharmonicity. Using an additional Debye spectrum with a low perturbed quantum anharmonicity term the high-temperature anomaly could be successfully modeled [5]. The change of the bulk modulus for the lithium diffusion was also discussed.

**References:** [1] A.W. Sleight, Curr. Opin. Solid State Mater. Sci. **3** (1998) 128. [2] H. Schulz, J. Am. Ceram. Soc. **57** (1974) 313. [3] M.S. Rahman, M.M. Murshed, T.M. Gesing, Z. Kristallogr. **229** (2014) 797. [4] M.E. Straumanis, S.S. Hsu, J. Am. Chem. Soc. **72** (1950) 4027. [5] M.M. Murshed, C.B. Mendive, M. Curri, G. Nénert, P.E. Kalita, K. Lipinska, A.L. Cornelius, A. Huq, T.M. Gesing, Mater. Res. Bull. **59** (2014) 170.

**Keywords:** bronzes, thermal expansion, Li diffusion



**MS15-P7** Growth, polymorphism and structure of Nd<sub>2</sub>MoO<sub>6</sub> Single Crystals

Olga A. Alekseeva<sup>1</sup>, Natalia I. Sorokina<sup>1</sup>, Igor A. Verin<sup>1</sup>,  
Alexander M. Antipin<sup>1</sup>, Elena P. Kharitonova<sup>2</sup>, Ekaterina I.  
Orlova<sup>2</sup>, Valentina I. Voronkova<sup>2</sup>

1. Shubnikov Institute of Crystallography RAS  
2. Moscow State University, Physical Department

email: olalex@crys.ras.ru

The Ln<sub>2</sub>Mo(W)O<sub>6</sub> compounds (1:1), so-called oxymolybdates, can be synthesized with all the rare-earth elements and attract the attention due to their chemical resistance, high refractive index, luminescence intensity. Earlier it was found that these molybdates have a tetragonal structure of La<sub>2</sub>MoO<sub>6</sub>-type or a monoclinic structure of Nd<sub>2</sub>WO<sub>6</sub>-type depending on the ionic radius of the rare earth element. In the case of large cations (La, Pr, Nd) the oxymolybdates synthesized at above 1000 °C have a tetragonal structure. Earlier the Nd<sub>2</sub>MoO<sub>6</sub> monoclinic phase was obtained for the first time under the firing at 900°C, which has the irreversible phase transition at 1010°C into the tetragonal phase.

The purpose of the present work was growth, study of polymorphism and structure of Nd<sub>2</sub>MoO<sub>6</sub> single crystals.

All the oxymolybdates single crystals were obtained by crystallization from a molten solution at a maximum temperature of 1250°C. The oxymolybdates with large cations (La, Pr, Nd) had a plate-like shape, the others crystallized as isometric prisms. The monoclinic Nd<sub>2</sub>MoO<sub>6</sub> single crystals were obtained by slow melt at 800 °C temperature.

X-ray diffraction study of two Nd<sub>2</sub>MoO<sub>6</sub> single crystals obtained at two different temperatures, were carried out using a diffractometer XCalibur S. Analysis of diffraction patterns from single crystal Nd<sub>2</sub>MoO<sub>6</sub> obtained at temperatures above 1000°C revealed the presence of additional lines not indicated within a unit cell with parameters established earlier:  $a=4.089$ ,  $c=15.99\text{\AA}$ . This contradiction was eliminated by fold increase of cell volume by choosing of the cell with the basis vectors  $a=a_0 + b_0$ ,  $b=-a_0 + b_0$ ,  $c=2c_0$  as a result of the tetragonal cell (sp. gr. I4<sub>1</sub>/acd) was obtained with  $a=5.664(1)$ ,  $c=31.621(1)\text{\AA}$ . The refinement of the structure of Nd<sub>2</sub>MoO<sub>6</sub> single crystals obtained at a temperature of about 800 °C revealed the monoclinic cell (sp. gr. I2/c) with  $a=15.903(1)$ ,  $b=11.391(1)$ ,  $c=5.527(1)\text{\AA}$ ,  $\beta=91.169(1)^\circ$ . The refined structural models of both tetragonal and monoclinic Nd<sub>2</sub>MoO<sub>6</sub> single crystals confirmed that oxymolybdate polymorphic transformations occur in an extremely low speed and appears continuously over a wide temperature range. The results clarify the structural models of tetragonal and monoclinic samples confirmed that oxymolybdates polymorphic transformations occur in an extremely low speed and appears continuously over a wide temperature range.

The study was supported by the RFBR (pr.no.14-02-00531) and pr. NSH-6617-2016-5.

**Keywords:** molybdates, single crystals, X-ray diffraction study

**MS15-P8** Crystal chemistry of the wylleite group of phosphate minerals

Frederic Hatert<sup>1</sup>

1. Laboratory of Mineralogy, University of Liège, Belgium

email: fhatert@ulg.ac.be

The wylleite group of minerals contains Na-Mn-Fe-Mg-Al-bearing phosphates which occur in rare-elements granitic pegmatites; their crystal structure is topologically identical to the alluaudite structure. However, the ordering of cations in wylleite-type phosphates induces a splitting of the M(2) and X(1) sites of alluaudite into the M(2a) M(2b) and X(1a) X(1b) sites, with a concurrent change of space group from C2/c to P2<sub>1</sub>/n. Three samples of minerals belonging to the wylleite group were structurally investigated: wylleite from the Buranga pegmatite, Rwanda (A), wylleite from the Malpensata pegmatite, Italy (B), and qingheite from the Santa Ana pegmatite, Argentina (C). Their crystal structures have been refined, based on single-crystal X-ray diffraction data, to  $R_f = 2.72\%$  (A),  $3.53\%$  (B), and  $2.46\%$  (C); unit-cell parameters are:  $a = 11.954(2)$ ,  $b = 12.439(2)$ ,  $c = 6.406(1)\text{\AA}$ ,  $\beta = 114.54(1)^\circ$  (A);  $a = 11.983(1)$ ,  $b = 12.423(1)$ ,  $c = 6.381(1)\text{\AA}$ ,  $\beta = 114.54(1)^\circ$  (B);  $a = 11.878(3)$ ,  $b = 12.448(2)$ ,  $c = 6.438(2)\text{\AA}$ ,  $\beta = 114.49(1)^\circ$  (C). The structure consists of kinked chains of edge-sharing octahedra stacked parallel to {101}. These chains are formed by a succession of M(2a)-M(2b) octahedral pairs, linked by slightly larger M(1) octahedra. Equivalent chains are connected in the  $b$  direction by the P(1), P(2a) and P(2b) phosphate tetrahedra to form sheets oriented perpendicular to [010]. These interconnected sheets produce channels parallel to  $c$ , channels that contain the large X sites. The X(1a) site is a distorted octahedron, whereas the X(1b) site can be described as a very distorted cube. The morphology of the X(2) site corresponds to a very distorted gable disphenoid with a [7 + 1] coordination, similar to the A(2)' site of the alluaudite structure. The structural features of these phosphates are compared to those of other wylleite-type phosphates: ferrosemaryite, roosemaryite, and qingheite-(FeII). These new structural data indicate that Al is predominant on the M(2a) site in the investigated samples, with Fe(II), Fe(III) or Mg on the M(2b) site. Variations of unit-cell parameters, of bond distances, and of distortion coefficients among members of the wylleite group are discussed in detail.

**Keywords:** phosphate minerals, wylleite group, crystal chemistry

**MS15-P9** Cell Dimensions of Titanium from 10 K to 290 KHåkon Hope<sup>1</sup>, Boris Kodess<sup>2</sup>

1. Department of Chemistry, University of California, Davis

2. ICS&amp;E-VNIIMS, Crystals Metrology Laboratory, Moscow 119361, Russian Federation

email: hhope@ucdavis.edu

We have measured the unit cell of Ti from 10 K to 290 K, using a Bruker area detector diffractometer. The three lowest temperatures were 10, 28 and 45 K. From 90 K to 290 K we used a Cryoindustries of America nitrogen cooler. Below 90 K we used a helium cooler from the same company. The sus for our measurements are about 0.00007 Å for *a* and 0.00017 Å for *c*. 290 K values are 2.95151 Å for *a* and 4.68483 Å for *c*. Corresponding 10 K values are 2.94650 and 4.67977 Å.

From 290 K to 45 K we see no unusual behavior, but at 28 K we measure the *c* axis to be longer than at 10 and 45 K. The *a* axis did not show any unusual behavior. This is at variance with earlier published measured and computed values, which showed negative thermal expansion for *c* below 170 K. Our crystal was of high purity, and the temperatures are reliable to better than 1 K. The measurements we have for comparison were performed with a capacitance dilatometer.

**Keywords:** Titanium, thermal expansion, 10 K to 290 K**MS15-P10** Structure Determination of Synthetic Shlykovite by Using Rotation Electron DiffractionZhehao Huang<sup>1</sup>, Jiho Shin<sup>1</sup>, Xiaodong Zou<sup>1</sup>

1. Berzelii Centre EXSELENT on Porous Materials, and Inorganic and Structural Chemistry, Department of Materials and Environmental Chemistry, Stockholm University, SE-106 91 Stockholm, Sweden.

email: zhehao.huang@mmk.su.se

Electron crystallography has attracted rapidly attention in recent years for structure solution of unknown crystals that are too small to be studied by single crystal X-ray diffraction. We developed rotation electron diffraction (RED) for collection and processing of 3-dimensional (3D) electron diffraction (ED) data. It combines fine electron beam tilt and coarse goniometer tilt to collect ED patterns semi-automatically with a large tilt range ( $\sim \pm 70^\circ$ ) [1, 2]. The RED method has been used for structural analysis of polycrystalline materials including complex zeolites [3], and would be useful for studying structures of rare and new minerals. For TEM investigations, the crystals are observed in high vacuum. It was found that crystal structures could be changed under such conditions due to the removal of water and organic molecules in the crystal. This problem could be solved if the samples are studied under cryogenic conditions, i.e. at liquid nitrogen temperature.

Recently, we are succeeded for the first time in synthesis of a mineral analogue to shlykovite ( $\text{KCaSi}_3\text{O}_9(\text{OH}) \cdot 3\text{H}_2\text{O}$ ) [4], which is one type of phyllosilicates and belongs to the mountainite family. The synthetic shlykovite crystals show a 2D nanosheet-like morphology. Therefore, the water molecule and organic molecules in the interlayer space are easily removed in high vacuum, which results in a different unit cell with that in the air. Hence, the structure of shlykovite was determined by using cryo-TEM, in which water molecules remained in the structure. By analyzing the reconstructed 3D reciprocal lattice, the space group and unit cell parameters of the synthetic shlykovite were determined as  $P2_1/c$  and  $a=6.59$  Å,  $b=7.03$  Å,  $c=26.99$  Å,  $\beta=95.1^\circ$ . The structure could be solved from the RED data. The combination of cryo-TEM and RED technique shows the capability for the analysis of crystals with flexible structures. It is complement to X-ray crystallography for studying crystals which have small sizes and unique morphology. The synthesis of shlykovite reveals a new route to synthesize natural minerals and can improve strategies toward the synthesis of new crystal structures.

[1] Wan, W.; Sun, J.; Su, J.; *et al. J. Appl. Crystallogr.*, **2013**, 46, 1863–1873.

[2] Zhang, D.; Oleynikov, P.; Hovmoller, S.; *et al. Z. Kristallogr.*, **2010**, 225, 94–102.

[3] Yun, Y.; Zou, X.; Hovmoller, S.; *et al. IUCrJ*, **2015**, 2, 267–282.

[4] Zubkova, N. V.; Filinchuk, Y. E.; Pekov, I. V.; *et al. Eur. J. Mineral.*, **2010**, 22, 547–555.

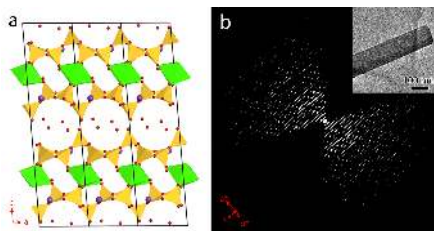


**Figure 1.** (a) Crystal structure of shlykovite viewed along the *b*-axis. Si: yellow tetrahedral; Ca: green octahedral; K: purple sphere; O: red sphere. (b) 3D reciprocal lattice of the synthetic shlykovite reconstructed from the RED data. Insert is the crystal from which the RED data was collected.

**Keywords:** electron crystallography, cryo-electron microscopy, electron diffraction, crystal structure, phyllosilicates, shlykovite.

## MS15-P11 Cronstedtite-6 $T_2$ , a non-MDO polytype

Jiří Hybler<sup>1</sup>

<sup>1</sup> Institute of Physics, Academy of Sciences of the Czech Republic, Na Slovance 2, CZ-18221 Praha, Czech Republic

email: hybler@fzu.cz

The new 6 $T_2$  polytype of cronstedtite was identified, together with known 2 $H_1$ , 2 $H_2$ , 3 $T$ , 1 $M$  and probably 2 $M_1$  polytypes in the mineral assemblage of an ore veinlet in the active quarry near Pohled, Czech Republic. The GPS co-ordinates of the locality are 49°35'50.326"N, 15°39'49.730"E [1].

Lattice parameters are  $a=5.4976(3)$ ,  $c=42.601(1)$  Å,  $Z=6$ , space group  $P3_1$ , composition  $(\text{Fe}^{2+}_{2.515} \text{Fe}^{3+}_{0.485}) (\text{Si}_{1.515} \text{Fe}^{3+}_{0.485}) \text{O}_3 (\text{OH})_4$ . The refinement converged to  $R_{\text{obs}} = 4.13\%$  for 3244 independent reflections [2]. The polytype belongs to the subfamily (Bailey's group) A.

The structure is built of edge-sharing octahedral (*Oc*) and corner-sharing tetrahedral (*Tet*) sheets forming the 1:1 layers (corresponding to OD packets) by sharing apical corners of *Tet* sheet. There are two independent 1:1 layers, where the odd one is shifted with respect of the even one by  $-(\mathbf{a} + \mathbf{a}_c)/3$  and raised by  $c/6$  of the hexagonal cell. The sextuple multiplicity is achieved by mapping this pair of layers by  $3_1$  axis repeatedly to two other equivalent positions raised by  $c/3$ ,  $2c/3$ . There are two tetrahedral and three octahedral sites per each 1:1 layer ( $T_1$ ,  $T_2$ ,  $M_1$ ,  $M_2$ ,  $M_3$  in even layers,  $T_{11}$ ,  $T_{12}$ ,  $M_{11}$ ,  $M_{12}$ ,  $M_{13}$  in odd layers), all in general positions. The  $M_3$ ,  $M_{13}$  octahedra are smaller than  $M_1$ ,  $M_2$ ,  $M_{11}$ ,  $M_{12}$ , thus *Oc* sheets in both layers are *meso-octahedral*. In even layers, however, the  $M_2$  octahedron is somewhat smaller than  $M_1$ , so the *Oc* sheet is "transitional" to a *hetero-octahedral* character. The occupancies of Si:Fe in *T* positions were refined to:  $T_1$ : 0.96:0.04(1),  $T_2$ : 0.63:0.37(1),  $T_{11}$ : 0.55:0.45(1),  $T_{12}$ : 0.89:0.11(1). Ditrigonalization angles  $\alpha$  are  $+11.4(5)^\circ$ , and  $+10.9(5)^\circ$ , in even and odd layers, respectively. Hydrogen positions were localized and geometries of hydrogen bonds linking the 1:1 layers were described. The structure is an example of OD structure of more than one kind of layers with a very low degree of desymmetrization. Cronstedtite-6 $T_2$  is a non-MDO polytype, because more than one kind of packet triplets can be distinguished in the stacking sequence.

Another, quite different sextuple non-MDO polytype 6 $T_1$  of the isostructural mineral lizardite [3] belongs to the group D.

The study was supported by the grant 15-0204S of the Czech Science Foundation.

### References:

- [1] Hybler, J., Sejkora, J., Vencík, V. (2016). DOI: 10.1127/ejm/2016/0028-2532
- [2] Hybler, J. (2016). Accepted in Eur. J. Mineral.
- [3] Hall, S. H., Guggenheim, S., Moore, P., Bailey, S. W. (1976). Can. Mineral. 14, 314-321.

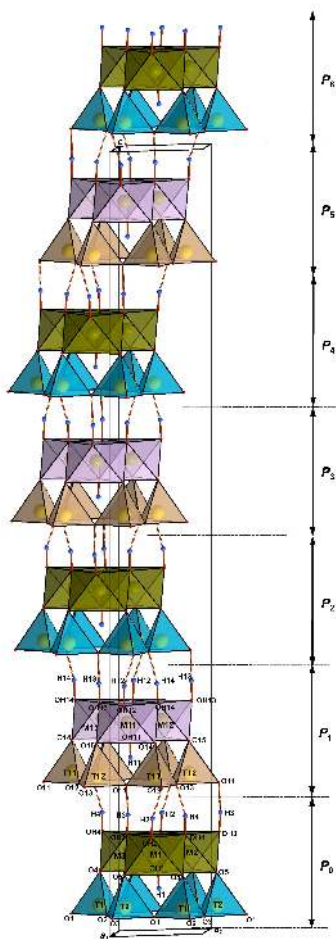


**Figure 1.** Structure of cronstedtite-6T<sub>2</sub>, side view, projection close to a<sub>0</sub>. For sake of clarity, only a small part of every OD packet (1:1 layer) is displayed: one ring of tetrahedra and three adjacent octahedra. Delimitations of packets ( $P_0$ ,  $P_1$ ,  $P_2$  ...) are indicated on the right side.

**Keywords:** Cronstedtite, 1:1 layer silicate, polytypism, non-MDO polytype 6T<sub>2</sub>, crystal structure

## MS15-P12 Chemical preparation, crystallographic characterization and vibrational study of condensed phosphates associated to Barium-Cesium $\text{BaCs}(\text{P}_3\text{O}_9)_2 \cdot 2\text{H}_2\text{O}$

Aziz KHEIREDDINE<sup>1</sup>, TRIDANE Malika<sup>1,2</sup>, BELHABRA Mustapha<sup>1</sup>, FAHIM Ismail<sup>1</sup>, MOUTAABBID Hicham<sup>3</sup>, MOUTAABBID Mohammed<sup>1</sup>, BELAAOUAD Said<sup>1</sup>

1. Laboratory of chemistry and physic of materials, University Hassan II- Casablanca, Morocco
2. Centre Régional des métiers d'enseignement et de formation Casablanca, Maroc
3. Minéralogie, de Physique des Matériaux, et de Cosmochimie (IMPMC), University Paris 06, France.

email: kheireddine.aziz@gmail.com

Methods of chemical preparation and XRD data are reported for the new condensed phosphates associated to Barium-Cesium  $\text{BaCs}(\text{P}_3\text{O}_9)_2 \cdot 2\text{H}_2\text{O}$ .  $\text{BaCs}(\text{P}_3\text{O}_9)_2 \cdot 2\text{H}_2\text{O}$  was prepared by the method of ion-exchange resin. This salt crystallizes in the monoclinic system, space group P2<sub>1</sub>/n  $a = 7.6992(2)$  Å  $b = 12.3237(3)$  Å  $c = 11.8023(3)$  Å,  $\beta = 101.181^\circ(3)$ ,  $M(20) = 1313.35$ ;  $F(20) = 1004.53$  and  $V = 333.95(2)$  (Å<sup>3</sup>), the vibrational study by IR absorption spectroscopy of the title compound reveals the presence of three bands and confirm the existence of non-equivalent positions of water molecules in the structure.

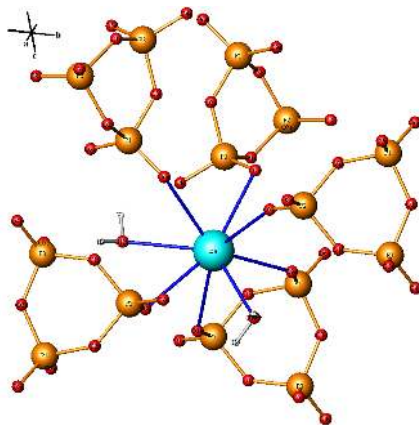


**Figure 1.** Projection of the structure Barium-Cesium  $\text{BaCs}(\text{P}_3\text{O}_9)_2 \cdot 2\text{H}_2\text{O}$

**Keywords:** condensed phosphates, ion-exchange resin, vibrational study

# MS15-P13 Structural peculiarities and structure-optical property relationships of doped ( $\text{Sr}_{0.61}\text{Ba}_{0.39}\text{Nb}_2\text{O}_6$ :Cr/Ni and $\text{SrMoO}_4$ :Tm/Ho) crystals

Galina M. Kuzmicheva<sup>1</sup>, Irina A. Kurova<sup>1</sup>, Lyudmila I. Ivleva<sup>2</sup>, Victor B. Rybakov<sup>3</sup>, A. Cousson<sup>4</sup>

**Keywords:** barium strontium niobate, scheelite, diffraction study, optical properties

1. Moscow Technological University, MITHT
2. Prokhorov General Physics Institute, Russian Academy Sciences
3. Lomonosov State University
4. Laboratoire Leon Brillouin, CEA Saclay

email: galina\_kuzmicheva@list.ru

Doping is one of the main ways to entrance properties of crystals. The aim of paper is to establish the role of doping of single crystals with initial compositions  $\text{Sr}_{0.61}\text{Ba}_{0.39}\text{Nb}_2\text{O}_6$  (sp.gr. P4bm) (SBN), grown by Czochralski, and  $\text{SrMoO}_4$  (sp.gr. I4/a) (SMO), grown by Stepanov, by  $\text{Cr}^{3+}$  and  $\text{Ni}^{3+}$ , and  $\text{Tm}^{3+}$  and  $\text{Ho}^{3+}$  ions, respectively.

The neutron diffraction analysis of SBN ( $\sim 5 \times 5 \times 5 \text{ mm}^3$ ) was carried out on diffractometer 5C2 (LLB, France;  $\lambda = 0.83 \text{ \AA}$ ). The refined compositions of SBN were found to be different from the initial charge compositions, wherein the doping enhances such differences. Analysis of cation-anion internuclear distances together with calculation of bond-valence sums showed that Nb1 and Nb2 are located in distorted octahedra with split vertices, forming a framework with three types of channels: Sr1 atoms are located in cuboctahedra (square channels), Ba2 and Sr2 atoms are located in distorted three-capped trigonal prisms and five-capped pentagonal prisms, respectively, with split vertices in base planes (pentagonal channels). Displacement of electron density in Nb1 and Sr2 polyhedra, responsible for covalent bond and second-order nonlinear susceptibility, has been revealed. It was found that  $\text{Cr}^{3+}$  ions occupy triangular cavities with distorted octahedral coordination and Ni ions are located in distorted semi-octahedra near Nb2 and Nb1 sites. It leads to appearance of additional energy levels, which enhances photo-refractive properties and results in shift of the absorption edge to longer wavelengths.

The X-ray diffraction analysis of SMO crystals ( $\sim 0.1 \times 0.1 \times 0.1 \text{ mm}^3$ ) was carried out on CAD-4 diffractometer ( $\text{MoK}\alpha$ , graphite monochromator). Introduction of dopants into the melt in the form of  $\text{RE}^{3+}\text{Nb}_2\text{O}_6$  ( $\text{RE}^{3+} = \text{Tm}, \text{Ho}$ ) with distorted scheelite structure (that is favorable for isomorphic substitution and maintenance of electrical neutrality leads to different behavior of  $\text{RE}^{3+}$  in SMO structure: to partial substitution of  $\text{Sr}^{2+}$  (in dodecahedra) and  $\text{Mo}^{6+}$  (in tetrahedra) ions by  $\text{Ho}^{3+}$  and  $\text{Nb}^{5+}$  ions near  $\text{Sr}^{2+}$  and  $\text{Mo}^{6+}$  defect sites. Spectroscopic investigations of  $\text{SMO:Tm}$  have shown that the maximum absorption cross section of  $\text{Tm}^{3+}$  lies at 795 nm and reaches  $1.1 \cdot 10^{-20} \text{ cm}^2$  for  $\pi$ -polarized radiation, higher than that in  $\text{Y}_3\text{Al}_5\text{O}_{12}$  and  $\text{LiYF}_3$  crystals.

This work was carried out of state task of the Ministry of Education and Science of Russian Federation (N 4.745.2014/K).

**MS15-P14** Structural and physicochemical characterization of Basic Calcium Carbonate (BCC)Christian L. Lengauer<sup>1</sup>, Manuel Ripken<sup>1</sup>, Florian Gallien<sup>2</sup>,  
Thomas Schlotterbach<sup>2</sup>

1. Department of Mineralogy and Crystallography, University of Vienna, Althanstrasse 14, 1090 Vienna, Austria

2. Onya GmbH, Gersheimstrasse 1-2, 9722 Gummern, Austria

email: christian.lengauer@univie.ac.at

This study reports investigations on physicochemical characterization, environmental stability and structural features of calcium carbonate hydroxide hydrate, labeled in literature [1,2] as basic calcium carbonate (BCC). Despite the fact of the relevance of BCC in calcium carbonate processing, structural knowledge of this metastable phase is still missing. Therefore, material, precipitated according to the synthesis route described later, was analyzed by means of powder X-ray diffraction (pXRD), thermal analyses (TA), chemical analyses, electron microscopic imaging (SEM) and spectroscopic methods.

The best conditions for the storage of calcium carbonate hydroxide hydrate (basic calcium carbonate - BCC) are in a bone dry non-heated environment. This is confirmed by powder X-ray (pXRD) analysis. Under humid conditions sample material transforms into vaterite-type calcium carbonate, while under a dry heating process it dehydrates and dehydroxylates to calcite-type calcium carbonate. Under ambient humidity and temperature conditions the dehydrated modification does not convert back to BCC, but also transforms to the vaterite-type calcium carbonate. High quality scanning electron microscopy (SEM) images of a rapidly converted vaterite-type calcium carbonate reveal imperfect pseudomorphs of vaterite after the platy BCC.

According to the observed and calculated weight losses of BCC and data from literature, one can state a mismatch with the prior reported chemical formula, which would require an overall weight loss of -14.9 wt% for (OH)<sub>2</sub> + 1.5H<sub>2</sub>O. As the observed weight loss is here proven to be -12.3 wt%, which is very close to the calculated value for a monohydrate (-12.2 wt%), one can give the corrected chemical formula as Ca<sub>3</sub>(CO<sub>3</sub>)<sub>2</sub>(OH)<sub>2</sub>.H<sub>2</sub>O for BCC.

Crystallographic analysis reveals the hitherto unknown structure of BCC determined by analyzing pXRD patterns. BCC crystallizes to a monoclinic lattice with space group Pc. The cell parameters of the pseudo-orthorhombic cell are *a* = 8.661(1) Å, *b* = 6.557(1) Å, *c* = 7.078(1) Å, *β* = 90.08(1)° and *V* = 401.97(4) Å<sup>3</sup>. The structure model shows similarities with those of portlandite, vaterite and hydromagnesite.

[1] Schimmel G. (1970) Naturwissenschaften, Jg. 57, 38-39.

[2] Matsushita et al. (1993) J. Ceramic Soc. Japan, 101, 895-899.

**Keywords:** BCC, calcium carbonate hydroxide hydrate

**MS15-P15** Study and Characterization of a Composite for Use in the Automotive Industry with the Use of X-ray Powder DiffractionKelly C.L. Lixandrão<sup>1</sup>

1. Federal University of ABC

email: kellycrislima@yahoo.com.br

The development of the automotive industry in the twentieth century has increased the production of motor vehicles, generating an increase of the national fleet, and the consumption of tires reached staggering numbers. By this reason, the amount of solid wastes generated and deposited in the environment has grown considerably. In order to minimize the impacts arising from this deposition, some environmental agencies have created resolutions to ensure proper disposal of scrap materials. [1]. At the end of its service life, the wasted tires, without shooting conditions or reforms, are difficult to recycle because the vulcanization process makes the material infusible and of difficult processability. When discarded in inappropriate locations, tires may serve as a medium for the development of disease vectors besides representing risk of fire, polluting the air with toxic fumes – containing pollutants such as carbon and sulfur – as well as releasing oil, which can contaminate the water table [2]. In order to reduce the amount sent to the environment and to generate an appropriate production cycle, the wasted tire was used as reinforcement in a polymeric matrix to be applied to the engine encapsulation of commercial vehicles. It is intended to provide a reduction of the piece weight and thus the vehicle, optimizing fuel consumption and reducing the emission of pollutants; additionally, it ensures the minimization of noise pollution through the noise attenuation by the composite. Acoustic analysis of transmission loss and external noise were performed to verify whether the material complies with the limits specified by the resolutions. The X-ray powder diffraction analysis was fulfilled to identify and quantify the different phases that composing the material.

**Keywords:** tire powder, X-ray diffraction, engine encapsulation.

## MS15-P16 Characterization of lone electron pair using Liebau density vector and Wang-Liebau eccentricity parameters

M. Mangir Murshed<sup>1</sup>, Cecilia B. Mendive<sup>2</sup>, Mariano Curti<sup>2</sup>,  
Thorsten M. Gesing<sup>1</sup>

1. Chemische Kristallographie fester Stoffe, Institut für Anorganische Chemie und MAPEX Center for Materials and Processes, Universität Bremen, Leobener Straße /NW2, D-28359 Bremen, Germany

2. Departamento de Química, Facultad de Ciencias Exactas y Naturales, Universidad Nacional de Mar del Plata, Dean Funes 3350, 7600 Mar del Plata, Argentina

email: murshed@uni-bremen.de

Compounds carrying cations with lone electron pair (LEP) show marked distortion in their coordination sphere, which is intimately related to the electronic distribution of the LEP. Hence, non-spherical but asymmetric LEPs are usually referred to be stereochemically active. It is still in search of a measure to quantify at which extend the LEP of a cation in a crystal structure is stereochemically active. Herein we approach the Wang-Liebau eccentricity (WLE) parameter [1] and the Liebau density vector (LDV) [2] to characterize the 6s<sup>2</sup> LEP of Bi<sup>3+</sup> cations in Bi<sub>3</sub>B<sub>2</sub>O<sub>9</sub> as a model compound. WLE is a vector term associated with all bonds in a given coordination, which measures the electronic deformation density of the LEP and directs along the line from the nucleus to the approximate center of the LEP charge density. The dimensionless length of the WLE parameter thus indirectly measures the degree of deformation of the associated LEP, and cannot be depicted graphically. LDV describes the length of a vector directed from the nucleus of an atom to the maximum electron density of the LEP. We have demonstrated on some mullite-type compounds that the direction of WLE and LDV are almost parallel as long as a localized electron density is obtained for LDV [2]. The ambient condition crystal structure of Bi<sub>3</sub>B<sub>2</sub>O<sub>9</sub> (P2<sub>1</sub>/c) [3,4] possesses four crystallographically different Bi-positions, where Bi1 and Bi3 are six-coordinated and, Bi2 and Bi4 are seven and eight coordinated, respectively, within Bi-O distance less than 330 pm. Both the WLE and LDV magnitudes for Bi1 and Bi3 are higher than those of the higher coordinated Bi2 and Bi4. A correlation between the LDV and the electron density of LEP determines the minimum localized electron density of LEP to be stereochemically active irrespective to the crystallographic position of the Bi-atom. With increasing temperature both the WLE and LDV decreased, indicating the decrease of stereochemical activity of the LEP.

**References:** [1] X. Wang, F. Liebau, Z. Kristallogr. 211 (1996) 437. [2] M. Curti, Th.M. Gesing, M.M. Murshed, T. Bredow, C.B. Mendive, Z. Kristallogr. 228 (2013) 629. [3] S.K. Filatov, Y.F. Shepelev, Y.V. Aleksandrova, R.S. Bubnova, Russ. J. Inorg. Chem. 52 (2007) 21. [4] A. Hyman, A. Perloff, Acta Crystallogr. 28 (1972) 2007.

**Keywords:** lone electron pair, Liebau density vector, Wang-Liebau eccentricity

## MS15-P17 Twinning is the key aspect of giant gypsum crystals in Naica

Fermin Otálora<sup>1</sup>, Dino Aquilano<sup>2</sup>, Marco Rubbo<sup>2</sup>, JuanMa García-Ruiz<sup>1</sup>

1. Laboratorio de Estudios Cristalográficos. Instituto Andaluz de Ciencias de la Tierra. CSIC-Universidad de Granada, Armilla, Granada, Spain

2. Dipartimento di Scienze della Terra, Università degli Studi di Torino, via V. Caluso 35, 10125, Torino, Italy

email: ferminotolara@gmail.com

The giant gypsum crystals discovered in 2000 at Naica (Mexico) have been since then a source of deep fascination not only because of their look, but also due to the wealth of scientific information that the mineralogical/crystallographic community can get from them. The first report explaining the extremely unusual size of these crystals [1] showed that they are only compatible with very low nucleation and growth rates under extremely steady conditions very close to equilibrium. These results lead to a deeper understanding of the nucleation and growth processes at very low supersaturation and to the definition of geological settings where nucleation and growth of giant crystals is plausible. Even the state of the art of our knowledge concerning the equilibrium morphology of gypsum was challenged [2] by these unique crystals growing in conditions very close to equilibrium, where no experiments can be performed in the laboratory.

After 14 years of study, [3] one question was still open. The presence of two clearly distinct crystal habits for gypsum in Naica (bulky crystals with a morphology close to the equilibrium one, and much longer crystals, called “beams”, up to 11 meters long) was reported, but left unexplained. Our last results show that the reason for the presence of the long crystals that make Naica so exceptional is related to twinning. All long crystals are 100 twins and the reentrant angle of the twin is the source of growth steps required for the extremely unusual development of the giant c-elongated beams. The origin and operation of this structurally controlled mechanism is explained.

[1] García-Ruiz, J.M., Villasuso, R., Ayora, C., Canals A. and Otálora, F. (2007): Formation of natural gypsum megacrystals in Naica, Mexico. *Geology*, 35, 327–330.

[2] Massaro, F.R., Rubbo, M. and Aquilano, D. (2010): Theoretical Equilibrium Morphology of Gypsum (CaSO<sub>4</sub>·2H<sub>2</sub>O). 1. A Syntectic Strategy to Calculate the Morphology of Crystals. *Crystal Growth & Design*, 10, 2870–2878.

[3] Otálora, F. and García-Ruiz, J.M. (2013): Nucleation and growth of the Naica giant gypsum crystals. *Chem Soc Rev.* 43, 2013–2026.



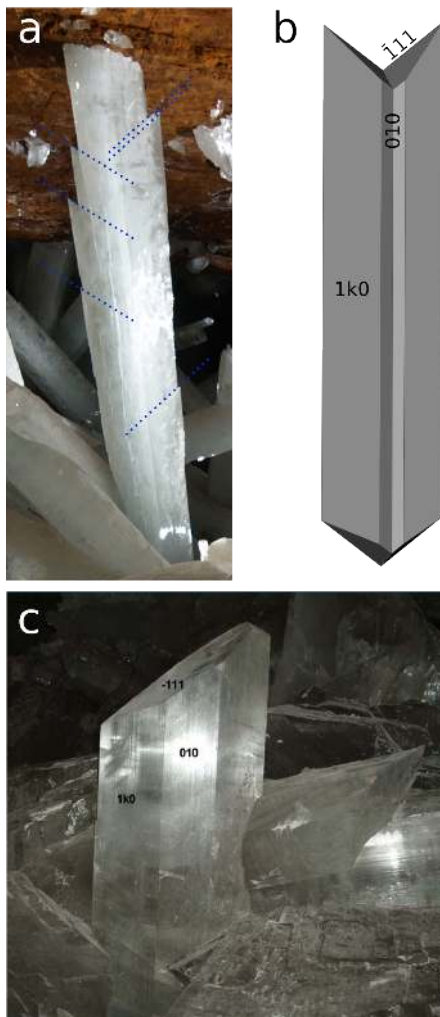


**Figure 1.** The two gypsum habits present in the Cave of Crystals at Naica. 10 meters long beam (a) showing the reentrant twin angle; sketch of the twin (b); 0.8 meters blocky crystal close to the equilibrium habit of gypsum (c).

**Keywords:** gypsum, twinning, growth mechanisms

## MS15-P18 Application of $\delta$ -recycling to multidomain tts-microdiffraction: The ilerdite case

Jordi Rius<sup>1</sup>, Carlos Frontera<sup>1</sup>, Oriol Vallcorba<sup>2</sup>

1. Institut de Ciència de Materials de Barcelona (CSIC), Campus de la UAB, 08193 Bellaterra, Catalonia, Spain

2. Alba Synchrotron, Barcelona, Spain

email: jordi.rius@icmab.es

In previous tts (*=through-the-substrate*) synchrotron microdiffraction experiments, a new aluminosilicate (code name: ilerdite) was detected in petrological polished thin sections from Tartareu (Lleida, Spain) [1]. The corresponding 2D patterns showed diffraction spots from multiple grains of ilerdite. The powder pattern was approximated by circularly integrating the 2D frames. The resulting metric of ilerdite was: Monoclinic with unit cell  $a = 6.398(1)$ ,  $b = 6.904(1)$ ,  $c = 9.427\text{\AA}$ ,  $\beta = 96.42(1)^\circ$ ,  $V = 414\text{ \AA}^3$ ,  $(\text{Ca}_{0.7}\text{Mg}_{0.3}\text{K}_3)(\text{Al}_1\text{Si}_9\text{O}_{16}) \cdot 5\text{H}_2\text{O}$ ,  $Z=1$ . Application of Patterson-function direct methods (PFDM) [2] to cluster intensities derived from whole-pattern matching gave the arrangement of the metal atoms. Due to the limited resolution of the 'powder' pattern (no reliable information from the high angle region) O atoms could not be located, so that a second tts-microdiffraction experiment at BL04 of ALBA synchrotron was performed. Details on the experimental set-up and the tts data collection mode can be found in [3]. In this experiment several microvolumes of ilerdite in different regions of the polished thin section were measured. The 2D diffraction patterns of three microvolumes were selected and processed. From this information, intensity data of six oriented ilerdite microcrystals were recovered (each microvolume contained more than one microcrystal). After multicrystal-merging, 200 single-crystal-like intensities were obtained. Application of PFDM ( $\delta$  recycling algorithm) in  $P2/m$  gave the model of the average structure which was confirmed by the subsequent LS refinement. Financial support of projects MAT2012-35247 and MAT2015-67593-P of MINECO is acknowledged. [1] Rius, J., Labrador, A., Crespi, A., Frontera, C., Vallcorba, O., Melgarejo, J.C. (2011) *J. Synchrotron Rad.* 18, 891-898. [2] Rius, J. (2014) *IUCrJ*, 1, 291-304. [3] Rius, J., Vallcorba, O., Frontera, C., Peral, I., Crespi, A., Miravittles, C. (2015) *IUCrJ*, 2, 452-463.

**Keywords:** tts-microdiffraction, multidomain, ilerdite, structure solution,  $\delta$  recycling, polished thin sections

**MS15-P19 HT phase transition in olivenite**Serena C. Tarantino<sup>1</sup>, Michele Zenna<sup>1</sup>, Athos M. Callegari<sup>1</sup>,  
Massimo Boiocchi<sup>2</sup>, Michael A. Carpenter<sup>3</sup>

1. Dipartimento di Scienze della Terra e dell'Ambiente, Università di Pavia, Italy
2. Centro Grandi Strumenti, Università di Pavia, Italy
3. Department of Earth Sciences, University of Cambridge, UK

email: serenachiara.tarantino@unipv.it

Olivenite group comprises several arsenates and phosphates minerals, such as eveite, olivenite, zincolivenite, libethenite and zincolibethenite. The members of this group crystallize in the orthorhombic  $Pnmm$  space group with the exception of olivenite, which crystallizes in the monoclinic  $P2_1/n$  space group. The monoclinic symmetry of olivenite has been ascribed to a cooperative Jahn-Teller effect involving  $Cu^{2+}$  in an octahedral ligand field, whereby electron-phonon coupling lowers the symmetry of the structure.

In this work, a natural olivenite single crystal was submitted to in situ HT single-crystal X-ray diffraction from room temperature to 500°C. Olivenite undergoes a structural phase transition from  $P2_1/n$  to  $Pnmm$  at ca. 200°C, and eventually becomes isostructural with the other members of the olivenite mineral group.

Instability of the electronic structure is the driving mechanism for a Jahn-Teller transition, but change in the structural state appears overtly as changes in lattice parameters, which have been analysed in terms of spontaneous strain. Moreover, the order parameter has been extracted from fractional coordinates by symmetry mode decomposition performed using the AMPLIMODES tool of the Bilbao Crystallographic Server.

There is a primary distortion (irrep  $GM4+$ ), which yields the observed symmetry break between the two phases, and the full symmetric distortion mode (irrep  $GM1+$ ). The amplitudes of the primary distortion is significantly large (0.8706 Å). It follows the typical law of an order parameter of a continuous phase transition  $Q \propto (T - T_c)^{0.25}$ , thus indicating that the transition conforms to Landau tricritical behavior. The spontaneous strain arising in the monoclinic phase is only non symmetry breaking as the shear strain associated to the primary distortion mode  $GM4+$  is negligible. Volume strain at room temperature is large and negative, as volume expansion with temperature is larger in the monoclinic than in the orthorhombic phase. Observed strain relationships are consistent with pseudoproper ferroelastic behaviour  $V_s \propto \text{Amp } GM4+^2$ .

Distortion of Cu polyhedra is quite high in the olivenite monoclinic phase at RT and goes towards a relative regularization with increasing  $T$  until the phase transition occurs. At temperatures around 500°C, the structure collapses due to dehydration and transform into the anhydrous form.

**Keywords:** olivenite, high temperature, single-crystal X-ray diffraction

**MS15-P20 Synthesis and Characterizations of new quaternary selenide  $Sn_4(In/Sb)_{14}Se_{25}$** Chi-Shen Lee<sup>1</sup>, Guan-Ruei Chen<sup>1</sup>

1. National Chiao Tung University

email: chishen@mail.nctu.edu.tw

New quaternary selenide  $Sn_4(In/Sb)_{14}Se_{25}$  was synthesized by a solid state chemistry reaction with stoichiometric mixture of elements ( $Sn:In:Sb:Se = 5:4:9:25$ ). The structure is constructed with two building units called  $NaCl^{100}$ -type () and  $NaCl^{111}$ -type (), respectively. Due to similar atomic numbers of indium, tin and antimony atoms, the valence and coordination environments of atomic sites were utilized to assign metal positions. Five-coordinated (square pyramid) sites in  $NaCl^{100}$  units were considered as mixed occupied  $Sn^{2+}/Sb^{3+}$ , while six-coordinated (octahedron) sites in  $NaCl^{111}$  units were assigned as  $In^{3+}/Sb^{3+}$ . The result gave a charge-balanced formula  $Sn_4In_5Sb_9Se_{25}$ .  $Sn_4In_5Sb_9Se_{25}$  crystallizes in the monoclinic space group  $C2/m$  in a new structure type and shows the property of preferred orientation with columnar appearance. This compound exhibits black color and physical property measurements suggest semiconducting property with a narrow band gap. The value of the band gap obtained by UV-Vis-NIR spectroscopy and the electrical conductivity is  $\sim 0.52$  eV. Band structure calculations from a model structure also showed the result of nearly semiconducting property. The as prepared compound is stable at room temperature under ambient condition. And it is melted and decomposed in temperature near 600°C under vacuum.

**Keywords:** crystal structure, selenide, solid state chemistry, crystallography

# MS15-P21 Synthesis, structure and band structure calculation of the new sodium sulfido ferrates $\text{Na}_2[\text{FeS}_2]$ and $\text{Na}_7[\text{Fe}_2\text{S}_6]$

Pirmin Stübke<sup>1</sup>, Caroline Röhr<sup>1</sup>

<sup>1</sup> Albert-Ludwigs-Universität Freiburg, Germany

email: pirmin@pyrite.chemie.uni-freiburg.de

In the course of a systematic study of alkali chalcogenido metalates, the new compounds  $\text{Na}_2[\text{FeS}_2]$  and  $\text{Na}_7[\text{Fe}_2\text{S}_6]$  were synthesized by heating natural pyrite and elemental sodium enclosed in corundum crucibles under an argon atmosphere at a maximum temperature of 800°C. In this reductive approach, lower iron valences were obtained extending once again the structural diversity of this well investigated class of compounds. The crystal structures were determined by means of single crystal X-ray diffraction. DFT+U band structure calculations were performed using the FP-LAPW method.

The orthorhombic compound  $\text{Na}_2[\text{FeS}_2]$  ( $\text{K}_2\text{MnS}_2$  structure type, space group  $Ibam$ ,  $a=643.3$ ,  $b=1140.4$ ,  $c=562.9$  pm,  $Z=4$ ,  $R1=0.037$ ) contains linear anionic chains of  $\text{FeS}_4$  tetrahedra connected via two opposite edges (Fig. a), relating it structurally to the mixed valent  $\text{Na}_2[\text{Fe}_2\text{S}_4]$  with corrugated chains [1].  $\text{Na}_2[\text{FeS}_2]$  is isotypic to the cobaltates  $A_2[\text{CoS}_2]$  ( $A=\text{Na}, \text{K}, \text{Rb}, \text{Cs}$ ) [2] and is the first alkali chalcogenido ferrate with anionic chains exclusively containing  $\text{Fe}^{\text{II}}$ .

Corresponding to the known magnetism of the cobaltates DFT calculations were carried out with antiferromagnetic spin ordering in the linear chains.

The triclinic diferrate  $\text{Na}_7[\text{Fe}_2\text{S}_6]$  (new structure type, space group  $P-1$ ,  $a=764.2$ ,  $b=1153.7$ ,  $c=1272.6$  pm,  $\alpha=62.3$ ,  $\beta=72.83$ ,  $\gamma=84.64^\circ$ ,  $Z=3$ ,  $R1=0.019$ ) contains binuclear  $[\text{Fe}_2\text{S}_6]^{7-}$  anions formed by two edge sharing  $\text{FeS}_4$  tetrahedra (Fig. b). Two crystallographically different  $[\text{Fe}_2\text{S}_6]^{7-}$  anions can be distinguished, one of them is centrosymmetric. Nevertheless, averaged terminal and bridging Fe-S distances are well comparable in both, indicating one  $\text{Fe}^{\text{II}}$  and one  $\text{Fe}^{\text{III}}$  in each dimer (Fig. c). This mixed valency is unique among the alkali chalcogenido metalate dimer compounds, previously containing only  $M^{\text{III}}$ , like e.g. the diferrates  $A_7[\text{Fe}_2\text{Q}_6]$  ( $A=\text{Na}, \text{K}, \text{Rb}, \text{Cs}$ ;  $\text{Q}=\text{O}, \text{S}, \text{Se}$ ) [3-6] and  $\text{Rb}_{12}[\text{Fe}_2\text{Q}_6](\text{Q}_2)_3$  ( $\text{Q}=\text{S}, \text{Se}$ ) [6].

Due to the antiferromagnetic spin ordering in the dimers in the reference compound  $\text{Na}_6[\text{Fe}_2\text{S}_6]$  [3], we found ferrimagnetic spin ordering for  $\text{Na}_7[\text{Fe}_2\text{S}_6]$  coinciding with its macroscopic magnetic behaviour.

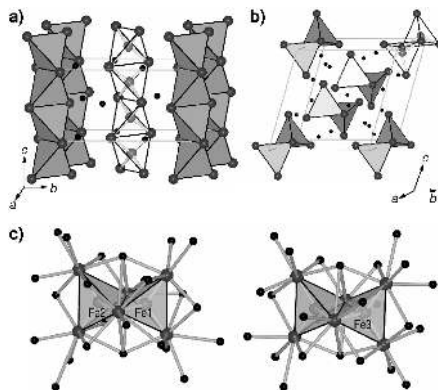


**Figure 1.** a) Unit cell of  $\text{Na}_2[\text{FeS}_2]$ . b) Unit cell of  $\text{Na}_7[\text{Fe}_2\text{S}_6]$ . c) Acentric dimer1 (left) and centrosymmetric dimer2 (right) with  $\text{Na}^+$  coordination. Bridging and terminal Fe-S bond lengths of dimer1 / dimer2:  $d_{\text{Fe-S}}^{\text{br}} = 234.7(3) / 235.4$  pm,  $d_{\text{Fe-S}}^{\text{t}} = 228.7(1) / 229.2(2)$  pm.

**Keywords:** chalcogenido ferrate, diferrate, band structure, magnetism

[1] K. Klepp, H. Boller. *Monatsh. Chem.* 112, 83-89 (1981).

[2] W. Bronger, C. Bomba. *J. Less-Common Met.* 158, 169-176 (1990).

[3] W. Bronger, U. Ruschewitz, P. Müller. *J. Alloys Compd.* 187, 95-103 (1992).

[4] G. Frisch, C. Röhr. *Z. Kristallogr.* 220, 135-141 (2005).

[5] M. Schwarz, M. Haas, C. Röhr, *Z. Anorg. Allg. Chem.* 369, 360-374 (2013).

[6] M. Schwarz, P. Stübke, C. Röhr (in prep.).

## MS15-P22 The biclinic crystal system – a hidden system in crystallography

Hejing Wang<sup>1</sup>, Jian Zhou<sup>2</sup>

1. School of Earth and Space Sciences, Peking University, Beijing 100871, China

2. Chinese Academy of Geological Sciences, Beijing 100037, China

email: hjwang@pku.edu.cn

It is well known that there are seven crystal systems, the cubic, hexagonal, trigonal, tetragonal, orthorhombic, monoclinic and the triclinic systems. From the orthorhombic to the triclinic systems, the crystal axial angles change from orthogonal ( $\alpha = \beta = \gamma = 90^\circ$ ) to oblique in one axis (e.g.  $\beta \neq 90^\circ$ ) to oblique in three axes ( $\alpha \neq \beta \neq \gamma \neq 90^\circ$ ). There is no oblique case in two axes (any two of  $\alpha$ ,  $\beta$  and  $\gamma \neq 90^\circ$  and with the remainder  $= 90^\circ$ ). That is strange. The biclinic crystal system ( $a \neq b \neq c$ ,  $\alpha \neq \beta \neq \gamma$  and  $\alpha$  (or  $\beta$  or  $\gamma$ )  $= 90^\circ$ ) is a real but being hidden system in crystallography. As  $\alpha$  (or  $\gamma$ )  $= 90^\circ$  ( $\beta \neq \gamma \neq 90^\circ$  or  $\beta \neq \alpha \neq 90^\circ$ ), kaolinite donates a real example of the biclinic crystal system [1]. The formation of the biclinic system is demonstrated by its equivalent biclinic-parallelepiped that is built from a pair of rectangles by shifting each other along their two edges (Fig. 1). The P1 and P-1 properties of space group are deduced from both twofold axis and mirror plane. Those formulae of the biclinic system are given for useful calculations including the metric tensor  $G$  and its reciprocal  $G^{-1}$ , volume  $V$ , reciprocal lattice parameters  $a^*$ ,  $b^*$ ,  $c^*$ ,  $\alpha^*$ ,  $\beta^*$  and  $\gamma^*$ , the relationships between the Miller indices, interplanar angle  $\Phi$ , vector length  $r$ , intervector angle  $\rho$  and the interplanar distance  $d$ . The transformations between the biclinic and the triclinic crystal systems arisen from a little axis-angle variations are exemplified with kaolinite, heulandite and anorthite. It is summarized from those transformations that the difference, in  $d$  spacing, less than  $0.05^\circ 2\theta$  in copper radiation will be no significance in distinguishing the biclinic from the triclinic system and *vice versa* [2]. It is worth noting that when use the regulations of the triclinic system to deal with these data of the biclinic system it is very easy to fall in a “no biclinic system” trap and layouts them into the triclinic system. Finally, the “missing” of the biclinic crystal system is because the P1 and P-1 space groups are classified into the triclinic system. One does not need to “refine” the data ( $a \neq b \neq c$ ,  $\alpha \neq \beta \neq \gamma$  and  $\alpha$  or  $\beta$  or  $\gamma = 90^\circ$ ) from the biclinic system to the triclinic system ( $\alpha \neq \beta \neq \gamma \neq 90^\circ$ ). These low grade crystal systems (bi- and triclinic) would make a plentiful crystal world.

### References

[1] Corlelis K, 2002, The manual of mineral science, 22th edition (New York, John wiley)

[2] Wang H, Zhou J, 2000, J. Appl. Crys. 33, 1128

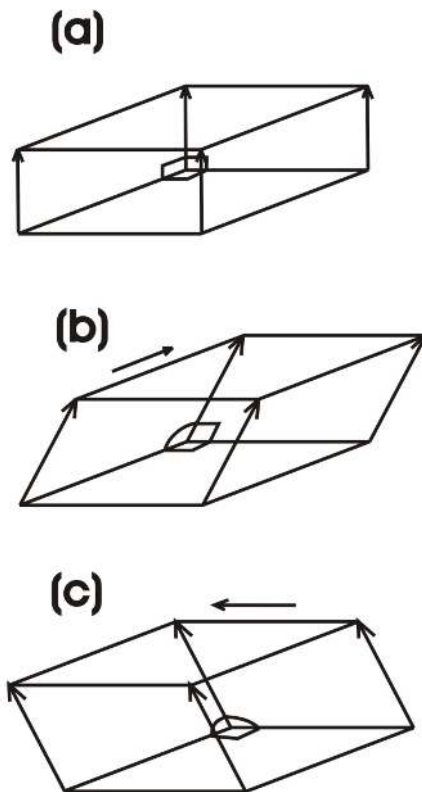


**Figure 1.** Formation of the biclinic parallelepiped. (a): orthorhombic parallelepiped, (b): monoclinic parallelepiped, (c): biclinic parallelepiped.

**Keywords:** crystal system, space group, formulae, kaolinite

**MS15-P23** *Crystal Structure of a New Coordination Polymer*Hamadene Malika<sup>1</sup>, Benhacine Mohamed El-Amin<sup>1</sup>, Bouacida Sofiane<sup>2</sup>, Merazig Hocine<sup>2</sup>

1. Laboratoire de Cristallographie-Thermodynamique, Faculté de Chimie, U.S.T.H.B, Alger, Algérie
2. Unité de Recherche de Chimie de l'Environnement et Moléculaire Structurale, Faculté des Sciences Exactes, Université des frères Mentouri, Constantine 1, 25000, Algérie

email: hamadene.m21@gmail.com

The oxalate dianion is one of the most studied ligands, capable of bridging two or more metal centres and creating inorganic polymers based on the assembly of metal polyhedra with a wide variety of one-, two - or three dimensional extended structures. Among the oxalate-based compounds M with the general formula  $AM(C_2O_4)_n \cdot n(H_2O)$  (A= alkali metal and, M= trivalent element), only a few crystal structures involving sodium metal have been reported in the literature with M=Yb [1]. As a continuation of work on mixed oxalate-based compounds with a tri- or bivalent element [2] a new coordination polymer, namely catena-poly[[diaquasodium(I)]- $\mu$ -oxalato- $k^4O_1O_2O_1'O_2'O_2'$ -[NaFe(C<sub>2</sub>O<sub>4</sub>)<sub>2</sub>(H<sub>2</sub>O)<sub>4</sub>]<sub>n</sub>], has been prepared and its crystal structure elucidated by single-crystal X-Ray diffraction analysis [3]. The compound crystallizes in the non centrosymmetrical space group  $I4_1$  ( $Z = 4$ ). The asymmetric unit contains one Na(I) atom and one Fe(III) atom lying on a fourfold symmetry axis, one oxalate ligand and two aqua ligands. Each metal atom is surrounded by two chelating oxalate ligands and two equivalent water molecules, in a *cis* arrangement. The structure consists of infinite one-dimensional chains of alternating FeO<sub>4</sub>(H<sub>2</sub>O)<sub>2</sub> and NaO<sub>4</sub>(H<sub>2</sub>O)<sub>2</sub> octahedra, bridged by oxalate ligands, parallel to the [100] and [010] directions, respectively (Fig. 1). Because of the *cis* configuration and the  $\mu_2$ -coordination mode of the oxalate ligands, the chains run in a zigzag manner. This arrangement facilitates the formation of hydrogen bonds between neighboring chains involving the H<sub>2</sub>O and oxalate ligands, leading to a two-dimensional framework. The resulting framework exhibits tunnels parallel to the c axis with an elliptic cross-section as shown in Fig. 1. The structure of this new one dimensional coordination polymer is shown to be unique among the A<sup>M</sup>M<sup>III</sup>(C<sub>2</sub>O<sub>4</sub>)<sub>2</sub>(H<sub>2</sub>O)<sub>n</sub> series. The thermal decomposition behavior has been studied by TG and DTA and gave as a final product the well-known ternary oxide NaFeO<sub>2</sub> [1] Chapélet-Arab B., Duviéubourg, L., Nowogrocki G., Abraham F., Grandjean S. (2006). *J. Solid State Chem.* **179**, 4029 [2] Kherfi H., Hamadène M., Guehria A., Dahaoui S. & Lecomte C. (2011). *Acta Cryst.* **C67**, m85 (2013). *Acta Cryst.* **E69**, m493 [3] Benhacine M.A., Hamadène M., Bouacida S., Mérazig H. (2016). *Acta Cryst.* **C72**, 243

**Keywords:** absolute structure, one-dimensional chains, new structural type

**MS15-P24** *Calcite (CaCO<sub>3</sub>) epitactic overgrowths on anhydrite (CaSO<sub>4</sub>) cleavage surfaces*Fernandez-Diaz Lurdes<sup>1,2</sup>, Iris Cuesta<sup>1,2</sup>, José Manuel Astilleros<sup>1,2</sup>, Manuel Prieto<sup>3</sup>

1. Department of Crystallography and Mineralogy, Complutense University of Madrid, Spain
2. Department of Geomaterials, Institute of Geosciences (UCM, CSIC), Spain.
3. Department of Geology, University of Oviedo, Spain

email: ishtar@ucm.es

The mineral replacement of calcium sulfate minerals by calcium carbonate (product phase is a common phenomenon in a wide range of Earth's surface and subsurface environments and often leads to the formation of pseudomorphs. The mineral replacement process is usually triggered by presence of carbonate-rich aqueous solutions in the system and involves the coupling of dissolution and crystallization reactions, according to reaction pathways that mainly depends on the specific calcium sulfate mineral and the concentration of carbonate in the aqueous solution. When the calcium sulfate mineral is anhydrite (CaSO<sub>4</sub>), the initial stages of mineral replacement reaction are characterized by the simultaneous formation of dissolution pits on anhydrite crystal surfaces and the oriented nucleation of calcite (CaCO<sub>3</sub>) crystals on these surfaces. The progress of the coupled dissolution-crystallization reactions eventually results in the formation of calcite pseudomorphs after anhydrite. In this work we investigate the crystallographic relationships observed during the development of these reactions between calcite crystals and the three main anhydrite cleavage surfaces, (100), (010) and (001). In all the investigated anhydrite cleavage surfaces, calcite crystals dispose one of their {104} faces in contact and parallel to the substrate. In the case of anhydrite (100) surface the better matching occurs with [001]<sub>Anh</sub>, [011]<sub>Anh</sub>  $\parallel$   $\langle 441 \rangle_{\text{Cal}}$ ,  $\langle 010 \rangle_{\text{Cal}}$ . As a consequence, most calcite crystals show this orientation. However, for a few calcite crystals the matching occurs so that [010]<sub>Anh</sub>, [011]<sub>Anh</sub>  $\parallel$   $\langle 441 \rangle_{\text{Cal}}$ ,  $\langle 010 \rangle_{\text{Cal}}$ . Although this second matching is characterized by a slightly higher misfit, this still is within the limits required for epitactic nucleation from solution. On anhydrite (010) surface, calcite crystals are oriented according to a similar pattern as observed on (100) surface. Most calcite crystals appear oriented so that [001]<sub>Anh</sub>, [011]<sub>Anh</sub>  $\parallel$   $\langle 441 \rangle_{\text{Cal}}$ ,  $2 \times \langle 010 \rangle_{\text{Cal}}$ . This orientation provides an excellent matching between the structures of both phases. However, also in this case a small number of calcite crystals are oriented with [100]<sub>Anh</sub>, [011]<sub>Anh</sub>  $\parallel$   $\langle 441 \rangle_{\text{Cal}}$ ,  $2 \times \langle 010 \rangle_{\text{Cal}}$ . Calcite crystals grown on anhydrite (001) also shown two main orientations, with [100]<sub>Anh</sub>, [110]<sub>Anh</sub>  $\parallel$   $\langle 441 \rangle_{\text{Cal}}$ ,  $\langle 010 \rangle_{\text{Cal}}$  and [100]<sub>Anh</sub>, [010]<sub>Anh</sub>  $\parallel$   $\langle 441 \rangle_{\text{Cal}}$ ,  $[48-1]_{\text{Cal}}$ .

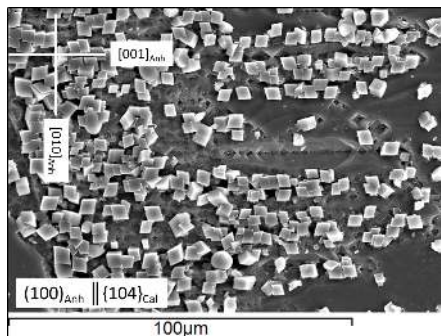


**Figure 1.** Calcite crystals growing on anhydrite (100) surface. Calcite crystals dispose one of their {104} faces in contact with the substrate. Most of calcite crystals are oriented with [001]<sub>Anh</sub> and [011]<sub>Anh</sub> parallel to  $\langle -441 \rangle_{\text{Cal}}$  and  $\langle 010 \rangle_{\text{Cal}}$ .

**Keywords:** Anhydrite, calcite, epitaxy, pseudomorph, mineral replacement

## MS16 Structure-property relationships in high pressure crystallography

Chairs: Andrzej Grzechnik, Paul Attfield

### MS16-P1 High-pressure studies of [4]helicene-TCNQ complex

Michał A. Dobrowolski<sup>1</sup>, Mateusz Piędzio<sup>1</sup>, Michał K. Cyrański<sup>1</sup>

<sup>1</sup> University of Warsaw

email: miked@chem.uw.edu.pl

[4]helicene is a chemical compound composed of four conjugated aromatic rings [see fig. 1]. The molecule is deviated from planarity. This feature is a result of steric interactions between C-H atoms six-membered aromatic rings. The interplanar angle between pairs of adjacent rings of [4]helicene molecule is 26.8°. This compound forms a charge-transfer complex with 7,7,8,8-tetracyanoquinodimethane (TCNQ), where [4]helicene is an electron pair donor and TCNQ is an acceptor. The molecules are arranged in stacks resulting in a sandwich-like columns. Forming a complex causes that the aforementioned angle is reduced to a value of 25.4°. In this report we present the synthesis and structural analyses of [4]helicene-TCNQ complex under different pressures. The complex was studied at atmospheric pressure, 0.44 GPa, 1.68 GPa and 2.1 GPa. Geometrical changes and intermolecular interactions of [4]helicene -TCNQ complex are analyzed under high-pressure.

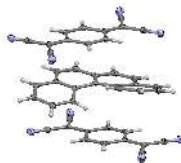


**Figure 1.** [4]helicene-TCNQ complex.

**Keywords:** [4]helicene, tetracyanoquinodimethane, high-pressure, X-ray diffraction, Raman spectroscopy

**MS16-P2** Stability of  $(\text{NH}_4)_2\text{V}_3\text{O}_8$  and  $\text{Cs}_2\text{V}_3\text{O}_8$  fresnoites at high pressures**Keywords:** mixed-valence vanadates, fresnoite structure, phase transition, high pressureAndrzej Grzechnik<sup>1</sup>, Hans-Conrad zur Loye<sup>2</sup>, Tie-Zhen Ren<sup>3</sup>,  
Karen Friese<sup>4</sup>

1. Institute of Crystallography, RWTH Aachen University

2. Department of Chemistry and Biochemistry, University of South Carolina, Columbia, United States

3. School of Chemical Engineering, Hebei University of Technology, Tianjin, China

4. Jülich Centre for Neutron Science, Forschungszentrum Jülich GmbH, Jülich, Germany

email: grzechnik@xtal.rwth-aachen.de

Vanadates  $\text{A}_2\text{V}_3\text{O}_8$  (A: K, Rb,  $\text{NH}_4^+$ , Cs) have the fresnoite structure ( $P4bm$ ,  $Z=2$ ) at atmospheric conditions [1-3]. They are built-up of layers of corner-sharing  $\text{V}^{5+}\text{O}_4$  tetrahedra and  $\text{V}^{4+}\text{O}_5$  tetragonal pyramids, separated by the  $\text{A}^+$  cations.  $\text{K}_2\text{V}_3\text{O}_8$  and  $\text{Rb}_2\text{V}_3\text{O}_8$  transform to incommensurate phases at low temperatures [4,5] due to rotations and displacements of rigid  $\text{V}^{5+}\text{O}_4$  and  $\text{V}^{4+}\text{O}_5$  polyhedra.

We have studied pressure-induced structural instabilities of  $(\text{NH}_4)_2\text{V}_3\text{O}_8$  and  $\text{Cs}_2\text{V}_3\text{O}_8$  using single-crystal x-ray diffraction in diamond anvil cells.  $(\text{NH}_4)_2\text{V}_3\text{O}_8$  undergoes a reversible phase transition at 3 GPa to a three-dimensional structure ( $P4/mbm$ ,  $Z=2$ ), formed by corner-sharing  $\text{V}^{5+}\text{O}_5$  trigonal bipyramids and  $\text{V}^{4+}\text{O}_6$  octahedra [1]. The chains of these corner-connected polyhedra form a framework with tunnels along the  $c$  direction. Vanadate framework structures formed of more than one type of coordination polyhedra are frequent at ambient conditions, their common structural feature being the presence of both corner- and edge-shared polyhedra. The framework of the high-pressure polymorph of  $(\text{NH}_4)_2\text{V}_3\text{O}_8$  is unique since all the polyhedra are exclusively connected via common corners.

$\text{Cs}_2\text{V}_3\text{O}_8$  undergoes a reversible phase transition at 4 GPa [3]. Up to the phase transition, the compression has little effect on the polarity of the structure. Above 4 GPa, the structure is still polar but the pseudo-symmetry with respect to the corresponding space group  $P4/mbm$  abruptly increases. Both structures consist of layers of corner-sharing  $\text{V}^{5+}\text{O}_4$  tetrahedra and  $\text{V}^{4+}\text{O}_5$  tetragonal pyramids, separated by the  $\text{Cs}^+$  cations. The unit-cell volumes, at which the phase transitions in  $(\text{NH}_4)_2\text{V}_3\text{O}_8$  and  $\text{Cs}_2\text{V}_3\text{O}_8$  occur, coincide with the unit-cell volume of  $\text{K}_2\text{V}_3\text{O}_8$  at atmospheric pressure.

The unit-cell volumes are reduced by 22% and 20% in  $(\text{NH}_4)_2\text{V}_3\text{O}_8$  and  $\text{Cs}_2\text{V}_3\text{O}_8$  upon compression to approximately 7.0 GPa and 8.6 GPa, respectively. The fact why modulated structures, like those in  $\text{K}_2\text{V}_3\text{O}_8$  and  $\text{Rb}_2\text{V}_3\text{O}_8$  at low temperatures [4,5], are not observed in the fresnoites with larger  $\text{NH}_4^+$  and  $\text{Cs}^+$  cations upon compression is explained by the suppression of rotations and displacements of the polyhedra around the  $\text{V}^{4+}$  and  $\text{V}^{5+}$  cations.

[1] A. Grzechnik et al., *Dalton Trans.*, 2011, **40**, 4572.[2] J. Yeon et al., *Inorg. Chem.*, 2013, **52**, 6179.[3] A. Grzechnik et al., *J. Solid State Chem.*, 2016, **238**, 252.[4] B.C. Chakoumakos et al., *J. Solid State Chem.*, 2007, **180**, 812.[5] R.L. Withers et al., *J. Solid State Chem.*, 2004, **177**, 3316.



### MS16-P3 High pressure synthesis of iron complex oxides in high oxidation state ( $\text{Fe}^{4+}$ , $\text{Fe}^{5+}$ ): mapping between localized and itinerant behavior

Fei Li<sup>1,2</sup>, Dariusz Jakub Gawryluk<sup>1</sup>, Ekaterina Pomjakushina<sup>1</sup>, Kazimierz Conder<sup>1</sup>

1. Laboratory for Scientific Developments and Novel Materials, Paul Scherrer Institute, CH-5232 Villigen PSI, Switzerland  
2. Laboratory for Multifunctional Ferroic Materials, Department of Materials, ETH, Vladimir-Prelog-Weg 4, CH-8093 Zurich, Switzerland

email: Fei.Li@psi.ch

In 1993 colossal magnetoresistance (CMR) was found in  $\text{La}_{1-x}\text{Ba}_x\text{MnO}_3$  at the Curie point where electrical resistance changes by orders of magnitude when a magnetic field is applied. Up to now, most of the known CMR materials are manganese based perovskites – mostly  $\text{La}_{1-x}\text{Sr}_x\text{MnO}_3$  or  $\text{SmBaMn}_2\text{O}_6$  [1]. Analysis of the potential map that was proposed by Kamata et al. [2] suggests that CMR could also be obtained in  $\text{A}_2\text{B}_2\text{FeO}_3$  (where  $\text{A}=\text{Na}, \text{K}, \text{Rb}$  and  $\text{B}=\text{Ca}, \text{Sr}, \text{Ba}$ ) perovskites. These proposed iron based compounds should display similar electrical transport properties to the manganese perovskites being in vicinity to metal-insulator border line in the potential map. Additionally, both families should be isoelectronic:  $\text{Fe}^{4+}$  and  $\text{Fe}^{5+}$  have the same electron configuration as  $\text{Mn}^{3+}$  and  $\text{Mn}^{4+}$  in  $\text{La}_x\text{Sr}_{1-x}\text{MnO}_3$ . To stabilize these unusually high oxidation states, and to achieve oxygen stoichiometry,  $\text{Sr}_{1-x}\text{A}_x\text{FeO}_3$  ( $\text{A}=\text{Na}, \text{K}$ ) have been synthesized by using a unique oxygen high pressure (HP) system recently relocated and already successfully used in our lab [3]. This HP system allows precise control of temperatures (up to 1200 °C), gas pressures (up to 2000 bars) and large production of materials ( $\text{cm}^3$ ). The synthesized materials are phase pure and have structure similar to the parent compound (space group  $Pm\bar{3}m$ ). Measurements of the magnetic susceptibilities and electric properties for these materials are currently underway. Determination of the magnetic structure of the materials by neutron powder diffraction has also been scheduled.

#### References

- [1] R. von Helmolt, J. Wecker, B. Holzapfel, L. Schultz and K. Samwer, *Phys. Rev. Lett.*, **71** (1993) 2331; H. Sakurai, T. Kolodiazny, Y. Michiue, E. Takayama-Muromachi, Y. Tanabe, H. Kikuchi, *Angew. Chem. Int. Ed.*, **51** (2012) 6653
- [2] K. Kamata et al., *Bulletin of the Tokyo Inst. of Techn.*, **120** (1974) 73
- [3] Ekaterina Pomjakushina, Vladimir Pomjakushin, Katharina Rols, Janusz Karpinski, and Kazimierz Conder, *Inorg. Chem.*, 2015, 54 (18), pp 9092–9097

**Keywords:** High pressure synthesis, CMR

### MS16-P4 Symmetry reduction in anti-perovskites at high pressure

Morten B. Nielsen<sup>1</sup>, Martin Bremholm<sup>1</sup>

1. Aarhus University

email: mbnielsen@chem.au.dk

Anti-perovskites of  $\text{AXB}_3$  stoichiometry with  $\text{A}$  = early period cation,  $\text{X}$  = group 13-15 anion and  $\text{B}$  = transition metal have in recent years been found to host as many interesting physical and structural properties as the vast perovskite family. While the anti-perovskites are much less common than their normal counterparts, they display superconductivity in the presence of ferromagnetic ions[1], topologically insulating states[2] and heavy fermion superconductivity[3]. Few high pressure structural studies on anti-perovskites exist, and it is worth investigating whether this class of materials follows the same structural trends at high pressure as the oxide perovskites.

A famous anti-perovskite is  $\text{CeSiPt}_3$ , a heavy fermion superconductor that crystallises in the non-centrosymmetric  $P4mm$  space group. Its properties have been investigated under pressure to a few GPa, but no structural studies on this or related compounds have been reported. In this study, we investigated the structure of  $\text{CeSiPt}_3$  and the newly synthesized isostructural  $\text{YBPt}_3$  to high pressures. Surprisingly, we observed a second-order structural phase transition in  $\text{YBPt}_3$  at 24 GPa that lowered the symmetry even further. It is interesting that pressure drives further structural distortion in this anti-perovskite system, since the oxide perovskite  $\text{PbVO}_3$  (which also displays the  $P4mm$  structure with similar  $c/a$  ratio at ambient pressure) undergoes a first-order transition at ~3 GPa with a large volume collapse (10.6%) to the ideal cubic  $Pm\bar{3}m$  perovskite structure[4].  $\text{CeSiPt}_3$  on the other hand does not undergo any changes in structure up to 45 GPa. We will present our structural results and rationalise the difference between the two otherwise chemically similar compounds through DFT calculations.

#### References:

- [1] T. He et al. *Nature*, 411, 54, 2001; [2] M. Klintonberg et al. *Appl. Phys. Res.* 6(4), 31, 2014 [3] E. Bauer et al. *Phys. Rev. Lett.* 92, 027003, 2004; [4] W. Zhou et al. *J. Phys. Cond. Matt.* 24, 435403, 2012;

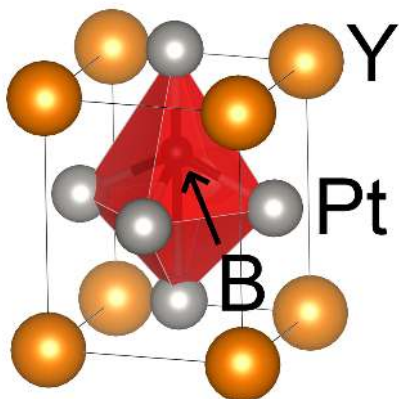


**Figure 1.** The non-centrosymmetric  $P4mm$  structure of  $YBPt_3$

**Keywords:** Anti-perovskite, phase transition, symmetry reduction, intermetallic

## MS17 Minerals, materials and polymorphs

Chairs: Håkon Hope, Elisa Nauha

### MS17-P1 Re-determination of four $CsCoPO_4$ crystal structures from single-crystal X-ray diffraction data

Maria Orlova<sup>1</sup>, Hannes Krüger<sup>1</sup>, Volker Kahlenberg<sup>1</sup>, Dmitry Michailov<sup>2</sup>, Albina Orlova<sup>2</sup>

1. Institute of Mineralogy and Petrography, University of Innsbruck, Austria

2. Department of Chemistry, State University of Nizhny Novgorod, Russia

email: maria.p.orlova@gmail.com

The crystal structures of the four known  $CsCoPO_4$  polymorphs have been reported by P. Henry [1] and H. Kawaji [2]. The structures were determined using synchrotron (phase 1-4) and neutron powder diffraction (phase 3) methods. Although the reported structures are correct and are in good agreement with known structural analogues, for example,  $CsZnPO_4$ , isotropic displacement parameters of some atoms seem to be questionable. For example,  $B_{11}$  of P1 of the phase 4 exhibits very low value of  $0.3(1) \text{ \AA}^2$ . In order to understand the nature of low displacement parameters and to obtain more precise structural information for  $CsCoPO_4$  polymorphs, a single crystal diffraction study has been performed. The compound undergoes three phase transitions at following temperatures: 280, 210, 30°C. It adopts two orthorhombic phases crystallizing in space group  $Pnma$  (phase 1) and  $Pn2_1a$  (phase 2), and two monoclinic phases, space group  $P12_1/a1$  (phase 3) and  $P12_11$  (phase 4). New structural data of all four polymorphs with anisotropically refined displacement parameters will be presented and compared with known powder diffraction data. **KEYWORDS** Phosphates, Polymorphism, Crystal structure, Structure solution, Single-crystal diffraction

[1] P. Henry, E. Hughes, M. T. Weller, J. Chem. Soc., Dalton Trans., 2000, 555-558

[2] H. Kawaji, Y. Ishihara, A. Nidaira, et al., J. Therm Analys. 92 2008, 451-455

The financial support of the Russian Science Foundation (Project No 16-13-10464) is gratefully acknowledged.

**Keywords:** Phosphates, Polymorphism, Crystal structure, Structure solution, Single-crystal diffraction

**MS17-P2 2D and 3D Titanium Phosphate Materials: Crystal Structure and Properties**

Santiago García-Granda<sup>1</sup>, Jorge García-Glez<sup>2</sup>, Camino Trobajo Camino Trobajo<sup>2</sup>, Zakariae Amghouz<sup>3</sup>, Sergei A. Khainakov<sup>3</sup>, Conchi O. Ania<sup>4</sup>, José B. Parra<sup>4</sup>, Artem A. Babaryk<sup>5</sup>, Iván da Silva<sup>6</sup>, Germán R. Castro<sup>7</sup>

1. Department of Physical and Analytical Chemistry, University of Oviedo-CINN, 33006 Oviedo, Spain
2. Department of Organic and Inorganic Chemistry, University of Oviedo-CINN, 33006 Oviedo, Spain
3. Scientific and Technical Services, University of Oviedo, 33006 Oviedo, Spain
4. INCAR-CSIC, 33080 Oviedo, Spain
5. Faculty of Chemistry, Taras Shevchenko National University of Kyiv, 01601 Kyiv, Ukraine
6. ISIS Facility, Rutherford Appleton Laboratory, Chilton, Oxfordshire OX11 0QX, UK
7. SpLine, Spanish CRG Beamline, ESRF, BP 220, 38043 Grenoble, France

email: sgg@uniovi.es

In 1990 Christensen *et al.* proposed the structure of titanium compound,  $\text{Ti}(\text{PO}_4)(\text{H}_2\text{PO}_4)\cdot 2\text{H}_2\text{O}$ , according with Clayden, but later the combined <sup>55</sup>SS-NMR and powder synchrotron X-ray diffraction data showed a different cell [1]. In 1995, the  $\gamma$ -ZrP was solved by Poojary *et al.*, confirming the model reported by Christensen. Later, the  $\beta$ -TiP showed that the structure of the  $\gamma$ -type layer is retained in the anhydrous compound. Layered titanium phosphate compounds intercalated with amines may be used as precursors in pillaring reactions [2]. Despite the many potential applications of these materials, including the synthesis of organic-inorganic nanotubes [3], their detailed structural features have remained poorly understood. In the last decade, we have combined chemical information, NMR spectroscopy and powder XRD data, and chemical modeling studies to describe the alkylamine templated  $\gamma$ -titanium phosphates, including the  $(\text{C}_2\text{H}_5\text{NH}_2)[\text{Ti}(\text{H}_{1.5}\text{PO}_4)(\text{PO}_4)]\cdot \text{H}_2\text{O}$  pseudotridimensional porous structure (fibrous morphology) that shows an unusual and very strong interlayer-hydrogen bond [4].

Layered  $\alpha$ - $\text{Ti}(\text{HPO}_4)_2\cdot \text{H}_2\text{O}$  ( $\alpha$ -TiP) and its propylamine intercalation product,  $\alpha$ - $\text{Ti}(\text{HPO}_4)_2\cdot 2\text{C}_3\text{H}_7\text{NH}_2\cdot \text{H}_2\text{O}$ , have been synthesized and characterized, their sorption capacity for europium(III) was investigated, and structure of  $\alpha$ - $[\text{Eu}(\text{H}_2\text{O})_9]_2\text{Ti}(\text{PO}_4)_2\cdot [(\text{H}_2\text{O})_6]_{1/3}$  has been proposed by DFT calculations. Tri-dimensional  $\text{Ti}_2\text{O}(\text{PO}_4)_3\cdot 2\text{H}_2\text{O}$  polymorphs ( $\rho$ -TiP and  $\pi$ -TiP) were prepared hydrothermally. The crystal structure of  $\Pi$ -phase was solved *ab initio* from synchrotron data, and the thermal transformation of  $\rho$ - $\text{Ti}_2\text{O}(\text{PO}_4)_3\cdot 2\text{H}_2\text{O}$  to  $\rho$ - $\text{Ti}_2\text{O}(\text{PO}_4)_3$  was monitored by HT-PXRD. The coordination environment of the hydrated titanium changes from octahedral to distorted tetrahedral, which explains the measurable thermally activated nitrogen-adsorption observed for the anhydrous phase. To our knowledge, the process described here constitutes the first example of nitrogen-fixation by an inorganic material far above room temperature.

**Acknowledgments.** Financial support from Spanish MINECO (MAT2013-40950-R), FICYT (GRUPIN14-060), and ERDF funding are acknowledged.

**References** [1] S. García-Granda, *et al.*, Inorganic Chemistry 49 (2010) 2630-2638; [2] L. Mafra, *et al.*, Chemistry of Materials 17 (2005) 6287-6294.; [3] J.A.

Blanco, *et al.*, Physica Status Solidi C 6 (2009) 2190-2194; [4] L. Mafra, *et al.*, Chemistry of Materials 20 (2008) 3944-3953.

**Keywords:** Titanium, phosphate, crystallography

## MS18 Structures of minerals, planetary and carbon materials at Earth and planetary conditions

[1] Chiavassa et al 2005 Astron. & Astroph. 432,547; Posch Th et al 2007 Astroph. J. 668, 993 [2] Ferrarotti and Gail 2005 Astron. & Astrophys. 430, 959 [3] Thompson et al. 2012 Journal of Non-Crystalline Solids 358 (5), 885 [4] Demyk, et al. A&A, 2000,364,170; B.T. Draine. 2003 Annu. Rev. Astron. Astroph., 41,1

**Keywords:** amorphous silicates, carbonates, powder diffraction, PDF

Chairs: Tiziana Boffa-Ballaran, Marco Merlini

### MS18-P1 Solid-gas carbonation of amorphous silicates: the origin of cosmic carbonates?

Sarah J. Day<sup>1,2</sup>, Stephen P. Thompson<sup>1</sup>, Aneurin Evans<sup>2</sup>

1. Diamond Light Source

2. Keele University

email: sjday15@googlemail.com

Silicates are the most abundant component of cosmic dust present in the universe, forming in the atmospheres of dying stars as primitive, structurally disordered grains. Throughout their lifetime dust grains are subjected to a number of physical processes leading to their evolution from highly disordered, refractory grains to the more complex crystalline mineral species that were present within the solar nebula. Of particular interest is the formation of crystalline Ca-rich carbonate minerals that have been identified in the spectra of evolved stars, protoplanetary disks and planetary nebulae [1]. Due to the absence of liquid water in these environments and that direct condensation of carbonates is unlikely, due their low condensation temperature [2] it is believed that carbonate species in such environments could form through solid-phase alteration of amorphous Ca-bearing silicates with gaseous CO<sub>2</sub>.

Amorphous cosmic silicate analogues are produced using a well-developed sol gel technique [3] in which the gels are dried under high-vacuum (~10<sup>-6</sup> mbar) to produce highly disordered, fine-grained powders of composition Mg<sub>1-x</sub>Ca<sub>x</sub>SiO<sub>3</sub>, where 0 ≤ x ≤ 1, analogous to the primitive silicates present within circumstellar and interstellar mediums [4]. Beamlines I11 and I12 at Diamond Light Source have been used to conduct synchrotron X-ray powder diffraction (SXPd) and Pair Distribution Function (PDF) measurements respectively, both in-situ and ex-situ. These measurements together provide an insight into the underlying structural mechanics that govern the carbonation reaction at the amorphous level as well as allowing a detailed study of the reaction kinetics and phase evolution.

The results of this research will be presented, focusing on the structural mechanisms involved with the carbonation of silicates in order to place constraints on the environmental conditions and initial silicate compositions favourable for carbonate formation.

#### References

## MS18-P2 Single Crystal High Pressure Diffraction at the Advanced Light Source

Christine M. Beavers<sup>1,2</sup>, Earl F. O'Bannon<sup>2</sup>, Andrew Doran<sup>1</sup>,  
Martin Kunz<sup>1</sup>, Quentin Williams<sup>2</sup>

1. Advanced Light Source, Lawrence Berkeley National Laboratory, Berkeley, CA USA

2. Department of Earth & Planetary Sciences, University of California Santa Cruz, Santa Cruz, CA USA

email: cmbeavers@lbl.gov

Beamline 12.2.2 at the Advanced Light Source, which was previously optimized for high pressure powder diffraction only, has undergone the substantial addition of a dedicated single crystal diffractometer. Positioned upstream of the existing endstation, the new endstation consists of a Stoe Stadi Vari diffractometer equipped with a RDI CMOS detector. The system was configured with high pressure diffraction in mind: a small sphere of confusion (10  $\mu$ m), a sample weight capacity compatible with DACs (1kg), and a detector phosphor optimized for 25keV. System details and commissioning experiment results will be shared.

**Keywords:** high pressure, single crystal

## MS18-P3 Deformation of single-crystals of water ice VI

Tiziana Boffa-Ballaran<sup>1</sup>, Anna S. Pakhomova<sup>1</sup>, Alexander Kurnosov<sup>1</sup>

1. Bayerisches Geoinstitut, Universitaet Bayreuth, Germany

email: Tiziana.Boffa-Ballaran@uni-bayreuth.de

Water ices form significant portion of the satellites which orbit the giant planets of our solar system. The formation, early evolution and internal structure of these icy satellites is of particular importance to planetary sciences as they include the only objects in the solar system, other than Earth, to show evidence of recent tectonic activity and volcanism. The aim of our study is to constrain the deformation mechanism of ice VI, an high-pressure polymorph of ice likely present in the deep interior of the large icy satellites, using high-pressure single-crystal X-ray diffraction. Two crystals of ice VI have been grown *in situ* inside a four-screw diamond anvil cell at room temperature from liquid water. The single-crystal X-ray diffraction experiments were performed at 1.2-1.4 GPa and room temperature. Because the two crystals refill the entire sample chamber, they are experiencing a uniaxial stress. As a consequence, broadening of different sets of reflections is observed with time and the evolution of such broadening has been monitored by measuring the profile of selected reflections using an Huber 4-circle diffractometer. After c.a. 20 hours, the appearance of an additional peak in the omega profiles of several reflections of one of the crystals was observed. The difference in the positions of the two peaks in the omega profiles,  $\Delta\omega$ , increases with time. The larger  $\Delta\omega$  was observed for planes oriented perpendicular to the (0 2 1) plane which instead remains sharp. Planes with smaller interplanar angles to the (0 2 1) have smaller  $\Delta\omega$  value. A further increase in pressure to 1.3 GPa also led to significant broadening of the reflections of the second crystal. These results suggest that the uniaxial compression leads to bending of the two crystals and consequent formation of randomly distributed dislocations resulting in broadening of the initial  $\omega$ -profiles. The energy associated with the elastic bending of the crystal lattice is reduced by rearranging the dislocations into a vertical wall to form low angle boundaries. The slip system, deformation mechanism and microstructural evolution of ice VI single crystal will be discussed.

**Keywords:** icy satellite, ice VI, high-pressure single-crystal diffraction

## MS19 Solid state oxygen fuel cell, hydrogen storage & battery materials

relation between the anionic redox process and the evolution of the O-O bonding in layered oxides.

**Keywords:** Li-ion battery, cathode, crystal structure, transmission electron microscopy

Chairs: Bernhard Frick, Kristina Edstroem

### MS19-P1 Advanced transmission electron microscopy for Li-ion battery cathodes

Artem Abakumov<sup>1</sup>

<sup>1</sup> Skolkovo Institute of Science and Technology

email: a.abakumov@skoltech.ru

Advanced transmission electron microscopy (TEM) is by far the most suitable and direct tool to view materials down to atomic scale. Recent progress in the electron diffraction methods, related to implication of electron diffraction tomography, and in the aberration-corrected scanning TEM imaging will be illustrated here with the examples of atomic structure investigation on cathode materials for Li-ion batteries. Precession electron diffraction and electron diffraction tomography provide quantitative diffraction data with substantially suppressed dynamical effects, enabling reliable structure solution and refinement. The electron diffraction experiments require very small quantity of material, typically less than  $1\text{ }\mu\text{m}^3$ , making this method applicable to virtually all samples extracted from electrochemical cells. Electron diffraction patterns can be taken at a very low electron dose, enabling investigation of the materials sensitive to the electron beam damage, such as polyanion Li-ion battery cathodes, particularly in their charged state. The capabilities of quantitative electron diffraction will be demonstrated using the  $\text{Li}_2\text{CoPO}_4\text{F}$ ,  $\text{Li}_2\text{FePO}_4\text{F}$  and  $\text{LiMn}_{0.5}\text{Fe}_{0.5}\text{PO}_4$  cathode materials. Aberration-corrected scanning  $0.5\text{ }\text{\AA}$  TEM (STEM) techniques deliver the information on the local structural state with sub-angstrom resolution. High angle annular dark field STEM (HAADF-STEM) imaging provides clear visualization of the cation positions, whereas annular bright field STEM (ABF-STEM) shows the location of the “light” elements, such as O and Li. HAADF-STEM method has been applied to investigate the capacity and voltage fading in the layered rock-salt type oxides, which are determined to large degree by the cumulative local structure changes upon continuous electrochemical cycling. A comparative HAADF-STEM study of the layered oxides in the Li-Ru-Ti-O and Li-Ru-Sn-O systems at different stages (pristine, fully charged, discharged and cycled over different number of times) allowed establishing the cation migration pathways and identifying the cation traps responsible for the degradation of the electrochemical performance. ABF-STEM visualizes changes in the oxygen sublattice upon Li extraction and provides direct observation of O-O peroxo dimers in  $\text{Li}_{1-x}\text{Fe}_{0.5}\text{Ir}_{0.5}\text{O}_3$  and O vacancy formation in  $\text{Li}_x\text{Fe}_{0.56}\text{TeO}_6$  helping us to establish the fundamental

**MS19-P2 Heterometallic single precursor of oxides for Na-ion battery cathode materials**Benoît Baichette<sup>1</sup>, Katharina M. Fromm<sup>1</sup><sup>1</sup>. University of Fribourg

email: benoit.baichette@unifr.ch

After decades of improvements of and investments in the Li-ion battery technology, attention has been shifted toward Na-ion battery, mainly because of sodium's low cost. A lot of different materials are investigated as potential cathode for Na-ion batteries, especially the layered oxides of transition metals,  $\text{NaT}_M\text{O}_2$  (with  $T_M = \text{Ti, V, Cr, Mn, Fe, Co, Ni, ...}$ ), which are traditionally synthesized via solid state techniques.

These solid state techniques involve high energy ball-milling of several precursors (usually sodium carbonate and transition metal oxide) followed by calcination at high temperature (800-1000°C) for long reaction times, (8-12 hours) [2]. This long and energy consuming process was required in order to obtain a homogeneous mixing of the precursors. Recently, it was reported that synthesizing heterometallic single precursor can reduce the duration and the calcination temperature due to the pre-organized precursor design [3]. The high temperature phase of lithium cobalt oxide (HT- $\text{LiCoO}_2$ ) was obtained using heterometallic Li-Co alkoxides/aryloxide complexes as precursors [3] at as low temperatures as 350-450°C instead of 600-900°C required for the solid state synthesis [4].

The crystal structure of  $\text{Na}_x\text{CoO}_2$  ( $x < 1$ ) has octahedral  $\text{CoO}_2$  layers and prismatic coordinated sodium ions (Figure 1)[1]. The content of sodium influences the crystal structure and the lattice parameters of the unit cell. In the end, the amount of sodium in the structure also determines the specific capacity of sodium ion batteries.

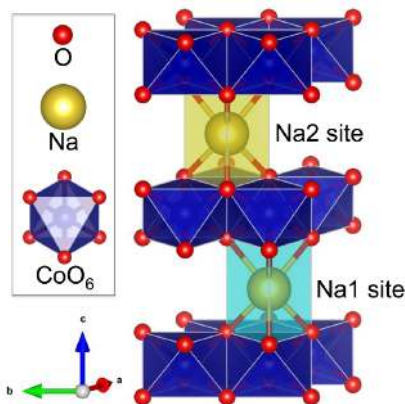
We synthesized the  $\text{Na}_x\text{CoO}_2$  starting from heterometallic complexes of sodium and cobalt. The method of heterometallic complexes is also applied to other transition metals: nickel, iron and manganese. The obtained oxides will be characterized and tested as sodium ion battery cathode materials. We will present our first efforts, results of syntheses and characterizations.

[1] Mo, Y., S.P. Ong, and G. Ceder, *Insights into Diffusion Mechanisms in P2 Layered Oxide Materials by First-Principles Calculations*. Chemistry of Materials, 2014. **26**: p. 5208-5214

[2] Takada, K., H. Sakurai, and E. Takayama-muromachi, *Superconductivity in two-dimensional  $\text{CoO}_2$  layers*. Nature, 2003. **422**: p. 53-55

[3] Brog, J.-P., A. Crochet, and K. M. Fromm, *Lithium metal aryloxide clusters as starting products for oxide materials*. 2012

[4] Shao-Horn, Y., et al., *Atomic resolution of lithium ions in  $\text{LiCoO}_2$* . Nature materials, 2003. **2**: p. 464-7

Figure 1. Crystal structure of  $\text{NaCoO}_2$  [1]**Keywords:** Na-ion battery



## MS19-P3 Molecular and Crystal Structures of Aminoalanes and Aminoboranes

Thomas Bernert<sup>1</sup>, Morten B. Ley<sup>1</sup>, Alexander Bodach<sup>2</sup>, Javier Ruiz-Fuertes<sup>3</sup>, Michael Fischer<sup>4,5</sup>, Michael Felderhoff<sup>1</sup>, Claudia Weidenhaller<sup>1</sup>

1. Max-Planck-Institut fuer Kohlenforschung, Kaiser-Wilhelm-Platz 1, D-45470 Muelheim an der Ruhr, Germany
2. Goethe-Universitaet Frankfurt am Main, Institut fuer Anorganische und Analytische Chemie, Max-von-Laue StraÙe 7, D-60438 Frankfurt am Main, Germany
3. Departament de Física Aplicada – ICMUV, Universitat de València, Dr. Moliner 50, E- 46100 Burjassot, Spain
4. Fachgebiet Kristallographie, Fachbereich Geowissenschaften, University of Bremen, Klagenfurter StraÙe, D-28359 Bremen, Germany
5. MAPEX Center for Materials and Processes, University of Bremen, Germany

email: bernert@mpi-muelheim.mpg.de

Compounds, bearing  $H^{\delta+}$  and  $H^{\delta-}$  species, are promising candidates for reversible hydrogen storage materials. This strategy has already been discussed, e.g. by Stephan and Erker [1] for Lewis-acid/base adducts, which show a reversible hydrogenation. Lewis-acid/base adducts of nitrogen and aluminium or boron could be economically and environmentally beneficial candidates for hydrogen storage, e.g. in  $NH_3BH_3$  [2, 3]. Within the group 13 elements, Lewis-acid/base adducts with different substituents often form molecular structures build up by dimers or trimers [Figure 1 (a)]. Since, the reactivity of these compounds towards small molecules like  $H_2$  [4] or  $CO$ , [5] strongly depend on the bond lengths between the corresponding Lewis acid and the base, a knowledge of their molecular structures is crucial for their applications.

Recently, we determined the crystal structure of diethylaminoalane by a combination of powder X-ray diffraction, Raman spectroscopy and DFT calculations [6]. This approach has led to a reliable molecular structure determination of diethylaminoalane in the solid state and to obtain further information about the environment and behavior of the Al-H bonds. This combination of techniques was also applied to characterise a phase transition of dimethylaminoalane [Figure 1 (b)] from a monoclinic to a plastic crystalline phase, where the molecules are found to be strongly disordered and arranged accordingly to the cubic  $a15$  phase, often adopted by liquid crystals. The analogous boron compound, dimethylaminoborane, is an example for a substance which can exist as dimer or as a trimer. For dimeric dimethylaminoborane, we were able to determine its monoclinic crystal structure and the second order phase transition to a triclinic phase by single crystal X-ray diffraction and in-situ X-ray powder diffraction. Our measurements confirm the cell parameters from [7], and led to the atomic positions.

### References:

- [1] D. W. Stephan, G. Erker (2010), *Angew. Chem., Int. Ed.*, 49, 46 - 76.
- [2] A. Staubitz *et al.* (2010), *Chem. Rev.*, 110, 4079 - 4124.
- [3] P. P. Power (2010), *Nature*, 463, 171 - 177.
- [4] Z. Xiong *et al.* (2008), *Nat. Mater.*, 7, 138 - 141.
- [5] J. A. B. Abdalla *et al.* (2015), *Angew. Chem., Int. Ed.*, 54, 5098 - 5102.

[6] T. Bernert *et al.* (2016), *Acta Crystallogr. B.*, 72, 232 - 240.

[7] P. J. Schapiro (1962), PhD Thesis, Refcode CSD: DMABDI.

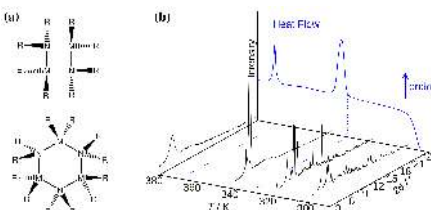


**Figure 1.** (a) Typical molecular structures of amino adducts of group 13 elements (M) with R = H or alkyl moieties. (b) *In-situ* diffractograms during heating of dimethylaminoalane together with DSC data.

**Keywords:** Solid-State Hydrogen Storage, Phase Transitions, Molecular Crystals, Aminoalanes, Aminoboranes

**MS19-P4** Structural design principles for close packed Na and Li solid-electrolytes built from mixed anion borane latticesMatteo Brighi<sup>1</sup>, Pascal Schouwink<sup>1</sup>, Yolanda Sadikin<sup>1</sup>, Radovan Cerny<sup>1</sup>

1. Laboratory of Crystallography, DQMP, University of Geneva, 24 Quai Ernest-Ansermet, CH-1211 Genève

email: matteo.brighi@unige.ch

Energy storage solutions on a large scale have long been identified as a primary target within renewable energy research. While various complex hydrides, such as the salts built from the  $[\text{BH}_4]^-$  anion, have shown high  $\text{Li}^+$  ionic conductivity, the compound family of the metal boranes are more promising contenders when it comes to Na-superionics and all-solid battery concepts. Very recently, the complex anion landscape of complex hydrides has been extended to include the carborane (CB)  $[\text{CB}_n\text{H}_{2n}]^-$ . When used to template close-packed ionic conductors, they show the highest reported  $\text{Li}^+$  and  $\text{Na}^+$  ionic conductivities of all reported complex hydrides<sup>1</sup> and are amongst the highest for Na solid electrolytes in general. Due to their quasi-spherical shape, this molecule easily forms the cubic close packed structure (ccp), an hard backbone to tailor vacancy concentration achieving high ionic mobility<sup>2</sup>, which is boosted additionally by well-known “paddle wheel effect”<sup>3</sup>. We present different approaches to design in particular Na-conducting solid electrolytes with ever lower operating temperatures. On the one hand, it is conceptually straightforward to rebuild benchmark conductors from the literature. In this sense, the ionic conductor  $\text{RbAg}_4\text{I}_5$  was taken as a template to reproduce its CB analogues, resulting in double cation phases containing alkali metals, and with an ideal composition of  $\text{CsA}_4(\text{CB}_n\text{H}_{2n})_5$  ( $\text{A} = \text{Li}^+, \text{Na}^+$ ) in the specific case of the parent phase  $\text{RbAg}_4\text{I}_5$ . The ionic mobility of the resulting new phases will be presented and related to the crystal structure. On the other hand, we show how the close packing of the anion lattice may be controlled by anion-mixing of CB  $[\text{CB}_{11}\text{H}_{12}]^-$  and dodeca-boranes  $[\text{B}_{12}\text{H}_{12}]^{2-}$ , both their Na-endmembers known to have superionic *ht*-phases. Making use of the knowledge of preferred coordination polyhedra in higher boranes, this approach allows us to control the occupancy of tetrahedral (T) and octahedral (O) vacancies by modifying the carborane – dodeca-borane ratio, made possible due to the different charges of the polyanions. A control of site occupancies in packed lattices is known to be the key point to achieve high ionic conductivities at a suitable temperature and therefore highly promising approach to tailor metal boranes for battery application.

**References:** 1. Tang et al *Energy. Environ. Sci.*, 2015, 8, 3637 2. Wang et al *Nat. Mat.* 2015, 14, 1026 3. Jansen *Angew. Chem. Int. Ed.* 1991, 30, 1547

**Keywords:** ionic conductor, solid electrolyte, Li battery, Na battery, closo-boranes, carboranes

**MS19-P5** X-ray Scattering Analysis of the Morphology of  $\text{TiO}_2$  (B) NanoparticlesXiao Hua<sup>1,2</sup>, Zheng Liu<sup>3</sup>, Peter G. Bruce<sup>4</sup>, Clare P. Grey<sup>1</sup>

1. University of Cambridge

2. Adolphe Merkle Institute

3. University of St. Andrews

4. University of Oxford

email: xiaohua716@gmail.com

The morphological characteristics of a nanomaterial, *i.e.*, geometric shape and dimension, and the arrangement of atoms, which both vary depending on specific nanostructures, have a considerable impact on properties such as electronic structure, ionic diffusion, and surface structure. It is, therefore, essential to determine the nanomorphology of the electrode materials so as to link shape with the electrochemical performance.

Conventional microscopy methods used to characterize the morphology of nanomaterials sometimes involve practical challenges arising from the aggregation of nanoscopic structure. In order to determine the morphology of a  $\text{TiO}_2$  (B) nanoparticle sample that shows excellent electrochemical performance<sup>1,2</sup>, we have performed a comprehensive X-ray scattering analysis of SAXS, PDF and XRPD data. The scattering pattern within a particular angular range encodes distinct structural features of the materials ranging from mesoscale to nanoscale. The combination of small- and wide-angle measurements therefore covers a full angular range that enables us to access a complete set of morphological and structural characteristics including size and shape via SAXS, particle asymmetry and long-range structure via XRPD, and short-range atomic ordering via PDF.

From the analyses, we conclude that the particles are oblate-shaped, contracted along the [010] direction<sup>3</sup>. This particular morphology provides not only a plausible rationale for the excellent electrochemical behavior of these  $\text{TiO}_2$  (B) nanoparticles, but also a structural foundation to model the strain-driven distortion induced by lithiation. A more complex displacement model incorporating this lithiation-induced strain was developed making use of the oblate particle model. It clearly shows the importance of determining the morphology of the nanoparticle so as to understand the lithiation mechanism and rationalize the rate performance of nanostructured materials.

**Reference:**

[1] Ren, Y.; Liu, Z.; Pourpoint, F.; Armstrong, A. R.; Grey, C. P.; Bruce, P. G. *Angew. Chem. Int. Ed.* 51 (2012) 2164-2167.

[2] Andreev, Y. G.; Panchmatia, P. M.; Liu, Z.; Parker, S. C.; Islam, M. S.; Bruce, P. G. *J. Am. Chem. Soc.* 136 (2014) 6306-6312.

[3] Hua, X.; Liu, Z.; Bruce, P. G.; Grey, C. P. *J. Am. Chem. Soc.* 137 (2015) 13612-13623.

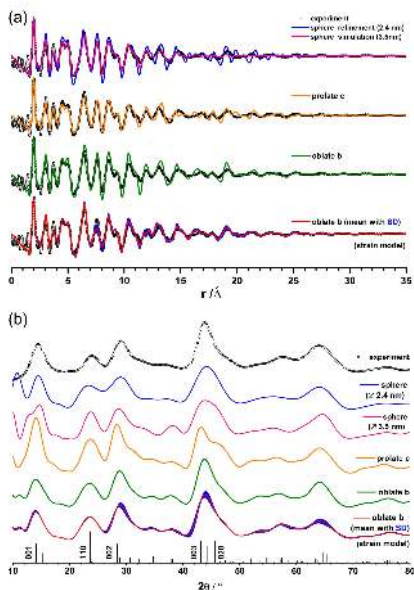


**Figure 1.** Comparison of (a) PDF and (b) XPRD data for the fully lithiated  $\text{TiO}_2(\text{B})$  nanoparticles between experiment and simulations using the PDF refined spherical, prolate c, oblate b, and the oblate b strain model averaged over 20 particles.

**Keywords:** PDF, SAXS, XRD, nanomaterials, batteries

## MS19-P7 Sn/C composite anode materials for high energy lithium/sodium ion batteries

Sivarajakumar Maharajan<sup>1</sup>, Nam Hee Kwon<sup>1</sup>, Katharina M. Fromm<sup>1</sup>

1. University of Fribourg, Switzerland

email: sivarajakumar.maharajan@unifr.ch

### Introduction:

Metallic tin (Sn) is one of the most promising anode materials for next-generation LIBs due to its high theoretical capacity of  $991 \text{ mAhg}^{-1}$  or  $7313 \text{ mAhcm}^{-3}$ , multiple times that of commercialized graphite anode materials ( $372 \text{ mAhg}^{-1}$  or  $833 \text{ mAhcm}^{-3}$ ). However, the huge volume expansion (up to 360%) consequently leading to the dramatic mechanical stress of Sn during cycling cause cracking and pulverization of the active material (refer Fig. 1). This also leads to the loss of conductivity at the electrode, resulting in quick capacity fading, which greatly hinders the practical application of Sn as anode material and thereby letting down its application in LIBs<sup>[2, 3]</sup>. It is therefore essential to control the volume expansion and thereby preventing the loss of active materials. A composite electrode which could facilitate a buffer volume to survive the volume expansion will be the call of the moment. We have adopted a novel synthesis method to form a nano-rattle composite anode made of Sn nano metal encapsulated into carbon shell as shown in figure 1.

### Reverse micelle micro emulsion synthesis:

A reverse micelle micro emulsion technique has been developed to form Sn encapsulated into silica shell where silica shell serves as substrate for carbon coating<sup>[4]</sup>. A non-structured carbon coating has been formed on silica shell. To enhance the conductivity and mechanical strength, the obtained  $\text{Sn@SiO}_2\text{@C}$  has been further heated to  $700^\circ\text{C}$  under Argon to obtain a well-structured carbon coated  $\text{Sn@SiO}_2$ . Further etching of  $\text{SiO}_2$  layer by treating with 10% HF creates a void between Sn nanoparticle and carbon shell, yielding  $\text{Sn@C}$  nano-rattles. Figure 3 shows the TEM picture showing Sn encapsulated into carbon shell with void in between. Also, the cyclic voltammetry shows the redox behaviour of Sn and  $\text{SiO}_2$ .

### Conclusion:

Sn/C nano-rattle composite anode material has been synthesised. However, the  $\text{SiO}_2$  removal is incomplete which hinders the redox behaviour contribution of Sn. Successful removal of  $\text{SiO}_2$  completely will be followed by making electrodes and assembling of half cells.

### References:

- [1] W.-J. Zhang, *Journal of Power Sources* **2011**, 196, 13-24.
- [2] J. O. Besenhard, J. Yang and M. Winter, *Journal of Power Sources* **1997**, 68, 87-90.
- [3] D. Aurbach, *Journal of Power Sources* **2000**, 89, 206-218.
- [4] M. Priebe and K. M. Fromm, *Particle & Particle Systems Characterization* **2014**, 31, 645-651.

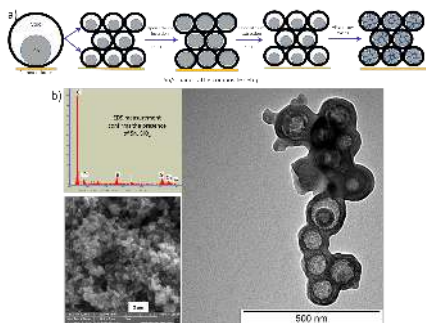


**Figure 1.** Sn/C nano-rattle set up to avoid volume expansion (a), SEM/EDS images with EDS measurement

**Keywords:** lithium ion batteries, sodium ion batteries, alloy based anode material

## MS19-P8 Temperature dependent structural studies of the oxygen ion conductor $\text{Pr}_{1.5}\text{Sr}_{0.5}\text{NiO}_{4+d}$ investigated by single crystal neutron diffraction

Sumit R. Maity<sup>1,2,3</sup>, Monica Ceretti<sup>3</sup>, Martin Meven<sup>4</sup>, Jurg Schefer<sup>2</sup>, Lukas Keller<sup>2</sup>, Winfried Petry<sup>1</sup>, Werner Paulus<sup>3</sup>

1. Heinz Maier-Leibnitz Zentrum (MLZ), Technische Universität München, Garching, Germany

2. Laboratory for Neutron Scattering and Imaging, Paul Scherrer Institut, Villigen PSI, Switzerland.

3. Institut Charles Gerhardt, UMR 5253, CNRS-University Montpellier, Montpellier, France

4. Institute of Crystallography, RWTH Aachen and Jülich Centre for Neutron Science (JCNS) at MLZ, Garching, Germany

email: sumit.maity@psi.ch

Mixed-ionic electronic conductors offer significant advantages over conventional cathodes especially in the intermediate temperature range for solid oxide fuel cell applications as well as for oxygen sensors. Ruddlesden-Popper type layered oxides which belong to the  $\text{K}_2\text{NiF}_6$  family are of great scientific interest in this field due to the interplay of the variable structure to tune functional properties. Among them,  $\text{Pr}_2\text{NiO}_{4+d}$  is a promising candidate as the compound shows the searched high oxygen mobility already at ambient temperature and the oxygen diffusion can be lowered by Sr doping.

Apical oxygen disorder is regarded as the fundamental prerequisite behind the high oxygen diffusion at moderate temperatures which is described by the phonon assisted diffusion mechanism. We explore the effect of Sr doping and temperature on apical oxygen dynamics in  $\text{Pr}_{1.5}\text{Sr}_{0.5}\text{NiO}_{4+d}$  by single crystal neutron diffraction. Our diffraction measurements at RT revealed a tetragonal crystal structure for  $\text{Pr}_{1.5}\text{Sr}_{0.5}\text{NiO}_{4+d}$  when no structural transitions were evidenced up to 800°C [1]. Large structural displacement factors were found for equatorial oxygens along the c-axis and for apical oxygens in the ab-plane with respect to the tetragonal unit cell (Fig.1a). Anisotropic displacement parameters are almost linearly increasing with temperature (Fig.1b). Comparisons of our results with undoped samples [2] show that Sr doping highly reduces the anisotropic movement both for the apical (Fig.1c) and equatorial oxygen atoms. To describe the oxygen disorder in the anharmonic approximation at different temperatures, the observed neutron scattering density of the averaged structure was also explored using the Maximum Entropy Method. These results confirm the anharmonic flat square behavior for apical oxygens with the normal parallel to the c-axis at RT. The outer diameter of the flat square almost reaches up to 0.5 Å which is much less than 2 Å observed for  $\text{Pr}_2\text{NiO}_{4.25}$  already at RT.

We conclude from the comparison of our observation in  $\text{Pr}_{1.5}\text{Sr}_{0.5}\text{NiO}_{4+d}$  with published results from undoped compounds, that the presence of interstitial oxygen atoms at RT is enhancing the diffusion process by providing a shallow diffusion potential for apical oxygens.

[1] S. Maity, Temperature dependent oxygen disorder in  $\text{Pr}_{2-x}\text{Sr}_x\text{NiO}_{4+d}$  by high resolution single crystal neutron diffraction in HeiDi, Master Thesis TUM (2015).

[2] M. Ceretti *et al.*, J. Mater. Chem. A (2015) 3, 21140.

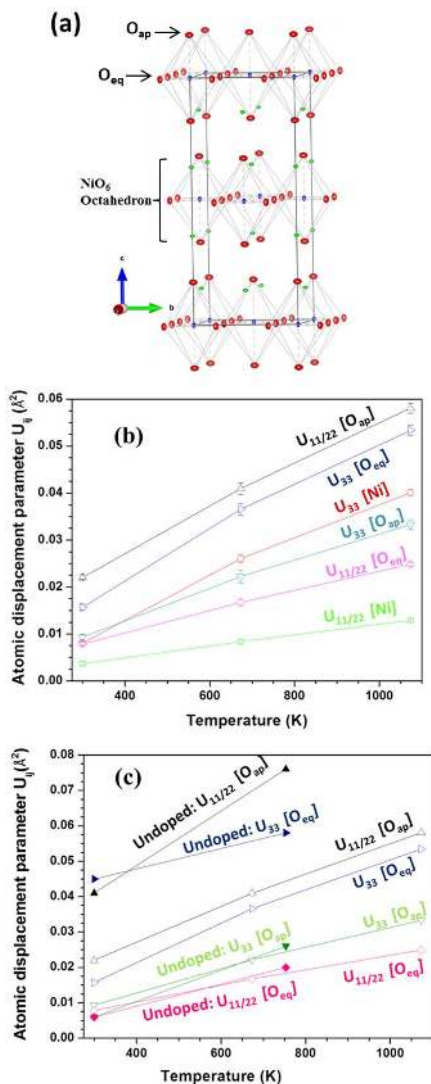


**Figure 1.** (a) Crystal structure of  $\text{Pr}_{0.5}\text{Sr}_{0.5}\text{NiO}_{4-d}$  in  $F4/mmm$  with anisotropic displacement parameters  $U_{eq}$  and (b) and (c) show the effect of temperature and Sr-doping on atomic displacements parameters in  $\text{Pr}_{0.5}\text{Sr}_{0.5}\text{NiO}_{4-d}$  measured by single crystal neutron diffraction at  $\text{HEiDi@MLZ-Garching}$ .

**Keywords:** Mixed-ionic electronic conductors (MIEC), Phonon assisted oxygen diffusion, Oxygen Disorder, Single crystal neutron diffraction

## MS19-P9 Crystal structure, microstructure and ionic conductivity of the cost-efficient sodium solid electrolyte $\text{Na}_5\text{YSi}_4\text{O}_{12}$

Wolfram Münchgesang<sup>1</sup>, Dörte Wagner<sup>2</sup>, Mykhaylo Motylenko<sup>3</sup>, Ulrike Langklotz<sup>2</sup>, Tina Nestler<sup>1</sup>, Anastasia Vyalikh<sup>1</sup>, Falk Meutzner<sup>1</sup>, Axel Rost<sup>2</sup>, Jochen Schilm<sup>2</sup>, Tilmann Leisegang<sup>1,4</sup>, Vladislav A. Blatov<sup>4</sup>, David Rafaja<sup>3</sup>, Dirk C. Meyer<sup>1</sup>

1. Technische Universität Bergakademie Freiberg, Institut für Experimentelle Physik, Leipziger Straße 23, 09596 Freiberg, Germany

2. Fraunhofer Institute for Ceramic Technologies and Systems IKTS, Winterbergstraße 28, 01277 Dresden, Germany

3. Technische Universität Bergakademie Freiberg, Institute of Materials Science, Gustav-Zeuner-Straße 5, 09596 Freiberg, Germany

4. Samara State Aerospace University, Samara Center for Theoretical Materials Science, Moskovskoye Shosse 34, Samara 443086, Russia

email: Wolfram.muenchgesang@physik.tu-freiberg.de

There exist a number of solid-electrolyte materials for sodium battery technologies characterized by intermediate complexity of the corresponding crystal structures. Beside the well-known sodium solid-electrolytes,  $\beta''$ -alumina and NASICON,  $\text{Na}_5\text{YSi}_4\text{O}_{12}$  is another promising phase with a high ionic conductivity. Its main advantage over the two above-mentioned structures is a lower production complexity and thus associated costs. However, very little is known about the correlation between the complex crystal structure, with their one-dimensional ion migration pathways, the microstructure and the interplay with  $\text{Na}^+$  ionic conductivity.

In this work, the phase content, the phase distribution, the migration pathways and the ionic conductivity of polycrystalline  $\text{Na}_5\text{YSi}_4\text{O}_{12}$ -based materials, obtained by a glass-ceramic process, have been analyzed by means of X-ray powder diffraction, scanning electron microscopy, solid-state nuclear magnetic resonance and electrical impedance spectroscopy. These experimental results were discussed with respect to theoretical considerations of the crystal structure, based on the bond valence method and the Voronoi-Dirichlet approach, and other  $\text{Na}^+$  conductors.

This work was financially supported by the BMWi within the project BaSta (0325563D) and the BMBF within the projects CryPhysConcept (03EK3029A) and SyNeSteSia (05K2014).

**Keywords:** ionic conductivity, solid electrolyte, ceramic, bond valence, Structure conductivity correlation

# MS19-P10 Experimental visualization of the Na diffusion paths in Na<sub>0.7</sub>CoO<sub>2</sub>, a prospective cathode material for Na-ion batteries

Marisa Medarde<sup>1</sup>, Medarde Marisa<sup>1</sup>, Mena Mattia<sup>2</sup>, Gaviolo Jorge<sup>2</sup>, Pomjakushina Ekaterina<sup>1</sup>, Kamazawa K<sup>3</sup>, Pomjakushin Vladimir<sup>2</sup>, Sheptyakov Denis<sup>2</sup>, Batlogg Bertram<sup>1</sup>, Ott Hans-Rudolf<sup>4</sup>, Mansson Martin<sup>5</sup>, Juranyi Fanni<sup>2</sup>

1. Laboratory for Scientific Developments and Novel Materials, Paul Scherrer Institut, 5232 Villigen PSI, Switzerland
2. Laboratory for Neutron Scattering and Imaging, Paul Scherrer Institut, CH-5232 Villigen PSI, Switzerland
3. Comprehensive Research Organization for Science and Society (CROSS), Tokai, Ibaragi 319-1106, Japan
4. Laboratory for Solid State Physics, ETH Zürich, CH-8093 Zürich, Switzerland
5. KTH Royal Institute of Technology, SE-100 44, Stockholm, Sweden

email: marisa.medarde@psi.ch

The layered cobaltite NaCoO<sub>2</sub> (0 < x < 1) has been extensively studied during the last decade due to the unusual evolution of its electronic and magnetic properties with the Na content (and hence the Co<sup>3+</sup>/Co<sup>4+</sup> ratio). Its phase diagram includes metallic and insulating phases, charge order, frustrated magnetism, and even a small region where superconductivity appears when H<sub>2</sub>O molecules are intercalated between the CoO<sub>2</sub> layers. Interestingly, this material has also attracted the attention of applied sciences due to its structural similarity with LiCoO<sub>2</sub>, which is one of the most common electrode materials in Li-ion batteries. In view of the larger abundance of Na in the earth crust with respect to Li and the increasing interest on cheaper Na-ion batteries for grid storage, we have investigated the Na-ion diffusion in Na<sub>x</sub>CoO<sub>2</sub> by means of NMR<sup>1</sup>,  $\mu$ SR<sup>2</sup>, elastic<sup>3</sup> and quasicrystalline<sup>4</sup> neutron scattering in order to assess the use of this material as cathode for solid-state rechargeable batteries.

For this purpose we choose the material with x=0.7, where the tendency of Na ions to form ordered superstructures might reduce the ionic conductivity. By combining these techniques we could establish the existence two structural transitions at T<sub>1</sub>=290K and T<sub>2</sub>=400K. Analyses of the anomalies in the Na-Na distances, the Debye-Waller factors and the scattering density in the paths connecting neighbouring Na sites unambiguously showed that both transitions are related to changes in the Na-ion mobility. Moreover, we found that ionic diffusion in this material occurs through the successive opening of first quasi-1D (T<sub>1</sub> < T < T<sub>2</sub>) and then 2D (T > T<sub>2</sub>) Na diffusion paths within the Na layers<sup>3</sup>. These findings provide new insight on the subtle mechanisms controlling the Na-ion diffusion in the NaCoO<sub>2</sub> series and indicate that even in the less favourable member of the family ion diffusion is already present at RT.

<sup>1</sup> Weller et al., PRL **102**, 056401 (2009)

<sup>2</sup> M. Månsson et al., Phys. Scr. **88** (2013) 068509

<sup>3</sup> M. Medarde et al., PRL **110** (2013) 266401

<sup>4</sup> F. Juranyi et al., EPJ Web Confs. **83** (2015) 02008

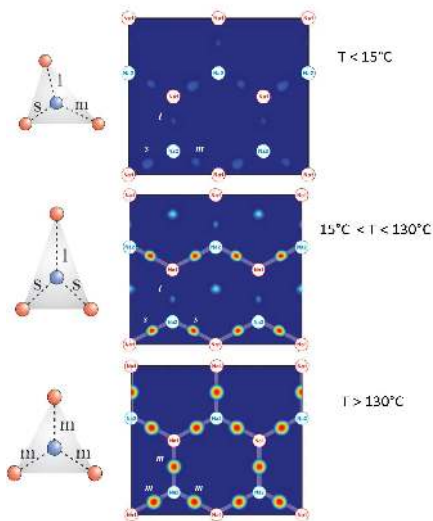


**Figure 1.** Na diffusion paths at different temperatures in one of the Na layers of Na<sub>0.7</sub>CoO<sub>2</sub> with partially occupied NaI (red) and Na2 (blue) sites<sup>3</sup>.

**Keywords:** Na batteries, Na diffusion, neutron powder diffraction



## MS19-P11 Advanced fuel cell component characterization by the development of *in-situ* SAXS flow cell

Olha Sereda<sup>1</sup>

1. Centre Swiss of Electronics and Microtechnology

email: osr@csem.ch

The most commonly used technique for structural characterization at the nanoscale is transmission electron microscopy (TEM). However, there are several limitations to this technique: the information is only obtained on a very small part of the sample and the contrast between support and supported catalyst nanoparticles can be very weak for certain systems like Pt nanoparticles on a high-Z metal oxide support. This can make it difficult to distinguish the catalyst nanoparticles from individual support crystallites. Moreover, due to the very short electron absorption length in condensed matter, TEM investigations cannot be performed *in situ* during operation. These limitations of TEM can be overcome by small-angle X-ray scattering (SAXS): even for very small beam diameters of a couple of hundred micrometers, the scattering curve contains information of hundreds of millions of catalyst nanoparticles [1]. The support contribution to the scattering curve can be subtracted: in case of anomalous SAXS (ASAXS), several energies are used close to the Pt LIII absorption edge in an energy-tunable synchrotron radiation, while in laboratory SAXS diffractometer, incident X-Ray energy is fixed and measurements of both support and catalyst on support are required. The results of *in-situ* ASAXS experiments on Pt/IrTiO<sub>2</sub> will be presented. The conventional model of spherical catalyst particles to incorporate the particle-support interference effect will be explained. Moreover, an experimental setup to perform *in-situ* SAXS experiments in a laboratory machine will be shown on Pt / Vulcan carbon system. [1] Binninger T., Garganourakis M., Han J., Patru A., Fabbri E., Sereda O., Kötzer R., Menzel A., Schmidt T.J. *Phys. Rev. Applied*, 2015, 3, 024012

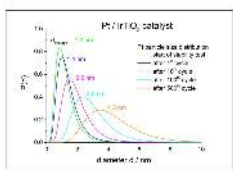


Figure 1. Evolution of the NPs size distribution

**Keywords:** small-angle X-ray scattering (SAXS), nanoscale characterisation

## MS19-P12 Anion Packing and Cation Mobility in Potential Solid Electrolytes $\text{Na}_2\text{B}_{12}\text{H}_{12-x}\text{I}_x$ and $(\text{A}_1\text{A}_2)\text{B}_{12}\text{H}_{12}$ ( $\text{A}_1 = \text{Li}, \text{Na}, \text{A}_2 = \text{Li}, \text{Na}, \text{K}, \text{Cs}$ )

Yolanda Sadikin<sup>1</sup>, Pascal Schouwink<sup>1</sup>, Matteo Brighi<sup>1</sup>, Radovan Černý<sup>1</sup>

1. Laboratory of Crystallography, Department of Quantum Matter Physics, University of Geneva

email: yolanda.sadinik@unige.ch

The application of solid state batteries would be technologically more viable if operating temperatures were to approach values that do not require costly heating systems. Materials exhibiting superionic conductivity at ambient temperature are needed to solve such issues. These concerns can be addressed through materials research, especially through new crystalline phases. Complex hydride compounds are superior candidates for battery solid electrolytes, in view of their high energy density and excellent electrochemical stability, and their applications in batteries have been demonstrated.<sup>[1]</sup> The complex hydride anions are susceptible to rotational disorder, hence, the so-called ‘paddle-wheel mechanism’<sup>[2]</sup> can be exploited to tailor superionic conductivity.

In compounds based on large complex anions, such as *closo*-boranes ( $\text{B}_{12}\text{H}_{12}$ )<sup>2-</sup>, the nearly spherical anions pack easily in *ccp*, *hcp* or *bcc* packing, creating conduction pathways built from continuous networks of tetrahedral and octahedral sites with their connectivity favorable for vacancy- and interstitially-driven cation mobility. The smaller cation (i.e.  $\text{Li}^+$  and  $\text{Na}^+$ ) is the mobile (conducting) species moving between the tetrahedral and octahedral sites.

The study of binary and ternary *closo*-borane compounds containing light alkali metals  $\text{Na}_2\text{B}_{12}\text{H}_{12-x}\text{I}_x$  and  $(\text{A}_1\text{A}_2)\text{B}_{12}\text{H}_{12}$  ( $\text{A}_1 = \text{Li}, \text{Na}, \text{A}_2 = \text{Li}, \text{Na}, \text{K}, \text{Cs}$ ) will be presented with the aim of exploring possible routes to stabilize the suitable anionic packing, which stabilizes superionic phases at room temperature. The experimental approach includes anion modification via partial iodination of  $(\text{B}_{12}\text{H}_{12})^{2-}$  anion, where H is substituted by I, and cation substitution, where the larger cation ( $\text{K}^+$ ,  $\text{Cs}^+$ ) occupies the octahedral site and stabilizes the *closo*-borane framework with significant conducting pathways (*bcc* or *hcp*). The types of anion packing and connectivity of interstitial sites will be discussed as important features in designing superionic conductors based on *closo*-boranes. AC conductivities obtained from impedance spectroscopy show that *hcp*-packed metal *closo*-boranes exhibit superionic conductivity at lower temperatures than their cubic *ccp*-packed analogues, as observed in  $h\text{-Na}_2\text{B}_{12}\text{H}_{12-x}\text{I}_x$  with  $x_1$  approaching 0.1 S cm<sup>-1</sup> at 360K.

### References:

- [1] A. Unemoto, M. Matsuo, S. Orimo, *Adv Funct Mater* 2014, 24, 2267.
- [2] A. Kvist, A. Bengtzelius in W. Van Cool, *Fast Ion Transport in Solids*. North Holland Pub. Co., Amsterdam, 1973, pp. 193-199.

**Keywords:** superionics, *closo*-boranes, solid electrolyte, anion packing



## MS19-P13 Ionic Liquids based on Crown Ethers as electrolytes for batteries

Hervé Yao<sup>1</sup>, Katharina M. Fromm<sup>1</sup>

<sup>1</sup> SCCER Heat and Electricity Storage, Chemistry Department, c/o University of Fribourg, Switzerland

email: herve.yao@unifr.ch

Room temperature ionic liquids (RTILs) are salts that are liquid at room temperature and that are usually composed of an asymmetrical organic cation and a large charge-delocalized anion which is poorly coordinated. They are non-flammable, and thermally as well as electrochemically stable.

These properties make them very interesting for many applications including green solvents for synthesis, catalysis, and electrolytes for ionic and electronic devices<sup>1</sup>. Crown ethers are able to strongly interact with alkali metal cations (Li<sup>+</sup>, Na<sup>+</sup>, K<sup>+</sup>) and have been used as additives in battery electrolytes in order to increase the ionic conductivity of the latter and to prevent electrolyte decomposition<sup>2,3</sup>. However, few studies have been done on crown ethers in the field of electrolytes.

This is why we propose to integrate them covalently as an alkali cation carrier<sup>4,5</sup> in the ionic liquid system. The aim of the project is thus to design and synthesize new Room Temperature Ionic Liquids (RTILs) based on crown ether moieties, to investigate their properties (flammability, thermal and electrochemical stability, conductivity, Li/Na-ion diffusion) and then to use them as electrolytes for rechargeable batteries. We will present their synthesis, structures and properties in this contribution.

### References:

<sup>1</sup>H. Ohno, *Electrochemical aspects of Ionics liquids*, John Wiley & sons, 2005

<sup>2</sup> Abouimrane, A.; Alarco, P J., *Journal of power source*, **2007**, 174, 1193-1196

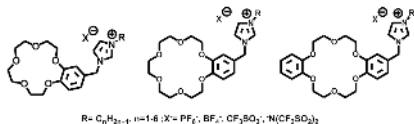
<sup>3</sup>Danil de Namor, Margot. A.; Abu Lebdeh. Y.; Davidson. I.; Armand. M., *Journal of Physical Chemistry*, **1994**, 98, 11796-11802

<sup>4</sup>Shu, Z.X.; McMillan, R S.; Murray, J J., *Journal of the Electrochemical Society*, **1993**, 140, 101-103

<sup>5</sup>Assuma, C.D.; Crochet. A.; Cheremond.Y.; Giese. B.; Fromm, K M., *Angewandte Chemie International Edition*, **2013**, 52, 4682-4685

**Figure 1.** New Ionic liquids based on crown ether building blocks.

**Keywords:** Ionic liquids, electrolytes, battery, crown ether



## MS19-P14 Can we predict Al ion conductors? A combination of crystallographic and energetic evaluation tools.

Falk Meutzn<sup>1</sup>, Tina Nestler<sup>1</sup>, Artem A. Kabanov<sup>2</sup>, Matthias Zschornak<sup>1</sup>, Wolfram Münchgesang<sup>1</sup>, Tilmann Leisegang<sup>1,2</sup>, Vladislav A. Blatov<sup>2</sup>, Dirk C. Meyer<sup>1</sup>

1. TU Bergakademie Freiberg, Institut für Experimentelle Physik, Leipziger Str. 23, 09599 Freiberg, Germany
2. Samara State Aerospace University, Moskovskoye Shosse 34, Samara 443086, Russia

email: falk.meutzn<sup>1</sup>@physik.tu-freiberg.de

Ionic conduction in crystalline oxides can be described as jumps of mobile ions between interconnected oxygen-coordinated crystallographic sites. Therefore, crystallographic evaluation tools can be utilised and combined into a high-throughput prediction method for crystalline ionic conductors. An energetic consideration in the end allows an in-depth analysis of the predicted ionic conduction process in order to verify the most-promising compounds.

Three approaches can be synergetically used to allow a time-efficient and consistent methodology for the identification of oxidic, crystalline aluminium ion conductors: Voronoi-Dirichlet partitioning (VDP) combined with data mining offers a fast high-throughput screening of crystallographic databases on the basis of a geometrical division of the crystal structure into domains assigned to each constituent of the structure, pointing towards possible void networks.

Bond-valence methodology (BVM) as a chemically motivated evaluation tool assists in the prediction process as the second step, determining the most probable migration ways by calculating bond-valence sums for each point in the crystal structure. Bond-valence energy landscape calculations then allow for an energetic estimation of jump energies.

The most promising structures are, eventually, fully electronically modelled by density functional theory (DFT) calculations *ab initio*. Calculating migration step energies subsequently enables a full assessment of jump energies from equilibrated structures as well as electronic conductivities and diffusion coefficients. As a very time-consuming method, DFT is applied as the final step.

This work presents the first results of the identification of promising oxidic Al-ion conductors involving all three approaches and their comparison.

This work is funded by the German BMBF (CryPhysConcept: 03EK3029A) and BMUB (BaSta: 0325563B).

**Keywords:** Voronoi-Dirichlet, Bond-Valence, DFT, Ionic conductors, data mining

## MS19-P15 Diffraction and XAFS - the multi-purpose beamline KMC-2

Götz Schuck<sup>1</sup>, Daniel M. Töbrens<sup>1</sup>, Susan Schorr<sup>1,2</sup>

1. Helmholtz-Zentrum Berlin für Materialien und Energie, Berlin, Germany
2. Institute of Geological Sciences, Freie Universität Berlin, Berlin, Germany

email: goetz.schuck@helmholtz-berlin.de

The beamline KMC-2 at BESSY II, Helmholtz-Zentrum, Berlin, Germany [1], operates a graded SiGe monochromator constructed of two independent crystals. With beam intensity stabilized to an accuracy of 0.3 % and energy resolution of  $E/\Delta E = 4000$  in the energy range of 4 – 15 keV, KMC-2 provides high-quality X-ray radiation suitable for demanding applications requiring energy resolution and accuracy. KMC-2 beamline consists of two end stations: "Diffraction" and "XANES". The beamline recently underwent significant modifications, both extending the range of possible applications and allowing for easier handling [2]. Semi-permanently mounted at KMC-2 is the "Diffraction" end station, a six-circle goniometer in  $\Psi$ -geometry. The instrument allows a wide range of scattering and diffraction measurements, including grazing incidence diffraction (GID), reciprocal space mapping, diffuse scattering, reflectometry, and powder diffraction. A scintillation point detector with motorized detector apertures allows high resolution experiments. An area detector provides reciprocal space coverage with high counting rates and low background. KMC-2 end station "Diffraction" is frequently used in powder diffraction experiments utilizing its abilities in anomalous scattering or its capability to mount a wide range of dedicated sample environments. KMC-2 "XANES" is a dedicated end station to investigate the short-range environment around selected atomic species in condensed matter by X-ray Absorption Spectroscopy. The end station "XANES" provides capabilities for XAFS,  $\mu$ XAFS, and X-ray fluorescence measurements with a flexible suite of detectors (three ionization chambers, Si-PIN photodiode, energy-dispersive detector) and sample environments with the capability to provide various possibilities for *in-situ* XAFS experiments. As only a short time is needed to switch between "XANES" and "Diffraction", it is possible to combine both end stations in the same beam time, making KMC-2 a very versatile beamline especially suited for a wide range of non-standard experiments. [1] www.helmholtz-berlin.de [2] Töbrens, D. M., Zander, S.: Journal of large-scale research facilities, 2, A49 (2016)

**Keywords:** instrumentation, synchrotron, X-ray absorption

# MS19-P16 Crystallochemical analysis of ion conductivity in K<sup>+</sup>-oxygen containing inorganic compounds.

Yelizaveta A. Timofeyeva<sup>1,2</sup>, Vladislav A. Blatov<sup>1,2</sup>, Natalia A. Kabanova<sup>1,2</sup>

1. Samara Aerospace University, 34, Moskovskoye shosse, Samara, 443986

2. Samara Center for Theoretical Materials Science, Ac. Pavlova St. 1, 443011 Samara, Russia

email: eliztimofeeva@mail.ru

A challenge for the materials science is the search for alternative cation-conductive materials, in particular, potassium- or sodium-conductive solid electrolytes, which can be used to create new prospective chemical sources of energy. One of the solutions of this problem is the processing of large amounts of structural data by means of special software based on modern methods of crystallochemical analysis.

The geometry of the migration channels is an important factor which determines the prerequisites for cation conductivity in the structure. In [1, 2] the promising lithium and sodium oxygen-containing compounds, possessing 1D, 2D, or 3D infinite systems of channels (the migration maps) available for Li<sup>+</sup> and Na<sup>+</sup>-cations respectively, have been found based on the Voronoi-Dirichlet approach.

In this work, we have analyzed all known ternary and quaternary potassium-oxygen-containing compounds (2729 compounds) from the Inorganic Crystal Structure Database (ICSD version 2015/1). The systems of voids and channels were found in the selected structures using the Voronoi-Dirichlet approach, which is implemented in the ToposPro program package [3]. In total, 231 compounds were found, whose structures allow free migration of potassium ions. Out of the 231 compounds, 53 substances are known as K<sup>+</sup>-solid electrolytes, while the remaining 178 compounds, which possess 1D, 2D, or 3D migration maps of K<sup>+</sup> cations (Fig. 1), have not been electrochemically studied so far. They can be used as precursors for the synthesis of new potassium-conductive solid electrolytes.

[1] Meutzner F., Kabanova N.A., Meyer D. C. et al. Chem. Eur. J. 2015. 21, 16601-16608.

[2] Blatov V.A., Ilyushin G.D., Ivanov-Schitz A.K. et al. Solid State Ion. 2008. 179, 2248-2254.

[3] V.A. Blatov, A. P. Shevchenko, D. M. Proserpio Cryst. Growth Des. 2014. 3576–3586 <http://topospro.com>.

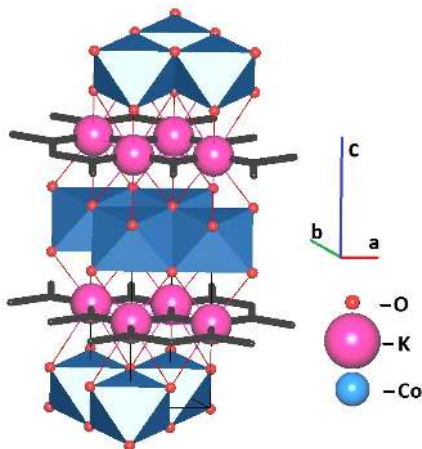


Figure 1. 2D migration map for K<sup>+</sup> cations in K<sub>0.61</sub>CoO<sub>2</sub>

**Keywords:** Crystallochemical analysis, solid electrolyte, Voronoi-Dirichlet approach, systems of voids and channels

**MS19-P17** New electrochemical cells for operando neutron diffraction of battery materialsKristina Edstroem<sup>1</sup>, William Brant, Matthew Roberts<sup>2</sup>

1. Uppsala University

2. Departments of Materials and Chemistry, University of Oxford, Parks Road, Oxford OX1 3PH, UK

email: Kristina.Edstrom@kemi.uu.se

The interest and frequency of performing operando neutron diffraction experiments for lithium ion batteries has increased significantly over the past few years. A major contributor to this is that the challenge to construct an electrochemical cell which balances both electrochemical performance, quality of the obtained diffraction pattern and cost of construction now is addressed. Up until now most work has been performed on, often complex, custom cells built to target a specific feature such as fast cycling at the cost of data quality or data quality with high material loading [1-3].

A significant amount of work has been performed within our group on developing multiple varieties of electrochemical cells for operando neutron diffraction. To this end we have newly designed two vastly different operando cells; a large wound 18650-like cell and a smaller, cheaper coin cell design. The 18650-like wound cell can contain up to 4 g of active material, is able to be cycled at faster rates and provides a diffraction pattern which is of high enough quality to extract accurate structural parameters. It does, however, require expensive deuterated electrolyte and specialised equipment. Alternatively, the coin cell design is cheap, does not require deuterated electrolyte, can provide good quality diffraction and reasonable electrochemical cycling rates. It is anticipated that the coin cell design will make neutron diffraction accessible to more research groups and also presents a viable cell design for operando neutron diffraction studies of sodium ion cells.

Using LiFePO<sub>4</sub>, LiNi<sub>0.5</sub>Mn<sub>1.5</sub>O<sub>4</sub> and Li<sub>0.18</sub>Sr<sub>0.66</sub>Ti<sub>0.5</sub>Nb<sub>0.5</sub>O<sub>3</sub> as case study materials this contribution will focus on the operando neutron diffraction results obtained from both cells, thus exploring the core strengths and potential of each design.

## References

[1] N. Sharma, X. Guo, G. Du, Z. Guo, J. Wang, Z. Wang, and V. K. Peterson. J. Am. Chem. Soc. 134 (2012), 7867 [2] M. Roberts, J. J. Biendicho, S. Hull, P. Beran, T. Gustafsson, G. Svensson and K. Edström. J. Power Sources 226 (2013), 249. [3] M. Bianchini, J.B. Leriche, J.L. Laborier, L. Gendrin, E. Suard, L. Croguennec, C. Masquelier, J. Electrochem. Soc., 160 (2013) A2176.

**Keywords:** operando, neutron diffraction, lithium-ion battery

**MS19-P18** A new high flux neutron backscattering spectrometer for research into the ns-dynamics of battery, fuel-cell and hydrogen storage materials.Bernhard Frick<sup>1</sup>, Markus Appel<sup>1</sup>

1. Institut Laue-Langevin, Grenoble

email: frick@ill.fr

The new neutron backscattering spectrometer IN16B at the Institut Laue-Langevin, Grenoble, with highest flux and signal-to-noise ratio for a high energy resolution spectrometer of its kind, is perfectly suited for studying diffusion and relaxation processes on the nanosecond time scale. In this poster we also present some instrumental aspects, but will mainly give examples to illustrate the possibilities for spectroscopy on materials which are of interest for fuel cells, battery materials or hydrogen storage.

IN16B has a standard energy resolution with Si111 analysers in backscattering of FWHM ~ 0.75 µeV in an energy transfer range of ± 30 µeV, thus exploring simultaneously a momentum transfer (Q) range between 0.2 and 1.8 Å<sup>-1</sup>. The Q-range can be doubled by using Si311 analysers and the resolution can be halved by using unstrained small crystals on the analyser sphere. Ongoing projects aim for an energy transfer range extension by a factor of 10 with BATS, BAcKscattering and Time-of-flight Spectrometer and a decade improvement of the energy resolution.

**Keywords:** neutron spectroscopy, energy related materials, dynamics, relaxation

## MS20 Materials for energy conversion and harvesting

Chairs: Manuel Hinterstein, Siegbert Schmid

### MS20-P1 Organic-inorganic hybrid perovskite $\text{CH}_3\text{NH}_3\text{PbI}_3$ : structural consequences of water absorption

Alla Arakcheeva<sup>1</sup>, Dmitry Chernyshov<sup>2</sup>, Massimo Spina<sup>1</sup>, László Forró<sup>1</sup>, Endre Horváth<sup>1</sup>

1. Laboratory of Physics of Complex Matter, Ecole polytechnique Fédérale de Lausanne, CH-1015 Lausanne, Switzerland  
2. SNBL, ESRF, 71 Avenue des Martyrs, 38043 Grenoble Cedex 9, France

email: alla.arakcheeva@epfl.ch

The organic-inorganic hybrid perovskite-like  $\text{CH}_3\text{NH}_3\text{PbI}_3$  (MAPbI<sub>3</sub>) is intensively studied owing to its rôle in energy conversion. In this compound, the linear methyl ammonium ( $\text{MA}^+$ ) cation is located in the centre of the cuboctahedra formed by I-atoms. Hence, statistical disorder over its different orientations can be expected. This allows a high flexibility of the structure symmetry with pressure, temperature and other conditions affecting the weak N-H...I hydrogen bonds, which maintain this cation inside the cubooctahedron. Indeed, the different tetragonal space groups, such as *I4/mcm* [1-4], *I4cm* [5,6] and *I4/m* [7], were reported previously even in the room temperature phase. MAPbI<sub>3</sub> is structurally unstable at ambient conditions. Air humidity provokes its gradual decomposition. We have studied the mechanism for the decomposition. Crystal structure of the pristine (**I**) and in wet air aged (**II**) samples has been investigated at 293 K with high precision single crystal XRD experiments using synchrotron radiation. We show [8] that different space groups, *I422* and *P4<sub>2</sub>2<sub>2</sub>*, characterize **I** and **II**, respectively. Both of them are subgroups of *I4/mcm*, which is commonly adopted for MAPbI<sub>3</sub>. The difference appears due to the changes in H-bonds induced by the H<sub>2</sub>O inclusion in the structure of the aged crystal **II**. This inclusion initiates the crystal decomposition, which can be described by the chemical reaction:  $\text{CH}_3\text{NH}_3\text{PbI}_3 + (\text{H}_2\text{O}) = \text{CH}_3\text{NH}_2 + \text{PbI}_2 + (\text{H}^+ + \text{I}^- + \text{H}_2\text{O})$ . The dashed contour in the figure 1 indicates the atomic part, which most probably leaves the structure leading to the decomposition.

[1] Y. Kawamura *et al.*, Journal of the Physical Society of Japan, **71**(7), 1694 (2002).

[2] Y. Yamada *et al.*, Journal of the American Chemical Society, **137**, 10456 (2015).

[3] Y. Dang *et al.*, CrystEngComm, **17**, 665 (2015).

[4] M.T. Weller *et al.*, Chem. Commun. **51**, 4180 (2015).

[5] C.C. Stoumpos *et al.*, Inorg. Chem. **52**, 9019 (2013).

[6] J. Xie *et al.*, Journal of Power Sources, **285**, 349 (2015).

[7] T. Baikie *et al.*, J. Mater. Chem. **A1**, 5628 (2013).

[8] A. Arakcheeva, D. Chernyshov, M. Spina, L. Forró, E. Horváth. *CH<sub>3</sub>NH<sub>3</sub>PbI<sub>3</sub>: precise structural consequences of water absorption at ambient conditions* Acta Cryst. B. (Submitted in April, 2016).

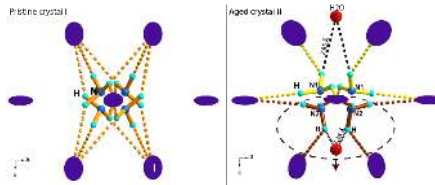


**Figure 1.** The N-H...I H-bonds in the pristine and the aged crystals. Four shown  $\text{NH}_3$  groups conform to four orientations of  $\text{MA}^+$ . In **I**, all  $\text{NH}_3$  groups are statistically present with probability of 25% for each one. In **II**,  $\text{N}_2\text{H}_5^+$  and  $\text{N}^+\text{H}_3$  are present with probability of 29.5% and 16.5%, respectively.

**Keywords:** crystal structure, hybrid organic-inorganic lead iodide, aged MAPbI<sub>3</sub>

## MS20-P2 Thermoelectric transport properties in magnetically ordered crystals

Hans Grimmer<sup>1</sup>

1. Laboratory for scientific developments and novel materials, Paul Scherrer Institut, WGHG/342, Villigen PSI, CH-5232, Switzerland

email: hans.grimmer@psi.ch

Thermoelectric transport properties of magnetically ordered crystals in an external magnetic field  $\mathbf{H}$  were investigated in [1, 2] from a space-time symmetry point of view. Crystals belonging to any of the 122 point groups may show electric resistivity, thermal conductivity, Seebeck and Peltier effect for  $\mathbf{H}=0$ , as well as the following effects linear in  $\mathbf{H}$ : Hall, Righi-Leduc, Nernst and Ettingshausen. The tensors describing these effects are invariant under space inversion  $\mathbf{I}$  and time inversion  $\mathbf{I}'$ ; their form can be found using Neumann's principle and the Onsager relations  $\Gamma_{\mu\nu}(\mathbf{H}) = \Gamma_{\nu\mu}(-\mathbf{H})$ , where  $\Gamma$  is a  $6 \times 6$  matrix giving the  $\mu\nu$ -gradient of the electrochemical potential and the heat current as functions of the electric current and the temperature gradient in the crystal.

Magnetically ordered crystals belong to one of the 90 magnetic point groups (MPGs) that do not contain time inversion  $\mathbf{I}'$  as a separate element. For  $\mathbf{H}=0$ , spontaneous Hall and Righi-Leduc effects appear for the 31 MPGs allowing ferromagnetism; spontaneous Nernst and Ettingshausen effects appear for 58 MPGs. Whereas magnetoresistance, magneto-heat-conductivity, magneto-Seebeck and magneto-Peltier effect are of even order in  $\mathbf{H}$  in magnetically unordered crystals, such effects linear in  $\mathbf{H}$  appear in case of magnetoresistance and magneto-heat-conductivity for the 66 MPGs allowing piezomagnetism, and in case of magneto-Seebeck and magneto-Peltier effect for all 69 MPGs that do not contain space-time inversion  $\mathbf{I}'$  as a separate element.

To find the forms of the tensors describing the effects in magnetically ordered crystals, Onsager relations were used in [1] as formulated in [3]:  $\Gamma_{\mu\nu}(\mathbf{H}, \mathbf{M}) = \Gamma_{\nu\mu}(-\mathbf{H}, -\mathbf{M})$ , where  $\mathbf{M}$  denotes the time averaged magnetization field describing the magnetic configuration.

Whereas the results of [1] and [2] agree for  $\mathbf{H}=0$ , some of the results obtained in [2] for the effects linear in  $\mathbf{H}$  are at odds with generally accepted results. The procedure used in [1] makes it easy to separate tensors into two parts being invariant and changing sign under  $\mathbf{I}'$ , respectively. Whereas [2] considers both parts as forming a single tensor, it will be shown that considering the two parts (which can be measured separately) as independent tensors leads to simpler and stronger results.

### References:

- [1] H. Grimmer (1993). *Acta Cryst.* **A49**, 763-771.
- [2] M. Seemann, D. Ködderitzsch, S. Wimmer & H. Ebert (2015). *Phys. Rev. B*, **92**, 155138.
- [3] S. Shtrikman & H. Thomas (1965). *Solid State Commun.* **3**, 147-150.

**Keywords:** Thermoelectrics, Transport properties, Onsager relations, Magnetic order

## MS20-P3 Structural characterisation of $\text{Cu}_2\text{Zn}(\text{Sn}_{1-x}\text{Ge}_x)\text{Se}_4$ by neutron diffraction.

Galina Gurieva<sup>1</sup>, Alexandra Franz<sup>1</sup>, Susan Schorr<sup>1,2</sup>

1. Helmholtz Zentrum Berlin für Materialien und Energie GmbH, Hahn-Meitner-Platz 1, D-14109 Berlin, Germany

2. Free University Berlin, Institute of Geological Sciences, Malteserstr. 74-100, Berlin, Germany

email: galina.gurieva@helmholtz-berlin.de

$\text{Cu}_2\text{ZnGeSe}_4$  and  $\text{Cu}_2\text{ZnSnSe}_4$  are quaternary semiconductors belonging to the adamantane compound family, contain only abundant elements, which makes these materials promising candidates for engineering on their base of different high-efficient and low-cost devices [1].  $\text{Cu}_2\text{ZnSn}(\text{S}_{1-x}\text{Se}_x)_4$  solar cells with Ge alloying recently reached efficiency of 8.4% [2]. CZTSe crystallizes in the kesterite type structure (space group) [3]. X-ray diffraction used for structural characterization of CZGSe was reported in the literature, and it suggests that it shows the stannite type structure (space group) [4]. In contrast to these findings recent first principal calculation predicts the kesterite type phase (space group) to be the ground state structure for this material [5]. A differentiation between the isoelectronic cations  $\text{Cu}^+$ ,  $\text{Zn}^{2+}$  and  $\text{Ge}^{4+}$  and consequently kesterite and stannite is not possible using X-ray diffraction due to their similar scattering power. But neutrons diffraction can solve this problem; the coherent scattering lengths are sufficiently different [6]. By this method our group could show that both  $\text{Cu}_2\text{ZnSnSe}_4$  and  $\text{Cu}_2\text{ZnGeSe}_4$  occur in the kesterite structure. [3, 7]. A detailed structural analysis of Zn rich off-stoichiometric (B-F and F-D type mixtures)  $\text{Cu}_2\text{Zn}(\text{Sn}_{1-x}\text{Ge}_x)\text{Se}_4$  powder samples, grown by solid state reaction, was performed by neutron diffraction at the fine resolution neutron powder diffractometer E9 at BER II ( $\lambda = 1.7986 \text{ \AA}$ , RT). Rietveld refinement of diffraction data using the FullProf suite software [8] lead to accurate values of  $a$  and  $c$  lattice constants and site occupancy factors. The latter have given insights into the cation distribution within the crystal structure of  $\text{Cu}_2\text{Zn}(\text{Sn}_{1-x}\text{Ge}_x)\text{Se}_4$  solid solutions with different  $x$  values. The correlated information about changes in lattice parameters and cation site occupancies, details on the existing intrinsic point defects and their concentrations will be discussed.

[1] K. Tanaka et. al., *Sol. Energy Mater. Solar Cells* **91** (2007) 1199

[2] Q. Guo et al., *Sol. Energy Mater. Sol. Cells*, **105** (2012) 132.

[3] S. Schorr, *Solar Energy Materials and Solar Cells*, **95** (2011) 1482.

[4] O.V. Parasyuk et. al., *J. Alloys Comp.* **329** (2001) 202-207.

[5] S. Chen et.al., *Phys. Rev. B*, **82** (2010), p. 195203 (8pp.)

[6] V.F. Sears, *Neutron News* **3** (3), 26-37, (1992).

[7] G. Gurieva, D.M. Többsen, M. Valakh, S. Schorr, *Phys and Chem of Solids*. Submitted.

[8] Juan Rodriguez-Carvajal and Thierry Roisnel, [www.ill.eu/sites/fullprof](http://www.ill.eu/sites/fullprof)

**Keywords:** CZTGe, neutron diffraction

## MS20-P4 Luminescent copper(I) complexes with chelating N<sup>^</sup>N and P<sup>^</sup>P ligands and application in light-emitting electrochemical cells (LECs)

Sarah Keller<sup>1</sup>, Alessandro Prescimone<sup>1</sup>, Fabian Brunner<sup>1</sup>, Edwin C. Constable<sup>1</sup>, Catherine E. Housecroft<sup>1</sup>

1. Department of Chemistry, University of Basel

email: sa.keller@unibas.ch

New lighting devices such as LECs (Light-Emitting Electrochemical Cells) and OLEDs (Organic Light-Emitting Diodes) promise considerable savings in terms of both energy and resources, due their generation of visible light as main product instead of heat with light only as a by-product. We here present light-emitting copper(I) complexes, which are a low-priced alternative to materials based on less abundant elements such as ruthenium or iridium. Encouraging results have been obtained by coordinating copper(I) with P<sup>^</sup>P chelating bisphosphanes such as POP (bis[(2-diphenylphosphino)phenyl] ether) and xantphos (4,5-Bis(diphenylphosphino)-9,9-dimethylxanthene), in combination with 2,2'-bipyridines, 2,2':6',2''-terpyridines and other chelating N<sup>^</sup>N-donors. The copper(I) systems are very susceptible to the steric demand of the ligands. In order to stabilize the  $d^{10}$  state of Cu(I) and protect it from being oxidized, the ligands should be coordinated in a tetrahedral geometry. While smaller ligands fail to prevent the tetrahedral complex structure from flattening, sterically too challenging ligands can lead to mixtures of heteroleptic [Cu(N<sup>^</sup>N)(P<sup>^</sup>P)]<sup>+</sup> with homoleptic [Cu(N<sup>^</sup>N)<sub>2</sub>]<sup>+</sup> and [Cu(P<sup>^</sup>P)<sub>2</sub>]<sup>+</sup> complexes. Especially substitution at the 6-position of the bipyridine has considerable impact on the stability and structural features of the heteroleptic [Cu(N<sup>^</sup>N)(P<sup>^</sup>P)]<sup>+</sup> complexes. Interesting complex structures were obtained by attaching various alkyl and CF<sub>3</sub>-groups, halogens, pyridine and aryl groups to the bipyridine. Depending on the steric demand and electronic properties of the bipyridine, the dihedral angle between the ligands as well as the torsion and tilting of the bipyridine rings (see angles I, II, III in **Fig. 1 a)**) vary. Furthermore, the coordinating bisphosphanes can adapt different conformers (see **Fig. 1 b)**), which is confirmed by crystal structures and supported by low-temperature NMR studies. For N<sup>^</sup>N = 2,2':6',2''-terpyridine, a fourfold as well as a rarely found fivefold coordination of the copper(I) center is present in the crystal structure. Further alteration of the ligands will provide much needed insights into the correlation between structural features of the complexes and important properties such as electroluminescence, lifetime of the excited state, quantum yield and ion mobility.

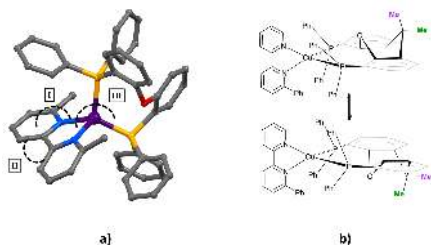


**Figure 1.** a) Characterizing angles of a typical Cu(POP)(bipyridine)<sup>+</sup> cation. b) Proposed conformers of [Cu(xantphos)(Phbpy)]<sup>+</sup> and interconversion pathway through inversion of the xanthene unit.

**Keywords:** Copper(I), Luminescence, Light-emitting electrochemical cells, LECs, bipyridine, bisphosphanes, conformers



## MS20-P5 The influence of mobile monovalent ions on structures and properties of multinary thermoelectric tellurides

Oliver Oeckler<sup>1</sup>, Paul Heitjans<sup>2</sup>, Stefan Schwarzmüller<sup>1</sup>, Andre Düvel<sup>2</sup>, Leonie Schmohl<sup>1</sup>, Matthias Jakob<sup>1</sup>, Alexander Kuhn<sup>1</sup>, Markus Nentwig<sup>1</sup>, Thorsten Schröder<sup>3</sup>

1. Universität Leipzig, Faculty of Chemistry and Mineralogy, IMKM, Scharnhorststr. 20, D-04275 Leipzig, Germany

2. Leibniz Universität Hannover, Institute of Physical Chemistry and Electrochemistry, Callinstr. 3-3a, D-30167 Hannover, Germany

3. Technische Universität München, Physik Department / Heinz Maier-Leibnitz Zentrum, Lichtenbergstr. 1, D-85748 Garching, Germany

email: oliver.oeckler@gmx.de

Crystal structures and thermoelectric properties in the system  $(\text{GeTe})_x\text{Sb}_3\text{Te}_3$  (GST materials) are dominated by high concentrations of vacancies associated with diffusion-controlled phase transitions.[1] Partially replacing Ge by twice the amount of monovalent cations  $\text{M}^+$  reduces the number of vacancies and yields stable compounds without reconstructive phase transitions. In the case of Li, the lattice thermal conductivity is as low as that of compounds with high vacancy concentrations, indicating that Li acts as a "pseudo vacancy".[2] Such materials reach thermoelectric figures of merit ZT up to ca. 1. Varying the ratio of  $\text{M}^+$ ,  $\text{Ge}^{2+}$  and  $\text{Sb}^{3+}$  enables the adjustment of the vacancy concentration and consequently the Li mobility. Thus,  $\text{LiGe}_{3.5}\text{Sb}_3\text{Te}_5$  or  $\text{LiGe}_{11.5}\text{Sb}_5\text{Te}_{15}$  exhibit lower thermal conductivities ( $0.4$  and  $1.6 \text{ W m}^{-1} \text{ K}^{-1}$ , respectively) than the vacancy-free variants  $\text{Li}_2\text{Ge}_3\text{Sb}_3\text{Te}_5$  and  $\text{Li}_2\text{Ge}_{11}\text{Sb}_5\text{Te}_{15}$  ( $1.3$  and  $2.5 \text{ W m}^{-1} \text{ K}^{-1}$ ).<sup>2</sup> As corroborated<sup>2</sup> by superionic Li-ion conductivity in  $\text{Li}_2\text{Te}$ , the mobility of Li may lead to PLEC (phonon liquid/electron crystal) behavior at elevated temperature.<sup>7</sup> Li solid-state NMR spectra clearly indicate Li mobility. Motional narrowing of the NMR signal sets in at temperatures slightly above room temperature. Compounds with vacancies exhibit higher Li mobilities, correlation times are in the order of magnitude of  $10^{-3} \text{ s}$  at ca.  $300 \text{ K}$  and less at higher temperatures.

Using Na instead of Li is also possible whereas samples with Cu contain precipitates of copper tellurides. The interplay of doping GST and nanoscale heterostructures leads to ZT values of 1.5 and higher.

Since SnSe emerged as a promising and cheap thermoelectric material,[3] related substitution strategies in the system Sn/Sb/Se seem intriguing.  $\text{SnSb}_3\text{Se}_4$  with a chain-like "sulfosalt" structure [4] is an n-type semiconductor with a high Seebeck coefficient; however, the ZT value is limited by the low electrical conductivity, similar to that of comparable sulfosalts. Formally adding Na<sub>2</sub>Se leads to p-type  $\text{Na}_2\text{SnSb}_3\text{Se}_4$  which crystallizes in a NaCl-type structure and is surprisingly stable against air and moisture.

[1] T. Rosenthal, M. N. Schneider, C. Stiewe, M. Döblinger, O. Oeckler, *Chem. Mater.* **2011**, 23, 4349.

[2] T. Schröder, S. Schwarzmüller, C. Stiewe, J. de Boor, M. Hölzel, O. Oeckler, *Inorg. Chem.* **2013**, 52, 11288.

[3] H. Zhang, D. V. Talapin, *Angew. Chem. Int. Ed.* **2014**, 53, 9126.

[4] P. P. K. Smith, J. B. Parise, *Acta Crystallogr. Sect. B* **1985**, 41, 84.

**Keywords:** thermoelectrics, tellurides, defects, 7Li NMR

## MS21 Structural disorder and materials' properties at ambient and non-ambient conditions

Chairs: Dmitry Chernyshov, Vaughan Gavin

### MS21-P1 HRXRD analysis of bonded Si / Si interface

Zoltán Balogh-Michels<sup>1</sup>, Zwiackier Kai<sup>1</sup>, Zhang Yucheng<sup>2</sup>, Jung Arik<sup>2,3</sup>, Flötgen Christian<sup>4</sup>, Chahine Gilbert<sup>5</sup>, Dommann Alex<sup>1</sup>, Erni Rolf<sup>2</sup>, von Känel Hans<sup>2,3</sup>, Neels Antonia<sup>1</sup>

1. Center of X-Ray Analytics, Empa, Swiss Federal Laboratories for Materials Science and Technology, 8600 Dübendorf, Switzerland

2. Electron Microscopy Center, Empa, Swiss Federal Laboratories for Materials Science and Technology, 8600 Dübendorf, Switzerland

3. Laboratory for Solid State Physics, ETH-Zürich, Schafmattstrasse 16, 8093 Zürich, Switzerland

4. EV Group, 4782 St. Florian/Inn, Austria

5. European Synchrotron, ESRF, Grenoble 38043, France

email: zoltan.balogh@empa.ch

Stress and strain can not only influence the structural behavior of the materials but can significantly alter their functional properties. The need for local, nanoscale characterization of stress levels and its correlation with other material properties increases rapidly. Scanning X-ray microscopy using synchrotron radiation is an emergent technique which can deliver fast, conclusive results with *submicrometer real space* resolution [1,2]. On the other hand the technique is limited in its *reciprocal space* resolution by the pixel size of 2D detectors. This is especially important if high quality single crystals have to be characterized. Modern laboratory instruments therefore offer the complementary capability owing to their higher reciprocal space resolution.

In this study we investigated the stress distribution in Si wafer pairs which were covalently bonded at room temperature [3]. The wafer bonds were analyzed by the “nanodiffraction” ID01 beamline at ESRF (F) [1] as well as by a Bruker D8 Davinci HRXRD instrument at EMPA (CH). Transmission electron microscopy (TEM) was used for morphological analysis. The specific wafer bond shown in Fig. 1 exhibited bulk bond strength, but contained a ~ 3 nm thick amorphous interfacial layer in their as-prepared form. After high temperature annealing a network of dislocations emerged to compensate for rotation and tilt of the two wafers.

The built-in stress at the interface caused some long range changes in the diffraction patterns, which can easily be distinguished by lower spatial resolution laboratory scale devices. The evaluation of the rocking curve FWHM going through the bonding interface cross section (X-ray beam size 50mm) shows the overall silicon crystal

quality summing up in strain and geometrical behavior (Fig.1a). At the interface, dislocations in the annealed specimens (Fig. 1b) caused a broadening of the Si(333) reflection (Fig. 1c).

[1] G.A. Chahine, M-I. Richard, R.A. Homs-Regoyo, T.N. Tran-Caliste, D. Carbone, V.L.R. Jacques, R. Grifone, P. Boesecke, J. Katzer, I. Costina, H. Djazouli, T. Schroeder and T.U. Schüllli, J. Appl. Cryst., 47 (2014) 762.

[2] C.V. Falub, M. Meduna, D. Chrastina, F. Isa, A. Marzegalli, T. Kreiling, A.G. Taboada, G. Isella, L. Miglio, A. Dommann and H. von Känel, Sci. Rep. 3 (2013) 2276.

[3] C. Flötgen, N. Razek, V. Dragoi and M. Wimplinger, ECS Transactions 64 (2014) 103.

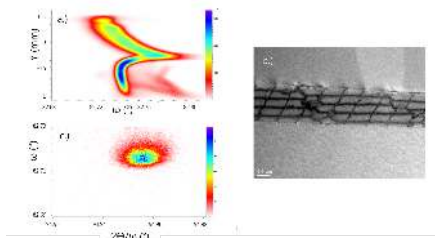


**Figure 1.** Spatially resolved RCs for an as prepared specimen showing strain/tilt components (a). TEM picture showing dislocation density patterns (b). Reciprocal space map (RSM) on the Si(333) reflection from the annealed Si/Si interface (c), the dislocations caused a more diffuse Bragg-peak.

**Keywords:** reciprocal space mapping, stress analysis, bonded silicon, dislocations

**MS21-P2** Synthesis, structures and luminescence properties of two gallium(III) complexes containing 5,7-dimethyl-8-hydroxyquinoline.

Orbett T. Alexander<sup>1</sup>, Orbett T. Alexander<sup>1</sup>, Mart-Mari Duvenhage<sup>2</sup>, Alice Brink<sup>1</sup>, Peter Muller<sup>3</sup>, Hendrik C. Swart<sup>2</sup>, Hendrik G. Visser<sup>1</sup>

1. Department of Chemistry, University of the Free State, PO Box 339, Bloemfontein, South Africa.

2. Department of Physics, University of the Free State, PO Box 339, Bloemfontein, South Africa.

3. Department of Chemistry, Massachusetts Institute of Technology, Massachusetts, USA.

email: orbettalexander@yahoo.com

Metal-quinolinates are known as key materials in the design of organic light emitting diode (OLEDs) devices since their discovery by Tang and Van Slyke back in 1987.<sup>1</sup> Quinolinol derivatives have been since envisaged as promising fluorophores. As a result, that has prompted growth in the science of these  $M(Ox)_3$  entities with other icosagens down the boron group such as gallium (Ga) and indium (In).<sup>2,3</sup> Not only has there been extensive research on the structural discrepancies of these type of complexes leading to isomerization (*mer/fac*), but also, the net effect (in the solid state) imposed by the guest molecules trapped in the unit cell. Crystallography in particular, provided an excellent technique for the investigation of the net effect in these complexes w.r.t. to inter-molecular interactions therein and the solvent species "trapped" within the crystal lattice.<sup>4</sup>

In this work, two complexes of  $M(Ox)_3$  ( $M = Ga(III)$ ,  $OxH = 5,7$  dimethyl-8-hydroxyquinoline) have been synthesized and characterized by <sup>1</sup>H NMR, <sup>13</sup>C NMR, single crystal X-ray Diffraction and SEM, and their photoluminescence properties evaluated. The fact that crystals were obtained with a different number of dichloromethane molecules in the crystal lattice, provides the rare opportunity to investigate solvent effects in photoluminescence.

1. C.W. Tang, S.A. Van Slyke, *Appl. Phys.*, 51, 913, **1987**.

2. P. E. Burrows, L.S. Sapochak, D. M. McCarty, S. R. Forrest, M.E. Thompson, *Appl. Phys. Lett.*, 64, 2718, **1994**.

3. M.M. Duvenhage, H.C. Swart, O.M. Ntwaeaborwa, H.G. Visser, *Optical Materials*, 35, 2366, **2013**.

4. M. Brinkmann, G. Gadret, M. Muccini, C. Taliani, N. Masciocchi, A. Sironi, *J. Am. Chem. Soc.*, 122, 5147, **2002**.

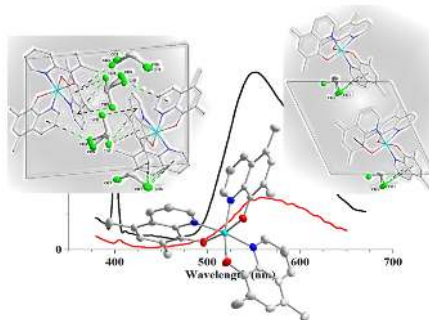


**Figure 1.** Crystallography as the decider in the optical behaviour of two gallium(III) complexes.

**Keywords:** Aluminium, Fluorescence, Quinolinol, OLEDs

**MS21-P3 Phase transitions of silicon under dynamic and non-hydrostatic conditions**

Eva-Regine Carl<sup>1</sup>, Jannik Richter<sup>2</sup>, Andreas N. Danilewsky<sup>2</sup>,  
 Rajani K. Vijayaraghavan<sup>3</sup>, Sean Kelly<sup>3</sup>, Patrick McNally<sup>3</sup>,  
 Zuzana Konopkova<sup>4</sup>, Hanns-Peter Liermann<sup>4</sup>

1. Institute of Earth and Environmental Sciences - Geology
2. Institute of Earth and Environmental Sciences - Crystallography
3. School of Electronic Engineering - Dublin City University
4. DESY

email: eva-regine.carl@geologie.uni-freiburg.de

Silicon represents one of the most important semiconductors in today's high-performance electronics. By the processing in the industry locally high pressures and temperatures emerge during the mechanical treatment and the wafer handling, leading to phase transitions under non-equilibrium conditions. This can result in a change of the electronic properties of the material, as well as the formation of cracks and the breaking of the wafers. We present time-resolved X-ray diffraction experiments under non-hydrostatic conditions that study in situ phase transformations of silicon. The experiments were conducted in a membrane-driven diamond anvil cell (mDAC) at the Extreme Conditions Beamline (ECB) P02.2 at PETRA III, DESY. We used powdered Si standard and added gold flakes for pressure determination. The compression rates varied around 0.04 GPa/s and the maximal pressure went up to 20 GPa. Most experiments were conducted at room temperature. After one experiment, the sample was heated up to 500 °C using a graphite resistance heater. During compression and decompression, diffraction patterns were collected every 10 seconds. For analysis, three-dimensional contour plots were created to get an overview of the experiment to define the onset of phase transitions. In order to identify the phases and to determine the lattice parameters, we performed a LeBail analysis on single diffraction patterns. All experiments reveal two phase transitions during compression. Between 4 and 7 GPa, Si-I transforms to Si-II. The next phase transition from Si-II directly to Si-V occurs between 13 and 15 GPa, skipping the stability field of Si-XI. Si-V remains then stable to maximal pressure. Upon decompression, Si-V transforms to Si-III and Si-XII. The approximate proportion of Si-III to Si-XII is 20:1. The mixture remains stable to 2 GPa. At ambient pressure, this recovered sample was heated up to 500 °C to obtain Si-XIII. During heating, the two phases remain stable. Furthermore, there is no evidence that the proportion changes with respect to the diffraction patterns. However, a Raman-analysis of the recovered samples reveals a strong variation of this proportion over the entire sample. After maintaining at 500 °C for 5 minutes, two new reflections occur at low diffraction angles up to 11 °2 $\theta$  that can be indexed to Si-IV. However, two other strong reflections of this phase at higher 2 $\theta$ -values are not observed. Being metastable, Si-IV could not be identified by a Raman-analysis.

**Keywords:** Silicon, non-hydrostatic

**MS21-P4 On the stacking disorder of an organic acid**

Christian Czech<sup>1</sup>, Edith Alig<sup>1</sup>, Kristoffer E. Johansson<sup>2</sup>, Jan Bats<sup>1</sup>,  
 Martin U. Schmidt<sup>1</sup>

1. Goethe-University, Institute of Inorganic and Analytical Chemistry, Max-von-Laue-Straße 7, 60438 Frankfurt am Main, Germany
2. University of Copenhagen, Institute of Pharmacy, Universitetsparken 2, DK-2100 Copenhagen, Denmark

email: cczech@chemie.uni-frankfurt.de

Crystals of the  $\alpha$ - and  $\beta$ -phase of 2-amino-hexanoic acid ( $C_6H_{13}NO_2$ ) frequently show diffuse streaks parallel to  $c^*$ , which indicates a stacking disorder in the layer structure. Order-disorder (OD) theory is used to derive possible stacking sequences. Lattice-energy minimisations by force fields and dispersion-corrected density functional theory (DFT-D) were performed on a set of ordered model structures. The calculated energies depend not only on the arrangement of neighbouring layers, but also of next-neighbouring layers. From the DFT-D energies stacking probabilities were calculated. According to the calculated stacking probabilities large models containing 100 double-layers were constructed. Their simulated diffraction patterns show sharp reflections for  $h + k = 2n$  and strong diffuse streaks parallel to  $c^*$  through all reflections with  $h + k = 2n + 1$ , which is in good agreement to experimental investigations.

**Keywords:** stacking disorder, lattice energy minimisations, force fields, DFT-D,

**MS21-P5** Neutron diffraction study of the deformation behavior of Mg-alloy-based compositesGergely Farkas<sup>1</sup>, Kristián Máthi<sup>2</sup>, Ján Pilch<sup>1</sup>, Peter Minárik<sup>2</sup>, Petr Lukáš<sup>1</sup>

1. Nuclear Physics Institute, ASCR, v. v. i.

2. Charles University in Prague, Department of Physics of Material, Czech Republic

email: farkasgr@gmail.com

Deformation mechanisms in Mg-Al-Ca alloy reinforced with short alumina fibres (30 wt. %) were studied in-situ using neutron diffraction method. Ceramic fibres were homogeneously distributed in the matrix and are arranged to parallel planes, inside which they have random orientations. Two type of sample were investigated: samples with parallel fibre plane orientation and perpendicular fibre plane orientation with respect to the loading axis. The fibres plane orientation was found to be a key parameter, which influences the acting deformation processes, such as twinning or dislocation slip.

Deformation curves shows that parallel fibre plane orientation has stronger influence on the increment of yield stress and tensile strength (600 MPa), that the perpendicular fibre orientation. Concurrently, the elongation is smaller. Mechanical properties of composite shows strong degradation at 200 °C and enhanced ductility up to 15% strain.

Results from in-situ neutron diffraction shows the lattice strain changes in the matrix and also in the reinforcement phase depending on macroscopic compressive deformation and stress. In case of parallel fibre plane orientation the increment of compressive lattice strain is lower in the matrix and higher in the fibres in comparison to perpendicular fibre orientation. This is a direct proof of Shear-lag model according to which the load transfer is more effective, when fibres close a small angle with the operating load.

At elevated temperature regardless of the fibre plane orientation, above 1% of deformation matrix's lattice strain start to show inverse behaviour. Compressive strain in the matrix rapidly decreases with compressive deformation, without a significant loss of macroscopic stress.

**Keywords:** metal matrix composite, internal lattice strain, neutron diffraction

**MS21-P6** Comprehensive Analysis of Disorder in NaLaF<sub>4</sub>, an Efficient Up-Conversion PhosphorRuggero Frison<sup>1</sup>, Thomas Weber<sup>2</sup>, Tara Michels-Clark<sup>3</sup>, Michal Chodkiewicz<sup>2</sup>, Christina Hoffmann<sup>2</sup>, Andrei Savici<sup>2</sup>, Anthony Linden<sup>1</sup>, Hans-Beat Bürgi<sup>1,6</sup>

1. Department of Chemistry, University of Zurich, CH-8057 Zurich

2. X-ray platform, Department of Materials, ETH Zurich, CH-8093 Zurich Switzerland

3. Lawrence Berkeley National Laboratory, Berkeley, CA 94720, USA

4. Biological and Chemical Research Centre, Department of Chemistry, University of Warsaw, Zwirki i Wigury 101, 02-089 Warszawa, Poland

5. Neutron Sciences Directorate, Oak Ridge National Laboratory, Oak Ridge, TN 37831, USA

6. Department of Chemistry and Biochemistry, University of Bern, CH-3012 Bern Switzerland

email: ruggero.frison@uzh.ch

NaLaF<sub>4</sub> is an efficient up-conversion phosphor [1] belonging to the family of rare earth-doped sodium lanthanide tetrafluorides where the nature of the photoactive sites can unambiguously be explained only in terms of a microscopic model of disorder [2]. X-ray and Neutron Diffuse Scattering (XDS, NDS), as *k*-space probes, provide statistically reliable data on atomic pair correlation functions and thus on deviations from the average periodic structure. Using high quality XDS and NDS datasets from the distinctive, planar diffuse scattering of NaLaF<sub>4</sub>, we calculated the 3D-Difference Pair Distribution Function (3D-ΔPDF), identified the various types of disorder and derived an abstract model of interatomic vectors [3]. It was then possible by means of Monte Carlo (MC) simulations to build and optimize large model crystals providing a specific atomistic disorder model for NaLaF<sub>4</sub>, whose Fourier transform gives an excellent fit to the experimental diffuse scattering. The distinct contrast displayed by the various atomic species with the two radiation types provides a better sensitivity to the different pair-wise correlations ultimately yielding more robust results.

[1] T. Kano, H. Yamamoto, Y. Otomo, *J. Electrochem. Soc.* (1972) 119, 1561-1564. [2] J.F. Suyver, J. Grimm, K.W. Krämer, H.U. Güdel, *J. Lumin.* (2005) 114, 53-59. A.Sarakovskis, J. Grube, A. Mishnev, M. Springis, *Opt. Mat.* (2009) 31, 1517-1534. [3] A. Aebischer, M. Hostettler, J. Hauser, K. Krämer, T. Weber, H.U. Güdel, H.B. Bürgi, *Angew. Chem. Int. Ed.* (2006) 45, 2802-2806. [3] T. Weber, A. Simonov, Z. Krist., (2012) 227, 238-247.

**Keywords:** photo-active materials, disorder, diffuse scattering

## MS21-P7 Unraveling Two-Dimensional Polymerization Propagation from Diffuse Scattering

Gregor Hofer<sup>1,2</sup>, Martin Kröger<sup>3</sup>, A. Dieter Schlüter<sup>1</sup>, Thomas Weber<sup>2</sup>

1. Laboratory of Polymer Chemistry, ETH Zurich, CH-8093 Zurich, Switzerland
2. X-Ray Platform D-MATL, ETH Zurich, CH-8093 Zurich, Switzerland
3. Polymer Physics, ETH Zurich, CH-8093 Zurich, Switzerland

email: gregor.hofer@mat.ethz.ch

A recent advance in polymer chemistry is two-dimensional polymerization [1]. This is achieved by pre-organizing trifunctional monomer molecules through crystallization followed by exposure of the crystal to intense light. This external trigger propels a thermally reversible photochemical reaction and genuine long-ranged ordered two-dimensional polymerization is accomplished.

The monomer molecules used in this study [2] crystallize in the chiral and polar space group *R*3. Polymerization occurs in the *ab*-plane of the crystal. Despite large structural changes during polymerization and depolymerization, the space group is preserved in this single-crystal-to-single-crystal transformation. Both, polymerization and depolymerization can be frozen in time by simply removing the crystal from the triggering source thus creating a disordered monomer/polymer single crystal. The highly polar solvent molecule 2-cyanopyridine is incorporated into the structure in an orientationally disordered manner. This disorder is altered by the polymerization reaction.

This contribution will address two-dimensional polymerization propagation by means of real crystal structure analysis. Three imaginable propagation models with different distributions of bonded monomer moieties are presented in Figure 1. Unlike Bragg scattering, diffuse scattering [3] is sensitive to the distribution of these bonded monomer moieties. High-resolution synchrotron measurements were done to record the diffuse scattering during the polymerization and depolymerization. Several different diffuse scattering features were observed and will be presented and qualitatively interpreted. The newly developed 3D- $\Delta$ PDF method [4] and Monte Carlo simulations will be employed to model the real structure. The combined results will reveal the type of polymerization propagation. Furthermore, additional aspects caused by the polymerization will be discussed, such as the overall change in the electric dipole momentum caused by the reorientation of the solvent molecules or the crystal quality.

[1] Payamyar, P., King, B. T., Öttinger, H. C., & Schlüter, A. D. (2016). *Chem. Commun.*, **52**, 18-34.

[2] Kory, M. J., Wörle, M., Weber, T., Payamyar, P., van de Poll, S. W., Dshemuchadse, J., Trapp, N., Schlüter, A. D. (2014) *Nat. Chem.*, **6**, 779–784.

[3] Welberry, T. R. & Weber, T. (2016). *Cryst. Rev.* **22**, 2–78.

[4] Weber, T., Simonov, A. (2012) *Z. Krist.*, **227**, 238–247.

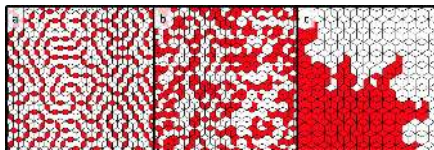


**Figure 1.** Schematic visualization of three imaginable propagation types. The image shows snapshots from (a) dimerization-like, (b) random-like and (c) nucleation-like polymerization propagations. Although all three models exhibit the same average structure, they have very different real structures.

**Keywords:** Disorder; Diffuse Scattering; PDF; Polymer

## MS21-P8 Order change and phase's redistribution in single crystal of Ni-based superalloy during hard cyclic viscoplastic deformation

Lembit Kommel<sup>1</sup>, Boris N. Kodess<sup>2</sup>, Igor L. Kommel<sup>1</sup>

1. Tallinn University of Technology, Department of Materials Engineering, 19086 Tallinn, Estonia
2. VNIIMS-ICS/E, 119361 Moscow, Russian Federation

email: lemmitt.kommel@ttu.ee

The X-ray investigation of cuts and spheres of complex alloyed single crystal (SC) of Ni-based superalloy ZS-32 have been carried out for samples with identical solidification parameters prior to identical casting conditions and after different levels of hard (tension-compression) cyclic viscoplastic (HCV) deformation. The microstructure evolution of the cast samples have been studied in a plane, parallel to solidification direction, using optical microscope (Nikon Microphot-FX) and scanning electron microscope (Zeiss EVO MA-15) equipped with energy dispersive spectrometer (EDS) system for local chemical composition determine of different phases. The lattice constant and atomic occupancy have been determined use Siemens and CCD single crystal diffractometer Xcalibur with MoK-alpha-radiation. The 7000-8000 Bragg reflections have been collected in full Ewald sphere. The micromechanical properties of the phases have been determined using the nanoindentation data (NanoTest NTX testing centre of Micro Materials Ltd.) after deformation. The results indicate that the interdiffusion of additive atoms have been found during HCV deformation at room temperature. It is shown that the phase's microstructure was homogenized and micromechanical properties changed. We suggesting that are due to result of atoms interdiffusion between different phases, which initiating via microstresses increase during HCV deformation. After deformation appear small pores and defects as result of atoms non balanced interdiffusion. Our experiments have shown the change in atomic order after deformation. We suppose that both the change in atomic order and the shift in the phase equilibria of Ni-based superalloys determine changes in the phase's micromechanical properties and evolution of microstructure characteristics. XRD peaks of the formation of a new proof of the formation of microstructural rafting, defects like micropores and grain boundaries. The material with SC microstructure becomes to polycrystalline microstructure. A mechanism of subsequent fracture includes the above-mentioned phenomena when occur the increasing of cumulative strain during HCV deformation.

**Keywords:** Order, Ni-based superalloy, interdiffusion, rafting, fracture mechanism

## MS21-P9 Relation between photoluminescence properties and crystalline structure of III-V semiconductor alloys grown by MOVPE

Tatiana Prutsikj<sup>1</sup>, Nikolay Makarov<sup>1</sup>, Giovanni Attolini<sup>2</sup>

1. Instituto de Ciencias, Benemerita Universidad Autonoma de Puebla, Puebla, Mexico
2. Istituto dei Materiali per l' Elettronica ed il Magnetismo, CNR, Parma, Italy

email: tatiana.prutsikj@correo.buap.mx

III-V semiconductor alloys, such as a ternary GaInP and a quaternary GaInAsP alloys, are important materials widely used in semiconductor lasers, solar cells, high electron mobility transistor (HEMT) and heterojunction bipolar transistors (HBT). It is well known that within III-V semiconductor epitaxial layers grown by Metalorganic Vapour Phase Epitaxy (MOVPE) technique a periodic composition fluctuation coexists with spontaneously-formed atomically-ordered clusters. The photoluminescence (PL) emission characteristics strongly depend on the crystalline structure. In particular, the PL emission of epitaxial III-V layers with atomic ordering is polarized and the polarization degree depends on the values of ordering parameter and elastic, biaxial strain.

We studied the PL emission polarization of the GaInP and GaInAsP epitaxial layers lattice matched to GaAs. We measured and calculated the integrated PL intensity as a function of polarization angle for the PL emission of two atomically ordered III-V alloys with different ordering parameters. We compared these measured and calculated PL polarization patterns for the PL propagating along the [001] direction, and along [1-10] and [110] directions. Our calculations show that if the alloy is almost lattice-matched to the substrate the PL emission from the layer (001) surface is polarized because of atomic ordering in the alloy, and the PL polarization degree is proportional to the ordering parameter. The polarization degree of the PL emission from the (001) surface reaches its maximum when the lattice parameters of the layer and the substrate match, and decreases proportionally to the value of biaxial strain. The PL from the edge planes is strongly polarized when the epitaxial layer is under a strong biaxial strain, thus the strong strain becomes a dominant factor in the polarization degree. We measured the polarization of the PL emission from the (001) surface the ordered GaInP and GaInAsP alloy at different temperatures and analyzed its temperature evolution within the range from 10 K to 300 K. We observed the change of the PL polarization pattern induced by thermal strain due to the difference between the thermal expansion coefficients of the layer and the substrate, and estimated the biaxial strain at different temperatures. Our measurements point out that the polarization of the PL emission from (001) plane increases with decreasing temperature because of the thermal variation of the epitaxial strain.

**Keywords:** III-V solid solutions, MOVPE, Photoluminescence



**MS21-P10** Crystallographic Investigation of Photo-Excited States in Molecular CrystalsNikolaj Roth<sup>1</sup><sup>1</sup>. Center for materials crystallography, Department of chemistry, Aarhus university, Denmark

email: nikolajroth@chem.au.dk

Materials with photo-switchable physical properties become increasingly studied for possible applications. These controllable properties, such as changes in magnetic susceptibility<sup>1</sup> and electric polarisation<sup>2</sup>, often come from electronically excited states of the constituent molecules of the crystals. The study of electronically excited states in molecules has traditionally been carried out using spectroscopic techniques, giving very accurate values for energy levels, but only rough estimates of the structural changes associated with the excitation. The structural investigation of these states can instead be carried out using the methods of photo-crystallography, a field which is currently seeing rapid development. By exciting a crystal with light, the resulting structural changes can be probed using x-ray and neutron diffraction techniques. Here, a long lived excited state of the photo-magnetic compound [Nd(DMF)<sub>2</sub>(H<sub>2</sub>O)<sub>2</sub>(μ-CN)Fe(CN)<sub>5</sub>]•H<sub>2</sub>O is investigated using single-crystal x-ray diffraction. The excitation is carried out using a new LED-based device which can easily be mounted on most diffractometers and present a cheap alternative to laser-based setups<sup>3</sup>. It is found that the excited state is more stable than previously thought<sup>4</sup>, as it can be kept for hours at 100K. [1] Gütlich, P et al. (2001) *Coord. Chem. Rev.* 219-221, 839-879 [2] Collet et al. (2003) *SCIENCE*, 300, 612-615 [3] Brayshaw et al. (2010) *J. Appl. Cryst.* 43, 337-340 [4] Svendsen et al. (2009) *Angew. Chem.* 121, 2818-2821

**Keywords:** photocrystallography, excited state, photo-induced**MS21-P11** Structural disorder in a magnetic pyrochlore oxideRomain Sibille<sup>1,2</sup>, Tom Fennell<sup>2</sup>, Monica Ciomaga Hatnean<sup>3</sup>, Elsa Lhotel<sup>4</sup>, David Keen<sup>5</sup>, Geetha Balakrishnan<sup>3</sup>, Michel Kenzelmann<sup>1</sup>

1. Laboratory for Scientific Developments and Novel Materials, Paul Scherrer Institut, 5232 Villigen, Switzerland
2. Laboratory for Neutron Scattering and Imaging, Paul Scherrer Institut, 5232 Villigen, Switzerland
3. Physics Department, University of Warwick, Coventry, CV4 7AL, UK
4. Institut Néel, CNRS and Université Joseph Fourier, BP 166, 38042 Grenoble Cedex 9, France
5. ISIS Neutron Facility, STFC Rutherford Appleton Laboratory, Chilton, Didcot, OX11 0QX, UK

email: romain.sibille@psi.ch

Insulating pyrochlore oxides of formula A<sub>2</sub>B<sub>2</sub>O<sub>7</sub> where A is a rare-earth magnetic ion and B is a transition metal ion or a group IV ion, have attracted much attention because both A and B form a network of corner-sharing tetrahedra, a wonderful landscape for the study of magnetic frustration in three dimensions [1]. Rare-earth ions having a strong uniaxial anisotropy constrained along the <111> direction of the cubic unit-cell (Pr<sup>3+</sup>, Tb<sup>3+</sup>, Dy<sup>3+</sup>, Ho<sup>3+</sup>) reverse, in theory, the role of ferromagnetic and antiferromagnetic couplings with regard to frustration [2]; the ferromagnetic case becomes highly frustrated, and can lead to the spin ice state [3], while the antiferromagnetic one is not. However, pyrochlore Ising antiferromagnets have proved able to markedly defy the expectations of long-range magnetic order. A famous example is the enigmatic terbium titanate, Tb<sub>2</sub>Ti<sub>2</sub>O<sub>7</sub>, which forms a so-called spin liquid state [4] with power-law spin correlations [5]. We report experimental studies on a related pyrochlore, Tb<sub>2</sub>Hf<sub>2</sub>O<sub>7</sub>, which displays striking similarities with the magnetism of Tb<sub>2</sub>Ti<sub>2</sub>O<sub>7</sub>, despite the existence of a substantial amount of structural disorder.

Firstly we present a detailed investigation of the crystal chemistry of Tb<sub>2</sub>Hf<sub>2</sub>O<sub>7</sub> using a combination of Resonant Contrast Diffraction (RCD) and high-resolution Neutron Powder Diffraction (NPD), both on powder samples. We show that these measurements unveil the existence of defects that affect the pyrochlore structure of Tb<sub>2</sub>Hf<sub>2</sub>O<sub>7</sub>. The neutron Pair Distribution Function (PDF) presents significant differences between the experimental function at low **r** values and the one calculated from the average structure (Figure 1), which points out local distortions around the defects. Secondly we demonstrate that the structural defects in this material influence the magnetic ground state, and that our experimental results can be related to theories on disordered pyrochlore magnets.

- [1] J. S. Gardner et al., *Rev. Mod. Phys.* 82, 53 (2010).
- [2] S. T. Bramwell et al., *J. Phys. Condens. Matter* 10, L215-220 (2012).
- [3] S. T. Bramwell and M. J. P. Gingras, *Science* 294, 1495 (2001).
- [4] J. S. Gardner et al., *Phys. Rev. Lett.* 82, 1012 (1999).
- [5] T. Fennell et al., *Phys. Rev. Lett.* 109, 017201 (2012).

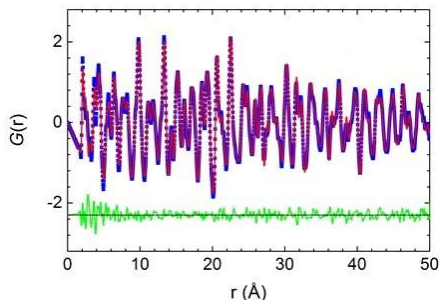


**Figure 1.** Pair Distribution Function obtained from neutron scattering measurements on GEM at ISIS.

**Keywords:** structural disorder, frustrated magnetism

## MS21-P12 Hysteresis in the solid-state phase transition in DL-Norvaline

Jun Xu<sup>1</sup>, Anthony Linden<sup>1</sup>, Hans-Beat Bürgi<sup>1,2</sup>

1. Department of Chemistry, University of Zurich, Switzerland

2. Department of Chemistry and Biochemistry, University of Bern, Switzerland

email: jun.xu@chem.uzh.ch

DL-Norvaline is an artificial and non-polar amino acid with chemical formula  $C_6H_{11}NO_2$ . DSC measurements show that it undergoes two temperature-dependent phase transitions, at about 188 K and 153 K.<sup>1,2</sup> It shows substantial disorder with three principal conformations of the propyl side chain in the room-temperature  $\beta$ -phase (A, B, C) and two main conformations (B, D) in the intermediate-temperature  $\alpha$ -phase.<sup>3</sup> The structure of the low-temperature phase is still unknown, due to crystal delamination before the  $\gamma$ -phase is observed.<sup>3</sup>

We have found that the onset of the  $\beta$  to  $\alpha$  phase transition can be delayed and is dependent on the cooling rate. Three crystals instantly cooled from room temperature, and nine crystals rapidly cooled within a few minutes, go through the first phase transition near 188 K. Slow cooling of 5 crystals in steps of 20 K from 300 K to 140 K and waiting 10 hours at each temperature during an X-ray data collection, reveals that the onset of the phase transition occurs only at lower temperatures, sometimes as low as 140 K, and in one case no transition occurred at all. The sluggish phase transition correlates with a different temperature dependence of the atomic displacement and site occupation parameters for the three molecular conformations, compared with those observed following fast cooling. As the temperature decreases, the population of the A conformation in the  $\beta$ -phase grows at the expense of the population of the B conformation, while that of the C conformation remains fairly constant.

In contrast, the populations of the B and D conformations in the  $\alpha$ -phase remain constant across the measured temperature range (140-180 K).

Crystals that were rapidly cooled below 188 K transformed to the  $\alpha$ -phase, but further rapid cooling to 140 K, which is below the temperature expected for transformation to the  $\gamma$ -phase, did not reveal any significant change of the unit cell or structural parameters, so no evidence for the formation of the  $\gamma$ -phase could be obtained.

### References:

<sup>1</sup> Chatzigeorgiou, P. et al., J. Phys. Chem. B 2010, **114**, 1294-1300.

<sup>2</sup> Ren, P. et al., J. Phys. Chem. B 2011, **115**, 2814-2823.

<sup>3</sup> C.H. Görbitz, J. Phys. Chem. B 2011, **115**, 2447-2453.

**Keywords:** Hysteresis

## MS21-P13 Determination of the crystal structure, composition and water uptake of the mixed ionic-electronic conductor



Andrea Fantin<sup>1</sup>, Tobias Scherb<sup>1</sup>, Janka Seeger<sup>2</sup>, Gerhard Schumacher<sup>1</sup>, Uta Gerhards<sup>3</sup>, Mariya E. Ivanova<sup>2</sup>, Wilhelm A. Meulenber<sup>2</sup>, Roland Dittmeyer<sup>1</sup>, John Banhart<sup>1</sup>

1. Helmholtz-Zentrum Berlin für Materialien und Energie GmbH, Hahn-Meitner-Platz 1, D-14109 Berlin, Germany
2. Forschungszentrum Jülich GmbH, D-52425 Jülich, Germany
3. Karlsruhe Institute of Technology, Hermann-von-Helmholtz-Platz 1, D-76344 Eggenstein-Leopoldshafen, Germany

email: andrea.fantin@helmholtz-berlin.de

The presented work on proton conducting materials will show new results on the structural characterization of substituted lanthanum tungstate:  $\text{La}_{5.4}\text{W}_{1-x}\text{Re}_x\text{O}_{12.6}$  with  $0 \leq x \leq 0.2$  in two different conditions (dry(Ar), wet-D<sub>2</sub>O(Ar)). Among the specimen series measured, the specimen without substitution ( $\text{La}_{5.4}\text{WO}_{12.6}$ ) and the one with highest Re-substitution level ( $x = 0.2$ ) will be in the focus of the presentation. Their comparison will be achieved considering neutron diffraction results, due to the insufficient contrast between W ( $Z = 74$ ,  $b = 4.86$  fm) and Re ( $Z = 75$ ,  $b = 9.2$  fm) against X-Rays.

The structural model of the undoped system  $\text{La}_{5.4}\text{WO}_{12.6}$  recently suggested will be thoroughly analyzed, independently confirmed, and taken as starting point to determine the position of Re atoms in the crystal structure. Anharmonic vibrations of the oxygen anions are for the first time found in LaWO-based systems and shortly discussed.

Neutron diffraction data was obtained from D2B (ILL, Grenoble), HRPT (SINQ, Villigen) and FIREPOD (BERII, Berlin) in the temperature range between 1.5 K and 1200 K.

Three models will be presented for the Re-substituted system within the  $Fm-3m$  space group: Re substituting W on the main W position (Wyckoff site  $4a$ ), Re substituting W on the shared La/W position (Wyckoff site  $48h$ ) and Re substituting W statistically on both sites. Substitution amount in the shared sites is reached refining site occupancy factors in a single-atom-per-site approach (average neutron scattering length). Restraining of the site occupancy factors according to electron probe micro-analysis composition was mandatory to decrease the degrees of freedom.

Notwithstanding the low Re amount (~1 atom per unit cell out of 32 cations and 55 oxygen anions) and the close neutron scattering length of Re to the main element La ( $Z = 57$ ,  $b = 8.24$  fm), the very details of the structure were unambiguously determined by the combination of thermogravimetry, neutron diffraction and electron probe micro-analysis. Surprisingly, even one single Re atom in such a large unit cell ( $\approx 1400 \text{ \AA}^3$ ) strongly influences the water uptake. This peculiar feature will be discussed in relation to the stoichiometry, the oxygen site occupancy factors and the bond lengths in wet and dry specimens.

**Keywords:** mixed ionic-electronic conductor, Re-substituted lanthanum tungstate, neutron diffraction, water uptake

## MS21-P14 Nanoscale order in the frustrated mixed conductor $\text{La}_{5.6}\text{WO}_{12.8}$

Tobias Scherb<sup>1</sup>, Simon A.J. Kimber<sup>2</sup>, Christiane Stephan<sup>3,4</sup>, Paul F. Henry<sup>2</sup>, Andrea Fantin<sup>1</sup>, Gerhard Schumacher<sup>1</sup>, Janka Seeger<sup>6</sup>, Justus Just<sup>1</sup>, Adrian H. Hill<sup>7</sup>, John Banhart<sup>1,8</sup>

1. Helmholtz-Zentrum Berlin (HZB)
2. European Synchrotron Radiation Facility (ESRF)
3. Freie Universität Berlin
4. Bundesanstalt für Materialforschung und -prüfung (BAM)
5. European Spallation Source (ESS)
6. Forschungszentrum Jülich (FZJ)
7. Johnson Matthey Technology Centre
8. Technische Universität Berlin

email: tobias.scherb@helmholtz-berlin.de

$\text{Ln}_6\text{WO}_{12}$  (Ln = Lanthanide) compounds are due to their mixed protonic/electronic conduction properties and their superior stability in acidic atmospheres highly potential materials for the use as gas separation membranes. We prepared pure samples of  $\text{La}_{5.6}\text{WO}_{12.8}$  which showed exceptional device performance and stability, and studied the crystal structure in detail by the complementary use of neutrons and photons. The performance at temperatures above  $T=600^\circ\text{C}$  is better than reported for other mixed conductors, and the comparable tiny water uptake ( $< 0.2$  weight %), measured by TGA, suggests an unusually effective mechanism for proton transport. We report a comprehensive investigation of the average and local structure of  $\text{La}_{5.6}\text{WO}_{12.8}$ . Synchrotron x-ray and neutron powder diffraction show that a cubic fluorite supercell describes the average structure, with highly disordered lanthanum and oxide positions. On average the tungsten sites are six-fold coordinated, and we detect a trace (3.7(1.3)%) of anti-site disorder. In addition to sharp Bragg reflections, strong diffuse neutron scattering is observed, which hints at short-range order. We consider plausible local configurations, and show that the defect chemistry implies a simple 'chemical exchange' interaction that favors ordered  $\text{WO}_6$  octahedra. Our local model is confirmed by synchrotron x-ray pair distribution function analysis and EXAFS experiments performed at the La K and W L3-edges. We show that ordered domains of around 3.5 nm are found, implying that mixed conduction in  $\text{La}_{5.6}\text{WO}_{12.8}$  is associated with a defective glassy-like anion sublattice. The origins of this ground state are proposed to lie in the non-bipartite nature of the fcc lattice and the pairwise interactions which link the orientation of neighboring octahedral  $\text{WO}_6$  sites. This 'function through frustration' could provide a means of designing new mixed conductors.

**Keywords:** neutron diffraction, PDF analysis, EXAFS

**Keywords:** invarium, coordination compound, validation

## MS22 Beyond multipolar refinement

Chairs: Alessandro Genoni, Simon Grabowsky

### MS22-P1 Identifying the correct metal atom in pairs of crystal structures of coordination compounds by aspherical-atom refinement

Claudia M. Wandtke<sup>1</sup>, Matthias Weil<sup>2</sup>, Jim Simpson<sup>3</sup>, Birger Dittrich<sup>4</sup>

1. Georg-August University Goettingen, Germany

2. TU Wien, Austria

3. University of Otago, New Zealand

4. Heinrich-Heine University Duesseldorf, Germany

email: claudia.wandtke@chemie.uni-goettingen.de

Experimental multipole refinements on compounds containing metal atoms push the limit of classical charge density studies for various reasons. [1] The situation is different when conventional diffraction data of limited resolution are to be modelled by transfer of Hansen/Coppens multipole parameters [2] predicted by density functional theory, used as fixed scattering factors. Such procedures [3 and references therein] have so far mainly been used for organic compounds. Here we continue these developments and extend their applicability to coordination compounds.

It has been shown recently that the independent atom model can provide misleading results and does not allow to distinguish between neighbouring 3d metals, whereas aspherical modelling permitted their identification solely from single crystal X-ray diffraction data. [4] While the method is based on the Hansen/Coppens multipole model, the iterations involved are conceptually similar to Hirshfeld-atom refinement. [5]

In our current study several further 3d-metal complexes were studied. These were examples of pairs of published structures with nearly identical lattice constants but different metal atoms, where the differing chemical composition might already be questioned on chemical grounds, and where only diffraction data are available (e.g. in the form of a CIF and deposited structure factors). It is shown that aspherical-atom refinement then permits to identify and confirm the chemically most plausible metal atom in these metal-organic compounds.

Schmøkel *et al.* *Z. Anorg. Allg. Chem.* 2013, 11, 1922.

Hansen and Coppens, *Acta Crystallogr. Sect. A* 1978, 34, 909.

Dittrich *et al.* *Acta Crystallogr. Sect. B* 2013, 69, 91.

Dittrich *et al.* *ChemPhysChem* 2015, 16, 412.

Jayatilaka and Dittrich, *Acta Crystallogr. Sect. A* 2008, 64, 383. Capelli *et al.* *IUCrJ* 2014, 1, 61.

**MS22-P2** Charge density and disorder in  $\text{Al}_2\text{Ru}$ Horst Borrmann<sup>1</sup>, Michael Wedel<sup>1,2</sup>, Lev Akselrud<sup>1,3</sup>, Miroslav Kohout<sup>1</sup>, Yu-Sheng Chen<sup>4</sup>, Tibor Koritsanszky<sup>5</sup>, Yuri Grin<sup>1</sup>

1. Max Planck Institute for Chemical Physics of Solids, 01187 Dresden, Germany
2. European Spallation Source, 22363 Lund, Sweden
3. Dept. of Inorg. Chem., Ivan Franco National University, Lviv, Ukraine
4. ChemMatCars, University of Chicago, USA
5. Dept. of Chem., Middle Tennessee State Univ., USA

email: borrmann@cpfs.mpg.de

The simple intermetallic compound  $\text{RuAl}_2$  exhibits remarkable physical properties, e.g. it is an unconventional semiconductor with narrow band gap [1]. In terms of structural features it is considered a parent structure and main building block for the family of Nowotny chimney Ladder (NCL) structures [2]. In contrast to the intriguing structures of most NCL compounds, the adopted  $\text{TiSi}_2$  type structure is 'well behaved' as it is not modulated and therefore composite structure approach needs not to be applied [3]. In order to avoid problems due to inelastic scattering with Ag-target X-ray sources and in order to collect Bragg intensities up to very high resolution, diffraction data were collected at beamline ID-15-B of the Advanced Photon Source applying 30 keV X-rays. Since a large fraction of possible Bragg reflections is systematically weak, special efforts were necessary in order to extract reliable intensities from measured images. The fundamental approach as implemented in EVAL15 finally gave very good results [4]. The independent atom refinement already derives a model with excellent agreement, however, a faint indication of specific disorder is revealed. After applying the multipolar model according to Hansen and Coppens using XD-2006 [5], charge transfer from Al atoms towards Ru is clearly derived.  $\text{Al}_2\text{Ru}$  obviously is a more adequate description in perfect agreement with Si,Ti as given in the early determination of the parent structure [6]. Details of chemical bonding along with interpretation of detected disorder in terms of stacking faults will be discussed. Similar deviations in typically well-known structures seem to be quite common and deserve careful consideration.

[1] D. Mandrus, V. Keppens, B.C. Sales, and J.L. Sarrao, *Phys. Rev.* **B58** (1998) 3712.

[2] D.C. Fredrickson, S. Lee, R. Hoffmann, and J. Lin, *Inorg. Chem.* **43** (2004) 6151.

[3] F.E. Rohrer, H. Lind, L. Eriksson, A.-K. Larsson, and S. Lidin, *Z. Kristallogr.* **215** (2000) 650.

[4] A.M.M. Schreurs, X. Xian, and L.M.J. Kroon-Batenburg, *J. Appl. Crystallogr.* **43** (2010) 70.

[5] T. Koritsanszky, P. Macchi, A. Volkov, L.J. Farrugia, C. Gatti, P. Mallinson, and T. Richter, XD-2006 A Computer Program Package for Multipole Refinement, Topological Analysis of Charge Densities and Evaluation of Intermolecular Energies from Experimental or Theoretical Structure Factors, 2007.

[6] F. Laves, and H.J. Wallbaum, *Z. Kristallogr.* **101** (1939) 78.

**Keywords:** intermetallic compounds, charge density, disorder

**MS23** Charge and spin density of materials at extreme conditions

Chairs: Nicola Casati, Philippe Guionneau

**MS23-P1** Vitamin C RevisitedNatalie T. Johnson<sup>1</sup>, Michael R. Probert<sup>1</sup>

1. Department of Chemistry, Newcastle University, Newcastle Upon Tyne, UK

email: N.Johnson5@newcastle.ac.uk

X-ray charge density (CD) studies are notorious for requiring high quality diffraction data to ensure the production of physically meaningful results. With continual improvements in both processing software and experimental hardware it may be useful to revisit previously studied compounds. This may afford the option to fully test these developments to discover additional subtleties in the structures. Alongside this, there is growing research into the reproducibility of CD refinements that have continued beyond the investigations into oxalic acid dihydrate<sup>1</sup>. This original study found that for four CD studies while significant features were reproducible in electron density maps, both '*peak shapes and locations of maxima differ in detail*', leading researchers to advise caution when interpreting experimental distributions.

Further concern was raised when discrepancies were found between the dipole moment calculated across half of 2,2'-(1,4-Phenylene)dimalononitrile<sup>2</sup>. When varying either the instrument or refinement procedure the calculated dipoles ranged from 0.84D to 5.36D. It is imperative that CD studies, as with other studies, be reproducible in order to be able to confidently draw conclusions about the electron density of molecules. However, it has previously been shown that the CD multipole parameters of chemical fragments of molecules are transferable between systems where the fragments are in similar environments<sup>3,4</sup>.

The availability of high quality crystals of vitamin C provide an ideal test case for our preliminary work into CD reproducibility. The CD of vitamin C has previously been studied at 120K<sup>5</sup> and refined to give good agreement with theoretical and neutron studies. New data will be presented along with an exploration of the reproducibility of charge density models.

An additional property of vitamin C that is of interest is that it crystallizes with  $Z' > 1$  which further allows the investigation into the transferability of multipole parameters between chemical moieties, an underlying requirement for the use of non spherical parameters in models derived from standard resolution datasets<sup>6</sup>.

1 P. Coppens et al., *Acta Cryst. A*, **1984**, **40**, 184-195

2 M. R. Probert, *private communication*, 2007

- 3 C. P. Brock et al., *Acta Cryst. B*, 1991, **47**, 789-797  
 4 V. Pichon-Pesme et al., *J. Phys. Chem.*, 1995, **99**, 6242-6250  
 5 M. Milaneso et al., *J Mol Struct-TheoChem*, 1997, **419**, 139-154  
 6 B. Ditttrich et al., *Angew. Chem. Int. Ed. Engl.*, 2004, **43**, 2718-2721

**Keywords:** charge density,

## MS23-P2 Charge Density Study of Distorting Tetrahedral and Octahedral Cu(II) Complexes

Ai Wang<sup>1</sup>, U. Englert<sup>1</sup>

1. RWTH Aachen, Landoltweg 1, 52056 Aachen

email: 744675445@qq.com

How to understand the intermolecular interactions (especially the hydrogen bond and halogen bond) in the context of crystal packing and the utilization of such understanding in the design of new solids with desired physical and chemical properties is one of the most flourishing fields in crystal engineering.<sup>[1]</sup> Based on the high resolution X-ray data, experimental charge density provides us one perspective to study the interaction existing between two molecules. Furthermore, for those transition metal complexes, which electrons of d-orbital is not fully occupied, experimental charge density also leaves people some kind of clues, which can help to figure out how the distribution of d-orbital's configuration in different coordination situation is.<sup>[2]</sup> In this work, we will present different charge settings for central metal and refinement strategies based on the different data banks in aspheric atomic density expansion<sup>[3]</sup> for distorting tetrahedral and octahedral coordinating surrounding Cu<sup>2+</sup>.

[1]Desiraju, G. R. *Crystal Engineering: The Design of Organic Solids*, Elsevier, 1989, Amsterdam.

[2]Mallinson, P. R., Koritsanzsky, T., Elkaim, E., Li, N., and Coppens, P. *Acta Cryst.* A44, 336(1988).

[3]Hansen, N. K. & Coppens, P. *Acta Cryst.*, A34, 909-921(1978).

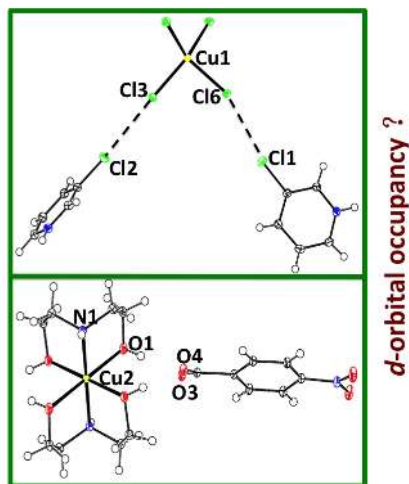


**Figure 1.** How are the d orbital populations distribution for distorting tetrahedral and octahedral Cu(II) complexes?

**Keywords:** Charge Density, d-orbital population, distorting tetrahedral and octahedral Cu(II) complexes

## MS24 Inorganic and metal-organic magnetic structures

Chairs: Georg Eickerling, Bo Iversen

### MS24-P1 Structure determination of coordination polymers of [Co(II)(Htrz)Cl<sub>2</sub>] by powder x-ray diffraction and x-ray absorption spectroscopy

I-Jui Hsu<sup>1</sup>, Bo-Hao Chen<sup>1</sup>, Yu-Chun Chuang<sup>2</sup>, Ling-Yun Jang<sup>2</sup>, Jin-Ming Chen<sup>2</sup>, Jey-Jau Lee<sup>2</sup>, Jyh-Fu Lee<sup>2</sup>

1. Department of Molecular Science and Engineering, National Taipei University of Technology

2. National Synchrotron Radiation Research Center

email: [ijuihsu@mail.ntut.edu.tw](mailto:ijuihsu@mail.ntut.edu.tw)

In developing advanced functional materials, the design and building of metal coordination polymers by forming polynuclear complexes is one way to synthesize potentially applicable materials in separation, catalysis, gas storage, molecular recognition, and magnetism. To achieve this purpose, one of strategies is using polydentate ligands such as 4,4'-bipyridine, pyrazine, and 1,2,4-triazole to chelate with transition metals. The spin crossover compound, [Fe(II)(Htrz)<sub>2</sub>(trz)] (BF<sub>4</sub>), (Htrz = 1,2,4-4H-triazol and trz = 1,2,4- triazolato), was one of the examples synthesized based on such concepts to increase the cooperative effect. However, such kinds of coordination polymers are often not easy to get good quality of single crystal for x-ray single crystal structure determination. Thus, *ab initio* structure determination from powder x-ray diffraction (XRD) data becomes one of important methods. Moreover, extended x-ray absorption fine structure (EXAFS) is an element specific technique to explore the local structure of metal site, which may assist to build a better model for further structure determination in XRD data. Here, we present the structure determination of coordination polymers of [Co(II)(Htrz)Cl<sub>2</sub>] (**1**) and its related compounds based on the combination with EXAFS and XRD data. The results indicate that complex **1** is crystallized in orthorhombic system with Ima2 space group, and the cell constants are  $a = 7.0882(2)$  Å,  $b = 11.7408(4)$  Å, and  $c = 6.7152(6)$  Å, with Co-N1 = 2.15(2) Å. The electronic structures and magnetism are also discussed in this report.

**Keywords:** EXAFS, XRD, coordination polymer



## MS24-P2 Interplay of structural complexity and magnetism in $\text{Pr}_2\text{NiO}_{4+\delta}$ single crystals.

Shantanu Mishra<sup>1,2</sup>, Jürg Schefer<sup>2</sup>, Lukas Keller<sup>2</sup>, Matthias D. Frontzek<sup>2</sup>, Monica Ceretti<sup>1</sup>, Werner Paulus<sup>1</sup>

1. Chimie et Cristalochimie des Matériaux (C2M), Institut Charles Gerhardt, Université de Montpellier, F-34095, France

2. Laboratory for Neutron Scattering and Imaging (LNS), Paul Scherrer Institut, 5232 Villigen PSI, Switzerland

email: shantanu.mishra@empa.ch

The discovery of high- $T_c$  superconductivity in substituted lanthanum cuprate, belonging to the Ruddlesden-Popper phase, fuelled a general interest in the structural and electronic properties of rare-earth transition metal oxides. In this regard, there have been few reports on electronic properties of  $\text{Pr}_2\text{NiO}_{4+\delta}$ . On the other hand, Ruddlesden-Popper-type structures reversibly intercalate oxygen ions, and may thus find application in high-performance solid-oxide fuel cells. It was reported that low-temperature oxygen mobility in such compounds is triggered by low-energy phonons<sup>[1]</sup>. Regarding this,  $\text{Pr}_2\text{NiO}_{4+\delta}$  is a promising candidate due to its superior low-temperature oxygen conductivity over currently employed materials. Associated with oxygen intercalation in  $\text{Pr}_2\text{NiO}_4$  is the emergence of structural complexity in the form of a long-range ordered oxygen superstructure, and partial oxidation of  $\text{Ni}^{2+}$  ions to  $\text{Ni}^{3+}$ . This motivates a deeper understanding of the influence of superstructure and transition metal valence states on the electronic properties of the non-stoichiometric compounds.  $\text{Pr}_2\text{NiO}_{4+\delta}$  presents a system where there could be multiple and complex ordering mechanism at play - including charge-, orbital- and spin-ordering - which presents a complex albeit fundamentally interesting physical system to study. Work towards this direction is expected to give insight into emergence of novel electronic properties via hole-doping in Ruddlesden-Popper phases.

We present here results of macroscopic magnetic measurements and single crystal neutron diffraction measurements on DMC and TriCS (SINQ) on three variants of the parent compound:  $\text{Pr}_2\text{NiO}_{4.12}$ ,  $\text{Pr}_2\text{NiO}_{4.25}$  and  $\text{Pr}_{1.5}\text{Sr}_{0.5}\text{NiO}_4$ , which is isoelectronic to  $\text{Pr}_2\text{NiO}_{4.25}$  but devoid of oxygen superstructure. Through a careful comparison of the experimental results, it is seen that while the general exchange interaction in the compounds is anti-ferromagnetic, the oxygen superstructure and transition metal valence states each play their own distinct role to bring about a complex magnetic order in these compounds (Figure 1).

[1] W. Paulus, H. Schober, S. Eibl, M. Johnson, T. Berthier, O. Hernandez, M. Ceretti, M. Plazanet, K. Conder and C. Lamberti, *J. Am. Chem. Soc.* 2008, 130, 16080-16085.

[2] S. Mishra, *M.Sc. Thesis*, Université de Montpellier, France and Paul Scherrer Institut, Switzerland, 2015, LNS-Report No. 255.

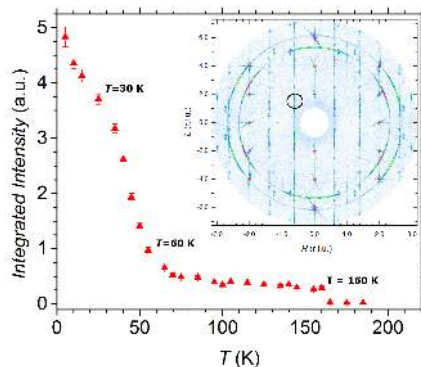


**Figure 1.** Temperature-dependent scan along  $(-0.62, k, 1.46)$  on  $\text{Pr}_2\text{NiO}_{4.25}$  single crystal, showing a three-step transition. The scanned magnetic peak is marked in the (HOL) reciprocal map, where a combined 2D and 3D magnetic order is seen<sup>[2]</sup>.

**Keywords:** Ruddlesden-Popper, Neutron Scattering, Magnetism, Oxygen Superstructure, Fuel Cell, Oxygen Transport

**MS24-P3** Electron density analysis in Quantum Magnets

Rebecca Scatena<sup>1</sup>, Leonardo H.R. Dos Santos<sup>1</sup>, Arianna Lanza<sup>1,2</sup>, Nicola Casati<sup>2</sup>, Björn Wehinger<sup>2</sup>, Christian Rüegg<sup>3</sup>, Mariusz Kubus<sup>1</sup>, Karl Krämer<sup>1</sup>, Lukas Keller<sup>3</sup>, Tom Fennell<sup>3</sup>, Alun Biffin<sup>3</sup>, Piero Macchi<sup>1</sup>

1. Department of Chemistry and Biochemistry, University of Bern, Freiestrasse 3, 3012, Bern, Switzerland  
2. Laboratory for Synchrotron Radiation, Paul Scherrer Institute, 5232 Villigen – PSI Switzerland  
3. Laboratory for Neutron Scattering and Imaging, Paul Scherrer Institute, 5232 Villigen – PSI Switzerland

email: rebecca.scatena@dcb.unibe.ch

We have investigated the correlation between the accurate electron density distribution and the magnetic properties of two metal-organic polymeric quantum magnets, the  $\{[\text{Cu}(\text{pyz})_2\text{Cl}(\text{BF}_4)]_n\}$  and the  $\{[\text{Cu}(\text{pyz})_2\text{Br}(\text{BF}_4)]_n\}$  ( $\text{pyz}$  = pyrazine), using high resolution single crystal X-ray diffraction and density functional theory (DFT) calculations in the crystalline state as well as in the gas phase on selected fragments of the framework. Topological Analysis based on Quantum Theory of Atoms in Molecules (QTAIM) has been applied to characterize the possible magnetic exchange coupling constants. Electron density analysis confirmed the orientation of the magnetic orbital. The magnetic properties have been examined and correlated with the topological and integrated properties of the electronic distribution. This has enabled the detailed rationalization of the experimental antiferromagnetic exchange coupling constants in terms of the interchain Cu-Cu interactions. Molecular orbital and spin density analysis have been used to identify the atomic and group sources of magnetism. In particular, halogens and pyrazine act as typical non-innocent ligands, with large part of the spin density developed on their atoms. In both cases, the experimentally observed antiferromagnetic coupling can be explained by the copper-copper super-exchange coupling mediated by the pyrazine ligands. Moreover, our results suggest a non-negligible coupling through the halogens although the electron density shows a much weaker interaction than the one observed along pyrazine. From this study, it is clear that systematic electron density analysis on transition metal compounds could lead to a better understanding of the super exchange mechanism with a topological description of the involved interactions.

**Keywords:** MOF quantum-magnets electron-density

**MS24-P4** Structural and magnetoelectric study of triethylmethylammonium tetrachloroferrate(III)

Martina Vrankić<sup>1</sup>, Sanja Burazer<sup>1</sup>, Zvonko Jagličić<sup>2</sup>, Ana Šantić<sup>3</sup>, Jasminka Popović<sup>1</sup>

1. Division of Materials Physics, Ruder Bošković Institute, Bijenička 54, 10 000 Zagreb, Croatia  
2. Institute of Mathematics, Physics and Mechanics, Jadranska 19, SI-1000 Ljubljana, Slovenia  
3. Division of Materials Chemistry, Ruder Bošković Institute, Bijenička 54, 10 000 Zagreb, Croatia

email: mvrankic@irb.hr

The novel organic-inorganic hybrids with a perovskite-type structure represent a potentially very attractive platform for interesting electrical and magnetic properties. In contrast to pure inorganic multiferroics, this class of materials exhibit new properties tuned by the nature of metal centers, organic cations and appropriate ligands. It was found that inorganic-organic hybrid compounds containing tetrabromoferrate(III) anion exhibit the ferroelectric and magnetic phase transitions resulting in a strong magnetodielectric coupling at ~360 K [1]. Namely, the combination of disordered cation and magnetic transition metal ion results in formation of a magnetodielectric molecule-based functional material above room temperature.

A dark-yellow polycrystalline sample of a triethylmethylammonium tetrachloroferrate(III) compound was produced by the wet chemical synthesis. Detailed high temperature in-situ X-ray powder diffraction in the range from RT to 400 K was utilized in order to follow the temperature-induced structural changes. Title compound crystallizes in hexagonal space group  $P6_3mc$  at RT where the organic cationic part is completely disordered. Both the  $\text{FeBr}_4^-$  anion and the organic cation lie on a hexagonal axis. It was found that structural phase transition of triethylmethylammonium tetrachloroferrate(III) was accompanied with changes in magnetic and electrical behaviour as shown in Figure 1. Since for most multiferroics, the magnetic phase transition temperature is much lower than the ferroelectric phase transition temperature, (finally resulting in a weak coupling between magnetic and ferroelectric orderings) this compound exhibiting transitions at similar temperatures shows potential for further investigations of magnetoelectric coupling.

1. Cai, H.-L., et al., *Above-Room-Temperature Magnetodielectric Coupling in a Possible Molecule-Based Multiferroic: Triethylmethylammonium Tetrabromoferrate(III)*. Journal of the American Chemical Society, (2012)**134**, 18487-18490.

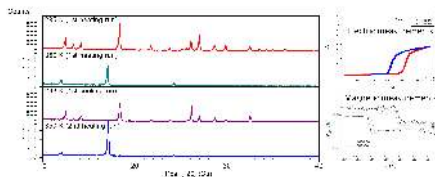


**Figure 1.** XRD, electric and magnetic measurements of triethylmethylammonium tetrachloroferrate(III) compound

**Keywords:** X-ray powder diffraction, organic-inorganic hybrid compounds, phase transition

**MS24-P5 Investigation on the low temperature distorted phase of  $\text{MgCr}_2\text{O}_4$**

Shang Gao<sup>1,2</sup>, Oksana Zaharko<sup>1</sup>, Tom Fennell<sup>1</sup>, Vladimir Tsurkan<sup>3,4</sup>, Christian Rueegg<sup>1,2</sup>

1. Laboratory for Neutron Scattering and Imaging, Paul Scherrer Institut, Switzerland
2. Department of Quantum Matter Physics, University of Geneva, Switzerland
3. Experimental Physics V, University of Augsburg, Germany
4. Institute of Applied Physics, Academy of Science of Moldova, Republic of Moldova

email: shang.gao@psi.ch

Despite extensive studies of the spinel  $\text{ACr}_2\text{O}_4$  systems, some basic questions still remain to be addressed [1-2]. What is the low temperature (LT) nuclear structure? How does this structural distortion influence the  $\text{Cr}^{3+}$  spin configuration? And, perhaps the most crucial one for understanding their spin dynamics, what is the exchange strength in the distorted phase? Here, using synchrotron/neutron diffraction and neutron scattering methods, we tried to answer these questions on  $\text{MgCr}_2\text{O}_4$ . Powder synchrotron diffraction shows that the LT structure belongs to the  $Fddd$  space group, which contradicts previous  $I4_1amd$  space group determined from neutron diffraction but is consistent with the magnetic resonance measurements on the related  $\text{ZnCr}_2\text{O}_4$  compound [3]. Based on  $Fddd$  space group, magnetic structure was solved from single crystal neutron diffraction data with both symmetry analysis and simulated annealing methods. Finally, we discussed the spin dynamics in  $\text{MgCr}_2\text{O}_4$  measured with both hot and cold triple-axis spectrometers.

- [1] S.-H. Lee, et. al., Nat. 418, 856 (2002)
- [2] K. Tomiyasu, et. al., Phys. Rev. Lett. 110, 077205 (2013)
- [3] V. N. Glazkov, et. al., Phys. Rev. B 79, 024431 (2009)

**Keywords:** spinel, spin-lattice coupling, neutron scattering, synchrotron x-ray diffraction

## MS24-P6 $\text{Mn}(\text{H}_2\text{O})_{1.5}(\text{C}_{14}\text{H}_8\text{O}_4)_n$ , a magnetic MOF with a double inorganic sub-network

Michel Francois<sup>1</sup>, Romain Sibille<sup>2</sup>

1. Institut Jean Lamour, Université de Lorraine, Nancy, France  
2. Laboratory for Scientific Developments and Novel Materials, Paul Scherrer Institut, Villigen, Switzerland

email: michel.francois@univ-lorraine.fr

Two new magnetic Metal Organic Frameworks (MOFs) were synthesized by solvothermal reaction in the system  $\text{Mn}-\text{C}_{14}\text{H}_8\text{O}_4$  (biphenyldicarboxylate = bpdcc)- $\text{H}_2\text{O}$ .  $\text{Mn}(\text{H}_2\text{O})_{1.5}(\text{C}_{14}\text{H}_8\text{O}_4)_n$  **1** (SG = C2/c, Z = 8, Dx = 1.67 g/cm<sup>3</sup>, a = 53.329(2) Å, b = 6.4911(2) Å, c = 7.4036(2) Å, b = 90.59(1)°, V = 2562.8 Å<sup>3</sup>, R<sub>1</sub> = 8.5% ), and  $\text{Mn}_2(\text{OH})_2(\text{C}_{14}\text{H}_8\text{O}_4)_n$  **2** (SG = P-1, Z = 1, Dx = 1.927 g/cm<sup>3</sup>, a = 14.2039(4) Å, b = 6.4785(1) Å, c = 3.4530(3) Å, a = 90.09(1)°, b = 96.84(2)°, g = 91.710(2)°, V = 315.34 Å<sup>3</sup>, R<sub>1</sub> = 6.8%). The crystal structures of **1** and **2** were solved from synchrotron powder diffraction data using optimization methods in direct space with the FOX program [1], and refined using the Rietveld method. The complexity of **1** needed additional information from IR spectroscopy and thermogravimetric analysis. Compound **1** has a lamellar structure built up from a double inorganic sub-network. It consists of two slabs of metallic ions differing by their hydration: (i) a layer of composition  $\text{Mn}(\text{H}_2\text{O})_2$ , already encountered in  $\text{Mn}(\text{H}_2\text{O})_2(\text{C}_6\text{H}_4\text{O}_4)_n$  [2], where manganese cations are inside an octahedral environment, and (ii) an original layer with composition  $\text{Mn}(\text{H}_2\text{O})$  where manganese is five-fold O-coordinated in a triangular deformed bi-pyramid. These two slabs are bridged by the benzene biphenyldicarboxylate molecule along the stacking direction corresponding to the long period of 53.32 Å. This original structure influences the magnetic properties. Alternative susceptibility shows two magnetic transitions attributed to the two sub-networks ordering at two different temperatures. Two anomalies at the same temperatures in the heat specific measurement confirm this scenario. Notably, only one magnetic hybrid compound featuring two different inorganic layers was reported before [3]. The layered structure of **2** is isorecticular with that of  $\text{Cu}_2(\text{OH})_2(\text{C}_8\text{H}_4\text{O}_8)_n$  [4]. The dicarboxylate molecules bridge the single inorganic slab with composition ' $\text{Mn}(\text{OH})_2$ ' where Mn atoms are in an octahedral environment.

[1] Favre-Nicolet V. and Cerny R., J. Appl. Crystallogr. 2002, 35, 734-743. [2] Sibille R., Mesbah A., Mazet T., Malaman B. and François M., Journal of Solid State Chemistry 186, 2012, 134-141 [3] Saines P. J., Melot B. C., Seshadri R. and Cheetham A. K., Chem. Eur. J. **2010**, 16, 7579-7585. [4] Abdelouhab S., François M., Elkaim E., Rabu P., Solid State Sciences 7 (2): 227-232 Feb 2005

**Keywords:** ab-initio structure, dicarboxylate, magnetic MOF.

## MS25 Quasicrystal and approximant: structure and properties

Chairs: Cesar Pay Gomez, Emilie Gaudry

### MS25-P1 Two-shell nanoclusters in intermetallic compounds: beyond the icosahedral core

Tatiana G. Akhmetshina<sup>1,2</sup>, Vladislav A. Blatov<sup>1,2</sup>

1. Samara National Research University, 34, Moskovskoye shosse, Samara, 443086, Russia  
2. Samara Center for Theoretical Materials Science, Ac. Pavlov St. 1, 443011 Samara, Russia

email: akhmetshina.tanya@yandex.ru

In this work, we apply the nanocluster method [1] to analyze all known intermetallic compounds containing two-shell nanoclusters with icosahedral core. Using the ToposPro program package [2] we have found all intermetallics with two-shell nanoclusters as primary nanoclusters or local configurations., we have analyzed in more details Mackay, Bergman, Bergman-based and two types of icosahedral-based 63-atom nanoclusters, which have been discovered for the first time using the nanoclustering procedure [3]. With the TTN collection [4] we have found that the four isomeric 63-atom clusters occur in 60 topological types of intermetallic compounds, and only two models of these clusters contain icosahedral inner polyhedron. We have also studied all kinds of isomeric Bergman-type 0@12@32 and 1@12@32 nanoclusters, which occur in intermetallics. Simplification of the nanocluster representations to their underlying nets revealed widespread topologies such as body-centered cubic (**bcc-x**), face-centered cubic (**fccu**), and hexagonal primitive (**hex**). We have performed topological analysis of these intermetallics in terms of local and overall binding of clusters. The statistical data on chemical composition of the nanoclusters and their topological descriptors are presented. We have found 23 and 3 different topologies for binding of the intermetallics composed of the Bergman clusters and 63-atom clusters, respectively. As a result, the correlations between topological parameters and chemical composition of the nanoclusters were found. For instance, if the inner icosahedron of a Mackay nanocluster consists of the same atoms and composition of the second shell is 30A+12B, the topology of underlying net is **bccu-x** in 82% cases. The results of our analysis are included to the set of the ToposPro topological collections.

[1] Vladislav A. Blatov *Struct. Chem.* **2012**, 23, 955-963.

[2] Vladislav A. Blatov, Alexander P. Shevchenko, and Davide M. Proserpio *Cryst. Growth Des.* **2014**, *14*, 3576-3586 <http://topospro.com>.

[3] Shevchenko, V. Ya.; Blatov, V. A.; Ilyushin, G. D. *Glass Physics and Chemistry*, **2013**, *39*, 3, 229-234.

[4] Arina A. Pankova, Tatiana G. Akhmetshina, Vladislav A. Blatov, Davide M. Proserpio *Inorg. Chem.* **2015**, *54*, 6616-6630.

**Keywords:** intermetallics, topology, nanoclusters

## MS25-P2 Brick tiling

Shelomo I. Ben-Abraham<sup>1</sup>, Dvir Flom<sup>1</sup>

<sup>1</sup>. Department of Physics, Ben-Gurion University of the Negev, POB 653, IL-8410501 Beer-Sheva, Israel

email: shelomo.benabraham@gmail.com

We present a three-dimensional analog of the two-dimensional table tiling [1] – a *brick tiling*. Its prototiles are standard bricks (henceforth "protobricks"), i.e. cuboids with edges of  $2^0 = 1$ ,  $2^1 = 2$  and  $2^{d-1} = 2^2 = 4$  units ( $d$  for dimension). They consist of  $2^{(d-1)d/2} = 2^{2 \times 3/2} = 2^3 = 8$  basic cubes and come in  $d! = 3! = 6$  orientations. A 3D brick is a *rep-tile*, i.e. a polyhedron that can be nontrivially tiled by smaller, congruent copies of itself. Thus it induces the inflation shown in the Figure. Moreover, we have devised a code identifying the basic cubes by  $6 \times 8 = 48$  "colors" and constructed a lattice substitution tiling that reproduces the brick tiling. We also discuss possible generalizations to arbitrary dimensions.

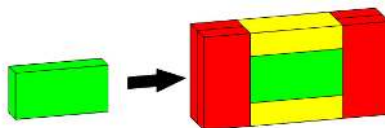


**Figure 1.** Three-dimensional brick inflation.

**Keywords:** brick tiling, lattice substitution tiling

## MS25-P3 First surface structure determination of a quasicrystalline approximant using combined surface x-ray diffraction and ab initio calculations.

Emilie Gaudry<sup>1</sup>, Corentin Chatelier<sup>1</sup>, Roberto Felici<sup>2,3</sup>, Jakub Drnec<sup>2</sup>, Marc de Boissieu<sup>4,5</sup>, Guillaume Beutier<sup>4,5</sup>, Laura Serkovic Loli<sup>1</sup>, Garry McGuirk<sup>1</sup>, Marie-Cécile de Weerd<sup>1</sup>, Julian Ledieu<sup>1</sup>, Vincent Fournée<sup>1</sup>

1. Institut Jean Lamour - Université de Lorraine CMRS UMR 7198
2. ESRF, Grenoble, France
3. CNR-SPIN, Area della ricerca di Tor Vergata, Via del fosso del cavaliere 100, Roma, Italy
4. Université Grenoble Alpes, Simap, Grenoble, France
5. CNRS Simap, Grenoble, France

email: emilie.gaudry@univ-lorraine.fr

Because of their large crystal cells, generally described as clusters assembly, the determination of quasicrystalline approximant surface structure is a challenging task. It results from the interplay between the selection of specific atomic planes at the surface and the preservation of atomic clusters up to the surface. Moreover, surface segregation and interatomic relaxations also play a role to decrease the surface energy.

In this work, we re-investigate the pseudo-10fold surface of the  $Al_{13}Co_4$  complex intermetallic compound (Fig. 1 left) [1,2], considered as a decagonal approximant, using both surface x-ray diffraction (SXRD) and density functional theory (DFT) calculations. SXRD has the advantage compared to dynamical low-energy electron diffraction (LEED-IV) that one can generally ignore multiple scattering, which makes data analysis more straight-forward. The determination of the surface structure by SXRD was only possible due to the large experimental dataset which could be recorded at ESRF – the largest experimental dataset ever analyzed with this technique – a consequence of the high density of crystal truncation rods and of the relatively low symmetry of the system.

Fits of the SXRD data allowed to discriminate among various surface models and pointed towards a bulk truncated surface at dense Al-rich puckered planes where protruding surface Co atoms are missing. Surface relaxations and exact atomic positions obtained by SXRD and complementary DFT calculations are very similar and give confidence in the analysis. In addition, the surface energy of the corresponding surface model could be estimated from DFT calculations with a rather low value of  $1.09 \text{ J/m}^2$ . This in turn allowed us to estimate interfacial energy differences, consistent with a complex interface structure. This study opens new perspectives for the determination of complex surface structures, such as quasicrystalline and related intermetallic surfaces.

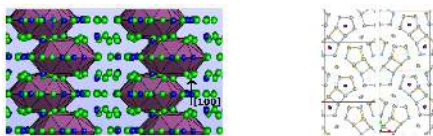


**Figure 1.** Left: Crystal structure of  $Al_{13}Co_4$  highlighting Henley-type clusters. Right: Comparison of positions of surface atoms deduced from SXRD (blue) and DFT (red-orange).

**Keywords:** approximant, surface structure, surface x-ray diffraction, calculations based on density functional theory

## MS25-P4 A complex pseudo-decagonal quasicrystal approximant solved by the strong reflections approach and refined against Rotation Electron Diffraction (RED) data

Sven Hovmöller<sup>1</sup>, Devinder Singh<sup>1</sup>, Benjamin Grushko<sup>2</sup>, Wei Wan<sup>1</sup>, Yifeng Yun<sup>1</sup>, Xiaodong Zou<sup>1</sup>

1. Department of Materials and Environmental Chemistry, Stockholm University, SE 10691 Stockholm, Sweden  
2. PGI-5, Forschungszentrum Jülich, 52425 Jülich, Germany

email: sven.hovmoller@mmk.su.se

The strong-reflections approach is valid on structures that contain similar atomic clusters and electron diffraction patterns with similar intensity distribution of reflections. It is based on the fact that the strongest reflections largely determine the atomic positions in a structure and represent the main structure features of a crystal. Thus, this approach can be used for structure solution. In the present study, the structure of the complex pseudo-decagonal (PD) quasicrystal approximant PD1 in the Al-Co-Ni alloy system was solved by phasing the strong reflections from rotation electron diffraction [1] (RED) data using the known PD2 structure [2]. The PD1 crystal is primitive and orthorhombic *Pnam*, with unit cell parameters  $a=37.7$ ,  $b=39.7$ ,  $c=4.1$  Å. Electron diffraction studies show that in reciprocal space, the positions of the strongest reflections and their intensity distributions are similar for both approximants. The high-resolution transmission electron microscopy (HRTEM) image after image processing with CRISP (crystallographic image processing program) shows that PD1 and PD2 intergrow with each other. The orientation relationship between PD1 and PD2 was found by comparing the Fourier transforms, calculated from the two regions in the HRTEM image. By applying the strong-reflections approach, the structure factor amplitudes and phases of PD1 were deduced from those of the known PD2 structure. The structure of PD1 contains 115 unique atoms (31 Co/Ni and 84 Al). They were located from a density map calculated from only the 15 (!) strongest unique reflections. As with other approximants in the PD series, PD1 is built of characteristic 2 nm wheel clusters with 5-fold rotational symmetry [3], which agrees with results from HRTEM images.

### References

- [1] Wei Wan et al. *J. App. Crystallogr.* **46** (2013) 1863-1873.
- [2] Devinder Singh et al. *J. App. Crystallogr.* **47** (2014) 215-221.
- [3] Devinder Singh et al. *J. App. Crystallogr.* **49** (2016) 433-441.

**Keywords:** quasicrystals, approximants, rotation electron diffraction, strong reflections approach

## MS25-P5 New binary and Cd-substituted barium mercurides: $\text{BaHg}_3$ , $\text{Ba}_3(\text{Hg}/\text{Cd})_{11}$ and $\text{Ba}_7(\text{Hg}/\text{Cd})_{32}$

Caroline Röhr<sup>1</sup>, Marco Wendorff<sup>1</sup>

1. Universität Freiburg, Institut für Anorganische und Analytische Chemie

email: caroline@ruby.chemie.uni-freiburg.de

Recently, we reported on the new binary Hg-rich Ba mercurides  $\text{BaHg}_3$  [1] and  $\text{Ba}_{20}\text{Hg}_{103}$  (together with a small Zn/Cd substitution) [2]. For the Ba-richer compounds in the range  $\text{BaHg}_3$  to  $\text{BaHg}_{-5}$  (and again their Cd-substituted derivatives) experimental (synthesis from stoichiometric amount of the elements at  $T_{\text{max}}$  of 800 to 900 °C) and crystallographic (single crystal) investigation also require a further revision of the Ba-Hg phase diagram [3] and the composition and structure of the 7:31 phases. Additionally, the new phase  $\text{BaHg}_3$  was obtained. It crystallizes with a new structure type in the rare space group *P4/ncc* ( $a = 1193.04(3)$ ,  $c = 958.02(5)$  pm,  $Z = 12$ ,  $R1 = 0.0461$ , fig. a). The three crystallographically different Hg atoms form holey distorted flat square pyramids, a structure motif which is similarly found in the 3:11 compounds (see below and fig. (b) and (c)) and in  $\text{K}_3\text{Hg}_{19}$  [4]. The Ba polyhedra exhibit coordination numbers of 12 and 14. The electronic bandstructure, which has been calculated within the framework of FP-LAPW theory, exhibits a pronounced pseudo band gap.

The phase width of the Cd-containing  $\text{La}_3\text{Al}_{11}$ -type structure (orthorhombic *Immm*, fig. (c)) reaches from the already described fully ordered phase  $\text{Ba}_3\text{CdHg}_{10}$  (9.1 % Cd, [5]) up to a Cd content of 47 % ( $\text{Ba}_3\text{Cd}_{3.2}\text{Hg}_{5.8}$ ). At the same 3:11 composition, but with a further reduced Cd proportion of only 3 %, the orthorhombic  $\text{Ba}_3\text{ZnHg}_{10}$ -type [2] (fig. (b)) was obtained, which also occurs with a very small Ga-content in  $\text{Ba}_3\text{Ga}_{0.2}\text{Hg}_{10.8}$  [5].

The composition and structure of the hexagonal '7:31' compounds (powder data for the mercuride [3], single crystal data film data for the cadmide [6]) were investigated for the whole Hg-Cd series. Herein, the formation of different types of orthorhombic and monoclinic superstructures (with complex twinning) was observed, which all exhibit  $M_3$  squares instead of disordered  $M_3$  triangles as common faces between the Ba(4) polyhedra (gold in fig. (d)) around the pseudo-hexagonal *c* axis, leading to a 7:32 instead of the originally reported 7:31 composition.

[1] M. Wendorff, C. Röhr, *J. Alloys Compd.*, **546**, 320 (2013).

[2] M. Schwarz, M. Wendorff, C. Röhr, *J. Solid State Chem.*, **196**, 416 (2012).

[3] G. Bruzzone, F. Merlo, *J. Less-Common Met.*, **39**, 271 (1975).



[4] E. Biehl, H. J. Deiseroth, *Z. Anorg. Allg. Chem.*, **625**, 389 (1999).

[5] M. Wendorff, C. Röhr, *Z. Naturforsch.* **68b**, 307 (2013).

[6] G. Bruzzone, M. L. Fornasini, *Acta Crystallogr. B30*, 317 (1974).

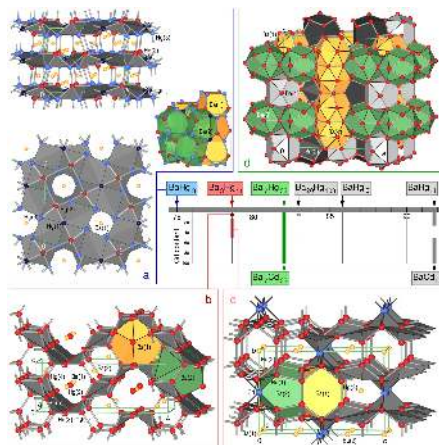


**Figure 1.** Phase widths and crystal structures of Ba mercurides and its ternary Cd derivatives: (a)  $\text{BaHg}_2$  (new structure type); (b, c): Cd-containing 3:11 phases of the  $\text{Ba}_2\text{ZnHg}_{10}$ - and the  $\text{La}_2\text{Al}_{11}$ -type, (d): polyhedra representation of the structure of the corrected pseudohexagonal 7:32 compounds.

**Keywords:** Mercurides, Synthesis, Bandstructure calculation

## MS25-P6 Two-dimensional oxide quasicrystals from perovskites

Stefan Förster<sup>1</sup>, Sebastian Schenk<sup>1</sup>, Klaus Meinel<sup>1</sup>, Rene Hammer<sup>1</sup>, Florian Schumann<sup>1</sup>, Wolf Widdra<sup>1,2</sup>

1. Institute of Physics, Martin-Luther-Universität Halle-Wittenberg

2. Max-Planck-Institut für Mikrostrukturphysik

email: stefan.foerster@physik.uni-halle.de

In addition to the well-known intermetallic and soft quasicrystals (QC), recently a two-dimensional oxide quasicrystal (OQC) has been discovered [1]. This OQC is derived from  $\text{BaTiO}_3$  thin films on a hexagonal Pt(111) substrate. Low-energy electron diffraction (LEED) reveals a twelve-fold rotational symmetry. Scanning tunneling microscopy (STM) at room temperature as well as at low temperatures (80 K) allow to resolve the atomic structure. The aperiodic structure is formed by primitive atomic arrangements in squares, triangles, and rhombs with a universal edge length of 0.69 nm. The resulting tiling is comparable to an ideal Stampfli-Gähler tiling [2]. In addition to this dodecagonal atomic arrangement, building blocks of squares, triangles, and rhombs are also found on  $(2+\sqrt{3})$  and  $(2+\sqrt{3})^2$  larger scales indicating the characteristic self-similarity of an ordered QC. The high-resolution STM measurements allow furthermore to identify phason flips on the atomic scale.

The observed interface-driven formation of a 2D OQC is not limited to this particular materials combination. Following an analogous preparation procedure, we show that  $\text{SrTiO}_3$  on Pt(111) develops an OQC as well. As a consequence of the 2% smaller lattice constant of  $\text{SrTiO}_3$  in comparison to  $\text{BaTiO}_3$ , the fundamental length of the  $\text{SrTiO}_3$ -derived OQC is 2% smaller. Nevertheless, the epitaxial alignment of the  $\text{SrTiO}_3$ -derived OQC with respect to the Pt(111) lattice as determined by LEED as well as the local atomic arrangement as measured by STM are identical with that of the  $\text{BaTiO}_3$ -derived OQC. Our results suggest that OQC formation is a general process of perovskite oxides on suitable substrates.

[1] S. Förster, K. Meinel, R. Hammer, M. Trautmann, and W. Widdra, *Nature* 502 (2013) 215.

[2] F. Gähler in: *Quasicrystalline Materials* (World Scientific, 1988)

This work is supported by the Deutsche Forschungsgemeinschaft (DFG) through SFB 762.

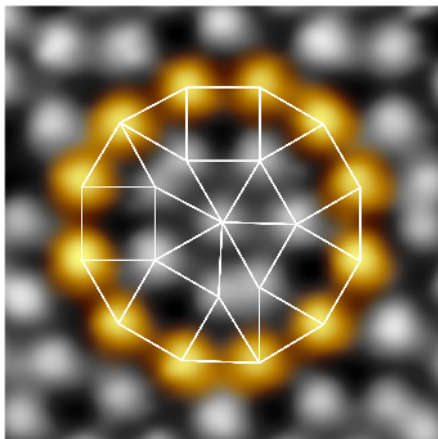


**Figure 1.** Atomically resolved STM image of the typical dodecagonal motif of the BaTiO<sub>3</sub>-derived OQC on Pt(111). A similar tiling is observed for the SrTiO<sub>3</sub>-derived OQC. 4x4 nm<sup>2</sup>, I=30 pA, U=0.1 V.

**Keywords:** Oxide quasicrystal, Bariumtitanate, Strontiumtitanate, STM, LEED

## MS25-P7 New approach to phasonic Debye-Waller factor.

Radosław Strzalka<sup>1</sup>, Ireneusz Buganski<sup>1</sup>, Paweł Kuczera<sup>1</sup>, Janusz Wolny<sup>1</sup>

1. Faculty of Physics and Applied Computer Science, AGH University of Science and Technology, Krakow, Poland

email: strzalka@fis.agh.edu.pl

The very serious concerns of scientists dealing with crystal structure refinement, including theoretical research, pertains to characteristic bias in calculated vs. measured diffraction intensities, observed particularly in weak reflections regime. We attribute it most distinctly to corrective factor for phasons, and give credible proofs of this in our presentation. The lack of consistent theory of phasons in quasicrystals manifests most spectacularly in a characteristic bias of fitted vs. observed diffraction intensities. In our presentation we show that the most commonly used exponential Debye-Waller factor for phasons fails in case of quasicrystals and propose a novel method of calculating the correction factor within a statistical approach. Our results obtained for model quasiperiodic systems show that phasonic perturbations can be successfully described. It is possible to include very weak reflections to a dataset during the structure refinement and fits of high quality are achievable.

By phonons we mean a rearrangement of atoms in the structure [1]. The calculations are performed for vertex decoration models based on 1D Fibonacci chain and 2D Penrose tiling. For such models, phasons can be introduced as flips of tiles violating matching rules. Such flips are easily recognized within statistical method based on average unit cell concept [2]. The probability distributions of atomic positions calculated against some reference lattice are sensitive to phason flips, which occur in their fragmentation as comparing to ideal shapes [3]. The level and manner of this fragmentation depends on the amount and type of flips introduced to the system. Including this in a definition of structure factor automatically solves the problem of phasons at the very basic level of calculating the diffraction pattern. Neither any multiplicative correction factor nor iterative fitting of parameters in the Gaussian's exponent is required. The only free parameter to fit would be a number of phason flips, which has a very physical grounds.

[1] de Boissieu M., Phonons, phasons and atomic dynamics in quasicrystals, Chem. Soc. Rev. 41, 6778-6786, (2012).

[2] Wolny J., The reference lattice concept and its application to the analysis of diffraction patterns, Philos. Mag. A77, 395-412, (1998).

[3] Wolny J., Buganski I., Kuczera P., Strzalka R., Pushing the limits of crystallography, submitted (2016).

**Keywords:** phasons, quasicrystals, correction factor

## MS26 Incommensurate modulated and composite phases

Chairs: Michal Dusek, Artem Abakumov

### MS26-P1 Structural complexity and O<sup>2-</sup> ordering in Pr<sub>2-x</sub>Sr<sub>x</sub>NiO<sub>4+δ</sub> studied by single crystal x-ray diffraction

Rajesh Dutta<sup>1,2</sup>, Avishek Maity<sup>1</sup>, Monica Ceretti<sup>1</sup>, Antoine Villesuzanne<sup>2</sup>, Werner Paulus<sup>1</sup>

1. Institut Charles Gerhardt, UMR 5253, CNRS-University Montpellier, 34095 Montpellier, France

2. ICMCB, UPR 9048, University Bordeaux, 33600 Pessac, France

email: rajeshatiitm@gmail.com

Ruddlesden-popper phases especially those with K<sub>2</sub>NiF<sub>4</sub>-type structure, are of particular interest, as they exhibit high ionic and electronic conductivity already at moderate temperatures. Among them, Pr<sub>2</sub>NiO<sub>4+δ</sub> phases have attracted much attention as promising materials, showing a rather wide range of oxygen non-stoichiometric and accommodating extra oxygen on interstitial lattice sites, suitable for membranes in next generation SOFCs. A high oxygen doping level has been shown to induce a special lattice dynamics, allowing the apical oxygen atoms to easily move to vacant interstitial sites on a shallow energy diffusion pathway<sup>[1,2]</sup>.

Hole doping in Pr<sub>2</sub>NiO<sub>4</sub>, either by substituting Pr with Sr cations or by O<sup>2-</sup> ion intercalation on interstitial lattice sites modifies the structural (ordering of O<sup>2-</sup> ions) and electronic ordering in Pr<sub>2-x</sub>Sr<sub>x</sub>NiO<sub>4+δ</sub>. We investigated the structural evolution of the complex electronic and structural ordering as a function of x and δ by scanning the whole reciprocal space using single crystal x-ray diffraction. The average structure changes from orthorhombic *Fmmm* (x = 0 and 0.125) to tetragonal *P4/2ncm* (x = 0.25 and 0.5) in Pr<sub>2-x</sub>Sr<sub>x</sub>NiO<sub>4+δ</sub>. Due to oxygen intercalation δ up to 0.25 and long-range ordering of those O<sup>2-</sup> ions, Pr<sub>2</sub>NiO<sub>4+δ</sub> forms complex superstructures with 2D-incommensurate modulation ( $q_{1,2} = \pm 0.83a^* + 0.49b^*$ ) in the (*hkn*, *n=integer*) reciprocal plane (Fig. 1), still present in the doped crystal (x = 0.125). More complex and different modulation exists in (*hkn*+1/2, *n=integer*) plane due to ordering along *c*-direction which as contrary disappears in doped crystal with x = 0.125. Four twin individuals are present in the as grown Pr<sub>2</sub>NiO<sub>4+δ</sub> single crystal which also makes the incommensurate modulation more complex whereas this modulation disappear gradually and new p-type superstructure reflections appear when entering to the tetragonal phase of Pr<sub>2-x</sub>Sr<sub>x</sub>NiO<sub>4+δ</sub> (x=0.25 and 0.5) with no modulated incommensurate superstructure.

#### Reference:

[1] M. Ceretti, O. Wahyudi, A. Cousson, A. Villesuzanne, M. Meven, B. Pedersen, J. M. Bassat and W. Paulus, *J. Mater. Chem. A*, 2015, 3 (42), 21140-21148.

[2] O. Wahyudi, M. Ceretti, I. Weill, A. Cousson, F. Weill, M. Meven, M. Guerre, A. Villesuzanne, J.-M. Bassat and W. Paulus, *CrystEngComm*, 2015 17, 6278-6285.

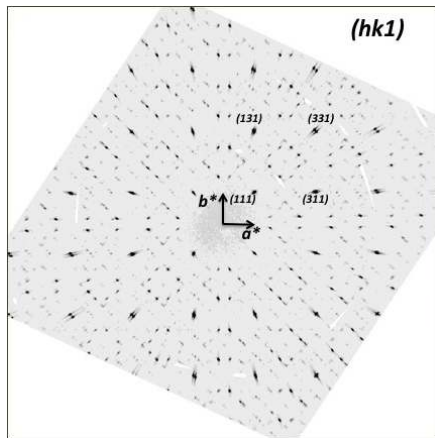


**Figure 1.** (*hk1*) reciprocal plane of Pr<sub>2</sub>NiO<sub>4.25</sub> containing incommensurate superstructure reflections along with main reflections @RT reconstructed from X-ray single crystal diffraction data obtained on a STOE STADIVARI diffractometer (Mo Kα  $\mu$ -focus) equipped with a 2D Pilatus detector.

**Keywords:** Hole doped, Incommensurate modulation, Oxygen/charge ordering

## MS26-P2 The mystery of the AuIn 1:1 phase

Laura C. Folkers<sup>1</sup>, Sven Lidin<sup>1</sup>

1. Centre for Analysis and Synthesis, Lund University, Naturvetarvägen 14, 223 62 Lund, Sweden

email: laura.folkers@chem.lu.se

Recently, the Gold Indium system has regained interest due to its importance for applications in soldering and nanowire growth. For these applications knowledge of the occurring components in the phase diagram is important. Earlier studies of this alloy were able to uncover most currently known compounds along with their crystal structures. Only the structure of the seemingly most straight-forward one, AuIn 1:1, has not been elucidated. Its lattice parameters are known from earlier experiments [1], but growth of single crystals has proved difficult.

The powder diffraction pattern contains unindexed peaks that cannot be explained by any known Au-In binary or by any known oxide or nitride. The problem is exacerbated by the tendency of the compound to amorphisize on grinding. Subsequent annealing at low temperature (400°C) however restores full crystallinity.

Differential thermal analysis (DTA conf. Fig. 1) reveals further surprises. On heating, a small endothermic peak appears at 440°C while a second endotherm at 515°C corresponds well with the reported melting point of AuIn ( $T_M = 510^\circ\text{C}$  [2]). On cooling only one exothermic peak can be observed, which, in position, corresponds to the low temperature exotherm at 440°C, but in size it corresponds to the high temperature endotherm at 515°C.

An electron diffraction study reveals weak satellites in AuIn, indicating that the structure may be incommensurately modulated [3].

In this study we will discuss structure models for AuIn and possible explanations for the thermal behaviour.

[1] K. Schubert, U. Rösler, M. Kluge, K. Anderko, L. Härle, *Naturwissenschaften*, **40**, (1953), pp.437

[2] I. Ansara, J.-Ph. Nabot, *CALPHAD*, **16**, (1992), pp. 13-18

[3] Wilder Carillo-Cabrera, unpublished work, (2014)

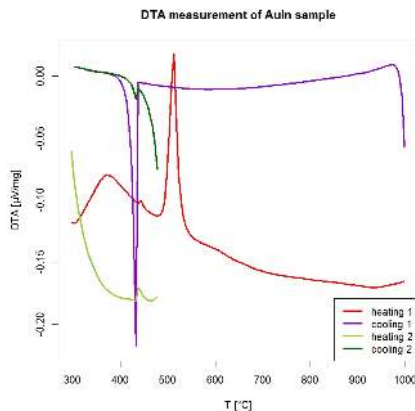


Figure 1. DTA curve showing a first melt at  $T = 440^\circ\text{C}$ , a second one at  $T = 515^\circ\text{C}$  and solidification at  $T = 436^\circ\text{C}$ .

**Keywords:** Intermetallics, modulation, powder diffraction

# MS26-P3 ErCu<sub>0.5</sub>Ga<sub>3.5</sub> – A (3+1)D-incommensurately modulated variant of the BaAl<sub>4</sub> type

Margarida S. Henriques<sup>1</sup>, Yuriy Verbovytsky<sup>2</sup>, Václav Petříček<sup>1</sup>,  
Michal Dušek<sup>1</sup>, Vasyli Kinzhybalov<sup>3</sup>, António P. Gonçalves<sup>4</sup>

1. Institute of Physics, Academy of Sciences of the Czech Republic, Na Slovance 2, 182 21 Prague, Czech Republic
2. Department No. 27, Karpenko Physico-Mechanical Institute of the NAS of Ukraine, Naukova str. 5, 79-060 Lviv, Ukraine
3. Institute of Low Temperature and Structure Research, Polish Academy of Sciences, Okólna str. 2, PO Box 1410, 50-950 Wrocław, Poland
4. CCTN, Instituto Superior Técnico, Universidade de Lisboa, Estrada Nacional 10, 2695-066 Bobadela LRS, Portugal

email: henriques@fzu.cz

Ternary intermetallic systems R-Cu-Ga were widely studied for all the rare earth metals and uranium [1,2]. The gallium rich intermediate phases RCuGa<sub>3</sub> were reported to crystallize as tetragonal or orthorhombically distorted derivatives of the BaAl<sub>4</sub>-type structure [3]. Moreover, some of these phases tend to form modulated structures due to disorder that might occur in the R and/or Cu/Ge crystal sublattices [4].

Single crystals of the ternary compound ErCu<sub>0.5</sub>Ga<sub>3.5</sub> were grown by the self-flux method. The structure of ErCu<sub>0.5</sub>Ga<sub>3.5</sub> was determined by single-crystal X-ray diffraction recorded at 120 and 300 K. The compound crystallizes in an incommensurately modulated (3+1)D structure, being related to the tetragonal BaAl<sub>4</sub>-type. The structure was refined in the monoclinic superspace group  $X2/m(\alpha,0,g)00$ , with modulation vector  $q = (0.184(2), 0, 0.347(1))$ ,  $a = 413.99(9)$ ,  $b = 963.83(11)$ ,  $c = 410.52(16)$  pm, and  $b = 90.11(1)^\circ$  at 120 K. The modulation wave occurs in the Ga/Cu disordered sublattice and  $q$  was found to be similar at both temperatures. Furthermore, analysis of the reciprocal pattern of ErCu<sub>0.5</sub>Ga<sub>3.5</sub> also indicates a twinning effect, described by a two-fold axis around  $a^*$ .

[1] Yu. Verbovytsky, A.P. Gonçalves, Chem. Met. Alloys 5 (2012) 129.

[2] Yu. Verbovytsky, A.P. Gonçalves, Intermetallics 33 (2013) 16.

[3] V.Ya. Markiv, et al., Dopov. Akad. Nauk Ukr. RSR, Ser. A 7 (1985) 76.

[4] Yu. Verbovytsky, M. Pasturel, T. Roisnel, A.P. Gonçalves, XIV Scientific Conference “Lviv Chemical Readings – 2013”, Book of Abstracts, Lviv, Ukraine, 26-29 May 2013, H5.

**Keywords:** incommensurate, occupation modulation, intermetallics

# MS26-P4 Staging superstructures in high- $T_c$ Sr/O co-doped La<sub>2-x</sub>Sr<sub>x</sub>CuO<sub>4+y</sub>

Pia J. Ray<sup>1</sup>, Niels H. Andersen<sup>2</sup>, Feng-Chen Chou<sup>3</sup>, Thomas B.S. Jensen<sup>2</sup>, Hashini E. Mohottala<sup>4,5</sup>, Christof Niedermayer<sup>6</sup>, Barret O. Wells<sup>4</sup>, Martin von Zimmermann<sup>7</sup>, Linda Ubdy<sup>1</sup>

1. Nano-Science Center, Niels Bohr Institute, University of Copenhagen, DK-2100 Copenhagen, Denmark
2. Physics Department, Technical University of Denmark, DK-2800 Kgs. Lyngby, Denmark
3. Center for Condensed Matter Sciences, National Taiwan University, Taipei 10617, Taiwan
4. Department of Physics, University of Connecticut U-3046,2152 Hillside Road, Storrs, Connecticut 06269-3046, USA
5. Department of Physics, University of Hartford, 200, Bloomfield Ave., West Hartford, CT-06117, USA
6. Laboratory for Neutron Scattering, ETHZ & PSI, CH-5232 Villigen PSI, Switzerland
7. Deutsches Elektronen-Synchrotron, Notkestraße 85 D-22607 Hamburg, Germany

email: pjay@bozack.dk

The very rich cuprate phase diagram continues to induce new investigations for the mechanism behind high- $T_c$  superconductivity in these materials. It is well known that the superconducting phase transition strongly depends on the hole content in the case of chemical substitution of La for Sr in La<sub>2-x</sub>Sr<sub>x</sub>CuO<sub>4</sub>, as well as for intercalation of O in La<sub>2</sub>CuO<sub>4+y</sub>.

We will here present results of elastic hard X-ray scattering experiments on the Sr/O co-doped La<sub>2-x</sub>Sr<sub>x</sub>CuO<sub>4+y</sub> family of compounds, in particular with  $x=0.00$ , 0.03, 0.065, and 0.09. Co-doping by superoxygenating the Sr doped compound opens up for a vast space of new and surprising phases. In particular, these samples all have the same superconducting critical temperature  $T_c = 40$  K independent of the Sr content, in contrast to oxygen-stoichiometric samples. We observe the superstructure known as staging - or hints of it - in all four samples. Staging is characterised by a number  $n$  referring to the periodicity of the intercalated oxygen layers in terms of CuO<sub>2</sub> spacings, and has only been investigated earlier in samples without Sr doping.

We find that the staging number  $n$  increases monotonically with Sr doping  $x$  despite the unchanged  $T_c$ . Furthermore, the transition temperature for the staging phase increases with  $x$ . This indicates a correlation between the randomly positioned Sr ions and the mobile oxygen interstitials, resulting in a stabilization of the staged phase with  $x$ , while the superconducting phase seemingly remains the same over varying  $x$ . This points to the interstitial oxygen that do not take part in the staging being responsible for the high- $T_c$  superconductivity in the samples.

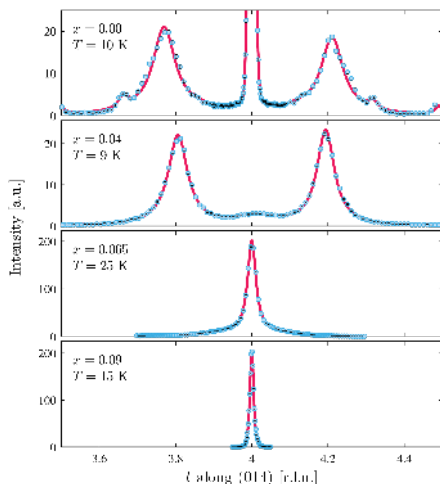


**Figure 1.** Examples of data fitted to several peak shapes in a single combined fit in order to obtain the reflection positions and intensities. Each set of peaks around the central (014) peak correspond to a staging related to the ordering of oxygen interstitials along the *c* axis.

**Keywords:** superconductivity, modulated crystal structure, staging, hard X-rays

**MS26-P5** When alternative layer stackings cause commensurate structures to co-exist the interpretation of the diffraction data need not be unique.

A. David Rae<sup>1</sup>

<sup>1</sup> Australian National University

email: [rae@rsc.anu.edu.au](mailto:rae@rsc.anu.edu.au)

Refinements of crystal structures with commensurate stacking faults should recognize that the structure is not everywhere the same and the structure can change coherently from one structure to another across an interface between adjacent layers. Assumptions are commonly used to constrain a refinement by placing the structure in a particular category consistent with the capabilities of a particular program. However this categorization can restrict the success of a refinement. The first assumption is that the options for a layer can be constructed using a symmetry operation commensurate with the crystal lattice and either a single reference layer or a single commensurately modulated structure. The second is that a clear distinction can be made between twinning and disorder. The twinning concept can include allo twins, ie the diffraction pattern has independent intensity contributions from different selections of layers corresponding to different ordered structures. Problems associated with these constraints are minimized when a single orientation of a single component structure dominates the diffraction data. However a systematic error still remains. Pseudo equivalent reflections of a disordered structure containing the various packing options can be used to project out the contributions to the scattering density from different irreducible representations of a commensurate parent structure and hence refine a correlation coefficient (range 0 to 1) between the component structures. Recent structure determinations will be used to illustrate this.

**Keywords:** polymorphs, stacking faults, refinement

## MS26-P6 Influence of the oxygen concentration on crystal growth and structure of the $\text{BaCuSi}_2\text{O}_{6\pm\delta}$ and

### $\text{Ba}_{1-x}\text{Sr}_x\text{CuSi}_2\text{O}_{6\pm\delta}$ spin dimer compounds

Natalija van Well<sup>1</sup>, Pascal Puphal<sup>2</sup>, Björn Wehinger<sup>1,3</sup>, Mariusz Kubus<sup>1,4</sup>, Dmitry Chernyshov<sup>1</sup>, Denis Sheptyakov<sup>1</sup>, Franz Ritter<sup>2</sup>, Wolf Assmus<sup>2</sup>, Cornelius Krellner<sup>2</sup>, Jürg Schefer<sup>1</sup>, Christian Rüegg<sup>1,3</sup>

1. Laboratory for Neutron Scattering and Imaging, Paul Scherrer Institute, CH-5232 Villigen, Switzerland

2. Physikalisches Institut, Goethe-Universität Frankfurt, D-60438 Frankfurt am Main, Germany

3. Department for Quantum Matter Physics, University of Geneva, CH-1211 Geneva, Switzerland

4. Department of Chemistry and Biochemistry University of Bern, CH-3012 Bern, Switzerland

5. Swiss-Norwegian Beam Lines at the European Synchrotron Radiation Facility, 38042 Grenoble, France

email: Natalija.van-well@psi.ch

By using the crystal growth method with  $\text{O}_2$ -partial pressure the new  $\text{Ba}_{1-x}\text{Sr}_x\text{CuSi}_2\text{O}_{6\pm\delta}$  mixed system can be prepared for  $x \leq 0.3$ . The crystal growth of  $\text{BaCuSi}_2\text{O}_{6\pm\delta}$  is also possible at a temperature of 1150°C by using an oxygen pressure of around 1 bar. The particular challenge of crystal growth of this material is that for the existing oxygen networks oxygen partial pressure operates as control parameter.  $\text{BaCuSi}_2\text{O}_{6\pm\delta}$  and  $\text{Ba}_{1-x}\text{Sr}_x\text{CuSi}_2\text{O}_{6\pm\delta}$  mixed crystals have the same tetragonal structure type *I4<sub>1</sub>/acd* down to low temperature, which has only one type of dimer layers. First results from single crystal structure diffraction of the new  $\text{BaCuSi}_2\text{O}_{6\pm\delta}$  show that, in contrast to Sr doped crystals of this mixed system, the incommensurate structure is present at low temperature (see Fig. 1).  $\text{BaCuSi}_2\text{O}_6$  is a model material for studying Bose-Einstein condensation (BEC) of magnons in high magnetic fields. It is also a quasi-two dimensional spin dimer system. The material is observed to have a singlet ground state in zero magnetic field with a large gap to the lowest excited triplet states [1, 2]. The quantum critical point at around 23 T and T=0 K separates the quantum paramagnetic regime from the ordered state [3, 4]. The investigation of the proportions of oxygen in the compounds shows a variation of the imbedded oxygen content ( $\pm\delta$ ). A detailed understanding of the crystal structure, the incommensurately modulated structure depending on the oxygen content will enable studying the spin dynamics of field-induced order states in this model magnetic compound of high current interest with only one type of dimer layers, showing the same distance between the Cu atoms, in the structure.

[1] Y. Sasago, K. Uchinokura, A. Zheludev, and G. Shirane, Phys. Rev. B 55, 8357 (1997) [2] C. Rüegg, D. F. McMorro, B. Normand, H. M. Rønnow, S. E. Sebastian, I. R. Fischer, C. D. Batista, S. N. Gvasaliya, C. Niedermayer, J. Stahn, Phys. Rev. Lett. 98, 017202 (2007) [3] M. Jaime, V. F. Correa, N. Harrison, C. D. Batista, N. Kawashima, Y. Kazuma, G. A. Jorge, R. Stern, I. Heinmaa, S. A. Zvyagin, Y. Sasago, K. Uchinokura, Phys. Rev. Lett. 93, 087203 (2004) [4] S. E. Sebastian, N. Harrison, C. D. Batista, L. Balicas, M. Jaime, P. A. Sharma, N. Kawashima, and I. R. Fisher, Nature (London) 441, 617 (2006)

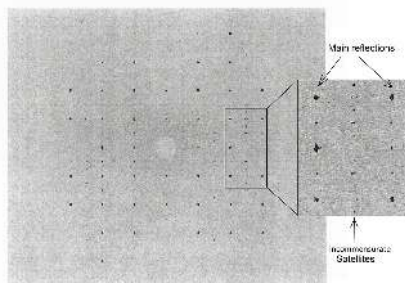


**Figure 1.** The first experimental (0kl) reciprocal space plane of  $\text{BaCuSi}_2\text{O}_{6\pm\delta}$  (1 bar) at 4.3K.

**Keywords:** growth with oxygen partial pressure, phase transition, spin dimer compounds



## MS27 Dynamical refinement of electron diffraction data

Chairs: Mauro Gemmi, Richard Beanland

### MS27-P1 Looking for the Potential in Digital Large-Angle Electron Diffraction Patterns

Richard Beanland<sup>1</sup>

1. University of Warwick

email: r.beanland@warwick.ac.uk

The sensitivity of convergent beam electron diffraction (CBED) to a crystal's structure and electron density has been known for a long time. The technique has the advantage of sampling material limited only by the size of the electron beam and the thickness of the specimen, i.e. a volume that can easily be less than 5000 cubic nanometres. However, the small electron wavelength of high energy electrons leads to very small Bragg angles, which severely restricts the convergence angle that can be used. The problem becomes worse for materials with larger lattice parameters, often with the result that insufficient information is obtained from CBED to do anything useful.

Computer control of transmission electron microscopes and digital image capture allows hundreds, or thousands, of CBED patterns to be collected automatically. The patterns can then be combined to construct a single 'digital' large-angle convergent beam electron diffraction (D-LACBED) pattern that has no restrictions due to Bragg angle. These patterns have a wealth of detail and, for example, symmetry determination becomes straightforward. Examples are given from materials that would be difficult or impossible using conventional CBED.

While analysis of the intensities in CBED patterns has been shown to yield information about crystal potentials – even providing sufficient detail to show the redistribution of electrons between atoms (i.e. bonding effects) – there has been less work on LACBED patterns. Careful experimentation and energy filtered imaging is needed for CBED work, since reliable answers usually require elastically-scattered intensities to be measured with accuracies better than 1%. For D-LACBED patterns, it may be hoped that the large amount of data contains some regions that are much more sensitive than others. Thus, the sensitivity of D-LACBED patterns to changes in the crystal potential is investigated using Bloch wave simulations. It is found that dynamical diffraction effects often produce large changes in the intensity of multiple diffracted beams from the variation of a single Fourier coefficient that describes the crystal potential. It thus seems possible that highly accurate measurement of crystal structure and bonding on a routine basis is readily achievable with a modern computer controlled TEM

without the need for energy filtering.

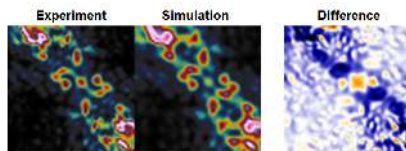


**Figure 1.** Experimental and simulated 111 D-LACBED pattern from the [110] zone axis of GaAs. The simulated pattern uses Kirkland scattering factors and is optimised for specimen thickness, Debye-Waller factor and absorption. Large differences in intensity remain (>30%), presumably due to bonding effects.

**Keywords:** D-LACBED, dynamical electron diffraction, refinement

## MS28 New approaches in electron crystallography

Chairs: Louisa Meshi, Xiaodong Zou

### MS28-P1 Ni-rich phases identification in GaAs nanowire devices by mean of Electron Diffraction Tomography

Jérémy David<sup>1</sup>, Francesco Rossella<sup>2</sup>, Mirko Rocci<sup>2</sup>, Mauro Gemmi<sup>1</sup>, Daniele Ercolani<sup>2</sup>, Lucia Sorba<sup>2</sup>, Fabio Beltram<sup>2</sup>, Stefano Roddaro<sup>2</sup>

1. Istituto Italiano di Tecnologia, Center for Nanotechnology Innovation@NEST, Piazza San Silvestro 12, 56127 Pisa, Italy

2. Scuola Normale Superiore and Istituto Nanoscienze-CNR, NEST, Piazza San Silvestro 12, 56127 Pisa, Italy

email: jeremy.david@iit.it

Rapid thermal annealing is a powerful tool for the preparation of ohmic contact at metal–semiconductor interfaces, and it can yield to complex inter-diffusion phenomena, as it has been extensively studied in the case of bulk GaAs<sup>[1]</sup>. We observed that the controlled thermal annealing of GaAs nanowire (NW) devices with Ni/Au electrodes promotes the diffusion of nickel into the nanowire, forming Ni-rich metallic alloy regions in the nanostructured body.

From EDS analysis, the content of nickel in the nanowires was variable, indicating the presence of different Ni-rich alloys in the transformed part of the NW. In order to identify which crystal phases form, the devices were designed on a 50nm SiN membrane transparent to a high energy electron beam, making the device observable in a TEM. Since the transformed part is very small, from 200 to 400 nm in the best scenario, phase identification using oriented zone axis patterns is critical. To avoid this problem we performed Electron Diffraction Tomography<sup>[2]</sup> data collection on the transformed region in parallel microdiffraction mode. In this experimental configuration a set of diffraction patterns are recorded while tilting the sample around the goniometer axis of the microscope, with a specific angular step (1° in this study) and within a variable angular range depending on the goniometer available. The illuminated area is minimized through a small condenser aperture, while the beam is kept always parallel. In our case with a 5 µm aperture we could illuminate a circle of 200 nm (see figure) in diameter, being sure that mainly the transformed region was diffracting. From the collected data the reciprocal space of the diffractive volume can then be reconstructed in three dimensions, allowing the determination of the lattice parameters of the diffracting crystal. For this purpose an angular range of only 60° was sufficient and although the patterns were noisy and “contaminated” by spurious spots coming from the surrounding part of the nanowire, the unit cell of several Ni-rich alloys could be determined.

Possible interpretation on which are the parameters that can play a role on the predominance of one of them over the others will be discussed.

[1] T.-J. Kim, P. H. Holloway, “Ohmic Contacts to II-VI and II-V Compound Semiconductors”, in *Processing of Wide Band Gap Semiconductors*, S.J. Pearton, 2001.

[2] U. Kolb, T. Gorelik, C. Kübel, M.T. Otten, D. Hubert, *Ultramicroscopy* 107, 507 (2007)

**Keywords:** Electron Diffraction Tomography, GaAs, Nanowires

**MS28-P2** Improved Accuracy of Unit Cell  
Determination for Rotation Electron  
Diffraction Data

Bin Wang<sup>1</sup>, Sven Hovmöller<sup>1</sup>, Xiaodong Zou<sup>1</sup>, Wei Wan<sup>1</sup>

<sup>1</sup>. Department of Materials and Environmental Chemistry,  
Stockholm University, Stockholm 106 91, SWEDEN

email: bin.wang@mmk.su.se

Electron crystallography can overcome the limitation of X-ray crystallography on crystal size, which is a few microns for modern synchrotron sources, and allow the structures of crystals down to nanometer sizes to be studied. Rotation electron diffraction (RED) was thus developed with the aim of accurate determination of 3D atomic structures of crystals of sub-micrometer sizes [1-2]. RED has shown to be powerful in phase identification and structure determination. More than 70 structures have been solved from the RED data [3]. In RED data collection, electron beam tilt and goniometer tilt are combined to rotate the crystal in a large range (typically 100 – 140 degrees) with a small step (0.1 ~ 0.2 degrees) and electron diffraction (ED) frames are collected for each tilt. In RED data processing, 3D reciprocal lattice of the crystal is reconstructed from the 2D ED patterns. The unit cell parameters are determined, and after indexing the diffraction intensities are output for structure determination and refinement.

In this work we aim at improving the processing of RED data, in particular the unit cell determination. Since the orientation matrix and unit cell determination are based on the positions of diffraction peaks, accurate determination of peak positions is very important for unit cell determination. In RED, the diffraction peaks are identified and the positions are determined according to the maximum intensities of the spots in 2D and 3D. Dynamic effects due to multiple scattering of electrons are known to distort electron diffraction data and they may change the distribution of diffraction peaks, i.e., peak shapes and profiles. Accuracy of peak positions determined using the maximum intensity may be affected accordingly. Therefore we introduced an alternative method for determining the peak positions using intensity weighted coordinates, i.e. the peak coordinates are calculated as the average of the coordinates of all the pixels of the reflection with intensities above a certain threshold, weighted using the intensities. By using the new peak positions for a RED data set of garnet it was shown that the accuracy of unit cell determination was improved.

References

- [1] D.L. Zhang, S. Hovmöller, P. Oleynikov, X. Zou, Z. Kristallogr, 2010, 225, 94-102.
- [2] W. Wan, J.L. Sun, J. Su, S. Hovmöller, X. Zou. J. Appl. Cryst., 2013, 46, 1863-1873.

[3] Y.F. Yun, X. Zou, S. Hovmöller, W. Wan, IUCrJ, 2015, 2, 267–282.

**Keywords:** Rotation Electron Diffraction, Peak Searching, Unit Cell Determination

## MS28-P3 Structural characterisation of complex zeolite structures using electron crystallography

Hongyi Xu<sup>1</sup>, Jiho Shin<sup>1,2</sup>, Peng Guo<sup>1</sup>, Xiaodong Zou<sup>1</sup>

1. Inorganic and Structural Chemistry and Berzelii Center EXSELENT on Porous Materials, Department of Materials and Environmental Chemistry, Stockholm University, SE-106 91 Stockholm, Sweden

2. Center for Ordered Nanoporous Materials Synthesis, School of Environmental Science and Engineering, POSTECH, Pohang 790-784, Korea

email: hongyi.xu@mmk.su.se

The structures of two new zeolites, PST-26 and PST-28 with super-complex structures were predicted, synthesized and confirmed.<sup>1</sup> The prediction of these two structures was achieved by the strong reflections approach<sup>2</sup> and model building, which provided essential information for targeted syntheses of these materials. Due to small energy differences, PST-26 and PST-28 could only be obtained as mixtures, together with a small amount of gismondine which makes structure confirmation by powder X-ray diffraction more difficult. By taking the advantage of electron crystallography, individual particles of PST-26 and PST-28 could be characterized in a transmission electron microscope (TEM) in order to verify their structures. Due to the large unit cell and the structure complexity of the materials, we cooled down the sample to liquid nitrogen temperature (-176°C) during TEM studies to (1) prevent the crystals from being distorted/damaged by the high vacuum inside the TEM column and (2) reduce electron beam damage. For both materials, electron diffraction patterns were collected along both [111] and [001] zone axes and compared against simulated electron diffraction patterns based on predicted models. By analysing the strong reflection distributions and the weak diffraction spots between the experimental and simulated electron diffraction patterns, the structures of as-synthesized PST-26 (*Im-3m*, *a* = 75 Å) and PST-28 (*Im-3m*, *a* = 85 Å) were successfully verified.<sup>1</sup> This work not only demonstrated the power of electron crystallography, but also shows the possibility to combine cryo-EM and electron diffraction techniques to study electron beam sensitive materials with complex structures such as micro-sized protein crystals.

### Reference:

1. Shin, J. and Xu, H. *et al.* Targeted Synthesis of Two Super-Complex Zeolites with Embedded Isorecticular Structures. *Angewandte Chemie International Edition* (2016).
2. Zhang, H. *et al.* Structure relations in real and reciprocal space of hexagonal phases related to i-ZnMgRE quasicrystals. *Philos. Mag.* **86**, 543-548, doi:10.1080/14786430500279658 (2006).
3. Guo, P. *et al.* A zeolite family with expanding structural complexity and embedded isorecticular structures. *Nature* **524**, 74-U143, doi:10.1038/nature14575 (2015).

**Keywords:** Electron crystallography, Zeolite, Electron microscopy, Cryo-EM, Method development

## MS29 Molecular interactions in crystal packing and molecular assemblies

Chairs: Kari Rissanen, Doris Braun

### MS29-P1 Molecular Structure, FT-IR and UV-Vis Spectra, NBO, NPA and Fukui Function Analysis of

5-((4-bromophenylimino)methyl)-3-methoxyphenol

Zeynep Demircioğlu<sup>1</sup>, Orhan Büyükgüngör<sup>1</sup>, Çiğdem Albayrak Kaştaş<sup>2</sup>

1. Ondokuz Mayıs University, Turkey
2. Sinop University, Turkey

email: zeynep.kelesoglu@omu.edu.tr

A new o-hydroxy Schiff base of the title compound was isolated and investigated by experimental (X-ray diffraction, FT-IR, UV-Vis) and theoretical (DFT, FT-IR, UV-Vis) methodologies. The experimental investigations of the compound indicated that the molecule seems to be in enol form and this is also supported by the results obtained from the theoretical density functional theory (DFT)'s calculations, performed both for the enol and keto tautomers of the title compound. Stability of the molecule arises from hyper conjugative interactions, charge delocalization and hydrogen bond interactions and these have been analyzed using natural bond orbital (NBO) analysis. Additionally, frontier molecular orbitals (HOMO, LUMO), molecular electrostatic potential (MEP), Mulliken population method, Natural Population Analysis (NPA) and Fukui function analysis have been studied.

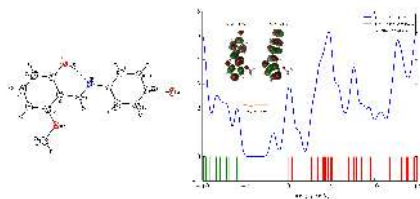


**Figure 1.** Molecular structure and calculated TDOS spectrum of the title compound.

**Keywords:** X-ray Diffraction Method, Natural Bond Analysis (NBO), Natural Population Analysis (NPA), Fukui Function Analysis

## MS29-P2 Spontaneous reduction of polydispersity and self-healing colloidal crystals

Urs Gasser<sup>1</sup>, Andrea Scotti<sup>1</sup>, Emily S. Herman<sup>2</sup>, Miguel Pelaez-Fernandez<sup>3</sup>, Jun Han<sup>4</sup>, Andreas Menzel<sup>4</sup>, L. A. Lyon<sup>5</sup>, Alberto Fernandez-Nieves<sup>3</sup>

1. Laboratory for Neutron-Scattering and Imaging, Paul Scherrer Institut, Villigen, Switzerland.
2. School of Chemistry and Biochemistry, Georgia Institute of Technology, Atlanta, USA.
3. School of Physics, Georgia Institute of Technology, Atlanta, USA.
4. Laboratory for Macromolecules and Bioimaging, Paul Scherrer Institut, Villigen, Switzerland.
5. Chapman University, Schmid College of Science and Technology, Orange CA, USA.

email: urs.gasser@psi.ch

Crystallization is often suppressed by the presence of point defects due to larger atoms or impurity particles. Surprisingly, colloidal pNIPAM hydrogels can overcome this limitation: A small number of large microgels can spontaneously deswell to fit in the crystal lattice of smaller but otherwise identical microgels, thus avoiding the occurrence of point defects [1]. We find this unique reduction of polydispersity and particle deswelling to be due to an osmotic pressure difference between the inside and the outside of the microgels [2]. Although pNIPAM is an uncharged polymer, pNIPAM microgels carry charged groups, remaining from particle synthesis, on their surface, and most of the corresponding counterions are bound to the particle. An osmotic pressure difference between inside and outside of a microgel builds up when the counterion clouds of neighboring particles overlap. With increasing concentration, this pressure difference exceeds the bulk modulus of the large microgels and makes them deswell, enabling crystallization without point defects. Compared to hard colloidal particles, this particle deswelling mechanism fundamentally changes the role of polydispersity in pNIPAM suspensions and possibly other soft polymer particles. We find the freezing point of bidisperse pNIPAM suspensions to be determined by particle deswelling: A reduction of polydispersity by deswelling of the large particles in the bidisperse suspensions is required for crystallization. Compared to monodisperse suspensions, this causes the freezing point to shift to higher concentrations.

[1] A. St. J. Iyer and L. A. Lyon, *Angew. Int. Ed.* **48**: 4562-4566 (2009).

[2] A. Scotti, U. Gasser, E.S. Herman, M. Pelaez-Fernandez, Jun Han, A. Menzel, L.A. Lyon, and A. Fernandez-Nieves, accepted for publication in *PNAS* (2016).

**Keywords:** crystallization, microgels, osmotic pressure, SANS, SAXS

## MS29-P3 Theoretical insights into the Rh...Rh interactions

Ferdit G. Groenewald<sup>1</sup>, Andreas Roodt<sup>1</sup>

1. University of the Free State

email: ferdichem@gmail.com

Our theoretical investigation focuses on Rh...Rh interactions with the first observation of this metallophilic interactions dates back to 1975. We theoretically investigate numerous Rh(I) structures, synthesised in our group, containing Rh...Rh interactions that yield infinite 1D chains brought upon by the directionality of these interactions. The neutral crystal structures exhibit Rh...Rh distances ranging from 3.254(3) Å to 3.617(3) Å, with ligands ranging in steric bulk and electronic properties. Our aim is to characterise these interactions and to determine why these differences in the Rh...Rh separations occur. In particular, we shed light onto if these geometrical changes are brought upon by changes in the electronic state of the metal center influenced by the coordinating ligands, the energies of the orbitals or due to changes in intermolecular interactions between adjacent ligands. Characterisation of the Rh...Rh interactions were determined from the properties of the Bond Critical Point (BCP) calculated with the Atoms in Molecules (AIM) theory. Electrostatic Surface Potentials were calculated to evaluate the electrostatic properties of the complexing monomers that could give additional insight into packing preferences in the solid state. Noncovalent Interactions (NCI) plots were utilised to shed light on additional interactions. This is to better our understanding of the influence of ligands on the Rh...Rh distances. Furthermore, these interactions yield interesting optical properties which is dependent on the Rh...Rh interactions that can induce shifts in the UV visible spectra as the interaction strength changes. Our work seem to bare commonalities with Pt(II) packing in the solid state. A summary of our work thus far will be presented and correlated with solid state X-ray crystallographic and spectroscopic data for a range of complexes wherein the electron donating properties of the ligands were systematically varied.

**Keywords:** Computational Chemistry, Metallophilic, Atoms in Molecules, Interaction

## MS29-P4 The Crystalline Sponge Method for the Unambiguous Structural Determination of Non-Crystalline Compounds: Reproducibility, Reliability and Versatility.

Lilian M. Hayes<sup>1</sup>, Dr Caroline E. Knapp<sup>1</sup>, Dr Neil J. Press<sup>2</sup>, Prof Derek A. Tocher<sup>1</sup>, Prof Claire J. Carmalt<sup>1</sup>

1. Department of Chemistry, University College London

2. Novartis Institutes for BioMedical Research, Basel, Switzerland

email: uccalha@ucl.ac.uk

The crystalline sponge method, first introduced by Fujita and co-workers in 2013,<sup>1</sup> provides a revolutionary way of investigating the structures of liquid and amorphous compounds previously not amenable to single-crystal X-ray diffraction studies. It involves the encapsulation of non-crystalline compounds of interest into the pores of a specific crystalline sponge – the metal-organic framework (MOF)  $[(ZnL)_3(\text{tris}(4\text{-pyridyl})\text{-}1,3,5\text{-triazine})_2 \bullet x(\text{solvent})]_n$ . Through the formation of guest – host interactions the guest may be rendered regularly ordered and thus capable of contributing to Bragg peaks and a diffraction pattern. As such, its structure may be solved alongside that of its host. Whilst implementation of the technique has not been without its difficulties, its applicability has been tested and its value clearly demonstrated. However, in order for the method to be applied routinely to compounds with a broad range of functionalities and size we must gain more understanding as to why this MOF acts so successfully as a crystalline sponge and apply these findings to the design and synthesis of alternative host frameworks.

Here we present a systematic study detailing the encapsulation of a range of chemically simple functionalised aromatic molecules and assess how guest – host and guest – guest interactions vary with specific functionality of guest molecules, such as aldehyde, halogen and nitrile groups. These include the formation of hydrogen bonds,  $\pi$  –  $\pi$  and CH –  $\pi$  interactions and those involving halogens. We also discuss the reproducibility of guest positioning within the void space and why certain positions may be favoured.

(1) Inokuma, Y.; Yoshioka, S.; Ariyoshi, J.; Arai, T.; Hitora, Y.; Takada, K.; Matsunaga, S.; Rissanen, K.; Fujita, M. *Nature* **2013**, 495 (7442), 461–466.

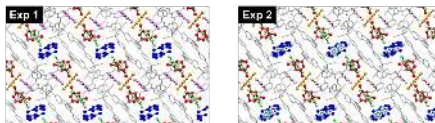


**Figure 1.** Plot of X-ray crystal structures of repeat encapsulation experiments with 1,3-dichlorobenzene. Guest molecules coloured to show the reproducibility of their locations in the framework (shown in grey).

**Keywords:** Crystalline Sponge,  $\pi$  –  $\pi$  interactions, guest – host complexes, metal organic frameworks

## MS29-P5 Inner and outer electrical field and dipole moment of a polar molecular crystal

Rolf Hesterberg<sup>1</sup>, Piero Macchi<sup>1</sup>, Jürg Hulliger<sup>1</sup>

1. University of Bern, Department of Chemistry and Biochemistry, Freiestrasse 3, 3012 Bern, Switzerland

email: rolf.hesterberg@dcb.unibe.ch

The inner and outer electrical field distribution and the macroscopic dipole moment are calculated for a polar molecular crystal such as 4-iodo-4'-nitro-biphenyl (INBP) crystallizing in Fdd2 (crystal class mm2). In INBP, the molecules pack head-to-tail parallel to the polar axis, leading to an ideal built up of opposite surface charge densities on the polar faces. At atmospheric ambient conditions, the surface charges can be compensated, implying a dipole opposed to the crystal dipole.

We simulated various nano-crystals of linear dimensions up to 20 nm, with and without surface charge compensation. We calculated, with gas-phase density functional theory, each molecule in the mean field generated by all the others in the nano-particle, thus enabling the calculation of an individual dipole moment for each molecule. This procedure is different from the classical calculation of an ideally infinite crystal and periodic boundary conditions. It was iterated until convergence was found (typically, within 10 cycles a root mean square smaller than 0.1 D on the molecular dipole is obtained).

The ideal crystal packing of this molecule is such that, at variance from other species, the molecular dipole is smaller (by about 20%) with respect to the molecular dipole in the gas phase. This is caused by the internal crystal field, which opposes the molecular dipole due to the lateral interactions that overwhelm the head-to-tail motif.

If the charge compensation is taken into account, two additional effects occur: the field generated by the surfaces enhances the molecular dipole but the additional dipole due to these charges contrast the crystal dipole (sum of molecular dipoles). As a result, the average molecular dipole increases, but the total dipole (i.e. sum of all molecular and surface dipoles) can be 80% smaller than the sum of the gas phase molecules. These results strongly depend on the surface definition, in particular at which distance from the external atoms the charge carriers will be accommodated. Because the nature of these particles is not known, and very likely strongly variable with the atmospheric conditions, the estimation is very approximate and the dipole compensation can be even much larger, thus reducing the observable crystal dipole to a very small value.

**Keywords:** Polar crystal, dipole moment, electrical field, surface charge density

**MS29-P6** Molecular interactions in crystal packing of dipeptide gels**Keywords:** Dipeptide gels, self-assemblyAnja Holzheu<sup>1</sup>, Katharina M. Fromm<sup>1</sup>, Aurelien Crochet<sup>1</sup>,  
Veronique Trappe<sup>2</sup>

1. University of Fribourg, Department of Chemistry, Chemin du Musée 9, 1700 Fribourg, Switzerland

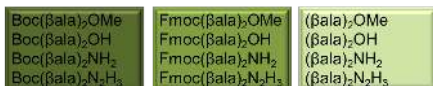
2. University of Fribourg, Department of Physics, Chemin du Musée 3, 1700 Fribourg

email: anja.holzheu@unifr.ch

A gel is defined as a non-fluid colloidal network or polymer that is expanded throughout its whole volume by a fluid<sup>1</sup>. This network can be obtained by either intermolecular - or by interfibrillar - crosslinks<sup>2</sup>. In general peptide hydrogels are a promising class of soft biomaterials for cell culture, regenerative medicine, or drug delivery applications having advantages in biocompatibility, biodegradability and injectability<sup>3,4</sup>. So far, many different longer peptide hydrogel systems like Max1 and P<sup>-24</sup> are well studied but the publications about dipeptide hydrogels are limited. Dipeptide gels have certain advantages over longer peptide gels being less cost intensive, more versatile and easier to synthesize in high quantities. The most commonly studied one is the Fmoc-Phe-Phe dipeptide<sup>5</sup>. The major driving force of the self-assembly of such peptides is proposed to be  $\pi$ - $\pi$  stacking. Other forces known to play a role are hydrophobic interactions, ionic interactions, hydrogen bonding and electrostatic interactions<sup>6,7</sup>. Nevertheless, a better understanding of the self-assembly process would allow a more rational design for specific applications. In our work, we found that a dipeptide based on two  $\beta$ -alanine groups, hence excluding  $\pi$ - $\pi$  stacking, was able to form a gel-like state. In order to explore this phenomenon, we specifically target the different driving forces by changing the protecting or end groups of the dipeptide. Additionally, solvents of different polarities, salts and pH are tested. The main goal is to synthesize the different dipeptide systems depicted in figure 1, to analyze their chemical, physical and mechanical characteristics, using techniques like Small-angle X-ray scattering, X-ray Single crystal - and X-ray powder diffraction, to show the major differences and to perform mathematical models.

**References**

- [1] J. V. Alemán et al., *Pure Appl. Chem.*, **2007**, *10*, 1801–1829
- [2] A. Dasgupta et al., *RSC Advances*, **2013**, *3*, 9117-9149
- [3] S. Marchesan et al., *Nanoscale*, **2012**, *4*, 6752-6760
- [4] W.Y. Seow et al., *Materials Today*, **2014**, *17*, 381-388
- [5] Thomas Liebmann et al., *BMC Biotechnology*, **2007**
- [6] M. Tena-Solsona et al., *J. Mater. Chem. B*, **2014**, *2*, 6192-6197
- [7] G. Fichmann et al., *Acta Biomaterialia*, **2014**, *10*, 1671-1682

**Figure 1.** Scheme of the different dipeptides



## MS29-P7 Crystal structure of the 1D coordination polymer [Fe(ebtz)<sub>2</sub>(CH<sub>3</sub>CN)<sub>2</sub>](BF<sub>4</sub>)<sub>2</sub>·2CH<sub>3</sub>CN

Maria Książek<sup>1</sup>, Robert Bronisz<sup>2</sup>, Marek Weselski<sup>2</sup>, Joachim Kusz<sup>1</sup>

1. Institute of Physics, University of Silesia, Katowice  
2. Faculty of Chemistry, University of Wrocław, Wrocław

email: maria.ksiazek@us.edu.pl

Spin crossover (SCO) depends on alteration of electronic structure of metal ion which can be triggered by the change of temperature, an application of pressure, by light irradiation or using pulsing magnetic field as well as by chemical perturbation.[1] SCO in octahedral iron(II) complexes is associated with the shift of two electrons between  $t_{2g}$  and  $e_g$  electronic levels. This results in alteration of magnetic, optical and dielectric properties. Transition from high spin HS(S=2) to low spin LS(S=0) state is accompanied by the reduction of Fe-donor distance from 2.0 to 2.2 Å. This becomes a source of perturbation which spreading on the crystal lattice may trigger further structural transformations within a complex molecule and in the network of intermolecular interactions.

[Fe(ebtz)<sub>2</sub>(C<sub>2</sub>H<sub>5</sub>CN)<sub>2</sub>](ClO<sub>4</sub>)<sub>2</sub> (1) represents an example in which SCO is associated with structural changes.[2] In this complex neighbouring Fe(II) ions are linked by 1,2-di(tetrazol-2-yl)ethane (ebt<sub>2</sub>). This bridging mode leads to formation of the polymeric chain. Adjusted polymeric chains form supramolecular layers which are parallel to each other. Nitrile molecules adopt uncommon orientation in relation to coordination octahedron. The angle Fe-N-C(nitrile) in HS is lesser than 150° (145.9° at 110 K). SCO in this complex is very abrupt and accompanied by wide hysteresis loop ( $T_{1/2}^{\downarrow} \approx 112$  K,  $T_{1/2}^{\uparrow} \approx 141$  K). It was found that HS→LS transition is associated with reorientation of propionitrile molecule (<Fe-N-C(nitrile) = 162.9° at 80 K).

On the poster will be presented the crystal structure and magnetic properties of 1D coordination polymer [Fe(ebtz)<sub>2</sub>(CH<sub>3</sub>CN)<sub>2</sub>](BF<sub>4</sub>)<sub>2</sub>·2CH<sub>3</sub>CN (2). In this complex the polymeric chains form supramolecular layers. Axially coordinated acetonitrile molecules are also directed towards space between layers. But the angle of Fe-N-C(CH<sub>3</sub>) fragment in HS of 2 is significantly greater (167.95°) than in 1 and after HS→LS transition increases only slightly (171.61°). SCO in 2 is more gradual and accompanied by a narrow hysteresis loop ( $T_{1/2}^{\downarrow} \approx 161.0$  K,  $T_{1/2}^{\uparrow} \approx 163.5$  K).

The work was supported by the Polish National Sciences Centre Grant No. DEC-2014/15/B/ST5/04771.

### Literature

[1] P. Gütlisch, H. A. Goodwin, *Top. Curr. Chem.*, **2004**, 233, 1-47; M. A. Halcrow, *Spin-Crossover Materials: Properties and Applications*, John Wiley & Sons, Ltd, **2013**.

[2] A. Białońska, R. Bronisz, *Inorg. Chem.*, **2012**, 51, 12630–12637.

**Keywords:** spin crossover, Fe(II) complexes

## MS29-P8 Quantitative estimate of cohesion forces

Michał Kaźmierczak<sup>1</sup>, Andrzej Katrusiak<sup>1</sup>

1. Adam Mickiewicz University in Poznań

email: kax@amu.edu.pl

Distance between van der Waals spheres is a handy variable for description of intermolecular contacts.<sup>1-3</sup> Its value vary between types of contacts but also within it. The idea behind presented research was to investigate the distribution of first, second and next shortest contacts with taking under consideration the type of contact. Changes of these distributions reflect role of specific types of interactions in the crystal structure (Figure 1). This information is extremely useful in crystal engineering and drug design because it sheds light on processes of molecular aggregation and phase transition.<sup>4</sup>

To describe investigated contacts two parameters were introduced: contact parameter  $\delta$  (distance between van der Waals spheres) and contact order  $n$  (position on list sorted by ascending value of contact parameter  $\delta$ ). The survey was conducted on structural models from Cambridge Structural Database.<sup>5</sup> For every investigated deposit ten shortest contacts were statistically analysed in terms of contact parameter  $\delta$  and contact order  $n$ . Obtained distributions were approximate by split Pearson VII function.

Tabulated data obtained by fitting model function allows to compare various types of intermolecular interactions. Distributions of contact parameter  $\delta$  as function of contact order  $n$  show also very important role of strongest intermolecular interaction during processes of molecular aggregation and phase transition.

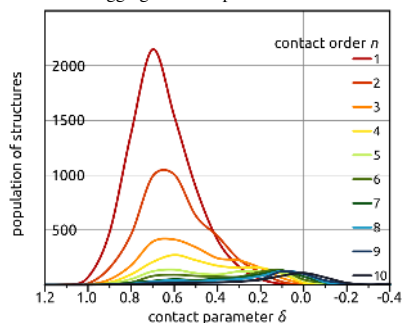


**Figure 1.** Distribution of contact NH...N in function of contact parameter  $\delta$  for 10 first contact orders  $n$ . The bin-width 0.1 Å was applied.

**Keywords:** intermolecular interactions, molecular assemblies, phase transition

**MS29-P9 Force field prediction of a reversal transition in molecular crystals**Khadidja Brahimi<sup>1</sup>, Juerg Hulliger<sup>1</sup><sup>1</sup>. Department of Chemistry and Biochemistry, University of Berne

email: khadidjab7@gmail.com

Polarity formation is a general growth feature of systems showing unidirectional self-assembly of polar building blocks into a bulk state [1]. Channel-type inclusion compounds, single component molecular crystals, solid solutions, optically anomalous crystals, inorganic ionic crystals, biological tissues and biomimetic composites investigated experimentally all showed domains of opposite polarities in their final grown state [2]. In this field, molecular crystals made of dipolar organic molecules growing into a *polar* crystals structure are subject to undergo a *reversal transition* and open up fascinating opportunities for computational and experimental studies. In the frame of a general theory on stochastic polarity formation, the analytical description demonstrates that the *reversal* will take place in that direction (sectors involving the polar axis) where 180<sup>0</sup> orientational defect formation is less endothermic [3]. Therefore, force field calculations of the energy of 180<sup>0</sup> defect formation at both types of faces, i.e (*hkl*) (*h,k,l* = +1,0,-1) may allow to predict which side of the polar axis should show *reversal* of most of the dipoles. This basic property of molecular crystals is exemplified by investigating real systems for which at first we describe the structures and the representative (*hkl*), (*h,k,l* = +1,0,-1) faces for which interaction energies are explicitly calculated by taking into account the specific symmetry of the lattice. Conceptually a quite simple procedure, the practical elaboration can be rather complicated, because of the presence of different sites which are symmetry independent at the surfaces of different (*hkl*) faces. The two chosen dipolar molecules are 1-chloro-4-nitrobenzonitrile and 1-bromo-4-cyanobenzonitrile. The molecules were selected as such to provide geometries and sizes which do not impose a significant surface site reconstruction (relaxation), when an 180<sup>0</sup> reversed attachment is considered. We will present the results of a structural and energetical analysis involving different faces where we may define a difference of energy when docking a molecule down or up, by looking at the values of this energy difference predictive for the polar behaviour of individual faces. This configurational study highlights a relationship between the symmetry of a surface and the *reversal transition* which may occur when growth proceeds.

**Keywords:** Polar molecular crystals, Polarity, crystal growth**MS29-P10 Halogen-halogen, halogen-oxygen, and dipolar interactions in a series of Re(I)(CO)<sub>3</sub> complexes with halogen-substituted nitrogen-donor ligands**Reza Kia<sup>1</sup>, Paul R. Raithby<sup>2</sup><sup>1</sup>. Chemistry Department, Sharif University of Technology, Tehran, 11155-3516, Iran<sup>2</sup>. Chemistry Department, University of Bath, Bath BA2 7AY, UK

email: rkia@sharif.edu

Intermolecular interactions are of significant interest in chemistry, mainly because they are responsible for stabilization of many important molecules such as DNA and proteins [1]. They have also important roles in the arrangement of molecular species in crystal packing. Therefore, they are one of the main foci in the field of crystal engineering because of their structural role on the physical properties of crystalline materials such as nonlinear optics, electrical, and magnetic properties [2]. In this study, the effect of different intermolecular interactions such as halogen...halogen, halogen...oxygen, and pi...pi interactions has been investigated on the crystal packing of Re(CO)<sub>3</sub> complexes with halogen-substituted nitrogen-donor ligands.

**References**

- 1) G. R. Desiraju, *Nature* 2001, 412, 397–400.
- 2) D. Braga, L. Brammer, N. Champness, *Cryst. Eng. Comm* 2005, 7, 1–19.

**Keywords:** Intermolecular interactions, Halogen interactions, Re(I) complexes

# MS29-P11 Insights into solution and solid-state coordinative properties of tantalum(V) and niobium(V) metal centres.

Renier Koen<sup>1</sup>, Hendrik G. Visser<sup>1</sup>, Andreas Roodt<sup>1</sup>, Johannes T. Nel<sup>2</sup>

1. Department of Chemistry, University of the Free State, Bloemfontein, 9300, South Africa

2. Nuclear Energy Corporation of South Africa, V-H2 Building, Pretoria, 0001

email: koen.renier87@gmail.com

Tantalum(V) and niobium(V) are two transition metals found in the vanadium triad in the periodic table, with very similar chemical properties, and always occur together in nature. Both elements have hard metal centres and the halido species are known to readily hydrolyse to form relatively unreactive oxido species, which severely inhibit bidentate ligand coordination to these metal centres.[1] Accordingly, in-depth investigations of the coordinative preferences of these elements remain elusive.

In this present investigation of tantalum(V) and niobium(V) complexes, a range of functionalized mono-charged bidentate ligands (*L,L'*-*Bid'*) has been used in synthesis, in an attempt to study the variation in activity and selectivity of coordination of *L,L'*-*Bid'* to the metal halides in both solid- and solution state. [*L,L'*-*BidH* = functionalized acetylaceton- (acacH), 8-hydroxyquinoline- (oxH) and tropolone (tropH) derivatives].

Two new stable (relatively hydrolysis resistant) synthons ( $(Et_4N)[NbCl_6]$  (see Figure 1 a) and  $(Et_4N)[TaCl_6]$ ) have been instrumental in the success of  $\beta$ -diketone and tropolone ligand coordination to tantalum and niobium metal centres.[2] Crystal structures have been obtained for numerous complexes, with examples including;  $[Nb(trop)_4Cl]$ ,  $[Ta(trop)_4Cl]$ ,  $(Et_4N)[NbOCl_5(tffa)]$  (see Figure 1 b),  $(Et_4N)[NbOCl_5(hfaa)]$  and  $(Et_4N)[NbOCl_5(btfa)]$ , where tropH = tropolone, tffaH = thenoyltrifluoroacetone, hfaaH = hexafluoroacetylacetone, btfaH = benzoyltrifluoroacetone and tffaH = trifluorofurylacetone. Differences in coordination modes and crystal packing of these isostructural complexes have been identified in an attempt to gain insight into these compounds to assist in predictions of properties for future use.

Additionally, to further evaluate the electronic environment experienced by the niobium(V) and tantalum(V) centres in these complexes, a solution-state kinetic study of the substitution reactions of  $[NbCl_6]^-$  and  $[TaCl_6]^-$  with a range of  $\beta$ -diketones as entering ligands was undertaken. These results will also be reported and correlated to entering ligand electronic characteristics.

representation of  $(Et_4N)[NbOCl_5(tffa)]$  (tetraethylammonium counter-ion omitted).

**Keywords:** hydrolysis, bidentate, kinetics, crystallization

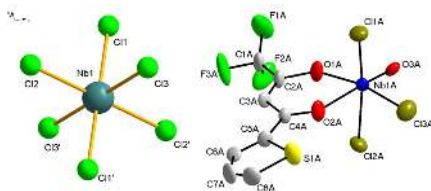


**Figure 1.** (a) Ball-and-stick representation of  $(Et_4N)[NbCl_6]$  (tetraethylammonium counter-ion omitted) (b) Ball-and-stick

## MS29-P12 Temperature structural studies of spin crossover 1D coordination polymer [Fe(4-amino-1,2,4-triazole)<sub>3</sub>]SO<sub>4</sub>

Joachim Kusz<sup>1</sup>, Robert Bronisz<sup>2</sup>, Krzysztof Drabent<sup>2</sup>, Andy Fitch<sup>3</sup>, Maciej Zubko<sup>4</sup>, Mikołaj F. Rudolf<sup>2</sup>, Marek Weselski<sup>2</sup>

1. Institute of Physics, University of Silesia, ul. Uniwersytecka 4, 40-007 Katowice, Poland
2. Faculty of Chemistry, University of Wrocław, ul. F. Joliot-Curie 14, 50-383 Wrocław, Poland
3. European Synchrotron Radiation Facility, B.P.220, Grenoble Cedex, France
4. Institute of Materials Science, University of Silesia, ul. 75 Pułku Piechoty 1a, 41-500 Chorzów

email: kusz@us.edu.pl

Spin crossover (SCO) usually occurs in octahedral 3d<sup>4-7</sup> transition metal complexes. SCO can be induced by change of temperature, application of pressure or by light irradiation and is accompanied by change of magnetic, optical and dielectric properties. What is important, transition from high spin (HS, t<sub>2g</sub><sup>4</sup>e<sub>g</sub><sup>2</sup>, S=2) to low spin (LS, t<sub>2g</sub><sup>6</sup>e<sub>g</sub><sup>0</sup>, S=0) form in iron(II) complexes is accompanied by shortening of Fe-ligand distance at about 0.2 Å. Although SCO phenomenon is of molecular nature, a perturbation produced by shrinkage of complex molecule (as a result of Fe-ligand bond shortening) spreads on the whole crystal lattice through intermolecular interactions. Therefore it was postulated that an incorporation of direct linkage between metal ions should enhance transmission of perturbation. Thus it should lead to the more cooperative spin transitions. Indeed, in the coordination polymers in which iron(II) ions are bridged by small and rigid ligands, SCO very often proceeds in narrow temperature range. In particular iron(II) complexes based on 1H,2,4-triazole or 4-amino-1,2,4-triazole (NH<sub>4</sub>trz) exhibit very abrupt spin transitions accompanied by hysteresis loops [1]. Unfortunately, synthesis of these type of complexes does not lead to the formation of crystalline samples suitable for single crystal X-Ray diffraction studies. Initially, postulated structure of one dimensional (1D) polymeric chains in which metal ions are bridged by three 1,2,4-triazole rings was supported by elucidation of crystal structure of copper(II) complexes [2].

The subject of performed studies are spin crossover 1D coordination polymers [Fe<sub>x</sub>Zn<sub>1-x</sub> (4-amino-1,2,4-triazole)<sub>3</sub>]SO<sub>4</sub> (for x=0.0, 0.09, 0.20, 0.40, 0.60, 1.00) that represent an examples of NH<sub>4</sub>trz based SCO systems containing divalent anion [3]. The complex exhibits complete one step, abrupt spin crossover slightly above room temperature and is accompanied by the hysteresis loop. Based on the synchrotron powder diffraction measurements we have determined the crystal structure of the studied compounds.

### Literature

- [1] M. M. Dirtu, C. Neuhausen, A.D. Naik, A. Rotaru, L. Spinu, Y. Garcia, Inorg. Chem., **2010**, 49, 5723-5736.
- [2] K. Drabent, Z. Ciunik, Chem. Commun., **2001**, 14, 1254-1255.
- [3] K. Drabent, R. Bronisz, M. F. Rudolf, Italian Physical Society Conference Proceedings, **1996**, 50, 15-18.

**Keywords:** Spin crossover, synchrotron powder diffraction study, Fe(II) compounds

## MS29-P13 Atom interaction propensities between atom types in crystal packings assessed by Hirshfeld surface analysis. The best partners and behaviors of several chemical functions, including oxygen, hydrogen, halogens and water are investigated.

Christian J.P. Jelsch<sup>1</sup>

1. CNRS, Lorraine University, France

email: christian.jelsch@univ-lorraine.fr

The partitioning of space with Hirshfeld surfaces enables to analyze and fingerprint molecular interactions in crystalline environments [1]. The decomposition of the crystal contact surface between pairs of interacting chemical species enables to derive an enrichment ratio [2]. This descriptor yields information on the propensity of chemical species to form intermolecular interactions with themselves and other species. The enrichment ratio is obtained by comparing the actual contacts in the crystal with those computed as if all types of contacts had the same probability to form.

The enrichments and contacts tendencies were analysed in several families of compounds, based on chemical composition and aromatic character. As expected, the polar contacts of type H...N, H...O and H...S, which are generally hydrogen bonds, show enrichment values larger than unity. In aromatic compounds, C...C contacts can display large enrichment ratios due to extensive π...π stacking occurrence in the crystal packings of heterocyclic compounds. The crystal packings of several families of halogenated compounds also highlights that hydrogen, notably the lowly polar H-C atoms are a preferred interaction partner for halogens [3].

In alcohols, the systematic large enrichment ratios of some interactions like the O-H...O hydrogen bonds suggests that these contacts are a driving force in the crystal packing formation. The same statement holds for the weaker C-H...O hydrogen bonds in ethers, esters and ketones, in the absence of polar hydrogen atoms. The over-represented contacts in crystals of oxygenated hydrocarbons are generally of two types: electrostatic attractions (H-bonds) and hydrophobic interactions between lowly polar groups. It was found in several cases that, in the presence of several oxygenated chemical groups, cross-interactions between different chemical groups (e.g. water/alcohols; alcohols/phenols) are often favored in the crystal packings.

While general tendencies can often be derived for many contact types, the outlier compounds are instructive as they display peculiar or rare features. The methodology allows also detecting outliers which can be structures with errors. The behavior of water in monohydrate compounds was also investigated

- [1] McKinnon, Jayatilaka & Spackman (2007). *Chem. Commun.* 3814-3816.
- [2] Jelsch, Eijsmont & Huder (2014). *IUCr J.* **1**, 119-128.
- [3] Jelsch, Soudani & Nasr (2015). *IUCr J.* **2**, 327-340.

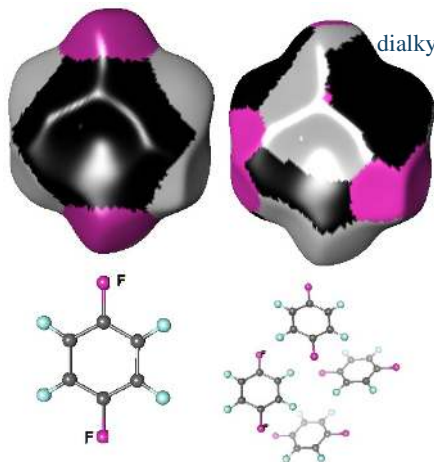


**Figure 1.** C<sub>6</sub>H<sub>4</sub>F<sub>2</sub> compound and its crystal packing. The Hirshfeld surface is colored according to the inner (left) and outer contact atom (right).

**Keywords:** hydrogen bond, halogens, crystal packing.

## MS29-P14 $\pi$ - $\pi$ Stacking motifs in dialkylbis{5-[(*E*)-2-aryldiazen-1-yl]-2-hydroxybenzoato}tin(IV) complexes

Anthony Linden<sup>1</sup>, Tushar S. Basu Baul<sup>2</sup>

1. Department of Chemistry, University of Zurich, Winterthurerstrasse 190, CH-8057 Zurich, Switzerland

2. Centre for Advanced Studies in Chemistry, North-Eastern Hill University, NEHU Permanent Campus, Umshing, Shillong 793 022, India

email: anthony.linden@chem.uzh.ch

Diorganotin(IV) complexes of 5-[(*E*)-2-aryldiazen-1-yl]-2-hydroxybenzoic acid (LHH') with the formula R<sub>2</sub>Sn(LH)<sub>2</sub> (R = methyl, *n*-butyl or *n*-octyl) are of interest because of their structural diversity in the crystalline state and their potential biological activity. Molecules of this class of compounds usually exhibit a skew-trapezoidal bipyramidal coordination geometry at the Sn-atom. The two planar extended carboxylate ligands, each with their two phenyl rings, lend themselves to  $\pi$ - $\pi$  stacking interactions. The diversity of supramolecular structural motifs formed by these interactions has been examined in detail for thirteen closely related complexes, which differ mainly in the substituents on the terminal phenyl ring [1]. While there are some recurring basic motifs amongst the observed stacking arrangements, such as dimers and step-like chains, variations through longitudinal slipping and inversion of the direction of the overlay add significant complexity in some of the structures (Fig. 1). The results of this motif analysis will be presented.

[1] A. Linden, T. S. Basu Baul, *Acta Crystallogr.* **2016**, C72, 313-325.

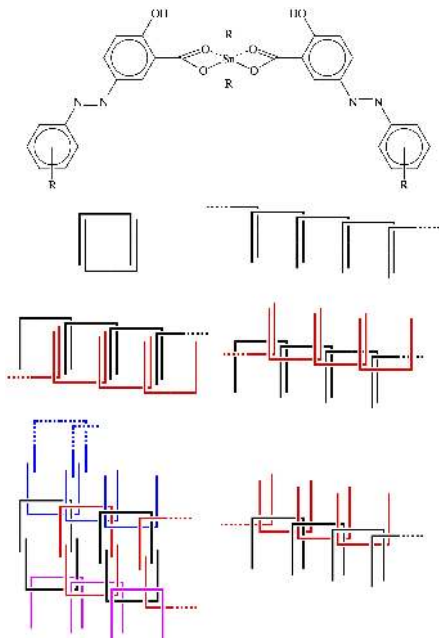


**Figure 1.** The class of diorganotin carboxylate complexes investigated and a cartoon of the  $\pi$ - $\pi$  stacking motifs discerned.

**Keywords:** supramolecular structures,  $\pi$ - $\pi$  stacking interactions, intermolecular interactions, packing motifs, diorganotin carboxylate complexes

## MS29-P15 Large supramolecular assemblies of a bowl-shaped host

Clive L. Oliver<sup>1</sup>

1. Department of Chemistry, University of Cape Town

email: clive.oliver@uct.ac.za

Nature is able to produce large, supramolecular assemblies of macromolecules with intricate complexities such as found in viruses and cellular membranes.<sup>1</sup> These complicated structures are held together by non-covalent interactions which are ultimately crucial in the functioning of these complex biological systems. Small-molecule supramolecular chemists are inspired by these complex supramolecular systems in nature, however, large, synthetic, multi-component ( $n > 3$ ) supramolecular assemblies which enclose chemical space are still relatively rare phenomena in the field of small-molecule, supramolecular chemistry. Atwood and MacGillivray reported the first example of such an assembly by showing that the bowl-shaped host molecule C-methylcalix[4]resorcinarene **1** can spontaneously assemble in a nitrobenzene solution to form a large, chiral, supramolecular assembly consisting of 6 molecules of **1** and 8 water molecules, the latter 'stitching' molecules of **1** into a hexameric assembly,  $\mathbf{1}_6(\text{H}_2\text{O})_8$  via O-H...O hydrogen bonds.<sup>2</sup> Despite the approximately 125 structures reported since this discovery containing **1** co-crystallised with various guest and/or solvent molecules, only one similar hexameric assembly of **1** was reported by Holman et al. where 6 of the 8 water molecules were replaced by 2-ethylhexanol molecules.<sup>3</sup> Hexameric assemblies of pyrogallolarenes and dodecameric assemblies of sulfonatocalix[4]arenes have also been reported. It is notable that in all these assemblies only one type of assembly per crystal structure was isolated in the solid-state. Here we present a crystallisation of **1** from 1-butanol, which yielded two different types of hexameric assemblies within the same crystal structure. Furthermore, the two unique assemblies are linked part of the time into a heterodimer of hexameric assemblies which we entitle a supra-heterodimer, a 38-component assembly consisting of 129 hydrogen bonds. To the best of our knowledge, the isolation of two different large, supramolecular assemblies ( $n > 3$ ) within the same crystal structure has not been observed before and neither has identical large supramolecular assemblies been shown to link into discrete units. In addition, we report a hexameric assembly of 1-propanol with **1** which increases the interior cavity size by simultaneous insertion of water and 1-propanol as the 'stitching' molecules, indicating a possible means of engineering the size of these cavities.

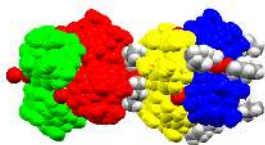


**Figure 1.** Space-filling representation of 38-component supra-heterodimer of 1

**Keywords:** large supramolecular assemblies, supra-heterodimer

## MS29-P16 Changes of LLT1, a ligand for human NKR-P1, with varied glycosylation and crystallization conditions

Tereza Skálová<sup>1</sup>, Jan Bláha<sup>2</sup>, Karl Harlos<sup>3</sup>, Jarmila Dušková<sup>1</sup>,  
Tomáš Koval<sup>1</sup>, Jan Stránský<sup>1</sup>, Jindřich Hašek<sup>1</sup>, Ondřej Vaněk<sup>2</sup>,  
Jan Dohnálek<sup>1</sup>

1. Institute of Biotechnology, Academy of Sciences of the Czech Republic, v.v.i., Průmyslová 595, 252 50 Vestec, Czech Republic

2. Department of Biochemistry, Faculty of Science, Charles University Prague, Hlavova 8, 128 40 Praha 2, Czech Republic

3. Division of Structural Biology, The Wellcome Trust Centre for Human Genetics, University of Oxford, Roosevelt Drive, Oxford OX3 7BN, United Kingdom

email: t.skalova@gmail.com

Natural killer (NK) cells are a type of lymphocytes which kill tumor, virally infected or stressed cells. Decision to kill a cell is made as a result of balance of signals from plenty of activating and inhibitory receptors on surface of the natural killer cells. LLT1 is a ligand expressed primarily on activated lymphocytes (including NK cells itself). It is a binding partner for NKR-P1, receptor on surface of NK cells. Both NKR-P1 and LLT1 have an extracellular part of C-type lectin like (CTL) fold. Receptors and ligands with CTL fold have not been yet excessively studied and their interactions are not still understood.

Here we would like to present four crystal structures of LLT1 which we have recently published [1]. LLT1 with homogenous GlcNAc<sub>2</sub>Man<sub>3</sub> glycosylation was expressed in HEK293S GnTI<sup>-</sup> cells [2]. The four LLT1 structures differ by its oligomeric state (monomeric, dimeric and hexameric [three dimers in compact packing]) under various pH. Monomeric and dimeric LLT1 crystal structures originate from protein deglycosylated after the first GlcNAc, while the hexameric form corresponds to LLT1 with the original GlcNAc<sub>2</sub>Man<sub>3</sub> glycosylation. The poster will present types of crystal interactions leading to formation of the four crystal structures.

This study was supported by BIOCEV CZ.1.05/1.1.00/02.0109 from the ERDF, by the Czech Science Foundation (project 15-15181S), by the Ministry of Education, Youth and Sports of the Czech Republic (grant LG14009), by Charles University (UNCE 204025/2012, SVV 260079/2014, GA UK 161216), BioStruct-X (EC FP7 project 283570) and Instruct, part of the European Strategy Forum on Research Infrastructures (ESFRI) supported by national member subscriptions.

[1] Skálová *et al.*, Acta Cryst., 2015, D71, 578-591. (Open access)

[2] Bláha *et al.*, Protein Expres. Purif. 2015, 109, 7-13.



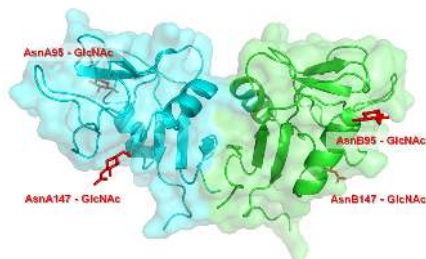


**Figure 1.** Structure of dimeric LLT1 with denoted positions of glycosylation sites.

**Keywords:** LLT1, C-type lectin like, NK receptors

## MS29-P17 A Three-Pronged Approach to Strong Halogen Bonds – Crystallographic, Solution and Computational Study of *N*-Halosuccinimide-Pyridine Complexes

Vladimir Stilinović<sup>1</sup>, Gordana Horvat<sup>1</sup>, Tomica Hrenar<sup>1</sup>, Vinko Nemec<sup>1</sup>, Dominik Cinčić<sup>1</sup>

1. Department of Chemistry, Faculty of Science, University of Zagreb

email: vstilinovic@chem.pmf.hr

Over the past couple of decades halogen bonds (XB) have transformed from an obscure intermolecular interactions known only to a handful of experts into an indispensable tool of crystal engineering rivaling even to hydrogen bond (HB). However, detailed studies of XB energetics are still quite scarcer than those for HB.

In our study we have used commercially available *N*-iodo-, *N*-bromo- and *N*-chlorosuccinimide (**NIS**, **NBS**, **NCS**) as halogen bond donors, succinimide (**S**) as an equivalent HB donor, and 7 *p*-substituted pyridines as halogen (or hydrogen) bond acceptors. The pyridines have been selected to cover as wide as possible range of Hammett coefficients (-0.88 to 0.66), while avoiding functionalities which could act as hydrogen bond donors. This has ensured a relatively large variability of XB acceptor qualities, while ensuring that the observed XB is the only strong intermolecular interaction. In order to provide a detailed description of the halogen bonding in these systems, *N*-halosuccinimides were crystallised with the pyridines in order to study the formed complexes in the solid state. Simultaneously, microcalorimetric measurements were made to study the formation of halogen bonded complexes in acetonitrile solution, and, extensive computations in order to study the deformation of electron density upon XB formation, as well as the effect of various geometric parameters on the energy of XB.

Solid state studies have shown that **NIS** and **NBS** form strong halogen bonds with all 7 pyridine derivatives. **NIS** is expectedly a better XB donor ( $N\cdots X$  distances 29-32% shorter than the sum of van der Waals radii for **NIS** and 23-29% shorter for **NBS**). In both cases the more nucleophilic pyridine nitrogen atoms were better XB acceptors forming shorter bonds. The scattering of the datapoints was larger in the case of **NBS** indicating wider and more shallow potential well for XB with **NBS**, as confirmed computationally. The differences in the measured bond lengths were mirrored in the stability of the **NIS**-pyridine complexes in the solution - the stability constants were found to vary by over three orders of magnitude from  $\log K = 4.003(9)$  for the complex exhibiting the shortest XB to  $\log K = 0.825(3)$  for the one with the longest bond. In comparison, **S** was found to produce hydrogen-bonded cocrystals only with the two strongest nucleophiles used, and the corresponding stability constants were nearly four orders of magnitude lower than those for halogen bonded complexes with **NIS**.

**Keywords:** halogen bond, supramolecular chemistry, *N*-halosuccinimides

## MS29-P18 $\beta$ -diketones and their derivatives in Rh(I) dicarbonyl and phosphine complexes

Getruida J.S. Venter<sup>1</sup>, Mohammed A.E. Elmakki<sup>1</sup>, Johan A. Venter<sup>1</sup>

<sup>1</sup> University of the Free State, PO Box 339, Bloemfontein 9300, South Africa

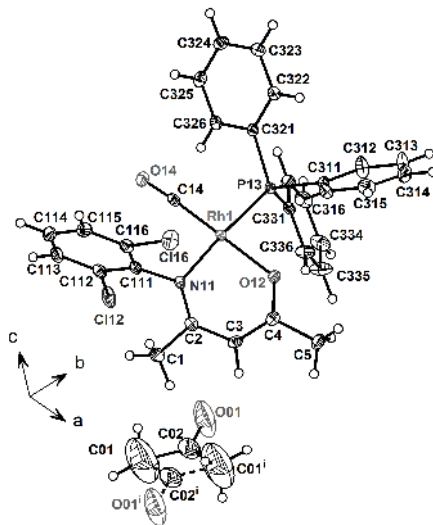
email: VenterGJS@ufs.ac.za

This study is concerned with the application of  $\beta$ -diketone derivatives, specifically enaminoketones and cupferron variants, as ligand systems and the influence of substitution on such ligands with regard to rhodium(I) complex formation. Enaminoketones contain nitrogen and oxygen donor atoms as well as an alkene functionality, and as such these electron-rich compounds are of interest in various areas, including application as liquid crystals [1], in fluorescence studies [2], the medical field [3,4] and with significant potential in homogeneous catalysis [5].

A range of crystal structures of the  $[\text{Rh}^{\text{I}}(\text{Bid})(\text{CO})(\text{PX}_3)]$  (where X is a combination of phenyl and cyclohexyl groups) complexes [6,7] as catalyst precursors will be discussed. Furthermore, the exchange between free and coordinated phosphine as indicated through nuclear magnetic spin transfer techniques will be highlighted.

### References

- [1] W. Pyżuk, A. Krówczyński and E. Górecka, *Mol. Cryst. Liq. Cryst.* **237** (1993), 75-84.
- [2] M. Xia, B. Wu and G. Xiang, *J. Flu. Chem.* **129** (2008), 402-408.
- [3] H.Y. Tan, W.K. Loke, Y.T. and Tan, N.-T. Nguyen, *Lab Chip* **8** (2008), 885-891.
- [4] W.J. Fanshawe, L.S. Crawley, S.R. Safir, G.E. Wiegand and E.C. Cooley, Substituted enaminoketones (1974), US3997530 (Patent).
- [5] V.A. Nair, M.M. Suni and K. Sreekumar *Proc. Indian Acad. Sci. (Chem. Sci.)* **114** (2002), 481-486.
- [6] G.J.S. Venter, G. Steyl and A. Roodt, *Z. Kristallogr.* **228** (2013), 410-412.
- [7] G.J.S. Venter, G. Steyl and A. Roodt, *Acta Cryst.* **E65** (2009), m1606-m1607.



## MS29-P19 Luminescence study of anthracene derivatives and their complexes with silver

Noémie Voutier<sup>1</sup>, Jing Chen<sup>1</sup>, Katharina M. Fromm<sup>1</sup>

<sup>1</sup>. Department of Chemistry, University of Fribourg, Chemin du musée 9, CH-1700 Fribourg, Switzerland

email: noemie.voutier@unifr.ch

An excimer, or excited dimer, is formed when a fluorophore in its ground state interacts with a fluorophore in its excited state. For this to happen, the two fluorophores should be within Van der Waals contact distance. The fluorescence of such dimer is usually shifted to lower energies, and shows a broader band. This difference in emission makes such a system an interesting candidate for sensor application<sup>1</sup>. Anthracene, due to its luminescence properties and possible formation of excimer, has been studied as sensor for selective recognition<sup>2,3</sup>. In our group, an isonicotinic derivative of anthracene has shown interesting fluorescence properties and was designed to be used as a luminescent tracer placed on an antibacterial implant coating<sup>4</sup>.

We here study the luminescence behavior of anthracene molecules functionalized with nicotinic and isonicotinic acid, and their complexes with silver. In a previous study, the isonicotinic derivative (fig 1. b) formed coordination polymers with silver<sup>5</sup> dependent on the solvent and anion considered. This compound showed excimer emission around 520nm in solid state, due to the stacking of the anthracene moiety. We are completing the study with the other 3 ligands (fig 1) and are interested in the influence of solvent molecules and anions in the solid state, therefore the packing of the molecules, on their luminescence.

### References:

- <sup>1</sup>H. N. Lee, Z. Xu, S. K. Kim, K. M. K. Swamy, Y. Kim, S.-J. Kim and J. Yoon, *J. Am. Chem. Soc.*, **2007**, 129, 3828
  - <sup>2</sup>F. Huang and G. Feng, *RSC Adv.*, **2014**, 4, 484
  - <sup>3</sup>S. Malkondou, D. Turhan and A. Kocak, *Tetrahedron Letters*, **2015**, 56, 162
  - <sup>4</sup>P. S. Brunetto and K. M. Fromm, *Chimia*, **2008**, 62, 249
  - <sup>5</sup>J. Chen, A. Neels and K. M. Fromm, *Chem. Comm.*, **2010**, 46, 8282
- We thank Anne Schuwey and the Laboratoire Central of the University of Fribourg for their precious help.

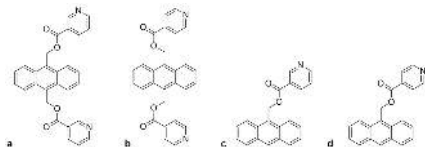


**Figure 1.** Structures of the anthracene derivatives a: anthracene-9,10-diylbis(methylene)nicotinate b: anthracene-9,10-diylbis(methylene)diisonicotinate c: anthracene-9-ylmethyl nicotinate d: anthracene-9-ylmethyl isonicotinate

## MS30 Hydrogen bonding from theory to applications

Chairs: László Fábián, Nikolett Bathori

### MS30-P1 Towards an Understanding of Hydrate Formation

Alankriti Bajpai<sup>1</sup>, Michael J. Zaworotko<sup>1</sup>

<sup>1</sup>. Department of Chemical and Environmental Sciences, University of Limerick, Limerick, Republic of Ireland

email: alankriti.bajpai@ul.ie

Hydrates constitute an important class of multicomponent crystals pertinent to both crystal engineering<sup>1-3</sup> as well as pharmaceutical science<sup>4</sup>. The occurrence of hydrates in molecules containing solely strong H-bond donors or H-bond acceptors in particular has thus far been understudied. A comprehensive investigation of hydrate formation in *N*-heterocyclic aromatic compounds that lack strong H-bond donor groups was therefore performed. A Cambridge Structural Database (CSD) survey of 5- and 6-membered *N*-heterocyclic aromatics, and hydrate screening experiments on a small set of compounds **1-11** (Figure 1) were conducted. The hydrate screening experiments involved: (i) crystallization from mixed solvent systems, (ii) slurry in water at ambient temperature, and (iii) exposure of anhydrous form to humid conditions (75% relative humidity at 40 °C). The results, which, when coupled with modelling experiments, provide much needed insights into the formation of hydrates and will be detailed.

### References:

1. Desiraju, G. R. *J. Chem. Soc., Chem. Commun.* **1991**, 426.
2. Infantes, L.; Fabian, L.; Motherwell, W. D. S. *CrystEngComm* **2007**, 9, 65.
3. Clarke, H. D.; Arora, K. K.; Bass, H.; Kavuru, P.; Ong, T. T.; Pujari, T.; Wojtas, L.; Zaworotko, M. J. *Cryst. Growth Des.* **2010**, 10, 2152.
4. Khankari, R. K.; Grant, D. J. W. *Thermochim. Acta* **1995**, 248, 61.

**Keywords:** Anthracene, excimer, solid state fluorescence, PXRD

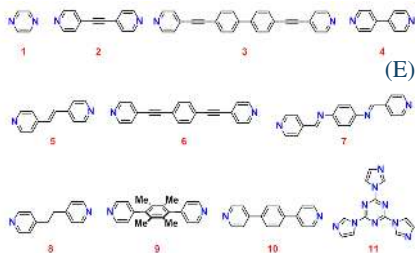


**Figure 1.** *N*-heterocyclic compounds investigated for hydrate screening.

**Keywords:** Crystal engineering, hydrogen bonding, hydrate screening

## MS30-P2 Theoretical and Experimental Investigation of (E)-2-([3,4-dimethylphenyl]imino)methyl)-3-methoxyphenol

Orhan Büyükgüngör<sup>1</sup>, Zeynep Demircioğlu<sup>1</sup>, Çiğdem Albayrak<sup>2</sup>

1. Department of Physics, Faculty of Arts and Sciences, Ondokuz Mayıs University, Samsun, Turkey

2. Department of Chemistry, Faculty of Arts and Science, Sinop University, Sinop, Turkey

email: orhanb@omu.edu.tr

The molecular structure and spectroscopic properties of the title compound were investigated by X-ray diffraction, FT-IR and UV-vis spectroscopy. The x-ray structure analysis showed that the molecule has O–H...N intramolecular hydrogen bonding and it adopts the enol-imine tautomeric form. This is also confirmed by the calculations made using density functional theory (DFT) method with B3LYP applying 6-31G(d,p) basis set, for both O–H...N interactions in enol-imine form and N–H...O interactions in keto-amine form.

The harmonic vibrational frequencies (FT-IR) were calculated and compared with the experimental values. The study of the highest occupied molecular orbital (HOMO) and lowest unoccupied molecular orbital (LUMO) analysis has been used to elucidate information regarding charge transfer within the molecule. Moreover, the calculation of Mulliken Population analysis and Natural Population analysis were provided to estimate partial atomic charges. Stability of the molecule arising from hyper-conjugative interactions and charge delocalization has been analyzed by using Natural Bond Orbital (NBO) analysis. The results of nonlinear optical (NLO) properties of the molecule showed that it exhibits good nonlinear optical (NLO) activity and so can be used as an effective optical material.

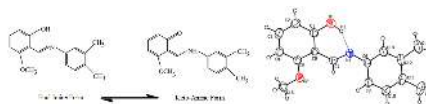


**Figure 1.** Enol-imine and keto-amine tautomeric forms (left) and the molecular structure (right) of the title compound.

**Keywords:** X-ray Diffraction, Density Functional Theory (DFT), Natural Population Analysis (NPA), Natural Bond Analysis (NBO), Chemical activity.

### MS30-P3 Charge density analysis of intermolecular interactions in the crystal structures of two molecular complexes of p-hydroxybenzoic acid

Maciej Kubicki<sup>1</sup>, Agata Owczarzak<sup>1</sup>

1. Faculty of Chemistry, Adam Mickiewicz University, Poznan, Poland

email: mkubicki@amu.edu.pl

Experimental charge density analysis, based on high-resolution diffraction data, has its own and high technical demands, but it gives - in return - an opportunity of deeper insight into the details of charge density distribution in the crystal, in particular into both, intra- and intermolecular interactions. It has been shown that this method can be very important for the hydrogen bond analysis, allowing for instance for the building of the hierarchy of the interactions.

We have performed high resolution diffraction studies of two molecular complexes: N-methyl piperidine betaine with p-hydroxybenzoic acid and trygonelline hydrate with p-hydroxybenzoic acid (Fig. 1). The charge density analysis of these structures together with the Atoms-In-Molecules description of the interactions will be presented.

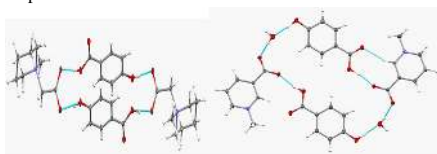


**Figure 1.** Main hydrogen bonding motifs in the structures of 1 (left) and 2 (right)

**Keywords:** charge density, hydrogen bonds, atoms-in-molecules

### MS30-P4 Gemfibrozil chain conformation and crystal packing requirements

Carl H. Schwalbe<sup>1,2</sup>, Miren Ramirez<sup>1</sup>, Barbara R. Conway<sup>3</sup>, Peter Timmins<sup>4</sup>

1. School of Life & Health Sciences, Aston University, Birmingham B4 7ET, U.K.

2. Cambridge Crystallographic Data Centre, 12 Union Rd., Cambridge CB2 1EZ, U.K.

3. School of Applied Sciences, University of Huddersfield, Huddersfield HD1 3DH, U.K.

4. Bristol-Myers Squibb, Reeds Lane, Moreton, Cheshire CH46 1QW, U.K.

email: carlschwalbe@hotmail.com

To pack efficiently, the antilipidaemic drug gemfibrozil (Gem, Fig. 1) must find interaction partners for both its highly polar carboxyl group and its bulky nonpolar dimethylphenyl group. These can be well separated if the intervening  $\text{Ph-O-(CH}_2)_3\text{-CMe}_2\text{-COO}$  linkages have an *all-trans* conformation. Structures of Gem free acid [1] and four salts [2] appear in the Cambridge Structural Database. Additionally, we have determined the structures of the adamantylammonium (GAdam), benzylammonium (GBenz), cyclobutylammonium (GCbut), cyclohexylammonium (GChex), and triethanolammonium (GTea) salts. In the free acid the first four link conformations are *trans* and the last two are *gauche*. A Mogul [3] search confirms that these values are preferred for the first five torsion angles, suggesting low energy, while the sixth has no preference. The same arrangement persists in most salts, creating ether  $\text{O}\cdots\text{carboxyl O}$  distances of 5.17-5.89 Å; but with Tris the Gem anions lengthen one such  $\text{O}\cdots\text{O}$  distance to 6.32 Å. Complexed with human transthyretin [4], where Gem occupies the thyroxine T4 binding site, the  $\text{O}\cdots\text{O}$  distances stretch almost 1 Å farther. In the latter two structures the carboxyl(ate) group is *trans* to the rest of the chain.

The carboxyl groups in paired molecules of the free acid form  $\text{R}_2^2(8)$  dimers. In (aryl)alkylammonium salts the ionic groups form ladders of hydrogen-bonded rings, either  $\text{R}_4^3(10)$  or alternating  $\text{R}_2^2(8)$  and  $\text{R}_4^4(12)$ . Cations with one or two OH groups build these into the chains of rings; but in the Tris salt the cations form hydrogen bonded layers [2], retaining two hydrogen bonds to one carboxylate O atom and one to the other. In the non-hydroxylated ladder-forming salts a correlation coefficient of 0.85 between the average of the two  $\text{O}\cdots\text{O}$  distances in Gem and the distance from the N atom to the most distant C atom in the cation suggests that there may be some mutual adaptation. In the transthyretin binding site Gem does not increase its number of hydrogen bonds, so any energy needed to stretch it must be supplied by packing interactions.

We thank the U.K. National Crystallography Service for data collection.

[1] B. Bruni et al. (2005) *Acta Cryst.* **E61**, o1989-o1991. [2] E.Y. Cheung et al. (2007) *J. Solid State*

*Chem.* **180**, 1068-1075. [3] I.J. Bruno et al. (2004) *J. Chem. Inf. Comput. Sci.* **44**, 2133-2144. [4] I. Iakovleva et al. (2015). *J. Med. Chem.* **58**, 6507-6515.

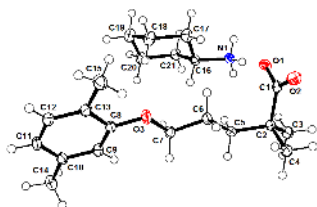


**Figure 1.** ORTEP drawing of the cyclohexylammonium salt of gemfibrozil

**Keywords:** gemfibrozil, chain conformation, crystal packing

## MS30-P5 Comparison of hydrates of 4,6-diaminopyrimidine with selected dicarboxylic acids (oxalic, malonic, succinic, glutaric and adipic)

Jan Fábry<sup>1</sup>, Irena Matulková<sup>2</sup>, Jana Mathauserová<sup>2</sup>, Ivan Němec<sup>2</sup>, Ivana Čisářová<sup>2</sup>

1. Institute of Physics, Academy of Sciences of the Czech Republic, Na Slovance 2, 182 21 Praha 8, Czech Republic, E-mail: fabry@fzu.cz

2. Faculty of Science, Department of Inorganic Chemistry, Charles University in Prague, Hlavova 2030/8, 128 43 Praha 2, Czech Republic

email: fabry@fzu.cz

The structures of  $2(\text{C}_4\text{N}_2\text{H}_7^+)\text{C}_2\text{O}_4^{2-} \cdot 4\text{H}_2\text{O}$ ;  $\text{C}_4\text{N}_2\text{H}_7^+ \cdot \text{C}_2\text{H}_3\text{O}_4^- \cdot \text{H}_2\text{O}$ ;  $2(\text{C}_4\text{N}_2\text{H}_7^+)\text{C}_3\text{H}_4\text{O}_4^{2-} \cdot 8\text{H}_2\text{O}$ ;  $2(\text{C}_4\text{N}_2\text{H}_7^+)\text{C}_3\text{H}_3\text{O}_4^{2-} \cdot 2\text{H}_2\text{O}$  and  $2(\text{C}_4\text{N}_2\text{H}_7^+)\text{C}_6\text{H}_8\text{O}_8^{2-} \cdot 8\text{H}_2\text{O}$  are compared. There are common features in the title structures: **1]** All of them are centrosymmetric. The molecules of ethanedioic, butanedioic and hexanedioic acid are situated on the inversion centres. **2]** In all the structures, there are N-H...N, N-H...O<sub>(acid)</sub>, N-H...O<sub>w</sub> and O<sub>w</sub>-H...O and O<sub>w</sub>-H...O<sub>w</sub> hydrogen bonds. The intermolecular hydrogen bonds are of moderate strength. **3]** There are graph set motifs  $R^2_2(8)$  in which the dicarboxylic groups and the primary and secondary amine groups are involved. The secondary amine group tends to form a somewhat shorter hydrogen bond with respect to the primary amine group. **4]** There is a growing complexity of arrangement of the water molecules towards the structures with a longer dicarboxylic molecule while it seems that the dependence on the parity of the number of carbon atoms in the dicarboxylic acid is present: in the structure with ethanedioic acid the water molecules form rows parallel to b axis; in the structure with hydrogen propanedioic acid the water molecules are linked in a pair of water molecules; in the structure with butanedioic acid the water molecules themselves form layers composed of annelated six-membered rings parallel to (0 1 0); in the structure with pentanedioic acid the water molecules themselves forms rows along b axis; in the structure with hexanedioic acid the water molecules themselves form columns parallel to b axis while each layer in the column contains 4 water molecules. This substructure corresponds to a section from structure of pure water though the hydrogens are ordered in the title structure.

### Acknowledgements:

This work was supported by the Czech Science Foundation (grant no. 14-05506S).

**Keywords:** hydrogen bonding, dicarboxylic acids, 4,6-diaminopyrimidine

## MS31 Crystal energy landscapes: computation and uses

Chairs: Anthony Reilly, Marcus Neumann

### MS31-P1 Quantifying Intermolecular Interaction Energies in Organic Clathrates at High Pressure

Espen Eikeland<sup>1</sup>, Solveig R. Madsen<sup>1</sup>, Maja K. Thomsen<sup>1</sup>, Jacob Overgaard<sup>1</sup>, Mark A. Spackman<sup>2</sup>, Bo B. Iversen<sup>1</sup>

1. Center for Materials Crystallography, Department of Chemistry and iNANO, Aarhus University, DK-8000 Aarhus C, Denmark
2. School of Chemistry and Biochemistry, M310 University of Western Australia, 35 Stirling Hwy, Crawley, 6009, Australia

email: eikeland@chem.au.dk

Molecular self-assembly is at the heart of the field of crystal engineering and supramolecular chemistry. Yet, it is striking that the fundamental chemistry governing even simple self-assembly processes are not well understood. To improve our understanding it is necessary to precisely quantify the different superimposed intermolecular interactions, such as dispersion and electrostatic energies. In this project novel *energy frameworks* [1] are used to study and eloquently illustrate host-guest interaction energies in three different hydroquinone clathrate systems containing formic acid, acetonitrile and methanol respectively, as the different guest molecules. The intermolecular interaction in these systems have been probed by subjecting single crystals to high external pressure, forcing the molecules closer together. In this way it is possible to observe how changing the guest molecule affect the compression of the host structure. For the hydroquinone – formic acid structure an interesting new pressure-medium-dependent phase transition is observed where the host structure collapse and the guest molecules migrate out of the cavities. The phase transition can be kinetically hindered using a non-hydrostatic pressure-transmitting medium, enabling the comparison of intermolecular energies in two polymorphic structures in the same pressure range [2]. For the hydroquinone – acetonitrile system the guest molecule is found to heavily influence the compression of the host structure until a phase transformation occurs above 4 GPa, where the guest molecule break the host symmetry, reducing the space group symmetry to P-1. *Energy frameworks* can be used to explain the nature of the phase transformations. A new analysis method combining void space analysis and equation of state calculations have been used to quantify the compression of the host cavities and how they are influenced by the presence of different guest molecules. In this way we show that in the hydroquinone – formic acid clathrate system the cavity volume is reduced by more than 50 % up to 4 GPa [2].

[1] M. J. Turner, S. P. Thomas, M. W. Shi, D. Jayatilaka, M. A. Spackman. *Chem. Commun.* 2015, 51, 3735–3738

[2] E. Eikeland, M. K. Thomsen, S. R. Madsen, J. Overgaard, M. A. Spackman, B. B. Iversen. *Structural Collapse of the Hydroquinone–Formic Acid Clathrate: A Pressure-Medium-Dependent Phase Transition* *Chem. Eur. J.* 2016, 22, 4061 – 4069

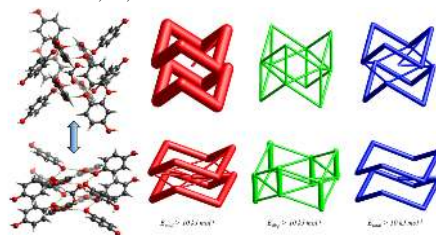


**Figure 1.** *Energy frameworks* for the hydroquinone - formic acid clathrate before (top row) and after (bottom row) the structural collapse of the host structure at 4 GPa. The electrostatic, dispersion and total interaction energies are colored red, green and blue, respectively.

**Keywords:** Energy frameworks, intermolecular energies, high-pressure crystallography, host-guest interactions, organic clathrates



## MS31-P2 *q*-GRID: a new method to calculate lattice and interaction energies for molecular crystals from electron densities

Joost A. van den Ende<sup>1</sup>, Niek J. J. de Klerk<sup>1</sup>, Johannes van de Haar<sup>1</sup>, Rita Bylsma<sup>1</sup>, Peter Grančič<sup>1</sup>, Gilles A. de Wijs<sup>1</sup>, Herma M. Cuppen<sup>1</sup>, Hugo Meekes<sup>1</sup>

1. Radboud University, Institute for Molecules and Materials, Nijmegen, The Netherlands

email: j.vandenende@science.ru.nl

Mapping of intermolecular interactions is a useful tool to obtain packing motives and insights in the relative stability of different crystal structures. Obtaining quantitative information on these interactions is, however, not straightforward. Often, the gas phase conformation and charge distribution of an isolated molecule are used as a starting point - for instance in the PIXEL method[1] - although many examples exist in which this approximation is not applicable. Here we present *q*-GRID[2], a newly developed and freely accessible tool ([www.theochem.ru.nl/qGRID](http://www.theochem.ru.nl/qGRID)) that is designed to calculate intermolecular interactions directly from conformations and the charge distribution as obtained within the crystal. The charge distribution on a grid is partitioned over the different molecules. For the electrostatic interactions, simply the Coulomb energy is determined by a summation over the grid points of the different molecules. Added to this are empirical dispersion and repulsion contributions. The sum of the three components leads to pairwise intermolecular interactions that perform very well in all three test systems studied; anthracene, isonicotinamide and DL-methionine.[2]

Two ways in which *q*-GRID can be used are, ranking the stability of different crystal structures on the basis of the lattice energy[3] and zooming in at specific interactions within a crystal. Fig. 1 is an example of the latter, it shows the dominant interactions in the five known polymorphic forms of isonicotinamide. Two different classes of dimer configurations can be clearly seen. The strongest one is an amide-connected dimer which is only present in the thermodynamically stable polymorph, Form I. Interestingly, metastable polymorphs only crystallize from solution when these amide-connected dimers are absent from the solution.[4] This can be understood with the results of Fig. 1, since this particular dimer has a stronger interaction energy than the other leading interactions. Currently, we are further developing *q*-GRID by more precisely treating the dispersion and repulsion energy terms. In the future we aim to use *q*-GRID for morphology and nucleation rate predictions.

[1] A. Gavezzotti, *Mol. Phys.*, 2008, 106, 1473

[2] Niek J. J. de Klerk, Joost A. van den Ende *et al.*, *Cryst. Growth Des.*, 2016, 16, 662

[3] Anthony M. Reilly, Joost A. van den Ende, Colin R. Groom *et al.*, *Acta Cryst. B*, submitted

[4] Samir. A. Kulkarni *et al.*, *Chem. Commun.*, 2012, 48, 4983

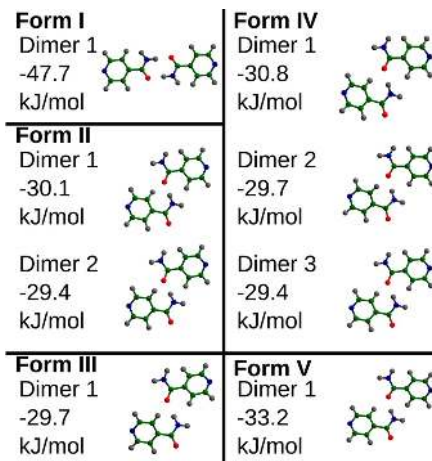


**Figure 1.** The strongest intermolecular interactions within the five different polymorphic forms of isonicotinamide as obtained with the *q*-GRID method. The strongest dimer in the thermodynamically stable polymorph, Form I, is much stronger than the strongest dimers in the metastable polymorphs.

**Keywords:** intermolecular interactions, computational tool, molecular crystals, charge distribution, polymorphism

**MS31-P3** Accurate and efficient representation of intramolecular energy in *ab initio* generation of crystal structures.

Isaac Sugden<sup>1</sup>, Claire Adjiman<sup>1</sup>, Constantinos Pantelides<sup>1</sup>

1. Faculty of Engineering, Department of Chemical Engineering, Imperial College London, UK

email: I.sugden@imperial.ac.uk

The CrystalPredictor I<sup>1,2</sup> and II<sup>3</sup> codes have been used to explore the space of crystal structures have been used successfully in several crystal structure prediction (CSP) investigations in recent years<sup>4</sup>, including in the series of blind tests organised by the Cambridge Crystallographic Data Centre<sup>5,6</sup> and in the prediction of the crystal structures of pharmaceutically-relevant molecules<sup>7,8</sup>. We present a summary of CrystalPredictor, focussing on improvements to the lattice energy evaluation that the most recent blind test<sup>9</sup>, as well as our own investigations into a variety of flexible polymorphic molecules, has prompted. These improvements aim to achieve greater accuracy in the initial ranking of potential crystal structures, while managing computational cost so that a thorough exploration of the search space is possible. Firstly we discuss non-uniform LAMs; an innovation in CrystalPredictor II that allows the most efficient use of computational effort to cover a flexible molecule's conformational space. We use blind test molecule 26 as an example. Secondly, we discuss the smoothing of the intramolecular potential, which improves accuracy in CrystalPredictor II by collating data from *ab initio* calculations. The impact of this approach is investigated based on a CSP study for flufenamic acid<sup>10</sup>.

(1) Karamertzanis, P. G.; Pantelides, C. C. *J Comput Chem* **2005**, 26, 304.

(2) Karamertzanis, P. G.; Pantelides, C. C. *Mol Phys* **2007**, 105, 273.

(3) Habgood, M.; Sugden, I. J.; Kazantsev, A. V.; Adjiman, C. S.; Pantelides, C. C. *J Chem Theory Comput* **2015**, 11, 1957.

(4) Pantelides, C. C.; Adjiman, C. S.; Kazantsev, A. V. *Top Curr Chem* **2014**, 345, 25.

(5) Day, G. M.; *et. al.* . *Acta Crystallogr B* **2009**, 65, 107.

(6) Bardwell, D. A.; *et. al.* *Acta Crystallogr B* **2011**, 67, 535.

(7) Vasileiadis, M.; Pantelides, C. C.; Adjiman, C. S. *Chem Eng Sci* **2015**, 121, 60.

(8) Vasileiadis, M.; Kazantsev, A. V.; Karamertzanis, P. G.; Adjiman, C. S.; Pantelides, C. C. *Acta Crystallographica Section B-Structural Science* **2012**, 68, 677.

(9) Reilly, A. M. *et. al.* *Acta Crystallographica Section B: Structural Science, Crystal Engineering and Materials* **2016**.

(10) Lopez-Mejias, V.; Kampf, J. W.; Matzger, A. J. *J Am Chem Soc* **2012**, 134, 9872.

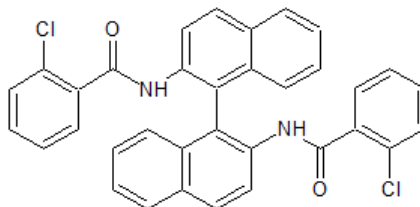


Figure 1. The flexible molecule 26

**Keywords:** Crystal energy, polymorphism

# MS31-P4 Stabilization of dynamically unstable crystal structures in the Decoupled Anharmonic Mode Approximation (DAMA)

Donat J. Adams<sup>1</sup>

<sup>1</sup> Reliability Science and Technology Laboratory Empa, Swiss Federal Laboratories for Materials Science and Technology Ueberlandstrasse 129 CH-8600 Dübendorf

email: donat77adams@gmail.com

The combination of experimental structure determination with *ab initio* simulations allows to refine structures with poor data. Still, this complementation is difficult, especially when it comes to crystal structures at high temperature or to temperature driven phase transitions: there the observed high temperature crystal structures often appear unstable once they are recalculated *ab initio*.

We therefore have developed a formalism (DAMA, [1,2]) that allows to calculate the vibrational free energy using DFT even for materials which exhibit negative curvature of the potential energy surface with respect to atomic displacements. Our novel solver allows to calculate the true vibrational states of the anharmonic potential in a non-perturbative way.

We apply the DAMA to the perovskite cryolite ( $\text{Na}_3\text{AlF}_6$ ) and investigate the phase transition from the  $P2_1/n$  to the  $Immm$  space group at a critical temperature between 710 and 950 K (experimental value 885 K [3]). We thus show that the free energy can stabilize crystal structures at finite temperatures which appear dynamically unstable at  $T = 0$ . Furthermore for cryolite we calculate the main axes of the thermal ellipsoid and can explain the experimentally observed increase of its volume for the fluorine by 250% at  $T_c$ .

Our calculations suggest the appearance of tunnelling states in the high temperature phase with a degenerate vibrational spectrum.

We compare our method to other approaches like the solution of effective Hamiltonians using Monte Carlo simulations or molecular dynamics, the SCAILD[4] and SSCHA [5]. We investigate the convergence of the vibrational DOS and of the critical temperature with respect of reciprocal space sampling using the polarizable-ion model.

From these very promising tests we conclude, the the DAMA formalism is computationally fast because it avoids statistical sampling and is completely *ab initio*. It is free of statistical uncertainties and independent of model parameters, but can give insight into the mechanism of temperature-driven structural phase transitions.

[1] Adams and Passerone, *submitted* (2016)

[2] Adams, *Solid State Ionics, in press* (2016)

[3] Yang et al. *Phys. Chem. Minerals* 19, 528 (1993)

[4] Souvatzis et al. *Phys. Rev. Lett.* 100, 095901 (2008)

[5] Errea et al. *Phys. Rev. B* 89, 064302 (2014)

[6] Zhong and Vanderbilt, *Phys. Rev. B* 53, 5047 (1996)

[7] Müller et al., *Z. Physik B Cond. Matt.* 84, 277 (1991)

[8] Bednorz and Müller, *Z. Physik B Cond. Matt.* 64, 189 (1986)

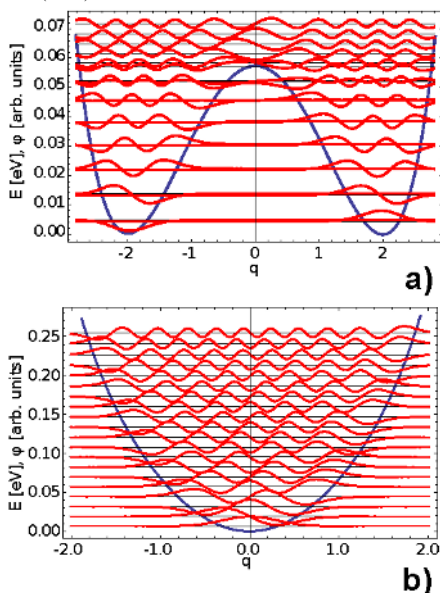


**Figure 1.** Eigenstates a) for the monoclinic and b) for the orthorhombic of cryolite, which due to delocalized ions in other crystals could give rise to physical properties such as multiferroicity [6], high dielectric constant [7] and superconductivity [8].

**Keywords:** High temperature crystal structure, vibrational ellipsoid, high temperature phase transition, *ab initio* calculations, free energy calculation, cryolite

## MS32 Polymorphs, cocrystals, solvates, salts: a jungle for scientists and industries

**Figure 1.** Primary cell of trospium triiodide

**Keywords:** Salt, Organic ions, X-ray diffraction, Structure, Crystallography,

Chairs: Catharine Esterhuysen, Martin Schmidt

### MS32-P1 Structural Characterization of Various Salts of Trospium: From Small Change of Anion to Huge Unit Cell

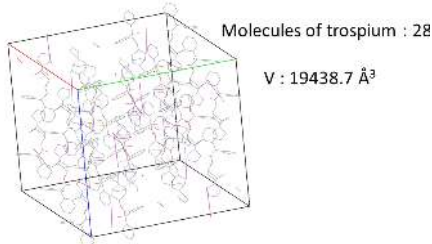
Martin Babor<sup>1</sup>, Eliška Skořepová<sup>1</sup>, Jan Čejka<sup>1</sup>

<sup>1</sup>. Department of Solid State Chemistry, University of Chemistry and Technology Prague, Czech Republic

email: baborm@vscht.cz

Trospium chloride (TCl) is a drug used to treat urge incontinence and frequent urination. Four different salts of trospium are known. They are trospium chloride, bromide, iodide and saccharinate. A detailed structure characterization is available only for TCl. In this work, a single-crystal X-ray diffraction was used for structure characterization. The salts of trospium were prepared in two different ways. Inorganic salts were made from a mixture of TCl with hydrobromic or hydriodic acid in varied ratio. Organic salts were prepared from a mixture of TCl and sodium salt of organic acid in ratio 1:1. New structures of four forms were solved (trospium iodide, triiodide and two polymorphs of trospium saccharinate). New structures and structure of TCl were compared to each other and high similarity was found among them. There is some small trend between the anion shape and the structure, but different anions create similar structure as well. An extreme example of the structure dependent variation on the anion is trospium triiodide, which crystallized in a really huge unit cell ( $V=19438.7 \text{ \AA}^3$ ) almost seventy times larger than in the other structures of the trospium salts.

This work was supported by the Grant Agency of Czech Republic, Grant no. 106/16/10035S and received financial support from specific university research (MSMT No 20/2016).



## MS32-P2 Rhenium Monomers vs. Manganese Dimers – what is driving the linkage ?

Alice Brink<sup>1</sup>, Pennie P. Mokolokolo<sup>1</sup>, Hendrik G. Visser<sup>1</sup>,  
Andreas Roodt<sup>1</sup>

<sup>1</sup>. Department of Chemistry, University of the Free State, P.O. Box 339, Bloemfontein 9300, South Africa.

email: brinka@ufs.ac.za

During the design of pharmaceuticals, in particular those containing a transition metal radionuclide, several factors should always be kept in mind, such as, the half-life of the radionuclide, type of radiation, oxidative state, stability and biological suitability of the organometallic complex as well as the final coordination mechanism of the ligand to the radionuclide [1-3].

Our interest in the tricarbonyl complexes of the Group 7 Manganese Triad, namely *fac*-[M<sup>I</sup>(CO)<sub>3</sub>] (M = Mn, Re and Tc) has resulted in several unexpected structural results [4-7]. The radionuclides of rhenium and technetium show distinct advantages for theranostics complexes [8] with the technetium diagnostic application, combined with the therapeutic potential of rhenium [9] as well as the anti-inflammatory potential of superoxide dismutase manganese mimics [10]. As always in pharmaceutical development the final coordination mode of the organometallic complexes in solid and solution are of importance and ideally identical.

We report here several monomer and dimeric complexes of the manganese, technetium and rhenium triad that have formed with identical ligand systems in the solid state. In solution state, however all complexes indicate monomer coordination stabilised by the coordinating solvents. The possible crystallization factors which drive this monomer vs. dimer solid state observation will be discussed as well the kinetic substitution of the *fac*-[Re/Mn(N,O-Bid)(CO)<sub>3</sub>(X)] (where N,O-Bid = N and O donor atoms of mono-negative bidentate ligands, X = methanol, aqua, acetone) on the 6<sup>th</sup> solvento position.

### References:

- [1] Liu, S., *Chem. Soc. Rev.*, 2004, 33, 445-461. [2] Liu, S., Edwards, D.S., *Top. Curr. Chem.*, 2002, 222, 259-278. [3] Volkert, W.A., Hoffman, T.J., *Chem. Rev.*, 1999, 99, 2269-2292. [4] Brink, A., Visser, H.G., Roodt, A., *Inorg. Chem.*, 2013, 52, 8950- 8961. [5] Brink, A., Visser, H.G., Roodt, A., *Inorg. Chem.*, 2014, 53, 12480-12488. [6] Marake, D.T., Mokolokolo, P.P., Visser, H.G., Brink, A., *Acta Cryst.*, 2015, C71, 423-429. [7] Mokolokolo, P.P., Brink, A., Visser, H.G., *Z. Kristallogra., NCS*, 2016, DOI 10.1515/ncrs-2015-0210. [8] Svenson, S., *Mol. Pharmaceutics*, 2013, 10, 848-856. [9] Can, D., Schmutz, P., Sulieman, S., Spingler, B., Alberto, R., *Chimia*, 2013, 67, 267-270. [10] Miriyala, S., Spasojevic, I., Tovmasyan, A., Salvemini, D., Vujaskovic, Z., St. Clair, D., Batinic-Haberle, I., *Biochimica et Biophysica Acta*, 2012, 1822, 794-814

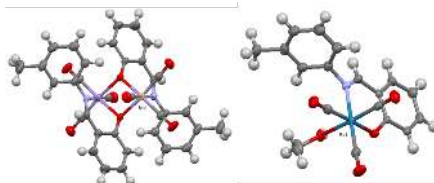


**Figure 1.** The manganese and rhenium dimeric / monomeric structures of *fac*-[M(N,O-Bid)(CO)<sub>3</sub>(X)] complexes.

**Keywords:** rhenium, manganese, tricarbonyl, dimerization, theranostics

**MS32-P3** A thermal gradient approach towards polymorph selection in thin filmsBasab Chattopadhyay<sup>1</sup>, Yves H. Geerts<sup>1</sup>

1. Laboratoire de Chimie des Polymères (LCP) Université Libre de Bruxelles CP 206/01 Boulevard du triomphe 1050 Brussels, Belgium

email: basab.chattopadhyay@ulb.ac.be

Polymorphism can be defined as the intrinsic ability of a solid material to exist in two or more crystal forms which may differ in the molecular conformation and/or crystal packing. The phenomenon is generally understood in terms of nucleation, i.e. once a nucleus of a given phase has appeared, growth continue in the same phase without any subsequent phase transition. Polymorphism is central to crystal science and is of great importance for industrial sectors like pharmaceuticals, fertilizers, explosives, pigments, and organic electronics because it has a dramatic influence on properties of materials. Although an extensive body of research is available in this topic, some elements key to the understanding of polymorphism is still missing. To this extent we sought to understand the role of heat flux in polymorphic control and phase transitions with a model system, acetaminophen. This is experimentally facilitated by a temperature gradient heating stage which essentially consists of two independent heating elements separated by a distance of 2.5 mm. One of the heating elements is set at a temperature, above the melting temperature (hot side) while the other at a temperature below the crystallization temperature (cold side) of acetaminophen. Structural evolution is then followed as thin films of acetaminophen are translated from the hot zone to the cold zone. Thin films are ideal model systems, because of the absence of convection, heat transport occurs only by diffusion. In this presentation, we report on the crystallization of polymorphs of acetaminophen as a function of thermal gradient parameters (magnitude of the gradient, sample velocity) in a thin film geometry. The thin film samples were displaced at a given rate ( $1 \leq v \leq 75 \mu\text{m/s}$ ) to control direction and the rate of crystal growth. This allowed us to decouple nucleation and growth. A detailed structural analysis combining polarized optical microscopy (POM) and X-ray diffraction (out-of-plane, in-plane) has been carried out to characterize different crystalline forms produced by the thermal gradient technique.

**Keywords:** Polymorphism, Thermal Gradient, Thin film, X-ray Diffraction

**MS32-P4** Re-investigating the structures of *trans*-[Cu(NO<sub>3</sub>)<sub>2</sub>(en)<sub>2</sub>] and *trans*-[Cu(NO<sub>3</sub>)<sub>2</sub>(pn)<sub>2</sub>]; Tales of twinning and a reversible phase change leading to a new polymorph.

Mark R.J. Elsegood<sup>1</sup>, Cameron L. Carpenter-Warren<sup>1</sup>, Muhammet Kose<sup>2</sup>

1. Chemistry Dept., Loughborough University, Loughborough, LE11 3TU, UK

2. Chemistry Dept., K. Maraş Sütçü Imam University, 46100, K. Maraş, Turkey.

email: m.r.j.elsegood@lboro.ac.uk

The structure of *trans*-bis(1,2-diaminoethane)-copper(II), [Cu(NO<sub>3</sub>)<sub>2</sub>(en)<sub>2</sub>], has been reported twice previously,<sup>1</sup> including once as a private deposition to the CSD. On both occasions the data were collected at room temperature with a 4-circle serial diffractometer and the *R* factors at ca. 4% suggest there is little more to understand. Our recent re-determinations at low temperature on a CCD area detector system reveal both merohedrally twinned and non-twinned diffraction patterns from a single batch of crystals. We will describe the handling of the twinning and hence a halving of the *R* factor.

The structure of *trans*-bis(1,2-diaminopropane)-dinitrato-copper(II), [Cu(NO<sub>3</sub>)<sub>2</sub>(pn)<sub>2</sub>], has also been reported twice previously.<sup>2,3</sup> As above, both determinations were at room temperature on serial diffractometers. The first determination did not include H atoms and had an *R* factor of 12.2%. The second however, did include H atoms and refined to *R*1 = 3.3%. A close inspection of the published ORTEP plot however, with hindsight, now provides clues to our new findings. A reduction in temperature leads to a loss of molecular symmetry and, primarily, a significant movement of both the nitrate ligands (Fig. 1). On re-warming the crystal, the original structure is obtained, albeit with a little de-lamination of the crystal. We will describe our experiments and the structural changes observed.

## References.

1. V. Manríquez, M. Campos-Vallette, N. Lara, N. González-Tejeda, O. Wittke, Guillermo Díaz, S. Diez, René Muñoz, and Lukas Kriskovic, *J. Chem. Cryst.*, (1996), **26**, 15.

2. A. Pajunen, *Suom. Kemistil. B.*, (1969), **42**, 15.

3. M.R. Sundberg, *Inorg. Chim. Acta*, (1994), **218**, 151.

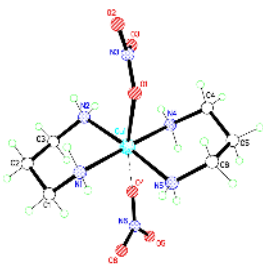


**Figure 1.** New unsymmetrical polymorph of  $[\text{Cu}(\text{NO}_3)_2(\text{pn})_2]$  at 160K.

**Keywords:** Polymorph, twinning, coordination complex.

## MS32-P5 Cocrystal Systems of Cyanopyridines and Carboxylic acids

Dennis Enkelmann<sup>1</sup>, Gregor Lipinski<sup>1</sup>, Klaus Merz<sup>1</sup>

<sup>1</sup>. Department of Inorganic Chemistry I, Ruhr-University Bochum, 44801 Bochum, Universitätsstrasse 150

email: dennis.enkelmann@rub.de

In the recent past, multicomponent crystals like cocrystals, salts and solvates became more and more interesting due to their upcoming applications in pharmaceutical use and materials science.<sup>1</sup> The understanding of the formation of those compounds is an essential part of crystal engineering to achieve more knowledge about multicomponent crystal aggregation and subsequently to use this information to tune chemical and physical properties of active pharmaceutical ingredients (API) like solubility, bioavailability, melting point and stability.<sup>2,3</sup>

In some cases it can be preferable to synthesize a cocrystalline compound instead of a salt, for example based on the poor predictability of salt structures in respect of their chemical and stoichiometric composition.<sup>4</sup> To select suitable compounds for targeted cocrystal growth, the  $\text{pK}_\text{a}$ -rule is a helpful tool. The  $\Delta\text{pK}_\text{a}$  of a two component system (defined as  $\Delta\text{pK}_\text{a} = \text{pK}_\text{a}(\text{base}) - \text{pK}_\text{a}(\text{acid})$ ) can give reliable information concerning cocrystal or salt formation.<sup>5-8</sup>

In order to study the applicability of this method, selected compounds were chosen for a cocrystal screening. Different cyanopyridines, acting as bases with relatively low  $\text{pK}_\text{a}$ -Values were intended to be formed into cocrystals via solution crystallization with selected carboxylic acids as cocrystal-former.

In our studies, the  $\text{pK}_\text{a}$ -rule turned out to be a very accurate instrument for a specific cocrystal approach. Depending on this rule we were able to design various cocrystals consisting of pyridine derivatives and carboxylic acids.

[1] D. Yan, A. Delori, G. O. Lloyd, T. Friščić, G. M. Day, W. Jones, J. Lu, M. Wei, D. G. Evans, X. Duan, *Angew. Chem.Int. Ed.*, **2011**, 50, 12483.

[2] P. Vishweshwar, J. A. McMahon, J. A. Bis, M. J. Zaworotko *J. Pharm. Sci.*, **2006**, 95, 499.

[3] N. Qiao, M. Li, W. Schlindwein, N. Malek, A. Davies, G. Trappitt, *Int. J. Pharm.*, **2011**, 419, 1.

[4] C.B. Aakeröy, M.E. Fasulo, J. Desper, *Mol. Pharm.*, **2007**, 4, 317.

[5] D.A. Haynes, W. Jones, W.D.S. Motherwell, *CrystEngComm* **2006**, 8, 830.

[6] M. J. A. Bowker, P.H. Stahl, C.G. Wermuth, *Handbook of Pharmaceutical Salts*, **2002**, VCH, Wiley-VCH: New York.

[7] R. Bhogala, S. Basavoju, A. Nangia, *CrystEngComm*, **2005**, 7, 551.

[8] K. Molčanov, B. Kojić-Prodić, *CrystEngComm* **2010**, 12, 925.

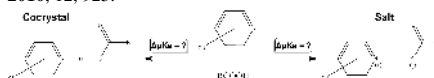


**Figure 1.**



**Keywords:** Cocrystal, Polymorphism, Intermolecular potentials, Hydrogen bonds, Carboxylic Acid, Cyanopyridine

## MS32-P6 Dehydration of paroxetine hydrochloride forms I and II

László Fábíán<sup>1</sup>, M. Fátima Pina<sup>2</sup>, Sarah J. Day<sup>3</sup>, Annabelle Baker<sup>3</sup>, Chiu C. Tang<sup>3</sup>, Min Zhao<sup>2</sup>, Duncan Q.M. Craig<sup>2</sup>

1. School of Pharmacy, University of East Anglia, Norwich, UK

2. University College London School of Pharmacy, London, UK

3. Diamond Light Source, Harwell Science and Innovation Campus, Didcot, UK

email: L.Fabian@uea.ac.uk

Paroxetine hydrochloride has two hydrate forms: a stoichiometric hemihydrate (form I) and a non-stoichiometric hydrate (form II). Both forms can be dehydrated to give two distinct anhydrous forms, which are isostructural with their respective parent hydrates.<sup>1,2</sup>

The water content and unit cell volume of form II change rapidly, continuously and without any noticeable hysteresis in response to changes in relative humidity at 30°C. Form I, on the other hand, shows a clear first order phase transition on heating, producing the pure dehydrated form after *ca.* 1 h at 100°C. Dehydrated form I converts back to hemihydrate form I at room temperature at relative humidities as low as 1%.

The dehydration process was monitored in-situ using synchrotron powder diffraction experiments. There was no evidence of any intermediate phase and the data allowed structure determination of form I dehydrate. It was revealed that both form I and its dehydrate are isostructural with the corresponding paroxetine hydrobromide forms.<sup>3</sup>

Comparison of the structures gives an explanation of the different stabilities and transformation kinetics observed. Form II contains solvent pockets separated by easy-to-open gates, and consequently it behaves as a channel hydrate. Molecular dynamics simulations show the mechanism of opening the gates, which are formed by hydrophobic rings with only weak intermolecular interactions between them. In form I, however, water molecules are separated from each other by strongly hydrogen-bonded chloride ions, so their removal is much more difficult. The dehydrates show poor hydrogen bond coordination,<sup>4</sup> which explains their low stability and easy conversion back to the isostructural hydrate form.

1. M. F. Pina, J. F. Pinto, J. J. Sousa, L. Fábíán, M. Zhao, D. Q. M. Craig, *Mol. Pharmaceutics* 2012, **9**, 3515.

2. M. F. Pina, M. Zhao, J. F. Pinto, J. J. Sousa, C. S. Frampton, V. Diaz, O. Suleiman, L. Fábíán, D. Q. M. Craig, *Cryst. Growth Des.* 2014, **14**, 3774.

3. P. S. Carvalho Jr., C. C. de Melo, A. P. Ayala, C. C. P. da Silva, J. Ellena, *Cryst. Growth Des.* 2016, **16**, 1543.

4. P. T. A. Galek, J. A. Chisholm, E. Pidcock, P. A. Wood, *Acta Cryst.* 2014, **B70**, 91.

**Keywords:** hydrates, dehydration

# MS32-P7 New cocrystals of Flurbiprofen and Proline: structural effect of enantiomorphism.

João L.A.F. Silva<sup>1</sup>, Pedro Paulo Santos<sup>1</sup>, Vânia André<sup>1</sup>, Filipa Galego<sup>1</sup>

<sup>1</sup>. Centro de Química Estrutural, Instituto Superior Técnico, U. Lisbon, Av. Rovisco Pais, 1049-001 Lisboa, Portugal

email: joao.luis@ist.utl.pt

Flurbiprofen (FBP) is a nonsteroidal anti-inflammatory drug (NSAID) with antipyretic and analgesic activities and a very low water solubility (8 mg/l).<sup>1</sup> The most common strategy to alter physical and chemical properties of Active Pharmaceutical Ingredients (APIs) is the search for multicomponent crystal forms, mainly salts and cocrystals. Because of their ionic character salts result in the increase of solubility of APIs but also in more stable products easy to recrystallize. When the intervenient molecules do not present adequate properties for salification a more recent approach to modify properties has been adopted: the growth of cocrystals. There are several definitions of pharmaceutical cocrystal, but in general it can be described as a combination of an API and a Generally Recognized As Safe (GRAS) chemical in a stoichiometric ratio, bound by non-covalent interactions. Zwitterionic compounds favor formation of H-bonds and, therefore, cocrystals. The nature of aminoacids (ionic or zwitterionic depending on pH) makes them good candidates to obtain both API salts and cocrystals. Proline (P) shows one of the largest zwitterionic pH ranges (1.80-10.63)<sup>2</sup> so it was chosen for the synthesis of new FBP cocrystals using Liquid Assisted Grinding. FBP has a strong tendency to form racemic compounds by direct interaction of (R)- and (S)-molecules, involving H-bonding in a carboxylic acid dimer.<sup>3</sup> When P is introduced the structure evolves into a trimer composed by a P molecule "sandwiched" between an (R)- and an (S)- FBP. This work registers differences in supramolecular arrangements obtained using D-proline (I) and L-proline (II) as coformer. In both cases the trimers form chains where P molecules interact by N-H...O<sup>carboxylate</sup> bonds. D-proline forms two O-H...O<sup>carboxylate</sup> interactions, one with S-FBP using the same O atom involved in the P-P interactions and a second with R-FBP involving the other O<sup>carboxylate</sup>. P amino group also participates in a N-H...O=C<sup>carboxylate</sup> bond with the next R-FBP molecule, assisting in the chain formation. If the conformer is L-proline the interactions with (R)- and (S)- molecules are reversed.

Acknowledgements: FCT (REC1/SEQ-QIN70189/2012, SFRH/BPD/78854/2011, UID/QUI/00100/2013).

1 - S.H Yalkowsky, R.M. Dannenfelser, The AQUASOL Database of Aqueous Solubility V.5, Tucson, AZ, Univ AZ, USA, 1992. 2 - A.Tilborg, B. Norberg, J. Wouters, *Eur. J. Med. Chemistry*, **74** (2014), 411-426. 3 - A.L.Grzesiak, A.J.Matzger, *J.Pharm.Sci.*, **96** (2007), 2978-2986.

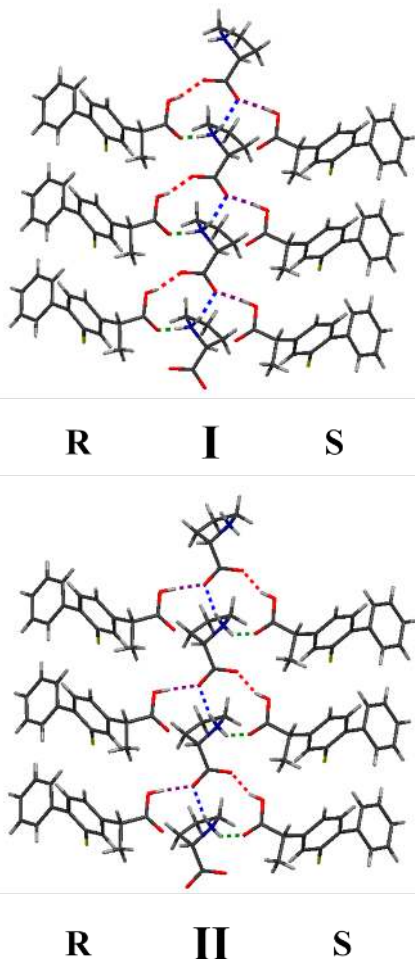


**Figure 1.** Supramolecular arrangements of racemic flurbiprofen with D-proline (I) and L-proline (II).

**Keywords:** cocrystals, flurbiprofen, enantiomorphism

**MS32-P8** X-ray structural analysis of sodium salt of acetylsalicylic acidMiroslava Dědová<sup>1</sup>, Jan Čejka<sup>1</sup><sup>1</sup>. Department of Solid State Chemistry, University of Chemistry and Technology Prague, Technická 5, Prague 6, Czech Republic

email: dedovam@vscht.cz

Pharmacological effects of acetylsalicylic acid have been known for a long time. Recently, new therapeutic uses of aspirin were discovered, and investigated, e.g. prevention of colon cancer or treatment of dementia. This promotes a detailed screening for new physical (polymorphs) and chemical (salts, co-crystals) forms of aspirin. An improved dissolution rate of the forms is a desirable property in order to decrease stomach wall damage.

Many patents are focused on the preparation of the sodium aspirin. Surprisingly, no structure of sodium aspirin has been solved yet. The sodium salt can be prepared by the reaction of acetylsalicylic acid with sodium bicarbonate. Both known and patented forms arise under very similar conditions - sodium acetylsalicylate dihydrate and anhydrate. Their preparation is very difficult and the reproducibility is fairly low due to ester hydrolysis. Therefore a new screening of salt preparation and crystallization was performed to achieve better reproducibility.

The preparation of sodium acetylsalicylate dihydrate was successful, the structure was determined by single-crystal X-ray diffraction. The dihydrate form was later dehydrated to sodium acetylsalicylate anhydrate. (not verified yet). The dehydration was studied by thermoanalytical methods (TGA/DSC). However, the structure of anhydrate has not been solved yet.

Further, a new form of sodium aspirin was discovered - sodium acetylsalicylate monohydrate. Its structure was determined by single-crystal X-ray diffraction. Unlucky, no attempts to reproduce the monohydrate form were successful.

This work was supported by the Grant Agency of Czech Republic, Grant no. 106/14/03636S.

**Keywords:** x-ray crystallography, salt formation, pharmaceuticals

**MS32-P9** Temperature-induced single-crystal-to-single-crystal polymorph transformation in cadmium(II) trimer with pyridine-4-propanamideBoris-Marko Kukovec<sup>1</sup>, Ivan Kodrin<sup>2</sup>, Marijana Đaković<sup>1</sup><sup>1</sup>. Division of General and Inorganic Chemistry, Department of Chemistry, Faculty of Science, University of Zagreb, Horvatovac 102a, HR-10000 Zagreb, Croatia<sup>2</sup>. Division of Organic Chemistry, Department of Chemistry, Faculty of Science, University of Zagreb, Horvatovac 102a, HR-10000 Zagreb, Croatia

email: bkukovec@chem.pmf.hr

Single-crystal-to-single-crystal (SCSC) transformations have been established as an interesting solid state phenomenon and have gained some interest, as the transformed structure can be also determined, providing insight into the possible mechanism of transformation [1]. SCSC transformations may be induced by external stimuli like heat, light or sorption/desorption of guest/solvent molecules and usually occur in metal-organic frameworks (MOFs). The studies of SCSC polymorph transformations of metal-organic compounds are scarce, but they start to gain attention [2]. The molecular structure of cadmium(II) coordination trimer with pyridine-4-propanamide (4-Propy),  $[\text{Cd}_3\text{Cl}_4(4\text{-Propy})_6](\text{CH}_3\text{CH}_2\text{COO})_3$  (**1**), consists of three cadmium(II) ions bridged with chloride ions; each is coordinated by two *N*-monodentate 4-propy ligands. Two water molecules are bound to the terminal cadmium(II) ions of the trimer, preventing further polymerization of the trimer units. High-temperature polymorph (**A**) of **1** crystallized in triclinic system (*P*-1 space group) at room temperature. SCSC transformation to low-temperature polymorph (**B**) of **1** occurred by cooling a single crystal to 150 K on a diffractometer (Fig. 1). Polymorph **B** crystallized in monoclinic system (*P*2<sub>1</sub>/*n* space group). In **A**, trimer units are linked via propanoate ions by N-H...O interactions, forming a 1D chain along the [0 1 1] direction. However, in **B**, similar 1D chains are assembled into a 2D network in the plane (0 1 0) due to the additional N-H...Cl interactions, present only in **B**. Therefore, lowering temperature enables the assembly of the 1D chains of **A** into 2D network of **B** by introducing different type of interaction (N-H...Cl). It seems that the transformation of **A** into **B** is possible due to slight change of the molecules' orientation in the structure of **A**, enabling the formation of N-H...Cl interactions in the same crystal, without a collapse of the crystal structure. This SCSC polymorph transformation was also studied by PXRD and DSC. The Hirshfeld surface analysis was performed to identify the interactions present in **A** and **B**, revealing differences between the two polymorphs. **References:** [1] J. P. Zhang, P. Q. Liao, H. L. Zhou, R. B. Lin, X. M. Chen, Chem. Soc. Rev. 43 (2014) 5789.; [2] D. Aulakh, J. R. Varghese, M. Wriedt, Inorg. Chem. 54 (2015) 8679. **Acknowledgment:** This work has been fully supported by Croatian Science Foundation under the project UIP-11-2013-1809.

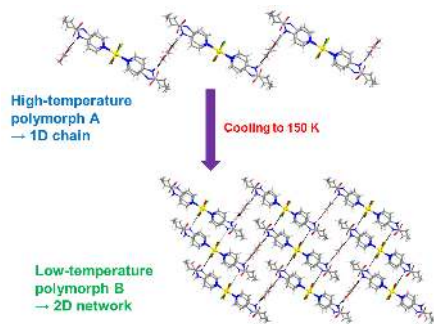


**Figure 1.** SCSC transformation of high-temperature polymorph A of  $[\text{Cd}_2\text{Cl}(\text{4-Propyl})_2](\text{CH}_2\text{CH}_2\text{COO})_2$  (1) into low-temperature polymorph B by cooling to 150 K

**Keywords:** single-crystal-to-single-crystal transformation, polymorph, cadmium(II) trimer

## MS32-P10 Polymorphism, what it is and how to identify it.

Sofia Martin Caba<sup>1</sup>, Jean-Pierre Brog<sup>1</sup>, Claire-Lise Chanez<sup>1</sup>, Aurelien Crochet<sup>1</sup>, Katharina M. Fromm<sup>1</sup>

<sup>1</sup>. Department of Chemistry, University of Fribourg, Switzerland

email: sofia.martincaba@unifr.ch

Polymorphism is a very important phenomenon not only in basic research, but certainly in pharmaceutical industry and materials science. Polymorphs possess different properties, for instance the solubility or the mechanical resistance can differ dramatically from one polymorph to the other – properties which can be crucial for their application. Hence, it is important to be able to control the formation of polymorphs and to understand their formation. We here gave some insights into the basic knowledge of polymorph formation and their identification and characterization in order to give an overview on the current state of the art. In order to give interested peoples a tool in hand to test their compounds for polymorphism, we established a series of flow sheets to follow, depending on the class of compounds, hoping that they are useful for many scientists who are not so well acquainted with polymorphism. The presented schemes resume thus the identification steps for polymorphs. It should also help to use the term polymorph correctly in order to reduce the number of publications in which this term is not used in a correct way.

**References:** J-P. Brog, C-L. Chanez, A. Crochet, K. M. Fromm, *RSC Adv.*, **2013**, 3, 16905-16931.

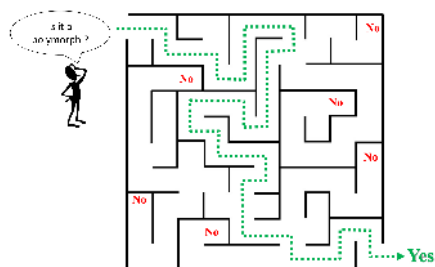


**Figure 1.**

**Keywords:** Polymorphism, organic, organometallic, inorganic.

**MS32-P11** Lead(II) acetate: anhydrous polymorphs, hydrates and by-products.  
Room temperature phosphorescence.

Francisco Javier Martínez-Casado<sup>1</sup>, Miguel Ramos-Riesco<sup>2</sup>, José Antonio Rodríguez-Cheda<sup>3</sup>, Fabio Cucinotta<sup>3</sup>

1. MAX IV Laboratory - Lund University (Sweden)

2. Fac. Químicas, Universidad Complutense de Madrid (Spain)

3. School of Chemistry, Newcastle University (UK)

email: francisco.martinez@maxiv.lu.se

Lead(II) acetate (hereafter referred to as  $\text{Pb}(\text{Ac})_2$ ) is a very common salt with many and varied uses throughout history: a) as a sweetener and sugar substitute (known as "sugar of lead"), despite its toxicity; b) in cosmetics, as a hair colouring product, and in skin whitening lotions; c) in medical uses, as an astringent and as a remedy for sore nipples, in solution with lead(II) oxide (Goulard's extract); d) in industrial uses, as a hydrogen sulfide detector, as a mordant in dyeing and textile printing, as a drier in paints and varnishes; etc. However, the behaviour of this -in principle- simple salt and its structures and decomposition process have remained unclear. In this sense, only lead(II) acetate trihydrate was characterized and solved to date.

In this study, we unravel the thermal behaviour and show the different compounds (hydrates and by-products) that appear for this salt. Thus, two enantiotropic polymorphs of the anhydrous salt, a novel hydrate (with  $\text{Pb}(\text{Ac})_2/\text{H}_2\text{O}$  ratio 2:1) and two decomposition products are reported (corresponding to the 3:1 and 1:1 stoichiometric mixtures of  $\text{Pb}(\text{Ac})_2/\text{PbO}$ ), being the structure of all of them solved for the first time. The compounds present a variety of molecular arrangements, being two-dimensional (2D) or one-dimensional (1D) coordination polymers. A thorough thermal analysis, by DSC and TGA, was also carried out and to study the behaviour and thermal data of the salt and its decomposition process, in inert and oxygenated atmospheres, identifying the phases and by-products that appear.

One of the most relevant aspects is the luminescence in two of the compounds: lead(II) acetate hemihydrate and tetralead(II) oxo-hexaacetate ( $3\text{Pb}(\text{Ac})_2/\text{PbO}$  ratio). These salts were analyzed by UV-Vis spectroscopy and were found to be phosphorescent at room temperature.

and  $\text{Pb}(\text{Ac})_2\text{-B}$  (c and d), respectively. The structures are presented along the axes  $a$  (a) and  $b$  (b), and parallel to the plane (102) (c), and along the axes  $b$  (d), respectively.

**Keywords:** Polymorphs, hydrates, by-products, lead(II) acetate, XRD, phosphorescence, DSC, TGA

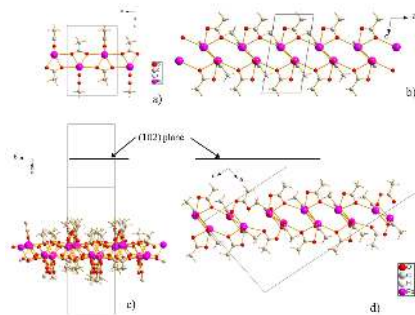


**Figure 1.** Crystal structures of anhydrous high and low temperature polymorphs of lead(II) acetate,  $\text{Pb}(\text{Ac})_2\text{-A}$  (a and b)

## MS32-P12 Can ionic liquids be the key for pharmaceutical polymorphic control? Gabapentin as a case study

Inês C.B. Martins<sup>1,2,3</sup>, Maria T. Duarte<sup>1</sup>, Luís M. Mafra<sup>2</sup>, Luís C. Branco<sup>3</sup>

1. Centro de Química Estrutural, Instituto Superior Técnico, Universidade de Lisboa, Lisbon, Portugal

2. CICECO, Universidade de Aveiro, Aveiro, Portugal

3. REQUIMTE, Faculdade de Ciências e Tecnologia, Universidade Nova de Lisboa, Monte da Caparica, Lisbon, Portugal

email: inesbmartins@tecnico.ulisboa.pt

For pharmaceutical industry, the delivery of an active pharmaceutical ingredient (API) as crystalline solid form occurs predominantly due to solubility, bioavailability and thermal stability considerations.[1] However, solids are often strongly affected by polymorphic conversions, which impacts the bioavailability and thus the drug efficacy, imposing great financial and patenting issues.[1] Having this in mind, it is extremely important to control this solid state phenomenon, or even avoid it, recurring to new alternatives (Figure 1). In the past years, ionic liquids (ILs) have been used, not only as green solvents for the synthesis and crystallization of organic compounds, but also as possible drug delivers, giving rise to the third generation of ILs, called API-ILs.[2] Gabapentin (Gaba) is an amino acid-based drug used to treat neurodegenerative diseases, such as epilepsy. This API is known to exhibit three polymorphs (Forms II, III and IV), which are easily interconverted,[3] making Gaba susceptible to adopt different physicochemical behaviors. In order to explore the role of ionic liquids as possible green and challenging alternative for polymorphic control, we studied the influence of selected ionic liquids in crystallization control process of Gaba and also prepared some API-ILs, through the combination with biocompatible counter-ions. We will present here some of the latest results from the crystallization process. The room temperature API-ILs obtained allowed to avoid polymorphism, transforming the solid API into a liquid. All the compounds were characterized by NMR, DSC and MS.

1. Stoimenovski J, MacFarlane DR, Bica K, Rogers RD: **Crystalline vs. Ionic liquid salt forms of active pharmaceutical ingredients: A position paper.** *Pharmaceutical Research* (2010) **27**(4):521-526.

2. Ferraz R, Branco LC, Prudêncio C, Noronha JP, Petrovski Z: **Ionic Liquids as Active Pharmaceutical Ingredients.** *ChemMedChem* (2011) **6**:975-985.

3. Braga D, Grepioni F, Maini L, Rubini K, Polito M, Brescello R, Cotarca L, Duarte MT, Andre V, Piedade MFM: **Polymorphic gabapentin: Thermal behaviour, reactivity and interconversion of forms in solution and solid-state.** *New Journal of Chemistry* (2008) **32**(10):1788-1795.

**Acknowledgements:** The authors acknowledge funding of the projects UID/QUI/00100/2013 and SFRH/BD/93140/2013 by Fundação para a Ciência e a Tecnologia.

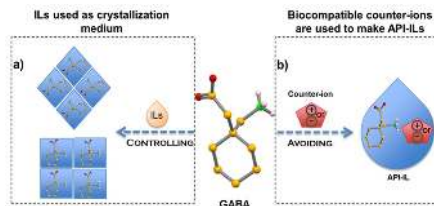


**Figure 1.** Schematic representation for polymorphic control (a) and avoidance (b) of Gabapentin.

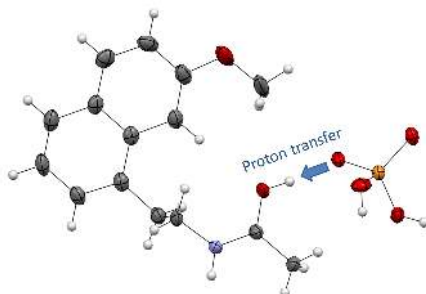
**Keywords:** Polymorphism, Ionic Liquids (ILs), API-ILs, Gabapentin

**MS32-P13 Agomelatine Phosphate: Salt or Co-Crystal?****Keywords:** pharmaceuticals, salt, co-crystal,  $\Delta pK_a$ , crystal structure, proton transferEliška Skořepová<sup>1</sup>, Michal Hušák<sup>1</sup>, Luděk Ridvan<sup>2</sup>, Tereza Hanyková<sup>1</sup><sup>1</sup>. Department of Solid State Chemistry, University of Chemistry and Technology Prague, Technická 5, 166 28, Praha 6, Czech Republic<sup>2</sup>. Solid State Development, Zentiva k.s., Czech Republic

email: eliska.skorepova@vscht.cz

The search for new solid forms of an active pharmaceutical ingredient (API) is an important step in a drug development. Often, an API has a low water solubility, which then leads to a low oral bioavailability. The problem can be solved by crystallizing the API together with another chemical, resulting either in salt or co-crystal formation. Salts and co-crystal are multicomponent solids but in different ionization states. In salts, there is a proton transfer between the molecular components, making it contain cations and anions. On the other hand, co-crystals are made up from neutral molecules held together by non-bonded interactions. One such API is agomelatine (AG), a melatonergic antidepressant. However, agomelatine is an amidic compound and, since amides are generally considered neutral and, for agomelatine, only co-crystals have been published, it was quite a surprise, when agomelatine, in the combination with phosphoric acid, produced a salt. Moreover, the  $\Delta pK_a$  calculation clearly indicated a co-crystal preference.<sup>a</sup> However, we were able to obtain synchrotron single-crystal diffraction data and solve the structure. The position of the acidic hydrogen was located in the difference Fourier map. Specifically, the amide oxygen was protonated. The proton transfer and the salt formation were also confirmed by solid state NMR and through CASTEP energy minimization. For pharmaceuticals, the determination whether the material is a salt or a co-crystal is interesting not only academically, but also from the regulatory point of view. Therefore, our findings may play a crucial role in the future development of the multicomponent solid phases of agomelatine.

This work was supported by the Grant Agency of Czech Republic, Grant no. 106/14/03636S and received financial support from specific university research (MSMT No 20/2016). We acknowledge the ESRF for provision of synchrotron radiation facilities and we would like to thank J. Wright for assistance in using beamline ID11.

**Figure 1.** The asymmetric unit of agomelatine phosphate



# MS32-P14 Structural characterization of tenofovir disoproxil fumarate Form I using X-ray and electron diffraction and a study of its conversion to related solid forms

Veronika Sládková<sup>1</sup>, Eliška Skořepová<sup>1</sup>, Jan Čejka<sup>1</sup>, Ondřej Dammer<sup>2</sup>, Bohumil Kratochvíl<sup>1</sup>, Petr Brázda<sup>3</sup>, Jan Rohlíček<sup>3</sup>

1. Department of Solid State Chemistry, University of Chemistry and Technology, Prague, Technická 5, 16628, Prague 6, Czech Republic

2. Department of Solid State Development, Zentiva k.s., U Kabelovny 130, 102 37, Prague, Czech Republic

3. Institute of Physics AS CR, v.v.i., Na Slovance 2, 182 21 Prague 8, Czech Republic

email: sladkovv@vscht.cz

Tenofovir disoproxil fumarate (TDF) is an orally delivered pharmaceutical compound used for the treatment of HIV and chronic hepatitis, which acts as an inhibitor of nucleotide reverse transcriptase. There are many solid forms of TDF described in patent literature; two of them we identified in drug products: Form I and Form A. It seems that during formulation the active pharmaceutical ingredient (API) undergoes partial to total conversion of TDF Form I to TDF Form A. The aim of the study was to propose a formulation of tablet containing pure TDF Form I. However, we observed that TDF Form I converted either to TDF Form A or recently described TDF Form I-1. We investigated, when and why did the conversion occur and whether the conversion could be avoided, and how. The influence of pH and possible interaction with excipients were studied. The conditions enabling using wet granulation in technology while preventing the undesired conversion were found. The stabilization was achieved either by replacement of used disintegrants or pH adjustment by acid addition to the current composition of formulation.

We also found that TDF Form I underwent the same non-reversible phase transformation to TDF Form I-1 both upon heating, as well as upon exposure to humidity. The phenomenon was observed by temperature resolved X-ray powder diffraction (XRPD), solid state NMR spectroscopy and DSC.

As neither structure of TDF Form I nor of TDF Form I-1 has been determined, we focused on structure solution by combining high quality XRPD, synchrotron single crystal XRD and electron diffraction. We were successful in indexing of the powder of TDF Form I, which was in agreement with the indexing of the microcrystals measured on synchrotron. Moreover, a structure of another tenofovir compound – tenofovir disoproxil phosphate, was successfully determined from single crystal XRD data.

**Acknowledgment:** This work was supported by the Grant Agency of Czech Republic, Grant no. 106/16/10035S and received financial support from specific university research (MSMT No 20/2016). We acknowledge the ESRF for provision of synchrotron radiation facilities and we would like to thank J. Wright for assistance in using beamline ID11.

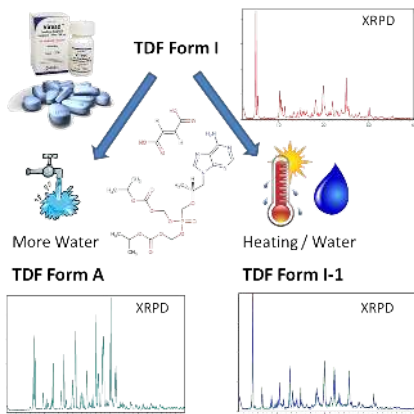


**Figure 1.** TDF Form I converted either to TDF Form A upon slurrying in water or to recently described TDF Form I-1 upon heating or exposure to water.

**Keywords:** pharmaceuticals, phase transformation, electron diffraction, x-ray powder diffraction, indexing

**MS32-P15** While you were screening...Elisa Nauha<sup>1</sup>, Louis Adriaenssens<sup>1</sup>, Nicholas Blagden<sup>1</sup>, Ian Scowen<sup>1</sup>

1. University of Lincoln, Joseph Banks Laboratories, Green Lane, Lincoln, LN6 7DL, UK

email: enauha@lincoln.ac.uk

Screening for crystal forms can be a laborious process where the desired results are sometimes fleeting. During the process new crystal forms which are not relevant to the research question but which are novel, perhaps challenging and of interest to the crystallographer are often found. Sometimes these discoveries lead to a new research direction and sometimes they are forgotten in desk drawers awaiting publication. I will present "undesired" crystal structures acquired while screening for other crystal forms.

**Keywords:** cocrystal, polymorph, solvate**MS32-P16** The exciting life of a small adenine moleculeDubravka Sisak Jung<sup>1</sup>, Tomislav Stolar<sup>2</sup>, Stipe Lukin<sup>2</sup>, Gordan Horvat<sup>2</sup>, Josip Pozar<sup>2</sup>, Graeme M. Day<sup>3</sup>, Mirta Rubcic<sup>2</sup>, Ivana Biljan<sup>2</sup>, Ivan Halasz<sup>4</sup>

1. DECTRIS Ltd., Baden-Daetwil, Switzerland

2. Department of Chemistry, Faculty of Science, University of Zagreb, Zagreb, Croatia

3. School of Chemistry, University of Southampton, Southampton, United Kingdom

4. Ruder Bošković Institute, Zagreb, Croatia

email: dubravka.sisak@dectris.com

Once known only as a component of DNA, modern chemistry successfully exploits nucleobase adenine for preparation of supramolecular and metallo-organic systems [1,2]. Although commercially available as a solid and widely used in synthesis of targeted entities, the characterization of adenine is still very limited, due to tautomersim, inability to grow single crystals and the poor quality of polycrystalline materials [3]. In our attempt to overcome these hindrances we have found out that the problem is far more complex, and that the solution surpasses the simple solid-state characterization. In order to untangle the somewhat conflicting results obtained during the study, a variety of experimental and theoretical techniques had to be used. The characterization started with a commercial adenine, which proved to be a mixture of two polymorphs, one known (**I**,  $P2_1/c$ ,  $Z'=2$ , [3]) and one unknown (**II**). In order to solve the structure of polymorph **II**, a strategy to purify the commercial batch had to be developed first. Subsequent structural analysis, against all odds, showed that the same tautomer as **I**, but with the symmetry was *Fdd2* with  $Z'=1$ . According to some authors, this suggests that the new form should be more stable. This seemed to comply with the quantitative analysis of several commercial batches, where most showed presence of polymorph **II** in excess. However, a series of experiments on polymorph occurrence conditions, interconversion and thermodynamic relationship recognized polymorph **I** with  $Z' = 2$  as the more stable form at room temperature, while polymorph **II** is favored at higher temperatures. Extensive theoretical calculations not only supported these experimental results, but also gave an insight into fine structural details that contribute to stability of a certain form. Although this study covered a good share of solid-state characterization, there are still questions open. Disordered structures and possible new polymorphs are a few that will be discussed to illustrate that isolation and identification of polymorphs continues to be a vital area of research in solid-state chemistry [4,5].

[1] Etter, M. C., Reutzel, S. M., Choo, C. G. (1993) *J. Am. Chem. Soc.* **115**, 4411. [2] Stylianou, K. C. *et al.* (2011) *Chem. Commun.* **47**, 3389. [3] Mahapatra, S. *et al.* (2008) *Cryst. Growth Des.* **8**, 1223. [4] Bernstein, J. (2011) *Cryst. Growth Des.* **11**, 632. [5] Bučar, D.-K., Lancaster, R. W., Bernstein, J. (2015) *Angew. Chem. Int. Ed.* **54**, 6972.

**Keywords:** adenine, polymorphism, structure determination, powder

## MS32-P17 Crystalline forms of dihydroergocornine salts

Radka Zajícová<sup>1</sup>, Jan Čejka<sup>1</sup>, Alexandr Jegorov<sup>2</sup>

1. Department of Solid State Chemistry, University of Chemistry and Technology Prague, Technická 5, Prague 6, Czech Republic

2. Teva Czech Industries s.r.o., Research Unit, Branišovská 31, 370 05 České Budějovice, Czech Republic

email: radka.zajicova@vscht.cz

Dihydroergocornine is a semi-synthetic ergot alkaloid, which is used in a mixture for the treatment of age-related cognitive decline and acute migraine. Due to the low solubility of dihydroergocornine in water, many pharmaceutically acceptable salts were reported, but for industrial production methanesulfonate salt was chosen. Most of the reported salts have not been characterized at all. Within this study we are growing crystalline forms of dihydroergocornine salts and their solvates. The crystalline forms are characterized mainly from structural and stability points of view. Samples are prepared by solution crystallization under various conditions and analysed by X-ray diffraction techniques. Up to date two solvates of dihydroergocornine mandelate were solved from SC-XRD data. According to experience with solvated structures of dihydroergocornine mesylate, the large number of dihydroergocornine mandelate solvates is expected. We assume this solid-state behaviour in all new salts and their solvates.

**Keywords:** solvates, X-ray diffraction, ergot alkaloids

## MS32-P18 The ISX Stage: A Novel Home-Lab Solution for Automated Screening of Crystallization Plates

Severine Freisz<sup>1</sup>, Vernon Smith<sup>1</sup>

1. Bruker AXS GmbH Oestliche Rheinbrueckenstrasse 49 76187 Karlsruhe, Germany

email: severine.freis@bruker.com

Recent developments in hardware and software are greatly increasing the capabilities of in-house diffraction systems making it more routine to obtain *de novo* structural information in the home lab. We have now introduced the D8 Venture solution for structural biology with the PHOTON II detector featuring the first CPAD for in-house X-ray crystallography. Our new microfocus source, the METALJET delivers beam intensity exceeding those of typical bending-magnet beamlines.

Very recently, we developed a fully automated solution for in situ crystal screening in plates: the ISX stage. This stage facilitates the investigation of a large number of crystals within the routine workflow of the crystallization lab. The combination of the sensitive PHOTON II detector and a high intensity X-ray source maximizes the diffraction signal from even the smallest, most weakly diffracting crystals. The ISX software provides an intuitive user environment to maximize the productivity of even occasional users.

The system can be quickly converted from the typical single crystal diffractometer to the completely motorized in situ crystal screening device leaving the KAPPA untouched and allowing you to revert just as quickly once you identified your favorite crystal on which you want to collect data. Here we present all the ISX stage features and data we collected in house.

**Keywords:** plate, screening, structural biology,

## MS32-P19 Oleonic Acid: A Case Study of the Control and Suppression of Solvate Crystals

REBECCA YIP<sup>1</sup>, Thanh-hà Nguyen<sup>1</sup>, Yuxin Zhang<sup>1</sup>, Herman H.Y. Sung<sup>1</sup>, Ian D. Williams<sup>1</sup>

1. Hong Kong University of Science and Technology (HKUST)

email: reyip1992@live.co.uk

Oleonic Acid (OA) a natural triterpene of pharmaceutical interest has been found to form solvate crystals from a wide range of solvents.[1][2] The control of solvate versus anhydrous phase formation is demonstrated for a variety of alcohols, with characterization by pXRD, TGA and single-crystal XRD. It appears that the product formation can be correlated to the temperature of crystallization. The potential of OA as a resolving agent for a variety of chiral alcohols has also been explored.

[1] Tong, H. Y.; Wu, H. B., Zheng, Y., Xi, J., Chow, A. h. I., Chan, C. K. *Int. J. Pharm.* **2008**, 355, 195-202.

[2] Froelich, A.; Gzella, A. K., *Acta Crystallogr E* **2010**, 66, o2690.

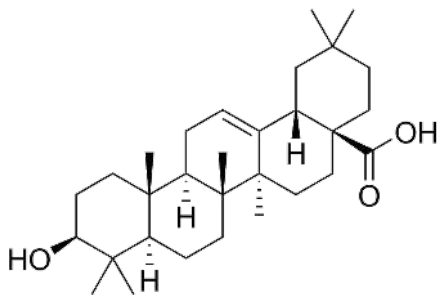


Figure 1. Oleonic Acid Structure

**Keywords:** Solvates, cocrystals

## MS32-P20 From 0D to 3D - The structural diversity of polyoxometalate catalysts

Kim D. von Allmen<sup>1,2</sup>, Anthony Linden<sup>1</sup>, Greta R. Patzke<sup>\*1</sup>

1. University of Zurich, Departement of Chemistry

2. Eidgenössische Materialprüfanstalt (Empa), Center for X-ray Analytics

email: kim.vonallmen@empa.ch

Polyoxometalates (POMs) are metal oxo clusters which are preferably formed by W, Mo and V in their high oxidation states. Among their remarkable spectrum of potential applications, POMs have widely been investigated as homogeneous and heterogeneous catalysts for organic reactions and as catalysts for artificial photosynthesis.[1] It was shown that the extent of Co/W disorder in the transition metal core of Co/Bi-sandwich type POMs based on the lacunary precursor  $\text{Na}_9[\text{B}-\alpha\text{-BiW}_9\text{O}_{33}]$  is a key feature for their activity as water oxidation catalysts (WOCs).[2] In order to understand the origin of the catalytic activity, POMs were prepared from  $\text{Na}_9[\text{B}-\alpha\text{-BiW}_9\text{O}_{33}]$  in the presence of Mn(II), Co(II), and Cu(II) cations. Efforts were made to prepare compounds with a specific composition of the transition metal core. Single crystal X-ray diffraction studies of the new transition metal containing POMs have revealed a large structural diversity of polyanions, which is due to  $\alpha$ - $\beta$  isomerization and partial decomposition of the lacunary precursor. Cross-linking of polyanions via supplementary d- or f-block counter cations resulted in the formation of 1D, 2D, and even 3D networks.[3] The polyanion  $[\text{Cu}_2(\text{H}_2\text{O})_2(\text{B}-\beta\text{-BiW}_{10}\text{O}_{35})]^{10-}$  crystallized with a 2D structure in the presence of  $\text{Na}^+$  and  $\text{K}^+$  cations, while  $\text{Rb}^+$  cations favored the crystallization of the 0D structure  $\text{Na}_6\text{Rb}[\text{Cu}_2(\text{H}_2\text{O})_2(\text{B}-\alpha\text{-BiW}_9\text{O}_{33/2})]$  from the same reaction mixture. The importance of the counter cations as structure-directing parameter could thus be highlighted.

The negative charge of polyanions can be exploited to prepare new compounds with interesting properties by introducing a transition metal complex as the counter cation. Crystals could be grown from  $[\text{Mn}_3(\text{H}_2\text{O})_3\{\text{As}_2\text{W}_{18}\text{O}_{66}\}]^{8-}$  as a potential WOC and the photosensitizer cation  $[\text{Ru}(\text{bpy})_3]^{2+}$ . Crystal structure determination confirmed the formation of  $[\text{Ru}(\text{bpy})_3]_4[\text{Mn}_3(\text{H}_2\text{O})_3\{\text{As}_2\text{W}_{18}\text{O}_{66}\}]$  from which crucial structural details could be deduced.

[1] D.-L. Long, R. Tsunashima, L. Cronin, *Angew. Chem. Int. Ed.* **2010**, 49, 1736. [2] F. Evangelisti, P.-E. Car, O. Blacque, G. R. Patzke, *Catal. Sci. Technol.* **2013**, 3, 3117. [3] K. von Allmen, H. Grundmann, A. Linden, G. R. Patzke, in preparation for submission.

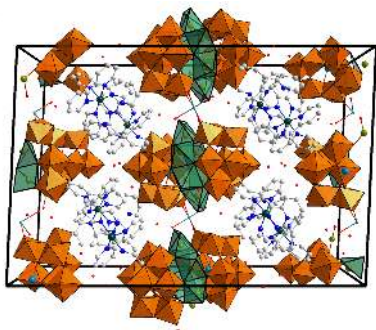


**Figure 1.** Packing diagram of the POM-PS-complex  $[\text{Ru}(\text{bpy})_3]_4[\text{Mn}_2(\text{H}_2\text{O})_4(\text{As}_2\text{W}_{18}\text{O}_{66})]$ :  $\text{WO}_6$  octahedra (orange), Mn (green), Ru (black).

**Keywords:** Polyoxometalates, Catalysts, Self-Assembling, Multidimensional Structures, Polymorphism

## MS33 Hot structures of small molecules

Chairs: Marijana Dakovic, Andreas Roodt

### MS33-P1 Syntheses and crystal structures of transition-metal bromide complexes with pyridine-type ligands: $[\text{MBr}_2(3\text{-cypy})_4]$ and $[\text{MBr}_2(3\text{-cypy})_2]_n$

Miriam Heine<sup>1</sup>, Lothar Fink<sup>1</sup>, Martin U. Schmidt<sup>1</sup>

<sup>1</sup> Goethe-Universität Frankfurt am Main, Institut für Anorganische und Analytische Chemie, Max-von-Laue-Straße 7, 60438 Frankfurt am Main, Germany

email: miriam.heine@t-online.de

In recent years numerous investigations on the syntheses and structural characterization of new coordination polymers based on transition-metals have attracted much attention due to their useful physical properties and their various potential applications [1]. We report the crystal structures of the ternary mixed complexes  $[\text{MBr}_2(3\text{-cypy})_4]$  and thermal intermediates  $[\text{MBr}_2(3\text{-cypy})_2]_n$  with  $\text{M}^{\text{II}} = \text{Co}, \text{Ni}$ , formed during decomposition. All crystal structures were determined by X-ray powder diffraction. In the ligand rich compounds the metal atoms are octahedrally coordinated by two bromide anions in trans-position and by four nitrogen atoms of the neutral co-ligands in order to build up discrete molecules (Fig. 1). Thermal decomposition induces the polymerization of these molecules: by release of two cyanopyridine molecules in the first step of thermal decomposition single chains are obtained where the  $\text{M}^{\text{II}}$ -ions are linked by pairs of bridging bromide cations in order to maintain the octahedral coordination at the metal atom. Further decomposition steps lead to the formation of double chains, bands and larger two dimensional networks [2], [3].

#### References:

- [1] Batten et al., Pure Appl. Chem 85, 1715, 2013
- [2] Krysiak et al., ZAAC 640, 3190, 2014
- [3] Zhao et al., 2015 in preparation

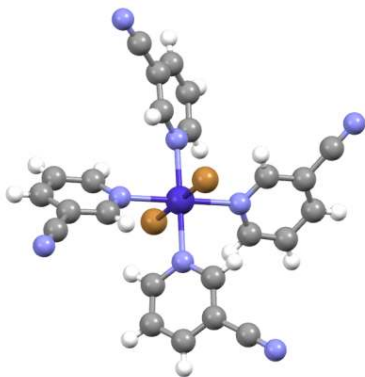


**Figure 1.** Molecular structure of the ligand rich precursor compound

**Keywords:** X-ray powder diffraction, crystal structures, structure relations, coordination polymers, condensed networks, substituted pyridine ligands, transition-metal halides

## MS33-P2 Crystal structure determination of two novel 1,2,4-triazolo[3,4-b]-1,3,4-thiadiazine and -thiadiazole derivatives by XRPD method

Filiz B. Kaynak<sup>1</sup>, Gülsüm Gündoğdu<sup>1</sup>, Melanie Müller<sup>2</sup>, Süheyla Özbey<sup>1</sup>

1. Hacettepe University, Faculty of Engineering, Department of Physics Engineering, Beytepe, 06800, Ankara, TURKEY

2. Ruhr University Bochum Institute for Geology Mineralogy and Geophysics Crystal Chemistry, 44721, Bochum, GERMANY

email: gulsen@hacettepe.edu.tr

In recent years, studies reporting anticancer activities of a number of fused 1,2,4-triazole derivatives such as triazolopyridazine, triazolothiazine, triazolothiadiazine have being attracting interest. In the light of these knowledge, we prepared new series of 1,2,4-triazolo[3,4-b]-1,3,4-thiadiazine and 1,2,4-triazolo[3,4-b]-1,3,4-thiadiazole derivatives and evaluated their possible anticancer activities [1]. The samples are originally synthesized in Hacettepe University, Faculty of Pharmacy, Department of Pharmaceutical Chemistry by Dr. Tozkoparan and her group.

In the presented research, we have obtained and determined crystal structures of two compounds by X-ray powder diffraction techniques. The synchrotron measurements of the samples have been done in Argonne National Laboratory on 11-BM beamline. Data sets were collected over the 1–40° 2θ range with a 0.001° step size at room temperature (295.0 K) with ( $\lambda \sim 0.459169\text{\AA}$ ) wavelength. This measurement from beamline 11-BM at APS allowed us to fully analyze this data.

The powder X-ray diffraction pattern of the samples were first indexed using the TOPAS 4.2 program. Structure determination of compound I was carried out using the simulated annealing method implemented in the program DASH (unit cell of compound 1:  $a=15.55645(11)\text{ \AA}$ ,  $b=8.61693(6)\text{ \AA}$ ,  $c=8.56702(6)\text{ \AA}$ ,  $\beta(^{\circ})=104.3270(4)$ , space group:  $P2_1$ ) and FOX program was used for compound II (unit cell of compound 2:  $a=6.373(3)\text{ \AA}$ ,  $b=11.362(5)\text{ \AA}$ ,  $c=14.089(6)\text{ \AA}$ ,  $\alpha(^{\circ})=80.175(1)$ ,  $\beta(^{\circ})=94.877(1)$ ,  $\gamma(^{\circ})=99.022(1)$ , space group:  $P-1$ ). XRD patterns are carefully analyzed by the Rietveld method using FullProf program and soft restraints was employed at the final stage of the refinement. Good agreement was achieved between calculated and experimental powder diffraction patterns at the final Rietveld refinement (Figure 1). So, the agreement factors support the correctness of the structures (for compound 1:  $R_{wp}=0.0694$   $R_p=0.05470$   $R_{exp}=0.0704$  and  $\chi^2=0.9705$ ).

Financial support to Gülsüm Gündoğdu of the Scientific and Technical Research Council of Turkey is gratefully acknowledged (grants 2214 A by TÜBİTAK one year research grant during PhD). We also thank Argonne National Laboratory for the synchrotron measurement of compound I and II using 11-BM mail-in Program.

[1] P. S. Aytac, I. Durmaz, D. R. Houston, R.Ç.-Atalay, B. Tozkoparan, Bioorganic & Medicinal Chemistry, Vol 24, Iss 4, 2016, 858–872.

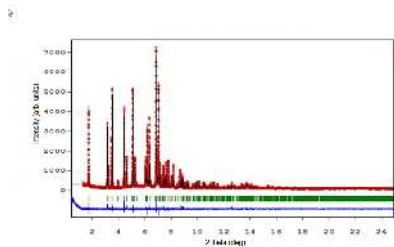


Figure 1. FullProf Rietveld refinement solution for compound 1.

**Keywords:** XRPD, Rietveld refinement, 1,2,4-triazole derivatives

## MS33-P3 New polynuclear Re-M cyanide complexes (M = Cu, Ag)

Monika K. Krawczyk<sup>1</sup>, Rahman Bikas<sup>1</sup>, Marta S. Krawczyk<sup>2</sup>

1. Faculty of Chemistry University of Wrocław, F. Joliot-Curie 14 St., 50-383 Wrocław, Poland

2. Department of Analytical Chemistry, Faculty of Pharmacy, Wrocław Medical University, Borowska 211A St., 50-556 Wrocław, Poland

email: monika.krawczyk@ifd.uni.wroc.pl

New class of mixed-metal square-shaped polynuclear clusters based on rhenium(I) phosphine complexes have been obtained. The heteronuclear complexes are comprising of the core that consists of Re and Cu or Ag atoms bridged by cyanide ligands resulting in the formation of cyclic structure with approximate square geometry. In studied complexes Re atoms are located in vertices of the square, while Cu or Ag atoms along with coordinated CN ligands form their sides.

Permanent address: Institute of Experimental Physics, University of Wrocław, M. Borna 9, 50-204 Wrocław, Poland Financial support: National Science Center (Grant NCN UMO-2013/11/N/ST5/01375)

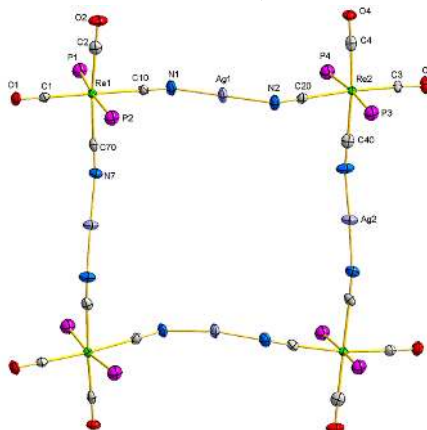


Figure 1. Structure of square-shaped  $[\text{Re}(\mu\text{-CN})\text{Ag}(\mu\text{-NC})(\text{CO})_2\text{P}]_4$  unit in studied complex. The aromatic rings attached to phosphorus atoms in  $\text{PPh}_3$  groups are omitted for clarity.

**Keywords:** rhenium complexes, cyanide complexes, heteronuclear clusters



## MS33-P4 Disappearing Superstructure in Crystals of Pentaphosphaferrocene-Based Supramolecules

Eugenia V. Peresyppkina<sup>1,2</sup>, Alexander V. Virovets<sup>1,2</sup>, Manfred Scheer<sup>1</sup>

1. Institute of Inorganic Chemistry, University of Regensburg, Germany

2. Nikolaev Institute of Inorganic Chemistry SB RAS, Novosibirsk, Russia

email: peresyp@niic.nsc.ru

Since 2002, we have been systematically investigating an inorganic analogue of ferrocene, pentaphosphaferrocene,  $[\text{Cp}^{\text{R}}\text{Fe}(\eta^5\text{-P}_5)]$  ( $\text{Cp}^{\text{R}} = \eta^5\text{-C}_5\text{R}_5$ ,  $\text{R} = \text{Me}$  ( $\text{Cp}^{\text{Me}}$ ),  $\text{CH}_2\text{Ph}$  ( $\text{Cp}^{\text{Bn}}$ ),  $\text{PhC}_4\text{H}_9$  ( $\text{Cp}^{\text{BIG}}$ )). It showed an unprecedented ability to assemble in giant supramolecules [1-7] when reacted to Cu(I) halides ( $\text{X} = \text{Cl}, \text{Br}, \text{I}$ ). These supramolecules reach 2.1–4.6 nm in size and can be isolated in astonishingly high yields. Their molecular structure is usually based on inorganic hollow cage, in which the *cyclo*- $\text{P}_5$  ring of the  $[\text{Cp}^{\text{R}}\text{Fe}(\eta^5\text{-P}_5)]$  ligand is coordinated to single or various aggregated CuX units. The single-layered cages often follow fullerene topology involving single CuX units [1-4]. The multi-layered cages [1-2, 6] are constructed of  $\text{Cu}_n\text{X}_m$  polynuclear fragments.

The X-ray structural analysis of these compounds faces many difficulties as low diffraction power, disorder in  $\text{Cu}_n\text{X}_m$  halide core, disorder of guest molecules and  $\text{Cp}^{\text{R}}$  ligands. The disorder can be interpreted as formation of solid solutions of co-crystallizing supramolecules with different, but similar structure. In some cases, we observed superstructural effects pointing to partial ordering. The aging of the crystals in the mother liquor unexpectedly leads the superstructure to disappear. For example, the diffraction pattern of freshly prepared  $(\text{CH}_2\text{Cl}_2)_{3,4} @ [(\text{Cp}^{\text{Bn}}\text{FeP}_5)_{12}(\text{CuI})_{54}(\text{MeCN})_{1,46}]$  demonstrates superstructural ordering accompanied with doubling of the triclinic unit cell (see figure 1, blue). In the supercell two crystallographically unique supramolecules are related by pseudo body-centering translation. While aging, the diffraction pattern shows as superstructural reflections gradually fade. The resulting subcell (figure 1, red) contains only one unique supramolecule [1]. Other examples will also be discussed.

This work was supported by ERC grant AdG339072-SELPHOS.

[1] F. Dielmann, C. Heindl, F. Hastreiter, E. V. Peresyppkina et al (2015) *Chem.-A Eur. J.*, **21**, 6208.

[2] S. Heindl E. V. Peresyppkina, J. Sutter, M. Scheer (2015) *Angew. Chem. Int. Ed.*, **54**, 13431.

[3] J. Bai, A. V. Virovets, M. Scheer (2003), *Science*, **300**, 781.

[4] M. Scheer, J. Bai, B. P. Johnson et al (2010), *Chem. Eur. J.*, **18**, 2092.

[5] C. Heindl, E. V. Peresyppkina, A. V. Virovets et al (2015) *J. Am. Chem. Soc.*, **137**, 10938.

[6] C. Schwarzmaier A. Schindler, C. Heindl et al (2013) *Angew. Chem. Int. Ed.*, **52**, 10896.

[7] E. Peresyppkina, C. Heindl, A. Schindler et al (2014) *Z. Kristallogr.*, **229**, 735.

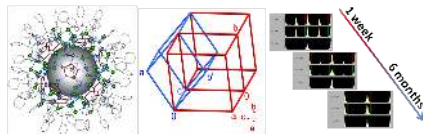


**Figure 1.** Structure-superstructure relation in  $(\text{CH}_2\text{Cl}_2)_{3,4} @ [(\text{Cp}^{\text{Bn}}\text{FeP}_5)_{12}(\text{CuI})_{54}(\text{MeCN})_{1,46}]$

**Keywords:** giant supramolecule, pentaphosphaferrocene, superstructure, single-crystal X-ray diffraction

# MS33-P5 Zn(II) and Cu(II) coordination polymers based on anthracene ligands: Luminescence and antimicrobial properties

Serhii I. Vasylevskiy<sup>1</sup>, Katharina Fromm<sup>1</sup>

<sup>1</sup>. Department of Chemistry, University of Fribourg, Chemin du Musée 9, 1700 Fribourg, Switzerland

email: serhii.vasylevskiy@unifr.ch

Anthracene derivatives have been widely studied during the last two decades as perspective materials for luminescence [1]. Moreover anthracene derivatives have been intensively investigated as an attractive building block and starting material in OLEDs (organic light-emitting diodes), due to their unusual photoluminescence and electroluminescence properties [1]. Coordination compounds of Cu(II) and Zn(II) have been developed *in vitro* as promising materials for antimicrobial properties against *Staphylococcus aureus*, *Bacillus subtilis*, *Escherichia coli*, *Pseudomonas aeruginosa* etc... [2,3]. In this work, new coordination polymers of Zn(II) and Cu(II) based on new anthracene derivatives (Figure 1) will be presented combining both luminescent and antimicrobial properties. The ligand (L1) was already investigated with Ag(I) in our group. While the shift of emission and the decrease of eximer band are observed upon coordination to silver ion in crystalline form, amorphous nanowires showed a large emission band for this system [4]. Three coordination polymers of Cu(II) and three of Zn(II) were obtained with ligands L1 and L2 by slow liquid diffusion technique. Crystalline structures of coordination compounds were obtained from X-ray single crystal measurements, and solved by SHELX-97 program. Further luminescent and antimicrobial properties will be investigated.

## References

[1] Jinhai Huang, Jian-Hua Su and He Tian., *J. Mater. Chem.*, 2012, **22**, 10977-10989. [2] Qing Yuan., *Journal of Inorganic Biochemistry*, 2009, **103**, 1156-1161. [3] Sudeep Goswami *et al.*, *J. Mater. Chem. B*, 2015 **3**, 7068-7078. [4] Jing Chen, Antonia Neels and Katharina M. Fromm., *Chem. Commun.*, 2010, **46**, 8282-8284.

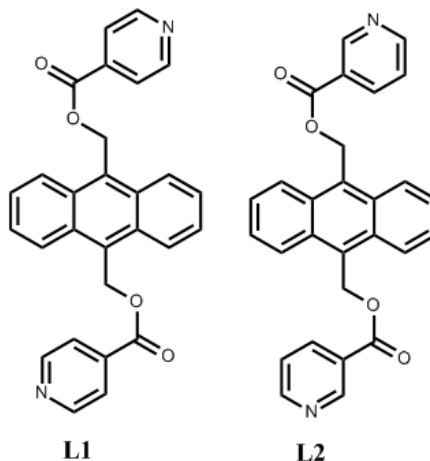


**Figure 1.** Ligands used for obtaining coordination polymers of Cu(II) and Zn(II). L1 = anthracene-9,10-diylbis(methylene) diisonicotinate; L2 = anthracene-9,10-diylbis(methylene) dinicotinate.

**Keywords:** Coordination polymers, antimicrobial properties, luminescence

**MS33-P6 Giant**  
**Pentaphosphaferrocene-Based**  
**Supramolecules as Molecular Containers**

Alexander V. Virovets<sup>1,2</sup>, Eugenia V. Peresyphkina<sup>1,2</sup>, Manfred Scheer<sup>1</sup>

1. Institute of Inorganic Chemistry, University of Regensburg, Germany

2. Nikolaev Institute of Inorganic Chemistry SB RAS, Novosibirsk, Russia

email: avvirovets@yahoo.com

An inorganic analogue of ferrocene, pentaphosphaferrocene,  $[\text{Cp}^{\text{R}}\text{Fe}(\eta^5\text{-P}_5)]$  ( $\text{Cp}^{\text{R}} = \eta^5\text{-C}_5\text{R}_5$ ,  $\text{R} = \text{Me}$  ( $\text{Cp}^{\text{R}}$ ),  $\text{CH}_2\text{Ph}$  ( $\text{Cp}^{\text{Bn}}$ ),  $\text{PhC}_6\text{H}_4$  ( $\text{Cp}^{\text{BtG}}$ )), is able to coordinate  $\text{Cu}^+$  and  $\text{Ag}^+$  cations resulting in either coordination polymers or in giant supramolecules [1-7]. The self-assembled supramolecules of 2.1 – 4.6 nm in diameter can be isolated in high yields using special crystallization technique. A tetrahedral coordination of  $\text{Cu}^+$  together with the predetermined five-fold symmetry of the *cyclo*- $\text{P}_5$  ligand favors the formation of giant cages with fullerene [1,2] or fullerene-like [3, 4] topologies.

Pentaphosphaferrocene-based supramolecules can play a role of molecular containers (Figure 1). The central cavities can include metallocene and cage molecules, fullerene  $\text{C}_{60}$ , molecules of metastable compounds such as white phosphorous and yellow arsenic [6]. The ability of  $\text{CuX}$  to aggregation allows adapting supramolecule to encapsulate cationic guest molecules like  $\text{Cp}^*\text{Co}^+$ . Even more sophisticated supramolecules with multi-layered inorganic core built up with hundreds of metal, halogen and P atoms [5, 6] can be obtained, where external and internal cores are formed *via*  $\sigma$ - and  $\pi$ -coordination of the planar  $\text{P}_5$ -ring to copper, respectively.

Alternative way to influence the structure of the supramolecule is to use salts of copper(I) and silver(I) with larger anions. First results show that single-layered quasi-spherical supramolecules with large central cavity can be obtained by using of  $\text{RSO}_3^-$  anions that can coordinate three metal atoms with donor oxygen atoms. The resulting inorganic  $\text{M-anion-Cp}^{\text{R}}\text{Fe}(\eta^5\text{-P}_5)$  core resembles an icosidodecahedron, which is however essentially vacant in metal cation positions. The  $\text{Cp}^*\text{-based}$  supramolecules encapsulate  $\text{Cp}^*\text{Fe}(\eta^5\text{-P}_5)$  molecules. Host-guest intermolecular interactions are discussed.

This work was supported by ERC grant AdG339072-SELFPHOS.

[1] F. Dielmann C. Heindl, F. Hastreiter, E.V. Peresyphkina et al (2015) *Chem.-A Eur. J.*, **21**, 6208.

[2] S. Heindl E. V. Peresyphkina, J. Sutter, M. Scheer (2015) *Angew. Chem. Int. Ed.*, **54**, 13431.

[3] J. Bai, A. V. Virovets, M. Scheer (2003), *Science*, **300**, 781.

[4] M. Scheer, J. Bai, B. P. Johnson et al (2010), *Chem. Eur. J.* **18**, 2092.

[5] C. Heindl, E. V. Peresyphkina, A.V. Virovets et al (2015) *J. Am. Chem. Soc.*, **137**, 10938.

[6] C. Schwarzmaier A. Schindler, C. Heindl et al (2013) *Angew. Chem. Int. Ed.*, **52**, 10896.

[7] E. Peresyphkina, C. Heindl, A. Schindler et al (2014) *Z. Kristallogr.*, **229**, 735.

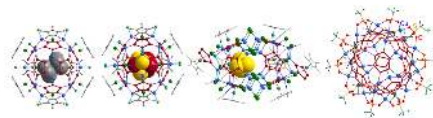


**Figure 1.** (left to right) Copper(I)-based supramolecules encapsulating molecules of ferrocene,  $\text{P}_5\text{S}_3$ , and  $\text{As}_4$ . Inorganic core of a supramolecule based on copper triflate.

**Keywords:** giant supramolecule, pentaphosphaferrocene, inclusion compound, host-guest interaction, intermolecular interaction, single-crystal X-ray diffraction

### MS33-P7 Small Angle Neutron Diffraction on the Vortex Lattice of Type II Superconductors

Jorge L. Gavilano<sup>1</sup>, Jonathan White<sup>2</sup>, Simon Gerber<sup>1</sup>, Nikola Galvan<sup>2</sup>, B. Biswas<sup>3</sup>, Daniel Mazzone<sup>2</sup>, Edwards Forgan<sup>4</sup>, Hazuki Kawano-Furukawa<sup>5</sup>

1. SwissFEL Photonic Group, Paul Scherrer Institut, Villigen PSI, Switzerland

2. Laboratory for Neutron Scattering and Imaging, Paul Scherrer Institut, Villigen PSI, Switzerland

3. Physics Department, University of Warwick, Coventry, United Kingdom

4. School of Physics and Astronomy, University of Birmingham, United Kingdom

5. Division of Natural/Applied Science, Ochanomizu University, Bunkyo-ku, Tokyo, Japan

email: jorge.gavilano@psi.ch

In type II superconductors in magnetic fields  $H_{c1} < H < H_{c2}$  the flux form a Vortex Lattice VL, whose geometry represents a delicate balance of the electronic Fermi surface features and pinning. This provides a very sensitive probe of some microscopic electronic properties which can be measured using small angle neutron scattering technique SANS. Below we describe selected results.

i)  $\text{YBa}_2\text{Cu}_3\text{O}_{7-\delta}$  with  $\delta=0, 0.15$  at 2 K and for fields of up to 16 T applied parallel to the crystal c-axis, we observe in the SANS data (see Fig. 1) a sequence of field-driven and first-order transitions between different VL structures. By rotating the field away from the c-axis, we observe each structure transition to shift to either higher or lower field dependent on whether the field is rotated towards the [100] or [010] direction. We argue that these transitions are determined by the Fermi Surface Morphology [1].

(ii)  $\text{KFe}_2\text{As}_2$ , and related materials. We find an intrinsic anisotropy of the superconducting state in this material. With the SANS technique we monitor the vortex and find a field dependent anisotropy, indicating multiband superconductivity. These results support that  $\text{KFe}_2\text{As}_2$  is Pauli limited for field applied in the basal plane.

iii) The flux-line lattice in  $\text{CaAlSi}$  has been studied by small-angle neutron scattering. A well-defined hexagonal flux-line lattice is seen just above  $H_{c1}$  in an applied field of only 54 Oe. A 30° reorientation of this vortex lattice has been observed in a very low field of 200 Oe. This reorientation transition is first-order and reflect nonlocal effects [3].

[1] J of the Phys Soc of Jpn, 84, 44709 (2015), by N Galvan, J White J. Lim et al.

[2] Phys Rev B **93**, 104527 (2016) S. Kuhn, H. Kawano-Furukawa, E. Jellyman et al.

[3] Phys. Rev. Lett. 108, 77001 (2012) P.K.Biswas MR Lee B. Balaktishnan et al.

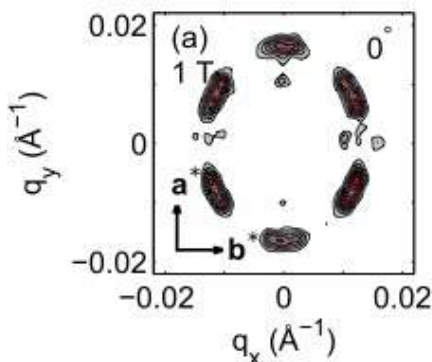


**Figure 1.** SANS diffraction pattern from a VL on  $\text{YBa}_2\text{Cu}_3\text{O}_{7-d}$  at 2K and an external field of 1T parallel to c

**Keywords:** SANS, Vortex Lattice, superconductors

## MS34 Molecular recognition, supramolecular chemistry and crystal engineering

Chairs: Chiara Massera, Carl Henrik Görbitz

### MS34-P1 Crystallization *in situ*, structural investigation, physicochemical properties of azetidine cocrystals with water

Grzegorz Cichowicz<sup>1</sup>, Łukasz Dobrzycki<sup>1</sup>, Michał K. Cyrański<sup>1</sup>,  
Roland Boese<sup>2</sup>

<sup>1</sup>. Czochralski Laboratory of Advanced Crystal Engineering,  
Faculty of Chemistry, University of Warsaw, Żwirki i Wigury 101,  
02-093 Warsaw, Poland

email: gcichowicz@chem.uw.edu.pl

The purpose of this study was to devise, obtain and determine the structures of cocrystals of azetidine with water. Azetidine is volatile liquid cyclic secondary amine with four membered ring. The crystal structure of the neat amine is known [1]. There is also an evidence that azetidine can co-crystallize with water and form sI type clathrate hydrate [2]. Using IR laser assisted *in situ* crystallization technique [3] two unknown polymorphs of azetidine and four hydrates were obtained. Azetidine forms hemi- and monohydrate crystal phases as well as two hydrates containing seven and twelve water molecules per one amine molecule. Hemihydrate has two transformation polymorphs with phase transition at the temperature below 170 K. In hepta- and dodecahydrates amine molecules interact with water lattice *via* non-covalent, hydrogen bonds N-H...O. Comparing unit cell parameters, crystal structure of heptahydrate can be considered as sI clathrate [4]. Information obtained from the X-ray diffraction experiment shown however that water molecules form three distinct cages what results is a new type of hydrate. Moreover heptahydrate crystallizes in different, Pm-3 space group than clathrate hydrate type sI which is Pm-3n. The comparison of azetidine heptahydrate crystal structure and clathrate hydrate type sI is presented in the figure below. Additionally all obtained solid phases were characterized with use of the Raman spectroscopy.

**Acknowledgements** The work has been supported by the National Science Center grant (NCN 2011/03/B/ST4/02591).

#### References

- [1] Bond, A. D., Davies, J. E., Parsons, S. (2008). *Acta Crystallogr. C*, **64**, 543.
- [2] Rosso, J. C., Caranoni, C., Carbonnel, L. (1975). *C. R. Acad. Sci. C*, **280**, 909.
- [3] Boese, R. (2014). *Z. Kristallogr.* **229**, 595.
- [4] Sloan, E. D., Koh, C. A. *Clathrate Hydrates of Natural Gases*, 3rd Edition, Taylor & Francis/CRC Press,

Boca Raton, FL, USA, (2008).

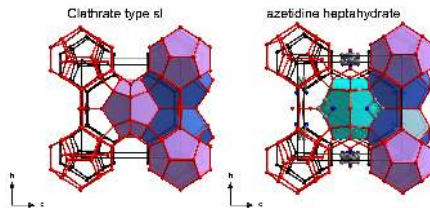


**Figure 1.** Crystal packing comparison of hydrate clathrate type sI and azetidine heptahydrate

**Keywords:** Hydrates, Clathrates, Azetidine, *in situ* crystallization, Crystal Engineering, Single Crystal Diffraction, Raman Spectroscopy

## MS34-P2 Mixed Metal Multinuclear Cr(III) Cage Compounds and Coordination Polymers Based on Unsubstituted Phenolate: Design, Synthesis, Mechanism, and Properties.

Aurelien Crochet<sup>1</sup>, Jean-Pierre Brog<sup>1</sup>, Katharina M. Fromm<sup>1</sup>

1. Department of Chemistry, University of Fribourg, Switzerland

email: aurelien.crochet@unifr.ch

The use of alkali aryloxide reagents in organo-metallic synthesis often depends on their solubility, a property derived from their structure. The regain of interest of alkali aryloxides also originates from the discovery of high-temperature superconducting compounds, which has generated a great interest in the formation of oxide materials and other ceramics. Thus, many alkoxides of yttrium and copper are common precursors for oxide materials. Moreover, the synthesis of heterobimetallic alkoxides has provided a facile route for obtaining soluble, volatile, and generally monomeric species. These heterobimetallic complexes can thus serve as valuable precursors for making mixed metal oxides. This is however not the only possible application for this type of compounds. These complexes can be used as starting compounds for the syntheses of more complex structures. In this work, the salt elimination and ligand exchange reaction of chromium(II) chloride with lithium phenoxide yields a mixed metal lithium-chromium(II) phenoxide. Using this latter as intermediately formed starting material and combining the substitution reaction with an oxidation process, we have gained access to new polynuclear chromium(III) aryloxide complexes. While a 1D coordination polymer based on chromium(III) is obtained in a first reaction by serendipity, the controlled addition of water to the Cr(II) complex leads to three new discrete chromium(III) cluster compounds. The use of deuterated species allowed to confirm the oxidation based on the addition of water by detection of H<sub>2</sub>, HD and D<sub>2</sub>. During these investigations, we have also identified a THF-adduct of chromium(II) chloride, used in the literature as precursor in numerous syntheses, but with a hitherto unknown structure.

A. Crochet, J.-P. Brog, and K. M. Fromm, *Cryst. Growth Des.*, **2016**, *16* (1), pp 189–199.

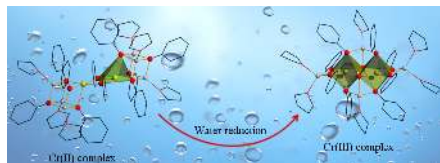


**Figure 1.** Oxidation of a Cr(II) complex by water and formation of a new Cr(III) complex and hydrogen.

**Keywords:** Chromium, oxidation, reduction, aryloxide, water

## MS34-P3 Fabrication of New MOFs *via* Rational Design of the Organic Building Block

Rajdip Dey<sup>1</sup>, Susan A Bourne<sup>1</sup>

1. Centre for Supramolecular Chemistry Research, Department of Chemistry, University of Capetown, 7700 Rondebosch, South Africa

email: rajdipdey@gmail.com

The fabrication of metal organic frameworks<sup>1</sup> (MOFs) is one of the current interest in the fields of supramolecular chemistry and crystal engineering, not only because of their intriguing architectures but also due to its multidirectional functional property.<sup>2</sup> Thus the synthesis and characterization of infinite one, two, and three dimensional (1D, 2D, and 3D) networks, with coordination space, has been an area of rapid growth. The applications of MOFs<sup>3</sup> can be enhanced by the incorporation of open metal sites into the framework. As a result, development of methodologies for the inclusion of various metal centres into MOFs are important. It has been found that the metal component in MOFs play a critical role in the material's property.<sup>4</sup> We have designed an important synthetic strategy and the use of metallogand building blocks to incorporate various metal centres into MOFs.

Here we have synthesised several MOFs by the solvo-thermal process in a reaction with different metal system (Cu(II), Ni(II), Mn(II), Co(II), Cd(II), Zn(II) and using different dicarboxylates (4,4',4'',4'''-benzene-1,2,4,5-tetratyltetrabenzoic acid, terphenyl-3,3'',5,5''-tetracarboxylic acid, 2,6-naphthalenedicarboxylic acid) and some newly designed N, N donor ligands. The compounds have been analysed by PXRD, TGA and the single crystal X-ray structure. The propensity of these compounds to absorb solvent & gas molecules commensurate with their porous structures are under study.

### References:

1. O. M. Yaghi, M. O'Keeffe, N. W. Ockwig, H. K. Chae, M. Eddaoudi and J. Kim, *Nature* 2003, **423**, 705.
2. S. Kitagawa, R. Kitaura and S. Noro, *Angew. Chem., Int. Ed.* 2004, **43**, 2334.
3. J. Hennessy, *Nature Materials*, 2015, **14**, 962.
4. R. Dey, R. Haldar, T. K. Maji and D. Ghoshal *Cryst. Growth & Des.*, 2011, **11**, 3905.

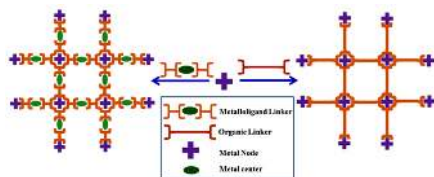


**Figure 1.** Scheme 1: The assembly of framework with an organic ligand linker versus a metallogand linker allowing for the incorporation of various metal centers into the MOF

**Keywords:** MOF, dicarboxylate, Supramolecular Chemistry, Crystal engineering

## MS34-P4 Ferrocene derivatives as potential mechanophores for stimuli-responsive materials

Michela Di Giannantonio<sup>1</sup>, Katharina M. Fromm<sup>1</sup>

1. Departement of Chemistry, University of Fribourg, Chemin du Musée 9, CH-1700 Fribourg, Switzerland

email: michela.digiannantonio@unifr.ch

Since long time ferrocene and its derivatives have attracted the attention of the scientific and technical community because of its fascinating chemistry. Due to its easy functionalization and unusual and attractive properties, ferrocene derivatives have found different applications in material science, such as sensors, catalysts, polymers, electro active materials and medicinal chemistry<sup>1,2</sup>. The aim is to synthesize linear polyurethane chains or linear poly(methyl methacrylate) with a number of covalently linked ferrocene units in the backbone. Upon exerting a mechanical stress (e.g. sonication in solution), we expect the polymer to break along the weakest bonds, i.e. the ferrocene moieties. In order to verify this hypothesis, we analyze the physico-chemical properties and changes of the polymers following sonication in solution or using techniques such as the atomic force microscope (AFM), in order to understand their potential as stimuli-responsive materials.

In collaboration with Prof. C. Weder (Adolphe Merkle Institute, Fribourg) the first mechanical tests in solution were performed with the linear polyurethane (Fc 3%) exploiting the ultrasound-induced degradation<sup>3</sup> to stretch the polymer and to selectively break the weak bonds. With the first results obtained by a kinetic study (Fig. 1) we can conclude that the ferrocene moiety could be a potential mechanophore in a linear polymer. The synthesized ferrocene-based polymers will be further studied exploiting the AFM<sup>4</sup> and other techniques to confirm these preliminary findings.

**References:** <sup>1</sup> S. Zhai, J. Shang, D. Yang, S. Wang, J. Hu, G. Lu, X. Huang, *J. Polym. Sci. Part Polym. Chem.* **2012**, *50*, 811–820.

<sup>2</sup> C. Herfurth, D. Voll, J. Buller, J. Weiss, C. Barner-Kowollik, A. Laschewsky, *J. Polym. Sci. Part Polym. Chem.* **2012**, *50*, 108–118.

<sup>3</sup> M. M. Caruso, D. A. Davis, Q. Shen, S. A. Odom, N. R. Sottos, S. R. White, J. S. Moore, *Chem. Rev.* **2009**, *109*, 5755–5798.

<sup>4</sup> N. Hosono, A. M. Kushner, J. Chung, A. R. A. Palmans, Z. Guan, E. W. Meijer, *JACS*, **2015**, *137*, 6880–6888.

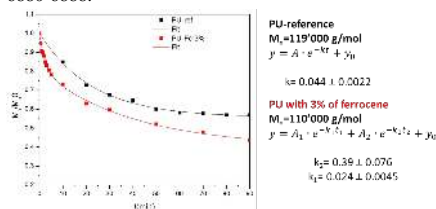


Figure 1. Ultrasound-induced degradation of a Fc-containing PU.

**Keywords:** polyurethanes, ferrocene, sonication

## MS34-P5 Multitopic precursors for oxide materials' synthesis.

Alba Finelli<sup>1</sup>, Aurélien Crochet<sup>2</sup>, Katharina M. Fromm<sup>3</sup>

1. Department of Chemistry, University of Fribourg, Chemin du Musée 9, 1700 Fribourg.

2. FriMat, Department of Chemistry, University of Fribourg, Chemin du Musée 9, 1700 Fribourg.

3. Department of Chemistry, University of Fribourg, Chemin du Musée 9, 1700 Fribourg.

email: alba.finelli@unifr.ch

The research interest in mixed metal oxides is increasing in material science, as they have multiple applications, such as in batteries, ceramics, pigments, high-Tc superconductors or transparent conductors. However, the two main challenges for the synthesis of such compounds are the lack of control on the ratio of the different metal components and the extreme conditions (up to 900 °C) that many of these oxides require during their traditional solid state synthesis. To overcome these issues, we propose a strategy for the synthesis of mixed metal complexes, which is based on precursors of coordination compounds, using the "multitopic ligand approach". The aim is to design specific ligands with selective coordination sites to bind different metal ions. Due to the metal ion preorganization in the precursor thus formed, the stoichiometry of the final oxide material can be controlled and the extreme synthesis conditions diminished (pressure or temperature). These new mixed metal complexes will be finally combusted to oxide materials with possible new features and ideally at the nanoscale, allowing to access new and better properties in their applications.

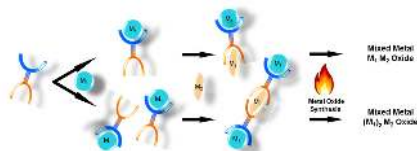


Figure 1. Multitopic ligand approach

**Keywords:** Inorganic chemistry, complexes, alkali, alkaline earth



**MS34-P6** Co-crystals of  
5,6-Dimethyl-2-thiouracil: further proof of  
the robustness of the *ADA-DAD*  
 $\text{N}-\text{H}\cdots\text{O}/\text{N}-\text{H}\cdots\text{N}/\text{N}-\text{H}\cdots\text{S}$ -synthon

Wilhelm Maximilian Hützler<sup>1</sup>, Ernst Egert<sup>1</sup>

<sup>1</sup> Institute of Organic Chemistry and Chemical Biology,  
Goethe-University Frankfurt am Main, Germany

email: huetzler@chemie.uni-frankfurt.de

One of the main goals in crystal engineering is the search for reliable non-covalent intermolecular interaction motifs ("synthons") for the design of new solids with desired properties.<sup>[1]</sup> The replacement of a strong hydrogen bond within a certain interaction with a weaker one, say  $\text{N}-\text{H}\cdots\text{O}$  with  $\text{N}-\text{H}\cdots\text{S}$ , may open up ways to new synthons.<sup>[2]</sup> Thereby, the robustness of the synthon still may be preserved due to the cooperativity of hydrogen bonding interactions.<sup>[3]</sup> Inspired by the cyanuric acid-melamine co-crystal, where an *ADA-DAD*  $\text{N}-\text{H}\cdots\text{O}/\text{N}-\text{H}\cdots\text{N}/\text{N}-\text{H}\cdots\text{O}$  interaction is observed (*A* = acceptor, *D* = donor), the title compound 5,6-dimethyl-2-thiouracil (DMTU) was selected for co-crystallization. DMTU contains an *ADA* hydrogen-bonding site involving an S-atom as an acceptor and, therefore, should be capable of forming a mixed *ADA-DAD*  $\text{N}-\text{H}\cdots\text{O}/\text{N}-\text{H}\cdots\text{N}/\text{N}-\text{H}\cdots\text{S}$  synthon with suitable coformers like 2,4-diaminopyrimidine (DAPY), 2,4,6-triaminopyrimidine (TAPY) or 2,4,6-triamino-1,3,5-triazine (melamine; MELA). Co-crystallization experiments yielded two solvates of DMTU, (I) and (II), one salt-hydrate and two co-crystal solvates with DAPY, (III) – (V), one co-crystal solvate and one co-crystal salt-solvate with TAPY, (VI) and (VII), and one co-crystal solvate with MELA, (VIII) (Fig. 1). The two solvates show the formation of dimers or tetramers in the crystal packing formed by either "pure"  $\text{R}^2_2(8)$   $\text{N}-\text{H}\cdots\text{O}$  hydrogen bonds in (I) or by a combination of "pure"  $\text{R}^2_2(8)$   $\text{N}-\text{H}\cdots\text{O}$  and "mixed"  $\text{R}^2_2(8)$   $\text{N}-\text{H}\cdots\text{O}$  and  $\text{N}-\text{H}\cdots\text{S}$  hydrogen bonds in (II). While DMTU showed an *AA-DD* motif with DAPY in (III) the synthesis of the desired *ADA-DAD* synthon was successful in co-crystals (IV) – (VIII). Moreover, due to a proton transfer along an  $\text{N}-\text{H}\cdots\text{N}$ -hydrogen bond in (VII), one of the two observed *ADA-DAD* interactions was changed into an *AAA-DDD* motif. The results demonstrate, that the *ADA-DAD*  $\text{N}-\text{H}\cdots\text{O}/\text{N}-\text{H}\cdots\text{N}/\text{N}-\text{H}\cdots\text{S}$  motif is a reliable synthon for the design of co-crystals of DMTU.

[1] Desiraju, G. R. (2013). *J. Am. Chem. Soc.* **135**, 9952–9967.

[2] Hützler, W. M. & Egert, E. (2015). *Acta Cryst.* **C71**, 229–238.

[3] Desiraju, G. R. (2011). *Angew. Chem. Int. Ed.* **50**, 52–59.

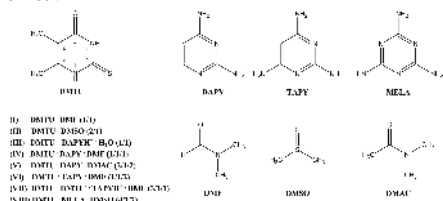


**Figure 1.** Structures of the compounds used and composition of the crystals.

**Keywords:** Co-crystals, crystal engineering,  $\text{N}-\text{H}\cdots\text{S}$  hydrogen bonds

## MS34-P7 New easily-synthesisable and modifiable organic materials for applications in luminescent devices

Sylvia E. Kutyla<sup>1</sup>, Mateusz Piędzio<sup>1</sup>, Katarzyna N. Jarzemska<sup>1</sup>, Radosław Kamiński<sup>1</sup>, Michał K. Cyrański<sup>1</sup>, Daniel T. Gryko<sup>2</sup>

1. Biological and Chemical Research Centre, Department of Chemistry, University of Warsaw, Żwirki i Wigury 101, 02-089 Warsaw, Poland

2. Institute of Organic Chemistry, Polish Academy of Sciences, Kasprzaka 44/52, 01-224 Warsaw, Poland

email: sekutyla@gmail.com

Arylboronic acids have found many applications in diverse areas of chemical science, such as organic synthesis, catalysis or crystal engineering. They can be also used as low-cost luminescent complexes (e.g., borinic-type compounds) for applications in optoelectronic devices.<sup>1</sup> Quite recently, we have introduced a new class of cheap, easily-synthesisable and modifiable organic luminescent materials based on ortho-phenylenediboronic acid.<sup>2,3</sup> The acid reacts with 8-hydroxyquinoline in high yield, both in solution and under mechanochemical conditions, and forms a brightly luminescent 8-oxyquinoline complex.<sup>3</sup> More importantly, the obtained complexes appeared to be electroluminescent. Similarly to the well-known borinic-based luminescent materials tuning of the emitted colour can be achieved mainly by modifications of the N,O-donor fragment.

Therefore, here we present a series of ortho-phenylenediboronic acid complexes<sup>4,5</sup> with luminescent N,O-donor compounds (Figure 1).<sup>4,5</sup> The latter species themselves contain phenyl fragment and imidazo[1,2-a]pyridine ring, and thus may easily form intramolecular hydrogen bonding, which enables a further proton transfer. The proton transfer is responsible for their luminescent properties and can be tuned via the phenyl ring substituent character and a solvent choice. In the complex with ortho-phenylenediboronic this proton transfer is disabled. Hence, we checked the impact of the complexation of boronic acid on luminescent properties of the selected N,O-donor species. All new complexes were crystallized and structurally characterized using X-ray diffraction technique. Additionally, we examined their luminescence properties both in solution and in the solid state. The experimental data were supported by periodic energetic calculations and TDDFT studies.

(1) Durka, K. et al. *J. Mater. Chem. C* 2015, 3, 1354. (2) Durka, K.; Jarzemska, K. N.; Kamiński, R. et al. *Cryst. Growth Des.* 2013, 13, 4181. (3) Jarzemska, K. N.; Kamiński, R. et al. *Acta Cryst* 2015 A71, s333. (4) Stasyuk, A. J. et al. *J. Org. Chem.* 2012, 77, 5552. (5) Stasyuk, A. J. et al. *J. Photochem. Photobiol. A* 2016, Volume 314, 198.

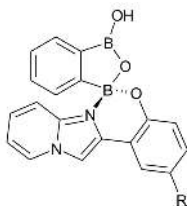
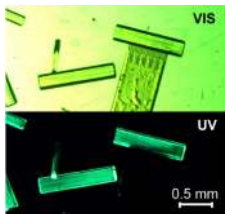


**Figure 1.** Luminescent properties of single crystals of new adducts (left panel). Schematic representation of new complexes based on ortho-phenylenediboronic acid and imidazo[1,2-a]pyridines (right panel).

**Keywords:** luminescent complexes, boronic acid, crystal engineering, spectroscopic properties

## MS34-P8 4,2':6',4'' and 3,2':6',3''-terpyridine Ligands – Coordination polymers with discrete, up to 3-dimensional assemblies

Y. Maximilian Klein<sup>1</sup>, Prescimone Alessandro<sup>1</sup>, Constable C. Edwin<sup>1</sup>, Housecroft E. Catherine<sup>1</sup>

1. University of Basel

email: Max.Klein@unibas.ch

Oligopyridines are well known building blocks in coordination chemistry. The popular 2,2':6',2''-terpyridine (tpy) building block adopts a bis(chelating) coordination in octahedral complexes, leading to mainly discrete compounds. By using the less common isomers 4,2':6',4''- and 3,2':6',3''-tpy in combination with a wide range of transition metals, it is observed that the N-atom of the inner pyridine ring does not participate in coordination.<sup>1</sup> Unlike tpy, 4,2':6',4''- and 3,2':6',3''-tpy ligands can no longer form chelates, but favour a variety of multinuclear and multidimensional structures. The ease of introducing substituents in the 4''-position of these tpy's enables facile modification, making the ligands bulkier, as well as introducing additional coordination sites. Taking this one step further, it is possible to synthesise tetra-dentate ditopic bis(tpy) tectons. In the reaction of 1,4-bis(*n*-octoxy)-2,5-bis(3,2':6',3''-terpyridin-4''-yl) benzene (figure) with Co(NCS)<sub>2</sub> a 3-dimensional {4<sub>2</sub>,8<sub>1</sub>} lvt net is obtained.<sup>2</sup> The assembly of 3-D nets or 2-D sheets as well as discrete assemblies will be presented.

### References

- 1 C. E. Housecroft, *Dalton Trans.*, 2014, **43**, 6594–6604.
- 2 Y. M. Klein, E. C. Constable, C. E. Housecroft and A. Prescimone, *CrystEngComm*, 2015, **17**, 2070–2073.

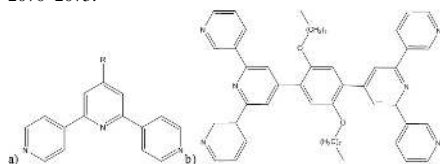


**Figure 1.** a) 4,2':6',4''-terpyridine with substituent R in 4'' position  
b) The ditopic ligand  
1,4-bis(*n*-octoxy)-2,5-bis(3,2':6',3''-terpyridin-4''-yl) benzene.

**Keywords:** Terpyridine, Multidimensional, Self Assembly

## MS34-P9 Self-organization of *para*-sulfonatocalix[*n*]arenes and selected aromatic amines in heteromolecular crystals: structural studies

Barbara Lesniewska<sup>1</sup>, Kinga Suwińska<sup>2</sup>, Anthony W. Coleman<sup>3</sup>

1. Institute of Physical Chemistry PAS, Kasprzaka 44/52, PL-01-224 Warszawa, Poland

2. Faculty of Mathematics and Natural Sciences, Cardinal Stefan Wyszyński University in Warsaw, Woycieckiego 1/3, 01-938 Warszawa, Poland

3. LMI, Université Lyon 1 CNRS UMR 5615, 43 bvd 11 Novembre, 69622 Villeurbanne, France

email: blesniewska@ichf.edu.pl

Supramolecular chemistry is an interdisciplinary field of science that deals with the design, formation and exploration of complex chemical systems of smaller building blocks joined by non-covalent intermolecular interactions. One of its tasks is to look for new molecular receptors, and acquiring knowledge about molecular recognition which involves the formation of selective bond between a receptor and the substrate molecules, resulting in the host-guest complex formation. The inclusion complexes of *p*-sulfonatocalix[*n*]arenes (*n* = 4, 6, 8) with aromatic amines (1,2-bis(4-pyridyl)-ethane, 1,3-bis(4-pyridyl)-propane, 1,10-phenanthroline) were obtained. *p*-Sulfonatocalix[*n*]arenes show a great ability to interact with the aromatic amines. The obtained supramolecular systems are organic salts formed from deprotonated calixarene and protonated guest molecules. Anion receptors form inclusion complexes with substrates mainly by  $\pi$ - $\pi$ , C-H... $\pi$  and N-H... $\pi$  interactions. New, not described before, conformations of the *p*-sulfonatocalix[8]arene anion was observed and it has been shown that this particular anion may substantially change its conformation depending on the type and the amount of complexed cations. In the obtained complexes, the mechanism of induced fitting is observed in cases where the substrate forces the conformational change of the receptor and the mechanism of mutual induced fitting is observed, when there is a mutual adjusting host and guest molecules. Ions and molecules in described supramolecular compounds contribute to the formation of various structural motifs, such as dimers, trimers, tetramers, infinite stacks, capsules, columns, polymeric chains (Fig.1), channels. The obtained inclusion complexes are characterized by diverse molecular packing in the crystal lattice and diverse topologies from simple, stepped and a "zig-zag" bilayers through the column packing to the three-dimensional network of intersecting channels. The obtained results show structural diversity of these compounds, a great richness of supramolecular chemistry, and demonstrate that these compounds are promising building blocks to construct further supramolecular architectures of high complexity. The information gained about the crystal and molecular structures of *p*-sulfonatocalix[*n*]arenes complexes with aromatic amines can contribute to the development of supramolecular chemistry, crystal engineering and also for materials chemistry, aimed at obtaining new functional materials.

**Keywords:** calixarene, host-guest complex

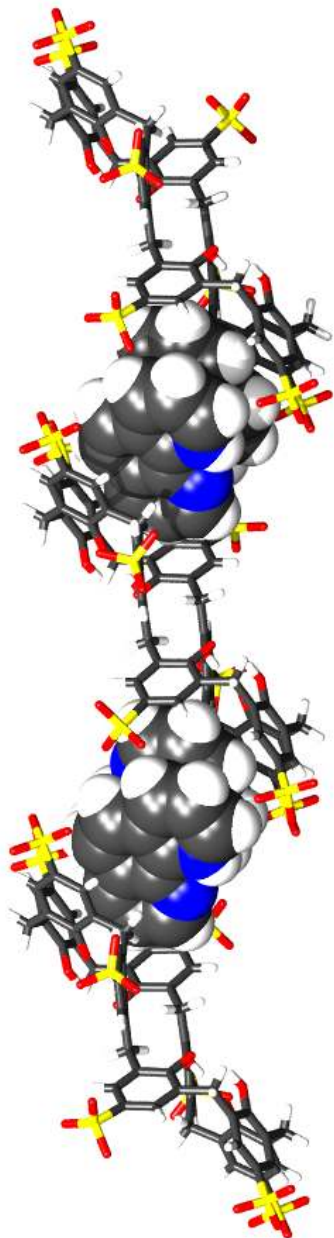


**Figure 1.** Inclusion polymer formed by *p*-sulfonatocalix[8]arene and 1,10-phenanthroline dimers.

## MS34-P10 pH-Dependant crystalline forms of pyridoxal – a comparative crystallographic and theoretical study

Paulina H. Marek<sup>1</sup>, Maciej Ciemny<sup>2</sup>, Izabela D. Madura<sup>1</sup>,  
Małgorzata Ogryzek<sup>2</sup>, Agnieszka Chylewska<sup>3</sup>

1. Warsaw University of Technology, Faculty of Chemistry, Noakowskiego 3, 00-664 Warsaw, Poland

2. University of Warsaw, Faculty of Physics, Pasteura 5, 02-093 Warsaw, Poland

3. University of Gdansk, Faculty of Chemistry, Wita Stwosza 63, 80-308 Gdansk, Poland

email: pau.marek@gmail.com

Vitamin B6 is unique among the B vitamins in that it is involved in the metabolism of all three primary macronutrients, namely proteins, lipids and carbohydrates and so it is aligned in high diversity of biochemical reactions.<sup>[1]</sup> In addition, it has been lately demonstrated that vitamin B6 has a second important function by being an effective antioxidant.<sup>[2]</sup>

The name 'vitamin B6' is a generic term for a group of six naturally occurring water-soluble vitamers, the 3-hydroxy-2-methylpyridine derivatives pyridoxine (PN), pyridoxal (PL) and pyridoxamine (PM) and their 5-phosphorylated derivatives. Every form of vitamin has proven ability to form complexes with a broad spectrum of metal ions. Nevertheless, no PL complexes nor salts have been characterized in the solid state by X-ray diffraction so far.<sup>[1]</sup> The only described form is a hemiacetal PL zwitterion<sup>[3, 4]</sup> and a platinum hexachloride salt with protonated form of PL hemiacetal.<sup>[5]</sup>

The current contribution contains structural characterization of pyridoxal hemiacetal chloride and semichloride obtained by crystallization from controlled pH water solutions. The comparison of molecular packing of three PL forms will be presented. The identification of important, directional intermolecular interactions in crystal structures will be supported by the Hirshfeld surface analysis. Additionally, in the case of pyridoxal hemiacetal semichloride where the proton transfer between two PL hemiacetal is observed, the nature of this interaction will be investigated by quantum chemical methods.

[1] J. S. Casas; M. D. Couce; J. Sordo, *Coord. Chem. Rev.*, **256** (2012) 3036.

[2] S. Mooney; H. Hellmann, *Phytochemistry*, **71** (2010) 495.

[3] S. P. S. Rao; H. Manohar; K. Aoki; H. Yamazaki; R. Bau, *J. Chem. Soc., Chem. Commun.* (1986) 4.

[4] S. P. S. Rao; H. Manohar; K. Aoki; H. Yamazaki, *J. Chem. Soc., Dalton Trans.*, (1987) 1009.

[5] J. H. K. A. Acquaye; M. F. Richardson, *Inorg. Chim. Acta*, **201** (1992) 101.

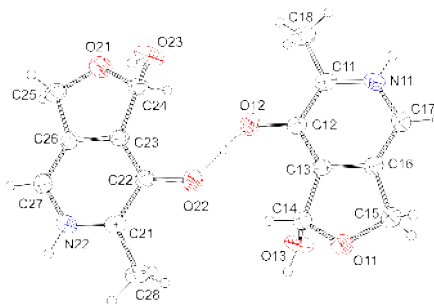


Figure 1.

**Keywords:** vitamin B, pyridoxal, proton sponge

## MS34-P11 Structural and spectroscopic investigations of cyclobutylamine and cyclobutylamine hydrates

Kamila Pruszkowska<sup>1</sup>, Łukasz Dobrzycki<sup>1</sup>, Michał K. Cyrański<sup>1</sup>, Roland Boese<sup>1</sup>

<sup>1</sup>. Czocharlski Laboratory of Advanced Crystal Engineering, Faculty of Chemistry, University of Warsaw, Żwirki i Wigury 101, 02-093 Warsaw, Poland

email: kpruszkowska@chem.uw.edu.pl

Clathrate hydrates are fascinating group of compounds where the guest molecules are trapped in the water cage. The most known example are clathrate hydrates of methane [1]. This research is focused on the supramolecular synthesis of compounds of this kind with cyclobutylamine as the guest molecule. The structure of the amine hemihydrate is already known. It crystallizes in monoclinic  $P2_1/n$  space group [2]. The crystal is stabilized by a hydrogen bond and weak van der Waals interactions. To screen the possibility of hydrate/clathrate formation and the amine/water ratios some preliminary XRD experiments have been made. The samples suitable for single crystal X-ray diffraction were grown with use of the *in situ* crystallization method assisted by IR laser [3]. In this way we were able to obtain crystals of the cyclobutylamine and its four new hydrates containing: 1.00, 6.43, 7.54 and 9.50 water molecules *per* one amine molecule [4]. Their crystal and molecular structures were solved with use of the X-ray diffraction experiment on single crystal. The structures containing larger amount of water (6.43, 7.54 and 9.50 hydrates) resembled clathrate hydrates of methane. Contrary to true clathrates the guest molecules interacted with the water framework via N...O hydrogen bonds. These structures are in addition severely disordered. All systems were also characterized using Raman spectroscopy.

**Acknowledgements** The work has been supported by the *National Science Center* grant (NCN 2011/03/B/ST4/02591).

### References

- [1] Dendy Sloan, Jr., E. "Clathrate Hydrates of Natural Gases" (Monticello, NY: Marcel Dekker, Inc 1990), 641 pp.
- [2] Allan, D. R. (2006). *Acta Cryst. E*, **62**, o751.
- [3] Boese, R. (2014). *Z. Kristallogr.* **229**, 595.
- [4] Dobrzycki, Ł., Pruszkowska, K., Boese, R., Cyrański, M. K. (2015). *Crystal Growth&Design*, in press.

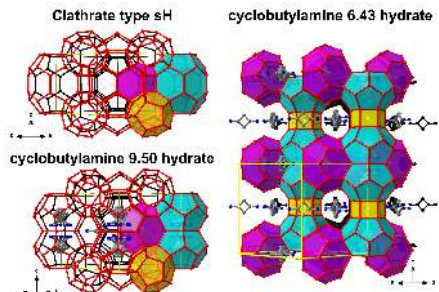


**Figure 1.** Packing diagrams of 6.43 and 9.50 hydrates of cyclobutylamine compared to structure of clathrate type sH

**Keywords:** Hydrates, Clathrahes, Cyclobutylamine, in situ crystallization, Crystal Engineering, Single Crystal Diffraction, Raman Spectroscopy

## MS34-P12 Using matched-molecular structures in the Cambridge Structural Database for crystal engineering

Anthony M. Reilly<sup>1</sup>, Ilenia Giangreco<sup>1</sup>, Jason C. Cole<sup>1</sup>, Gregory P. Shields<sup>1</sup>, Neil Feeder<sup>1</sup>, Colin R. Groom<sup>1</sup>

1. The Cambridge Crystallographic Data Centre

email: reilly@ccdc.cam.ac.uk

With over 800,000 small-molecule crystal structures, the Cambridge Structural Database (CSD) features a wealth of information for understanding molecular packing and crystal engineering. Within this vast dataset are numerous pairs of molecules related by a single well-defined structural transformation. In drug discovery, analysis of such pairs is used to understand how structural modifications will affect the properties of a molecule. This type of investigation is not common for crystal structures, but has the potential to provide critical insights into how simple chemical transformations affect the structure and properties of solid forms.

In this presentation, we outline the process of finding over 100 million matched molecular pairs in the CSD. We will then highlight the potential of this dataset to inform on crystal engineering in a variety of ways. One example is to explore how transformations around acyclic single bonds (*e.g.* a terminal methyl group becoming a Cl atom) affect the packing of a molecule. There are over 12,000 such transformations represented in the CSD, which allows us to determine which functional-group changes are more or less likely to disrupt or change the packing of a molecule in the solid state.

**Keywords:** CSD, matched molecular pairs, isostructurality

## MS34-P13 Rational engineering of protein surfaces to improve crystallization while preserving solubility

Shikha Singh<sup>1</sup>

1. Biological Sciences, Columbia University in the city of New York

email: shikhasingh.bhu@gmail.com

Obtaining diffraction quality crystals remains the bottleneck for structure elucidation of most proteins using X-ray crystallography, which is the most precise method for atomic-resolution structure determination. A better understanding of crystallization should therefore help us identify both problematic areas of the process and potential solutions to this critical barrier. The simple observation that some proteins crystallize with minimal effort, while others are entirely resistant to crystallization, suggests that crystallization propensity is an intrinsic property of an individual protein. Based on our previously published work, we hypothesized that the principal determinant of this propensity is the prevalence on the protein surface of low-entropy epitopes with high intermolecular interaction potential. To find such "crystal packing epitopes", we developed a simple topological scheme to identify local sequence motifs that are statistically overrepresented in crystal-packing interfaces in the Protein Data Bank. All residues within a minimum contact distance between chains are identified and then grouped into an ascending hierarchy ranging from the simplest elementary binary interacting epitopes to complete binary interprotein interaction interfaces. For counting and averaging purposes, protein chains are redundancy-downweighted to account for homologous chains forming similar crystals, as evaluated by a dot-product-like Packing Similarity Score. We show that introducing such "overrepresented crystal packing epitopes" into ten crystallization-resistant proteins generally improves their crystallization propensity without reducing their stability or solubility in aqueous salt or polyethylene glycol solutions. In some cases, their solubility is even improved, demonstrating that protein crystallizability and solubility are fundamentally separable properties. The most effective crystal-packing epitopes identified in our studies to date contain high-entropy polar sidechains constrained in low-entropy conformations by local interactions, so the mutations that we have used to improve crystallization generally involve introducing rather than removing high-entropy sidechains from the protein surface. Our results open a new approach to probabilistic engineering of protein surfaces to simultaneously enhance their stability, solubility, and crystallization propensity.

**Keywords:** protein crystallization, protein engineering, x-ray structure determination, crystallization-epitope engineering, data mining



**MS34-P14** 3-pyrroline hydrates: *in situ* crystallization and structural investigations

Patryk Rzepinski<sup>1</sup>, Łukasz Dobrzycki<sup>1</sup>, Michał K. Cyrański<sup>1</sup>,  
Roland Boese<sup>1</sup>

1. Czochralski Laboratory of Advanced Crystal Engineering,  
Faculty of Chemistry, University of Warsaw, Żwirki i Wigury 101,  
02-093 Warsaw, Poland

email: przepinski@chem.uw.edu.pl

3-pyrroline (2,5-dihydropyrrole,  $C_4H_7N$ ) is a cyclic amine, liquid at ambient conditions. Using the *in situ* crystallization technique [1] assisted by IR laser focused radiation we obtained two hydrates of 3-pyrroline (three- and hexahydrate) presented in the figure below. The trihydrate crystallizes in  $P2_1/c$  space group ( $V=690 \text{ \AA}^3$ ) with  $H_2O$  molecules forming layers. The amine molecules are attached to these layers via N...O hydrogen bonds. The hexahydrate belonging to  $P2_1/m$  space group ( $V=538 \text{ \AA}^3$ ) contains 3D network of interacting water molecules. In the structure the amine molecules are incorporated to this network thus the hexahydrate is example of semicathrate [2]. This structure is isostructural with hexahydrate of pyrrolidine [3] - saturated analogue of 3pyrroline. Contrary to the pyrrolidine hexahydrate however, corresponding structure with 3-pyrroline does not undergo order-disorder phase transition. In all presented structures containing 3-pyrroline water molecules are disordered what manifests in alternative positions of hydrogen atoms similarly like in the hexagonal ice  $I_h$  crystal structure.

**Acknowledgements** The work has been supported by the National Science Center grant (NCN 2011/03/B/ST4/02591).

**References**

- [1] Boese, R. (2014). *Z. Kristallogr.*, **229**, 595.
- [2] Fowler, D. L., Loebenstein, W. V., Pall, D. B., Kraus, C. A. (1940). *J. Am. Chem. Soc.*, **62**, 1.
- [3] Dobrzycki, Ł., Taraszevska, P., Boese, R., Cyrański, M. K. (2015). *Crystal Growth & Design*, **15**, 4804.

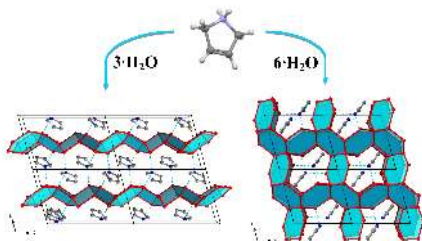


**Figure 1.** Packing diagrams of pyrroline tri- and hexahydrate

**Keywords:** Hydrates, Clathrates, 3-pyrroline, *in situ* crystallization, Crystal Engineering, Single Crystal Diffraction, Raman Spectroscopy

**MS34-P15** Separation of alcohol isomers by Host-Guest Chemistry

Nicole Sykes<sup>1</sup>, Luigi R. Nassimbeni<sup>1</sup>, Hong Su<sup>1</sup>, Susan A.  
Bourne<sup>1</sup>, Edwin Weber<sup>2</sup>

1. University of Cape Town

2. Technische Universität Bergakademie Freiberg

email: nixsykes@gmail.com

Host-Guest chemistry is a useful separation technique when the components of a targeted mixture have similar boiling points, rendering distillation inefficient.

We have chosen pairs of alcohols from a total of 14 isomers of propanol (2 isomers), butanol (4 isomers) and pentanol (8 isomers), which have close normal boiling points. Starting with equimolar mixtures of the selected pairs, we have exposed the guest mixtures to diol host compounds

(3,3'-bis(9-hydroxy-9-fluorenyl)-2,2'-binaphthyl and 9,9'-(Biphenyl-2,2'-diyl)difluorene-9-ol).

The crystal structures of the inclusion compounds with the single alcohol isomer and that of the targeted mixture have been elucidated. The non-bonded interactions in the structures have been analysed with the programme Crystal Explorer and the thermal characteristics of all the crystalline compounds have been measured by thermal gravimetry (TG) and differential scanning calorimetry (DSC).

Selectivity curves and the effect of multiple hosts have been analysed in order to understand the effect of changes to the mother liquors from which the crystals were grown.

The analysis of the percentage of each guest which was entrapped, was obtained from the refined crystal structures and confirmed independently by NMR spectroscopy and gas-liquid chromatography.

**Keywords:** host-guest, isomer, selectivity, inclusion, alcohols

## MS34-P16 Structural chemistry of piperidine hydrates

Paweł Socha<sup>1</sup>, Łukasz Dobrzycki<sup>1</sup>, Michał K. Cyrański<sup>1</sup>, Roland Boese<sup>1</sup>

<sup>1</sup>. Czocharlski Laboratory of Advanced Crystal Engineering, Faculty of Chemistry, University of Warsaw, Żwirki i Wigury 101, 02-093 Warsaw, Poland

email: psocha@chem.uw.edu.pl

The aim of this report was to investigate the possibility of creating hydrates or clathrates for piperidine-water system. Piperidine is a heterocyclic aliphatic amine with six-membered ring. Crystal structure of the amine is known, molecules build columns in crystal lattice [1]. Hydrates were crystallized on the diffractometer, using *in situ* crystallisation technique with IR laser [2]. Five hydrates have been received during the project, consisting of 0.50, 2.00, 8.10, 9.75 and 11.00 water per one amine molecule. Structures of hydrates were determined with single crystal X-ray diffraction. Interestingly, hydrates with high concentration of water were very similar to gas clathrates [3], however there were hydrogen bonds between amine and water in crystal lattice and the water framework including positions of H<sub>2</sub>O molecules was disordered. What is more, piperidine hydrates consisting 9.75 and 11.00 water were isostructural with an analogue structure of *tert*-butylamine hydrates [4, 5]. Packing diagrams of these two structures are presented in the Figure below. Moreover, piperidine hydrate 8.10 were isostructural with *iso*-propylamine hydrate 8.00 [6, 7]. All synthesised crystals were also characterised with Raman spectroscopy and X-ray powder diffraction.

**Acknowledgements** The work has been supported by the National Science Center grant (NCN 2011/03/B/ST4/02591).

### References

- [1] Parkin, A., Oswald, I. D. H., Parsons S. (2004). *Acta Crystallogr. B.*, **60**, 219.
- [2] Boese, R. (2014). *Z. Kristallogr.* **229**, 595.
- [3] Sloan, E. D. "Clathrate Hydrates of Natural Gases", Marcel Dekker, New York, USA, 1990.
- [4] McMullan, R. K., Jeffrey, G. A., Jordan, T. H. (1967). *J. Chem. Phys.*, **47**, 1229; Jeffrey, G. A. (1969). *Acc. Chem. Res.*, **11**, 344.
- [5] Dobrzycki, Ł., Taraszewska, P., Boese, R., Cyrański, M. K., Cirkel, S.A. (2015). *Angewandte Chemie International Edition*, **54**, 10138.
- [6] McMullan, R. K., Jeffrey, G. A., Panke, D. (1970). *J. Chem. Phys.*, **53**, 3568.
- [7] McMullan, R. K., Jordan, T. H., Jeffrey, G. A. (1967) *J. Chem. Phys.*, **47**, 1218.

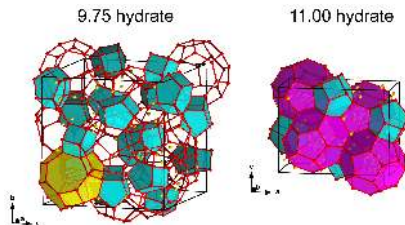


**Figure 1.** Unit cell content of 9.75 and 11.00 hydrates of piperidine. Alternative positions of H<sub>2</sub>O molecules indicating disorder of water framework are presented as yellow spheres.

**Keywords:** Hydrates, Clathrates, Piperidine, *in situ* crystallization, Crystal Engineering, Single Crystal Diffraction, Raman Spectroscopy

## MS34-P17 Selective Encapsulation of Neutral Molecules by *endo*-Functionalized Molecular Tubes

Arto Valkonen<sup>1</sup>, Wei Jiang<sup>2</sup>, Kari Rissanen<sup>1</sup>

1. University of Jyväskylä, Department of Chemistry, P.O. Box 35, FI-40014, Jyväskylä, Finland

2. South University of Science and Technology of China, Department of Chemistry, No. 1088 Xueyuan Blvd, Nanshan District, Shenzhen, 518055, P. R. China

email: arto.m.valkonen@jyu.fi

Biological functions heavily rely on selective recognition of neutral molecules. As in an enzyme binding pocket and a membrane channel, catalysis and transportation are initiated by selective recognition. These natural receptors select guest molecules with complementary size and shape which can fill the cavity appropriately. In the meantime, the converging functional groups in the cavity pose another level of selectivity: the substrate must be electrostatically complementary to the functional groups in the cavity as well. Thus, high binding selectivity and/or affinity to neutral molecules are achieved by combining the cavity and the converging functional groups. For example, *endo*-functionalized receptors reject the guests with appropriate shape but inappropriate electrostatic surface, and show a high binding affinity to the guests with both shape and electrostatic complementarity.[1,2]

The title compounds of this presentation, *endo*-functionalized molecular tubes, have rarely been reported in the literature.[2] Recently, it has been demonstrated that naphthalene and the bisnaphthalene cleft are very good scaffolds for constructing molecular receptors. [3-5] On this basis, we reported molecular tubes with *endo*-functionalized urea and thiourea groups and carefully studied their molecular recognition behaviour to neutral molecules.[2,6] In this presentation our continued efforts to encapsulate neutral guests inside these *endo*-functionalized molecular tubes and the obtained crystallographic results are demonstrated.

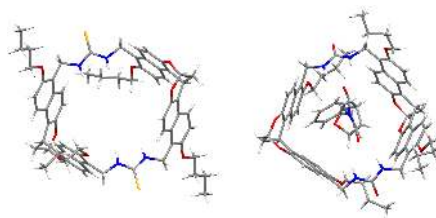


**Figure 1.** A structure of *endo*-functionalized thiourea derivative (left) and urea derivative with neutral guest molecule inside (right).

**Keywords:** Molecular tubes, neutral guest molecules, *endo*-functionalization

[1] S. Mecozzi, J. Rebek, Jr., *Chem. Eur. J.*, 1998, **4**, 1016–1022.

[2] G. Huang, A. Valkonen, K. Rissanen, W. Jiang, *Chem. Commun.*, in press. DOI: 10.1039/C6CC00349D.

[3] Z. He, G. Ye, W. Jiang, *Chem. Eur. J.*, 2015, **21**, 3005–3012.

[4] Z. He, X. Yang, W. Jiang, *Org. Lett.*, 2015, **17**, 3880–3883.

[5] F. Jia, Z. He, L.-P. Yang, Z.-S. Pan, M. Yi, R.-W. Jiang, W. Jiang, *Chem. Sci.*, 2015, **6**, 6731–6738.

[6] G. Huang, Z. He, C.-X. Cai, F. Pan, D. Yang, K. Rissanen, W. Jiang, *Chem. Commun.*, 2015, **51**, 15490–15493.

## MS34-P18 Coordination Frameworks of Tetrakis[*meso*-(3,5-biscarboxyphenyl)]-Metalloporphyrin with Polynuclear Metallic Nodes

Israel Goldberg<sup>1</sup>, Bharat Kumar Tripuramallu<sup>1</sup>

1. School of Chemistry, Tel Aviv University

email: goldberg@post.tau.ac.il

Metal organic frameworks deserve increasing attention as an emerging class of porous functional materials in recent years. The most successful design strategy for constructing these crystalline frameworks is to take advantage of the versatile geometry of organic building units (linkers) and metal centers (uni- and multinuclear connecting nodes), which greatly influence the resulting architectures of the formed framework. Tetrapyrrole macrocycles or porphyrin building blocks are quintessential for forming quadrangular open frameworks, owing to their bulkiness and D<sub>4h</sub> symmetry. Multiple functionality of the organic linkers is important for promoting expansion of the formed framework in three dimensions.

Prior to this study formulation and characterization of octacarboxy porphyrin-based metal organic frameworks have enjoyed a rather slow progress in view of the synthetic difficulty in obtaining sizeable crystalline samples, as polycrystalline or amorphous solids are most frequently the outcome of common preparative procedures. On rare occasions, when small crystallites became available, their structural characterizations by X-ray diffraction technique required access to synchrotron radiation sources due to the weak diffraction power of such crystals and high content of the disordered solvent trapped in the channel-perforated lattice.

This work provides an insight into an improved synthetic methodology of crystalline framework solids with the fast-reacting octa-topic tetrakis(3,5-dicarboxyphenyl) metalloporphyrin linker and a variety of metallic nodes, using NaOH as a modulator to enhance crystal growth. During the supramolecular reaction the hydroxyl ions supplied by the NaOH compete with the carboxylate anions for coordinating to the metal (or metal cluster), slowing the reaction rate between the metal ions and the porphyrin, and thus enhancing crystal growth of the solid polymeric product. Here we describe crystalline framework materials of the octa-carboxy porphyrin ligand obtained with a series of metal centers, including lanthanoid and transition metal ions, as Pr, Eu, Gd, Tb, Mn, Fe, In and Ga, as well as Na centers. The structural diversity of the framework architectures and of the interaction synthons will be discussed.

B. K. Tripuramallu and I. Goldberg, *Cryst. Growth Des.* **2016**, *16*, 1751-1764.

B. K. Tripuramallu, H. M. Titi, S. Roy, R. Verma and I. Goldberg, *CrystEngComm* **2016**, *18*, 515-520.

**Keywords:** metal-organic-frameworks

## MS35 Simulation of dynamics in molecular compounds

Chairs: Anders Østergaard Madsen, Markus Meuwly

### MS35-P1 Martensitic solid-to-solid transitions in amino acid crystals: what insight can simulations bring to the table?

Herman M. Cuppen<sup>1</sup>

1. Institute for Molecules and Materials, Radboud University

email: h.cuppen@science.ru.nl

Many molecular compounds exhibit polymorphism: the ability to crystallize in different crystal structures. The polymorphic forms determine crystal properties such as the solubility rate, which is key in dose determination in a pharmaceutical context. Understanding of solid-to-solid transitions between different polymorphic forms is the first step in controlling the polymorphic stability of a compound.

Polymorphic transitions are driven by a free energy difference. If the relative stability of different polymorphic forms changes reversibly as a function of temperature, one speaks of enantiotropically related polymorphic forms. In the case of transformations in which the parent and daughter phase have similar structures, there is an ongoing debate whether the transformation mechanism is martensitic or occurs through nucleation and growth. I will present advanced Molecular Dynamics (MD) simulations of two enantiotropically related polymorphic forms of DL-norleucine:  $\alpha$  (room temperature) and  $\beta$  (low temperature), which are thought to transform through a martensitic mechanism by sliding along two cell axes. I will show that the mechanism of the transition occurs through a cooperative movement of bilayers via an intermediate state [1,2]. Although the layers move in a concerted fashion, the results further indicate that local fluctuations in the conformations of the aliphatic chains play a crucial role in keeping the cooperative mechanism sustainable at large length scales (see figure). The results suggest a mechanism where formation of a nucleus of the new phase occurs through cooperative motion, which then grows through propagation in a wave-like manner through the crystal [3]. At the length scale of the initial size of the cluster, classical nucleation theory and the cooperative mechanism could naturally come together.

References:

[1] J.A. van den Ende and H.M. Cuppen *Cryst. Growth Des.*, 2014, *14*, 3343

[2] J. A. van den Ende, M.M.H. Smets, D.T. de Jong, S.J.T. Brugman, B. Ensing, P.T. Tinnemans, H. Meekes, and H. M. Cuppen *Faraday Disc.*, 2015, *179*, 421

[3] J. A. van den Ende, B. Ensing, and H. M. Cuppen *CrystEngComm*, accepted

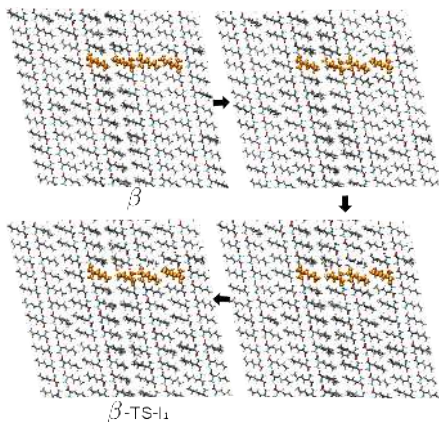


**Figure 1.** The initial stages of the  $\beta$  to  $\alpha$  transition through intermediate state II towards the first transition state as obtained by Nudged Elastic Band calculations. A large simulations cell is used to assess the deviations from perfect cooperative motion.

**Keywords:** phase transitions, molecular dynamics simulations, DL-norleucine, martensitic

## MS35-P2 Single Crystal Structures and Spectroscopic Analysis in Metal Complex Dynamics

Andreas Roodt<sup>1</sup>, Hendrik G. Visser<sup>1</sup>, Alice Brink<sup>1</sup>, Marietjie Schutte-Smith<sup>1</sup>, Pennie Mokokolo<sup>1</sup>, Dumisani V. Kama<sup>1</sup>, Angelo Frei<sup>2</sup>, Roger A. Alberto<sup>2</sup>

1. University of the Free State, Bloemfontein, SOUTH AFRICA

2. University of Zurich, Zurich, SWITZERLAND

email: RoodtA@ufs.ac.za

Since many dynamic processes (still) occur at the molecular level and at metal cores, fundamental understanding of structural behavior, and the associated influence on (kinetic) properties are of continued and prime importance. In this presentation we emphasize this in conjunction with an *integrated mechanistic approach* to evaluate bonding and reactivity, utilizing small molecule crystal structure data, spectroscopic techniques and reaction kinetics, to counteract trivialized conclusions often based on thermodynamic observations alone [1].

As example, we focus on dynamics in small coordination compounds utilised as model radiopharmaceuticals, in particular incorporating the  $^{99m}\text{Tc}$ ,  $^{188}\text{Re}$ ,  $^{186}\text{Re}$  isotopes [2,3]. We discuss some basic characteristics, and the dynamics of the versatile synthon *fac*- $[\text{M}(\text{CO})_3]^+$  and complexes thereof, which include its low-valent, low-spin, kinetically 'inert' organometallic core and the high potential for *in vivo* stability. This starting material and its characteristics must be well understood both in terms of structure and the dynamics therein, before utilization is possible. It coordinates many types of ligands and allows bifunctional chelator ligand design which determines different properties and significantly influences the reactivity in these organometallic molecular materials [1, 3-4].

The above arguments also hold for the dynamics in other processes, in particular homogeneous catalysis [4].

This presentation will underline some of these aspects of small coordination compounds, and illustrate the importance of structure and kinetics and concurrent different processes/ factors which may significantly influence the course of the reaction and the dynamics therein [1, 3-4].

[1] Roodt, A., Visser, H.G. & Brink, A. *Crystallogr. Rev.* **2011**, 17, 241-280.

[2] Alberto, R., Schibli, R., Waibel, R., Abram, U. & Schubiger, A.P. *Coord. Chem. Rev.* **1999**, 901-919.

[3] Examples: Brink, A., Visser, H.G. & Roodt, A. *Inorg. Chem.* **2014**, 53, 12480-88; Twala, T.N., Schutte-Smith, M., Roodt, A. & Visser, H. G. *Dalton Trans.* **2015**, 44, 3278-88; Schutte, M., Kemp, G., Visser, H.G. & A. Roodt. *Inorg. Chem.* **2011**, 50, 12486-98.

[4] Example: Warsink, S., Venter, J.A. & Roodt, A. *J. Organomet. Chem.* **2015**, 775, 195-201.

**Keywords:** Small Molecules, Reaction Mechanism, Kinetics, Dynamics, Spectroscopy

# MS35-P3 What happens when thermal motion is frozen? A case study of polymorph stabilities for Gallic Acid Monohydrate

Ioana Sovago<sup>1</sup>, Anna Hoser<sup>1</sup>, Arianna Lanza<sup>2</sup>, Anders Madsen<sup>1</sup>

1. University of Copenhagen, Chemistry Department

2. University of Bern, Department of Chemistry and Biochemistry

email: ioana.sovago@chem.ku.dk

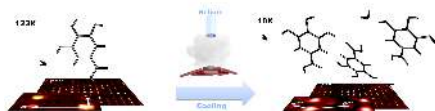
There is a paramount effort from both theoretical and experimental sides in establishing the structures and properties of all the polymorphs that a system can adopt. However, many theoretical studies, including crystal structure prediction (CSP) methods are typically performed at 0 K and effects of thermal motion are neglected. Because vibrational effects play an important role in assessing the stability of structure, the theoretically predicted structures are often not observed experimentally. A polymorph of gallic acid monohydrate (GAM) was a target of the fifth crystal structure prediction blind test.<sup>1</sup> Of the six targeted systems, GAM was the only one which could not be predicted in the lowest-energy range by any of the 14 contributing groups. Here we show that GAM is a very complex system, and the lack of predictability is due to the neglect of vibrational estimates, combined with the comparison with room-temperature structures. We demonstrate that target polymorph IV is commensurately modulated at 10 K and disordered at higher temperatures. The GAM system is enantiotropic, leading to changes in stability as a function of temperature. Single crystal high resolution X-ray data were collected at four different temperatures (10K, 95K, 123K and 175K). Accurate atomic and anisotropic displacement parameters were derived from aspherical atom refinement. The experimental data were further analysed by refinement of a lattice-dynamical model derived from periodic DFT/B3LYP calculations.<sup>2</sup> This combination of theoretical modelling and experimental data allows us to derive vibrational entropies, and to assess the free energies as a function of temperature. Furthermore, some of the H atoms were disordered, which explains why the predicted hydrogen-bond network was ambiguous. This disorder further helps stabilizing the structure by enhancing the entropy of the system. Therefore, comparing CSP determined at 0K with experimentally structures based on room temperature measurement can often be misleading and structures determined at lowest available temperature is vital for such studies.

## References:

1. D. A. Bardwell, C. S. Adjiman, Y. A. Arnaudova, E. Bartashevich, S. X. M. Boerrigter, D. E. Braun, A. J. Cruz-Cabeza, G. M. Day, R. G. Della Valle, G. R. Desiraju, et al., *Acta Cryst. B* **2011**, 67, 535–551.
2. A. A. Hoser, A. Ø. Madsen, *Acta Cryst A*, **2016**, A72, 206–214

**Figure 1.** Gallic acid monohydrate form IV transformation under cooling. Three molecules are present in the asymmetric unit at 10 K

**Keywords:** lattice-dynamic, vibrational entropy



## MS36 Crystallography in solid state reactions and catalysis

Chairs: Fernando Lahoz, Krešo Bučar

### MS36-P1 Solvent-free solid-state synthesis of lanthanide complexes monitored by in-situ XRPD

Laure Guenee<sup>1</sup>, Bahman Golesorkhi<sup>2</sup>, Claude Piguet<sup>2</sup>

1. Laboratory of crystallography, DQMP, University of Geneva, Switzerland

2. Department of Inorganic Chemistry, University of Geneva, Switzerland

email: laure.guenee@unige.ch

Lanthanide complexes with organic ligands are good candidates for applications in different technologies, especially for their tunable luminescence properties. However, the presence of solvent (water) molecules in the coordination sphere of the metal may dramatically affect the photophysical properties (luminescence) of the target complex. Moreover, the presence of solvate molecules may change the crystal packing and the crystal structure of the solid, which can in turn modify the physical properties in the solid state. In this context, the usual synthetic reaction performed in solution may found some limitations such as low stability constant, competition with solvent molecules depending of the chemical affinity (especially when water is present), and solubility problems. Solvent-free solid state synthesis can be a welcome alternative to overcome these limitations. Well-known in solid state chemistry for the preparation of inorganic materials, this procedure recently received a renewal of interest for the synthesis of polymeric metal organic frameworks, and for the complexation of lanthanide salts with N heterocycles amines [1]. We present here some solvent-free solid state syntheses (using grinding and thermal treatment) of non-polymeric lanthanide complexes with tridentate terpyridine or bis-benzimidazole-pyridine based ligands. In-situ XRPD experiment is exploited to follow the reaction and to monitor the formation of the resulting complex (figure 1). Comparison with analogous compounds combined with crystal structures solved ab-initio using the Fox program [2] are applied for extracting the pertinent molecular structures. Our ultimate goal is the synthesis of new solvent free complexes, which are not yet accessible in solution.

[1] Müller-Buschbaum K. *Z. Anorg. Allg. Chem.* 2005, 361, 811-828.

[2] Favre-Nicolin V., R. Cerny *J. Appl. Cryst.*, 2002, 35, 734-743.

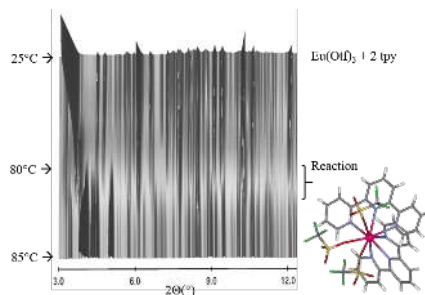


**Figure 1.** In-situ XRPD pattern (heating) and crystal structure of the complex  $[\text{Eu}(\text{Tpy})_2(\text{OTf})_3]$  formed.

**Keywords:** lanthanide complexes, in-situ XRPD, solid state synthesis



# MS36-P2 Dynamic temperature-rate dependent in-situ dehydration of cavansite $(\text{Ca}(\text{VO})(\text{Si}_4\text{O}_{10}) \cdot 4\text{H}_2\text{O})$

Martin Fisch<sup>1</sup>, Georgia Cametti<sup>1</sup>, Thomas Armbruster<sup>1</sup>, Nicola Casati<sup>2</sup>

1. Institute of Geological Sciences, University of Bern, 3012 Bern, Switzerland

2. Swiss Light Source, Paul Scherrer Institute, 5232 Villigen, Switzerland

email: martin.fisch@geo.unibe.ch

We have investigated non-equilibrium dehydration dynamics of cavansite  $(\text{Ca}(\text{VO})(\text{Si}_4\text{O}_{10}) \cdot 4\text{H}_2\text{O})$  with extremely fast time-resolved high-temperature (HT) synchrotron powder X-ray diffraction (XRD). For the first time, an in-situ dehydration experiment of a zeolite-like material was carried out with both distinct heating rates (3K/min and 10K/min) and particle sizes (crystals < 25 µm, and between 25 and 50 µm) in open 0.3 mm capillaries.

Cavansite consists of sheets of  $\text{SiO}_4$  tetrahedra, linked by intercalated vanadyl-units, with Ca and 4  $\text{H}_2\text{O}$  molecules as extra-framework occupants. Previous in-situ HT single-crystal XRD experiments [1], from which the structures of static intermediate phases were obtained, indicate three dehydration steps at 348, 448 and 623 K, each associated with release of 1  $\text{H}_2\text{O}$ .

Our preliminary results (Fig. 1) indicate that the non-equilibrium dynamic dehydration behavior is mainly influenced by the heating rate. At steps 1 and 2, the different grain sizes behave similarly whereas different heating rates yield distinct results. The volume discrepancy with respect to quasi-equilibrated single-crystal data [1] can be explained by the fact that intermediate equilibria are not reached [2]. At step 3, dV/dT of the fine particles is steeper than of the coarse ones, which is likely due to shorter  $\text{H}_2\text{O}$  diffusion paths within the small crystals, becoming increasingly important at higher temperature. This assumption is also valid within the two 10K/min runs, in which small particles react slightly faster. The opposite behavior within the 3K/min rates seems striking. However, it is known that increasing  $\text{pH}_2\text{O}$  retards dehydration of zeolite-like materials [3,4]. Here,  $\text{pH}_2\text{O}$  is mainly controlled by the denser packing of the smaller crystals. The coarse-grained sample reacts faster because of lower  $\text{pH}_2\text{O}$ . At lower temperature (3K/min rate), the influence of  $\text{pH}_2\text{O}$  is governing the dehydration, whereas it is governed by diffusion path lengths at higher temperature (10K/min).

Temperature is a thermodynamic variable often used to change and probe materials. Our data show that not only different heating rates but also particle size, packing density and atmosphere should be considered in this type of experiments.

[1] Danisi R.M. et al., Am. Mineral. 87 (2012) 1874–1880; [2] Martucci A. et al., Eur. J. Mineral. 28(1) (2016) 5–13; [3] Bish D.L. & Wang H.W., Phil. Mag. 90(17) (2010) 2425–2441; [4] Wang H.W. & Bish D.L., Phys. Chem. Minerals 39 (2012) 277–293

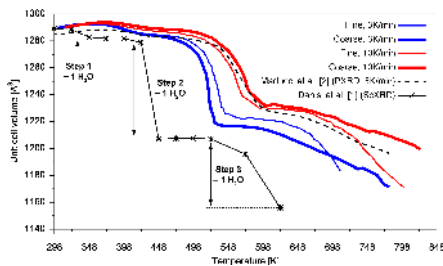


**Figure 1.** Unit cell volumes vs. temperature: 3K/min runs are shown in blue, 10K/min in red. Thin lines correspond to the < 25 µm, thick ones to the 25 < x < 50 µm sample. PXRD data at 5K/min [2] with unspecified crystal size are indicated by the dashed line, single-crystal XRD data of [1] with stars.

**Keywords:** PXRD, zeolite-like material, in-situ high-temperature, non-equilibrium, dehydration dynamics

# MS36-P3 Red-light activated photoCORMs of Mn(I) species bearing symmetric substituted 2,2'-azopyridines.

Emmanuel Kottelat<sup>1</sup>, Albert Ruggi<sup>1</sup>, Fabio Zobi<sup>1</sup>

1. University of Fribourg, Chemistry Department

email: emmanuel.kottelat@unifr.ch

Carbon monoxide (CO) has been acknowledged as a fundamental neurotransmitter in humans and there is a growing interest in its pharmacological or medical applications. As nitric oxide and hydrogen sulfide, CO is endogenously produced in animals. These neurotransmitters are involved in several cellular, physiological and pathological pathways, such as vasodilatation, endothelial injuries, inflammation. Organometallic carbonyl complexes are best suited to play the role of CO carriers. Targeting of the molecules to local injuries can thus be achieved by modifying the coordination sphere of the metal ion via a proper selection of ligands or by appending CO releasing molecules (CORMs) to biomolecules. Manganese-based CORMs, for example, are activated by exposure to UV-light and are known as photoCORMs<sup>[1]</sup>. One of the great challenges in the design of photoCORMs lies in their sensitivity to visible light. Most of known photoCORMs have suffered from this fundamental drawback with few exceptions. In particular the group of Mascharak<sup>[2]</sup> has endeavored to develop rational strategies to visible light-activated CORMs and has introduced a series of carbonyl Mn(I) complexes with conjugated ligands of the 2-pyridyl-N-(2-methylthiophenyl) methylenimine and 2-phenylazopyridine type which show MLCT bands with maxima at ca. 585 nm. These molecules represent probably the most significant improvement the field has seen in the recent years. In this work, we report the synthesis, characterization and photochemical behaviour of the above mentioned complexes. The systematic substitution of the 2,2'-azopyridine with weak donating to strong deactivating substituents (EWG) lead to the progressive bathochromic shift of the MLCT absorption band maximum from 625 nm to 693 nm (Fig. 1). Exposure of solutions of complexes 1-5 to low-power visible light ( $\geq 625$  nm, red light) resulted in CO photorelease as evidenced by the myoglobin assay. Furthermore, the MLCT band of complexes with strong EWG tails beyond the visible region of the spectrum in the near infrared and in one case photodecomposition could also be promoted at 810 nm. References: [1] Kottelat, E.; Chabert, V.; Crochet, A.; Fromm, K. M.; Zobi, F., *Eur. J. Inorg. Chem.*, **2015**, 34, 5628-5638 [2] Chakraborty, I.; Carrington, S. J.; Mascharak, P., *Acc. Chem. Res.* **2014**, 47, 2603-2611

**Keywords:** CO Releasing Molecules, Manganese, azopyridine

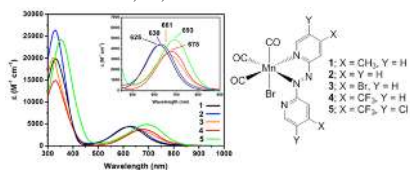


**Figure 1.** Electronic absorption spectra (left) and the molecular structure of  $[\text{MnBr}(\text{azpy})(\text{CO})_3]$  species presented in this work (right).

**MS36-P4** Focusing-optics laser assembly for modern photocrystallography: technical design and performanceRadosław Kamiński<sup>1</sup>, Sylwia E. Kutyla<sup>1</sup>, Katarzyna N. Jarzemska<sup>1</sup><sup>1</sup>. Biological and Chemical Research Centre, Department of Chemistry, University of Warsaw, Żwirki i Wigury 101, 02-089 Warsaw, Poland

email: rkaminski@chem.uw.edu.pl

Photocrystallography is defined as a set of crystallographic techniques applied to study light-induced dynamic processes occurring in crystals. Over the last several years there is a rapid growth in this field, including studies on chemical reactions,<sup>1</sup> low-temperature metastable states,<sup>2</sup> and even on electronic excited states.<sup>3</sup> Many of these investigations are performed employing synchrotron sources where it is easier to install light delivery devices when compared to home diffractometers, for which a limited set of solutions currently exists.<sup>4,5</sup>

Consequently, here we describe our own setup for the purpose of conducting photocrystallographic experiments using home diffractometers. The whole system consists of adjustable laser-focusing optics and a holder, which can be conveniently mounted as additional sample conditioning device (Figure 1). Current setup is designed to work best with Bruker-type diffractometers, yet can easily be extended for other types of commercially available SXD machines. The holder allows for implementation of various optics (with different focusing lengths), but more importantly, for reducing the goniometer-collision areas to absolute minimum (the assembly does not obstruct fixed-chi goniometer). The laser light is delivered through the fibre optics, which assures full flexibility in choosing the light source. Thus, one can equally well attach large-box high-power lasers and simple LEDs (which can be controlled by our home-made electronics). In our opinion, the designed laser assembly has certain advantages over other solutions tested previously, especially in terms of X-ray safety (the light source can be stored outside the radiation-safety enclosure), and available flexibility in selecting the laser wavelength.

The laser assembly has been tested by performing various solid-state transformations. These included either well-known [2+2] photo-dimerization reactions of cinnamic acid derivatives,<sup>1</sup> or metastable linkage isomers in nickel(II) complexes.<sup>6</sup> The experimental results shall be presented here in details, together with the technical aspects of the laser assembly.

(1) Benedict, J. B.; Coppens, P. J. Phys. Chem. A 2009, 113, 3116. (2) Hatcher, L. E.; Raithby, P. R. Acta Cryst. 2013, C69, 1448. (3) Jarzemska, K. N.; Kamiński, R. et al. Inorg. Chem. 2014, 53, 10594. (4) Brayshaw, S. K. et al. J. Appl. Cryst. 2010, 43, 337. (5) Cox, J. M. et al. J. Phys. Chem. A 2015, 119, 884. (6) Warren, M. R. et al. Chem. Eur. J. 2014, 20, 5468.

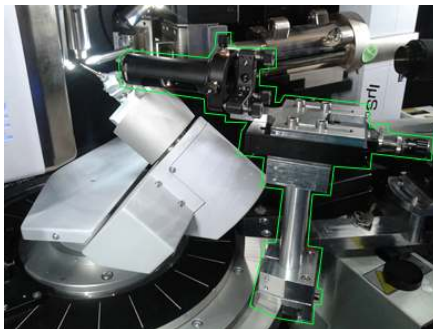


**Figure 1.** New versatile laser-focusing assembly (outlined in green) as mounted on the single-crystal diffractometer.

**Keywords:** photocrystallography, laser assembly, photo-induced transformations

**MS36-P5** Revisiting the structure and synthesis of technetium heptoxide

Daniel Mast<sup>1</sup>, Bradley C. Childs<sup>1</sup>, Keith Lawler<sup>1</sup>, Henrik Braband<sup>2</sup>, Frederic Poineau<sup>1</sup>, Kenneth R. Czerwinski<sup>1</sup>, Alfred P. Sattelberger<sup>3</sup>

1. Department of Chemistry, University of Nevada, Las Vegas, Las Vegas NV 89154, USA
2. Department of Chemistry, University of Zurich, Zurich, Switzerland
3. Energy Engineering and Systems Analysis Directorate, Argonne National Laboratory, Lemont, IL 60439, USA

email: mastd1@unlv.nevada.edu

There are two binary oxides of technetium which have been characterized in the solid state. Technetium dioxide,  $\text{TcO}_2$ , crystallizes in a distorted rutile structure and is the starting point for many synthesis routes. Technetium heptoxides,  $\text{Tc}_2\text{O}_7$ , forms one of the few molecular binary metal oxides, the others including:  $\text{RuO}_4$ ,  $\text{OsO}_4$  and  $\text{Mn}_2\text{O}_7$ . In water,  $\text{Tc}_2\text{O}_7$  forms the common pertechnetate anion but in air the volatile solid decomposes to produce the red compound(s). It has been suggested that the red compound could be  $\text{HTcO}_4$  or  $\text{Tc}_2\text{O}_5$ .

In the context of the ongoing investigation into the nature of the red compound the structure and synthesis of  $\text{Tc}_2\text{O}_7$  were revisited.  $\text{Tc}_2\text{O}_7$  was synthesized by a sealed tube reaction of  $\text{TcO}_2$  in a dry oxygen environment. Single crystal X-ray diffraction results confirmed the originally proposed structure of the molecular solid with smaller lattice parameters than originally determined. With new lattice parameters, the work of Fang et al. [CrystEngComm, 2016, 18, 328-33] was revisited and effects of modeling the Pulay stress using an equation of state fit for flexible materials such as molecular solids is demonstrated. The structural stability, electronic structure and bond characteristics of  $\text{Tc}_2\text{O}_7$  were investigated by DFT analysis. In addition, gas chromatography-mass spectrometry of  $\text{Tc}_2\text{O}_7$  was performed to narrow the field of potential candidates for the red compound.

**Keywords:** Technetium oxide, molecular solid, crystallography

**MS36-P6** Mechanisms of mechanochemical salt formation by *in situ* real time X-ray powder diffraction.

Adam A.L. Michalchuk<sup>1,2,3</sup>, Ivan A. Tumanov<sup>3,4</sup>, Simon A.J. Kimber<sup>5</sup>, Elena V. Boldyreva<sup>3,4</sup>, Colin R. Pulham<sup>1,2</sup>

1. EPSRC Centre for Continuous Manufacturing and Crystallisation
2. EaStChem School of Chemistry, University of Edinburgh, UK
3. Novosibirsk State University, Novosibirsk, Russia
4. Institute of Solid State Chemistry and Mechanochemistry SB RAS, Novosibirsk, Russia
5. European Synchrotron Radiation Facility (ESRF), Grenoble 38000, France

email: adam.michalchuk@ed.ac.uk

Mechanochemistry is becoming increasingly popular as a tool for multi-component crystallisation and solid-state chemistry. This increase in popularity has largely been due to the increased efficiency, yields and environmentally benign nature of these processes as compared to solution-based equivalents. While mechanochemistry does offer considerable benefits, it can also induce structural or chemical transformations that may be undesired and unexpected. Such transformations can cause serious issue for industrial and academic applications. In order to prevent unwanted transformations (and similarly, promote desired ones), a better understanding of the mechanisms that underpin mechanochemistry must be understood.

In the present work the ball milling of glycine + oxalic acid dihydrate was followed by *in situ*, real-time X-ray powder diffraction (XRPD). The present work suggests that both salt products – glycinium semi-oxalate and bis(glycinium) oxalate – form concomitantly. A comparison of the dynamics of this process to previous *ex situ* work[1] highlights mechanistic discrepancies between *in situ* and *ex situ* mechanochemical investigations. Interestingly, the quantities of the final crystallisation product could be fine-tuned by controlling particle size. This suggests that, in contrast to solution based methods, a mechanochemical reaction is driven by local reactant “concentrations” as opposed to their global “concentrations”. This, in combination with the XRPD-derived dynamic curves, is used to provide a working model for mechanochemical multi-component crystallisation. Such work is crucial for the further development of mechanochemical technologies in academic and industrial application. It is only through obtaining a better understanding of these processes that they can ultimately be controlled.

This work was supported by Edinburgh University Global Research Scholarship, EPSRC CMAC, grant 1828 from the Russian Ministry of Science and Education and ESRF CH-4313.

[1] I Tumanov, A Achkasov, E Boldyreva, and V Boldyrev (2011) *CrystEndComm*, 2213

**Keywords:** Mechanochemistry, Multi-component crystals, mechanisms

## MS36-P7 Spontaneity of heterogeneous (solid/gas) chemical reactions: Theoretical study of dimensionality changes induced by ammonia in zinc phosphates

Francisco J. Rey-García<sup>1</sup>, Santiago García-Granda<sup>1</sup>

<sup>1</sup>. Department of Physical and Analytical Chemistry, University of Oviedo - CINN, 33006 Oviedo, Spain.

email: franrey.asturies@gmail.com

Previous researches in our group [1] shown that two-dimensional zinc phosphate  $\text{NH}_4\text{Zn}_2(\text{PO}_4)(\text{HPO}_4)$  (**1**), via ammonia vapor interaction at room temperature, transforms to a one dimensional novel compound  $\text{NH}_4\text{Zn}(\text{NH}_3)\text{PO}_4$  (**2**). By ammonia desorption (in air at room temperature) **2** transforms to  $\text{NH}_4\text{ZnPO}_4$  (**3**). The structures of three compounds include extra-framework ammonium cations to the 4-fold coordinated zinc ( $\text{ZnO}_4$  tetrahedra for **1** and **3**, and  $\text{ZnO}_3\text{N}$  tetrahedra for **2** and phosphorus ( $\text{PO}_4$  tetrahedra) with bi-, mono- or three-dimensional linkages, respectively for **1**, **2** or **3**. To our knowledge, the process described here constitutes the first example of dimensionality change in the solid phase promoted by a solid-gas interaction at room temperature in metal phosphates. The thermodynamics of the transformation between these three compounds can shown why this reactions have been played. In order to obtain the theoretical values of  $\Delta G^0$ , the corresponding values of  $\Delta H^0$  and  $\Delta S^0$  have been calculated. For the enthalpy calculation, the suite *Quantum Espresso* [2] was used, applying DFT methodology with plane waves and pseudopotentials. For the entropy, only the gas contribution was calculated (ideal crystal approximation), and the software *Gaussian 03* [3] was used for this computation, applying also DFT methodology, but, in this case, with the hybrid functional B3LYP and the 6,31-G(d,p) basis. The theoretical methodology was tested by studying the formation of the crystalline chlorides of the two first groups of periodic table, and some transition metals. The test results are in agreement with the experimental data available for  $\Delta G^0$ , and allow us to validate the method.

**Agreements:** I wish to thank to Economy and Competitive Minister of Spain Government for the financial support of this work (MAT2013-40950-R) and my grant (BES-2014-068080).

### REFERENCES

- [1] Zakariae Amghouz, Beatriz Ramajo, Sergei A. Khainakov, Iván da Silva, Germán R. Castro, Jose R. García and Santiago García-Granda. *Chem. Commun.*, 2014, 50, 6729
- [2] P. Giannozzi, *et. al.*, *J.Phys.:Condens.Matter*, 21, 395502 (2009).
- [3] *Gaussian 03*, Revision C.02, M. J. Frisch *et. al.*, *Gaussian, Inc.*, Wallingford CT, 2004.

**Keywords:** DFT, Theoretical calculations, zinc phosphates, dimensionality changes, thermodynamics, heterogeneous reactions

# MS36-P8 Synthesis of New Functional, Catalytic Materials by Thermal Decomposition of Ag(I)/Yb(III) Bimetallic From Magnesium Precursor to Mesoporous Material Coordination Networks

Khai-Nghi Truong<sup>1</sup>, Ulli Englert<sup>1</sup>

1. Institute of Inorganic Chemistry, Working group for Crystallography and Structural Chemistry, RWTH Aachen University, Aachen, Germany

email: khai.truong@ac.rwth-aachen.de

Bimetallic coordination networks facilitate the preorganization of the two cations in three-dimensional space. The nanoscale, predefined distribution of the different metal cations is used to design new catalytic materials. Thermal decomposition of those bimetallic networks, *e.g.* removal of the organic linker, results in a bimetallic metal/metal oxide compound. Those decomposition compounds have been analysed by X-ray powder diffraction, SEM-SEI, SEM-BSE, EDX and XRF.

In previous works, a non-commercial acetylacetone derivative has been used successfully as an organic linker [*Dalton Trans.* **2012**, 41, 4664–4673]. The decomposition compound containing silver and ytterbium oxide exhibited catalytic activity towards the decomposition reaction of nitrous oxide, N<sub>2</sub>O, at 500 °C (commercially-available catalyst: 600 °C). The aims of the new project were to optimize the catalyst system by using cheaper, commercially-available ligands, such as EDTA (see scheme), and try to decrease the reaction temperature.

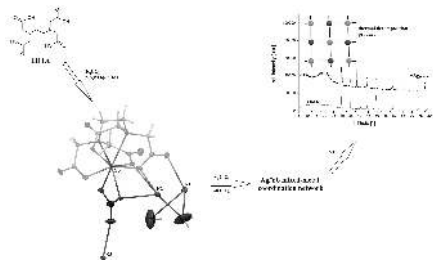


**Figure 1.** Schematic illustration of the synthesis path starting from ethylenediaminetetraacetic acid going to Ag nanoparticles and Yb<sub>2</sub>O<sub>3</sub>.

**Keywords:** Mixed-metal polymers, MOF, Catalysis, N<sub>2</sub>O decomposition, Ag nanoparticles, X-ray powder diffraction, Single-Crystal XRD, Rare-earth metal

# MS36-P9

## Controlled Stepwise Synthesis of a Cu MOF: Decomposition of Ag(I)/Yb(III) Bimetallic From Magnesium Precursor to Mesoporous Material

Qianqian Guo<sup>1</sup>, Ulli Englert<sup>1</sup>

1. Institute of Inorganic Chemistry, RWTH Aachen University, Aachen, Germany

email: qianqian.guo@ac.rwth-aachen.de

A three-dimensional copper metal-organic framework (MOF) has been synthesized from a magnesium precursor and copper sulfate crystallized in space group *F*<sub>2</sub>3. The effective free volume calculated by PLATON analysis after removing the entire guest molecules amount approximately 54.8 percent of the crystal volume (8773 Å<sup>3</sup> of 16007 Å<sup>3</sup> unit cell volume). Topological analysis was carried out by *GTECS3D* to obtain an insight in to the structure [*Z. Kristallogr. Suppl.*, **2012**, 32, 117.]. The structure can be viewed as a 4-connected topology with a Vertex symbol 3.3.10<sub>2</sub>.10<sub>2</sub>.10<sub>2</sub>, which corresponds to a *lcu* net. The 3D intersecting channel system has a cross section of approximately 9 Å. In addition, the oxygen atoms of sulfate ions and methyl groups from the ligand are exposed toward the channel, which facilitate the trapping of polar guests.

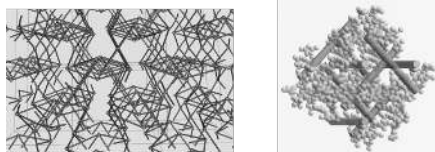


**Figure 1.** lcu network structure of the Cu MOF (left); 3D channel net running along the *a*, *b* and *c* axes (right).

**Keywords:** Metal Organic Framework, Copper, Mesoporous Material, Polar Guests

## MS37 Molecular compounds and MOFs at ambient conditions and under high pressure

Chairs: Francesca Fabbiani, Wendy Queen

### MS37-P1 Metal-Hydride Organic Frameworks (HOF)-new solids for gas adsorption and separation

Sanja Burazer<sup>1</sup>, Jasminka Popović<sup>1</sup>, Anton Meden<sup>2</sup>, Andreas Gierlinger<sup>2</sup>, Yaroslav Filinchuk<sup>3</sup>, Radovan Cerný<sup>4</sup>

1. Division for Materials Physics, Ruder Bošković Institute, Bijenička c. 54, 10000 Zagreb, Croatia
2. Faculty of Chemistry and Chemical Technology, University of Ljubljana, Vecna pot 113, 1000 Ljubljana, Slovenia
3. Institute of Condensed Matter and Nanosciences, Université catholique de Louvain, Place L. Pasteur 1, 1348 Louvain-la-Neuve, Belgium
4. Laboratory of Crystallography, DQMP, University of Geneva, 24 Quai Ernest-Ansermet, CH-1211, Geneva, Switzerland

email: Sanja.Burazer@irb.hr

Due to daily increase in energy demand it is a great task to explore and use a sustainable and carbon-free energy systems. Hydrogen, as clean and easily productive (from water and renewable energy) is possible future energy carrier. Problem of its safe and efficient storage can be solved by solid state storage-through chemical bonding in crystalline compounds or by physical adsorption in porous materials[1].

Metal-hydride organic frameworks (HOF) are a novel hybrid materials designed by combining molecular building blocks of light-weight complex hydrides with organic linkers developed for coordination frameworks. They will be based on crystal engineering principles of coordination frameworks and have new properties (guest-host interactions, dehydrogenation properties) defined by the nature of the unique complex-hydride ligands. HOFs present new type of frameworks due to flexibility of the  $\text{BH}_4^-$  which allows other cation coordination than usually available in coordination frameworks. Also, directional anionic ligands other than hydrides can be used. We used imidazoles or its derivatives because the metal-imidazolate-metal angle of  $145^\circ$  is very similar to metal-borohydride-metal angle observed in  $\text{Mg}(\text{BH}_4)_2$ [2].

We will present first results on mono- and bi-metallic mixed anion (borohydride and imidazolate) frameworks

based on  $\text{Zn}^{2+}$  node and light alkali metal cations ( $\text{Li}^+$ ,  $\text{Na}^+$ ). For synthesis we used ball-milling procedure under inert atmosphere, solvent free and liquid-assisted grinding with different solvents (DMF, DMSO, THF, acetonitrile). Starting reactants were  $\text{NaBH}_4$ , NaIm, Him, 2-MeIm,  $\text{ZnCl}_2$  or other metal cation versions[3].

Final products are polycrystalline and usually containing several novel crystalline phases of uncertain chemical composition, so we performed synchrotron high temperature *in-situ* powder diffraction measurements on prepared compounds (T-ramping)[4]. Structure solution was carried out by combining information obtained from electron density maps provided by Direct Methods and several direct space approaches such as Simulated annealing and Parallel tempering[5].

[1] David, W. I. F., *Faraday Discuss.* 2011;151:399-414.

[2] Filinchuk Y., Richter B., Jensen T.R., Dmitriev V., Chernyshov D., Hagemann H. *Angew. Chem. Int. Ed.*, 2011, 50, 11162.

[3] Friscic T., *Chem. Soc. Rev.* 2012, 41, 3493-3510.

[4] Cerny R., Filinchuk Y., *Z. Kristallogr.* 2011, 226, 882.

[5] V. Favre-Nicolin and R. Cerny, *FOX, J. Appl. Cryst.*, 2002, 35, 734-743.

**Keywords:** metal-hydride organic frameworks, mechanochemistry, *in-situ* powder diffraction



**MS37-P2** New high-symmetry layered cocrystal of tetranuclear zinc benzoateÉva Kováts<sup>1</sup>, Gábor Bortel<sup>1</sup>, Emma Jakab<sup>2</sup>, Sándor Pekker<sup>1,3</sup>

1. Institute for Solid State Physics and Optics, Wigner Research Centre for Physics, Hungarian Academy of Sciences, H-1525 Budapest, P.O.Box 49, Hungary
2. Institute of Materials and Environmental Chemistry, Research Centre for Natural Sciences, Hungarian Academy of Sciences, H-1525 Budapest, P.O.Box 17, Hungary
3. Faculty of Light Industry and Environmental Engineering, Óbuda University, Doberdó út 6, H-1034 Budapest, Hungary

email: kovats.eva@wigner.mta.hu

Zinc-oxocarboxylates are well-known compounds as possible catalysts or luminescent materials [1]. Tetranuclear oxo clusters are in the center of interest because of their role as secondary building blocks in metal-organic frameworks (MOFs) [2]. MOFs with high porosity are widely studied as storage materials for small molecules. Despite of this property there is a lack of studies of intermolecular interactions in simplified systems of building blocks of the frameworks. Detailed study of the supramolecular interactions in high-symmetry tetranuclear zinc benzoate cocrystal helps to understand the nature of basic interactions between the host frameworks and guest molecules in MOFs. Fullerene molecules are good candidates to study supramolecular interactions because they have the ability to form various cocrystals with high-symmetry organic and metal-containing molecules [3].

Here we show the preparation, crystal structure and thermal stability of a new high-symmetry fullerene-zinc benzoate cocrystal.  $C_{60}$ -basic zinc benzoate cocrystal was prepared from toluene solutions of the constituents by slow evaporation of the solvents. The trigonal structure of the single crystals consists of alternating fullerene and basic zinc benzoate layers. Fullerenes are ordered in a hexagonal closed packed sheet at room temperature in which all fullerenes are surrounded with six adjacent  $C_{60}$  molecules with center-to-center distances similar to distances in neat  $C_{60}$  crystals. The monomolecular fullerene layers are fully separated from each other by layers of ordered benzoate molecules. This complex supramolecular assembly is stabilized by incorporated solvent molecules. The thermal stability study based on thermogravimetry mass spectrometry shows that two sets of solvent molecules are built into the cocrystals. In the oxocarboxylate layers strongly bonded toluene molecules are built in between benzoate groups of adjacent molecules. Further disordered toluene molecules with weaker interaction can also be found in the structure.

This work has been supported by the grant OTKA NK105691.

[1] Lewinski, J.; Bury, W.; Dutkiewicz, M.; Maurin, M.; Justiniak, I.; Lipkowsky, J. *Angew. Chem. Int. Ed.* 2008, 47, 573. [2] Li, h., Eddaoudi, M., O'Keeffe, M., Yaghi, O.M., *Nature*, 1999, 402, 276. [3] Pekker, S.; Kováts, É.; Oszlányi, G.; Bényei, Gy.; Klupp, G.; Bortel, G.; Jalsovszky, I.; Jakab, E.; Borondics F.; Kamarás, K.; Bokor, M.; Kriza, G.; Tompa, K.; Faigel, G. *Nat. Materials*, 2005, 4, 764.

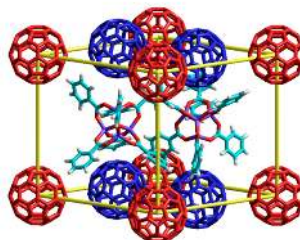


**Figure 1.** Layered crystal structure of  $C_{60}$ -basic zinc benzoate cocrystal

**Keywords:** MOF, fullerene, cocrystal

### MS37-P3 Alternatives to “co-crystal – salt” transitions in glycine co-crystals at low temperature and high pressure: two new examples as a follow-up to a glycine – glutaric acid study

Evgeniy A. Losev<sup>1,2</sup>, Boris A. Zakharov<sup>1,2</sup>, Elena V. Boldyreva<sup>1</sup>

1. Institute of Solid State Chemistry and Mechanochemistry SB RAS, Kutateladze 18, Novosibirsk, 630128, Russia

2. REC-008, Novosibirsk State University, Pirogova 2, Novosibirsk, 630090, Russia.

email: losev.88@mail.ru

The effects of temperature and pressure on the co-crystals of glycine with DL-tartaric and phthalic acids (**GT** and **GP**, respectively) have been studied by X-ray diffraction and Raman spectroscopy in a comparison with those in **GG**. Like for **GG**, for both **GT** and **GP** neither cooling nor increasing pressure resulted in a co-crystal to salt transition. On cooling, no phase transitions were observed in **GT** or **GP**, contrasting the situation with **GG**. On hydrostatic compression both **GT** and **GP** underwent reversible phase transformations, accompanied by fracture. In the high-pressure phases the main structural framework was preserved, the number of crystallographically independent molecules in the unit cell increased; the type of intermolecular H-bonds linking DL-tartaric molecules into dimers in **GT** changed in every second dimer from hydroxy-group to hydroxy-group in the low-pressure phase for the hydroxy-group – carboxy-group in the high-pressure phase.

The work was supported by the Russian Foundation for Basic Research (RFBR) (Grants No. 14-03-31866 mol\_a, 16-33-60089 mol\_a\_dk), and RAS (Project 44.3.4).

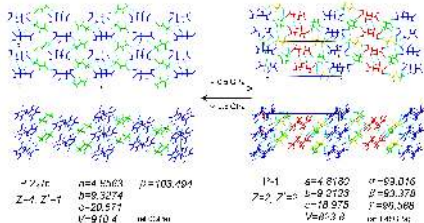


**Figure 1.** Structural changes in GT due to the phase transition at high pressure.

**Keywords:** glycine, co-crystal, hydrogen bond, high-pressure

### MS37-P4 Synthesis, Structures and Luminescence Properties of Metal-Organic Frameworks Based on Lithium- Lanthanide and Terephthalate

Mohammed S. M. Abdelbaky<sup>1</sup>, Zakariae Amghouz<sup>1,2</sup>, Santiago García-Granda<sup>1</sup>, José R. García<sup>1</sup>

1. Departamentos de Química Física y Analítica y Química Orgánica e Inorgánica, Universidad de Oviedo-CINN, 33006 Oviedo, Spain.

2. Servicios Científico-Técnicos, Universidad de Oviedo-CINN, 33006 Oviedo, Spain.

email: saidmohammed.uo@uniovi.es

Lanthanide MOFs (LnMOFs), as an important subclass of advanced functional materials, which can be synthesized using a wide range of lanthanide cations and organic ligands, they have been investigated in the fields of coordination chemistry, not only for their diverse architectures due to high coordination numbers and big ionic radii of lanthanide cations, but also for the potential applications in field of luminescence [1]. Among these compounds, the lithium-based MOFs [2] are attracting particular interest in being the promising candidates for replacing the conventional electrode in Li-ion batteries, exhibiting a high reversible specific capacity and excellent cyclability [3]. Novel metal-organic frameworks assembled from Ln(III), Li(I) and rigid dicarboxylate ligand, formulated as [LiLn(BDC)<sub>2</sub>(H<sub>2</sub>O)·2(H<sub>2</sub>O)] (**MS1-6,7a**) and [LiTb(BDC)<sub>2</sub>] (**MS7b**) (Ln = Tb, Dy, Ho, Er, Yb, Y, <sup>0.96</sup>Eu, <sup>0.04</sup>Y, <sup>0.93</sup>Tb, <sup>0.07</sup> and H<sub>2</sub>BDC = terephthalic acid), were obtained under hydrothermal conditions. The isostructural **MS1-6** crystallize in monoclinic P2<sub>1</sub>/c space group. While, in the case of Tb<sup>3+</sup> a mixture of at least two phases was obtained, the former one (**MS7a**) and a new monoclinic C2/c phase (**MS7b**). All compounds have been studied by single-crystal and the bulk characterized by powder X-ray diffraction (PXRD). The structures of **MS1-6** and **MS7a** are built up of inorganic-organic hybrid chains. While, the structure of **MS7b** is constructed from double inorganic chains. Both **MS1-6,7a** and **MS7b** structures possess a 3D framework with 1D trigonal channels running along the a and c axis, containing water molecules and anhydrous, respectively. Topological studies revealed that **MS1-6** and **MS7a** have a new 2-nodal 3,10-c net, while **MS7b** generates a 3D net with unusual β-Sn topology. The photoluminescence properties Eu- and Tb-doped compounds (**MS5-6**) are also investigated, exhibiting strong red and green light emissions, respectively, which are attributed to the efficient energy transfer process from the BDC ligand to Eu<sup>3+</sup> and Tb<sup>3+</sup>.

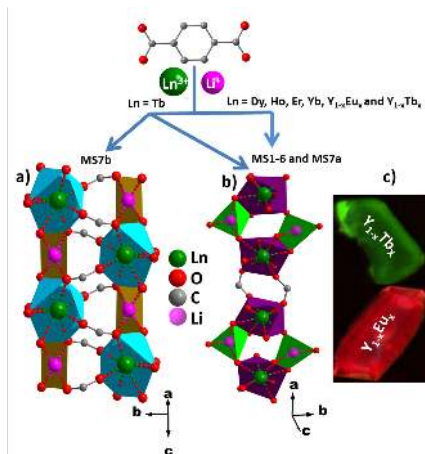


**Figure 1.** Perspective view of the infinite chains along the *c* and *a* axis for MS7b (a) and MS1-6 (b). The optical microscopic images under UV-light of single-crystals of Eu- and Tb-doped compounds (c).

**Keywords:** lanthanide-organic frameworks, dicarboxylate, hydrothermal, crystal structure, topology, photoluminescence

## MS37-P5 Testing soft donor-acceptor intermolecular interactions with high pressure.

Fabio Montisci<sup>1</sup>, Arianna Lanza<sup>1,2</sup>, Nicola Casati<sup>2</sup>, Piero Macchi<sup>1</sup>

1. Departement für Chemie und Biochemie, Universität Bern

2. Paul Scherrer Institute

email: fabio.montisci@dcb.unibe.ch

Weak intermolecular interactions have a fundamental role in diverse fields such as protein folding, enzymatic reactions, supramolecular chemistry, and crystal engineering. Hydrogen bonding interactions, among the most common interactions and ubiquitous in biological systems, have been therefore extensively studied. However, several non-hydrogen bonding interactions have received less attention and still need to be carefully investigated since they can also play a significant role in molecular self-assembly and single-crystal-to-single-crystal modifications (e.g. polymorphism and solid-phase chemical reactions). Among these,  $\text{NO}_2 \cdots \text{NO}_2$  interactions are particularly interesting and somehow controversial; the nature of the interaction has been debated, but various results suggest that it is indeed attractive and comparable in energy to a weak hydrogen bond.

In this preliminary work, the crystal structure of 4-amino-4'-nitrophenyl was studied at different temperatures and different pressures, aiming to observe the behaviour of  $\text{NO}_2 \cdots \text{NO}_2$  contacts under extreme conditions, when significant changes of stereo-electronic properties can occur due to the smaller volumes in which molecule are confined. A pressure-induced phase transition was observed above 1.6 GPa, associated with a severe rearrangements of the molecular packing, mainly driven by a  $\text{NO}_2 \cdots \text{NO}_2$  interaction. Several high-pressure DFT calculations were also performed in order to select new possible study subjects in which the nitro-nitro distances may reach smaller values.

**Keywords:** high pressure, intermolecular interactions

**MS37-P6** *Ab initio* crystal structure determination, thermal behaviour, and magnetic characterization of a new nickel coordination polymer based on carboxyethylphosphonic acid and 4,4'-bipyridine.

Rafael Mendoza-Meroño<sup>1</sup>, Eva Fernández-Zapico<sup>1</sup>, Iván da Silva<sup>2,3</sup>, Jose Montejo-Bernardo<sup>1</sup>, David Martínez-Blanco<sup>4</sup>, Santiago García-Granda<sup>1</sup>, José R García<sup>1</sup>

1. Departments of Physical-Analytical Chemistry and Organic-Inorganic Chemistry, University of Oviedo-CINN, 33006 Oviedo, Spain

2. Current address ISIS Facility, Rutherford Appleton Laboratory, Didcot, Oxfordshire OX11 0QX, UK.

3. SpLine-BM25, ESRF (European Synchrotron Radiation Facility), 6 rue Jules Horowitz, 38000 Grenoble, France.

4. Scientific and Technical Services, University of Oviedo, 33006 Oviedo, Spain

email: rafam80@gmail.com

The phosphonate type ligands have been widely used in the design and synthesis of new coordination polymers due to its strong ability to coordinate with transition and rare-earth metals under a set of different reaction conditions. These materials have a great interest not only due to their structural variety but also for their potential application in catalysis, gas storage, as magnetic materials, ion exchange, photoluminescent devices, intercalation chemistry, as sorbents, and in biomedical and biological process [1]. In this work we have obtained a crystalline powder aggregates of a new nickel coordination polymer  $\text{Ni}_2(\text{HPPA})_2(4,4'\text{-bipy})_2(\text{H}_2\text{O})$  by hydrothermal synthesis, and their crystal structure has been *ab initio* determined from synchrotron powder data. The compound shows a layer structure in *bc* plane, with Ni atoms in two different environments. The loss of the coordinated water by heating leads to the apparition of an anhydrous phase, which remains stable when cooling down to room temperature. Synthesized material presents a paramagnetic behaviour until 10 K, showing some trends of being magnetically ordered below 2 K.

[1] a) Clearfield, A.; Demadis, K. (Eds.), Metal Phosphonate Chemistry: From Synthesis to Applications. RSC Publishing, Cambridge, UK, **2011**; b) Brunet, E.; Colón, J. L.; Clearfield, A. (Eds.), Tailored Organic-Inorganic Materials. John Wiley & Sons, New York, **2015**.

**Keywords:** Nickel phosphonates, Hydrothermal synthesis, *Ab initio* crystal structure determination, Thermal characterization, Magnetic characterization.

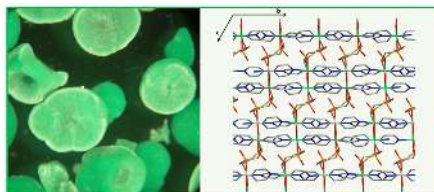


**Figure 1.** Morphology of the crystalline aggregates for the compound. (Zoom 1.6x) and packing diagram in *bc* plane, with a view of the 4,4'-bipyridine chains along *b*-axis, connected by the PPA ligands.

### MS37-P7 Structure-versus-luminescence Reversibility and Solvent Adsorption Properties of a 3D Porous Supramolecular Metal–organic Frameworks Studied by Synchrotron X-ray Powder Diffraction

Hwo-Shuenn Sheu<sup>1</sup>, Yu-Chun Chuang<sup>1</sup>, Chung-Kai Chang<sup>1</sup>,  
Chih-Chieh Wang<sup>2</sup>, Gia-Bin sheu<sup>2</sup>, Mei-Lin Ho<sup>2</sup>, Ru-Hsio Liao<sup>3</sup>,  
Gene-Hsiang Lee<sup>4</sup>

1. National synchrotron radiation research center, Hsin-chu, Taiwan.
2. Department of Chemistry, Soochow University, Taipei, Taiwan.
3. Department of Chemistry and Biochemistry, National Chung Cheng University, Chia-Yi, Taiwan.
4. Instrumental Center, National Taiwan University, Taipei, Taiwan.

email: hsheu@nsrrc.org.tw

A three-dimensional (3D) porous supramolecular architecture,  $\{[\text{Zn}(\text{bdc})(\text{dpds})]\cdot 0.62(\text{MeOH})\cdot 2\text{H}_2\text{O}\}_n$  (**1**), with a 2D layered-like metal–organic framework (MOF) has been synthesized. Adjacent layers are assembled via two types of  $\pi$ – $\pi$  interactions, the sandwich-type  $\pi_{\text{pyridyl}}-\pi_{\text{benzene}}-\pi_{\text{pyridyl}}$  and  $\pi_{\text{pyridyl}}-\pi_{\text{pyridyl}}$  fashions to afford a 3D porous supramolecular architecture. Controlled heating of the as-synthesized crystal **1** at  $\sim 120^\circ\text{C}$  causes de-solvated species of  $\{[\text{Zn}(\text{bdc})(\text{dpds})]\}_n$  (**1a**). The de-solvated compound shows the same structure as that of **1** with the nonexistence of solvated MeOH and water molecules. The de-solvated **1a** generates the re-hydrated crystal of  $\{[\text{Zn}(\text{bdc})(\text{dpds})]\cdot 1.1(\text{H}_2\text{O})\}_n$  (**1b**) upon exposure to water. The water ab-/de-sorption phenomenon by cyclic TG measurement suggests the complete reversibility upon re-/de-hydration between **1a** and **1b**, associated with reversible temperature-dependent light emission properties. Moreover, **1a** also displays interesting reversible water, methanol and ethanol vapor ad-/de-sorption behavior correlated with the polarity of the pore surface in **1a** to the corresponding adsorbate molecules. The crystal structures of as-synthesis, dehydration and rehydration forms were studied by *in situ* synchrotron X-ray powder diffraction.

**Keywords:** Synchrotron Radiation, Powder X-ray Diffraction, MOF, Luminescence

### MS37-P8 Magnesium Imidazolate – a First Porous Zeolitic Imidazolate Framework with Alkali and Alkaline Earth Metals

Damir A. Safin<sup>1</sup>, Koen Robeyns<sup>1</sup>, Yaroslav Filinchuk<sup>1</sup>

1. Institute of Condensed Matter and Nanosciences, Université catholique de Louvain, Place L. Pasteur 1, 1348 Louvain-la-Neuve, Belgium

email: damir.a.safin@gmail.com

Zeolitic imidazolate frameworks (ZIFs) are an outstanding class of MOFs, constructed from tetrahedrally configured transition metal cations linked through bridging imidazolate (Im) spacers. ZIFs are structurally isomorphous to zeolites since the metal–Im–metal angle is similar to the Si–O–Si angle ( $145^\circ$ ) in the latter compounds. This feature was exploited to produce a huge variety of porous transition metal-based ZIFs. Our initial goal was to combine Im and alkali metal borohydrides in the same structure with the formation of porous borohydride compounds, where Im serves as a structural unit of the framework, while borohydride anions provide with a functionality. However, alkali and alkaline earth metal-based imidazolates are not structurally characterized so far. Thus, the coordination chemistry of Im towards alkali and alkaline earth metal cations remains a challenge. With this in mind and inspired by the storage properties of ZIFs, we have recently turned our attention to Im-based coordination compounds with  $\text{Li}^+$ ,  $\text{Na}^+$  and  $\text{K}^+$  [1]. Unfortunately, these imidazolates form dense and hypercoordinated structures. The coordinative demand of the metal cation increases with an increase of the ionic radii. The  $\text{Li}^+$  cation exhibits a strong propensity to form heteroleptic structures, while the  $\text{K}^+$  cation allows to coordinate the Im ring through the  $\pi$ -system.

Our next challenge was to obtain magnesium imidazolate ( $\text{MgIm}_2$ ), which, based on the nature of  $\text{Mg}^{2+}$  as well as its coordination chemistry, was considered as a much more promising complexing agent in comparison with alkali metal cations. While, the freshly synthesized  $\text{MgIm}_2$  was found to be amorphous, annealing at relatively high temperatures yields the crystalline and porous  $\text{MgIm}_2$ .

Herein, we present our results on the synthesis, characterization and some properties of newly obtained  $\text{MgIm}_2$ .

[1] D. A. Safin, K. Robeyns, N. A. Tumanov, V. Ban, Y. Filinchuk, *Dense Hypercoordinated vs. Porous ZIFs of Alkali and Alkaline Earth Metals: Single Source Precursors for Hybrid Borohydrides*. 42<sup>nd</sup> International Conference on Coordination Chemistry, July 3–8, 2016, Brest, France.

**Keywords:** zeolitic imidazolate framework, magnesium imidazolate, porous structure, crystal structure, physical properties

## MS37-P9 High-Pressure Guest Included Phase Transitions, Amorphisation and Negative Linear Compressibility on a Porous Copper-Based Metal Organic Framework

Charlie J. McMonagle<sup>1</sup>, Priyanka Comar<sup>1</sup>, Euan K. Brechin<sup>1</sup>, Mark R. Warren<sup>2</sup>, David R. Allan<sup>2</sup>, Stephen A. Moggach<sup>1</sup>

1. EaStCHEM, The Centre for Science at Extreme Conditions, University of Edinburgh, Edinburgh, EH9 3JJ, UK

2. Diamond Light Source Ltd., Harwell Science & Innovation Campus, Diamond House, Oxfordshire, OX11 0DE, UK

email: c.j.mcmongale@ed.ac.uk

Porous materials such as zeolites and porous organic polymers have long been considered good candidates for storing and separating molecules based on their size. More recently, metal organic frameworks (MOFs) have attracted further interest with many aspects of their functional and mechanical properties investigated.<sup>1</sup> The porous channels found in MOFs are ideal for the uptake of guests of different shapes and sizes, and with careful design they can show high selectivity for particular species from a mixture.<sup>2</sup> Adsorption properties of MOFs have been thoroughly studied,<sup>3</sup> however obtaining in depth 'structural' insight into the adsorption/desorption mechanism is not so common place.

Over the last 6 years, we have been using high-pressure crystallographic techniques to explore the uptake of guest species in the pores of MOFs. This is done by selecting a hydrostatic medium that can penetrate the pores on increasing pressure and has revealed unexpected flexibility,<sup>4</sup> explained unusual adsorption phenomena under milder gas pressures, and increased reactivity in MOFs.<sup>5</sup>

Here, we present a high-pressure and low-temperature crystallographic study on the Cu-based MOF, bis[1-(4-pyridyl)butane-1,3-dione]copper(II), (CuPyr-I) which crystallises in the rhombohedral space group *R*-3. Under ambient temperature and pressure, the structure of CuPyr-I is composed of Jahn-Teller distorted octahedral Cu-centres, which link via the dione linkers to form a one-dimensional porous framework material. On increasing pressure to 3.34 GPa using methanol as a hydrostatic medium, CuPyr-I undergoes an isosymmetric single-crystal to single-crystal phase transition which results in a doubling of the *a*- and *b*-axes, while the *c*-axis displays negative linear compressibility caused by a subtle twisting of the framework in order to accommodate the uptake of methanol into the pores. In comparison, on direct compression using a nonpenetrative hydrostatic medium (FC-70), amorphisation occurs above 1.60 GPa, with no associated phase transition.

1. Bennett, T. D. et al. *Crystengcomm* **2015**, *17* (2), 286-289.

2. Herm, Z. R. et al. *Science* **2013**, *340* (6135), 960-964.

3. Zhou, H.-C. et al. *Chemical Reviews* **2012**, *112* (2), 673-674.

4. Moggach, S. A. et al. *Angew. Chem. Int. Ed.* **2009**, *48* (38), 7087-7089.

5. Graham, A. J. et al. *J. Am. Chem. Soc.* **2014**, *136* (24), 8606-8613.

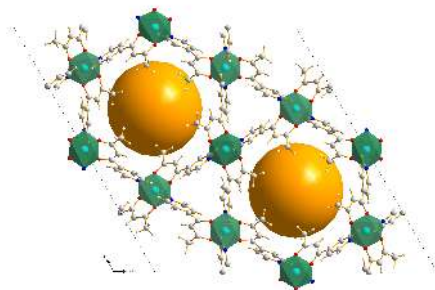


**Figure 1.** The ambient pressure structure of CuPyr-I viewed perpendicular to the *a*, *b* face. This is a one-dimensional porous material with large channels 9 Å in diameter at their widest point, shown in the figure by the orange spheres.

**Keywords:** MOF, High Pressure, Phase Transition

**MS37-P10** Crystal structures of novel polydentate N,O-ligandsStanislava Todorova<sup>1</sup>, Vanya Kurteva<sup>1</sup>, Boris Shivachev<sup>2</sup>, Rositsa P. Nikolova<sup>2</sup><sup>1</sup>. Institute of Organic Chemistry with Centre of Phytochemistry, Bulgarian Academy of Sciences, Acad. G. Bonchev str., bl. 9, 1113 Sofia, Bulgaria<sup>2</sup>. Institute of Mineralogy and Crystallography "Acad. Ivan Kostov", Bulgarian Academy of Sciences, Acad. G. Bonchev str., bl. 107, 1113 Sofia, Bulgaria

email: stodorova@orgchem.bas.bg

Polydentate molecules are of growing interest as they are widely applied as scaffolds in the combinatorial synthesis of artificial receptors for ions with medical and environmental potential. Among the broad variety of synthetic molecules, polyazaoxa ligands have received special attention due to their outstanding coordination abilities. A particular goal involves the construction of ligands with an appropriate order and predictable arrangement of two or more molecular components with possibility to form hydrogen bonds, which play the pivotal role in molecular recognition by synthetic receptors.

Herein, we present a study on the crystal structures of a series of novel polydentate N,O-ligands possessing unsymmetrical urea fragments attached to a *p*-cresol scaffold. The compounds are obtained by a fast and simple protocol from *p*-cresol-based symmetrical bis-amine, phosgene, and primary amine. Their structures are assigned by 1D and 2D NMR spectra in solution and by single crystal XRD in solid phase. Ortep drawings of selected crystal phases are presented on Figure 1.

The ligands can be generally divided in two groups: open-chain substituted aromatics with at least one unsymmetrical urea unit (a) and fused aryloxazinones with unsymmetrical urea fragment (b). The concept is to design polydentate ligands with variable coordination abilities controlled by the difference in the molecule geometry.

The single crystal XRD analysis showed that the open-chain substituted molecules are oriented towards optimal intramolecular H-bonding of the ureas' heteroatoms, while the preferred geometry of oxazinones is driven by intermolecular bonding.

The financial support by Swiss National Science Found (SupraMedChem@Balkans.Net, IZ7420\_160515, SCOPES), Bulgarian Science Fund, infrastructure projects UNA-17/2005, DRNF-02-13/2009, and DRNF-02/01, and by Bulgarian Academy of Sciences, project Support for the young scientists in BAS 2016, is gratefully acknowledged.

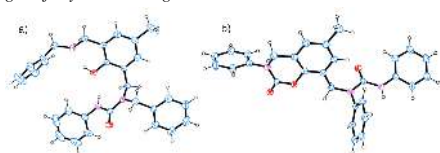


**Figure 1.** ORTEP drawings of selected samples

**Keywords:** polydentate N,O-ligands , singal crystal XRD

**MS37-P11** Symmetry in MOF synthesis: A new network topology from a heterotritopic linkerPhilipp Urban<sup>1</sup>, Noelle R. Catarineu<sup>1</sup>, Maureen B. Morla<sup>1</sup>, Omar M. Yaghi<sup>1,2</sup><sup>1</sup>. Department of Chemistry, University of California, Berkeley, Berkeley, California 94720, United States<sup>2</sup>. King Abdulaziz City for Science and Technology, Riyadh 11442, Saudi Arabia

email: p.urban@berkeley.edu

Metal-organic frameworks (MOFs) are crystalline materials, composed of inorganic clusters or coordination spheres (secondary building units, SBUs), connected by organic linkers through strong bonds. Most of the linkers employed in MOF synthesis are highly symmetric, leading to structures with only a few network topologies, aiming for a high network transitivity.<sup>[1]</sup> A reason for this is that for linkers with identical functional groups, a pH exists that allows reversible bond formation to the metal centers, hence facilitating crystal growth. Here we report the use of a heterotritopic linker which leads to a stable, porous MOF (BET surface area 2140 m<sup>2</sup>g<sup>-1</sup>) with a new network topology (named tto). MOF-910 crystallizes in the trigonal spacegroup *R*-3c with lattice parameters *a* = 47.239(2) Å and *c* = 27.1216(12) Å. The structure (Figure 1) consists of hexagonal channels 28 Å in diameter constructed from infinite helical SBUs of Zn<sup>2+</sup> ions ligated by the oxygen and nitrogen atoms of the linker, which bears a benzoate, a semiquinonate and a pyridonate functional group.

The structure is achiral, as it contains an equal amount of left- and right-handed helical SBUs. The semiquinonate and the pyridonate group align together at the same SBU with the benzoate group bridging to the opposing SBU. The benzoate is disordered, showing two distinct conformations. Despite the differences of the pK<sub>a</sub> values of the functional groups (benzoate: 4.2; catecholate: 9.5; pyridonate: 11),<sup>[2,3]</sup> synthetic conditions could be derived which led to a homogeneous, stable product. These results show the potential of extending the variety of known MOFs constructed with new network topologies utilizing much higher complexity in the organic linker molecules than previously achieved.

[1] M. Li, D. Li, M. O'Keeffe, O. M. Yaghi, *Chem. Rev.* **2014**, *114*, 1343.

[2] E. P. Serjeant, B. Dempsey, *Ionization Constants of Organic Acids in Aqueous Solution*; Pergamon Press: Oxford, 1979.

[3] J. A. Joule, K. Mills, *Heterocyclic Chemistry*, 5th ed.; John Wiley& Sons, Ltd.: West Sussex, U.K., 2010; pp 143.



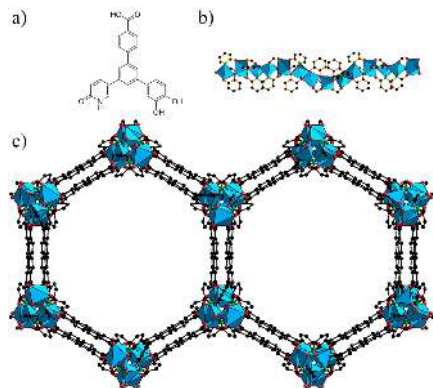


**Figure 1.** a) Heterotritopic linker. b) Section from helical SBU. c) Structure of MOF-910 viewed along the *c*-axis along the hexagonal channels. Color scheme: Zn, blue; C, black; O, red; N, green. Hydrogen atoms omitted for clarity.

**Keywords:** Metal-organic frameworks, Single-crystal X-ray diffraction, Disorder

## MS37-P12 Reticular Synthesis and Structural Trends of Novel Cd(II) Coordination Polymers Based on N-donor Bridging Ligand

Mansoureh Zahedi<sup>1,2</sup>, Ulli Englert<sup>1</sup>

1. Institute of Inorganic Chemistry, RWTH Aachen University, Landoltweg 1, 52074 Aachen, Germany

2. Department of inorganic chemistry, Faculty of chemistry, Tabriz University, Tabriz, Iran

email: mzahedi83@gmail.com

The rational design and syntheses of coordination polymers have attracted great attention from chemists not only because of their intriguing structural diversities and aesthetical topologies but also due to their interesting properties and potential applications as functional materials in gas storage/separation, heterogeneous catalysis, magnetism, photochemistry [1-4]. since the bulk properties of these materials are closely related to their structures, it is important to understand the factors such as coordination geometries of metal ions and the resulting secondary inorganic building blocks, spatial arrangements of organic building blocks, interpenetration, anions and solvents, which control their topologies. Taking the above discussion into account, in this study, we have systematically investigated construction, structural and property feature comparison of some new coordination polymers composed of a long and rigid N-donor, bipyridine, linker ligand (L) towards  $CdX_2$  ( $X = CH_3COO^-, I^-, \dots$ ). The X-ray crystallography results display considerable structural differences in Cd (II) geometry. It includes one-dimensional ladder like polymeric chains with seven coordination numbers for Cd (II) metal center in the present of acetate anion, meanwhile, the tetrahedral geometry with zigzag chains have been seen with Iodide one.

### References:

- [1] J.L.C. Rowsell, O.M. Yaghi, *Micropor. Mesopor. Mater.* 2004,**73**, 3.
- [2] Y. Ma, L. Zhang, G. Peng, C. Zhao, R. Dong, C. Yang and H. Deng *CrystEngComm*, 2014,**16**, 667-683.
- [3] R. Patra, H. Titi and I. Goldberg, *CrystEngComm*, 2013, **15**, 7257-7266.
- [4] P. Wang, R. Fan, X. Liu, L. Wang, Y. Yang, W. Cao, B. Yang, W. Hasi, Q. Su and Y. Mu *CrystEngComm*, 2013,**15**, 1931-1949.

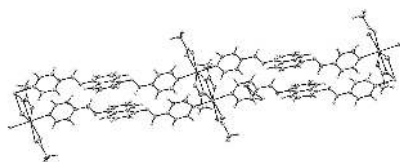


**Figure 1.** One dimensional structure of  $[Cd(L)(OAc)_2]$

**Keywords:** Coordination polymer, Bridging Ligand, Cadmium salts, X-ray Crystallography

## MS37-P13 A Flexible Interpenetrated pcu Coordination Network Formed by Mixed Ligands

**Keywords:** Flexible, Interpenetrated, pcu

Mohana Shivanna<sup>1</sup>, Dr.QingYuan Yang<sup>2</sup>, Prof. Michael J Zaworotko<sup>3</sup>

1. Mr. Mohana Shivanna, Doctor of philosophy, crystal engineering resrach group at University of Limerick, Ireland

2. Dr.QingYuan Yang, Post doctoral student, crystal engineering research group at university of limerick

3. Prof. Michael J. Zaworotko, Crystal engineering research group, University of Limerick

email: mohana.shivanna@ul.ie

**Abstract:** Metal–organic materials (MOMs), also known as porous coordination polymers (PCPs) or metal-organic frameworks (MOFs), are receiving attention thanks to their amenability to design and properties [1, 3]. The pore size and chemistry of MOMs makes them excellent candidates for applications in storage, separation, sensing, and catalysis [2]. Flexible MOMs can exhibit behavior such as swelling, stepwise uptake, gate-opening and breathing which can be induced by stimuli such as solvent, pressure, heat and light [ 4, 5]

Here, we report a two, three-fold interpenetrated **pcu** network with general formula  $[Zn_4(L_1)_4(L_2)_2] \cdot DMF$  ( $L_1=1,4$ -bis(4-carboxyphenyl)benzene; $L_2=1,4$ -bis(4-pyridyl)benzene), or  $L_2=3,6$ -Di(4-pyridinyl)-1,2,4,5-tetrazine) based on axially coordinated zinc “paddle-wheels”, that exhibits dynamic structural transformations induced by guest incorporation and removal. X-ray structures highlight the highly flexible nature of the framework and reveal that phase transformations involve the movement or rotation of the biphenylene dicarboxylate ligands. The coordination geometry of a zinc paddle-wheel unit is considerably changed without bond breakage.

### References:

- 1 Kitagawa, S. *et al.*, *Chem. Soc. Rev.* **2005**, *34*, 109
- 2 Nugent, P. *et al.*, *Nature.* **2013**, *495*, 80
- 3 Sakata, Y. *et al.*, *science* . **2013**, *339*, 193
- 4 Schneemann, A. *et al.*, *Chem. Soc. Rev.* **2014**, *43*, 6062
- 5 Mason, A. J. *et al.*, *Nature.* **2015**, *527*, 357

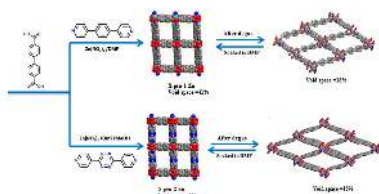


Figure 1(a) and (b) An illustration of the interpenetrated pcu nets formed by Zn (II) and reversible phase transformations induced by guests.

**Figure 1.** (a) and (b) An illustration of the interpenetrated pcu nets formed by Zn (II) and reversible phase transformations induced by guests.

## MS38 Nanomaterials & graphene

Chairs: Adrià Gil-Mestres, Michael Woerle

### MS38-P1 Synthesis of Ag@SiO<sub>2</sub> nanorattles for controlled Ag<sup>+</sup> release

Sarah-Luise Abram<sup>1</sup>, Katharina M. Fromm<sup>1</sup>

<sup>1</sup> Department of Chemistry, University of Fribourg, Chemin du Musée 9, 1700 Fribourg, Switzerland

email: sarah-luise.abram@unifr.ch

Medical progress and an ageing world population have led to an increasing use of foreign materials inside the human body. Consequently also the number of infections related to these implants has grown significantly.<sup>1</sup> Antimicrobial coatings that prevent the formation of infectious biofilms on the surface of the implants could make an important contribution to overcome that issue. Silver is known for its good antimicrobial and biocompatible properties and could thus play an important role in the fight against implant infections, especially if they are caused by antibiotic resistant bacteria.<sup>2</sup>

This project investigates Ag@SiO<sub>2</sub> nanorattles as antimicrobial agent for implant coatings. These nanoparticles are characterized by a void between a silica shell and a Ag nanoparticle as cargo.<sup>3</sup> The silica shell protects the Ag cores from aggregation and prolongs the release of the antimicrobial active Ag<sup>+</sup> ions. Moreover it provides reactive sites to functionalize the nanocontainers in order to attach them covalently to implant surfaces or to incorporate them into polymer materials.

We have developed two different synthetic routes to Ag@SiO<sub>2</sub> nanorattles of different sizes. The microemulsion method<sup>4</sup> gives access to nanorattles with a diameter of ca. 25 nm (Fig. 1, top) that were evaluated for their Ag<sup>+</sup> release properties, antimicrobial potential and for their impact on cells of the immune system.<sup>5</sup>

The second synthetic approach is based on the coating of Ag nanoparticles with silica under classical Stöber conditions followed by a surface protected etching protocol<sup>6</sup>. This results in Ag@SiO<sub>2</sub> nanorattles with a diameter of ca. 80 nm (Fig. 1, bottom). Cytotoxicity tests showed a good biocompatibility. Their antimicrobial efficiency is currently under investigation.

Silver-containing silica nanorattles thus fulfill several requirements for the development of novel antibacterial nanocoatings on biomaterial surfaces.

<sup>1</sup>S. Veerachamy, T. Yarlagadda, G. Manivasagam, P. Yarlagadda *Proc IMechE Part H: J Eng in Med*, **2014**, 228, 1083-1099

<sup>2</sup>S. Eckhardt, P. Brunetto, J. Gagnon, M. Priebe, B. Giese, K. M. Fromm, *Chem. Rev.*, **2013**, 113, 4708-4754

<sup>3</sup>M. Priebe, K. M. Fromm, *Chem. Eur. J.* **2015**, 21, 3854-3874

<sup>4</sup>M. Priebe, K. M. Fromm, *Part. Part. Syst. Charact.* **2014**, 31, 645-651

<sup>5</sup>M. Priebe, J. Widmer, N. Suhartha, S.-L. Abram, I. Mottas, A. Woischnig, P. Brunetto, N. Khanna, C. Bourquin, K. M. Fromm, *Nanomedicine* **2016**, submitted

<sup>6</sup>F. Hu, Y. Zhang, G. Chen, C. Li, Q. Wang, *small* **2015**, 11, 985-993

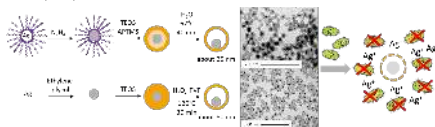


**Figure 1.** Synthesis and antimicrobial Ag<sup>+</sup> release of Ag@SiO<sub>2</sub> nanorattles: microemulsion method (top) and Stöber conditions followed by surface protected etching (bottom).

**Keywords:** nanocontainers, nanorattles, antimicrobial surfaces, silica, silver

## MS38-P2 Dual-Responsive Lipid Nanotubes: Two-Way Morphology Control by pH and Redox Effects

Leyla T. Yildirim<sup>1</sup>, Hande Unsal<sup>2</sup>, Judith Schmidt<sup>3</sup>, Yeshayahu Talmon<sup>3</sup>, Nihal Aydogan<sup>2</sup>

1. Hacettepe University Physics Engineering Department, Beytepe, 06800, Ankara, Turkey

2. Hacettepe University Chemical Engineering Department, Beytepe, 06800, Ankara, Turkey

3. Technion-Israel Institute of Technology, Department of Chemical Engineering, Haifa, 3200003, Israel

email: tatar@hacettepe.edu.tr

Lipid nanotubes are the preferred structures for many applications, especially biological ones. Here, we presented a two-way reversible morphology control of the nanotubes formed by the novel molecule AQUA ( $C_{27}H_{59}NO_4$ ). The diameters of the AQUA nanotubes are  $110 \pm 20$  nm, and their lengths are 4–8  $\mu$ m. AQUA has both pH-sensitive and redox-active characters provided by the carboxylic acid and anthraquinone groups. Upon chemical reduction, the nanotubes turned into thinner ribbons and this structural transformation was significantly reversible. Nanotube morphology can additionally be altered by decreasing the pH below the pKa value of the AQUA. The molecular length of AQUA is calculated as  $\sim 2$  nm, and when this value is combined with the information gained from the XRD and cryo-TEM analysis such that the nanotubes have a multi-layered structure. The number of layers is either 2 or 3 and the total wall thickness is 4–6 nm at pH 9, this proves the claims that the d-spacing value of  $\sim 2$  nm in the XRD spectrum gives the thickness of one layer in the tube walls and the wall structure is composed of symmetrical monolayers with a little space between them at pH 9. Decreasing the pH caused the gradual unfolding of the nanotubes and the inter-layer distance in the nanotube's walls increased. This morphological change is fast and reversible at a wide pH range (Fig. 1).

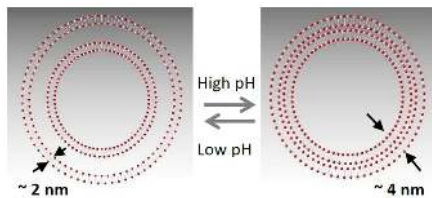


**Figure 1.** Schematic representation of the effect of pH on the membrane structure

**Keywords:** Lipid nanotube, Stimuli response, Redox-active, pH-sensitive, Conductive, XRD, TEM

## MS38-P3 Design of polymer-silver nanocomposites for biomedical applications

Milène P.L. Tan<sup>1</sup>, Katharina M. Fromm<sup>1</sup>

1. University of Fribourg, Department of Chemistry, Chemin du Musée 9, 1700 Fribourg.

email: milene.tan@unifr.ch

In the last decades, polymeric materials have attracted a significant interest in the biomedical field especially in their use as implants. With the emergence of new multi-drug resistant bacteria and despite the advanced sterilization procedures, the contamination of implant surfaces by bacteria is a new challenge to overcome.<sup>1</sup> Then, the design of new antibacterial/bactericidal surfaces in order to prevent bacterial adhesion and biofilm formation is an important task.

Silver has already been proven to be effective against bacterial infections even at low concentration (0.1–10 ppm).<sup>3</sup> Furthermore, it has been demonstrated that nano-sized silver could be even more efficient due to a better interaction with bacteria and a more long-term activity compared to ionic silver.<sup>4</sup> For these reasons, silver nanoparticles (NPs) will be exploited in the framework of this project.

The poly(N-isopropylacrylamide) (PNiPAAm) is widely studied for biomedical applications especially in tissue engineering owing to its good biocompatibility and thermosensitivity with a lower critical solution temperature (LCST) close to 32°C. Practically, the polymer is readily soluble under this temperature but above, it becomes insoluble and precipitates out.<sup>5</sup> In the context of this work, the polymer was synthesized by RAFT polymerization in order to provide silver binding site. Several nanocomposites with different ratios of silver/polymer have been prepared. Different techniques have been used to study these materials such as transmission electron microscopy, dynamic light scattering, thermogravimetric analyses, inductively coupled plasma, x-ray photoelectron spectroscopy.

<sup>1</sup>L. Guo, W. Yuan, Z. Lu, C. Li, *Colloids and Surface A: Physiochem. Eng. Aspects*, **2013**, 439, 69–83.

<sup>2</sup>J. Hasan, R. J. Crawford, E. P. Ivanova, *Trends in Biotechnology*, **2013**, 31, 295–308.

<sup>3</sup>S. Silver, L. T. Phung, G. Silver, *J. Ind. Microbiol. Biotechnol.*, **2006**, 33, 627–634.

<sup>4</sup>J. R. Morones, J. L. Elechiguerra, A. Camacho, K. Holt, J.B. Kouri, J.T. Ramirez, M.J. Yacaman., *Nanotechnology*, **2005**, 16, 2346–53.

<sup>5</sup>B. Jeong, A. Gutowska, *TRENDS in Biotechnology*, **2002**, 20, 305–11

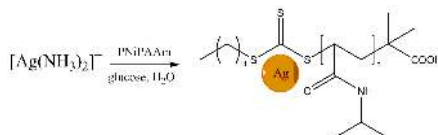


**Figure 1.** Synthesis of the nanocomposite

**Keywords:** Silver, nanoparticles, polymer

## MS39 X-Ray diffraction on the $\mu$ s to ps time scale

Chairs: Semën Gorfman, Michael Wulff

### MS39-P1 Time-Resolved Crystallography from femtoseconds to microseconds at the laser driven X-ray plasma source in ELI beamline

Borislav Angelov<sup>1</sup>, Jakob Andreasson<sup>1</sup>

1. Institute of Physics, ELI Beamlines, Academy of Sciences of the Czech Republic, Na Slovance 1999/2, CZ-18221 Prague, Czech Republic

email: borislav.angelov@eli-beams.eu

The novel laser driven plasma X-ray sources will allow for time resolved X-ray scattering and diffraction on a femtosecond to microsecond time scale. Unlike large scale facilities such as synchrotrons, intensive lasers can be used for the generation of short X-rays pulses in a setup of much smaller size that will be suitable for implementation in a laboratory. The femtosecond laser driven emission of X-ray pulses from plasma (XPS) offers higher time resolution for fast kinetic measurements than continuously emitting sources. The ELI beamlines facility is planned to start operation by the end of 2016 in Dolní Brezany, Czech Republic. The first users are planned for 2018. ELI beamlines will give a unique advantage for time resolved crystallography and wide angle scattering from crystalline samples, including proteins. The generated pulses will span approx. 100 fs with a repetition rate of 1 kHz. The intensity of the X-ray pulses on the sample will be  $\sim 10^6$  ph/pulse at 10.8 KeV. The scattered and diffracted by the crystal X-rays will be counted using a DECTRIS Eiger 1M area detector which operates at the same frame rate as the source, i.e. 1 kHz. Such setup can be combined with several pump probe lasers to study the fast kinetics for example in proteins relevant to plant photosystems or vision in animals. To obtain a representative statistics from the measurements, it will be necessary several repetitions to be done. Because of the interdisciplinary nature of the fields and of the ELI beamlines facility regular discussions between experts in the field of high power laser-matter interaction and potential users, as well as young scientists, are organized.

References: I. B. Rus ; F. Batysta ; J. Čáp ; M. Divoký ; M. Fibrich, et al. "Outline of the ELI-Beamlines facility", Proc. SPIE 8080, Diode-Pumped High Energy and High Power Lasers; ELI: Ultrarelativistic Laser-Matter Interactions and Petawatt Photonics; and HiPER: the European Pathway to Laser Energy, 808010, 2011; doi:10.1117/12.890392

**Keywords:** laser plasma X-rays, diffraction, fast kinetics, Eiger detector

### MS39-P2 Time-resolved Local Dynamics Measurement of Supersaturated Solution by Diffracted X-ray Tracking

Yufuku Matsushita<sup>1</sup>

1. The University of Tokyo, Graduate School of Frontier Sciences, Kashiwa, Japan

email: 8113178469@mail.ecc.u-tokyo.ac.jp

Recently, the micro scale structure of the supersaturated solution are receiving a lot of attention in nucleation and crystal growth process of inorganic, organic and protein compounds. In particular, the crystallization and nucleation process from supersaturated solution is known as a local phenomenon and instantaneous process. The observation of supersaturated solution is required a local structure and time resolved behaviour[1]. In this study, we approached to observe the time resolved micro scale dynamics of protein solution by Diffracted X-ray Tracking (DXT) as known as single molecule measurement method. This method is able to direct observation of local solution dynamics for Target solution by detecting angular rotational displacement of a single gold nanocrystal (approximately 100 nm) with pico-meter scale positional accuracy and micro-second time resolution. For target sample, we choose a inorganic (Sodium acetate) and Protein supersaturated solution (Lysozyme). From detailed DXT analysis, we observed the crystal precursor state solution both of inorganic and protein compounds are containing slow and fast dynamics. In particular the fast diffusion corresponded relaxation process of supersaturated state of nano scale clusters which is a important factor of maintenance of metastable supersaturated condition, driving force of morphology determination of final product from crystallization and nucleation process from supersaturation. And the force-field values of this diffusion behaviour are detected as  $10^{-15}$  and  $10^{-18}$  Newton scale in inorganic and protein supersaturated solution, respectively. From this study, DXT measurement results and detailed analysis process for a protein solution such as crystal precursor metastable state of solution are concerned that this technique is a powerful tool for observing nano-scale molecular dynamical structures and its local dynamics in bulk solution. For next work, we will planning to tackle research in order to determine the morphology control factor of final products and inhibit techniques of nucleation by DXT, and instantaneous observation of nucleation process by Pump-and-probe measurement.

[1] Y. Matsushita, H. Sekiguchi, K. Ichiyanagi, N. Ohta, K. Ikezaki, Y. Goto, and Y. C. Sasaki, "Time-resolved X-ray Tracking of Expansion and Compression Dynamics in Supersaturating," *Nat. Publ. Gr.*, no. November, pp. 1–8, 2015.

**Keywords:** Supersaturated solution, Diffracted X-ray Tracking

### MS39-P3 From Micromolecules' to Macromolecules' Structural Dynamics Properties: Ultrafast Chiroscopy with Synchrotron and Free Electron Laser Radiation

Simone A. Techert<sup>1</sup>, Sreevidya Thekku-Veedu<sup>1</sup>, Sadia Bari<sup>1</sup>,  
Rebecca Boll<sup>1</sup>, Zhong Yin<sup>1</sup>, Darina Storozhuk<sup>1</sup>, Philipp Busse<sup>2</sup>,  
Dirk Raiser<sup>2</sup>

1. DESY  
2. MPIPB

email: simone.techert@desy.de

Common for all time-resolved x-ray experiments is the applied pump / probe scheme, where an optical pump-laser initiates a reaction whose structural time evolution is then investigated by x-ray probe pulses at various time delays. X-ray photon-in / photon-out techniques are based on diffraction or spectroscopic techniques like near edge spectroscopy or x-ray emission spectroscopy. Meanwhile x-ray spectroscopic techniques probe the local environment around specific atoms in a molecule - such as orbitals, diffraction studies reveal the structure of the bulk of periodic systems. In the present contribution we will give an overview of our strategy utilizing the pulsed characteristics of X-ray sources, in particular synchrotrons and free electron lasers, to gain structural dynamics information of micro- and macromolecules on their time scales of reactivity which ranges from femtoseconds to milliseconds. Method wise, *Chiroscopy* will be introduced and discussed in the context of time-resolved X-ray diffraction / X-ray scattering and X-ray spectroscopy. In a new concept of photon-assisted reaction trigger we will introduce an experimental strategy to overcome the paradigm of optical light initiation for time-resolved X-ray scattering experiments and what it means for chiroscopy. Finally, we will summarize our efforts in systematizing the characteristic structural changes in molecular systems during chemical reactions to some kind of "periodic table" of structural dynamics allowing predicting reaction properties in chemistry and biochemistry from a time-dependent structural point of view.

References: S. Bari, R. Boll, S. E. Canton, L. Glaser, K. Idzik, K. Kubicek, D. Raiser, S. Thekku Veedu, Z. Yin, S. Techert, *High flux X-ray sources and Free Electron Lasers for studying ultrafast time structure imprints in complex chemical and biochemical reactions*, in: X-ray Free Electron Lasers, eds. U. Bergmann, P. Pellegrini, Oxford University Press, in press (2016) and references therein.

**Keywords:** time-resolved x-ray crystallography

### MS40 New detectors for high energy x-ray applications

Chairs: Heinz Graafsma, Lothar Strüder

#### MS40-P1 3D energy dispersive detector (pnCCD) for ultra-hard x-rays Laue diffraction: In situ analysis of lattice deformation in polycrystalline Copper

Ali Abboud<sup>1</sup>, Jozef Keckes<sup>2,3</sup>, Mohammad Shokr<sup>1</sup>, Amir Tosson<sup>1</sup>,  
Lothar Strüder<sup>1</sup>, Manuela Klaus<sup>2</sup>, Christopher Klaus<sup>2</sup>, Ullrich  
Pietsch<sup>1</sup>

1. Department of Physics, University of Siegen, Siegen, Germany  
2. Montanuniversität Leoben, Leoben, Austria  
3. Material Center Leoben Forschungs GmbH, Leoben, Austria  
4. PnSensor GmbH, Munich, Germany  
5. Helmholtz-Zentrum Berlin for Materials and Energy, Berlin, Germany

email: aliabbouds@hotmail.com

The deformation behavior of individual grains in a large grained polycrystalline Cu sample is studied during in situ tensile loading. The Laue diffraction experiment was carried out at the EDDI beamline (@ Bessy II) using ultra-hard x-rays (5 to 160 keV) and a 3D energy dispersive pnCCD detector. The recorded Laue-patterns as a function of tensile loading shows the evolution of spatially well-defined Laue spots into streaking ones. The pnCCD was used to record the position and the energy spectrum of each diffraction peak in all of the collected Laue patterns in a single shot experiment, which allowed to index all Laue spots and assign them to individual grains simultaneously. The two-fold information yields the crystal cell orientation of each individual grain and its relative orientation with respect to the surrounding grains, i.e. the texture of the probed region. Results show that the grains rotate around the loading axis until the preferred slip direction is aligned with the tensile direction. This phenomena is accompanied by a continuous expansion of the lattice parameters followed by a rapid strain release resulting in internal stress relaxation, while the strain increases again at very high strain levels. In addition, the energy profile of the elongated Laue spots shows that in most cases rotational strain was the main response of the grains with respect to external strain.

**Keywords:** hard x-rays, pnccd, polycrystalline, copper, in-situ energy dispersive x-ray diffraction

## MS41 The use of X-ray, electron and neutron scattering in nanoscience

Chairs: Christian Lehmann, Julian Stangl

### MS41-P1 Structure determination and charge density analysis of nanostructured, disordered MoS<sub>2</sub>-based layered compounds with organic cations

Alexander S. Goloveshkin<sup>1</sup>, Alexander A. Korlyukov<sup>1</sup>, Natalia D. Lenenko<sup>1</sup>, Alexandre S. Golub<sup>1</sup>, Ivan S. Bushmarinov<sup>1</sup>

1. A.N.Nesmeyanov Institute of Organoelement Compounds of Russian Academy of Sciences

email: golov-1@mail.ru

Molybdenum disulfide is a layered material demonstrating properties interesting for different applications. A charge transfer onto the MoS<sub>2</sub> layers induces the transformation of semiconductive 2H-modification to "metallic" 1T-MoS<sub>2</sub>. The 1T-structure, however, is stable only in the presence of negative charge on the MoS<sub>2</sub> sheets: for example, in intercalation compounds with organic cations. In these compounds, the stabilization of the negative charge on the MoS<sub>2</sub> layers may depend on the interactions between the sulfide layers and organic cations, and the aim of the current study is to determine the structure of such intercalates and the energy of the interactions within them.

Recently [1], we have studied (R<sub>3</sub>N)MoS<sub>2</sub> (R= H, alkyl) using the "supercell approach" developed by C. Ufer for full-pattern modeling of turbostratically disordered clays. We found that many of intercalation compounds are not fully turbostratic and have short-range correlations between MoS<sub>2</sub> layer positions. These correlations were successfully modeled assuming that the turbostratic disorder is actually exhibited by stable bilayer fragments [2].

In this work, we used this "bilayer-supercell" model to refine the powder patterns of new intercalation compounds of MoS<sub>2</sub> with cations containing aromatic and aliphatic fragments. We obtained the preferred geometry and relative positions of MoS<sub>2</sub> layers and the orientation of aromatic molecules in the interlayer space for compounds with urotropine, phenanthroline and tris-methylphenylammonium cations. We found that compounds with substituted  $\alpha$ -amino-naphthalene cations formed turbostratic structure without correlations between MoS<sub>2</sub> layers positions.

The PW-DFT-d calculations based on cell geometries obtained with "bilayer-supercell" approach were used for final verification and charge density determination. Then, we studied the calculated structures within the framework

of R.F.W. Bader's quantum theory of atoms in molecules. Finally, we quantified binding energy of cation-sulfide sheets interactions. To summarize, we found the geometric and energetic characteristics of different weak interactions between organic cations and MoS<sub>2</sub> layers (Fig. 1).

[1] A.S. Goloveshkin, N.D. Lenenko, V.I. Zaikovskii, A.S. Golub, A.A. Korlyukov, I.S. Bushmarinov, *RSC Adv.*, **2015**, *5*, 19206-19212

[2] A.S. Goloveshkin, I.S. Bushmarinov, A.A. Korlyukov, M.I. Buzin, V.I. Zaikovskii, N.D. Lenenko, A.S. Golub, *Langmuir*, **2015**, *31*, 8953-8960

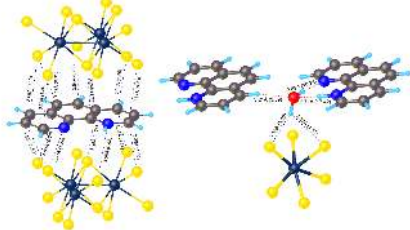


**Figure 1.** Weak interactions in (PhenH<sup>+</sup>·H<sub>2</sub>O)(MoS<sub>2</sub>)<sub>10</sub>:  $\pi$ ...S contacts (left part), hydrogen bonds (right part). Distance between non-hydrogen atoms, forming interaction, and its energy in kcal/mole (in brackets) are labeled.

**Keywords:** molybdenum disulfide, powder diffraction, layered materials, Rietveld refinement, charge density



## MS41-P2 X-ray scattering-based studies of nano/bio-structures with hierarchical order for nanomedicine applications

Cinzia Giannini<sup>1</sup>, Davide Altamura<sup>1</sup>, Dritan Siliqi<sup>1</sup>, Teresa Sibillano<sup>1</sup>, Liberato De Caro<sup>1</sup>, Stella Pastore<sup>1</sup>, Massimo Ladisa<sup>1</sup>

1. Institute of Crystallography - CNR/IC Bari, Italy

email: cinzia.giannini@ic.cnr.it

The application of nanotechnology in medicine offers numerous exciting possibilities in healthcare. The current and promising applications of nanomedicine include, but are not limited to, *drug delivery*, *theranostic* and *tissue engineering*, which are among the many beneficiaries of nanotechnology. Some of these opportunities are becoming realities or are being used today, while others are generating promise in their early phases of development and are expected to experience vigorous growth in the foreseeable future. As recognition of the importance of this exciting field, it was expected that the global market of nanoscale applications in the medical field could have grown to \$70 - \$160 billion by 2015.<sup>1,2</sup> So far, regarding drug delivery, there are over two dozen nanotechnology-based therapeutic products approved by Food and Drug Administration (FDA) for clinical use, and more are in clinical trials.<sup>3-5</sup> The majority of these products are composed of a non-targeted delivery system (e.g. liposomes and polymers) and a drug, and are therefore considered first generation nanotherapeutics<sup>6</sup>.

In the present work, small and wide angle X-ray scattering techniques have been adopted to characterize the morphology and structure of:

- “nanoparticles in solution”<sup>7</sup>
- “self-assembled PEGylated tetra-phenylalanine derivatives”<sup>8</sup>
- “collagen tissues”
- “mineralized tissues”<sup>9</sup>

### References

1. Jain KK. The Handbook of Nanomedicine. Humana Press; Totowa: 2008. p. p353.
2. Occupational Health & Safety Report: Nanomedicine Market to Surpass \$160 Billion by 2015. <http://ohsonline.com/articles/2009/06/29/report-on-nanomedicine-market.aspx> (6/1/2010)
3. Wagner V, Dullaart A, Bock AK, Zweck A. NAT. BIOTECHNOL. 2006;24:1211–1217.
4. Zhang L, Gu FX, Chan JM, Wang AZ, Langer RS, Farokhzad OC. CLIN. PHARMACOL. THER. 2008;83:761–769.
5. Davis ME, Chen Z, Shin DM. NAT. REV. DRUG DISCOV.2008;7:771–782.
6. Riehemann K, Schneider SW, Luger TA, Godin B, Ferrari M, Fuchs H. ANGEW. CHEM. INT. Ed. 2009;48:872–897.
7. Sibillano T, De Caro L, Altamura D, Siliqi D, Ramella M, Boccafocchi F, Ciasca G, Campi G, Tirinato L, di Fabrizio E and Giannini C. SCI REPORT 4, Article number: 6985 (2014)
8. Diaferia C, Mercurio F A, Giannini C, Sibillano T, Morelli G, Leone M, Accardo A SCI REPORT(submitted)
9. Altamura D, Pastore S, Raucci MG, Siliqi D, De Pascalis F, Nacucchi M, Ambrosio L. and Giannini C

ACS APPLIED MATERIALS & INTERFACES (in press, 2016)

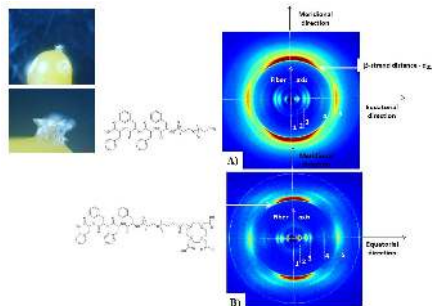


**Figure 1.** (a) and (b) show the two-dimensional SAXS pattern collected on self-assembled PEGylated tetra-phenylalanine fibers. A photo of the typical fiber is also displayed.

**Keywords:** SAXS, WAXS, nano/bio structures, hierarchical order, nanomedicine

# MS41-P3 Anomalous x-ray diffuse scattering from nanoparticles in single crystalline Ti alloys

Václav Holý<sup>1</sup>, Jana Smilauerová<sup>2</sup>, Dominik Kriegner<sup>1</sup>, Petr Harcuba<sup>2</sup>

1. Department of Condensed Matter Physics, Charles University in Prague, Czech Republic

2. Department of Material Physics, Charles University in Prague, Czech Republic

email: vasekholy@gmail.com

Metastable  $\beta$ -titanium alloys are the most prospective and versatile group of titanium alloys, as they exhibit high specific strength and good fatigue and corrosion resistance. The properties of these materials are substantially affected by alloying elements, which affect the martensitic phase transition to hexagonal  $\omega$  phase, which is observed as particles of around 10-20 nm in size uniformly dispersed throughout the  $\beta$  matrix. The chemical composition of the  $\omega$  nanoparticles and their changes during ageing from the starting quenched structure is of particular interest, since the out-diffusion of alloying atoms from the volumes of the growing nanoparticles controls the kinetics of the particle growth. We have investigated the evolution of the chemical composition of the  $\omega$  nanoparticles in single crystals of Ti+8%Mo during annealing at various temperatures, using anomalous x-ray diffraction and diffuse scattering. In this experiment we measured diffuse x-ray scattering around the diffraction peaks of the  $\omega$ - and  $\beta$ -phases for various energies in the range  $\pm 100$  eV around the MoK absorption edge, after various annealing steps. From the reciprocal-space maps of scattered intensity taken at various energies we extracted the energy dependences of the intensity scattered into various reciprocal-space points around the chosen reciprocal lattice point (RELP). Figure shows atypical reciprocal-space intensity distribution around the (006) $\beta$  RELP (panel a) and the energy dependences of the intensities extracted from rectangular regions 1-3 (b). From the data we were able to determine the densities of the Mo atoms in various iso-strain volumes around a  $\omega$ -nanoparticle and together with elasticity theory simulations we reconstructed the profile of the Mo density around the particle. From the data taken at the  $\omega$  RELP we found that a nanoparticle consists of a core with higher Mo content and a shell with almost no Mo atoms.

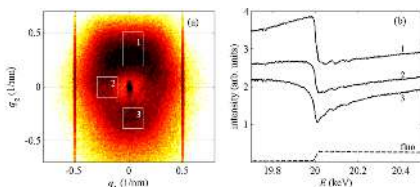


**Figure 1.** (a) Reciprocal-space map around the (006) $\beta$  maximum at 19.95 keV. (b) Energy dependences of the intensity extracted from the regions denoted by white rectangles in panel (a).

**Keywords:** Anomalous x-ray scattering, diffuse scattering, nanoparticles, Ti alloys

# MS41-P4 Multiple Bragg reflections of neutrons accompanying a strong allowed reflection at a constant neutron wavelength

Pavol Mikula<sup>1</sup>, Miroslav Vrána<sup>1</sup>, Jan Šaroun<sup>1</sup>, Jan Čapek<sup>2</sup>

1. Nuclear Physics Institute ASCR, v.v.i., 25068 Rez, Czech Republic

2. Faculty of Math. and Physics, Charles University, Ke Karlovu 5, 121 16 Prague, Czech Republic

email: mikula@ujf.cas.cz

In our contribution, the neutron diffraction results of particular studies of multiple Bragg reflection (MBR) effects accompanying a strong Si(111) reflection in the cylindrically bent perfect crystal at the neutron wavelength of 0.162 nm will be presented. Contrary to a common view that MBR effects could be considered negligible or represent maximally a few percent of an effect related to a single allowed reflection, it is shown that in the case of a homogeneously deformed perfect single crystal (in our case of cylindrically bent Si crystal) and particular diffraction geometry they can be even several times higher. For searching the MBR effects, the method of azimuthal rotation of the crystal lattice around the scattering vector of the primary reflection for a fixed wavelength was used. Cylindrically bent perfect crystal slab of Si was set in the symmetric transmission geometry for diffraction on the lattice planes (111). It has been found that multiple Bragg reflections realized in bent perfect crystals can provide intensive highly monochromatic beams which are parallel to the diffracted beam corresponding to the primary reflection. The present investigation points out on the necessity of considering the presence of MBR effects in accurate measurements of primary reflection intensities, namely, in the case of deformed single crystals.

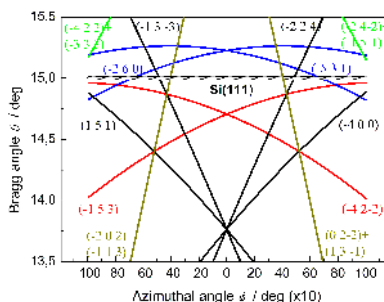


**Figure 1.** Plot of the azimuth-Bragg angle relationship for 111 primary reflection of the diamond structure at the vicinity of the Bragg angle of 15° as used in the experiment. Indexes are related only to the secondary reflections.

**Keywords:** Multiple reflections, neutron diffraction, bent perfect crystals

## MS41-P5 Neutron scattering investigations of microstructure in Al-Zn-Mg-Cu alloy prepared by spark plasma sintering

Vasyly Ryukhtin<sup>1</sup>, Přemysl Málek<sup>2</sup>, Přemysl Beran<sup>1</sup>, Pavel Strunz<sup>1</sup>, Orsolya Molnáróvá<sup>2</sup>

1. Nuclear Physics Institute v.v.i., Řež 25068, Czech Republic  
2. Department of Physics of Materials, Charles University, 121 16, Prague 2, Czech Republic

email: ryukhtin@ujf.cas.cz

Aluminum alloy samples (5.3 wt.% Zn, 2.1 wt.% Mg and 1.3 wt.% Cu) were compacted by spark plasma sintering (SPS) process from atomized powder with particle mean size of about 50  $\mu\text{m}$ . The material was prepared by same SPS procedure at various temperatures (425  $^{\circ}\text{C}$   $\div$  550  $^{\circ}\text{C}$ ). Scanning electron microscopy (SEM) images show quite complex structure of precipitates - as inside grains as well as at grain boundaries. The morphology of the phases remains complex after SPS sintering (Fig. 1 a). Small-angle neutron scattering (SANS) was applied for studying of this microstructure, since this method is very efficient for bulk investigations and it does not require any special samples preparation. High resolution double bent crystal SANS instrument MAUD [1] was utilized for studying of this alloys. The measured scattering curves obey power law with exponent quite close to -2 (see Fig. 1 b) in whole Q-range of MAUD. Such scattering behavior was observed for sedimental rocks with microstructure formed by surface fractal mesoporosity [2]. Other interpretation of such scattering is that clusters of intermetallic phases and pores form size distribution which correspond to scattering from fractal surface [3]. However neutron powder diffraction practically was not able to detect any intermetallic phase on strong background of  $\alpha$ -Al.

### Acknowledgements

This research was supported by GAČR program 14-36566G (AdMat). Also we would like to thank to Hanka Becker (TU Bergakademie Freiberg) for preparation of the samples.

### References

1. P. Mikula, P. Lukas, F. Eichhorn, *J. Appl. Cryst.* **21**, 33 (1988)
2. Radlinski, A.P. *Rev. Miner. Geochem.* **63**, 363 (2006)
3. Schmidt, P.W. *J. Appl. Crystallogr.* **15**, 567 (1982)

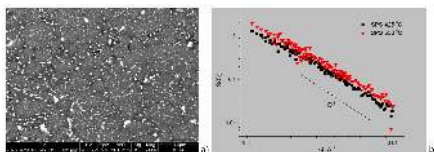


**Figure 1.** Electron micrograph of compacted at 425  $^{\circ}\text{C}$  (a) and SANS from the alloys compacted by SPS at different temperatures (b).

**Keywords:** small-angle neutron scattering, neutron diffraction, aluminum alloys

## MS41-P6 The High Energy Material Science and High Resolution Diffraction Beamlines at PETRA III

Diana Thomas<sup>1</sup>, Olof Gutowski<sup>1</sup>, Florian Bertram<sup>1</sup>, René Kirchhof<sup>1</sup>, Karthick Perumal<sup>1</sup>, Ann-Christin Dippel<sup>1</sup>, Genziana Bussone<sup>1</sup>, Abhisakh Sarma<sup>1</sup>, Uta Rütt<sup>1</sup>

1. DESY, Photon Science, Notkestr. 85, 22607 Hamburg, Germany

email: diana.thomas@desy.de

In this contribution the potential use of high energy X-ray diffraction (50 - 200 keV) and high resolution diffraction in the hard X-ray regime (5.4 - 29.4 keV) for *in situ* and *in operando* studies of nanostructured materials will be highlighted. The physics hutch of P07 operated by DESY is equipped with a heavy load diffractometer and a surface and interface diffractometer, which can be used together with an additional tilt monochromator for scattering on liquid surfaces and interfaces. Due to the high penetration depth of high energy X-rays relatively thick samples can be investigated in transmission geometry, but also grazing incidence scattering experiments can be done making use of the large reciprocal space accessible due to the high photon energies. A set of compound refractive lenses allows focusing of the X-ray beam down to  $2 \times 30 \mu\text{m}^2$  at the sample position allowing measurements of multi-layer systems, nano-rods and quantum dots. At the high resolution diffraction beamline P08 experiments on solids and liquids can be performed. For solid materials a high precision 6-circle diffractometer (Kohzu) is used, whereas liquid samples can be investigated by use of a specially designed liquid diffractometer. To achieve a high energy resolution of  $10^{-5}$  a high resolution large offset monochromator (LOM) is installed, which is also used to separate P08 from the adjacent beamline P09 and suppress higher harmonics. Using compound refractive lenses the beamline can be operated in a collimating, focusing or microfocusing mode with beam sizes between  $1500 \times 100 \mu\text{m}^2$  and  $20 \times 2 \mu\text{m}^2$ . Depending on the scientific problem (large q-range or high q-resolution) P07, P08 or a combination of both beamlines is most suitable. In this presentation a few highlight examples of the best use of the beamlines will be shown, e.g. *in situ* study of surface oxidation and growth of nanostructured layers.

**Keywords:** X-ray diffraction, beamline

## MS42 Advances in neutron scattering under non-ambient conditions

### MS42-P2 FALCON - A Laue diffractometer for ambient and non-ambient neutron structural analysis

Michael Tovar<sup>1</sup>, Lisa Diestel<sup>1</sup>, Hans-Jürgen Bleil<sup>1</sup>, Katharina Fritsch<sup>1</sup>, Klaus Habicht<sup>1</sup>, Dirk Wallacher<sup>1</sup>, Gail N. Iles<sup>2</sup>, Susan Schorr<sup>1,3</sup>

1. Helmholtz-Zentrum Berlin für Materialien und Energie

2. ANSTO, Sydney

3. FU Berlin, Germany

email: [tovar@helmholtz-berlin.de](mailto:tovar@helmholtz-berlin.de)

End of 2015 the FALCON Laue diffractometer at the Berlin neutron source BERII started. It was developed in collaboration with the ILL, Grenoble. The diffractometer is designed for fast neutron data acquisition of single crystals and makes use of a white ("pink") neutron beam with wavelength band of 0.8-3.2 Å. Pattern acquisition is performed by means of a backscattering and a transmission detector consisting of four iCDD cameras each. The detectors cover an active area of 400x400 mm<sup>2</sup>. Acquisition time depending on sample is about half up to three minutes. The sample is mounted on an irelec cradle allowing sample positioning and orienting. A chamber for sample cooling is in progress and will open up the possibility for Laue data acquisition down to temperatures of about 60K. The instrument set-up as well as some worked examples will be shown in detail.

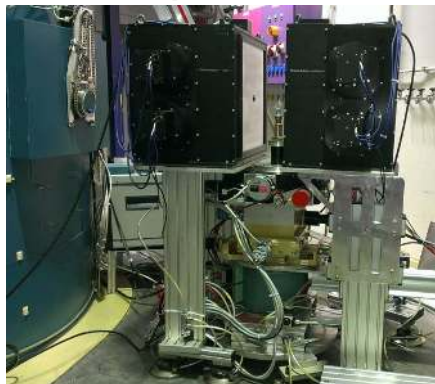


Figure 1. FALCON - Fast Acquisition Laue Camera for Neutrons

**Keywords:** Neutron diffraction, Laue technique

Chairs: Jiri Kulda, Stefan Klotz

### MS42-P1 Neutron diffraction on methane and hydrogen hydrates under high pressure

Umbertoluca Ranieri<sup>1,2</sup>, Livia E. Bove<sup>1,3</sup>, Stefan Klotz<sup>1</sup>, Thomas C. Hansen<sup>2</sup>, Michael M. Koza<sup>2</sup>, Philippe Gillet<sup>1</sup>, Dirk Wallacher<sup>1</sup>, Andrzej Falenty<sup>3</sup>, Werner F. Kuhs<sup>3</sup>

1. Ecole Polytech Fed Lausanne, Inst Cond Matter Phys, EPSL, CH-1015 Lausanne, Switzerland

2. Institut Laue-Langevin, CS 20156, 38042 Grenoble, France

3. IMPMC, CNRS-UMR 7590, Université Pierre & Marie Curie, 75252 Paris, France

4. Experimental Physics, Saarland University, D-66041 Saarbrücken, Germany and Department Sample Environments, Helmholtz-Centre Berlin for Energy and Materials, Hahn-Meitner-Platz 1, D-14109 Berlin, Germ

5. IGZG Abteilung Kristallographie, Universität Göttingen, Goldschmidtstrasse 1, 37077 Göttingen, Germany

email: [umbertoluca.ranieri@epfl.ch](mailto:umbertoluca.ranieri@epfl.ch)

Gas hydrates are crystalline solids composed of water and gas. They have attracted considerable attention over the past decade both for their geophysical relevancy [1] and for their possible application to gas storage [2]. Pressure is a key parameter in the study of these systems as gas hydrates are believed to exist at pressure in nature and the gas content is found to increase in gas hydrates as their crystalline structure rearranges upon compression. In addition, high-pressure studies on gas hydrates offer new possibilities to explore water-gas interactions.

We will present recent work on methane and hydrogen hydrates at high pressure performed by neutron diffraction in the GPa range [3]. Several issues including the gas content in the different high-pressure structures will be discussed.

[1] J. S. Loveday and R. J. Nelmes, Phys. Chem. Chem. Phys. 2008 10, 937–950.

[2] V. V. Struzhkin et al., Chem. Rev. 2007, 107, 4133–4151.

[3] U. Ranieri et al. in preparation.

**Keywords:** neutron diffraction, high-pressure, gas hydrates

## MS42-P3 News from the Swiss Spallation Neutron Source SINQ: Diffraction at Non-Ambient Conditions

Christian Rüegg<sup>1,2</sup>, Romain Sibille<sup>1</sup>, Jürg Schefer<sup>1</sup>, Vladimir Pomjakushin<sup>1</sup>, Denis Sheptyakov<sup>1</sup>, Lukas Keller<sup>1</sup>, Emmanuel Canevet<sup>1</sup>, Tobias Panzner<sup>1</sup>, Oksana Zaharko<sup>1</sup>

1. Laboratory for Neutron Scattering and Imaging, Paul Scherrer Institute

2. Department of Quantum Matter Physics, University of Geneva

email: christian.rueegg@psi.ch

We present news from the Swiss Spallation Neutron Source SINQ and its instruments for neutron diffraction. The neutron diffraction group operates four instruments: the single-crystal diffractometer ZEBRA, the two powder diffractometers HRPT and DMC, and the strain scanner POLDI as shown in Fig. 1.

The new neutron single-crystal diffractometer ZEBRA, which replaces the TriCS instrument, is now in commissioning phase. It will allow crystallographic and parametric studies (temperature, magnetic and electric fields, pressure). ZEBRA is designed to achieve high peak-to-background ratio and to operate in high magnetic fields up to 11 Tesla. The instrument is aimed at resolving challenges emerging in systems that are available as small crystals only and requiring extreme sample environments.

The applications of the thermal high-resolution multi-detector powder diffractometer HRPT are high-resolution refinements of chemical and magnetic structures as well as phase analysis of novel materials. Recently HRPT was equipped with computer controlled sample changers of eight (RT) and five (1.7-310 K) samples with sample rotation, which significantly increases the efficiency of operation. The exclusive stroboscopic mode allows measurements of crystal structures as a function of time with time resolution down to 10ms.

The cold neutron powder diffractometer DMC is complementary to HRPT and ZEBRA and is designed for high-intensity measurements of weak magnetic intensities. Its recent success in mapping the reciprocal space of single crystals prompts the development of a new high-efficiency two-dimensional neutron detector, which will be available in the near future. A new non-magnetic sample table allows fields up to 6 Tesla.

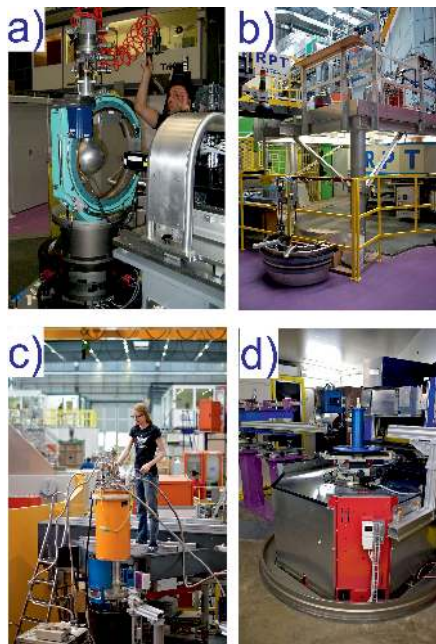


**Figure 1.** Diffraction instruments at the Swiss Spallation Neutron Source SINQ: a) ZEBRA, b) HRPT, c) DMC and d) POLDI.

**Keywords:** neutron diffraction, instrumentation, pressure, magnetic fields

## MS43 Combining x-ray diffraction and other techniques for in situ and operando studies

Chairs: Helmut Ehrenberg, François Fauth

### MS43-P1 Advances in the X-ray Rotation-Tilt Technique

Jürgen Bauch<sup>1</sup>, Stefan Enghardt<sup>1</sup>, Mirko Heckert<sup>1</sup>

<sup>1</sup> TU Dresden, Institut für Werkstoffwissenschaft

email: juergen.bauch@tu-dresden.de

The X-Ray Rotation Tilt technique (XRRT) [1-2] is an X-ray microdiffraction method in which X-ray interference patterns are produced by directing a monochromatic X-ray or synchrotron beam of high intensity and small diameter onto a monocrystalline region of a sample. Each diffracting lattice plane defines a set of concentric cones with a half opening angle equal to  $90^\circ - Q_{hkl}$ , whereas  $Q_{hkl}$  denotes the BRAGG angle. If the incident monochromatic X-ray beam coincides with a generatrix of the interference cone, then the diffracted line on the diametrically opposite side of the cone can generate a small spot on a detector. By moving the sample in a specific way (several rotation-tilt movements whilst the rotation of the sample and detector is constrained to one synchronous rotation around a common axis) it is possible to accumulate such spots on a detector system (e.g. X-ray film, image plate or CCD area detector) which faces the sample (Fig. 1 top). These reflections in entirety form the so-called XRRT lines on the detector. Fig. 1 (bottom) shows an example of an XRRT pattern.

This technique can be applied to a wide range of analytical problems in materials diagnostics, e.g. high-accuracy determination of crystallographic orientations and lattice constants, determination of dislocation density and decrease in symmetry, precision determination of residual stress/strain and phase identification in micro regions. The applicability of the method will be demonstrated by highlighting the results of some selected examples measured on functional materials. For example, the measurement of the transition from the cubic high temperature phase of Barium titanate to the tetragonal room temperature phase shows clearly a well-marked decrease of symmetry in the XRRT-Patterns in Fig. 1 (bottom). By using a new tool based on focal curves it is now possible to automatically determine the orientation and position of the sample from one single pattern. In this example, it permits the determination of the lattice constants of the two  $\text{BaTiO}_3$ -Phases and the direction of the strain during the structural phase transition (Fig. 1 bottom right). This new tool also facilitates the evaluation of XRRT-Patterns of more complex crystal structures, where a manual indexation of the reflections is usually not feasible.

[1] Ullrich, H.-J.; Greiner, W.: Patent WP 139 671, Berlin 1977

[2] Bauch, J.; Ullrich, H.-J.; Reiche, D.: Acta Cryst. Vol. A55 (1999), Supplement

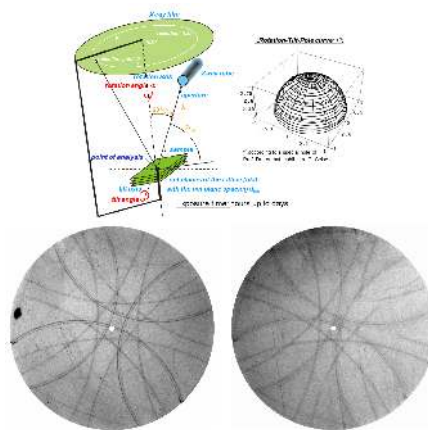


**Figure 1.** Principle of the X-ray-Rotation-Tilt Method (top). XRRT pattern of  $\text{BaTiO}_3$  at 20°C (bottom left) and at 130°C (bottom right). The white dot marks the rotation center which is close to the 100-pole.

**Keywords:** X-ray Microdiffraction, X-ray Rotation-Tilt Technique, crystallographic orientation, lattice constants, dislocation density, residual stress/strain



## MS43-P2 Investigation of thermal stability of Cu/W multilayers by in-situ x-ray diffraction

Claudia Cancellieri<sup>1</sup>, Frank Moszner<sup>1</sup>, Mirco Chiodi<sup>1</sup>, Songhak Yoon<sup>1</sup>, Daniel Ariosa<sup>2</sup>, Jolanta Janczak-Rusch<sup>1</sup>, Lars Jeurgens<sup>1</sup>

1. Empa, Swiss Federal Laboratories for Materials Science and Technology, Überlandstrasse 129, Dübendorf CH-8600, Switzerland

2. Instituto de Física, Facultad de Ingeniería, Universidad de la República, Herrera y Reissig 565, C.C. 30, Montevideo 11000, Uruguay

email: claudia.cancellieri@empa.ch

Interfacial effects can dominate multilayer structure and properties leading to unusually large strains and frequently stabilization of metastable structures. The total Gibbs energy of nanomultilayered (NML) systems is indeed strongly governed by the excess energy contributions originating from the very high density of internal interfaces (i.e. grain boundaries and phase boundaries) [1]. Consequently, NML systems are intrinsically thermodynamically unstable, especially towards higher temperatures. Furthermore, the thermal expansion mismatch between the alternating nanolayers and the substrate can impose huge thermal stresses during heating which, if relaxed by plastic deformation, can also cause a degradation of the nano-laminated structure upon heating. In this work, we report on the delicate interplay between the (residual) stresses, texture, grain size and epitaxy in Cu/ W NML upon thermal treatment at different temperatures in a controlled atmosphere. Alternating nanolayers of Cu and W with individual thicknesses varied between 5-20 nm were prepared by magnetron sputter deposition on an Al<sub>2</sub>O<sub>3</sub> (C- and R-oriented) and Si-substrate [2]. The thermal stability of Cu/W nano-multilayers up to 900 °C has been in-situ investigated by X-ray diffraction (see Figure). The individual layer thickness and the relative in-plane and out of plane orientations are found to have an important effect in the thermal stability of the system. The initial stress state of the multilayer can change considerably upon thermal annealing. The microstructure evolution upon heating is the result of the interplay between the thermally induced stress, including the role of the substrate, and the growth-related internal stress. Different techniques including high-resolution scanning electron microscopy, X-ray photoelectron spectroscopy were also employed to study the thermal effect on the morphology and microstructure. It follows that the individual layer thickness and (in-plane and out-of-plane) textures in the as-deposited state have a pronounced effect on the thermal stress evolution of the individual Cu and W nanolayers upon thermal annealing; i.e. the accumulated thermal stresses in the individual Cu and W nanolayers are superimposed on the intrinsic growth stresses and become relaxed at around  $T \sim 750^\circ\text{C}$ , which coincides with the thermal activation of W migration along internal interfaces (i.e. phase and grain boundaries) [2].

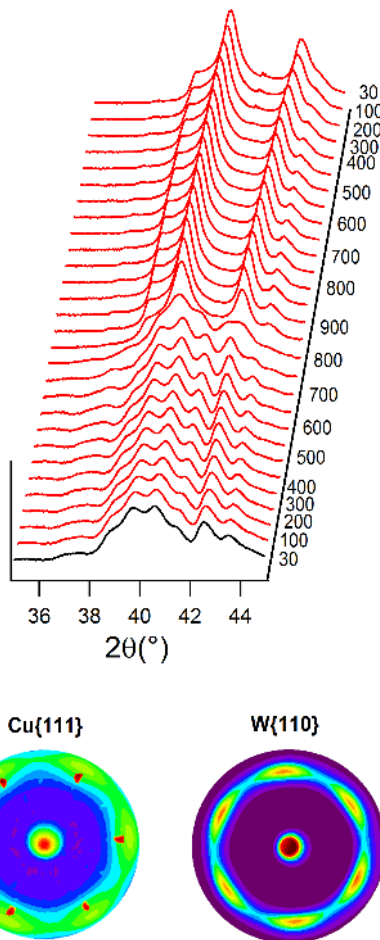


**Figure 1.** Structural evolution of W(110) and Cu(111) superlattice reflections upon thermal treatment (during heating from room temperature till 900°C and cooling). On the bottom, room temperature pole figures of Cu and W indicating precise crystallographic relation between the layers.

**Keywords:** X-ray diffraction, Microstructure, Morphological stability



## MS43-P3 An Add-on Device for Automated *In Situ* Screening

Angela Criswell<sup>1</sup>, Colin Acheson<sup>1</sup>, Pierre Le Magueres<sup>1</sup>, Thom Hendrixson<sup>1</sup>, Cheng Yang<sup>2</sup>, Zhao Zijian<sup>3</sup>, Joseph D. Ferrara<sup>1</sup>

1. Rigaku Oxford Diffraction
2. Beijing Liangjia Deshi Technology Ltd. Co.
3. Rigaku Beijing Corp

email: [angela.criswell@rigaku.com](mailto:angela.criswell@rigaku.com)

*In situ* screening of crystallization trials continues to be a topic of importance. *In situ* screening allows one to determine if the crystal-like object in a trial is salt, protein or something else of interest. Furthermore, crystal quality can be assessed before cryoprotection is attempted, providing a means to better optimize this step. Finally, some crystals are well-behaved enough that complete or nearly-complete data sets can be collected *in situ*, eliminating the need for harvesting and cryoprotection altogether.

In this presentation we will show results from a newly developed automated *in situ* screening system designed specifically to work with legacy Rigaku diffractometers, extending their utility. The system is easy to install and deinstall so one can go from collecting data on cryo-protected samples to *in situ* screening in minutes. The system uses the same software as the Rigaku Oxford Diffraction PXScanner, CrystalEyes, making the transition between dedicated and part time systems easy.

**Keywords:** in situ crystallography

## MS43-P4 Enol-imine/keto-amine tautomerism of (E)-4-[(2-hydroxybenzylidene)amino]phenyl benzenesulfonate

Muharrem Dinçer<sup>1</sup>, Namık Özdemir<sup>2</sup>, Reyhan Kağıt<sup>3</sup>, Osman Dayan<sup>3</sup>

1. Department of Physics, Faculty of Arts and Sciences, Ondokuz Mayıs University, 55139, Samsun, Turkey
2. Department of Secondary School Science and Mathematics Education, Faculty of Education, Ondokuz Mayıs University, 55139, Samsun, Turkey
3. Department of Chemistry, Faculty of Arts and Sciences, Çanakkale Onsekiz Mart University, 17020, Çanakkale, Turkey

email: [mdincer@omu.edu.tr](mailto:mdincer@omu.edu.tr)

The title Schiff base compound has been obtained from the reaction of 4-aminophenyl benzenesulfonate and salicylaldehyde, and characterized by spectroscopic and single-crystal X-ray diffraction techniques. Quantum chemical calculations employing density functional theory (DFT) method with the 6-311++G(d,p) basis set were performed to study the molecular, spectroscopic and enol-imine/keto-amine tautomerization mechanism of the compound. There exists a good correlation between experimental and theoretical data. The tautomerization mechanism was investigated in the gas phase and in solution phase using the polarizable continuum model (PCM) approximation. The energetic and thermodynamic parameters of the enol-imine → keto-amine transfer process show that the single proton exchange is unfavored in all cases. However, the reverse reaction seems to be feasible with a very low barrier height and is supported by negative values in enthalpy and free energy changes for all cases.

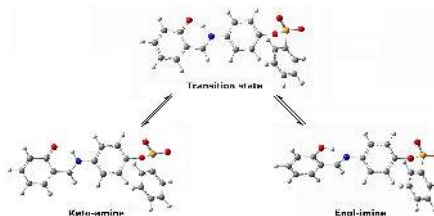


**Figure 1.** Tautomerization of the title compound.

**Keywords:** Crystal structure, DFT, Enol-imine/keto-amine tautomerism

## MS43-P5 Thermal Polymorphism and Decomposition of $M(\text{BH}_4)_2$ ( $M = \text{Sr}$ , $\text{Ba}$ and $\text{Eu}$ ) studied by in situ XRPD, FTIR and DFT Calculations

Emilie Didelot<sup>1</sup>

1. Laboratoire de Cristallographie, Université de Geneve

email: emilie.didelot@unige.ch

The renewed interest in metal borohydrides over the past few years is owed (i) to their high volumetric and gravimetric hydrogen content and (ii) high mobility of charge carriers commonly used in batteries, in particular  $\text{Li}^+$  and  $\text{Na}^+$ . Here, the thermal polymorphism and decomposition of  $M(\text{BH}_4)_2$  ( $M = \text{Sr}$ ,  $\text{Ba}$  and  $\text{Eu}$ ) is studied by combining in situ X-ray powder diffraction (XRPD) with FTIR and ab initio solid state calculations.

We have optimized a halide-free synthesis method for bivalent metals, and carried out a detailed investigation of the temperature-dependent crystal structure of three halide-free borohydrides  $M(\text{BH}_4)_2$  ( $M = \text{Eu}$ ,  $\text{Sr}$ ,  $\text{Ba}$ ) as well as their thermal decomposition.<sup>1</sup> The absence of remnant solvent molecules has been verified by FTIR. Synchrotron radiation - XRPD collected on a 2D detector (SNBL, ESRF) while heating the sample has allowed to separate various sets of diffraction peaks in a multiphase sample and to solve ab initio crystal structures of novel polymorphs and decomposition product after hydrogen release. Due to the limits imposed by powder diffraction in these cases a given structural model cannot always be chosen unambiguously. Where more than one chemically sensible structure was determined we performed solid state calculations (DFT) to optimize structural features and inspect the resulting energies. Two alkali metals ( $\text{Sr}$  and  $\text{Ba}$ ) and one bivalent rare earth ( $\text{Eu}$ ) crystallize in structures derived from known structure types based on a *hcp* of anions (rutile and  $\alpha\text{-PbO}_2$  types) and on simple cubic packing of anions (*ccp* packing of cations) as in  $\text{CaF}_2$  type.

Halide free compounds show higher thermal stability than the previously reported materials obtained from chloride based synthesis.<sup>2-4</sup> The thermal decomposition route of all three borohydrides is rather complex involving unidentified phases, but in the cases of  $\text{Sr}$  and  $\text{Eu}$  results in  $M_2(\text{BH}_4)\text{H}_3$ , a first compound containing hydride in two anions, as a simple hydride and as a complex borohydride.

**Keywords:** borohydride, in situ x-ray powder diffraction, DFT calculation, IR spectroscopy, hydride

## MS43-P6 The Application of Silver X-ray's in Single Crystal Diffraction

Alexandra Griffin<sup>1</sup>, Fraser White<sup>1</sup>

1. Rigaku Oxford Diffraction

email: Alex.griffin@rigaku.com

Rigaku Oxford Diffraction has a range of high-flux, low maintenance micro-focus sources to suit even the most challenging of samples. Weakly diffracting proteins and small molecule crystals can be studied using **Nova** ( $\text{Cu}$ ) sources. The Nova source is ideal for absolute structure determination on pure organic compounds. Samples that suffer from absorption can be looked at with the **Mova** ( $\text{Mo}$ ) source, which also opens up the possibility to perform charge density experiments, as well as high pressure studies. The new Rigaku Oxford Diffraction micro-focus silver source, **Silva**, extends the ability to study a wider range of samples than using traditional copper or molybdenum wavelengths.

The shorter wavelength of the silver source (0.56 Å compared to 0.71 Å for molybdenum) means that it is now possible to measure very highly-absorbing samples, obtain better completion on high pressure setups, and choose to either push the resolution limits of charge density experiments, or perform single-theta charge density measurements. Here we describe a variety of experiments with the Silva source and its enhancements over other wavelengths with the results showing that, in many cases, silver radiation outperforms in terms of data quality and data collection time over other available wavelengths.



**Figure 1.** The Silver Microfocus Source

**Keywords:** Silver, X-ray Diffraction, High pressure, Charge Density

### MS43-P7 Solid-state reactivity explored *in situ* by synchrotron radiation on single crystals of SrFeO<sub>2.5</sub> during electrochemical oxygen intercalation

Avishek Maity<sup>1</sup>, Rajesh Dutta<sup>1</sup>, Bartosz Penkala<sup>1</sup>, Monica Ceretti<sup>1</sup>, Angélique Letrouit-Lebranchu<sup>1</sup>, Dmitry Chernyshov<sup>2</sup>, Werner Paulus<sup>1</sup>

1. Institut Charles Gerhardt, UMR 5253, Université de Montpellier, 34095 Montpellier, FR  
2. BM01A, SNBL, ESRF, 71-Avenue des Martyrs, Grenoble, FR

email: avishek.maity@univ-montp2.fr

Due to the high performance of modern x-ray and neutron diffractometers, the chemical reactivity of solids is studied today routinely under *in situ* conditions on polycrystalline samples in specific reaction chambers. This technique became the standard characterization not only for battery systems but also for catalysis and many other applications. Following up chemical solid-state reactions on single crystals would be even more powerful, as it would allow to scanning the whole reciprocal space. Recent developments concerning fast and low-noise 2D-detectors, together with a high primary beam quality, especially available at large scale facilities but also via  $\mu$ -focus type x-ray sources using standard laboratory equipment, present a huge potential for the study of solid-state reactions on single crystals in real time. It allows to obtain valuable information about diffuse scattering and weak super-structure reflections, as well as microstructural aspects, partially impossible to access by powder diffraction.

We report here on the electrochemical oxygen intercalation reaction on SrFeO<sub>2.5</sub>, followed up *in situ* by x-ray diffraction in a dedicated, miniaturized electrochemical cell, mounted on the BM01A goniometer. We were especially interested to structurally explore the phase diagram of SrFeO<sub>3-x</sub> at ambient temperature, as it is interesting from a crystal chemistry point of view. We report here on the characterization of intermediate phase products in course of the reaction and related changes in the twin structure. In addition, all involved phases show interesting physical properties, beside their outstanding performance as oxygen membranes in SOFCs for energy storage and conversion.

#### Reference:

[1] Maity A., Dutta R., Penkala B., Ceretti M., Letrouit-Lebranchu A., Chernyshov D., Perichon A., Piovano A., Bossak A., Meven M and Paulus W 2015 Solid-state reactivity explored *in situ* by synchrotron radiation on single crystals: from SrFeO<sub>2.5</sub> to SrFeO<sub>3</sub> via electrochemical oxygen intercalation *J. Phys. D: Appl. Phys.* **48** 504004

**Keywords:** *in situ* diffraction, non-stoichiometric oxides, synchrotron radiation, diffuse scattering, twinning, chemical reactivity of solids, electrochemistry

### MS43-P8 Synchrotron Experiments in Large Volume Presses at High Pressure and High Temperature at different Spinels

Christian Lathe<sup>1</sup>, Michael Wehber<sup>1</sup>, Jörn Lauterjung<sup>1</sup>

1. GFZ German Research Centre for Geosciences, Telegrafenberg, 14473 Potsdam, Germany

email: lathe@gfz-potsdam.de

For geoscientists, material scientists, physicists and chemists it is very important to study the samples under extreme conditions. It is necessary to use *in-situ* X-ray diffraction experiments at synchrotron beamlines because of the high intensity and the broad energy range to figure out the stability of minerals under high pressure and temperature, the determination of bulk moduli, the thermal expansion, phase diagrams, and the behaviour of kinetic measurements.

The Large Volume Presses were located at the Hamburger Synchrotron Laboratory (HASYLAB) at the DORIS III storage ring. The experiments were carried out using the high pressure multi anvil devices MAX80 (F2.1) and MAX200x (W2). The F2.1 beamline was a bending magnet beamline with a critical energy of 16.6 keV and an energy range up to 75 keV. The W2 beamline was a hard-wiggler beamline with a critical energy of 26.4 keV and an energy range up to 150 keV. Energy-dispersive X-ray diffraction was used to determine the pressure and temperature induced volume change. Isothermal experiments were performed up to 15 GPa at ambient temperature.

Many spinels show phase transformations under pressure (Funamori et al. 1998 [1], Irifune et al. 2002 [2]) and are used as model structures for deep earth mineralogy and for a better understanding of underlying high-pressure phase transition mechanisms. It is widely accepted that the behavior within the transition zone of the Earth's interior (410-670 km depth) is strongly linked to the properties of minerals showing spinel or pseudospinel structure.

The pressure dependence of the thermal expansion coefficient is examined on three different spinels, while systematically varying the iron contents. All three minerals, Magnetite (Fe<sup>2+</sup>Fe<sup>3+</sup><sub>2</sub>O<sub>4</sub>), Franklinite (Zn<sup>2+</sup>Fe<sup>3+</sup><sub>2</sub>O<sub>4</sub>) and Gahnite (Zn<sup>2+</sup>Al<sup>3+</sup><sub>2</sub>O<sub>4</sub>) adopt the normal spinel structure. Derived from compression experiments using MAX80 apparatus up to 5 GPa at temperatures of 298, 500, 700, 900 and 1100 K.

[1] Funamori, N., Jeanloz, R., Nguyen, H., Kavner, A., Cadwell, W.A., Fujino, K., Miyajima, N., Shinmei, T., and Tomioka, N. (1998) High-pressure transformation in MgAl<sub>2</sub>O<sub>4</sub>. *Journal of Geophysical Research*, 103, 20813-20818.

[2] Irifune, T., Naka, H., Sanehira, T., Inoue, T., and Funakoshi, K. (2002) *In situ* X-ray observations of phase transitions in MgAl<sub>2</sub>O<sub>4</sub> spinel to 40 GPa using multi-anvil apparatus with sintered diamond anvils. *Physics and Chemistry of Minerals*, 29, 645-654.

**Keywords:** Synchrotron, High Pressure, High Temperatures

## MS43-P9 New Facility for Long Duration Experiments at Diamond Light Source

Claire A. Murray<sup>1</sup>, Jonathan Potter<sup>1</sup>, Sarah J. Day<sup>1</sup>, Annabelle R. Baker<sup>1</sup>, Stephen P. Thompson<sup>1</sup>, Jon Kelly<sup>1</sup>, Christopher G. Morris<sup>2</sup>, Sihai Yang<sup>2</sup>, Hilary Kennedy<sup>3</sup>, Chiu C. Tang<sup>1</sup>

1. Diamond Light Source, Harwell Science and Innovation Campus, Didcot, OX11 0DE, UK
2. School of Chemistry, University of Manchester, Manchester, M13 9PL, UK
3. School of Ocean Sciences, Bangor University, Menai Bridge, Anglesey, LL59 5AB, UK

email: [claire.murray@diamond.ac.uk](mailto:claire.murray@diamond.ac.uk)

The high brightness beamline I11 at Diamond Light Source is a dedicated powder diffraction instrument which has been in user operation for a number of years. Equipped with multi-analysing crystals (MAC) and fast position-sensitive detectors, it is routinely used for high-resolution and time-resolved experiments [1-3]. Recently, a new facility for long duration experiments (LDE) has been added. Now in operation mode, this facility houses the necessary hardware and equipment for multiple LDE studies. These experiments are mounted on a large sample table equipped with adjustable linear drives to automatically and periodically move sample cells in and out of the beam and the Pixium area detector. LDE are set up and left in place with programmed automated data collections over periods of months or years. Sample environments such as electrochemical cyclers, incubators, heating stages, environmental chambers and high pressure gas cells are accommodated for user operation.

To complement the existing I11 facilities, the LDE hutch opens up new opportunities for those experiments which require weeks to months of periodically monitoring "slow" changes, up to two years. It is of particular benefit to research areas where important information on the development of phases over time cannot be obtained via ex-situ methods. Areas that benefit include studies of crystallization, battery materials, gas storage, mineral evolution, seasonal effects, thermal and electrical cycling and corrosion science. With a versatile design and many automated features such as robotic sample changers, the upgraded beamline is used by many academic researchers from diverse scientific backgrounds and industries. Recent results from LDE experiments on cement have revealed a new type of cement which is up to 50% more effective than previously proposed barrier solutions for containing nuclear waste in deep geological disposal facilities [4].

### References:

- [1] S. P. Thompson, J. E. Parker, J. Potter, T. P. Hill, A. Birt, T. M. Cobb, F. Yuan, and C. C. Tang, *Review Sci. Inst.* 2009, 80, 075107, [2] S.P. Thompson, J.E. Parker, J. Marchal, J. Potter, A. Birt, F. Yuan, R.D. Fearn, A.R. Lennie, S.R. Street and C.C. Tang, *J. Synchrotron Rad.*

2011, 18, 637, [3] J.E. Parker, S.P. Thompson, T.M. Cobb, F. Yuan, J. Potter, A.R. Lennie, S. Alexander, C.J. Tighe, J.A. Darr, J.C. Cockcroft and C.C. Tang, *J. Applied Crystallog.* 2011, 44, 102, [4] <http://www.bbc.co.uk/news/science-environment-35571793>

**Keywords:** Powder Diffraction, In-situ Measurements, Synchrotron Instrumentation

### MS43-P10 Characterization of amorphous high-surface area magnesium carbonate (Upsalite) using laboratory diffractometer

Olga Narygina<sup>1</sup>, Marco Sommariva<sup>1</sup>, Sara Frykstrand<sup>2</sup>, Johan Forsgren<sup>2</sup>

1. PANalytical B.V., Almelo, The Netherlands

2. Division for Nanotechnology and Functional Materials, Department of Engineering Sciences, The Ångström Laboratory, Uppsala University, Uppsala, Sweden.

email: olga.narygina@panalytical.com

Micro- and mesoporous inorganic solids with a large surface areas and controllable pore size are extensively studied due to the numerous potential applications for this type of materials as catalysis and sorption media, for gas storage and separation, as vaccine adjuvants and drug delivery vehicles, in regeneration of bone tissue, in cosmetics, etc. Need for the materials with a disordered interconnected pore network easily accessible for external components, possibility of *in situ* loading of the pores with active agents during synthesis process as well as reduction of production cost and environmental impact are the driving forces for the development of template-free synthesis of porous materials. Recently Frykstrand et al. [1,2] reported the formation of a mesoporous, extraordinary moisture-absorbing, amorphous, high-surface area magnesium carbonate (Upsalite) synthesized without the use of surfactants as pore forming agents. In the attempt to understand the pore formation mechanism in Upsalite and to characterize the properties of this novel material a number of experimental techniques, including electron microscopy, X-ray scattering and spectroscopy techniques, infrared spectroscopy, were used. The outcome of this comprehensive study will be published separately (Cheung et al., in preparation). Here we present the results of small-angle X-ray scattering (SAXS) and total X-ray scattering for pair distribution function (PDF) study of Upsalite.

PDF analysis enabled characterization of short and long-range order in the amorphous Upsalite. The majority of PDF features are explained by magnesium carbonate alone, but the quality of the fitting is improved by including MgO. The PDF results are in agreement with the high-resolution TEM and XPS suggesting composite nature of Upsalite (MgO/MgCO<sub>3</sub>).

SAXS experiment confirmed the mesoporous structure of Upsalite. Furthermore, using SAXS at controlled temperature and relative humidity the water sorption process and its effect on the pore structure of Upsalite was characterized *in situ*.

[1] Forsgren J, Frykstrand S, Grandfield K, Mihranyan A, Strømme M (2013) PLoS ONE 8(7): e68486. doi:10.1371/journal.pone.0068486

[2] Frykstrand S, Forsgren J, Mihranyan A and Strømme M (2014) Micropor. Mesopor. Mat. **190**, 99. DOI: 10.1016/j.micromeso.2013.12.011

**Keywords:** mesoporous, Upsalite, SAXS, PDF, *in situ*

### MS43-P11 Formation and high-temperature stability of metastable (Cr,Zr)<sub>2</sub>O<sub>3</sub>/(Zr,Cr)O<sub>2</sub> nanocomposites

David Rafaja<sup>1</sup>, Christina Wüstefeld<sup>1</sup>, Gintautas Abrasonis<sup>2</sup>, Stefan Bräunig<sup>1</sup>, Carsten Baecht<sup>2</sup>, Milan Dopita<sup>2</sup>, Matthias Krause<sup>2</sup>, Sibylle Gemming<sup>2</sup>

1. Technische Universität Bergakademie Freiberg, Institute of Materials Science, Germany

2. Helmholtz-Zentrum Dresden-Rossendorf, Dresden, Germany

3. Department of Condensed Matter Physics, Charles University Prague, Czech Republic

email: rafaja@ww.tu-freiberg.de

Successive crystallization of amorphous Cr-Zr-O thin films, formation of the (Cr,Zr)<sub>2</sub>O<sub>3</sub>/(Zr,Cr)O<sub>2</sub> nanocomposites and thermally induced changes in the hexagonal crystal structure of metastable (Cr,Zr)<sub>2</sub>O<sub>3</sub> were investigated by means of *in situ* high-temperature synchrotron diffraction experiments up to 1100°C. The thin films of Cr-Zr-O were deposited at room temperature using reactive ion beam sputtering from zonal Cr-Zr targets under oxygen flow. The resulting amorphous Cr-Zr-O solid solutions contained up to 15 at.% Zr. During the annealing in vacuum, the Cr-Zr-O solid solutions decomposed into two metastable phases, Cr-rich (Cr,Zr)<sub>2</sub>O<sub>3</sub> and Zr-rich (Zr,Cr)O<sub>2</sub>, which crystallized in hexagonal and tetragonal structure, respectively. With increasing Zr content in amorphous Cr-Zr-O, the start of the phase segregation and crystallization was shifted from 600°C at 3 at.% Zr to 1000°C at 15 at.% Zr. With the aid of the *in situ* high-temperature synchrotron powder diffraction experiments, it was found that the metastable Cr<sub>2-2x</sub>Zr<sub>x</sub>O<sub>3-x</sub> can accommodate up to approx. 3 at.% Zr. The zirconium atoms occupy partially the Wyckoff positions 6b in the corundum-like crystal structure of Cr<sub>2</sub>O<sub>3</sub> that are empty in the stoichiometric chromium oxide. The incorporation of Zr into the crystal structure of Cr<sub>2</sub>O<sub>3</sub> inflated the elementary cell and modified the thermal expansion of Cr<sub>2-2x</sub>Zr<sub>x</sub>O<sub>3-x</sub>. The tetragonal structure of zirconia was stabilized by chromium. The phase segregation during the crystallization led to the formation of (Cr,Zr)<sub>2</sub>O<sub>3</sub>/(Zr,Cr)O<sub>2</sub> nanocomposites. The size of crystallites in these nanocomposites decreased with increasing Zr content from 60 nm to 30 nm and increased only slightly at the highest annealing temperatures. In summary, this contribution illustrates the microstructure design in nanocomposites on the example of metastable chromium and zirconium oxides.

**Keywords:** Cr-Zr-O nanocomposites, *in situ* high-temperature synchrotron diffraction, metastable Cr(2-2x)Zr(x)O(3-x)

# MS43-P12 Structural response of melt-spun poly(3-hydroxybutyrate) fibers to heat and stress investigated by wide-angle X-ray diffraction (WAXD) and small-angle X-ray scattering (SAXS)

Felix A. Reifler<sup>1,2</sup>, Rudolf Hufenus<sup>2</sup>

1. Empa, Swiss Federal Laboratories for Materials Science and Technology, Center for X-ray Analytics, Überlandstrasse 129, 8600 Dübendorf, Switzerland

2. Empa, Swiss Federal Laboratories for Materials Science and Technology, Laboratory for Advanced Fibers, Lerchenfeldstrasse 5, 9014 St. Gallen, Switzerland

email: felix.reifler@empa.ch

Poly(3-hydroxybutyrate) (P3HB) is produced by bacteria as intracellular carbon and energy storage compound. P3HB is sustainable, biocompatible and biodegradable, and it qualifies for the use in numerous textile and medical applications due to its exceptional properties as well as reasonable production costs via a relatively simple biosynthesis process. The brittleness of native P3HB and its rapid thermal degradation at temperatures just above the melting temperature, however, makes melt-spinning of P3HB into fibers a challenging task. The issue has been previously addressed in the scientific literature, but at the laboratory scale only, and up to now, melt-spinning of P3HB at large scale is not feasible.

By performing studies regarding the effects of additives and of modifications of the draw-off unit on the melt-spinning performance of P3HB, we succeeded in developing an upscalable melt-drawing method for P3HB fibers, leading to fibers exhibiting promising tensile strengths up to 215 MPa.

In the equatorial 2Theta scan of the WAXD patterns of these fibers, we observed a series of local maxima and postulated a highly ordered amorphous phase, which is kinetically trapped between the aligned lamellae of the crystalline  $\alpha$ -phase [1]. This is in contrast to the previous literature, where diffraction signals in this region are commonly described as one reflection, assigned to the so-called "β-form" of P3HB. In our model, the local maxima in the 2Theta scan correspond to preferred distances between polymer chains that are oriented nearly parallel to, but irregularly arranged along the fiber direction.

For the present study, P3HB fibers are subjected to various tensions and temperatures. The intensities of the highly oriented (020) and (110) reflections, e.g., decrease with increasing tension (Fig.1). Simultaneously, the intensity of the reflections assigned to the highly ordered amorphous phase is considerably increasing. Cyclic change of load reveals a high degree of reversibility for these phenomena, which supports our model of the highly ordered amorphous phase described above. This and more results of *in-situ* WAXD and SAXS experiments to trace the structural response of the P3HB fibers will be presented.

[1] Hufenus R, Reifler FA, Fernandez-Ronco MP, Heuberger M. Eur Polym J. 2015; 71:12-26.

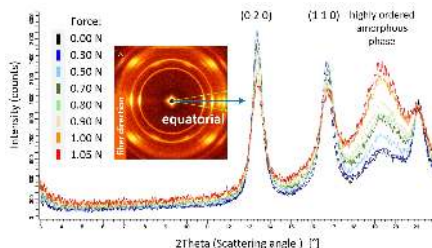


**Figure 1.** Structural response of a P3HB fiber to increasing tensional forces. 2Theta scans of equatorial sectors in the WAXD pattern. Under load, the orientation of the amorphous phase is enhanced, to the disadvantage of the orientation in the crystalline phase.

**Keywords:** fiber, melt-spinning, biopolyester, biopolymer, wide-angle X-ray diffraction, WAXD, small-angle X-ray scattering, SAXS

### MS43-P13 HEIMDAL@ESS – Going beyond a classical neutron powder diffractometer

Jürg Schefer<sup>1</sup>, Sonja L. Holm<sup>2,3</sup>, Mads Bertelsen<sup>2,3</sup>, Kim Lefmann<sup>2</sup>, Paul Henry<sup>4</sup>, Björn C. Hauback<sup>5</sup>, Mogens Christensen<sup>6</sup>

1. Laboratory for Neutron Scattering and Imaging (LNS), Paul Scherrer Institut, Villigen PSI, Switzerland
2. Nanoscience Center, Niels Bohr Institute, University of Copenhagen, Denmark
3. ESS Design Update Programme, Denmark
4. ESS-AB, Science Division, Lund, Sweden
5. IFE, Physics Department, Kjeller, Norway
6. Department of Chemistry & iNano, University of Aarhus, Denmark

email: jurg.schefer@psi.ch

HEIMDAL is a multiple length scale instrument designed for the ESS. It combines three instrumental techniques: Investigating the atomic distances by powder diffraction (NPD), the subsequent longer ones by a small angle scattering (SANS) and the mm-range by neutron imaging (NI). It is using a thermal and a cold neutron guide to have two different optics as needed by diffraction and small angle scattering. Our proposal allows covering a wide length scale as well as a time window appropriate to study chemical and physical processes under working conditions. Many future materials will have physical properties given by the characteristics of the structure, but depending on various length scales not covered by a standard NPD instrument. Atomic-, nano-, meso-, and microstructure will be essential. Heterogeneous catalysts build just one group of such materials: Catalytic nano-sized crystallites worked into a microporous matrix, and both – nanocrystals and matrix – are relevant to the efficiency of the catalytic process. Understanding of such materials often involves external stimuli e.g. light activation, gas flow, elevated temperature or magnetic field. Today, structural information on functional compounds is collected in sequence, often after the process has taken place and therefore only under similar, but not identical conditions on the different length scales. As a consequence of the HEIMDAL layout, we need cold and thermal neutrons from the butterfly moderator. With our novel two-guide concept, it is possible to adapt the optics in respect of size, divergence and wavelength spectra. Having an adjustable pulse length, HEIMDAL will also outperform as a powder diffractometer with easily adaptable resolution optimal for in-situ and in-operandi investigations. It takes full advantage of the long ESS pulse to maximize the intensity. We will discuss here the updated guides, the chopper layout (discussed in [1]) and the detector concepts for NPD, SANS and NI parts [2], also foreseen in other diffraction instruments at ESS. We present first data analysis procedures for our 2D data in this poster.

[1] S.L. Holm et al., Nuclear Instrument and Methods (2016) 782, 1-8.

[2] I. Stefanesc et al., <http://arxiv.org/abs/1607.02324> (July 11, 2016)

**Keywords:** ESS, Neutron Diffraction, in-situ, in-operandi, materials science

### MS43-P14 STOE InSitu HT2 – a new in-situ reaction chamber in Debye-Scherrer geometry

Thomas Hartmann<sup>1</sup>, Sascha Correll<sup>1</sup>

1. Stoe & Cie GmbH, Hilpertstr. 10, D-64295 Darmstadt, Germany

email: hartmann@stoe.com

STOE & Cie GmbH in Darmstadt, Germany, has developed a new equipment for their STOE STADI P powder diffractometer series, the InSitu HT2. This new reaction chamber in Debye-Scherrer geometry is mounted on a vertical setup Goniometer with Mo K $\alpha$  radiation and offers the user a horizontal capillary with up to 2mm inner diameter to expose the sample to high temperatures up to 1600 K and a gas flow through the capillary of 10 - 100 ml/min.

The sample volume is in the area of some mm<sup>3</sup>, only, offering real micro sample investigations under non-ambient conditions and reactive gases. First test measurements with a carbon coated Pt – Ru catalyst [1] under oxygen atmosphere at T from RT – 300°C showed impressively that the STOE InSitu HT2 fills a gap in the field of commercial available in-situ cells in transmission geometry.

Figure 1 shows the appearing RuO<sub>2</sub> reflections with those of the Pt-Ru alloy and the carbon matrix.

[1] C. Roth, N. Martz and H. Fuess., *Phys. Chem. Chem. Phys.*, **2001**, 3, 315-319.

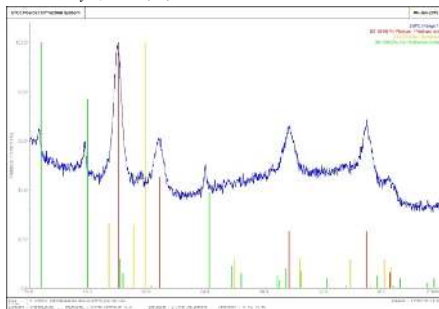


**Figure 1.** X-ray pattern at 250° (blue) with the markers for Pt (red), Ru (yellow), and RuO<sub>2</sub> (green)

**Keywords:** XRPD, non ambient methods, X-Ray diffraction, in situ measurements, reaction chamber



## MS43-P15 Comparative analysis of *ex-situ* and *in-operando* X-ray diffraction experiments for lithium insertion materials

Siegbert Schmid<sup>1</sup>, William R. Brant<sup>1,2</sup>

1. School of Chemistry, The University of Sydney

2. Department of Materials Chemistry, Ångström Laboratory, Uppsala University, Uppsala 751 21, Sweden

email: siegbert.schmid@sydney.edu.au

A comparative study of *ex-situ* and *in-operando* X-ray diffraction experiments using the fast lithium ion conductor  $\text{Li}_{0.18}\text{Sr}_{0.66}\text{Ti}_{0.5}\text{Nb}_{0.5}\text{O}_3$  will be presented. *Ex-situ* analysis of synchrotron X-ray diffraction data suggests that a single phase material exists for all discharges to as low as 0.422 V. For samples with higher lithium content, it is possible to determine the lithium position from the X-ray data. However, *in-operando* X-ray diffraction reveals a kinetically driven two phase region on cycling below 1 V. Monitoring the change in unit cell dimension during electrochemical cycling showed a reduction in the rate of unit cell expansion part way through the first discharge and during the second discharge, caused by a drop in lithium diffusion into the bulk material for higher lithium contents. A more significant change is a jump in the unit cell expansion once the lithium content exceeds one lithium ion per vacant site, caused by damping of octahedral rotations. This provides a link between lithium content and octahedral rotations. Using *in-operando* diffraction may therefore enable to determine the strength of octahedral rotations in defect perovskites and allow correlations with the large variance of ionic conductivities in these materials.

### References

- [1] W. R. Brant, D. Li, Q. Gu & S. Schmid, *J. Power Sources* **302**, 126 – 134 (2016). Comparison of *ex-situ* and *operando* X-ray diffraction techniques for investigating lithium insertion defect perovskite  $\text{Li}_{0.18}\text{Sr}_{0.66}\text{Ti}_{0.5}\text{Nb}_{0.5}\text{O}_3$ .
- [2] W. R. Brant, S. Schmid, A. Kuhn, J. Hester, M. Aydeev, M. Sale & Q. Gu, *ChemPhysChem*, **13**, 2293-2296 (2012). Rapid lithium insertion and location of mobile lithium in the defect perovskite  $\text{Li}_{2y}\text{Sr}_{1-x-y}\text{Ti}_{1-2x}\text{Nb}_{2x}\text{O}_3$ .

**Keywords:** lithium insertion, X-ray diffraction, in-operando

## MS43-P16 PHOENIX: a tender energy beamline for in-situ X-ray studies

Camelia N. Borca<sup>1</sup>, Reto Wetter<sup>1</sup>, Christophe Frieh<sup>1</sup>, Katja Henzler<sup>1</sup>, Jacinta Xto<sup>1</sup>, Markus Janousch<sup>1</sup>, Thomas Huthwelker<sup>1</sup>

1. Paul Scherrer Institut

email: camelia.borca@psi.ch

The PHOENIX beamline at the Swiss Light Source is specially designed for in-situ experiments covering an energy range of 400 to 8000 eV. This energy range provides opportunity to study light elements (e.g. O, Na, Mg, Al, S, Cl ... Fe) using X-ray absorption spectroscopy (XAS). The high photon flux delivered by an elliptical undulator can be focused to 2.5  $\mu\text{m}^2$  using X-ray mirrors. Topics addressed by users include environmental [1] and energy research [2], biology [3] and catalysis [4-5], as well as art preservation [6]. Experiments can be performed in two flexible vacuum end-stations, providing ample opportunity for in situ studies.

For the in-house research we focus on in situ studies of aqueous carbonate nucleation using a variety of liquid cells with precise control of the pH value, temperature and saturation index. For fast XAS measurements (ms and above) we use liquid jets [7] and for slow measurements (min to hrs) we have developed in-situ titration cells as well as flow-through cells which allow simultaneous XAS and XRD measurements. The first results obtained on  $\text{CaCO}_3$  and  $\text{Ca(Mg)CO}_3$  nucleation and growth in aqueous environments will be presented. The measured XAS spectral features contain information on the local order around Mg/Ca atoms, while the XRD spectra unveils the phase transformation in time of the pure and Mg doped Ca carbonates.

For further information about the beamline: <https://www.psi.ch/sls/phoenix/phoenix>

Contact: thomas.huthwelker@psi.ch, camelia.borca@psi.ch

- [1] S. Pin et al., *J. of Phys. Chem.*, 2013, 117, 8368-8376
- [2] G. Nurk et al., *J. Power Sources* 2013, 240, 448-457
- [3] J. Czaplá-Masztafiak et al., *Biophysical J.* 2016, 110(6), 1304-1311
- [4] M.W. Tew et al., *J. Cat.* 2011, 283(1), 45-54
- [5] A. Vjunow et al., *Journal of the Am. Chem. Soc.* 2014, 136(23), 8296-8306
- [6] E. Cato et al., *Microchem. J.* 2016, 126, 18-24
- [7] M. Brown et al., *J. Phys. Chem. Lett.* 2012, 3, 231-235

**Keywords:** X ray absorption

## MS44 Total scattering: pdf analysis and diffuse scattering in X-Ray, neutron and electron diffraction

Chairs: Václav Holý, Cinzia Giannini

### MS44-P1 Cooperation or competition? Multiprobe PDF analysis of local and long-range instabilities in A-site doped SrTiO<sub>3</sub>

Stefano Checchia<sup>1,2</sup>, Marco Scavini<sup>1</sup>, Michela Brunelli<sup>2</sup>, Mauro Coduri<sup>3</sup>, Mattia Allietà<sup>1</sup>

1. Università degli Studi di Milano - Dipartimento di Chimica, Milano, Italia

2. Swiss-Norwegian Beamlines at the European Synchrotron Radiation Facility (ESRF), Grenoble, France

3. European Synchrotron Radiation Facility (ESRF), Grenoble, France

email: stefano.checchia@unimi.it

Local structural order in perovskites can take a number of forms, and its relationship to both the crystallographic structure and the physics of the material lends itself to an even greater number of interpretations. Recent pair distribution function (PDF) approaches to disorder in perovskites have managed to explain some relations between short-range order and electric behaviour and to give new views on structural phase transitions [1,2].

We present a multiprobe PDF study of Sr<sub>1-x</sub>Pr<sub>x</sub>TiO<sub>3</sub> (0<x<0.150), a perovskite with a significant relaxor ferroelectric response at room temperature. A composition-driven phase transition occurs via gradual stabilization of the nonpolar antiferrodistortive mode with doping [3]. Also, the continuous temperature dependence of the TiO<sub>6</sub> octahedral tilt resembles the SrTiO<sub>3</sub> critical behaviour. But although the ferroelectric and antiferrodistortive instabilities are commonly regarded as competitive, in this case the onset and magnitude of the dielectric permittivity peak are insensitive to high Pr concentration, which should promote antiferrodistortion. In fact, recent theoretical work proposed cooperation between the ferroelectric and antiferrodistortive instabilities in large-tilted structures [4]. The increased tetragonal strain observed alongside octahedral tilt, moreover, might prompt an analogy to the polar strain in ferroelectric SrTiO<sub>3</sub> films (e.g.[5]).

To assess the compatibility of local atomic displacements and long-range antiferrodistortive structure, we have undertaken a combined X-ray and neutron total scattering study. We collected PDF-quality XRPD data at the ID22 beamline (ESRF) and neutron TOF data at GEM (ISIS). Large-box models were provided by Reverse Monte Carlo joint refinement of

real- and reciprocal-space neutron data. The resulting atom displacement and tilt angle distributions were compared to the results of small-box modelling on both X-ray and neutron PDF data. Besides a possible picture for the coexistence of local atomic displacements and antiferrodistortive structure, we discuss reliability and downsides of the joint analysis method used.

[1] M.S. Senn et al., arXiv:1512.03643 (2015)

[2] K. Datta et al., *Phys. Rev. B* 93, 064102 (2016)

[3] S. Checchia et al., *Acta Cryst. A* 71(a1), s151-s151 (2015)

[4] U. Aschauer & N.A. Spaldin, *J. Phys. Condens. Matter* 26(12), 122203 (2014)

[5] A. Vasudevarao et al., *Phys. Rev. Lett.* 97, 257602 (2006)

**Keywords:** pair distribution function, total scattering, reverse monte carlo, perovskite, ferroelectric, relaxor

## MS44-P2 Analysis of short range phenomena in novel materials using the PDF-method

Philipp Hans<sup>1</sup>, Reinhard B. Neder<sup>2</sup>, Nastaran Hayati-Roodbari<sup>3</sup>,  
Paul Kautny<sup>4</sup>, Klaudia Hradil<sup>1</sup>

1. X-ray Centre, Vienna University of Technology
2. Crystallography and Structural Physics, Friedrich-Alexander-Universität Erlangen-Nürnberg
3. Materials Science and Physics, University of Salzburg
4. Institute of Applied Synthetic Chemistry, Vienna University of Technology

email: philipp.hans@tuwien.ac.at

In the present contribution we will show results of pair distribution function (PDF) studies on amorphous materials. The pair distribution function contains information on the occurrence of all atom-to-atom distances in the substance.

The samples consist of so called host materials for organic-light-emitting-diodes (OLEDs) and are applied as amorphous films. In this amorphous state their electronic structure seemingly gets altered in a way required to induce the light emittance in the blue region. The molecular structure of the molecules is known and these molecules possess a large degree of freedom with respect to internal torsion. The initial expectation was that the light emitting state is caused by collective torsion of neighbouring molecules.

Initial PDF data were collected on an inhouse powder diffractometer with Mo-radiation. The experimental PDF does not show correlations beyond intramolecular distances. This indicates that the material is highly disordered and does not show correlated tilts between neighbouring molecules. Refinements with the DISCUS-Suite confirm the local torsion and the lack of correlations.

**Keywords:** amorphous organic materials, PDF-analysis, glass structure

## MS44-P3 In-situ measurements of average and local structures in hydrogen gas environment at BL22XU in SPring-8

Akihiko Machida<sup>1</sup>, Naoyuki Maejima<sup>1</sup>, Tetsu Watanuki<sup>1</sup>,  
Hyunjeong Kim<sup>2</sup>, Kouji Sakaki<sup>2</sup>, Yumiko Nakamura<sup>2</sup>

1. Synchrotron Radiation Research Center, National Institutes for Quantum and Radiological Science and Technology, Sayo, Hyogo 679-5148, Japan
2. Research Institute of Energy Frontier, National Institute of Advanced Industrial Science and Technology, Tsukuba, Ibaraki 305-8565, Japan

email: machida@spring8.or.jp

Hydrogen absorbing alloys are considered as potential hydrogen storage materials for several applications such as stationary energy storage system. The absorbed hydrogen atoms largely expand the metal lattice and induce a structural phase transition on the hydrogenation reaction. From a nanoscale structural point of view, a large number of crystallographic defects, such as dislocations, are formed during hydrogen absorption/desorption cycles and they influence the properties of hydrogen absorbing alloys. Therefore, thorough structural studies on the hydrogen absorbing state are essential for improving the material properties as well as for preparing novel alloys. However, those are challenging tasks because the hydrogen absorbing states of alloys usually arise in the pressurized hydrogen gas environment. Furthermore, average structural information from conventional methods is not sufficient to elucidate the mechanism of hydrogen absorption, and therefore local structural information is also necessary.

In order to investigate the structural change of hydrogen absorbing alloys during hydrogen absorption/desorption processes, we have developed in-situ setup for x-ray diffraction experiments at BL22XU in SPring-8. Using a large imaging plate (IP) detector and high energy x-rays about 70 keV, we can also obtain x-ray total scattering data ( $Q_{\text{max}} \sim 27 \text{ \AA}^{-1}$ ) for the atomic pair distribution function (PDF) analysis, which is one of powerful methods to investigate structures in an atomic scale. PDFs obtained from BL22XU show peaks even above 100 Å allowing us to investigate even intermediate range structural features related to the crystallographic defects or crystal lattice distortion. Recently, we have developed time-resolved measurement setup using an amorphous-Si detector from PerkinElmer. This setup enables us to study change in both average and local structures of hydrogen absorbing alloys in either equilibrium or non-equilibrium states with hydrogen gas pressure up to 1 MPa. We succeeded in obtaining the PDF of  $\text{La}(\text{Ni},\text{Al})_5$  intermetallic compounds on hydrogen absorption process with short accumulation time of 0.25 sec. In this presentation, we will introduce our experimental setup and evaluation of obtained PDFs, and present some preliminary results on the hydrogen absorbing alloys.

This work is supported by Photon and Quantum Basic Research Coordinated Development Program from the Ministry of Education, Culture, Sports, Science and Technology, Japan.

**Keywords:** x-ray total scattering, in-situ measurement, hydrogen absorbing alloys

**MS44-P4** Diffuse scattering analysis of sodium fluorosilicateErik Stronks<sup>1</sup>, Hans-Beat Bürgi<sup>1,2</sup>, Anthony Linden<sup>1</sup><sup>1</sup>. Department of Chemistry, University of Zürich, Winterthurerstrasse 190, CH-8057 Zürich<sup>2</sup>. Department of Chemistry and Biochemistry, University of Bern, Freiestrasse 3, CH-3012 Bern

email: erik.stronks@chem.uzh.ch

Many crystalline materials with interesting properties show correlated disorder, e.g. relaxor ferroelectrics and super ionic conductors<sup>1</sup>. Diffuse X-ray scattering analysis is one of few means to elucidate the crystal structure at the nano- and micrometer length scale. However, methods to derive a disorder model, including both data processing and analysis, are strongly lagging behind those for average structure determination. We will present some data processing techniques and our attempts at modeling the diffuse scattering of crystalline sodium fluorosilicate. The diffuse scattering data of Na<sub>2</sub>SiF<sub>6</sub> has been symmetry averaged using the Laue group  $-3m\bar{1}$ . Outlier rejection based on Blessing<sup>2</sup> has been applied in order to remove artifacts and spurious peaks. For background correction we have developed a least squares procedure by which the background is estimated from the data without the need of background measurements. A user definable set of spherical harmonic functions of degree  $l$  and order  $m$  are used as the least squares basis functions. The background estimate,  $B$ , can be expressed as:

$$B(r^{rec}, \theta, \varphi) = Rad(r^{rec}) \sum_l A_{lm} Y_{lm}(\theta, \varphi) \quad (1)$$

here  $B$  is the background fit which is a function of the distance from the reciprocal space origin  $r^{rec}$ , and the two polar angles  $\theta$  and  $\varphi$ .  $Rad$  is a radial function describing the radial dependence of the background intensity,  $A_{lm}$  are the set of coefficients to be determined in the least squares procedure and  $Y_{lm}$  are the real spherical harmonic functions that were provided by the user. The first sum is over the spherical harmonic degrees  $l$  from  $l=0$  to  $l$  and the second sum is over spherical harmonic orders  $m$  from  $m=-l$  to  $l$ . Figure 1 shows the symmetry averaged  $hk0$  layer before and after background correction. In order to be able to use 3D-APDF<sup>3</sup> analysis for disordered crystal structure modeling the Bragg peaks would ideally have to be deconvoluted from the diffuse intensities. We will present our attempts at doing so.

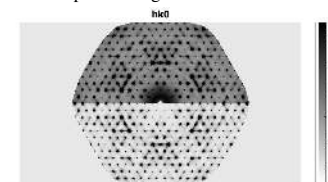


**Figure 1.** Symmetry averaged  $hk0$  layer before (top) and after (bottom) background correction

**Keywords:** background fitting, least squares

**MS44-P5** Diffuse scattering in the high  $T_c$  superconductor,  $\text{HgBa}_2\text{CuO}_{4+\delta}$ Thomas R. Welberry<sup>1</sup><sup>1</sup>. Australian National University, Research School of Chemistry

email: welberry@rsc.anu.edu.au

The properties of many technologically important materials are intimately associated with the inherent disorder that exists in their crystal structures. Examples include: alloys, shape-memory alloys, ferroelectrics, fast ion conductors, semi-conductors, to high  $T_c$  superconductors, zeolites and inclusion compounds and even pharmaceuticals. To understand these materials it is insufficient to know their average unit cell structure as revealed by Bragg scattering. It requires additional knowledge of their local or nanoscale structure — information that can only be obtained from the *diffuse scattering* component of the total scattering. It is perhaps quite surprising that while there have been many studies of single-crystal diffuse scattering for alloys and ferroelectric materials, for example, there have been very few for high  $T_c$  superconductors. However, Izquierdo *et al* [1] have recently reported quite detailed diffuse scattering patterns obtained from a single crystal of  $\text{HgBa}_2\text{CuO}_{4+\delta}$ , showing that for these materials too such information is quite accessible.

However, though obtaining diffuse scattering data is now feasible for most crystalline materials, interpreting and analyzing the data remains problematical. Izquierdo *et al* developed a model to try to explain the diffraction patterns they had observed but although their ‘best fit’ model captured some of the attributes of the observed diffraction pattern, some key features were poorly modeled. In the work described we have developed a model that satisfactorily accounts for the details of the observed diffraction pattern. This is significantly different from the published model and hence has implications for understanding the structure-property relationship of this important material.

[1] Izquierdo *et al.* (2011), *Journal of Physics and Chemistry of Solids*, 72: 545–548.

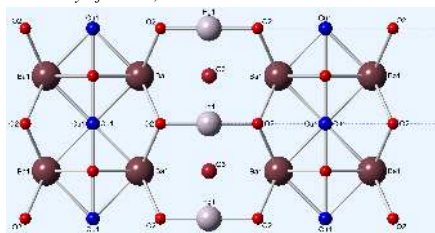


**Figure 1.** The average structure of the high  $T_c$  superconductor,  $\text{HgBa}_2\text{CuO}_{4+\delta}$ . View down  $[010]$  showing how the planar  $\text{HgO}_2$  layer is sandwiched between two  $\text{Ba}_2\text{CuO}_4$  layers.

**Keywords:** Diffuse scattering, SCDS, high temperature superconductivity, computer simulation, bond-valence

**MS44-P6** Measurement and calculation of thermal diffuse scattering of molecular crystals: A case study of the anti-tuberculosis drug pyrazinamideAnders Østergaard Madsen<sup>1</sup>, Nanna Wahlberg<sup>1</sup>, Alexei Bosak<sup>2</sup>1. University of Copenhagen  
2. European Synchrotron Radiation Facility

email: madsen@chem.ku.dk

Experimental information on the properties of phonons is traditionally obtained from inelastic neutron and inelastic X-ray scattering measurements. These experiments are time-consuming, and last at least a few days, and the information obtained gives only limited information about the phonon eigenvectors. The study of thermal diffuse scattering (TDS) offers a much faster route to obtain information about the low-frequency phonons, which has become feasible thanks to the advent of third generation synchrotrons in combination with large single-photon count detectors. The interpretation of TDS in the case of molecular crystals has been hampered by the lack of sufficiently accurate models of the lattice dynamics in crystals. Within recent years, it has become feasible to perform periodic DFT calculations of the lattice dynamics. Here, we demonstrate the calculation and analysis of TDS of pyrazinamide, a polymorphic tuberculosis drug. The polymorphs of pyrazinamide is an enantiotropic system, and the change in relative stability of the polymorphs with temperature is driven by differences in the acoustic phonons, which leads to differences in entropy. We examine the TDS patterns of these systems and discuss their features in relation to lattice-dynamical models derived from DFT calculations.

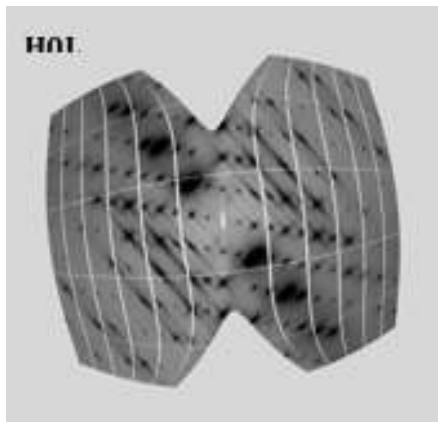


**Figure 1.** Results from a recent diffraction experiment on a pyrazinamide single crystal in the polymorphic delta-phase at room temperature showing a strong thermal diffuse scattering signal in the H0L plane.

**Keywords:** Thermal diffuse scattering, polymorphism, phonons

**MS44-P7** X-ray diffraction studies of crystal structure and strain distribution in nanowiresJulian Stangl<sup>1</sup>

1. Johannes Kepler University Linz

email: julian.stangl@jku.at

Semiconductor nanowires exhibit a number of special properties making them interesting both for fundamental science as well as for different applications ranging from solar cells to fast transistors. In III-V semiconductors, the observation of hexagonal polytypes has spurred investigations of this crystal structure, which cannot be fabricated in bulk (at least not stable under ambient conditions). Some materials show a change in band alignment from indirect to direct fundamental band gap, such a behavior has also been predicted in the SiGe system. In this presentation, we will highlight the structural investigation of hexagonal Si material fabricated in nanowires, using high resolution x-ray diffraction. Analysis of the diffuse x-ray diffraction patterns from the core-shell wires using finite element method yields the unit cell properties of hexagonal (lonsdaleite) silicon.

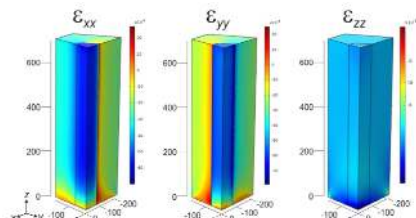


**Figure 1.** Finite element model simulations of the strain distribution in GaP core/ hexagonal Si shell nanowires.

**Keywords:** nanowires, hexagonal Si, diffuse scattering

## MS44-P8 Structural investigation of mullite-type $\text{Al}_4\text{B}_2\text{O}_9$ by electron diffraction

Haishuang Zhao<sup>1</sup>, Kristin Hoffmann<sup>2,3</sup>, Yaşar Krysiak<sup>1</sup>, Bastian Barton<sup>1</sup>, Hartmut Schneider<sup>2</sup>, Thorsten M. Gesing<sup>3</sup>, Reinhard X. Fischer<sup>2</sup>, Ute Kolb<sup>1</sup>

1. Institute of Inorganic and Analytical Chemistry, Johannes Gutenberg University Mainz, Jakob-Welder-Weg 11, D-55128 Mainz, Germany

2. Crystallography, Department of Geosciences, University of Bremen, Klagenfurter Straße, D-28359 Bremen, Germany

3. Institute of Inorganic Chemistry, University of Bremen, Leobener Straße /NW2, D-28359 Bremen, Germany

email: hzhao@uni-mainz.de

Structural characterization of materials is a key step to understand their physical properties in order to optimize industrial applications. Electron diffraction, as opposed to X-ray powder diffraction, can provide atomic structure information from a single nanocrystal. It has advantages in the case of structures with large unit cells, pseudosymmetry, superstructures, low crystallinity and for impure or multi-phase samples. Automated electron diffraction tomography (ADT), combines nano diffraction, tilt series acquisition and electron beam precession to derive a three-dimensional atomic structure with data bearing minimal dynamic scattering artifacts.<sup>1,2</sup>

The published crystal structure of  $\text{Al}_4\text{B}_2\text{O}_9$ , an industrially important mullite-type ceramic material, was constructed from a model of the known boralsilite structure and refined from X-ray powder diffraction data.<sup>3</sup> Due to the pseudo-orthorhombic unit cell and the complexity of the structure, Rietveld refinement results were not ideal, leading to unclear occupancies of two oxygen atoms.

ADT data reconstruction delivered monoclinic unit cells in space group  $C2/m$  ( $a = 14.8 \text{ \AA}$ ,  $b = 5.5 \text{ \AA}$ ,  $c = 15.1 \text{ \AA}$ , and  $\beta = 90.6^\circ$ ). *Ab-initio* structure solution of  $\text{Al}_4\text{B}_2\text{O}_9$ , using direct methods, delivered all atoms directly from solution. The well-resolved potential map clearly shows one fully occupied oxygen position but no significant signal for the second postulated oxygen in the other channel. For samples prepared with an initial excess of boron, some crystals revealed modulated streaking in  $b^*$  direction, which has been assigned to a superstructure with a threefold  $b$ -axis and an additional disorder. The modeling of different layer stacking along  $b$  direction and diffraction simulations were carried out with software package DISCUS<sup>4</sup> leading to electron diffraction patterns resembling the experimentally observed streaking.

### References

- 1 U. Kolb, T. Gorelik, C. Kübel, M. T. Otten and D. Hubert, *Ultramicroscopy*, 2007, **107**, 507–513.
- 2 U. Kolb, T. Gorelik and M. T. Otten, *Ultramicroscopy*, 2008, **108**, 763–772.
- 3 R. X. Fischer, V. Kahlenberg, D. Voll, K. J. MacKenzie, M. E. Smith, B. Schnetger, H.J. Brumsack and H. Schneider, *Am. Mineral.*, 2008, **93**, 918–927.
- 4 T. Proffen and R. B. Neder, *J. Appl. Crystallogr.*, 1997, **30**, 171–175.

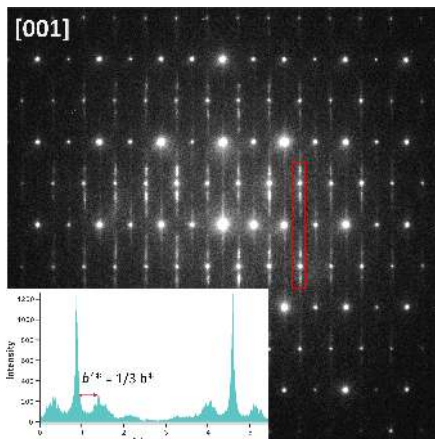


**Figure 1.** Modulated diffuse scattering in the electron diffraction pattern of  $\text{Al}_4\text{B}_2\text{O}_9$ .

**Keywords:** Electron crystallography, Automated electron diffraction tomography, Mullite-type structure

## MS45 Measuring data quality

Chairs: Phil Evans, Alexandre Urzhumtsev

### MS45-P1 Current Status of Microfocus X-ray Sources for Chemical and Biological Crystallography

Juergen Graf<sup>1</sup>, Holger Ott<sup>2</sup>, Tobias Stuerzer<sup>2</sup>, Severine Freisz<sup>2</sup>,  
Andreas Kleine<sup>1</sup>, Joerg Wiesmann<sup>1</sup>, Carsten Michaelson<sup>1</sup>

1. Incoatec GmbH  
2. Bruker AXS GmbH

email: graf@incoatec.de

Modern microfocus X-ray sources define the state-of-the-art for most applications in X-ray diffraction. These sources are usually combined with multilayer X-ray mirrors which are excellent X-ray optical devices for beam shaping and preserving the brightness of the source.

Microfocus rotating anode generators and liquid metal jet systems deliver flux densities in the range of  $10^{11}$  photons/s/mm<sup>2</sup>. However, these sources are expensive and need regular and sometimes time-consuming maintenance. Low power microfocus sealed tube sources, such as the Incoatec Microfocus source *lμS*, represent an interesting low-maintenance alternative to rotating anode generators. Power loads of several kW/mm<sup>2</sup> in anode spot sizes of < 50 μm deliver a small and bright beam. Flux densities of up to  $10^{10}$  photons/s/mm<sup>2</sup> can be achieved in a focused beam suitable for most protein crystals and poorly diffracting small molecule samples. The latest generation of the *lμS*, the *lμS* 3.0, is the first microfocus X-ray source that is optimized for X-ray diffraction resulting in a gain in intensity of about 30% compared to its predecessor.

In this presentation, we will be reviewing the current performance levels of different microfocus X-ray sources. Further, we will be discussing the main features of the newest generation of the *lμS*. We will be presenting selected results to demonstrate the impact of these modern microfocus X-ray sources on the data quality for applications in chemical and biological crystallography.

**Keywords:** X-ray optics, microfocus X-ray source, new XRD technology, multilayer thin films

### MS45-P2 2D spherical-polar visualization of data completeness using equal-volume units of reciprocal space

James Foadi<sup>1</sup>, Gwyndaf Evans<sup>1</sup>

1. Diamond Light Source Ltd, Oxfordshire, UK

email: james.foadi@diamond.ac.uk

In Macromolecular Crystallography (MX) completeness plays an important role in the assessment of data quality. Lack of completeness often results in the distortion of the related electron density map, with the ensuing difficulty in the building of a macromolecular model. Data completeness is typically quantified as percentage in spherical resolution shells; the specific region of the reciprocal space covered by the data is not normally reported in plots. This poses little or no problem when dealing with data from a single crystal, but becomes a complication when multiple crystals are involved. In the BLEND software [1] for the management of multiple crystals, for instance, the specific selection of groups of crystals is mainly guided by the criterion of isomorphism, while data completeness, especially related to reciprocal space coverage, is only dealt with after many trial-and-error combinations. One of the reasons why completeness is calculated only as a function of resolution is that the number of reflections in the case of MX is very high, thus requiring CPU or GPU intensive tools for their visualization. Even when computing resources make this feasible, three-dimensionality does not immediately render data completeness as an overall function of reciprocal space, because multiple rotations are needed to highlight regions poor in reflections. Here we introduce a new type of completeness diagram made out of two 2D plots, a resolution-dependent (radial) and an angular-dependent one. An example of the two plots is shown in Figure 1. This diagram gives an instantaneous and immediately intuitive picture of data completeness in terms of specific coverage of reciprocal space. Two or more diagrams related to individual crystals can be added without loss of information as data multiplicity is displayed by gradient or hue colouring. The main algorithmical innovation behind the creation of these diagrams is the one used already in the field of robotics, more specifically in the rotational movement of robotic parts. One of the problems addressed and solved in that field is the partition of a spherical region of space in regions of equal volumes [2]. The same type of partition, this time applied to the crystallographic reciprocal space, has been used for the completeness diagrams presented in this work.

[1] J. Foadi et al. (2013) - Acta Cryst D [2] G. Yang & I-M Chen (2006) - IEEE Trans on Robotics

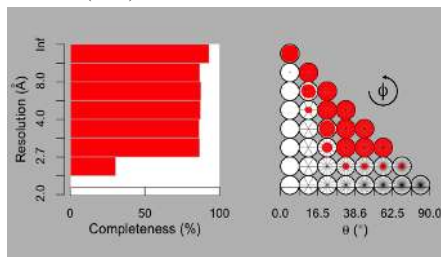




**Figure 1.** Diagrams to represent data completeness in reciprocal space. The plot on the left is a traditional completeness in resolution shells. The plot on the right provides angular (spherica-polar) completeness on the same data

**Keywords:** data completeness, reciprocal space representation, multiple crystals, BLEND

## MS45-P3 Advances in Data Quality in Area Detector Diffraction Experiments.

Mathias Meyer<sup>1</sup>

1. R&D CSG group, Rigaku Oxford Diffraction (Poland) Sp. z o. o., Ul. Szarskiego 3, PL-54-609 Wrocław, Poland

email: mathias.meyer@rigaku.com

Achieving good, reliable data for structure research and subsequent publication is the end goal for most users of single crystal diffraction equipment. It is important that all factors affecting data quality of are taken in to consideration and to understand how best to control them.

The following elements of the diffraction experiment will be discussed:

a) The hardware, which revolves around notions of absolute detectivity, overhead, readout speed, minimizing systematic errors and diffractometer access. Advances in area detector technology and data collection approaches will be presented. Rigaku Oxford Diffraction's new generation of HPC detectors will be described. The CCD camera generation S2 with 'Smart Sensitivity Control' will be put in context of existing CCD detectors.

b) Selecting the sample, method of mounting and protection environment is controlled mainly by the user. This presentation offers suggestions on how to select your sample whilst being conscious of the fixed characteristics of your diffractometer.

c) The experimental procedure comprises the choice of wavelength, the geometric strategy, the mode of scan and detector operation and the decision on absolute detectivity vs. redundancy. Rigaku Oxford Diffraction's CrysAlisPro software implements the fifth generation of strategy software with new features for data quality: The 'Intelligent Measurement System' optimizes experiment conditions for CCD and HPC systems.

d) The data reduction software which should be optimized at extracting consistent area detector data not only under good conditions, but also under real life flaws of the practical experimental procedure e.g. twinned samples. A new data reduction approach for twins, is highlighted, and can significantly improves the data quality of small molecule and protein twins.

**Keywords:** Area detector, data quality, single crystal diffraction

**MS45-P4** On the application of leverage analysis to parameter precision using area detector strategiesPascal Parois<sup>1</sup>, Richard I. Cooper<sup>1</sup>

1. University of Oxford, Chemistry research laboratory, 12 Mansfield road, Oxford, UK

email: pascal.parois@chem.ox.ac.uk

Analysis of the influence of measurements on an existing crystallographic model allows the identification of the most useful additional data to measure to improve the precision of specific model parameters. We show that as a result of the distribution of those diffraction measurements in reciprocal space, the technique is more appropriate for certain parameters and derived functions when using an area detector. Remeasurement of specific diffraction peaks from single crystals in order to improve the precision of specific parameters is considered in the context of data collection strategy using an area detector. By considering strategies for recollecting small sets of data, we show that certain parameters are more amenable to being optimized in this manner.

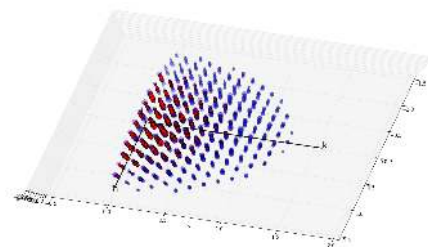


**Figure 1.** Estimated improvement in variance  $\Delta V$  of all the reflections ( $h,k,l$ ) in real space ( $u,v,w$ ). The area of the discs is proportional to  $\Delta V$  on a non linear scale. The red reflections are part of an optimised short data collection strategy calculated by our software to optimise the variance of a C-H bond.

**Keywords:** Error analysis, Diffraction experiment strategy, Area detectors

**MS45-P5** XtaLAB Synergy: Fast, Precise, Intelligent.Fraser J. White<sup>1</sup>, Alexandra Griffin<sup>1</sup>, Dyanne Cruickshank<sup>1</sup>, Mathias Meyer<sup>2</sup>, Damian Kucharczyk<sup>2</sup>

1. Rigaku Oxford Diffraction, Sevenoaks, UK

2. Rigaku Oxford Diffraction, Wroclaw, Poland

email: fraser.white@rigaku.com

Performing data collections which are not only high quality but also efficient is a key requirement of diffractometer users around the world, either to enable high throughput, or simply maximise data quality in a given time. The new XtaLAB Synergy represents improvements in both hardware and software design. Advancements have been made not only in the microfocus sources but also in the goniometer hardware. The sample environment has been completely redesigned allowing ample space for easier access or incorporation of specialist equipment. The combination of these enhancements leads to better data quality in shorter data collection times for both weakly and strongly diffracting crystals. Ensuring the best possible use of the diffractometer hardware and the data it provides requires high performance software. The CrysAlisPro software package is under continual development in order to provide enhanced automation features, new options for sample screening, data collection and improvements to data processing algorithms. We compare the previous generation of Rigaku Oxford Diffraction diffractometer technology to the XtaLAB Synergy.



**Figure 1.** The XtaLAB Synergy with Atlas S2 detector

**Keywords:** hardware, diffractometer, high-speed, efficient

## MS46 Computational tools for theoretical chemistry in crystallography

380. [BB1]Вопросы те же, что и в русской версии

**Keywords:** Topological analysis, self-catenated motifs, coordination networks

Chairs: Martin Lutz, Martyn Winn

### MS46-P1 Topological analysis of self-catenated motifs in coordination networks

Aleksandr A. Garin<sup>1</sup>, Eugeny V. Alexandrov<sup>1</sup>, Davide M. Proserpio<sup>1,2</sup>, Vladislav A. Blatov<sup>1</sup>

1. Samara Center for Theoretical Materials Science (SCTMS), Samara State Aerospace University named after academician S.P. Korolyov (National Research University), Moskovskoye Shosse 34, Samara 443086

2. Dipartimento di Chimica, Università degli Studi di Milano, Via C. Golgi 19, 20133 Milano, Italy

email: alexgarinx@gmail.com

In the last decade, the phenomenon of self-catenation became widespread in structures of coordination compounds<sup>1</sup>. Self-catenation is the entanglement of circular fragments of the same atomic net. Despite the prevalence of the phenomenon among coordination polymers, neither total number of self-catenated structures, nor their topological characteristics (topological type, methods of entanglements of rings) are known yet. The modern crystallochemical approaches in the analysis of such structures are construction of Hopf ring net<sup>2</sup> as well as splitting of the atomic net on the individual entangled motifs<sup>3</sup>. Both approaches are automated and implemented in the program package ToposPro (<http://topospro.com>)<sup>4</sup>. Thus, our work was devoted to the topological analysis of self-catenated motifs in framework coordination polymers by the ToposPro tools.

At the first step, we have extracted the crystal structural information from the Cambridge Structural Database (version 5.35)<sup>5</sup> for more than 15,000 structures of 3-periodic coordination polymers. Analysis of the structures without topologically dense structural groups (atomic clusters), more than 250 self-catenated frameworks were found. For them we have analyzed all possible ways for splitting into subnets (the most typical of which are – dia, srs, hcb, sql, 4T13) and the topology of entanglements by constructing Hopf's ring net. Using the results we have found general crystallochemical principles of the self-catenation realization.

1. X.-J. Ke, D.-Sh. Li, M. Du *Inorg. Chem. Comm.*, **2011**, *14*, 788. 2. E.V. Alexandrov, V.A. Blatov, D. M. Proserpio *Acta Cryst.*, **2012**, *A68*, 484. 3. Sh.-L. Xiao, G.-H. Cui, V.A. Blatov, J.-Ch. Geng, G.-Yu. Li *Bull. Korean Chem. Soc.*, **2013**, *34*, 1891. 4. V.A. Blatov, A.P. Shevchenko, D.M. Proserpio *Cryst. Growth Des.* **2014**, *14*, 3576. 5. F. H. Allen *Acta Crystallogr.* **2002**, *B58*,

**MS46-P2** The taxonomy of rod-packing coordination networks (CNs)Andrey V. Goltsev<sup>1</sup>, Eugeny V. Alexandrov<sup>1</sup>, Vladislav A. Blatov<sup>1</sup>, Davide M. Proserpio<sup>1,2</sup>

1. Samara Center for Theoretical Materials Science (SCTMS), Samara State Aerospace University named after academician S.P. Korolyev (National Research University), Samara, Russia
2. Dipartimento di Chimica, Università degli Studi di Milano, Milano, Italy

email: andregoltsev@gmail.com

CNs and metal-organic frameworks (MOFs) attract a great interest due to their promising applications. MOFs possess a wide number of useful properties, e.g. adsorption and catalytic activity, magnetic susceptibility, ionic and electronic conductivity[1]. At present time, more than 18500 3-periodic CNs have been synthesized and their number is steadily growing. The combination of organic ligands, metal cations and secondary building units (SBUs) allows to obtain new coordination polymers every day. Molecular groups (clusters), chains, layers and frameworks can serve as finite and polymeric SBUs. The coordination networks constructed by rod SBUs have been called rod packing (RP) MOFs[2]. The classification of structures by a range of descriptors is of major importance for establishing correlations between structure, composition and properties and for design of new materials. Such taxonomy for RP MOFs still does not exist, and it is the main goal of our work.

Using ToposPro[3], we have extracted from CSD 5.36[4] the crystal data for 2767 RP MOFs. For each structure we have determined the number of sets of parallel rods and their mutual orientation. For each such set, the orthogonal projection has been constructed. To characterize the packing pattern, the topological type has been assigned to 2-periodic net in the orthogonal projection.

It was found that the 2658 RP MOFs consist of only one set of parallel rods. Two, three, and four sets are observed in 96, four, and one structures, respectively. Classification of the rod packings is performed in accordance to the patterns described in [2,5]. In addition, we classified the RP MOFs in more details by a series of descriptors: topological types of rod and framework, composition and coordination properties of SBUs. These values will be deposited in the knowledge database of topological and geometrical relationships in RP MOFs and they will be used for prediction of new functional RP MOFs[6].

1.R. J. Kuppler, D. J. Timmons, Q.-R. Fang, J.-R. Li, T. A. Makal, M. D. Young, D. Yuan, D. Zhao, W. Zhuang, H.-C. Zhou, *Coord. Chem. Rev.*, **2009**, 253, 3042

2.N.L. Rosi, J. Kim, M. Eddaoudi, B. Chen, M. O'Keeffe, O.M. Yaghi, *JACS*, **2005**, 127, 1504

3.V.A. Blatov, A. P. Shevchenko, D. M. Proserpio, *Cryst. Growth Des.*, **2014**, 14, 3576, [www.topospro.com](http://www.topospro.com)

4.C.R. Groom, I. K. Bruno, M. P. Lightfoot, S. C. Ward, *Acta Cryst.*, **2016**, B72, 171

5.M. O'Keeffe, S. Andersson, *Acta Cryst.*, **1977**, A33, 914

6.E.V. Alexandrov, A.P. Shevchenko, A.A. Asiri, V.A. Blatov, *CrystEngComm*, **2015**, 17, 2913

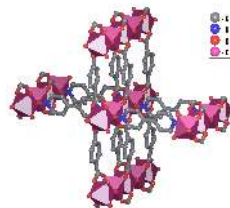


**Figure 1.** The crystal structure of  $[\text{Co}_2(\text{BDC})_2(\text{BPNO})_2]$  with a parallel 1-periodic rods. <sup>a</sup> 1,4-benzene-dicarboxylate <sup>b</sup> 4,4-bipyridyl-N,N-dioxide

**Keywords:** Metal-organic frameworks (MOFs), coordination networks (CNs), secondary building units (SBUs), Cambridge Structural Database (CSD), classification, rod packing, database, topological descriptors

## MS46-P3 DSR - Modelling Disorder with new GUIs for ShelXle and Olex2

Daniel Kratzert<sup>1</sup>

1. Albert-Ludwigs-Universität Freiburg

email: daniel.kratzert@ac.uni-freiburg.de

DSR - Modelling Disorder with new GUIs for ShelXle and Olex2

One of the remaining challenges in single-crystal structure refinement is the proper description of disorder in crystal structures. DSR<sup>[1]</sup> (Disordered Structure Refinement) performs semi-automatic modelling of disordered moieties using SHELXL<sup>[2]</sup>. It contains a database that includes molecular fragments and their corresponding stereochemical restraints and a fitting procedure to place these fragments on the desired position in the unit cell. The program is also suitable for speeding up model building of well-ordered crystal structures. Writing a special DSR command into the SHELXL .res file of the target structure instructs DSR on where to place and how to orient a molecular fragment from the fragment database in the unit cell (Figure 1).

\r\n

Recent features to DSR such as two new Graphical user interfaces (GUIs) in ShelXle<sup>[4]</sup> and Olex2<sup>[3]</sup> as the main GUIs for SHELXL are presented. With the new GUI, the user has full control over every aspect of the model building while keeping the procedure as simple as possible. Also additional checks were added to keep restraints in the database consistent.

\r\n

The software can be downloaded at [5].

\r\n

[1] D. Kratzert, J. J. Holstein, I. Krossing, J. Appl. Cryst. **2015**, 48, 933–938.

\r\n

[2] G. M. Sheldrick, Acta Cryst. **2015**, C71, 3–8.

\r\n

[3] L. J. Bourhis, O. V. Dolomanov, R. J. Gildea, Howard, Judith A K, H. Puschmann, Acta Crystallogr A Found Adv **2015**, 71, 59–75.

\r\n

[4] C. B. Hübschle, G. M. Sheldrick and B. Dittrich, J. Appl. Cryst. **2011**, 44, 1281–1284.

\r\n

[5] <https://www.xs3.uni-freiburg.de/research/>

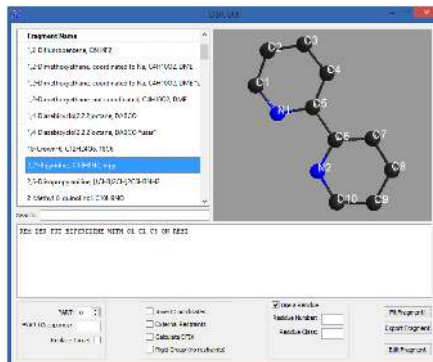


Figure 1.

**Keywords:** DSR, SHELXL, disorder, molecular database, computer programs, Python, C++

## MS46-P4 Selection of most promising hypothetical zeolite frameworks for the synthesis of new zeolites

Ekaterina D. Kuznecova<sup>1</sup>, Olga A. Blatova<sup>1</sup>

1. Samara Center for Theoretical Materials Science (SCTMS), Samara State Aerospace University named after academician S.P. Korolyov (National Research University), Moskovskoye Shosse 34, Samara 443086

email: kuznecova.ekaterina.d@gmail.com

Nowadays there are more than 300000 hypothetical zeolites structures in databases [1,2], whose nets are generated and optimized for energy, but only about 0.05% of them exist in nature or have been obtained in the laboratory. The aim of our work is to search for additional criteria for determination if hypothetical nets can be realized in real zeolites, and, respectively, which of them are the most likely to be synthesized.

Using the program package ToposPro [3], which implements the method of presenting zeolite framework as a packing of tiles (elementary cages) [4], we have decomposed all 230 known zeolite frameworks into tiles and found how the tiles associate to each other. A similar analysis was performed for hypothetical zeolites. According to [4], the tile packing (a way of connecting tiles without sharing atoms) features a method of the framework assembling by a polycondensation mechanism. We can expect that the most prospective hypothetical frameworks for the synthesis will be those, which have the similar method of assembling as in natural zeolites; this condition severely limits the choice. For example, the BRONZE database, which includes 274611 zeolite frameworks [1], comprises 8050 structures containing tiles of the **t-can** type (Figure 1a); 2132 of them can be built as packings of **t-can** (Fig. 1b,c). Comparative analysis allowed us to find eight hypothetical frameworks, where the arrangement of the **t-can** tiles and the way, in which they bind to each other, are the same as in real zeolites (ERI, LIO, LTL, OFF). These eight frameworks can be recommended as potential targets for synthesis.

In a similar way, we have analyzed packings of other types of tiles in hypothetical zeolite frameworks, and prepared a general list of the most prospective of them.

1. The Database on Prospective Zeolite Structures. <http://www.hypotheticalzeolites.net/>.
2. Pophale, R.; Cheeseman, P. A.; Deem, M. W. *Phys. Chem. Chem. Phys.* 2011, 13, 12407 <http://www.hypotheticalzeolites.net/DATABASE/DEEM/index3302403>
3. V.A. Blatov, A.P. Shevchenko, D.M. Proserpio *Cryst. Growth Des.* 2014, 14, 3576.
4. V. A. Blatov, G. D. Ilyushin, Davide M. Proserpio, *Chem. Mater.* 2013, 25, 412



Figure 1. Tile t-can (a) local connection of t-can (b) and the ERI framework assembled as a packing of t-can (c).

**Keywords:** zeolites, hypothetical zeolites, tilings

## MS46-P5 Reduction by deduction – How to prioritize crystallization experiments

Max Pillong<sup>1</sup>, Corinne Marx<sup>1</sup>, Wicker Jerome<sup>2</sup>, Cooper Richard<sup>2</sup>, Wagner Trixie<sup>1</sup>

1. Novartis Institute of Biomedical Research  
2. Department of Chemistry, University of Oxford

email: max.pillong@novartis.com

Computational tools have found an increasing use throughout various topics and fields in chemistry. From the prediction of physicochemical properties<sup>1</sup>, reaction types and products<sup>2</sup> or biological affinities towards macromolecules<sup>3</sup> up to the high-dimensional problem of crystal structure prediction, so-called *Machine Learning* models experience a steady increase in application. *Machine Learning* models are considered a collection of algorithms that can be used to find regularities, irregularities and correlations in data sets independent of their dimensionality. The resulting mathematical constructs can then be used to predictively characterize previously unseen data. In crystallography, recent studies have set out to use such algorithms in order to predict general crystallinity of small molecules<sup>4</sup>, their crystallization propensity in different solvents<sup>5</sup>, or the crystallization conditions of proteins<sup>6</sup>.

The most important prerequisite for a high-performing machine learning model is a sufficiently large data set of high integrity. Unfortunately, due to the lack of negative results in commonly used collections like the CSD, crystallization data suited for machine learning tasks is sparse. Therefore, several years back we set out to record both positive and negative results for every crystallization attempt made in the analytics group at the Novartis Institute for Biomedical Research. This data is stored in an SQL data base equipped with a touch-screen based graphical user interface, enabling easy access for both experimenter as well as programmer.

Next to numerous statistical analyses, we set out to use machine learning for the prediction of suitable conditions to crystallize small, drug-like molecules. In particular, we focused on the prediction of organic solvents to crystallize a given compound in. While the individual performances of the first generation of machine learning models for this were rather frugal, a newly devised ensemble approach embodying additional data allows us to rationalize our crystallization experiments and thus significantly reduce the experimental effort required to yield crystalline materials.

- [1] Alzghoul A., et al. (2014) *J Chem Inf Model* **54**, 3302-403
- [2] Schneider N., et al. (2016) *J Med Chem* (10.1021/acs.jmedchem.6b00153)
- [3] Reker D., et al. (2014) *PNAS* **111**, 4067-72
- [4] Wicker J.P., Cooper R. (2015) *CrystEngComm* **17**, 1927-34
- [5] Hosokawa K., et al. (2005) *ChemPharmBull* **10**, 1296-99
- [6] Rupp B., Wang J. (2004) *Methods* **34**, 390-407

**Keywords:** crystallization, machine learning, database, statistical analysis

**MS46-P6** Crystal structure, Hirshfeld surfaces and DFT computation of (E)-(5-methylfuran-2-yl) (morpholino) methanone oxime

Ersin Temel<sup>1</sup>, Aydın Demircan<sup>2</sup>, Medine Çolak<sup>2</sup>

1. Department of Electric and Energy, Technical Sciences Vocational High School, Giresun University, TR-28000, Giresun/Turkey

2. Department of Chemistry, Faculty of Arts and Science, Niğde University, TR-51240, Niğde, Turkey

email: ersin.temel@giresun.edu.tr

N-hydroxy amidoximes are one of the most important amidine derivatives with synthetic utility and various biological applications. They have been used extensively as starting materials for the preparation of nitrogen-rich heterocyclic compounds. Characteristically, they can also react or cyclize with electrophiles such as aldehydes, ketones, carboxylates, and acids. In practice, they have applications in drugs, dyes, polymers, and many other materials as well.

With this work, we provide a synthesis of N-hydroxy amidoxim from the reaction between furfurylimidoyle chloride and N-morpholine [1]. The structure of (Z)-(5-methylfuran-2-yl) (morpholino) methanone oxime was investigated with experimental (X-ray single crystal technique, NMR and FT-IR spectroscopic techniques) and theoretical (DFT) techniques. The compound crystallizes in monoclinic space group P2<sub>1</sub>/c. Crystal structure is stabilized by inter-molecular O-H...N and C-H...O hydrogen bonds. The Hirshfeld surface was drawn for visualizing the van der Waals distances and to determine the interaction sites. It is understood that O-H...N and C-H...O type hydrogen bonds are dominant interactions on the packing. When 2D fingerprint plot are partitioned, H-H interactions are seen to be the most dominant interactions with percentage of 60.2. And then O-H/H-O interactions with 20.0% and C-H/H-C interactions with 12.0% come. The puckering amplitude for the six-membered ring was determined as Q=0.572(3)Å. The gas phase geometry optimization and vibrational frequencies calculations were carried out using density functional theory (DFT) incorporated in B3LYP with 6-311++(d,p) basis set. The detailed vibrational assignments were performed on the basis of the potential energy distributions (PED) of the vibrational modes. Additionally, HOMO-LUMO energy gap, natural bond orbital (NBO) analysis and nonlinear optical (NLO) properties of the compound were performed.

**Acknowledgement:** We would like to thank TUBITAK (PN: 113T136) and Giresun University for financial support of this work.

[1] A. R. Katritzky, L. Huang, M. Chahar, R. Sakhuja, C. D. Hall, *Chem. Rev.* **2012**, 112, 1633–1649; P. Vitale, S. Tacconelli, M. G. Perrone, P. Malerba, L. Simone, A. Scilimati, A. Lavecchia, M. Dovizio, E. Marcantoni, A. Bruno, P. Patrignani *J. Med. Chem.* **2013**, 56, 4277–4299; V. Mercalli, M. Giustiniano, E. Del Grosso, M. Varese, H. Cassese, A. Massarotti, E. Novellino, and Gian Cesare Tron, *ACS Comb. Sci.* **2014**, 16, 602–605.

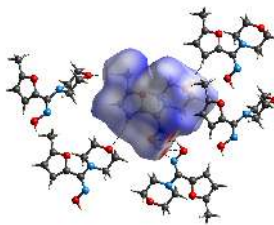


**Figure 1.** The Hirshfeld surface mapped with  $d_{\text{norm}}$

**Keywords:** Single crystal X-ray diffraction, Density Functional Theory, Hirshfeld Surfaces, Spectroscopic Methods



## MS47 Teaching & Education

Chairs: Helen Stoeckli-Evans, Howard Flack

### MS47-P1 Modern web technologies as tools in teaching crystallographic group theory

Zoran Štefanić<sup>1</sup>

1. Ruder Bošković Institute, Bijenička 54, 10000 Zagreb, Croatia

email: zoran.stefanic@irb.hr

The concept of symmetry is central to crystallography. Although symmetry is ubiquitous around us, it takes some conceptual effort to leverage this everyday knowledge in understanding why the molecules pack the way they pack in crystals. Group theory on the other hand is a mathematical formalism describing symmetry. In the crystallographic context it comes in the form of point, plane and space groups. As with any abstract concept to be learned, it is easier to understand by visualization.

Today there are plenty of excellent libraries for visualization of data in 2D (like for example d3.js<sup>1</sup>). Even the HTML standard has evolved in the way that it now natively supports drawing on its canvas. Combined with some great capabilities of the general purpose library for crystallographic computations such as cctbx<sup>2</sup> it can be used to bring the visualization of space group patterns to a very broad audience, practically everyone and everywhere. This undertaking was conceived originally as a help in teaching the course “Group theory in crystallography” to graduate students of chemistry.

1. <https://d3js.org/>

2. R. W. Grosse-Kunstleve, N. K. Sauter, N. W. Moriarty and P. D. Adams, *J. Appl. Cryst.* **35** (2002) 126-136.

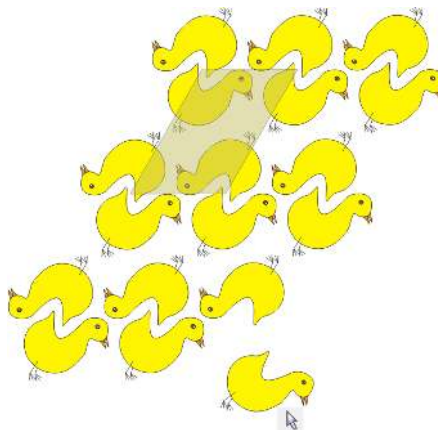


**Figure 1.** Trying to arrange objects interactively in „crystal“ packing can be more instructive than learning group theory formalism just through theorems and formulas.

**Keywords:** teaching group theory, web visualization,

## MS48 Crystallography in art and cultural heritage

Chairs: Alicja Rafalska-Lasocha, Helen Stoeckli-Evans

### MS48-P2 X-ray powder diffractometry in the study of heritage objects from Polish museums

Alicja Rafalska-Lasocha<sup>1</sup>, Marta Grzesiak-Nowak<sup>1</sup>, Wiesław Łasocha<sup>1,2</sup>

1. Faculty of Chemistry Jagiellonian University, 30-060 Krakow, Ingardena 3, Poland

2. Jerzy Haber Institute of Catalysis and Surface Chemistry PAS, 30-239 Kraków, Niezapominajek 8, Poland

email: rafalska@chemia.uj.edu.pl

X-ray-based techniques continue to be the preferred methods for scientific analysis of material composition of the objects of cultural heritage. Within this group, X-ray fluorescence (XRF) and X-ray powder diffraction (XRPD), due to their non-destructive nature, are the most popular and well-established methods in the field of heritage science. These scientific studies provide support for archaeologists, art historians, and conservators as they continue to expand their knowledge about heritage objects housed in museums and private collections. Information about the composition of heritage objects facilitates the understanding of historical events, manufacturing techniques, and provenance. In addition, the obtained results can assist in the formation of better preventive conservation strategies for the valuable ancient collections.

The XRF technique, usually applied as the first step of an investigation, provides information about the elemental composition of a sample, whereas XRPD enables identification of its phase composition. It is often difficult to identify the presence of a certain compound on the basis of XRF alone; thus, the results obtained by this technique usually require clarification or confirmation by XRPD.

Structure-oriented Powder Diffractometry group at the Faculty of Chemistry, Jagiellonian University, is involved in XRPD investigations of metallic archaeological objects (seals, coins, spearheads, jewellery) [1] and painting materials used by famous Polish painters [2] such as Henryk Siemiradzki, Aleksander Gierymski, Rafał Hadziewicz whose works are housed in a great number of museums. In our study we investigated works from the collections of the National Museum in Krakow. The obtained results and various case studies involving the use of XRPD will be presented with the aim of illustrating some of the possibilities and limitations encountered when analysing the objects of cultural heritage.

[1] M. Wołoszyn, E. M. Nosek, J. Stepiński, A. Rafalska-Lasocha, W. Łasocha, E. Bielańska, *The seals*

*from Czeremno (Cherven Towns, eastern Poland) – chemical analysis and metallurgical examination.*, Archeologia Polski, LX:2015, 123–152

[2] A. Rafalska-Łasocha, M. Grzesiak-Nowak, D. Sarkowicz, W. Łasocha, *The use of XRPD for the investigation of historic pigments and painting materials in works by Henryk Siemiradzki*, J. Anal. At. Spectrom., 2015, 30, 751–758

**Keywords:** XRPD, cultural heritage, XRF

## MS49 How to....: crystallization for small and large molecules

Chairs: Aurelien Crochet, Andrew Maloney

### MS49-P1 Growing single crystals using thermal recrystallization

Philipp P. Nievergelt<sup>1</sup>, Bernhard Spingler<sup>1</sup>

<sup>1</sup> Department of Chemistry, University of Zurich, Switzerland

email: philipp.nievergelt@chem.uzh.ch

Growing of suitable single crystals is fundamental for the determination of the X-ray structure. Quite often, only an X-ray analysis reveals the composition of a compound. We have written a tutorial about the growth of single crystals, however this publication only discusses isothermal methods such as vapour diffusion or layering of different solvents.[1] There are very few reports about molecular single crystals that were grown by slow cooling.[2, 3]

We have now studied for a series of very different compounds the growth of single crystals by thermal crystallisation with the help of the CrystalBreeder. For thermal recrystallization, it is essential to know the solubility in the chosen solvent at a selected temperature in order to obtain supersaturation at the cooling step. We observed that thermal recrystallization can be performed very fast – suitable carbamazepine and *p*-amino benzoic acid single crystals could be obtained only within one day – more importantly the obtained crystal quality for these compounds was excellent. Furthermore, we only used small amounts (as little as 1 mg) of material which is of course very advantageous.

[1] B. Spingler, S. Schnidrig, T. Todorova, F. Wild, *CrystEngComm* **2012**, *14*, 751.

[2] R. W. Seidel, J. Graf, R. Goddard, I. M. Oppel, *Acta Cryst.* **2011**, *E67*, m236.

[3] T. Notake, K. Nawata, H. Kawamata, T. Matsukawa, H. Minamide, *Opt. Mater. Express* **2012**, *2*, 119.

**Acknowledgement:** We thank Technobis for providing us with the CrystalBreeder and Dr. Carmen Guguta for many helpful discussions.

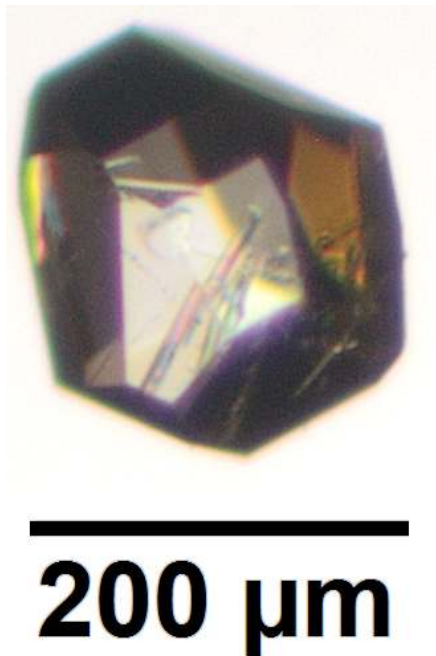


Figure 1. Carbamazepine crystal grown in isopropyl alcohol within six hours

**Keywords:** Crystal growth, carbamazepine, *p*-amino benzoic acid, polymorphs, single crystals, thermal recrystallization

## MS50 History of ECA, history of crystallography: contributions to and of crystallography

triclinic crystal, developing expressions for conditions of appearance and for intensities of the principal and subsidiary diffraction maxima. He found conditions under which the intensity of subsidiary maxima became negligible. Brixxy proposed a number of crystallographic terms in Croatian, many of them being nowadays in use.

**Keywords:** X-rays, X-ray diffraction, Bernardo Brixxy

Chairs: Menahem Kaftory, Peter Paufler

### MS50-P1 Franciscan Brixxy, the first Laue's follower in Croatia

Stanko Popović<sup>1,2</sup>, Branko Hanžek<sup>1</sup>

1. Croatian Academy of Sciences and Arts, Zagreb, Croatia

2. Physics Department, Faculty of Science, University of Zagreb, Croatia

email: spopovic@phy.hr

Laue discovered diffraction of X-rays in 1912 and the Braggs determined the first crystal structures in 1913. Soon after that, Bernardo Brixxy (1882-1945) published papers, in Croatian, on properties and interference of X-rays. The titles of the papers and journals, translated in English, are: X-rays and new discoveries, *Croatian Education*, Society of Croatian Writers, Zagreb, **3**(1916) 155-160, 251-258, 368-375; Theory of interference of X-rays in a general case, *Educational Journal*, Society of Croatian Teachers, Zagreb, **26**(1917) 1-17; Cathode and X-rays, *Our Thought*, Croatian and Slovenian Franciscans, Sarajevo, **32**(1918) 94-100. Brixxy was graduated in theology, mathematics and physics at the University of Zagreb. He was the author of textbooks and papers published in Croatian and German journals. Brixxy described in detail the collected knowledge on X-rays, the main facts being as follows. The point of impact of cathode rays on a solid is the source of X-rays, which propagate along straight lines by the speed of light. The absorption of X-rays in a material depends on its chemical composition. X-rays are *inhomogeneous*, showing a spread of wavelengths. The impact of X-rays on a solid causes the emission of secondary rays: b-rays, *diffuse* X-rays (*i.e.* incoherent scattering) and characteristic, *homogeneous*, X-rays. The wavelengths of the characteristic X-rays depend on the chemical elements contained in the solid. The emission of characteristic X-rays can be induced in an element if its atomic number is smaller than that of the element which is the source of primary X-rays. The nature of X-rays is very similar to that of light, as both radiations exhibit interference, diffraction and polarization. The wavelength of X-rays is comparable to the distance among neighbouring atoms in the crystal. The interference maxima appear in directions for which X-rays, coherently scattered by atoms in the crystal, are in phase. Brixxy compared Laue's theory of interference of X-rays and W. L. Bragg's theory of reflection of X-rays (considered as particles) from crystal lattice planes. He elaborated a rigorous theory of interference of X-rays scattered by a

the 1990s, the incidence of *S. flexneri* has increased in the United Kingdom [10]. In the United States, *S. flexneri* has been reported as the most common serotype in the 1990s [11]. In the United Kingdom, *S. flexneri* has been reported as the most common serotype in the 1990s [12]. In the United States, *S. flexneri* has been reported as the most common serotype in the 1990s [11].

The purpose of this study was to determine the prevalence of *S. flexneri* in the United Kingdom. The study was conducted in the United Kingdom, where *S. flexneri* is the most common serotype. The study was conducted in the United Kingdom, where *S. flexneri* is the most common serotype.

The study was conducted in the United Kingdom, where *S. flexneri* is the most common serotype. The study was conducted in the United Kingdom, where *S. flexneri* is the most common serotype.

The study was conducted in the United Kingdom, where *S. flexneri* is the most common serotype. The study was conducted in the United Kingdom, where *S. flexneri* is the most common serotype.

The study was conducted in the United Kingdom, where *S. flexneri* is the most common serotype. The study was conducted in the United Kingdom, where *S. flexneri* is the most common serotype.

The study was conducted in the United Kingdom, where *S. flexneri* is the most common serotype. The study was conducted in the United Kingdom, where *S. flexneri* is the most common serotype.

The study was conducted in the United Kingdom, where *S. flexneri* is the most common serotype. The study was conducted in the United Kingdom, where *S. flexneri* is the most common serotype.

The study was conducted in the United Kingdom, where *S. flexneri* is the most common serotype. The study was conducted in the United Kingdom, where *S. flexneri* is the most common serotype.

The study was conducted in the United Kingdom, where *S. flexneri* is the most common serotype. The study was conducted in the United Kingdom, where *S. flexneri* is the most common serotype.